Euratom
European Commission

**Nuclear fission safety
programme
1992-94**

Radiation protection research action

Final report

Volume 2

EUR 16769 DE/EN/FR

Comisión Europea
Europa-Kommissionen
Europäische Kommission
Ευρωπαϊκή Επιτροπή
European Commission
Commission européenne
Commissione europea
Europese Commissie
Comissão Europeia

Euratom

Programa
SEGURIDADDE LA FISIÓN NUCLEAR
Plan de «Investigación en materia de protección contra las radiaciones»

Program
SIKKERHED I FORBINDELSE MED KERNESPALTING
Programmet »Forskning vedrørende Strålingsbeskyttelse«

Programm
SICHERHEIT BEI DER KERNSPALTUNG
Aktion „Strahlenschutzforschung"

Πρόγραμμα
ΑΣΦΑΛΕΙΑ ΣΤΗΝ ΠΥΡΗΝΙΚΗ ΣΧΑΣΗ
Δράση «'Ερευνα στον τομέα της Ακτινοσταυίας»

NUCLEAR FISSION SAFETY
programme
Action 'Radiation protection research'

Programme
« SÛRETÉ DE LA FISSION NUCLÉAIRE »
Action «Recherche en radioprotection»

Programma
SICUREZZA DELLA FISSIONE NUCLEARE
Azione «Ricerca sulla radioprotezione»

Programma
VEILIGHEID VAN KERNSPLIJTING
Actie „Onderzoek Stralingsbescherming"

Programa
SEGURANÇA DA CISÃO NUCLEAR
Acção «Investigação no domino da protecção contra radiações»

1992-1994
Final report

Volume 2

1997   EUR 16769 DE/EN/FR

Zahlreiche weitere Informationen zur Europäischen Union sind verfügbar über Internet, Server Europa (http://europa.eu.int).

A great deal of additional information on the European Union is available on the Internet. It can be accessed through the Europa server (http://europa.eu.int)

De nombreuses autres informations sur l'Union européenne sont disponibles sur Internet via le serveur Europa (http://europa.eu.int).

Bibliographische Daten befinden sich am Ende der Veröffentlichung.

Cataloguing data can be found at the end of this publication.

Une fiche bibliographique figure à la fin de l'ouvrage.

Printed in Belgium

INHALTSVERZEICHNIS

―――――

TABLE OF CONTENTS

―――――

TABLE DES MATIERES

―――――

A2   Transfer and behaviour of radionuclides in the environment.

A2A IUR

A21   Environmental behaviour of radionuclides in situations meriting particular attention for long-term behaviour or post-acident conditions.

A22   Natural radioactivity in the environment and its pathways to man.

FI3P-CT920035-A22 . . . . *991*
        Pathways of radionuclides emmited by non nuclear industries.

        1   Lembrechts   RIVM
        2   Germain   CEA - FAR
        3   Travesi Jiménez   CIEMAT
        4   Ortins   Direcção-Geral do Ambiente
        5   García-León   Univ. Sevilla
        6   McGarry   RPII
        7   Ortins   Direcção-Geral do Ambiente
        8   Dahlgaard   Lab. Risø
        9   Heaton   Univ. Aberdeen
        10 Zagyvai   TUBUD.INT

FI3P-CT930075-A22 . . . . *1059*
        Investigation on exposure to natural radionuclides in selected areas affected by
        U-processing.

        1   Belot   CEA - FAR
        2   Röhnsch   BFS
        3   Massmeyer   GRS

A23   Influence of speciation, chemical modification, changes in physico-chemical
        properties and biological conversion.

FI3P-CT920010-A23 . . . . *1085*
        The bio-availability of long-lived radionuclides in relation to their physico-chemical
        form in soil systems.

        1   Lembrechts   RIVM
        2   Wilkins   NRPB
        3   Cremers   Univ. Leuven (KUL)
        4   Merckx   Univ. Leuven (KUL)
        5   Staunton   INRA - Montpellier
        6   Berthelin   CNRS
        7   Mocanu   ROIAP
        8   Szabó   NRIRR *(PECO contract)*

FI3P-CT920022-A23 . . . . *1169*
        Investigations and modelling of the dynamics of environmental HT/HTO/OBT levels
        resulting from tritium releases.

        1   Bunnenberg   ZSR
        2   Belot   CEA - FAR
        3   Kim   Univ. München - Technische
        4   Dertinger   KfK
        5   Eikenberg   Inst. Paul Scherrer
        6   Uchrin   HAS.II
        7   Paunescu   IFIN

A24   The behaviour of accidentally released radionuclides, evaluation of the reliability of transfer parameters and experimental studies.

1	Howard	ITE
2	Assimakopoulos	Univ. Ioannina
3	Crout	Univ. Nottingham
4	Mayes	Inst. MacAulay Land Use Research
5	Voigt	GSF
6	Vandecasteele	CEN/SCK Mol
7	Zelenka	UAB.FAGR
8	Hove	Univ. Norway - Agricultural
9	Hinton	Inst. Paul Scherrer

A25   The role of retention and release of radionuclides in natural ecosystems and in marginal agricultural areas.

1	Minski	IMPCOL
2	Rauret	Fundació "Bosch i Gimpera"
3	Ronneau	Univ. Louvain (UCL) - LLN

1	Wirth	BFS
2	Moberg	Inst. Nat. of Radiation Protection
3	Bergman	Swedish Defense Research Establish.
4	Palo	Univ. Agricultural Sci. of Sweden
5	Impens	Faculté Sciences Agronom. Gembloux
6	Belli	ENEA
7	Feoli	CETA
8	Nimis	Univ. Trieste
9	Antonopoulus-Domis	Univ. Thessaloniki
10	Pietrzak-Flis	CLRP Warsaw

1	McGarry	RPII
2	Horrill	NERC
3	Nielsen	Lab. Risø
4	Johanson	Univ. Umeå - Agr.Sci. - Dep. Forestry
5	Veresoglou	Univ. Thessaloniki

A26   Development of countermeasures to reduce the contamination in the environment and
       to impede its transfer to man.

VOLUME 2

B11   Interpretation of low dose and low dose rate effects with the help of microdosimetry.

FI3P-CT920027-B11 . . . . *1705
         Biophysical models for the effectiveness of different radiations.

         1   Paretzke   GSF
         2   Goodhead   MRC
         3   Terrissol   ADPA
         4   Leenhouts   RIVM
         5   Von Sonntag   Inst. Max-Planck
         6   Smith   Univ. London
         7   O'Neill   MRC

FI3P-CT920041-B11 1769
         Specification of radiation quality at nanometre level.

         1   Colautti   INFN - Legnaro
         2   Watt   Univ. St. Andrews
         3   Harder   Univ. Göttingen
         4   Leuthold   GSF
         5   Izzo   Univ. Roma - Tor Vergata
         6   Kraft   GSI
         7   Pszona   SINS.PL

B12   Repair and modification of genetic damage and individual radiosensitivity.

FI3P-CT920007-B12 1823
         Molecular basis of radiosensitivty.

         1   Lohman   Univ. Leiden
         2   Bridges   MRC
         3   Bootsma   Univ. Rotterdam - Erasmus
         4   Moustacchi   CIR
         5   Thacker   MRC
         6   Backendorf   Univ. Leiden
         7   Eckardt-Schupp   GSF
         8   Szumiel   ICHTJ
         9   Szymczyk-Wasiluk   WMS

FI3P-CT930080-B12 1889
         Radiation ionduced mitotic aneuploidy.

         1   Parry   Univ. Wales, Cardiff
         2   Tanzarella   CNR
         3   Kirsch Volders   Univ. Bruxelles (VUB)

B13   Cellular, molecular and animal studies to determine the risk of stochastic somatic
       effects of radiation with respect to low dose, low dose rate and radiation quality.

FI3P-CT920011-B13 1923
         Cytogenetic and molecular mechanisms of radiation myeloid leukaemogenesis in the
         mouse.

         1   Janowski   VITO
         2   Cox   NRPB
         3   Huiskamp   ECN

B14   Assessment of genetic risks in man.

FI3P-CT920005-B14 . . . . *2389*
        Radiation-induced genetic effects in mammals and the estimation of genetic risks in
        man: a concerted approach using theoretical, epidemiological, cytogenetic,
        biochemical and molecular methods.

        1   Sankaranarayanan   Univ. Leiden
        2   Tease   MRC
        3   Jacquet   CEN/SCK Mol
        4   Streffer   Univ. Essen
        5   Czeizel   WHO

FI3P-CT920055-B14 . . . . *2433*
        Genetic risks associated with exposure to ionizing radiation.

        1   Favor   GSF
        2   Van Buul   Univ. Leiden
        3   Cattanach   MRC
        4   de Rooij   Univ. Utrecht
        5   Miró Ametller   Univ. Barcelona - Autónoma
        6   Eeken   Univ. Leiden
        7   Hulten   EBHA

B15   Action of radionuclides on target cells in relation to radionuclide metabolism and
        studies on biological models for radionuclide-induced cancer.

FI3P-CT920021-B15 . . . . *2487*
        Dose assessment early cellular and late carcinogenic effects of exposure to radon and
        its progeny.

        1   Fritsch   CEA - Paris
        2   Collier   UKAEA

FI3P-CT920051-B15 . . . . *2513*
        Induction of osteosarcoma and leukaemia by bone-seeking alpha-emitting
        radionuclides.

        1   Höfler   GSF
        2   Harrison   NRPB
        3   Wright   MRC
        4   Erfle   GSF
        5   Skou Pedersen   Univ. Århus
        6   Höfler   Univ. München - Technische

B2   Non-stochastic Effects of Radiation.

B21   Radiation syndromes and their treatment after exposure of large parts of the body.

FI3P-CT920008-B21 . . . . *2545*
        Research on the management of accidentally radiation exposed persons.

        1   Fliedner   Univ. Ulm
        2   Wagemaker   Univ. Rotterdam - Erasmus
        3   Covelli   ENEA
        4   Jammet   CIR

B33   Transfer of radionuclides in utero.

        Dosimetry and effects of parental, fetal and neonatal exposure to incorporated
        radionuclides and external radiation.

        1   Harrison   NRPB
        2   Henshaw   Univ. Bristol
        3   Van den Heuvel   VITO
        4   Lord   Inst. Paterson
        5   Visser   TNO - Delft
        6   Tejero   Univ. Madrid - Complutense
        7   Bueren   CIEMAT
        8   Archimbaud   CEA - Bruyères-le-Chàtel

VOLUME 3

C   **RISKEN DER STRAHLENEXPOSITION UND IHRE BEWÄLTIGUNG**
     RISKS AND MANAGEMENT OF RADIATION PROTECTION

C1   **Assessment of human exposure and risks.**

C12   Exposure to natural radioactivity and evaluation of parameters influencing these risks.

        Retrospective assessment of radon exposure from long-lived decay products.

        1   Vanmarcke   CEN/SCK Mol
        2   McLaughlin   Univ. Dublin - College
        3   Falk   Inst. Nat. of Radiation Protection
        4   Poffijn   Univ. Gent
        5   Fehér   HAS.RIAE *(PECO contract)*
        6   Samuelsson   Univ. Lund

        Characteristics of airborne radon and thoron decay products.

        1   Porstendörfer   Univ. Göttingen
        2   Poffijn   Univ. Gent
        3   Vanmarcke   CEN/SCK Brussels
        4   Akselsson   Univ. Lund
        5   Falk   Inst. Nat. of Radiation Protection
        6   Tymen   Univ. Brest
        7   Ortega   Univ. Catalunya - Politécnica
        8   Lebecka   CMI
        9   Kobal   IJS
       11   Schuler   Inst. Paul Scherrer

FI3P-CT920061-C12 . . . . *3019*
       Study of the different techniques to mitigate high radon concentrations level disclosed
       in dwelling.

1	Sabroux	CEA - IPSN
2	Torri	ENEA
3	Ortins	Direcção-Geral do Ambiente
4	Quindós Poncela	Univ. Cantabria
5	Kritidis	NCSR "Demokritos"
6	Proukakis	Univ. Athens (Not yet submitted)

FI3P-CT920064d-C12 . . . . *3069*
       Radon sources models and countermeasures.

1	Miles	NRPB
2	De Meijer	Univ. Groningen
3	Andersen	Lab. Risø
4	Wouters	CSTC-WTCB
5	Ball	NERC
6	De Meijer	Univ. Groningen
7	Hubbard	Inst. Nat. of Radiation Protection
8	Balek	BIJO
9	Cosma	NPL.RO

FI3P-CT930074-C12 . . . . *3159*
       Evaluation of the combined helium/radon in soil gas mapping methodology as an
       indicator of areas in which elevated indoor radon concentrations may be found.

1	Madden	RPII
2	O'Connor	Geological Survey (Irish)
3	Van den Boom	ENMOTEC GmbH
4	Porstendörfer	Univ. Göttingen

C13   Comparative assessment of exposure and risks.

FI3P-CT920019-C13 . . . . *3219*
       Comparative assessment and management of radiological and non-radiological risks
       assiciated with energy systems.

1	Dreicer	CEPN
2	Friedrich	Univ. Stuttgart
3	Uijt de Haag	RIVM

FI3P-CT920064e-C13 . . . . *3249*
       Studies related to the expression of the detriment associated with radiation exposure.

1	Muirhead	NRPB
2	Schneider	CEPN

FI3P-CT930065-C14 . . . . *3473*
　　　Risk estimates of lung cancer from the follow-up of uranium miners.

　　　1　Chmelevsky　　　　　GSF
　　　2　Tirmarche　　　　　　CEA - FAR
　　　3　Muirhead　　　　　　NRPB
　　　4　Darby　　　　　　　　ICRF
　　　5　Kunz　　　　　　　　　NIPHE.CRH

FI3P-CT930066-C14 . . . . *3529*
　　　International collaborative study of cancer risk among nuclear industry workers.

　　　1　Cardis　　　　　　　　IARC
　　　2　Sztanyik　　　　　　NRIRR
　　　3　Cesnek　　　　　　　SEP

C2　　Optimisation and management of radiation protection.

C2A ICRP

FI3P-CT920004-C2A *3547*
　　　Development of fundamental data for radiological protection.

　　　1　Smith　　　　　　　　ICRP

C21　　Optimisation of radiological protection.

FI3P-CT920033-C21 . . . . *3555*
　　　Alara in installations.

　　　1　Lefaure　　　　　　　CEPN
　　　2　Zeevaert　　　　　　CEN/SCK Mol
　　　3　Pfeffer　　　　　　　GRS
　　　4　Wrixon　　　　　　　NRPB

C22　　Reduction of patient exposure in medical diagnostic radiology.

FI3P-CT920014-C22 . . . . *3597*
　　　Digital Medical Imaging: Optimization of the dose for the examination.

　　　1　Malone　　　　　　　Hosp. Federated Dublin Voluntaries
　　　2　Faulkner　　　　　　Hosp. Newcastle
　　　3　Busch　　　　　　　　Univ. Heidelberg
　　　4　Jankowski　　　　　　IOM
　　　5　Shehu　　　　　　　　Inst. Onkologjise

FI3P-CT920020-C22 . . . . *3653*
　　　Quality assurance parameters and image quality criteria in computed thomography.

　　　1　Jessen　　　　　　　Univ. Århus - Hospital
　　　2　Ortins　　　　　　　Direcção-Geral do Ambiente
　　　3　Schneider　　　　　　Univ. München
　　　4　Moores　　　　　　　IRS Ltd.

III B

FOLGEN DER STRAHLENEXPOSITION DES MENSCHEN; IHRE ABSCHÄTZUNG, VERHÜNTUNG UND BEHANDLUNG

CONSEQUENCES OF RADIATION EXPOSURE TO MAN; THEIR ASSESSMENT, PREVENTION AND TREATMENT.

CONSEQUENCES POUR L'HOMME DE L'EXPOSITION AUX RAYONNEMENTS, EVALUATION, PREVENTION ET TRAITEMENT
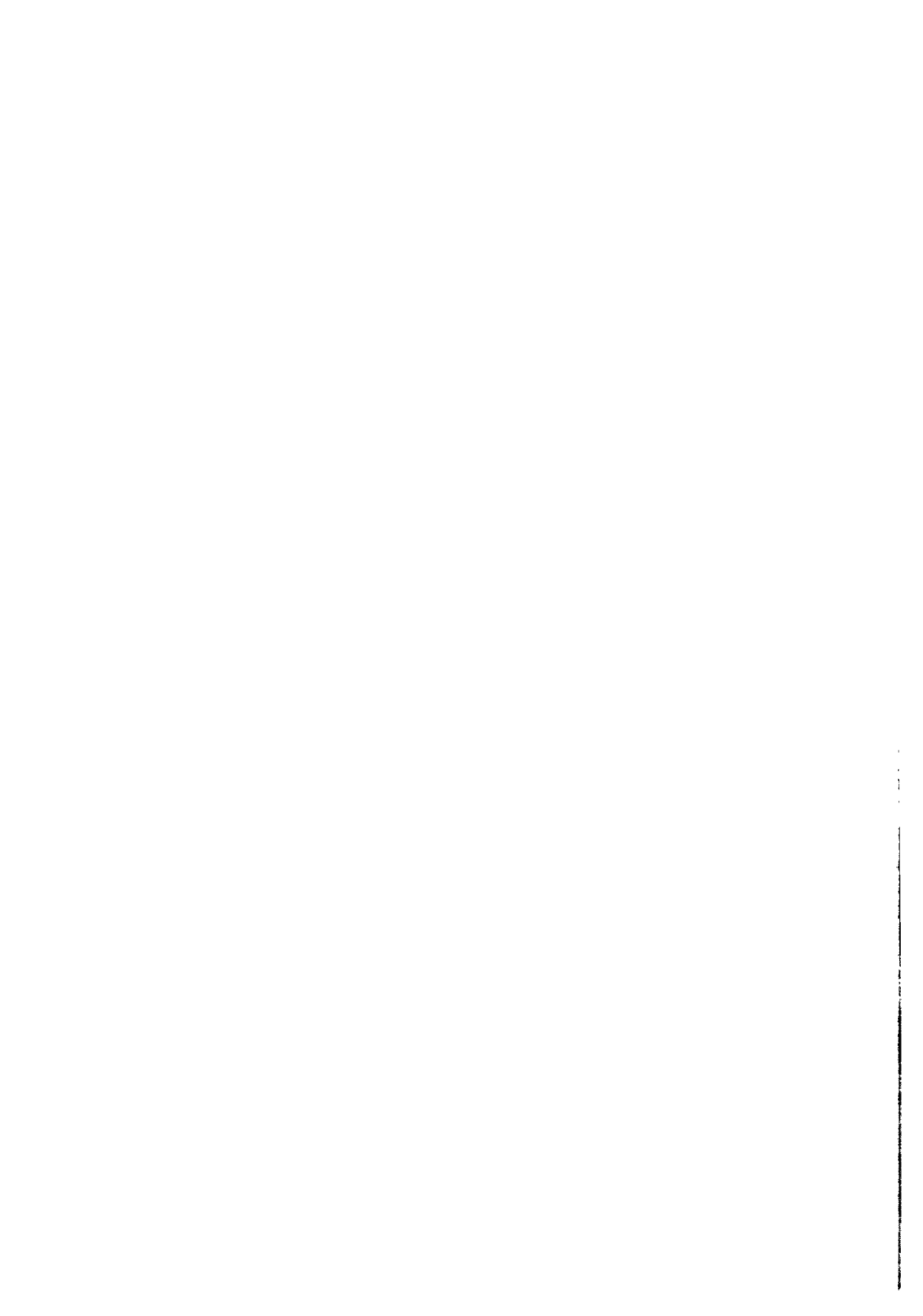
FINAL REPORT

Contract: F13P-CT920030   Sector: B1A

Title: Co-operative research on late somatic effects of ionizing
radiation in the mammalian organism

1)   Maisin   EULEP

I.   **Summary of Project Global Objectives and Achievements**

The objective of the European Late Effects Project Group (EULEP)
is to improve the understanding of late biological effects of
exposure to ionising radiation.   Its work consists of the
standardization and development of methodology in the member
institutions, the coordination and promotion of co-operative
research by means of task groups, and the organisation of
training activities, workshops and symposia.   There are now 26
laboratories participating in this work.   From these are drawn
129 Associate Members and, from other laboratories, there are
currently 57 Corresponding Members who are participating to the
work of EULEP.

Work on the Standardisation and Development of Methodology has
been carried out by the following committees:

- Committee of External Radiation Dosimetry and Techniques
- Committee of Internal Radiation Dosimetry and Techniques
- Committee on Cell and Molecular Pathology

The co-ordination of collaborative research work between the
member institutions has been organised by means of a number of
problem-orientated task groups and special task group actions,
which are devoted to specific problems and which have their own
defined goals.

A more recent objective has been the establishment of an archive
of long-term radiobiological studies, consisting of a
comprehensive database and decentralized specimen archive.

EULEP   is   concerned   to   promote   the   training   of   young
radiobiologists. High priority continues to be attached to the
support of scientific exchange visits between laboratories for
the purpose of acquiring technical expertise. The means by which
EULEP achieves its stated objectives is reviewed regularly, and
it has maintained sufficient flexibility in its organisation to
meet changing requirements.

II. Objectives for the reporting period

(a) to develop the programme of standardisation and development of methodology through the committees;

(b) to promote the co-ordination of research by the task groups and special task group actions, including the review of existing work and the establishment of new task groups and actions as opportunities presented themselves;

(c) to continue the development of the European Radiobiological Archive;

(d) to continue an ongoing review of the future structure and activities of EULEP, in the light of changing requirements in radiation protection research.

III. Progress achieved including publications

STANDARDISATION AND DEVELOPMENT OF METHODOLOGY

Committee of Cell and Molecular Pathology

During the passed period, the Committee of Pathology and the Committee of Molecular Biology have merged in order to bridge the interests of classical morphological pathology and experimental molecular biology. The Committee has organized several symposia, workshops and slide seminars.

The annual slide seminar of 1992 was held on November 6 at Neuherberg on the "Pathology of immune-related diseases". Professor Müller-Hermelink (Würzburg) gave an excellent overview on the pathogenesis of immunopathic diseases. Professor Baroni demonstrated the role of expression of cell adhesion molecules and cytokines in human thymus and thymomas. Professor Feller (Lübeck) gave an overview of the interactions in the cytokine network during the maturation of lymphoid cells and the role of the disturbance of this network in the pathogenesis of malignant lymphoma. Dr Feichtinger (Innsbruck) and Professor Boniver (Liège) demonstrated their experimental models of AIDS. In addition, problem cases of liver pathology in rats from Professor Bannasch (Heidelberg) were discussed.

The slide seminar of 1993 was held in November at Neuherberg, and dealt with the "Pathology of Certain Strains of Transgenic Mice". Contributions included a detailed introduction to the approach of using transgenic animals by W Engström; aspects of B-cell lymphomas in mice carrying activated myc or ras oncogens by P Pattengale; and the use of transgenic mice in the study of liver neoplasia and pre-neoplasia by P Bannasch; mammary and urino-genital neoplasia and hyperplasia by G W H Stamp; neurological degeneration by A Aguzzi, and bone tumours by A Luz and J Schmidt. In 1994, the topic of the slide seminar and workshop was: "Pathology of Soft Tissue Tumors".

In 1993, the committee organised at the occasion of the General Assembly of Reisensburg a workshop on "Pathology of Transgenic Mice". Several experts gave talks covering many aspects of the application of transgenic mice, especially the study of the pathogenesis of malignant lymphomas and mammary neoplasia. In 1994, the committee organized a symposium on programmed cell death apoptosis.

The committee organised three meetings between EULEP and the Biological Effects Task Group of the US DOE: the first one was held in Paris, France in October 1992: the second one at Heidelberg in April 1994 and the third one in Albuquerque, New Mexico, USA in 1995. The meeting in Paris concerned "Acute and Late Effects on the Lung from Inhaled Radioactive Materials and External Radiation". The second workshop covered liver pathology, including comparative aspects in animals and man, caused by radiation and also chemicals. The third workshop concerned the hematopoietic system. It included a general discussion on the status of pathology efforts in radiation pathology of both sites of the Atlantic.

The new colour edition of the EULEP Pathology Atlas has now been published. It is felt that this complements other existing pathology atlases very well. It is the intention of the committee to proceed immediately to preparing the second volume, which would cover all remaining topics not included in the first.

Committee of External Radiation Dosimetry

The committee of X-ray dosimetry decided that a seventh dosimetry intercomparison would be performed, using TLD which would be read at TNO Arnhem, now a new voting member laboratory of EULEP. It was necessary to continue such exercises, in order to check both the accuracy and precision of dosimetric measurements among member laboratories, and the homogeneity of the dose delivered. It was also essential to be able to provide special assistance where discrepancies were discovered, so that these could be rectified.

In addition, the activities of the committee have been focused on the characteristics of phantoms simulating experimental animals of various sizes. In this context the EULEP phantoms have also been included in the ICRU report 48 (1993) on Phantoms and Computational Models in Therapy, Diagnosis and Protection. As a follow-up of the studies with the rectangular and cylindrical rat phantoms, dose distributions have been studied in more realistic phantoms. For unilateral and bilateral irradiation with 300 kV X-rays of the real shape phantoms, maximum to minimum doses values in the trunk amounted to 2.5 and 1.25 respectively. These values are appreciably higher than those reported earlier (Zoetelief *et al*, 1985, Int. J. Radiat. Biol. 47, 81-102) for phantoms with simple geometry.

Other activities of the EULEP Dosimetry Committee are concerned with the assessment of dose distributions employing Monte Carlo calculations and the introduction of new thermo-luminescent material for the determination of the absorbed dose.

Committee of Internal Radiation Dosimetry

During this contract period, the Committee continued to support standardisation activities by means of inter-laboratory consultations for its five Tasks Groups.

Several members of the Committee of Internalradiation Dosimetry have been active in assisting ICRP to revise its biokinetic models, as required for updating different ICRP publications. As members of the ICRP task group on internal dosimetry, and in some cases as members of Committee 2, EULEP scientists were playing lead roles in the development of new biokinetic models for radionuclide behaviour in adults, children and in the fetus. Much of this work has now been published as ICRP publications 66, 67 and 69. Members of the committee had also accepted invitations during the year to provide specialist advice to the CEC multi-national contract on reduction of risk.

The Committee has considered the direction which its future activities might take during the next four years. These activities will include the continuation of its role in the standardization of methods and in the international work on dosimetric models and dose coefficients, and could also include training courses in internal dosimetry, perhaps in collaboration with EURADOS; the preparation of state of the art reports on topics related to internal dosimetry, for example the uncertainties attached to dosimetric parameters; and a feasability study of the practicability of preparing a comprehensive international database containing all the available information on radionuclide biokinetics in humans and animals.

EULEP Radiobiology Archive

EULEP has now established the database for the archive of long – term animal experiments performed in European laboratories. It has been developed in collaboration with the National Radiobiological Archives of the US DOE. Much of the information, and the associated histological material, is irreplaceable and must be preserved after the scientists concerned retire or the institutes change their interests. Moreover, the materials offer possibilities for future use by molecular techniques.

A list of all communicated experiments has been republished, including exposure conditions, treatments, dosimetry and species used. The data have been computerized for 40 large-scale studies comprising more than 70,000 animals, giving information on survival and pathology. This is available both in a purpose-

designed system, which facilitates browsing, combining sets of data, and statistical evaluations, and also on Paradox software, to make it compatible with the US DOE database. A collection of reprints of the relevant published papers is also being made.

For the establishment of an archive of pathological materials, a questionnaire will be circulated to establish what is available and in what form. It will be necessary, to decide what can be preserved, and where since a centralized compository is not envisaged. Both paraffin blocks and slides have a limited life, and their likely future use has to be evaluated.

Concerning the prospects of issuing teaching slides in radiobiology, a first set of teaching slides is now available and most probably the demand for such services will increase and should be carefully considered for the future.

Symposia and training activities

A symposium entitled "Acute and Late Effects on the Lungs from Inhaled Radioactive Materials and External Radiation" was held on 4 October 1992, during the 24th Annual Meeting of the European Society for Radiation Biology at Erfurt, Germany. There were eight invited presentations covering the field of acute and late effects caused by inhaled radioactive materials as well as by external radiation of the lung. The first part covered aspects of the new respiratory tract dosimetry model proposed by the ICRP task group; there were related presentations on particles deposition and clearance and on cells at risk. The second part of the symposium was devoted to radon, including recent animal experiments as well as epidemiological investigations. Abstracts of the symposium were published in the EULEP Newsletter 73, May 1993.

In June 1994, EULEP organised a meeting entitled "Genetic Predisposition of Radiosensitivity". The meeting was held in conjunction with the Annual Meeting of the European Society for Radiation Biology in Amsterdam. There were eight invited presentations covering cellular phenomena determining radiosensitivity: the molecular basis of DNA repair; the role of the P53 gene; tumourigenesis in transgenic mice; heriditary disease; damage during prenatal development; sensitivity of human deploid fibroblasts and lymphocytes; and the Beck With-Wiedemann syndrome genetic predisposition to cancer.

A symposium on "Molecular Analysis of Development and Neoplasia: Homologous Recombination and Knock-Out Approaches" was held in March 1994 at Reisensburg during the General Assembly.

In May 1995, EULEP organised a training course in Saclay, France on the techniques which are currently used to study cell apoptosis.

EULEP will contribute to the ILEG symposium in Würzburg in 1995

EULEP will contribute to the ILEG symposium in Würzburg in 1995 on "Long-term animal studies. Archiving and results of continuum exposure."

EULEP/EBMT Study on Late Effects after Total Body Irradiation

A retrospective study has been completed in collaboration with the European Bone Marrow Transplantation Group, based on reports from 29 European centres. It was based on 258 patients who survived more than 5 years. The average whole-body dose was 9.3 Gy in a single dose or 10.9 Gy fractionated. The data were collected on report forms drawn up by experts from the different centres and from EULEP. They indicated full recovery of clinical performance and social activity in 84-88% of transplanted patients.

Late deaths caused by complications other than recurrent disease were due to graft-versus-host disease (GVHD) with infections, AIDS, a secondary tumour and late cardiac insufficiency. Severe disabilities were caused by chronic GVHD, lung fibrosis, sicca syndrome, osteoporosis, autoimmune disorders and epilepsy. Secondary tumours were limited to skin and mucosa and were not life-threatening; the spectrum was similar to that seen in organ transplanted patients, indicating the importance of immune suppression as compared to radiation.

Serious complications that occur in most patients treated with radiation were defects in growth and development, infertility and cataracts. There was an increased risk of chronic liver disease, and children had a higher risk of hypothyroidism.

This retrospective analysis has provided a clear indication of clinical performance following total body irradiation, and is of assistance in the design of a future multi-centre prospective study. A detailed report has been published in the EULEP Newsletter 75 (February 1994).

Co-ordination of Collaborative Research

The future of EULEP task groups has been the subject of an in-depth review. It was generally recognised that part or all of the co-ordination activities of some of the former task groups had in one sense been superseded by the establishment of multi-national contracts. Accordingly some task groups have been disbanded during the past years, having completed and published their joint work - these are the groups working on osteosarcoma, haemopoietic neoplasia, cell biology of leukaemia, CNS vascular task group on late radiation necrosis, radon, reduction of risk, fetal dosimetry. In the cases of bone, reduction of risk and CNS, new groups have been established.

Selected reports on progress achieved by some of the task groups are as follows:

Radiation-Induced Carcinogenesis in the Liver

The possible combined effects of the initiator diethylnitrosamine (DEN) and neutrons on the induction of foci adenomas and carcinomas in C57BL/Cnb mouse liver were evaluated. The rate of appearance of foci increased significantly at different time intervals when a neutron dose of 0.125 Gy was administered 7 days before or after a dose of 1.25 μg DEN. No significant differences were observed in the total surface of foci and/or adenomas and carcinomas when increasing doses of neutrons were given 7 days before or after the administration of 1.25 or 2.5 μg DEN. An additional experiment is in progress in order to determine the relative biological effectiveness of 6.3 MeV neutrons in the induction of liver tumours in C57BL mice exposed at 7 and 21 days of age. Mice were exposed to increasing doses (0.125, 0.25, 0.5 and 1.0 Gy) of 6.3 MeV neutrons and to 1, 2 and 3 Gy of X rays. Today the 1336 treated mice are dead and the histological slides of the most important tissues and organs have been analysed.

Pathogenesis of Fibrosis (Bladder)

The experimental planning of the comparison of strains is based on functional, cystometric studies. One objective is to correlate bladder function and morphology, i.e. to compare the quality and degree of morphological changes in different dose groups and at different time points with the equivalent cystometric response in different strains of mouse. Typical changes, observed by all three laboratories, consisted of a thickening of different layers of the bladder wall as well as a focal degeneration and dissection of the urothelium. It was agreed that each laboratory will attempt to quantify these changes morphometrically in 5 animals 180 days after irradiation to the ED_{80}, compared to 5 controls, as a basis for determining if this method of analysis is appropriate for evaluation of the entire study.

The collagen isotype staining protocol was adapted for this study, and the specificity of antibodies tested in a range of control tissues. Determination of the extent and intensity of the immunoreaction by image analysis showed that constant conditions at every step in the procedure are required: therefore it was decided that this part of the experiment will be performed at Neuherberg for slides from all three laboratories. The method for detecting TGF-β is being optimized and will be standardized.

Cell kinetic experiments have been undertaken, and different cell labelling methods compared. The interpretation of cell kinetics in the urothelium is complicated by the very low rate of cell production and by the presence of multinucleated cells. Continuous labelling experiments are therefore required for a

meaningful analysis, covering a range of labelling time intervals.

CNS/Vascular Task Group

Meetings were held in December 1993, March 1994 and December 1994. The former reviewed progress over a wide area of collaborative studies, including the relationship between the β-astrocyte and the O-2A glial progenitor cell, studied in the brain and spinal cord respectively. Physiological measurements of blood flow, blood volume and permeability in the whole brain had shown close agreement with the results of morphometric assessment in the cortex. Regarding the tissue injury unit in the CNS, besides a loss of endothelial cell nuclei, the enlargement of the nucleus in approximately 50% has been noted after 25 Gy. Lymphocytes and leucocytes migrate into the parenchyma early during the pathogenesis of necrosis. Potentially useful markers for cytokine expression would be evaluated, one aim being to see if oligodendrites die by apoptosis.

A proposal for a new EULEP task group on endothelial effects has been prepared to study the mechanism of late vascular injury by the selective irradiation of the vascular endothelium in the CNS rat model. This can be made possible by irradiating endothelial cells *in vivo* with α-particles, using the $^{10}B(n,\alpha)$ reaction. Boronated compounds are available which do not penetrate the blood-brain barrier, so that the dose to parenchymal cells is some 2.5 times less then the dose to the endothelium itself. It was agreed to begin by comparing X-rays with neutrons plus different boron compounds, looking at changes in endothelial and glial cell populations, scoring the tissue injury unit by histology, and estimating clonogenic survival of glial cell progenitors *in vitro*. The last of these will permit a comparison of the biological dosimetry of the parenchymal tissue compartment, using boron compounds which do or do not penetrate the blood-brain barrier. Additional studies using X-irradiation will allow the evaluation of new techniques for the immunohisto-chemical determination of apoptotic cell death in endothelial and glial cells, and for measuring vascular permeability of amino-isobutyric acid by quantitative autoradiography.

The objective of the joint *EULEP-EURADOS Task Group on Deposition and Clearance of Inhaled Particles in the Human Respiratory Tract* is to promote and facilitate discussion and collaboration between European Laboratories involved in the development of improved human respiratory tract models for intakes of radionuclides. Its approach is to identify important areas of uncertainty, and to stimulate experiments to address them.

The Task Group held five meetings during the period 1991-1995. Several members of this Task Group were also members of the ICRP Task Group on Respiratory Tract Models and considerable effort was devoted to finalising the new *Respiratory Tract Model* which

was adopted by ICRP in 1993 and published as ICRP Publication 66 in January 1995. Considerable effort was also devoted to the further development of the personal computer software, LUDEP, to calculate doses to organs from inhalation of radionuclides, in particular members collaborated in the production of a French language version. Several Task Group members are also involved in reviewing the biokinetics of inhaled compounds of a wide range of elements, in order to give guidance on parameters to be used in the ICRP Respiratory Tract Model to derive inhalation doses.

Experimental studies were carried out to quantify aspects of human respiratory tract deposition and clearance. Deposition measurements focused on areas where data are sparse, e.g. partition of air between nose and mouth, total deposition in subjects with lung disease. Clearance studies continued to focus on particle retention in the bronchial tree, because of the high radiosensitivity attributed to the bronchial epithelium. The most recent studies indicate that retention is related to particle size, and this was taken into account in the ICRP model.

A standardisation exercise, sponsored by EULEP as a Task Group activity, was successfully carried out to investigated difference in results reported by the Karolinska Institute in Stockholm and the GSF in Frankfurt for the deposition and bronchial clearance of particles. The human studies were also complemented by investigations in rats and dogs, in which the site of deposition is more easily specified. A three-year study of the retention of particles in the alveolar region of the human lung was also completed.

The results of much of this work is described in the 8 papers listed in Part A of the attached publications list.

Since inhalation represents one of the two major routes of intake of radionuclides into the human body, there is still a vital need for a European Task Group, such as this, to continue to gather and interpret new information which may be used for the improvement of dose calculations for doses from inhaled radionuclides. It is, thus, important that the work of this Task Group should be continued under the EULEP-EURADOS contributions to Fourth Framework Programme.

The *Task Group on the Interspecies Comparison of Lung Clearance* has as objective the coordination of multispecies comparisons of the clearance of standardised radioactive particles from the lungs of animals of different species, including whenever possible *Homo Sapiens,* in order to demonstrate the validity, or otherwise, of extrapolating animal data to humans. Interspecies comparisons of the clearance of inhaled, or instilled, ionic ^{57}Co and monodisperse, porous- or solid ^{57}Co$_3$O$_4$ particles have been carried out in baboons, dogs, guinea pigs, HMT and Fischer-344 rats, hamsters and CB/H mice. These data have shown that in all species there is a relatively large rapid clearance of material from the lung plus a long-term retention phase of more than 100 days in all species. However, the kinetics of the long-term phase differed significantly among the species. In all species

ionic cobalt is taken up specifically by collagen in cartilaginous structure, such as the tracheal rings.

The kinetics of intracellular particle dissolution *in vitro* has been compared in cultured alveolar macrophages from dogs, rats, mice, cattle, baboons and humans using uniform $^{57}Co_3O_4$ particles. The results have confirmed that alveolar macrophages from all species dissolve the particles more rapidly than extracellular fluids; but there are species differences with alveolar macrophages from dog and baboon showing higher dissolution rates than those from humans, cattle or rats. This interspecies comparison of particle dissolution in alveolar macrophages *in vitro* can only partially explain the observed differences in *in vivo* dissolution and the subsequent absorption of dissolved particle material from the lungs to blood.

A further interspecies comparison of the lung clearance of physically and chemically uniform particles of terbium oxide, involving humans, monkeys, dogs, rats and mice is now in progress in six member laboratories using agreed and standardised protocols.

This Task Group continues to carry out very valuable work some of which have been described in the 18 papers cited in Part B of the publications list.

The *Task Group on the Evaluation of New Chelators*, was originally called the Task Group on Reduction of Risk of Late Effects from Incorporated Radionuclides but when much of the work was transferred to a CEC Multinational Contract in 1992, it was renamed and the terms of reference altered to avoid overlap with the contract. The current terms of reference are to maintain a watching brief on developments in the whole area of treatments designed to enhance the natural rate of elimination from the human body of the most highly toxic radionuclides, *eg*. thorium, uranium, neptunium, caesium, as well as plutonium and americium, and to propose new studies designed to evaluate promising new agents or approaches.

During the past four years studies, partially funded by the CEC or under the aegis of EULEP, have resulted in considerable progress concerning the decorporation of actinides from the body. Attention has been devoted principally to the testing of analogues of siderophores in the rat. The most promising substance so far, code-named 3,4,3-LI(1,2-HOPO) is substantially more effective than DTPA, the current agent of choice, after the deposition of plutonium nitrate, plutonium tributylphosphate or thorium nitrate in the lungs, and plutonium, americium and thorium nitrate at simulated wound sites. The greatest differences were observed after wound contamination. Recent studies have shown that the ligand is also more effective than DTPA after the intravenous injection of neptunium. Preliminary studies of the toxicity of 3,4,3-LI(1,2-HOPO) in the baboon have provided no evidence of adverse side effects but comprehensive toxicity testing, now under discussion, is required before its use in humans. Alternative syntheses of 3,4,3-LI(1,2-HOPO),

designed to substantially increase the yield, are under investigation. Other analogues eg. DFO-HOPO and TREN-(Me-3,2-HOPO) have also been shown to be more effective than DTPA after wound contamination.

The administration of Zn-DTPA in drinking water has been shown to be an effective method for removing inhaled transportable forms of plutonium and americium from the rat. This work, stimulated by previous studies after intravenous injection of these actinides, also confirmed the absence of histological damage to the kidneys, liver and gastrointestinal tract at therapeutically effective doses.

Several phosphonic acid derivatives have been examined for the decorporation of uranium. Some have been partially successful in so far that the kidney content was reduced tenfold after their immediate administration. However, delayed treatment was not effective and the development of more potent substances remains an important aspect of the radiation protection of the worker.

In its work the Task Group has built up and maintained strong links with other organisations throughout the world, notably the University of California, Berkeley and the Lawrence Berkeley Laboratory.

Regular reports of the Task Group meetings have appeared in the EULEP Newsletter and some of the work is described in the 20 papers cited in Part C of the publications list.

The Task Group continues to play an important role in keeping abreast of developments in methods for the treatment of serious internal contamination by radionuclides and in recognising the needs for further research and proposing appropriate experimental programmes, and this need will continue into the period of the Fourth Framework Programme.

A *Task Group on Radon* was created in 1992 with the objective of conducting intercomparison studies in radon exposure facilities for animals in Europe. Four standardisation exercises in which rats were exposed to radon daughters in the exposure chambers of the CEA at Limoges, France at TNO, Holland and AEA, Harwell, UK and the rats were evaluated independently by each of the three groups of workers. The results showed that the three groups were in reasonable agreement with each other, especially in respect to the measurement of the potential alpha energy concentrations (PAEC) and that all three laboratories could produce exposure data which were comparable to each other. The work was completed in late 1993, at which time the group was disbanded. Some of the results were reported in the publication listed in Part D of the publications list.

A new *Task Group on the Standardisation of Bone and Bone Marrow Dosimetry* was formed in 1993 by scientists from five laboratories in the UK and Germany. The purpose of this Task Group is the development of methods for determining dose distribution within the skeleton, principally for α-particle emitting radionuclides.

The specific work areas have included, at the GSF, Neuherberg, Germany, the study of the effects of osteosarcomagenic doses of ^{224}Ra on the proliferation and differentiation of skeletal cells *in vitro*; the retention of ^{88}Y, ^{169}Er and ^{227}Th after parenteral administration; and the continuation of the epidemiological study on German ankylosing spondylitis patients, and its extension to patients from the former East Germany. AEA, Harwell, UK has continued the studies of the comparative uptake of thorotrast in monkey and human bone marrow, including marrow from Japanese patients using x-ray fluorescence spectrometry.

Work at Bristol University includes examination of the distribution of natural α-particle emitters in autopsy samples of human bone and in children's teeth and human fetal samples obtained from West Cumbria, Bristol in the UK and Kiev in Ukraine; the CD34 antibody is being used to map the distribution of stem cell in adult and fetal bone marrow. Work is also being undertaken at the Paterson Institute, Manchester on the distribution of bone marrow stem cells prior to assessing the microdistribution of α-particle doses to potential leukaemogenic or osteosarcomagenic target cells. NRPB have continued with the comparative study of the toxic effects of ^{233}U, ^{239}Pu, and ^{241}Am in animals; work is also in progress using autoradiography to calculate doses to different regions of bone and to relate the incidence of tumours with the distribution of dose.

The work of this Task Group is partly described in the 12 papers listed in Part E of the publications list.

Publications

Part A. *EULEP-EURADOS Task Group on Deposition and Clearance of Inhaled Particles in the Human Respiratory Tract*

1. Bailey M. R., EULEP-EURADOS Task Group Reports. EULEP Newsletter **64**. 46-49 (1991); **66**, 5-9 (1992); **71**, 29-33 (1993); **78**, 15-19 (1994).

2. Bailey M. R., Bath September 1993. *Radiat. Prot. Dosim.*, **53**, 107-114 (1994).

3. Bailey M. R. and Roy M., ICRP Publication 60 Annexe E: Clearance of Particles from the Respiratory Tract. *Annals of the ICRP*, **24**, 301-413 (1994).

4. Bailey M. R., Dorrian M-D and Birchall A., *J. Aerosol. Med. in the press*.

5. Malarbet J. L., Bertholon J. F., Becquemin M. H., Taieb G., Bouchikhi A. and Roy M., *Radiat. Prot. Dosim.*, **53**, 179-182 (1994).

6. Roy M., Malarbet J. L., Becquemin M. H., Bouchikhi A. and Bertholon J. F., Bath September 1993. *Radiat. Prot. Dosim.*, **53**, 115-118 (1994).

7.   Stahlhofen W., Schleuch G. and Bailey M. R., *Radiat. Prot. Dosim., in the press.*

8.   Stahlhofen W., Schleuch G. and Bailey M. R., *Ann. Occup. Hyg.* **38** Suppl.1, 189-193 (1994)

Part B. *Task Group on the Interspecies Comparison of Lung Clearance*

9.   Kreyling W. G., André, Collier C. G., Ferron G. A., Métivier H. and Schumann G., *J. Aerosol Science.,* **22**, 509-535 (1991).

10. Collier C. G., Hodgson A., Gray S., Noody J., and Ball A., *J. Aerosol Sci.,* **22**, 537-549, (1991).

11. Kreyling W. G., Nyberg K., Nolibé D., Collier C. G., Camner P., Heilmann P., Lirsac P., Lundborg M. and Matejkova, *Inhalation Toxicology,* **3**, 91-100 (1991).

12. Collier C. G., Pearce M. J., Hodgson A. and Ball A., *Environ. Health Perspect.,* **97**, 109-113, (1992).

13. Heilmann P., Beisker W., Miaskowski U., Camner P. and Kreyling W. G., *Environ. Health Perspect.,* **97**, 115-120, (1992).

14. Kreyling W. G., *Environ. Health Perspect.,* **97**, 121-126, (1992).

15. Poncy J-L., Métivier H., Dhilly M., Verry M., and Masse R., *Environ. Health Perspect.,* **97**, 127-130, (1992).

16. Ansoborlo E., Chalabreysse J., Henge-Napoli M-H., and Pujol E., *Environ. Health Perspect.,* **97**, 139-144, (1992).

17. Nyberg K., Johannson U., Johannson A. and Camner P., *Environ. Health Perspect.,* **97**, 149-152, (1992).

18. Lundberg M., Falk R., Johannson A., Kreyling W. G. and Camner P., *Environ. Health Perspect.,* **97**, 153-158 (1992)

19. Kreyling W. G., Beisker W., Miaskowski U., Neuner M. and Heilmann P., *Environmental Hygiene III,* (N. H. Seemayer and N. Hadnagy (Eds.)), Springer Verlag, Heidelberg, pp 19-22, (1992).

20. Kreyling W. G., Cox C., Ferron G. A. and Oberdörster G., *Exp. Lung Res.,* **19**, 445-467, (1993).

21. Kreyling W. G. and Covelli V., *EULEP Newsletter,* **73**, 13-23 (1992).

22. Patrick G., Kreyling W. G., Poncy J-L., Collier C. G., Godleski J. J., Duserre C., Striling C. and Brain J. D., *Inhalation Toxicology*, **6**, 225-240, (1994).

23. Harper R. A., Stirling C., Townsend K. M. S., Kreyling W. G. and Patrick G., *Exp. Lung Res.*, **20** 143-156 (1994).

24. Hodgson A., Stradling G. N., Foster P. P., Kreyling W. G. and Pearce M. J., In, *Portsmouth 1994: Proceedings of the IRPA Regional Congress on Radiological Protection*, Nuclear Technology Publishing, Ashford, Kent, pp193-196, (1994).

25. Lundborg M., Johar U., Johannson A., Eklund A., Falk R., Kreyling W. G. and Camner P., *Exp. Lung Res.*, **21**, *in the press* (1995).

26. Morgan A., Kellington J. P., Morris K. J., Collier C. G. and Hodgson A., *Inhalation Toxicology, in the press* (1995).

Part C. *Task Group on the Evaluation of New Chelators*

27. Taylor D. M. and Volf V., Plzen Medical Reports, Suppl. 62/1990 pp 101-102.

28. Stradling G. N., Gray S. A., Moody J. C., Hodgson A., Raymond K. N., Durbin P. W., Rodgers S. J., White D. L. and Turowski P. N., *Int. J. Radiat. Biol.*, **59**, 1269-1277 (1991).

29. Stradling G. N., Moody J. C., Gray S. A., Ellender M. and Hodgson A., *Human Exp. Toxicol.*, **10**, 15-20, (1991).

30. Bhattacharyya M. H., Breitenstein B. D., Métivier H., Muggenburg B. A., Stradling G. N. and Volf V., *Radiat. Prot. Dosim.* **41**(1) (1992) (Nuclear Technology Publishing, Ashford, Kent, ISBN 1 870965 22 1) pp.49).

31. Stradling G. N., Gray S. A., Ellender M., Moody J. C., Hodgson A., Pearce M. J., Wilson I., Burgada R., Bailly T., Leroux Y. G. P., Manouni D. E., Raymond K. N. and Durbin P. W., *Int. J. Radiat. Biol.*, **62**, 487-497, (1992).

32. Stradling G. N., Gray S. A., Ellender M., Pearce M., Wilson I., Moody J. C. and Hodgson A., *Human Exp. Toxicol.*, **12**, 233-239, (1993).

33. Volf V., Burgada R., Raymond K. N. and Durbin P. W., *Int. J. Radiat. Biol.*, **63**, 785-793, (1993).

34. Stradling G. N., Gray S. A., Moody J. C., Pearce M. J., Wilson I., Burgada R. Leroux Y. G. P., Raymond K. N. and Durbin P. W., *Int. J. Radiat. Biol.*, **64**, 134-14 (1993).

35. Poncy J-L., Rateau G., Burgada R., Bailly T., Leroux Y. G. P., Raymond K. N. Durbin P. W. and Masse R., *Int. J. Radiat. Biol.*, **64**, 431-436 (1993).

36. Rencova J., Volf V., Jones M. M., Singh P. K. and Bubenikova D., *Plzen Medical Reports, Suppl.* 68/1993 pp 11-13.

37. Volf V., Rencova J., Jones M. M. and Singh P. K., *Plzen Medical Reports, Suppl.* 68/1993 pp 59-61.

38. Stradling G. N., *Radiat. Prot. Dosim.* **53**, 297-304, (1994)

39. Gray S. A., Stradling G. N., Pearce M. J., Wilson I., Moody J. C., Burgada R., Durbin P. W. and Raymond K. N., *Radiat. Prot. Dosim.*, **53**, 319-322 (1994).

40. Pacquet F., Poncy J-L., Rateau G., Burgada R., Bailly T., Leroux Y., Raymond K. N. Durbin P. W. and Masse R., *Radiat. Prot. Dosim.* **53**, 323-326, (1994).

41. Fritsch P., Herbreteau D., Moutairou K., Lantenois G., Richard-Le Naour H., Grillon G., Hoffschir D., Poncy J-L., Laurent A. and Masse R., *Radiat. Prot. Dosim.*, **53**, 315-318, (1994).

42. Archimbaud M., Henge-Napoli M-H., Lilienbaum D., Desloges M. and Montagne C., *Radiat. Prot. Dosim.*, **53**, 327-330, (1994).

43. Rencova J., Volf V., Jones M. M. and Singh P. K., *Radiat. Prot. Dosim.*, **53**, 311-313, (1994).

44. Stradling G. N., Gray S. A., Pearce M. J., Wilson I., Moody J. C., Burgada R., Durbin P. W. and Raymond K. N., *Human Exp. Toxicol. in the press*

45. Stradling G. N., Task Group Report on Reduction of Risk of Late Effects from Incorporated Radionuclides, *EULEP Newsletters*, **68**, 15-21 (1992); **72**, 3-18 (1993); **75**, 35-45 (1994); **78**, 12-14 (1994); **79**, 10-22 (1995).

46. Stradling G. N., Gray S. A., Pearce M. J., Wilson I., Moody J. C. and Hodgson A., *NRPB Memorandum M-534* (1995).

Part D. Task Group on Radon

47. Strong J. C., Morlier J. P., Groen J. S., Bartstra R. W. and Baker S. T., Nuclear Technology Publishing, Ashford, Kent, ISBN 1 870965 30 2. (*Radiat. Prot. Dosim.*, 56(1-4), 1994) pp 259-262 (1994).

Part E.   Task Group on the Standardisation of Bone and Bone Marrow Dosimetry

48.   Ellender M., Haines J. W. and Harrison J. D., *Human and Exp. Toxicol., in the press* (1995).

49.   Henshaw D. L., Allen J. E., Keitch P. A. and Randle P. H., *Int. J. Radiat. Biol., in the press* (1995).

50.   Henshaw D. L., Allen J. E., Keitch P. A., Salmon P. L. and Oyedepo C., In *Health effects of internally deposited radionuclides: Emphasis on Radium and Thorium*, Heidelberg, Germany 18-22 April 1994.

51.   Humphreys J. A. H., Priest N. D., Ishikawa Y., Townsend S. K. and McInroy J. F., In *Health effects of internally deposited radionuclides: Emphasis on Radium and Thorium*, Heidelberg, Germany 18-22 April 1994.

52.   Ishikawa Y., Humphreys J. A. H., Priest N. D., Mori T. and Kato Y., In *Health effects of internally deposited radionuclides: Emphasis on Radium and Thorium*, Heidelberg, Germany 18-22 April 1994.

53.   Müller W. A., Luz A. and Linzer U., *Radiat. Res.*, **138**, 412-422, (1994).

54.   Müller W. A., Luz A. and Linzer U., In *Health effects of internally deposited radionuclides: Emphasis on Radium and Thorium*, Heidelberg, Germany 18-22 April 1994.

55.   Priest N. D., Humphreys J. A. H., Ishikawa Y. and Kathren R., In *Health effects of internally deposited radionuclides: Emphasis on Radium and Thorium*, Heidelberg, Germany 18-22 April 1994.

56.   Salmon P. L., Henshaw D. L., Allen J. E., Keitch P. A. and Fews A. P., TASTRAK, *Radiat. Res.*, **140**, 63-71, (1994)

57.   Schmidt J., Heermeier K., Linzer U., Luz A., Silbermann M. Linve E. and Erfle V., *Radiat. Environ. Biophys.* **33**, 69-79, (1994).

58.   Wick R. R. and Gössner W., *Environ. Intern.* **19**, 467-473 (1993)

59.   Wick R. R., Chmelevsky D. and Gössner W., In *Health effects of internally deposited radionuclides: Emphasis on Radium and Thorium*, Heidelberg, Germany 18-22 April 1994.

60. EULEP Newsletter: 9 issues were published during the period 1.9.92 to 30.6.95 (Nos. 71-79).

61. Report of Joint BETG/EULEP Workshop on Lung Pathology (1993), resulting from a workshop held on 12-13 October 1992 in Paris.

62. Pathology of neoplasia and preneoplasia in rodents, edited by P. Bannasch and W. Gössner, Schattauer, Stuttgart, New-York.

63. Hopewell J.W., Calvo W., Jaenke R., Reinhold H.S., Robbins M.E.C. and Whitehouse E.M., Rec.Res.Can.Res., **130**, 1-16, (1993).

64. Calvo W., Rec.Res.Can.Res., **130**, 175-188, (1993).

65. Hopewell J.W., Res.Adv.Space Res., **14**, 435-442, (1994).

66. Maisin J.R., Vankerkom J., De Saint-Georges L., Janowski M., Lambiet-Collier M. and Mattelin G., Rad.Res., **133**, 334-339, (1993).

67. Maisin J.R., Vankerkom J., De Saint-Georges L., Janowski M., Lambiet-Collier M. and Mattelin G., Rad.Res., **142**, 78-84, (1995).

68. Bouffler S.D., Silver A.R.J., Papworth D., Coates J. and Cox R., Genes Chrom.Cancer, **6**, 98-106 (1993).

69. Bouffler S.D., Silver A.R.J. and Cox R., BioEssays, **15**, 409-412, (1993).

70. Goodhead D.T., Thacker J. and Cox R., Int.J.Radiat.Biol., **63**, 543-556, (1993).

71. Bouffler S.D., Silver A., Finnon P., Morris D., Rance E. and Cox R., In: Chadwick K.H., Cox R., Leenhouts H.P. and Thacker J., eds. Molecular Mechanisms of Radiation Mutagenesis and Carcinogenesis, Office for official publications of the European Communities, Luxembourg, (1994).

72. Thacker J. and Cox R., In: Chadwick K.H., Cox R., Leenhouts H.P. and Thacker J., eds. Molecular Mechanisms of Radiation Mutagenesis and Carcinogenesis, Office for official publications of the European Communities, Luxembourg, (1994).

73. Cox R., Int.J.Radiat.Biol., **65**, 57-64, (1994).

74. Cox R., Int.J.Radiat.Biol., **66**, 643-647, (1994).

75. Silver A.R.J., Meijne E., Huiskamp R. and Cox R., In:
     Proceedings of the 8th International Conference of the
     International Society of Differentiation, Oct. 22-26,
     Hiroshima, Japan, (1994).

76. Silver A.R.J., Bouffler S., Finnon P., Rance E. and Morris
     D., Rad.Prot.Dosim., **52**, 461-464, (1994).

77. Silver A. and Cox R., Proc.Natl.Acad.Sci., **90**, 1407-1410,
     (1993).

78. Bouffler S., Kemp C., Balmain A. and Cox R., Cancer Res.,
     55, 3883-3889, (1995).

Title: Biophysical models for the effectiveness of different radiations.

1)   Paretzke   GSF
2)   Goodhead   MRC
3)   Terrissol   ADPA
4)   Leenhouts   RIVM
5)   Von Sonntag   Max-Planck Inst.
6)   Smith   Univ. London
7)   O'Neill   MRC

I. Summary of Project Global Objectives and Achievements

The global objectives of this co-ordinated project concentrate on efforts to improve with experimental, computational, and system analytical studies the present knowledge on the form of the relevant biological dose-time-effect curves especially in the low dose regime of radiation protection and its dependency on the dose rate, fractionation, type of radiation (X, gamma, alpha, beta, neutrons and mixed fields), and on the influence of environmental factors The scientific approach to develop an appropriate integral mechanistic model for radiation carcinogenesis was differentiated into the development of several models for the different levels of biological complexity, namely for the production of primary and secondary physical and early chemical changes in the DNA (by Terrisol et al., O'Neill et al., v. Sontag et al., Smith et al.), the formation of mutations (e.g. HPRT-) and chromosome aberrations (by Goodhead et al.), the induction of late somatic effects in experimental animals and man by such early effects including intercomparison with the mechanistic action of UV-light (by Leenhouts et al., Paretzke et al.). Particular emphasis was given to the improvement of track structure simulations codes, the study of biochemical reactions, and modelling of the induction of cancer by alpha emitters. In all areas of research good experimental and theoretical progress could be achieved during this period.

In **project 1 (GSF)** the cross section basis for the interaction of protons and electrons could be improved by using truncated Drude functions for the fit of single shell contributions to oscillator strength distributions for condensed water and by measuring low energy electron emission differential in energy and angle from very clean solid target surfaces. The simulation of the geometry of the DNA molecules in a cell nucleus was improved to form a nucleosome, six of which are wrapped around in a spiral to form a DNA fibre, which, in turn, can even form arbitrary "loops". Extensive track structure calculations were performed and successfully compared to experimental data for the absolute yields of SSBs, and DSBs, and of deletions in DNA molecules after irradiation with photons, alpha particles, or protons of various energies. A comprehensive literature study was made regarding existing semi-mechanistic models for carcinogenesis including single-, two-, and multiple-step models, and tolerance distribution models, which showed for a wide variability of parameter combinations of the same multi-step model good agreement with existing experimental data. Finally, a comparison of models and data was made regarding the probability of causation for lung cancer after exposure to radon daughter products.

Project 2 (MRC-Phys) has achieved progress in several areas·

a) Because track structure analyses are a crucial element in the modelling of biological effectiveness of different radiations, comparisons were made between different available electron track simulation codes to test the robustness of conclusions drawn from their analyses. Wide regions of close quantitative agreement were found. However, also differences became apparent over small dimensions that may be important for chemical modelling.

b) Computational and classification methods have been developed for the quantitative estimation of spectra of DNA-damage complexity from both direct ionizations in the DNA and also local water radiolysis products in the highly-scavenging cellular environment. These have been applied initially to electron irradiations, while corresponding liquid-water/chemical track codes are being developed for heavier ions.

c) Experimental data on *hprt* mutagenesis, as a paradigm for modelling, have been obtained for a variety of cell types, particularly for irradiation by slow α-particles such as from radon. These have revealed, *inter alia,* the very large effect that single-track inactivation can have in determining the frequency of viable mutants.

d) the ionization-clustering properties of radiation tracks, leading to clustered molecular damage to DNA as well as spatial and temporal correlations over larger sub-cellular distances, have been revealed by track analyses, and their consequences appear to be manifest experimetally as substantial differences between slow high-LET α-particles, such as from radon, and low-LET radiations. These quantitative, and sometimes also qualitative, differences include spectra of initial DNA damage, its repairability, efficiency for mutation induction, proportion of complex chromosome aberrations and induction of genomic instability These notable features of α-particles exist even for single tracks and therefore should be directly applicable in extrapolation to environmentally low doses and low dose rates.

In **project 3 (ADPA)** the objective was to simulate more precisely the physical and chemical steps of the DNA irradiation in the cell environment. For the primary interactions of radiation higher order structures of DNA were included. To study the role of water radicals, oxygen, scavengers and chemical repair, all chemical reactions between water radio-chemical species, radicals and added scavengers with sub-molecular units of DNA were taken into account. The code CPA100 was implemented in the computer of partner 2 who simulated the transport of electron up to 100 keV in liquid water as a function of space and time. The code was also employed for comparisons with other codes, for simulation of chemical reactions, to introduce water shells on DNA structures, and for statistical investigations. During this contract period our previosnly straight DNA segment model was modified into nucleosomal DNA. The physico-chemical and chemical codes were improved to take into account large amount of atoms, species and molecules able to diffuse and to react with each other. The nucleosome core unit has been modelled as a 146 basepairs helical DNA, containing 9056 atoms, wound around the histones. These latter being considered here as absorbing energy but being chemically inactive. All the nucleosome atoms are specified by their co-ordinates and their van der Waals radii. The yields of strand breaks for electrons were calculated for a nucleosome target in liquid water. ^{125}I was chosen as the source of radiation because it was possible to localize its position in the DNA structure. Iodine atoms were consideres individually, but uniformly distributed among all the thymine bases of the nucleosome by replacing their methyl group (71 positions in the model).

During the physical step all events located inside the van der Waals radius of a DNA atom are scored as direct interactions on DNA while other water interactions create new species and radicals. Molecules of scavengers (Tris, DMSO, etc.) were "added" randomly accordingly to the specified concentration inside a "working sphere". To evaluate the DNA damage by simulation we used the following assumptions: during the first 10^{-15}s, when an ionisation was

located inside the van der Waals radius of a phosphate-group or sugar atom, it was stored as a direct single-strand break (SSB), and subsequently the event was removed from the initial track. From 10^{-5}s to 10^{-8}s, when a deoxyribose-monophosphate reacts, it was transformed in a sub-product and could not react twice per decay; the event was scored as an indirect SSB. The number of damaged DNA nucleotides in the nucleosome unit per ^{125}I decay for the direct effect as well as for the indirect effect resulting from later chemical reactions in the working sphere were calculated. The results show that about 40% of the sugar-phosphate groups are damaged directly during the physical phase, but only 14% react during the chemical phase (up to 10^{-8}s), mainly with OH radical, which is the reason for the SSB creation. The DMSO reduced the number of DNA damages with a similar ratio on all nucleotides Comparison of the mean values of the number of SSB per decay with experimental data show that the relative number of indirect DSBs seems to be larger than that for directly produced (0.6 over 0.2) as compared to the relative number for SSBs (2.6 over 1.5). This is due to the fact that an indirect SSB associated with a direct one was scored as an indirect DSB. The mean value of about 1 DSB per decay reported from many experiments results from the fact that in about 20% of all decays more than 1 DSB was produced. Differentiating between directly and indirectly induced DSBs leads to quite interesting results which could perhaps give hints for the assumed correlation between the number of DSBs and cell death. We can observe here a result already mentionned in the literature: 0.5M of DMSO reduce the indirect effect by 50%.

In the framework of **project 4 (RIVM)** for quantitative description of radiation effectiveness a relatively simple model (TRAX) was developed and used to calculate the effectiveness of different radiation types. The model provides a track segment description of the primary particle involved in the radiation effect and of the secondary particles generated, and can estimate the radiation effectiveness of a radiation effect for each track segment, using the specific geometry of the target involved. A "diffusion" parameter is used to simulate the relevant physico-chemical processes involved in the radiation action. Using TRAX the radiation effectiveness of different effects was calculated, such as for single-hit detectors and for DNA damages. The results show the importance both, a), of the radiation type and, b), of the target geometry on the radiation effect. Further, the results show that the well known "humped" behaviour of the RBE-LET relationship for cell killing and mutations, which is primarily caused by a changing linear term of the dose-effect relationship, can be explained assuming that DNA double strand breaks are the crucial primary lesions for these cellular effects.
Furtheron, a stationary CHO cell system was used to especially investigate the quadratic term of the dose-effect relationship for gamma rays, for ultraviolet radiation (UV), and for combinations of these radiations. The results were explained assuming that the quadratic term was caused by a dual hit mechanism for both gamma and UV radiation. The different nature of the primary lesions involved in the effects (i.e. DNA "breaks" for gamma radiation and dimers for UV-radiation) was reflected in differences in repair. The combined exposure experiments showed an extra effect from interaction of gamma and UV radiation produced sublesions. This extra lesion was not significant for lower dose rates.
Finally, in relation with carcinogenesis, RIVM investigated a two-mutation model (TMC), which accommodates for the multi-stage character of tumour development. Several data sets of tumour induction by radiation in animals and man for a variety of exposure conditions were fitted using the model. Although in the current project the TMC model could only be investigated preliminarily, the results were promising. In principle, the TMC model links DNA-molecular and cellular damage with tumour formation. The model can show features of the relative or the absolute age projection risk model, and sometimes of the single-somatic mutation model, depending of the radiation and tumour involved. The model accounts for the multistage character of carcinogenesis and links spontaneous tumour incidence with radiation risk. The model in its present form allows investigation of the involvement of radiation in

different stages during carcinogenesis. The model, therefore, can be of importance for the dervation of radiation risk estimates of lifetime exposures to low doses of ionizing radiation

The work undertaken in **project 5 (MPI)** to further elucidate aspects of the chemical effects of ionizing radiation on DNA has realized several objectives: One focus was the phenomenon of radical-site transfer from purine-base OH-adduct radicals to transfer the radical site to the sugar moiety, as well as the inverse event. Purine-nucleoside-derived products were identified which result from the complex subsequent reactions.The influence exerted by the presence of a phosphate group with respect to the propensity of an H-atom to be abstracted at the DNA deoxyribose moiety by an OH-radical, relative to the hypothetical phosphate-free situation, is not well known, and this question was studied in hydroxyalkyl phosphates as model compounds. Finally, studies were performed in connection with those on the action of dioxygen and other oxidants, notably nitroaromatic compounds, on the resulting radicals as well as on other model-compound reaction systems.

It came as a surprise when in our study on the γ-radiolysis of 2'-deoxyadenosine, two products that must have sugar-moiety-derived radicals as their precursors were observed as major ones, alongside the previously reported products free adenine, adenine-derived formamidopyrimidine (A-Fapy), and 8-hydroxy-AdR. These newly-observed products are the 8,5'-cyclodeoxynucleoside and the 5'-aldehyde. The total yield of these products may reach G values close to or even exceeding G(OH), and a strong variation of their yields with the pH, occurs in a pH range 8 to 10 where 2'-deoxyadenosine has no pK_a. At the maximum of G(dA-consumption) as a function of pH, i. e. at about pH 9.5, G(dA-consumption) is about twice that of G(OH). This shows that there exists an important amplification effect, and it is concluded that intermediate radicals must play a role which are capable of reacting with dA. At present, mechanistic details are not yet clear. This conclusion is of relevance to DNA radiolysis where products related to the 8,5'-dA-cyclonucleoside are well-documented.

A further series of experiments was devoted to the polynucleotide poly(A). The products unaltered adenine and A-Fapy were determined straight after irradiation, as well as after various periods of time of heating the samples to 95°C. The results show that some of the adenine is released during and/or very shortly after irradiation, and that there is much further release upon heating. The total G(adenine) of 1.3×10^{-7} mol J^{-1} is quite high, higher perhaps than would be expected considering the proportion of promt OH-attack at the deoxyribose moiety.

The rate constants for the reaction of OH-radicals with glycerol-1-phosphate and glycerol-2-phosphate were redetermined by the thiocyanate competition method and found to be considerably smaller than the values available to date in the literature. Our values are 1.4×10^9 dm^3 mol^{-1} s^{-1} at pH 4 (for the first molecule $k=2.0 \times 10^9$ dm^3 mol^{-1} s^{-1} at pH8; 1.1×10^9 dm^3 mol^{-1} s^{-1} at pH 4; for the second molecule :$k = 1.6 \times 10^9$ dm^3 mol^{-1} s^{-1} at pH 8).

In order to obtain further information regarding the mode of action of oxidants on deoxyribose-centered DNA radicals, the propensities of some model-system α-alkoxyalkyl radicals to follow the oxidation pathway versus the fragmentation pathway, have been studied. a-Monoalkoxyalkyl radicals from 1,4-dioxan, tetrahydrofuran, dimethyl ether (all three are models for 2'-deoxyribose C(4')), as well as the radicals from 1,3-dioxan (model for deoxyribose C(4') and C(1'), were produced radiolytically in aqueous solution. In the presence of oxygen, these radicals are converted into the corresponding peroxyl radicals.

In response to the request from projects 1 and 3 we have been glad to supply values of the rate constants for the reaction of the OH-radical with some DNA model compounds that we have determined or redetermined.

The objectives of **project 6 (UoL)** have been to exploit thin-film technology in order to carry out proton transmission measurements in condensed organic materials, in order to verify experimentally those where there are deficiencies in interaction cross sections. Measurements

were made in the energy range 3 - 15 keV in films of different thickness followed by comparison with computed transmission factors using the TRIM-code. Langmuir-Blodgett (LB) films were used as thin organic foils which have particular importance in microdosimetry because they can form precisely defined nanometre thicknesses from a variety of molecules which have biological relevance.One ultimate goal was to determine experimental W-values over a range of charge-particle energies in a number of realistic biological systems. For this, it was necessary to measure energy loss in the film, as well as to find ways of collecting all the charge produced as a result of this energy loss. The novelty of this new methodology has resulted in slow progress because of the need to produce films of the highest quality. All the technical difficulties associated with the prime objectives have been overcome during the reporting period. Separate measurements of proton transmission through unsupported films and charge production in selected thicknesses of supported films have clearly shown the value of studying these condensed organic materials. In this regard, the original aims of the project have been met. Three areas of activity relating to radiation effects in LB films have been persued.

(a) PROTON TRANSMISSION THROUGH NANOMETRE ORGANIC FILMS: Protons in the energy range 3 - 15 keV were selected with an energy resolution of ~ 2% from a spectrum of energies scattered off a heated tantalum foil. This beam was collimated down to a diameter of 1.5 mm and restricted to a current of $\leq$ 2 nA in order to prevent thermal damage to the organic LB film samples. Transmitted protons were detected by a Single Channel Electron Multiplier (SCEM) whose entrance cone was maintained at -2.5 kV, and which subtended an angle at the sample of 27.5 $\pm$ 2.5 degrees. The response of the detector was first normalized to the beam current measured upstream of the energy analyzer. Multilayer samples of polymerized (12,8) diacetylene were prepared to span a 750 lines per inch copper mesh. The coverage of the mesh by these films was 100% over an approximately circular area of diameter ~8 mm, i.e. - much larger than the beam diameter. Transmission through film thicknesses of 21,23 and 25 layers (corresponding to thicknesses of 63, 69 and 75 nm) was normalized to that through the mesh alone. An unsupported area of film of 25 x 25 μm^2 was therefore achievable using support mesh wires that were 7.5 μm thick. This gave an open area ratio of 55%. Computations of proton transmission through such films was made using the lastest version (1992) of the TRIM code. The results show significant disagreements between computed and measured values at all energies except the lowest (3 keV), where the film ticknesses are on the order of the proton range. The estimated magnitudes of simple corrections to the experiments and calculations are not likely to explain the large discrepancy between measured and calculated transmissions. More important factors are the deposition of thin carbon, or other organic, deposits due to less-than-UHV vacuum conditions, the formation of neutral atomic hydrogen by low energy protons on exiting the LB film, and incorrect low energy cross section data used by TRIM.

(b) CHARGE PRODUCTION AND TRANSPORT FOLLOWING ENERGY DEPOSITION: This aspect of the project used supported LB films in order to develop the optimum design of electrodes and electronic amplification needed to reliably record the production of pico-Coulombs of charge. Irradiation of the films was achieved using a 2.5 MBq source of [241]Am α-particles. Films of (12,8) diacetylene were prepared with thicknesses of 50 layers (150 nm) on an insulating substrate between appropriate electrodes. Application of a bias voltage between the electrodes then enabled charge resulting from energy deposition by an ionizing particle to be collected. The response to α-particle energies between 5.5 and 3.5 MeV, when normalised to unit solid angle show that the larger stopping power at low energies is reflected in a larger charge production rate in the films, as expected, and encourages the prospect of being able to measure W-values in LB films by measuring charge production in unsupported films simultaneously with energy loss.

(c) POLYMERIZATION IN NANOMETRE (12,8) DIACETYLENE FILMS USING GAMMA RADIATION: A monomer film of (12,8) diacetylene (DA) will polymerize under the action of both UV and gamma photons. Estimates of the sensitivity were made using ^{60}Co photons for irradiation, and optical absorption at 490 nm as the indicator of monomer-polymer conversion. For films having thicknesses 72 nm, 144 nm and 150 nm (24, 48 and 50 layers) the optical density per layer shows a consistent and quasi-linear increase with absorbed dose up to about 10 kGy, and a more gradual increase thereafter. The sensitivity of (12,8) DA films towards polymerization, as quantified by optical absorption, is not likely to be sufficient for use as a dosimeter at protection levels but could find use as the basis for an industrial or therapy instrument. Radiation effects in these films for other purposes, however, have been shown to provide dosimetric data a nanometre levels which are not otherwise obtainable in condensed organic media.

In **project 7 (MRC-Chem)** the major objective of the studies was to gain a better understanding of the influence of the chemical stages in the development of DNA damage induced by radiation of different quality and its relationship to biological consequences. Experimental evidence is presented for the effects of radiation on mammalian cells, that the severity of complex damage in DNA increases with increasing LET, as predicted from biophysical models (GSF, MRC-Phys, ADPA). The severity of the damage is decreased if scavengers of diffusible water radicals produced in the close environment of cellular DNA are used, and this decreased severity is reflected in reduced cellular readiosensitivity. Evidence from plasmid DNA model system, which mimic the cellular environment, have emphasised the increased complexity of DNA damage for high LET radiation when comparing γ- to α-radiation. From comparison of the yield of DNA-protein crosslinks(DPC) induced by γ. and α-radiation, it is inferred that they do not reflect complex damage. Furthermore, oxygen reduces the level of DPC. The radiobiological significance of DPC is therefore open to question. Preliminary findings on the direct effects of radiation have indicated that hole migration occurs in DNA but only over short distance (a few base pairs) so that the track fingerprint is not lost due to migration processes in DNA. The major type of DNA damage from ionisation of DNA bases is base modification with a low level of strand breaks involving radical transfer processes. These studies have also provided several benchmark quantities such as yields of double strand breaks, DPC, and non-scavengeable yields which are essential for development of more sophisticated models of radiation effects.

Head of project 1 : Dr. Paretzke

II. Objectives for the reporting period

1.   To improve the quantification of the electron emission cross sections used in charged particle track structure computer codes for the condensed phase in biological matter by empirical theoretical models and by experimental data

2.   To improve and to couple to the initial physical stage the computer simulation of the diffusion and of the chemical reactions of species newly created in the physical stage of the formation of a charged particle track.

3.   To improve the geometrical description of the DNA molecule and its super-structures in track structure codes.

4.   To investigate the capabilities and problems of various approaches to the mathematical modelling of radiation carcinogenesis by multi-step models.

5.   To improve the programme structure of the track structure simulation code PARTRAC.

6.   To continue collaboration with other highly qualified partners within and outside (in Europe and USA) this contract for improvements of the depths and widths of the models as well as for particular applications

III. Progress achieved including publications

The work performed during the reporting period covered all 6 objectives mentioned above and consisted mainly of theoretical analyses, computations, model calculations, etc., but for topic 1 ("emission cross sections") also experimental data were obtained to guide the derivation of theoretical approximations and generalizations.

(1a) THEORETICAL ELECTRON CROSS SECTIONS IN LIQUID WATER.
Electron cross sections in liquid water are an essential ingredient to the simulation of the effects of ionising radiation on DNA in cells, their dependence on primary electron energy T, on energy transfer E, and on momentum transfer q was quantified. The approach was based on a method proposed by Ritchie et al. (1978), Hamm et al. (1975), and Ritchie et al. (1991) in which electron cross sections are derived from the dielectric function for liquid water. The latter has been calculated by applying the Kramers-Kronig relations on the optical reflectance of photons determined by measurements with photons in the energy range of 7.6 eV to 25.6 eV (Heller et al. 1974). The imaginary part of the dielectric function describing the light absorption, was approximated by these authors by a sum of so-called Drude functions:

$$\in_2 (E) = E_p^2 \sum_n \frac{f_n \gamma_n E}{(E_n^2 - E^2)^2 + \gamma_n^2 E^2}$$

where f_n is the oscillator strength, γ_n the width, and E_n the resonance energy. E_p denotes the "plasma energy" assumed as 6.8 eV for liquid water. Each Drude function is assumed to represent an ionisation or excitation in water. Due to the analytical form of the Drude function, however, there are also contributions below the resonance energy E_n. In the case of

ionisations, this parameter is identified with the ionisation energy of the corresponding shell Therefore, this approach is not in accordance with the law of energy conservation In our approach this deficiency is avoided by truncating the Drude functions for the ionisation part below the threshold energies E_n. The parameters were chosen such that the following sum rule was fullfilled

$$\int_0^\infty E \, \epsilon_2 \cdot dE = \frac{\pi \cdot Z \cdot E_p^2}{2}.$$

The binding energies for the five shells were chosen to be 10 9, 13.5, 16 2, 32, and 540 eV. To avoid sharp edges at the threshold energies E_n and to simulate the width of the valence band for the liquid, the resonance energy was identified with the threshold energy for ionisations of shell n and it was assumed to be distributed according to a Gaussian function with a width of 1 eV. This value is in agreement with band structure calculations for cubic ice by Zaider et. al (1989, 1994).

Another shortcomming of the method mentioned above was an unrealistic distribution of the dielectric function over the shells of the water molecules Therefore, in the present approach additional constraints were imposed on the parameters f_n and γ_n. These were derived from experimental results obtained by X-ray electron spectroscopy (Shibaguchi et al 1977, Berkowitz 1979, Siegbahn 1974) and the known high energy transfer behaviour of the electron cross sections. Further, relativistic and exchange corrections were imposed.

For the contribution of excitations to the imaginary part of the dielectric function, in the present approach a parametrisation similar to the one proposed by Kutcher and Green (1976) was used. As there is a significant uncertainty in the partitioning into ionisations and excitations for energy transfers larger than 12 eV, where the excitation and the ionisation levels overlap, the parametrisation of Kutcher and Green was changed to allow a better fitting of the ionisation part. However, the total oscillator strength attributed to excitations has not been changed. The present approach yielded the parametric fit of the imaginary part of the dielectric function for zero momentum transfer as shown in Fig. 1.

The real part of the dielectric function was obtained by applying the Kramer-Kronig relations and by performing an analytical continuation in the complex E-plane. To derive cross sections for electron scattering, the obtained approximation of the dielectric function for zero momentum transfer had to be extrapolated to non vanishing momentum transfers For this purpose, E_n was replaced by $E_n + q^2/(2m_e)$, with m_e being the electron mass, and the constants f_n by functions of q. Here the procedure of Hamm et al. (1975) was followed closely. Finally, the differential inverse mean free path (dimfp) or macroscopic cross section was obtained according to Hamm et al. (1975) by

$$\frac{d\mu}{dE} = \frac{1}{\pi T a_o} \int_{p-}^{q+} \frac{dq}{q} \frac{\epsilon_2 (E,q)}{\epsilon_1^2 (E,q) + \epsilon_2^2 (E,q)}.$$

Results are shown in Fig. 2. The total inverse mean free path is obtained by integration over the energy transfer. For primary energies above 100 eV, results are similar to those obtained by Ritchie et al. (1978). However as shown in Fig. 3, for energies below 20 eV, where the excitations contribute significantly, the results of the two approaches deviate by a factor of up to two.
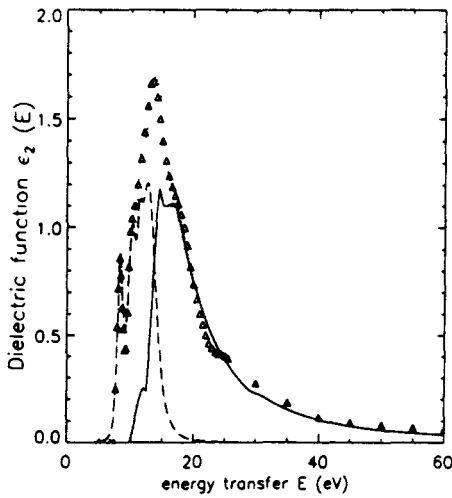
Fig. 1 : Imaginary part of the dielectric function for zero momentum transfer from optical measurements (open triangles), by Ritchie et al. (closed triangles) and by the present approximation (dotted line). The broken line gives the excitation part, the solid line the ionisation part of this work.
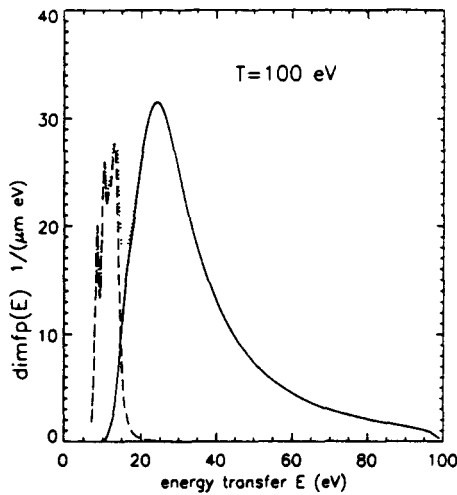
Fig. 2 : Inverse mean free path differential in energy transfer as derived in this work for a primary electron energy of 100 eV. Shown are the contributions due to ionisations (solid line), excitations (dashed line), and the total imfp (dotted line).
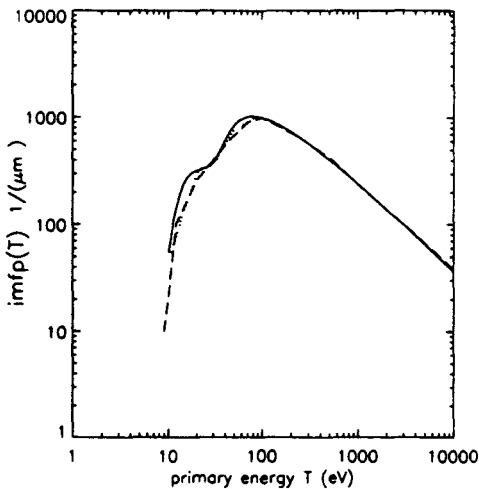
Fig. 3 : Inverse mean free path in liquid water as derived by the present approach (solid line), by Ritchie et al. (1978, dashed line), and by Hamm et al. (1975, dotted line).

(1b) EXPERIMENTAL ELECTRON CROSS SECTIONS IN CONDENSED MATTER To guide the development of theoretical equations describing electron emission also energy and angle differential data for low energy electron emission from clean surfaces under controlled conditions were measured using "Time of Flight" -energy analysis The pulsed particle beam (I_A = 5 pA, f = 2 MHz, pulse width $\leq$ 0.5 ns) traversed the thin target foil positioned perpendicular to the beam direction. Electron spectra were measured from enerergies as low as 0.1 eV up to approximately 100 eV with a resolution $\Delta E/E$ better than 10%. All experiments were performed in the Radiological Physics Laboratory of Battelle Northwest Laboratories, Richland, USA, under UHV conditions with a chamber pressure in the 10^{-10} torr region

Commercially produced, self-supporting carbon foils with nominal thicknesses of 3 $\mu g/cm^2$ and 5 $\mu g/cm^2$ were used These foils were thoroughly cleaned by sputtering with 3 kV Ar-ions until no furhter changes in the low energy range of the spectrum could be observed. Doubly differential secondary electron spectra were measured for impact energies from 500 keV/amu up to 2 MeV/amu for H^+, H_2^+ and H_3^+ projectiles. The electrons emerging from the target were detected for an angular range of 25°$\leq \theta \leq$155°

Figures 4 and 5 display measured secondary electron emission spectra in forward (25°$\leq \theta \leq$75°) and backward (105°$\leq \theta \leq$155°) directions obtained for 1 MeV proton impact on a 10 $\mu g/cm^2$ carbon foil The following features were observed. (a) electrons originationg from carbon K-Auger transitions are observed at energies below 250 eV, (b) single electron "plasmon decay" may contribute to the 'hump' at about 20 eV, (c) low energy electrons originate from soft collisions near the surface and energy degraded high energy electrons produced by hard collisions deeper in the material These form the 'true secondary electron peak' which contains $\approx$85% of all emitted electrons. Note the energy shift of the peak maximum with angle, (d) the hard collision component of the low energy emission primarily contributes the low energy tail for electrons emitted in forward direction, (e) little dependence on projectile energy is seen in the spectra

First experiments were performed using a 1.5 μm Mylar foil which was glued on a target holder. As Mylar is an insulator, electrical charging of the target, even at beam currents lower than 1 pA, prevented any low energy electron emission from the irradiated surface. Using a biased filament close to the target, electrons were sprayed on the charged surface to compensate for the remaining positive charge. The filament bias voltage was adjusted in a way that no electrons from the filament reached the detector. The influence of the filament potential on the electron energy distribution needs further investigation. Sputtering appeared to destroy the insulating properties of the surface Electron emission could be observed even without spraying additional electrons. Experiments will be conducted using lower sputtering energies, thus damaging only a thinner surface region, in order to explore the influence of structural damage by sputtering. Several attempts were made to mount thin DNA-foils provided by Prof. A. Rupprecht (Univ.Stockholm, Sweden). However, unfortunately foils proved to be not suitable in the environment neccessary for electron emission studies. During pump-down and baking, the DNA dried and turned into brown powder. It appears to be more promising, to dry DNA solution in a deepening on the target holder before putting the target in the vacuum system. Such experiments are planned for the furture
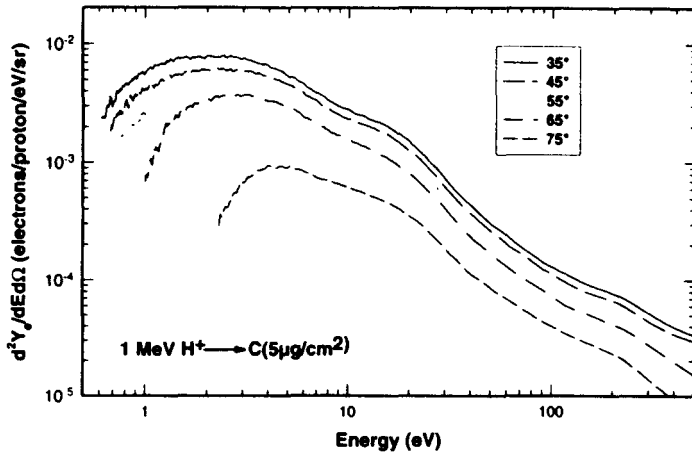
Fig. 4 Double differential electron emission cross sections in forward directions induced by 1 MeV protons on a 5μg/cm² carbon foil.
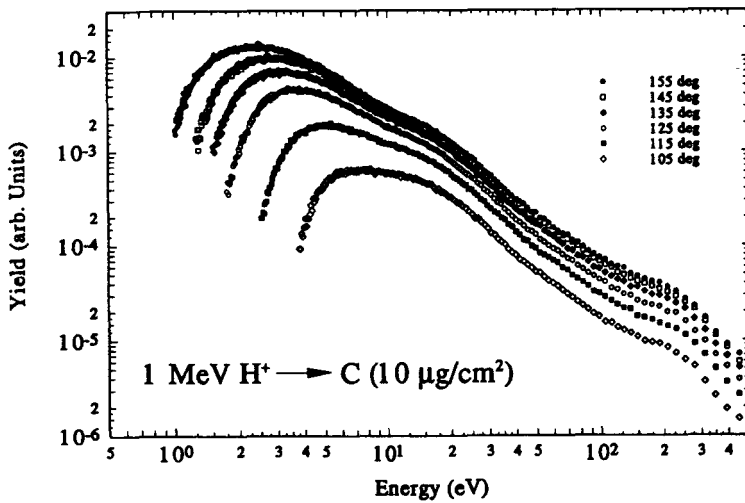
Fig.5 Double differential electron yields in backward directions induced by 1 MeV protons on a sputter cleaned carbon foil (10μg/cm²).

(2) INTERACTIONS OF RADIATION INDUCED RADICALS IN WATER WITH DNA A literature review was performed to model the interactions of radiation induced radicals in water with DNA. The developed model consists of two submodels, the first describing the prechemical stage ($0-10^{-12}$s) and the second the chemical stage ($10^{-12}-10^{-6}$s) The submodel on the prechemical stage consists of three parts describing ionisations, excitations, and subexcitation electrons The submodel on the chemical stage describes reactions of the radicals with each other, with a scavenger, and with DNA molecules.

a) Prechemical stage: The submodel on the prechemical stage is mainly based on the work performed at the Oak Ridge National Laboratory (Turner et al. 1980, 1983, 1988, Bolch et al 1988) The primary product of an ionisation H_2O^+ was assumed to migrate before reacting with a water molecule. The migration distance is sampled from a three-dimensional Gaussian distribution with a standard deviation of 0 7 nm in each of the three cartesian directions. The relative coordinates between the two reaction products H_3O^+ and OH^- are sampled from a three-dimensional Gaussian distribution with a standard deviation in each of the three cartesian directions of 0.3 nm. Excitations of molecules in liquid water were considered to result in three different processes: relaxation, dissociation and autoionisation. In 86 5% of all A^1B_1 excitations, the molecule is assumed to relax, i e. to return to its initial, unperturbed state, and otherwise to dissociate. Two types of dissociations are considered, resulting either in H and OH or in two OH and H_2. The positions of the dissociation products are sampled from assumed distance distributions. The excitation B^1A_1 is assumed to relax in 55% of all cases and otherwise to lead to a dissociation. Rydberg A+B, Rydberg C+D and dissociative excitations, and excitations of the diffuse band are assumed to relax in 49% of all cases, to lead to a dissociation in 3.6%, and otherwise to be followed by an autoionisation. Electrons with energies below 10 eV were considered to thermalize and then to become hydrated. The propagation distance during thermalisation was assumed to be a function of electron energy The distance ranges between 33 nm for an electron energy of 10 eV and negligeable distances for energies below 0.1 eV

b) Chemical stage· The chemical stage starts with a spatial distribution of the species e^-_{aq}, H_3O^+, OH, H, and H_2. The simulation of the diffusive motion is based on the work performed at the Oak Ridge National Laboratory (Turner et al. 1983, Wright et al. 1985, Turner et al. 1988, Bolch et al. 1988, Klots et al. 1990). The diffusion is modeled in discrete time steps of 3 ps . The jump distances are calculated from known diffusion constants and are for the initial species in the range of 0.21 nm for OH to 0 41 nm for H_3O^+. Fourteen interactions between the initial species and further reaction products are considered. The species are assumed to interact if they are closer to each other than a given distance, called "reaction radius". For a diffusion-controlled reaction the reaction radius was calculated in a simple manner from the diffusion coefficients of the reaction partners and the reaction rate constant. Reaction rate constants have been obtained by a literature review. The derived reaction radii vary between 0.001 nm for the reaction between OH and H_2O_2 and 1.3 nm for the reaction between H_3O^+ and OH^-. Since the jump distances in the simulation of the diffusion process are in the same order of magnitude as the reaction radii, the above indicated simple model had to be modified. The concept of so called "reduced reaction radii" was introduced The validitiy of the concept and its parameters has still to be analysed by comparing the calculation results with experimental results for the time-dependent yields of OH and e^-_{aq} after radiation exposures of liquid water.

The presence of a scavenger was modelled by a Russian roulette process for OH in which the probability of survival after each time step is proportional to the scavenging capacity Reactions between radicals and e^-_{aq} on one side and constituents of the DNA (desoxyribosemonophosphate and the four bases) on the other side were also modelled by the concept of "reduced reaction radii". In a first step, experimental reaction constants were taken from Buxton et. al (1988). According to these data, the most reactive constituents are guanine

and thymine For OH the reaction radius with desoxyribosemonophosphate is by a factor of four lower than with these two bases, for H and e^-_{aq} the difference is even larger In a first approach the response of the DNA to attacks by radicals was modelled according to discussions with C v Sonntag An OH-reaction with the sugar moiety is assumed to lead to a strand break in 60% of the cases In the case of a reaction with a base, a probability for strand breakage of 10% was assumed.

(3) DNA COMPUTER MODEL AND MODEL CALCULATIONS WITH PARTRAC A comprehensive DNA target model has been developed which describes five orders of B-DNA structure (nucleotide, helix, nucleosome, chromatin fibre and chromatin fibre loop) on an atomic level. The DNA model starts from the atomic co-ordinates of the four nucleotides in B-DNA stacked in a random or a selected sequence yielding the DNA helix The nucleosome comprises 146 nucleotide pairs of a DNA helix wrapped 1.8 times around a cylindrical representation of the histone octamer Two adjacent nucleosomes are connected by linker DNA determined by its length and the parameters of the chromatin fibre (radius, repeat length, number of nucleosomes in this repeat length, corresponding number of turns, the tilt angle) Fig. 6 shows a 'zigzag' formation of a chromatin fibre with 2 nucleosomes per 20 nm repeat length and 60 bp linker DNA. For the generation of chromatin fibre loops, one linear and two curved fibre elements are introduced comprising the atoms inside one repeat length of a linear chromatin fibre. These three elements can be stacked offering smooth connections of the lower order DNA structures. Fig. 7 shows a chromatin fibre loop of 67 elements comprising together about 90,000 nucleotide pairs in a 'cross linker' chromatin structure in which the linker DNA traverses the chromatin fibre

The DNA model has been implemented in the biophysical model PARTRAC. In PARTRAC, the DNA target in the cell nucleus is superimposed with spatial patterns of ionisation and excitation events generated in a Monte Carlo simulation of electron interactions in water Spatial coincidences of these events with atoms of the DNA strand are further analysed in terms of single and double strand breaks due to direct interaction. Additionally, the production of water radicals, its time dependent evolution, and diffusion to DNA target atoms is considered resulting in DNA lesions due to indirect interaction For the implementation of the DNA model, much effort was necessary to limit the computing times as well as the memory and storage space requirements to an acceptable amount. First calculations with the DNA model in PARTRAC have been performed for two chromatin fibre structures, both of them consist of almost 70,000 randomly distributed and oriented chromatin fibre loops of about 300 nm length and 200 nm width to describe the entire DNA ($3.6 \cdot 10^{12}$ Dalton) inside a cell nucleus. One target describes a solenoid type chromatin fibre structure of 6 nucleosomes per 11 nm repeat length in one turn, the other is a cross linker model of 7 nucleosomes per 13 nm repeat length in 2 turns displayed in Fig. 7 Tracks were calculated for electrons with energies between 100 eV and 30 keV generating random patterns of energy deposition events inside the nucleus. In all calculations, almost 4 % of about 35,000 ionisations plus excitations were found inside the van der Waals radii of DNA atoms. Hit atoms of the strand were considered to produce a strand break, hits on different strands with a distance of not more than 10 nucleotide pairs as double strand breaks (DSBs), hits at neighbouring nucleotides of the same strand were taken as one strand break.

Form the large number of numerical results, distributions of the DNA fragment size resulting from pairs of DSBs due to direct interaction of a single primary electron are given in Fig. 8 The DNA fragment size distributions reflect the geometrical structure of the DNA target as well as spatial distribution of the events in the tracks. The DNA fragment size distributions in Fig. 8 are given for two chromatin fibre structures resulting from 1 keV electrons. In the solenoid model, pronounced peaks are found at fragment lengths of about 80 bp, 180 bp and around 1200 bp corresponding to DSBs in adjacent turns of the DNA around the nucleosome, adjacent pieces of linker DNA and adjacent solenoidal turns. In the cross linker model, a far
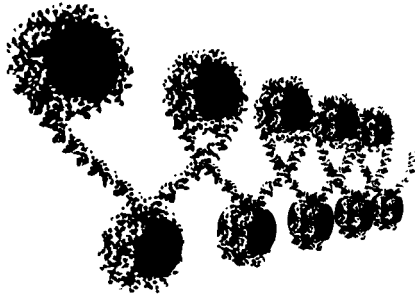
Fig. 6: **Zigzag Chromatin Fibre Model**
Parameters:
0° tilt angle
20 nm repeat length

2 nucleosomes per 1 turn
60 bp linker length
15 nm fibre radius

Fig. 7: **Chromatin Fibre Loop Model**
67 fibre elements in cross linker structure
Parameters:
0° tilt angle
13 nm repeat length

7 nucleosomes per 2 turns
48 bp linker length
15 nm fibre radius
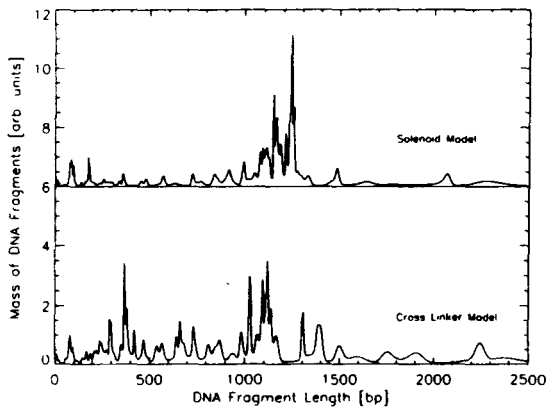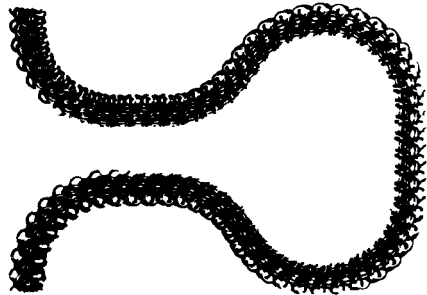
Fig. 8: **DNA Fragment Size Distribution**
due to direct interaction from 1 keV electrons for a cross linker model of the
chromatin fiber (parameters as in Fig.2) and a solenoid model of the chromatin
fiber with the parameters:
6 nucleosomes per 1 turn
40 bp linker length
15 nm fibre radius

20° tilt angle
11 nm repeat length

greater number of fragments with lengths between 200 and 1200 bp is found The help of E. Pomplun KFA-Julich, for providing his nucleosome model being a basis of our DNA model development is gratefully acknowledged.

(4) BIOPHYSICAL MULTISTAGE MODELLING Several biologically motivated, mechanistic models of tumor genesis for bridging the gap between mutation rates and observed cancer incidence were considered This type of model was proposed e.g. by Armitage and Doll, and by Moolgavkar, Venzon and Knudson (MVK model); their aim was a quantitative description of tumor development in biological terms like cell growth, cell death and mutation rates. It has been shown that they give a good description of a wide range of human and animal tumors. In this approach the application to epidemiological data is one of the sources of input to risk analysis. Another possible source of information is molecular biology.

The classical Armitage-Doll model assumens n mutational stages, not taking into account growth and death processes of the various intermediary cells. The age dependence of the tumor incidence in this model is a power law, with the exponent $n - 1$ The MVK model is a special case of clonal expansion models in which intermediary cells are allowed to divide, and die. Often, only two rate limiting mutations are considered, with one intermediary stage

We concentrated here on these clonal expansion models, of which there are two versions in use:

- The"epidemiological approximation", which is assumed in many studies of human cancer, it models the net growth rate of the intermediary cells only. After an initial period it gives an exponential growth of hazard with age.
- The "exact formulation" derived by modelling the birth-death process of the intermediate cells. In this case the exponential growth eventually levels off to a constant hazard.

The epidemiological approximation was rederive using differential equations for expectation values. Explicit hazard functions for short time exposure to radiation were given. Although we restricted ourselves to modelling cancer incidence of adults, we had to model also childhood in order to calculate the initial condition of how many intermediate cells are in the organism at the age of 20 years (assuming an initial condition would introduce another free parameter). For this we used linear growth from birth. An analysis was made which effects of radiation on the parameters of the model might be determined from incidence data. It was shown that only a subset of parameter combinations of the MVK model can be determined from epidemiological data sets [7]. Therefore we derived hazard functions with an unconventional set of parameters from the formulas of Moolgavkar et.al. for both, the spontaneous rate and for short time exposure. The parameters were chosen in such a way, that each of it determined characteristics of the hazard function which are easy to monitor. We feel this is a good safeguard against running into local extrema in the fitting procedure. Applications of the formulas derived to various human and animal tumors were analysed.

For analysis of the probability of causation of lung cancer by inhalation of radon and its daughter products different models were analysed (ICRP-Report 50, NCRP, BEIR-IV-Report, Jacobi-model). The S-cohort of the Czech Uranium miner was taken for comparison of these models, and it was found that these models differ less from each other than the varions epidemiological data sets for different underground miners [10]. Mathematical functions were derived in this analysis to quantify PC-tables and figures. As an example the predictions of Jacobi's model for the excess relative risk after exposure to 100 WLM are given in fig. 9.
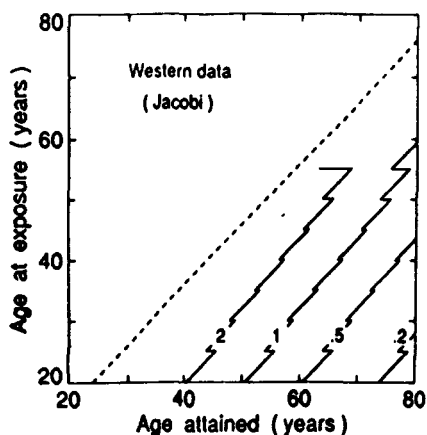
Fig. 9: Predictions for the excess relative risk for lung cancer incidence as a function of age at exposure and age at diagnosis after 100 WLM exposure to radon daughter products based on Jabobi's model

Publications

[1] H. Nikjoo, M. Terrissol, R.N. Hamm, J.E. Turner, S.Uehara, H.G. Paretzke, D.T. Goodhead. "Comparison of energy deposition in small cylindrical volumes by electrons generated by Monte Carlo track structure codes for gaseous and liquid water". Radiat. Prot. Dosim. 52, 161-165 (1994).

[2] H. Nikjoo, D.T. Goodhead, D.E. Charlton, H.G. Paretzke. "Energy deposition in cylindrical targets by monoenergetic electrons, 10 eV to 100 keV". MRC Monograph 94/1, MRC Radiobiology Unit, Chilton, Didcot (1994).

[3] H.G. Paretzke, D.T. Goodhead, I.G. Kaplan, M. Terrissol. "Track structure quantities". In: Atomic and Molecular Data for Radiotherapy and Radiobiology. IAEA TECDOC-799, pp. 633-721 (1995).

[4] H.G. Paretzke, M. Inokuti, D.T. Goodhead, M. Terrissol, L.H. Toburen, J. Botero, N. Kocherov, R.K. Janev. "Atomic and Molecular data needs for Monte Carlo track structure calculations of radiation induced damage in biological substances". IAEA Report INDC (NDS)-295 (1994).

[5] D.T. Goodhead, H.P. Leenhouts, H.G. Paretzke, M. Terrissol, H. Nikjoo and R. Blaauboer. "Track structure approaches to the interpretation of radiation effects on DNA". Radiat. Prot. Dosim. 52, 217-223 (1994)

[6] A. Ottolenghi, M. Merzagora, L. Tallone, M. Durante, H.G. Paretzke, W.E. Wilson, (1995). "The quality of DNA double-strand breaks: a Monte Carlo simulation of the endstructure of strand breaks produced by protons and alpha particles", Radiat. Environ. Biophys., in press.

[7] A. Ottolenghi, M. Merzagora, H.G. Paretzke. "DNA Complex lesions induced by protons and alpha particles: Track structure characteristics determining LET and particle dependence". Submitted to Radiat. Environ. Biophys.

[8] W.F. Heidenreich and H. Paretzke. On the parameters of the MVK model. Submitted to Rad. Environ. Biophys.

[9] W.F. Heidenreich, P. Jacob, H.G. Paretzke. "Exact solutions of the clonal expansion model and their application to the tumor incidence of the atomic bomb survivors". Submitted to Radiat. Environ. Biophys.

[10] D. Chmelevsky, D.Barklay, A.M. Kellerer, L. Tomasek, E. Kunz, V. Placek. "Probability of causation for lung cancer after exposure to radon progeny: A comparison of models and data". Health Phys. 67 (1994) 15-23.

Head of project 2:   Dr. Goodhead

II.   Objectives for the reporting period

1.   Assess robustness of track scoring results, at the nanometre level, by comparisons using Monte Carlo transport codes from different workers.
2.   Extend electron transport code for electrons from 100 keV up to the MeV region.
3.   Develop methods for incorporating main chemical pathways in track structure modelling of damage to DNA for comparison with experimental data, for electrons and charged particles.
4.   Survey available information on *hprt* mutagenesis and supplement with new experiments where appropriate.
5.   Accumulate data on track structure, DNA damage and single-track survival probabilities required for understanding and modelling mutagenesis and related cellular effects.
6.   Measure and evaluate role of single-track-survival factor in limiting mutation frequencies of high-LET α-particles.
7.   Continue collaborative support to partner MRC (Chem) for special radiation sources and configurations.
8.   Compare theoretical analyses from track structure with experimental data on biological effectiveness, develop hypotheses and tests of underlying mechanisms and consider implications.

III.   Progress achieved, including publications

The project consisted of a general strategy towards biophysical understanding and modelling of the relative effectiveness of radiations of different qualities and extrapolation to low doses not experimentally accessible. The related components of the work were (a) track structure analyses of radiations of different qualities, (b) experimental investigations and data analysis of *hprt* mutagenesis (as a paradigm), cell inactivation, DNA damage and other cellular effects and (c) comparative analysis of biological effects in relation to the microscopic features of the tracks.

(a)   Track structure calculations

Our previous analyses of track structure had concentrated on frequency distributions of energy deposition in defined small volumes for comparison with experimentally observed biological effectiveness of different radiations. Initially these analyses were based on track structure codes for water vapour (adjusted to unit density) because these were most firmly founded on experimental data. Recognising that the ionization (and excitation) yields would be substantially different in liquid water and that stochastic properties at the level of small numbers of interactions in very small volumes would depend substantially on the water phase, the analyses were carried out in terms of energy deposition rather than numbers of ionizations. In this way it was anticipated that the frequency distributions for vapour would be reasonably representative of those for liquid, except at the smallest energies (such as for single ionizations or excitations) or smallest (nanometre) volumes. With this underlying assumption, analyses from the vapour codes, when compared quantitatively to radiobiological data for different radiations and conditions, led to clear hypotheses on the biological importance of clustered damage at the DNA, or slightly supra-DNA levels [1,2]. Current

evidence appears to justify this assumption since similar frequency spectra of energy-deposition clusters are calculated to occur with tracks in liquid [3,4].

Hence it has become necessary to understand in more detail the nature of the molecular damage to DNA within the clusters. Clean double-strand breaks are just one simple class of a spectrum of clustered DNA damage of potentially widely varying molecular complexity and biological severity. In order to model quantitatively damage from radiation tracks that lead to mutations, chromosome aberrations and other long-term biological effects it is necessary to follow the track chemistry within and between clusters of ionizations in the highly scavenging, short-diffusion, cellular environment.

Within this contract the justification and needs of this approach have become more clear and tools have been developed to make it more achievable and accurate.

Before the period of this contract we had established an extensive data base on absolute frequencies of energy deposition in cylindrical volumes of dimensions <1 to >100 nm for a wide variety of different radiations, simulated by MOCA8b and MOCA14 Monte Carlo codes (from partner GSF), to act as a guide towards the biologically critical features of radiation quality and the nature and quantities of relevant initial molecular damage in cells. Calculations also included preliminary evaluations of DNA strand breakage from direct ionizations in the DNA. As more advanced evaluations of DNA damage are approached, including more realistic descriptions of the DNA and simulations of chemical pathways in the cellular environments, it has become particularly important to judge the reliability of the Monte-Carlo track-structure simulations at the very high spatial resolution required. Our previously established data base has allowed standardised-scoring comparisons with electron tracks from four additonal water transport codes world wide. Large-statistics scoring routines were applied for target diameters of initially 2 and 25 nm [3] and subsequently 10 nm as well as other criteria of comparison [4]. Good agreement was shown between the different codes in many situations, but some substantial differences were revealed over distances of a few nanometres, especially for larger energy depositions that may cause more complex and biologically-severe clustered damage in DNA. These were not explicable simply as differences between 'vapour' and 'liquid' codes, nor were they entirely eliminated even when only relative frequencies for different electron energies were considered. The differences are likely to be of some significance in attempts to follow the detailed chemical processes.

In collaboration with S. Uehara, electron interaction cross sections have been extended from 100 keV (the limit of MOCA8b) up to several MeV to allow simulation of these higher energy electrons. The new code KURBEC has been fully described [5]. This codes was included in the above comparisons.

Initial methods have now been developed for incorporation of water radiolysis products, from radiation tracks (using CPA100 code; with partner ADPA) in the highly-scavenging cellular environment, into our previous evaluations of DNA strand breakage from direct ionizations in the DNA [6a,b]. These allow qualitative and quantitative estimation of the spectrum of types of DNA damage, including the molecular complexities of clustered damages composed of multiple strand breaks, base damages and other chemical changes, which may be of particular biological significance by virtue of reduced reparability and hence greater severity [2]. Much more advanced spatial descriptions of the DNA molecule have also under developed, (in collaboration with J. Goodfellow and Y. Umrania) to include precise

optimization of the positions of the bound water molecules as well as the DNA atoms [7a] and to investigate their influence on DNA damage [7b].

We have collaborated also in the development of the PITS codes as a potential standardized code format for simulation of tracks from positive ions, comparison of consequences of different secondary electron transport options, phase effects, etc. [8]. The code is currently being formulated particularly to provide tracks of protons and α-particles in liquid water in both the initial form of the 'physical' track as ionizations and excitation, and its conversion to the 'chemical' track of early reactive species. This will allow initial simulations of molecular spectra of clustered DNA damage by direct and indirect ionizations from these high-LET radiations for comparison with low-LET radiations and observed biological effectiveness.

As an initial approach to incorporating track dimensions into simulations of chromosome aberrations resulting from radiation-induced breaks, radial distributions of ionizations around charged particle tracks have been evaluated [9] for use in simulations of aberration formation based on the assumption of pair-wise exchanges between breaks [10].

(b)   Experimental studies of radiation quality in cellular systems

The conventional view of radiation carcinogenesis assumes that radiation acts directly as an initiator by a mutation, or large chromosomal rearrangement, as one of the early critical steps in multi-stage carcinogenesis. [There is scope for alternative hypotheses based on radiation-induced instability and experimental evidence for these are increasing. However, such mechanisms are beyond the scope of the present contract.] The *hprt* mutation system has previously been identified as a particularly suitable paradigm for mechanistic understanding and modelling of radiation mutagenesis because of the extensive quantitative information that exists on radiation-parameter dependencies and molecular characterization of early mutations. A partial literature survey was undertaken for pertinent data on *hprt* radiation-mutagenesis, with emphasis on studies revealing dependence on radiation quality, dose and time [11]. Direct experiments were commenced to fill some of the notable gaps in available information. These include the effects of reduced dose rate for high-LET radiations and dependence on oxygenation for both low- and high-LET radiations. We have completed our experiments with V79 cells on dose-rate dependence for high-LET α-particles (121 keV μm^{-1}) and comparison with chromosome aberrations induction and cell inactivation under similar conditions. These showed that under favourable plateau-phase culture conditions there is very little dose-rate dependence (in the conventional direction, if at all) for *hprt* mutagenesis, although we did get anomalous results with unfavourable culture in our initial mutation experiments with titanium-walled dishes [12]. Comparative data, obtained under similar experimental conditions, for induction of dicentric and ring chromosome aberrations and for cell inactivation (all in glass-walled dishes) showed small, but significant, reduction in effect at the lower dose rates, in accordance with conventional expectations. For investigation of modification of mutagenesis by lack of oxygen at the early chemical stage of track damage, a 20-dish system has been constructed for irradiation of cells on our α-particle irradiator under conditions of controlled gassing, as well as control of other environmental and scavenging conditions.

We have also measured *hprt* mutagenesis by α-particles in a variety of other cell types, most notably of the haemopoietic system to ascertain the generality of induced

frequencies and radiation quality dependence. Generally, induced mutation frequencies for various developmental stages of B cells were found (in collaboration with S. Griffiths and M. Greaves) to be similar or somewhat lower than those in human fibroblastic or V79 cells, although in the particular radio-sensitive pre-B stage no induced mutations could be detected with either α-particles or X-rays [13]. Notable features of X-ray dose responses at other stages were the high-power dependence on dose (D^2-D^4) and no evidence of a linear term. Alpha-particle induced mutations are being measured also in L5178Y lymphoma cells and human lymphocytes (with B. Bridges and J. Cole) following suggestions of enhanced sensitivity to α-particles in view of observations of an association between lymphocyte mutations and household radon concentrations. Our results to date do not indicate particularly high mutation frequencies after *in vitro* irradiation [14].

For interpretation and modelling of data on mutagenesis, or other viable cellular consequences, for α-particles it is essential to evaluate the probability (S_1) that a cell will survive the passage of a single α-particle and therefore remain capable of expressing any genetic damage. We have established these S_1-factors for a wide variety of cell types for α-particles (particularly at 121 keVμm^{-1}) and we find that they vary from 0 (for mouse pre-B cells) through 10-20% for mouse haemopoietic stem cells, 30-60% for mouse multipotential, multimyeloid or transformed pre-B cell lines and normal mature B-cells, and 60->90% for normal and established fibroblasts [13,15,16,17]. This factor can clearly have a substantial, greater than ten-fold, influence on the final mutation frequencies for high-LET radiations. In the extreme case of pre-B cells, that are extraordinarily prone to apoptosis after X-rays giving a D_o of only 0.3 Gy [18], apparently every α-particle is lethal, the inactivation RBE is <1 and no induced mutants at all are detectable [13]. S_1-factors for radiosensitive fibroblasts, such as human AT cells and irs hamster mutants, are also being evaluated to establish the degree to which they may be responsible for the apparent reduced dependence of cellular effects on radiation quality. For accurate evaluation of the S_1-factors, we now routinely include in our experiments confocal microscope measurements of the dimensions of the living cells, and their nuclei, under the conditions of irradiation.

Other cellular effects have also been investigated under our standard conditions of 121 keVμm^{-1} α-particles in collaborative experiments to ascertain the extent to which the track structure features relevant to mutagenesis may or may not also be relevant to other endpoints and cell types, including cell transformation [19]. Results have included the observation that single α-particles can induce in a cell, with high probability, an ongoing genomic instability that can manifest itself as new chromosome aberrations in all subsequent cell generations [20]. This has raised the possibility, supported by some additional evidence, that *hprt* and other mutations can arise by similar delayed and untargetted mechanisms. An additional ability of single α-particles appears to be to induce at first metaphase a high proportion of complex chromosome aberrations, involving three or more break points in two or more chromosomes [21]. This observation should place particular new quantitative constraints on chromosome aberration mechanisms and track structure features that should aid future modelling and understanding.

Our experimental work on radiation quality included collaborations throughout with partner MRC (Chem) on a variety of fronts to aid in establishment of the yield, nature and reparability of initial radiation damage to DNA, with special emphasis on clustered damage and the chemical environment of the DNA. Our supporting role has been particularly with respect to α-particle irradiation configurations (see partner's report, including references) and

initial consideration of conditions for ultrasoft X-rays of 0.3 to 1.5 keV. These are a means of enriching for the clustered-ionization contributions from the low-energy electrons that occur in all low-LET irradiations [22]. It has been hypothesized from earlier evidence that these low energy electrons are the biologically-dominant component of all low LET radiations, but this remains controversial and the evidence to date is not yet conclusive [23].

(c)   Comparative analysis of track features with biological effectiveness

Understanding and quantification of radiation-induced mutagenesis, and other cellular effects, requires that track features be considered at both the DNA and cellular levels [24,25,26]. Clusterings of initial ionizations at the DNA level or slightly larger (5-10 nm) have been suggested as important features in determining the radiation quality dependence [2,27]. In recent years it has become apparent that the total yield of DNA double-strand breaks, as conventionally measured by a variety of techniques, has very little dependence on radiation quality of γ-rays, hard X-rays or heavy ions even when the track properties are varied enormously on both the cellular and molecular scales. This may be due to fairly small clusters, such as from low energy electrons, being dominant in producing 'dsb' as a broad class of measurable damage [28]. These relative numbers of initial dsb correlate very poorly with final cellular effects, including mutations, which show high relative biological effectiveness for densely ionizing radiations. We have suggested that this may be due to differential reparability of clustered damage including dsb of varying degrees of severity at the level of the DNA and immediately surrounding structures [1,2,29]. Our theoretical, experimental and comparative work has continued attempts to refine and evaluate this hypothesis and its implications, including in collaboration with partner MRC (Chem).

(d)   **Publications**

[1]   D.T. Goodhead. "Initial events in the cellular effects of ionizing radiations: clustered damage in DNA". Int. J. Radiat. Biol. 65, 7-17 (1994).
[2]   D.T. Goodhead, J. Thacker and R. Cox. "Effects of radiations of different qualities on cells: molecular mechanisms of damage and repair". Int. J. Radiat. Biol. 63, 543-556 (1993).
[3]   H. Nikjoo, M. Terrissol, R.N. Hamm, J.E. Turner, S. Uehara, H.G. Paretzke, D.T. Goodhead. "Comparison of energy deposition in small cylindrical volumes by electrons generated by Monte Carlo track structure codes for gaseous and liquid water". Radiat. Prot. Dosim. 52, 161-165 (1994).
[4]   H. Nikjoo, S. Uehara. "Comparison of various Monte Carlo track structure codes for energetic electrons in gaseous and liquid water". In: Computational Approaches in Molecular Radiation Biology, eds. M. Varma, A. Chatterjee (Plenum) pp. 167-186 (1994).
[5]   S. Uehara, H. Nikjoo and D.T. Goodhead. "Cross sections for water vapour for Monte Carlo electron track structure code from 10 eV to MeV region". Phys. Med. Biol. 38, 1841-1858 (1993).
[6a]   H. Nikjoo, P. O'Neill, M. Terrissol, D.T. Goodhead. "Modelling of radiation-induced DNA damage: the early physical and chemical events". Int. J. Radiat. Biol. 66, 453-457 (1994).
[6b]   H. Nikjoo, M. Terrissol, P. O'Neill. "Modelling of initial yield of DNA strand breaks induced by low LET radiation". Int. J. Radiat. Biol. 65, 123 (1994) [Abstr.].
[7a]   Y. Umrania, H. Nikjoo, J.M. Goodfellow. "A knowledge-based model of DNA hydration". Int. J. Radiat. Biol. 67, 145-152 (1995).

[7b]   H. Nikjoo, Y. Umrania, J.M. Goodfellow. "Influence of hydration shell of DNA in estimation of contributions by scavengeable and non-scavengeable effects". 42nd Ann. Meeting of Radiat. Res. Soc. (Radiation Research Society, Oak Brook), p. 203 (1994) [Abstr.].

[8]   W.E. Wilson, J.H. Miller, H. Nikjoo. "PITS: A code system for positive ion track simulation" In: Computational Approaches in Molecular Radiation Biology, Monte Carlo Methods, eds. M.N. Varma and A. Chatterjee (Plenum Press), 137-154 (1994).

[9]   H. Nikjoo. "The calculation of ionization distributions around charged particle tracks". MRC Monograph 93/1, MRC Radiobiology Unit, Chilton, Didcot (1993).

[10]   A.A. Edwards, V.V. Moiseenko, H. Nikjoo. "The repair of DNA breaks and the formation of chromosomal aberrations". Int. J. Radiat. Biol. 66, 633-638 (1994).

[11]   D. Baines. "Radiation-induced mutation". M.Sc. Thesis, University of St. Andrews (1992).

[12]   D.L. Stevens, S. Marsden, R.E. Wilkinson, A. Stretch, D.A. Bance, D.T. Goodhead. "A study of high LET dose-rate effects on V79-4 plateau-phase cells". Int. J. Radiat. Biol. 65, 133 (1994) [Abstr.] Also, 42nd Ann. Meeting of Radiat. Res. Soc. (Radiation Research Society, Oak Brook), p. 142 (1994) [Abstr.]

[13]   S.D. Griffiths, S.J. Marsden, E.G. Wright, M.F. Greaves, D.T. Goodhead. "Lethality and mutagenesis of B lymphocyte progenitor cells following exposure to α-particles and X-rays". Int. J. Radiat. Biol. 66, 197-205 (1994).

[14]   M. Thompson, J. Cole, D.T. Goodhead, B.A. Bridges. "Mutagenesis of human lymphocytes by alpha particles". 42nd Ann. Meeting of Radiat. Res. Soc. (Radiation Research Society, Oak Brook), p. 161 (1994) [Abstr.].

[15]   S.A. Lorimore, D.T. Goodhead and E. Wright. "Inactivation of haemopoietic stem cells by slow α-particles". Int. J. Radiat. Biol. 63, 655-660 (1993).

[16]   S.J. Marsden, S.D. Griffiths, S.A. Lorimore, D.T. Goodhead. "The sensitivity of murine haemopoietic cells of alpha particles and X-rays". 42nd Ann. Meeting of Radiat. Res. Soc. (Radiation Research Society, Oak Brook), p. 141 (1994) [Abstr.].

[17]   S.J. Marsden, S.A. Lorimore, D.T. Goodhead, E. Wright. "Viability of haemopoietic cells after exposure to low doses of ^{238}Pu α-particle irradiation at different linear energy transfers". Int. J. Radiat. Biol. 65, 145 (1994) [Abstr.].

[18]   S.D. Griffiths, D.T. Goodhead, S.J. Marsden, E.G. Wright, S. Krajewski, J.C. Reed, S.J. Korsmeyer, M. Greaves. "Interleukin 7-dependent B lymphocyte precursor cells are ultrasensitive to apoptosis". J. Exp. Med. 179, 1789-1797 (1994).

[19]   A.J. Mill, S.C. Hall, D.T. Goodhead, L.A. Allen, A. Butler, M.M. Lehane, S. Marsden, D.L. Stevens. "Dose-rate effects for transformation of C3H 10T½ cells irradiated with α-particles". Int. J. Radiat. Biol. 65, p. 145 (1994) [Abstr.].

[20]   M.A. Kadhim, S.A. Lorimore, K.M.S. Townsend, D.T. Goodhead, V.J. Buckle, E.G. Wright. "Radiation-induced genomic instability: delayed cytogenetic aberrations and apoptosis in primary human bone marrow cells". Int. J. Radiat. Biol. 67, 287-293 (1995).

[21]   C.S. Griffin, S.J. Marsden, D.L. Stevens, P. Simpson, J.R.K. Savage. "Frequencies of complex chromosome exchange aberrations induced by ^{238}Pu α-particles and detected by fluorescence *in situ* hybridization using single chromosome-specific probes". Int. J. Radiat. Biol., 67, 431-439 (1995).

[22]   H. Nikjoo, D.T. Goodhead, D.E. Charlton, H.G. Paretzke. "Energy deposition in cylindrical targets by monoenergetic electrons, 10 eV to 100 keV". MRC Monograph 94/1, MRC Radiobiology Unit, Chilton, Didcot (1994).

[23] D.T. Goodhead. "Soft X-ray radiobiology and synchrotron radiation". In: Synchrotron Radiation and the Biosciences, Eds. B. Chance *et al.* (Oxford University Press, Oxford) pp. 683-705 (1994).

[24] D.T. Goodhead. "Consequences of radiation track structure for low level radiation effects". In: Int. Conf. on Radiation Effects and Protection, Mito, Japan (Japan Atomic Energy Research Institute, Tokyo) pp. 21-30 (1992).

[25] H.G. Paretzke, D.T. Goodhead, I.G. Kaplan, M. Terrissol. "Track structure quantities". In: Atomic and Molecular Data for Radiotherapy and Radiobiology. IAEA TECDOC-799 pp. 633-721 (1995).

[26] H.G. Paretzke, M. Inokuti, D.T. Goodhead, M. Terrissol, L.H. Toburen, J. Botero, N. Kocherov, R.K. Janev. "Atomic and Molecular data needs for Monte Carlo track structure calculations of radiation induced damage in biological substances". IAEA Report INDC(NDS)-295 (1994).

[27] D.T. Goodhead, H.P. Leenhouts, H.G. Paretzke, M. Terrissol, H. Nikjoo and R. Blaauboer. "Track structure approaches to the interpretation of radiation effects on DNA". Radiat. Prot. Dosim. **52**, 217-223 (1994).

[28] H. Nikjoo, D.E. Charlton and D.T. Goodhead. "Monte Carlo track structure studies of energy deposition and calculation of initial DSB and RBE". Advances in Space Research **14**, 161-180 (1994).

[29] D.T. Goodhead. "Molecular and cell models of biological effects of heavy ion radiations". Radiat. Environ. Biophys. **34**, 67-72 (1995).

Head of project 3: Dr. Terrissol

II. Objectives for the reporting period

Our objective was to build a model able to simulate the more precisely possible the physical and chemical steps of the DNA irradiation in the cell environment. For the primary interactions of radiation we intended to include higher order structures of DNA instead of water cylinder.To study the role of water radicals, oxygen, scavengers and chemical repair, we intended to take into account all chemical reactions between water radio-chemical species, radicals and added scavengers with sub molecular units of DNA.

Another goal was to port our code on the MRC computer, to allow a more easy use for the development of our common research.

III. Progress achieved including publications

We have port the code CPA100 to MRC-Phys (partner 2) who simulates the transport of electron up to 100 keV in liquid water, as a function of space (3 co-ordinates) and time. The code was employed for comparisons with other codes (see publication n° 4), simulate the chemical (see publications n° 1 and 10), to begin introduction of water shells on DNA structures (see publication n° 11), and to do statistical investigations.

During this contract period we begun to develop our straight DNA segment model towards nucleosomal DNA. It is an important step, since the replication of nucleosom units lead to chromatin fibre. The physico-chemical and chemical codes were improved to take into account such large amount of atoms, species and molecules able to diffuse and react together.

The nucleosome core unit has been modelled as a 146 basepairs helical DNA, containing 9056 atoms, wound around the histones. These latter being considered here absorbing energy but inactive chemically. All the nucleosom atoms are known by their co-ordinates and their van der Waals radius. The yields of strand breaks for electrons is obtained by placing the nucleosome target in liquid water.

To build and test our model, ^{125}I was chosen as the source of radiation because it is possible to localise its position in the DNA structure. Iodine atoms were considered individually, but uniformly distributed among all the thymine bases of the nucleosome by replacing their methyl group (71 positions in the model).

Complete transport of electrons is done with a 4-dimensional (x,y,z,t) code, previuously described and simulatiing all individual interactions. Due to lack of data, the cross-sections for DNA were assumed to be similar to those for liquid water: at places of double helix atoms, liquid water with density 1.3 was assumed. Slowing-down of electrons is then simulated in the nucleosom and in the working sphere filled with liquid water at normal density. (see Fig. 1)
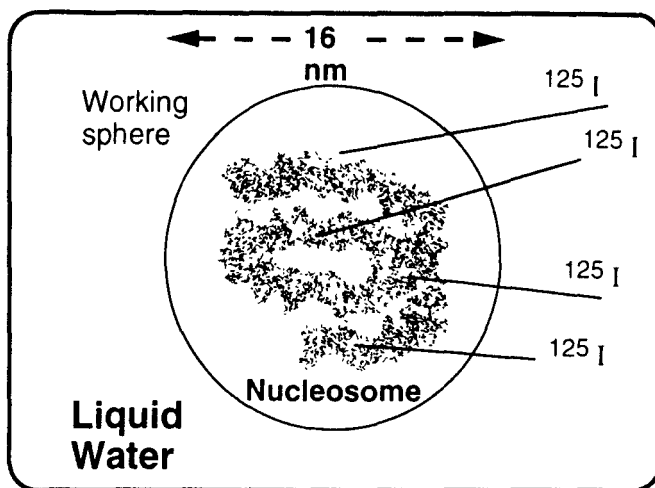
Figure1: Schematic representation of the simulation model.

During the physical step (up to 10^{-15} s.) all events located inside the van der Waals radius of a DNA atom are scored as direct interactions on DNA while other water interactions create species and radicals.

Then, molecules of scavengers (Tris, DMSO, ...) are added randomly (accordingly to the desired concentration) inside the working sphere. For a 1M concentration, e.g., about 690 molecules of scavenger are considered. As time increases, from 10^{-15} s. to 10^{-6} s., all water species e^-_{aq}, OH·, H·, H_3O^+, H_2O_2, OH$^-$, H_2 , HO_2 diffuse and react between themselves as well as with scavenger and DNA sub-units. For the latter reactions we adapted experimental data (Table-1) taken from the literature.

Table I : Reactions radii in nanometers of main water species with themselves and DNA sub-units calculated from reaction rate constants.

	OH·	e-aq	H·	OH-
OH·	0.141	0.452	0.269	
H·	0.269	0.287	0.094	0.0002
e-aq	0.452	0.08	0.287	
H_3O^+		0.166		0.944
H_2O_2	0.0006	0.256	0.0014	
Deoxyribose-monophosphate	0.085	0.0003	0.0006	
Adenine	0.288	0.265	0.0019	
Cytosine	0.288	0.382	0.017	
Guanine	0.425	0.413	0.000	
Thymine	0.302	0.53	0.011	
DMSO	0.202		0.0002	
Tris	0.071			
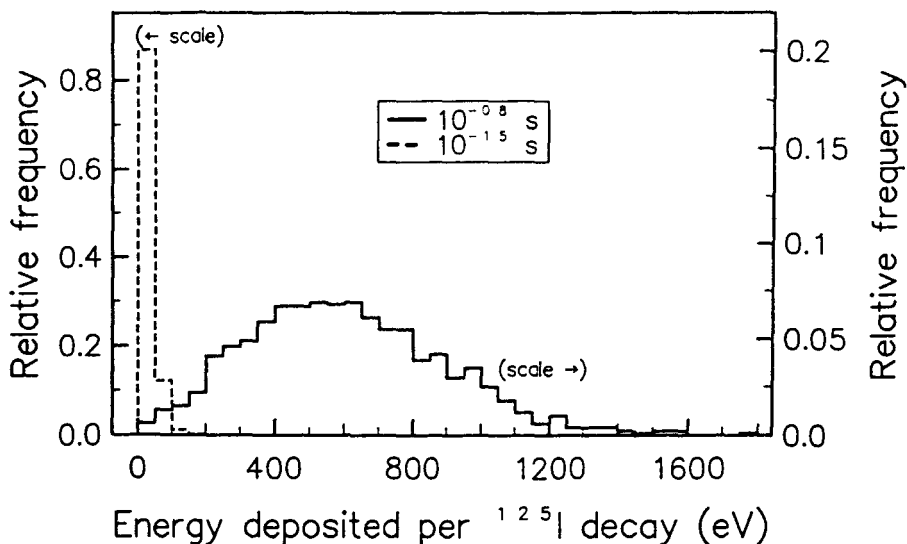
Figure 2. Frequency distribution of the size of energy deposition events during the physical phase (10^{-15} s) and after.

Fig. 2 shows that during the physical phase (at about 10^{-15} s after the decay) only very small amounts of energy (an average of 40 eV per decay) were deposited on DNA target atoms whereas a large fraction of absorbed energy (about 680 eV per decay in the working sphere) was transferred to secondary electrons interacting and depositing this energy at later times e.g. via radicals. The number of ionisations and excitations per ^{125}I decay created during the physical phase is given in Table II for the nucleosome and the working sphere.

Table II : Mean number of ionisations and excitations per ^{125}I decay in the nucleosome and the working sphere.

	Nucleosome	Working sphere
Ionisations	3.3	38.9
Excitations	1.2	20.7

The yield of water species, free radicals and solvated electrons created during the physico-chemical stage in the working sphere per ^{125}I decay at 10^{-12} s and 10^{-8} s are shown in Table III. These figures clearly indicate that OH radicals play an important role during the chemical phase since more than 90% of them have reacted with other species or DNA

nucleotides The effect of DMSO can be seen not only directly on OH yield, but indirectly on all other species yield.

At 10^{-12} s the G-values are about 5 for e^-_{aq}, OH· and H_3O^+ and around 1 for H· From Table I, we see that nearly all reactions involving e^-_{aq} give temporary OH- ion reacting strongly with H_3O^+. Then all these reactions have to be considered in a model.

Table III : Main water species present in the working sphere per ^{125}I decay at different times.

	e^-_{aq}	OH·	H·	H_3O^+	H_2O_2	OH$^-$	H_2
at 10^{-12} s	23	31.1	14.4	27.3	6.4	0	2.48
at 10^{-8} s	12	2.3	5.2	21	8.9	0.7	4.9
with 0.5M DMSO	6.5	0.0	6.4	13.2	6.7	0.3	4.2

To evaluate the DNA damage by simulation in order to compare with experiment our model is able to do any assumptions. At present, the exact mechanisms leading to damage are not completely elucidated and for first evaluation we used the following assumptions: during the physical step (10^{-15} s), when an ionisation was located inside the van der Waals radius of a phosphate-group or sugar atom, it was stored (time, co-ordinates and energy deposited on this atom) as a direct single-strand break (SSB), and subsequently the event was removed from the initial track. From 10^{-15} s to 10^{-8} s when a deoxyribose-monophosphate reacts, it was transformed in a sub-product and could not react twice per decay, the event was scored as an indirect SSB (time, co-ordinates and total energy deposited in the working sphere by the Auger electrons belonging to the decay).

In Table IV, the number of damaged DNA nucleotides in the nucleosome unit per ^{125}I decay for the direct effect as well as for the indirect effect resulting from later chemical reactions in the working sphere are given. The numbers show that about 40% of the sugar-phosphate groups are damaged directly during the physical phase, but only 14% react during the chemical phase up to 10^{-8} s, mainly with OH radical, which is the reason for the SSB creation. The DMSO reduces the number of DNA damage with a similar ratio on all nucleotides.

Table IV : Number of damaged DNA nucleotides in the nucleosome unit per ^{125}I decay.

	Phos.	Sugar	Aden.	Cytos.	Gua.	Thym.
Excit. up to 10^{-12} s	0.17	0.33	0.14	0.09	0.12	0.26
Ionis. up to 10^{-12} s	0.43	0.86	0.31	0.28	0.31	0.74
Chemical reactions up to 10^{-8} s	2.65		2.59	3.31	5.02	5.40
Number of nucleotides present	292	292	73	73	73	73
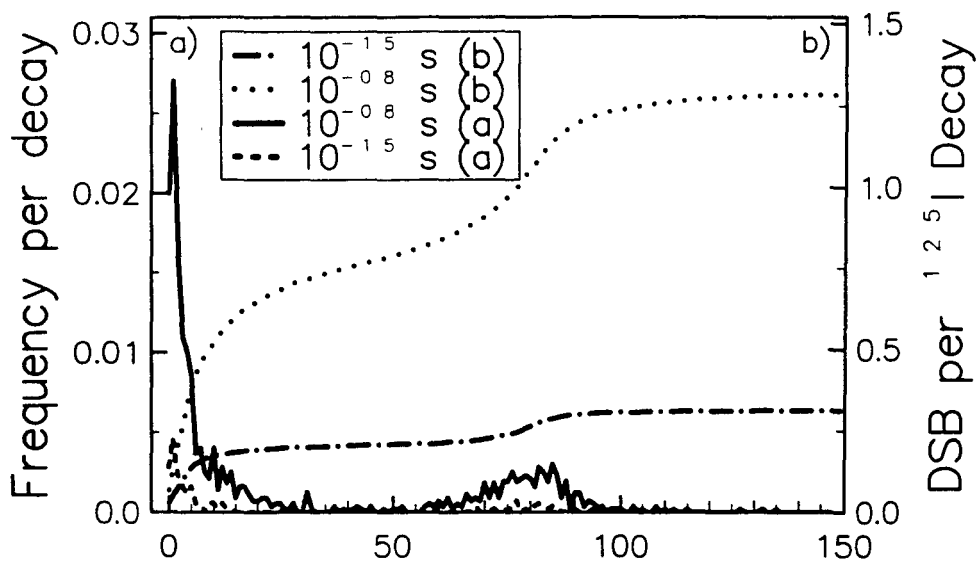
Figure 3. Spatial distribution of ssb and dsb yield as a function of the distance between contributing ssbs. a) Distance in basepairs betweeen two dsb. b) Distance in basepairs between two ssb forming a dsb.

A characteristic of the ^{125}I radiation as well as the nucleosome model can be seen in Fig. 3. In most case when one decay induced two DSB the distance between the two DSB was found to be less than 20 basepairs. This reflects the short range action of ^{125}I. The second maximum at about 80 basepairs is expected from the fact that the DNA helix has completed one turn around the histons after 80 basepairs. Quantitatively, the same results are found by considering the calculated DSB yield as a function of the distance between the two contributing SSB.

Fig. 4 gives the relative number of decays inducing different types of breaks per decay. Low energy values correspond to high fractions of no break or simple SSBs whereas with increasing amounts of energy deposited in the target the former decreases very steeply and a more complex break pattern is observed. A continuous increase can be seen with two or more DSB. These results are similar to those of figure 4 of Charlton and Humm (1988). However in this study strand breaks were scored as the sum of the direct and indirect effects and the total energy was the energy deposited in the working sphere. Charlton and Humm (1988) used the direct action of radiation only for strand break calculations.
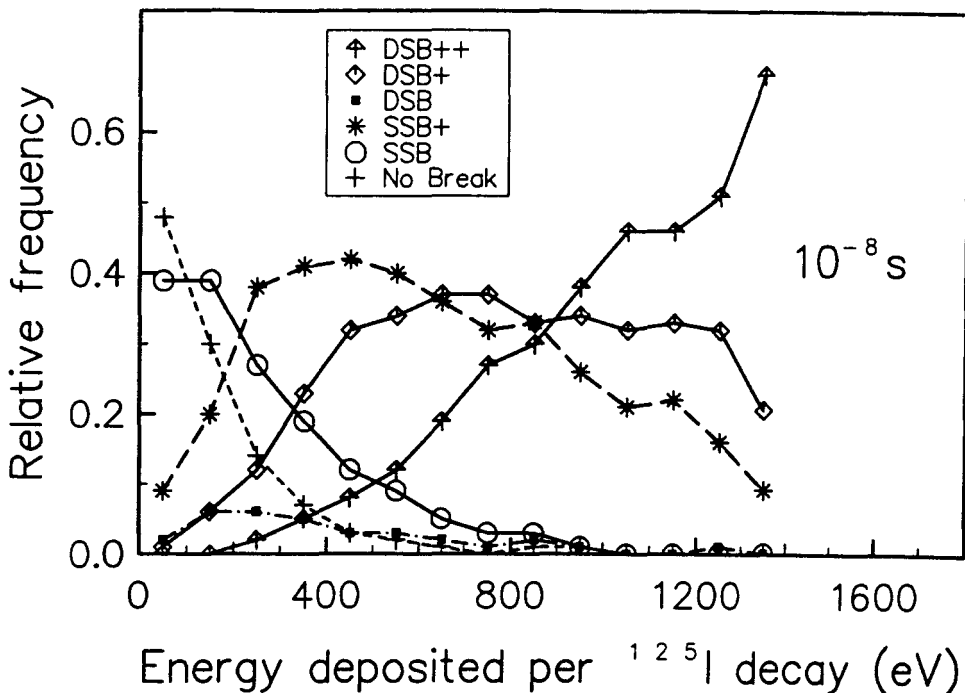
Figure 4. Break pattern induced by a total number of 5680 decays. 'SSB': one single ssb; 'SSB+': two or more ssb on one strand; 'DSB': one dsb; 'DSB+': one dsb plus additional ssb; 'DSB++': two or more dsb.

Table V : Comparison of calculated mean numbers of SSB and DSB per ^{125}I decay with experimental data.

Break	Direct	Indirect	Total	Experiment
SSB	1.55	2.65	4.2	3 - 6
DSB	0.2	0.6	0.8	0.9 - 1.2
with 0.5M DMSO	Indirect SSB: 1.3		Indirect DSB: 0.3	

Comparisons of the mean values of the number of SSB per decay with experimental data are shown in Table V. The relative number of indirect DSBs seems to be larger than that for directly produced (0.6 over 0.2) compared to the relative number for SSBs (2.65 over 1.55). This is due to the fact that an indirect SSB associated with a direct one was scored as an indirect DSB. The mean value of about 1 DSB per decay reported from many experiments results from the fact that in about 20% of all decays more than 1 DSB was produced. Differentiating between directly and indirectly induced DSBs leads to quite interesting results which could perhaps give hints for the assumed correlation between the number of DSBs and

cell death. We can observe here a result already mentionned in the literature: 0.5M of DMSO reduce by 50% the indirect effect.

An atomic scale nucleosome target model has been constructed and used with electron track structure in order to study DNA damage. To model such a long chain of events from the very early physical to the beginning of biological step a number of assumptions had to be incorporated. Simulation of events until 10^{-6} second after irradiation requires a full set of physical and chemical input data: (a) Geometrical data : three-dimensional co-ordinates of all atoms and molecules involved in the structure of a nucleosome. (b) Physical data : atomic structure, energy levels, bond strengths, van der Waals radii, reorganisation schemes, fluorescence and Auger yields, elastic and inelastic total and double differential cross-sections for all channels, etc. (c) Physico-chemical data : desexcitation, recombination, internal conversion, molecular dissociation, thermalization, solvation, attachment, etc. (d) Chemical data : complete description of reactions, diffusion coefficients and reaction rates as a function of temperature and concentration. These parameters need to be known in the cellular environment, e.g. the solvation of e^-_{aq} in the hydration shell of DNA which is different from bulk water.

To reflect more realistic cellular condition it is intended to use more realistic DNA electronic interaction cross-sections, to extend the nucleosome model to simulation of the chromatin fibre and to simulate electron transport in this complex chemical environment.

Publications

1- H. NIKJOO, M. TERRISSOL : " Monte Carlo track structure studies of the chemical modification of initial damage in DNA". Conference on Pathways to Radiation Damage in DNA, Oakland University, Rochester, Michigan , June 1992.

2- E. POMPLUN, M. TERRISSOL : "A nucleosome model for the simulation of DNA strand break experiments" 25th Meeting of the European Society for Radiation Biology, Stockholm University, Sweden, June 1993.

3- D.T. GOODHEAD, H.P. LEENHOUTS, H.G. PARETZKE, M. TERRISSOL : "Track structure approaches to the interpretation of radiation effects in DNA". Radiation Protection Dosimetry, 52, N° 1-4, pp 217-223, (1994)

4- H. NIKJOO, M. TERRISSOL , R.N. HAMM, J.E. TURNER, S. UEHARA, H.G. PARETZKE, D.T. GOODHEAD : " Comparison of energy deposition in small cylindrical

volumes by electrons generated by Monte Carlo track structure codes for gaseous and liquid water" Radiation Protection Dosimetry, 52, N° 1-4, pp 165-169 (1994).

5- M. TERRISSOL, E. POMPLUN : "Computer simulation of DNA incorporated 125 Iodine Auger cascades and of the associated radiation chemistry in aqueous solution", Radiation Protection Dosimetry, 52, N° 1-4, pp 177-181, (1994).

6- E. POMPLUN, M. TERRISSOL : "Low-energy electrons inside active DNA models. a tool to elucidate the radiation action mechanisms", Radiation Environmental Biophysics, 33, pp 279-292, (1994)

7- M. INOKUTI, H.G. PARETZKE, D.T. GOODHEAD, M. TERRISSOL, L. TOBUREN, J. BOTERO, N. KOCHEROV and R.K. JANEV : "Atomic and Molecular data needs for Monte Carlo track structure calculations of radiation induced damage in biological substances" IAEA Report INDC(NDS)-295, Vienna, (1994)

8- M. TERRISSOL : "Modelling of radiation damage by I-125 on a nucleosome" Int. J. Radiat. Biol., vol 66, n° 5, pp 447-451, (1994)

6- M. TERRISSOL, E. POMPLUN : "A nucleosome model for the simulation of DNA strand break experiments" in "Computational Approachses in Molecular Radiation Biology: Monte-Carlo Methods", M.N. Varma and A. Chatterjee, Eds, pp 243-250, Plenum, New-York, (1994)

10- H. NIKJOO, P. O'NEILL, M. TERRISSOL and D.T. GOODHEAD : "Modelling of radiation induced DNA damage: the early physical and chemical events" Int. J. Radiat. Biol. vol 66, n° 5, pp 453-457 (1994)

11-H. NIKJOO, M. TERRISSOL and J.M. GOODFELLOW : « A Model of DNA Hydration Sheel Based on Cristallographic Data. » 43rd Meeting of the Radiation Research Society, San Jose, California, April 1995

12- H. PARETZKE, D.T. GOODHEAD, I.G. KAPLAN and M. TERRISSOL : "Track structure quantities" in "Atomic and Molecular Data for Radiotherapy and Radiobiology" IAEA TecDoc-799, Vienna, pp 633-721 (1995)

Head of project 4: Dr H.P. Leenhouts

II. Objectives for the reporting period
The aim of the RIVM contribution to the project is to continue the development of a comprehensive model for the analysis and interpretation of radiation effects at cellular, organ and animal level on the basis of specific radiation damage in DNA. The model is intended to provide a framework for analysis of the the effectiveness of different radiation types for cellular effects and the influence of radiation on the development of tumours and cancer.
The ultimate goal is to provide insight into the dose-time-effect relationships for late radiation effects, in general, and the extrapolation of radiation effects at high doses to the estimated radiation risks at low doses and dose rates.
The activities are:
1. the development and application of a track structure model (TRAX) for radiation energy deposition to calculate the effectiveness of different radiation types for different radiation effects.
2. cellular experiments to investigate and compare the quadratic term of the dose-effect relationship for gamma rays and ultraviolet radiation (UV) with special attention for the influence of repair.
3. development and application of a two-mutation carcinogenesis model (TMC) to relate cellular effects with tumour formation and to investigate the role of radiation in the development of tumours.

III. Progress achieved including publications

Introduction
One of the most important aspects of radiation protection is the estimation of risks of low doses and dose rates. This estimation has to be derived from epidemiological data at relatively high doses and high dose rates. For the extrapolation to low doses use has to be made of a dose-effect relationship. These relationships should include the different effectiveness of different radiation types and the influence of repair, when comparing effects at high dose rates with chronic irradiation regimes.

In a previous contract a radiobiological model (RBM) was developed to explain and interpret cellular radiation effects on the basis of the induction of crucial DNA damage by the radiation. In the model the crucial damage for ionizing radiation was assumed to be DNA double-strand breaks with, in general, a linear-quadratic dose-effect relationship $(\alpha D + \beta D^2)$. The linear term is especially dependent on the type of radiation used, while the quadratic term is primarily dependent on dose rate and repair.

In the reported period the relation between the linear term and radiation type was investigated using the track structure model TRAX (section 1). The applicability of the RBM model and especially the behaviour of the quadratic dose term (βD^2) with repair was experimentally investigated using stationary CHO-cells (section 2). In these experiments radiation effects of gamma radiation were compared with effects of ultraviolet radiation (UV). Further, a relation between cellular effects and tumour development was investigated using a two-mutation model for radiation tumour induction (section 3). The organisation of a scientific seminar is described in section 4.

1. Radiation track structure model TRAX

As the energy absorption after exposure to ionizing radiation is not homogeneous, the radiation effectiveness varies with the type of radiation and depends on the distribution of energy deposition and the type of sensitive target. For quantitative description of this radiation effectiveness use of a single parameter, such as stopping power or LET, seems to be too simple. For this problem Monte Carlo methods are used for a complete slowing down of energy events and all physico-chemical products involved in the radiation effect are followed for their contribution in the radiation effect (see ref. 5 and the activities of partners 1 and 3). These procedures are very time consuming and difficult to perform for all radiation types. In this project RIVM used an intermediate method to calculate the effectiveness of different radiation types. The model TRAX (ref. 17) uses the following concepts:
1. the model provides a track segment analysis of the primary particle(s) involved in the radiation effect as it slows down and also of the secondary particles generated;
2. for each track segment a calculation is made of the average stopping power, track radius and energy loss per event, and its dose contribution in the radiation effect;
3. for an given type of effect, the effectiveness per unit dose is calculated, using the specific geometry of the target, the characteristics of the track segment, and a "diffusion" parameter to simulate the physico-chemical processes involved in the radiation effect;
4. the effectiveness of the radiation ultimately is calculated as the dose average of the effectiveness of all track segments.

The mathematical concepts of TRAX were justified by comparing some of the intermediate radiation-physical results, such as stopping power and slowing down spectrum, with literature data. Using TRAX the effectiveness of single-hit detectors for electrons, protons and ions of various energies relative to gamma rays could be calculated (ref. 14). An example is shown in fig. 1.
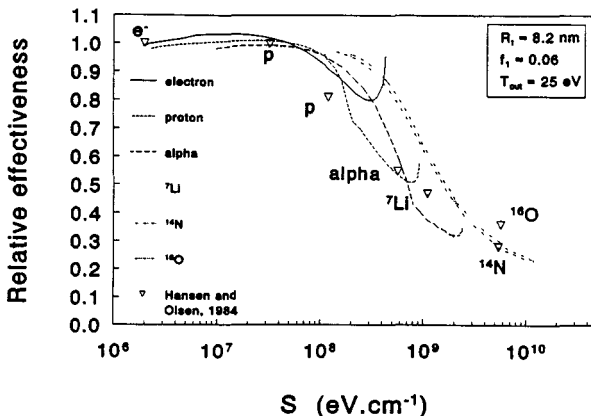
Fig. 1. Relative effectiveness of several radiation types for FWT 60 dye film calculated using TRAX. In the corner some model parameters used in the fit are given.

The results show that stopping power is not sufficient to define the radiation effectiveness, but that different particles of the same stopping power showed different effectiveness. TRAX

turned out to be rather flexible to simulate this behaviour. The model was used to calculate cellular effects, assuming that cell killing and mutations are caused by DNA double-strand breaks. In fig. 2 the relative effectiveness of radiation induced cell killing for a spectrum of stopping powers and particles is shown (ref. 14).
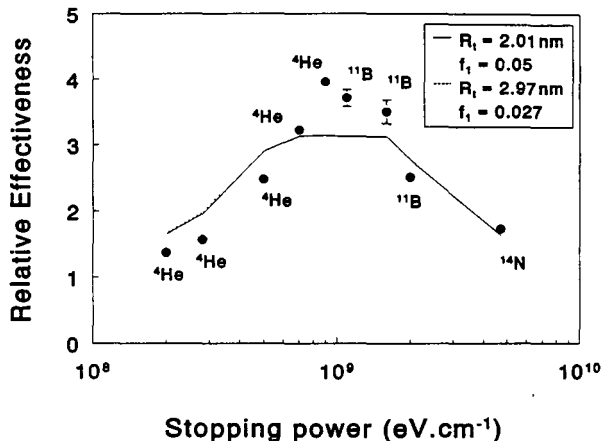
Fig. 2. Relative effectiveness of inactivation of human fibroblasts for heavy ions, experimentally and calculated using TRAX. Some model parameters are given in the corner.

The results clearly show the importance both of the radiation type and of the target geometry in the radiation effect. Further the results show that the well known humped behaviour of the RBE-LET relationship for cell killing and mutations, which is primarily caused by a changing linear term of the dose-effect relationship, can be explained assuming that DNA double strand breaks are the crucial primary lesions for these cellular effects.

2. CHO cell experiments

An experimental approach was used to investigate the influence of time on the dose-effect relationships for cell killing and mutations with emphasis on the quadratic term (βD^2) of the general linear-quadratic dose-effect relationship. An important question to be answered is, whether the quadratic term can be described by a two-hit phenomenon and how repair changes this term. To avoid influence of the variation of radiation sensitivity in different phases of the cell cycle a stationary cell system was necessary.

An experimental method of Nelson et al. (Cell Tissue Kinet. 17 (1984) 411-425) was used to bring the CHO cells in a stationary phase, which lasted for several days. In this phase the CHO cells were suitable for irradiation procedures up to several days without changes in the cell sensitivity. The cells were irradiated with ^{60}Co gamma rays, or with ultraviolet radiation (UV), with a wavelength of about 300 nm, or with combinations of these radiations. Standard experimental procedures were designed to investigate cell killing and the induction of HPRT mutations after immediate and delayed plating (ref. 16).

Important conclusions of the experiments were:
- The experimental results of gamma radiation could well be explained using RBM. In the model it is assumed that DNA double strand breaks are responsible for cell killing and mutations, and have, in general, a linear-quadratic dose-effect relationship ($\alpha D + \beta D^2$).
- The dominating effect of time was a change of the β-term. In the present project the effect of time was studied experimentally for cell killing using two or more irradiation fractions given after each other. If the time between the fractions was small (i.e. within several minutes), the irradiation effect of the two fractions was more than the sum of the effect of each fraction given separately (i.e. synergism). The synergism decreased, when the time between the fractions was increased. The results could be explained assuming interaction of the β-terms of the fractions. The change of effect with time (halve value time about 2 h) was in agreement with the change of the radiation effect with dose-rate as found by Metting et al. (Radiat. Res. 103 (1985) 204-212) in the same cell system (ref. 2 and 24).
- UV-effects could be described assuming, in principle, purely quadratic exposure-effect relationships. For cell killing in stationary cells two cell populations with distinct sensitivity difference were detected. For mutation induction these sensitivity differences were not showing up (see figure 3). These results could be explained using an extension of the RBM model for UV-effects. The primary lesions of UV are assumed to be pyrimidine dimers, i.e. single strand DNA lesions. Cell killing and mutations of UV are assumed to be caused by pairs of pyrimidine dimers, which have a purely quadratic exposure-effect relationship.
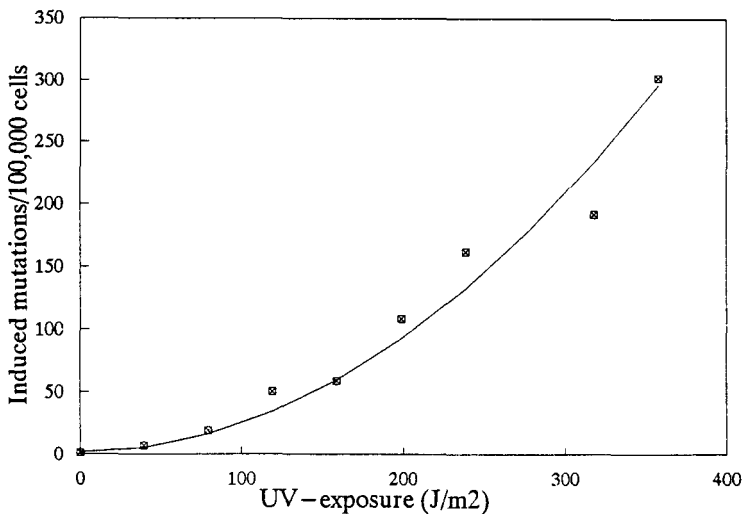
Fig. 3. Mutation rate, corrected for survival, of stationary CHO cells after exposure to UV.

- Repair involved in delayed plating experiments resulted in a lower radiation effect similarly for mutations and cell killing, both for gamma rays and for UV radiation. For gamma radiation the change of delayed plating repair was only 30% and had a halve value time of about 3 h, but for UV the change was more than 90% with a halve value time of

about 30 h. This difference can be ascribed to the different primary lesions involved.
- The effect of combined exposure to gamma rays and UV was investigated especially for mutations. When the time between the fractions is small (within several minutes) the effect of the combined exposure was more than the sum of the effects of the UV and gamma rays separately (synergism). The synergistic contribution was proportional with the product of UV exposure and gamma dose (see fig. 4).
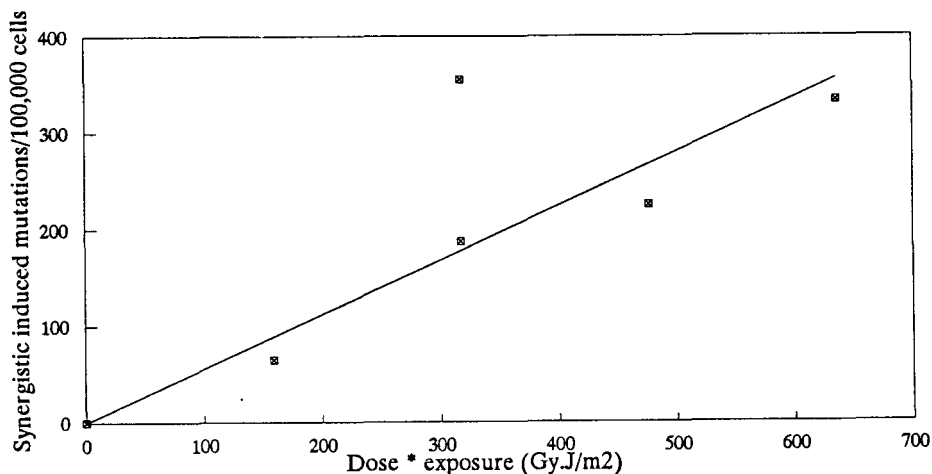
Fig. 4. The synergistic contribution of the mutation rate after combined exposure to gamma rays and UV.

The observed effects could be explained assuming interaction of gamma ray induced single strand damage (i.e. single-strand "breaks") and UV induced single strand lesions (i.e. pyrimidine dimers). An attempt was made to characterize the interaction damage as UV type or gamma type of damage, on the basis of its behaviour with delayed plating. The results were not conclusive, but in favour of a UV type of damage.
- When the time between the gamma and UV fraction was long enough (i.e. more than 24 h) a significant synergism could not be detected any more. This implied that interaction at cellular level is not expected to be important when long irradiation exposures are involved.

In relation with the experimental results attention was paid to the problem of the linear-quadratic form of the dose relationship of the induction of DNA double-strand breaks at doses relevant for cellular radiobiology, as proposed by RBM. It was found from analysis of literature, that, the interaction of single strand "breaks" necessary for the quadratic term could well take place over distances larger than a few DNA base pairs on the basis of biological processes such as the processing of DNA repair and replication. This may lead to a quadratic term which is larger than estimated on the basis of purely physical considerations (ref. 6, 11). Also the involvement of other types of single strand damage than single strand

breaks in the β-term cannot be excluded. These processes should be taken into account when modelling cellular dose-effect relationships from first principles.

The results of the TRAX model and CHO cell experiments support the assumption that the dose-effect relationship for radiobiological effects could readily be explained assuming a double-hit radiation mechanism. The molecular model for ionising radiation and its extension for UV is very suitable for describing dose-effect relationships of cell killing and mutations.
For application of cellular dose-effect relationships in e.g. carcinogenesis models (see section 3) the most important conclusions are:
- the dose-effect relationship for ionising radiation, in general, is linear-quadratic ($\alpha D + \beta D^2$), both for cell killing and mutations;
- for lower dose rates the β-term becomes lower, and β is negligible for dose rates lower than 0.1 Gy per hour;
- for low dose rates the linear term (αD) is dominating;
- different radiation types are characterised by different α-coefficients;
- for more densely ionising radiation the α-term is larger than for sparsely ionising radiation;
- a close correlation can be expected between cell killing and mutation induction;
- for UV radiation a purely quadratic exposure-effect relationship is expected, both for cell killing and mutations;
- the effect of combined exposure to ionizing radiation and UV can be more than the sum of the effects of each radiation separately, when a significant quadratic term for both types of fractions is observed and the time between the fractions is small;
- synergistic interaction between UV and gamma radiation is negligible, when the time between the fractions is large (more than 1 day) or when low dose rates are involved.

3. Two-mutation carcinogenesis model (TMC)

For radiation protection purposes the extrapolation of epidemiolological data of relatively high doses to estimation of risks at low doses, in general, is made using a linear dose relationship. However, many animal experimental results on radiation tumours indicate non-linear dose-effect relationships. Further, a linear dose relationship does not take account of the multi-stage nature of carcinogenesis.
In this project a two-mutation model (TMC) is used as a relatively simple model to accommodate for the multi-stage character of tumour development, with a limited number of parameters to be fitted. A schematic diagram of the model is given in figure 5 (ref. 2, 7, 12).
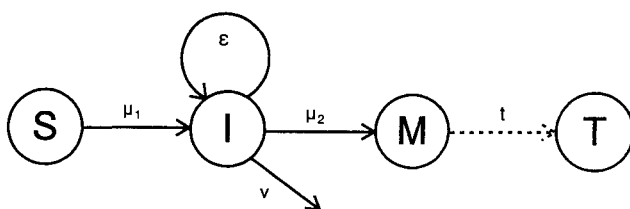
Fig. 5. Schematic diagram of the two-mutation carcinogenesis model TMC.

Shortly, the carcinogenic process can be described as follows: a normal cell has to be transformed by two distinct mutations (probabilities μ_1 and μ_2) to become malignant; in the intermediate stage (I) cells undergo clonal expansion (ϵ) resulting in an increased number of cells or may die (probability v) in the course of time; once a cell is malignant, after a distinct time period the cell grows into a detectable tumour. Radiation interacts with this process by changing (increasing) the mutation probabilities and, possibly, by changing the expansion rate. In the model the age and dose dependence of tumour formation are defined. The model predicts an intimate relation between spontaneous tumours and radiation sensitivity, and gives a relation between the cellular radiation effect and radiation induced tumours. The RBM model of cellular effects (see section 2) was used to define the influence of radiation at cellular level.

In the current project period the TMC model could only be investigated preliminary. The following results are reported:
- the model could be used to describe dose-effect relations of lung tumours in two types of animals and for different radiations (X-rays, gamma rays, neutrons and radon) (ref. 2, 7). Only limited age dependent tumour incidence data were available for this analysis. In the model, the changes of cellular effects for different radiation types and different dose rates were reflected in the tumour formation, in agreement with exprimental data.
- the model was used to explain the age dependent bone tumour formation after injection of beagles with various levels of internal α-emitters (e.g. ^{226}Ra) with lifetime irradiation of the animal (ref. 9, 12). In this case both the age and dose dependence could be well fitted (see fig. 6).
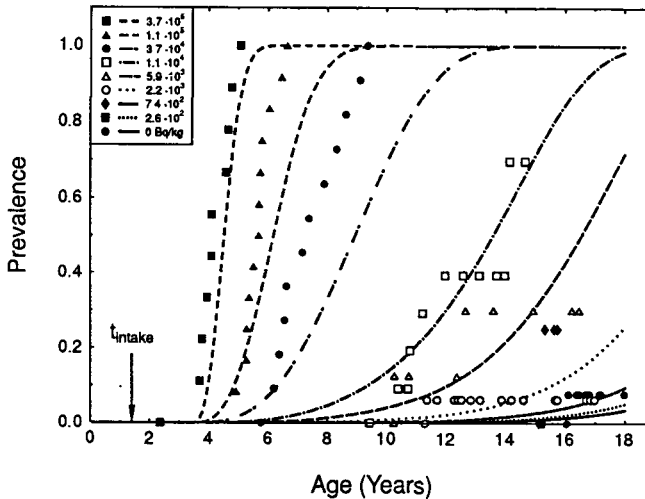
Fig. 6. Age dependence of osteosarcoma's in beagles for 8 injections of ^{226}Ra and control, fitted by the TMC model.

The conclusion of these results was that the spontaneous incidence of bone tumours is

very important for the radiation sensitivity, and a non-linear, almost purely quadratic dose-effect relationship for bone tumours was found using the model, although the dominant radiation is α-radiation and the radiation induced mutations were assumed to be linearly related with dose.
- the TMC model was used to test the possibility to describe skin tumours in mice exposed to 6 levels of continuous exposure to UV radiation (ref. 15) (see figure 7).
  In this case of UV exposure using a quadratic dose-effect relationship for cell mutations in the model resulted in a significantly better fit than using a linear one. Note that a purely quadratic dose-effect relationship for UV induced HPRT-mutations in CHO cells was found experimentally (see section 2).
- the model also was used to describe the dose-effect relationship of bone tumour induction tumours in female radium dial painters, who ingested large amounts of radioactive radium (ref. 7, 13). A strong quadratic dose dependence of tumour induction was observed, in accordance with the epidemiological data.

The first investigations to describe radiation induced tumours using the TMC model were very promising and deserve further attention. The model was fitted to several data sets with a variety of exposure conditions. Further research on the model for understanding of radiation induced carcinogenesis and for the risk estimation of radiation risks is recommended. Up to now, no significance could be attached to the parameters found in the analyses.
In principle, the TMC model links DNA-molecular and cellular damage with tumour formation. The model shows features of a relative and absolute age projection risk model, and of a single-somatic mutation model, depending of the radiation and tumour involved. The model accounts for the multistage character of carcinogenesis and links spontaneous tumour incidence with radiation risk. The model in its present form allows an easy investigation of the involvement of radiation in different processes during carcinogenesis. The model, therefore, can be of invaluable importance for the derivation of radiation risks of lifetime exposures from acute and high dose epidemiological data.

4. Symposium on Molecular Mechanisms in Radiation Mutagenesis and Carcinogenesis

During the contract period a symposium on "Molecular Mechanisms in Radiation Mutagenesis and Carcinogenesis" was organised in Doorwerth from 19-23 April 1993, with a significant involvement of RIVM. The proceedings were issued in 1994 (ref. 3).

Publications

1. H.P. Leenhouts and K.H. Chadwick. Radiation cancer risk: implications from a two-stage model of carcinogenesis. In: Proceedings of Fukui Workshop on Health Risks: Perspectives and Research. T. Sugahara, K. Torizuka et al., eds. Health Research Foundation, Kyoto (1993) pp.83-87.
2. H.P. Leenhouts and K.H. Chadwick. A two-mutation model of carcinogenesis: analysis of radiation induced lung tumours in animals an implications for risk evaluation. RIVM report no. 749251001, Bilthoven (1993).
3. Molecular Mechanisms in Radiation Mutagenesis and Carcinogenesis. K.H. Chadwick, R. Cox, H.P. Leenhouts and J. Thacker, eds. EUR 15294, Luxembourg (1994).
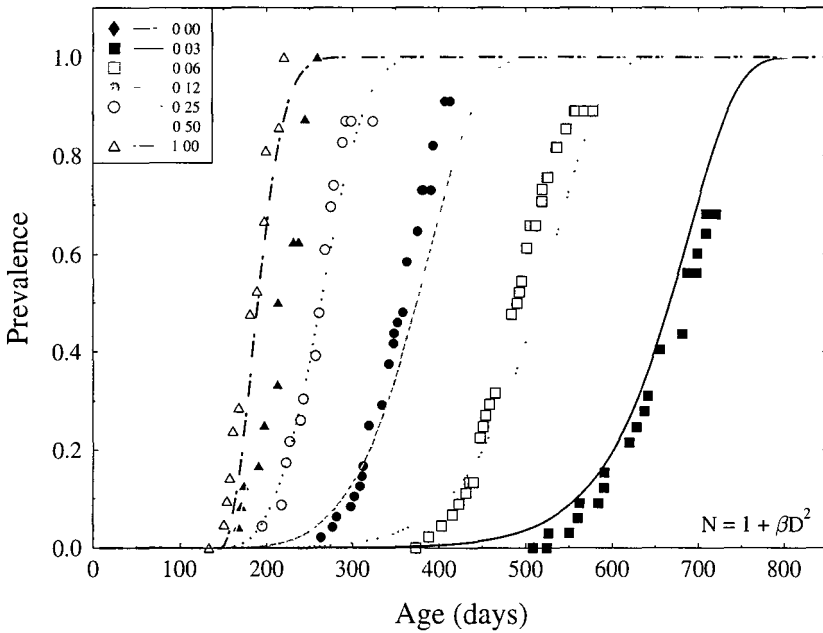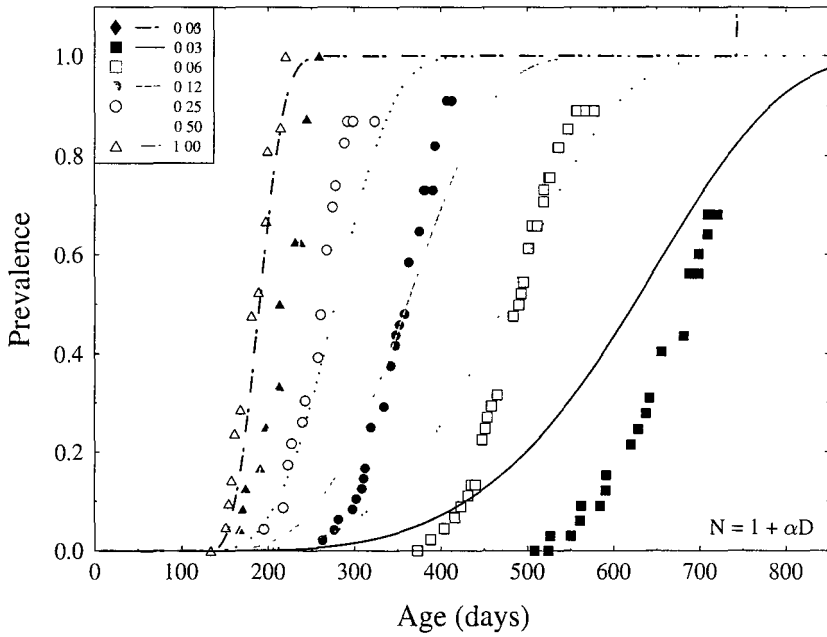
Fig. 7. Skin tumours in mice after lifetime exposure to 6 levels of UV, experimentally and fitted by the TMC model, using a linear (upper panel) or a quadratic (lower panel) dose-mutation relationship.

4. H.P. Leenhouts and K.H. Chadwick. A two-mutation model for radiation induced cancer: biological basis and implications for risk analysis. In: Molecular Mechanisms in Radiation Mutagenesis and Carcinogenesis. K.H. Chadwick, R. Cox, H.P. Leenhouts and J. Thacker, eds. EUR 15294, Luxembourg (1994), pp. 299-304.

5. D.T. Goodhead, H.P. Leenhouts, H.G. Paretzke, M. Terrisol, H. Nikjoo and R. Blaauboer. Track structure approaches to the interpretation of radiation effects on DNA. Radiat. Prot. Dosim. 54, 217-223 (1994).

6. K.H. Chadwick and H.P. Leenhouts. DNA double strand breaks from two single strand breaks and cell cycle radiation sensitivity. Radiat. Prot. Dosim. 52, 363-366 (1994).

7. H.P. Leenhouts and K.H. Chadwick. A two-mutation model of radiation carcinogenesis: application to lung tumours in rodents and implications for risk evaluation. J. Radiol. Prot. 14, 115-130 (1994).

8. H.P Leenhouts and K.H. Chadwick. Analysis of radiation induced carcinogenesis using a two-stage carcinogenesis model; implications for dose-effect relationships. Radiat. Prot. Dosim. 52, 465-469 (1994).

9. H.P. Leenhouts, L.B. Venema, G.M.H. Laheij and K.H. Chadwick. Use of a two-mutation carcinogenesis model for the analysis of bone tumours induced by internal emitters: implications for low dose risks. In: Health Effects of Internally Deposited Radionuclides: emphasis on radium and thorium. G. van Kaick, A. Karaoglou and A.M. Kellerer, eds. World Scientific, Singapore (1995) pp. 197-201.

10. K.H. Chadwick, H.P. Leenhouts, G.M.H. Laheij and L.B. Venema. The implications of a two-mutation carcinogenesis model for internal emitters. In: Health Effects of Internally Deposited Radionuclides: emphasis on radium and thorium. G. van Kaick, A. Karaoglou and A.M. Kellerer, eds. World Scientific, Singapore (1995) pp. 353-360.

11. K.H. Chadwick and H.P. Leenhouts. On the linearity of the dose-effect relationship of DNA double strand breaks. Int. J. Radiat. Biol. 66, 549-552 (1994).

12. L.B. Venema and H.P. Leenhouts. A two-mutation model of carcinogenesis: application to ^{226}Ra induced osteosarcoma prevalence in beagles. RIVM report no. 610065001, Bilthoven (1994).

13. G.M.H. Laheij and H.P. Leenhouts. Beschrijving van een twee-staps carcinogenese model met fitprocedure (in Dutch). RIVM report no. 610065003, Bilthoven (1994).

14. R.O. Blaauboer and H.P. Leenhouts. TRAX: a track structure model for nanometer resolution in calculating the response of several single-hit and biological detectors to different radiations. RIVM report no. 610065002, Bilthoven (1994).

15. L.B. Venema and H.P. Leenhouts. Analysis of UV skin carcinomas using a two-mutation carcinogenesis model and implications for risk estimation. In: RIVM Annual Report 1995, Bilthoven. pp. 153-157.

16. H.P. Leenhouts and M.J. Sijsma. Dose-effect relationships of survival and HPRT mutations in stationary CHO cells after gamma and UV irradiation. RIVM report no. 610065004, Bilthoven (1995).

17. L.B. Venema and H.P. Leenhouts. Application of a two-mutation carcinogenesis model to UV induced skin tumours in albino hairless mice. RIVM report no. 610065005, Bilthoven (1995).

II. Objectives for the reporting period

The work undertaken in the effort to further elucidate aspects of the chemical effects of ionizing radiation on DNA has realized several objectives. One focus has been the phenomenon of radical-site transfer from purine-base OH-adduct radicals to transfer the radical site to the sugar moiety, as well as the inverse event. Purine-nucleoside-derived products have been identified that result from the complex subsequent reactions.

The influence exerted by the presence of a phosphate group with respect to the propensity of an H-atom to be abstracted at the DNA deoxyribose moiety by an OH-radical, relative to the hypothetical phosphate-free situation, is not well known, and this question was to be studied in hydroxyalkyl phosphates as model compounds. These studies in connection with those on the action of dioxygen and other oxidants, notably nitroaromatic compounds, on the resulting radicals as well as on other model-compound reaction systems, constitute a further focus.

III. Progress achieved, including publications.

It is generally accepted that in their reactions with DNA and its low-molecular-weight models the 2'-deoxynucleosides, OH-radicals add mainly to the base moiety, and only a relatively small fraction abstract an H-atom from the sugar moiety Hence it came as a surprise when in our study on the γ-radiolysis of 2'-deoxyadenosine, two products that must have sugar-moiety-derived radicals as their precursors were observed as major ones, alongside the previously reported products free adenine, adenine-derived formamidopyrimidine (A-Fapy), and 8-hydroxy-AdR. These newly-observed products are the 8,5'-cyclodeoxynucleoside 1 and the 5'-aldehyde 2.
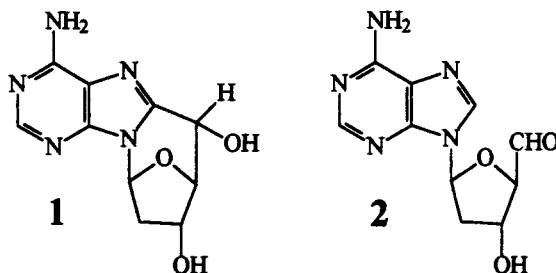
Material isolated from N_2O-saturated irradiated solutions and characterized by [1]H- and ^{13}C-nmr has been used for reference in the quantification of these products Figures 1 and 2 show their G values as a function of the pH.
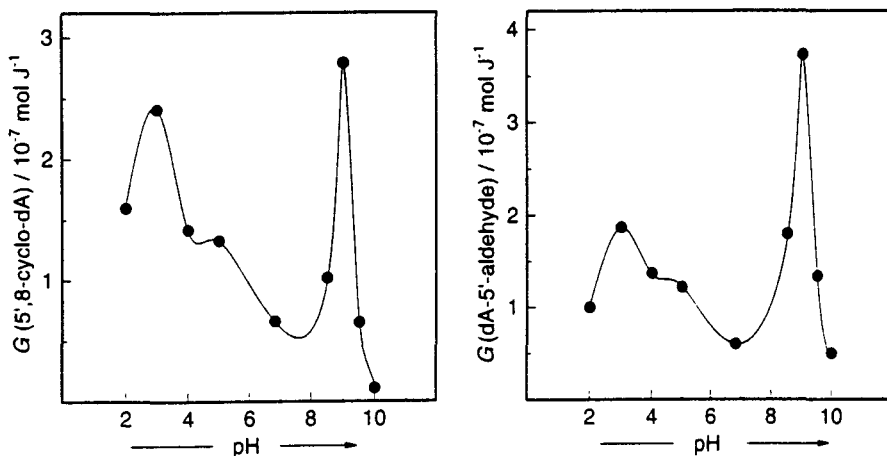
Figure 1. pH Dependence of the G value of adenine 8,5'-cyclodeoxynucleoside 1.

Figure 2. pH Dependence of the G value of adenine 2'-deoxynucleoside-5'-aldehyde 2.

It can be seen from these Figures that (i) the total yield of these products may reach G values close to or even exceeding $G(OH)$, and that (ii) a strong variation of their yields with the pH occurs in a pH range (8 to 10) where 2'-deoxyadenosine has no pK_a. Further information is contained in Figure 3 where $G(dA$-consumption) is plotted as a function of pH. At the maximum, i.e. at about pH 9.5, $G(dA$-consumption) is about twice that of $G(OH)$. This shows that there exists an important amplification effect, and it is concluded that intermediate radicals must play a role which are capable of reacting with dA. At present, mechanistic details are not yet clear. Attempts to obtain potentially valuable information using the pulse radiolysis technique failed because the relevant first-order reactions are too slow to be monitored by this fast technique (reactions kinetically of second order, i.e. radical-termination, predominate over the relatively slow first-order ones which are of interest here). However, it can be firmly stated that the first step of these reactions must be the addition of the OH-radical to the nucleobase, and that radical transfer to the sugar moiety (intra- or intermolecularly) occurs at a subsequent stage. This conclusion is of relevance to DNA radiolysis where products related to the 8,5'-dA-cyclonucleoside are well-documented.
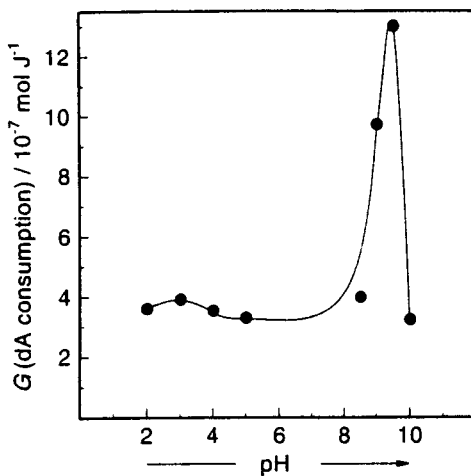
Figure 3. pH Dependence of the G value of 2'-deoxyadenosine consumption.
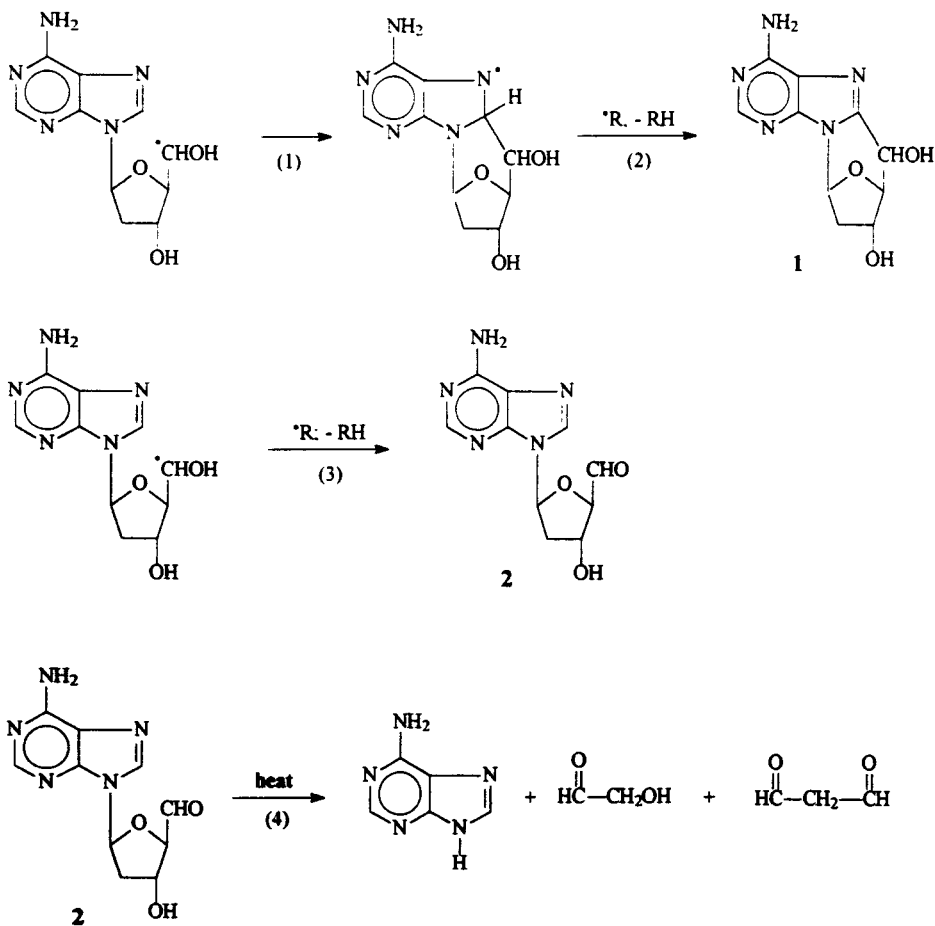
The formation of 1 is considered to be by way of the C(5')-radical which may add to the N(7)-N(8) double bond (reaction 1) In a subsequent step the N(7) radical thus formed disproportionates with other radicals, giving rise to the 8,5'-cyclodeoxynucleoside 1 (reaction 2) We have further isolated an additional product whose ^{1}H- and ^{13}C-nmr data are compatible with the 5'-aldehyde 2. It is formed in a disproportionation reaction (reaction 3) It is noteworthy that this compound gives a positive thiobarbituric-acid test for "malonaldehyde" with 30% efficiency. To rationalize this reaction, one may consider acid hydrolysis of 2 followed by a retroaldol reaction (overall reaction 4) These results pose the interesting question as to whether processes similar to those formulated here contribute to the so-called "malonaldehyde" found in γ-irradiated DNA.

In the case of the 2'-deoxyguanosine, Buchko et al (*Int. J. Radiat. Biol.* **63**, 669 (1993)) have reported the formation of (2S)-2,5'-anhydro-1-(2'-deoxy-β-D-erythro-penta-furanosyl)-5-guanidinylidene-2-hydroxy-4-oxoimidazolidine **3** in the presence of O_2
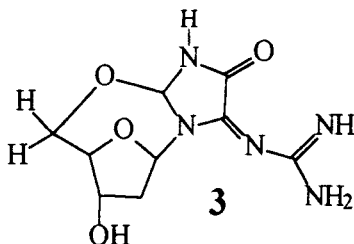
This product can be assayed with 1,2-naphthoquinone-4-sulfonate (formation of a fluorescent dye). We have now shown on the basis of this assay that the yield of this product is about the same in N_2O/O_2 (4:1) and O_2-saturated solutions, despite the fact that under the latter conditions the OH-radical yield is only half of the former. This indicates that a further intermediate is required for the formation of **3** which is more abundant in O_2-saturated solutions. As this is likely to be O_2^-, experiments have been carried out in the presence of the enzyme superoxide dismutase which reduces the steady-state concentration of O_2^-. Under these conditions **3** is no longer formed. This is an important finding with respect to the potential role of O_2^- of taking part in the radical-induced degradation of DNA under oxic conditions. The superoxide radical is known to be potentially a major intermediate under these conditions, and the observation reported here may be the key to an explanation of the contribution of O_2^- to oxic DNA degradation by ionizing radiation.

A further series of experiments was devoted to the polynucleotide poly(A). The products unaltered adenine and A-Fapy were determined straight after irradiation, as well as

after various periods of time of heating the samples to 95 °C The data are shown in Figures 4 and 5
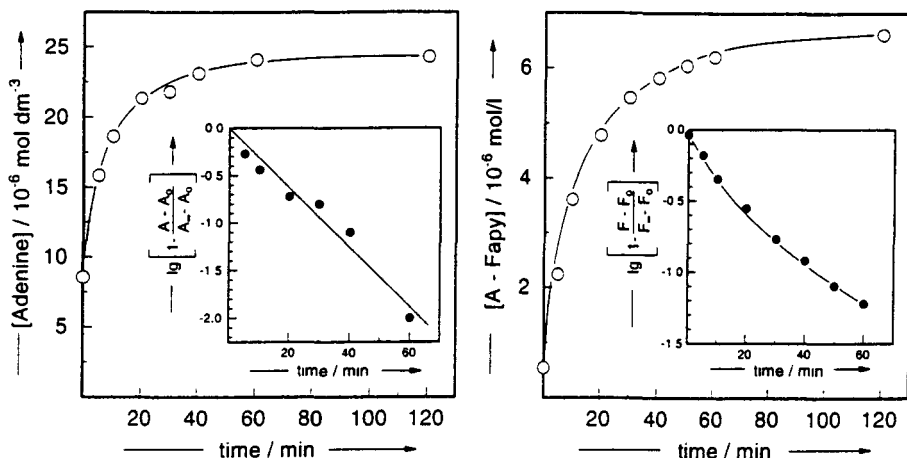
Figure 4 Instant appearance and delayed release of unaltered adenine upon heating at 95 °C.
Inset· the release reaction is approximately first-order (A = adenine concentration).
Figure 5 Instant appearance and delayed release of the product A-Fapy upon heating at 95 °C.
Inset. the release reaction is not monophasic first-order (F = A-Fapy concentration).

It is seen that some of the adenine is released during and/or very shortly after irradiation, and that there is much further release upon heating The total G(adenine) of 1 3 x 10^{-7} mol J^{-1} is quite high, higher perhaps than would be expected considering the proportion of prompt OH-attack at the deoxyribose moiety, and the question arises as to whether there is more than one type of precursor. The trivial case would be OH-radical-induced damage at the deoxyribose moiety, followed by immediate as well as delayed base release, phenomeno-logically similar to what we have previously observed with poly(U) where, however, there are several kinetic components and deoxyribose radicals are formed by radical transfer from uracil-OH-adduct radicals. This kind of sequence is doubtful in the case of poly(A). Here, only two kinetic components, one immediate and one delayed, are in evidence. The latter may be linked to unstable, altered sugars or adenine hydrates which may also be the precursors of the A-Fapy.

Compared to the direct attack of the OH-radical at hydroxyl-group-bearing molecules such as deoxyribose, unaffected by phosphate-ester functions, the presence of such functions, as in DNA, is bound to have an effect on the distribution of the H-atom abstraction reaction at

the various positions, by activating certain C-H bonds in the sugar moiety while deactivating others. A number of alkyl and hydroxyalkyl phosphates, being relatively simple model compounds in this respect, were chosen for this study It is possible to differentiate between the different positions of attack by examining the reducing (toward tetranitromethane or nitroaromatic compounds) or oxidizing (toward N,N,N',N'-tetramethylphenylene-diamine) nature of the resulting radicals. To this effect, the rate and extent of the buildup of a characteristic spectral absorbance, depending on the probe reagent, is measured by pulse radiolysis.

With alkyl phosphates, the OH-radical reacts preferentially by H-atom abstraction a to the phosphate function. The resulting α-phosphatoalkyl radicals are moderately efficient one-electron-reducing agents toward nitro compounds They react with tetranitromethane by addition to form transient adducts with absorption maxima near 300 nm. The rate constants for the decay of these adducts which is reflected by the appearance of the corresponding α-hydroxyphosphates and of nitroform anion, have been determined by optical and/or electric-conductance detection. The stability of these tetranitromethane adducts varies considerably with the chain length (methyl > ethyl > isopropyl) and their number (trialkyl > dialkyl > monoalkyl) of the substituents. Additional formation of conductance due to proton formation during or after the decay of the tetranitromethane-adduct radicals is tentatively attributed to the hydrolysis of the a-hydroxyphosphates. α-Phosphatoalkyl radicals derived from trimethyl, triethyl, triisopropyl, and diethyl phosphates also react with p-nitroacetophenone, though much more slowly than diffusion-controlled ($k < 5 \times 10^7$ dm^3 mol^{-1} s^{-1}), possibly through adduct formation, as one-electron reduction of the nitroacetophenone to its transient anion radical was not observed (witness the absence of its characteristic absorption spectrum in pulse radiolysis).

The rate constants for the reaction of OH-radicals with glycerol-1-phosphate **4** and glycerol-2-phosphate **5** have been redetermined by the thiocyanate competition method and found to be considerably smaller than the values available to date in the literature. Our values are 1.4×10^9 dm^3 mol^{-1} s^{-1} at pH 4 (**4:** $k = 2.0 \times 10^9$ dm^3 mol^{-1} s^{-1} at pH 8; 1.1×10^9 dm^3 mol^{-1} s^{-1} at pH 4; **5:** $k = 1.6 \times 10^9$ dm^3 mol^{-1} s^{-1} at pH 8). Using the chemical probes N,N,N',N'-tetra-methylphenylenediamine and tetranitromethane, the distribution of OH-attack over the carbon atoms of the glycerol moiety can be obtained. In contrast to the alkyl phosphates, the α position is disfavoured in the glycerophosphates. One may therefore say that the tendency to undergo H-atom abstraction increases along the series -CHR- < -CH(OPO$_3^{2-}$)- < -CH(OH)-. The radical distribution for the glycerol monophosphates is shown in Table 1.

Table 1 Relative abundances of carbon-centered radicals formed through H-atom abstraction by the OH-radical from glycerol-1-phosphate **4** and glycerol-2-phosphate **5** at the time of their generation

Compound	pH	α (%)	β (%)	γ (%)
Glycerol-1-phosphate **4**	4	15	35	50
Glycerol-1-phosphate **4**	8	11	39	50
Glycerol-2-phosphate **5**	8	7	93	-

As in the case of the alkyl phosphates, these α-phosphatoalkyl radicals react with tetranitromethane by forming transient adducts which have nitroxyl radical character The β-phosphatoalkyl radicals eliminate inorganic phosphate in a fast process (k > 10^6 s^{-1}). The γ-phosphatoalkyl radical undergoes base-catalyzed dehydration (k_{obs} = 1 8 x 10^5 s^{-1} at pH 10 6).

In order to obtain further information regarding the mode of action of oxidants on deoxyribose-centered DNA radicals, the propensities of some model-system α-alkoxyalkyl radicals to follow the oxidation pathway versus the fragmentation pathway, have been studied. a-Monoalkoxyalkyl radicals from 1,4-dioxan, tetrahydrofuran, dimethyl ether (all three are models for 2'-deoxyribose C(4')), as well as the radicals from 1,3-dioxan (model for deoxyribose C(4') and C(1')), were produced radiolytically in aqueous solution. In the presence of oxygen, these radicals are converted into the corresponding peroxyl radicals. In the case of 1,4-dioxan, the bimolecular decay of the latter gives rise to 1,4-dioxan-2-one (G value in terms of 10^{-7} mol J.$_1$: 0.4), 2-hydroxy-1,4-dioxan (0.4), ethane-1,2-diol monoformate (0.6), ethane-1,2-diol diformate (2.8), and formaldehyde (0.6), as well as to traces of peroxidic products. The action of the oxidant 4-nitrobenzonitrile shows some resemblance to that of oxygen in that the formation of an adduct is observed as well (one might have expected outright electron transfer to prevail in the case of the nitroaromatic). The adducts are N-alkoxyaminoxyl-type radicals, which show absorption maxima near 310 nm and decay very slowly, with rate constants in the range 0.4 - 1.0 s^{-1}. In contrast, the reaction of the α-dialkoxyalkyl radical from 1,3-dioxan (formed in a proportion of 32%) with 4-nitrobenzonitrile leads to the rapid formation of the radical anion of this nitroaromatic.

The N-alkoxyaminoxyl-type radicals react with ascorbate (k = 2 x 10^4 dm^3 mol^{-1} s^{-1}) and show a very low reactivity toward O_2 (k < 10^3 dm^3 mol^{-1} s^{-1}), but are rapidly reduced by the radical anion of 4-nitrobenzonitrile (k ≈ 10^9 dm^{-3} mol^{-1} s^{-1}).

The products from 1,4-dioxan irradiated in the presence of 4-nitrobenzonitrile in N_2O-saturated aqueous solution are 1,4-dioxan-2-one (G value, 0.3), 2-hydroxy-1,4-dioxan (2.5),

The products from 1,4-dioxan irradiated in the presence of 4-nitrobenzonitrile in N_2O-saturated aqueous solution are 1,4-dioxan-2-one (G value, 0.3), 2-hydroxy-1,4-dioxan (2 5), ethane-1,2-diol monoformate (2 1), ethane-1,2-diol diformate (0 7), formaldehyde (2.1), as well as 4-nitrosobenzonitrile and other reduction products of the nitroaromatic. The products can be accounted for on the basis of a fragmentation of the aminoxyl radical by (i) heterolysis of the (ether)C-ON(aromatic) bond (corresponding to 45% one-electron oxidation of 1,4-dioxan-2-yl) and (ii) homolysis of the (ether)CO-N(aromatic) bond (corresponding to 55% formation of 1,4-dioxan-2-oxyl which undergoes further fragmentation). The situation is similar in the case of the alkoxyalkyl radicals derived from the other substrates investigated.

The results indicate that fragmentation reactions involving the carbon skeleton of organic radicals are important not only in the case of peroxyl radicals, but that they can also be induced by nitroaromatic sensitizers. In the living cell, the reduction of the long-lived sensitizer radical-adducts by compounds such as ascorbate, giving rise to (toxic) hydroxylamine-type products, may compete with the homolytic or heterolytic fragmentation of the N-alkoxyaminoxyl radicals.

The radiation-induced formation of malonaldehyde and malonaldehyde-like products in DNA (oxygenated aqueous solution) is still not entirely understood. These products are assayed by means of the thiobarbituric-acid (TBA) test, Essentially all of the TBA-reactivity attributable to low-molecular-weight (DNA-free) material is represented by malonaldehyde, with no indication of the formation of any base propenals which, in contrast, in the form of the thymine and adenine propenals, are the main products of bleomycin/Fe/O_2 action on DNA. A considerable part of the TBA-reactive material remains bound to the DNA.

The kinetics of the colour formation in the TBA-assay reveals an interesting complexity. Oxygen-satureted and N_2O/O_2 (4:1)-saturated solutions behave differently. In O_2-saturated solution, the kinetics is practically the same as that observed with malonaldehyde alone. Since from γ-irradiated DNA, the amounts of free malonaldehyde and DNA-bound TBA-reactive material are of roughly comparable size, the kinetics of the colour formation would have deviated markedly from the observed first-order behaviour if the DNA-bound material were reacting as fast as the base propenals do, or as slowly as the material from monomeric purine deoxynucleosides does. N_2O/O_2 (4:1)-saturated DNA solutions, on the other hand, while following the same kinetics initially, then show a further increase of colour formation that continues at a very slow rate, without reaching a well-defined endpoint. This indicates that here the TBA-reactive DNA-bound products must be different from those under

O_2 alone. The suggested explanation is that in O_2-saturated solution the superoxide radical takes part in the transformation of the oxygen-fixated lesions effected by the OH-radical, and that these products are different from those produced where the peroxyl radicals mainly react with each other.

In response to the request from a fellow research group also participating in this network project, we have been glad to supply values of the rate constants for the reaction of the OH-radical with some DNA model compounds that we have determined or redetermined, see Table 2.

Table 2. Determination of rate constants for the reaction of hydroxyl radicals with DNA model compounds. The literature values are taken from G. V. Buxton, C. L. Greenstock, W P Helman, and A. B. Ross, *J. Phys. Chem. Ref. Data*, 17, 513-886 (1988)

Substrates	$k(OH + S)$ $dm^3\ mol^{-1}\ s^{-1}$	Method	Literature values $dm^3\ mol^{-1}\ s^{-1}$
2-Deoxyribose	$2\ 3 \times 10^9$	KSCN	2.5×10^9
Thymine	5.5×10^9	KSCN	$6\ 4 \times 10^9$
Thymidine	5.1×10^9	KSCN	4.6×10^9
Thymidine-5'-phosphate	4.4×10^9	KSCN	$5\ 2 \times 10^9$
2'-Deoxyguanosine	6.7×10^9	Buildup kinetics at 520 nm	not available
2'Deoxyguanosine-5'-phosphate	6.1×10^9	Buildup kinetics at 520 nm	$6\ 8 \times 10^9$

The following papers have grown out of our work funded under the auspices of the Network Project

(1) C. von Sonntag Topics in free-radical-mediated DNA damage. purines and damage amplification - superoxide reactions - bleomycin, the incomplete radiation mimetic. *Int. J. Radiat. Biol.* **66**, 485-490 (1994).

(2) C Nese, M N. Schuchmann, S. Steenken, and C von Sonntag. Oxidation vs. fragmentation in radiosensitization. Reactions of a-alkoxyalkyl radicals with 4-nitrobenzonitrile and oxygen. A pulse radiolysis and product study. *J. Chem. Soc. Perkin Trans. 2*, 1037-1044 (1995).

(3) M. N. Schuchmann, M. L Scholes, H. Zegota, and C. von Sonntag. Reaction of hydroxyl radicals with alkyl phosphates and the oxidation of phosphatoalkyl radicals by nitro compounds. *Int. J. Radiat. Biol.*, in the press.

(4) D. Langfinger, R. Wagner, R. Rashid, H.-P Schuchmann, and C. von Sonntag. Bleomycin vs. OH-radical-induced malonaldehydic-product formation from DNA. In preparation.

(5) M. Hess, M. N. Schuchmann, R. Wagner and C. von Sonntag. Radiolysis of 2'-deoxyadenosine in aqueous solutions - a model for OH-radical-induced purine damage in DNA. In preparation.

Head of Project 6. Dr Smith.

II. Objectives for the reporting period

The objectives have been to exploit thin-film technology in order to carry out charged particle (proton) transmission measurements in condensed organic materials, in order to verify experimentally those areas where there are deficiencies in interaction cross sections. Measurements will be made in the energy range 3 - 15 keV in films of different thickness, to be followed by comparison with computed transmission factors using up-to-date (TRIM) codes
Methods are to be developed for the detection of ionization charge in such films, as a prelude towards the determination, in later projects, of W-values in condensed quasi-biological material.

III. Progress achieved, including publications

The intention behind this contribution has been to use nanometre thick organic films, prepared by the Langmuir-Blodgett (LB) method, as the basis for measuring quantities which have relevance to the microdosimetry of charge-particle-induced radiation damage. LB films have particular importance in microdosimetry because they can form condensed, organic films of precisely defined nanometre thicknesses from a variety of molecules which have biological relevance. In certain cases these films can be made to conduct charge, thereby leading to the possibility of developing a new form of dosimetry based on condensed organic material. It is, furthermore, possible to attach other biological molecules to such films and to form molecular layers of molecules which do not otherwise lend themselves to the LB technique.

One ultimate goal is to advance the determination of experimental W-values over a range of charge-particle energies in a number of realistic biological systems. For this, it is necessary to measure energy loss in the film, as well as to find ways of collecting all the charge produced as a result of this energy loss. The work done so far is a preparation towards the achievement of this goal. The first steps have been the selection of precise incident proton energies and beam currents together with some initial progress towards the development of methods for the collection of secondary charge. Future activity will be directed towards the analysis of transmitted proton energy and to the bringing together of those techniques for making simultaneous measurements

Two major objectives have therefore been set in the present work:-

1) the measurement of charged particle (proton) transmission at low energies in condensed organic systems together with a comparison with the best available codes and

2) a refinement of the techniques for extracting charge produced by incident charged particles in thin LB films.

In both cases, the novelty of this new methodology has resulted in slow progress because of the need to produce films of the highest quality. All the technical difficulties associated with the prime objectives have been overcome during the reporting period. Separate measurements of (1) proton transmission through **unsupported** films and (2) charge production in selected thicknesses of **supported** films have clearly shown the value of studying these condensed organic materials in the context of the overall aim of the program, and have pointed the ways forward for future, and more

sophisticated, measurements In this regard, the original aims of the project have been met Three areas of activity relating to radiation effects in LB films have been persued.

Proton transmission through nanometre organic films

Protons in the energy range 3 - 15keV were selected with an energy resolution of ~2% from a spectrum of energies scattered off a heated tantalum foil This beam was then collimated down to a final diameter of 1.5mm and restricted to a current of ≤ 2nA in order to prevent thermal damage to the organic LB film samples. Transmitted protons were detected by a Single Channel Electron Multiplier (SCEM) whose entrance cone was maintained at -2.5kV, and which subtended an angle at the sample of 27.5 ± 2.5 degrees. The response of the detector was first normalized to the beam current measured upstream of the energy analyzer.

Multilayer samples of polymerized (12,8) diacetylene were prepared to span a 750 lines per inch copper mesh. The coverage of the mesh by these films was 100% over an approximately circular area of diameter ~8mm, i.e. - much larger than the beam diameter. Transmission through film thicknesses of 21,23 and 25 layers (corresponding to thicknesses of 63, 69 and 75 nm) was normalized to that through the mesh alone. An unsupported area of film of 25 × 25 μm² was therefore achievable using support mesh wires that were 7 5 μm thick. This gave an open area ratio of 55%.

Computations of proton transmission through such films was made using the lastest version (1992) of the TRIM code together with the appropriate geometry and beam parameters used in the measurements.
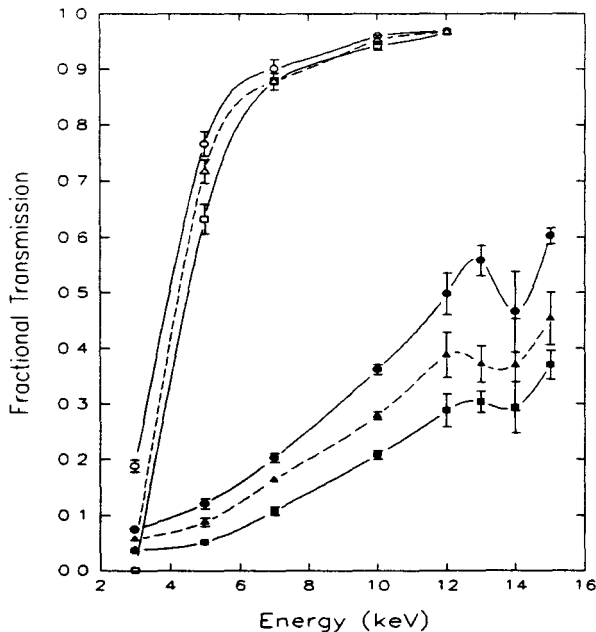
Figure 1: *Fractional transmission of protons through unsupported (12,8) PDA films of thickness 630nm (O), 690nm (Δ) and 750 (□) nm. Upper curves (open symbols) are TRIM computations. Lower curves (solid symbols) are experimental results*

Figure 1 shows the significant disagreements between computed and measured values at all energies except the lowest (3 keV), where the film thicknesses are on the order of the proton range. Error bars on the measured values reflect the reproducibility of several experimental runs, while uncertainties in the computed values reflect imprecise knowledge of:

(a) beam spread of the incident beam between final collimator and sample. An increase of 100% in beam diameter above 1.5mm will increase the solid angle subtended to 32 degrees (from 27.5), and increase transmission by ~15% at the lowest energy. Any effect will be much reduced at higher energies.
(b) geometrical solid angles between sample and detector. Errors here could arise because of an overestimated sensitive area of detector cone which, in any case, cannot be greater than 11.4mm. Any reduction in the area of the detector will decrease the solid angle and with it, the transmission. Errors which arise due to (a) and (b) go in opposite directions and would tend to cancel out if both were present.
(c) proton scatter off the mesh wires after transmission through the film. Typical values of proton energy loss in the film, as calculated by TRIM, suggests that any such effect of scatter would not be least at the lowest energy of 3 keV, which is what is observed.
(d) error in the scatter geometry due to attraction by -2 5kV into the detection cone of low energy protons which would otherwise have remained undetected. Substantial error here would be corrected by decreasing the experimental transmission, thereby leading to a larger discrepancy between computed and experimental values.

The estimated magnitudes of corrections (a-d) are therefore not likely to explain the large discrepancy between measured and calculated transmissions. More important factors are the following:

(e) deposition of thin carbon, or other organic, deposits due to less-than-UHV vacuum conditions. Visual inspection of the films after each series of run showed no evidence of either damage or deposit, although a discolouration was observed many weeks after measurements had been taken. It was not possible to produce a consistent agreement between the TRIM and experimental results over this energy range using any thickness, or any likely composition, of a carbonaceous deposit. However, there is approximate agreement at 3 keV, where the proton range is comparable with the film thicknesses. Disagreement caused by an increase in the effective thickness of the LB film system due to any unwanted deposit would be likely to be most pronounced at the lower energies. This is not what is observed.

(f) the formation of neutral atomic hydrogen by low energy protons on exiting the LB film. Although the sensitivity of the SCEM towards neutral species is not known, it is likely to be negligible for slow, ground state hydrogen but could be significant for fast or excited state atoms. The largest difference between experimental and calculated transmission is observed at about 7 keV and decreases up towards 15 keV but also down towards 3 keV. This effect has to be considered as a possible reason for the disagreement showing, perhaps, a highest rate of hydrogen production at 7 keV where the energy on exit is ~ 2 keV.

(g) incorrect low energy cross section data used by TRIM.
The variation in transmission with film thickness provides the most significant difference between experimental data and TRIM calculations. As the incident proton energy increases above 3 keV, the TRIM calculations show a decreasing discrimination between thicknesses, while the experimental data show an increasing effect, even though there is an overall increase in

transmission with energy in both cases. Since the film thicknesses are incremented by only 8 - 10% each time, any effects due to possible surface contamination of the films or the production of atomic hydrogen should be negligible. It is therefore likely that there are some deficiencies in the cross section data used by TRIM at these energies.

Charge production and transport following energy deposition

This aspect of the project used supported LB films in order to develop the optimum design of electrodes and electronic amplification needed to reliably record the production of pico-Coulombs of charge. Irradiation of the films was achieved using a 2.5 MBq source of ^{241}Am α-particles

Films of (12,8) diacetylene were prepared with thicknesses of 50 layers (150nm) on an insulating substrate between appropriate electrodes. When polymerized with uv light, the conjugated bonds made an easy conduction path within the layers. Application of a bias voltage between the electrodes then enabled charge resulting from energy deposition by an ionizing particle to be collected.

Figure 2 shows the response to α-particle energies between 5.5 and 3.5 MeV when normalised to unit solid angle . The larger stopping power at low energies is reflected in a larger charge production rate in the films, as expected, and encourages the prospect of being able to measure W-values in LB films by measuring charge production in unsupported films simultaneously with energy loss.
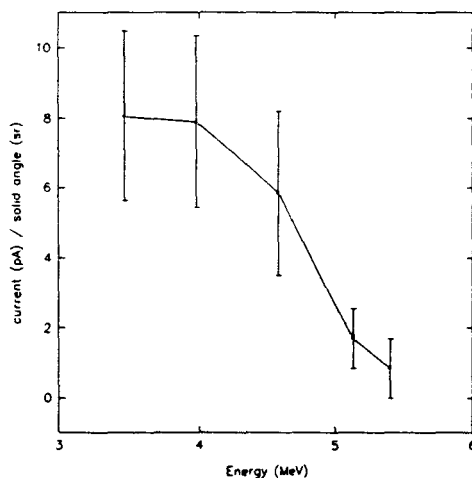
Figure 2: Collected current normalised to unit solid angle, from 150 nm of (12,8) PDA irradiated by α-particles from a 2.5 MBq ^{241}Am source.

Polymerization in nanometre (12,8) diacetylene films using gamma radiation

A monomer film of (12,8) diacetylene (DA) will polymerize under the action of both uv and gamma photons. Estimates of the sensitivity were made using ^{60}Co photons for irradiation, and

optical absorption at 490nm as the indicator of monomer-polymer conversion. For films having thicknesses 72nm, 144nm and 150nm (24, 48 and 50 layers) the optical density per layer shows a consistent and quasi-linear increase with absorbed dose up to about 10 kGy, and a more gradual increase thereafter.
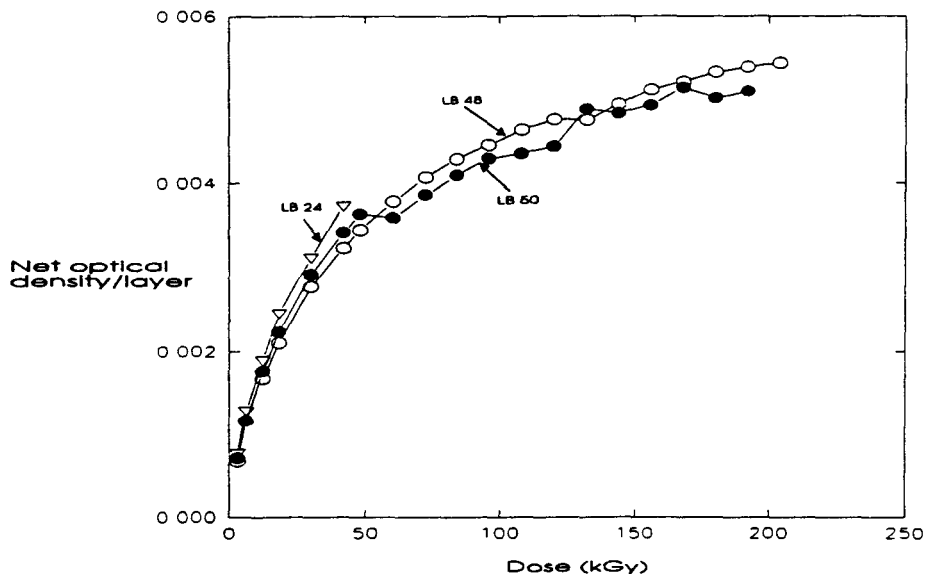
Figure 3: Normalized response of (12,8) DA films composed of 24,48 and 50 layers to ⁶⁰Co γ-rays. Optical Density is measured at 490nm.

The sensitivity of (12,8) DA films towards polymerization, as quantified by optical absorption, is not likely to be sufficient for use as a dosimeter at protection levels (Figure 3) but could find use as the basis for an industrial or therapy instrument.

Radiation effects in these films for other purposes, however, have been shown to provide dosimetric data at nanometre levels which are not otherwise obtainable in condensed organic media.

PUBLICATIONS:

1. "Monte Carlo calculations of radical proximity functions around thermalizung positrons in water
   M A Hill and F A Smith,   Materials Science Forum 105 1581 (1992)
2. "Calculation of initial and primary yields in the radiolysis of water"
   M A Hill and F A Smith,   Radiat. Phys. Chem 43(3) 265 (1994)
3. "Is the response of the Fricke dosimeter constant for high energy electrons and photons?"
   M A Hill and F A Smith,   to be published in Radiat.Phys.Chem (1995)
4. "Consideration of radiation-induced polymerization of diacetylene LB films for dosimetry"
   N Mod Ali, C E Tucker and F A Smith,   to be published in Thin Solid Films (1995)
5. "Nanometre organic films in the service of radiation dosimetry"
   F A Smith, M A Hill, C E Tucker and J Oriel,   10th ICRR (1995)

Head of project 7: Dr. O'Neill

II   Objectives for the reporting period

1)   To establish the yield for the induction of double strand breaks (dsb) in V79-4 and CHO cells using γ- and α-irradiation and to assess their repairability.
2)   To assess the influence of radical scavengers on the induction and reparability of DNA double strand breaks (dsb) by α- and γ-irradiation of V79-4 mammalian cells and its relevance to damage complexity.
3)   To determination the yield of DNA- protein crosslinks induced in V79-4 mammalian cells by α- and γ-irradiation to assess the influence of target volume.
4)   To compare damage induced in plasmid DNA under various radical scavenger conditions which mimic the cellular environment.
5)   To gain insight into DNA damage induced by ionisation using 193nm light as model for direct effects of radiation.

These approaches yield information on the complexity of DNA damage and the influence of the chemical environment [2]. The information is being used to develop models (with MRC (Phys) and ADPA) to simulate the chemical processes in the development of track structure modelling.

III. Progress Achieved, including Publications

These studies have been carried out in collaboration with MRC (phys) who provide the expertise for α-irradiations of mammalian cells and dosimetry.

(i)   The effects of radiation quality on cellular DNA damage

The radiobiological effectiveness (RBE) for the induction of dsb in V79-4 mammalian cells by α-particles was established using three different methods for the analysis of dsb, namely sedimentation, non-denaturing elution and pulsed field gel electrophoresis (PFGE). The induction of DNA dsb was determined in V79-4 mammalian cells following irradiation by ^{60}Co γ-rays or ^{238}Pu α-particles (average LET 120 kev μm^{-1}) under aerobic conditions. The induction of dsb was found to be linearly dependent on the dose with the RBE for α-particles of 0.85 ± 0.14 (sedimentation) and 0.68 ± 0.12 (elution) compared with ^{60}Co γ-rays [1].

A discrepancy which has existed in the literature concerning the RBE for dsb induction by α-particles has been suggested to reflect the method of dsb determination. The method of PFGE for determination of dsb induction was set-up to enable access to dose ranges which approach those used for cellular inactivation. Using the PFGE method [3,10], the RBE for induction of dsb in V79-4 and CHO cells by α-particles has been verified to be ~ unity at radiation doses of < 10 Gy. Therefore, the RBE for dsb induction by α-particles is~1 and independent of the method for assaying for dsb. A possible discrepancy between these findings and those of Kampf and Eichorn is the centrifugation speed and the absence of proteinase k in their lyse solution so that the DNA may still be associated with protein.

The timecourse and extent of rejoining of radiation-induced dsb were determined over a 3 hr period at 310K following irradiation of V79-4 cells under aerobic conditions. With low LET radiation, > 90% of the dsb are rejoined within the 3 h repair period. The ability of the cells to rejoin dsb induced by α-irradiation is significantly reduced with only 30-50% rejoined within 3 hr. With low LET radiation, the kinetics of rejoining is distinctly multi-component whereas with high LET radiation the majority of dsb rejoining occurs within 1 hr [1,3].

The RBE for cellular inactivation at the 1% survival level was determined to be 4.0, a value which is comparable with that obtained from comparison of the residual yields of dsb. From the D_0-value of 0.68 Gy for α-irradiation, the average number of tracks which pass through the nucleus is calculated to be 4.7 tracks/lethal lesion. Therefore the average number of tracks which pass through the cell is significantly greater than the average number of lethal lesions per cell. Further, based upon the residual yield of dsb at 3 hr it is estimated that ~ 7 residual dsb/cell nucleus/lethal event, are produced for α-irradiation. Under hypoxic conditions, the RBE-values for induction of dsb and cellular inactivation (10% level) by α-particles are ~ 3.0 and ~ 11.8 respectively.

It is suggested that the yield of residual damage reflects the lesion severity whereby it has been hypothesised that the clustering of damage from the energy deposition events increases with increasing LET of the radiation (MRC (phys)). Therefore different types of dsb are produced whereby chemical modifications of the DNA in the vicinity of the breaks may influence their subsequent reparability. With α-irradiation, the proportion of these more complex damages is greater than those produced by low LET radiation [1,3]. Therefore different types of dsb are produced with differences in the associated damage (base modifications, ssb) in the vicinity of the dsb.

2) The influence of radical scavengers on cellular DNA damage induced by
α-irradiation - properties of non-scavengeable dsb

This study was undertaken to assess the protective effect of dimethyl sulphoxide (DMSO) against both high and low linear energy transfer (LET) radiations on the induction and rejoining of DNA double strand breaks (dsb) and inactivation of V79-4 Chinese hamster cells [4,9]. The cells were exposed under aerobic conditions as monolayers to either low LET photons (^{60}Co γ-rays) or high LET alpha particles (^{238}Pu) at 277K. Prior to determination of DNA dsb, it was necessary to establish the effect of additives upon the ability of the cells to remain as monolayers using confocal microscopy. The effect of DMSO upon V79-4 cells as monolayer was found to cause the cells to round up from a cell thickness of ~ 5 μm to a thickness of ~ 14 μm but still remain attached. The optimum concentration of DMSO was established to be 0.5 mol dm^{-3} since at higher concentrations, the cells detached.

The initial yield of DNA dsbs, determined by elution under non-denaturing conditions, are linearly dependent on dose. When the irradiation was carried out in the presence of DMSO (0 - 0.6 mol dm^{-3}), the initial yields of dsb induced by both γ- and α-irradiation decrease. Since DMSO changes the morphology of the cell, this protection by DMSO with α-particles may be due to chemical scavenging or dose attenuation. The scavenger, 2-methyl-2-propanol (t-BuOH), which is ~ 10 less effective at scavenging water radicals was used as the control to check the effect of morphological changes of the cells. At a low concentration of 0.1 mol dm^{-3} of t-BuOH, the morphology of the cells is similar to that in the presence of DMSO. From

the negligible effects of t-BuOH on cell survival, it is confirmed that the effect of DMSO is chemical protection through scavenging of water radicals, namely OH radicals. With γ-irradiation at [DMSO] > 0.6 mol dm^{-3}, a further decrease in the yield of dsb occurs. DMSO (0.5 mol dm^{-3}) reduces the initial yield of dsb by (50±5)% and (32±4)% for photons and alpha particles respectively. DMSO protects more effectively against cellular inactivation and dsb induction at low LET compared with α-irradiation with protection factors (P.F.) of 1.7 and 1.4 respectively for survival and 2.0 and 1.5 respectively, for dsb.

After incubation of the irradiated cells for 3h at 310K following high LET irradiation, the residual yield of dsb is reduced by < 13% (from 70% to 60% of the initial yield) when the irradiations were carried out in the presence of 0.5 mol dm^{-3} DMSO. With γ-irradiation in the presence of 0.5 mol dm^{-3} DMSO, 90% of the dsb are rejoined by 3h incubation at 310K. Therefore, the non-scavengeable dsbs (do not involve water radicals to produce the actual breaks) induced by α-particles are not significantly rejoined within 3h in contrast to rejoining of the majority of the non-scavengeable dsb induced by γ-irradiation. From comparison of the dsb and survival data for α-irradiation, it is inferred that the damage severity is reduced by DMSO through minimising the formation of OH-induced sugar/base modifications in the vicinity of non-scavengeable dsbs.

It is suggested that only the scavengeable (and less severe) damage is rejoined in the absence of DMSO and that this component of damage involves the OH radical as a precursor. From a comparison of the dsb and survival data, these studies give indirect support for the increased severity of damage induced by α-particles. It is inferred that DMSO reduces the severity of dsb induced by radiation, especially α-radiation, through minimising the formation of hydroxyl radical-induced sugar/base modifications in the vicinity of dsbs. These shifts in damage severity to less complex damage are reflected in the radiosensitivity of the cells to α-irradiation. These studies raise the question as to whether the changes in the spectrum of damage severity is subtle and may only involve moderate increases in the number of localised lesions.

3)   DNA - protein crosslinks induced by α-particles - target size

It has been proposed from track structure approaches that the critical target volume and the size of the ionisation cluster increase with increasing LET of the radiation. These studies were undertaken to assess the induction of radiation-induced DNA- protein crosslinks in V79-4 cells with γ- and α-irradiations [5, 6]. This type of damage would represent a target size for the energy deposition events of 5-10nm. The technique for determination of DNA- protein crosslinks (DPC) is based upon the nitrocellulose filter binding assay used by Oleinick and co-workers.

The induction of DPC in V79-4 cells under hypoxic conditions by α- and γ- radiation is similar with an RBE of 0.93 for α-particles as shown in Figure 1. For both radiations the yield of DPC is reduced in the presence of oxygen with oxygen enhancement ratios (OER) of 0.8 and 0.5 for γ- and α-irradiations respectively. As shown in Figure 1, the RBE for induction of DPC under aerobic conditions by α-particles is 0.5. To overcome any problems in the size of DNA involved in DPC due to dsb, the average size of the DNA attached to the protein was determined to be ~15kb pairs for both radiations. This size is restricted through shearing and not the accumulation of dsb.
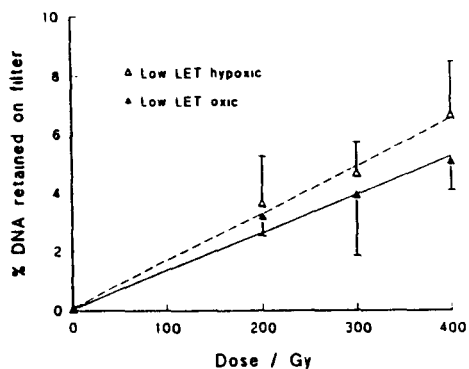
LOW LET RADIATION   HIGH LET RADIATION
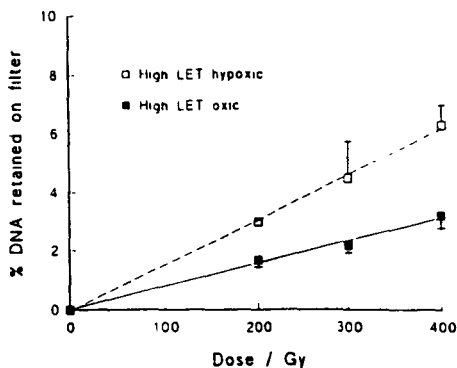
Figure 1 The dose dependence for the induction of DPC in V-79 mammalian cells by γ- and α-radiation

Although the yields of DPC under hypoxic conditions are similar for both radiations, oxygen appears to protect partially against the formation of DPC especially for α-particles. This reduction occurs for radiations which produce more severe damage. The RBE for α-particle induction of DPC is in contrast to the RBE values generally determined for cell inactivation, mutations and several other biological end-points. The mechanism remains outstanding for their formation although oxygen may act by intercepting the radical species involved in the formation of DPC , thereby reducing the efficiency for their production. Whether the precursor radicals to DPC results from species produced on DNA or protein by less severe events remains an open question. For instance, the yield of single strand breaks, an indicator of less severe damage, decreases on increasing LET of the radiation.

4)   Formation of clustered lesions by radiation - induction of S1 nuclease   sensitive sites in mammalian cells

From our experimental studies and track modelling (MRC-Phys) [1,7,9], high LET radiation is thought to produce more complex DNA damage. If these more complex DNA damages, which do not contain a dsb, are partially denatured, it is thought that they may be substrates for the enzyme, S1 nuclease. These S1 nuclease sensitive sites (sss) may result in an enhanced level of dsb. Monolayers of V79-4 cells were exposed to γ- and α-irradiation, lysed and treated with S1 nuclease to convert sss into dsb assayed by neutral filter elution. With high LET radiation the dsb yield is increased by ~40% following the S1 nuclease treatment. Contrastingly, the yield of dsb from γ-irradiation is essential independent of S1 nuclease treatment. It was inferred from these studies [8] that the complexity of DNA damage increases with increasing LET of the radiation. With α-radiation, base damages associated with other base damage or ssb on the complementary strand may be converted to dsb. Since the yield of

base damage is expected to be much greater than that for dsb, it is inferred that only very severe complex damage is recognised as sss and that less severe clustered damage (e.g. involving base modifications) are not recognised by S1 nuclease.

5)   Radiation induced strand breakage of plasmid DNA - complexity of damage

The induction of DNA dsb and ssb in plasmid DNA under different scavenger conditions has been determined following γ-and α-irradiation as shown in Figure 2.   At low scavenger concentrations, the major damage is induced by the OH radical. Evidence for increased density of clustered events in the aqueous phase is obtained from the lower yield of ssb/Gy with α-irradiation since fewer OH radicals escape the cluster and become homogeneously distributed in the solution when compared with γ-irradiation. The yield of ssb and dsb decrease on increasing scavenging capacity of the solution. Increasing the scavenging capacity reduces the diffusion distance of water radicals. Under conditions of high scavenger concentrations, which mimic the scavenging capacity of the cellular environment, the ratio of dsb:ssb is greater for α-irradiations than for γ-irradiations as shown in Figure 3.   These differences are indirect evidence for increases in probability that energy deposition events yield a dsb, a very simple form of complex damage. The RBE for dsb induction by α-particles under conditions that mimic the cellular environment is ~ unity. The yields of dsb at high scavenger are similar to those determined in V-79 cells and this similarity adds weight to the assumption on cell mimetic conditions. Treatment of the radiation damage DNA with S1 nuclease does not lead to increased levels of strand breakage, indicating that sss are not produced in significant yields.
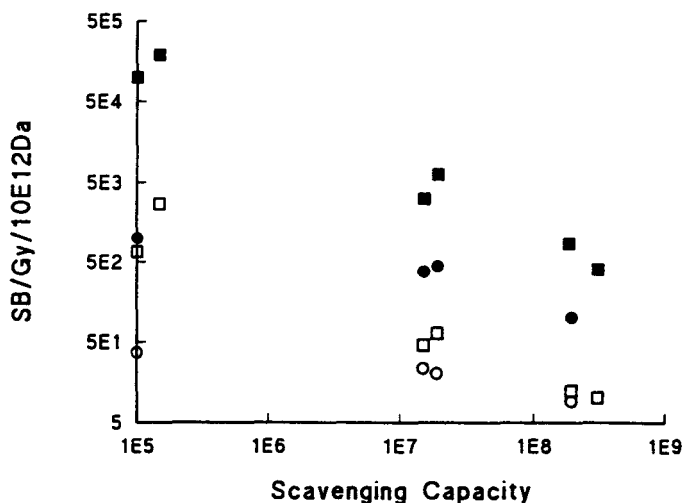
Figure 2 The dependence of the yield of ssb (closed symbols) and dsb (open symbols) on scavenging capacity for irradiation of plasmid DNA with γ- (squares) and α- (circles) radiation

The change in DNA damage severity is mirrored in these solution studies and provide a useful method to examine in more detail damage complexity, a factor which may influence significantly the efficiency of DNA damage processing.

ssb/dsb (y-axis: 0, 20, 40, 60, 80, 100, 120, 140, 160)

x-axis labels: 1e5 γ, 1e5 α, 1.5e7 γ, 1.5e7 α, 3e8 γ, 2e8 α

scavenging capacity
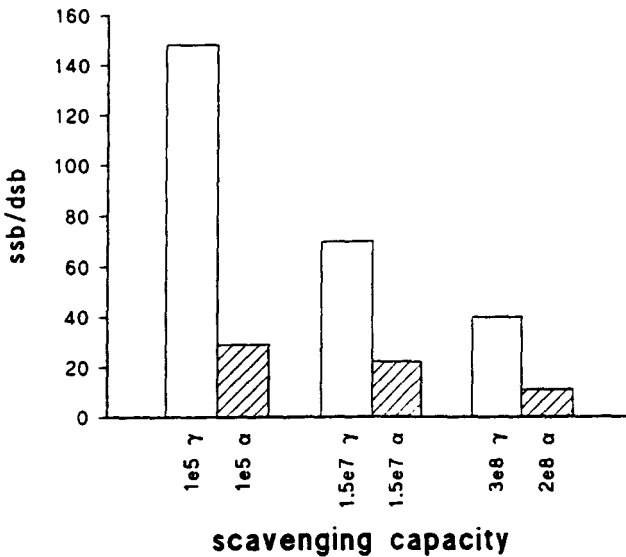
Figure 3 The ratio of ssb:dsb on scavenging capacity for plasmid DNA irradiated with γ-(open) and α- (hatched) radiation. Tris was used as the scavenger in aqueous solution.

6) Damage induced in DNA by 193nm light- models for direct effects

At present very little information exists on the properties of the species and chemical events which occur following ionisation of DNA. To simulate ionisation events in DNA and establish the chemical pathways of the resulting radicals, photo-ionisation of DNA with 193nm light has been used to model direct events of radiation. These studies give insight into the free radical chemistry following ionisation and in particular, the potential for oxidised DNA base moieties to act as precursors to strand breakage.

Irradiation of DNA with 193nm light results in its photo-ionisation involving a monophotonic process with the formation of a base radical cation and a hydrated electron (ϕ pI=0.048-0.065) [11,12]. Although > 50% of the photo-ionisation events initially occur at guanine in DNA, migration of the 'hole' from the other bases to guanine occurs to yield predominantly its radical cation or its deprotonated form. From sequence analysis, the data reveals that 193nm light induces single strand breaks (ssb) in double stranded DNA preferential 3' to a guanine residue. However it has previously been reported that 193nm light yields very low yields of ssb (<2% of the yield of e^-aq). The distribution of these ssb at guanine is non-random, showing a dependence on the neighbouring base moiety. The efficiency of ssb formation at non-guanine sites is estimated to be at least one order of magnitude lower. With single stranded DNA, the ssb occur also preferentially at guanine but the distribution between the different guanine sites is different to that with double stranded DNA. The preferred cleavage at guanine is consistent with migration and localisation of the electron loss centre at guanine. It is argued that singlet oxygen and the photo-ionised phosphate group of the sugar moiety are

not major precursors to ssb. At present, the mechanisms of strand breakage is not known although a guanine radical or one of its products remain potential precursors. Therefore ionisation of the bases leads to hole migration over a few base pairs with localisation at guanine predominantly. The guanine species or a product lead with low efficiency to strand breakage. From these preliminary findings, it appears that ionisation events in the bases lead to base damage.

References

1.   Jenner T J, deLara C M, O'Neill P and Stevens D L. The induction and rejoining of DNA double strand breaks in V79-4 mammalian cells by γ- and α irradiation. *Int. J. Radiat. Biol. 64*, 265-273 (1993).

2.   O'Neill P and Fielden E M. Primary three radical processes in DNA. *Adv. Radiat. Biol. 17*, 53-120 (1993).

3.   Jenner T J, deLara C M, Stevens D L, Burns N A and O'Neill P. The induction of DNA double strand breaks in V79-4 cells by γ- and α radiations - Complexity of damage. *Radiat. Prot. Dosim. 52*, 289-293 (1994).

4.   deLara C M, Jenner T J, Marsden S J, Townsend K M S and O'Neill P. The protective effect of DMSO on double strand break induction in V79 cells by ^{238}Pu α-particles. Abstract 18th L H Gray Conference, April 1994

5.   Jenner T J, O'Neill P and Stevens D L. Formation of DNA-protein crosslinks in mammalian cells following high and low LET irradiation. Abstract 18th L H Gray Conference, April 1994.

6.   Jenner T J, O'Neill P and Stevens D L. Induction of DNA protein crosslinks in V79-4 mammalian cells following γ- and α-irradiation. 42nd Annual Meeting of the Radiation Research Society, Nashville, 1994. p.154.

7.   Nikjoo H, O'Neill P, Terrissol M and Goodhead D T. Modelling of radiation-induced DNA damage: the early physical and chemical events. *Int. J. Radiat. Biol. 66*, 453-458 (1994).

8.   Cunniffe S, O'Neill P and Stevens D L. Induction of S1 nuclease sensitive sites in mammalian cells following high and low let radiation. Abstract Int. J. Radiat. Biol. (1995) in press.

9.   deLara C M, Jenner T J, Townsend S K M, Marsden S J and O'Neill P. The effect of DMSO on the induction of DNA double strand breaks in V79-4 mammalian cells by α-particles. *Radiat. Res.* (1995) in press.

10.   Burns, N. Investigation of radiation-induced DNA double strand breaks and repair in cellular DNA using pulsed field gel electrophoresis, M.Sc dissertation, University of St. Andrews. (1992).

11.   Melvin, T., Plumb, M.A., Botchway, S.W., O'Neill, P. and Parker, A.W. 193nm Light induces single strand breakage of DNA predominantly at guanine. *Photochemistry and Photobiology*, 61, 584-591, (1995).

12.   Melvin, T., Plumb, M.A., Botchway, S.W. O'Neill, P. and Parker, A.W. The distribution of single strand breakage at guanine initiated by 193nm light is different for single and double stranded DNA.In 'Radiation Damage in DNA: structure/function Relationships at Early times', A.F. Fuciarelli and J.D. Zimbrick (Eds.), (1995) pp. 175-184.

.

Title: Specification of radiation quality at the nanometre level.

1	Colautti	INFN - Legnaro
2	Watt	Univ. St.Andrews
3	Harder	Georg-August Univ. - Göttingen
4)	Leuthold	GSF - Neuherberg
4	Izzo	Univ. Roma - Tor Vergata
6)	Kraft	GSI - Darmstadt
7)	Pszona	SINS.PL

I.   Summary of Project and Global Objectives

The common aim of this international research group is "research concerning the best possible way of specifying radiation quality for radiobiology and radiation protection by a single physical parameter expressing the track structure". The quoted definition of the group's aim can be easily recognised as an old but urgent target because the application fields of radiation protection and radiotherapy require a physical parameter which can predict its biological efficiency. That aim is difficult because the parameters studied in the past, especially the unrestricted LET and the lineal energy y for a reference volume size of about 1μm, have been proven to be too "rough" to play a role as indicators of track structure at nanometre level. But nanometre is the scale of the critical target of radiation effects, as both molecular biology and radiobiological analysis suggest.

The renewal of this old aim was motivated by new ideas which appeared to describe more adequately the meaningful track parameters at nanometre level (restricted LET and linear primary ionisation) The research on the gas detector physics allows to design microdosimetric instruments able to measure ionisation distributions near the particle track with nanometre resolution and the recent advances in technology suggests the possibility to develop a nano-dosimeter in condensed phase. Modern Monte-Carlo codes, are able to simulate the interaction of particles with the matter at nanometre level. This supports both experimental and theoretical research.

Global objectives of the project concern:

i) to study a gas detector able to measure the ionisation produced by a charged particle in nanometric volumes in order to validate, on experimental bases, the *invariance theorem*;

ii) to study the possibility to manufacture tissue-equivalent gas counters able to simulate nanometric volumes;

iii) to assess the consequences of the assumption of the linear primary ionisation as quality parameter for radiobiology and radioprotection;

iv) to asses the consequences of the assumption of the restricted LET as quality parameter for radiobiology and radioprotection;

v) to investigate the feasibility of an absolute dosimeter based on linear primary ionisation as radiation quality parameter;

vi) to investigate the physical bases of the so called *invariance theorem*;

vii) to calculate, by using Monte Carlo energy transport codes, the ionisation induced in nanometric volumes by charged particles of different energy and charge;

viii) to investigate the possibility to measure radical separation at nanometer level by using ESR technique;

ix) to evaluate existing experimental data and perform new measurements of double differential δ-electron emission cross-sections in heavy ion atom collisions in order to improve our knowledge of the physical phenomena which underlie the radiobiological radiation damage;

x) to improve the Jet Counter experimental set-up to performe nanodosimetric measurements (PECO project).

Calculations performed have confirmed that the fluctuations of the energy deposition in nanometre-sized targets traversed by charged particles are peculiar. Long-range δ-rays escape from very small targets, so that the δ-ray contribution to energy deposition is dominated by short-range δ-rays with energies not larger than about 100 eV. Thus the fluctuations of energy deposition is described by the Poissonian distribution of the number of the primary particle combined with the energy deposition distribution of the low-energy δ-rays. Since the low-energy δ-ray component results to be identical for all types and energies of the primary particle (*invariance theorem*), the absorbed energy fluctuations per traversing particle can be described by only one variable, namely the linear primary ionisation density of the primary particle. Monte Carlo calculations have shown that these findings are valid for a very wide range of proton energies, namely from few hundred of keV to 100 MeV.

As first step to extend the investigation to solid state targets, calculation have been performed to simulate δ-ray emission induced by ions passing thin foils of low-Z material. Calculations have been compared with experimental data. Comparison points out that the error induced by the assumption of gas phase cross-section for simulation of solid state media is tolerable in first order. These findings suggest that the energies fluctuation peculiarities calculated in nanometre gas targets could occur similarly in condensed target.

A well-known representative for linear primary ionisation density is the restricted LET_Δ (with $\Delta = 100$ eV). Therefore calculations have been performed to evaluate the dose-mean values of restricted LET both for the core and the δ-ray halo of charged particle tracks. Moreover radiobiological data have plotted against LET_{100}.

Averaged values of physical track structure (linear primary ionisation density and restricted LET included) and microdose parameters, important e.g. in radiobiology, nuclear medicine, high and low LET radiotherapy, radiochemistry and radiological protection, have been compiled as a ready reference for use in the interpretation of damage mechanisms and for quantifying radiation effects. Moreover, from study of quality parameters active at nanometre level, a new interpretation, based on the primary ionisation density, has been made of the main mechanisms of the radiation action. Validation has been found in the ability to explain unusual radiation effects. A new system of unified dosimetry has been suggested and described quantitatively.

As consequence of these calculated data and phenomenological modelling of the radiation action, a new generation of instruments should be required to assess the radiation risk. However, before of investing in that, it is necessary to validate on experimental bases the calculation data which support the thesis that linear primary ionisation density or LET_{100} are the best parameters to use for the radiation risk assessment.

Gas detectors have been designed and manufactured to investigate experimentally the ionisation distributions in nanometric volumes positioned at variable nanometric distances from a charged particle track. The mean ionisation yield in nanometric volumes around an α-particle track has been measured. This experimental investigation, which we call *track-nanodosimetry*, has been performed with two different detectors and a third detector is under preliminary experimental testing. This technological effort is due to the necessity to minimise the ionisation spectral distortions due to boundary effects, like secondary electron emission from detector walls, and due to the statistical fluctuation in the electronic avalanche inside the counter. The experimental results suggest that it is possible to perform track-nanodosimetry, with an electron counter, with sensitive volumes as small as 10-20 nanometres in diameter. For investigating the ionisation track with smaller volumes, a positive ion counter is necessary.

In the last period of the contract the experimental validation of calculated data at nanometre scale has been enriched by the work performed with a *jet-counter*-based device. This experimental set-up has been shown to be able to measure the mean energy deposition in nanometric gas volumes.

Parallel to ionisation measurements in gas devices, the possibility to investigate the track structure in solid DNA on a nanometre scale has been studied. This approach is based on local electron-spin

densities measurements. The experimental tools used have been the ESR and the observation of fast and slow components of the radiophotoluminescence decay.

Finally some basic physics characteristics, on which the future risk assessment monitors will be designed, have been studied both for scintillator and gas devices. For gas devices, both Monte Carlo calculations and experimental investigation has been performed to study the behaviour of electrons in radial electrical fields at low gas pressures. The role of the electrical field gradient has been understood and a simple analytical model, to take it into account, has been proposed. Moreover the so-called non-equilibrium behaviours of the electron swarm near the anode and the cathode walls have been investigated. The findings will allow to design gas devices able to measure properly the ionisation created in nanometric volumes by an external radiation field.

Head of project 1: dr. P. Colautti

II. Objectives for the reporting period

To study a gas detector able to measure the ionisation produced by a charged particle in nanometric volumes in order to validate, on experimental bases, the invariance theorem.
To study the possibility to manufacture tissue-equivalent gas counters (TEPC) able to simulate nanometric volumes.

III. Progress achieved including publications

We will show hereafter the progress achieved in the two lines of research: study and development of an experimental set-up able to perform track-nanodosimetry and study of TEPC physics.

TRACK-NANODOSIMETRY

Measuring single ionisation events in nanometric gas volumes is in principle possible with gas counters. Gas detectors working in pulse mode can measure ionisation distributions. The two main experimental problems are:
- to measure few electrons, possibly one;
- to obtain the information on the initial position of the electron within a few nanometres of uncertainty.
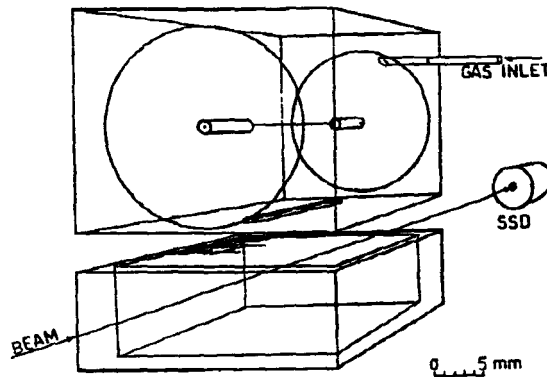
Figure 1

The last problem is fundamentally related to the diffusion of electrons in gas which depends on the gas pressure (**P**) and the path travelled (**X**). The standard deviation of the diffusion probability around the electron is given by the relation: $\sigma \propto \sqrt{\dfrac{1}{E/P}} \cdot \sqrt{\dfrac{X}{P}}$ where **E/P** is the reduced electrical field. However in microsimetry we are interested in the simulated lengths rather than in the real lengths in the gas. Therefore the equivalent diffusion is:

$$\sigma(nm) = 0.316 \cdot D \cdot E_q \cdot \sqrt{X \cdot P} \qquad (1)$$

where **X** (mm) is the length travelled in the gas by the electron, **P** is the gas pressure in Torr, **D** is the diffusion constant in mm for 1 cm of drift at 1 Torr of pressure and $\mathbf{E_q}$ is the equivalence ratio for the gas used, namely $E_q = \dfrac{d(nm)}{d(mm)}$ at unity of pressure. Equation (1) shows that the detection precision of the single electron improves by decreasing the gas even if the electron diffusion increases at low pressures. That means that is a good policy decreasing the gas pressure to perform track-nanodosimetry. The factor before the squared root in the equation (1) is a characteristic of the counting gas and its value has a minimum for **E/P** near to 1 volt /cm Torr and it is 2.1 for propane, 1.5 for methane, 1.4 for the carbon dioxide and 1.2 for DME (dimethylether). That

means that in order to obtain a position uncertainty of about 1 nanometre it is necessary to work at about 1 Torr of pressure or less and with drift lengths of about 1 millimetre.
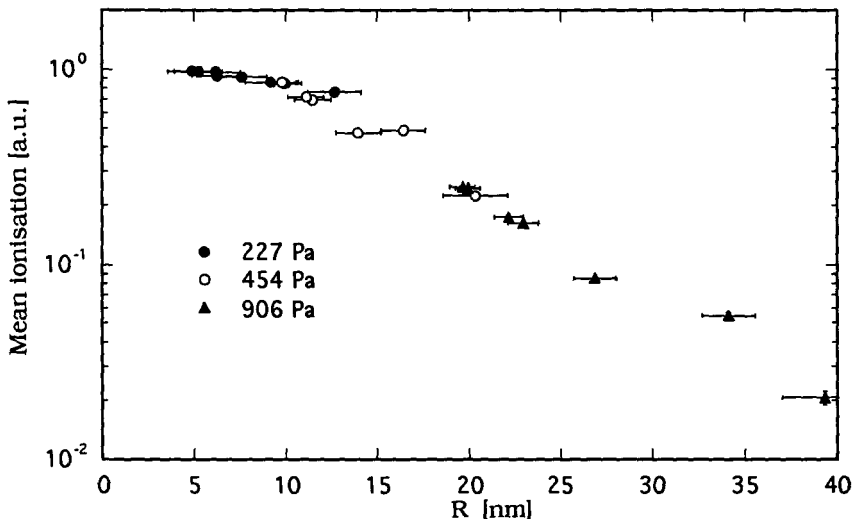
Figure 2

Following these considerations we have manufactured the track detector of figure 1. It is made up of two parts: a small drift region to minimise the electron diffusion and a relative large multiplication region to get a gain high enough at low pressure. A stainless steel block has been drilled to obtain a cylindrical cavity of 20.4 mm in diameter. The proportional counter is almost tangent to the lower side of the block in which a 25 mm long, 1 mm large and 0.5 mm thick slit has been milled. Through the slit, the multiplication region communicates with the drift region which is 4 mm deep. Behind there is a 10 mm deep well to trap the scattered electron. An electroformed mesh of copper with 45 wires per inch and 88% of transparency closes the well and defines the lower side of the diffusion region; an identical mesh is attached on the upper side in order to prevent the electrical field distortions due to slit. The particle beam travels at the centre of the drift region parallel to the slit and it hits a solid state detector, the signal of which opens a coincidence gate for the proportional counter. The counter pulses are produced by the ionisation events which are in the region defined by the projection of the slit into the drift region. All the track detector can be moved in the direction perpendicular to the beam by means of a micrometric screw, so that the distance between the particle track and the slit can be determined with a precision better than 0.01 mm.

With this detector we measured the ionisation yielded by a ^{244}Cm α-particle at different distances from the track (pub. 1). In figure 2 the measured mean ionisation is plotted towards the mean distance of the sensitive volume from the particle track. The plot is the sum of three different measurements made at three different pressures of the propane-based tissue-equivalent gas mixture. This was necessary because of the relevant electronic noise due to backscattered and secondary emitted electrons. The electronic noise in fact increased with R for a given gas pressure, preventing to measure far from the particle track. By increasing the gas pressure the electron diffusion changes and the sensitive volume increases, because of that the ionisation fluctuations are different. Therefore with this detector it was not possible to evaluate the consistency of the data (by comparing data collected at the same position but with different gas pressures) and the relevance of the electron diffusion in the measurements

A second detector was manufactured (figure 3). The stainless steel block was dug out all around the proportional counter. The new counter had a new drift region with an high transparency. The electronic background due to δ-ray backscattering and to secondary electron emission (SEE) from the drift region walls was calculated. The calculated data showed that the electronic background

increases with the distance from the track, as in the previous measurements and in agreement with the new experimental data, but it was estimated to be less than 7%. The electron noise was in fact rather low, allowing even for measurements rather far from the particle track (pub. 5). Thanks to that, it was possible to compare measurements collected at different gas pressures.
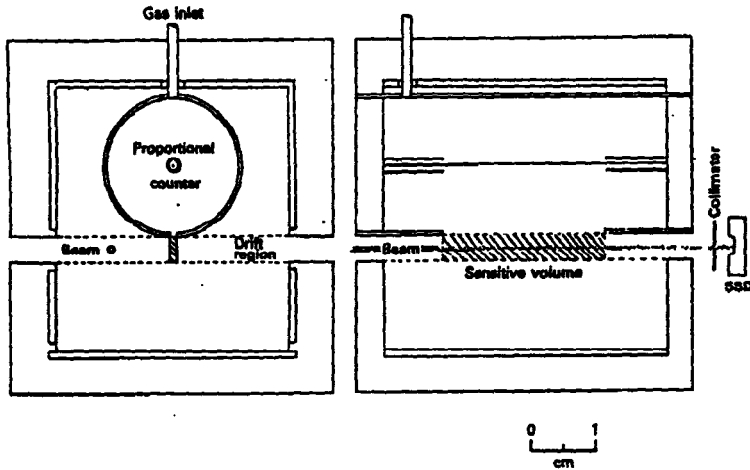
Figure 3

Figure 4 shows the mean ionisation against R for a ^{244}Cm α-particle in propane gas at three different gas pressures. Since the proportional counter gas gain was not known with enough precision, the data are relative and only the curve shapes are meaningful. The lines in figure 4 are power best fits of the data. For the two lower pressures the ionisation decreases with the square root of **R**, for the highest pressure with a power of **R** bigger than 2. This suggest that at low pressure there is a smoothing effect due to the electron diffusion.
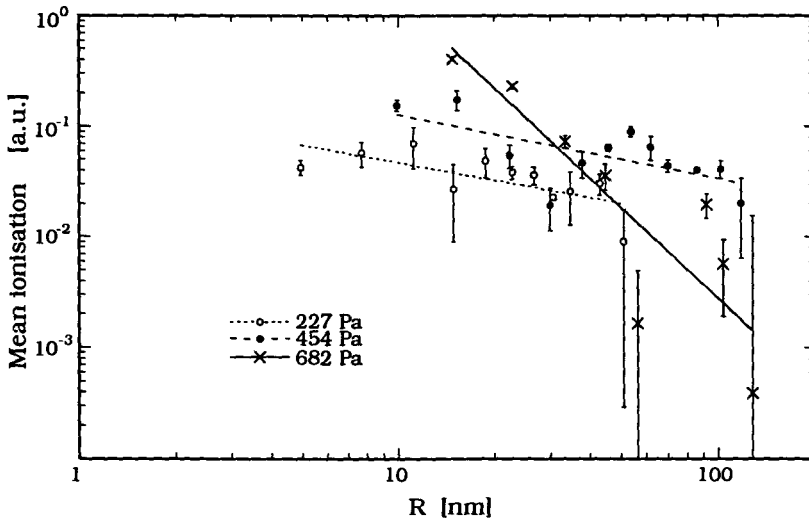
Figure 4

Because of that some features of the experimental curves, like the broad maximum at 10-15 nm at 227 Pa of pressure, are doubtful. Moreover the electronic pulse fluctuations were clearly

dominated by the electronic avalanche statistics inside the proportional counter rather than by the absorbed energy fluctuations inside the sensitive volume.

In order to understand better the electron transport in low-pressure gas detectors, we have therefore opened a collaboration with the research group of P.Segur of the Centre de Physique des Plasmas of Toulouse. Monte Carlo calculations show that the electrons move not in equilibrium with the electrical field when they are close to the electrode walls. This phenomenon increases at low gas pressures. Therefore the electron transmission efficiency through a slit can not be studied by using only the Einstein's relation about the electron diffusion (on which is based the equation 1). More sophisticated Monte Carlo calculations are necessary to optimise the detector resolution.

The other problem risen from the data was the very poor energy resolution of the proportional counter. In order to overtake this problem, we have opened a collaboration with the research group of A.Breskin of the Physics Department of the Weizmann Institute of Science of Rehovot. A single-electron counter (SEC) has been manufactured. It is capable of measuring the ionisation yield by separately counting each single electron, released in the ionisation process. It is free of gas gain fluctuations of the counter. It can therefore efficiently measure the ionisation yield in nanometric volumes and its fluctuations. This could also allow for a better evaluation of the SEE contribution to the ionisation yield and for better data analysis (slit electron transmission efficiency evaluation, discrimination by spurious events and so on). The SEC will substitute the cylindrical proportional counter of the detectors in figures 1 and 3.

The SEC (figure 5) consists of a long drift column with a conical part at the bottom, connected through a small aperture to the SV (sensitive volume). An electron multiplier based on the principle of a multistep avalanche chamber (MSAC) detects the electrons which arrive one by one at the end of the column. In figure 5 the SEC and its counting system are sketched. Electrons created within the SV are collected into the drift volume and diffused under a suitable reduced electric field. Due to longitudinal diffusion the electrons arrive at the MSAC at different time intervals. The MSAC is made of four meshes which define three regions of different reduced electric fields: when an electron arrives at the first region an electronic avalanche is generated, due to the high reduced electric field. The avalanche is then transferred through the second region, without further multiplication, into the third region where it is multiplied again. In such a manner a very high gas gain ($> 10^6$) can be obtained, which allows for an efficient detection of the electron. Other configurations, which use more meshes, can be used in order to maximise the gas gain and to minimise the secondary electron emission.
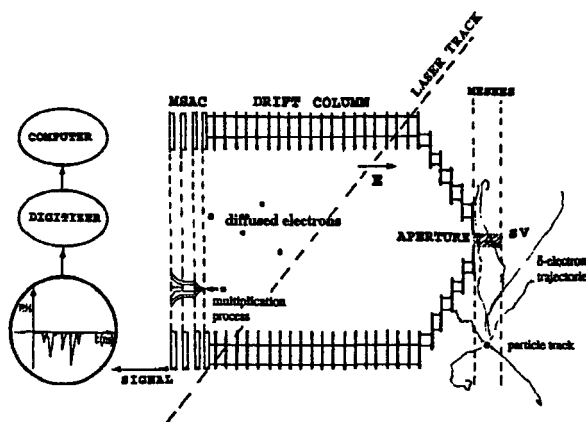
Figure 5

The final signal from the MSAC has a width of only a few tens of nanoseconds, therefore two electrons separated in time by the same order as the pulse width produce avalanches which can be detected separately with a fast digitizer. A long drift column, in our case 200 millimetres, ensures good separation by diffusion and therefore high detection efficiency. The column diameter has to be large enough to minimise the probability of electron loss because of the lateral diffusion. The column we have manufactured is made of a stack of stainless-steel disks of 90 mm internal diameter. The 2 mm thick stainless-steel discs are separated by 3 mm insulator discs. The uniformity of the electric field inside the column is assured by a voltage divider. The electron drift uniformity assures low electron losses. These are checked experimentally with a UV laser beam which diagonally crosses the drift column, passing through two holes opened in the drift column wall. In figure 5 the electrons created by the laser along its track are plotted versus their arrival time. The electrons randomly created near the MSAC arrive after about 1 μs and the last electrons, created near the bottom of the drift column, after about 5 μs. All the electrons created in between these two extreme positions expand over intermediate time intervals. The plateau, in the counted electrons against time plot, indicates that, on the average, the same number of electrons arrives per unit of time, which means that no distortions occurred along the drift path. This experimental test is able to evaluate even the electron losses due to attachment.

The counting electron efficiency of the SEC depends on the gas used and on its pressure, on the reduced electrical field of the drift column and on its length. In figure 6 the counting efficiency of a 200 mm drift column is plotted against the initial number of electrons released at the bottom of the column (pub. 8). The gas was pure propane at 400 Pa of pressure. Figure 6 shows that with low values of **E/p** there is a good and constant efficiency up to 15 electrons. That means that the sensitive volume can not contain more than 15 electrons, otherwise we loose resolution. The SEC puts an upper limit for the simulated volume and for ionisation density. This limit can be overtaken by increasing the drift column length or by using a "colder" gas like dimethylether.
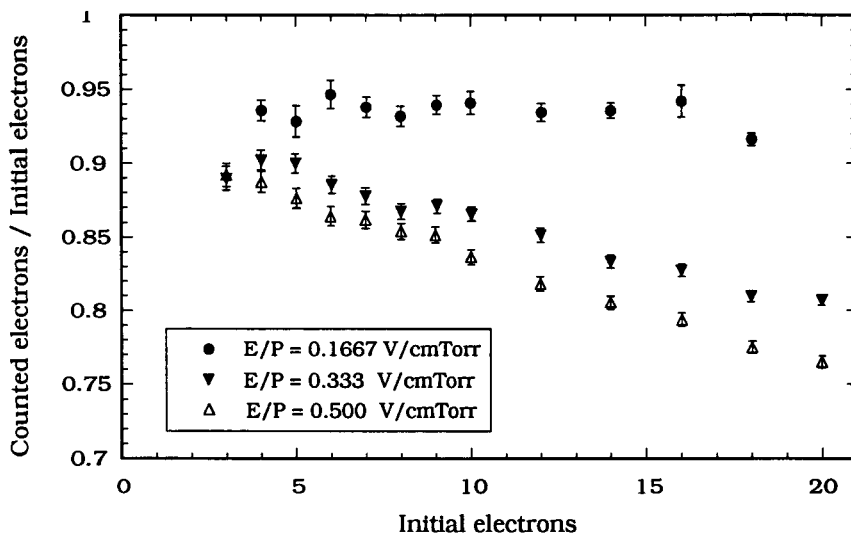
Figure 6

The efficiency of a track-nanodosemeter depends even on the efficiency of collecting the electrons, generated inside the sensitive volume, through the slit. Figure 4 suggests that the electron transmission efficiency depends on the gas pressure. Monte Carlo models have been developed to simulate the electron transmission efficiency trough a slit. Calculations have been compared with experimental data.

The experiments were made with pure propane at 300 Pa (2.25 Torr). A small quantity of TMAE under controlled flow conditions was added in order to increase the ionisation yield. Then the

sensitive volume has been scanned with a Nd-YAG laser beam of 0.5 mm of diameter. In such a manner, free electrons of 4 eV of energy have been generated along the laser track (pub. 12). Figure 7 shows the efficiency of transferring electrons through a slit of 6 mm. The agreement with calculated data is good. The little bit higher efficiency measured inside the slit is probably due to secondary effects due to TMAE.

The status of art of this experiment suggests that the experimental track-nanodosimetry is feasible with simulated volumes not smaller than 10-20 nm. At smaller simulated volumes a smoothing effect occurs, due to non-equilibrium phenomena. The minimum volume, which can be used, depends on the gas, being close to 20 nm for propane and perhaps close to 10 nm for dimethylether. These conclusions are qualitative since the work on the detector is in progress. However this resolution seems to be already enough to check experimentally the so called "invariance theorem", which states that the ratio between the total ionisation and the primary ionisation is constant, in volumes less than about 20 nm of size, with respect to charge and velocity of the primary particle.

This experimental set-up can measure nanodosimetric track features both in the penumbra and in the core of charged particles. However some limitations come from the upper measurable number of electrons. When propane gas is used, the track core is open to the experimental investigation only for protons (E > 200 keV) and alpha particles (E > 1 MeV). These performances can be improved by increasing the length of the SEC, by using other gases and by substituting the MSAC with a position-sensitive detector, so that the electrons arriving at the same time, but in different positions, can be separately measured.
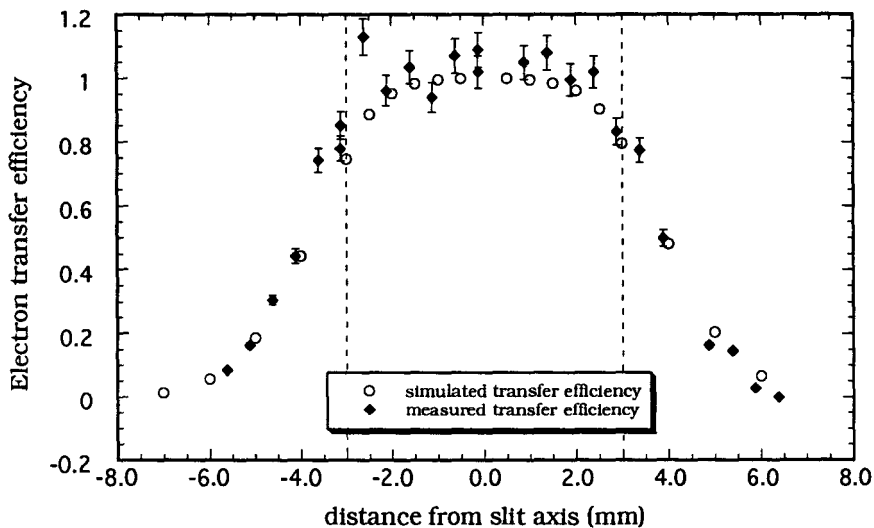
Figure 7

In order to investigate experimentally the ionisation fluctuation features about a charged particle track with simulated volumes smaller than 10 nm, another technique is advisable. We have investigated with Monte Carlo simulations the possibility to measure the ionisation distribution by counting the single positive ions instead of the electrons (publ.13). This experimental technique, which will use a differential pumping system to maintain a good vacuum in the ion counter and few hundreds of Pa in the sensitive volume, looks to be very promising for very small volumes since it should have a spatial resolution much better than 1 nm.

MICRODOSIMETRY AT NANOMETRE LEVEL WITH TEPCs

As far as nanodosimetric track features are relevant for the biological radiation action (hence for the radiation quality), it is necessary to monitor the radiation field with detectors sensitive to nanometric features. A good monitor of the radiation quality is the tissue-equivalent proportional counter (TEPC). However in order to simulate nanometric dimensions TEPCs have to work at very low gas pressures or they have to be very small. In both cases the reduced electrical field inside the detector is not constant and it reaches very high values.

All the gas gain models, used to describe the electron avalanche inside a TEPC, assume that the electron swarm is in equilibrium with the electrical field. This assumption was soon recognised to be valid only for reduced fields of less than few hundreds Volt cm^{-1} $Torr^{-1}$. TEPCs able to simulate nanometric dimensions work very beyond this limit; near their anode wires the reduced electrical field reaches values up to 10^5 Td (1Td=0.33 V/cm·torr) and the field gradients are very high.

Based on the experimental set-up developed in the previous European project, experimental measurements about the variation of the gas gain inside a TEPC have shown that the reduced ionisation coefficient α/N does not depends only on the reduced electrical field E/N (pub. 3). During this project an extensive study has been performed to investigate the features of the electron avalanche inside a TEPC (pub. 4, 7, 9). First aim was to understand the role of the electrical field gradient in a TEPC.

The gain of a cylindrical proportional counter at the equilibrium can be written as:

$$\ln G = K \int_{S_1}^{S_a} \frac{\alpha(S)}{N} \frac{1}{S^2} dS$$

where $K = \dfrac{V}{\ln \dfrac{c}{a}}$

c and a are the cathode and anode radius respectively, S_a is the reduced electrical field at the anode surface S_1 is the reduced electrical field for which α/N is zero, α/N is the reduced ionisation coefficient and N is molecular density of the counter gas.
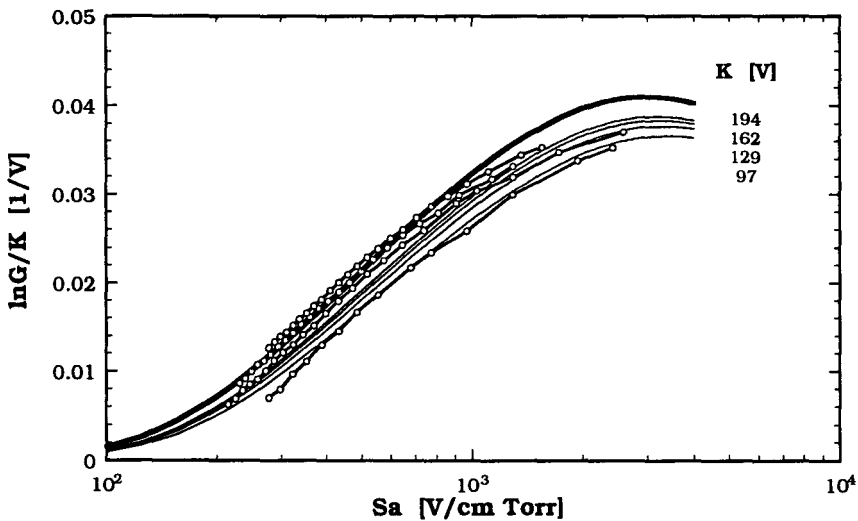
Figure 8

On the other words, the total gain in a cylindrical gas counter is the integration of the reduced ionisation coefficient over the avalanche size, which occupies a volume going from the anode surface to the avalanche limit r_l (where the reduced electrical field has the value of S_l). Since the value of the reduced ionisation coefficient at S_l is zero by definition, the reduced gain is a function of S_a only: $\ln G/K = f(S_a)$. However experimental data and Monte Carlo calculations suggest that the reduced gain depend not only on S_a but even on K.

In figure 8 the experimental data collected with a TEPC (open circles) are plotted against the reduced electrical field at the anode surface for different K values (pub. 9). The data stay clearly on different curves; the equilibrium equation (Campion's) gives on the contrary only one curve (thick line). In order to take into account the experimental data, a new model has been developed which is in good agreement with the experimental data. In this model (thin lines in figure 6) the reduced gain depends on K as it follows:

$$\frac{\ln G}{K} = \frac{L}{M v_i (1 - m)} \left(e^{-M S_a^{m-1}} - e^{-M S_c^{m-1}} \right)$$

where M is:

$$M = \frac{L}{v_i} K \left(e^{v_i / K} - 1 \right)$$

v_i is the effective ionisation potential of the gas, L and m are constants depending only on the gas used.

Monte Carlo calculations confirm the findings of this model. Therefore in general we can write that $\ln G/K$ is a function both of S_a and K, namely: $\ln G/K = f(S_a, K)$. When the electron swarm energy depends only on the reduced electrical field and on its gradient, we can say that it is in a *quasi-equilibrium* situation. However near the cathode and anode walls other physical phenomena take place, which prevent so far the use of simple analytical formulas to describe satisfactorily the electronic transport inside the TEPC.
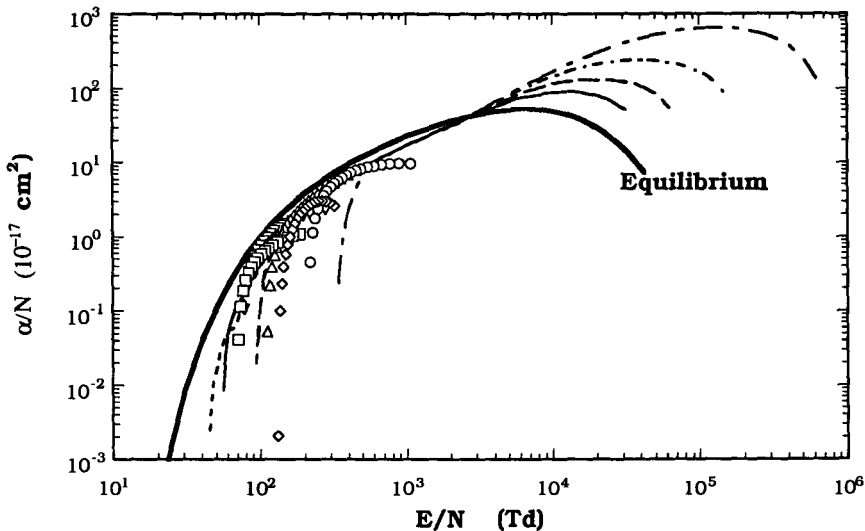
Figure 9

In figure 9 the values which the reduced ionisation coefficient takes at different radial positions inside a cylindrical proportional counter are plotted against the values of the reduced electrical field at those radial positions. Symbols are experimental data, thin lines calculated Monte Carlo data and the thick line points out the expected equilibrium behaviour (pub. 7). The TEPC was filled with a gas mixture Ar-CH_4 (90-10); for this gas mixture we know in fact very well the basic physical data and therefore Monte Carlo data are more reliable. Experimental data could be collected only for low and intermediate values of E/N. The agreement with calculated data is good (the hooks of the experimental data at the end of the curves are artefacts due to limitations of the experimental approach). Both experimental and calculated data were collected at the same value of K.

Clearly the electron swarm does not follow the equilibrium curve. However, since all the data were taken at the same K value, the data were expected to stay on a single *quasi-equilibrium* curve. This is the case indeed, but only for intermediate values of E/N (calculated data between 10^3 and 10^4 Td). That means that the electron swarm is in *quasi-equilibrium* condition only in the intermediate region between the cathode wall and the anode wire. Near the two electrodes other non-equilibrium phenomena occur, because of them the gain depends even on the gas pressure and on S_a independently.

These findings say that the electronic avalanche, when the gas pressure decreases, starts at higher E/N values than expected at the equilibrium and the gain around the anode wire is higher. On the other words, in a TEPC working at low pressure the electronic avalanche is more confined than expected, with respect both to equilibrium and to *quasi-equilibrium* equations, around the anode wire.

In this part of the project we aimed to study the physics of a TEPC, in order to design TEPCs able to simulate properly equivalent lengths less than 1 µm. The analytical model which takes into account the electrical field gradient, and gives the first *quasi-equilibrium* equation to calculate the gas gain, improves considerably the Campion's formula. Experimental work is necessary to evaluate better the range of validity of this model. The non-equilibrium effects near the detector boundaries are relevant at very low gas pressure. A further effort is necessary to determine the physical parameters which govern these effects.

Publications

1. P.Colautti, G.Talpo and G.Tornielli
Measurements of Ionization Distributions at Nanometre Level
Biophysical Modelling of Radiation effects, ed. by K.H.Chadwick, G.Moschini and M.N.Varma, Adam Hilger Bristol,Philadelfia and New York, pp. 269-276 (1992).

2. P.Colautti, G.Talpo and G.Tornielli
Microdosimetry as Specification of the Radiation Quality
Topics on Biomedical Physics. ed. by L.Andreucci, Word Scientific Publ. Singapore, New York and London, (1992).

3. P.Colautti, V.Conte, G.Talpo, G.Tornielli and M.Bouchefer
A Method to Investigate the Working Characteristics of New Microdosimetric Detectors which Use Low Gas Pressure
Nuclear Instruments and Methods, NIM A 321, 392-402(1992).

4. P.Segur, P.Colautti, C.Moutarde, V.Conte, G.Talpo and G.Tornielli
Comparison Between Experimental and Theoretical Determination of the Space Variation of the Gas Gain Inside Low-Pressure TEPC's
Radiation Protection Dosimetry 52, 65-71 (1994).

5. P.Colautti, G.Talpo, G.Tornielli, A.Akkermann and A.Breskin
Measurements of Ionization Distributions Around a Particle Track at a Nanometre Level.

Radiation Protection Dosimetry 52, 329-334 (1994).

6. P.Colautti, V.Conte, G.Talpo and G.Tornielli
Radiation Quality, Microdosimetry and Track Structure
Physica Medica X, suppl.1, 15-18 (1994).

7. P.Colautti, V.Conte, M.Guli, G.Talpo, G.Tornielli, B.Boutruche, C.Moutarde and P.Segur
The electronic Avalanche in Proportional Counters
Radiation Protection Dosimetry 61, 257-262 (1995).

8. A.Breskin, R.Chechik, P.Colautti, V.Conte, A.Pansky, G.Talpo, G.Tornielli
A Single-Electron Counter for Nanodosimetry
Radiation Protection Dosimetry 61, 199-204 (1995).

9. P.Segur, P.Olko, P.Colautti
PC-Report, chapter three: *Numerical Modelling*
Int. Workshop on Advances in Radioprotection Measurements, Chalk River (Canada) 3-6 October 1994 (to be published in Radiation Protection Dosimetry 61, n°4)

10. P.Colautti and P.Pihet
New Trends in Microdosimetry: Implications for Radiation Protection
Invited paper at International Conference on *Radiation Protection and Medicine* , Montpellier 28-30 June 1995. Published in the conference proceedings, 1995.

11. P.Colautti, N.Brassard, V.Conte, A.Courdi, J.Herault, G.Tornielli and P.Chauvel
Microdosimetric Depth Measurements in the Nice Fast Neutron Therapeutic Beam.
Third biennial meeting on physics in clinical radiotherapy (ESTRO), Gardone Riviera, Italy 8-11 October 1995.

12. L.De Nardo
Un Rivelatore per Nanodosimetria di Traccia
Thesis, University of Padova, Physics Department , Academic Year 1994-1995.

13. S.Shchemelinin, A.Breskin, R.Chechik, A.Pansky, P.Colautti, V.Conte, L.De Nardo and G.Tornielli
Ionisation Measurements in Small Gas Samples by Single Ion Counting
Report WIS-95/35/Aug.-PH. Submitted to Nuclear Instruments and Methods in Physics Research A

Head of project 2:   **Dr. Watt**

II.   **Objectives for the reporting period.**   **1992-1995.**
The overall objectives for improved radiation protection were broad, aimed at determining the dominant biophysical mechanisms responsible for induction of biological effects in mammalian cells and to define better quality parameters. The detailed objectives were:
(i)   to explore methods of validating the quality parameter 'the mean free path for linear primary ionisation, λ_i' proposed along with dose-restricted LET, $L_{100, D}$, as a fundamental descriptor of radiation effects.
(ii)   to complete a model for biological effectiveness to be applied to 'unified' dosimetry.
(iii)   to define the desired response for, and explore approaches to the design of, a new generation of instrumentation to measure the new quantities.
(iv)   to re-appraise the consequences of the results for the current ICRP system of risk control.

III.   **Progress achieved including publications.**
Fundamental to the success of the program is the establishment of a reliable biological data base and a compilation of all quantities likely to be required for the analysis of track structure and radiation quality. Some of these quantities e.g ' the mean free path for linear primary ionisation' and the dose restricted LET, $L_{100, D}$, are not available in the literature for the range of radiation types to be analysed.

3.1   **Data-base of radiobiological effects [1].**
A data-base has been compiled of survival, transformations, mutations, dicentric chromosomes aberrations and DNA dsb's induced by ionising radiations has been compiled for a number of cell lines. The literature survey is up to 1995. The data-base is in two major parts.
(i)   Physical parameters.
This includes the radiation type and energy at the relevant point of biological impact; the dose and dose-rate; the appropriate track parameters of dose and track average LET and their restricted values, β^2, z^2/β^2, charged particle range, δ-ray maximum energy and maximum range.
(ii)   Radiobiological data
From the curves of biological effect are determined the: initial and final slopes: α (Gy^{-1}), β (Gy^{-2}) The slopes quoted are as determined by the original authors whenever available, whereas for other older data linear quadratic fitting is used to determine the initial slope [ ]

3.2   **Quantities for the generalised dosimetry of ionising radiations [2-7].**
Averaged values of physical track structure and microdose parameters, important e.g. in radiobiology, nuclear medicine, high and low LET radiotherapy, radiochemistry and radiological protection, have been compiled as a ready reference for use in the interpretation of damage mechanisms and for quantifying radiation effects The calculated results are for a liquid water medium which is also a good analogue to soft tissue and light organic media. In the tables are listed quantities for electrons, 50 eV to 30MeV; characteristic K_α X-rays from carbon to uranium; commonly used radioisotope sources of [241]Am, ^{137}Cs, ^{60}Co gamma rays and for continuous X-ray spectra (up to 300kVand for 26MV); Auger electron and beta-emitter radionuclides including tritium and carbon-14, heavy charged particles having specific energies of 0.1 keV/u to 1 GeV/u for 74 ion types ranging from protons, deuterons, tritons, [3]He and alpha-particles to uranium ions. Aggregate effects in liquid water are taken into account implicitly in the calculations. Novel methods have been developed to determine information at low velocities where experimental information is sparse. Results are presented for

instantaneous particle energies and for averages over the charged particle equilibrium spectra. The latter are of special relevance to radiation dosimetry. Quality parameters calculated are β^2, z^2/β^2, linear primary ionisation and the mean free path between ionisations; LET; track and dose-restricted LET with 100 eV cut-off; relative variances; delta-ray energies and ranges; ion energies and ranges and kerma factors. The microdose quantities of lineal energy and specific energy and their dose distributions are included. Concentrations of charged particles are given because of their relevance to estimating indirect effects in radiochemistry. A complete compilation of the data is to be published by Taylor and Francis (early 1996) to make the information generally available. Of particular interest in the present project are the quality parameters λ_i and $L_{100, D}$

3.3   Preliminaries to modelling.

Prior to modelling, and as a guide to the direction it should take, information was sought directly from published cell survival data for various biological end-points e.g. inactivation, chromosome aberrations, mutations and oncogenic transformations. The approach used was to extract cross-sections for induction of the specified end-points by tracks in the charged particle equilibrium spectrum generated by the incident radiation field. Use of effect cross-sections has two distinct advantages: (i) they provide a means of using the tracks as probes to search for structure within the sub-cellular targets and (ii) they can be expressed as functions of various possible contenders for quality parameters to determine which best unifies the data for all radiation types. Furthermore the data for different biological targets can be unified by taking ratios with respect to the recorded saturation cross-sections thereby providing a means of grouping all the information into the minimal number of curves. These results, obtained solely from the experimental data, provide a clear indication of the quantities and mechanisms to be used in modelling of radiation effects in a generalised way. The relevance to development of a better system of risk control in radiation protection and of the response functions for the required new related instrumentation are obvious.

Conclusions reached from the analyses are:

1.   Radiation quality is best expressed in terms of the 'mean free path for primary ionisation'. $L_{100, D}$ is closely related to this parameter (Harder).

2.   Double strand breaks (dsbs) in the intracellular DNA of mammalian cells are the dominantly important lesion for the end-points of cell inactivation, chromosome aberrations, mutations and oncogenic transformations

3.   There are multiple sensitive sites, identified as DNA segments, amounting to 15-20 sites at risk upon a charged particle track traversal of the cell nucleus. The probability of damaging all sites is an order of magnitude larger for fast heavy charged particles than for electrons - because of the interplay of particle range and the value of the mean free path for damage (averaged over the spectrum of equilibrium electrons generated).

4.   Action is found to be caused by *single tracks*, at doses up to several tens of grays. Consequently the concept of an $\alpha D + \beta D^2$ response has no scientific basis except possibly at very large doses   If it is accepted that action is due to single tracks, then a mechanism must be proposed to explain the observation of sigmoid cell survival curves. Repair has been widely suggested as the explanation for the curved response. For electrons and photons, it is well-established that the shape of survival curves is dose-rate dependent - attributable to indirect (scavengable) action. In the present contract, a time-dependent repair capability, linked to the cell cycle, is hypothesised and is being explored (see section 3.4.3 below).

5.   The magnitude of the saturation ('overkill') effect cross-section for normal mammalian cells is determined by the projected cross-sectional area of the DNA at risk multiplied by the multiplicity factor for segment overlap (see 3 4.4) i.e. ~ 50 μm^2 for fast heavy particles and ~ 4 μm^2 for equilibrium electron spectra.

6.   For fast heavy charged particles, delta-rays are found to have almost negligible effect $\leq$ 10^{-4} per electron.   For slower, heavy particles ($Z > 6$), in the saturation region, the delta ray yield becomes so large that the effect cross-section increases by up to a factor of three times the saturation level. However the damage efficiency of an individual δ-ray remains at $\leq 10^{-4}$. The reason proposed is that electrons are only efficient at inducing DNA dsbs at the very end of their range when the mean free path for primary ionisation is near 2nm (~ 100 eV); their range is only a few nm, they have to stop in the DNA and they have to produce two ionisations which correlate exactly with the double-strands in the DNA.   The very small probability of achieving all these requirements is consistent with the $< 10^{-4}$ quoted above.

7.   As the δ-rays normally play such a minor role and since the 'mean free path for primary ionisation' (the zeroth moment of energy transfer) is found to be the optimal quality parameter it follows that absorbed dose and therefore LET are not relevant parameters for specifying the direct (unscavengable) effects of ionising radiations.   This is probably true also for indirect (scavengable) action because of the combined effects of geometrical proximity, the line source of radicals, competing reactions, and intrinsic efficiency for single strand breakage in the DNA.

8.   RBE's plotted conventionally as a function of LET are shown to lie on independent curves for each radiation type and, therefore, it is invalid to draw a single curve through values of RBE obtained for different radiation types (and different LET's).   In the past it has been demonstrated that RBE reaches a maximum value, for any fast heavy charged particle type, when $z^2/\beta^2 \sim 2000$. z^2/β^2 is not applicable to slow heavy particles. However this can now be replaced by the more general rule that maximum RBE for any specified end-point for mammalian cells, will occur when the net 'mean free path for primary ionisation' is equal to 2 nm.   For mean free paths less than 2nm, saturation occurs and so the δ-ray effects discussed in 6 above for slow particles do not alter this conclusion.

9.   As the effect-crossection is an absolute measure of the biological effect for the irradiation conditions used, hence a system of dosimetry based on the equilibrium charged particle fluence weighted appropriately for the quality defined in terms of the 'mean free path for primary ionisation' will provide a measure of the absolute biological effectiveness. Better control over the effectiveness of radiation fields of any type should be attainable.   RBE's, quality factors and radiation weighting factors in their present form should become redundant.

10.   Consideration of the foregoing conclusions implies strongly that the basic mechanism of radiation damage to normal mammalian cells is due to the correlation between randomly produced ionisations spaced at $\sim$2 nanometres along single charged particle tracks in the equilibrium spectrum with the similarly spaced strands of the intranuclear DNA.   A template action is proposed.   Ionisations at other orientations do not fulfill this requirement and so absorbed dose and conventional microdosimetry, even at the nanometre level, do not comply with the requirement although it may be possible to derive approximate adjustments using probability functions.   The biological effect is found to depend on the *number* of such events, the energy transfer per event (and therefore absorbed dose and LET) plays no role.   On the basis of the present argument it seems unlikely that clustering plays a special role beyond that found for the singly spaced ionisations, except possibly in the severity of damage at the break.

These results are deduced directly from the trend of effect cross-sections derived from analyses of the extensive literature on cell surviva curvesl.

Modelling the proposed mechanism is of value to indicate methods of testing the conclusions reached, to provide a scientific framework for specifying instrument response functions and design; for resolving the extrapolation to low doses near environmental levels and to indicate the direction and requirements for validating a new system of risk control in radiation protection

3.4 Modelling of Biological Effectiveness. [8,9]

Basically the problem is to determine the yield of DNA double strand breaks for single tracks. Damage is presumed to be caused by direct ionisation, indirect radical action and combined direct and indirect action.

3.4.1 Direct (non-scavenging) action.

The biological effect cross-section is given as:

$$\sigma_B = \sigma_S . \varepsilon(\lambda) \quad - - - - - (1)$$

The meaning of the quantities in equation (1) are given in section 3.4 4

3.4.2 Indirect (radical) scavenging action.

The modelling scheme used to determine the indirect contribution to strand damage in the DNA in mammalian cell nuclei is based on analogy with damage to enzymes in solution. First the transition of damage from the solid to liquid phases at different concentrations of enzyme targets (known to be inactivated by single target, single hit kinetics) was investigated. The respective contributions from direct and indirect action can then be separated. Results obtained in this laboratory for the inactivation of dihydro-orotate dehydrogenase by Cu K_α X-rays at different doses and dose-rates and for the inactivation of ribonuclease by X-rays of various LET, for a range of concentrations in solution and in the dry state, have been supplemented by data taken from the literature. A simple model of the radiation action has been derived. The cross-section for enzyme inactivation by indirect action, σ_{ind}, is obtained by solving the differential rate equations to get:

$$\sigma_{ind} = \sigma_r . v_r . t_r . \overline{L_{100,\,T}} . G \times 10^5 \quad - - - - - (2)$$

Equation (2) allows for decay of radicals after the end of the irradiation time. σ_r is the interaction inactivation cross-section for radicals having mean diffusion velocity v_r. t_r is the mean lifetime of radicals = $1/(k_2 C_{z,0} + k_3 Q)$ where $C_{z,0}$ is the initial concentration of enzyme targets, Q is a radical scavenger of arbitrary concentration and the k's are reaction rate constants. G is the value for production of the relevant radicals per 100 eV energy expenditure in the solution. $L_{100,\,T}$ is the restricted LET in keV/μm averaged over the equilibrium charged particle field. Equation (2) succeeeds in correlating all the data within the range of concentrations, radical scavenger, and LET tested. Further attention to dose rate effects is required. From the results, information is obtained on the role of the dose-rate; on diffusion lengths, on the type of radical predominantly responsible (OH) for the inactivation and on scavenging of radicals. Since water radicals are thought to be the main cause of indirect damage in mammalian cells it is a simple step to deduce from the enzyme results the probability of induction of single and double strand breaks in the DNA by making the assumption that basically the same radical kinetics are involved and then applying Poisson probabilities Certain parameters are left 'free' to enable transfer from the enzyme in solution to the intra-cellular fluid. The results can be tested against reported experimental measurements of the yields of DNA double-strand breaks.

3.4.3 Repair of damage, U(t_r/t_r) function [20].

The duration of the irradiation, the nature of the cell population, whether it is synchronised or asynchronised, and the link to the position in the cell cycle are important factors in determining the shape of the cell survival curve in the present model. Further study is being pursued to investigate the validity of the proposed function and to extract values for the mean repair times.

3.4.4 Model for cell inactivation by ionising radiation: probability of double-strand breaks in intracellular DNA [20].

$$\frac{\sigma_B}{\sigma_S} = [\varepsilon_{dsb}(\lambda) + (\frac{\sigma_{ssb}}{\sigma_S})^2 + 2.\varepsilon_{ssb}(\lambda).(\frac{\sigma_{ssb}}{\sigma_S})].U(t_i/t_r)$$

$$\sigma_S = [\sigma_{g,DNA}.n_0.\frac{\overline{R}}{d}] \quad - - - (3)$$

n_0 = number of dsb segments at risk per track traversal (~ 15 for fast ions).
d = mean chord length through the cell nucleus.
R = the mean projected range of the relevant tracks. If $R > d$, $R/d = 1$ which allows for the reduced number of DNA segments at risk for 'stopper' and 'insider' tracks (in microdosimetry terminology).
$\sigma_{g,DNA}$ = the projected area of the intranuclear DNA - varies with cell type.
σ_S = the saturation cross-section = $\sigma_{g,DNA} n_0.R/d$
$\varepsilon_{dsb}(\lambda)$ = the efficiency of dsb production by direct action.
$\varepsilon_{dsb}(\lambda) = e^{-\lambda_0/\lambda}(1-e^{-1 0/\lambda})^2$; $\lambda_0=1.8$ nm and λ = mfp for linear primary ionisation.
$\varepsilon_{ssb}(\lambda) = 1-e^{-1.0/\lambda}$ = efficiency for ssb production by direct action in a single DNA strand.
$\sigma_{ssb} = a_1.e^{-a2}.(1-e^{-a3 L})$. a_1 is a radical interaction cross-section determined by the diffusion length. a_2 is a scavenging efficiency for radicals and $a_3 L_{T,100}$ is the mean number of reactions with DNA strands.
$U(t_i / t_r)$ = probability that dsb's remain unrepaired. t_i = duration of irradiation; t_r = mean repair time.

3.4.5 Discussion of models [10,29].

 An extensive review of the many models of radiation damage was completed, attention being given to 5 main types: lethal and potentially lethal (Curtis); pairwise lesion interaction (Harder); cellular track structure (Katz); hit-size effectiveness (Bond and Varma) and the present linear ionisation model (Watt).   Test criteria used for comparison were, the induced initial slopes and final slopes of the survival curves; the number of parameters and their meaning, the basic concepts involved.   Further mathematical techniques were applied to enable the calculated results from the models to be compared on a unified plot to explore deviations from the straight line thereby emphasising regions of difference and the degree of importance.   Fits of the models were made to bench-mark data to identify the suitability of parameters used and for intercomparison of the models Comparisons were also made of the first and second derivatives of the calculated survival curves.   The conclusions were not encouraging. Most of the models can fit the experimental data by adjusting free parameters. Most of the models are suitable for interpolative purposes but not suitable for extrapolation to low doses.   The linear ionisation model is selected here because it is derived directly from the experimental observations and has a repair component.   Testing the validity of models has long been known to be a major problem.   Some support for the validity of a model can be found in its ability to predict and explain unusual dosimetric observations as described below.
With the acceptance that double-strand breaks in the DNA are key lesions, it would appear that a good test for models can now be made against the experimental data for single and double strand break production now becoming available.

3.4.6   Applications as test of validity.

3.4.6.1   Inverse dose-rate effect [11].

An explanation for the mechanism of the so-called 'inverse dose-rate effect' (IDRE) observed by (Hill et al in 1982) for transformations in mouse fibroblasts irradiated with fission neutrons emerges naturally from the proposed model using λ_i as a quality parameter. The effect is attributable to the different degree of damage caused by direct and indirect action and to the duration of the irradiation linked to the position in the cell cycle combined with the repair capability. IDRE is expected to occur only for neutrons and fast heavy charged particles in unsaturated damaging conditions. Consequently it should not be observed for natural alpha particles at energies near or < 4.0 MeV but should be seen for accelerated alpha particles   Also it is not expected to be detectable for photon and electron irradiations because the yield of dsb's per track is much lower, repair is more efficient and therefore the overall effect is lost in the statistical errors. Dose-rate is not directly concerned in the effect. It is the duration of the irradiation that is predicted to be important combined with the relative proportions of direct and indirect effects. For low dose-rates , the irradiation time is usually extended compared with that at higher dose-rates. The role of time could be tested by fixing the dose-rate but varying the irradiation time and expressing the results for equal doses.

3.4.6.2   Auger electron cascades from incorporated radionuclides and resonance absorption in bound phosphorus [12,13; 19-21].

Electron-emitting radionuclides, especially those decaying by Auger-electron emission, are known to be excessively damaging when incorporated into the nuclear component of mammalian cells. The subject is of considerable topical interest because of the importance in nuclear medicine as well as the general implications for radiation protection. Conventional dosimetry is widely recognised as being inadequate to quantify the observed effects. The claim is made that Auger electron emitters such as ^{125}I exhibit the damage properties of high LET particles.   When the cell survival curves are interpreted using effect cross-sections it is found that [77]Br and ^{125}I produce saturation damage thereby reducing their observed effectiveness which when compared external beam irradiations in the unified scheme leaves a satisfactory safety factor for radiation protection purposes. The apparently excessively large effectiveness found in the conventional system is simply due to the multiplicity of electrons emitted in the Auger electron cascade, some of which are in the saturation region ($\lambda_i \sim$ 2nm). These factors are automatically allowed for in the fluence-based system used here. The efficiency of dsb production per decay due to direct effects by ^{125}I incorporated into the DNA of mammalian cell nuclei is about 1.25%
In collaboration with Kobayashi et al, two key experiments were analysed in terms of track structure parameters to obtain information on the excessive damage observed upon the production of inner shell vacancies at the resonance energy of bound phosphorus and for bromine incorporated into DNA   The relative damage enhancement factor due to resonance in phosphorus is 1.32. Additional Auger electron cascade events induced at resonance contribute about 35% to the total effect cross-section. In the bromine experiments, the intrinsic effectiveness is shown to be less than that for phosphorus   The effects were adequately quantified by the equilibrium electron fluences generated, combined with a quality specification determined from the net mean free path for linear primary ionisation. This was not possible with conventional dosimetry.

3.4.6.3   High LET therapy [14].

Much discussion has ensued on the optimum type of accelerated ion to be used in high LET particle therapy.   From the mechanisms proposed here, the maximum RBE will always occur when the mean free path for linear primary ionisation of the charged particle is uniquely equal to ~2nm in the cell nucleus.   [The corresponding LET's are multi-valued viz: p, 75 keV/μm; α, 125 keV/μm; ^{12}C, 217 keV/μm; ^{20}Ne, 254 keV/μm; ^{40}Ar, 340 keV/μm}.   Consequently the same bio-physical therapeutic advantage will be the same for any ion type under the foregoing conditions.   Other factors to be considered are the ranges over which the 2nm spacing can be sustained in the cell nucleus and the possible effects on surrounding healthy tissue of the delta-ray penumbra emitted by slow ions in the region of saturated damage.   The delta ray contribution does not alter the position of the maximum RBE.

3.4.6.4   Proposed system of risk control for Radiological Protection [18,22,28].

On the basis of the unified system of 'dosimetry' proposed an improved system of 'dose' limitation based on fluence can be constructed for better risk control.   When compared with the current legally adopted system, points of anomaly emerge e.g. the inappropriateness of the same ICRP radiation weighting factor of 20 for fast neutrons, heavy accelerated ions and natural alpha particles.   Neutrons at their most damaging can never be as effective as the most damaging heavy particles, for equal fluences.   The significant differences in effectiveness with photon energy for X and gamma rays and fast electrons per unit fluence is appropriately quantified.   In the case of neutron irradiations, the evaluation leads to a simple smooth effect curve which harmonises with the histogram of radiation weighting factors recommended by ICRP making the latter step function obsolete.

The ICRP risk coefficients, R_{ICRP}, are currently:

1)   for radiation workers the risk which corresponds to a dose limit of 20 mSv per year is determined from the cancer risk coefficient (R_{ICRP}) of 4×10^{-2} Sv^{-1} (called the 'nominal probability coefficient' by ICRP) to be equal to $20\times10^{-3}\times4\times^{-2} = 8\times10^{-4}$ per year

2)   for the general population the dose limit is 1 mSv per year and the cancer risk coefficient (R_{ICRP}) is 5×10^{-2} Sv^{-1} which corresponds to a risk of $1\times10^{-3}\times5\times10^{-2} = 5\times10^{-5}$ per year.

Risk factors, R_f per unit fluence, proposed in the new system, are related to the current ICRP risk factors by .

$$R_{f,\,\gamma} = R_{ICRP}\cdot\frac{K_{f,\,v_c}\cdot Q_{v_c}}{\sigma_{B,\,v_c}}\cdot\sigma_{B,\,\gamma}$$

$$R_{f,\,n} = R_{ICRP}\cdot K_{f,\,n_c}\cdot\frac{Q_{f,\,n_c}}{\sigma_{B,\,n_c}}\cdot\sigma_{B,\,n}$$

$$R_{Tot} = R_{f,v_c}\cdot\phi_{\gamma} + R_{f/n}\cdot\phi_{n} \quad ----\ (4)$$

where K's are kerma factors, Q's are quality factors for the reference radiations, subscript 'c'. R_{Tot} , the net risk for a mixed field of photons and neutrons., can be obtained by substituting the cross-section ratios determined from equation (5).

3.5   Instrumentation for absolute dosimetry [15,27].

From the cross-sections for inactivation of mammalian cells, empirical response functions can be derived in the form:

$$\frac{\sigma_B}{\sigma_S} = a.\lambda^{-b} \quad - - - - - - (5)$$

valid for $\lambda > 1.8$ nm, where a (~ 0.34 for photons; 1.84 for heavy particles) and b (~ -1.28 for photons and -1.18 for heavy particles) are constants.   This response is obtained directly from the biological data and is independent of modelling. On the other hand, from the model, one can conclude that an instrument designed to have an appropriate number of pairs of sensitive sites (~ 20) spaced at about two- nanometres and triggered by coincident ionisations in a pair will have a response equal to the initial damage to a sensitive site in a mammalian cell.   The response will be independent of radiation type. It is the *number* of pairs triggered that appear to matter, not the energy deposition.   Initial approaches to achieving such a detector, within limited available resources, have concentrated on studies in nanometre depletion layers in n-type MOSFET semi-conductors.

Another device being studied utilises the doping concentration of thin scintillators to achieve the desired spacing of two nanometres combined with mathematical interpretation of the probability of the appropriate pairs of scintillation centres being triggered.   A feasibility study on the likelihood of success has been published and experimental work is proceeding.

References.

(1)   A data-base of published biological results for interpretation of damage mechanisms   Alkharam A.S. University of St. Andrews Report Biophys/10/95. University of St. Andrews, St. Andrews, Fife KY16 9SS. U.K.

(2)   Quantities for generalised dosimetry of ionising radiations in Biology, Medicine and Protection.   [Track structure data for ionising radiations in liquid water]. Part 1: Electrons and Photons. Watt D.E.   St. Andrews University Report, Biophys/10/89. Abstr. in Int. J. Radiat. Biol. 58, 917, 1990.   Revised, 6/1995. To be published, Taylor and Francis, London, 1996.

(3)   Ibid.: Part 2. Heavy charged particles, 0.5 keV/u to 1 GeV/u.   Watt, D.E University of St. Andrews. Report Biophys /2 /1993, Revised 1994. To be published Taylor and Francis, London, 1996.

(4)   Ibid.. Part 3: Neutrons 0.5keV to 100 MeV.   Watt D.E. St. Andrews University Report: Biophys /11/1993   Revised Jan. 1995. To be published Taylor and Francis, 1996.

(5)   Stopping Powers and Ranges for Protons and Alpha Particles. ICRU Report 49. Berger, Inokuti, Andersen, Bichsel, Powers, Seltzer, Thwaites and Watt. 1994. International Commission on Radiation Units and Measurements, 7910 Woodmont Ave. Bethesda, Maryland 20814, USA.

(6)   Charged particle track structure parameters for application in radiation biology and radiation chemistry   Watt D.E. and Alkharam A.S. Int.J.Quantum Chemistry· Quantum Biology Symposium 21, 195-207, 1994.

(7)   Heavy particle track structure parameters for biophysical modelling   Watt D.E. Nucl. Instr. and Methods in Physics Research B. 93, 215-221, 1994.

(8)   Observed cellular effects lead to a track 'core' model of radiation action. Watt D.E., Kadiri L.A. and Glodic S. Workshop on 'Biophysical modelling of radiation effects',

Watt D.E. Padua, Italy. September 2-7, 1991. Chapter 7, 201-209. Adam Hilger, 1992.

(9) An empirical model for induction of double-stranded breaks in DNA by the *indirect* effects of ionising radiations. Watt, D.E. and Hill, S.A. 11th Symposium in Microdosimetry, Sept. 1992. Radiat. Protect. Dosim. 52, nos.1-4, 17-20, (1994).

(10) Dose as a damage specifier in radiobiology for radiation protection. Watt D.E., Alkharam A.S., Child M.B. and Salikin M.S. Radiat. Res. 139,(2), 249-251 1994.

(11) Comment on radiation effects with special reference to transformations. Watt D.E. Letter to the Editor. Int. J. Radiat. Biol. Vol 61, No.2, 263-267, 1992.

(12) Comment on the damage induced by monoenergetic X-rays at the resonance absorption energy of intracellular phosphorous in yeast cells. Jin,T., Watt,D.E. and Kobayashi, K. 4th Intn. Conf. on Biophysics and Synchrotron Radiation. Aug.30th-Sept.5th, 1992. Tsukuba, Japan.

(13) Damage induced by monochromatic synchrotron X-rays at the resonance absorption energy of intracellular phosphorous in yeast cells. Jin,T., Watt,D.E. and Kobayashi, K. Applied Radiation and Isotopes: International Journal of Radiation Applications and Instrumentation, Part A.45,(7), 767-772, 1994

(14) Assessment of components of radiation action by relativistic nuclei. Watt D.E. and Storey J. BARN, 1992. Conf. on Biological Applications of Relativistic Nuclei, Clermont- Ferrand, France, Oct.14-16, 1992. Eds. J.P.Alard and J.C.Montret. Report No. PCCF RI 9308, 1992. Laboratoire de Physique Corpusculaire, Universite Blaise Pascal, IN2P3 CNRS, 63177 Aubiere Cedex.

(15) A feasibility study of scintillator microdosimeters for measurement of the bioeffectiveness of ionising radiations. D.E.Watt and A. Alkharam. Workshop on Advances in Radiat. Measurements, AECL/CEC/DOE Chalk River, Oct 3rd-6th. 1994 Radiat. Prot. Dosim. (in press), 1996.

(16) Microdosimetry: biophysical quality of ionising radiations at the sub-cellular level. Watt, D.E. Invited opening presentation to the 6th European Symposium on Radiopharmacy and Radiopharmaceuticals. March 5th to 8th , 1995, Graz Austria.

(17) Proposals for a unified system of bio-effectiveness and its consequences in practice for radiobiology, radiation protection, particle therapy and nuclear medicine. Watt, D.E. ARR Meeting, University of St. Andrews, April 5th-7th, 1995.

(18) Bio-effectiveness in nanometre sites for an improved system of risk control in radiation protection. Salikin, M.S. and Watt, D.E. ARR Meeting, St. Andrews, April 5th-7th, 1995.

(19) Unified Dosimetry: Biophysical effectiveness of incorporated electron-emitting Radionuclides. 3rd. Int. Symp. on Biophysical Aspects of Auger Processes. Aug. 24-25, 1995. Univ. of Lund, Sweden. submitted to Acta Oncologica.

(20) Physical specification of the biological effectiveness of electrons from incorporated radionuclides. Khan, S. and Watt, D.E. Poster P01-15, Tenth Int. Congress of Radiat. Research, Würzburg, Germany, Aug.27-Sept.1, 1995

(21) Cross-sections for the biological effectiveness of electrons in mammalian cells. Watt, D.E. and Khan, S. 3rd. International Symposium on Biophysical Aspects of Auger Processes, University of Lund, Sweden. Aug.24-25, 1995.

Other indirectly related publications.
(22) Preparation of A-150 tissue-equivalent plastic films. Saion, E.B. and Watt, D E. Phys. Med. Biol. 37, (12), 2303-2308, 1992.

(23) Calculation of effective stopping power of ions generated by neutrons in tissue constituents. Saion, E.B. and Watt D.E. Pertanika 15, (1), 55-59, 1992.

(24) Inherent calibration of microdosemeters for dose distributions in lineal energy. Crossman J.S.P. and Watt D.E. Radiat. Protect. Dosim. 55 (4) 295-298, 1994.

(25) Endo-microdosimeters for the control of radiation effectiveness in therapy applications. Crossman, J.S.P., Foster, C.J. and Watt, D.E. Workshop on Advances in Radiat. Measurements, AECL/CEC/DOE Chalk River, Oct 3rd-6th. 1994. Radiat. Protect. Dosim. (in Press), 1996.

(26) Yields and quality of photoneutron fields in the vicinity of high energy therapy machines. Al-Janabi M., Crossman J.S.P., Foster C.J., Robertson M. and Watt D.E. Radiat. Protect. Dosim. 52, No. 1-4, 119-122, 1994.

PhD theses:

(27) Advances in semiconductor device design for radiation detection in medical and industrial application. A. M. Yusuf. PhD thesis, 1992. Univ.of St. Andrews, Fife, Scotland, UK.

(28) An improved system of damage limitation for better risk control in radiological protection near environmental level. Salikin S.Md. Ph.D. thesis, University of St. Andrews, Dept. of Physics and Astronomy, St. Andrews, Fife KY16 9SS. U.K.

Head of project 3: Prof. Harder

Introduction

The dose-effect relationships for all known biological effects of ionizing radiation - from long-known effects like radiation-induced mutations or cell death up to effects studied more recently such as cell transformation or change of gene expression - show a well-established common phenomenon: they depend on „radiation quality", i. e. on the composition of the given radiation field from particles of various types and energies [1, 2]. Consequently, it is generally accepted that radiation quality has to be accounted for in practical decisions such as the setting of dose limits for radiation protection or the prescription of target doses in radiotherapy. There is also common agreement that the key to understand the mechanism(s) causing these influences, and to quantify these influences more specifically than by the statement of particle types and energies, has to be found by accounting for the „track structure", i. e. the topologic pattern of the ionizations and excitations produced along the pathes of these particles through matter.

But this general insight is already the essence of what has been commonly accepted. Still not solved in a satisfying way is the question whether the pattern of energy deposition along particle pathes can be effectively represented by a widely applicable and commonly acceptable *quantitative parameter* of radiation quality. Remarkable changes of opinion have recently occurred. The parameter „unrestricted linear energy transfer", L_∞, frequently abbreviated as „LET", by which ICRP had characterized radiation quality over many years [3], was criticized in a common task group report of ICRP and ICRU [4], and a few years later ICRP *abandoned* its long-standing practice of associating the „quality factor", by which body doses of different radiation qualities are weighted, with LET [5]. ICRU maintained the Q(LET) approach for the realm of radiation protection measurement [5]. After this, the community of microdosimetry has been left with the unsolved question whether some more suitable physical parameter of particle track structure could be found to do the service in which LET has failed.
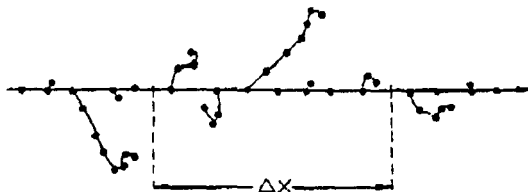
Figure 1 a
Definition of unrestricted LET:
$L_\infty = \lim_{\Delta x \to 0} \Delta E_\infty / \Delta x$. The deposited energy ΔE_∞ comprises all delta rays irrespective of their range
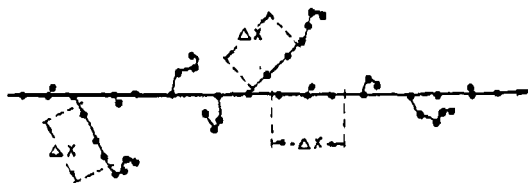
Figure 1 b
Definition of restricted LET:
$L_\Delta = \lim_{\Delta x \to 0} \Delta E_\Delta / \Delta x$. Delta rays with initial kinetic energies $\geq \Delta$ are excluded from ΔE_Δ. These long-range delta rays are characterized by their own L_Δ values

The idea of the present research project, grown during the history of microdosimetry [6], was to make a new attempt into the task of finding a commonly acceptable parameter of radiation quality. There were new, encouraging facts, namely the observation that the important topological effects of track structure, such as the proximity between physical energy deposition events or of the molecular lesions arising from them, are to be sought on the *nanometre* scale. This was indicated by the structures of DNA and other biomolecules and was shown specifically by biophysical experiments with ultrasoft X-rays [7], whose photoelectrons have ranges of the order of 10 nm. If nanometres were the relevant scale for the track structure pattern to be resolved, it became immediately clear that the role of the long-range delta rays, which are

carried away from the path of the primary particle (the „track core") over micrometer or even millimeter distances, had to be reconsidered. The resulting idea was to modify the LET concept by excluding kinetic energies transferred to delta rays if these energies exceed a *cut-off value* Δ, thus arriving at the definition of *restricted linear energy transfer*, L_Λ (see fig. 1).In this concept, going back to Burch [8] but left almost unconsidered for many years, the short-range delta rays are treated as an integral part of the „track core", but the long-range delta rays are approximately regarded as if they constitute an independent, superimposed electron radiation field with own values of restricted LET, and their statistical correlation with the primary particles' pathes is treated as negligible. It has been the task of the present research project, which came out of discussions on the symposium on microdosimetry in Rome, 1989, to investigate the implications and the range of applicability of the restricted LET concept [16].

Thus the present report aims at the question whether restricted LET has the desirable properties enabling it to take over the role left open after the abandonment of unrestricted LET, i. e. to serve as a physical parameter of radiation quality able to predict the magnitude of effects for a given dose of any type of radiation. Fortunately, a theoretical background represented by the „independence theorem" and by the regularities of the compound Poisson distribution has been available, and there has been invaluable help from other members of the EC research project group coordinated by Dr. Colautti. As we will see, restricted LET is showing the features of a widely useful physical parameter of radiation quality.

Theory

There is more than one biophysical model of the mechanism by which particle track structure may influence the yield per unit dose of radiobiological effects. The „threshold" model requires a minimum of energy deposition per particle traversal through a target. The „interaction" model makes the efficiency of a particle traversal dependent on the probability of pairwise interaction between primary molecular lesions, i. e. of a second order reaction. The model of „multiply damaged sites" attributes enhanced molecular effects to particle traversals with higher degree of localized molecular damage. These models have in common that the efficiency of a particle traversal does not simply depend on the mean value, but on the stochastic distribution or „fluctuation" of energy deposition per particle traversal. Even at a low mean value of energy deposition, the distribution function would attribute some probability to traversals with sufficiently high amount of energy deposition, for instance due to low-energy delta rays accompanying the traversal of high-energy electrons.

Thus, the demand to be put on a useful physical parameter of radiation quality would be to represent the *fluctuation*, not only the mean value of energy deposition per particle traversal. It is long known [9] that the main features of the track structure of an ionizing particle are (1) the pearl-chain-like sequence of the interactions of the primary particle with matter, whose number on a given track segment is *Poisson distributed*, and (2) the branch tracks of the secondary electrons or delta rays, whose initial energies are distributed according to *collision kinematics* (see fig. 1). Therefore, the distribution of the energy deposition in a given target due to a particle traversal is a *compound Poisson distribution*, whose variance is given by two factors, the mean value of the Poisson distribution of the number of primary ionizations, and the variance of the energy deposition associated with a delta ray branching off from the spot of a primary ionization. In a paper of fundamental importance, Kellerer and Chmelevsky [9] have shown that the latter variance is strongly increasing with increasing maximum energy of the delta rays
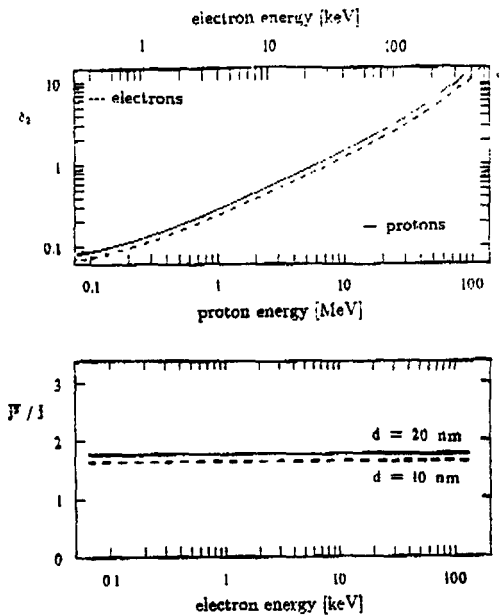
Figure 2

Fluctuation of energy deposition by electrons and protons in targets with total reabsorption of the delta particles (upper panel, Kellerer and Chmelevsky [9]) and in cylinders with finite diameter (lower panel, Bartels [16]). The ordinate is the quotient of the second and first distribution moment of energy deposition (upper panel) resp. of the number of ions (lower panel) associated with one particle traversal

and therefore with increasing energy of the primary particle (see fig. 2). After this analysis, it appeared hopeless to characterize the whole of the fluctuation of energy deposition per particle traversal by the single parameter unrestricted LET, and this caused the verdict of the latter by ICRU 40 [4].

However, Kellerer and Chmelevsky had treated a special geometrical case, namely a target of laterally infinite width, able to *completely reabsorb* all delta rays originating from the path of the primary particle (see fig. 1), and already in their Monte Carlo calculations for varying target diameters the picture changed. The other extreme, targets with diameters of the order of ten nanometres, was treated by our group, which was interested in radiation action on biomolecules and had seen the expression of track structure effects of ultrasoft X-rays [7]. For target cylinders of 10 and 20 nm diameter, our Monte Carlo calculations showed a completely new regularity, namely the *independence* of the delta-ray fluctuation contribution from the energy of the primary particle [10]. This striking new feature (see fig. 2) was due to the *escape of the long-range delta rays* from the target in which they were generated, so that their influence on the fluctuation of energy deposition within this target was practically eliminated. The dominating part of the fluctuation of energy deposition per delta ray which now remained was made up from *short-range delta rays completely reabsorbed* in the nanometre target.

This constancy of the delta-ray contribution to the fluctuation of energy deposition in a nanometre target meant that the second of the two above-mentioned contributions to the variance of the compound Poisson distribution, the delta-ray contribution, was *invariable*, so that only the contribution of the fluctuation of the number of primary ionizations remained as a variable depending on type and energy of the primary particle. But since the number of primary ionizations on a given track segment is *Poisson* distributed, and Poisson distributions have only one parameter (the mean value), the only remaining variable parameter is their *mean* number, which is simply the product of the mean linear primary ionization density and the mean target thickness. Therefore, the specific geometrical feature of nanometre targets, namely the escape of the long-range delta rays, *eliminates* the fundamental difficulty treated by Kellerer and Chmelevsky, and it re-establishes the notion that radiation quality can be described by a *single* physical parameter, although full account is given to the fluctuation of energy deposition per particle traversal through the target.
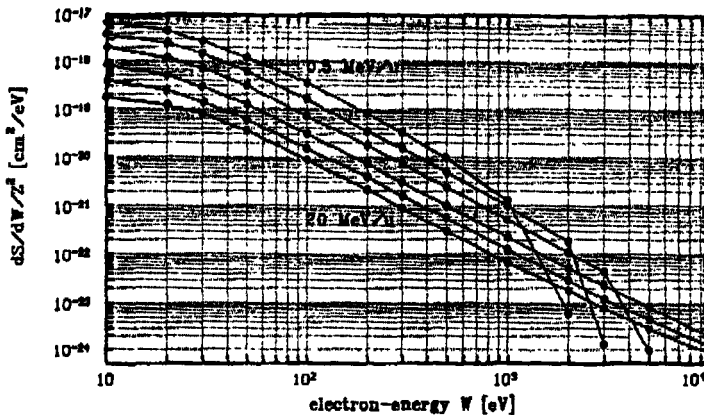
Figure 3

Initial spectrum of secondary electrons released from water vapor by light ions of charge Ze and specific energy 0.5 - 20 MeV/u [14].

Therefore, the most direct choice of a suitable parameter would certainly be the mean linear primary ionization density, but we have chosen to use a parameter practically proportional to it [11], the restricted linear energy transfer with a low value of the cut-off energy Δ, for instance $\Delta = 100$ eV. Restricted LET does not present difficulties with the definition of ionization which may arise in the case of non-gaseous materials, furthermore it is well tabulated in applications of the Bethe theory [12, 13], and it is a known concept introduced already in ICRU 16 [1]. The delta rays with initial kinetic energies exceeding value Δ are treated as an independent admixture to the radiation field, which is justified due to their longer ranges. The choice of the cut-off energy Δ has to warrant both that restricted LET is closely proportional to linear primary ionization density, and that the tracks of delta rays with higher initial energies are sufficiently delocalized from their place of origin; therefore $\Delta = 0$ would not be a good choice.

But before we embark into practical applications, there is the necessity to check that the constancy of the delta-ray contribution to the fluctuation of energy deposition is a phenomenon of sufficient generality This important check has been performed in various ways. The main trend of the spectral cross section for the generation of delta rays is shown in fig. 3. At initial delta-ray energies below 100 eV the relative spectral shape is practically independent from the energy (and also from the kind) of the primary particle ("invariance theorem"). That this must be systematically so is shown by Bethe-type collision theory [15]; the unspecific shape of the initial spectrum of low-energy delta rays is caused by the mechanism of "glancing collisions" between the primary particle and the atoms with which it interacts. Furthermore, we have evaluated Monte Carlo results from other groups, which had calculated the energy deposition in nanometre targets, to demonstrate the correctness of our conclusion that there exists a unique dependence of the energy deposition spectrum per particle traversal on linear primary ionization density respectively restricted LET (fig. 4).

We can therefore conclude that, for nanometre targets, the unspecific shape of the spectrum of the not-escaping, low-energy delta-rays causes the delta-ray contribution to the fluctuation of energy deposition per particle traversal to be practically *invariant*, so that linear primary ionization density, respectively restricted LET, remains as the single variable parameter of this fluctuation and thereby of radiation quality.
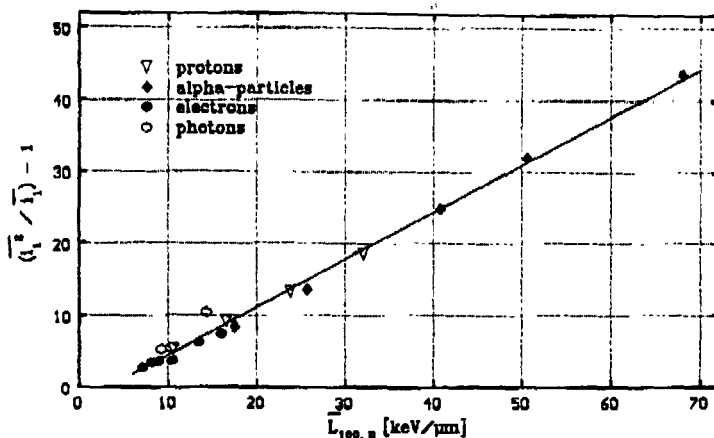
Figure 4

Relation between ($\bar{i}_1{}^2 / \bar{i}_1 - 1$) and $\bar{L}_{100,D}$ for different types of radiation. i_1 is the number of ionizations in a nanometre target per particle traversal.
Target dimensions: diameter 10 nm, length infinite (electrons) resp. 10 nm
(all other particles)

Applications

In order to support the practical use of restricted LET, part of this project was devoted to supply numerical values of restricted LET and its mean values for given radiation fields. We started from extensive tabulations of the track core values L_{100}^{core} for various ions [13]. The dose-mean values $\bar{L}_{100,D}^{delta}$ and $\bar{L}_{100,D}^{core+delta}$ were then calculated and tabulated [17, 18], since the dose mean is of interest in relation with radiation yields per unit dose, which are linearly related with restricted LET. The delta particle values were obtained from Monte Carlo calculations. The resulting restricted LET was calculated as

$$\bar{L}_{100,D}^{core+delta} = (\frac{L_{100}^{core}}{L_\infty}) \, L_{100}^{core} + (1 - \frac{L_{100}^{core}}{L_\infty}) \, \bar{L}_{100,D}^{delta}$$

Some examples of the resulting values are given in figs. 5 - 7

In order to test the applicability of $\bar{L}_{100,D}$ as a parameter of radiation quality, the linear yield coefficients α for some well-known cellular endpoints (dicentric chromosomes, cell transformation and yield of DNA double-strand breaks) were plotted in dependence upon $\bar{L}_{100,D}$ (figs. 8 - 10). According to biophysical theory [16], the slope with increasing restricted LET reflects intratrack pairwise lesion interaction along the tracks of the primary ions and the long-range delta rays, while the amplitude of the ordinate intersection reflects LET-independent contributions such as pairwise interaction along the short-range delta-ray tracks. The linear shape of these plots - more or less precisely confirmed, dependent on data accuracy - supports the theoretical model of pairwise lesion interaction [19], because this predicts the linear dependence of yield coefficient α on dose-mean restricted LET, and simplifies interpolation for other radiations, e. g. for neutrons with any given spectra.
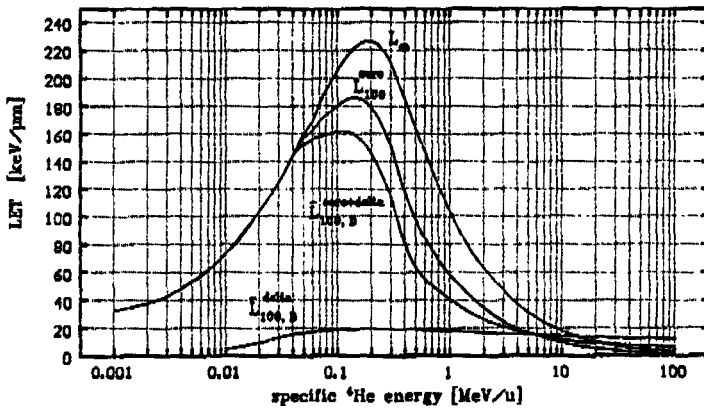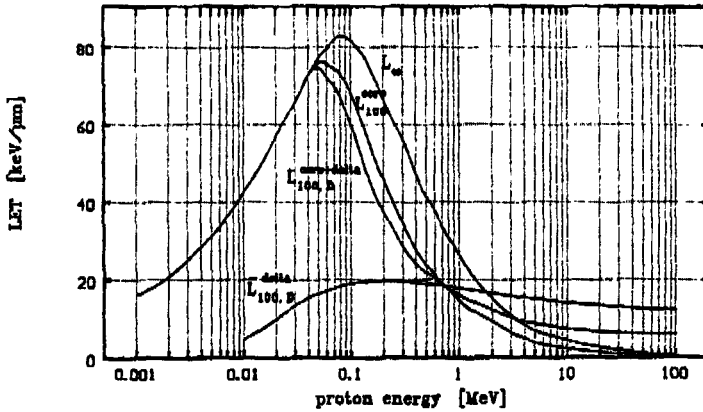
Figures 5 und 6   LET characteristics of protons and alpha particles: L_∞, L_{100}^{core}, $\bar{L}_{100,D}^{-delta}$ (dose mean restricted LET of the long- range delta rays) and $\bar{L}_{100,D}^{-core+delta}$ (dose mean restricted LET of the total track structure)
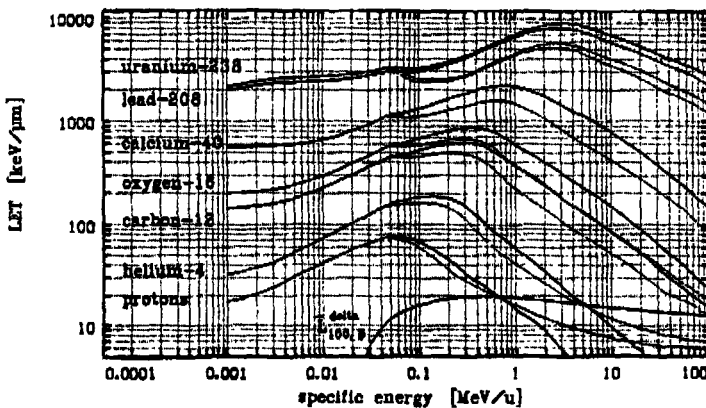
Figure 7 L_{100}^{core} (full curves), $\bar{L}_{100,D}^{-core+delta}$ (dotted curves) and $\bar{L}_{100,D}^{-delta}$ for light and heavy ions at various values of their specific energy
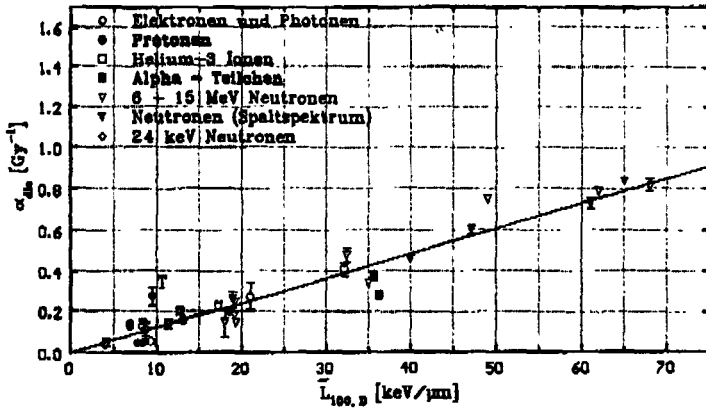
Figure 8

Linear yield coefficient α_{dic} for the production of dicentric chromosomes in human lymphocytes (37 publications) in dependence upon $\bar{L}_{100,D}$
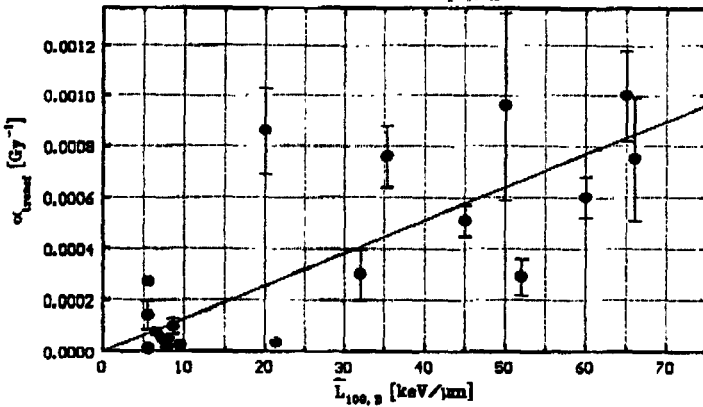
Figure 9

Linear yield coefficient α_{transf} for cell transformation in C3H10T1/2 cells (20 publications) in dependence upon $\bar{L}_{100,D}$
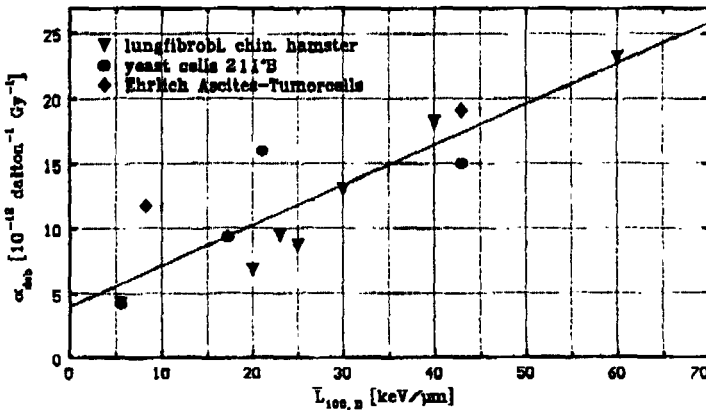
Figure 10

Linear yield coefficient α_{dsb} for double-strand break production, measured by sucrose gradient centrifugation (12 publications) in dependence upon $\bar{L}_{100,D}$

Conclusions

The long-standing task of representing particle track structure by a single microdosimetric parameter able to predict RBE values is going to be solved. The reason is that, for particle tracks traversing nanometre targets, the fluctuation of energy deposition obeys a simple regularity: Long-range delta rays escape from very small targets so that the delta-ray contribution to energy deposition is dominated by the short-range delta rays with energies not larger than about 100 eV. Their initial spectra, however, are almost independent from type and energy of the primary particle, due to the mechanism of „glancing collisions". Thus the fluctuation of energy deposition per particle traversal is described by a Poisson distribution of the number of primary ionizations, combined with an energy deposition distribution per low-energy delta ray, which is *identical* for all types and energies of the primary particle (invariance theorem).

This permits to describe the fluctuation of energy deposition by a single variable, the linear primary ionization density or the restricted LET of the primary particle respectively the separately treated long-range delta ray. For practical applications, tabulations of $L_{100,D}$ have been prepared, and $L_{100,D}$ has been successfully used as a parameter to systematize the radiation quality dependence of the radiobiological yields for certain well-known endpoints. Especially for neutrons, a clear system for the specification of radiation quality has thereby been developed. Other endpoints will be analyzed in continuation of this work.

Finally, we should consider the relationship with other proposed methods of quantifying particle track structure for biophysical purposes. Monte Carlo patterns of inelastic interactions of ionizing particles of varying type and energy in and around biomolecules such as the DNA, the nucleosome, the chromatin fiber etc. have repeatedly been compared with product yields such as the yield of DNA double strand breaks, but the general law behind the dependence of these yields on particle track structure has not become obvious. The present result, that restricted LET is the only parameter with which the pattern of these interactions in a nanometre region is varying, might be helpful to systematize these results.

Another proposal for a parameter which might possess predictive power with respect to the changes of radiobiological yields with radiation quality is „lineal energy" [2]. It is well known that this parameter suffers from the „insider" artefact if the reference volume is of the usual order of 1 μm, but there are ongoing attempts to minimize the reference volume down into the region of tens of nanometres. At this level, lineal energy should converge with restricted LET [11] and might well be regarded as its experimental equivalent.

References

[1] International Commission on Radiation Units and Measurement
Linear Energy Transfer
ICRU Report 16, Washington (1970)

[2] International Commission on Radiation Units and Measurement
Microdosimetry
ICRU Report 36, Bethesda, Maryland (1983)

[3] International Commission on Radiological Protection
Recommendations of the ICRP
ICRP Publication 26, Pergamon Press (1977)

[4] International Commission on Radiation Units and Measurement
The Quality Factor in Radiation Protection
ICRU Report 40, Bethesda, Maryland (1986)

| 5| International Commission on Radiological Protection
1990 Recommendations of the ICRP
ICRP Publication 60, Pergamon Press (1991)

| 6| Harder, D.
Physikalische Grundlagen zur RBW verschiedener Strahlenarten
Biophysik $\underline{1}$ (1964) 225 - 258

| 7| Virsik, R. P., Schäfer, Ch., Harder, D., Goodhead, D. T., Cox, R. and Thacker, J.
Chromosome aberrations induced in human lymphocytes by ultrasoft Al_k and C_k X-rays
Int. J. Radiat. Biol. 38 (1980) 545 - 557

| 8| Burch, P. R. J.
Some physical aspects of relative biological efficiency
Brit. J. Radiol. $\underline{30}$ (1957) 524 - 529

| 9| Kellerer, A. M. and Chmelevsky, D.
Criteria for the Applicability of LET
Radiat. Res. $\underline{63}$ (1975) 226 - 234

|10| Harder, D., Blohm, R. and Keßler, M.
Restricted LET remains a good parameter of radiation quality
Radiat. Prot. Dosim. $\underline{23}$ (1988) 79 - 82

|11| Blohm, R. and Harder, D.
Restricted LET: Still a good parameter of Radiation Quality for Electrons and Photons
Radiat. prot. Dosim. $\underline{13}$ (1985) 377 - 381

|12| International Commission on Radiation Units and Measurements
Stopping Powers for Electrons and Positrons
ICRU Report 37, Bethesda, Maryland (1984)

|13| Watt, D. E.
Track structure data for ionizing radiations in liquid water
Part 2: Heavy charged particles; 100 eV/A to 1 GeV/A
University of St. Andrews, Scotland, UK
University Report: BIOPHYS/1/93, Revision 2 (1994)

|14| Leuthold, G.
Startspektrum der Sekundärelektronen
Private communication, GSF Neuherberg (1994)

|15| Bichsel, H.
Charged particle-matter interactions
In: Atomic, Molecular, and Optical Physics Reference Book

|16| Bartels, E. R., and Harder, D.
The microdosimetric regularities of nanometre regions
Radiat. Prot. Dosim. $\underline{31}$ (1990) 211 - 215

|17| Bartels, E. R.
Der beschränkte lineare Energietransfer als statistische Kenngröße der Teilchenbahn-
struktur in der Strahlenbiophysik
PhD Thesis, University of Göttingen, 1995

|18| Bartels, E. R., and Harder, D.
Restricted LET represents particle track structure in nanometre targets
Poster, 10th Int. Congr. Rad. Res., Würzburg 1995

|19| Harder, D., Virsik-Peuckert, R. P. and Bartels, E. R.
Theory of intratrack pairwise lesion interaction
Radiat. Prot. Dosim. $\underline{52}$ (1994) 13 - 16

Head of project 4: Dr. Leuthold

II. Objectives of the reporting period.

The energy range for the Monte-Carlo calculations of ionisation distributions by single secondary electrons in small nanometer volumes was extended from 10 MeV up to 100 MeV and from 200 keV down to 10 keV proton energy

III. Progress achieved and final report.

Microdosimetric regularities of nanometer regions (E.R. Bartels and D. Harder Rad. Protec. Dos. Vol. 31 No 1/4 p. 211-215 (1990)) deal with the contribution of secondary electrons and was formulated in the 'invariance theorem'.

The 'invariance theorem' predicts the independence of some moments of the ionisation distribution of single secondary electrons in nanometer volumes with proton energy. This concerns the first moment, i.e. the mean number of ionisations in the target and the ratio of the second moment of the distribution to the first moment.

Monte-Carlo calculations were performed to simulate the random passage of protons through small spherical targets with diameters from 2 nm up to 50 nm. The target material is water vapor. Below 100 keV proton energy the analytical functions given by M.E. Rudd (Rad. Protec. Dos. Vol.31, p.17-22, (1990)) for the ejection of secondary electrons from different shells were used. Above 10 MeV the differential ionisation cross sections calculated with a computer code by B. Senger (B. Senger, Z. Phys. D, Vol. 9, p.79-89 (1988)) were applied. The proton started uniformly distributed from a circular area of the same diameter as the sphere. Below 1 MeV proton energy 10000 proton tracks were generated for each sphere diameter, above 1 MeV 20000 tracks and at 100 MeV 50000 tracks.

From the ionisation distributions the moments were calculated. Figure 1 and 2 show the results of the calculations for the mean number of ionisations and the ratio of the second moment to the first moment of the distributions in the proton energy range from 10 keV up to 100 MeV for sphere diameters from 2 nm up to 50 nm. A constant behaviour can be seen for small diameters over nearly the whole range of proton energy. For higher target diameters a systematic deviation is found due to the deminished kinetic energy of the secondary electrons with decreasing proton energy. Therefore the mean number of ionisations decreases and the ionisation distributions become narrower. At 10 keV the datapoints coincide independent of the sphere diameter.

In conclusion, the 'invariance theorem' is fulfilled over a wide range of proton energies and is a contribution to specify radiation quality at nanometer level by a single parameter (e.g. primary ionisation). Deviations at lower proton energies play no important role as in this region primary ionisation is predominant.
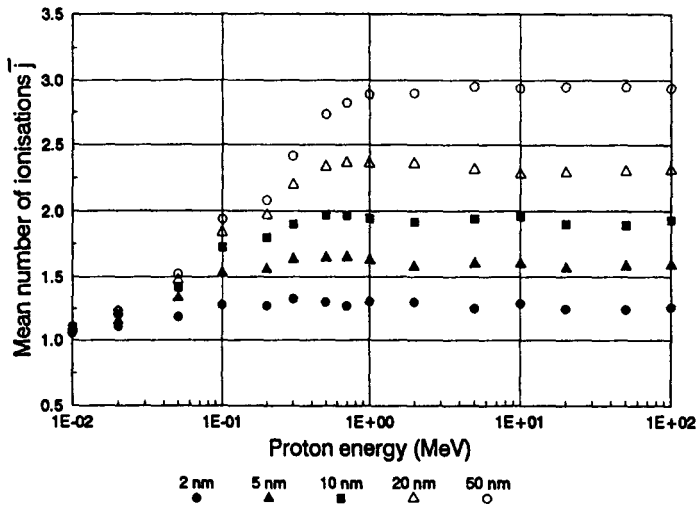
Figure 1: Mean number of ionisations $\bar{j}$ caused by single secondary electrons as function of proton energy in spherical targets.
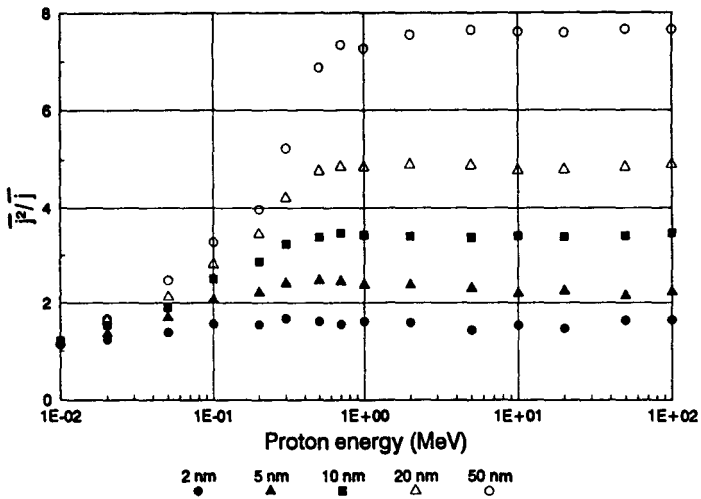
Figure 2: Ratio of the second moment $\overline{j^2}$ to the first moment $\bar{j}$ of the ionisation distribution caused by single secondary electrons as function of proton energy in spherical targets.

Head of project 5 : Dr. Izzo

II. Objectives for the reporting period.

The main objective was study of the track structure in solid DNA on a
nanometer scale by physical techniques which included ESR spectroscopy,
optical spectroscopy and electrical conductivity measurements. The
particular focus of research was the relation between the Radiation
Quality and the local spin densities. The local spin densities were to be
investigated by means of spin resonance and by observation of fast and
slow components of radiophotoluminescence (scintillation) decay. The
programme provided for doing the measurements on samples of dried DNA
with light, medium and heavy mass ions as well as gamma rays.

III. Progress achieved including publications.
1. ESR Measurements
1. a. General

The group in Rome has based its investigations of track structure on the
measurement of the local quantities, such as the mean path between
ionizing interactions λ (as diverse from global quantities), which was
proposed as the single physical parameter expressing the track structure.
The experiments particularly dealt with the changes in the properties of
ESR spectral lines (shapes, widths and relaxation times). The ESR
techniques **complement and supplement** the computational and experimental
techniques used by other teams in the group. The use of ESR in studies of
tracks left in solids by heavy charged particles has been expanded and
further developed by us. The technique used by the group in Rome is one
of the 'post mortem' analyses on an irradiated specimen, when fast
processes following immediately the act of deposition of energy, have run
their courses. What remain are processes characterized by time
constants sufficiently long to be resolved by the available equipment. We
have tried these techniques first on polyethylene, before trying the
natural polymer, DNA.
It is possible to measure the mean spacing of radicals in the cluster
or, in case of heavy ionizing particles in which the individual clusters
are overlapping, mean spacing within the track. The ESR investigations
need to be compared and correlated with the results of Monte Carlo
computation of the **spatial distribution of radicals** as discrete events of
high energy deposition. In Rome there were developed some novel methods
of interpretation of annealing of radicals. Annealing, which can be
closely controlled removes the pairs of radicals, separated by a distance
less than a certain length, selected at will, thus permitting the
experimenter to estimate not only the **mean spacing** in the cluster but
also the **first moment of the interradical spacing distribution.** With the
extension in the future of the existing set of measurements we hope to
find what law is followed by the radical spacing as a function of
restricted energy loss. Furthermore, the information on the linear free
radical density on a local scale gives an estimate of the **indirect action**
of radiation, which may interest those who are concerned with the study
of absolute biological effectiveness of radiation.
The **cluster sizes** were obtained from the measurements of local and mean
spin densities, because a difference between these two quantities is an
evidence of clustering. We have repeated the measurement of clustering

for a variety of DNA as well as other materials (nucleotides and nucleosides). The clustering measurements were poorly reproducible, until it was found that the dominant factor controlling the changes was amount of water in the structure of DNA. The sizes of clusters for a given radiation dose can be used as sensitive probes for the amount of water molecules attached to the various parts of DNA structure. This discovery was not pursued, however, because it falls completely outside the scope of the project.

2. Study of irradiated DNA.
2.a. Materials and methods
Studies were carried out on the formation and disappearance of trapped radicals and electrons in solid DNA at temperatures of liquid nitrogen. This is important for radiobiology, because of the key·role of DNA damage for the induction of cancer, for the mutations and for the reproductive cell death. The DNA was exposed *in vacuo* at about 90 K to beams of 40 and 60 MeV protons, 40 MeV alpha particles, as well as 1.25 MeV photons. The bulk radiation doses for charged particles ranged from about 0.05 kGy to about 0.5 MGy. For γ-ray irradiations with 1.25 MeV photons the doses were contained in the range from about 10 Gy to 50 kGy. The DNA from herring sperm was dried and moisture content checked by conductivity measurement according to and also chemically by Karl Fisher method. The sodium salts of calf thymus DNA and herring testes DNA were also, less extensively, studied.

The ESR spectrometry of the irradiated DNA and its constituents has been already studied for many years and we were interested in the ESR spectra only so far as they provided information on the track structure. The samples during the irradiation, storage and the read-out were kept at temperatures slightly above 90 K. In particle irradiations the samples in form of lightly compressed powder were placed in metal target holders covered with very thin Havar foil beam window and exposed to accelerator vacuum. The only contact of irradiated material with air was when the powder was transferred after irradiation to the ESR silica tubes, a procedure performed manually under liquid nitrogen and lasting 10 - 20 seconds. The silica tubes were then sealed. In γ-ray irradiations , on other hand, the samples remained all time in sealed tubes. Some measurements were carried out also on frozen wet DNA with an access of oxygen.

The samples stored after irradiation in liquid nitrogen were read by an X-band double cavity ESR spectrometer (Bruker ED200) with variable temperature cavity attachment.

The moisture content of the samples designated as 'dry' was below 2%. The samples were dried by gentle heating (40°C) in vacuum for at least three days, sometimes accompanied by ultrasonic agitation.

The ESR readout of radical concentration was done using a dual cavity and a freshly prepared DPPH substandard for comparison. The substandard itself was checked against the ruby standard provided by NBS. Corrections were applied for the nonuniformity of the microwave field, for the changes in the filling factor and for the nonuniformity of the modulating field along the cavity height.

2.b. Linewidth determination
It is well known that the radicals are accumulated in local separate

groupings (clusters) and that with an increase in absorbed dose the clusters grow, and are coming closer to each other before they start to overlap. This is illustrated in Figure 1 which shows the build-up curves of local (upper curve) and average (lower curve) spin densities for dry herring sperm DNA exposed to 40 MeV protons. The average radical density or bulk density is the total number of free spins divided by the mass of the sample, while the local density corresponds to the density within the clusters. The local density can be found from the broadening of the ESR lines or from the values of characteristic relaxation times Figure 2 shows parts of the build-up curves (average densities only) for wet frozen herring sperm DNA bombarded with 40 MeV protons. Percentages indicate the amounts of water. The wet DNA hopefully approximates better the nucleic acid *in vivo* than the dry preparation. These curves were obtained after heating the ice to about 140 K, which procedure eliminates the OH· radicals. For both dry and wet DNA the signal saturation of carbon radicals is reached at about $2 \cdot 10^5$ Gy.

The width of the line ΔH_L appears in the graphs as dX . The doses are correspondingly 5 kGy, 0.2 MGy and 0.5 MGy. The approximate local radical densities C can be found from $C = \Delta H_L / k$, where $k = 9.3 \cdot 10^{-24}$ [Tesla.cm^3]

2.c. Saturation behaviour
The microwave power saturation curves indicate that the dry herring sperm DNA saturates at the microwave power levels of about 120 mW after proton irradiation and at 160 mW after γ-ray irradiation. This difference may be just an experimental error, as the estimated uncertainty of these determinations is ±15 %. Measurement of microwave power saturation levels in dry herring testes Na-DNA and also in dry calf thymus Na-DNA gave similar results.

2.d. Thermal annealing of the samples
The isochronous annealing curves (2 hrs intervals) were obtained for herring sperm and for calf thymus varieties of DNA (γ-ray dose). In the herring sperm DNA, after warming from −117 ˚C to −10˚C, the radical density was reduced 11 times from the initial value. No single Arrhenius activation energy could be sensibly attributed to this process of fading. However, investigations using the data for herring sperm DNA irradiated with 60 MeV protons in a slightly narrower range of temperatures, indicate that the Arrhenius activation energy changes apparently from 0.52 eV to 0.39 eV. The non-constancy of activation energy eliminates a possibility of a monomolecular reaction eliminating the radicals (e.g. auto-fragmentation) and we interpret the process of thermal fading as a recombination between a pair of radicals originally separated by a few interstitial distances or, more probably, as a a recombination between a radical and detrapped electron, the traps having a spectrum of depths.

3. Observation of trapped electrons in solid DNA
The electrons are created in abundance during the irradiation, slowed down and stored, most likely, in intermolecular traps. Dry DNA is not a glass, but most of conclusions, excluding those referring to the trapping in ices, are applicable to dry solids as well. We have observed the trapped electrons in the irradiated dry and wet species of DNA, using the ESR as well as an optical detector (PM tube) and observed their release from traps in the temperature range 90 − 200 K, accompanied by light emission in the visible part of the spectrum and near UV. It is suggested

that this light emission is associated with the radical-electron recombination, which leaves *in situ* a non-radical anion. The electron trap depth depends upon sample thermal history, which is most likely a consequence of an initial broad spectrum of trap depths. The ESR spectrum of a sample of DNA shows a narrow electron peak superposed on the spectrum of carbon radicals in DNA. This peak fades with an increase in the temperature and the activation energy for this process changes with the radiation dose received by sample.

4 Scintilation monitors sensitive to dE/dx.
4.a. Introduction.
The scintillations produced by charged particles in organic phosphors can be decomposed into two components, which do not differ in respect of wavelength of emitted light, but which decay according to different kinetic laws. One of these two components, called the 'fast', decays exponentially with a time constant in the range from a few units to about 100 of nanoseconds, depending upon the molecular structure of the emitter, being almost independent of the initial ionization density. The second component, which follows, has a decay waveform generally not exponential. Among the various approximations to the actual shape of decay I(t) frequently employed is (1) :

(1) $I(t) = M/\{[1+Alog(1+t/t_m)]^2 \times (1+t/t_m)\}$

where constants A and M depend upon the scintillator and, to some extent, also on the nature of the exciting and ionizing particle.

 The parameters of the track of the charged particle and the structure of ionization clusters enter the eq. (1) through the characteristic time t_m,
(2) $t_m = 0.25\ r_o^2/D_T$
where r_o is mean radius of the particle track and D_T is the diffusion coefficient of molecules of the scintillator in the excited triplet state. The parameters of the track, specific energy loss, effective charge of the particle are thus influencing the decay characteristics of the slow component of scintillations. A very useful summary of dependence of specific intensities of both components of luminescence on the stopping power for ions with Z= 1,2 and 7 has been, given by Lopez da Silva. The ratio of intensities of these components determines the shape of the scintillation pulse and serves as the base for discrimination between the signals from heavy charged particles and those of photons or electrons.

This report describes progress in the development of a scintillation radiation monitors capable of indicating the flux of heavy charged particles and their specific energy loss dE/dx. One is a 'direct' digitizer. The other one, far more complex is based on a single photon counting principle (SPC) and permits to observe the shape of light pulses too fast to be directly digitized.

4.b. Technical description of direct digitizer.
For recording of the scintillation waveform a very fast transient capture system (direct digitizer) has been built. It is based on an Analog-to-Digital converter, which digitizes the signal from a PM tube and stores it in Random Access Memory. The conversion starts on arrival of a trigger signal and continues for 5-10 μs, depending on amount of RAM on board. After the digitization of a pulse, the data are transferred to the

computer and eventually reconstructed off line and processed by decomposition of the sampled decay curve into components. The fastest ADC tried had a sampling rate of 100 MHz, with the resolution of 8 bits i.e. 4 % accuracy. With a train of samples in 10 ns intervals the computer resolved the fast and slow decays in naphtalene (90 ns and 330 ns respectively) and was just able to resolve both components in anthracene (36 ns and 410 ns). The speed of ADC appears sufficient only for the slow component in many other scintillators. With arrival of faster ADCs (400 MHz sampling rate) a large number of available scintillators will fall into the range of the instrument. In reconstruction were used the algorithms for deconvolution and decomposition of Marquardt. The value dE/dx can be found from formulas and graphs given by Lopez da Silva, if integrals of both light components are known.

4.c. Single Photon Counting Lifetime Measurements

The single photon counting measurement relies on the concept that the probability distribution for emission of a single photon, following an excitation event, yields the time dependence of luminescence intensity arising as a result of the excitation i.e. particle induced scintillation. By sampling the single photon emission following a large number of excitations of scintillation it is possible to construct then the probability distribution of light emission as the function of time elapsed after excitation . This is done with the help of a time-to-heightconverter and a multichannel analyzer so that the PM tube is used solely to determine the instant of arrival of photon at the photocathode. The timing arrangement was that of the 'start' being determined by a Thin Film Detector (TFD) while the 'stop' was obtained from a PM tube coupled to the scintillating materiaml under test. The actual arrtangementof components was dictated by the need to optimize the timing resolution (2.6 ns) and the signl-to noise ratio. The stop detector was based on a fast phototube, it could use a small piece of solid scintillator or a liquid. The electronic system of the SPC was assembled from NIM modules.

The accumulated spectrum, stored in the memory of computer acting as a multichannel analyzer, was subject to processing, including shift of time origin, smoothing and optional deconvolution and, finally, separation into fast and slow scintillation components.

4.d. Experimental Test Of Equipment.

The directly digitized detector was tested with a number of scintillators including anthracene, naphthalene, a solution of fluoranthene in xylene and others, including a commercial scintillator NE213. While the slow component of scintillations could be always digitized and integrated, particularly under proton and alpha particle bombardment, only for naphthalene there was a satisfactory resolution of both emissions , as liquid scintillators, outgassed and kept under argon were poured into a small cylindrical silica vessel. The tests were performed with photon radiations and also with α particles from a ^{241}Am source. The use of SPC yielded a number of light decay curves for solid and liquid scintillators. The use of SPC provides, at least in principle, an accurate determination of the both components of scintillation. The characterization of the radiation is thus possible if the medium has some scintillating properties, far from being a good scintillator in a sense used in the technology of detectors.

5. Discussion and conclusions

From the physical point of view it was necessary to find indicators of action of radiation resulting in a single or multiple ionization within a sensitive volume of the target. Looking for such indicators we have chosen formation of radicals, stable on a time scale which permits to make the measurements. We have assumed that in the conditions prevailing during the irradiations with unpolarized targets or beams the distribution of radicals has the same form as that of ionizations or excitations. Radicals sufficiently close together, of the order of nanometers or tens of nanometers interact between themselves sufficiently strong bto modify the easily observable ESR spectrum. Being so close together the radicals themselves are becoming distorted and their equilibrium shape undergoes change. More information can be made available with the judicious application of annealing: In annealing the radicals which are sufficiently close recombine i. e. vanish as entities detectable by ESR. One should keep in mind that in irradiated DNA and related compounds electrons are stored in electron traps, which after release can replace the electron missing from the bond. This type of recombination process has been little studied and requires not only fulfillment of quantum mechanical conditions but also a penetration of a potential barrier by tunnelling. By taking the census of radicals before and after the annealing we had obtained the information on the distances between the radicals.

The second technique which has been used by the group of Rome was related to the scintillation method of detecting radiation and and to the process of energy transfer between the molecules of scintillator . The use is made of the two components of radiophotoluminescence. The fast or 'prompt' component comes from the deexcitation of scintillation solute. The properties of the scintillator 'have no time' to be reflected in the characteristics of light emitted as the fast component. According to the model of mechanism of scintillation of Voltz and Lopes da Silva the ratio of intensities of prompt (fast) and delayed (slow) components depends upon dE/dx of the heavy charged particle beam. The quantities dE/dx and λ are closely related. Determination of the λ of unknown radiation requires thus simple measurements of the components of radiophotoluminescence. We have reported here the work on development of a prototype of a device which can perform this task.

So far we have reported the work in which only light ions were involved. We were unable to gain access to heavy ion beams during the duration of the project.

RADICAL CLUSTER BUILD-UP

Local radical density

Average radical density

Herring sperm DNA

Separate clusters | Small overlap | Large overlap | No separate clusters

RADICAL DENSITY [cm⁻³]

DOSE [Gy]
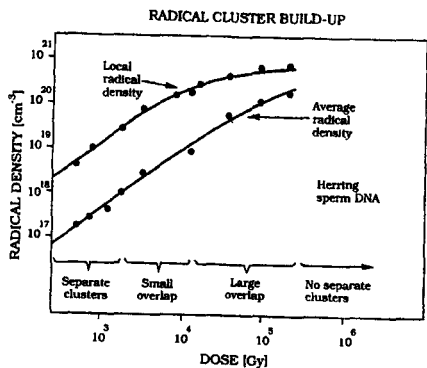
Fig. 1. Irradiation with 40 MeV protons

BUILD UP CURVES FOR DNA

Spins/g

50%

33%

~0%

Dose [Gy]
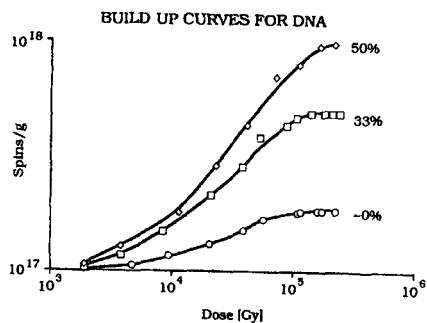
Fig. 2. Wet herring sperm DNA. The moisture content is indicated near the corresponding graph. 40 MeV protons

DNA 5 kGy 40dB

Δx=1.1769 mT

x=0.338338 T

1.5 mT

0.33 T

Dose: 5 kGy

DNA 200 kGy 40dB

Δx=2.5293 mT

x=0.339162 T

1 5 mT

0.33 T

Dose: 0.2 MGy

DNA 50 kGy 40dB

Δx=2.6953 mT

x=0 339211 T

1 5 mT

0 33 T
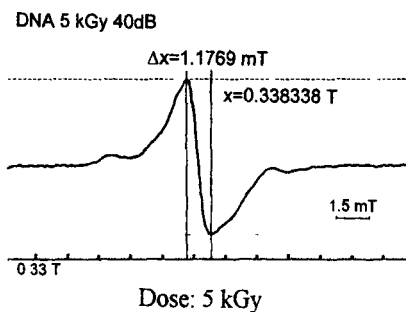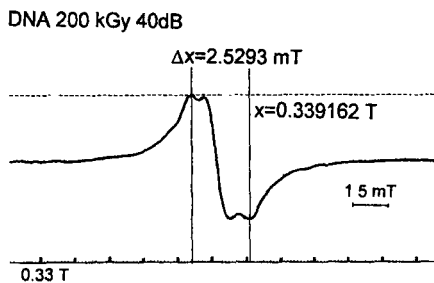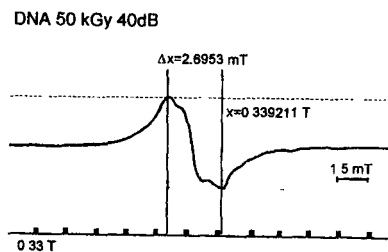
Dose: 0.5 MGy

Fig. 3. ESR spectrum of dry herring sperm DNA

Fig. 4. Isochronal thermal annealing of herring sperm DNA irradiated with protons

Fig. 5. Post-irradiation luminescence of irradiated DNA

DNA22+TRAPPED
ELECTRONS

TEMP.= -126°C
A=4 dB

Fig. 6. ESR spectrum of irradiated
DNA + trapped electrons

Fig. 7. Directly Digitizing Monitor. The signal applied to input is
digitized and stored in a Random Access Memory
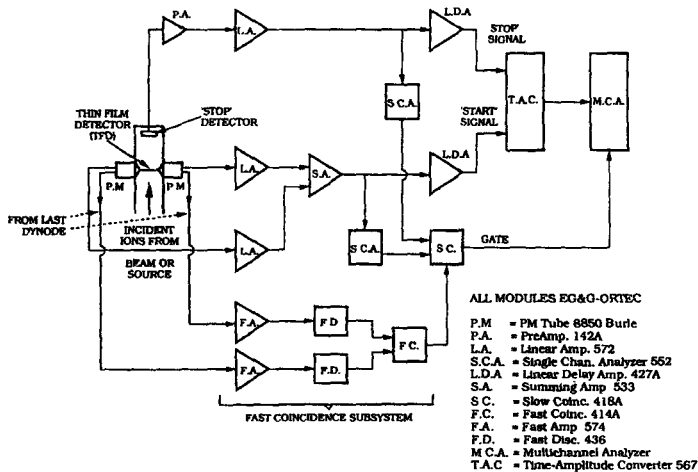
Fig. 8. Single photon counting electronics for lifetime measurements

LIGHT DECAY FOR NAPTHALENE
BOMBARDED WITH 20 MeV PROTONS

——— Total light
– – Fast component
· · · · · Slow component
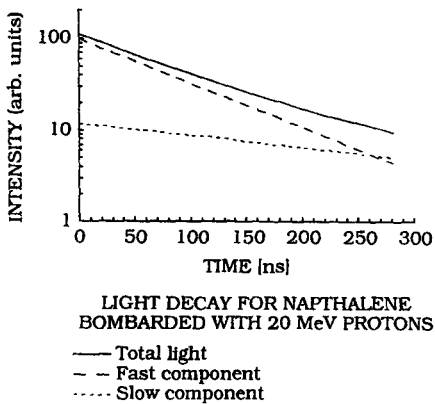
Fig. 9. Light decay for naphthalene
bombarded with 20 MeV protons.
Measured with Direct Digitizer.

LIGHT DECAY CURVES FOR NE102A
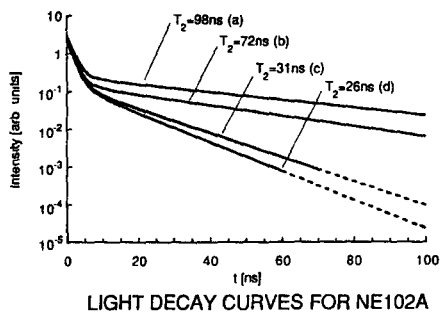
Fig. 10. Light decay for plastic scintillator
NE102A shows different decay times of
the slow component T_2.

PUBLICATIONS

1. Finestre di ESR sul panorama della scala di dimensioni nanometriche (with G. Izzo and J. Holowacz). Proc. Congr. SIRR, Capri, 1992.
2. Features of radiation field on a nanometer scale measurable by ESR (with G. Izzo and J. Holowacz). Proc. Eleventh Symp. on Microdosimetry, Gatlinburg Tenn., 1992.
3. Radical pair formation by radiation of low and high LET (G. Izzo, K.V. Ettinger and J. Holowacz). III° Convegno Nazionale del Gruppo Italiano di Risonanza di Spin Elettronico, Alghero, 24-27 Sett. 1993.
4. On the magnetic RF field in some resonant system used in the radical local density determination by saturation method (with J. Holowacz). Appl. Radiat. Isotopes 44, 373-376, 1993.
5. Investigation of a specialized S-band spectrometer for ESR dosimetry (with C. Franconi, J. Holowacz, M. Bonori and R. F. Laitano). Appl. Radiat. Isotopes 44, 351-355, 1993.
6. Some local radical densities in irradiated solids (K. V. Ettinger, G. Izzo, J. Holowacz, A. Canichella and A. Soriani). III° Convegno Nazionale del Gruppo Italiano di Risonanza di Spin Elettronico, Alghero, 24-27 Sett. 1993.
7. Electron Spin Resonance windows onto the nanometer landscape. G. Izzo, K. V. Ettinger and J. Holowacz. Radiation Prot. Dosimetry 52, 61-63, 1994.
8. Post-irradiation features of radiation field measurable by ESR in polyethylene. G. Izzo, J. Holowacz and K. V. Ettinger. Physica Medica 10 (Suppl.), 23-25, 1994.
9. New development in scintillation monitoring for dose and dE/dx. K. V. Ettinger, G. Izzo, J. Holowacz and D. Harder. Presented at Joint Conf. SIRR, AIFB, GIR. Pisa, Nov. 1994. To be published.
10. Investigation of radiation damage in DNA, using trapped species. G. Izzo, K. V. Ettinger, B. Nicoletti, J. Holowacz, S. Trivisonne, F. Bordi, A. Canichella and S. Agnolin. Presented at Joint Conf. SIRR, AIFB, GIR. Pisa, Nov. 1994. To be published.
11. New trends in scintillation detectors for dose and radiation quality monitoring purposes. K. V. Ettinger, G. Izzo, J. Holowacz and D. Harder. Accepted for Rad. Prot. Dosimetry, 1995.
12. Trapped species: radicals, electrons and their clusters as indicator of radiation Damage in DNA (K. V. Ettinger, G. Izzo, J. Holowacz, A. Soriani, S. Trivisonne and A. Canichella, University of Rome "Tor Vergata"; S. Agnolin, Ethicon, Pomezia, Italy). Proc. 4th International Symposium on ESR Dosimetry and Application, Munich, May 1995. To be published.
13. The slow component of scintillations in various materials measured with SPC (K.V. Ettinger, G. Izzo, J. Holowacz). To be published.

ACKNOWLEDGMENT

Head of project 6: Dr. Kraft

II. Objectives for the reporting period

- Measurement of double differential δ-electron emission cross sections in heavy ion atom collisions. Comparison with theoretical descriptions.

- Development of semi-empirical formulae for emission cross sections with reasonable accuracy to be used as input to MC calculations.

- MC calculations of radial dose distributions and specific energy deposition in small sites with theoretical and semiempirical heavy-ion cross sections.

III. Progress achieved including publications

- Experimental:

  The emission of δ-electrons in collisions of heavy ions with atoms and simple molecules was systematically investigated. Electron production cross sections differential in electron energy and emission angle were measured using ions from Neon up to Lead with charges from 7^+ up to 26^+.

- Theoretical:

  Semiempirical formulae have been developed to describe the double-differential δ-electron emission cross section for collisions of light ions with various noble gas and water vapour targets. Monte Carlo simulations have been performed using the improved cross sections as well as theoretical ones.

Measurements of the δ-electron emission in heavy ion atom collisions

The process of electron emission in the intermediate projectile energy range of the *UNILAC–* accelerator at the *GSI* in Darmstadt (*FRG*) have been investigated. The double differential cross sections, $d^2\sigma/dE_e d\Omega_e$, from heavy ion atom collisions has been measured systematically as a function of the electron emission energy, E_e and the electron emission angle, ϑ_e, for various collision systems. Various projectiles (Ne, Ar, Ni, Kr, Xe, Au, Bi, Pb) and gas targets (He, Ne, Ar, Xe, SF_6, H_2O, C_5H_{12}) were used. The projectile energy, E_P was chosen in the narrow range between 5.4 and 6.0 MeV/u. The projectile charge states, q, spanned a wide range from Ne^{7+} up to Pb^{26+}. The energy spectra of the electrons emitted in the heavy ion atom collisions were collected with two electrostatic hemispherical sector analysers in the energy range $0.3 \le E_e \le 12$ keV. The detectable emission angles cover the range $27.5^0 \le \vartheta_e \le 145^0$ with respect to the beam axis.

The experimental results can be described by incoherent addition of Binary Encounter and Three Body Encounter processes.

Binary Encounter electron emission from collisions with fully stripped ions up to Ar^{18+} shows the expected scaling behaviour. The cross sections scale with $(E_P/q)^2$ and can be described with theories like the Impulse Approximation.

For highly charged and partially stripped ions unexpected structures in the double differential cross sections have been observed. The spectral shape differs considerably from bare projectiles with the same net charge. An enhancement of Binary Encounter electrons in forward direction was observed. This dramatic deviation from simple theories like Binary Encounter Approximation and First Born Approximation were attributed to quantum mechanical interferences of the scattered target electrons in the screened Coulomb potentials of the projectile (Rainbow and Glory scattering). Thus, in the case of partially stripped heavy ions ($Z_P > 10$) colliding with gaseous targets for the electron emission cross sections no simple semi–empirical formulae could be obtained so far.

The internal structure of the target is of minor importance. Both single and double differential cross sections scale linearly with the number of target electrons.

The process of Three Body Encounter electron emission can be described as multiple scattering of target electrons in the two centre potential of target and projectile nucleus. It results in the production of low energy electrons at large impact parameters so that partially stripped ions can be viewed as a point charge. The Three Body Encounter double differential cross section can be described by an empirical expression.

Semi-empirical formulae

In addition to the formula derived for the Three Body Encounter electrons semiempirical expressions were developed to describe the double differential cross section in collisions of protons and light ions such as helium, carbon, oxygen and neon with He, Ne, Ar and H_2O targets. They are based on the Binary Encounter Approximation cross sections with semi–empirical corrections to better describe backward and forward emission as well as the creation of low-energy electrons. The corrections were fitted to achieve a reasonable agreement over a wide range of experimental data.

For protons this was done in accordance with Rudd's recommendations for energy–differential proton cross sections. The cross sections for helium and heavier ions were then multiplied with an effective projectile charge according to the Barkas formula.

The total δ-electron cross section can change as much as 50% when going from theoretical values to semiempirical ones. This is mainly due to the reduction of electrons with energies below the ionization maximum of water. Hence this would not affect the radial dose distribution very much but it does well influence the mean free path between subsequent primary ionizations. Therefore the precise knowledge of the δ-electron cross section at low electron energies is of great importance because it enters directly into the probability of primary ionization by the heavy projectile.

MC calculations

Based on the semi–empirical cross sections MC calculations were performed in order to obtain radial dose distributions. Compared with calculations based on the Binary Encounter Approximation the differences are about 5-20% at distances of 1nm.

In addition simulations of the specific and dose-mean lineal energy deposition in small sites corresponding to sub-micrometer spheres and cylinders were performed as a function of the distance from the ion path. The results were compared with measurements reported in the literature. The projectiles comprise protons, Li, Ge and U. The calculations for light ions reproduce within 20% the observed long-range flat tail caused by far reaching δ-electrons. Good quantitative agreement can also be obtained for very small and zero distance. For the heavier projectiles large discrepancies of a factor of 2-3 (overestimation at small, underestimation at large distances) were found that could be attributed to the inaccurately known primary cross section as well as to potential saturation effects in the detectors at zero distance.

As a first step to extend our investigations to solid state targets additional calculations have been performed to simulate δ-electron emission induced by ions passing thin foils of low-Z material like carbon. The simulations were compared with δ-electron spectra under 42^0 after 0.5 and 1.5 MeV/u alpha particle impact reported in literature. Although gas-phase cross sections are used the quantitative agreement between MC and experiment is quite good. The improvements in the description of the primary δ-electron angular distribution have been important to make this comparison possible. These findings indicate that the error induced by the assumption of gas phase cross sections for simulation of solid state media is tolerable in first order.

Publications

M. Krämer, G. Kraft, Calculations of heavy ion track structure, Radiat Environ Biophys (1994) 33:91-109.

U. Ramm, Ph.D. thesis, Univ. Frankfurt/Main, 1994.

U. Ramm, Binary encounter electron emission in collisions of highly charged ions with He gas targets, NIM B98 (1995) 359-362.

U. Ramm et al., Abnormal q^2-scaling of electron emission in high energetic argon-helium collisions, in preparation for J. Phys. B.

U. Ramm et al., Projectile charge state dependence of binary encounter electron emission in heavy-ion helium-collisions, in preparation for J. Phys. B.

Head of project 7: Dr. Pszona Stanislaw

II.   Objectives for the reporting period

1.   To improve the quality of the equipments incorporated in the experimental set up.

2.   To assembly a new modified experimental set up, Jet Counter (JC), for the nanodosimetric studies.

3.   To study the characteristics of the simulated nanometre sizes in a modified Jet Counter.

4.   To achieve the experimental readiness for two types of the experiments, namely:

-    for measuring the delta electron spectra generated by charged particles interacting with a nanometre site size,

-    for determination of the frequencies of creation of single and multiple number of ions within the nanometre size sites.

III.   Progress achieved including publications

(Ad 1)   Modernization of the Jet Counter

The following basic replacements and modifications were done:

-    turbo-molecular pump 200 l/s has been installed (which replaced the 2000P type diffusion pump). By this the "clean vacuum", which is necessary for the proper functioning of an electron multiplier "channeltron" has been achieved.

-    the deflecting electrodes were added to the electron gun for the optimalization of electron beam position in respect to gas jet.

-    the PC based multiscaler device was applied which replaced the old inoperative equipment.

-    the new power stabilized electronic system for the electron gun was elaborated and installed.

All these steps improved the quality of the components and allowed to modify the experimental set up, for studies the characteristics of simulated nanometre sites and which in the next period, the basic nanodosimetric experiment will be carry out.

(Ad 2)   *Description of the modified Jet Counter*

The general idea of JC is explained on Figure 1. A simulated nanometre size, SNS, is obtained by a short lasting gas jet. The gas jet is created due to pulse operated valve, PZ, which injects gas from a volume, R, over a valve, trough a nozzle with a 1 mm diameter orifice to an interaction chamber, IC, placed below a valve. A gas jet instead of constant flow gives higher instant gas density without disturbing the work of the counting devices and without necessity of using a pumping unit with high speed. Furthermore, placing the counting devices close to SNS gives a better chance as compared to previous attempt to handle efficiently the transport of ions and electrons to the detecting systems. The SNS is adjusted by changing the gas pressure in volume, R, or as it has been verified during recent experiments by varying the amplitude of pulse wich control a valve (with constant gas pressure in volume, R). The range of SNS, in unit density scale, has been determine experimentally by the transmission method applied to known energy monoenergetic electron beam. It has been shown (1) that the possible range of simulated nanometre sizes obtained by this technique extend to up to 250 nm.

When a SNS is irradiated by a charged particles, positive ions created within this nanometre site are directed by an electric field Ew with weak electric field strenght (to avoid secondary ionisations) toward the another area with Eh where they are accelerated and detected by a channeltron. The time sequences of the pulses from a channeltron, CH2, are registered by a fast digitizing osciloscop, D, and than analysed by a PC computer. The ions have to reach the acceleration area after a time when the gas pressure inside the IC is enough low. For this purpose the distance between the SNS and a detector of ions, CH2, will be experimentally verified.

(Ad 3)   *Characteristics of nanometre simulated size*

In an experiment, done with JC, the geometrical characteristics of the SNS have been studied. For this purpose an electron gun, EG, was madified by adding the deflection plates which make possible to identify the shape of gas jet. The experiment can be explained based on in Fig.1. The pencil beam of 1 keV electrons travers the gas jet (air in this experiment) and the transmitted electrons are detected by an electron multiplier ":channeltron", CH1, and than recorded by a multiscaler. Because of the pulse character of the gas jet, the electron beam and a multiscaler are synchronized in time. By deflecting of electron beam with respect to an orifize of a nozzle and corresponding positioning of a channeltron, CH1, (on Fig.1 at plane perpendicular to gas jet stream) the transmission ratio of passed electrons can be found. Based of such procedure the profile of a gas jet has been found. For simplicity the measurements were done for air.The results are shown on Fig.2. Horizontal axis - x/d, vertical axis - t/r., where x is linear deflection of electron beam with respect of the nozzle axis, d - is the diameter of an orifice of the nozzle, t- is the thickness of air jet and r - is the range of 1 keV electrons in air. The t/r values are derived from transmission curve of Rao (see references in (1)). As seen from this figure the air jet has pronounced component straight ahead of a nozzle within two diameter of the orifice and a "plateau " for x/d $>$ than 2. This simply means that the jets are expanding but the total mass of injected gas remain constant. In the next experimental step a system of an additional diaphragme will be applied to modify the shape of molecular beam to get higher directional effect.

In a second experiment, the range of SNS around 2 -5 nm, has been investigated in order to check a method of monitoring such thicknesses. For this purpose 100eV electron beam was applied for studying an attenuation effect of air jet which was controlled by pressure in R chamber. The results are seen on Figure 3. for different air pressure in R. From data of Iskef, range, r, of 100eV electron in air is 0.5 μ_cm^{-2} (with precision of 25%), this is equivalent to

5 nm in unit density scale. From the transmission curves, Fig. 3. a ratio of t/r has been calculated and the thicknesses of air jets for 20, 50 and 100 Torr were calculated to be 2.4 nm, 4 nm and 5.6 nm respectively. This means that with 100eV electrons we can firmly control the SNS in the range of single nanometre (in unit density scale).

When a pressure of gas in the chamber, R, over the valve is controlled then for known number of jets the pressure of gas is changing to a new lower value. The resulting p can be converted to a number of mollecules injected in each jet to interaction chamber, IC. The results for air gives $3.7 \ 10^{17}$ molecules per jet, for 1013 hPa of an initial pressure in R. This gives 20 μg per jet. This is the upper limit of mass of gas which correspond to about 250 nm simulated size. The lower limit is of mass of gas in a single jet can be adjusted on the level of ng and this correspond to a tenth of nanometre.

(Ad 4)   Delta- electron spectra - the experiments with Jet Counter

The delta-rays spectra generated by charged particles especially at the lower part of electron energy spectra i.e below 100 eV are of special interest for studies the validity of the "invariance theorem" which has been postulated by D. Harder. The performances of JC for delta - electron spectra measurements have been tested by scattering experiment of 1000eV monoenergetic electrons on thick carbon foil. In such experiment, the electron energy analyser was installed inside a IC chamber in position of CH1. (see Fig.1). The results is shown on Fig.4. The experiments with monoenergetic electrons of 700 eV interacting with SNS of 11 and 36 nm have been done and the results reported in (1). Based on these experiments the L_r (LET restricted with locality r) were estimated equal to 15.5 and 14.4 eV/nm respectively. The experiments with protons is planned in the next framework.

Set up for investigation of the number of ionisations within a nanometre site

For proper interpratation of the biological effects of ionising radiations of the different qualities the detailed description of interaction pattern at nanometre sized volumes is of great importance. At these sub-cellular sized volumes the number of interactions per particle passage are low, therefore the number of created ions instead of energy deposition have to be investigated. (1).

A set up as schematically shown on Fig.1 has been assembled for testing as a device for registration of the ionisations created in SNS by a charged particle. A 1keV electron beam was used to generate the ionisations in 50nm SNS in nitrogen. The first results have confirmed that the most critical parameters for such measurements is the efficiency of registrations of ions by a channeltron CH2. The efficiency of ions counting by a channeltron has been thoroughly analysed as a crucial for this method because it needs to be close to 100 %. Otherwise the efficiency for counting a group of n ions will be low according to dependence η^n where η is the counting efficiency for counting of single ion. Based on the data of manufacturers of the channeltrons, around 50% efficiency for a 5keV ions is declared, which means 25% for double and 12,5 % for triple ions counting efficiency respectively. Therefore in the course of this investigations the modification as shown on Fig. 5 has been foreseen, which will be tested in the next phase of the experiment.

Publications

1. S.Pszona and R. Gajewski, *An approach to experimental microdosimetry at the nanometre scale*. Radiat. Prot. Dosim. 52(1-4), 427-430 (1994).
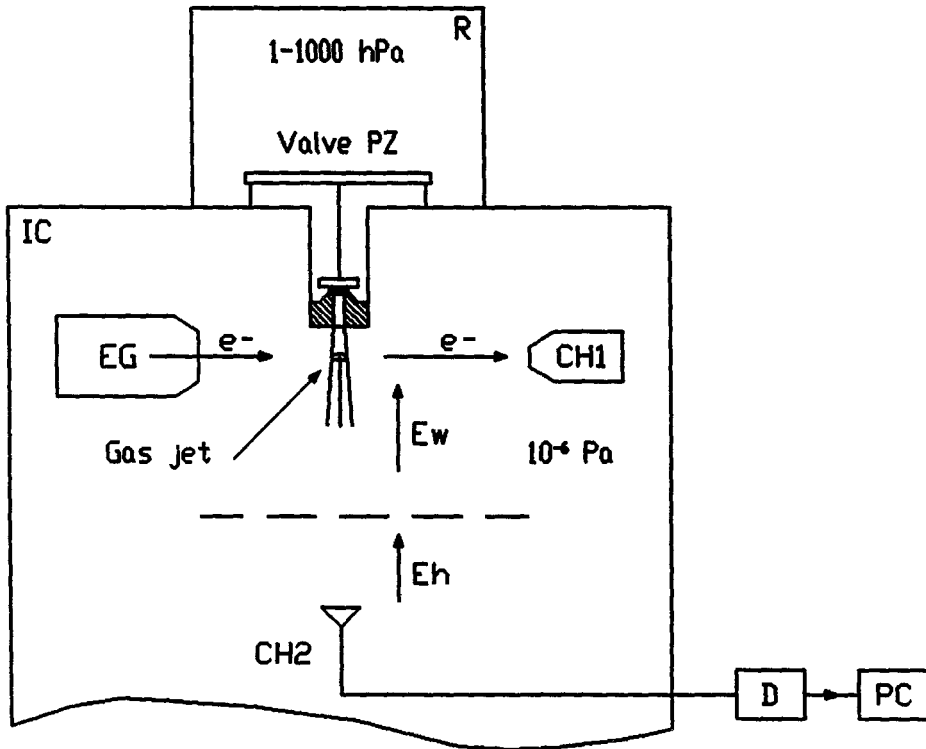
Figure 1. Schematic view of the Jet Counter; EG, electron gun; CH1, electron multiplier; PZ, valve; CH2, ion detector; D, digitizer; PC, personal computer.
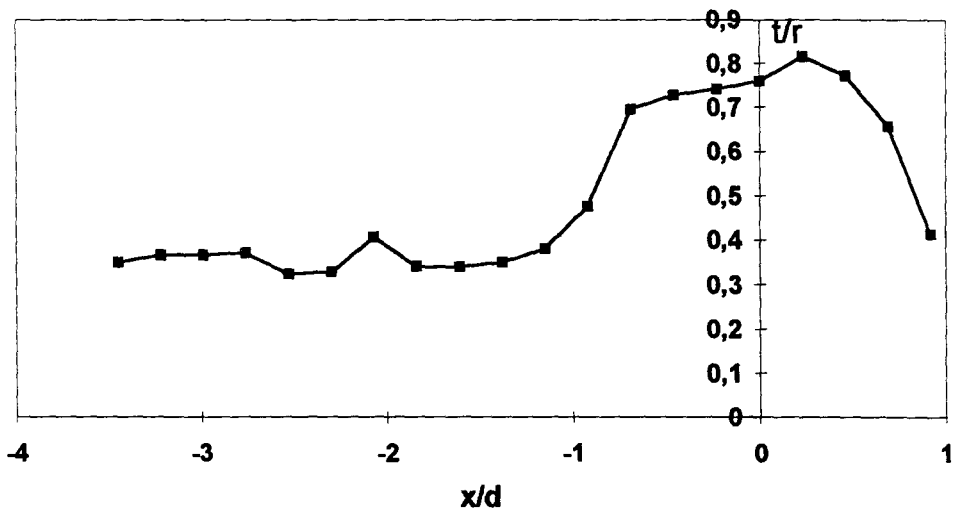
Figure 2.   The profile of air jet, x/d - ratio of a linear deflection of electron beam from a nozzle axis to diameter of an orifice; t/r - ratio of thickness of gas jet to range, r, of electrons.
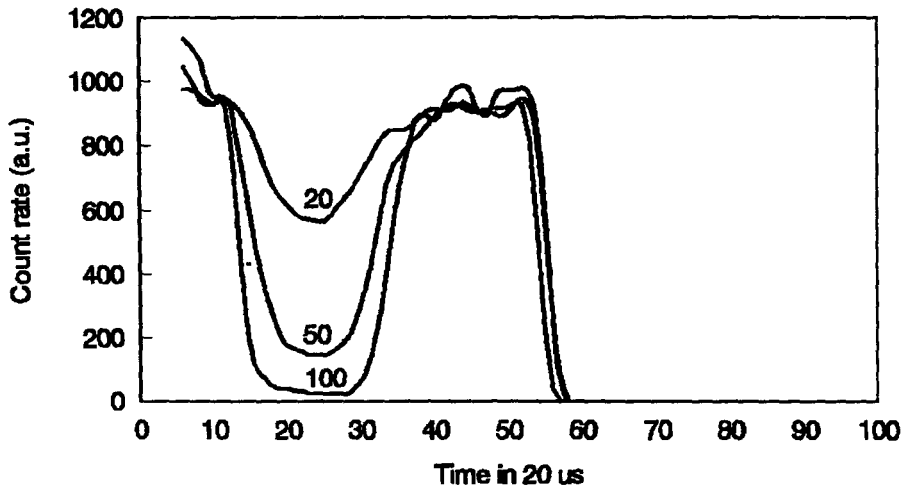
Figure 3.   Attenuation effects of 100eV electrons by air jets - timing chart, for different air pressure in volume R above the valve PZ.
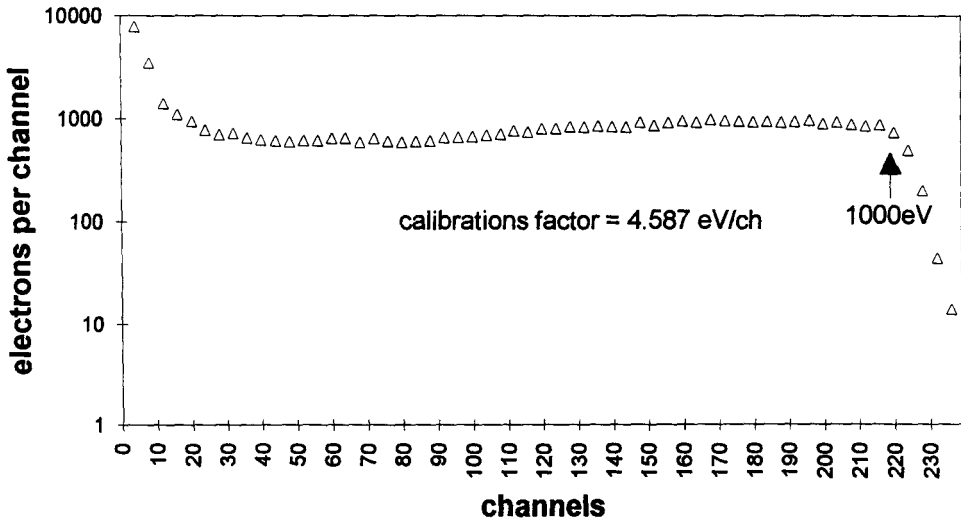
Figure 4.   The energy spectrum of scattered electrons from a thick carbon foil irradiated by 1keV monoenergetic electrons. Scattering angle 130 deg.
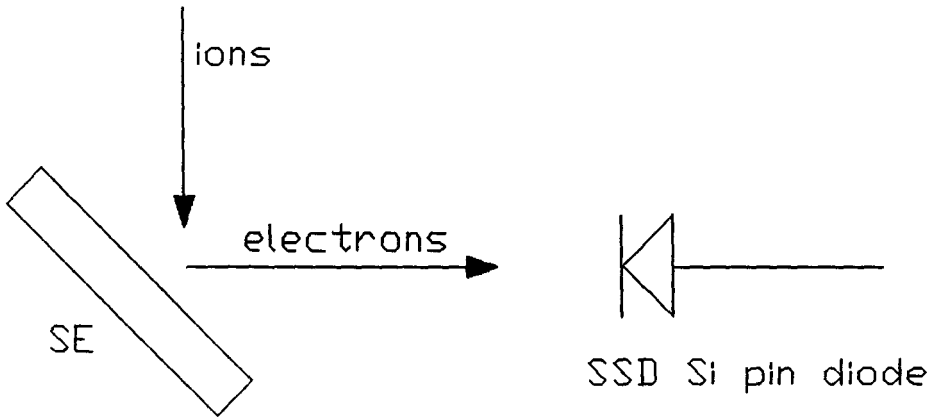
Figure 5.   The modification of a detecting system for ions, SE - secondary emmission foil, SSD - silicon pin diode.
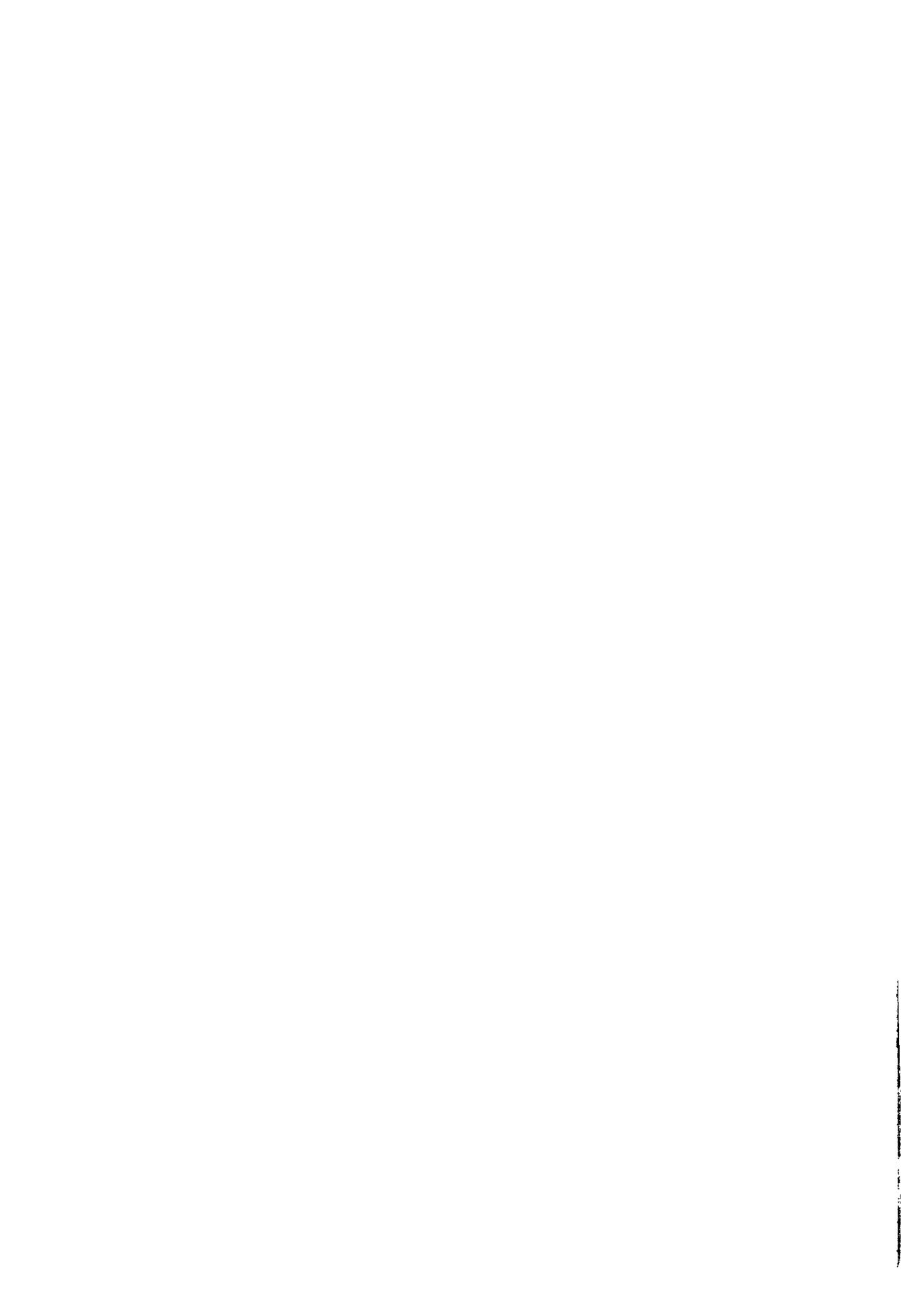
Contract: F13PCT920007   Duration: 1.9.92 to 30.6.95   Sector: B12

Title: Molecular basis of radiosensitivity.

1)   Lohman   Univ. Leiden
2)   Bridges   MRC
3)   Bootsma   Univ. Rotterdam - Erasmus
4)   Moustacchi   CIR
5)   Thacker   MRC
6)   Backendorf   Univ. Leiden
7)   Eckardt-Schupp   GSF
8)   Szumiel   ICHTJ
9)   Szymczyk-Wasiluk   WMS

I. Summary of Project Global Objectives and Achievements
Global objectives

(i)   Identification of radiosensitive individuals both in the normal population and with known radiosensitive genetic disorders.

(ii)   Understanding of the cellular response to radiation.

Achievements

(i)   The single cell microgel (comet) assay has been successfully employed to demonstrate individual sensitivity to induction of radiation induced DNA strand breaks in human T-lymphocytes, and to investigate the role of radical scavengers to counteract strand break formation. The latter has been achieved by modulation of dietary levels of vitamin C in a panel of normal volunteers. In addition, radiation induced cytotoxicity and micronuclei have been assayed to investigate potentially lethal and clastogenic damage to identify radiosensitive in-dividuals in the normal population as well as ataxia-telangiectasia (AT) heterozygotes. With respect to AT, evidence has been gained from a panel of 16 probands, their sibs and parents that mutation frequency in T-cells might be of prognostic value. A collection of radiation sensitive fibroblast cell lines has been established to investigate the possibility that chromosome damage can provide an early measurement of individual radiosensitivity. Three unique radiosensitive individuals have been identified not exhibiting the clinical features of AT. Analysis of their fibroblasts reveals AT-like radiosensitivity and in one case defective double strand break rejoining. These individuals probably carry mutations in human genes (different from AT) which affect radiosensitivity.
In Fanconi anemia (FA) cells an unbalanced cytokine production was demonstrated. In particular abnormalities in tumor necrosis factor α (TNFα) appear to be a general characteristic associated with FA and FA heterozygous individuals as revealed from a systematic study in FA families. The abnormally high production of TNFα is also seen in AT cell lines and might contribute to the enhanced apoptotic response of FA and AT cell lines. Surprisingly the induction of apoptosis by radiation was drastically reduced in AT and FA compared to normal

cells and this was associated with a lack of p53 induction. Altered expression of p53 may affect genes that regulate genomic stability and therefore be relevant to the phenotype of FA and AT syndromes.

(ii) Different and complementary strategies have been used in the different laboratories to study cellular responses to radiation.

A. Cloning of repair genes.

Mammalian genes

Isolation of genes relevant for cellular responses, is indispensible to understand the mechanisms of radiation sensitivity. During the course of the project a comprehensive set of radiosensitive mutants has been isolated. These mutants have been used to clone DNA repair genes by DNA transfection or positional cloning. The human gene correcting the radiosensitive XRS mutants is located on chromosome 2. Yeast artificial chromosomes (YACs) from this region of chromosome 2 were isolated and the complementing YAC identified. During the course of this work a candidate gene (Ku80) mapping to this region, was identified; analysis of human-hamster hybrids confirmed that Ku80 was consistently present in complementing hybrids. Expression of Ku80 in XRS cells was shown to complement all the defects characteristic of these mutants. Taken together these results identify Ku80 as the the product of XRCC5.

Ku 80 is a subunit of the heterodimer Ku protein being the DNA-end binding component of DNA dependent protein kinase (DNA-Pk). This raises the possibility that either Ku70 (the other subunit of Ku) or DNA-Pk itself, might be defective in mutants (Ionising Radiation complementation groups 4,5 and 7) exhibiting a similar phenotype to XRS mutants. Mutants lacking DNA-Pk activity (complementation group 7) were used to introduce YACS encoding DNA-Pk: two YACs were able to complement and the results therefore identify DNA-Pk as the product of XRCC7.

The human gene complementing irs1 radiosensitive cells is located on chromosome 7. The region of chromosome 7 carrying the gene, was mapped and the location of the putative XRCC2 gene was refined to an interval of 7q36. YACs of these region were isolated and one YAC was shown to complement.This YAC was used to identify PCR derived c-DNA clones. which are currently being employed to isolate the gene.

In the yeast S.cerevisiae the RAD 6 gene plays a central role in postreplication repair, mutagenesis and sporulation. The gene encodes a ubiquitin-conjugating enzyme. Sequence homology to the RAD6 yeast repair gene has been exploited to clone human homologs HHR6A and B. Using a similar approach 7 additional human repair genes were cloned: two human homologs of the yeast nucleotide excision repair (NER) gene RAD23 (HHR23A and B) and the human counterparts of the yeast recombination repair genes RAD52 (HHR52) and RAD54 (HHR54). Very recently two human homologs of the recombination repair gene rad 21$^+$ from the yeast S.pombe were identified and c-DNAs cloned. Presently the possibility is investigated that the HHSR21A gene is involved in the radiosensitive Nijmegen Breakage Syndrome because the gene maps to a candidate genomic region for this disorder.

The human homolog of the S.cerevisiae crosslink repair gene PSD2/SNM1 was cloned. Expression vectors carrying the full lenght c-DNA, are currently used for complementation of various mammalian mutants defective in crosslink repair.

Yeast genes

Six S.pombe genes have been cloned that prevent cell cycle progression after DNA damage(' checkpoint'rad genes). For one of the genes (rad 3) a human homolog has been identified which is related to, but distinct from AT. Genetic analysis of checkpoint genes has revealed a complex pathway with many proteins acting in a complex. Analysis of rad24 mutants has revealed a defect in the spindle assembly checkpoint which links (for the first time) the

mechanisms preventing mitosis after either DNA damage with inhibition of spindle formation. The human ERCC6 gene is defective in cells of CS complementation group B shown to be impaired in the preferential repair of active genes. The high conservation displayed by all NER genes analyzed to date permitted the identification of the S.cerevisiae homolog of ERCC6 (designated RAD26). In analogy with CS group B rad26 disruption is viable and impairs transcription-coupled repair, but, in discordance with CS, does not induce any UV-sensitivity. This suggests that the global genome repair is the major determinant of cellular resistance to genotoxicity in lower organisms.

The REV2 gene confering resistance to UV and ionizing radiation, was cloned and characterized. Genetic analysis has revealed pleitropic phenotypes of REV2 mutants.

B. Functional analysis of encoded proteins and identification of proteins in cell free in vitro systems.

During the course of the project, products of mammalian repair genes involved in NER and repair of radiation induced damage, have been purified and characterized with regard to functional domains and interaction with other proteins. The presence of an NER enzyme complex harbouring the products of ERCC1, and the correcting activities for ERCC4, ERCC11 and XPF gene mutants was demonstrated by an in vitro assay. It is postulated, that this complex functions both in nucleotide excision repair and recombinational repair and may play a role in strand incision.

Mutations in ERCC3 and ERCC2 are responsible for xeroderma pigmentosum group B and D respectively. Both proteins are part of a multiprotein complex (TF11H) required for transcription initiation and excision repair. Part of the clinical symptoms of the corresponding disorders which were difficult to interpret on basis of a repair defect, can now be explained as the result of a subtle impairment of transcription. Besides XPB and XPD the TFIIH factor contains an uncloned repair protein implicated in the newly identified TTD-A complementation group. It was found that the XPB and XPD proteins are responsible for the bidirectional helix-unwinding capacity of the complex. It is proposed that TFIIH may locally melt the DNA around the site of the lesion e.g. for loading the NER incision complex onto the DNA template. The selective association of mutations in TFIIH subunits with the peculiar clinical features of CS and TTD was further corroborated with the discovery of the first TTD family falling in the rare XP/CS group XP-B. This supports the idea that subtle transcriptional defects affecting the expression of a selective set of genes are responsible for the spectrum of CS and TTD features that lack a rational explanation based on a NER defect. Sofar no clear evidence has been found for a stable interaction of the CSB protein and known NER and transcription factors. XP-C cells exhibit the opposite repair phenotype of CS: namely a defect in the global genome repair pathway. The XP complementation group C protein was found in a very tight complex with the HHR23B gene product. The HHR23B protein is for a considerable part made up of a very strongly conserved repeat sequence also present as a C-terminal extension of one of the ubiquitin-conjugating enzymes. This provides a link between this gene and the ubiquitin pathway.

In vitro assays using plasmid DNA and cell-free extracts have been developed and employed to identify proteins involved in the repair of DNA double-strand breaks induced by restriction enzymes (DSBs). Substrates with homologous ends and non-homologous ends have been investigated. Using a substrate with homologous ends DSB rejoining is stimulated by an activity called REP-1 which increases the turnover of the first intermediate of a ligation step. The REP-1 protein differs from from another ligase associated protein, XRCC1. Recently, the rejoining of non-homologous ends by mammalian extracts has been demonstrated for the first time. The rejoining ocurs via different menchanisms involving either direct repeats, or blunting (or filling) of single stranded overhangs followed by ligation.

C. Topography of DNA repair.

A reliable quantification of DNA damage is a prerequisite to estimation of risks resulting from different irradiation conditions and to analysis of repair. Conceivably, DNA sequence and chromatin structure may affect induction and repair of radiation induced DNA damage. To analyse the distribution of DSB breaks in the yeast S.cerevisiae and mammalian cells, pulse field gel electrophoresis and computer analysis of DNA profiles have been employed. Gamma radiation of yeast and mammalian cells resulted in a random induction of DSB. In contrast, treatment of yeast and mammalian cells with neutron beams of various energies resulted in DNA profiles, inconsistent with the random breakage model. A model accounting for the (nonrandom) occurrence of DSB clusters is in better agreement with the results. The analysis of DSB repair kinetics in radiosensitive mutants may give hints to the functions of the mutated genes. In the yeast S.cerevisiae the predominant pathway for DSB repair is homologous recombination. However, using rad 52 and HDF1 (putative homolog of Ku-heterodimer) mutants, evidence has been obtained for the presence of additional minor DSB repair pathways in yeast.

Convincing evidence has been obtained for intragenomic heterogeneity of repair. Two repair subpathways have been distinguished: a (transcription independent) global genome repair pathway and a trancription coupled repair pathway specific for lesions (including ionizing radiation induced damage) in the transcribed strand of active genes. Specific genetic factors have been identified in both pathways: XP-C cells perform transcription coupled repair only, whereas CS cells are defective in this repair pathway but proficient in global genome repair. The contribution of the global genome and transcription coupled repair pathways to the removal of structurally different UV-induced lesions have been studied in normal, XP-C and CS cells. The results suggest that the defect in CS relates more to a transcription defect than a repair defect and that the significance of transcription coupled repair for removal of lesions depends on the type of lesion and the dose employed. Permeabilized cells have been utilized to study the role of chromatin structure in UV-induced repair by in vitro reactions. Transcription and replication activities are tightly associated with chromatin lacking the majority of cellular proteins. Also the polymerization step of NER is associated with chromatin; the association of incision activity with chromatin has not yet been demonstrated.

D. Mutagenesis.

The major types of mutations induced by ionizing radiation are large deletions and rearrangements. Analysis of several X-ray and high LET radiation induced mutations in the HPRT gene indicate that many mutants have lost the whole gene and mapping of breakpoints requires molecular probes outside the gene. In the case of X-rays, large deletions were formed by processes of illegitimate recombination. Taken together, the data show a broad distribution of sizes of deletion for both radiation qualities and suggest that α-particles induce more complex mutations than X-rays (more data are needed to verify this possibility). Since some of the deletions extend over a 3 Mb region, a much larger region than previously suspected, the results confounds predictions suggesting that hemizygous genes such as HPRT cannot detect very large mutations.

Site-specific breaks were introduced in mammalian cells, by electroporation of restriction endonucleases and their consequences assessed in survival and mutation assays. AT was shown to be sensitive reinforcing the view that the defect in this syndrome relates to the processing of DNA breaks. A similar approach with plasmids in yeast has revealed that radiosensitive mutants may differ either in efficiency and/or fidelity of DSB repair. To investigate the effect of radiation on intrachromosomal recombination, experiments are initiated to construct normal and radiosensitive hamster cell lines containing selectable markers.

Sequence analysis at the deletion breakpoints in spontaneous HPRT mutants in Fanconi anemia

(FA) cells, revealed features typical for V (D) J recombinase-mediated cleavage and joining. This suggests that illegitimate recombination may become active in FA pathology.

UV-induced mutations at the HPRT gene have been analysed in repair proficient and deficient hamster cells. A clear correlation was found between repair phenotype and distribution of mutations. Furthermore the data suggested that the distribution of mutations was determined by repair as well as different fidelities of replication of damaged leading and lagging strand.

E. Effects of radiation on cell proliferation and differentiation.

Human keratinocytes were used to identify genes and factors involved in radiation response. A new family of radiation responsive genes was identified and studied. SPRR genes code for precursor proteins of the cornified cell envelope, a structure typical for terminally differentiated keratinocytes and play an essential role in the barrier function of the skin. The expression of SPRR genes tightly regulated during the maturation of epidermal cells, is disturbed by UV- and ionizing radiation. SPRR's are small rigid proteins which can form cross-bridges between rather flexible meshes of crosslinked loricrin molecules. Variations in the concentration of the different classes of SPRR proteins, which can be dictated by external stress (e.g. radiation), inflammation, skin aging or tissue inherent factors, determines the rigidity of the cornified envelope. It is suggested that SPRR's are part of a genetic program which has evolved as a defence mechanism against environmental stress. Several transcription factors and signal transduction pathways involved in the regulation of these genes have been identified.

F. Generation of repair deficient mouse models

Using the recently developed technology of gene targeting in mouse stem cells transgenic mice with mutated repair genes were generated . Although ERCC1 mice are viable they have a severely reduced lifespan (KO <4 weeks, subtle mutant 4 weeks to 6 months depending on the genetic background). An unexpected feature exhibited by these mice is the high frequency of poly- and aneuploidy observed in several internal organs. In view of the likely dual functionality of ERCC1 in NER and in mitotic recombination it is plausible that the unexpected symptoms are derived from the recombination defect. The mice are extremely sensitive to genotoxic agents and completely deficient in NER. Mouse models mimicking mutations in XPB/ERCC3 and CSB/ERCC6 found in XP-B and CSB patients respectively and mice carrying a defect in HHR6A and 6B genes (postreplication repair), were generated. In addition mouse models are being generated for the XPD/ERCC2, the HHR23A and 23B genes and the HHR52 and 54 (recombination repair) genes.

Head of project 1: Prof. Dr. Lohman

II. Objectives for the reporting period
1. Topography of DNA repair.
    To assess the role of chromatin structure in DNA repair by investigating induction and repair of structural different DNA lesions in different genomic regions of mammalian cells and by studying (in vitro) repair of DNA damage in intact chromatin.
2. Molecular analysis of mutations.
    To determine spectra of genetic changes at the DNA level in the endogeneous HPRT and APRT genes in UV-irradiated normal and repair deficient cell lines.
3. Isolation and characterization of repair deficient mutants.
    To expand the collection of repair deficient rodent cell lines and to characterize mutants with regard to known complementation groups and biochemical defect.
4. Cloning of repair genes.

III. Progress achieved including publications
1. **Topography of DNA repair.**
    It is obvious that the condensed structure of DNA in chromatin may affect the induction and repair of DNA lesions across the genome. Biochemical methods have been developed to measure frequencies of DNA lesions as well as repair events in specific sequences. Our efforts have been focussed on the induction and repair of DNA lesions in transcriptionally active genes and inactive genes in repair proficient and deficient mammalian cells. Different assays employing either specific repair enzymes (T4 endonuclease V, UvrABC excinuclease), single stranded DNA specific enzymes (nuclease S1) or antibodies (anti BudR) have been applied to detect various DNA photolesions (UV-induced cyclobutane pyrimidine dimers (CPD), 6-4 pyrimidone photoproducts (6-4 PP), DNA single strand breaks (SSB)) as well as BudR containing DNA in defined sequences. The assay is either based on the cutting at damaged sites in DNA or on the isolation of DNA fragments containing BudR labelled repair patches.
    In a series of experiments we have made a comparison between the repair kinetics of 6-4 PP and CPD in active and inactive genes in human and hamster cells. The results can be summarized as follows: (i) Both in human and hamster cells 6-4 PP are induced at 3-fold lower frequency in both active and inactive genes compared to

CPD; as a consequence repair kinetics of CPD and 6-4 PP are determine at 10 J/m^2 and 30 J/m^2 respectively. (ii) Repair of 6-4 PP occurs faster in active housekeeping genes (ADA, HPRT, DHFR) than in X-chromosomal inactive genes (Factor IX, 754 gene). Also the rate of repair of 6-4 PP exceeds the rate of repair of CPD, no preferential repair of 6-4 PP in the transcribed strand of active genes was observed. Yet it is clear that 6-4 PP are target for transcription coupled repair as under conditions of defective global repair (i.e. in XP-C cells) 6-4 PP are selectively removed from the transcribed strand. (iii) Our results strongly suggest that the significance of transcription coupled repair for removal of DNA lesions depends on the type of lesions and on the dose employed. At high dose initiation of transcription is severely inhibited and therefore transcription coupled repair is eiher inactive or very slow. This implicates that at low doses the contribution of transcription coupled repair to removal of lesions from active genes becomes much more important. Since ionizing radiation induced DNA damage is target for transcription coupled repair and ionizing radiation efficiently inhibits transcription initiation, the effect of transcription coupled repair on radiosensitivity (as deducted from experiments with relatively high dose of X-rays) might be underestimated. Sofar not much information is available on heterogeneity of repair of radiation induced strand breaks in general and the role of transcription coupled repair. We have explored the specific conversion of single strand DNA breaks into double strand breaks by nuclease S$_1$ (under conditions of high ionic strength) to measure the induction of radiation induced damage in different genomic regions. To avoid aspecific breakage as much as possible, preparation of DNA and enzymatic steps are carried out in agarose blocks. Finally, the DNA is separated by pulse field electrophoresis and blotted onto membranes. Preliminary results indicate that DNA damage in cells irradiated with 5 Gy is detectable in the amplified DHFR locus.

Much of the activities involved in replication and transcription, are compartmentalized in the nucleus. The coupling of transcription to repair and the organization of transcription units into 'factories' by association to a nucleoskeleton, stresses an important role of nuclear architecture in DNA repair. To study the role of nuclear architecture in DNA repair we prepared chromatin with preserved structure and function (replication and transcription) and we analysed the capacity of chromatin to repair in the absence of added extract. The experiments demonstrate that the repair synthesis step in nucleotide excision repaire is firmly asociated with chromatin. This chromatin associated repair activity is not due to transcription coupled repair, but may reflect the concentration of global repair activity at the nucleoskeleton. With regard to localization of incision activities the experiments are inconclusive as these activities are not detected or inactivated in the chromatin even under very mild conditions of chromatin preparation.

2. Mutagenesis.

It is conceivable that the accelerated removal of DNA lesions from the transcribed strand of active genes in mammalian cells has its reflection on mutagenesis. The molecular nature of mutations induced by UV light has been investigated in HPRT mutants from various Chinese hamster cell lwith different repair capacities. Among the HPRT mutants analyzed from repair proficient cells (two cell lines, i.e. V79 and CHO) all possible classes of base pair changes were present, the majority being transversions. Since almost all HPRT mutations occur at dipyrimidine sites, it is likely that they are caused by UV-induced photoproducts (CPD and/or (6-4) photoproducts) at these sites. In repair proficient cells, over 85% of the HPRT mutations could be

attributed to lesions in the non-transcribed strand of the HPRT gene. Thus the data on the strand distribution of mutations in both genes are consistent with the hypothesis that strand specific repair of CPD in expressed mammalian genes is associated with strand specificity for mutation induction: the selective removal of CPD from the transcribed strand of the HPRT gene would account for the presence and the absence of a strand bias in mutations, respectively. In vivo the selective repair of CPD in the transcribed strand of the p53 gene in UV-B irradiated hairless mice is in accordance with the notion that the majority of p53 mutations in skin tumors is caused by photolesions in the poorly repaired nontranscribed strand.

The absence of global genome and transcription coupled repair results in a dramatic change in the HPRT mutation spectrum compared to repair proficient conditions as mutations consist almost solely of GC > AT transitions. The majority of the base pair changes in repair deficient cells are caused by photoproducts in the transcribed strand of the HPRT gene. Thus the absence of DNA repair affects the mutation spectrum in two ways: it alters the types of UV-induced mutations as well as the strand distribution of mutations. These observations are best explained by assuming that under repair proficient conditions CPD give the major contribution to mutagenesis, whereas under repair deficient conditions mutations are mainly caused by 6-4PP which are known to be highly mutagenic. Nevertheless it is still possible that the strand bias in HPRT mutations seen in repair proficient rodent cells, is actually due to strand specific repair of 6-4PP at the low UV-dose used for mutation induction experiments.

The effect of defective preferential repair on mutagenesis was assessed in the UV-sensitive hamster cells UV61. The UV-sensitivity in this cell line is complemented by the human ERCC6/CSB gene which is mutated in CS patients. In UV61 cells repair of CPD in the transcribed strand of active genes is delayed, a repair phenotype also observed in the moderately UV-sensitive cell line RH1-26 (complemented by ERCC2/XPD). But in contrast to the latter, UV-induced mutagenesis in UV61 is enhanced compared to wildtype cells and strongly biased toward the transcribed strand. A possible explanation is, that in addition to defective CPD repair, also removal of 6-4 PP from active genes is delayed. A defect in 6-4 PP repair would be consistent with the 6-4 PP repair phenotype observed in CS cells.

3. Isolation and characterization of repair deficient mutants.

A collection of rodent mutants sensitive to DNA damaging agents including UV, ionizing radiation and cross-linking agents, has been established during the course of the project. Several X-ray sensitive rodent cell lines have been been isolated and characterized with regard to complementation group and biochemical defect. Several of these mutants represented new complementation groups. One complementation group displays the characteristics of Ataxia telangiectasia (AT) cells (such as radioresistant DNA synthesis (RDS)) and these mutants (V-C4,V-E5,V-G8) serve as a hamster model for AT and the Nijmegen Breakage Syndrome (NBS). However by introducing a single chromosome 11, the region carrying the human AT gene has been excluded to complement the AT-like hamster mutants. This suggests that these mutants are not defective in the gene homologous to AT and most likely are defective in another closely related gene, i.e. NBS. Fusing of the AT-like hamster mutants with their parental V79 cells showed only partial complementation of RDS but complete complementation of the radiosensitivity. In contrast to intraspecies hybrids, a full complementation of RDS as well as radiosensitivity was achieved in hybrids of AT-like hamster mutants and human cells, suggesting that radiosensitivity and RDS are

pleiotropic effects of the same afflicted gene.

Another X-ray sensitive Chinese hamster V79 cell mutant (V-C8) which is also hypersensitive to MMC, shows RDS following γ-irradiation a feature of ataxia-telangiectasia (AT) cells. The mutant turned out to be defective in DSB, but not in SSB repair. The increased sensitivity to X-rays is accompanied by sensitivity to several radiomimetic agents. Moreover, spontaneous MMC-resistant revertants show a normal response to X-ray induced cell killing, suggesting that the observed phenotype results from a single mutation. These revertants, however, show RDS again suggesting that RDS and X-ray sensitivity can be complemented independently. Complementation analysis with mutants belonging to different complementation groups, revealed that VC-8 is a unique X-ray sensitive mutant.

4. Cloning repair genes.

In order to isolate the gene complementing the defect in AT-like hamster mutants, micro cell-mediated chromosome transfer was used. At least 20 independent hybrid clones between the mutants and each one of the human chromosomes 1,2,4,5,15,17 or 18 were isolated. All hybrid clones remained X-ray sensitive except two hybrids with chromosome 4 and 15 showing intermediate sensitivity. In situ hybridization revealed that this partial correction was due to the presence of a mouse chromosome. In the two hybrids RDS was corrected in the one carrying chromosome 4, but not in the one with chromosome 15.

Microcell mediated chromosome transfer has been used to correct AT cells. The radiosensitivity of AT-D (and AT-C) cells was corrected by chromosome 11 only in spite of the reported correction of AT-D by multiple c-DNAs (mapping to different chromosomes than chromosome 11). Our findings demonstrate, that for establishing cDNAs as AT candidate genes, chromosome studies are needed to exclude aspecific correction.

RAD52 group genes in the yeast Saccharomyces cerevisiae are involved in the recombinational repair of double-strand breaks in DNA. Mutants in this group are sensitive to ionizing radiation, usually have a block in meiotic recombination and also show reduced levels of some types of mitotic recombination. The most extreme phenotype is shown by RAD51, 52 and 54 mutants. To study the evolutionary conservation of the RAD52 group genes we isolated the RAD51 and RAD54 homologs of the distantly related yeast strain Schizosaccharomyces pombe: rhp51 and 54. Both genes show a remarkable similarity at the amino acid level with their homologs in S. cerevisiae (69% and 54% identity, respectively). Gene disruption experiments indicate that rhp51 and 54 are not essential for viability. Both mutants are extremely sensitive for ionizing radiation. In contrast to S.cerevisiae rad51 and 54 mutants, the S.pombe mutants also show a strongly reduced survival after UV-irradiation, suggesting that in this yeast strain part of the UV-damage is removed by recombinational repair. Degenerated primers based on conserved amino acid sequences of S.cerevisiae RAD52 and its counterpart from S.pombe, rad22, were used to clone part of the mouse RAD52 homolog by RT-PCR. The amplification product was used to isolate full-length cDNA clones from man and mouse. The identity between the human and mouse RAD52 homologs is 69% and the overall similarity 80%. The homology of the mammalian proteins with their counterparts from yeast is somewhat less and primarily concentrated in the N-terminal region. Low amounts of RAD52 RNA were observed

in adult mouse tissues. A relative high level of expression was obeserved in mouse testis and thymus tissue, suggesting that the mammalian RAD52 protein, like its

homolog from yeast, plays a role in recombination. The mouse RAD52 gene is located near the tip of chromosome 6 in region G3. The human equivalent maps to region p13.3 of chromosome 12. Until now this human chromosome has not been implicated in any of the rodent mutants with a defect in the repair of double-strand breaks. The presence of RAD52 group homologs in S.pombe and in mammals, strongly suggest that, at least, part of the recombinational repair pathway in S.cerevisiae is conserved in evolution. Overexpression of the RAD52 gene in E.coli has lead to the purification of the protein and the generation of antibodies.

5. Mouse models

Constructs are being made to knock out the RAD52 gene in ES cells to generate transgenic mice.

The location of the HPRT gene on the X-chromosome prevents the recombinational events which can result in loss of heterozygosity. In order to be able to detect these events another marker gene for mutagenesis studies has been selected i.e. the APRT gene. A transgenic mouse is generated in which one of the two APRT alleles has been inactivated by homologous recombination.

The HHR23B protein has been shown to be tightly associated with the XP-C protein. We are currently in the process of generating a HHR23B transgenic mouse to (i) investigate the phenotype of a defective HHR23B gene and (ii) to cross with the XP-C mouse.

Publications

Busch, D.B., M.Z. Zdzienicka, A.T. Natarajan, N.J. Jones, W.I.J. Overkamp, A. Collins, D.L. Mitchell, M. Stefanini, R. Riboni, R. Bliss Albert, N. Liu and L.H. Thompson (1995) A FAECB Chinese hamster overy cell mutant, UV40, that is sensitive to diverse mutagens and represents a new complementation group of mitomycin C sensitivity, Mutation Res., subm.

Cock, J.G.R. de, E.C. Klink, P.H.M. Lohman and J.C.J. Eeken (1992) Absence of strand-specific repair of cyclobutane pyrimidine dimers in active genes in Drosophila melanogaster Kc cells, Mutation Res., 274, 85-92.

Cock, J.G.R. de, E.C. Klink, W. Ferro, P.H.M. Lohman and J.C.J. Eeken (1992) Neither enhanced removal of cyclobutane pyrimidine dimers nor strand-specific repair is found after transcription induction of the ß₃-tubilin gene in a Drosophila embryonic cell line Kc, Mutation Res., 293, 11-20.

Cock, J.G.R. de, A. van Hoffen, J. Wijnands, G. Molenaar, P.H.M. Lohman and J.C.J. Eeken (1992) Repair of UV-induced (6-4)photoproducts measured in individual genes in the Drosophila embryonic Kc cell line, Nucl. Acids Res., 20, 4789-4793.

Eeken, J.C.J., A.W.M. de Jong, M. Loos, C. Vreeken, R. Romeijn, A. Pastink and P.H.M. Lohman (1994) The nature of X-ray-induced mutations in mature sperm and spermatogonial cells of Drosophila melanogaster, Mutation Res., 307, 201-212.

Hafezparast, M., P. Kaur, M.Z. Zdzienicka, R. Athwal, A.R. Lehmann and P.A. Jeggo (1993) Sub-chromosomal localisation of a gene (ERCC5) involved in double strand

break repair to the region 2q34-36, Som. Cell Mol. Genet., 19, 413-421.

Helbig, R., E. Gerland, M.Z. Zdzienicka and G. Speit (1995) The pattern of mutations induced by neocarzinostatin and methyl methanesulfonate in the ataxia-telangiectasia-like Chinese hamster cell line V-E5, Mutation Res., 336, 307-316.

Helbig, R., M.Z. Zdzienicka and G. Speit (1995) The effect of the defective DNA double-strand break repair on mutations and chromosome aberrations in the Chinese hamster cell mutant XR-V15B, Radiation Res., in press.

Hoffen van, A, J. Venema, R. Meschini, A.A. van Zeeland, and L.H.F. Mullenders (1995) Transcription -coupled repair removes both cyclobutane pyrimidine dimers and 6-4photoproducts with equal efficiency and in a sequential way from transcribed DNA in xeroderma pigmentosum group C fibroblasts. The EMBO J. 14, 360-367

Hoffen van, A., A.T.Natarajan, L.V. Mayne, A.A. van Zeeland, L.H.F. Mullenders, and J. Venema (1993) Deficient repair of the transcribed strand of active genes in Cockayne's syndrome. Nucleic Acids Res. 21,5890-5895

Jackson, D.A., A.S. Balajee, L.H.F. Mullenders, and P.R.Cook (1994) Sites in human nuclei where DNA damage by ultraviolet light is repaired: visualization and localization relative to the nucleoskeleton. J. Cell Sci 107, 1745-1752.

Jongmans, W., J. Wiegant, M. Oshimura, M.R. James, P.H.M. Lohman and M.Z. Zdzienicka (1993) Human chromosome 11 complement ataxia-telangiectasia cells but does not complement the defect in AT-line Chinese hamster cell mutants, Hum. Genet., 92, 259-264.

Jongmans, W., G.W.C.T. Verhaegh, K. Sankaranarayanan, P.H.M. Lohman and M.Z. Zdzienicka (1993) Cellular characteristics of Chinese hamster cell mutants resembling ataxia telangiectasia cells, Mutation Res., DNA Repair, 294, 207-214.

Jongmans, W., G.W.C.T. Verhaegh, N.G.J. Jaspers, M. Oshimura, E.J. Stanbridge, P.H.M. Lohman and M.Z. Zdzienicka (1995) Studies on phenotypic complementation of ataxia-telangiectasia cells by chromosome transfer, Am. J. Hum. Genet., 56, 438-443.

Kalle, W.H.J., A-M. Hazekamp-van Dokkum, P.H.M. Lohman, A.T. Natarajan, A.A. van Zeeland and L.H.F. Mullenders (1993) The use of streptavidin coated magnetic beads and biotinylatd antibodies to investigate induction and repair of DNA damage: Analysis of repair patches in specific sequences of UV irradiated human fibroblasts. Analytical Biochemistry 208, 228-236

Koken, M.H.M., C. Vreeken, A.A.M. Bol, Ngan Ching Cheng, I. Jaspers-Dekker, J.H.J. Hoeijmakers J.C.J. Eekens (1992) Homolog of the xeroderma pigmentosum complementation-group B correcting gene, ERCC3, Nucl. Acids Res., 20, 5541-5548.

Lohman, P.H.M., B. Morolli, F. Darroudi, A.T. Natarajan, J.A. Gossen, J. Venema, L.H.F. Mullenders, E.W. Vogel, H. Vrieling, and A.A. van Zeeland (1992) Contributions from molecular/biochemical approaches in epidemiology to cancer risk

assessment and prevention. Env. Health Perspectives 98, 155-165

Lohman, P.H.M., K. Sankaranarayanan and J. Ashby (1992) Choosing the limits to life, Nature 357, 185-186.

Muris, D.F.R., C. Vreeken, A.M. Carr, B.C. Broughton, A.R. Lehmann, P.H.M. Lohman and A. Pastink (1993) Cloning the RAD51 homologue of Schizo-saccharomyces pombe, Nucl. Acids Res., 21, 4586-4591.

Muris, D.F.R., O. Bezzubova, J-M. Buerstedde, C. Vreeken, A.S. Balajee, C.J. Osgood, C. Troelstra, J.H.J. Hoeijmakers, K. Ostermann, H. Schmidt, A.T. Natarajan, J.C.J. Eeken, P.H.M. Lohman and A. Pastink (1994) Cloning of human and mouse genes homologous to RAD52, a yeast gene involved in DNA repair and recombination, Mutation Res., 315, 295-305.

Mullenders, L.H.F., R.J. Sakkers, A. van Hoffen, J. Venema, A.T. Natarajan and A.A. van Zeeland (1993) Intragenomic heterogeneity of UV-induced DNA repair: relationship to chromatin structure and transcriptional activity. In DNA repair mechanisms, Alfred Benzon Symposium , 35, 247-254

Mullenders, L.H.F., J.A. Venema, A. van Hoffen, R.J. Sakkers, A.T. Natarajan and A.A. van Zeeland (1992) Genomic heterogeneity of UV-induced repair: relationship to higher order chromatin stucture and transcriptional activity. In 'Radiation research', vol II, (Eds.Dewey W.C.,Edington M., Fry R.J.M., Hall E.J., Whitmore G.F.) 155-159.

Mullenders, L.H.F., A.-M. Hazekamp-van Dokkum, W.H.J. Kalle, H. Vrieling, M.Z. Zdzienicka, and A.A. van Zeeland (1993) UV-induced photolesions, their repair and mutations. Mutation Research 299, 271-276

Mullenders, L.H.F, R.J. Sakkers. and H.H. Kampinga (1994) Chromatin structure, hyperthermia and repair of UV-induced DNA photolesions in mammalian cells.In ' Chromosomal Alterations. Origin and Significance' (G.Obe and A.T.Natarajan, Eds) 21-30 Springer Verlag, Berlin

Mullenders, L.H.F. and C.A. Smith (1994) DNA repair in specific sequences and genomic regions. In 'Methods to assess DNA damage and repair. Interspecies comparisons' (R.G Tardiff, P.H.M.Lohman, G.N.Wogan , Eds.) 141-156 Scientific group on Methodologies for the Safety Evaluation of Chemicals (SGOMSEC), John Wiley and Sons,Chicester, U.K.

Overkamp, W.J.I., M.A. Rooimans, I. Neuteboom, P. Telleman, F. Arwert and M.Z. Zdzienicka (1993) Genetic diversity of mitomycin C-hypersensitive Chinese hamster cell mutants: A new complementation group with chromosomal instability, Somatic Cell and Molec. Genetics, 19, 431-437.

Pergola, F., M.Z. Zdzienicka and M.R. Lieber (1993) V(D)J recombination in mammalian cell mutants defective in DNA double-strand break repair, Mol. Cel. Biol., 13, 3464-3471.

Ruven, H.J.T., R.J.W. Berg, C.M.J. Seelen, J.A.J.M. Dekkers, P.H.M. Lohman, L.H.F. Mullenders and A.A. van Zeeland (1993) Ultra-violet induced cyclobutane pyrimidine dimers are selectively removed from transcriptionally active genes in the epidermis of the hairless mouse. Cancer Res. 53, 1642-1645

Ruven, H. J.T., C.M.J. Seelen, P.H.M. Lohman, H. van Kranen, A. A. van Zeeland, and L.H.F. Mullenders (1994) Strand-specific removal of cyclobutane pyrimidine dimers from the p53 gene in the epidermis of UVB-irradiated hairless mice. Oncogene, 9, 3427-3432.

Sakkers, R.J., A.R. Filon, J.F. Brunsting, H.H. Kampinga, L.H.F. Mullenders and A.W.T.Konings. (1993) Heat-shock treatment selectively affects induction and repair of cyclobutane pyrimidine dimers in transcriptionally active genes in ultraviolet-irradiated human fibroblasts. Radiation Res. 135, 343-350

Sakkers, R.J., A.R. Filon, J.F. Brunsting, H.H. Kampinga, A.W.T. Konings and L.H.F. Mullenders (1995) Selective inhibition of repair of active genes by hyperthermia is due to inhibition of global and transcription coupled repair pathways. Carcinogenesis , 16, 743-748

Sakkers, R.J., A.R. Filon, H.H. Kampinga, A.W.T. Konings and L.H.F. Mullenders (1995) Repair of UV-induced pyrimidine 6-4 pyrimidone photoproducts is selectively inhibited in transcriptionally active genes after heat treatment of human fibroblasts. Int. J. Radiation Biology 5, 495-499

Studzian, K., P. Telleman, G.P. van der Schans and M.Z. Zdzienicka (1994) Mutagenic response and repair of cis-DDP-induced DNA cross-links in the Chinese hamster V79 cell mutant V-H4 which is homologous to Fanconi anemia (group A), Mutation Res., 314, 115-120.

Telleman, P., W.J.I. Overkamp, N. van Wessel, K. Studzian, L. Wetselaar, A.T. Natarajan and M.Z. Zdzienicka (1995) A new complementation group of mitomycin C-hypersensitive Chinese hamster cell mutants that closely resembles the phenotype of Fanconi anemia cells, Cancer Res., 55, 3412-3416.

Telleman, P., W.J.I. Overkamp and M.Z. Zdzienicka (1995) Spectrum of spontaneously occurring mutations in the HPRT gene of the Chinese hamster V79 cell mutant V-H4, which is homologous to Fanconi anemia group A, Mutagenesis, subm.

Venema, J., Z. Bartosová, A.T. Natarajan, A.A. van Zeeland and L.H.F. Mullenders (1992) Transcription affects the rate but not the extent of repair of cyclobutane pyrimidine dimers in the human adenosine deaminase gene, J. Biol. Chem., 267, 8852-8856

Verhaegh G.W.C.T., N.G.J. Jaspers, P.H.M. Lohman and M.Z. Zdzienicka (1993) Co-dominance of radioresistant DNA synthesis in a group of AT-like Chinese hamster cell mutants, Cytogenet. Cell Genet., 63, 176-180.

Verhaegh, G.W.C.T., N.G.J. Jaspers, P.H.M. Lohman and M.Z. Zdzienicka (1994) The relation between radiosensitivity and radioresistant DNA synthesis in ionizing

radiation-sensitive rodent cells mutants, In: Molecular Mechanisms in Radiation Mutagenesis and Carcinogenesis Proc. Symp (K.H. Chadwick, R. Cox, H.P. Leenhouts and J. Thacker, eds.), Published by the European Commission, 23-28.

Verhaegh, G.W.C.T., W. Jongmans, B. Morolli, N.G.J. Jaspers, G.P. van der Schans, P.H.M. Lohmand and M.Z. Zdzienicka (1995) A novel type of X-ray-sensitive Chinese hamster V79 cell mutant with radioresistant DNA synthesis and defective DNA double-strand break repair, Mutation Res., in press.

Verhaegh, G.W.C.T., W. Jongmans, N.G.J. Jaspers, A.T. Natarajan, M. Oshimura, P.H.M. Lohman and M.Z. Zdzienicka (1995) A gene which regulates DNA replication in response to DNA damage is located on human chromosome 4q, Am. J. Hum. Genet., in press.

Vreeswijk, M.P.G., A. van Hoffen, B.E. Westland, H. Vrieling, A. A. van Zeeland, and L.H.F. Mullenders (1994) Analys of repair of cyclobutane pyrimidine dimers and pyrimidine(6-4) pyrimidone photoproducts in transcriptionally active and inactive genes in Chinese hamster cells. J.Biol.Chem., 16, 31858-31863.

Vrieling, H., L.H. Zhang, A.A. van Zeeland and M.Z. Zdzienicka (1992) UV-induced *hprt* mutations in a UV-sensitive hamster cell line from a complementation group 3 are biased towards the transcribed strand, Mutation Res., 274, 147-155.

Zdzienicka, M.Z., J. Venema, D.L. Mitchell, A. van Hoffen, A.A. van Zeeland, H. Vrieling, L.H.F. Mullenders, P.H.M. Lohman and J.W.I.M. Simons (1992) (6-4) Photoproducts and not cyclobutne pyrimidine dimers are the main UV-induced mutagenic lesions in Chinese hamster cells, Mutation Res., DNA Repair, 273, 73-83.

Zdzienicka, M.Z., G.W.C.T. Verhaegh, W. Jongmans, N.G.J. Jaspers, M. Oshimura, M.R. James and P.H.M. Lohman (1993) AT-like radiosensitive rodent cell mutants: An alternative approach to the isolation of the AT gene(s), in: Ataxia-telangiectasia workshop V (R.A. Gatti and R.B. Painter, eds.), Nato ASI Series, Vol. H 77, 87-97.

Zdzienicka, M.Z., W. Jongmans, G.W.C.T. Verhaegh, N.G.J. Jaspers, G.P. van der Schans and M. Oshimura (1994) Functional complementation studies with X-ray-sensitive mutants of Chinese hamster cells closely resembling Ataxia-telangiectasia cells, Int. J. Radiat. Biol., 66, 189-195.

Zdzienicka, M.Z. and A. Pastink (1994) Cloning of mammalian DNA repair genes, In: Radiopathology and Radiation Protection, The State of the Art, 1, 11.

Zdzienicka, M.Z. and W. Jongmans (1994) Rodent cell mutants as a tool towards the identification of human genes involved in the cellular defence mechanisms against ionizing radiation, In: Molecular Mechanisms in Radiation Mutagenesis and Carcinogenesis Proc. Symp (K.H. Chadwick, R. Cox, H.P. Leenhouts and J. Thacker, eds.), Published by the European Commission, 11-16.

Zdzienicka, M.Z. (1995) Mammalian mutants defective in the response to ionizing radiation-induced DNA damage, Mutation Res., 336, 203-213.

Zdzienicka, M.Z., J. Venema, D.L. Mitchell, A. van Hoffen, A.A. van Zeeland, H. Vrieling, L.H.F. Mullenders, P.H.M. Lohman, and J.W.I.M. Simons (1992) (6-4) Photoproducts and not cyclobutane pyrimidine dimers are the main UV-induced mutagenic lesions in Chinese hamster cells. Mutation Research, 273, 73-83

Zdzienicka, M.Z., W. Jongmans, M. Oshimura, A. Priestly, G.F. Whitmore and P.A. Jeggo (1995) Complementation analysis of the murine scid cell line, Radiation Res., 143, 238-244.

Zeeland, A.A. van, L.H.F. Mullenders, M.Z. Zdzienicka and H. Vrieling (1993) Influence of strand-specific repair of DNA damage on molecular mutation spectra, In: DNA Repair Mechanisms (V.A. Boh, K. Wassermann and K.H. Kraemer, eds.), Proceedings Alfred Benzon Symposium No. 35, Munksgaard, Copenhagen, pp. 117-125

Zeeland van, A.A., L.H.F. Mullenders, M.Z. Zdzienicka and H. Vrieling (1993) Gene specific repair and molecular mutation spectra, In: Frontiers of Photobiology (A. Shima, M. Ichihashi, Y. Fujiwara and H. Takebe, eds.), Proceedings of the 11th Intern. Congr. on Photobiology, Kyoto, Japan, 7-12 September 1992, Elsevier Science Publishers, pp. 375-378.

Zeeland van, A.A., H. Vrieling, J. Venema, A. van Hoffen, P. Menichini, M.Z. Zdzienicka, P.H.M. Lohman and L.H.F. Mullenders (1994) DNA repair and mutagenesis, In: Molecular Mechanisms in Radiation Induced Mutagenesis and Carcinogenesis (K.H. Chadwick, R. Cox, H.P. Leenhouts and J. Thacker, eds.), Europ. Commission Publ., Luxembourg, pp. 3-10.

Head of project 2: Prof. Bridges

II. Objectives for the reporting period

<u>Identification of radiosensitive individuals</u>

To carry out investigations of A-T variants and other radiation-sensitive individuals using the single cell microgel assay and other established techniques.

<u>Cloning of human DNA repair genes</u>

To clone and characterize the hamster *xrs* (XRCC5) radiosensitivity gene.

To characterize *Schizosaccharomyces pombe* genes, to study them as models for human genes, in particular in relation to their involvement in the cell cycle, and to use them to clone corresponding human genes.

III. Progress achieved including publications

<u>Identification of radiosensitive individuals</u>

(1) Ataxia-telangiectasia (A-T) has remained of considerable interest as the model for human cellular and clinical radiosensitivity. We have extended our investigations of the genotype/phenotype interaction to include a summary of the clinical, clastogenic and cellular (for both fibroblasts and T-lymphocytes) sensitivity, and the mutation frequency to 6-thioguanine resistance in circulating T-cells for a panel of 16 probands, their sibs and parents. While none of these features was strongly prognostic, the mutation frequency gave indications that it might prove of value. Our recent contribution to the cloning of the ATM gene has shown the utility of these combined clinical, cellular and molecular studies in revealing the nature of the human gene defect which generates the dramatic radiosensitivity.

(2) Other Specific Instances of Radiosensitivity:

(a) 180BR is a fibroblast cell line derived from a leukemia patient who died from radiation morbidity following radiotherapy. He did not have the clinical features of A-T, and although his cells showed a level of sensitivity similar to A-T, they could be distinguished from A-T by the absence of radiation resistant DNA synthesis - a cellular diagnostic of the syndrome. We have shown that the fibroblasts are severely defective in the repair of radiation induced double strand breaks and chromosome damage. This individual represents the first case of a human defective in this mode of repair.

(b) 290BR is a cell line derived from a second radiosensitive leukemia patient with a similar clinical response but who did not succumb. The fibroblasts have an A-T like level of radiosensitivity and defect in radiation resistant DNA synthesis. He is not thought to be an A-T patient as defined clinically and genetically. He may thus well represent a second distinct entity from A-T as far as

radiation sensitivity is concerned. There is no defect in the repair of double strand breaks or interphase chromosome damage.

(c) XP14BR is a culture developed from a xeroderma pigmentosum patient from complementation group C who reacted badly to radiotherapy. These cells are A-T like in the level of radiosensitivity but have normal radiation resistant DNA synthesis. We have successfully introduced in the full length XP-C gene by DNA transfection into an SV40 immortalised cell line and corrected its UV sensitivity but not its ionising radiation sensitivity. We may thus have identified another human gene(s) for radiosensitivity.

Following an intensive search for ionising radiation sensitivity in other XP cell lines we have confirmed only one such instance in a fibroblast culture from XP3BR, which belongs to complementation group G. Cellular heterogeneity was demonstrated when T-cells and a B-cell derived lymphoblastoid line from this patient were shown to have a normal radiation response.

(3) General Studies

(a) The establishment of a panel of radiation sensitive fibroblast cell lines of unique origin has made it possible for us to demonstrate the possibility that chromosome damage, as detected on FISH analysis, can provide an early measure of individual radiosensitivity.

(b) We have used the single cell microgel "Comet' assay to demonstrate individual sensitivity to the induction of radiation induced single strand breaks and the importance of radical scavanging levels in its repair.

Cloning of DNA repair genes

(1) Mammalian genes

A positional cloning strategy has been utilised to clone the gene defective in the radiation sensitive hamster *xrs* mutants. The first step of this approach involved the identification of chromosome 2 as a complementing human chromosome. The complementing gene was then sub-localised to the region 2q33-35, and a complementing human-hamster hybrid constructed, which contained less than 5 Mb of human DNA. Using a variety of procedures, yeast artificial chromosomes (YACs) from this region of chormosome 2 were isolated and a YAC contig constructed, which spanned the region of human DNA present in the complementing hybrid. The next stage of our cloning strategy involved the identification of a complementing YAC. However, a candidate gene mapping to this region was identified, and analysis of the hybrids that we had constructed for our localisation studies, confirmed that the candidate gene, Ku80, was consistently present in complementing hybrids and absent in non-complementing hybrids. Finally, Ku80 cDNA was cloned into a mammalian expression vector, introduced into *xrs* cells by DNA transfection, and shown to

complement all the defects characteristic of these mutants including their radiosensitivity, defects in double strand break rejoining and V(D)J recombination, and absence of DNA end-binding activity. Taken together the results identifed Ku80 as the product of XRCC5. Ku80 sequences were present in some YACs within our contig, and two of these YACs introduced into *xrs* cells by protoplast fusion have also been shown to complement the defects of these cells.

Ku80 is one subunit of the heterodimeric Ku protein. Additionally, Ku itself has been identified as being the DNA end-binding component of DNA dependent protein kinase (DNA-PK). It was therefore anticipated that the *xrs* mutants might lack DNA-PK activity. In collaboration with Dr. S. P. Jackson, a sensitive assay was developed to examine the lower levels of DNA-PK found in rodent cells compared to human cells. Using this assay, *xrs* cells were found to be lacking DNa-PK acitivity confirming that Ku functions *in vivo* as the end-binding component of DNA-PK. DNA-PK activity was also restored in *xrs* cells complemented by the human Ku80 gene. These results raised the possibility that either Ku70, the other subunit of Ku, or DNA-PK$_{cs}$, the catalytic component of DNA-PK, might be defective in other mutants with similar phenotypes to the *xrs* mutants. Three complementation groups of radiosensitive mutants with defects in double strand break rejoining and properties similar to the *xrs* mutants have been identifed (Ionising Radiation complementation groups 4, 5, and 7). Recently, a fourth group (group 6) has also been reported. We therefore examined these mutants, and found that the two mutants belonging to group 7 (V-3 and *scid* cells) contained normal levels of DNA end-binding activity, but were lacking DNA-PK activity, indicative of a defect in DNA-PK$_{cs}$. DNA-PK$_{cs}$ has a 14 Kb cDNA and a full length cDNA has not yet been obtained. To examine complementation, we therefore took an alternative approach of introducing YACs encoding DNA-PK$_{cs}$ into V-3 cells by protoplast fusion. Using this approach we identifed two YACs able to complement the radiosensitivity, defect in V(D)J recombination and deficiency in DNA-PK activity of V-3 cells. These results therefore identified DNA-PK$_{cs}$ as the product of XRCC7, the gene defective in the mouse *scid* cell line.

In recent work, we have commenced a molecular analysis of these two genes. The hamster Ku80 cDNA has been cloned and sequenced, and shows 78% homology at the amino-acid level to the human gene. The Ku80 gene from the *xrs* mutants is currently being sequenced using RT-PCR, and mutations have been identified in three out of the six mutants. All the *xrs* mutants are revertible at high frequency following azacytidine treatment, which has led to the suggestion that a "silent", methylated copy of the Ku80 gene is present in the parent hamster cell line. Our results to date are supportive of this hypothesis, since revertants contain both a mutant and wild type transcript. Partial cDNAs encoding the kinase domain of the DNA-PK$_{cs}$ gene from hamster and mouse have also been cloned and sequenced and show

approximately 80% homology to the human gene. Sequencing of this region from *scid* and V-3 cells is currently underway.

(2) *S. pombe* genes

(a) We have cloned and sequenced several genes potentially involved in the direct repair response of cells to radiation damage in fission yeast. One of these , rad18, is involved in a novel pathway of repair of uv damage as well as having a role in the repair of IR damage. The genes identified are conserved in S. cerevisiae and one human homolog has been identified, indicating that the gene products which underlie the repair pathways defined by the original mutants are conserved.

(i) The S. pombe rad2 gene is a member of a small class of structure specific endonucleases and we have identified the functional human homolog. This gene is identical to the MF-1 nuclease involved in lagging strand DNA synthesis, and suggests an intimate relationship between DNA repair and DNA replication which has not been previously exposed.

(ii) The rad18 gene is a member of the SMC group of proteins which have a structure reminiscent of myosins, are involved in DNA dynamics and are thought to act as "motor proteins". We have cloned a homolog from S. cerevisiae and anticipate that the same gene is conserved in mammalian cells. Genetic analysis demonstrates that rad18 is an essential gene. This is the first potential force generating protein identified in DNA repair.

(b) We have identified the pathway in fission yeast that prevents cell cycle progression after DNA damage. Six genes have been cloned and sequenced including all the "checkpoint rad" group of genes that are central to all the DNA structure checkpoints. Many of these proteins are conserved in S. cerevisiae and for one, rad3, we have identified a human homolog, demonstrating for the first time the conservation of the checkpoint pathways in metazoan cells. The human rad3 homolog is related to, but distinct from the ATM gene defective in ataxia telangiectasia patients, cells from whom are defective in G2 checkpoints and display radio resistant DNA synthesis

(i) Extensive genetic analysis of deletion and point mutants of the checkpoint genes has revealed a complex pathway and allowed us to build a sophisticated model for the DNA structure checkpoints. The model predicts that many of the checkpoint proteins act in a complex. We have identified physical interactions between two of the checkpoint proteins,

rad1 and rad17, and have evidence from two hybrid studies that other proteins in the pathway may also interact.

(ii) Analysis of chk1, a potential protein kinase suggests that it acts towards the end of the checkpoint pathway, and we have shown that its over-expression can prevent cell cycle progression. Rad24, one of two 14-3-3 protein homologs in S. pombe, is involved in the radiation checkpoint response and appears to act in parallel with chk1, possible by stabilising the active form of chk1. Further analysis of rad24 mutants with other DNA damage response genes has identified a genetic interaction with a casein kinase II homolog. Further analysis demonstrated that this genetic analysis resulted from a defect in the spindle assembly checkpoint in rad24 cells, which links for the first time the mechanisms preventing mitosis after either DNA damage or inhibition of spindle function.

Publications

Radiosensitive individuals

Arlett, C. F. (1992). Human cellular radiosensitivity - the search for the holy grail or a poisoned chalice. *Advances in Radiation Biology* **16**: 273-292.

Bridges, B. A., Arlett, C. F., Kuller, L. H., Modan, B., Boice, J., Jr., Miller, R. W., Wagner, L. K., Hall, E. J., Geard, C. R., Brenner, D. J., Land, C. E., Swift, M., Morrell, D., Massey, R. B. and Chase, C. L. (1992). Risk of breast cancer in ataxia-telangiectasia (1). *New Engl. J. Med.* **326**(20): 1357-1361.

Hsieh, C.-L., Arlett, C. F. and Lieber, M. R. (1993). V(D)J recombination in ataxia telangiectasia, Bloom's Syndrome, and a DNA ligase I-associated immunodeficiency disorder. *J. Biol. Chem.* **268**: 20105-20109.

Cole, J. and Arlett, C. F. (1994). Cloning efficiency and spontaneous mutant frequency in circulating T-lymphocytes in ataxia-telangiectasia patients. *Int. J. Radiat. Biol.* **66**: S123-S131.

Green, M. H. L., Lowe, J. E., Cole, J., Waugh, A. and Arlett, C. F. (1994). The modulation of DNA damage in human lymphocytes by dietary Vitamin C supplementation. Molecular mechanisms in radiation mutagenesis and carcinogenesis Eds. K. H. Chadwick, R. Cox, H. P. Leenhouts and J. Thacker. Luxembourg, European Commission. 85-89.

Green, M. H. L., Lowe, J. E., Waugh, A. P. W., Aldridge, K. E., Cole, J. and Arlett, C. F. (1994). Effect of diet and vitamin C on DNA strand breakage in freshly isolated human white blood cells. *Mutation Res.* **316**: 91-102.

Attard-Montalto, S. P., Saha, V., Kingston, J. E., Plowman, P. N., Taylor, A. M. R., Arlett, C. F., Bridges, B. A. and Eden, O. B. (1995). Increased

radiosensitivity in a child with T-cell non Hodgkin's lymphoma. *Med. Pediatric Oncol.* : in press.

Badie, C., Arlett, C., Iliakis, G. and Malaise, E. P. (1995). Compararative studies of chromosome breaks (PCC), exhange chromosome aberrations (PCC/FISH) and DNA double-strand breaks in three different human fibroblast cell lines. Proceedings of the Xth International Congress of Radiation Research, Wurzberg,

Badie, C., Iliakis, G., Foray, N., Alsbeih, G., Pantellias, G. E., Okayasu, R., Cheong, N., Russell, N. S., Begg, A. C., Arlett, C. F. and Malaise, E. P. (1995). Defective repair of DNA double-strand breaks and chromosome damage in fibroblasts from a radiosensitive leukemia patient. *Cancer Res.* **55**: 1232-1234.

Badie, C., Iliakis, N., Foray, N., Alsbeih, G., Cedervall, B., Chavaudra, N., Pantelias, G., Arlett, C. and Malaise, E. P. (1995). Induction and rejoining of DNA double strand breaks and interphase chromosome breaks in two hypersensitive and one normal human fibroblast cell lines after exposure to x-rays. *Radiat. Res.* : in press.

Foray, N., Arlett, C. F. and Malaise, E. P. (1995). The dose-rate effect on induction and repair rate of radiation-induced DNA double-strand breaks in a normal and an ataxia-telangiectasia human fibroblast cell line. *Biochimie* : in press.

Green, M. H. L., Lowe, J. E., Aldridge, K., Waugh, A. P. W., Clingen, P. H., Cole, J. and Arlett, C. F. (1995). Protection of human lymphocytes against endogenous and ionising radiation-induced DNA strand breakage: Studies with the comet assay. *Env. Mut. Res. Comm.* **16**(3): 255-261.

Russell, N. S., Arlett, C. F., Bartelink, H. and Begg, A. C. (1995). Use of fluorescence *in situ* hybridization to determine the relationship between chromosome aberrations and cell survival in eight human fibroblast strains. *Int. J. Radiat. Biol.* **68**: 185-196.

Savitsky, K., Bar-Shira, A., Gilad, S., Rotman, G., Ziv, Y., Vanagaite, L., Tagle, D. A., Smith, S., Uziel, T., Sfez, S., Ashkenazi, M., Pecker, I., Frydman, M., Harnik, R., Patanjali, S. R., Simmons, A., Clines, G. A., Sartiel, A., Gatti, R. A., Chessa, L., Sanal, O., Lavin, M. F., Jaspers, N. G. J., Taylor, M. R., Arlett, C. F., Miki, T., Weissman, S. M., Lovett, M., Collins, F. S. and Shiloh, Y. (1995). A single ataxia telangiectasia gene with a product similar to PI 3-kinase. *Science* **268**: 1749-1753.

Mammalian genes

Taccioli, G. E., G. Rathbun, Y. Shinkai, E. M. Oltz, H. Cheng, G. Whitmore, T. Stamato, P. Jeggo and F. W. Alt (1992). Activities involved in V(D)J recombination. *Current Topics in Microbiol. Immunol.* **182** : 108-114.

Jeggo, P. A., M. Hafezparast, A. F. Thompson, B. C. Broughton, G. P. Kaur, M. Z. Zdzienicka and R. S. Athwal (1992). Localization of a DNA repair gene (XRCC5) involved in double-strand break rejoining to human chromosome 2. *Proc. Natl. Acad. Sci. USA* **89** : 6423-6427.

Hafezparast, M., G. P. Kaur, M. Zdzienicka, R. S. Athwal, A. R. Lehmann and P. A. Jeggo (1993). Sub-chromosomal localisation of a gene (XRCC5) involved in double strand break repair to the region 2q34-36. *Somatic Cell Molec. Genet.* **19** : 413-421.

Jeggo, P. A., M. Hafezparast, A. F. Thompson, G. P. Kaur, A. K. Sandhu and R. S. Athwal (1993). A hamster-human sub-chromosomal hybrid cell panel for chromosome 2. *Somatic Cell Molec. Genet.* **19** : 39-49.

Taccioli, G. E., G. Rathbun, E. Oltz, T. Stamato, P. A. Jeggo and F. W. Alt (1993). Impairment of V(D)J recombination in double-strand break repair mutants. *Science* **260** : 207-210.

Dahm-Daphi, J., E. Dikomey, C. Pyttlik and P. A. Jeggo (1993). Reparable and non-reparable DNA strand breaks induced by X-irradiation in CHO K1 cells and the radiosensitive mutants xrs1 and xrs5. *Radiation Biology* **64** : 19-26.

Harvey, C. B., M. F. Fox, P. A. Jeggo, N. Mantei, S. Povey and D. M. Swallow (1993). Regional localization of the lactase-phlorizin hydrolase gene, LCT, to chromosome 2q21. *Annals of Human Genetics* **57** : 179-185.

Darmoul, D., M. Fox, C. Harvey, P. Jeggo, J. R. Gum, Y. S. Kim and D. M. Swallow (1994). Regional localisation of DPP4 (alias *CD26* and *ADCP2*) to chromosome 2q24. *Somatic Cell Molec. Genet.* **20** : 345-351.

Hafezparast, M., C. G. Cole, G. P. Kaur, R. S. Athwal and P. A. Jeggo (1994). An extended panel of hamster-human hybrids for chromosome 2q. *Somatic Cell Molec. Genet.* **20** : 541-548.

Taccioli, T. G., T. M. Gottlieb, T. Blunt, A. Priestley, J. Demengeot, R. Mizuta, A. R. Lehmann, F. W. Alt, S. P. Jackson and P. A. Jeggo (1994). Ku80: product of the *XRCC5* gene. Role in DNA repair and V(D)J recombination. *Science* **265** : 1442-1445.

Jeggo, P. A. (1994). Induction of mutations, chromosome aberrations and recombination by ionising radiation in IR group 5 mutants. *In* "Molecular mechanisms in radiation mutagenesis and carcinogenesis". Luxembourg, European Commission. 17-22.

Jeggo, P. A., A. M. Carr and A. R. Lehmann (1994). Cloning human DNA repair genes. *Int. J. Radiat. Biol.* **66** : 573-577.

Finnie, N. J., T. M. Gottlieb, T. Blunt, P. A. Jeggo and S. P. Jackson (1995). DNA-dependent protein-kinase activity is absent in xrs-6 cells - implications for site-specific recombination and dna double-strand break repair. *Proc. Natl. Acad. Sci. USA* **92** : 320-324.

Blunt, T., N. J. Finnie, G. E. Taccioli, G. C. M. Smith, J. Demengeot, T. M. Gottlieb, R. Mizuta, A. J. Varghese, F. W. Alt, P. A. Jeggo and S. P. Jackson (1995). Defective DNA-dependent protein kinase activity is linked to V(D)J recombination and DNA repair defects associated with the murine *scid* mutation. *Cell* **80** : 813-823.

Ross, G. M., J. J. Eady, N. P. Mithal, C. Bush, G. G. Steel and P. A. Jeggo (1995). DNA strand break rejoining defect in *xrs* -6 is complemented by transfection with the human *Ku80* gene. *Cancer Res.* **55** : 1235-1238.

Thompson, L. H. and P. A. Jeggo (1995). Nomenclature of human genes involved in ionizing radiation sensitivity. *Mutation Res.* : in press.

Jeggo, P. A., Taccioli, G. E. and S. P. Jackson (1995). Manage à trois: double strand break repair, V(D)J recombination and DNA-PK. *Bioessays*: in press.

Jackson, S. P. and P. A. Jeggo (1995). DNA double-strand break repair and V(D)J recombination: involvement of DNA-PK. *TIBS*: in press.

Blunt, T., Taccioli, G. E., Priestley, A., Hafezparast, M., McMillan, T., Liu, J., Cole, C. C., White, J. Alt, F. W., Jackson, S. P., Schurr, E., Lehmann, A. R. and P. A. Jeggo (1995) A YAC contig encompassing the XRCC5 (Ku80) DNA repair gene and complementation of defective cells by YAC protoplast fusion. *Genomics* in press.

S. pombe **genes**

Al-Khodairy, F. and Carr, A.M. (1992) DNA repair mutants defining G2 checkpoint pathways in *schizosaccharomyces pombe*. *EMBO J.,* **4,** 1343-1350.

Murray, J.M., Doe, C.L., Schenk, P., Carr, A.M., Lehmann, A.R. and Watts, F.Z. (1992) Cloning and characterisation of the *S. pombe rad15* gene, a homologue to the *S. cerevisiae RAD3* and human *ERCC2* genes. *Nuc. Acids Res.,* **20,** 2673-2678.

Carr, A.M., Green, M.H.L. and Lehmann, A.R. (1992) Checkpoint policing by p53. *Nature,***359**, 486.

Enoch, T., Carr, A.M. and Nurse, P. (1992) Fission yeast genes involved in coupling mitosis to completion of DNA replication. *Genes and Devel.*, **6**, 2035-2046.

Barbet, N.C. and Carr, A.M. (1993) Fission yeast wee1 protein is not required for DNA damage-dependent mitotic arrest. *Nature*, **364**, 824-827.

Carr, A.M., Sheldrick, K.S., Murray, J.M., Al-Harithy, R., Watts, F.Z. and Lehmann, A.R. (1993) Evolutionary conservation of excision repair in *Schizosaccharmomyces pombe*: evidence for a family of sequences related to the Saccharomyces cerevisiae RAD2 gene. *Nuc. Acids Res.*, **21**, 1345-1349.

McCready, S., Carr, A.M. and Lehmann, A.R. (1993) Repair of cyclobutane pyrimidine dimers and 6-4 photoproducts in the fission yeast, *Schizosaccharomyces pombe. Molec. Microbiol.*, **10**, 885-890.

Muris, D.F.R., Vreeken, K., Carr, A.M., Broughto, B.C.Lehmann, A.R., Lohman, P.H.M. and Pastink, A. (1993) Cloning the *RAD51* homologue of *Schizosaccharomyces pombe. Nuc. Acids Res.* **21**, 4586-4591.

Al-Khodairy, F., Fotou, E., Sheldrick, K.S., Griffiths, D.J.F., Lehmenn, A.R.. and Carr, A.M. (1994) Identification and Characterisation of new elements involved in checkpoints and feedback controls in fission yeast. *Mol. Biol. of the Cell*, **5**, 147-160.

Carr, A.M., Schmidt, H., Kirchoff, S., Muriel, W.J., Sheldrick, K.S., Griffith, D.J., Basmacioglu, C.N.Subramani, S., Clegg, M., Nasim, A. and Lehmann, A.R. (1994) The *rad16* gene of *Schizosaccharomyces pombe*: A homologue of the *RAD1* gene of *Saccharomyces cerevisiae Molec and Cellular Biol.*, **14**, 2029-2040.

Murray, J.M., Tavassoli, M., Al-Harithy, R., Sheldrick, K.S., Lehmann, A.R., Carr, A.M. and Watts, F.Z. (1994) Structural and functional conservation of the human homolog of the *S. pombe rad2* gene, which is required for DNA repair and Chromosome segregation. *Molec. and Cellular Biol.*, **14**, 4878-4888.

Ford, J.C., Al-Khodairy, F., Fotou, E., Sheldrick, K.S., Griffiths, D.J.F. and Carr, A.M. (1994) 14-3-3 protein homologs required for the DNA damage checkpoint in Fission Yeast. *Science*, **265**, 533-535.

Al-Khodairy, F., Enoch, T., Hagan, I.M. and Carr, A.M. (1995) The *S. pombe hus5* gene encodes a ubiquitin conjugating enzyme for normal mitosis. *J. Cell Science*, **108**, 475-486.

van Heusden, G.P.H., Griffiths, D.J.F., Ford, J.C., Chin-a Woeng T.F.C., Schrader, P.A.T., Carr, A.M. and Steensma, H.Y.(1995) The 14-3-3 proteins encoded by the *BMH1* and *BMH2* genes are essential in the

yeast Saccharomyces cerevisiae and can be replaced by a plant homologue. *Eur. J. Biochem.* **229**, 45-53.

Carr, A.M., Moudjou, M., Bentley, N.J. and Hagan, I.M. (1995) The *chk1* pathway is required to prevent mitosis following cell cycle arrest at 'start'. *Curr. Biol.* **In press**.

Griffiths, D.J.F., Barbet, N.C., McCready, S., Lehmann, A.R., and Carr, A.M. (1995) Fission yeast *rad17*: a homologue of budding yeast *RAD24* that shares regions of sequence similarity with DNA polymerase accessory proteins. *EMBO J.* **In press**.

Lehmann, A.R., Walicka, M., Griffiths, D.J.F., Murray, J.M. Watts, F.Z., McCready, S. and Carr, A.M. (1995) The *rad18* gene of *Schizosaccharomyces pombe* defines a new subgroup of the *SMC* superfamily involved in DNA repair. *Mol. Cell. Biol.* **In press**.

Muris, D.F.R., Vreeken, K., Carr, A.M., Smidt, C., Lohman, P.H.M. and Pastink, A. (1995) Isolation of the *Schizzosaccharomyces pombe RAD54* homolog, *rhp54+*, a gene involved in the repair of radiation damage and replication fidelity. *J. Cell Sci.* **In press.**

Head of project 3: Prof. Dr. D. Bootsma

II. Objectives for the reporting period

The long-term interest of our research has been understanding of the molecular mechanism and biological impact of the nucleotide excision repair (NER) system, one of the major repair pathways in the cell. At least three severe human syndromes are associated with NER defects: xeroderma pigmentosum (XP), Cockayne syndrome (CS) and trichothiodystrophy (TTD). The application of recombinant DNA techniques has permitted the cloning of a number of NER genes involved in these disorders, has revealed strong evolutionary conservation and has contributed to the partial elucidation of the NER reaction mechanism. In addition to extending the cloning and functional analysis of NER genes and the molecular defect in NER syndromes, one of our new goals was to apply the same approaches to other complex repair pathways, notably recombination and postreplication repair. The specific objectives can be summarized as follows:
(i) Cloning and characterization of additional human repair genes. (ii) Functional analysis of the encoded proteins, involving purification of the (overexpressed) proteins, assay for activity using an *in vitro* repair system or microneedle injection into mutant cells, analysis of specific functions and interaction with other polypeptides of the DNA repair, recombination or replication machinery. (iii) Generation of a mouse model for XP/CS and other repair deficiencies based on targeted gene replacement in totipotent ES-cells from which germline chimera's and eventually homozygous mouse mutants can be derived. Such repair-deficient mouse strains are invaluable for assessing the biological role of repair in carcinogen-induced tumorigenesis, as an experimental model for XP and CS (etiology, treatment and prevention of the disease), for risk assessment of heterozygotes and for the sensitive screening of radiation and chemical agents for their carcinogenic and mutagenic potential *in vivo*.

1. Cloning of Repair Genes

Two strategies were followed for the isolation of repair genes:

a.　DNA transfection to repair-deficient rodent (at least 10 different complementation groups) and human cells followed by selection of UV-resistant transformants and 'rescue' of the correcting gene. This resulted in the past in the cloning of *ERCC1*, *XPBC/ERCC3* and *CSBC/ERCC6*.

b.　Sequence homology to cloned repair genes of lower eukaryotes, particularly yeast (*S.cerevisiae* and *Schizosaccharomyces* pombe).
This approach was applied to the *S.cerevisiae RAD6* gene, which plays a central role in postreplication repair, damage-induced mutagenesis and sporulation. The 172 amino acids RAD6 protein is a ubiquitin-conjugating enzyme (E2) that *in vitro* (poly)ubiquitinates histones. By evolutionary walking based on nucleotide sequence homology we have cloned two human *RAD6* homologs (designated *HHR6A* and *HHR6B*) using the *Schizosaccharomyces pombe* and *Drosophila melanogaster* genes

as "intermediates". *HHR6A* and *B* probably function in chromatin remodelling. Immunoelectronmicroscopy suggests that both proteins are associated with euchromatin. Subsequently, we have isolated 3 additional genes: two human homologs of the yeast NER gene *RAD23* (*HHR23A* and *HHR23B*) and the human counterpart of the yeast recombination repair gene *RAD54* (*HHR54*).

Very recently small parts of two human homologs of the recombination repair gene *rad21*[+] from *Schizosaccharomyces pombe*, which encodes an essential nuclear phosphoprotein were identified in the database. Subsequently, the full length cDNA of human and mouse *HHSPR21A* were cloned. The A gene seems to be ubiquitously expressed as expected for a repair gene and it was mapped to 8q24. This part of the chromosome may contain also the gene involved in Nijmegen breakage syndrome. Presently, we are investigating the possibility that the *HHSPR21A* gene is involved in this disorder. Also the *HHSPR21B* cDNA is being isolated.

A human homolog of the *Saccharomyces cerevisiae* crosslink repair gene PSO2/SNM1 was cloned. This gene resides on 10q25. Presently, the full-length cDNA is inserted in mammalian expression vectors to permit transfection to various mutants defective in the repair of DNA crosslinks. This includes some of the Fanconi's anaemia complementation groups and a number of rodent mutants (in collaboration with Dr. Zdzienicka in the Leiden group).

A human gene encoding a protein with extensive homology to the presumed XPE nucleotide excision repair factor was identified and subsequently isolated. This gene was assigned to 16q22-23, close to (but probably not within) the region where very recently the gene for Fanconi anaemia group A is mapped.

Finally, part of the human homolog of *RAD1* was cloned using a PCR-based strategy. This gene was previously shown by Thompson to be identical to *ERCC4* and may be implicated in XPF.

2. Functional Analysis

The *ERCC1* gene corrects the repair defect of rodent group 1 mutants and encodes a 297 amino acid (aa) protein). Mutation analysis suggests that *ERCC1* has distinct roles in the repair of UV-lesions and in the processing of cross-links. By using an *in vitro* repair system we demonstrated the presence of an enzyme complex in mammalian cell extracts, harbouring the products of the *ERCC1, ERCC4, ERCC11* and *XPFC* genes. We postulate that this complex, like the one in *S.cerevisiae* involving the RAD1 and RAD10 proteins, functions both in NER and recombinational repair, and may play a role in strand incision.

The *ERCC3* gene corrects UV-sensitive rodent mutants of group 3. The gene appeared very strongly conserved, which permitted isolation of the *Drosophila* and yeast (*S.cerevisiae* and *S. pombe*) homologs. Gene disruption in yeast indicated that ERCC3[sc] participates in a process essentional for viability in addition to its role in NER. Transfection and microinjection experiments demonstrated that mutations in *ERCC3* are responsible for xeroderma pigmentosum (XP) complementation group B, a very rare form of XP that is simultaneously associated with Cockayne's syndrome (CS). Using microinjection of the gene, 2 new patients were assigned to this group. In spite of the severe NER deficiency, both patients have not developed skin cancer (in striking contrast to the sole known XP-B case) even at relative advanced age. This points to

the involvement of additional factors for cancer proneness.

In collaboration with the laboratory of J-M. Egly (Strasbourg) the ERCC3 protein was found to be part of a multiprotein complex (TFIIH) required for transcription initiation of most structural genes and for NER. This defines the additonal, hitherto unknown vital function of the gene, suspected from parallels with the yeast and Drosophila *ERCC3* homologs. Importantly, the complex in fact appeared to contain at least 4 proteins implicated in different XP/CS complementation groups. Part of the clinical symptoms of the corresponding disorders that were difficult to interpret on the basis of a DNA repair defect can now be explained as the result of a subtle impairment of transcription.

The TFIIH factor contains XPB/ERCC3 and XPD/ERCC2 and the uncloned repair protein implicated in the newly identified TTD-A complementation group. In close collaboration with the group of Egly (Strasbourg), who is interested in the role in transcription, we have found that the XPB and XPD proteins are responsible for the bidirectional helix-unwinding capacity of the complex. This leads us to propose that TFIIH may locally melt the DNA around the site of the lesion e.g. for loading the NER incision complex onto the DNA template. A dominant mutation in ERCC3 as well as antibodies against ERCC2 and ERCC3 induced a complete abrogation of repair and transcription in injected fibroblasts confirming a role of both proteins in these processes *in vivo*. The selective association of mutations in TFIIH subunits with the peculiar clinical features of CS and TTD was further corroborated with the discovery of the first TTD family falling in the rare XP/CS group XP-B. This supports our idea that subtle transcriptional defects affecting the expression of a selective set of genes are responsible for the spectrum of CS and TTD features that lack a rational explanation based on a NER defect.

In further support for this idea of transcription syndromes we have identified a mutation in a TFIIH subunit in at least one Pollitt Syndrome patient with normal NER which we anticipated to suffer from a 'transcription only syndrome'.

The *ERCC6* gene, was cloned after extensive genomic DNA transfection to a member of the moderately UV-sensitive rodent group 6. The -for transfection cloning- very large gene ($\geq$ 85 kb) encodes a protein of 1493 amino acids. *ERCC6* is after *ERCC2* and *ERCC3* the third DNA helicase in mammalian NER. No equivalent of *ERCC6* is known in any species. Transfection experiments revealed that the gene specifically corrects the repair defect in cells of CS complementation group B shown to be impaired in the preferential repair (the transcribed strand of) active genes. The *CSBC/ERCC6* gene is the first cloned gene specifically implicated in this subpathway of NER. The high conservation displayed by all NER genes analyzed to date permitted the identification of the *S.cerevisiae* homolog (designated *RAD26*). In analogy with CS group B *rad26* disruption is viable and impairs transcription-coupled repair, but, in discordance with CS, does not induce any UV-sensitivity. This explains why this yeast mutant was not isolated before and suggests that the global genome repair is the major determinant of cellular resistance to genotoxicity in lower organisms.

To investigate the function of CSB in transcription-coupled repair possible stable interactions between CSB and all known NER factors and many transcription-initiation factors were examined. With the possible exception of XPG no evidence for a stable interaction was observed. Also immuno-depletion of CSB from a repair-competent Manley extract did not have an effect on the repair capacity indicating that the CSB protein is not essential for in vitro NER and not complexed with an indispensable component. Analysis of double mutants in yeast

affected in both the global genome and in transcription-coupled repair demonstrated that the latter NER subpathway is not totally dependent on CSB at least in S.cerevisiae (in collaboration with Dr. J. Brouwer, Leiden).

In collaboration with the group of Hanaoka (Japan) we have found that the HHR23B gene product resides in a very tight complex with the XP complementation group C protein. Intriguingly, the genes for both proteins also co-localize probably within 650 kb on 3p25.1, whereas the *HHR23A* gene was assigned to 19p13.2. Both HHR23 proteins harbour an N-terminal ubiquitin-like domain, that may have a chaperon function in complex assembly. The XPC-HHR23B complex, which has an exceptionally high affinity for ssDNA, is specifically involved in the global genome NER subpathway.

We found that the HHR23B protein is for a considerable part made up of a very strongly conserved repeat sequence also present as a C-terminal extension of one of the ubiquitin-conjugating enzymes. This provides a second link between this gene and the ubiquitin pathway. Also the majority of HHR23B and probably all HHR23A molecules (approx. 10^6/cell) appear not to be complexed with XPC ($\sim 5.10^4$ molecules/cell). This supports the idea that these abundant proteins may have an additional function. By immunofluorescence XPC and HHR23B were found to be nuclear proteins. Finally, large quantities of the HHR23A and B products were purified to enable X-ray diffraction analysis to determine their 3-D structure.

3. Generation of repair-deficient mouse models

Using the recently developed technology of gene targeting in totipotent embryo derived mouse stem cells (ES-cells) we have inactivated one of the alleles of *ERCC1* and *3*. Because of the possible vital role of both genes also constructs were made which induce more subtle mutations and -in the case of *XPBC/ERCC3*- mimick one of the mutations found in an XP-B patient. For each gene and type of mutation several homologous ES recombinants were obtained and injected intro mouse blastocysts. After implantation into pseudo-pregnant foster mother a number of *ERCC1* and *ERCC3* chimeric mice were born. Germ-line transmission was obtained for subtle and knock-out mutations in the *ERCC1* gene. Although these mice are viable they have a severely reduced lifespan (KO <4 weeks, subtle mutant <10 weeks), probably due to (a combination of) liver, spleen and kidney insufficiency. An additional unexpected feature exhibited by these mice -for which no human disorder is known yet- is the high frequency of poly- and aneuploidy observed in several internal organs (notably liver and kidney), which may be a sign of premature ageing. In view of the likely dual functionality of ERCC1 in NER and in mitotic recombination it is plausible that the unexpected symptoms are derived from the recombination defect. The mice are extremely sensitive to genotoxic agents and completely deficient in NER. Mouse models mimicking mutations in *XPB/ERCC3* and *XPD/ERCC2* found in XP-B and XP-D patients are being generated. One of these mutants (intended to mimic a splice-mutation in XP-B patient XP11BE) appeared inviable in a homozygous state in mice, consistent with the vital transcription role of the protein.

Several new targeting constructs for obtaining viable (i.e. patient-mimicking) mutations in the XPD and XPB genes were made and have been used to obtain homologous recombinants in mouse ES cells. Using the 'in-out' HPRT targeting strategy developed by Melton c.s. ES cells were obtained carrying only a single XPB pointmutation, without the presence of a dominant

marker, which may interfere with proper expression of the targeted gene. These and other ES cells are being injected into mouse blastocysts for the generation of corresponding mouse mutants.

We were able to generate homozygous CSB/ERCC6 deficient mice (mimicking one allele of CS-B patient). All repair parameters (UV survival, UDS, repair of transcribed strands of active genes) are conform the human CSB defect, a total inactivation of the transcription-coupled NER subpathway. However, remarkably, the other clinical hallmarks of CS are not or only marginally manifest, such as the severe neurologic and developmental impairment. CSB mice are physically, sexually and neurologically normal as far as tested. Only male -/- mice seem to have a 25% reduced body weight. Studies to investigate cancer predisposition are in progress.

Also inactivation of the postreplication repair gene *HHR6B* appeared to be fully viable, presumably because of functional redundancy with the strongly homologous *HHR6A* gene, for which chimeric mutant animals were obtained recently. Crossing should reveal what is the phenotype for defects in both genes. Interestingly the *HHR6B*$^{-/-}$ mice were found to be male-sterile. This confirms our early findings that this gene may be involved in the complex chromatin alterations in spermatogenesis, since specifically this stage seems to be impaired. Thus this is the first mouse model for infertility.

Also viable mice with a complete inactivation of the postreplication repair gene HHR6A were obtained. These mice fail to show an overt defect. Crossing with the already previously generated male-infertile HHR6B-/- mice yielded as yet no offspring with both of the mammalian RAD6 homologs inactive. This suggests that such a defect is incompatible with rodent development. The specific deficiency in the spermatogenesis of the HHR6B-/- males was further pinpointed using immunohistochemical methods (in collaboration with Dr. A. Grootegoed, EUR). All available evidence is consistent with our idea that the gross chromatin alterations in the final stages of spermatogenesis are impaired.

For the HHR54 recombination repair gene viable ES transformants were generated with inactivating mutations in both alleles, indicating that a null mutants is not incompatible with live at least at the cellular stage.

Publications:

A.R. Lehmann, J.H.J. Hoeijmakers et al.
Workshop on DNA repair.
Mutat. Res. 273: 1-28 (1992).

L. Ma, G. Weeda, A.G. Jochemsen, D. Bootsma, J.H.J. Hoeijmakers and A.J. van der Eb.
Molecular and functional analysis of the XPBC/ERCC-3 promoter: Transcription activity is dependent on the integrity of an Sp1 binding element.
Nucl.Acids Res. 20: 217-224 (1992).

M.H.M. Koken, E.M.E. Smit, I. Jaspers-Dekker, B.A. Oostra, A. Hagemeijer, D. Bootsma and J.H.J. Hoeijmakers.
Localization of two human homologs, HHR6A and HHR6B, of the yeast DNA repair gene

RAD6 to chromosome Xq24-25 and 5q23-31.
Genomics 12: 447-453 (1992).

C. Troelstra, R.M. Landsvater, J. Wiegant, M. van der Ploeg, G. Viel, C.H.C.M. Buys and J.H.J. Hoeijmakers.
Localization of the nucleotide excision repair gene ERCC-6 to human chromosome 10q11-21.
Genomics 12: 745-749 (1992).

A.P.M. Eker, W. Vermeulen, N. Miura, K. Tanaka, N.G.J. Jaspers, J.H.J. Hoeijmakers and D. Bootsma.
Xeroderma pigmentosum group A correcting protein from Calf Thymus.
Mutat.Res. 274: 211-224 (1992).

J.H.J. Hoeijmakers and D. Bootsma.
DNA repair: two pieces of the puzzle.
Nature Genetics 1: 313-314 (1992).

E. Park, S.N. Guzder, M.H.M. Koken, I. Jaspers-Dekker, G. Weeda, J.H.J. Hoeijmakers, S. Praksh and L. Prakash.
RAD25 (SSL2), a yeast homolog of the human xeroderma pigmentosum group B DNA repair gene, is essential for viability.
Proc.Natl.Acad.Sci.USA 89: 11416-11420 (1992).

C. Troelstra, A. van Gool, J. de Wit, W. Vermeulen, D. Bootsma and J.H.J. Hoeijmakers.
ERCC6, a member of a subfamily of putative helicases is involved in Cockayne's syndrome and preferential repair of active genes.
Cell 71: 939-953 (1992).

M.H.M. Koken, C. Vreeken, S.A.M. Mol, N.C. Cheng, I. Jaspers-Dekker, J.H.J. Hoeijmakers, J.C.J. Eeken, G. Weeda and A. Pastink.
Cloning and characterization of the Drosophila homolog of the xeroderma pigmentosum complementation group B correcting gene ERCC3.
Nucl.Acids Res. 20: 5541-5548 (1992).

J.H.J. Hoeijmakers, C. Troelstra and G. Weeda.
DNA repair genes and syndromes from man to yeast.
Alfred Benzon Symposium vol. 35. V.A. Bohr, K. Wassermann, K.H. Kraemer and J.H. Thaysen, eds. Munksgaard, Copenhagen pp 27-41, (1993).

G. Weeda, J.H.J. Hoeijmakers and D. Bootsma.
Genes controlling nucleotide excision repair in eukaryotic cells.
BioEssays 15, 394-403 (1993).

M.H.M. Koken, J.H. Odijk, M. van Duin, M. Fornerod and D. Bootsma.
Augmentation of protein production by a combination of the T7 RNA polymerase system and ubiquitin fusion.
-Overproduction of the human DNA repair protein, *ERCC1*, as a ubiquitin fusion protein in *Escherichia coli*.
Biochem. Biophys. Res. Comm. 195, 643-653, (1993).

J.H.J. Hoeijmakers.
Nucleotide excision repair I: from *E.coli* to yeast.
TIG 9, 173-177, 1993).

J.H.J. Hoeijmakers
Nucleotide excision repair II; from yeast to mammals.
TIG 9, 211-217 (1993)

W. Vermeulen, J. Jaeken, N.G.J. Jaspers, D. Bootsma and J.H.J. Hoeijmakers.
Xeroderma pigmentosum complementation group G associated with Cockayne's syndrome.
Am.J.Hum.Genet. 53, 185-193 (1993).

M. Stefanini, W. Vermeulen, G. Weeda, S. Giliani, T. Nardo, M. Mezzina, A. Sarasin, J.I. Harper, J.H.J. Hoeijmakers and A.R. Lehmann.
A new nucleotide excision repair gene associated with the genetic disorder trichothiodystrophy.
Am. J. Hum. Genet. 53, 817-821 (1993).

M. Molinete, W. Vermeulen, A. Bürkle, J. Ménissier-de Murcia, J.H. Küpper, J.H.J. Hoeijmakers and G. de Murcia.
Overproduction of the poly(ADP-ribose)polymerase DNA binding domain blocks alkylation-induced DNA repair synthesis in mammalian cells.
EMBO J. 12. 2109-2117, (1993).

C. Troelstra, W. Hesen, D. Bootsma and J.H.J. Hoeijmakers.
Structure and expression of the excision repair gene *ERCC6*, involved in the human disorder Cockayne's syndrome group B.
Nucl. Acids Res.: 21, 419-426 (1993).

G. Weeda and J.H.J. Hoeijmakers.
Genetic analysis of nucleotide excision repair in mammalian cells.
Seminars in Cancer Biol. 4, 105-117 (1993).

J.H.J. Hoeijmakers, G. Weeda, C. Troelstra, M.H.M. Koken, P.J. van der Spek and D. Bootsma.
Molecular analysis of human DNA repair genes and syndromes.
Int.J.Cancer 53, 162-163 (1993).

L. Schaeffer, R. Roy, S. Humbert, V. Moncollin, W. Vermeulen, J.H.J. Hoeijmakers, P. Chambon and J-M. Egly.
DNA repair helicase: a component of BTF2 (TFIIH) basic transcription factor. (research article)
Science 260, 58-63 (1993).

A.J. van Vuuren, E. Appeldoorn, H. Odijk, A. Yasui, N.G.J. Jaspers, D. Bootsma, and J.H.J. Hoeijmakers.
Evidence for a repair enzyme complex involving ERCC1, and the correcting activities of ERCC4, ERCC11 and the xeroderma pigmentosum group F.
EMBO J. 12, 3693-3701 (1993)

D. Bootsma and J.H.J. Hoeijmakers.
DNA repair engagement with transcription (News and Views).
Nature 363, 114-115 (1993)

W. Vermeulen, R.J. Scott, S. Potger, H.J. Müller, J, Cole, C.F. Arlett, W.J. Kleijer, D. Bootsma, J.H.J. Hoeijmakers and G. Weeda.
Clinical heterogeneity within xeroderma pigmentosum associated with mutaions in the DNA repair and transcription gene ERCC3.
Am. J. Hum. Genet. 54, 191-200 (1994)

E. Eveno, O. Chevallier-Lagente, A. Benoit, M. Carreau, W. Vermeulen, J.H.J. Hoeijmakers, M. Stefanini, A.R. Lehmann, C. A. Weber, M. Mezzina and A. Sarasin.
Correction by the *ERCC2* gene of UV sensitivity and repair deficiency phenotype in a subset of trichothiodystrophy cells.
Carcinogenesis, 15, 1493-1498 (1994)

A.J. van Vuuren, W. Vermeulen, L. Ma, G. Weeda, E. Appeldoorn, N.G.J. Jaspers, A.J. van der Eb, J.H.J. Hoeijmakers, and S. Humbert, L. Schaeffer, and J-M. Egly
Correction of xeroderma pigmentosum repair defect by basal transcription factor BTF2/TFIIH.
EMBO J. 13, 1645-1653 (1994).

L. Schaeffer, V. Moncollin, R. Roy, A. Staub., M. Mezzina., A. Sarasin, G. Weeda, J.H.J. Hoeijmakers, and J-M. Egly
The ERCC2/DNA repair protein is associated with the class II BTF2/TFIIH transcription factor.
EMBO J. 13, 2388-2392 (1994).

D. Busch, C. Greiner, K. Lewis Rosenfeld, R. Ford, J. de Wit, J.H.J. Hoeijmakers, and L. H. Thompson.
Complementation group assignments of moderately UV-sensitive CHO mutants isolated by large scale screening (FAECB).
Mutagenesis 9, 301-306 (1994).

L-B. Ma, A. Westbroek, A.G. Jochemsen, G. Weeda, A. Bosch, D. Bootsma, J.H.J. Hoeijmakers, and A.J. van der Eb.
Mutational analyis of ERCC3, involved in DNA repair and transcription initiation: identification of domains essential for the DNA repair function.
Molec. Cell. Biol. 14, 4126-4134 (1994).

C. Masutani, K. Sugasawa, J. Yanagisawa, T. Sonoyama, M. Ui, T. Enomoto, K. Takio, K. Tanaka, P.J. van der Spek, D. Bootsma, J.H.J. Hoeijmakers, and F. Hanaoka.
Purification and cloning of a nucleotide excision repair complex involving the xeroderma pigmentosum group C protein and a human homolog of yeast RAD23.
EMBO. J. 13, 1831-1843 (1994).

D. Bootsma, and J.H.J. Hoeijmakers.
The molecular basis of nucleotide excision repair syndromes.
Mutation Res. 307, 15-23 (1994).

S. Keeney, A.P.M. Eker, T. Brody, W. Vermeulen, D. Bootsma, J.H.J. Hoeijmakers, and S. Linn.
Correction of the DNA repair defect in xeroderma pigmentosum group E by injection of a DNA damage binding protein.
Proc. Natl. Acad. Sci. USA, 91, 4053-4056 (1994).

S. Humbert, H. van Vuuren, Y. Lutz, J.H.J. Hoeijmakers, J-M. Egly, and V. Moncollin.
Characterization of p44/SSL1 and p34 subunits of the BTF2/TFIIH transcription/repair factor.
EMBO J. 13, 2393-2398 (1994).

P.J. Van der Spek, E.M.E. Smit, H.B. Beverloo, K. Sugasawa, C. Matsutani, F. Hanaoka, J.H.J. Hoeijmakers, and A. Hagemeier.
Chromosomal localization of three repair genes: the xeroderma pigmentosum group C gene and two human homologs of yeast RAD23.
Genomics, 23, 651-658 (1994).

J.H.J. Hoeijmakers and A.R. Lehmann
Nucleotide excision repair among species, in: 'Methods to assess DNA damage and repair: Interspecies comparisons' (R.G. Tardiff, P.H.M. Lohman, and G.N. Wogan eds.) John Wiley & Sons, Ltd., Sussex. pp 57-82 (1994).

M. Carreau, E. Eveno, X. Quilliet, O. Chevalier-Lagente, M. Stefanini, W. Vermeulen, J.H.J. Hoeijmakers, A. Sarasin, and M. Mezzina.
Rapid complementation assay for DNA repair-deficient human cells.
Carcinogenesis, 15, 1493-1498 (1994)

A.J. van Gool, R. Verhage, S.M.A. Swagemakers, P. van der Putte, J. Brouwer, C. Troelstra, D. Bootsma, and J.H.J. Hoeijmakers.

RAD26, the functional *S.cerevisiae* homolog of the Cockayne syndrome B gene *ERCC6*.
EMBO J. 13, 5361-5369 (1994).

D.F.R. Muris, O. Bezzubova, J-M. Buerstedde, K. Vreeken, A.S. Balajee, C.J. Osgood, C. Troelstra, J.H.J. Hoeijmakers, K. Ostermann, H. Schmidt, A.T. Natarajan, J.C.J. Eeken, P.H.M. Lohmann, and A. Pastink.
Cloning of human and mouse genes homologous to *RAD52*, a yeast gene involved in DNA repair and recombination
Mutat. Res. 315, 295-305 (1994).

J.H.J. Hoeijmakers.
Human nucleotide excision repair syndromes: molecular clues to unexpected intricacies.
Eur. J. Cancer, 30A, 1912-1924 (1994).

J.H.J. Hoeijmakers and D. Bootsma.
DNA repair: Incisions for excision.
Nature, 371, 654-655 (1994)

R. Roy, J.P. Adamczewski, T. Seroz, W. Vermeulen, J-P. Tassan, L. Schaeffer, E.A. Nigg, J.H.J. Hoeijmakers and J-M. Egly.
The Mo15 cell cycle kinase is associated with the TFIIH transcription-DNA repair factor.
Cell, 79, 1093-1101 (1994)

R. Roy, L. Schaeffer, S. Humbert, W. Vermeulen, G. Weeda, J-M. Egly.
The DNA-dependent ATPase activity associated with the Class II basic transcription factor BTF2/TFIIH.
J. Biol. Chem. 269, 9826-9832 (1994).

M.K.K. Shivji, A.P.M. Eker, and R.D. Wood.
DNA repair defect in complementation group C and complementing factor from HeLa cells.
J. Biol. Chem. 269, 22749-22757 (1994).

C. Troelstra and N.G.J. Jaspers
Ku starts at the end
Current Biol. 4, 1149-1151 (1994)

A.R. Lehmann, D. Bootsma, S.G. Clarkson, J.E. Cleaver, P.J. McAlpine, K. Tanaka, L.H. Thompson, and R.D. Wood.
Nomenclature of human DNA repair genes.
Mutat. Res. 315, 41-42, (1994)

D. Bootsma, K.H. Kraemer and J.E. Cleaver: Addendum in:
The Metabolic and Molecular Bases of Inherited Disease, chapter 148 Xeroderma Pigmentosum and Cockayne Syndrome (Scriver, C.R., Beaudet, A.L., Sly, W.S., and Valle, D., eds.) Vol

III, pp. 4393-4419, McGraw Hill, New York, 1994.

W. Vermeulen, A.J. van Vuuren, E. Appeldoorn, G. Weeda, N.G.J. Jaspers, A. Priestly, C.F. Arlett, A.R. Lehmann, M. Stefanini, M. Mezzina, A. Sarasin, D. Bootsma, J-M. Egly and J.H.J. Hoeijmakers.
Three unusual repair deficiencies associated with transcription factor BTF2(TFIIH). Evidence for the existence of transcription syndromes.
Cold Spring Harbor Symp. Quant. Biol. 59, 317-329, (1994).

J.H.J. Hoeijmakers.
Nucleotide excision repair: molecular and clinical implications.
in: 'DNA repair mechanisms: Impact on Human diseases and Cancer', Series 'Molecular Biology Intelligence Unit' (J-M, H Vos, ed), R.G. Landes Company, Biomedical Publishers, pp 125-150, (1995).

B.C. Broughton, A.F. Thompson, S.A. Harcourt, W. Vermeulen, J.H.J. Hoeijmakers, E. Botta, M. Stefanini, M. King, C. Weber, J. Cole, C.F. Arlett, A.R. Lehmann.
Molecular and cellular analysis of the DNA repair defect in a patient with xeroderma pigmentosum complementation group D with the clinical features of xeroderma pigmentosum and Cockayne syndrome.
Am. J. Hum. Genet. 56, 167-174 (1995).

X.W. Wang, H. Yeh, L. Schaeffer, R. Roy, V. Moncollin, J-M. Egly, Z. Wang, E.C. Friedberg, M.K. Evans, B.G. Taffe, V.A. Bohr, G. Weeda, J.H.J. Hoeijmakers, K. Forrester, and C.C. Harris
p53 modulation of TFIIH-associated nucleotide excision repair activity.
Nature Genetics 10, 188-194 (1995)

P.J.M. Hendriksen, J.S. Hoogerbrugge, A.P.N. Themmen, M.H.M. Koken, J.H.J. Hoeijmakers, B.A. Oostra, T. van der Lende and J.A. Grootegoed.
Post-meiotic expression of X- and Y-specific genes during spermatogenesis in mouse.
Developmental Biology (in press)

D. Bootsma, G. Weeda, W. Vermeulen, H. van Vuuren, C. Troelstra, P. van der Spek, and J.H.J. Hoeijmakers
Nucleotide excision repair syndromes: molecular basis and clinical symptoms.
Phil. Trans. R. Soc. Lond. B 347, 75-81 (1995)

L-B. Ma, J.H.J. Hoeijmakers, and A.J. van der Eb.
Mammalian Nucleotide Excision Repair
Biochim. Biophys. Acta (in press, 1995).

A.J. van Vuuren, E. Appeldoorn, H. Odijk, S. Humbert, A.P.M. Eker, N.G.J. Jaspers, V. Moncollin, J.-M. Egly and J.H.J Hoeijmakers.

Partial characterization of the DNA repair protein complex, containing the ERCC!, ERCC4, ERCC11 and XPF correcting activities.
Mutat Res. 337, 25-39 (1995).

M. Carreau, E. Eveno, X. Quilliet, O. Chevalier-Lagente, A. Benoit, B. Tanganelli, M. Stefanini, W. Vermeulen, J.H.J. Hoeijmakers, A. Sarasin, and M. Mezzina.
Development of a new easy complementation assay for DNA repair-deficient human syndromes using cloned repair genes.
Carcinogenesis, 16, 1003-1009 (1995).

N.G.J. Jaspers and J.H.J. Hoeijmakers
Nucleotide excision repair in the test tube.
Current Biology 5, (1995), in the press.

D. Bootsma and J.H.J. Hoeijmakers
DNA repair: from the clinical to the molecular level and back
Louis Jeantet Award Lecture (1995). Les Cahiers de la Foundation Louis Jeantet, 1995, in press.

A. Nagai, M. Saijo, I. Kuraoka, T. Matsuda, N. Kodo, Y. Nakatsu, T. Mimaki, M. Mino, M. Biggerstaff, R.D. Wood, A. Sijbers, J.H.J. Hoeijmakers and K. Tanaka.
Enhancement of damage-specific DNA binding of XPA by interaction with the ERCC1 DNA repair protein.
Biochem. Biophys. Res. Comm. 211, 960-966, (1995).

M.L. Roller, A.C. Lossie, M.H.M. Koken, E.M.E. Smit, A. Hagemeijer, S.A. Camper.
Localization of sequences related to the human RAD6 DNA repair gene on mouse Chr 11 and 13.
Mammalian Genome 6, 305-306, (1995).

W. Jongmans, G.W.C.T. Verhaegh, N.G.J. Jaspers, M. Oshimura, E.J. Stanbridge, P.H.M. Lohman and M.Z. Zdzienicka.
Studies on phenotypic complementation of ataxia-telangiectasia cells by chromosome transfer.
Am. J. Hum. Genet. 56, 438-443, (1995).

K. Savitsky, A. Bar-Shira, S. Gilad, G. Rotman, Y. Ziv, L. Vanagaite, D.A. Tagle, S. Smith, T. Uziel, S. Sfez, M. Ashkenazi, I. Pecker, M. Frydman, R. Harnik, S.R. Patanjali, A. Simmons, G.A. Clines, A. Sartiel, R.A. Gatti, L. Chessa, O. Sanal, M.F. Lavin, N.G.J. Jaspers, A.M.R. Taylor, C.F. Arlett, T. Miki, S.M. Weissman, M. Lovett, F.S. Collins and Y. Shiloh.
A single ataxia telangiectasia gene with a product similar to PI-3kinase
Science, 268, 1749-1753, (1995).

Head of project 4: Dr. E. Moustacchi

II. Objectives for the reporting period

Informations on   i) activation of a wide range of genes and of signalling pathways associated to alterations of the cellular phenotype following treatment by radiations among other DNA damaging agents and   ii) a better definition of the molecular nature of spontaneous and induced-mutagenic events, have led to a complex but probably more realistic view of the cellular response to genotoxic treatment including radiations. Findings from our group on Fanconi anemia taken as a paradigm for altered control of differentiation and cell cycle in association with a DNA repair defect have contributed to this enlarged perspective. Some of our observations on FA have been extended to ataxia telangectasia (AT), another human genetic disease also characterized by chromosomal instability, sensitivity to genotoxic agents, cell cycle anomalies and cancer predisposition.

III. Progress achieved including publications

1. Alterations in the control of genes expression in FA and AT syndromes

We have previously shown (1992) that among the various growth factors examined, the constitutive and induced production of interleukin-6 (IL-6) was defective in FA. Moreover, the addition of this cytokine to the culture medium of FA lymphoblasts and fibroblasts increased to almost a normal level their resistance to cytotoxicity of DNA cross-linking agents. The other anomalie detected in the cytokine network balance concerns the tumor necrosis factor alpha (TNF-α). This protein, which enhances intra and extracellular O_2^- production and induces DNA breakage, is overproduced by FA lymphoblasts from the four FA genetic complementation groups. Indeed up to an eight-fold increase in TNF-α is observed in the growth medium of FA cells. Addition of TNF-α antibodies partially corrects the FA hypersensitivity to treatment by DNA cross-linking agents. Moreover, treatment of FA cells with IL-6 no only restores an almost normal sensitivity of FA cells but aslo simultaneously reduces the TNF-α overproduction in FA lymphoblasts. No anomalies at the molecular level (Southern and Northern blot analyses) were detected for the TNF-α gene and its mRNA. The *in vivo* situation was investigated by assaying TNF-α levels in the serum from FA homozygotes and their parents (obligate heterozygotes). In contrast to normal healthy donors or to aplastic anemia patients in whom serum TNF-α is present only in trace amounts, all 36 FA patients and 21 FA heterozygotes monitored showed a significantly higher level of TNF-α activity. The same is true in the AT patients examined whereas XP patients respond normally in this respect. Consequently abnormal TNF-α production seems to be associated with the two "chromosomal instability" syndromes FA and AT. Since growth factor deprivation, TNF-α treatment or DNA damage can trigger apoptosis, we monitored the apoptotic response of FA and AT cell lines. We showed that in both syndromes the spontaneous rate of apopotosis is slightly but repeatedly more elevated than in normal cell cultures. Surprisingly, the apoptosis induced by g-rays is drastically reduced in FA and in AT cells in conditions where the frequency of apoptotic cells is increased in a dose-dependent manner in normal cells.

Since the induction of apoptosis by radiation is a p53-dependent mechanism, the induction of this protein was examined in FA cells. We observed that the p53 protein is not radio-induced in FA cells belonging to 4 genetic complementation groups. The same impairement in

p53 induction is observed not only after γ-irradiation but also after UVB-irradiation, an agent known to cause oxidative stress. These observations are in line with recent reports showing that at least certain cell lines from AT and Bloom syndrome, the two other chromosome breakage syndromes, may be also defective for radiation-induced increase of the p53 protein. As the p53 tumor suppressor gene encodes a transcriptional activator whose targets include genes that regulate genomic stability, cellular response to DNA damage and cell cycle progression, it is clear that altered expression of p53 is likely to be relevant to the phenotype of such syndromes. It should be also kept in mind that, as recently shown by others, p53 can bind to several transcription factors including transcription-repair factors.

On the other hand, the relationship between p53-dependent and p53-independent apoptotic cell death, as well as the cell cycle checkpoints induced by DNA damaging agents were explored in hematopoietic cells. A set of M1 myeloblastic leukemia cell lines including wild thype p53 or being null for p53 expression or expressing p53ts and bcl2-transgenes were compared. It is shown that the kinetics of apoptotic cells death induced by γ-irradiation correlates with the rapidity of exit from γ-ray-induced G2 arrest for all the different hematopoietic cell types. More important, we demonstrate that in addition to a role in apoptosis and G1 arrest, wild type p53 positively controls the exit from the γ-ray-induced G2 checkpoint. This new function of p53 is a component of the physiological pathway by which p53 exerts its role in γ-rays-induced apoptosis. Considering that mutations in the p53 genes are one of the most common genetic changes found in human neoplasia, the activation of p53 mutants by DNA damaging agents may play an important role in determining the radiosensitivity of tumor cells.

In conclusion, our results on FA and AT syndromes largely contributed to the idea of genetic defects resulting in anomalies in intracellular signalling pathways. On the basis of our data, we proposed that the wild type gene product mutated in these syndromes controls the expression of a network of genes involved in the development of the hematopoietic system (including those coding for specific interleukins and TNF-α) and in the processing of DNA lesions The recent partial cloning of the AT genes (Science, June 1995) by Shilo's group brings strong support to this notion. Indeed the AT gene appears to encode a putative protein that is similar to eucaryotic phosphatidylinositol-3' kinase. This enzyme mediates cellular responses to several mitogenic growth factors and to factors triggering cellular differentiation.

2. Cloning of a gene possibly indirectly involved in the FA response to DNA damaging agents

In the case of FA, at the moment, only the group C gene has been molecularly cloned in Buchwald's laboratory (Nature, 1992) Mutations have been identified in the cDNA of FAC patients. However the absence of homology with any known protein and its cytoplasmic localization (D'Andrea's group, Proc Natl. Acad. Sci. USA, 1995 ; Youssefian, Proc. Natl. Acad. Sci. USA, 1995) renders problematic the understanding of this function

On the basis of the complementation of FA group D cells for their hypersensitivity to DNA cross-linking agents by a genomic DNA fragment, a cDNA encoding human dynamin II has been isolated and characterized in our group. This cDNA is ubiquitously expressed, and is a member of the large GTP-binding protein family. Alteration(s) in the properties of this motor protein hDYNII may account for a number of the FA cells features. Indeed, in addition to the GTP-binding domain, the hDYNII protein contains a noticeable number of consensus motifs for p34 Cdc2 kinase phosphorylation which may indicate a potential role at the G2/mitosis transition. However the hDYNII message is normaly expressed in the FAD cells analyzed and mutations were not detected by sequencing the corresponding DNA of the FAD patients. Moreover, attempts to complement the hypersensitivity of FAD cells with hDYNII were unsuccessfull due to alterations in the growth of cells after transfection. For all these reasons, it

is not possible to equate the hDYNII gene with the FAD gene. The possible connection between the function of this new gene and FA, which is clearly associated with a G2/M cell cycle defect, remains an open question to be explored.

In this general context, it can be recalled that a variety of cDNA's introduced into AT cells were found by others to complement the radiosensitivity of these cells. Such cDNA include for instance the gene for phospholipase A2 (Ziv *et al.*, Somat. Cell. Molec. Genet., 1995) or the truncated IkB-α, an inhibitor of the transcriptional activator NFk-B (Jung et *al.*, Science, 1995). These genes are not mutated in AT patients. Thus, cellular sensitivity of both AT and FA cells can be modulated by a number of physiological factors not directly related to the mutated gene product.

In conclusion, this general approach also emphasized the complexity of the network of genes involved in the cellular response to DNA damaging agents and led to the isolation of a gene, hDYNII, involved in vital functions.

3. Genomic instability in FA

The involvment of DNA repair processes in governing genomic instability emerged from the realization that the defects in nucleotide excision repair in cells from xeroderma pigmentosum patients were accompanied by hypermutability by DNA damaging agents. More subtil defects in the processing of DNA lesions as experienced by AT or FA cells were known to be associated to chromosomal abnormalities. In 1990, we reported that in normal human lymphoblasts, the vast majority of spontaneous and psoralen-photoinduced mutations at the hypoxanthine phosphoribosyl transferase (HPRT) locus are base substitutions (Papadopoulo *et al.*, Proc. Natl. Acad Sci. USA, 1990). In contrast, we have shown that in FA lymphoblasts, mutants are the result of deletions of HPRT coding sequences. Moreover, the variant frequency at the glycophorin A (GPA) locus is significantly increased in erythrocytes of FA patients as compared with age-matched healthy donors. Since GPA variants reflect essentially structural deletions, rearrangements and mutations leading to allele loss, the increased frequency of GPA variants is consistent with the enhanced deletion frequency at the HPRT locus. To obtain information on the mechanism(s) underlying the genomic rearrangements in FA, we examined the sequences at the breakpoint of deletions in spontaneous and induced HPRT mutants. The results show that a significant proportion of deletions involving a loss of a given exon are identical and that two deletions of different size have the same 3' breakpoint. Interestingly, it appears that in most of the mutants there is a common deletion signal sequence, which suggests that the mutations in the FA gene(s) may lead to an aberrant site-specific cleavage activity that might be responsible for the deletion proneness and the chromosomal instability characteristic of the FA pathology. From the similarity or even identity of the signal sequence at some of the breakpoints with the consensus heptamer which directs cleavage and joining in the assembly of immunoglobulin and T-cell receptor genes, we speculate that steps in common with the V(D)J recombinational process may be illegitimately involved in FA cells. *In vitro* studies with suitable constructs are undertaken in order to test this possibility.

More generally, inactivation (or malfunctioning) of p53 could lead to alterations in mutation frequencies resulting from inefficient nucleotide excision repair and genomic instability as exemplified by recent studies performed by others on cells from p53-deficient mice. The unravelling of the interactions between the gene products involved in the response to DNA damaging agents will have to take into account such possible links between alterations in expression of crucial genes and the specific genetic consequences.

List of relevant publications:

F. ROSSELLI, J. SANCEAU, J. WIETZERBIN & E MOUSTACCHI.
Abnormal lymphokine production : A novel feature of the genetic disease Fanconi anemia. I :
Involvement of interleukin-6
Human Genet., **89**, 42-48 (1992).

J.S. HOFFMANN, E. MOUSTACCHI, G. VILLANI and E. SAGE.
In vitro DNA synthesis by DNA polymerase I and DNA polymerase α on single-stranded
DNA Containing either purine or pyrimidine monoadducts.
Biochem. Pharmacol., **44**, 1123-1129 (1992).

E. SAGE, E. CRAMB & B.W. GLICKMAN.
UV damage distribution of the *LacI* gene of *Escherichia coli* analysed with various probes on
an automated DNA sequencer : correlation with mutation spectrum.
Mutation Res., **269**, 285-300 (1992).

S. NOCENTINI
Cellular responses to hematoporphyrin-induced photooxidative damage in Fanconi anemia,
xeroderma pigmentosum and normal human fibroblasts.
Mutation Res., **284**, 275-285 (1992).

Workshop on DNA repair.
A.R. LEHMANN, J.H J HOEIJMAKERS, A.A. VAN ZEELAND, C M.P. BACKENDORF,
B.A. BRIDGES, A. COLLINS, R.P.D. FUCHS, G P MARGISON, R. MONTESANO, E.
MOUSTACCHI, A.T. NATARAJAN, M. RADMAN, A. SARASIN, E. SEEBERG, C.A.
SMITH, M. STEFANINI, L H. THOMPSON, G P. VAN DER SCHANS, C.A. WEBER &
M.Z. ZDZIENICKA.
Mutation Res., **273**, 1-28 (1992).

O. RIGAUD, D PAPADOPOULO & E. MOUSTACCHI.
Decreased deletion mutation in radioadapted human lymphoblasts.
Radiation Res., **133**, 94-101 (1993).

E. SAGE.
Distribution and repair of photolesions in DNA : Genetic consequences and the role of
sequence context.
Photochem. Photobiol., **57**, 163-174 (1993).

E. SAGE, E A DROBETSKY & E MOUSTACCHI.
8-methoxypsoralen induced mutations are highly targeted at cross-linkable sites of
photoaddition on the non-transcribed strand of a mammalian gene.
EMBO J., **12**, 397-402 (1993).

S. ROUSSET, S. NOCENTINI, R.M. SANTELLA, F.P. GASPARRO & E MOUSTACCHI.
Immunological probing of induction and repair of 8-methoxypsoralen photoadducts in DNA
from Fanconi anemia and normal human fibroblasts : Quantitative analysis by electron
microscopy.
J. Photochem. Photobiol., Part B, **18**, 27-34 (1993).

S. BOITEUX, A.T. YEUNG & E. SAGE.
Enzymatic recognition and biological effects of DNA damage induced by 3-carbethoxypsoralen plus UVA.
Mutation Res., DNA Repair, **194**, 43-50 (1993).

D. PAPADOPOULO, A. LAQUERBE, C. GUILLOUF & E. MOUSTACCHI.
Molecular spectrum of mutations induced at the *HPRT* locus by a cross-linking agent in human cell lines with different repair capacities.
Mutation Res., DNA Repair, **294**, 167-177 (1993).

C. GUILLOUF, A. LAQUERBE, E. MOUSTACCHI & D. PAPADOPOULO.
Mutagenic processing of psoralen monoadducts differ in normal and Fanconi anemia cells.
Mutagenesis, **8**, 355-361 (1993).

M. SALA-TREPAT, J. BOYSE, P. RICHARD, D. PAPADOPOULO & E. MOUSTACCHI.
Frequencies of *HPRT* mutants in T-lymphocytes and of glycophorin A variants in erythrocytes of Fanconi anemia patients and control donors.
Mutation Res., **289**, 115-126 (1993)

E. SAGE.
Molecular basis of UV and psoralens mutagenesis.
J. Photochem. Photobiol., Part B, **20**, 211-217 (1993).

M. CAVAZZANA-CALVO, F. LE DEIST, G. DE SAINT BASILE, D. PAPADOPOULO, J.P. DE VILLARTAY & A. FISCHER
Increased radiosensitivity of granulocyte macrophage colony-forming units and skin fibroblasts in human autosomal recessive severe combined immunodeficiency.
J. Clin. Invest., **91**, 1214-1218 (1993)

O. GILLARDEAUX, O. PERIN-ROUSSEL, S. NOCENTINI and F. PERIN.
Characterization and evaluation by ^{32}P-postbalelling of psoralen-type DNA adducts in hela cells
Carcinogenesis, 15, 89-93 (1994).

O. RIGAUD & E. MOUSTACCHI.
Radioadaptation to the mutagenic effect of ionizing radiation in human lymphoblasts: Molecular analysis of *HPRT* mutants.
Cancer Res., 54, 1924S-1928S (1994).

F. ROSSELLI, J. SANCEAU, E. GLUCKMAN, J. WIETZERBIN & E. MOUSTACCHI.
Abnormal lymphokine production · A novel feature of the genetic disease Fanconi anemia. II : Spontaneous overproduction of tumor necrosis factor a. A possible tool in detecting heterozygous individuals
Blood, 83, 1216-1225 (1994).

C. DIATLOFF-ZITO, E. DUCHAUD, E. VIEGAS-PEQUIGNOT, D. FRASER & E. MOUSTACCHI.
Identification and chromosomal localization of a DNA fragment implicated in the partial correction of the Fanconi anemia group D cellular defect.
Mutation Res., 307, 33-42 (1994).

E. LEVY, C. BAROCHE, J.M BARRET, C ALAPETITE, B. SALLES, D. AVERBECK & E. MOUSTACCHI.
Activated *ras* oncogene and specifically acquired resistance to cisplatin in human mammary epithelial cells, induction of DNA cross-links and their repair.
Carcinogenesis, 15, 845-850 (1994).

E. DROBETSKY, E. MOUSTACCHI, B. GLICKMAN & E. SAGE.
The mutational specificity of simulated sunlight at the *APRT* locus in rodent cells.
Carcinogenesis, 15, 1577-1583 (1994).

D.R. ROBINSON, K. GOODALL, R.J. ALBERTINI, J.P. O'NEILL, B. FINETTE, M. SALA-TREPAT, E. MOUSTACCHI, Ad D. TATES, D.M. BEARE, M.H.L. GREEN & J. COLE.
An analysis of *in vivo hprt* mutant frequency in circulating T-lymphocytes in the normal human population : a comparison of four datasets.
Mutation Res., 313, 227-247 (1994)

F. ROSSELLI, E. DUCHAUD, D AVERBECK and E MOUSTACCHI.
Comparison of the effects of DNA topoisomerase inhibitors on lymphoblasts from normal and Fanconi anemia donors.
Mutation Res., 325, 137-144 (1994).

E. DUCHAUD, A. RIDET, Y. DELIC, E. CUNDARI, E. MOUSTACCHI & F. ROSSELLI.
Altération de la réponse apoptotique radioinduite chez les individus homozygotes et hétérozygotes pour l'ataxie télangiectasie
C. R. Acad. Sci. Paris, Sciences de la Vie, 317, 983-989 (1994).

C. ALAPETITE, E. LEVY & E. MOUSTACCHI.
Le test des comètes : Aspects techniques.
Path. Biol., 42, 930-931 (1994).

E. MOUSTACCHI.
Biologie cellulaire et moléculaire de l'anémie de Fanconi.
Médecine/Sciences, 10, 979-985 (1994).

O RIGAUD, D. PAPADOPOULO & E. MOUSTACCHI.
Deletion mutations are decreased in irradiated human lymphoblasts adapted to ionizing radiation.
in *European Commission Radiation Protection : Molecular mechanisms in radiation mutagenesis and carcinogenesis*, Eds : K.H. Chadwick, R Cox, H.P. Leenhouts, J. Thacker, pp. 117-119 (1994).

F. ROSSELLI, A. RIDET, T SOUSSI, E. DUCHAUD, C ALAPETITE and E. MOUSTACCHI.
P53-dependent pathway of radio-induced apoptosis is altered in Fanconi anemia.
Oncogene, 10, 9-17 (1995).

A. LAQUERBE, E MOUSTACCHI, J C. FUSCOE & D. PAPADOPOULO.
The molecular mechanism underlying formation of deletions in Fanconi anemia cells may involve a site specific recombination.
Proc. Natl. Acad. Sci. USA, 92, 831-835 (1995)

A. LAQUERBE, E. MOUSTACCHI & D. PAPADOPOULO.
Genotoxic potential of psoralen cross-links versus monoadducts in normal human lymphoblasts.
Mutation Res., 346, 173-179 (1995).

C. GUILLOUF, F ROSSELLI, K KRISHNARAJU, E. MOUSTACCHI, B. HOFFMAN & D.A. LIEBERMANN
P53 involvement in control of G2 exit of the cell cycle : Role in DNA damage-induced apoptosis.
Oncogene, 10, 2263-2270 (1995).

C. DIATLOFF-ZITO, A J E. GORDON, E. DUCHAUD & G. MERLIN.
Isolation of a ubiquitously expressed cdna encoding human dynamin II, a member of the large GTP-binding protein family.
Gene (1995) (in press).

O. RIGAUD, A. LAQUERBE & E MOUSTACCHI.
Radioadaptation to the mutagenic effect of ionising radiation in human lymphoblastoid cells : DNA sequence analysis of $HPRT^-$ mutants.
Radiation Res. (1995) (in press)

A. LAQUERBE, C GUILLOUF, E MOUSTACCHI & D. PAPADOPOULO.
The mutagenic processing of psoralen photolesions leaves a highly specific signature at an endogenous human locus.
J. Mol. Biol. (1995) (in press).

S. NOCENTINI.
Comet assay analysis of DNA break repair in normal and deficient human cells exposed to radiations and chemicals. Evidence for a repair pathway specificity of DNA ligation.
Radiation Res. (1995) (in press).

Head of project 5: Dr. Thacker

II. Objectives for the reporting period

To characterize further the cellular phenotypes of a series of radiosensitive (repair-deficient) cell lines derived in this laboratory (the *irs* lines). To use positional cloning methods to map and clone the human gene complementing the radiosensitive *irs1* line, and to initiate similar studies with the *irs3* line. To use cellular and cell-free methods to identify mechanisms of rejoining of the major radiation-induced damage, the DNA double-strand break. To fractionate biochemically cell and tissue extracts and substantially purify the proteins involved in rejoining both homologous and non-homologous DNA break sites. To complete the molecular analysis of X-ray induced mutations of the *HPRT* gene of primary human fibroblasts; to carry out a parallel study of α-particle induced mutagenesis, including the mapping and sequencing of the breakpoints of large deletions and rearrangements.

III. Progress achieved including publications

Progress towards cloning the human gene complementing the *irs1* radiosensitive line (provisionally named the *XRCC2* gene) has been substantial. We have firstly mapped the gene to human chromosome 7 using a panel of hybrids constructed from the fusion of *irs1* with a human lymphoblastoid line. Many of these hybrids had as their only human material this chromosome, and revertants of the hybrids co-ordinately lost the resistant phenotype and their chr.7 material. Some of these hybrids on further growth spontaneously reduced the size of the chr.7 material, but we have also used radiation-reduction-fusion with one of these hybrids to further localize the gene. The region of chr.7 carrying the gene was mapped using a panel of probes previously localized to specific regions of chr.7q (collaboration with Drs. S. Scherer and L-C. Tsui, Hospital for Sick Children, Toronto), and with available microsatellite markers from the Genethon project. This refined the localization of the *XRCC2* gene to an interval of 7q36 (size approx. 3-5 Mb).
To reduce the interval containing the gene still further, more radiation-reduced hybrids were generated: one of these was sufficiently small to carry only one marker site. The single

marker was then used to derive a set of YACs, and these YACs were fused back to the *irs1* cells to assay for the presence of the *XRCC2* gene. One YAC was found to carry the gene as shown by functional complementation, and a series of derivatives of this YAC were then used to delimit the gene to sub-megabase levels. A restriction map of the YAC and its derivatives, isolated using a fragmentation vector, was derived using rare cutting enzymes on pulsed-field gels. Additionally this YAC was used to identify a large series of PCR-derived cDNA clones hybridizing to the YAC sequence (direct selection method; collaboration with Drs. S. Scherer and L-C. Tsui, Hospital for Sick Children, Toronto). Many of these cDNAs have been sequenced and mapped back to the YAC. These procedures have identified 2 previously known but unassigned genes as well as other candidate genes for *XRCC2*. Functional complementation of full-length cDNAs is being used to finally identify the gene.

A similar project has been started with the *irs3* line: we have made hybrids and are refining the human chromosomal localization. In addition to this cloning work we have further characterized the *irs* lines, particularly extending previous mutation studies to show that *irs1* has a hyper-mutable phenotype. However, unlike some other radiosensitive lines, none of the lines *irs1, irs2* and *irs3* has a defect in V(D)J recombination (collaboration with Dr. E.A. Hendrickson, Brown University, Rhode Island U.S.A.).

We have developed a highly sensitive assay for the rejoining of DNA double-strand breaks (DSB) by mammalian cell-free extracts, and have succeeded in biochemically fractionating tissue and human cell extracts to analyse the nature of the proteins involved. Two types of DNA substrates carrying breaks have been used: (i) substrates with simple cohesive ('homologous') ends, generated with a single restriction enzyme, and (ii) substrates with non-homologous ends to more closely simulate radiation-induced DSB (generated with two different restriction enzymes). Using a substrate with homologous ends we previously reported an activity that stimulates DSB rejoining many fold, called REP-1. This protein has now been shown to increase the turnover of the first intermediate of a ligation reaction, the stable adenylation complex. DSB rejoining correlates with increased turnover of this complex. In this respect REP-1 acts through a completely different mechanism from other ligase-stimulatory substances, such as polyethylene glycol. Partially purified cellular fractions that are capable of rejoining DSB do not show the adenylation complex, and can disrupt the complex formed by a purified ligase. The REP-1 protein is not the same as another recently-identified ligase-associated protein, XRCC1. Several biochemically distinct complexes have been identified which differ in their sensitivity to REP-1, and show characteristic patterns of rejoined products. Such fractions have been shown to be devoid of ligase I, XRCC1 and the Ku protein by Western analysis. Recently, we have also identified and purified a human protein which may a candidate for a novel DNA ligase.

The rejoining of non-homologous substrates by mammalian cell extracts has been demonstrated for the first time, with efficiencies depending on the specific DNA termini present. Efficient rejoining has been found, for example, of two 3' termini using a mechanism that is dependent on nearby direct sequence repeats. Other types of non-homologous ends commonly rejoin through either the blunting or infilling of single-stranded overhangs, followed by blunt-end ligation. The optimal conditions of these rejoining reactions (temperature, salt concentration, cofactor dependence) have been defined. The fractionation of tissue extracts has substantially purified the proteins involved.

Site-specific breaks have also been introduced in mammalian cells, by electroporation of restriction endonucleases under defined conditions, and their consequences assessed in survival and mutation assays. It was shown for example that 4 human cell lines representing a range of radiosensitivities have a comparable sensitivity to endonucleases that give blunt-ended DSB in the cell. These cell lines also represent specific human disorders, namely (in order of sensitivity) Bloom's syndrome < ligase I-deficiency (line 46BR) < ataxia-telangiectasia (A-T). This is the first time that A-T has been shown to be sensitive to an agent inducing only DSB in DNA, reinforcing the view that the defect in this syndrome relates to the processing of DNA breaks. The importance of DSB end structure was addressed by treatment of cells separately with a large number of different restriction endonucleases, generating all possible types of end structure. No correlation in survival or mutagenic effectiveness was found for specific types of end-structure (e.g., endonucleases generating blunt-ended breaks, that might be expected to be more difficult to repair, were not uniformly more effective). However, it was found by careful assessment of the lifetime and activity of endonucleases in simulated cellular conditions, that this was the main determinant of effectiveness. This factor had not been considered before, and our findings reconcile much of the confusing and conflicting data in the literature regarding the effectiveness of endonucleases introduced into cells.

We have undertaken a major study of radiation mutagenesis in primary human fibroblasts. Although these cells are difficult to work with, because of their finite lifespan, we have succeeded for the first time in analysing the molecular changes in a number of large mutations. A set of X-ray-induced mutants of the *HPRT* gene were characterized previously to give a mutation spectrum and to show that large deletions are formed by processes of illegitimate recombination. We have now carried out a comparable study of mutants induced by high LET radiation, using an in-house α-particle source from 238-plutonium. We have considerable expertise in irradiating cells with this source and have derived a large number of α-particle-induced *HPRT* mutants for analysis. A mutation spectrum was derived using sets of PCR primers to define the presence/absence of multiple sites across the 44-kb gene. This analysis has revealed that a major fraction of the mutants (63%) carry large genetic changes and the remainder are point mutations. Further analysis of the large mutations shows that these mostly have breakpoints lying outside the gene, suggesting differences in mechanism from spontaneous mutations. The use of markers outside the gene in the Xq26 chromosomal region, derived for PCR analysis both by ourselves and others, has refined the localization of deletion breakpoints in both the previous X-ray-induced mutants and the new α-particle-induced set. The data show a broad distribution of sizes of deletion for both radiation qualities and that some of the deletions extend over a 3 Mb region, a much larger region than previously suspected. This result confounds predictions of others suggesting that hemizygous genes such as *HPRT* cannot detect very large mutations. In collaboration with our cytogenetics group, we have found that one α-particle-induced mutant carrying a large molecular deletion also has a chromosomal exchange in the region of Xq26 (i.e., it is a complex mutation). Five of the large deletions having at least one breakpoint within *HPRT* were analysed at the DNA sequence level; since sequence information was available on only one side of the deletion junctions the technique of RAGE (rapid amplification of genomic DNA)-PCR was used. Surprisingly two of these mutations were found to be more complex than expected: on sequencing across the junctions, unknown DNA was found, showing that

either insertions or other forms of rearrangement had occurred. The resolution of other junctions revealed that two of the mutations also had short direct repeats at the deletion sites, suggesting as for some X-ray mutants that the mechanism involved illegitimate recombination. Our results may be tentatively interpreted to suggest that α-particles induce more complex mutations than X-rays, but more data are needed to verify this possibility.

Publications

Fairman, M.P., A.P. Johnson and J.Thacker (1992) Multiple components are involved in the efficient joining of double stranded DNA breaks in human cell extracts. *Nucleic Acids Res.*, **20**, 4145-4152.

Thacker, J., J. Chalk, A. Ganesh & P. North (1992) A mechanism for deletion formation in DNA by human cell extracts: the involvement of short sequence repeats. *Nucleic Acids Res.*, **20**, 6183-6188.

Ganesh, A., P. North and J.Thacker (1993) Repair and misrepair of site-specific DNA double-strand breaks by human cell extracts. *Mutation Res.*, 299, 251-259.

Morris, T. and J. Thacker (1993) Formation of large deletions by illegitimate recombination in the HPRT gene of primary human fibroblasts. *Proc. Natl. Acad. Sci. USA*, **90**, 1392-1396.

Goodhead, D.T., J. Thacker & R. Cox (1993) Effects of radiations of different qualities on cells: molecular mechanisms of damage and repair. *Int. J. Radiat. Biol.*, **63**, 543-556.

Morris, T., W. Masson, B. Singleton & J. Thacker (1993) Analysis of large deletions in the *HPRT* gene of primary human fibroblasts using the polymerase chain reaction. *Somatic Cell Molec. Genet.*, **19**, 9-19.

Simpson, P., T. Morris, J. Savage & J. Thacker (1993) High-resolution cytogenetic analysis of X-ray induced mutations of the HPRT gene of primary human fibroblasts. *Cytogenet. Cell Genet.*, **64**, 39-45.

Costa, N.D., Masson, W.K. and Thacker, J. (1993) The effectiveness of restriction endonucleases in cell killing and mutagenesis. *Somat. Cell Molec. Genet.*, **19**, 479-490.

Costa, N.D. and Thacker, J. (1993) The response of radiation-sensitive human cells to defined DNA breaks. *Int. J. Radiat. Biol.*, **64**, 523-529.

Thacker, J. (1993) Fingerprinting of mammalian cell lines with a single PCR primer. *Biotechniques*, **16**, 252-253.

Thacker, J., Ganesh, A., Stretch, A., Benjamin, D.M., Zahalsky, A.J., and Hendrickson, E.A. (1993) Gene mutation and V(D)J recombination in the radiosensitive *irs* lines. *Mutagenesis*, **9**, 163-168.

Fairman, M.P., A. Johnson, R. Mason, J. Chalk and J. Thacker (1994) The rejoining of double-strand breaks in DNA by human cell extracts. In: *Molecular Mechanisms in Radiation Mutagenesis and Carcinogenesis*, (Eds: K.H. Chadwick, R. Cox, H.P. Leenhouts and J. Thacker), European Commission, Luxembourg, pp.47-52.

Costa, N.D., W.K. Masson and J. Thacker (1994) Mutation induction by agents that generate DNA double-strand breaks at defined sites. In: *Molecular Mechanisms in Radiation Mutagenesis and Carcinogenesis*, (Eds: K.H. Chadwick, R. Cox, H.P. Leenhouts and J. Thacker), European Commission, Luxembourg, pp.137-142.

Singleton, B., T. Morris, W. Mason and J. Thacker (1994) Molecular analysis of *HPRT* mutations induced by ionising radiations in primary human fibroblasts. In: *Molecular*

Mechanisms in Radiation Mutagenesis and Carcinogenesis, (Eds: K.H. Chadwick, R. Cox, H.P. Leenhouts and J. Thacker), European Commission, Luxembourg, pp.157-162.

Simpson, P., T. Morris, J. Savage and J. Thacker (1994) Cytogenetic and molecular analysis of X-ray induced mutations of the *HPRT* gene of primary human fibroblasts. In: *Molecular Mechanisms in Radiation Mutagenesis and Carcinogenesis*, (Eds: K.H. Chadwick, R. Cox, H.P. Leenhouts and J. Thacker), European Commission, Luxembourg, pp.163-168.

Thacker, J., and R. Cox (1994) Mutagenesis and genomic instability: carcinogenesis and the modelling of cancer risk. In: *Molecular Mechanisms in Radiation Mutagenesis and Carcinogenesis*, (Eds: K.H. Chadwick, R. Cox, H.P. Leenhouts and J. Thacker), European Commission, Luxembourg, pp.313-317.

Thacker, J. (1994) Cellular radiosensitivity in ataxia-telangiectasia. *International Journal of Radiation Biology*, **66**, S87-S96.

Thacker, J. (1994) The study of responses to 'model' DNA breaks induced by restriction endonucleases in cells and cell-free systems: achievements and difficulties. *International Journal of Radiation Biology*, **66**, 591-596.

Thacker, J., C.E. Tambini, P.J. Simpson, L-C. Tsui and S.W. Scherer (1995) Localization to chromosome 7q36.1 of the human *XRCC2* gene, determining sensitivity to DNA-damaging agents. *Human Molecular Genetics*, **4**, 113-120.

Thacker, J., and R.E. Wilkinson (1995) The genetic basis of cellular recovery from radiation damage: response of the radiosensitive *irs* lines to low-dose-rate irradiation. *Radiat. Res.*, in press.

Head of project 6:   Dr. Backendorf

II. Objectives for the reporting period

It has now been firmly established that exposure of living cells to radiation results in rapid changes in gene expression. Although many of the genes which are affected are involved in major cellular processes such as proliferation, differentiation and cell death, the physiological significance of these changes is still poorly understood. We have studied these radiation effects in epidermal keratinocytes derived from human skin for the following reasons: human skin constitutes one of the most radiosensitive organs of our body, probably because cell proliferation, differentiation and death have to be tightly regulated in order to permit epidermal maturation. Interference of radiation with these essential processes is thus readily visible by changes in gene expression. During a previous contract period we have isolated a novel class of genes (by differential screening of keratinocyte cDNA libraries) whose expression was strongly affected by exposure of keratinocytes to radiation (*SPRR* genes). The objectives for the reporting period were to unravel the molecular function of these gene products and to identify signal transduction cascades and transcription factors involved in the regulation of these genes.

III. Progress achieved including publications

a. The function of the SPRR gene family

As mentioned above, the *SPRR* genes were originally identified by differential screening of cDNA libraries obtained from UV irradiated human keratinocytes. Later on it was shown that the expression of these genes was also affected by other DNA damaging agents such as 4-NQO and ionizing radiation and by the tumor promoting agent TPA. Furthermore the expression of these genes was tightly regulated during keratinocyte terminal differentiation (an apoptotic process) both *in vivo* and *in vitro* (1,3,6). A first indication for a possible function for these genes, which code for small **proline rich** (SPRR) proteins, was obtained after assigning these genes to human chromosome 1q21 (5). This region of the human chromosome contains a large number of genes involved in keratinocyte differentiation. The *SPRR* gene family mapped between the loci of involucrin and loricrin. Both genes are, as is the case for the *SPRR* genes, expressed specifically in terminally differentiating keratinocytes and code for precursor proteins of the cornified cell envelope, a strong insoluble structure synthesized beneath the plasma membrane at late stages of squamous differentiation. When the protein sequence of the different members of the *SPRR* family were compared to the involucrin and loricrin sequences it was realized that the N- and C-terminal domains of these proteins were highly homologous, suggesting that these proteins had similar functions (4). This assumption was confirmed by direct biochemical evidence showing that the 3 different classes of *SPRR* genes code indeed for cornified envelope precursor proteins (6). The same genes have now also been cloned by two other groups (with the use of antibodies raised against isolated cornified envelopes). The corresponding proteins have been denominated "cornifins" and "pancornulins"

by these authors. An interesting recent observation in our group was that in contrast to involucrin and loricrin, which are expressed in all squamous epithelia, the expression of the different members of the *SPRR* gene-family is not uniform but characteristic for a specific epithelium (6). For instance SPRR1 is uniformly expressed in suprabasal cells in plantar and palmar epithelium, whereas in hairy epithelium it is restricted to appendageal areas. SPRR3 is strongly expressed in mucosal epithelium but not at all in the skin. As *SPRR* genes are also induced by radiation and other external damaging agents, it ensues that expression of SPRR's is variable and depends both on internal factors (determined by the tissue itself) and on external factors (e.g. stress, inflammation). Besides it is interesting to mention that *SPRR* expression changes during the normal aging process of the skin (2).

Recently a model for the structure of the outer two-thirds (cytoplasmic side) of the human epidermal cornified envelope was proposed by Dr. Peter Steinert (NIH). In this model the SPRR's fulfil the function of bridging molecules (cross-bridges) between flexible meshes of crosslinked loricrin molecules (whether SPRR's can also cross-bridge with involucrin is not yet known and awaits the determination of the structure of the inner part of the cornified envelope). As can be deduced from their aminoacid sequence (rich in proline) SPRR's can be viewed as small rigid globular proteins (with an estimated rigidity of SPRR2 > SPRR1 > SPRR3). It has been suggested that the amount of SPRR cross-bridging between the rather flexible (glycine-rich) loricrin molecules will determine the flexibility characteristics of the cornified envelope. As the expression of the SPRR's is influenced by external agents which cause epidermal injury (e.g. radiation) and as increased rigidity of the cornified envelope might mean better protection, it is likely that the *SPRR* genes are part of a protective response of our body to external stress.

b. Transcription factors involved in SPRR gene expression

The realisation that the *SPRR* gene family is likely to be part of a genetic system which has evolved in order to protect our body from external stress such as radiation, has opened the way to the analysis of the molecular factors which mediate this response. Knowledge of these genetic factors would be of outermost interest not only from a scientific point of view but also from the point of view of radiation protection and risk assessment. In order to identify transcription factors involved in these radiation responses the promoter regions of the 3 members of the SPRR gene-family have been isolated and genetic methods such as deletion mapping and site-directed mutagenesis have been used to identify important regulatory elements in the promoter region (3). Subsequently a beginning has been made with the identification of the transcription factors which can bind to these sequences. Sofar most of our work has concentrated on the *SPRR2A* gene. The most surprising outcome of this analysis was that the regulation of this gene appears to be extremely complicated and involves the synergistic action of at least 4 different classes of transcription factors (manuscript in preparation). As all of these transcription factor binding sites are essential for expression of this gene after the cells have been induced to terminal differentiation they have been denominated TDE's (terminal **d**ifferentiation **e**lement):

a) TDE-1 contains two octamer boxes arranged in a head to head fashion. These sequences are recognized by the POU family of transcription factors. From site directed mutagenesis studies and from bandshift analysis it appears that the OCT-11 transcription factor is involved in *SPRR2A* regulation allthough keratinocytes express many POU factors (e.g. OCT-1, OCT-2 and OCT-6). We have recently been able to isolate a human OCT-11 cDNA from a keratinocyte library, which will allow us to study the involvement of this factor in the radiation response in more detail.

b) TDE-2 contains an ISRE (interferon stimulated response element). Mutations, in this sequence, which are known to inhibit interferon stimulation, also block completely the regulated expression of the *SPRR2A* gene. In bandshift experiments with extracts from human keratinocytes two specific ISRE complexes are observed. These complexes are strongly induced after interferon gamma treatment as is the expression of the *SPRR2A* gene. Supershifts identified IRF-1 and IRF-2 as the responsible transcription factors. IRF-1 is a recently identified tumor suppressor gene whereas IRF-2 behaves more like an oncogene. Our results are the first indication of an involvement of these transcription factors in terminal differentiation.

c) TDE-3 contains an ETS binding site and is partly overlapping with TDE-2. The family of *ETS* genes encodes transcription factors which recognize a similar consensus sequence and are characterized by a specific protein sequence, the ETS domain. ETS transcription factors are involved in development and differentiation where they are often found as components of larger transcription factor complexes. ETS transcription factors are often activated by external (physiological and non-physiological) agents. At present it is not yet clear which member(s) of the ETS transcription factor family is (are) expressed in keratinocytes and involved in the regulation of the SPRR gene.

d) TDE-4 contains a novel sequence rich in T's and G's which has been named TG box. Deletion of this sequence or point mutations completely abolish *SPRR2A* expression. In a bandshift experiment with the TG box two specific complexes are observed. Supershifts with specific antibodies seem to indicate that the corresponding transcription factor might be identical or related to HLTF (a recently identified helicase like transcription factor with high homology to the yeast *rad16* repair gene). However more experiments are needed to confirm the implication of this factor in terminal differentiation and radiation response.

Although the multitude of transcription factors necessary for *SPRR2A* expression might be surprising at first sight, one should realize that *SPRR* genes are part of an apoptotic process (terminal differentiation is a process of programmed cell death) which by definition has to be very strictly regulated (once initiated there is no return, the cell will die). Only under specific conditions, characterized by a given configuration of transcription factors (determined either by tissue inherent conditions or by external stress factors), the expression of these genes is allowed. As expression of *SPRR* genes and the formation of the cornified cell envelope is directly linked with cell death, it appears that at least under certain conditions of external damage the cell chooses to die rather than trying to repair the damage which has been afflicted. This propensity to terminal differentiation is likely to be responsible for the rather high radiosensitivity of these cells. It should be clear that deregulation of these processes

might play a significant role in carcinogenesis.

Besides the transcription factors and signal transduction cascades essential for SPRR expression we have also identified molecular factors which can interfere with the strictly regulated expression of this important gene family. For instance ectopically expressed c-JUN is a powerful inhibitor of *SPRR2A* expression. This inhibition is not mediated via an AP-1 binding site. Probably downregulation by c-JUN is achieved via protein-protein interactions. It is possible that JUN interferes with the synergistic action of the positively acting transcription factors mentioned above (maybe by a squelching mechanism). We have recently obtained evidence that inhibition of *SPRR2A* expression by JUN is mediated by the RAS signal transduction cascade. Activated RAS inhibits *SPRR2A* expression. This inhibition can be relieved by cotransfection of an negatively dominant c-JUN mutant. The RAS signal transduction cascade appears to play an important role in determining the balance between proliferation and differentiation in human keratinocytes. In collaboration with the group of Prof. JL Bos (University of Utrecht) we have obtained indications that this balance might be determined by the balance between active and inactive forms of p21-RAS (7). In a number of cases the RAS signaling pathway has been implicated in the UV response. Whether this pathway is also involved in the response of human keratinocytes to radiation remains to be established.

c) Publications:

1. Gibbs, S., Lohman, F., Teubel, W., van de Putte, P. and Backendorf, C. (1990). Characterization of the human spr2 promoter: induction after UV irradiation or TPA treatment and regulation during differentiation of cultured primary keratinocytes. Nucleic Acids Research 18: 4401-4407

2. Garmyn, M., Yaar, M., Boileau, N., Backendorf, C. and Gilchrest, B. (1992). Effect of aging and habitual sun exposure on the genetic response of cultured human keratinocytes to solar-simulated irradiation. J. Invest. Dermatol. 99: 743-748

3. Gibbs, S. (1992) Interference of UV light with gene regulation in epidermal keratinocytes. PhD thesis. University of Leiden.

4. Backendorf, C. and Hohl, D. (1992) A common origin for cornified envelope proteins. Nature Genetics 2: 91

5. Gibbs, S., Fijneman, R., Wiegant, J., Geurts van Kessel, A., van de Putte, P. and Backendorf, C. (1993). Molecular characterization and evolution of the SPRR family of keratinocyte differentiation markers encoding small proline rich proteins. Genomics 16: 630-637

6. Hohl, D., de Viragh, P., Amiguet-Barras, F., Gibbs, S., Backendorf, C. and Huber, M. (1995). The small proline-rich proteins constitute a multigene family of differentially regulated cornified cell envelope precursor proteins. J.Invest.Dermatol. 104: 902-909.

7. Medema, J.P., Sark, M.W.J., Backendorf, C. and Bos, J.L. (1994). Calcium inhibits EGF-induced activation of p21-RAS in human primary keratinocytes. Mol.Cell.Biol. 14: 7078-70854

Head of project 7: Dr. F. Eckardt-Schupp, GSF-Forschungszentrum Neuherberg

II. Objectives for the reporting period:

Our objective was to develop techniques based on pulsed-field gel electrophoresis (PFGE) and computer-based evaluation procedures to quantify DNA double-strand breaks (DSB) induced by various radiation qualities in *S. cerevisiae* and mammalian cells and assess their spatial distribution. Furthermore, we used the techniques to study the efficiency of DSB repair, e.g. the reconstitution of high molecular weight DNA, in various radiosensitive diploid yeast strains and mammalian cell lines. In parallel, we studied the fidelity of restriction enzyme-mediated DSB and double-stranded gaps in a yeast centromeric plasmid transformed into haploid yeast strains differing in their repair capacities. A further task was the structural and functional analysis of the *REV2 (=RAD5)* gene of *S. cerevisiae* controlling error-free as well as error-prone processing of UV- and X-ray induced DNA damage.

During the period 1992/95 we have addressed the following topics:

1. Development of electrophoresis assays and appropriate evaluation procedures for the analysis of DSB in yeast and mammalian cells;

2. Analysis of the spatial distribution of DSB after irradiation with sparsely ionizing radiation and after damage repair;

3. Determination of the DSB induction frequency in yeast and various mammalian cell lines after ionizing irradiation under various irradiation conditions;

4. Determination of DSB repair kinetics in radioresistant and radiosensitive yeast strains and mammalian cell lines;

5. Use of the method to demonstrate non-random distribution of DSB induced by densely ionizing radiation;

6. Studies on the fidelity of repair of DSB and gaps in a yeast plasmid transformed into radioresistant and radiosensitive yeast strains;

7. Cloning and molecular analysis of the *REV2 (=RAD5)* gene of yeast;

8. Functional analysis of the *REV2* gene: diverse role in mutagenesis

III. Progress achieved including publications

1. Development of electrophoresis assays and appropriate evaluation procedures for the analysis of DSB in yeast and mammalian cells.

A reliable quantification of DNA damage is a prerequisite to the estimation of risks resulting from different irradiation conditions and to the analysis of damage repair. Types of DNA damage which result in fragmentation of the DNA molecules, either directly (DSB) or after enzymatic damage processing (S1 nuclease-sensitive sites or base damage) are generally analyzed via an evaluation of the change in the molecule length distributions of treated as

compared to untreated samples Most methods for a quantitative evaluation used so far rely on the assumption that the resulting breaks are distributed randomly within the analyzed genomic samples. If this assumption holds, a so-called random breakage model allows the quantification of breaks. However, if this assumption is invalid, its use for quantification is errorprone. Therefore, for a given sample it is necessary to check the validity of the random breakage model before it is applied to quantification. We have developed methods, which allow to test whether a tentative model for the spatial distribution of breaks is valid under given circumstances. In case the model holds, the method is then used for a reliable and fast quantification of breaks

In the yeast *S. cerevisiae* all intact chromosomal molecules and their radiation-induced fragments can be separated according to size by PFGE. Ethidium bromide-staining of the gels and measurement of the fluorescence intensity distribution yields DNA mass profiles which comprise the peaks of the intact chromosomal molecules and fragments of heterogeneous length. This distribution of DNA mass in the gel lanes versus migration distance is monitored by use of a CCD camera and an image analysis device Next, using arbitrary values for the frequencies of DSB per unit length, expected DNA mass distributions are calculated on the basis of a random breakage model. These distributions are transformed into distributions in migration distances using a calibration curve for the relationship between molecule length and migration distance valid in the gel The shape of the bands corresponding to intact chromosomal molecules can be simulated with the aid of a modified Lorentzian distribution. Finally, the calculated profiles are normalized to the same area as observed profiles and the two profiles are compared using a least square procedure. During an optimization procedure, the value for the DSB frequency yielding the best fit between observed and calculated distribution is then determined. If the agreement between observed and calculated profiles after optimization of the model parameters is still poor, this is treated as an incidence for a deviation of the actual distribution of DSB from a random distribution Satisfying agreement between both profiles indicates that the random breakage model can be used for a quantitative evaluation of the DSB frequency. A similar method has been established for DSB analysis in mammalian cell DNA Intact mammalian chromosomal molecules are too long to enter the gel during electrophoresis, therefore, only the size distribution of fragments small enough to enter the gel can be analyzed. This restricts the quantification of DSB to samples irradiated with at least 50 Gy

2. Analysis of the spatial distribution of DSB after irradiation with sparsely ionizing radiation and after damage repair.

Although with sparsely ionizing radiation the pattern of energy deposition within a cell nucleus is expected to be stochastic, it seemed conceivable that radical-mediated DSB induction is influenced by the structure and condensation status of the chromatin Evaluation of profiles obtained from yeast cells irradiated with sparsely ionizing radiation both under oxic and hypoxic conditions resulted in a good agreement between calculated and observed DNA mass distributions, and the quality of fit was not influenced by the irradiation conditions This indicates that a higher proportion of radical-mediated breaks does not result in a change in the spatial distribution of DSB as detectable with the method used The localization of a DSB with respect to sequence context or relative distance to other DSB might have an impact on its reparability We investigated therefore, whether DNA profiles obtained from γ-irradiated yeast cells which were allowed to repair the DNA damage during a post-irradiation incubation agreed still with the calculated profiles predicted assuming a random distribution of breaks. We

found no indications for a poorer agreement than observed in samples that were irradiated only (see Fig 1)
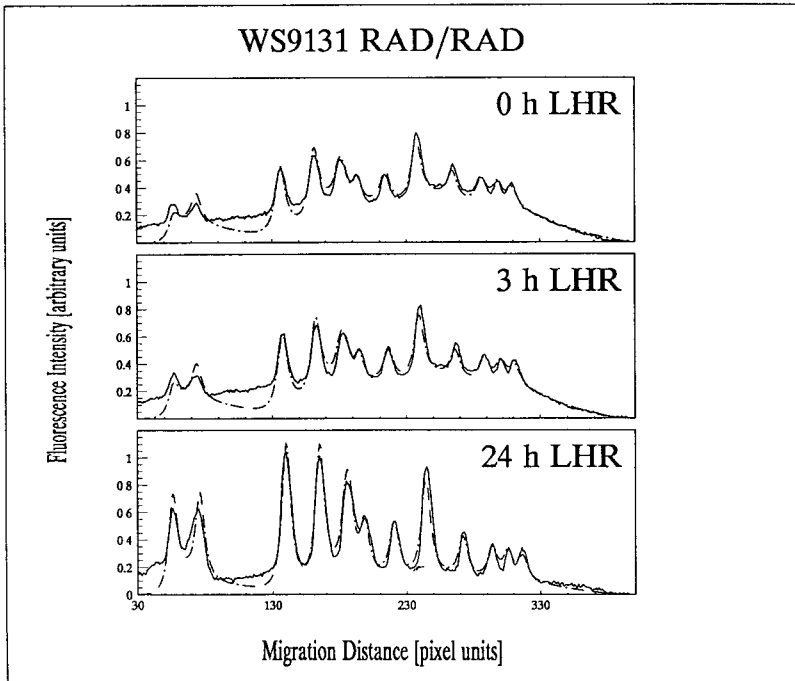
Fig. 1
Observed (solid line) and best-fitting calculated (dotted line) DNA mass distributions obtained from wildtype cells irradiated with 300 Gy under oxic conditions and kept for 0, 3 and 24h under non-growth conditions.

3. Determination of the DSB induction frequency in yeast and various mammalian cell lines after sparsely ionizing irradiation under various irradiation conditions.

In case the random breakage model holds, the evaluation procedure can be used for a quantitative DSB analysis In yeast the frequency of DSB induced by γ-radiation was determined as ($1\ 01 \pm 0\ 06$) and ($2\ 75 \pm 0\ 10$) DSB per 10^9 Gy x bp when irradiated under hypoxic conditions or oxic conditions, respectively No significant strain-specific variations in these values were detected. To validate the new technique, pulsed field gels were also blotted and hybridized to chromosome-specific gene probes The frequency of DSB as calculated from the diminution of the hybridization signals in the chromosomal bands compare well to those obtained by the other method.
In exponentially growing cells of the cell lines V79 (Chinese hamster), KE37/1 (human) and L929 (mouse) the DSB frequencies after γ-irradiation under oxic conditions was determined as ($5\ 0 \pm 0\ 4$), ($3\ 9 \pm 0\ 6$) and ($6\ 3 \pm 0\ 9$) DSB per 10^9 Gy x bp. The reason for these deviations is

not clear. One possible explanation is that the relative cell cycle distribution in exponentially growing cells of these lines differs, having an impact on the actual or apparent DSB frequency However, detailed analysis of DSB induction in synchronized populations of L972 cells showed that the influence of the cell cycle position is very small (variations in the induction frequency are lower than 20%). These data are in contrast to data obtained the so-called FAR method for DSB measurement, where the DSB frequency is inferred from the fraction of DNA able to enter the gel With this method, errors arise if molecules are inhibited from entering the gel although they are small enough, e.g. because of replication eyes and other structures.

4. Determination of DSB repair kinetics in radioresistant and radiosensitive yeast strains and mammalian cell lines.

We tested several radioresistant wildtype yeast strains for their ability to repair γ-ray-induced DSB during a post-irradiation incubation under non-growth conditions. These strains exhibited biphasic exponential repair kinetics, with $t_{1/2}$ values of 3-4h for the fast component and 11-15h for the slow component (for an example, see Fig. 2). Interestingly, the kinetics of repair is identical for DSB induced under oxic and hypoxic conditions, provided that the initial level of damage is the same. These data indicate that the reparability of the breaks is not influenced by the oxygen status during irradiation.

The analysis of DSB repair kinetics in radiosensitive mutants may give hints to the functions of the mutated genes. In yeast, the predominant pathway for DSB repair is homologous recombination This pathway depends on the Rad52 protein, and studies in *rad52* point mutants have long been interpreted in terms of a total deficiency of the cells to repair DSB However, using a diploid homozygous *rad52::TRP* disruption mutant, we observed a reproducible decrease of the frequency of DSB per unit molecule length of about 30% during the first 3h of repair incubation (Fig 2), whose velocity agrees well with the fast component of repair in wildtype cells. In contrast to data obtained by others in point mutants, we did not observe an increased unspecified DNA degradation after irradiation of the cell It remains to be tested whether these differences are due to different phenotypes of point and disruption mutants Yeast cells bearing mutations in the *REV2 gene* exhibit moderately enhanced radiosensitivity and show a very pleiotropic phenotype with regards to mutation induction. We tested whether deficiencies in DSB repair can be observed in diploid homozygous *rev2-1* strains. Although the final level of residual damage after 24h of repair incubation is similar to that obtained in wildtype cells, the kinetics of repair are drastically different. Recently, it has been demonstrated that the radiosensitivity of three complementation groups of radiosensitive mutant rodent cell lines is due to a defect in a component of the Ku-heterodimer-DNA-PK-complex. In yeast, a putative homologue to the Ku-heterodimer has been identified, and the gene *HDF1* encoding one of the subunits is cloned and sequenced We have shown that deletion of the *HDF1* genes enhances the radiosensitivity of the cells only in the absence of homologous recombination, i e. in a *rad52* background or in stationary haploid cells. These data may hint at the presence of additional minor DSB repair pathways in yeast. In preliminary experiments on DSB repair in *rad52 hdf1* double mutants a very small, if at all, decrease in the DSB frequency during post-irradiation incubation was observed. In collaboration with M. Zdzienicka, Leiden, we have begun to analyze DSB repair kinetics in various radiosensitve mutant rodent cell lines

Fig. 2
Kinetics of DSB repair under non-growth conditions [LHR] in a wildtype (WS9131),
rad52Δ and hdf1Δ derivatives

5. Use of the method to demonstrate non-random distribution of DSB induced by densely ionizing radiation.

In contrast to the results obtained using sparsely ionizing radiation, after treatment of yeast cells with neutron beams of various energies, the resulting DNA mass distributions could not be predicted with sufficient accuracy. It was shown that the observed distributions resulting from irradiation of cells with these densely ionizing radiations were broader than expected after random induction of DSB Thus, the random breakage model is inappropriate for the description of the spatial distribution of neutron-induced DSB Based on microdosimetric considerations, a new model was developed that accounts for the occurrence of clusters of DSB Implementation of this modified model in the evaluation program and its application to the analysis of measured DNA mass distributions resulted in a clearly improved agreement of the calculated spectra with the observed profiles as compared to the employment of the random breakage model This indicates deviations from randomness in the spatial distribution of neutron-induced DSB Our approach allows the computation of the resulting DNA mass distributions and, hence, the quantitative analysis of non-randomly induced DSB detectable after exposure of yeast cells to densely ionizing radiation We found an average of $(3\ 7 \pm 0\ 5)$ DSB per 10^9 Gy x bp after irradiation in air, which leads to a relative biological effectiveness (RBE) of approximately 2 7 for neutrons for the induction of DSB

Also in mammalian cells (V79) an analysis of the observed DNA mass profiles after induction of DSB by very densely ionizing radiations, such as beams of accelerated charged particles (Calcium ions, 6 9 MeV/u, LET $\approx 2\ 1$ x 10^3 keV/μ or Uranium ions, 9 MeV/u, LET ≈ 14 x 10^3 keV/μ, respectively), revealed a marked overdispersion of the resulting DNA mass distributions Any attempt to calculate corresponding profiles employing a random breakage

spectra are characterized by an excess of fragments both in the low as well as in the very high molecular weight regime, as compared to the amount of medium-sized molecules (Fig.3) In view of this excess of short fragments, one may speak of damage clustering, but one must note that, due to technical limitations, the observations refer to DSB separated by more than about 20 kb Track structure calculations suggest multiple damage on a nanometer scale that may correspond to much shorter fragments, but such fragments are not detectable with the present approach Nevertheless, it was found that after treatment of cells with very densely ionizing radiations, a considerable amount of DNA mass is contained in very small fragments that are partially lost during the preparation of the samples This observation and the fact that also a large fraction of DNA mass is contained in very large molecules that are not able to enter the gel prevented an unequivocal quantification of DSB induced by accelerated charged particles However, a simple model was developed that accounts for clustering of DSB which allows at least an empirical description of the resulting DNA mass distributions With the aid of this model, possible implications on the determination of RBE values for the induction of DSB by very densely ionizing radiations were assessed
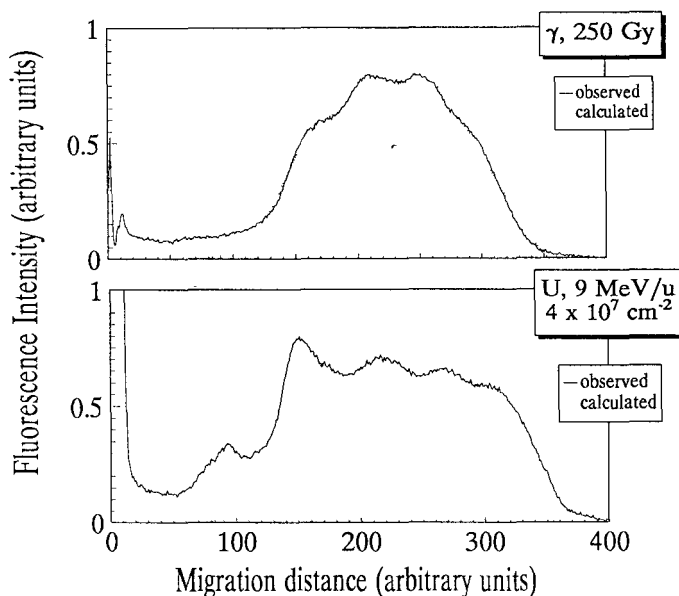
Fig. 3

Observed DNA mass distribution (solid lines) after treatment of cells with γ-rays (upper panel) and accelerated Uranium ions (lower panel). Exposures are as indicated. Wheras for the case of sparsely ionizing radiation an excellent agreement between observed and the calculated distributions (dotted lines) could be achieved, with densely ionizing radiation the agreement is rather poor.

6. Studies on the fidelity of repair of DSB and gaps in a yeast plasmid.

Commonly, X-ray sensitivity of yeast and mammalian cell mutants is explained by some deficiency in DSB repair Applying the PFGE technique we have analyzed DSB repair kinetics under non-growth conditions in various yeast strains, and we found the situation to be rather complex. Two different though closely related diploid repair-competent yeast strains (D7 and BKO) with significant differences in their sensitivities towards gamma-rays, both under oxic and hypoxic conditions of irradiation, show nearly identical efficiencies in the reconstitution of chromosomal length DNA ("DSB repair") after 24 hours as quantified by PFGE, but different time courses of repair. Under identical experimental conditions, the *rev2-1* diploid mutant exhibiting medium radiosensitivity, is capable of restoring chromosomal length DNA to a level similar the wild-type diploid after 24 hours of repair, however, the time course is much slower. A similar effect was found for a *rad18-1* diploid strain (E.M. Geigl and F. Eckardt-Schupp, Curr. Genet. 20, 33-37, 1991). We asked the question whether a reduced fidelity of DSB repair is possibly the cause for the enhanced radiosensitivity in strains with delayed DSB repair. We established an experimental system which allows to study the correctness of repair of restriction enzyme-induced DSB and small gaps (DSG, 169 bp) with sticky ends in the plasmid YpJA18. The plasmid contains two selectable recombinant yeast genes (*TRP1, URA3*) and is transformed, either circular or cut in the *URA3* gene by the restriction enzyme(s), NcoI and/or ApaI, into haploid yeast strains (*trp1-289, ura3-52*) differing in their capacities for repair of X-ray damage (see Table 1).

In repair-competent strains, both DSB and DSG are repaired with high efficiencies (as deduced from the transformation frequencies of the manipulated plasmids) and fidelities (as deduced from *URA3* gene function) presumably by recombination with the chromosomal *URA3* gene. In *rev2* point- and deletion-mutants the efficiency is similar to the wild-type strain, but the frequency of correctly repaired plasmids differs from the wild-type frequency considerably. In the point mutant *rev2-1* and deletion mutant *rev2Δ* the gap is restored in only 18% and 26% of the transformants as compared to wild-type strains. In contrast (and to our surprise) the DSB is restored with wild-type fidelity in the deletion mutant, but in the *rev2-1* point mutant in only 20% of the transformants. Obviously, the Rev2 protein is required for the fidelity control of the repair of DSB and DSG in plasmid DNA, and possibly of yeast chromosomal DNA as well In a *rad18* mutant the DSB are repaired correctly in 95% of the transformants whilst the value for DSG is about 80%. In contrast, mutants of the *RAD52* group with very reduced transformation efficiencies for the linearized plasmids show very reduced frequencies of correctly repaired lesions (<5 %).

Misrepaired plasmids were isolated for DNA sequence analysis of the junction sites. Misrepaired plasmids in the *rev2Δ* as well as the *rev2-1* point mutant showed similar results: In most of the plasmids the 5' and 3' termini of the gaps were simply joined either exactly or with deletions or insertions of nucleotides without restoration of the 169 bp sequence. Most of the DSB were joined with errors at the junction site. Plasmids isolated from the *REV2* wild-type strain, which did not restore the *URA3* function, have correctly restored the gap by recombination and DSB were repaired by ligation without alterations at the junction sites. Obviously, second site events caused the ura⁻ phenotype. Assuming a similar situation for radiation-induced DSB in chromosomal DNA, further analysis of the fidelity of DSB and DSG repair will improve our understanding of the molecular mechanism(s) of DSB repair. It is of particular interest to elucidate the role of the Rev2 protein in the processes of DSB and gap repair

Plasmid	Uncut		ApaI-DSB		ApaI-NcoI DSG	
Yeast strain	URA⁺TRP⁺/TRP⁺	%	URA⁺TRP⁺/TRP⁺	%	URA⁺TRP⁺/TRP⁺	%
Wildtype	370/372	100	400/408	98	584/600	97
rev2-1	173/188	92	111/555	20	146/796	18
rev2Δ	297/300	99	288/300	96	78/300	26
rad18Δ	299/300	100	285/300	95	240/300	80
rad50-1	498/570	87	12/300	4	6/300	3
rad51-1	546/600	91	5/176	3	6/192	3
rad54-1	528/600	88	4/185	2	4/198	2

Table 1
Restriction enzyme-induced double-strand break/gap repair in different yeast strains transfected with modified YpJA18 plasmid

7. Cloning and molecular analysis of the *REV2 (RAD5)* gene

The *REV2* gene was cloned by complementation of a *rev2-1* point mutation The gene was sequenced and genomically disrupted yielding sensitivity to UV and ^{60}Co-γ -rays in the range found for various *rev2 point* mutants Independently, the gene was cloned and analyzed by R. Johnson et al., Molec. Cell Biol 12(9), 3807-18, 1992. The *REV2* transcript has a length of 3.4 kb corresponding to the ORF of 3419 bp. The putative Rev2 protein possesses 7 helicase domains, two zinc fingers and a leucin zipper. Recently results by Prakash et al. (J Biol Chem 269, pp 28259-28262, 1994) on the purified protein showed no helicase activities but a functional nucleotide binding site
In continuation of the detailed biological analysis regarding the *REV2* gene function in repair and mutagenesis (Siede and Eckardt-Schupp Mutagenesis 1(6), 471-474, 1986) the regulation of the gene in response to DNA damage and various growth conditions was of particular interest The experimental approaches turned out to be difficult. First, the gene shows a very low expression, in comparison with the *RAD10* transcript level we estimated at most 1 *REV2* mRNA molecule per cell Second, the *REV2* transcripts are masked by the 28S RNA in Northern blot analysis, and third, even highly purified mRNA did not reveal clear bands without extra smear. We established RT-PCR using agarose gel electrophoresis and ethidium bromide for the detection and quantification of the reverse transcribed *REV2* DNA fragment and obtained some indication for an increase in the *REV2* transcript levels in response to UV and heatshock. However, the method is not sufficiently sensitive, and therefore we establish a new method using polyacrylamide gels and the GATC system for detection (Heller et al. Electrophoresis 89, ed. Radula, B J , Munich)

8. Functional analysis: Role of the *REV2* gene in mutagenesis.

Known for more than 20 years, still not understood, but of considerable interest are the remarkable locus- and allele-dependent effects of rev2 mutations on mutagenesis, since the role of the Rev2 protein might relate to chromatin structure influencing repair and mutagenesis The *REV2* gene exhibits a minor role for mutation fixation at specific ochre alleles (i.e arg4-17, his5-2) in genes coding for proteins and a very pronounced role for mutation avoidance in t-RNA genes. Qualitatively similar results were reported for the *RAD6* and *RAD18* genes (Cassier-Chauvat, C. and Fabre, F., Mutation Res , 254, 247-258, 1991)

We use an experimental system which allows the distinction of intragenic revertants of ochre alleles and extragenic suppressors, e.g t-RNA mutants by colony colour (Siede et al , Mol Gen Genet, 190, 406-412, 1983). We have investigated the spontaneous and UV-induced reversion and suppressor frequencies of various ochre alleles, using interruption mutants *rev2Δ* in two different wild-type strains and (non-isogenic) *rev2-1* and *rev2ts* point mutants. The following results were obtained·

- The *REV2* gene product has no influence on the spontaneous reversion of the ochre alleles arg4-17, his5-2, lys2-1

- The UV-induced reversion of the *lys2-1* allele is independent of the *REV2* function, whereas the reversion of the allele *arg4-17* dependend on the Rev2 protein. In *rev2-1* and *rev2ts* mutants the effect on UV-induced reversion frequencies seems to be more pronounced than in rev2Δ mutants.

- The *REV2* gene product has a remarkable influence on reducing the spontaneous and UV-induced ochre suppressor frequencies of both *lys2-1* and *arg4-17* alleles in repair competent wild type yeast As compared to the wild type strains the spontaneous mutations of tRNA genes are 15 to 100 fold enhanced in *rev2* mutants dependent on both the ochre and the *rev2* alleles investigated (Fig. 4)

- In repair competent haploid yeast the UV-induced suppressor mutations are lower than the spontaneous values (app. 1×10^{-6}) and show no increase above approximately 5×10^{-7} up to 100 J/m^2 In contrast, in *rev2* mutants suppressor frequencies increase in a dose-dependent fashion to more than 10^{-4} at 60 J/m^2, dependent on the allele analyzed.

The pleiotropic phenotypes of *rev2* mutants on survival, efficiency and fidelity of DSB repair and mutagenesis may indicate the association of the Rev2 protein with several complexes composed of different sets of proteins differing in their biological function

The considerable differences in the mutability of ochre alleles at structural gene loci and tRNA genes in *rev2* as well as *rad6* and *rad18* deletion mutants might hint at a role of the proteins of these genes with different RNA polymerases (Pol II for mRNA and Pol III for tRNA transcription) and/or different chromatin structures at the structural as compared to tRNA gene loci.
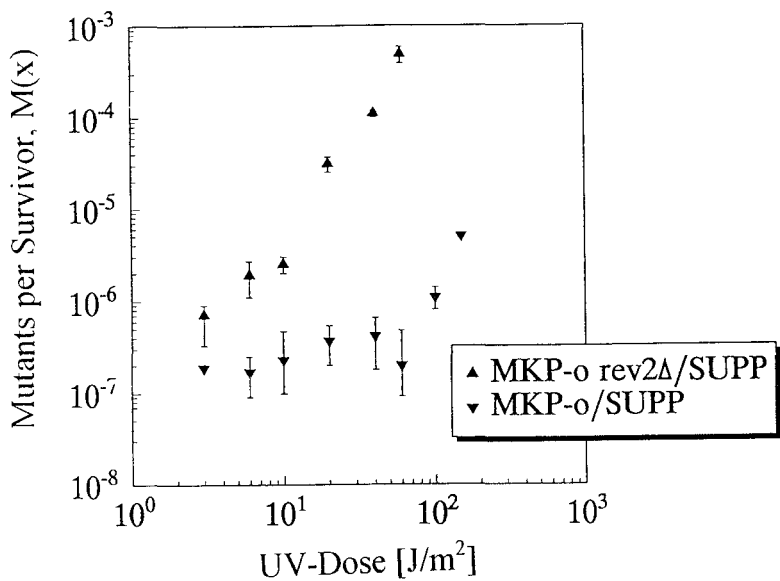
Fig. 4
The UV-induced frequencies of mutants per survivor, M(x), for extragenic suppressors of the lys2-1 ochre allele, are plotted against the UV dose. The spontanous frequencies (1.1 ± 0.6) x 10⁻⁶ and (1.5 ± 0.4) x 10⁻⁵ for the strain MKP-o (REV2) and, respectively, the strain MKP-o rev2Δ, have been substracted to yield the UV-induced frequencies.

List of publications relevant for the project

Ahne, F., Baur, M., Eckardt-Schupp, F. (1992) The *REV2* gene of *Saccharomyces cerevisiae*: cloning and DNA sequence Curr Genet 22, 277-282

Ahne, F, Jha, B., Biebel, A., Eckardt-Schupp, F. (1994) Vector-mediated analysis of DNA repair fidelity in *Saccharomyces cerevisiae*. In Molecular Mechanisms in Radiation Mutagenesis and Carcinogenesis, Chadwick, K.H., Cox, R, Leenhouts, H.P., Thacker, J (Eds) European Commission, Luxembourg, Report EUR 15294, pp 59-64

Eckardt-Schupp, F., Ahne F. (1993) Bridge-building between mathematical theory and molecular biology The *REV2* Gene as paradigm Mutation Res., 289, 39-46

Eckardt-Schupp, F, Ahne, F Friedl, A.A., Jha, B. (1995) Which role has the *REV2* gene product for DSB repair in yeast? J Biochem. Supplement 21A, p323

Friedl, A A., Beisker, W., Hahn, K., Eckardt-Schupp, F., Kellerer, A M. (1993) Application of pulsed-field gel electrophoresis to determine gamma ray-induced double-strand breaks in yeast chromosomal molecules Int J. Radiat. Biol. 63, 173-181

Friedl, A A. (1994) Entwicklung von Simulationsmethoden und deren Anwendung zur quantitativen und qualitativen Analyse von DNA-Doppelstrangbrüchen in niederen und höheren Eukaryonten, PhD Thesis, Ludwig-Maximilian Universitat, München

Friedl, A.A., Kraxenberger, A., Eckardt-Schupp, F. (1994) Approaches to the analysis of the possible influence of chromatin structure on gamma ray-induced DNA damage. In. Molecular Mechanisms in Radiation Mutagenesis and Carcinogenesis, Chadwick, K.H., Cox, R., Leenhouts, H.P., Thacker, J. (Eds.), European Commission, Luxembourg, Report EUR 15294, pp 67-72

Friedl, A A, Kraxenberger, A, Eckardt-Schupp, F (1995) Use of pulsed-field gel electrophoresis for studies of DNA double strand-break repair in the yeast *Saccharomyces cerevisiae*, in. Techniques for Studies of DNA Repair and Mutagenesis, E.C. Friedberg (Ed.), Methods: A Companion to Methods in Enzymology 7, 205-218 Academic Press, Inc. San Diego

Friedl, A.A., Kraxenberger, A., Eckardt-Schupp, F. An electrophoretic approach to the assessment of the spatial distribution of DNA double strand breaks. Electrophoresis, in press

Jha, B, Ahne, F., Eckardt-Schupp, F. (1993) The use of double marker shuttle vector to study DNA double-strand break repair in wild-type and radiation sensitive mutants of the yeast *Saccharomyces cerevisiae*. Curr Genet 23, 402-407

Kraxenberger, A., Friedl, A.A., Kellerer, A.M. (1994) Computer analysis of DNA profiles in pulsed-field gels for the assessment of double-strand breaks in yeast. Electrophoresis, 15, 128-136

Kraxenberger, A., Weber, K.J, Friedl, A.A., Eckardt-Schupp, F, Kellerer, A.M. Clustering of heavy ion induced DNA double-strand break in mammalian cells. Dependence of DSB-RBE on the method of DSB analysis (In preparation for Int.J.Radiat.Biol.)

Siede, W, Dianova, I., Friedberg, A.S., Friedl, A.A. Eckardt-Schupp, F, Friedberg, E.C (1995) Characterization of G1 checkpoint arrest in *S. cerevisiae* following treatment with DNA- damaging agents J Chem. Biochem Supplement 21A, p344

Siede, W., Friedl, A.A , Dianova, I , Eckardt-Schupp F., Friedberg, E.C.:The *Saccharomyces cerevisiae* Ku autoantigen homolog affects radiosensitivity only in the absence of homologous recombination (submitted to Genetics)

Wöhl, T , Baur, M., Friedl, A.A. Lottspeich (1992) Chromosomal localization of the Hyp2-gene in *Saccharomyces cerevisiae* and use of pulsed-field gel electrophoresis for detection of irregular recombination events in gene disruption experiments. Electrophoresis, 13˙651-653

Contract: FI3PCT930080   Duration: 1.7.93 to 30.6.95   Sector: B12

Title: Radiation induced mitotic aneuploidy.

1)   Parry   Univ. Wales Swansea
2)   Tanzarella   CNR
3)   Kirsch Volders   Univ. Bruxelles (VUB)

I. Summary of Project Global Objectives and Achievements

The objectives of the project were:

1)   To develop methodologies capable of characterising, identifying and quantifying aneuploidy induction in radiation exposed somatic cells, particularly in the low dose region. Such methods should be capable of characterising numerical chromosome changes in both interphase and metaphase progeny cells.

2)   Using the methods developed in 1) to determine the mechanisms by which ionising radiation induces numerical chromosome changes.

3)   To determine whether there are low dose thresholds for radiation induced aneuploidy and to compare aneuploidy dose response curves with those for radation induced structural chromosome changes.

The major achievements of the project were:

1)   Demonstration that ionising radiation of various LET values induces both chromosome loss and non-disjunction leading to aneuploidy in somatic cells.

2)   At low doses of ionising radiation induced non-disjunction appears to be the predominant mechanism leading to aneuploidy.

3)   Radiation induced aneuploidy results from radiation induced interactions with centromeric DNA and non-DNA targets, probably including components of the mitotic spindle.

In view of the role of chromosome aneuploidy during tumour progression it is of major importance that we determine the influence of low doses of ionising radiation upon numerical changes during progression.

Overview of Projects: Radiation Induced Mitotic Aneuploidy

Genome stability (i.e. chromosome number and structure) is dependant upon the coordinated functioning of the mitotic and meiotic cell division cycles. Critical events include chromosome replication and segregation which involve the functioning of a series of inter-related cell organelles and coordinated activities such as the synthesis and functioning of the proteins of the nuclear spindle and the attachment and movement of the chromosomes on the spindle apparatus. Modifications of the activity of the cell division apparatus and critical chromosome functions may lead to aberrations of chromosome segregation and the protection of cells with abnormal chromosome numbers, whether a multiple of the complete karyotype (polyploidy) or individual deviations from the normal number of individual chromosomes (aneuploidy).

During mitotic cell division aneuploidy may occur by a variety of malsegregation events, the most important of which are:-

a)   Chromosome loss, for example when a chromosome is dislocated from the mitotic splindle and expelled as a micronucleus. Such a process may lead to the formation of 2n and 2n-1 progeny cells. This event may be detected by the observation of micronuclei in interphase cells or by the presence of hypodiploid metaphase cells.

b)   Chromosome non-disjunction occurs when both copies of a chromosome segregate to the same pole of a dividing cell resulting in 2n+1 and 2n-1 progeny cells. Non-disjunction events may be detected by the observation of both hypodiploid and hyperdiploid metaphases and interphases in progeny cells.

The aim of the project was to develop an understanding of the effects of ionising radiations upon the fidelity of chromosome segregation. Numerical chromosome changes may lead to substantial changes in the behaviour of progeny cells and there is now extensive data to implicate aneuploidy in the etiology of tumour fomation in somatic cells and in birth defects such as Downs Syndrome (trisomy of chromosome 21) when they occur in germ cells.

During the progression of tumour cells to malignancy the homozygosity of mutant oncogenes and numerical chromosome changes has been a consistent observation. It is thus of considerable importance to determine whether low doses of ionising radiation induce numerical chromosome changes which may result in the homozygosity of active oncogenes.

Unlike the induction of point mutations and chromosome structural aberrations where the predominant target is the DNA, the potential targets for modification leading to aneuploidy are diverse. During mitosis, these theoretically include; the chromosomes themselves (particularly the centromeres and telomeres), the kinetochore proteins, microtubule synthesis and assembly, the formation of the division spindle, the synthesis and functioning of the polar bodies, the movement of the segregating chromosomes on the spindle and membrane modifications. A critical feature of the project has been to develop an understanding of whether ionising radiation interacts with cellular targets of importance to the induction of aneuploidy.

Currently, we have little information on the nature of the dose response curve for radiation induced somatic aneuploidy. This lack of understanding of the nature of the molecular events which result in radiation induced aneuploidy means that we cannot predict whether a threshold exists for the induction of numerical chromosome changes following radiation exposure. A number of studies upon radiation induced micronucleus formation in cultured cells indicate that they are induced by ionising radiation with dose response curves that show no evidence of a threshold (for example Brooks *et al* 1990). However, micronuclei may arise from both whole chromosomes (aneuploidy) or the presence of chromosome fragments. If micronuclei data are to be used to provide information on the dose response relationships of radiation induced aneuploidy it is necessary to distinguish between micronuclei containing whole chromosomes and chromosome fragments. Micronuclei arising from whole chromosomes and fragments may be distinguished on the basis of size, the presence of centromeric DNA and the presence of kinetochore proteins using appropriate molecular probes.

The objectives of the project were:-

1)   To develop methodologies capable of characterising, identifying and quantifying the aneuploidy induction in somatic cells following ionising radiation particularly in the low dose region. Methods are necessary to investigate numerical chromosome changes in both interphase and metaphase progeny cells.

2)   Using the methods developed in 1) to determing the mechanisms by which ionising radiation induces numerical chromosome changes.

3)   To determine whether there are dose thresholds for radiation induced anueploidy and to compare aneuploidy dose response curves with these for radiation induced chromosome structural aberrations.

The project was planned by the collaborators to cover a research period of 3 years. However, funding was provided for only 2 years and it was thus difficult for the collaborators to achieve all these aims. In spite of the time and funding limitations, the collaborators have achieved major progress in both method development and identifying the importance of non-disjunction as a mechanism for inducing aneuploidy following low doses of ionising radiation.

During the project the collaborating laboratories integrated their research in a manner which allowed the investigation of the induction of numerical chromosome changes using mouse/human cell hybrids, hamster and human fibroblasts and human lymphocytes. These cell types were utilized with a variety of protocol variations which included:

1)   Time of exposure in the cell cycle

2)   Sampling and fixation times

The endpoints developed and evaluated for the quantification of the induction of numerical changes included:

i)   Micronucleus induction, with evaluation of the nature of the chromosomal material using the antikinetochore Crest antibody and centromeric probes

ii)   Chromosome counts of the whole karyotype

iii) Counts of specific chromosomes using whole chromosome paints in metaphase cells and centromeric probes in interphase cells.

The results obtained demonstrated that micronuclei may be induced by ionising radiation at doses as low as 0.5Gy of both X-ray and proton irradiation. The micronuclei induced were predominantly kinetochore and centromere negative, indicating that they arose from chromosome structural aberrations. When micronuclei were classified into those arising from structural aberrations and those arising from whole chromosome loss it is clear that both types are induced by ionising radiation in a dose-dependent manner.

Analysis of radiation induced chromosome aneuploidy using whole or specific chromosome counts indicated that substantially higher frequencies of induction are observed than detected in the micronuclei assessments. Such data indicates that a major event involved in the generation of radiation induced aneuploidy is non-disjunction leading to both hypodiploidy and hyperdiploidy. Clearly, the adequate assessment of radiation induced aneuploidy requires the use of methodologies which are capable of quantifying the consequences of induced non-disjunction rather than the induction of chromosome loss alone. With the availability of *in situ* probes for the detection of both whole chromosomes and the centromeres of specific chromosomes the collaborators were able to directly evaluate radiation induced non-disjunction. These studies demonstrated that chromosome non-disjunction is the most important mechanism leading to aneuploidy following low doses (currently down to 0.125 Gy) of ionising radiation. The collaboration allowed the evaluation of radiation induced non-disjunction for 6 individual pairs of chromosomes 7 + 11, 2 + 8 and 1 + 17.

To investigate the role of cellular targets other than the chromosomal DNA in the etiology of aneuploidy the Swansea Laboratory compared the induction of chromosome structural and numerical aberrations in Chinese hamster cell lines with differing capacities to repair DNA damage. These studies demonstrated that following ionising radiation exposure there was a higher frequency of structural chromosome damage in repair defective cell cultures compared with repair proficient cell cultures. In contrast, there was little or no difference in the dose response for the induction of numerical chromosome changes in those cell lines of differing repair capabilities so far evaluated. Such data clearly indicate that at least a proportion of the induced aneuploidy measured in our studies is derived from ionising radiation damage to targets other than that to the chromosomal DNA. Such observations indicate that currently characterised DNA repair activities are not major factors for consideration in the risk-evaluation of radiation induced aneuploidy. It would be of considerable theoretical and practical interest to determine the factors which are of significance in influencing the frequencies of aneuploidy during tumour progression.

Although it is clear from our data that a significant proportion of radiation induced aneuploidy is derived from damage to non-DNA targets there is also evidence from the work of the Roma Laboratory that radiation interaction with the centromeric DNA is also of importance in producing numerical changes. Micronuclei containing kinetochore positive and

FISH negative signals appear to be unique to radiation induced cells suggesting a sensitivity of the centromeric regions of chromosomes to radiation induced disturbances which result in chromosome induced malsegregation. It is thus of importance to determine the relative contributions of chromosomal and non-chromosomal damage in the etiology of radiation induced aneuploidy.

By the end of the project period i.e. June 1995, it was not possible to adequately address the question of potential thresholds for radiation induced aneuploidy. The collaboration resulted in the development of suitable methodologies i.e. the analysis of chromosome segregation in binucleate cells, which would have been used to analyse the dose response relationship if time had been available.

In view of the role of chromosome aneuploidy during tumour progression, it is of major importance that we determine the influence of low dose ionising radiation upon numerical changes during progression.

Head of Project 1. Professor J M Parry

II   Objectives of the Swansea Laboratory 1.7.93 to 30.6.95

1)   To evaluate potential cultured cell test systems for their suitability for the study of radiation induced aneuploidy.

2)   To develop methods in an appropriate test system capable of detecting and quantifying radiation induced aneuploidy of specific chromosomes using fluorescence *in situ* hybridisation with whole chromosome paints in metaphase cells and centromere-specific probes in interphase cells.

3)   To estimate the capacity of ionising radiation to induce aneuploidy in cultured cells.

4)   To determine the relative contributions of chromosome loss and non-disjunction in the induction of aneuploidy by ionising radiations.

5)   To investigate the mechanisms of radiation induced aneuploidy and to determine the cellular targets critical to induction.

6)   To investigate potential thresholds of radiation induced aneuploidy.

III   Progress achieved

1)   Methods were successfully developed based upon fluoresence *in situ* hybridisation (FISH) to detect and quantify aneuploidy in metaphase and interphase cells.

2)   Ionising radiation was shown to induce chromosome loss and non-disjunction.

3)   Non-disjunction was shown to be the predominant mechanism leading to aneuploidy at low doses of ionising radiation.

4)   Studies in repair defective cells indicated that DNA repair makes little or no contribution to the levels of aneuploidy induced by ionising radiation indicating a major contribution of non-DNA targets.

5)   Little progress was made on potential thresholds during the limited time scale of the project.

Publications

Ellard, S., P. Wilcox and J. M Parry (1995). "Chromosome painting" *Mutagenesis* **10**. 62-63 (1995)

Bourner, R., T. Hermine, S. Ellard, E. M. Parry and J. M. Parry (1995). "The use of fluorescent *in situ* hybridisation technology in the detection of numerical and structural chromosomal aberrations in cultured human lymphocytes". *Mutagenesis* **10**. 63.

Ellard, S., M. Plumstead, S. Toper, G. Stamp, P. Wilcox, E. M. Parry and J. M. Parry (1995). "A comparison of conventional metaphase analysis of giemsa-stained chromosomes with multi-colour fluorescence *in situ* hybridization analysis using probes for chromosomes 1, 2 and 3 to detect chromosome aberrations" *Mutagenesis* **10**. 71-72.

Jones, C., S. Ellard, W. E. Evans and E. M. Parry (1995). "Micronucleus frequencies induced *in vitro* in human immunomagnetic separated lymphocyte subsets". *Mutagenesis* **10**. 73.

Parry, J. M., R. Fielder and A. McDonald (1994). "Thresholds for aneuploidy inducing chemicals". *Mutagenesis* **9**. 503-504.

Parry, E. M., L. Henderson and J. M. Mackay (1995). "Recommended procedures for the detection of induced aneuploidy". *Mutagenesis* **10**. 1-4.

Meeting Presentations

Bourner, R., T. Hermine, S. Ellard, E. M. Parry and J. M. Parry. "The use of fluorescent *in situ* hybridisation technology in the detection of numerical and structural chromosome aberrations in cultured human lymphocytes". *Genetical Society, Swansea, March 1994.*

Ellard, S. and E. M. Parry. "A comparison of immuno-fluorescent labelling of kinetochore proteins and FISH using centromeric and telomeric DNA probes for micronucleus analysis". *Genetical Society, Swansea, March 1994.*

Project 1a

Radiation induced aneuploidy in human lymphocytes

III.   **Main Results Obtained**
(Methodology, Results, Discussion)

The initial studies of the Swansea Laboratory involved the use of the mouse/human cell hybrid R3-5 which carries a single copy of human chromosome 2. The single human chromosome in R3-5 was hybridised with a biotin labelled Oncor total human DNA probe. The probe was revealed with avidin-FITC followed with biotinylated anti-avidine and avidin-FITC. The cells were scored for the number of human chromosomes present following low dose of X-rays. Radiation induced mitotic aneuploidy was scored for the presence of 0 (loss), 1 and 2 (gain) human chromosomes.

These initial studies indicated that up to 10% of untreated cells contained modifications of chromosome number. Such a high frequency of spontaneous aneuploidy was considered to be inappropriate for the study of radiation induced aneuploidy in the low dose region. Based upon these initial studies primary human cells were used for further analysis and to evaluate the suitability of a number of probes for various human chromosomes and to develop protocals for the quantification of both chromosome loss and gain.

Methods

Heparinised whole blood samples from healthy female donors were irradiated with X-rays at a dose rate of 1.47 Gy/minute. Cultures were grown at 37° under a 5% CO_2 atmosphere in RMP1 1640 medium supplemented with 20% foetal calf serum and 1.4% phytohaemagglutinin. Cultures were grown for 2 hr. Cells were harvested and given a brief (10 min) hypotonic treatment (0.075 M KCl) and fixed three times in 4:1 methanol: acetic acid. Fixed cells were dropped on to clean, polished slides, allowed to dry and stored at -20°C.

Slides were immersed in acetone (10-20 min), air-dried, treated with RNase (100μg/ml in 2 x SSC, pH 7.0) for 1 h at 37°C, washed three times in 2 x SSC, treated with proteinase < [0.5 μg/ml in 2mM $CaCl_2$, 20mM Tris-HCl, pH 7.4), rinsed twice in 2 x SSC and dehydrated through an ethanol series.

FISH was carried out using chromosome-specific "paint" probes obtained from Cambio and for the purpose of the project we selected probes for chromosomes 2 and 8 being suitable for further studies. FITC-labelled chromosome 2 specific paint and biotin labelled chromosome 8 paints were employed. The probes required immunological detection and were revealed with (a) goat anti-FITC and rabbit anti-goat FITC and (b) avidin-Texas Red followed by biotinylated anti-avidin and avidin-Texas Red respectively. All slides were counterstained with DAP1. Slides were mounted in Vectashield anti-fade and visualised using an Olympus fluorescence microscope equipped with a triple-band pass filter to allow the simultaneous observation of both labelled chromosomes and counterstain. The images of the FISH stained chromosomes were captured on a Perceptive Instruments Imge Analysis Station. The frequencies of chromosome 2 and 8 and exchanges involving both chromosomes were determined.

Results

An example of the data obtained from exposing human lymphocytes to X-ray doses of 0 and 5.88 Gy are illustrated in Table 1. The data for chromosomes 2 and 8 demonstrates an increase in hyperdiploidy at doses of 1.47 Gy and above. The data also demonstrated that the further analysis of X-ray induced hyperdiploidy should involve doses in the region of 0 to 1.5 Gy. In contrast to the dose-dependent increase in hyperploidy the frequencies of hypodiploidy were variable and not dose-dependent indicating that the predominant aneugenic event induced by X-rays was non-disjunction rather than chromosome loss.

To compare the relative induction of chromosome structural with numerical aberrations we have also evaluated the frequencies of exchanges involving chromosome 2 and 8 detectable in the cells evaluated for hypodiploidy and hyperdiploidy. The data obtained from these analyses demonstrate significant increases the frequencies of exchanges observed following X-ray exposure (Table 2).

Our data demonstrated that X-ray doses of 0.5 Gy induced hyperdiploidy and chromosome exchanges. The predominant mechanism of induced aneuploidy appears to radiation induced non-disjunction. To further evaluate the role of non-disjunction in radiation induced aneuploidy we investigated the distribution of centromere-specific signals in binucleate human lymphocytes sampled 24 hours after the addition of the actin inhibitor cytochalasin B. Centromere-specific signals for chromosomes 2 and 8 were detected using probes supplied by Oncor.

Table 3 illustrates an example of the data obtained when human lymphocytes were irradiated with X-ray doses of 0 to 2 GY. The data demonstrate a significant increase in non-disjunction of chromosomes 2 and 8 at doses above 0.5 GY. These data using interphase cells confirm the results of the metaphase studies that ionising radiation is capable of inducing non-disjunction leading to aneuploid progeny cells.
Although it is clear from our data that a significant proportion of radiation induced aneuploidy is derived from damage to non-DNA targets there is also evidence from the work of the Roma Laboratory that radiation interaction with the centromeric DNA is also of importance in producing numerical changes. Micronuclei containing kinetochore positive and FISH negative signals appear to be unique to radiation induced cells suggesting a sensitivity of the centromeric regions of chromosomes to radiation induced disturbances which result in chromosome induced malsegregation. It is thus of importance to determine the relative contributions of chromosomal and non-chromosomal damage in the etiology of radiation induced aneuploidy.

By the end of the project period i.e. June 1995, it was not possible to adequately address the question of potential thresholds for radiation induced aneuploidy. The collaboration resulted in the development of suitable methodologies i.e. the analysis of chromosome segregation in binucleate cells, which would have been used to analyse the dose response relationship if time had been available.

Table 1

The induction of radiation induced hypodiploidy and hyperdiploidy of chromosomes 2 and 8 in human lymphocytes.

X-ray dose Gy	cells scored	Chromosome 2		Chromosome 8		Total loss	Total gain	% loss	% gain
		loss	gain	loss	gain				
0	350	11	0	14	0	25	0	7.1	0
0.74	200	5	0	8	0	13	0	6.5	0
1.47	200	14	2	14	3	28	5	14.0	2.5
2.94	200	9	2	6	3	15	5	7.5	2.5
5.88	128	4	3	4	3	8	6	6.3	4.7

Table 2

**The induction of radiation induced exchanges involving
Chromosomes 2 and 8 in human lymphocytes**

X-ray dose Gy	Cells Scored	Chromosome 2	Chromosome 8	Total	%
0	350	2	1	3	0.85
0.74	200	0	0	0	0
1.47	200	3	10	13	6.5
2.94	200	22	24	46	23
5.88	121	55	50	105	86.8

Project 1.b

Role of DNA repair activity upon the induction of numerical and chromosome aberrations by ionising radiations

Following our observation that ionising radiation induced aneuploidy at low doses of exposure we undertook a study of the role of DNA repair activity into the induction of numerical and structural aberrations. The role of repair was assessed by the use of the Chinese hamster cell lines V79 and its repair deficient mutant *irs*1 (Jones *et al* 1987).

Induced structural and numerical chromosome aberrations were assessed by the use of the binucleate cell micronucleus assay. This involved the use of cytochalasin-B to inhibit the formation of actin and thus allow the completion of nuclear division without the completion of cytokinesis. Micronuclei present in binucleate cells were classified as to their origin i.e. whether they contained whole chromosomes or chromosome fragments as detected by the immunostaining for the presence of kinetochore protein.

Method

Monolayer cultures of repair proficient parental cell line V79.4 and the repair mutant *irs*1 were initiated with 2.8 x 10^5 cells in petri dishes for 24 hours. The cells were then irradiated at a dose rate of 1.6/min and incubated with cytochalasin B (3μg/ml) for 16 hours (V79.4) or 20 hours (*irs*1). The different incubation times were based upon the respective cell cycle times for the two cell cultures. Cells were harvested and aliquots centrifuged onto slides. Slides were briefly air dried and fixed in 90% methanol for 10-20 min.

Slides were immuno-labelled according to the protocol described by Ellard *et al.*, 1991. Briefly, slides were incubated with a commercial antikinetochore antibody (Antibodies Incorporated, Davies, USA) diluted 1:1 with PBS for 45 min. Slides were then washed and treated with a secondary anti-human IgG antibody (FITC conjugated) diluted 1:100 with PBS. Slides were stained with primulin and mounted in 1:200 DAPI:antifade solution.

Kinetochore labelled slides were analysed using an Olympus BH2 microscope fitted with RFL fluorescence equipment. 1000 or more binucleated cells were scored for micronuclei and a minimum of 100 of them examined for kinetochore positive signals. The ratio of binucleate to total cell number was ascertained to give an indication of the nuclear division index.

Results

The V79 cell line used in our experiments had a control frequency of micronuclei of approximately 15 micronuclei per 1000 binucleate cells of which approximately 30% were kinetochore positive and 70% were kinetochore negative. All of the radiation sensitive Chinese hamster cell lines we initially examined had higher levels of micronuclei in untreated cultures; up to 90 per thousand in *irs*1. However, the relative proportions of kinetochore positive to negative micronuclei was approximately 30:70 respectively in all the cultures.

Figure 1 demonstrates the induction of kinetochore negative micronuclei by ionising radiation of up to 2Gy in both the repair proficient V79 cell line and the repair deficient cell

line. In V79 the slope of the induction curve was 40.1 micronuclei per 1000 binucleate cells per Gy whereas in *irs*1 the slope of the induction curve was 96.6 micronuclei per 1000 binucleate cells per Gy. Clearly there was a substantially greater induction of kinetochore negative micronuclei presumably produced by chromosome fragments in the radiation sensitive repair deficient cell line.

Figure 2 demonstrates the induction of kinetochore positive micronuclei by ionising radiation in the two cell lines. As can be seen from Figure 2 the slopes of induction of kinetochore positive micronuclei were virtually identical i.e. V79 6.75 micronuclei per 1000 binucleate cells per Gy and *irs*1 6.0 micronuclei per 1000 binucleate cells per Gy. These data indicate that there was no difference in the slope of induction of kinetochore positive micronuclei produced by whole chromosome loss in either the wild type or the repair deficient cell line.

Discussion

The *irs*1 mutant had a background frequency of kinetochore positive micronuclei approximately 3-fold higher than the wild type V79 which was virtually identical to its radiation sensitivity (Jones *et al* 1987). The increased sensitivity of *irs*1 is clearly reflected in the elevated induction of chromosome structural damage by radiation exposure as reflected by the increased sensitivity of induction of kinetochore negative micronuclei. We suggest that in this DNA repair defective cell line (described in detail in Jones *et al* 1990) an increased proportion of radiation induced DNA lesions result in chromosome damage compared to the wild type V79 cell line.

The induction of whole chromosome aneuploidy as reflected by kinetochore positive micronuclei is in marked contrast to the induction of structural aberrations. The kinetics of induction of whole chromosome loss was identical in the two cell lines irrespective of their DNA repair status. The observations presented here indicate that DNA repair activity has little or no influence upon the induction of aneuploidy by ionising radiations. Such observations suggest that the cellular targets for ionising radiation induced aneuploidy are <u>not</u> the DNA of the chromosomes. The specific targets involved remain to be elucidated. However, our previous studies of the effects of ionising radiation upon dividing cells suggest that the spindle apparatus is probably the most important cellular target (Parry *et al* 1985).

References

Ellard *et al* (1991). *Mutagenesis* **6**, N6, 461-470.

Jones *et al* (1987). *Mutation Res*. **183**, 279-286.

Jones *et al* (1990). *Mutagenesis* **5**, 15-23.

Parry *et al* (1985). *Mutation Res*. **150**, 369-381.

FIGURE 1

**RADIATION INDUCED CREST NEGATIVE MICRONUCLEI
IN BINUCLEATED CHINESE HAMSTER CELLS
WILD TYPE V79-4 AND ITS IRS1 MUTANT**
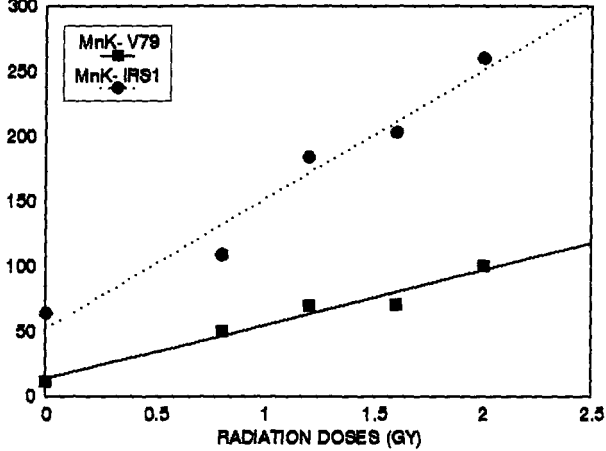
SLOPES:

V79.4 = 41.7 K- Mn /1000 cells/ Gray

IRS1 = 96.8 K-Mn /1000 cells/ Gray

FIGURE 2

**RADIATION INDUCED KINETOCHORE + MICRONUCLEI
IN BINUCLEATED CHINESE HAMSTER CELLS
WILD TYPE V79-4 AND ITS IRS1 MUTANT**
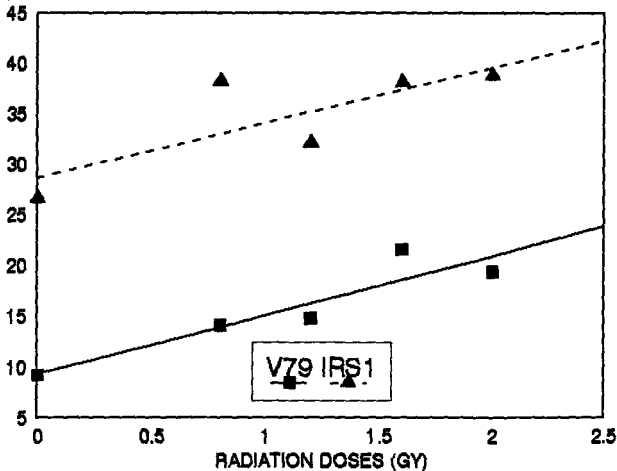
SLOPES:

V79.4 = 5.8 K+ Mn /1000 cells/ Gray

IRS1 = 5.4 K+ Mn /1000 cells/ Gray

Head of Project 2: Prof. C. Tanzarella

II.   Objectives

To study the effect of ionizing radiation on the induction of chromosomal malsegretation, human primary fibroblasts (MRC-5) and Chinese hamster cells (C1-1) were irradiated with low LET X-rays and high LET, low energy protons.

Three objectives were investigated:

A)   Induction of chromosome loss and non-disjunction.
B)   Persistence of micronuclei at several fixation times after irradiation.
C)   Mechanism(s) responsible for chromosome loss induction in human fibroblasts.

III.   Progress achieved including publications

MATERIALS AND METHODS

The Chinese hamster cell line (C1-1) was routinely maintained in Ham's F-10 medium supplemented with 10% fetal serum, antibiotics and L-glutamine in a 5% CO_2 atmosphere at 37° C. Cells were irradiated with low LET X-rays (Gilardoni apparatus, 250 kV, 6 mA, 70 cGY/min.) or high LET low energy protons.

For X-rays two types of protocols were adopted:

-    In a dose-range finding experiment, cells were grown for 24h on coverslips in 35 mm Petri dishes and subsequently irradiated with 12.5, 25, 50, 100 cGy of X-rays.   Cytochalasis-B (3ug/ml) was added immediately after X-ray irradiation, and kept for a further 20 hrs. before fixation.   Cells were stained with antikinetocore antibody (Antibody Inc., CA).

-    To study the persistence of cytogenetic damage, cytochalasin-B was added immediately (I FIX) or, in turn, 20 hrs. (II FIX) and 40 hrs. (III FIX) after X-ray-irradiation. The cultures were kept in the presence of cytochalasin-B for 20 hrs., then fixed and stained with antikinetochore antibody.

For protons, only one type of protocol was carried out:

-   About 18 hrs. before irradiation 4×10^6 cells were plated in each stainless-steel Petri dish and grown at 37°C as monolayer attached to a maylar foild (52 um thick; 133 mm area) at the dish. Two or three dishes were irradiated for each dose point. Irradiation was carried out at the radiobiological facility of the 7 MV Van de Fraaff CN accelerator at the Laboratori Nazionali di Legnaro of the Instituto Nazionale di Fiscia Nucleare (INFN), using 31 KeV monoenergetic proton beams in air. Cells were irradiated with 12.5, 25, 50 75, 100 and 150 cGy. Immediately after irradiation cells were detached by trypsin treatment and seeded in chamber slides, then cytochalasin-B (3ug/ml) was added and kept for further 20 hrs. before fixation. Cells were stained with antikinetocore antibody.

MN and CREST positive MN were scored in 500 BN cells for each experimental point/experiment.

Human primary fibroblasts (MRC-5) were cultured in MEM medium, 10% fetal serum, antibiotics and L-glutamine in a 5% atmosphere at 37° C. Fibroblasts were irradiated with 12.5, 25, 50, 100 cGy of X-rays for induction of chromosomal loss and non-disjunction.

Three types of protocols were carried out:

-   To study chromosome loss, Cytochalasin-B was added immediately after treatment and cells were fixed 24 hrs. later for FISH staining with centromeric DNA cocktail probe. FISH positive micronuclei were scored in 500 BN cells.

-   Non-disjunction was scored in the daughter nuclei of binucleated cells with FISH staining with alphoid-specific probes for chromosomes 7 and 11 (ONCOR).

-   Aiming at evaluating the possible mechanism responsible for chromosome loss, MRC-5 were exposed to 12.5, 25 and 50 cGy X-rays and incubated in the presence of Cytochalasin-B for 24 hours, then fixed and stained with CREST antibody. MN were recorded for the presence/absence of CREST signal. Slides were fixed again and stained according to FISH technique with centromeric DNA cocktail probe; the same MN analyzed for CREST signal were scored with FISH staining.

RESULTS

A) Induction of chromosome loss and non-disjunction:
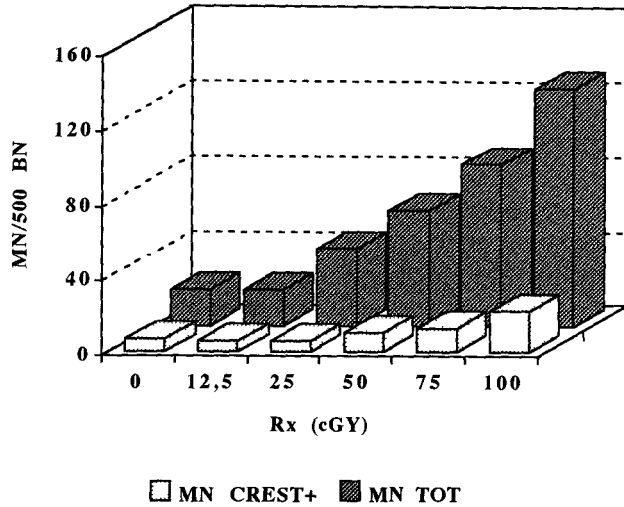
FIG.1. shows that X-rays induced MN in a dose-related manner in Cl-1 cells. The frequency of CREST positive MN scored in BN cells 20 hrs after treatment was at least 15% of total induced MN by all X-rays doses except 12.5 cGy.(Results from 3 experiments.)
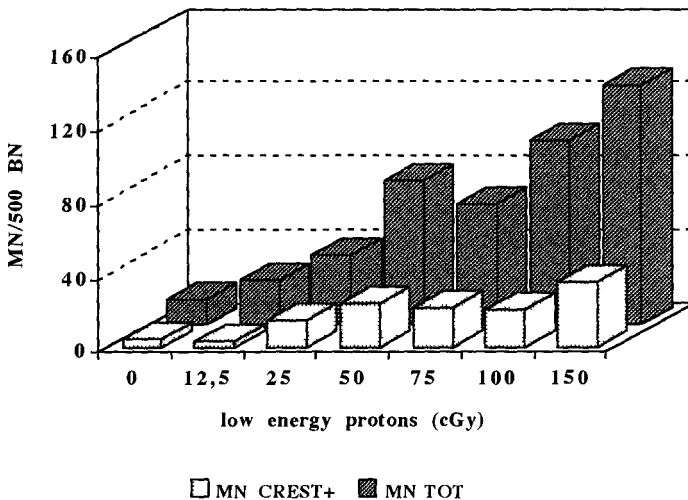
FIG.2. Frequency of MN and CREST positive MN scored in Cl-1 BN cells 20 hrs after   irradiation with protons.(Results from 1 experiments.)

FIG.3

MN/500 BN

160
120
80
40
0

0   12,5   25   50   75   100

Rx (cGy)

☐ MN FISH+   ▓ MN TOT
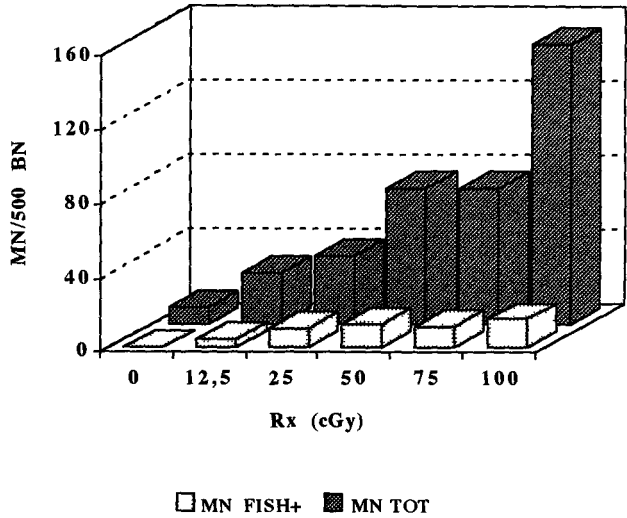
TAB.1

Chromosome loss   G1 irradiation

Dose (Gy)	nCB	%o MNCB	MN scored	%C+
0.000	3733	16.6	62.0	31.7
0.125	2500	34.8	107.0	20.0
0.250	2000	59.0	121.0	25.4
0.500	2500	93.0	222.0	17.6
1.000	1500	148.0	222.0	11.9

FIG.3 and TAB.1 A frequency ranging from 12% to 20% of MN containing centromeric regions were detected in X-irradiated <u>human fibroblasts</u> when stained with centromeric DNA cocktail probes and alphoid-specific probes. (Results from 3 experiments.)

TAB.2

Chromosome non-disjunction

Dose (Gy)	nCB	Cromosoma 7			Cromosoma 11			7+11
		(2+2) CB	(1+3) CB	%ND CB	(2+2) CB	(1+3) CB	%ND CB	%ND CB
0.00	1500	1495	5	0.33	1489	11	0 73	1.06
0.125	1000	993	7	0.7	989	11	1.1	1.8
0.25	1500	1493	7	0.46	1481	19	1.26	1.72
0.50	1500	1489	11	0.73	1474	26	1.73	2.46

TAB.2 gives the number of MRC-5 binucleates analysed and the frequencies of uneven distribution of the four signals between the two daughter nuclei (%NDCB) after FISH labelling with two chromosome specific centromeric probes.Chromosome 11 was more involved than chromosome 7 in both spontaneously and radiation-induced non-disjunction.After irradiation with 0.5 Gy a statistically significant (p=0.0125) increase in the frequency of non-disjunction was seen.
(Results from 3 experiments.)

B) Persistence of micronuclei at several fixation times from the low doses of irradiation.
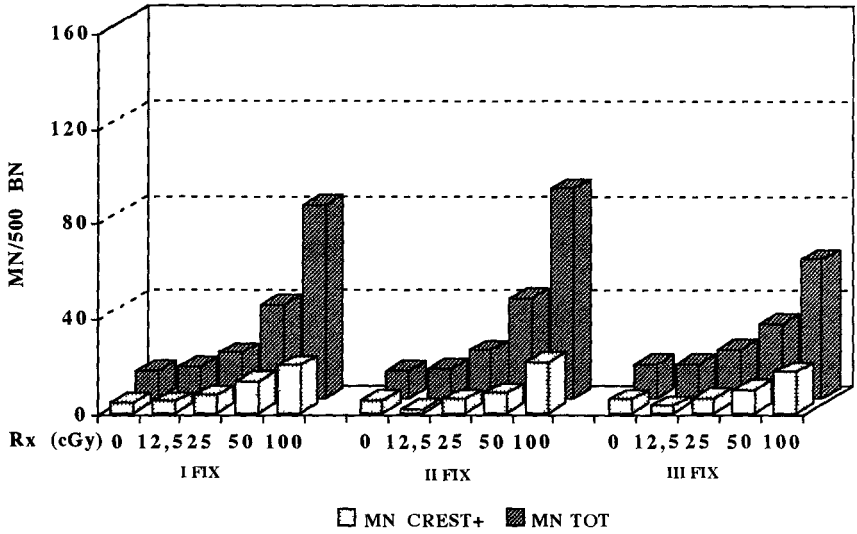
FIG.4 shows the frequency of MN and CREST positive MN in <u>Cl-1</u> BN cells irradiated at different dose of X-rays and harvested at different times after irradiation (20 hrs.40 hrs, 60 hrs.).The frequency of MN, both CREST positive and negative, was higher at the first and second fixation time (20 and 40 hrs) in comparison to the third (60 hrs), for doses of 25, 50 and 100 cGy.(Results from 5 experiments.)

C) Mechanism(s) responsible for chromosome loss in human fibroblasts.

Raggi-X	MN analizzati	MN CREST- FISH-	MN CREST+ FISH-	MN CREST- FISH+	MN CREST+ FISH+
0 cGy	39	23 (58)	-	3 (7.7)	13 (33)
12.5 cGy	59	42 (77)	4 (6.7)	2 (3.3)	11 (18.6)
25 cGy	81	57 (70)	6 (7.4)	3 (3.7)	18 (22 2)
50 cGy	83	71 (85)	7 (8 4)	1 (1 2)	4 (4.8)

TAB.3 Comparison between CREST and FISH staining performed on the same induced MN in <u>MRC-5</u> cells 24 hrs after X-irradiation.
As expected,ionizing radiation induced mainly MN negative detected following CREST and FISH staining. Interestingly, a percentage between 6.7 and 8.5% of induced MN appeared positive for CREST and negative for FISH staining (number in brackets represents percentages)

DISCUSSION

In our experiments, both low LET X-rays and high LET low energy protons, were able to induce MN CREST + and FISH+ in hamster cells as well as in primary human fibroblasts. Although the majority of induced MN results negative according to the well known clastogenic activity of ionizing radiation, values of about 15% and 30% of MN resulted CREST-positive for X-rays and protons respectively.
Molecular cytogenetic techniques have been very recently used to study not only chromosome loss but also the fate of specific chromosomes at cell division in mammalian cells.
It has been reported that non-disjunction may arise at doses of chemical compounds not able to induce significant number of micronuclei. However, up to now no data are available on this issue in mammalian cells exposed to radiations.
With the aim of studying the effect of low doses (from 12.5 to 100 cGy) of X-rays , centromeric probes for chromosome 7 and 11 were used to evaluate the distribution of these chromosomes in the main nuclei of irradiated binucleated cells.
Our data indicate that non-disjunction occured at higher extent compared to chromosome loss for both chromosomes probed. This may suggest that

chromosomal non-disjunction is the main mechanism leading to spontaneous and low dose radiation-induced aneuploidy and strengthenes the usefulness of study nondisjunction in combination with chromosome loss.

To study the kinetics of persistence/delayed expression of CREST-positive MN, hamster cells were irradiated and harvested at several cell division after irradiation. The frequency of this class of micronuclei was higher in treated compared to untreated cells, irrespective of the fixation time. However, it should be noted that at the later fixation time (about three cells division) the frequency of CREST-positive MN was lower than that observed at the second fixation time.This may indicate that cells mantain a condition prone to either persistence of induced CREST-positive MN or formation of new chromosomal or cellular damage leading to CREST-positive MN.

We cannot rule out the possibility that chromosomal non-disjunction which arise at higher extent than chromosomal loss, may determine a cellular condition leading to delayed instability several cellular division after irradiation.

Mechanism(s) responsible for radiation induced malsegregation are not understood. Our preliminary results in human fibroblasts indicated that radiation

induced a class of MN detected as CREST-positive, FISH-negative wich may be possibly explained by damage clusterized to centromeric regions which prevents the hybridization with the centromeric probe or by centromeric protein displacement.

However, the role played by assembly, structural integrity and functionality of kinetochores in radiation-induced chromosomal malsegregation need to be further investigated. In conclusion , our results showing induction of MN positive for both CREST and FISH staining, seem to exclude DNA damage as a major target in the X-ray-induced aneuploidy.

Publications

-Sgura, A., Antoccia, A.,De Dominicis, A.,Degrassi, F. and Tanzarella, C..
Radiation induced mitotic aneuploidy in rodent and human cultured cells.
VII Convegno Nazionale Societa' Italiana per le Ricerche sulle Radiazioni,
24-26 novembre 1994. p. E 14.
-Sgura,A., Antoccia, A.,Degrassi, F. and Tanzarella, C..
Radiation induced chromosomal loss and non-disjuction in human cultured fibroblast.
Atti Convegno Congiunto p. 92, 2-6 Ottobre 1995, Montesilvano Lido (PE).
-M.Kirsch-Volders, I.Tallon, C. Tanzarella, A. Sgura and J. Parry.
Chromosome non-disjunction as a major mechanism for in vitro aneuploidy induction by X-rays in primary human cells. Mutagenesis (in press).

Head of Project 3: Dr. Kirsch-Volders

II.   Objectives

This two year project aimed at the development of sensitive methods to analyse the importance of radiation (X-rays) induced aneuploidy (versus chromosome breakage) in vitro in human lymphocytes.

Different methodologies were first compared and applied:

-       Cytochalasin-B blocked micronucleus assay with fluorescence in situ hybridisation (FISH) using a pan-centromeric probe.

-       FISH using chromosome-specific centromeric probes for chromosomes 1 and 17 in cytochalasin-B blocked binucleated cells.

-       Chromosome counting performed on second metaphase cells.

A series of questions were addressed:

-       Is aneuploidy induction cell cycle dependent?

-       Is chromosome loss more or less frequent than chromosome non-disjunction?

-       Does a threshold exist for radiation induced chromosome loss/non-disjunction?

III.   Progress achieved including publications

1)   Modification and development of (cyto-) genetic methods for the detection of chromosome loss and chromosome non-disjunction

Irradiated cells will be delayed in their progression through the cell cycle. The extent of the delay depends on the stage of exposure; cells near mitosis are more delayed than those earlier in the cell cycle. To overcome this difficulty different fixation times (74 and 78 hours) were compared for cells irradiated during G_1 and G_2 phase, being respectively 20 and 42 hours after starting cultivation (Buckton and Evans, 1973; Watt and Stephen, 1986).

The first method used to evaluate radiation induced aneuploidy was the micronucleus assay using FISH but although earlier studies (Eastmond et al., 1993) have shown the sensitivity of this method for the detection of aneugens, for certain agents like ionising irradiation the technique does not seem satisfactory.

Firstly, clastogenic mutagens may break the double stranded DNA molecule at the centromeric region leading to "false" centromer-positive micronuclei. The development of a tandem labelling method provides us with a more sensitive technique for the discrimination between aneuploidy and chromosome breakage. Validation of the method is in progression. Mitomycin C, carbendazim and methylmethanesulfonate were tested.

Secondly, non-disjunction will not be detected by the micronucleus assay since only aneugenic events leading to chromosome lagging will give rise to micronuclei. To score non-disjunction in the subsequent interphase following the exposure a FISH methodology using chromosome-specific centromeric probes was developed in cytochalasin-B blocked binucleated lymphocytes.

Materials and methods

Cell cultures and irradiation protocol

Human venous blood was collected from two healthy donors in heparin containing vacutainers (Becton Dickinson). Lymphocyte cultures containing 0.4 ml whole blood and 4.9 ml Ham's F-10 medium supplemented with 15% Foetal Calf Serum (Gibco) and 2% phytohemagglutine (PHA 16, Wellcome Diagnostic, U.K.) were incubated at 37°C for 74 or 78 hours. For the preparation of metaphase chromosomes RMPA medium (Gibco) containing 1% bromodeoxyuridine (Serva) was used instead of Ham F-10 medium in order to score chromosomes in their second division.

The cells were exposed to 0.5, 1 and 2 Gy kVp X-rays (15 mA, 0.1 mm Cu filter) at a dose rate of 1 Gy/min at the G_1 and the G_2 stages of the cell cycle, here respectively 20 and 42 hours after starting cultivation (Buckton and Evans, 1973; Watt and Stephen, 1986).

Cytochalasin-B blocked micronucleus assay

After 44 hour incubation at 37°C, cytochalasin-B was added at a final concentration of 6 μg/ml (Van Hummelen and Kirsch-Volders, 1990). The cells were harvested at different sampling times (74 and 78 hours). Cells were subjected to a cold hypotonic

treatment (0.075 M KCl), immediately centrifuged and fixed three times with fixative (methanol:acetic, 3:1). The fixed cells were dropped onto slides using Pasteur pipettes, air dried and stored at -20°C.

Metaphase preparation

Colcemid (Gibco) was added to the cultures 1 hour prior to fixation. Cells were given a hypotonic treatment with 0.075 M KCl and fixed three times in 3:1 methanol: acetic acid. The slides were stained with Hoechst 33258 (Sigma) and 5% Giemsa (Merck) in Sörenson buffer.

Fluorescence in situ hybridisation (FISH) using a pan-centromeric probe

The 30 Nucleotide oligomer, shown to hybridise to the conserved region of the alpha satellite DNA present at centromeres of all human chromosomes (Meyne et al., 1989) was used. This 30 oligonucleotide (SO-aAllCen: Synthetic oligomer-a All Centromeres) was synthesised with Gene Assempbpler Plus® (Pharmacia). The probe was 3'end-labelled by terminal deoxynucleotidyl transferase (Gibco) with biotin-16-dUTP (Boehringer-Mannheim). The cells were pretreated with pepsin (Sigma) (0.005% in 10 mM HCl). Cells and probe were denatured simultaneously on a hot plate at 80°C for 3-4 min. Following overnight hybridisation immunofluorescence detection of the probe was performed by means of avidin-FITC (Vector Laboratories, Burlingane, CA, USA) and biotinylated goat anti-avidin (Vector Laboratories, Burlingane, CA, USA). After dehydration in ethanol series, the slides were counterstained with propidium iodide (5 μg/ml) and p-phenylenediamine antifade solution.

FISH with chromosome-specific centromeric probes for chromosome 1 and 17

Probes for centromeric regions of chromosomes 1 and 17 were used. The probes were labelled by nick translation according to the instructions of the suppliers (Life Technologies, BRL). FISH was performed as described by Pinkel et al. (1986) with some modifications. Slide were treated with RNase (0.1 mg/ml in 2xSSC) and pepsin (0.005% in 10 mM HCl). The slides were denatured in 70% formamide/2xSSC for 2 min. and dehydrated with ethanol (50%, 75% and 100%). The probes were denatured at 90°C and placed on each slide. Following an overnight hybridisation at 37°C in a moist chamber, the slides were washed with 60% formamide in 2xSSC at 45°C. Detection of the biotinylated-labelled probe as performed by means of avidin-FITC and biotinylated anti-avidin antibodies, the digoxigenin-labelled probe was detected using a mouse anti-digoxigenin antibody (Boehringer Mannheim) followed by a TRITC-conjugated goat anti-mouse antibody (Sigma). The cells were counterstained with 4',6-diamido-2-phenylindole (DAPI) (Boehringer Mannheim) in an antifade solution.

Tandem labelling with chromosome specific DNA probes

Probes for two different regions of chromosome 1 were used: for the pericentromeric region a classical satellite probe (pUC1.77), for the centromeric region an alpha satellite probe (pSD21-1 or pE25b). The probes were labelled by nick translation according to the instructions of the suppliers (Life Technologies, BRL). The pSD21-1 was digoxigenin purchased labelled from Oncor. FISH was performed as described by Pinkel et al. (1986) with some modifications. Slides were treated with RNase (0.1 mg/ml in 2xSSC) and pepsin (0.005% in 10 mM HCl). The slides were denatured in 70% formamide/2xSSC for 2 min. and dehydrated with ethanol (50%, 75% and 100%). The probes were denatured at 90°C and placed on each slide. Following an overnight hybridisation at 37°C in a moist chamber, the slides were washed for 3 min. in three changes of 2xSSC and either 50%, 55%, 60% or 66% formamide at 43°C. Then the slides were rinsed twice in 2xSSC at 43°C and once in 4xSSC/0.5% Tween 20 at room temperature. Detection of the biotinylated-labelled probe was performed by means of avidin-FITC and biotinylated anti-avidin antibodies, the digoxigenin-labelled probe was detected using a mouse anti-digoxigenin antibody (Boehringer Mannheim) followed by a TRITC-conjugated goat anti-mouse antibody (Sigma). The cells were counterstained with 4',6-diamido-2-phenylindole (DAPI) (Boehringer Mannheim) in an antifade solution.

Criteria for scoring

Micronuclei were identified according to the criteria of Heddle (1973) with some modifications. They were scored in binucleated cells, having less than a third of the diameter of either macronucleus and sufficiently separated from them. Per culture 1000 binucleated lymphocytes (CB) were analysed for the presence of one, two or more micronuclei (MN).

For the analysis of the fluorescence in situ hybridisation, the preparations were examined with a Leitz Dialux 20 fluorescence microscope equipped with a filter (Leitz I3, excitation at 450-490 nm, emission at 520 nm) to visualise the fluorescein-labelled probe and the orange-red propidium iodide-stained nuclei. The specificity of the probes was evaluated using metaphase cells. The micronuclei in binucleated lymphocytes (CB) were examined for the presence of one or more spots for the centromeric oligonucleotide probe and are classified as centromere-positive (C$^+$MN) or centromere-negative (C-MN). For the chromosome specific probes macronuclei were examined for the number of spots for each probe.

Metaphases in second division were scored for numerical chromosome aberrations and classified in three groups: (1) diploid when containing 46 chromosomes, (2) hypoploid when containing either 44 or 45 and (3) hyperploid when containing either 47 or 48 chromosomes.

2) Cell cycle dependent induction of aneuploidy

For the different endpoints variation in cell cycle sensitivity was observed. Concerning C^+MN G_1 cells seemed to be more sensitive than G_2 cells (Table 1). Moreover, exposure during G_1 phase resulted in a dose dependent increase which was not observed in G_2 exposed cells. The rates of non-disjunction (Table 2) and hyperdiploid cells (Table 3) were higher after G_2 than G_1 phase exposure. This suggests that both G_1 and G_2 cells are sensitive towards the induction of chromosome malsegregation by X-rays but that different targets might be involved.

3) Comparison of chromosome loss and chromosome non-disjunction

By comparing the frequencies of hyperdiploidy (Table 3) with the frequencies of chromosome loss (Table 1) and of chromosome non-disjunction (Table 2) one might estimate the relative contribution of chromosome loss versus non-disjunction to aneuploidy in human lymphocytes. Figure 1 made an attempt to quantify these events in lymphocytes irradiated in G_1. Since hypodiploidy could in part be due to technical artifacts, the total aneuploidy was considered to be equal to the double of the hyperdiploidy frequency. A correction factor (23/2) was applied to the hyperdiploidy data obtained with chromosome painting and to the frequencies of chromosome non-disjunction as well. Frequencies of chromosome loss were derived from the frequencies of centromere-positive micronuclei per 1000 biocleated cells. This comparison indicates that only a small fraction of the spontaneous and radiation induced aneuploidy is detected using the micronucleus assay. Non-disjunction seems to be a far more important mechanism leading to spontaneous and radiation induced aneuploidy.

4) Threshold for aneuploidy

A methodology to examine the existence of thresholds for compounds inducing chromosomal loss and non-disjunction was developed in our laboratory on flow sorted micronuclei and binucleated cells (Elhajouji, et al., 1995). our results obtained on X-ray induced aneuploidy combined with the knowledge of thresholds for chemical agents enable us to speculate about the existence of a threshold for radiation induced chromosome loss/non-disjunction.

Indications for the existence of a possible threshold for radiation induced aneuploidy might be hard to reveal.

Concerning chromosome loss, as demonstrated for chemically induced

aneuploidy, a high number of micronuclei have to be analysed with a fluorescent centromeric probe. However, since with radiation, the DNA is regarded as the main target for radiation induced genetic damage most of the micronuclei are the result of clastogenic events (centromeric-negative). Moreover, these events increase fast with dose, demonstrating a linear quadratic dose response for X-rays and a linear one for high LET irradiation. This will make it extremely difficult to collect enough micronuclei to study the dose dependent increase of C+MN.

Our study indicates that non-disjunction might be a far more important mechanism than chromosome loss for the induction of radiation induced aneuploidy. Still this effect is very limited and has to be studied in binucleated cells. Only a small increase was observed after irradiation of relative high doses (1 Gy).

Conclusion

On the basis of the observed results, one may hypothesise about the targets involved in X-rays induced aneuploidy. The comparison of the results obtained by the different scoring methods indicates that X-rays induced aneuploidy probably arises by means of interaction with several targets. As pointed out by the micronucleus assay, where higher frequencies of chromosome loss were observed in G_1 phase, aneuploidy during the G_1 phase might be preferentially attained by interaction with DNA targets. The higher levels of aneuploidy in G_2 phase, as observed with chromosome specific probing on interphases and chromosome counts on metaphases, on the other hand, suggest that additional non DNA targets might be involved in this stage of the cell cycle. Obviously interaction with the spindle apparatus should be considered but DNA targets at the level of both centromeres and the nuclear membrane attached telomeres should not be overlooked.

Publications

Elhajouji, A. P. Van Hummelen, and M. Kirsch-Volders (1995)
Indications for a threshold of chemically induced aneuploidy in vitro in human lymphocytes. Environmental and Molecular Mutagenesis, in press.

Kirsch-Volders, M. I. Tallon, C. Tanzarella, A. Sgura, T. Hermione, E. M. Parry, and J. M. Parry (1995) Chromosome non-disjunction is a major mechanism for in vitro aneuploidy induction by X-rays in primary human cells. Mutagenesis, submitted.

Tallon, I. L. Verschaeve, and M. Kirsch-Volders (1995) Cell cycle dependent aneuploidy induction by X-rays in vitro in human lymphocytes. Microscopy Research and Technique, submitted.

Tallon, I. L. Verschaeve, and M. Kirsch-Volders (1995) Evaluation of the in vitro aneuploidy induction by X-rays using different endpoint scoring methods. In preparation.

References

Buckton, K. E. and H. J. Evans (1983) Methods for the analysis of humane chromosome aberrations. World Health Organization, Geneva.

Eastmond, D. A., D. S. Rupa, H. W. Chen, and L. Hasegawa (1993) Multicolor fluorescence in situ hybridization with centromeric DNA probes as a new approach to distinguish chromosome breakage from aneuploidy in interphase cells and micronuclei, in B. K. Vig (Ed.) Chromosome segregation and aneuploidy, Springer-Verlag Berlin Heidelberg, pp. 377-390.

Elhajouji, A. P. Van Hummelen, and M. Kirsch-Volders (1995) Indications for a threshold of chemically induced aneuploidy in vitro in human lymphocytes. Environmental and Molecular Mutagenesis, in press.

Heddle, J. A. (1973) A rapid in vivo test for chromosomal damage. Mutation Res. 18, 187-190.

Meyne, J., L. G. Littlefield, and R. K. Moyzis (1989) Labelling of human centromeres using an alphoid DNA consensus sequence: application to the scoring of chromosome aberrations, Mutation Res., 226, 75-79.

Pinkel, D. T. Staume, and J. W. Grauw (1986) Cytogenetic analysis using quantitative

high sensitivity fluorescence hybridization. Proc. Natl. Acad. Sci. USA 83, 2934-2938.

Van Hummelen P., and M. Kirsch-Volders (1990) An improved method for the 'in vitro' micronucleus test using human lymphocytes. Mutagenesis, 5, 13-28.

Watt, J. L. and G. S. Stephen (1986) Lymphocyte culture for chromosome analysis. In Rooney, D. E. and B. H. Czepulkowski, eds. Human cytogenetics, a practical approach. IRL Press, Oxford, pp. 39-55.

TABLE 1.

Frequencies of centromere-positive micronuclei [‰C+CB] as a measure for chromosome loss in cytochalasin-B blocked lymphocytes.

Dose (Gy)	G1 irradiation					G2 irradiation				
	nCB	‰MNCB	MN scored	%C+	‰C+CB	nCB	‰MNCB	MN scored	%C+	‰C+CB
74 hours										
0.0	2000	13	77	53	7					
0.5	2013	97	227	20	19	2000	120	213	13	16
1.0	2010	217	314	17	37	1000	197	338	8	16
2.0	2017	484	270	11	54	2012	397	352	13	51
78 hours										
0.5	2013	98	190	15	15	2105	124	229	8	10
1.0	2025	186	338	14	26	2030	258	435	13	33
2.0	2019	486	530	14	70	2002	436	277	7	31

TABLE 2.

Frequencies of chromosome non-disjunction by chromosome specific centromere probing on interphase in cytochalasin-B blocked binucleates.

fixation at 78 hours		number of spots						
		Chromosome 1				Chromosome 17		1+17
Dose (Gy)	nCB	(2+2) CB	(1+3) CB	% NDCB	(2+2) CB	(1+3) CB	% NDCB	% NDCB
0.0	490	482	8	1.6	490	0	0.0	1.6
G1 irradiation								
0.5	571	562	9	1.6	571	0	0.0	1.6
1.0	636	629	7	1.1	634	2	0.3	1.5
2.0	624	612	12	1.9	622	2	0.3	2.2
G2 irradiation								
0.5	690	683	7	1.0	684	6	0.9	1.9
1.0	411	405	6	1.5	410	1	0.2	1.7
2.0	501	497	4	0.8	497	4	0.8	1.6

% NDCB: percentage of nondisjunction in binucleates is the number of binucleates when uneven (but $\Sigma=4$) distribution of spots for either chromosomes

* Chi-square test: $p < 0.05$

TABLE 3.

Aneuploidy frequences in second metaphase limphocytes.

chromosome counts of the whole metaphase on human lymphocites G1 and G2 irradiation; fixation at 78 h.

	Dose (Gy)	n cells	% hypodiploid	% hyperdiploid
	0.00	200	15.5	3.5
G1	0.50	200	10.0	3.0
	1.00	199	15.0	6.5
	2.00	200	35.0	6.5
G2	0.50	200	10.0	4.5
	1.00	200	13.5	7.0
	2.00	112	13.8	9.2

Figure 1.

Estimation of the relative contribution of chromosome loss versus non-disjunction to aneuploidy in human limphocytes.

Dose (Gy)	chromosomoe loss % C+MNCB [1]	nondisjunction % NDCB [2]	Aneuploidy % Aneuploidy [3]
0	0.7	18.4	7
0.5	1.9	18.4	6
1	3.7	17.3	13
2	5.4	25.3	13

[1]   Chromosome loss; derived from the ‰ C+MNCB (table 1)
[2]   Total non-disjunction frequences derived from the frequencies observed for two chromosomes (1 and 17) (table 2) using a correction factor of 23/2
[3]   Aneuploidy; since hypodiploidy could be due to technical artefacts, the total aneuploidy was considered to be equal to the double of the hyperdiploidy frequency (table 2).
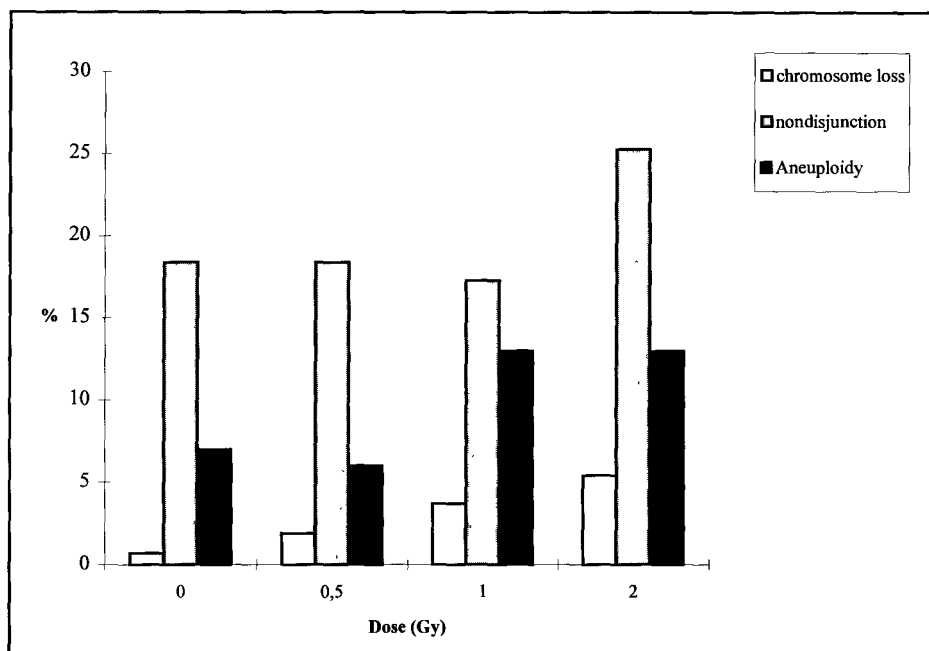
Title: Cytogenetic and molecular mechanisms of radiation myeloid leukaemogenesis in the mouse.

2)   Cox   NRPB
3)   Huiskamp   ECN

I. Summary of Project Global Objectives and Achievements

Global objectives

The global objectives of this project were to gain a detailed understanding of the mechanisms and genetics of radiation-induced acute myeloid leukaemia (AML) in the mouse through collaborative animal, cytogenetic and molecular investigations. Specific aims of the work included the resolution of a) the role of telomere and telomere-like repeat (TLR) DNA sequences in AML-associated somatic and germ line processes; b) dose-rate and radiation quality effects on AML induction; c) early cytogenetic events in AML and d) the patterns and mechanisms of leukaemogenic response in hybrid mice and, similarly, in lymphoma-prone mice deficient in the *p53* tumour suppressor gene.

Achievements

The principal objectives in all aspects of the work have been achieved; in most areas this was dependent upon close collaboration and exchange of biological material between NRPB and ECN.

The original hypothesis that recombinogenic TLR sequences in murine haemopoietic cells act to direct AML-associated chromosome (ch)2 breakage/rearrangement after radiation has been supported by DNA cloning and subsequent fluorescence *in situ* hybridization (FISH) cytogenetic studies. A molecular model of specific TLR sequence recombination has been developed in order to explain the genesis of these ch2 events. Ch2 allele loss and the associated deletion breakpoints have been defined by a study of loss of heterozygosity (LOH) for ch2 microsatellite loci in the AMLs of F1 hybrid mice; ch2 allele loss in these F1 AMLs showed no parental specificity. Also, in CBA/H AMLs, somatic telomere rearrangement and limited erosion has been shown to accompany leukaemogenic development. Good progress was made in the identification of murine DNA clones encoding the microsatellites that show close linkage to AML-associated ch2 breakpoints.

Dose-rate effects on CBA/H AML induction by x-rays and 1 MeV fission neutrons have been determined at single doses; these data were broadly consistent with prevailing views in radiological protection on dose-rate and radiation quality effects on radiation leukaemogenesis.

Subsequent cytogenetic studies revealed that ch2-mediated leukaemogenesis processes do not differ significantly after high and low LET radiations; also, that there is no obvious contribution to myeloid leukaemogenesis from high LET-induced genomic instability.

Studies on the status of early ch2 events in the haemopoietic systems of x-irradiated mice provided further support for the involvement of telomeric rearrangement and ch2 radiosensitivity in radiation leukaemogenesis but implied that, in the absence of further genomic changes, ch2 deletion/rearrangement does not have major effects on haemopoietic cell proliferation *in vivo*. These studies together with evidence obtained on clonal evolution in one AML suggest that the terminal region as well as an interstitial region of ch2 may encode genes involved in myeloid leukaemogenesis.

Molecular analysis of germ line TLR sequences provided strong evidence for their germ line hypervariability in the mouse. The initial observation of a possible association between locus-specific TLR polymorphism and AML-susceptibility in one CBA/H colony was however shown by subsequent colony re-screening and by investigation of a satellite colony to be a chance finding determined by the high germ line mutation rate of these sequences. In addition, studies on ch2 LOH in the AMLs of hybrid mice showed that the characteristic interstitial DNA losses were not obviously subject to *cis*-acting genetic or epigenetic effects. By contrast, cytogenetic studies with CBA/H, C57Bl and their F1 hybrid raised the possibility that a dominant *trans*-acting genetic trait expressing as a high frequency of induction of terminal chromosomal exchanges may serve to phenotypically identify murine susceptibility to AML. In general accord with this, initial data obtained on the incidence of AML in irradiated F1 hybrid mice were suggestive of dominant inheritance of AML susceptibility from the CBA/H parent..

Finally, in a collaborative study between NRPB and the Univ. of Glasgow (UK) it was shown that the tumorigenic radiosensitivity of lymphoma-prone mice deficient in the *p53* tumour suppressor gene was likely to be associated with a defect in checkpoint control in a late rather than an early phase of the cell cycle. This defect resulted in the high frequency *in vivo* induction of whole chromosome gain and loss in the haemopoietic system but appeared not to influence the overall induction of structural chromosome changes.

Head of project 2:   Dr R Cox

II. Objectives for the reporting period

      The principal role of NRPB was to take the lead in cytogenetic/molecular studies on the mechanisms and genetics of murine radiation leukaemogenesis. Attention was focused on: (a) the role of telomeric DNA sequences in the induction of AML-associated chromosome(ch) 2 deletions/rearrangements; (b) the effects of radiation quality on AML cytogenetics; (c) the characterisation of early cytogenetic events in AML induction; (d) the cytogenetic/molecular mapping of ch2 breakpoints in AMLs of hybrid mice; (e) possible mechanisms of genetic predisposition to AML; (f) the role of the *p53* gene in radiation-induced haemopoietic neoplasia. Work on topics (b), (d) and (e) was performed in close collaboration with staff at ECN, Petten.

III. Progress achieved including publications

1.   Conventional Cytogenetic and Fluorescence *in situ* hybridization (FISH) Studies

a)   *Cytogenetic characterisation of AML-associated radiosensitive chromosomal sites*

      Following clues from previous cytogenetic analyses of murine radiation-induced AML and *in vivo/in vitro* irradiated haemopoietic cells, attention was given to establishing the relationship between the pattern of region-specific ch2 deletion/rearrangement and the presence of interstitial telomere-like repeat (TLR) sequence arrays on this chromosome.

      A series of TLR sequences were cloned from size-selected DNA restriction fragments and microdissected ch2 material using polymerase chain reaction (PCR) methodologies. Two of these TLR clones together with synthetic linear telomeric DNA, ie. $(TTAGGG)_n$ were used in FISH analyses in order to map ch2 telomeric sequence arrays in relation to radiation-induced ch2 breakpoints. Telomeric DNA having a simple linear arrangement of the TTAGGG motif hybridized almost exclusively to terminal chromosomal regions with only weak FISH signals at interstitial sites. In sharp contrast a genomic TLR clone, ptel300, having an inverted and

interrupted telomeric structure, ie. $(TTAGGG)_n$ - $(CCCTAA)_n$ hybridized strongly to interstitial telomeric arrays throughout both mouse and human genomes. The interstitial TLR arrays were mapped to G-band regions of mouse ch2 (principally the B, C and F regions) and statistical analysis of the data demonstrated a strong correlation between interstitial ch2 TLR arrays, radiation-sensitive fragile sites and breakpoints in AML. It was concluded that AML-associated ch2 breakage was expressed preferentially in genomic regions rich in inverted arrays of TLR sequence.

On the basis of the specific DNA sequence of the informative ptel300 clone, a recombinational model involving G-quartet formation in DNA stem loops was developed to account for the apparent fragility of these specific arrays.

A series of other TLR clones were isolated from interstitial sites in murine DNA but the sequence of these allowed no further comment upon mechanisms of TLR sequence fragility. A TLR clone from microdissected ch2 DNA was however distinct in that it showed ~60% flanking sequence homology with a mobile element (*HetA*) from Drosophila in which it is involved in telomere function and chromosome break healing. It remains uncertain whether this *HetA*-like sequence plays a role in murine leukaemogenesis.

In other preliminary FISH studies inconclusive evidence was obtained that interstitial TLR array expansion in murine haemopoietic cells may be associated with radiation-induced damage and, in collaborative studies with Univ. of Aarhus (F. Pedersen and H. Moving), ptel300 sequences have been introduced into a murine haemopoietic cell line with a view to further exploring the mechanisms of TLR-mediated chromosomal radiosensitivity.

b)   *Cytogenetic characterisation of AML induced by different qualities of radiation*

A number of x-ray and α-particle induced CBA/H AMLs provided by NRPB collaborators (C. Kowalczuk and M. Ellender) were shown to carry ch2 deletions similar to those previously described. A more extensive collaborative survey of neutron-induced AMLs is nearing completion. AMLs were induced by ECN Petten and G-banded chromosome preparations were scored at NRPB with the aid of automated systems. Of 13 tumours studied 12 (92%) showed ch2 losses with, possibly, a greater proportion showing large deletions than seen after x-rays. With the exception of this, no evidence of radiation quality effects in respect of AML cytogenetics was observed. Non-passaging unstable chromosome damage was apparent in one neutron-induced AML and occasional chromatid damage was seen in others. No evidence was however obtained to support the hypothesis that high LET-induced genomic instability in haemopoietic cells makes a significant contribution to radiation leukaemogenesis.

c)   *Analysis of early cytogenetic events in the haemopoietic system*

A large scale experiment was performed using serial sacrifice of 3 Gy x-irradiated CBA/H mice in order to follow stable haemopoietic chromosomal changes and clonal evolution over a post-irradiation period of 15 months. Cytogenetic scoring and analysis of the oldest animals has yet to be completed but G-band data have been obtained from a total of 650 cells from animals 1-6 months post-irradiation. These data fully confirmed previous indications on the elevated radiosensitivity of CBA/H ch2 and showed this chromosome to contain ~2.5x more induced

breakpoints in stable aberrations than expected from its size; it was also shown that ch6 was ~1.7x over-involved in aberrations while chs X, Y and 18 were under-involved.

Analysis of the aberration spectrum obtained showed interstitial deletions in ch2 were more frequent than that predicted by the genome-wide data. Importantly, the absence of any obvious *in vivo* clonal growth advantage in the majority of cells containing ch2 deletions/rearrangements implies a) that ch2 is directly radiosensitive and b) that these events are not rate limiting or specific determinants of myeloid leukaemia development in individual animals. Further rate limiting genomic events are clearly needed for AML development and no evidence was obtained to suggest that these are detectable by G-band analysis. Chromosome painting techniques have been developed to explore these problems in greater depth.

d)   *Cytogenetic approaches to assessing and genetically mapping AML susceptibility in the mouse*

In CBA/H mice genome-wide terminal (telomeric) chromosomal translocations were the most common radiation-induced aberrations observed in haemopoietic cells of 3 Gy x-irradiated animals 1 month post-irradiation. Preliminary investigations with ECN Petten on the induction of these terminal translocations in AML-insensitive C57Bl mice revealed a significantly lower frequency than seen in AML-sensitive CBA/H. Importantly, x-irradiated CBA/H x C57Bl F1 mice showed a CBA-like terminal translocation frequency. Given the role of telomeric instability in AML development it is possible that this *trans*-acting cytogenetic trait is genetically linked to AML susceptibility and, if so, leukaemogenic radiosensitivity will tend to be inherited in a dominant or co-dominant fashion. Some support for this contention was obtained from F1 leukaemogenesis studies at ECN Petten (see ECN contribution).

In addition, the implication that terminal chromosomal translocations are specifically involved in the early phases of AML development in some animals was supported by detailed studies on one AML where the karyotype was shown to evolve from a primary t(2;11) translocation involving the terminus of ch2 to an apparently typical secondary ch2 deletion, i.e. del 2(C3F1). Previous studies suggest that other AMLs may also follow this pathway, thus further implicating the ch2 terminus in leukaemogenic processes. Since induced terminal translocations may act as a simple phenotypic marker for genotypic murine AML-susceptibility it may be possible using cytogenetic analysis of an irradiated backcross panel of mice to genetically map the dominant germ line locus involved.

e)   *Cytogenetic analysis of induced haemopoietic tumours in CBA/H x C57Bl F1 mice*

As part of a major collaboration with ECN Petten, cytogenetic analyses were performed on haemopoietic tumours arising in x-irradiated CBA/H x C57Bl F1 mice, G-banded preparations from ECN being scored at NRPB. To date, 20 tumours (not all yet confirmed as AML) have been analysed and 11 of these (55%) showed clear evidence of ch2 deletion. Tetraploidy tended to be more prevalent in these F1 tumours than in those of parental CBA/H and some secondary chromosomal changes have been observed. However, for those confirmed F1 AMLs, chromosome breakpoint data show an acceptable correlation with molecular analyses by loss of heterozygosity for microsatellites (see 2b below) and, in general, are not inconsistent with breakpoint data previously obtained from CBA/H AMLs.

f)   *Analysis of spontaneous and radiation-induced chromosomal abnormalities in lymphoma-prone p53 deficient mice*

A collaborative study with C. Kemp and A. Balmain (CRC, Medical Oncology Dept., Univ. of Glasgow) sought to establish a correlation between the patterns of tumorigenic and chromosomal radiosensitivity in wild type and *p53* tumour suppressor gene-deficient mice. Using direct bone marrow cytogenetic techniques based on those developed for CBA/H studies, the frequency of spontaneous exchange-type aberrations was found to be strongly influenced by germ line *p53* gene copy number. The frequency of spontaneous aberrations was greatest in null(-/-) mice, least in wild type (+/+) and intermediate in heterozygotes (+/-). Radiation-induced (3 Gy γ-ray) stable aberrations scored at 2 and 4 weeks did not however follow this simple pattern and no statistically significant differences in the frequency of induced chromosomal rearrangements/deletions was observed between the three genotypes. Assessment of spontaneous and radiation-induced sister chromatid exchange and G2 chromatid damage/repair in short term T-cell cultures also failed to demonstrate a significant effect of *p53* gene copy number. Overall, these data provided no support for the conventional view that *p53* plays a critical role in DNA damage response via its control of an early cell cycle checkpoint.

In sharp contrast a clear defect in the post-irradiation control of chromosome number was clearly apparent in *p53* deficient mice (+/- and -/-). These observations, together with *in vitro* T-cell data on the lack of radiation-induced mitotic delay in *p53* heterozygotes and nulls, point towards a critical role for p53 protein at a G2/M cell cycle checkpoint involved in the correct ordering of chromosomes on the mitotic spindle. Overall, the results obtained imply that increased tumorigenic radiosensitivity in *p53*-deficient mice correlates with increased sensitivity to the induction of whole chromosome gain/loss; previous studies on *p53* allele status in spontaneous and radiation-induced tumours in these mice provide some molecular support to this hypothesis.

2.   Molecular Studies

a)   *Telomeric sequence variation and AML susceptibility in CBA/H mice*

Southern analysis screening of normal CBA/H DNA using an oligonucleotide with the telomeric sequence $(TTAGGG)_4$ identified four genomic variants within the CBA/H colony maintained at the Medical Research Council, Radiobiology Unit, Chilton, UK. The variants were distinguished by the presence or absence of 4.7 and 5.5 kb telomere-like repeat (TLR) *Sau3A/MboI* restriction fragments. A maximum of 20-25% of irradiated CBA/H mice develop AML. Since one of the TLR variant sequences was found in both normal and tumour cell DNA of 23/25 animals presenting with AML and this variant constituted approximately 20% of Chilton mice, some form of germ-line TLR locus-associated AML predisposition seemed possible.

The principal source of uncertainty surrounding this proposal was the temporal discrepancy between AML induction (1978-1990) and colony screening (1990-92) which might allow for germ line TLR sequence mutation and subsequent genetic drift. A small breeding study with TLR variants provided some evidence of irregular inheritance of the TLR loci of interest but could not explain the stable maintenance of four mouse genotypes over many generations. This would be necessary to account for the long-standing consistency of AML radiosensitivity

in the CBA/H Chilton colony and in satellite colonies such as that established at ECN Petten in 1981.

In order to address these uncertainties collaborative TLR locus screening of the Petten CBA/H mouse colony was performed with ECN, the Chilton colony was similarly re-screened twice (1992 and 1993). In addition, in collaboration with ECN the leukaemic spleens and normal brains of x-irradiated ECN mice were analysed for TLR genotype. These studies revealed that while germ line TLR sequence polymorphism is frequent in CBA/H mice, there is no genetic link between specific TLR locus polymorphism and murine susceptibility to radiation-induced AML. Overall, it was judged that the four specific TLR variants originally noted in the Chilton colony arose through mutation/recombination but were present for only a short period. Between 1990 and 1993 the Chilton colony returned, presumably by breeding selection, to a single genotype and it was this same genotype that was represented in all mice in the Petten colony. Thus, the original germ line TLR correlation with AML-development was judged to be a chance finding.

During the course of this study pulsed field gel electrophoretic (PFGE) analysis of CBA/H telomeric *Sau3A* restriction fragments of between 200bp and 150 kb revealed very high germ line mutation rates which were greatest for fragments >50 kb (probably representing terminal telomeric arrays). The hypervariability of these arrays resulted in each mouse having a different genotype in spite of the highly inbred nature of the colony.

Prior to obtaining these results and terminating the study, some TLR clones had been isolated from the potentially informative restriction fragments. In no case was it possible however to recover full length restriction fragments in any of the vector systems used (plasmid, cosmid or λ bacteriophage). The inherent instability of these sequences in host bacteria appears to be a major limiting factor in all such cloning studies.

b)   *Somatic telomere sequence changes in CBA/H AML*

Collaborative studies on x-ray and neutron induced CBA/H AMLs from ECN were conducted in order to determine whether somatic telomere sequence changes were a consistent molecular feature of the leukaemogenic process and also to ascertain whether, as in human neoplasia, extensive shortening of terminal telomeres accompanies leukaemia transformation.

A total of 8 AMLs and the normal brain tissue of their hosts were analysed by PFGE using the $(TTAGGG)_4$ oligomeric DNA probe. Somatic telomere rearrangement and/or restriction fragment amplification was found to be common in radiation-induced AML. Four AMLs showed unambiguous evidence of rearrangement of telomeric *Sau3A* restriction fragments in the range 6-150kb and for *SalI* restriction fragments in the range 250-700 kb, which will include some interstitial telomeric arrays, all AMLs showed differences when compared with the normal host tissue. It is reasonable to suggest that some of these molecular changes to telomeric arrays are associated with the gross telomere-associated ch2 events that characterise early AML development. Locus-specific DNA probes for ch2 breakpoints in AML will however be necessary to resolve this important issue and these are being sought through the molecular analysis of ch2 loss of heterozygosity in AMLs of CBA/H x C57Bl F1 animals (see 2c below).

PFGE analysis of terminal telomeres also revealed that telomere shortening of up to ~10kb accompanied leukaemogenic development in 7/8 radiation-induced AMLs. This degree of telomere erosion is proportionately much less than has been reported for human neoplasms. Since the average length of terminal telomeres in CBA/H was ~100 kb it may be that the erosion noted does not make a major contribution to the molecular pathology of murine AML. Since however the analyses revealed evidence of considerable variation in terminal telomeric length between different CBA/H chromosomes, chromosome-specific effects of telomere erosion cannot be discounted.

c)   *Loss of chromosome 2 heterozygosity in AMLs of CBA/H x C57Bl F1 mice*

G-band cytogenetic analysis of radiation-induced CBA/H AML has identified the critical deleted segment of one copy of ch2 as the region between breakpoint sites in bands C and F. A smaller proportion of AMLs show larger deletions spanning from band C to band H which includes the terminus of ch2. Precise molecular mapping of chromosomal deletions in inbred mice is problematical but, in the tumours of hybrid (F1) mice, deleted chromosomal segments may be readily resolved since genetically linked polymorphic markers that are heterozygous in normal parental DNA are reduced to homozygosity in tumours by region-specific DNA deletion. Such loss of heterozygosity (LOH) provides a powerful tool with which to distinguish which parental allele is lost, the extent of that loss and, given sufficient markers, the precise position of the deletion breakpoints.

In a major collaborative study with ECN, haemopoietic tumours were identified in x-irradiated ♀ CBA/H x ♂ C57Bl F1 mice. DNA prepared at ECN was subject to ch2 LOH analysis at NRPB using a PCR technique to resolve simple sequence length polymorphisms in characterised and mapped ch2 microsatellite loci. The choice of these mouse strains was governed by their differential sensitivity to AML induction and their genetic divergence.

A total of 37 informative polymorphic microsatellite loci distributed throughout ch2 were initially identified in the two parental strains and confirmed in normal DNA from all AML-bearing F1 animals. These loci were analysed in 15 radiation-induced F1 AMLs. These analyses failed to identify ch2 microsatellite LOH in 5/15 (33%) while such losses were clearly apparent in the remaining 10 (67%). Of the 10 AMLs showing ch2 LOH, 5 had lost a linked set of CBA/H alleles while the remaining 5 had lost a linked set of C57Bl alleles. Thus, there appears to be no obvious indication of *cis*-acting parental strain (genetic) nor parent of origin (epigenetic) effects on AML-associated ch2 deletion.

Proximal ch2 breakpoints in all 10 AMLs showing ch2 LOH were shown to cluster in a ~5 cM interval of the ch2 C band. Eight AMLs had distal F region breakpoints within a ~2.5 cM interval and 2 had sub-telomeric H region breakpoints within a ~6.5 cM interval. Ongoing LOH studies with other markers seek to map more precisely these deletion breakpoints. These molecular data on ch2 breakpoints were in general accord with cytogenetic analyses and add much credence to the original hypothesis that radiation-induced murine AML development proceeds via region-specific ch2 breakage.

These data do not however allow comment on whether the specificity of ch2 breakage is determined by the presence of recombinogenic DNA sequences (interstitial telomeric arrays?)

and/or whether the close proximity of AML-associated genes to the breakpoints is important. In order to address this question microsatellites flanking these ch2 breakpoints have been used to screen by PCR for the presence of potentially informative clones within a bacterial artificial chromosome (BAC) library of large murine DNA inserts. This library has been shown to contain almost all the ch2 microsatellite DNA clones of interest. These are currently being isolated from sub-pools of the library and when available will be used as probes to screen CBA/H and F1 AMLs by FISH and PFGE to determine whether any encode ch2 breakpoint sequences. DNA sequences at these ch2 breakpoints and in the flanking regions will serve to guide future work.

In conjunction with these analyses, size-selected restriction fragments from normal CBA/H DNA have been screened by microsatellite PCR to direct plasmid cloning strategies. The microsatellite positive DNA libraries were divided into sub-pools and re-screened for the breakpoint-flanking loci of interest; individual clones are in the process of isolation and will supplement those from the BAC library noted above.

In addition to being used for DNA cloning, a DNA restriction fragment size-selection strategy was employed to determine the methylation status of DNA in the region of ch2 breakpoints. The methylation-sensitive and -insensitive restriction enzyme isoschizomers *Sau3A* and *MboI* were used to prepare size-selected CBA/H DNA and evidence for changes in DNA methylation status was sought by screening DNA fractions for consistent changes in respect of informative microsatellite representation. Preliminary results in respect of a microsatellite locus within the ch2 band C breakpoint interval of 5 cM suggest that this region may be subject to differential DNA methylation which may reflect the status of the two alleles. Further evidence on the role of DNA methylation in site specific ch2 breakage in AML will be sought when DNA clones representing breakpoint regions are available.

Publications

Ellender, M, Robbins, L, Bouffler, S D and Harrison, J D. (1992). Induction of osteosarcoma and leukaemia by [239]Pu, [241]Am and [233]U in CBA/Hmice. EULEP Newsletter 67: 25-26.

Bouffler, S, Silver A R J, Coates, J. Papworth, D and Cox, R (1993). Murine radiation myeloid leukaemogenesis; the relationship between interstitial telomere-like repeat sequences and chromosome 2 fragile sites. Genes, Chrom. Cancer 6: 98-106.

Bouffler, S, Silver , A R J and Cox, R (1993). The role of DNA repeats and associated secondary structures in genomic instability and neoplasia. Bioassays 15: 409-412.

Silver, A R J and Cox, R (1993). Telomere-like DNA polymorphisms associated with genetic predisposition to acute myeloid leukaemia in irradiated CBA mice. Proc. Natl. Acad. Sci USA 90: 1407-1410.

Goodhead, D T, Thacker, J, and Cox, R (1993). Effects of radiation of different qualities on cells: Molecular mechanisms of damage and repair. Int. J. Radiat. Biol. **63**, 543-556.

Silver, A R J, Bouffler, S, Finnon, P, Rance, E, Morris, D and Cox, R (1994). Site specific chromosome damage and myeloid leukaemogenesis in the CBA mouse. Rad. Prot. Dosim. 52: 461-464.

Bouffler, S D (1994). Whole chromosome hybridization. Int. Rev. Cytol. 153: 171-232.

Bouffler, S D, Silver, A R J, Finnon, P, Morris, D, Rance, E and Cox, R (1994). Cytogenetic and molecular studies on the initiation of myeloid leukaemia in irradiated CBA mice. In Chadwick, K H, Cox, R, Leenhouts, H P and Thacker, J, eds. Molecular Mechanisms of Radiation Mutagenesis and Carcogenesis. Office for Official Publications of the European Communities, Luxembourg (1994).

Thacker, J and Cox, R. (1994). Report on Discussions. In Chadwick, K H, Cox, R, Leenhouts, H P and Thacker, J, eds. Molecular Mechanisms of Radiation Mutagenesis and Carcinogenesis. Office for Official Publications of the European Communities, Luxembourg (1994).

Silver, A R J, Meijne, E, Huiskamp, R and Cox, R. (1994). Studies on telomere involvement in murine radiation-induced myeloid leukaemia. Proceedings of the 8th International Conference of the International Society of Differentation. Oct 22-26. Hiroshima, Japan 1994.

Cox, R. (1994). Molecular mechanisms of radiation oncogenesis. Int. J. Radiat. Biol.**65**: 57-64.

Cox, R. (1994). Human cancer predisposition and the implications for radiological protection. Int. J. Radiat. Biol. **66**: 643-647.

Bouffler, S D, Kemp, C J, Balmain, A and Cox, R. (1995). Spontaneous and ionizing radiation-induced chromosomal abnormalities in p53-deficient mice. Cancer Research 55: 3883-3889.

Lohman, P H M, Cox, R and Chadwick K H (1995). Role of molecular biology in radiation biology. Int. J. Radiat. Biol. (in press).

Cox, R. (1995). Genetic predisposition to cancer and radiation risk. Proceedings of 10th ICRR, Wurzburg. Aug 28-Sept 1 1995 (in press).

Meijne, E I M, Silver, A R J, Bouffler, S D, Morris, D J, Winter van Kampen, E, Spanjer, S, Huiskamp, R and Cox, R (1995). The role of telomeric sequences in murine radiation-induced acute myeloid leukaemia. Genes Chrom. Cancer (accepted for publication).

Bouffler, S D, Breckon, G and Cox, R. (1995). Chromosomal mechanisms and telomeric regions in the murine radiation acute myeloid leukaemia. Genes Chrom Cancer (submitted).

Clark, D, Meijne, E I M, Bouffler, S D, Huiskamp, R, Skidmore, C, Cox, R, and Silver, A R J (1995). Polymorphic microsatellite analysis or recurrent chromosome 2 deletions in acute myeloid leukaemia induced by radiation in F1 hybrid mice. Genes, Chrom. Cancer (submitted).

Head of project 3:   Dr Huiskamp

II. Objectives for the reporting period

The principal role of ECN was to take the lead in life-span animal studies relating to radiation quality effects and the mechanisms/genetics of murine radiation leukaemogenesis. Attention was focused on a) the effects of dose-rate of x-rays and fission neutrons on the induction of murine AML; b) the characterisation of chromosome 2 abnormalities in fission neutron induced AML; c) the possible involvement of germ line telomere-like repeat sequences in murine AML-predisposition; d) the x-ray induction of tumours in hybrid mice and the provision of chromosomal and DNA preparations of AMLs for detailed analyses.

Work on topics b), c) and d) was performed in close collaboration with staff at NRPB with E. Meijne of ECN spending a 6 month working visit at NRPB on a CEC-supported training bursary.

III. Progress achieved including publications

a)   *AML induction in CBA/H by x-rays and fission neutrons*

During the reporting period ♂ CBA/H mice from the Petten colony were exposed to x-rays and 1 MeV fission neutrons according to the schedule of Table 1.

Table 1 AML in x-ray and fission neutron exposed CBA/H mice

Exposure conditions	#Mice	#Alive	Estimated AML	#AML	Incidence
2 Gy X-rays (600 mGy/min)	90	0	16	21	0.233
2 Gy X-rays (3 mGy/min)	220	36	-	23	0.105
3 Gy X-rays (300 mGy/min)	100	0	20	17	0.170
400 mGy Neutrons (100 mGy/min)	140	2	15	17	0.121
400 mGy Neutrons (0.5 mGy/min)	160	26	15	21	0.131
Sham-irradiated controls	210	27	0	0	0.0

No animals were lost during the extended periods of the low dose-rate exposures and all animals were carefully monitored throughout their life-span. Complete analysis of AML induction after these exposures is not yet available. The inherent constraints of experimental design, the mean life-span of animals and subsequent pathological evaluation are such that the study period exceeds that of the formal contract. This work is therefore continuing. Based, however, on the gross pathology of irradiated animals provisional classification and quantification of induced AML has been possible and these data are given in Table 1.

For x-rays, AML incidence was found to be significantly reduced at a dose rate of 3 mGy min^{-1} when compared with 600 mGy min^{-1} and the data suggest a low LET dose-rate reduction factor for leukaemogenesis of ~2 at 2 Gy. In contrast for 1 MeV fission neutrons no difference in AML induction at a total dose of 400 mGy was observed between exposures at 100 mGy min^{-1} and 0.5 mGy min^{-1}, ie. a dose rate factor for high LET leukaemogenesis of ~1. These data add support to current radiological protection judgements on dose and dose rate effects for radiation leukaemogenesis. G-banded chromosomal preparations from a set of neutron induced AMLs were made together with high molecular weight DNA contained in agarose plugs (normal host brain and leukaemic spleen preparations). This material was subject to detailed cytogenetic and molecular analysis in collaboration with NRPB. The results of these studies are given in the report of NRPB and are only briefly noted here.

G-banded chromosome preparations of 20 neutron-induced AMLs were prepared. Analyses of 13 of these were completed and 12 showed ch2 deletions; the extent of the deleted ch2 region ranged from G-bands D-F to A2-H3. Thus, neutron-induced myeloid leukaemogenesis appears to proceed via the same ch2 deletion pathway as that reported by NRPB for x-rays and α particles. Importantly, no evidence was obtained to suggest that high LET-induced genomic instability contributes to neutron leukaemogenesis. Analysis of high molecular weight DNA from AMLs and their normal host tissues showed that somatic telomere rearrangements were common in AML but that significant telomere shortening did not appear to accompany leukaemogenic development.

b)   *Germ line telomere-like repeat (TLR) sequence variation in CBA/H Petten mice*

Following the NRPB finding that there may be an association between germ line TLR variation and AML-susceptibility in the CBA/H Chilton colony, mice from the satellite colony at Petten were appropriately screened in collaboration with NRPB. No such specific TLR variation was seen amongst 43 randomly selected Petten mice. Analyses of these TLR loci in the normal (brain) and leukaemic (spleen) tissues of animals bearing radiation-induced AML also provided no evidence to link germ line TLR loci with AML-susceptibility. Thus, although germ line telomere sequence polymorphism was common in CBA/H Petten mice none showed association with AML susceptibility. These data together with those obtained from the NRPB re-screen of the Chilton colony provided strong evidence against the TLR-AML genetic association originally proposed. Accordingly, the original ECN intention of identifying and selecting specific CBA/H TLR variant mice for breeding and leukaemogenesis studies was not pursued. Greater attention was given therefore to the study of radiation leukaemogenesis in hybrid mice (see below).

c)   *Radiation tumorigenesis in CBA/H x C57Bl F1 hybrid mice*

For the reasons given in the report of NRPB, the provision of radiation-induced tumours from F1 hybrids of genetically divergent laboratory mice offers great benefits in respect of resolving tumour-associated DNA deletion at the molecular level. In this way it was anticipated that ch2 deletion in radiation-induced AML of F1 hybrids could be analysed in detail. Since the two parental strains chosen for the study differ markedly in their inherent susceptibility to AML induction (CBA/H-sensitive; C57Bl-resistant), the AML yield from irradiated F1 animals would also allow comment on whether genetically determined murine AML-susceptibility is inherited as a recessive or dominant trait.

Following initial screening of parental animals for ch2 encoded microsatellite polymorphisms, ♀ CBA/H were mated with ♂ C57Bl and randomly selected F1 progeny (♀ and ♂) were 3 Gy x-irradiated according to Table 2. These animals are currently being followed throughout their life-spans and the data of Table 2 summarise the current position in respect of tumour induction overall.

Table 2 Radiation tumorigenesis in ♀ CBA/H x ♂ C57Bl F1 mice

Exposure conditions	#Mice	#Alive	Estimated AML	#Tumours
A* 3 Gy X-rays(600 mGy/min)	360	213	19	64
B* 3 Gy X-rays(600 mGy/min)	200	165	10	19
Sham-irradiated controls	100	96	0	2

* group A - parental animals not identified; group B - parental animals identified for DNA analysis and breeding if required.

The majority of F1 animals remain alive and detailed histology on those induced tumours that have arisen has yet to be completed. Nevertheless, it is already apparent that the rate of induction of haemopoietic neoplasia in F1 animals is high. In total, 1408 animal organs have been prepared for histopathology of which, 890 are paraffin-embedded; 80 animals have been fully processed including pathological analysis. In these studies 1250 mice have also been used in transplantation/passaging studies on induced tumours.

The principal haemopoietic neoplasm appearing in irradiated F1 animals is of the lymphosarcoma type but others show the gross histopathology of AML. Suspected AMLs were transplanted in F1, C57Bl and CBA/H recipient mice. These transplanted AMLs were very aggressive in F1 mice and leukaemia appeared in the host within 3-5 weeks; in contrast AML of the parental CBA/H mouse required ~3 months for expression in transplanted syngeneic hosts. F1 AMLs and lymphosarcomas induced graft versus host effects in C57Bl but not in CBA/H; to date, no F1 leukaemias have appeared in either of these transplanted parental strain animals.

The estimated AML yield of Table 2 was based on the conservative assumption that the AML-susceptibility of CBA/H (~20% after 3 Gy x-rays) would be expressed as a recessive genetic trait such that AML incidence in irradiated F1 would be around 5%. While the study is

incomplete and the full histopathology of suspected AML is pending, it is currently judged that the induced AML incidence in F1 animals will be substantially greater than 5% and may be as high as 15%. If this estimate is confirmed, then the AML-susceptibility of the CBA/H parental strain is being expressed in the F1 hybrid as a dominant or co-dominant genetic trait. This would accord with the finding by NRPB of the dominant expression of CBA/H-like telomere-associated chromosomal exchanges in the haemopoietic systems of irradiated F1 animals.

For the collaborative element of this study, G-banded chromosome spreads and high molecular weight DNA were prepared at ECN and transferred to NRPB for analyses. The results from these cytogenetic and loss of ch2 heterozygosity studies are reported by NRPB. In brief, 10/15 (67%) suspected F1 AMLs were characterised by CBA/H-like deletions with breakpoints that clustered in short chromosomal intervals in the C and F (8/10) or C and H (2/10) G-band regions of one of the two copies of ch2.

Although these molecular analyses also showed that ch2 deletion in F1 AML is not obviously biassed by strain of origin (genetic) or parent of origin (epigenetic) effects, such influences on radiation leukaemogenesis may be imposed by other regions of parental genomes. In order to take account of these possibilities F1 animals were produced from the cross, ♀ C57Bl x ♂ CBA/H, ie. the reverse of that reported above. To date, 40 such F1 animals have been 3 Gy x-irradiated and all remain alive. The tumour incidence recorded in this second study will be compared with that of the animals of Table 2 and cytogenetic/molecular studies will be performed as appropriate.

Publications

Silver, A R J, Meijne, E, Huiskamp, R and Cox, R. (1994). Studies on telomere involvement in murine radiation-induced myeloid leukaemia. Proceedings of the 8th International Conference of the International Society of Differentation. Oct 22-26. Hiroshima, Japan, 1994.

Meijne, E I M, Silver, A R J, Bouffler, S D, Morris, D J, Winter van Kampen, E, Spanjer, S, Huiskamp, R and Cox, R (1995). The role of telmoreic sequences in murine radiation-induced acute myeloid leukaemia. Genes Chrom. Cancer (accepted for publication).

Clark, D, Meijne, E I M, Bouffler, S D, Huiskamp, R, Skidmore, C, Cox, R and Silver A R J (1995). Polymorphic microsatellite analysis of recurrent chromosome 2 deletions in acute myeloid leukaemia induced by radiation in F1 hybrid mice. Genes, Chrom. Cancer (submitted).

1)   Natarajan   Univ. Leiden
3)   Ortins   Direcção-Geral do Ambiente
4)   Bryant   Univ. St. Andrews
5)   Pantelias   NCSR "Demokritos"
6)   Benova   NCRRP

I. Summary of Project Global Objectives and Achievements

a) Introduction

Ionizing radiations induce different types of lesions in the cellular DNA of which DNA double strand breaks (DSBs) are considered to be the most important ones involved in the formation of chromosomal aberrations. The aims of the current project include (a) an assessment of initial damage at chromosomal level, its repair/mis-repair and their relationship to the yields of observed chromosomal aberrations in human lymphocytes and cultured rodent cells, (b) to identify the factors responsible for increased radiosensitivity of human (A-T) and rodent mutant cells (c) the relationship between the yield of stable and unstable chromosome aberrations as well as their elimination during proliferation (d) chromatin structure in relation to induction and distribution of aberrations in Chinese hamster cells, (e) the role of modifiers on the yield of radiation induced chromosomal aberrations and (f) the influence of low dose adaptation to a subsequent challenge dose of radiation in human lymphocytes .

In addition to classical chromosome analysis, techniques of premature chromosome condensation (PCC), poration of cells with streptolycin-O, fluorescent in situ hybridization (FISH) using chromosome specific DNA libraries as well as region specific DNA probes have been employed in this project. Under the PECO project, Bulgarian scientists were trained in some of these techniques.

b) Relationship between initial damage and the yield of aberrations:

Using PCC method it is possible to determine the frequency of induced chromosome breaks per mammalian genome per Gy and this appears to be around 3 in human lymphocytes as well as Chinese hamster cells (Leiden, Athens). If the repair of DSBs is completely inhibited by Ara A, both during irradiation and during fusion with mitotic cells, the frequency of breaks increases by a factor of 2 indicating that at chromosomal level one can only recover about 6 to 12 % of DNA DSBs induced per cell (Leiden). One interesting observation was that when mitotic HeLa cells were used for fusion, the frequencies of PCC fragments were twice of that found when mitotic CHO cells were used, which implies that mitotic promoting factors are high in HeLa cells which leads to rapid condensation of chromatin (Athens). More experiments to confirm this observation have to be carried out using different types of mitotic cells, which may help in a more accurate estimate of induced fragments as determined by PCC.

c) Factors responsible for increased sensitivity in radio-sensitive cell lines:

Several cell lines are available with increased radiosensitivity. These include human cells derived from ataxia telangiectasia patients and mutants isolated from Chinese hamster cells. In some of these cell lines , such as xrs mutants, a direct correlation can be drawn between their inability to repair DNA DSBs and their radiosensitivity (St. Andrews, Leiden). However, cell lines such as A-T, hamster mutant cell lines such as VC4, irs 2 etc., there is no demonstrable defect in DSB repair but an increased radiosensitivity is found. One of the characteristics of these cell lines is that, unlike wild type cells, when irradiated in G1, both chromosome and chromatid types of aberrations are encountered (Leiden) which may indicate that repair of some lesions other than DSBs may be deficient in these cells and indeed, VC4 cells are sensitive to short wave UV as well (Leiden). When treated with restriction endonucleases (REs) or fast neutrons, the response of G1 cells for induction of chromosome aberrations, the response is very similar to wild type cells in these mutants (Leiden). In contrast, in G2 cells an increased frequency of chromatid breaks following treatment with X-rays or REs have been observed (St. Andrews). This discrepancy may be due to the fact that different cell cycle stages were studied and further studies are needed to clarify this point.

The initial yield of radiation induced breaks measured by PCC in radiosensitive (irs-1) and wild type cells (V79) is very similar and the rejoining of breaks occurs with similar kinetics ($t_{1/2}$ = 26.2 min.), however chromosome ring formation is higher in irs-2 cells compared to wild type cells indicating that mis-repair is higher in the mutant cells (Athens). This characteristic is very similar to that found in AT cells in which DSB repair is similar to normal human cells, but the fidelity of repair is poor. The repair of DSBs in xrs5 and CHO cells showed no difference in the fast component but a large difference in the slow component of the repair (Athens).

Characterization of nuclear extracts of xrs5 and CHO cells indicated clear differences in two proteins of MW 31.8 and 32.2 Kdal as determined by PAGE electrophoresis (St. Andrews). These proteins are thought to represent members of histone H1 family associated with DNA. Southern-Western blotting studies using ^{32}P labelled DNA showed that these proteins have a lower degree of DNA binding in xrs5 compared to CHO cells.

d) Relationship between the yields of stable and unstable aberrations and their elimination during proliferation:

The availability of chromosome specific DNA libraries has made detection of chromosomal translocations easy by the technique of fluorescence in situ hybridization (FISH). Since these "painting" probes are very specific to individual pair of chromosomes, any translocations involving these chromosomes can be easily detected (Leiden). Following irradiation of human lymphocytes with different doses of X-rays, the yields of dicentrics and translocations have been estimated. The frequencies of translocation were found to be about 1.5 times more than that of dicentrics (Leiden) an observation which has been confirmed by many other laboratories . The increase in the frequencies of translocations is mainly due to the contribution of terminal, interstitial and complex translocations, which can, in addition to reciprocal translocations can be detected by chromosome "painting"..

The yield of radiation induced translocations is controlled by three factors, namely, chromosome number, chromosome arms and the number of induced breaks. The higher yield of translocations than the dicentrics can be due to the several metacentric chromosomes present in human karyotype. In order to check the role of these factors, mouse chromosome specific DNA libraries were generated for # 1,11 and 13 by flow sorting a complex translocation involving these three chromosomes (Leiden). The frequencies of translocations are very similar to that of dicentrics in mouse and this may be due to the fact that all mouse chromosomes are acrocentrics namely single arms (Leiden) This observation is confirmed by other studies (Sofia).

Using long term culture of irradiated human lymphocytes, the elimination of cells carrying dicentrics or translocations was monitored. The detection of cells in first, second and third mitoses was made possible by culturing the cells in the presence of BrdU. The frequencies of dicentrics and fragments were reduced by 50% for each cell division whereas the frequencies of translocations as detected by FISH remained constant (Leiden)

The frequencies of dicentrics in x-irradiated human lymphocytes can be increased by about a factor of 2 by post treatment incubation in inhibitors of DNA repair, such as cytosine arabinoside (ara C) or 3 aminobenzamide (3 AB). However, under the same experimental conditions, the frequencies of translocations are not influenced (Leiden). This indicates that unstable (dicentrics) and stable aberrations (translocations) originate by different mis-repair mechanisms. However, when irradiated lymphocytes are post-treated with ara A, the yields of both dicentrics and translocations increased. Since araA inhibits both very fast as well as other components of rejoining of DNA DSBS, its potentiation of the yield of translocations indicate that translocations are most probably formed during the fast component of the chromosomal repair process (Leiden).

e) Chromatin structure in relation to induction and distribution of radiation induced aberrations:

It is generally assumed that ionizing radiations induce DNA lesions randomly among the chromosomes and the aberrations are also induced randomly among and along the chromosomes. Chinese hamster primary cells offer a very good system for such a study as the chromosomes have very defined heterochromatic (condensed) and euchromatic (relaxed) regions among the chromosomes and all chromosomes are easily identifiable. By X-irradiating Chinese hamster embryonic cells in G2 stage in the presence of araA one can inhibit repair of all the chromatid breaks and the yield obtained thus, will give an estimate of initial break frequencies. The frequencies of breaks were found to be not proportional to the length of the chromosomes and heterochromatic regions had fewer breaks in comparison to euchromatic regions. When the repair of breaks was monitored over a period of four hours, euchromatic regions were found to repair faster than heterochromatic regions (Natarajan). Similar heterogeneity was also found when G1 cells were irradiated, especially heterochromatic regions of X chromosome rarely participated in exchanges (Leiden).

The influence of telomeric sequences on the induction and formation of induced chromosomal aberrations has been investigated. While in most of the mammalian species the telomeric sequences are confined to the terminal ends of the chromosomes, Chinese hamster cells have large blocks of telomeric sequences distributed intercalarily (Leiden). A high proportion of RE induced aberrations was found to involve regions containing telomeric sequences (Leiden).

Following X-irradiation only breaks which appear after a S phase are capped with telomeric sequences. This preliminary observation needs confirmation (Leiden).

f) Role of modifiers on the yield of radiation induced chromosomal aberrations:

Hyperthermia brings about a large number of changes including chromatin configuration in cells leading to modification of cellular response to ionizing radiation. The influence of hyperthermia before or after irradiation in CHO cells was studied using the technique of PCC. There was a significant reduction in the repair of chromosome damage if the cells were heated after irradiation (probably due to inactivation of repair enzynmes) and increased damage if cells were heated before irradiation (due to relaxation of the chromatin (Athens)).

The mechanism of radio-sensitization by incorporated BrdU was found to have two components, one by increasing the frequencies of induced DSBs (which can be quenched by treating with 1M acetone) and the other by interfering with the DNA repair/damage fixing processes (Athens). Post incubation of irradiated mouse splenocytes in BrdU containing medium did not have influence on the yield of dicentrics, though the presence of BrdU appeared to alter the cell cycle progression, thus resulting in an *apparent* sensitization due to BrdU (Sofia).

g) Studies on low dose effects and adaptive response:

It has been shown that when stimulated human lymphocytes are irradiated with a very low dose of radiation and challenged subsequently with a higher dose, the yield of chromosomal aberrations is lower than expected and this phenomenon is called adaptive response. There have been several reports about the variability of results obtained in such experiments. In general, most individuals show an adaptive response, some do not show such a response and some even respond with a synergistic effect. In the present project, blood samples from five controls, five uranium mine workers exposed occupationally to high dose (about 25 cSv) and five workers exposed to low levels (< 11.5 cSv) were irradiated to an adaptive dose of 5 cGy followed by 3 Gy of gamma rays after five hours in G1 stage. Chromosome type of aberrations were scored. 4 out of 5 controls and workers exposed to low levels of radiation and 2 out of 5 exposed to high levels of radiation showed an adaptive response (Sacavem). There was no correlation between the occupational exposure and response to adaptation, indicating that this phenomenon is very complex one and the mechanism(s) by which adaptation is manifested is not fully understood.

Training of scientists from East European countries (PECO project):

During this project, two scientists from National Institute of Radiation Hygiene and Radiation Biology, Sofia were trained in Leiden. The technique of fluorescent in situ hybridization was introduced in the Bulgarian laboratory and the necessary equipments were provided. This methodology is at present operational in that laboratory.

Head of project 1: Prof. Natarajan

II. Objectives for the reporting period

(a) Studies designed to understand the relation between initial chromosome damage observed by PCC and those recovered in the first metaphase following irradiation
(b) Studies aimed at mapping distribution of X-ray induced lesions among the chromosomes and their repair
(c) Relative frequencies of radiation induced dicentrics and translocations in human and mouse lymphocytes
(d) Studies designed to check as to whether the DNA repair processes involved in the formation of stable and unstable aberrations are the same or different
(e) Studies on the influence telomeric sequences on induced chromosomal aberrations

III. Progress achieved including publications

1. Introduction

Ionizing radiation induces different types of DNA lesions such as single strand breaks (SSBs), double strand breaks (DSBs), base damage and DNA -protein cross-links. Among these, DSB appears to be the most important lesion for the induction of chromosomal aberrations though under DNA repair deficient conditions, other lesions such as base damages may also be involved (Natarajan *et al.*, 1993). There are some basic questions which need to be answered with regard to the induction of aberrations by radiation, such as (a) What is the relationship between initial DNA DSBs and observed chromosomal damage cytologically , b) are the initial chromosomal lesions distributed randomly among the genome, and is there any heterogeneity with regard to the repair of these lesions among the chromosomes or chromosomal regions, (c) are some chromosomes more prone for radiation induced chromosomal aberrations than others (d) do the symmetrical and asymmetrical exchanges following radiation formed at equal proportions ? and (e) is there any influence of DNA repeat sequences (such as telomeric repeats) on the formation of induced CAs ? Recent studies using techniques of chromosome banding, premature chromosome condensation, FISH using both chromosome specific libraries and telomeric sequences have been very useful in answering these questions to some extent.

2. Materials and methods

1. *Cell types used:*

a) *Chinese hamster cells:* Primary Chinese hamster embryonic cells (CHE), Chinese hamster ovary (CHO) cells, and lung fibroblast (V79) cells were cultured in a routine way using Ham's F10 medium supplemented with new-born or foetal calf serum and antibiotics (Balajee *et al.*, 1994).

b) *Mouse splenocytes:* Splenocytes from mouse were freshly isolated and cultured in RPMI 1640 medium supplemented with 20% HL, 6% bovine calf serum and antibiotics in the presence of concanavalin A (Pharmacia, 2.5 μg/ml) and 5 bromo- 2'-deoxyuridine (Sigma final concentration 5μM). Cells were harvested 41h after initiation (Boei *et al.*, 1994)

1. *Human peripheral blood lymphocytes:* Either isolated frozen lymphocytes or whole blood was used for the experiments. The lymphocytes were cultured in a routine way in the presence of PHA (Welcome) and 5-bromo-2' deoxyuridine (10 μM final concentration) and fixed at 48h after initiation.

2. *Cytological preparations:* These were made by routine air-dry procedure, which included colcemid pre-treatment, harvesting, hypotonic shock, fixation in aceto-methanol (1:3). Slides for in situ hybridization were stored at -20°C.

3. *Premature chromosome condensation:* This was achieved by fusing lymphocytes with mitotic Chinese hamster ovary cells in the presence of 55% polyethylene glycol - M.wt. 1450, Sigma, (Vyas *et al.*, 1991).

4. *Staining of chromosomal preparations:* For analysis using light microscope, the slides were stained in 5% aqueous Giemsa for 10 min. For identification of second division lymphocytes, the slides were stained with Fluorochrome plus Giemsa technique.

5. *Chromosome specific DNA libraries:*

   i) *Human:* Chromosome libraries were purchased from American Type Culture Collection (ATCC) or from Dr. J. Gray, Livermore. The isolation and purification of probe DNA has been described earlier (Natarajan *et al.*, 1992). Probes were labelled by nick translation using Bio-16-dUTP as one of the triphosphates in the reaction mixture.

   ii) *Mouse:* Chromosome specific DNA libraries were generated by us (Boei *et al.*, 1994). Primary embryonic cultures from a mouse carrying a translocation comprising chromosomes 1, 11, 13 were set up and the translocation carrying metacentric chromosomes were flow sorted. DNA was isolated from this compound chromosomes ,purified, and restricted. Ligation of linker/adapter was carried out and amplified by PCR. The probes were directly labelled during PCR, by replacing 200 μM dTTP with 150 μM Bio-11-dUTP (Sigma) and 50 μm dTTP (Boei *et al.*, 1994).

   iii) *Telomeric repeats:* These sequence was generated by PCR which was carried out in the absence of template using primers (TTAGGG)$_5$ and (CCCTAA)$_5$. Staggered annealing of primers provided single strand template for extension by Taq polymerase. This was followed by PCR. The probes were labelled by nick translation using bio-16-dUTP or digoxigenin 11-dUTP (Balajee *et al.*, 1994).

6. *In situ hybridization:* The method employed is described in Natarajan et al., (1992). The slides were viewed under a fluorescent microscope equipped with a triple filter (Omega).

7. Irradiation: Chinese hamster cells were irradiated at room temperature using an Muller machine operated at 200 kV and 8 mA at a dose rate of 2.0 Gy/min.

8. Treatment with DNA repair inhibitors: 9-ß-D-arabinofuranofuranosyladenine

(Ara A) which is known to be a very efficient inhibitor of repair of DNA DSBs was used in some of the irradiation experiments. 100 μM Ara A alone in the case of Chinese hamster

cells and in combination with coformycin (10 μmol.) in the case of human blood lymphocytes was added to cultures 30 min. before irradiation and washed off at different times depending on the experimental protocol.

3 aminobenzamide (3 AB) and cytosine arabinoside (araC) were used to study the influence of inhibitors on the yield of dicentrics and translocations. araC (5×10^{-5}M) was washed off 2h. following irradiation and the lymphocytes were cultured in the presence of deoxycytidine (10^{-4}M) till fixation. A final concentration of 10mM 3AB was used which remained in the medium throughout the culture period.

Results and Discussion:

A) Relation between initial radiation DNA damage and observed chromosome damage:

Under repair proficient conditions of DNA repair, DNA DSBs are considered to be the lesion leading to chromosomal aberrations induced by ionizing radiation. The estimate of DSBs induced by X-rays is around 40 to 80 per mammalian cell per Gy (Natarajan *et al.*, 1980). In human lymphocytes irradiated in Go stage, the frequencies of aberrations observed at the first division metaphase are very low (about 1% of the initial damage). If the lymphocytes are fused with mitotic cells immediately following X-irradiation about 3 excess fragments/cell/Gy are observed (Vyas et al., 1991). However, in the PCC technique repair of damage takes place during fusion and further incubation and thus the values obtained reflects the residual damage following a 45 min. repair. The formation of most of the exchange aberrations takes place during this period. In order to obtain an estimate the initial damage observable at chromosomal level, we have employed Ara A in combination with coformycin. Ara A is a known inhibitor of repair of DNA DSBs. Lymphocytes were pre-incubated for 30 min with Ara A (100 μM) prior to irradiation and fused with mitotic CHO cells in the presence of Ara A and incubated further in the presence of Ara A. By this method, it is expected that no repair takes place during the post fusion incubation, thus giving an estimate of initial chromosomal damage. A value of 5 excess breaks per Gy/lymphocyte was observed (Natarajan *et al.*, in preparation). Thus, only 6.25 to 12.5% of DSBs induced by X-rays result in visible chromosomal breaks at the PCC level. If the lymphocytes are pre- and post incubated in Ara A for two hours and allowed to recover in normal medium, about 75% of the breaks (estimated in PCCs in the presence of Ara A) form chromosomal aberrations (dicentrics, rings, translocations and fragments) as detected in the first mitotic metaphases .

B) Distribution of X ray induced lesions among the chromosomes and their repair.

It is generally assumed that ionizing radiation induced DNA lesions are randomly distributed among the chromosomes. It has been recognized from early studies that heterochromatic regions can respond differently from euchromatic regions to clastogenic damage. We have employed Chinese hamster embryonic fibroblasts, which have defined heterochromatic regions among their chromosomes to study the problem of heterogeneity of induction of damage by X-rays (Slijepcevic and Natarajan, 1994). In these cells, the long arms of X-chromosome, Y, 9, 10 chromosomes and short arms of chromosomes 5,6 and 7 are heterochromatic. Exponentially growing cells were X-irradiated (1 Gy) in the presence or absence of Ara A. The cells were allowed to recover 30 min. to facilitate those at mitosis could be excluded in the analysis. Following this, cells were fixed immediately (following 30 min. colcemid) at recovery times of 1,2, 3 and 4 hours. The cells irradiated in the presence of ara A were recovered in the medium containing Ara A. The number of breaks

and gaps in different chromosomes were scored for individual chromosomes. In the presence Ara A, there was no evidence of any rejoining of breaks over 4 h. The expected frequencies of breaks and gaps for individual chromosomes were calculated on the basis of relative chromosome length and random distribution and compared with the observed frequencies. Euchromatic chromosome 1 which represents 20.44% of the genome had about 35 % of damage, whereas chromosomes 6,7, 9,10, X and Y (which contain heterochromatin) had fewer aberrations than expected. Condensed chromatin appears to be resistant to radiation induced damage in comparison to uncondensed chromatin. This has been demonstrated earlier for human lymphocytes as well (Vyas *et al.*, 1991).

The repair of chromosome damage was also followed up to 4 h. in different chromosomes and there were some clear differences, e.g., chromosomes 8 and 9. They are of similar size, chromosome 8 and 9 being totally euchromatic and heterochromatic respectively. 12% and 56% of unrepaired damage was estimated in chromosome 8 and 9 respectively. Differences in the kinetics of repair was also found among the chromosomes indicating that the repair kinetics varies between eu- and hetero-chromatin (Slijepcevic and Natarajan,1994).

C) Non-random distribution of X-ray induced aberrations among the chromosomes of Chinese hamster embryonic cells.

The distribution of chromosome break points (exchange and deletion) from X-irradiated G1 cells was analyzed in G banded chromosomes (Slijepcevic and Natarajan., 1994). More break points were mapped to G-light bands (79.8%) than to G-dark bands (20.2%). Chromosomes 5 and 8 had more chromosome exchange break points than expected on the basis of chromosome length. X chromosome had more deletion break points and less exchange break points. The deficiency in the exchange break points in the long arm of X-chromosome is mainly due to the formation of distinct chromocentre thus limiting interaction with other chromosomes.

D) Frequencies of X-ray induced dicentrics and translocations.
i) *Human peripheral blood lymphocytes*:

Two major classes of aberrations induced by ionizing radiation in G0 or G1 cells are recognized, namely stable (balanced translocations) and unstable (dicentrics, rings and fragments). It was generally assumed that reciprocal translocations and dicentrics are formed in equal proportions following X-irradiation. Earlier studies relied on G banding techniques to quantify the frequencies of translocations. Recently introduced technique of fluorescent in situ hybridization (FISH) using human chromosome specific DNA libraries has considerably increased the resolution of detecting translocations.

In our initial study (Natarajan *et al.*, 1992) we employed two cocktails of DNA libraries of three human chromosomes (1,3,X and 2,4,8) to paint the chromosomes to detect X-ray induced translocations. It became obvious that in addition to reciprocal translocations, other types of translocations such as terminal translocations and interstitial translocations were encountered. When all types of translocations are taken into account, their frequencies were found to be 1.5 to 2 times more than the frequencies of dicentrics induced by a given dose of X-rays (Natarajan *et al.*, 1992). This observation was later confirmed by others. The question arose as to this increased frequency of translocations in comparison to dicentrics is due to misclassification of some of the dicentrics in the category of translocations and the contamination of second division cells, in which translocations and not dicentrics are likely to occur. Experiments designed to check these questions,(i.e., scoring of only first cell division and simultaneous painting with centromeric probes) showed clearly that the

increased frequencies observed translocations is not an artifact. Since at high doses of radiation or treatment with bleomycin or restriction endonucleases lead to complex aberration it became necessary to formulate a system of nomenclature for the structural aberrations detected by chromosome painting. Such a system called **PAINT** (Protocol for Aberration Identification and Nomenclature Terminology) was developed by a group of cytogeneticists (Tucker et al., 1994,). With this system, all exchange aberrations (dicentrics, fragments, all types of translocations) involving painted chromosomes and others can be evaluated simultaneously,thus, this system may prove useful in biological dosimetry of absorbed radiation dose in case of accidents.

ii) *Persistence of chromosome aberrations in different post-irradiation division* .

In order to estimate as to what proportion of stable and unstable aberrations pass through cell divisions, aberrations were analyzed by fluorescent in situ hybridization in the first three post irradiation (0 and 2 Gy) divisions. Lymphocytes were grown in the presence of BrdU, collected at different sampling times (47, 70 and 91 h) and analyzed using an alphoid centromeric probes and PCR amplified DNA libraries for chromosomes # 2 and 8. Following differential staining of sister chromatids , the analyzed cells were identified to be either in the first, second or third mitosis after irradiation. The frequencies of both dicentrics and fragments showed a reduction of about 50% after each cell generation whereas translocations were more persistent. Cells within the same post-irradiation division showed higher aberration frequencies when derived from later sampling times, indicating a delay in the progression of highly aberrant cells. As a result, the frequencies of dicentrics and fragments remained rather constant in different sampling times, if the cell cycle parameter is not taken into account. Thus, the average generation time of the lymphocytes had a clear effect on the obtained aberration frequencies. The combination of FISH technique with the differential staining of sister chromatids with Hoechst offers the possibilities to study the persistence of induced aberrations for three subsequent cell divisions (Boei, et al., 1995).

iii) *Mouse lymphocytes*:

Since laboratory mouse is used as a model for assessing human genetic risk to ionizing radiation, it is necessary to estimate the induction of translocations in mice. Unlike human chromosomes, it is difficult to identify individual chromosomes of mouse as all of them are acrocentric and not very different in length which makes it impossible to flow sort them. Fortunately, there are several mouse strains carrying complex or Robertsonian translocations which could be used for flow sorting. Cells derived from a mice strain carrying a translocation involving chromosomes 1, 11 and 13 were used by us for flow sorting and constructing chromosome specific DNA libraries (Natarajan *et al.*, 1993, Boei *et al.*,1994). We have generated dose response curves for induction of dicentrics and translocations in the splenocytes of X-irradiated mice. Since mouse chromosomes, except Y carry a prominent heterochromatic block near the centromere, it is not difficult to identify dicentric chromosomes in DAPI stained preparations, thus avoiding use of centromere specific DNA probes. Unlike human lymphocytes, the frequencies of translocations induced by X-rays are very close to the frequencies of dicentrics in mouse splenocytes (Boei *et al.*, 1994). This difference between the two species may be due to the characteristic karyotypic feature, (i.e., all acrocentrics) of mouse in comparison to human.

One of the problems encountered in the irradiated splenocytes of mice is the interpretation of Robertsonian fusion like figures as to whether these represent dicentrics or translocations. This can be resolved by probing chromosomal preparations with telomeric repeat sequences by FITC, with simultaneously staining with DAPI or propidium iodide (Fig. 1 A&B). The latter helps in identifying the centromeric heterochromatin and thus dicentric chromosomes

and the fragments contain two pairs of telomeric signals (Boei and Natarajan, in preparation).

E) Mis-repair process leading to the formation of dicentrics and translocations: Are they different ?

When human blood lymphocytes are X-irradiated in the presence and post-incubated with different types of inhibitors of DNA repair or agent which modifies the structure of the chromatin, an up to two fold increase in the frequencies of induced dicentrics is encountered. These agents include cytosine arabinoside-araC, 3 aminobenzamide, caffeine (Stoilov *et al.*,1994), Sodium butyrate . The increase in the frequency of dicentrics can be due to an increase in the frequency of initial X-ray induced DNA lesions or in the inhibition of repair of induced lesions. The latter will allow the unrepaired DNA lesions (DSBs) to interact, thus producing an increased frequency of dicentrics, by mis-repair process. It is of interest to check whether such inhibitors, which increase dicentric frequency do also increase the frequencies of translocations. We have employed ara C or 3 aminobenzamide to study their influence on the frequencies of X-ray induced dicentrics and translocations (using chromosome painting techniques). The results indicated that there was an increased frequencies of translocations over the dicentrics in X-irradiated lymphocytes. The inhibitors had no influence in the frequencies of induced translocations, while the frequencies of dicentrics increased by about a factor of 2 (Natarajan et al., 1994). These observations indicate that the mis-repair process leading to dicentrics and translocations may be different.

F. Influence of DNA repeat sequences on the formation of chromosome aberrations.

There are several repeat sequences present interdispersed among the chromosomes which may provide as hot spots for aberration formation. One such sequence is the telomeric repeats i.e., TTAGGG. In primary cells these repeats are confined to telomeric regions and in transformed cells, there are intercalary telomeric repeats present. Intercalary telomeric repeats have been suggested to be more prone for chromosome breakage and recombination .

Chinese hamster embryonic primary cells contain telomeric sequences at both ends of all the chromosomes.In addition all chromosomes except 1 and 2 have telomeric repeats present near the centromeric region. Chromosomes 8 and 10 are entirely painted by telomeric probes. In transformed Chinese hamster cells, CHO 9, the telomeric sequences at the end of the chromosomes are not detectable. Localization of telomeric sequences adjacent to centromeric regions was seen in many chromosomes, except for the two long pairs of chromosomes which were completely devoid of any telomeric signals. In Chinese hamster cells treated with restriction endonucleases a clear association between the aberrations and intercalary telomeric sequences has been found (Balajee *et al.*, 1994). Since most of the chromosomes of CHO cells have telomeric sequences present near the centromeres, as expected a large proportion of dicentrics contained two signals. However, when the two long pairs of chromosomes were involved in dicentrics, there were telomeric sequences present indicating that the apparent dicentrics are complex rearrangements. The number of fragments containing telomeric sequences in CHO cells was much higher than expected on random basis. Besides, some of the fragments hybridized totally with telomeric probes and the signals were so intense suggesting an amplification of the telomeric sequences in these cells.

We have generated DNA libraries for the Chinese hamster chromosomes and have probed Alu I treated cells with painting probes and telomeric probes. The results from painting probes alone indicated that many of the chromosomes in CHO and V79 cells contain translocations (Balajee *et al.* 1995). Besides, there appears to be hot spots for aberrations along the chromosomes .

Publications:

1. Balajee, A.S., and Natarajan, A. T., 1993. Restriction endonucleases *do* induce sister chromatid exchanges in Chinese hamster ovary cells, Mutation Research. 302, 25-31.
2. Balajee, A.S., Oh, H.J., and Natarajan, A.T., 1994. Analysis of restriction enzyme-induced chromosome aberrations in the interstitial telomeric repeat sequences of CHO and CHE cells by FISH. Mutation Research, 307, 307-313.
3. Balajee, A.S., Dominguez,I., and Natarajan A.T. (1995) Construction of Chinese hamster chromosome specific DNA libraries and their use in the analysis of spontaneous chromosome rearrangements in different cell lines. Cytogenetics & Cell Genetics. 70, 95-101.
4. Boei.J.W.A., Balajee, A.S., de Boer, P, Rens, W., Aten, J.A., Mullenders,L.H.F. and Natarajan.,A.T. 1994. The construction of mouse chromosome -specific DNA libraries and their use for the detection of X-ray induced aberrations. International J. radiation Biology, 65,583-590.
5. Boei, J.J.W.A., Vermeulen, S and Natarajan, A. T., (1995) Detection of chromosomal aberrations in the first three post-irradiation divisions of human lymphocytes. Mutation Research (in press).
6. Boei, J.J.W.A and Natarajan, A.T. (1995) Detection of chromosome malsegregation to the daughter nuclei in cytokinesis-blocked transgenic mouse splenocytes. Chromosome Research, 3,45-53.
7. Darroudi, F., Farooqi, Z, Benova, D. and Natarajan, A.T.(1992). The mouse splenocyte assay, an in vivo/in vitro system for biological monitoring: studies with X-rays, fission neutrons and bleomycin. Mutation Res. 272,237-248.
8. Dominguez, I., Pannerselvam, N., Escalza, P, Natarajan, A.T. and Cortes, F. (1993). Adaptive response to radiation damage in human lymphocytes conditioned with hydrogen peroxide as measured by the cytokinesis-block micronucleus technique. Mutation res. 301. 135-141.
9. Farooqi, Z., Darroudi, F. and Natarajan, A. T. (1993) Use of fluorescence in situ hybridization for the detection of aneugens in cytokinesis blocked mouse splenocytes. Mutagenesis 8, 329-334.
10. Natarajan, A. T (1993) Mechanisms of induction of mutations and chromosome aberrations. Env. Health Prospectives 101, suppl. 3. 225-229..
11. Natarajan, A.T., Darroudi, F and Ramalho, A.T. (1995) Cytogenetic indicators of radiation damage. In: "The Treatment of Radiation Injuries" Armed Forces Radiobiology Research Institute, Washington, USA. (in press).
12. Natarajan, A. T., Darroudi, F., Vermeulern, S., and Wiegant, J. (192) Frequencies of X-ray and fast neutron induced chromosome translocations in human peripheral blood lymphocytes as detected by in situ hybridization using chromosome specific DNA libraries. In: Low Dose Irradiation and Biological Defence Mechanisms. Eds. Sughara, T., Sagan, L., and Aoyama, T. Excerpta Medica, Elsevier, Amsterdam, 343-346.
13. Natarajan, A. T., Darroudi, F., Jha, A.N., Meijers, M., and Zdzienicka, M.Z., 1993, Ionizing radiation induced DNA lesions which lead to chromosomal aberrations.Mutation Research, 299, 297-303.
14. Natarajan, A.T., Tucker, J.D., and Sasaki, M.S. (1993) Monitoring cytogenetic damage in vivo. In: Methods to assess DNA Damage and Repair: Inter-species Comparisons. Eds. R.G.Tardiff, P.H.M. Lohman and G.N.Wogan. John Wiley & Sons. Ltd. New York. 95-106.
15. Natarajan, A. T., Vermeulen, S., Grigorova, M., Boei, J.J.W.I., Sakamoto-Hojo, E.T.,

Oh. H.J., and Darroudi, F. (1994). Fluorescence in situ hybridization in cytogenetic studies. In: Chromosomal Alterations: Origin and Significance. Ed. G. Obe and A.T. Natarajan, Springer Verlag, Heidelberg, pp.50-56.

16. Natarajan, A.T., Vyas, R.C., Darroudi, F., and Vermeulen, S. 1992. Frequencies of X-ray induced chromosome translocations in human peripheral lymphocytes as detected by *in situ* hybridization using chromosome specific DNA libraries.International J. Radiation Biology, 61, 199-203.

17. Natarajan, A. T., Balajee, A.S., Boei, J.J.W.A., Chatterjee, S., Darroudi, F., Grigorova, M., Oh, H.J., Slijepcevic, P., and Vermeulen, S, (1994). Recent Developments in the assessment of chromosomal damage. International J. Radiation Biology, 66, 615-623.

18. Slijepcevic, P., and Natarajan, A.T.,1994., Distribution of X-ray induced G2 chromatid damage among Chinese hamster chromosomes: influence of chromatin configuration.Mutation Research, 323, 113-119.

19. Slijepcevic, P. and Natarajan, A. T., 1994, Distribution of radiation induced G1 exchange and terminal deletion break points in Chinese hamster chromosomes as detected by G banding.International J. Radiation Biology , 66, 747-755.

20. Stoilov, L.M., Mullenders, L.H.F., and Natarajan, A. T. 1994. Caffeine potentiates or protects against radiation-induced DNA and chromosomal damage in human lymphocytes depending on temperature and concentration. Mutation Research, 311, 169-174.

21. Tucker, J.D., Morgan, W.F., Awa, A.A., Bauchinger, M., Blakey D., Cornforth, M.N., Littlefield, L.G., Natarajan, A.T., and Shasserre, C., 1994, A system of nomenclature for structural aberrations detected by chromosome painting. Cytogenetics and Cell Genetics 68, 211-221.

Head of project 3: Dr. Ortins

II. Objectives for the reporting period

Assessment of cytogenetic damage on individuals in Portuguese uranium mines and studies of the adaptive response for radiation-induced chromosomal aberrations on low and highly exposed workers of Portuguease uranium mines.

III. Progress achieved including publications

1. Introduction
      Several studies show that small doses of ionising radiation induce an adaptive response to subsequent high doses. As we are doing cytogenetic studies of people working on Portuguese uranium mines for biomonitoring purposes, we use this opportunity to know if that people were more or less adapted to subsequent ionising radiation doses.
      For these studies we address the following questions:
1. Can the dose received by miners, function like a prime dose for an adaptive response when they have a subsequent high exposition dose and this equal or different for low or high exposed individuals.
2. What is the capacity for adaptive response of lymphocytes from miners when they are primed with a low dose of 5 cGy and exposed at a challenge dose of 300 cGy.

2. Material and Methods
      The control group was composed by workers non-miners from one region with low level of background radiation (Table 1). Two groups of miner workers were selected on the base of their historical monitoring doses, one as low exposed (Table 2) and another as

high exposed (Table 3).

· TABLE 1
Control workers non-exposed

No.	Age	Sex	Smoke	Dose (cSv)
1	49	M	N	1.28
2	44	M	N	1.01
3	42	M	N	1.12
4	46	M	N	1.26
5	44	M	N	1.15

Table 2
Uranium miners workers selected as low level exposed

No.	Age	Sex	Smoke	Dose (cSv)
1	42	M	N	9.9
2	45	M	N	8.9
3	45	M	N	7.8
4	48	M	N	9.4
5	37	M	N	11.5

Table 3
Uranium miners workers selected as high level exposed

No.	Age	Sex	Smoke	Dose (cSv)
1	41	M	N	24.7
2	43	M	N	25.9
3	44	M	N	25.5
4	40	M	N	19.5
5	45	M	N	24.7

The induction of adaptive response was done on all groups on G_1, with 5 cGy and the challenge dose was done 5 hours after with 300 cGy of γ rays (^{60}Co.).
Heparinized blood samples from each donor were collected by venepuncture and whole blood cultures were made.
The peripheral lymphocytes blood cultures were set up in 15 ml glass bottles adding 0.5

ml of whole blood to 5 ml of RPMI 1640 medium containing 15% of new-born calf serum, 2 mM L-glutamine, 100 U/ml of penicillin, 100 μg/ml of streptomycin and 2% of PHA and kept at 37°C. Five hours after beginning of the cultures the lymphocytes in glass bottles were irradiated with a priming dose of 5 cGy from a Cobalt source gamma rays, and 5 hours later irradiated with a challenge dose of 300 cGy. The lymphocytes were then cultured till 48 hours and for the last 2 hours the cells were treated with 1 μg/ml colcemid. Lymphocytes were collected, treated with 75 mM potassium chloride for 10 min and fixed in 3:1 methanol acid acetic mixture.

Fixed cells were dropped onto clean slides and stained with Hoechst plus Giemsa in order to distinguish first division metaphases.

Coded slides were analysed for chromosome type aberrations and 200 metaphases were scored for each data point.

Results

The results obtained in the experiments for all groups are presented in Tables 4-6 and Figs. 1-3.

We saw that in the control group composed by 5 workers non-miners from one region with low level of background, 4 of them show adaptive responses, when we look for chromosomal type aberrations frequency induced by a challenge dose of 300 cGy on peripheral lymphocytes pre-exposed to an adaptive dose of 5 cGy Gamma rays (Table 4 and Fig. 1).

The two groups of uranium mine workers selected as low and as high level exposed, display a different frequency of adaptive response (Tables 5-6 and Figs. 2-3).

In the group of 5 uranium mine workers low level exposed, 4 of them show adaptive response, and in the group of 5 uranium mine workers high level exposed only 2 of them show adaptive response.

TABLE 4

CHROMOSOMAL TYPE ABERRATIONS FREQUENCY INDUCED BY A CHALLENGE DOSE OF 300 cGy ON PERIPHERAL LYMPHOCYTES PRE-EXPOSED TO AN ADAPTIVE DOSE OF 5 cGy GAMMA RAYS ON CONTROLS NON-EXPOSED

Treatment Doses

No.	0 cGy	5 cGy	300 cGy	5+300 cGy	Expected
1	0.005	0.015	0.7458	0.714	0.755
2	0	0.01	0.7867	0.746	0.796
3	0.015	0.025	0.8034	0.774	0.813
4	0.005	0.015	0.6856	0.650	0.695
5	0.01	0.015	0.7231	0.735	0.728

Counted 200 cells per point.
Expected = sum of the 2 individual treatments minus the control

Table 5
CHROMOSOMAL TYPE ABERRATIONS FREQUENCY INDUCED BY A CHALLENGE DOSE OF 300 cGy ON PERIPHERAL LYMPHOCYTES PRE-EXPOSED TO AN ADAPTIVE DOSE OF 5 cGy GAMMA RAYS ON URANIUM MINERS WORKERS SELECTED AS LOW LEVEL EXPOSED.

Treatment Doses

No.	0 cGy	5 cGy	300 cGy	5+300cGy	Expected
1	0.01	0.03	1.308	1.275	1.328
2	0.049	0.035	1.386	1.23	1.371
3	0.04	0.02	1.26	0.866	1.24
4	0.025	0.03	1.063	1.145	1.068
5*	0.03	0.05	0.830	0.810	0.850

Counted 200 cells per point.
Expected = sum of the 2 individual treatments minus the control

TABLE 6

CHROMOSOMAL TYPE ABERRATIONS FREQUENCY INDUCED BY A CHALLENGE DOSE OF 300 cGy ON PERIPHERAL LYMPHOCYTES PRE-EXPOSED TO AN ADAPTIVE DOSE OF 5 cGy GAMMA RAYS ON URANIUM MINERS WORKERS SELECTED AS HIGH LEVEL EXPOSED.

Treatment Doses

No.	0 cGy	5 cGy	300 cGy	5+300cGy	Expected
1	0.025	0.025	1.43	1.378	1.43
2	0	0.015	1.405	1.195	1.42
3	0.015	0.015	1.265	1.56	1.265
4*	0.065	0.025	0.565	0.62	0.525
5*	0.03	0.025	0.565	0.59	0.535

Counted 200 cells per point
*= Challenge dose 200 cGy.
Expected = sum of the 2 individual treatments minus the control

Fig 1

CONTROL WORKERS NON-EXPOSED

Legend: 0 cGy, 5 cGy, 300 cGy, 5+300 cGy, Expected

Y-axis: Aberrations/cell
X-axis: Donor number

Fig 2

URANIUM MINERS WORKERS SELECTED AS LOW LEVEL EXPOSED

Legend: 0 cGy, 5 cGy, 300 cGy, 5+300 cGy, Expected

Y-axis: Aberration/cell
X-axis: Donor number

Fig 3

URANIUM MINERS WORKERS SELECTED AS HIGT LEVEL EXPOSED

Legend: 0 cGy, 5 cGy, 300 cGy, 5+300 cGy, Expected

Y-axis: Aberration/cell
X-axis: Donor number

Discussion

Our observations show the ability of peripheral lymphocytes of the mine workers to display adaptive response after induction with a small dose of 5 cGy on G_1 and a challenge dose of 300 cGy. Because the small number of miners studied we can not say that the difference of adaptive response between low and high level exposed is significative.

We saw on some mine workers, (2 low level exposed and 2 high level exposed) that the frequency of chromosomal type aberrations after 5 cGy is less than background. If this is confirmed on more cases it means some kind of adaptation to small doses that we did not see on the control group.

Publications

Pereira Luís, J.H. and V. Póvoa (1992) Individual variability of adaptive response of human lymphocytes primed with low dose gamma rays, In: Low dose irradiation and biological defense mechanisms (eds. T. Sugahara, L.A. Sagan and T. Aoyama), Elsevier Science Publishers, pp. 315-317.

Silva, M.J., J.H. Pereira Luís (1993) Dose-response relationship for gamma-radiation induced micronuclei in cytokinesis blocked human lymphocytes, European Society of Human Genetics, Proc. 25th Annual Meeting, Barcelona, Espanha.

Piper, J., M.J. Silva, J.H. Pereira Luís (1993) Yield and distribution of micronuclei in CB human lymphocytes after gamma-radiation, Proc. Concerted Action on Automation in Cytogenetics, Vimeiro, Portugal.

Pereira Luís, J.H. (1993) Assessment of cytogenetic damage on individuals working on Portuguese uranium mines, Proc. CEC Meeting on studies in radiation induced chromosomal aberrations, Naxos, Grecia.

Silva, M.J., M.G. Boavida, J. Piper, J.H. Pereira Luís (1994) Dose dependence of radiation-induced micronuclei in cytokinesis-blocked human lymphocytes, Mutation Res., 322, 117-128.

Pereira Luís, J.H. (1994) Intercalibraçao em dosimetria citogenética, Proc. do V Congreso Nacional de la Sociedade Espanhola de Proteccion Radiologica, pg. 601-604, Santiago de Compostela, Espanha.

Head of project 4: Dr. Bryant

II. Objectives for the reporting period

1) To study of the mechanisms involved in conversion of specific types of DNA double-strand breaks (dsb) into chromosomal aberrations, especially in the radiosensitive mutant Chinese hamster (e.g. *xrs5, irs2*) and human AT cell lines.

2) To investigate the putative structural or chromatin differences in radiosensitive mutant cell lines by analysis of DNA binding properties of nuclear proteins.

3) To investigate the possibility of altering radiosensitivity by complemention using the technique of introducing cell or nuclear extracts into irradiated and restriction endonuclease treated porated cells.

4) To study the repair of dsb in xrs5 and CHO cells in detail using a recently developed filter elution technique able to detect specific damage in chromatin loops.

III. Progress achieved including publications

Studies on chromosomal responses of AT and mutant radiosensitive cell lines.

Ataxia telangiectasia cells
The chromosomal responses of lymphoblastoid AT cells to gamma-radiation and to the restriction endonucleases (RE) *PvuII* and *BamHI* have been studied in order to test the possibility that AT cells have a dsb processing defect. We have shown that RE treatment of porated human cells mimics the clastogenic effect of radiation in causing both break and exchange-type aberrations. Our results show that like gamma-rays, PvuII induces a higher frequency of aberrations in AT than normal cells (by a factor of 5) at both 5 and 24 h sampling times (figures 1a and b). Dsb induced by PvuII (blunt-ended) were found to be much more effective than cohesive-ended dsb in causing chromosomal aberrations, as found previously for rodent cells.
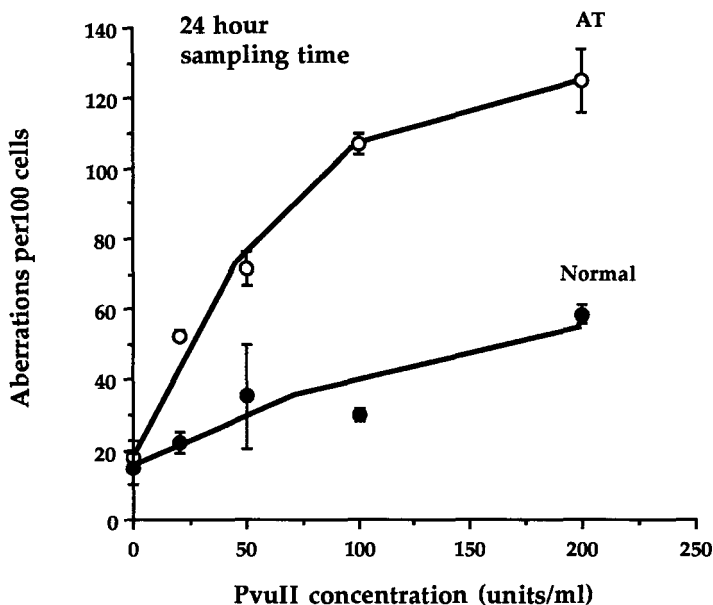
Figure 1b. Frequencies of chromosomal aberrations in ataxia telangiectasia and normal lymphoblastoid cells after treatment with PvuII, and sampled at 24h following treatment (Redrawn from Liu and Bryant 1993).

irs2 and VC4 cells
We found (Bryant et al 1993, Mutagenesis, 8, 141-147) that radiosensitive *irs2* cells, which have normal rejoining of radiation-induced dsb, yield a 2-4 fold higher break and exchange-type chromosomal aberration frequency as compared to the wild-type V79 parental cell line when porated with streptolysin O and treated with PvuII. The frequencies of dsb induced by PvuII was the same in irs2 and V79 cells as measured by neutral elution.

VC4, shown by cell fusion and colony assays to be in the same complementation group as irs2 (Thacker and Wilkinson 1991, Mutation Res. 254, 135-142) shows higher levels of radiation-induced chromosomal aberrations (Zdienicka et al, 1989, Cancer Res. 49, 1481-1485) but has been reported to show normal response to restriction endonucleases (AluI and BamH1), a normal cellular and chromosomal response to neutrons, but a 4-5 fold elevated sensitivity to UV (Natarajan et al 1993, Mutation Research, 299, 297-303).

Our own experiments showed that, in contrast to the results of Natarajan et al (1993) VC4 cells showed a 5-6 fold elevated chromatid aberration frequency to PvuII treatment as compared with the WT parental line (Figure 2 and Bryant and Liu, 1994, International Journal of Radiation Biology, 66, 597-601).

We therefore conclude that VC4, irs2 and AT cells, which are all highly chromosomally radiosensitive but show normal dsb rejoining, carry a dsb carry a defect which causes them to convert a higher proportion of radiation or restriction endonuclease induced dsb into visible chromatid breaks and exchanges.
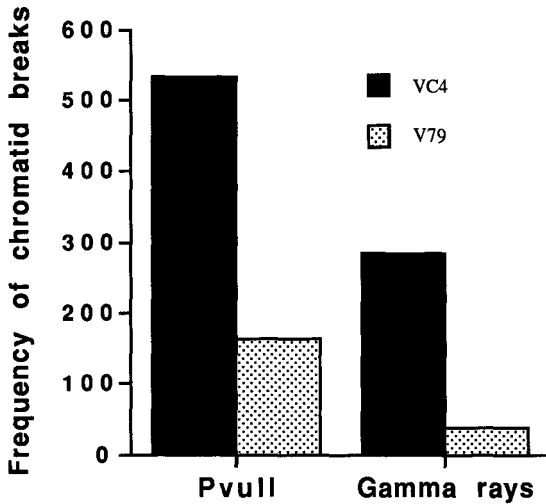
Figure 2. Frequencies of metaphase chromatid breaks in irradiated (1.54 Gy) and restriction endonuclease (PvuII; 2.5 units/ml) treated VC4 cells (redrawn from Bryant and Liu, 1994).

Studies on nuclear extracts of radiosensitive cells.

Nuclear extracts of xrs5 and CHO cells
Nuclear protein extracts were derived from CHO and *xrs5* cells by a detergent free system involving the sequential washing of nuclei released by homogenisation with buffers of increasing ionic strength. Spermine hydrochloride (6mM) was also included to facilitate nuclear protein removal and maintain a compact DNA structure during extraction. The two ionic strength fractions: 100mM KCl and 250 mM $MgCl_2$ were used. A protein binding assay involving the binding of ^{32}P labelled calf thymus DNA to the extracts was performed on extracts derived from non-irradiated cells and extracts from cells exposed to 10 Gy gamma rays followed by 30 minutes incubation at 37°C prior to extraction. The results from the non-irradiated fractions are shown in figure 3. The irradiated fractions gave similar results although both the 250 mM fractions were greater than the non-irradiated fraction. It is noticeable that the 100 mM extracts show non-specific linear binding to DNA whilst 250 mM extracts approximate to normal inverse exponential enzyme kinetics. Comparative regression analysis of the data gives the relative binding activity of *xrs5* fractions compared to CHO fractions (Table I). No difference is observed between the 100 mM extracts whilst the 250 mM extracts show a reduced DNA binding activity of *xrs5* proteins.
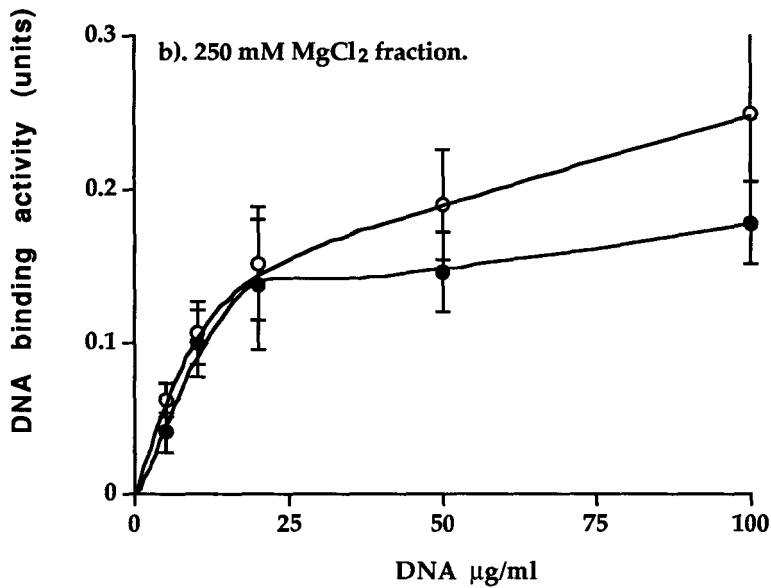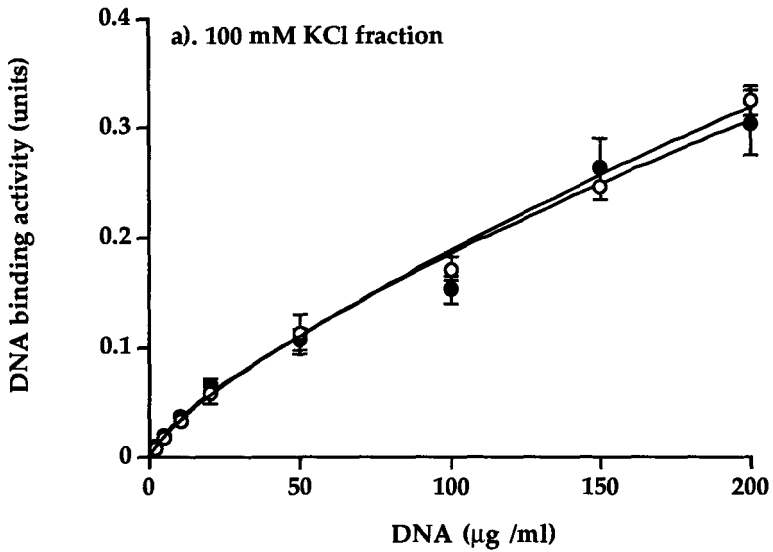
Figure 1. DNA binding activities of non-irradiated extracts of CHO (open symbols) and *xrs5* (closed symbols) versus an increase in the concentration off calf thymus DNA. a) 100 mM KCl fraction b) 250 mM MgCl2 fraction. Error bars show standard error of the mean of 4-8 experiments. (from P. J. Johnston, PhD Thesis, University of St Andrews, 1994).

	Relative DNA binding activity.	R^2	P
100 mM	0.938	95.3%	<0.001
100 mM (irradiated)	1.080	91.1%	<0.001
250 mM	0.724	71.4%	<0.001
250 mM (irradiated)	0.666	90.5%	<0.001

Table I. Relative DNA binding activity of *xrs5* extracts compared to CHO extracts. R^2 is the correlation coefficient and P is the confidence value of the analysis of regression. Figures derived from the correlation of individual data points from 3-7 independent experiments (from P. J. Johnston, PhD Thesis, University of St Andrews, 1994).

From Table II it is apparent that there are differences between CHO and *xrs5*. In addition to binding more DNA per μg of extract, CHO extracts have a reduced initial rate. This would indicate that the affinity of individual binding sites is reduced.

	Δ (units μg^{-1} ml^{-1})	V_{max} (units)	K_m (μg ml^{-1})
CHO	0.016 ($\pm$0.0029)	0.290 ($\pm$0.084)	18.58 ($\pm$3.66)
Xrs5	0.027 ($\pm$0.0115)	0.199 ($\pm$0.026)	14.95 ($\pm$5.93)
CHO (irradiated)	0.019 ($\pm$0.00200)	0.356 ($\pm$0.087)	18.57 ($\pm$3.38)
Xrs5 (irradiated)	0.037 ($\pm$0.0150)	0.241 ($\pm$0.050)	17.87 ($\pm$5.28)

Table II Kinetics of DNA binding by 250 mM extracts. Where Δ = initial rate of binding, V_{max} is the maximum amount of DNA bound per μg extract, K_m = Michaelis constant which is the concentration of DNA required to give half V_{max}. Results show the standard error of the mean of 3-4 independent experiments (from P. J. Johnston, PhD Thesis, University of St Andrews, 1994).

Therefore it appears that CHO extracts have more DNA binding sites per μg than *xrs5* extracts, but that these sites have a lower affinity for DNA. This results in the Michaelis constant showing only a slight variability between cell lines. These kinetic evaluations can only be taken as approximate since the extract fractions studied are still relatively crude and can not be expected to follow ideal Michaelis-Menten kinetics. This is apparent in the large errors associated with the values.

In further experiments, nuclear extracts of xrs5 and CHO cells were prepared in detergent-free buffer in a Dounce homogeniser. Spermine hydrochloride was added at 6mM to increase protein removal and to maintain chromatin structure. Nuclei were then subjected to sequential extraction with ionic buffers of varying strengths (100-2000mM). We previously reported differences in DNA binding between proteins from xrs5 and CHO extracted at 250mM MgCl$_2$. During the reporting period we extended these data by increasing the ionic concentration of nuclear extraction buffers to either 600 or 1000mM NaCl we showed that further proteins were extracted and clear differences were observed in two proteins of MW 31.8 and 32.2 Kdal as determined by PAGE electrophoresis. Minor changes in other bands were also observed.

The 31.8 and 32.2 Kdal bands (Figure 3) are thought to represent members of the histone H1 family associated with DNA. South-Western blotting using ^{32}P labelled DNA (Figure 1) showed that these proteins exhibit a lower degree of DNA binding in xrs5 than in CHO, confirming the general observation we have made, namely that xrs5 show a reduction in the apparent amount of DNA bound. The proteins have not yet been characterised although this will be carried out in the future. We have suggested that these proteins with altered DNA binding properties may relate to the reported altered chromosome and perinuclear structure in the xrs5 mutant.

The fact that the DNA binding properties of several proteins appears to be altered suggests a defective control mechanism in xrs5 which may be responsible for the post-translational modification of specific proteins. One possibility being investigated is that xrs 5 possesses altered protein kinase(s) or that the control of these is changed. The recent observation that the XRCC5 gene product has homology with the human Ku 80 protein, a DNA end binding protein which has protein kinase affinity may be significant in the context of our findings.
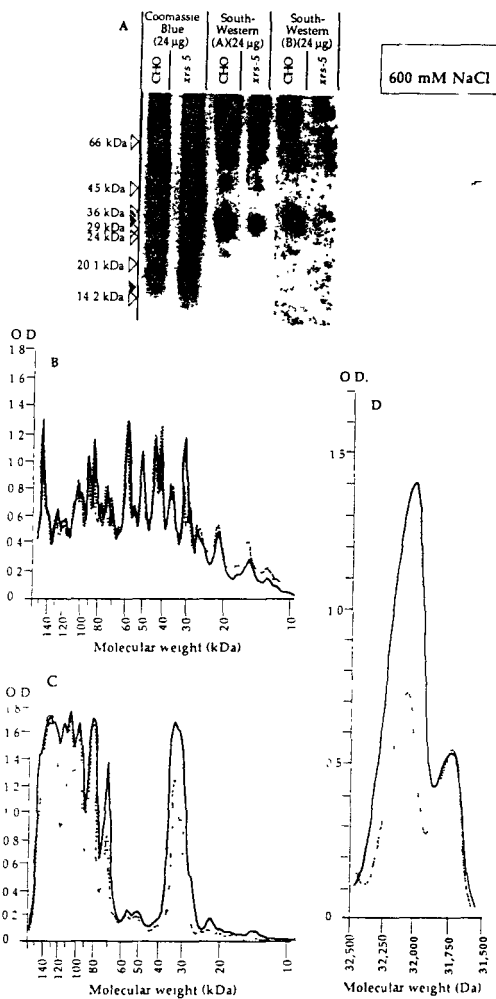
Figure 3. PAGE separation of 600 mM nuclear extract and South-Western blotting. Equal amounts of nuclear extract from xrs5 and CHO cells were loaded on gels. The resultant separated proteins were either stained with (A) Coomassie blue or South-Western blotted (type A = non-competitive, type B = competitive. Marker protein molecular weights are indicated by open triangles. Closed triangles represent the positions of major DNA binding bands of purified calf-thymus histone H1. (B) densitometric trace of Coomassie blue electrophoretograph, (C) densitometric trace of South-Western blot (type A) and (D) expanded trace of the Coomassie blue electrophoretograph of p32.2 and 31.8. Solid line = CHO, dotted line = xrs5. The Y axis represents the optical density of the bands. The X axis represents the approximate molecular weights of the bands as calculated from the position of the marker proteins.

Introduction of wild-type cell nuclear extracts into damaged cells

xrs5 cells

To date attempts to complement the defect in *xrs5* by introduction of wild type (CHO derived) proteins by streptolysin-O induced poration and measurement of damage by the micronucleus assay have been unsuccessful. The identification of biochemically altered proteins may enable complementation to occur. However, solubility of some proteins extracted under high salt conditions has prevented relevant experiments.

Ataxia telangiectasia cells

Nuclear extracts prepared form lymphoblastoid normal AT cells have been tested for DNA ligase, nuclease, and topoisomerase activity using an in vitro plasmid assay. The extracts were shown to have strong topoisiomerase activity, but no detectable ligase or nuclease activity. When nuclear extracts (prepared by Dounce homogenisation) from normal cells were porated (using streptolysin O) into gamma-irradiated AT cells and the frequencies of chromosomal aberrations measured, no decrease was detected. However, when nuclear extracts were porated into cells treated simultaneously with Pvu II, frequencies of chromatid aberrations (principally breaks) were 5 fold lower than in cell porated and treated with PvuII alone (Figure 4). When AT cells were treated with PvuII and nuclear extract from AT cells, no decrease in breaks was observed. Thus functional complementation is observed but at this stage the nature of the protein or factor responsible for this decrease in aberrations is not known. Since the extracts showed no ligase activity in the in vitro assays we assume that the protein (or factor) in the extract is not a DNA ligase. Also, introduction of T4 ligase into AT cells did not reduce the frequency of aberrations in PvuII treated cells.
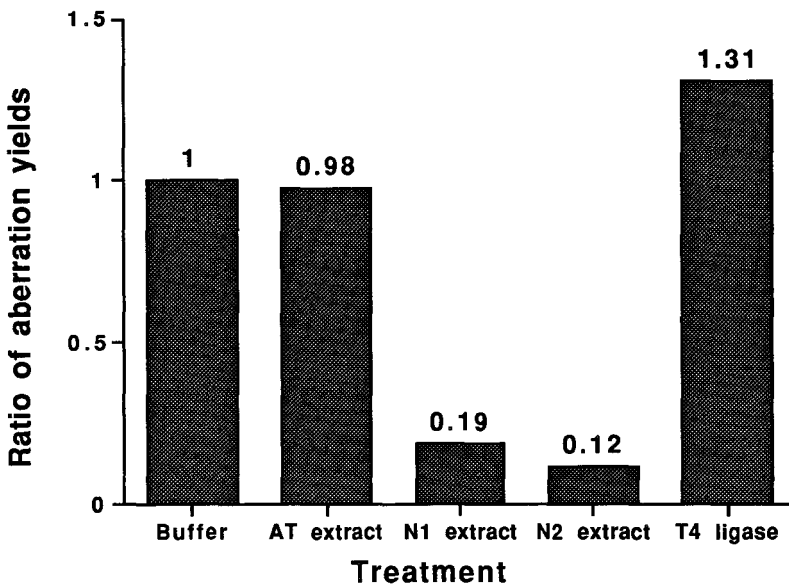
Figure 4. A comparison of the ratios of yields of PvuII (125 units/ml) induced chromosomal aberrations to the control (in the presence of buffer) in streptolysin (0.3 units/ml) porated AT cells. Cells were treated with: Buffer alone (HBSS/BSA), AT extract, Normal cell extracts (N1 and N2 represent two independent experiments), or T4 ligase. Chromosomal aberrations were analysed in colcemid blocked cells at 5h after treatment.

DNA double-strand break repair in xrs5 cells using non-ionic filter elution (NINFE)

Measurement of dsb induction and repair by neutral filter elution involves the disruption of chromatin and nuclear matrix of the cell by ionic detergents and protease. The harsh treatment removes the higher order chromatin structures which would interfere with elution of DNA containing dsb.

In these experiments we adopted the approach of lysing cells in non-ionic detergent in the presence of 2M salt (Johnston and Bryant, 1994, Int. J. Radiat. Biol. 66, 531-536). This procedure (NINFE) results in histone depleted structures (essentially nuleoids) that retain the higher order nuclear matrix organisation, including chromatin loops. Elution from such looped structures would only be possible if 2 or more dsb lie in a looped domain.

Evidence suggests that the nuclear organisation of xrs5 may be different from the WT CHO cell line. Therefore using NINFE we examined the induction and repair of dsb after irradiation in these cell lines. Experiments showed that the elution with NINFE was 5 times reduced compared to normal (ionic-detergent) filter elution (INFE). There was no significant difference in induction of breaks in xrs5 and CHO with NINFE. This indicates that the loop size is similar in xrs5 and CHO confirming reports by Schwartz et al 1993, Mutagenesis, 8, 105-108).

Repair of dsb analysed by NINFE (200Gy) showed no fast component but a large difference in slow repair analysed up to 16h. CHO showed a slow exponential component t1/2=5h. It is possible that the defect in xrs5 in the result of dsb misrepair. The release of dsb joined at the nuclear matrix which would be registered as repair by INFE but not by NINFE which would still measure the release of a fragment. Sequential treatment with NINFE and INFE showed that xrs5 accumulated elevated frequencies of dsb indicating that misjoining of matrix related dsb does not occur.

Repair of multiple dsb/loop may require an additional repair system which may have a requirement for a structural component. The multiple lesion repair seems to be defective in xrs5. The 60Kbp loops are clustered in 2-7Mbp looped domains and these larger units have been implicated in cellular sensitivity. That 50% elution occurs after 200Gy suggests that it is in these loop clusters rather than 60kbp loops that dsb are detected by NINFE.

Publications over the period of the grant.

Bryant, P.E. (1992) Induction of chromosomal damage by restriction endonuclease in CHO cells porated with streptolysin O. Mutation Research, 268, 27-34.

Macleod, R.A.F., and Bryant, P.E. (1992) Effects of adenine arabinoside and coformycin on the kinetics of G2 chromatid aberrations in X-irradiated human lymphocytes. Mutagenesis, 7, 285-290.

Bryant, P.E. (1992) Mimicking radiation with restriction endonucleases. British Journal of Radiology,Supplement 24, 35-38.

Bryant, P.E. and Johnston, P.J. (1993) Restriction endonuclease induced DNA double-strand breaks and chromosomal aberrations in mammalian cells. Mutation Research, 299, 289-296.

Johnston, P.J., and Bryant, P.E. (1993) Chromosome damage induced by nanomolar concentrations of bleomycin in porated mammalian cells. Biochemical Pharmacology, 45, 569-572.

Bryant, P.E., Jones, N.J. and Liu, N. (1993) Radiosensitive Chinese hamster irs 2 cells show enhanced chromosomal sensitivity to ionising radiation and restriction endonuclease induced blunt-ended double-strand breaks. Mutagenesis, 8, 141-147.

Liu, N. and Bryant, P.E. (1993) Response of ataxia telangiectasia cells to restriction endonuclease induced DNA double-strand breaks: I. Cytogenetic characterization. Mutagenesis, 8, 503-510.

Bryant, P.E. and Slijpecevic, P. (1993) G2 chromatid aberration kinetics and possible mechanisms. Environmental and Molecular Mutagenesis, 22, 250-256.

Bryant, P.E. (1994) Responses of radiosensitive mutant mammalian cells to restriction endonuclease induced DNA double-strand breaks. In "Chromosomal alterations: Origin and Significance", Eds. G. Obe and A.T. Natarajan, Springer Verlag, pp 160-168.

Mateos, S., Slijepcevic, P., MacLeod, R.A.F. and Bryant, P.E. (1994) DNA doouble-strand break repair in xrs5 cells is more efficient in the G2 than in the G1 phase of the cell cycle. Mutation Research DNA Repair Reports, 315, 181-187.

MacLeod, R.A.F., Voges, M., Bryant, P.E. and Drexler, H.G. (1994) Chromatid aberration dose response, dispersal and kinetics, in G2 human lymphocytes treated with bleomycin: comparison with equivalent X-irradiation reveals formation of a novel class of heavily damaged cells. Mutation Research, 309, 73-81

Liu, N. and Bryant, P.E. (1994) Enhanced chromosomal response of ataxia telangiectasia cells to specific types of DNA double-strand breaks. International Journal of Radiation Biology, 66, S115-S121.

Bryant, PE. and Liu, N. (1994) Responses of radiosensitive repair-proficient cell lines to restriction endonucleases. International Journal of Radiation Biology. 66, 597-601.

Johnston, P.J. and Bryant, P.E. (1994) A component of DNA double strand break repair is dependent on the spatial orientation of the lesions within the higher order structures of chromatin. International Journal of Radiation Biology, 66, 531-536.

Riches, A. C., Herceg, Z., Bryant, P.E. and Wynford-Thomas, D. (1994) Radiation-induced transformation of SV40-immortalised human thyroid epithelial cells by single and fractionated exposure to gamma-irradiation in vitro. International Journal of Radiation Biology, 66, 757-765.

Slijepcevic, P. and Bryant, P.E. (1995) Absence of terminal telomeric FISH signals in chromosomes from immortal Chinese hamster cells. Cytogenetics and Cell Genetics, 69, 87-89.

Symonds, R.P., Clark, BJ., George, W.D., Bryant, P.E. and Connor, J.M. (1995) Thrombocytopenia, absence of radii (TAR) syndrome: a new increased cellular radiosensitivity syndrome. Clinical Oncology, 7, 56-58.

Head of the project 5: Dr. Pantelias

II. Objectives for the reporting period
  1. To elucidate the mechanisms of chromosomal aberration formation through the analysis of induction and repair of radiation-induced damage in interphase cells by means of the PCC technique.
  2. To study radiosensitization processes and the nature of cell-cycle-dependent fluctuations in radiosensitivity.
  3. To study the nature of the variability in human radiosensitivity and the enhanced G_2 chromatid radiosensitivity in tumour cells and in cells from cancer prone individuals.

II. Progress achieved

In recent years evidence has been accumulated implicating dsb as the initial lesions leading to chromatin fragmentation, chromosome aberration formation and, ultimately, to reproductive cell death. Yet, factors and processes that determine transformation of radiation-induced DNA damage to lethal chromosome aberrations and intrinsic cell and cell-cycle stage relative radiosensitivity, are not well understood. It is usually assumed that cells would sustain the same amount of initial damage per unit amount of DNA at all times during the cell cycle, but the efficiency with which dsb are repaired would affect the formation of chromosomal aberrations (deletions or exchanges) and determine, therefore, relative radiosensitivity. The kinetics of repair, however, have been reported to be similar throughout the cell cycle. In particular, when cells are irradiated at metaphase, their chromosomes appear undamaged despite the presence of gross dsb, reported to rejoin at rates comparable to those observed in exponentially growing cells. Furthermore, radiosensitive mutant cell lines (e.g. irs1. irs2, irs3 isolated from V-79 cells) display increased sensitivity to ionizing radiation-induced killing without exhibiting measurable alterations in the rejoining of dsb. Ataxia telangiectasia (AT) cells are also known to have normal repair of radiation-induced dsb but show 2-3 fold higher frequency of radiation-induced chromosomal aberrations than normal human cells.

These disparities can only be understood assuming that the factors or processes which convert radiation-induced molecular lesions into lethal chromosome aberrations are cell-type and cell-cycle-stage dependent and independent from the rejoining rate of dsb.

1. **Induction and repair of radiation-induced chromosome fragments in the radiosensitive mutant irs-1 and wild-type V79 interphase cells.**

Induction and rejoining of interphase chromosome breaks were measured using premature chromosome condensation after exposure of plateau-phase V79 and *irs-1* cells to X-rays.

There was no difference in the induction of interphase chromosome breaks per Gy between the radiosensitive *irs-1* mutant cells and the wild type V79 cells despite the large differences in their radiosensitivity; an induction of 2.85 ± 0.05 breaks/cell/Gy was measured in both cell lines. Also, rejoining of interphase chromosome breaks proceeded in the two cell lines with similar kinetics ($t_{1/2} = 26.2$ min). In contrast, ring chromosome formation was higher in *irs-1* cells, as compared to wild-type V79 cells (0.78 versus 0.44 after 6h of repair). These results confirm previous observations suggesting that a general deficiency in the rejoining of DNA dsb is unlikely to be a direct cause of the increased radiosensitivity of *irs-1* cells, and are consistent with the hypothesis that the increased radiosensitivity of these cells derives from an increase in the probability of misrepair.

2. Radiosensitization processes
2.1. Hyperthermia at above or below 42.5 °C affects different forms of radiation-induced interphase chromosome breaks.

A large number of alterations have been observed in cellular structures and functions after exposure to heat and have been considered in the mechanism of heat-induced radiosensitization and cell killing. However, a direct causal relationship between alteration in nuclear architecture and the various effects of heat treatment was not possible since interphase chromatin and the nucleoli could not be visualized by means of conventional cytogenetic techniques.
Using the PCC method we have shown that exposure of interphase cells to elevated temperatures (42-45 oC) induces dramatic changes in chromatin conformation and a reduced ability of chromatin to condense and of the nucleoli to disintegrate under the influence of factors provided by the mitotic PCC inducer cells.
The effect of such alterations in nuclear architecture on the induction and repair of radiation-induced interphase chromosomal aberrations were thoroughly investigated (Pantelias and Iliakis, manuscripts in preparation). Plateau phase CHO cells pre-exposed to heat (45.5 °C) for up to 15 min in fresh growth medium without serum, were irradiated and either analyzed immediately or returned to the incubator at 37 °C in their conditioned medium. At various times thereafter (up to 24 h), flasks were trypsinized and assayed by means of the PCC method for excess chromosome fragments. Alternatively, cells were first irradiated and subsequently allowed for repair either at 37 or at 41 or 42 °C for up to 6h. The results obtained clearly indicated a significant reduction in the ability of cells to repair radiation-induced chromosome damage if kept at elevated temperatures after irradiation. The experiments also indicated an increase in the induction by radiation of chromosome damage in cells heated before irradiation, but not significant alterations in the rate of repair. An increase in misrepair and ring chromosome formation, however, was observed as chromatin condensation was increased by increasing heat treatment time before irradiation. These results contrast observations at the DNA level which show a dramatic reduction in DNA repair in pre-heated (45.5 °C) cells and no delay in DNA repair of incubated at either 41 or 42 °C after irradiation.
The modification by heat in the induction and repair of interphase chromosome damage parallels results obtained at the cell level under similar treatment conditions and indicate the possible importance of heat-induced chromatin alterations in the mechanism of heat-induced radiosensitization.

2.2 BrdU radiosensitization derives mainly from repair inhibition /damage fixation.

We measured the contribution of increased DNA double-strand break (dsb) and interphase chromosome break induction in BrdU-mediated radiosensitization in exponentially growing and plateau-phase Chinese hamster ovary cells using an approach developed by Webb *et al.* The approach is based on the scavenging capacity of acetone for hydrated electrons, which are thought to react with bromine and form excess DNA and chromosome damage in BrdU-containing cells. In irradiated exponentially growing cells, acetone (1M) removes the majority of excess DNA dsb induced in the presence of 4 iM BrdU, but does not restore cell radiosensitivity to the levels observed in BrdU-free cells. Although BrdU radiosensitizes cells by decreasing both D_o and D_q of the survival curve, acetone only restores D_o to levels measured in BrdU-free cells, but leaves D_q at levels measured in BrdU containing cells. In plateau-phase cells, acetone removes the majority of excess DNA dsb and interphase chromosome breaks induced in the presence of 4 iM BrdU but has only a small effect on BrdU-mediated radiosensitization to killing. These observations suggest that increased DNA damage production has a variable contribution in BrdU radiosensitization: it constitutes a major, albeit not the sole, component in the radiosensitization of the exponentially growing cells, but only a minor component in the radiosensitization of plateau-phase cells. The results suggest that BrdU radiosensitization does not derive exclusively from increased DNA damage induction and support our previous hypothesis invoking repair inhibition/damage fixation as a component in the mechanism of radiosensitization. The results further suggest that repair inhibition is a major component in BrdU radiosensitization in exponentially growing cells, but the main cause of radiosensitization in plateau-phase cells.

3. Mitosis-promoting factors (MPF) activity influence transformation of radiation-induced DNA damage into lethal chromosomal aberrations.

In an early report (Pantelias 1986, *Radiat. Res.*, 105, 341-350) it was concluded that changes in chromatin conformation immediately after irradiation affect the probability of conversion of DNA lesions into lethal chromosomal aberrations. Since changes in chromatin conformation associated with cell-cycle progression and the process of premature chromosome condensation are predominantly the result of mitosis promoting factors (MPF) acting on interphase chromatin, we examined the contribution of MPF activity level in the transformation of radiation-induced DNA damage to chromosome aberrations (Cheng and al., 1993).

We measured mitosis promoting factors activity in two cell lines, CHO and HeLa, extensively used at mitosis as inducers in the essay of premature chromosome condensation, to study the yield and the repair kinetics of radiation damage in interphase chromosomes of diverse cell lines. We found a 2.5-fold higher MPF activity in HeLa as compared to CHO mitotic cells per mg of crude extract protein. HeLa mitotic cells, when used as inducers of premature chromosome condensation, uncovered two times more interphase chromosome breaks in irradiated, non-stimulated human lymphocytes as compared to CHO mitotic cells. A two-fold increase in the yield of interphase chromosome breaks with HeLa mitotics was also observed in G_1 cells from plateau phase CHO cultures. MPF activity, therefore, may be a contributing factor of the process that transforms radiation-induced DNA damage to chromosome breaks, and subsequently to other types of lethal chromosome aberrations.

We hypothesize that the level and the control in cell cycle of MPF activity influence transformation of radiation-induced DNA damage to lethal chromosome aberrations and provide means of measuring a parameter with predictive potential. Differences in MPF activity or in the regulation of chromatin condensation under the influence of MPF may underlie cell-type and cell-cycle stage relative radiosensitivity as well as variability in human radiosensitivity.

4. Abrupt alterations in chromatin condensation cause misrepair and lead to potentiation of cell killing.

Cell radiosensitivity in CHO cells in the time interval between mitosis and G1 was examined. During this short time period (~2h), the surviving fraction of CHO cells exposed to 6 Gy X-rays increased more than two orders of magnitude. This represents the most rapid change in radiosensitivity measured throughout the cell cycle. It was investigated whether this rapid change in radiosensitivity is associated with alterations in DNA dsb rejoining and whether it is accompanied by an increase in the formation of chromosome aberrations. For the experiments, mitotic CHO cells obtained by shake-off were used. Cells were irradiated either at mitosis or after they entered G_1. To prevent progression into S, cells were incubated in conditioned medium obtained from unfed plateau-phase cultures. Under these conditions, cells divided and entered G_1 but did not progress further through the cycle. Despite the large differences in radiosensitivity, rejoining of dsb, as measured using asymmetric field inversion gel electrophoresis, proceeded with similar kinetics in cells irradiated at mitosis and in cells irradiated in G_1. Under the conditions employed, irradiated mitotic cells divided and entered G_1 in the time interval allowed for repair, whereas irradiated G_1 cells remained in G_1 phase. Contrary to the results at the DNA level, formation of ring chromosomes, as measured in G_1 using the PCC assay, was dramatically higher in cells irradiated at mitosis. The results are consistent with the hypothesis that abrupt alterations in chromatin condensation cause misrepair and lead to cell killing potentiation.

5. Further support to the hypothesis that abrupt alterations in chromatin condensation, rather than reductions in dsb rejoining, enhance radiation-induced cell killing.

A complementary set of experiments was carried out using tsBN2, a mutant of baby Hamster Kidney cells (BHK21), with a temperature-sensitive defect in the regulatory mechanism for chromosome condensation. Chromatin condensation, similar to that occurring at metaphase, is induced in tsBN2 cells during S phase by transfer from the permissive (33.5 °C) to the non-permissive (40 °C) temperature. This model system allows the evaluation of the effect of chromatin condensation on dsb rejoining and cell killing in cells irradiated during S phase. S phase populations were obtained by growing cells sequentially in low-serum and isoleucine-free medium, and cells were selected by centrifugal elutriation. These cells were resynchronised at G_1/S border by a 18h incubation with 2.5 mM hydroxurea, and used 4h after release of the block. Induction and rejoining of dsb was examined using asymmetric field inversion electrophoresis. Incubation at the non-permissive temperature caused a reduction in the survival curve shoulder and an increase in the slope. However, a concomitant reduction in the rate of DNA dsb rejoining was not observed.

6. MPF activity of inducer mitotic cells but not the type of fusogen used affects the radiation yield of interphase chromosome breaks in the premature chromosome condensation assay.

HeLa mitotic cells, as already referred in #3, when used as inducers of PCC uncover two times more interphase chromosome breaks in irradiated, non-stimulated human lymphocytes or plateau-phase CHO cells as compared to CHO mitotic cells. Since it was also found a 2.5 fold higher MPF activity in HeLa as compared to CHO mitotic cells per mg of crude extract protein, MPF activity may be a contributing factor of the process that transforms radiation-induced DNA damage into lethal chromosome aberrations. It is speculated, therefore, that the level and the control in the cell cycle of MPF activity may influence the radiosensitivity of cells to killing. In addition, these results suggest that a direct comparison between the yields of interphase chromosome breaks measured in different laboratories may not be possible unless PCC inducer cells with similar MPF activity are used. It was also examined the initial yields and the kinetics of rejoining of PCC fragments in plateau CHO cells fused with CHO mitotic cells by means of either Sendai virus or PEG. It was found a yield of 2.2 chromosome breaks/cell/Gy independently of the method used to induce PCC. Furthermore, rejoining of interphase chromosome breaks proceeded with identical kinetics in cells fused using either Sendai virus or PEG. Thus, the origin of mitotic cells but not the fusogen used seem to affect the yields of interphase chromosome breaks measured after radiation expo

7. Residual DNA dsb and chromosome damage, rather than induction values, explain the radiosensitivity of a hypersensitive human fibroblast cell line.

Experiments were carried out to measure and correlate in a quantitative manner cell survival and DNA dsb in three fibroblast cell lines (HF19, AT2 and 180BR) irradiated in the plateau phase of growth and assayed either immediately (IP) or 24h later (DP). Under the same conditions, the interphase chromosome breaks were also analyzed using the PCC assay and the results were correlated to those obtained at the DNA and the chromosome levels. The mean inactivation dose measured after IP are 1.36, 0.43 and 0.67 Gy for HF19, AT2 and 180BR, respectively. The inactivation doses measured after DP are 2.72, 0.58 and 0.86 Gy, respectively. The yields of DNA dsb, as measured by pulsed-field gel electrophoresis, were found similar in all three cell lines. In contrast, rejoining kinetics were significantly slower in 180BR cells compared to HF19 and AT2 cells. Induction of interphase chromosome breaks was found similar in HF19 and 180BR cells, but residual damage was 43% of the initial in 180BR and 9.7% in HF19 cells.

It was concluded that the radiation-sensitive fibroblast culture 180BR, established from an acute lymphoblastic leukaemia patient who died following radiotherapy, is defective in the repair of radiation-induced DNA double-strand breaks and that residual DNA damage and chromosome damage, rather than induction values, explain the radiosensitivity of the 180BR human fibroblast cell line.

2.8. Radiation-induced chromosomal damage in primary tumour cells and in peripheral blood lymphocytes of cancer patients in comparison with that induced in normal cells.

It has been reported that human tumour cells or cells from cancer-prone individuals, compared with those from normal individuals, show a significant higher yield of chromatid breaks and gaps at metaphase after G2 X-irradiation. Such an enhanced G2 chromatid radiosensitivity could result from a) a greater radiation-induced initial damage; b) a greater inherent chromatid instability; c) a decreased radiation-induced G2 block, allowing less time for DNA repair; and d) an impaired capacity to repair the DNA damage.

In an attempt to elucidate the mechanisms underlying the enhanced G2 chromatid radiosensitivity, the PCC technique has been used by our group to study induction and repair processes of radiation-induced chromosomal damage directly in the Go and G2 without having cells proceed to mitosis. In this way, the yields obtained are not subjected to cell cycle kinetics or other confounding factors of the conventional metaphase chromosome analysis.

Tumour specimens from human colon carcinomas were minced, digested for 1h with pronase, collagenase and deoxyribonuclease, and the cells were disaggregated for 0.5h with trypsin. In order to study the initial radiation-induced chromosomal damage in pure tumour cells, the cell mixture was then treated with CEA antibody binding, and sorted. The isolated cells were then irradiated in ice at various doses up to 4 Gy and fused immediately after with HeLa mitotic cells. A linear dose-response curve was obtained and the initial yield of excess chromosome fragments per cell per Gy, in Go cells, was similar to that obtained in normal primary cells.

In other experiments peripheral blood lymphocytes from breast cancer patients were used to study the induction of initial chromosomal damage in Go as well as in G2 phase. The yields obtained for chromosome and chromatid damage were found to be similar to those obtained in lymphocytes from healthy individuals.

Publications

1. Iliakis, G., Y. Wang, G.E. Pantelias, and L. Metzger (1992). Mechanisms of radiosensitization by halogenated pyrimides: Effect of BrdUrd on repair of DNA breaks, interphase chromatin breaks and potentially lethal damage in plateau-phase CHO cells. *Radiation Research*, 129, 202-211.

Iliakis, G, G.E. Panetlias, R. Okayasu, and W.F. Blakely (1992) Induction by H_2O_2 of DNA and interphase chromosome damage in plateau phase CHO cells. *Radiation Research*, 131, 192-203.

Pantelias, G.E., G. Iliakis, C.D. Sambani, and G. Politis (1993). Biological dosimetry of absorbed radiation by C-banding of interphase chromosomes in peripheral blood lymphocytes. *International Journal of Radiation Biology*, 63, 349-354.

Okayasu, R., G.E. Pantelias, and G. Iliakis (1993). Increased frequency of formation of interphase ring-chromosomes in radiosensitive *irs-1* cells exposed to X-rays. *Mutation Research*, 294, 199-206.

Cheng X., G.E. Pantelias, R. Okayasu, N.G.E. Cheong, and G. Iliakis (1993). Mitosis-promoting factor activity of inducer mitotic cells may affect radiation yield of interphase

chromosome breaks in the premature chromosome condensation assay. *Cancer Research*, <u>53</u>, 5592-5596.

Pantelias G.E. (1994).   Factors determining the yields of radiation-induced chromosome aberrations as visualized by means of premature chromosome condensation in interphase cells. In: **Chromosome aberrations: Origin and Significance,** G. Obe and N.T. Natarajan (eds.). Springer Verlag, p. 140-149.

Wang Ya, G.E. Pantelias, and G. Iliakis (1994). Mechanism of Radiosensitization by Halogenated Pyrimidines: The contribution of excess DNA dsb and interphase chromosome breaks in BrdU radiosensitization may be minimal in plateau-phase CHO cells. *International journal of Radiation Biology*, <u>66</u>, 133-142.

Badie,C., G. Iliakis, N. Foray, G. Alsbeih, G.E. Pantelias, R.Okayasu, N. Cheong, N. S. Russell, A.C. Begg, C.F. Arlett, and E. P. Malaise (1995).   Defective repair of DNA double-strand breaks and chromosome damage in fibroblasts from a radiosensitive leukaemia patient. *Cancer Research,* <u>55</u>, 1232-1234.

Head of project 6: Dr. Benova

II. Objectives for the reporting period

1. The introduction of the fluorescence *in situ* hybridization (FISH) technique with mouse specific DNA libraries in the Bulgarian laboratory.
2. Investigations of gamma-rays induced chromosome aberrations (CA) in mouse splenocytes.
3. Investigations of gamma-rays induced CA in mouse bone-marrow cells 24 h after irradiation.
4. Investigations of gamma-rays induced CA in mouse differentiating type spermatogonia 26 h after irradiation.
5. Studies on the influence of the radioprotector WR 2721 (S-2-[3-aminopropilamino]ethyl phosphorothioic acid) on the level of CA in differentiating spermatogonia.
6. Investigations of the sensitivity of mice with T(7;17) 3 BKM translocation - homozygous and heterozygous.

III. Progress achieved including publications

No significant difference was observed in the spontaneous level of CA in mouse splenocytes, bone-marrow cells and differentiating spermatogonia (Tables 1, 4 and 5). The spontaneous frequency of CA was, however, increased in mouse splenocytes when BrdUrd was added 19-20 h after culture stimulation at a final concentration of 5 uM. The cultures were harvested at the 44th hour (Table 1). The BrdUrd effect was not found when the cultures were harvested at the 36th hour (Table 1). This could be due to the presence of BrdUrd during two or more S phases in a proportion of cells fixed at 44 h. . As one can see in Table 2, at 44h fixation time most of the cells were in the 2nd or 3rd mitosis. This means that BrdUrd has been present mostly during G_1 or S phase of the 2nd or 3rd mitosis.

When the splenocytes were irradiated with 3.0 Gy ^{137}Cs gamma-rays, the effect of BrdUrd was also to be dependent on the time of fixation (Table 3). Since the cells were irradiated before the BrdUrd incorporation into the chromosomes, it could be speculated that it needed more time to stabilize some aberrations which usually do not reach the metaphase. This can explain the positive effect of BrdUrd at 44 h fixation time opposite to the negative one at 36 h. It is necessary to collect more data on this problem We also

think that the decrease of the yield of CA in the last group of Table 3 was due to the extremely low radiosensitivity of one of the two mice). However, if one takes the combined average of the two fixation times, there is no difference in the yield of dicentrics between the cultures grown in the presence or absence of BrdUrd,

The frequencies of CA in mouse splenocytes increase with the gamma-rays dose (Table 3). Our present observations indicate that the dicentrics scored in C-banded metaphases and the translocations determined by FISH are of almost equal frequencies when the splenocytes were irradiated with 2.0 Gy. There is a tendency the 3.0 Gy-induced translocation frequency to be higher than the frequency of dicentrics (Table 3).

The preliminary data on the frequency of CA in mouse bone-marrow cells 24 h after irradiation shows an increase with the dose of the gamma-rays (Table 4). As the bone-marrow cells' population is a very heterogeneous one and the different cell lines have very variable cell cycles, it is not possible under the present conditions to determine the number of the replication cycle of the analyzed cells after the irradiation. The low yield of chromatid-type aberrations shows that many of them have been in G_1 or S phase at the time of irradiation (Table 4). The ratio dicentrics : translocations was roughly 1 : 1.

Table 5 shows the dose-response study in differentiating spermatogonia (A_1 - A_4, In and B spermatogonia). The chromosome-type fragments increase with the dose but the dicentrics do not. As the length of the cell cycle of these cells varies between 26 and 30 h it might be presumed that due to the mitotic delay, a sub-population of these cells had not been in the G_1 at the time of irradiation. But the yield of the chromatid-type aberrations is very low. Our attempts to analyze metaphases 30 h and more after irradiation were not successful most probably due to interphase death. Cell elimination (apoptosis) of rodent testis cells is a common phenomenon after irradiation.

The radioprotector WR-2721 decreases the yield of abnormal differentiating spermatogonia harvested 26 h after gamma-irradiation with 1.0 and 2.0 Gy. The influence of WR-2721 was most explicit on the yield of the fragments.

The background frequency of CA in mice homozygous for the reciprocal translocation T(7;17) is higher compared to normal mice (Table 1). However, no difference was observed in the yields of CA in bone-marrow cells of normal and translocated mice (homo- and heterozygous) when they were irradiatied n *in vivo* with 3.0 Gy gamma-rays (Table 4). The ratio dicentrics : translocations was equal in the three groups. It was about 1 : 1. It could be suggested that the dose of gamma-rays was too high for some differences in the radiosensitivity to be manifested.

Publications:
1. **Benova, D., M. Grigorova, T. Nikolova, I. Georgieva, M. Bulanova, I. Rupova, R. Hristova, A. Yagova, and R. Kusheva** (1995) Radiation induced chromosome aberrations in mouse splenocytes, bone-marrow cells and differentiating spermatogonia, - a report at the Radiation Safety and Protection, CEC Contractors Meeting, Skavsjoholm, Sweden, June 25-27 1995.
2. **Grigorova, M. , J.J.W.A. Boei, A. van Duyn-Goedhart, A.T. Natarajan, and P.P.W. van Buul** (1995) X-ray induced translocations in bone marrow cells of *scid* and wild type mice detected by fluorescent in situ hybridization using mouse chromosome specific DNA libraries, Mutation Res., 331, 39-45.

3.   van Buul, P.P.W., D.G. de Rooij, I.M. Zandman, **M. Grigorova**, and A.M. van Duyn-Goedhart (1995) X-ray induced chromosomal aberrations and cell killing in somatic and germ cells of scid mice, Int. J. Radiat. Biol., 69, 549-553.
4.   van Buul, P.P.W., I.M. Zandman, **M. Grigorova**, J.J.W.A. Boei, and A.T. Natarajan (1995) Mitotic and meiotic detection of radiation induced translocations in mouse stem cell spermatogonia using fluorescence *in situ* hybridization, Chromosome Res., 3, 1-6.

Table 1

A study on the spontaneous frequency of chromosomal aberrations in mouse splenocytes

Genome	Fixation time (h)	BrdUrd substituted chromosomes (5 µM)	Mice No.	Cells scored	Abnormal cells %	Chromosomal aberrations %				Total aberrations %
						Fragments (chromosomal type)	Dicentrics	Metacentrics	Fragments (chromatid type)	
Normal	44	-	7	1300	1.0	0.9	0.07	-	0.07	1.0
Normal	44	+	5	986	3.8	2.2	0.6	1.5	-	4.3
Normal	36	-	1	200	1.0	1.0	-	-	-	1.0
Normal	36	+	1	200	-	-	-	-	-	-
T(7;17) homozygous	44	-	6	1200	2.6	1.6	0.4	-	0.7	2.7
T(7;17) homozygous	44	+	3	600	4.2	2.1	0.5	2.3	0.2	5.1

Table 2

Cell cycle analysis in BrdUrd substituted chromosomes of mouse splenocytes

Groups	Fixation time (h)	Mice No.	Cells scored	% of cells in		
				1st	2nd	3rd mitosis
Control	44	2	200	10.0 (8-12)	54.0 (46-62)	36.0 (26-47)
3.0 Gy γ-rays	44	2	273	40.7 (38-44)	59.3 (56-62)	-
2.0 Gy γ-rays	40	2	200	55.5 (53-58)	44.5 (42-47)	-
Control	36	1	200	73.5	26.5	-
2.0 Gy γ-rays	36	1	200	65.0	35.0	-
3.0 Gy γ-rays	36	2	200	84.5 (75-94)	15.5 (6-25)	-

Table 3

Gamma-rays induced chromosome aberrations in mouse splenocytes

Dose Gy	Fixation time (h)	Mice No.	Cells scored	C-banding							FISH technique			
				Abnormal cells %	Fragments %	Dicentrics %	Meta-centrics %	Minutes %	Trans-locations %	Total aberrations %	Transloc.% (Terminal/Reciprocal/Interstitial)	For the whole genome	Meta-centrics %	For the whole genome
0.5	44	2	219	1.3	0.9	0.4	-	-	-	1.3	-	-	-	-
1.0	44	6	1200	8.8	5.3	2.8	1.1	-	0.1	9.3	-	-	-	-
2.0	44	4	800	20.0	12.9	10.5	2.9	-	0.1	26.4	2.8(1.2/1.6/0) 2 mice;316 cells	10.4	0.3	1.1
2.0	36	2	400	29.0	23.6	19.8	3.3	0.25	0.5	47.5				
2.0+ BrdUrd	36	1	200	29.0	18.0	25.0	4.0	-	0.5	47.5	6.1(1.8/3.7/0.6) 1 mouse;165 cells in 1st mitosis	22.6	0.6	2.2
3.0	44	3	600	36.0	24.1	27.3	3.7	0.2	0.5	55.8	9.5(3.0/6.5/0) 3 mice;459 cells	35.2	0.2	0.7
3.0+ BrdUrd	44	2	360	48.3	39.3	34.1	10.5	1.5	2.5	87.9	10.8(5.4/5.4/0) 2 mice; 111 cells in 1st mitosis	40.0	-	-
3.0	36	2	400	54.0	44.1	39.3	4.5	-	1.5	89.4	12.4(7.6/4.8/0) 2 mice;430 cells	45.9	2.2	8.1
3.0+ BrdUrd	36	2	400	38.5	26.3	28.5	5.8	1.0	0.25	61.9	11.6(5.5/5.5/0.6) 1 mouse;310 cells in 1st mitosis	42.9	2.6	9.6

Gamma-rays induced chromosome aberrations in mouse bone-marrow cells

Table 4

Genome dose (Gy)	Mice No.	Cells scored	Abnormal cells %	Chromosome type aberrations %						Chromatid type aberrations %		FISH technique	
				Frag-ments	Dicen-trics	Meta-centrics	Minutes	Translo-cations	Exch-anges	Frag-ments	Total aberra-tions %	Translocations % (Terminal/Reciprocal/Interstitial)	For the whole genome
Normal 0	5	1000	0.7	0.6	-	-	-	-	-	0.1	0.7		
Normal 2.0	2	385	26.5	16.4	9.4	2.1	0.25	1.5	1.8	5.6	36.0		
Normal 3.0	4	400	51.7	44.7	38.5	3.5	0.25	-	2.7	4.1	93.9	8.9(4.7/4.2/0) 2 mice; 189 cells	32.9
T(7;17) homozygous 3.0	2	224	42.5	40.1	34.3	-	-	0.5	0.4	6.7	8.2	9.2(5.0/4.2/0) 2 mice; 341 cells	34.0
T(7;17) heterozygous 3.0	2	295	44.2	28.9	32.6	3.1	0.5	1.3	2.0	14.2	82.5	9.1(4.5/4.6/0) 2 mice; 295 cells	33.7

Table 5

Gamma-rays induced chromosome aberrations in differentiating type spermatogonia and influence of radioprotector WR-2721

Groups, Dose (Gy)	Mice	Cells scored	Abnormal cells %	Chromosome type aberrations %				Chromatid type aberrations %		Total aberrations %
				Frag-ments	Dicen-trics	Meta-centrics	Minutes	Ex-changes	Frag-ments	
0	4	722	1,2	1,2	-	-	-	-	-	1,2
0,5	5	884	4,0	3,6	0,6	-	-	-	-	4,2
1,0	8	1343	8,4	7,1	0,9	0,2	-	0,7	0,3	9,2
WR+1,0	5	800	5,1	4,5	0,5	0,2	-	0,2	0,1	5,5
2,0	4	483	17,7	15,5	0,5	1,0	-	2,1	1,5	20,6
WR+2,0	5	879	10,2	8,4	0,7	0,3	0,1	1,6	0,2	11,3

Final Report
1992 - 1994

Contract: F13PCT920028   **Duration: 1.9.92 to 30.6.95**   **Sector: B13**

Title: Radiation-induced processes in mammalian cells: principles of response modification and involvement in carcinogenesis.

1)	Van der Eb	Univ. Leiden
2)	Sarasin	CNRS
3)	Devoret	CNRS
4)	Rommelaere	DKFZ
5)	Bertazzoni	CNR
6)	Thomou-Politi	NCSR "Demokritos"
7)	Herrlich	KfK
8)	Simons	Univ. Leiden
9)	Russev	BAS

I. Summary of Project Global Objectives and Achievements

Ionizing radiation and UV light induce a variety of effects in mammalian cells, including point mutations, DNA rearrangements, cell death and sometimes cancer. The mechanisms involved in the induction of the various responses are only partially understood. It is becoming clear that apart from viral induction indirect mechanisms play a role as well. The purpose of this research proposal, in which 9 European laboratories have collaborated, was to gain an understanding of the responses that are induced in cells after exposure to ionizing radiation and UV light.

To be able to investigate the mechanism of mutation induction by DNA-damaging agents, it is important to know the variability in spontaneous mutation induction. The group of **Simons** has investigated the rate of spontaneous mutations in undamaged cells under different growth conditions. It was found that the mutation rate indeed is not constant but can vary considerably (approximately 30-fold). This indicates that rigorous standardization is required in studies on mutation induction. With this knowledge the Simons group has investigated indirect ionizing-radiation (IR)-induced mutation in mouse lymphoma cells. The induction of genetic instability by IR appears extremely heterogeneous in contrast to their previous findings with chemicals. Possibly the "cell cycle status" of the cells at the moment of radiation is of influence. In addition, Simons *et al.* have shown that stress-induced secreted proteins can induce genetic instability. Thus, the stress response might contribute indirectly to carcinogenesis.

The **Sarasin** group has investigated the mechanism of induction of point mutations in human cells. The research was focused on the question whether UV-

induced mutation spectra differ in fibroblasts from Xeroderma pigmentosum group D (XP-D) patients, who are prone to UV-induced skin cancer (as most XP patients), and in fibroblasts from Trichothiodystrophy (TTD)/XP-D patients who are not tumour-prone. (In the TTD/XP-D patients the same gene, ERCC-2, is affected as in the classical XP-D patients). No significant differences in UV-induced mutation spectra were found. The results of the Sarasin group indicate that the difference in tumour-proneness in response to UV is not due to differences in induction of point mutations. Furthermore, Sarasin *et al.* compared mutation spectra of the p53 tumour suppressor gene isolated from XP skin tumours, non-XP skin tumours and non-XP internal tumour. Their findings firmly underline the importance of UV-induced DNA lesions in the process of skin carcinogenesis. The molecular basis of the difference between tumour-prone and non-tumour-prone XP patients was also investigated by the **Van der Eb**-group. While most XP patients are tumour-prone, a subset exists who are "resistant" to UV-induced skin cancer. It was found that fibroblasts of the two categories of XP-patients are identical in most UV-induced responses, including induction of signal transduction pathways, but they differ in two UV-induced phenomena: not only do they fail to show the Enhanced-reactivation (ER) response after UV irradiation, as reported previously, but they also fail to induce expression of the ornithine decarboxylase (ODC) gene. The ODC gene is one of the genes that is activated by UV. In addition, a specific inhibitor of ODC can effectively block the ER-response indicating a pivotal role for ODC in this phenomenon.

The laboratory of **Herrlich** has investigated several aspects of the cellular response to radiation. UV light induces the activation of pre-existing transcription factors, including the AP-1 factors cJun and cFos. Activation of these factors appeared to depend on signal transduction pathways triggered by growth-factor receptors. Therefore, the crucial question has been investigated how growth-factor receptors are activated by UV radiation. Sofar, they have identified three pathways contributing to UV-induced gene transcription of which at least two seem to involve growth factor receptors. Interestingly, UV is a much more potent inducer than other genotoxic agents such as X-ray, MNNG, MMS and H_2O_2. A second line of research concerns the mechanism of UV-induced stabilization of p53. It was found that this stabilization is independent of the signal-transduction route leading to AP-1 activation.

Genomic instability is not only reflected by increased rates of point mutations but also of chromosomal aberrations, such as translocation, recombination and amplification. In the course of a study of the biological and genetical properties of XP and TTD cells, the group of **Bertazzoni** has identified a clonal chromosomal rearrangement in an XP-C fibroblast strain, which apparently reflected a preneoplastic state (anchorage-independent growth). Selection for anchorage independent growth has now led to the isolation of several more XP clones with chromosomal abnormalities. Continued culturing of one of the clones led to further chromosomal rearrangements, suggesting that the initial abnormality was the first step in the development of aneuploidy. The Bertazzoni group in addition investigates the role of poly-(ADP-ribose)polymerase (ADPRP) in mammalian cells.

In the reporting period the involvement of ADPRP in apoptotic cell death was investigated. It turned out that ADPRP indeed plays a role, and is activated by the appearance of small-sized DNA fragments formed during apoptosis.

The **Rommelaere** group has focused on the mechanism of radiation-induced DNA amplification, using Parvoviruses as a model. Parvoviruses can undergo viral DNA amplification in carcinogen-treated cells in the absence of viral replication proteins. Since p53 is known to protect cells against amplification of cellular genes, the group has investigated whether p53 plays a role in selective viral DNA amplification. It was found that not only parvoviral DNA amplification but also parvoviral replication are much less efficient in cells that express wild-type (wt) p53 than in cells lacking wt p53. This indicates that expression of wt p53 protects cells against viral infection. Thus, parvovirus replication may constitute an early marker of neoplastic transformation.

The molecular basis of recombination was subject of study of the **Devoret** group who are studying the BTCD gene, previously called Kin17, a mouse gene isolated by the group on the basis of cross-reactivity of the BTCD protein with antisera against *E.coli* RecA protein. Studies on the properties of the BTCD protein revealed that it is a nuclear protein that binds preferentially to curved DNA. It associates preferentially with curved DNA present at illegitimate recombination junctions on chromosomes, which suggests that it may play a role in recombination. Expression of the mouse BTCD gene in *E.coli* renders these bacteria sensitive to UV-light. Possibly BTCD competes with some DNA repair proteins in binding to DNA.

The laboratory of **Thomou-Politi** has investigated the effects of low doses of IR on expression of the CD_2 gene, which codes for a T-cell-specific surface antigen. Expression of CD_2 is enhanced by IR, and it may serve as a sensitive indicator for exposure to low radiation doses. Since CD_2 appears to be involved in cell-cell adhesion, signal transduction and T-cell differentiation, the effect of IR on stimulation of T-cell activation was studied. Low doses of IR indeed not only cause an increase in the level of CD_2 mRNA in T-lymphocytes but also enhance the response of the cells to mitogenic stimulation.

Finally, in the summer of 1994 the group of **Russev** from Sofia, Bulgaria, has joined the contract. The research of this group deals with the mechanism of inhibition of replicon initiation by gamma irradiation or topoisomerase II inhibitors. Specifically, the group focussed on (1) the effect of gamma-rays and topo II poisons on chromatin structure, (2) the effect of protein synthesis inhibitors and protein phosphorylation on replicon initiation suppression by these treatments. Their results led them to propose a model in which the transient hampering of replicon initiation during S phase by genotoxic agents leading to double strand breks is at first detected by poly(ADP-ribosyl) synthetase. Subsequently, the signal will be transmitted by various phosporylations.

Head of project 1: Prof.Dr. Van der Eb

II. Objectives for the reporting period

1. Characterization of UV-inducible phenomena in human cells

2. Radiation-induced carcinogenesis in transgenic mice

The objective of this investigation is to gain insight into the molecular nature of radiation-induced carcinogenesis. In project 1 the UV- or X-ray-induced responses are analyzed in cell cultures derived from individuals which are resistant to (UV-induced) carcinogenesis or, in contrast, are highly susceptible to (spontaneous) cancer induction. Project 2 makes use of tumor-prone transgenic mice which carry an activated oncogene or tumor-prone knock-out mice which carry one or two inactivated alleles of a tumor suppressor gene. These mice are used to investigate the kinetics and mechanism of radiation-induced carcinogenesis.

III. Progress achieved including publications

1. Characterization of UV-inducible phenomena in human cells

Exposure of human cells to UV or ionizing radiation results in the induction of a number of stress responses, including the Enhanced reactivation (ER) of UV-treated virus and Enhanced mutagenesis (EM) of untreated virus. Two of our recent observations have provided evidence that the ER phenomenon might be involved in, or co-regulated with, events leading to cancer induction. The evidence is (1) that ER is absent in cells derived from Xeroderma pigmentosum patients that did not develop skin cancer in sunlight-exposed areas, as well as in cells derived from UV-sensitive but non-cancer-prone Trichothiodystrophy patients; (2) that a super-induction of ER occurs in cells derived from patients with hereditary cancer-prone syndromes. These results not only indicate that cancer induction may be causally related with ER, but that actually ER might serve as a prognostic marker for cancer-proneness in families affected by these disorders.

Work in the reporting period has focused on the suitability of ER as a prognostic marker and the molecular mechanisms that are co-regulated with ER and

might be aberrant in ER⁻ and ER^super+ cells.

ER, a putative prognostic marker?

We have assessed the ER characteristics of various individuals of families afflicted with a certain disease. Firstly, we checked the ER in an "XP-family". In this particular case two brothers are XP patients with a defect in the XP-B gene. Both are ER⁻ and have not developed skin cancer in a UV-exposed area. In addition we examined the ER-response of fibroblasts from a sister, the mother and father. The cells from both females are ER⁺ whereas the father is ER⁻. The father is coincidently carrier of one defect XP-B allele. Since XP is a recessive disorder, he does not carry the disease and hence he provides the first fibroblasts that are not UV-sensitive but display the ER⁻ phenotype. Nevertheless, also in this case the ER⁻ trait is still linked genetically to at least one defect XP allele. Secondly, the induction of the SOS-like responses ER and EM were also investigated in the DNA repair deficiency Trichothiodystrophy (TTD). In contrast to xeroderma pigmentosum, TTD patients do not develop skin cancer. The induction of ER and EM was studied in TTD cells showing normal, intermediate or high sensitivity to UV-C. Interestingly, TTD cell lines with normal or high UV sensitivity exhibit induction of EM, whereas in all TTD cells the ER response is absent. Unexpectedly, TTD cell lines with intermediate UV sensitivety showed hardly if any induction of EM. These results suggest that also in TTD the ER⁻ phenotype is transmitted as a genetic trait, which in this case could possibly be linked to a mutated ERCC2 gene. Furthermore, the induction of the ER response was studied in UV-exposed skin fibroblasts derived from Li-Fraumeni syndrome (LFS) patients. LFS is characterized by a germ-line mutation of one allele of p53, giving rise to the early onset of various types of cancer. Abnormally high levels of ER were observed in UV-treated skin fibroblasts derived from five different LFS families. Interestingly, a study of cells from various generations of a LFS family revealed that cells from afflicted individuals, carrying one mutated p53 allele, exhibit abnormally high ER levels. In contrast, normal ER levels were observed in cells derived from unafflicted individuals, carrying wild type p53 alleles. These results show that inheritance of a mutated p53 tumor-suppressor gene correlates with the induction of abnormally high levels of ER. These observations indicate that a tumor-suppressor gene somehow might be involved in the process of the induction of SOS-like responses.

In addition, the induction of the ER response was investigated in cells from members, belonging to various generations of family with high incidence of breast/ovarian and also of colon and stomach cancer (Lynch type II syndrome). Sofar, no mutation in any known tumor-suppressor gene has been found in this family. Abnormally high ER levels were not only noticed in cells from afflicted individuals, but, unexpectedly, also in unafflicted siblings. These results confirm that abnormally high ER levels are inherited as a genetic trait. Since abnormally high ER levels are also observed in unaffected persons, which are still rather young for developing cancer, the ER response may possibly be used as a biological prognostic marker to identify carriers of certain hereditary cancer-prone syndromes that are characterized by germ-line mutations in tumor-suppressor genes.

Molecular mechanisms co-regulated with ER

Induction of Enhanced Recombination

In various hereditary cancer-prone syndromes genomic instability has often been observed, which might be caused by recombinogenic events. It is conceivable that the ER response could be due to the transient activation of recombination mechanisms. In order to investigate whether this might be the case, we studied the induction of recombination in ER^+, ER^{super+} and ER^- cells with the use of two HSV-1 mutants.

Preliminary results show that in UV-treated normal cells Enhaced Recombination follow similar kinetics as those of ER and EM. Furthermore, in ER^- cells we noticed lower levels of Enhanced Recombination than in normal ER^+ and ER^{super+} cells. These results indicate that ER and Enhanced Recombination might be closely related processes.

Further molecular mechanisms co-regulated with ER

UV-mediated induction of mRNA levels has in the past been reported for numerous genes. In the reporting period we checked a number of these genes, among them c-jun, c-fos, HSP70, BTCD/kin17 and collagenase. All are normally induced by UV in both ER^+ as well as ER^- cells. One gene, ODC, was the exception since we could not detect enhanced mRNA levels of this gene in any of the ER^- cells we tested. Nor can we find induction of ODC at the protein level (both in amount and activity). In ER^+ cells, but also in ER^{super+} cells, ODC is normally induced: a maximal mRNA level is reached 24 hours post-UV irradiation at the time point where ER reaches its maximum. To determine whether a more causative relation might occur between ODC expression and ER we made use of a specific inhibitor of ODC. This inhibitor irrevisibly binds to and inactivates ODC. Indeed, addition of this inhibitor can completely block the ER response, suggesting a role for ODC in this phenomenon. ODC is the key regulator of polyamine biosynthesis . In addition it has been reported that ODC is a transcriptional target for c-myc and, moreover, enhanced expression of ODC itself can transform NIH 3T3 cells. Efforts to assess the status of c-myc prior to and following UV irradiation have sofar been unsuccessful. Neither at the level of mRNA (Northern blotting and RT-PCR) nor at the level of protein (immunoprecipitation and Western blotting) have we been able to detect any c-myc. This is probably due to the exceedingly low levels of c-myc in non-established fibroblasts.

Finally, we have initiated experiments to study the genomic stability in relation to ER. Disturbed genomic stability is an important factor contributing to carcinogenesis. If ER^+ and ER^- cells might differ in the ability to maintain genomic stability this would most certainly be an important finding. In our initial efforts we have focused on DNA amplification frequencies (AF) in SV40-transformed ER^+ and ER^- fibroblasts. The DNA-AF was determined via the amount of PALA resistance. Cells can become PALA resistant by amplifying the CAD gene. Using FISH analysis we confirmed that in our hand PALA-resistant colonies indeed carried an amplified CAD gene (10-15 copies). Preliminary experiments indicate that the spontaneous AF is slightly higher in ER^+ than ER^- fibroblasts. UV can enhance the AF in ER^+ cell lines up to 40x, whereas in the ER^- cell lines the AF

can be enhanced only up to 5x. Currently, we are focusing on recombination assays in the SV40-transformed fibroblasts as well as radiation-induced chromosomal aberrations in the non-established fibroblasts (see above).

Impaired repair capacity in skin fibroblasts from hereditary cancer-prone syndromes:
Repair studies in aniridia, Dysplastic Nevus syndrome and
Von Hippel-Lindau syndrome cells.

During the course of our experiments on the induction of SOS-like responses in aniridia (AN), Dysplastic Nevus syndrome (DNS) and Von Hippel-Lindau syndrome (VHL) cells we noticed that certain cell lines exhibited a reduced capacity to produce HSV-1 after UV-C treatment of the cells. This observation indicated that the repair capacity of these cells could possibly be impaired. In order to investigate whether this might be the case the survival of UV-C-exposed cells and the Host Cell Reactivation (HCR) of UV-C-irradiated HSV-1 were studied in normal, AN, DNS and VHL cell lines. Some of the UV-C treated AN, DNS and VHL cell lines exhibited normal or slightly lower cell survival, suggesting lower repair capacity. That this is the case was clearly demonstrated when HCR of HSV-1 was studied. AN cell lines exhibited normal, intermediate or low HCR. Heterogeneity of the HCR of HSV-1 was also noticed in various DNS cell lines, whereas two investigated VHL cell lines exhibited an extremely low HCR. These results indicated an impairment of the mechanism to repair DNA damage in AN, DNS and VHL cells. A study on the kinetics of removal of CPD's revealed that they are slower removed from the DNA in AN, DNS and VHL cells than noticed in normal cells. These results suggest that the repair capacity in AN, DNS and VHL cells is impaired.

Li-Fraumeni syndrome.

A more extended study was performed with skin fibroblasts derived from patients suffering from the Li-Fraumeni syndrome. During the course of our experiments on the induction of SOS-like responses in UV-C-treated Li-Fraumeni syndrome (LFS) cells, we noticed that the UV-C-irradiated cell lines also exhibited a reduction of the capacity to produce virus. This indicated that the repair capacity of Li-Fraumeni cells could possibly also be impaired. Primarily the survival of UV-C-exposed cells derived from five different LFS families was studied. It was found that the survival of the UV-C-exposed LFS cell lines is much lower for UV-doses higher than 6.0 J.m^{-2}, than that observed in normal cells. In the same cell lines HCR of UV-C-irradiated HSV-1 was studied. In all LFS cell lines HCR of HSV-1 is much lower than that observed in normal cells. It has been shown that in LFS cells one allele of p53 is mutated and that it is involved in the surveillance process of damaged DNA to stop cell proliferation. In order to demonstrate that the presence of one mutated allele is sufficient to impair the repair capacity of LFS cells, HCR of HSV-1 and the cell survival and HCR of HSV-1 was studied in UV-C-treated cells derived from unafflicted and afflicted individuals from a LFS family. It was found that the survival of UV-C-treated cells from afflicted individuals is much lower than that of cells from unafflicted and normal ones. HCR of UV-C-irradiated HSV-1 was much lower in cells from afflicted family members, carrying

one mutated p53 allele, whereas normal HCR was observed in cells from unafflicted ones with wild type p53 alleles. These results indicated that indeed a p53 gene might possibly be involved in the DNA repair mechanism, resulting in the impaired repair capacity in LFS cells from afflicted individuals. In order to further characterize some of the LFS cell lines, the following repair parameters were studied:

1) Unscheduled DNA Synthesis (UDS), 2) The kinetics of removal of CPD's in genome overall and gene specific repair and 3) Induction of chromosomal aberrations.

In UV-C-treated LFS cell lines from 5 different families similar levels of UDS were noticed as those found in normal cells. UDS predominantly determines sensitivity to 6-4 photoproducts, indicating that removal of CPD's might be impaired in LFS cells. The kinetics of removal of CPD's was studied in cell lines from unafflicted and afflicted individuals from a LFS family. Genome overall repair in cells from unafflicted individuals is the same as that in normal cells, whereas slower kinetics of removal of CPD's was found in cells from afflicted ones. Gene specific repair was studied in the active house keeping gene ADA and the inactive 754 locus in two UV sensitive LFS cell lines. We noticed that in both LFS cell lines CPD's are removed with slower kinetics from the active ADA gene than in normal cells. Unexpectedly, one LFS cell line exhibited hardly any removal of CPD's from the inactive 754 locus even 24 hours after UV treatment.

In addition, abnormally high levels of chromosomal aberrations were found in the same LFS cell line after exposure to X-rays. Unexpectedly, higher spontaneous levels of SCE's were found in this cell line, whereas exposure to UV-C-light resulted in higher frequency of SCE's than that in normal cells. Furthermore, this cell line exhibit abnormal condensation of its chromosomes.

Family with high incidence of Breast, Ovarium and Colon Cancer (LYNCH Type II).

During the course of experiments on the induction of SOS-like responses in cell lines from a family suffering from a high incidence of breast, ovarium, colon, and stomach cancer (Lynch type II syndrome) we noticed higher sensitivity to UV-C of the cells than in normal cells. This indicated that also in this hereditary cancer-prone syndrome the repair capacity could possibly be impaired. In order to investigate this further, the HCR of UV-C-exposed HSV-1 was studied in cells derived from afflicted and not yet afflicted individuals, belonging to various generations of this family. Lower HCR of HSV-1 was not only observed in cells from afflicted individuals, but also in cells derived from sofar unafflicted siblings. This observation indicates that cells from even unafflicted siblings exhibit lower HCR of HSV-1, which could possibly be inherited as a genetic trait in this family.

Lower HCR of HSV-1 in cells from a family with high incidence of breast cancer.

Increased sensitivity to UV-C-light was also observed in cells derived from individuals belonging to a family suffering from a high incidence of breast cancer. This observation suggests that also in this cancer-prone family the DNA repair capacity could be possibly be impaired. In order to investigate whether this is the case, HCR of UV-C-treated HSV-1 was performed in cells from this breast cancer

family. Lower HCR was found in cells from afflicted and even unafflicted individuals than that in normal cells. Even cells derived from patients with sporadic breast cancer performed lower HCR of UV-C-irradiated HSV-1.

These results show that cells from various hereditary cancer-prone syndromes often exhibit heterogeneity of their DNA repair capacity, resulting possibly in induction of mutations and finally carcinogenesis. Besides the high levels of ER often observed in cells from various cancer-prone syndromes, an impaired DNA repair capacity can possibly be used as an additional prognostic marker to identify carriers in families with hereditary cancer-prone syndromes. This information can be applied for risk assessment of such individuals of exposure to carcinogenic or genotoxic agents.

Stabilization of p53 is in repair deficient cells different from that in normal ones.

We studied the stabilization of p53 in UV-exposed normal, XP and TTD cells. In UV-treated normal cells complete stabilization of p53 was observed during the first 4 hours and then p53 was degraded with similar kinetics as that in unirradiated cells. Stabilization of p53 persists much longer in repair deficient XP and TTD cells than in normal cells. Furthermore, the stabilization of p53 was found to be dose-dependent in normal and XP cells. These observations indicate that unremoved DNA damage could possibly cause the induction of transient stabilization of p53.

2. Radiation induced carcinogenesis in transgenic mice

Eμ-*pim-1* transgenic mice were treated with different doses of X-Rays. In all doses tested (4x1.5Gy, 4x1.0Gy, 4x0.5Gy) Eμ-*pim-1* mice were significantly more susceptible to develop a lymphoma due to the treatment than wild type mice. The majority of tumors are monoclonal T-cell lymphoma's as determined by immunofluorescence staining of cell surface markers on freeze sections. Rearrangements of the T-cell receptor gene showed that most tumors are of (mono)clonal origin. On RNA-level we do observe a general high *c-myc* expression and one case of N-*myc* overexpression. Interestingly, we also observe overexpression of *mdm-2* in the majority of tumors. Nearly all tumors show a simultaneous increase in cell proliferation (as measured by BrdU-incorporation) and apoptosis (DNA-end labeling), suggesting a high turn-over rate of the tumor cells. The results sofar indicate that we have a set of nearly identical tumors, which represent an excellent model to investigate the involvement of onco-/tumorsuppressor genes in the process of lymphomagenesis. We are continuing this study with the Differential Display technique and try to identify new genes involved in this process.

Currently new experiments are in progress in which APC knock-out mice and wild type control mice have been treated with X-Rays (5Gy). By now nearly all APC knock-out mice have developed multiple intestinal tumors and in some cases a breast tumor, wheras in the wild type mice only one lymphoma has developed as

yet. The tumors will be studied with respect to tumor type, cellgrowth-rate and apoptosis. Besides, the molecular changes that have led to tumor formation will be investigated.

Publications

Libin Ma, Geert Weeda, Aart G. Jochemsen, Dirk Bootsma, Jan H.J. Hoeijmakers and Alex J. van der Eb. Molecular and functional analysis of the XPBC/ERCC-3 promoter: transcription activity is dependent on the integrity of an Sp1-binding site. Nucl.Acids Res. 201(1992) 217-224.

Bernd Stein, Peter Angel, Hans van Dam, Helmut Ponta, Peter Herrlich, Alex J. van der Eb and Hans Rahmsdorf. Ultraviolet light induced c-jun gene transcription: two AP-1-like binding sites mediate the reponse. Photochem and Photobiol. 55(1992)409-415.

P.J. Abrahams, A. Houweling and A.J. van der Eb. High levels of Enhanced reactivation of Herpes Simplex virus in skin fibroblasts from various hereditary cancer-prone syndromes. Cancer Research 52(1992)53-57.

Hans van Dam, Monique Duyndam, Robert Rottier, Anne Bosch, Lydia de Vries-Smits, Peter Herrlich, Alt Zantema, Peter Angel and Alex J. van der Eb. Heterodimer formation of cJun and ATF-2 is responsible for induction of c-jun by the 243 amino acid adenovirus E1A protein. EMBO J. 12 (1993)479-487.

Theo van Laar, Wilma Steegenga, A.G.Jochemsen, Carrol Terleth and Alex J. van der Eb. Bloom's syndrome cells GM1492 lack detectable protein but exhibit normal G1 cell-cycle arrest after UV-irradiation. Oncogene 9 (1994)981-983.

Libin Ma, Antonia Westbroek, Aart G. Jochemsen, Geert Weeda, Anne Bosch, Dirk Bootsma, Jan H.J. Hoeijmakers and Alex J. van der Eb. Mutational analysis of ERCC3, which is involved in DNA repair and transcription initiation: identification of domains essential for the DNA repair function. Mol.Cell.Biol. 14(1994)4126-4134.

B. Klein, A.R. Filon, A.A. van Zeeland and A.J. van der Eb. Survival of UV-irradiated vaccinia virus in normal and Xeroderma pigmentosum fibroblasts: evidence for repair of UV-damaged viral DNA. Mut.Res. 307(1994)25-32.

Libin Ma, Ellen D. Siemssen, Mathieu H.M. Noteborn and Alex J. van der Eb.
The Xeroderma pigmentosum group B protein ERCC3 produced in the baculovirus system inhibits DNA helicase activity. Nucleic Acids Res. 22(1994)4095-4102.

Libin Ma, The Xeroderma pigmentosum group B protein ERCC3. Thesis, November 1994.

P.J. Abrahams, R. Schouten, T. van Laar, A. Houweling, C. Terleth and A.J. van

der Eb. Different regulation of p53 stability in UV-irradiated normal and DNA repair deficient human cells. Mut.Res. 336 (1995) 169-180.

Wilma Steegenga, Avi Shvarts, Theo van Laar, Alex J. van der Eb and AG Jochemsen. Altered phosphorylation and oligomerization of p53 in adenovirus type 12-transformed cells. Oncogene 11(1995)49-57.

Wilma T. Steegenga, Theo van Laar, Avi Shvarts, Carrol Terleth, Alex J. van der Eb and A.G. Jochemsen. Distinct modulation of p53 activity in transcription and cell-cycle regulation by the large (54kDa) and small 21kDa) adenovirus E1B proteins. Virology 212 (1995) in press.

Libin Ma, and Alex J. van der Eb. Mammalian nucleotide excision repair. BBA - Review in Cancer 1995, in press.

P.J. Abrahams, A. Houweling, P.D.M. Cornelissen-Steijger, F. Arwert, B.M. Pinedo and A.J. van der Eb. Inheritance of abnormal expression of SOS-like response in hereditary cancer-prone syndromes. Submitted for publication.

P.J. Abrahams, P.D.M. Cornelissen-Steijger, A. Houweling, R. Filon, L.H.F. Mullenders, N.G.J. Jaspers, A.H. Bootsma, A. de Klein, A.A. Van Zeeland, and A.J. van der Eb.Impaired repair capacity in skin fibroblasts from various hereditary cancer-prone syndromes. Submitted for publication.

Head of project 2: Dr. Sarasin

II. Objectives for the reporting period

1. We have determined the mutation frequency and the mutation spectra of a UV-irradiated shuttle vector replicating in normal, XPD and TTD/XPD SV40-transformed fibroblasts. In XPD and TTD/XP cells the mutation frequencies were much higher compared to wild-type cells. The mutation spectra was, however, more similar between TTD/XP and normal cells than with XPD cells. Complementation of XPD and TTD/XPD cells with the wild type ERCC2 gene allows the mutation frequency to be decreased to the level of wild type cells.

2. The p53 protein is stabilized in normal, XPD and TTD/XP cells after UV-irradiation. The half-life of the protein is higher in normal and TTD/XPD than in XPD cells, but the amount of UV-light necessary to detect this increase is higher in wild type cells than in XPD or TTD/XPD cells. In all cases, the p53 protein still exhibits a wild type conformation. The low p53 half-life in XPD may explain part of the cancer-proneness in this disease compared to the genetically related TTD/XPD syndrome.

III. Progress achieved including publications

The general aim of our project was to study at the molecular level the genetic modifications induced by radiations which will lead to cancer initiation. Among these genetic changes, point mutations are those we have studied in more details.

The biological model we have used is based on human diseases where hypersensitivity to UV is associated with a very high level of skin cancer in xeroderma pigmentosum patients (XP) while it is not associated with abnormal level of cancer in trichothiodystrophy (TTD) patients. The paradox in these two diseases is linked to the fact that some XP or TTD patients exhibit mutations on the same ERCC2 repair gene. Mutations in this gene are responsible for the XPD and the TTD/XPD diseases and the defect in nucleotide excision repair. Therefore, our aim was to understand the response towards ultraviolet irradiation in XPD and TTD/XPD cultured fibroblast cells.

In order to fulfill our aim, two general strategies have been followed : we studied the mutation frequency and mutation spectra in these patient'cells using a new shuttle vector we have developed in our laboratory and we analysed the oncogene and

tumor suppressor gene modifications in the UV-induced tumors from normal and XP individuals.

1. Analysis of mutagenesis at the molecular level using shuttle vector :

Most of the experiments using shuttle vectors in human cells are carried out with the pZ189 plasmid which is based as a target sequence on the supF tRNA gene. This target is very interesting but the putative presence of secondary structures and eventually of single-stranded areas renders it difficult to consider this sequence as a "classical" cellular gene. Since part of our projects deals with the analysis of mutation spectra in mammalian cells subjected to various treatment we developed a new shuttle vector based on a mutagenesis target rarely used in higher eukaryotes: the lac Z' gene. This gene represents about 150 base pairs and can be screened easily in bacteria by complementation on the lac operon. The absence of mutation on the plasmid leads to blue bacterial colonies while a mutation changing the amino-acid leads to a white colony.

We have constructed the pR2 plasmid where the lac Z' gene is located between the promoter and the coding sequence of the kanamycin resistance gene, used for bacterial selection. This target is very stable and a spontaneous mutation frequency of about 10^{-4} is observed in several transformed human cells. In order to validate the pR2 vector for mutagenesis studies we irradiated it with UV-light (254 nm) at various fluences from 0 to 1000 $J/m^{2\cdot}$ The mutation frequency can be increased by a factor greater than 70. The majority of mutations (> 90 %) are point mutations located at dipyrimidine sites. The substitution hot spots are at C-C sequences leading to C to T transitions, as already observed with other model systems.

To study the relationships between mutagenesis and carcinogenesis, we compared the mutations and their frequency induced by ultraviolet irradiation at 254 nm (UV-C) in XPD (GM-08207B/XP6BE), TTD/XPD (TTD1VI-LAS-KMT11) and wild type (MRC-5V1) human cells.

After verification of UV hypersensitivity and DNA repair defect of the immortalized XPD and TTD cell lines compared to a wild type cell line, UV-induced mutagenesis was studied with the shuttle vector pR2, carrying the target lacZ' gene. The UV-mutation frequencies in XPD and TTD cells were similar and significantly increased compared to normal cells. Sequence analysis of 312 independent mutant plasmids revealed that more rearrangements were induced in TTD cells (16 %) than in XPD (5 %) and normal cells (1 %), while XPD cells exhibited a 2-fold higher rate of tandem mutations compared with TTD and normal cells. In the three cell lines, a predominance of G:C to A:T transitions was found, especially in XPD cells (87 %) and most mutations were targeted on dipyrimidine sites, chiefly on the cytosine at 5'-TC-3' sites. The types of UV-induced point mutations in TTD cells were, however, more similar to those found in normal cells than those found in XPD cells. XPD mutations were preferentially located in 5'-TCpur-3' sites, while mutations in normal and TTD cells were mostly at 5'-TCC-3' sites. Analysis of mutation spectra revealed differences in the location of the mutational hotspots between the three lines.

Although the mutation frequency of the UV-irradiated pR2 vector is much higher in TTD and XPD cells than in normal cells, the mutation spectrum is closer between TTD and normal cells as compared to XPD cells. These dissimilarities could contribute to explain some differences between the two syndromes.

In order to ascertain that the mutations on the ERCC2 DNA repair gene are really responsible for the hypermutagenicity towards UV, we stably corrected XPD and TTD/XPD cells by an expression vector containing the wild type ERCC2 gene. After selection, we isolated wild-type ERCC2-containing XPD and TTD/XPD clones and characterized them as a function of their UV-sensitivity. These cells were corrected to wild-type level for UV-sensitivity, unscheduled DNA synthesis and host-cell reactivation. When transfected with UV-irradiated pR2 plasmid, the mutation frequency in these corrected XPD and TTD/XPD cells went back to wild type level. These results demonstrate clearly that the ERCC2 mutations are the only cause of UV-sensitivity, low DNA repair level and high mutation rate after UV-irradiation. The success in fully complementing cultured cells from these patients by expressing the wild type version of the repair gene allows us to propose a possible gene therapy for the xeroderma pigmentosum patients.

2. Gene modifications in UV-induced human skin tumors

We have used human diseases associated with hypersensitivity to ultraviolet light (UV) and other genotoxic agents as a model for understanding the mechanism of DNA repair and carcinogenicity in humans. Among UV-sensitive patients, xeroderma pigmentosum (XP), Cockayne's syndrome (CS) and trichothiodystrophy (TTD) are the most studied ones. They have been very useful to allow isolation and characterization of human DNA repair genes. The major paradox in these human diseases is linked to the fact that XP patients are in almost 100 % of cases cancer-prone individuals (they develop numerous skin cancers in sun-exposed parts of the body) while photosensitive TTD patients, which carry mutations on the same gene as XP patients (either the ERCC2 or the ERCC3 gene) never develop skin cancers. A major effort of this work was to try to understand this paradox and the various cellular processes which either facilitate or inhibit tumorigenesis.

Xeroderma pigmentosum (XP) patients are clinically characterized by a very high incidence of skin cancers on exposed skin, at an early age. XP cells in vitro are strongly deficient in excision-repair and highly mutagenized by UV-light. We were, therefore, interested in measuring mutation frequency and in determining mutation spectra in patient'tumors exposed to UV-lesions. We chose to look at oncogene activation in skin tumors with the idea that more mutations, particularly of the ras gene family, would be found in XP tumors where lesions remain unrepaired compared to normal individuals. Our results clearly show that more than a 2-fold significantly higher mutation frequency (50 %) of the ras genes was found in XP in contrast to control tumors (22 %).

The majority of the mutations were found at codon 12 of all three ras genes with a preponderance for N-ras in XP samples. The mutation spectra indicate that all

mutations found were located opposite pyrimidine-pyrimidine sequences which represent a hot spot for UV-induced DNA lesions. Most of the mutations were of the type expected from studies performed in vitro with model systems. This high mutation frequency in XP was accompanied by a very high level of Ha-ras and c-myc gene amplification and rearrangement. All these data are consistent with a fundamental role of unrepaired UV-induced DNA lesions as an initating event in human skin tumors on exposed parts of the body.

The p53 gene is frequently mutated in human cancers and represents a good target for studying mutation spectra since there are more that a hundred potential sites for phenotypic mutations. Using reverse transcription PCR and single strand conformation polymorphism (SSCP) to analyze over 40 XP skin tumors (mainly basal and squamous cell carcinomas), we have found 40 % (19/46) containing at least one point mutation on the p53 gene. Indeed 4 XP tumors contained point mutations on the two alleles of the p53 gene. All the mutations were located at dipyrimidine sites, essentially at C-C sequences, which are hot spots for UV-induced DNA lesions. 60 % of these mutations were tandem CC to TT mutations considered to be a unique signature of the presence of unrepaired UV-induced lesions and are not observed in internal human tumors. All the mutations, except two, must be due to translesion synthesis of unrepaired dipyrimidine lesions left on the non-transcribed strands. These results show for the first time the existence of preferential repair of UV lesions (either pyrimidine dimers or pyrimidine (6-4) pyrimidones) on the transcribed strand in human tissues.

We have compared the mutation spectra on the p53 tumor suppressor gene isolated from XP skin tumors, non-XP skin tumors (both being basal and squamous cell carcinomas) and non-XP internal tumors (from a p53 data base containing more than 2000 independent mutations). Interestingly in the three cases, the majority of point mutations occurs at G:C base pairs and corresponds to C to T transitions (47 % in internal tumors, 74 % in non-XP skin tumors and 87 % in XP skin tumors). These transitions are almost exclusively located opposite pyrimidine-pyrimidine sequences in skin tumors (95 % in non XP and 100 % in XP) while they are located at random in internal tumors.

This result confirms the initial role of UV-induced pyrimidine-pyrimidine lesions in skin tumor development even in non-XP patients. The molecular signature of UV-induced DNA lesions being the presence of tandem C-C to T-T double transitions, we compared this type of mutations in the three classes of tumors. In internal tumors, less than 1 % tandem mutations was found while this number increases spectacularly to 10 % and 60 % for non XP and XP skin tumors. This result demonstrates clearly the role of unrepaired lesions in the initiation of carcinogenesis. In XP tumors, 100 % of C-C to T-T tandem mutations were only due to unrepaired lesions on the non-transcribed strand of the p53 gene, while it was only 30 % in non-XP individuals. This difference is highly significant and is probably due to the fact that the very low repair activity detected in XP cells should be limited to the transcribed strand of active genes.

The specificity of p53 mutation spectra in skin tumors clearly demonstrates the

fundamental role of unrepaired UV-induced DNA lesions in the initiation of skin carcinogenesis in humans. This study confirms that the p53 gene is a particularly appropriate candidate for the correlation of mutation spectra with specific genotoxic agents. The mutation spectra we found on the UV-irradiated pR2 shuttle vectors replicated in human cells are similar to those found in XP tumors. The molecular dissection of the mechanism of mutation induction using model system, such as shuttle vector, can help us to explain those mutations found in human tumors.

In conclusion, the initial aim of this project has been nicely fulfilled. The use of UV-irradiation which leads to specific mutation fingerprint and the availability of cultured cell lines isolated from cancer-prone patients have allowed us to show that unrepaired DNA lesions, present on the non-transcribed strand of key genes, are directly responsible of activating oncogenes such as the ras family or tumor suppressor genes such as the p53 one. These mutations will rapidly initiate the carcinogenesis process in the XP syndrome. The absence of cancer in the TTD/XPD syndrome is still debated. The use of specific techniques we have developed in this work may help one to resolve the paradox of DNA repair syndromes.

PUBLICATIONS

Daya-Grosjean, l., C. Robert, C. Drougard, H.G. Suarez and A. Sarasin. High mutation frequency in ras genes of skin tumors isolated from DNA-repair deficient xeroderma pigmentosum patients. Cancer Research (1993) 53: 1625-1629.

Dumaz, N., C. Drougard, A. Sarasin and l. Daya-Grosjean. Specific UV-induced mutation spectrum in the P53 gene of skin tumors from DNA repair deficient xeroderma pigmentosum patients. Proceedings of the National Academy of Sciences, USA, (1993) 90: 10529-10533.

Hoffschir, F., M. Vuillaume, l. Sabatier, M. Ricoul, l. Daya-Grosjean, S. Estrade, R. Cassingena, A. Sarasin and B. Dutrillaux. Decrease in catalase activity and loss of chromosome 11p arms and of catalase activity in the course of SV40-transformation of human fibroblasts. Carcinogenesis (1993) 14: 1569-1572.

Madzak, C., J. Armier, A. Stary, l. Daya-Grosjean and A. Sarasin. UV-induced mutations in a shuttle vector replicated in repair deficient trichothiodystrophy cells differ with those in genetically-related cancer prone xeroderma pigmentosum. Carcinogenesis (1993) 14: 1255-1260.

Michelin, S., L. Daya-Grosjean, F. Sureau, S. Said, A. Sarasin and H.G. Suarez. Characterization of a c-met proto-oncogene activated in human xeroderma pigmentosum cells after treatment with N-methyl-N'-nitro-N-nitrosoguanidine (MNNG). Oncogene (1993) 8: 1983-1991.

Stefanini, M., P. Lagomarsini, S. Giliani, T. Nardo, E. Botta, A. Peserico, W.J. Kleijer, A.R. Lehmann and A. Sarasin. Genetic heterogeneity of the excision repair defect associated with trichothiodystrophy. Carcinogenesis (1993) 14: 1101-1105.

Stefanini, M., W. Vermeulen, G. Weeda, S. Giliani, T. Nardo, M. Mezzina, A. Sarasin, J.I. Harper, C.F. Arlett, J.H.J. Hoeijmakers and A.R. Lehmann. A new nucleotide excision repair gene associated with the disorder trichothiodystrophy. American Journal of Human Genetic (1993) 53: 817-821.

Dumaz, N., A. Stary, T. Soussi, 1. Daya-Grosjean and A. Sarasin. Can we predict solar ultraviolet radiation as a causal event in human tumors by analysing the mutation spectra of the p53 gene? Mutation Research (1994) 307: 375-386.

Mezzina, M., E. Eveno, O. Chevalier-Lagente, A. Benoit, M. Carreau, W. Vermeulen, J.H.J. Hoeijmakers, M. Stefanini, A.R. Lehmann, C.A. Weber and A. Sarasin. Correction by the ERCC2 gene of UV-sensitivity and repair deficiency phenotype in a subset of trichothiodystrophy cells. Carcinogenesis (1994) 15: 1493-1498.

Schaeffer, 1., V. Moncollin, R. Roy, A. Staub, M. Mezzina, A. Sarasin, G. Weeda, J.H.J. Hoeijmakers and J.M. Egly. The ERCC2/DNA repair protein is associated with the class II BTF2/TFIIH transcription factor. EMBO J. (1994) 13: 2388-2392.

Vermeulen, W., A.J. van Vuuren, M. Chipoulet, 1. Schaeffer, E. Appeldoorn, G. Weeda, N.G.J. Jaspers, A. Priestley, C.F. Arlett, A.R. Lehmann, M. Stefanini, M. Mezzina, A. Sarasin, D. Bootsma, J.-M. Egly and J.H.J. Hoeijmakers. Three unusual repair deficiencies associated with transcription factor BTF2 (TFIIH). Evidence for the existence of a transcription syndrome. Cold Spring Harbor Symposium (1994) LIX, 317-329.

Carreau M, E. Eveno, X. Quilliet, O. Chevalier-Lagente, A. Benoit, B. Tanganelli, M. Stefanini, W. Vermeulen, J.H.J. Hoeijmakers, A. Sarasin and M. Mezzina. Development of a new and easy complementation assay for DNA repair deficient human syndromes. Carcinogenesis (1995) 16:1003-1009.

Lafarge-Frayssinet C, Daya-Grosjean 1., Estrade S., Frezouls G., Sarasin A and Cassingena R. Cellular genes possibly involved in the transformation process of the human melanoma cell line XP44 RO (Mel). Anti Cancer Res. (1995) 15, in press.

Eveno, E., F. Bourre, X. Quilliet, O. Chevalier-Lagente, R. Len, A.P.M. Eker, W.J. Kleijer, O. Nikaido, M. Stefanini, J.H.J. Hoeijmakers, D. Bootsma, J.A. Cleaver, A. Sarasin and M. Mezzina. Different removal of UV-photoproducts in genetically-related xeroderma pigmentosum and trichothiodystrophy diseases. Cancer Research (1995), in press .

Marionnet, C., A. Benoit, S. Benhamou, A. Sarasin and A. Stary. Characteristics of UV-induced mutation spectra in human XP-D/ERCC2 gene-mutated xeroderma pigmentosum and trichothiodystrophy cells. J. Mol. Biol. (1995), in press.

Daya-Grosjean, l., N. Dumaz and A. Sarasin. The specificity of P53 mutation spectra in sunlight induced human cancers. J. Photochem. Photobiology (1995) 28:115-124.

Takayama, K., Salazar, E.P., Broughton, B.C., Lehmann, A.R., Sarasin, A., Thompson, l.H. and Weber, C.A. Defects in the DNA repair and transcription gene ERCC2 (XPD) in trichothiodystrophy. 1995. Submitted to Human Molecular Genetics.

Head of project 3: Dr. Devoret

II. Objectives for the reporting period

Our project was to look for mammalian proteins affecting gene expression with the prospect that the expressed proteins would change the cell's sensitivity to radiations. We aimed at finding some mouse proteins binding to gene regulatory regions. Many gene regulatory regions display intrinsic DNA curvature. A strong correlation between curvature and in vivo strength of promoters (or replication origins) was shown for several biological systems. Consequently, we looked for a mouse protein that would recognize and bind to curved DNA.

One of the best studied proteins that recognize and bind to curved DNA is H-NS, a protein present in thé E. coli nucleoid. H-NS regulates the expression of about 40 genes in response to various environmental signals. It has been proposed that H-NS acts in E coli as a transcriptional regulator through its preferential binding to curved DNA.

Our project was to test whether a mouse protein that we have isolated during the period of the present contract would bind to curved DNA in vivo. In short, we wanted to assess whether our mouse protein would substitute in E. coli for the natural bacterial H-NS protein in regulating gene expression. In the course of this project, we indeed discovered that a mouse protein, denoted Btcd (Binding To Curved DNA), can functionally mimic the prokaryotic H-NS protein, a regulator of gene expression.

III. Progress achieved including publications

Properties of BTCD gene. Btcd protein binding to curved DNA

The BTCD gene was shown to be present in human and mouse cells. It is located on mouse chromosome 2, band A, near the vimentin gene and on human chromosome 10p.

We have reported before that Btcd, previously called kin17, is a nuclear zinc-finger protein. The property of Btcd to bind to curved DNA was assessed using various DNAs: pBR322 segments, synthetic oligonucleotides, and mammalian curved DNA sequences found at hot spots of illegitimate recombination.

Expression of mouse Btcd protein in an hns- mutant of E. coli restores cell motility.

Escherichia coli bacteria lacking H-NS protein are non-motile because H-NS positively regulates the formation of flagellae. When the mouse Btcd protein was produced in hns- bacteria, most H-NS defective cells recovered motility.

Mouse Btcd protein represses the E. coli bgl operon.

Fermentation of salicin, a ß-glucoside, occurs when the bgl operon repressed by H-NS is derepressed. This the case in hns- E. coli. E. coli hns- bacteria that ferment salicin form red colonies on indicator color plates with salicin whereas hns+ bacteria, which do not ferment salicin, produce white colonies. When the mouse Btcd protein was produced in E. coli hns- white colonies were formed, indicating that the mouse Btcd protein prevented expression of the E. coli bgl operon.

A more quantitative assay than the color plate technique was used. We directly assayed the ß-glucosidase produced after addition of an inducer. Again, the mouse Btcd protein was shown to inhibit the induction of ß-glucosidase.

Mouse Btcd and prokaryotic H-NS act in synergy to repress a mutated bgl promoter resistant to H-NS.

A mutation, called bglR11, renders the bgl promoter insensitive to H-NS protein. Likewise, we found that the mutated promoter was insensitive to repression by Btcd. However, if Btcd and H-NS were both produced in E. coli, expression of bgl was again strongly repressed. Such a synergistic action of two proteins, a bacterial and a mouse one, suggests that Btcd and H-NS bind to the bgl promoter at two distinct binding sites. The first, [A], is bound by the two proteins. The second, [B], is normally bound by H-NS and is likely located at the bglR11 site. A third site, [C], is specific for Btcd.

Functional substitution of H-NS by Btcd is dependent on Btcd binding ability.

The functional replacement of H-NS by Btcd protein can be related to their common ability to bind to curved DNA. Btcd1 protein, a mutant Btcd protein deleted of its zinc-finger, and thus showing reduced DNA binding, failed to substitute for H-NS. Moreover, we checked and demonstrated that the bgl regulatory region contains curved DNA and that Btcd attaches preferentially to the curved bgl regulatory region.

Btcd renders bacteria sensitive to UV-light.

We tested if the expression of Btcd would influence bacterial sensitivity to UV-radiation. We have observed that when Btcd was expressed, E coli bacteria became more sensitive to UV-light.
We conclude that Btcd might compete with the activity of some DNA repair genes in binding to DNA.

CONCLUSIONS

Our work demonstrates that Btcd, a mouse protein, shares basic properties with the prokaryotic protein H-NS, a regulator of gene expression. There is a growing list of mammalian proteins involved in DNA metabolism that can substitute for their counterparts in E. coli. These are: DNA ligase, methyltransferase, thymidylate synthase, 3-meADE-DNA glycosylase, and DNA polymerase I. It is clear that the ability of those mammalian proteins to substitute for E. coli proteins

depends, among other factors, on their particular interactions with DNA and also with other cellular proteins involved as co-factors in the same biochemical reaction.

Substituting a mouse protein for H-NS in E. coli will permit us to isolate Btcd mutants altered in their binding activity to curved DNA. These mutants may help us to identify the DNA binding domains of Btcd protein. Such a test may also be useful to search for other mammalian proteins which can bind to curved DNA and regulate gene expression.

Some recent work from the groups of Egly, Sarasin and Hoeijmakers, show that some repair deficiencies in humans are dependent upon the presence or not of a factor controlling transcription. These findings open new vistas on a general mechanism, proposed by Hanawalt and coworkers, that links repair to gene transcription. Btcd protein might also be involved in that pathway. This has to be tested in the near future.

PUBLICATIONS

Dutreix M, Burnett B, Bailone A, Radding CM, Devoret R (1992) A partially deficient mutant, recA1730, that fails to form normal nucleoprotein filaments. Mol. Gen. Genet. 232:489-497

Devoret R. (1992) Les fonctions SOS ou comment les bactéries survivent aux lésions de leur ADN. Annales de l'Inst. Pasteur Actualités 1:11-20

Bagdasarian MM, Bailone A, Angulo J, Scholz P, Bagdasarian M, Devoret R (1992) PsiB, an anti-SOS protein, is transiently expressed by the F sex factor during its transmission to an Escherichia coli K12 recipient. Mol. Microbiol. 6:885-893.

Tissier A (1992) Etude du gène KIN17, un gène de souris impliqué dans une réponse cellulaire aux agents génotoxiques et dans la recombinaison génétique. Diplôme d'Etudes Approfondies, Paris V p.:1-50

Martin B, Ruellan JM, Angulo JF, Devoret R, Claverys JP (1992) Identification of the recA gene of Streptococcus pneumoniae. Nucleic Acids Res. 20:6412

Araneda S, Angulo J, Devoret R, Touret M, Sallanon M (1993) Identification of a Kin nuclear protein immunologically related to RecA protein in the rat CNS. C.R.Acad. Sci. Paris, Sciences de la vie/Life sciences 316:593-597.

Asai T, Sommer S, Bailone A, Kogoma T (1993). Homologous recombination-dependent initiation of DNA replication from DNA damage-inducible origins in Escherichia coli. The EMBO J. 12:3287- 3295

Devoret R (1993) Mécanisme de la mutagénèse SOS chez les bactéries.Médecine/Sciences 9:I-VII.

Sommer S, Knezevic J, Bailone A, Devoret R (1993a) Induction of only one SOS operon, umuDC, is required for SOS mutagenesis in Escherichia coli. Mol. Gen. Genet. 239:137-144.

Sommer S, Bailone A, Devoret R (1993b) The appearance of the UmuD'C protein complex in Escherichia coli switches repair from homologous recombination to SOS mutagenesis. Mol. Microbiol. 10:963-971

Mazin A, Milot E, Devoret R, Chartrand P (1994a) Kin17, a mouse nuclear protein, binds to bent DNA that are found at illegitimate recombination junctions in mammalian cells. Mol. Gen. Genet. 244:435-438

Mazin A, Timchenko T, Ménissier-de Murcia J, Schreiber V, Angulo JF, de Murcia G, Devoret R. (1994b) Kin17, a mouse zinc finger protein that binds preferentially to curved DNA. Nucleic Acids Res. 22:4335-4341

Timchenko T, Bailone A, Devoret R (1995) A curved-DNA-binding protein from mouse can substitute in E. coli for the nucleoid H-NS protein. (Submitted to EMBO J)

Head of project 4: Dr. Rommelaere

II. Objectives for the reporting period

Parvovirus replication as a marker of cell transformation.

One of the main objectives of our project was the identification and characterization of cellular factors which are modified, expressed or repressed as a result of cellular transformation by ionizing radiation. The autonomous parvoviruses H-1 and MVM were proposed as probes to detect such modified factors. This proposal was based on results obtained previously, showing that various virally and physicochemically transformed human and rodent cells of different tissue origin (among which cells transformed by ionizing radiation) and tumour-derived cells are more susceptible to parvovirus replication than the untransformed normal cells or respective short-lived cells cultured from healthy tissue (for a review see Rommelaere and Cornelis 1991, J. Virol. Meth. 33, 233-251). We have shown that viral DNA amplification as well as gene expression are upregulated in transformed cells (J. Virol. 62, 1679-1686, 1988; J. Virol. 65, 4919-4928, 1991). Consequently, the P4 promoter and viral DNA replication were proposed as probes to identify cellular factors which are expressed as a result of oncogenic transformation by γ-rays and cellular and viral oncogenes.

III. Progress achieved including publications

Amplification of parvoviral DNA as marker of cell transformation

We have previously shown that overall replication of H-1 and MVM DNA was strongly stimulated in *in vitro* transformed and tumour-derived human fibroblasts and epithelial cells compared with normal parental cells or cells derived from healthy tissue neightbouring the tumour. In all systems tested, the sensitization of transformed cells to parvoviruses did not appear to result from a more efficient virus uptake. Consistently, the greater sensitivity of a series of transformed human and rat fibroblasts or epithelial cells to the killing effect of parvovirus MVM or H-1 correlated with their enhanced capacity to support virus replication as compared to the normal parental cells.

Parvoviral DNA replication is a multistep process. The first step of parvoviral (H-1; MVM) DNA amplification consists in the conversion of virion single-stranded DNA to a double stranded replicative form (RF). This process was followed by inoculation of ^{32}P-labelled virus. The proportion of parental label in double-stranded DNA was similar for normal and transformed human fibroblasts, suggesting that their

differential capacity to amplify MVM DNA can probably be ascribed to a post-conversion step of replication. The pool of RF molecules is amplified by a process obligatory (autonomous parvoviruses) generating concatemeric double-stranded DNA species. Amplification of RF DNA was greatly stimulated in several transformed human fibroblasts. Both monomer and dimer-length RF molecules accumulated in the SV40-transformed human fibroblasts infected with MVM. In contrast, little if any RF DNA replication could be detected in untransformed parental fibroblasts. Therefore, RF DNA amplification appears to constitute a limiting event of parvovirus replication in normal fibroblasts which is stimulated in transformed derivatives.

p53 is a determinant of the preferential replication of parvovirus MVM and H-1 in transformed cells

An unscheduled cellular gene amplification is frequently observed in neoplastic cells and represents one of the various manifestations of genomic instability, a hallmark of neoplastic transformation. It has recently been shown that gene amplification may occur in cells with inactivated p53 tumor suppressor activity but not in wt p53 expressing cells (Livingstone et al., 1992, Cell 70, 923-936; Yin et al., 1992, Cell 70, 937-948). However, p53 seems necessary but not sufficient for gene amplification, since some cells with normal wt p53 function are still permissive for gene amplification probably because a regulatory step downstream of p53 has been inactivated. We have addressed the question whether the greater ability of transformed versus normal cells for parvovirus replication (see above) could be explained, at least in part, by the absence of wt p53 expression in many *in vivo* and *in vitro* transformed human cells. In other terms, it was analyzed whether wt p53 constitutes a negative regulator of the parvovirus life cycle.

One of the numerous manners to isolate factors involved in parvovirus replication and as a consequence possibly also cell transformation, is to compare cells able or not to sustain virus replication. The human erythroleukemia cell line K562 was found extremely sensitive to parvovirus H-1 infection (survival less than 10^{-6}). Yet, three independent resistant subclones could be isolated which survived infections of 100 plaque forming units per cell. Most surprisingly, the three subclones all expressed wild-type p53, while the parental K562 cells do neither express p53 at the RNA nor at the protein level. Thus wt p53 expression may be associated with a parvovirus resistant phenotype (Telerman et al., 1993). Unfortunately, the resistant clones had lost their parvovirus-specific receptors and were persistently infected with H-1 which rendered them useless for further analysis.

The negative role of p53 on H-1 replication in the K562 cell system was confirmed by a strategy which circumvents the use of virus as a selective agent. Upon a challenge with the drug N-(phosphonacetyl)-L-aspartate (PALA), human cells expressing p53 accumulate in G_1 whereas cells expressing a mutated p53 gene or do not express p53 at all pass the G_1/S block imposed by the drug, enter the S-phase and die, or occasionally survive owing to the amplification of the gene carbamoyl-phosphate synthetase-aspartate transcabamoylase-dihydroorotase. Derived from a tumour, K562 cells are supposed to display gene instability. Because of the great susceptibility of the parental cells after infection with H-1, rare spontaneously formed revertants re-expressing wt p53 may be isolated following treatment of K562 cultures

with PALA. Several PALA-resistant K562 clones could indeed be isolated. Western blot analysis revealed that a wt p53 protein was expressed in several of them. We have previously shown that the cellular susceptibility to parvovirus-induced killing parallels several steps of the viral life cycle such as viral DNA amplification and gene expression. The survival of the PALA-resistant p53-expressing cells survived at least $2x\ 10^4$ times better than the parental cells and the survival of one such subclone even reached $2x10^{-1}$. Consequently, a correlation could be established between the cellular ability for parvovirus replication, the absence of wt p53 expression, and the unscheduled gene amplification.

With the aim at confirming if the latter conclusion had general significance, it was further analysed whether the expression of endogenous wt p53 in some other human cell and rat systems would also correlate with limitations to viral DNA replication and cytotoxicity. In collaboration with Dr. M. Tainsky (Houston) we have analyzed three pairs of fibroblast cultures from Li-Fraumeni patients for their sensitivity to parvovirus attack. Low-passage cultures express a wt and a mutant p53 allele (mt/wt), whereas high-passage cells express only a homozygous mutant gene (Yin et al., 1992, Cell 70, 937-948). The three low-passage cultures could not be distinguished from a series of normal human fibroblasts (wt/wt) with respect to resistance to H-1 induced cytotoxicity suggesting that the wt p53 was not fully inactivated by the coexpressed mutant form. In contrast, the high-passage and as a consequence immortalized Li-Fraumeni cultures were significantly more susceptible to H-1 infection and were able to amplify larger amounts of viral DNA than their respective mt/wt cells. We have previously shown that immortalization of normal human fibroblasts by SV40 was not associated with a greater susceptibility to H-1 induced cytotoxicity (Chen et al., 1986; Cancer Res. 46, 3574-3579). Indeed, short-living SV40 transformed human fibroblasts were as sensitive to H-1 induced lysis as their immortalized derivatives.

In collaboration with M. Oren (Revohot), a series of related embryo rat fibroblasts lines were analyzed expressing or not functional endogenous p53 (Telerman et al, 1993). All cells overexpressed ectopic p53 miniproteins which were able to inactivate or not the endogenous wt p53 by oligomerization (see Shaulian et al., 1992, Mol. Cell Biol., 12, 5581-5592). The former cultures were susceptible to H-1 infection whereas the cells in which a miniprotein was expressed which failed to oligomerize endogenous p53, were more resistent (Telerman et al., 1993). Not unexpectedly, the greater susceptibility to parvovirus correlated with higher viral amplification levels. In summery, the present data suggest that in three different cell systems expression of endogenous wt p53 correlates with restrictions to parvovirus replication.

wt p53 downregulates the parvoviral P4 promoter.

When overexpressed, wt p53 can act as a positive regulator of genes bearing a specific p53 binding site, and as a negative regulator of a great number of genes devoid of such a sequence. Given the negative activity of p53 on virus replication, it was assessed whether wt p53 downregulates the pivotal P4 promoter of H-1 and MVM which lack a consensus p53 binding site. Cotransfections were performed in various cell lines with plasmids expressing either a wt or a mutant human p53 c-DNA and a

plasmid bearing the reporter gene CAT under control of the MVM P4 promoter. CAT expression was repressed in the presence of wt p53 but not in that of mutant p53. The region of the P4 promoter mediating the p53 response could be localized to a small region of the promoter containing the active TATA box. Thus, downregulation of the P4 promoter might be responsible for whole or part of the negative effect that wt p53 exerts on the viral life cycle. The question whether this downregulation has physiological significance remains to be answered and is currently under investigation.

Transient activation of the P4 promoter.

While cells stably *in vitro* transformed cells display higher P4 promoter activities than normal untransformed cells, we were, despite considerable efforts, unable to detect transient modifications in P4 promoter activity in cells exposed to low doses of ionizing radiation. Thus, the enhanced capacity of parvoviruses to replicate in pre-irradiated cells is not likely to be ascribed to a transient upmodulation of the P4 promoter. A region containing the palindromic ends and the early promoter is sufficient to allow a transient parvoviral DNA replication follwing cell exposure to physicochemical agents (reference Yalkinoglu et al., 1991, J. Virol. 65, 3175-3184). Thus, parvoviral DNA replication rather than promoter activation may constitute the primary event underlying the enhanced virus capacity.

In Vitro DNA replication of parvovirus DNA

From the foregoing, we may conclude that parvoviruses take advantage of factors provided by oncogenic transformed cells which promote their replication. In order to facilitate the identification and functioning of putative replication-promoting factors, an *in vitro* replication system was developed. Such a system may allow us to analyze viral DNA replication as a function of transformation, differentiation or cell cycle. The assay is based on the *in vitro* DNA replication system which has been developed for SV40, and uses cytoplasmic extracts and monomeric RF DNA as substrate. The viral nonstructural protein NS-1 which is required for viral DNA amplification *in vivo,* was purified from recombinant baculo-and vaccinia viruses. Preliminary results obtained with extracts from highly permissive transformed mouse fibroblasts showed that the processing of monomer RF to dimer RF DNA occurs in the presence, but not in the absence of the viral replication factor NS-1. Moreover, we have shown that NS-1 is able to resolve covalently closed right-hand ends of MVM, and by doing so stimulates a subsequent strand displacement reaction. The latter results are consistent with predictions made by current models of parvovirus DNA replication.

p53 will be the prime candidate to be tested in the replication system. Several forms of the protein will be used. A recombinant baculovirus will be constructed expressing a natural alternatively spliced form of murin p53 and will be compared to the already available normal spliced form of mouse p53 for its ability to interfere with the parvovirus replication machinery. There are strong indications that the alternatively spliced form of mouse p53 plays a role distinct from the normal form and may specifically inhibit cellular DNA replication. Moreover, a human wt p53 and a temperature-sensitive mutant will be compared. By means of south-western blotting and

screening of expression libraries, nucleolin, an abundant nuclear protein was identified which specifically interacted with single-stranded virion DNA (Barrijal et al., 1992, Nucleic Acids Res. 20, 5053-5060). It will be analyzed whether nucleolin modulates viral DNA replication. Extracts from γ-ray irradiated cells will be used to monitor viral DNA replication. From published data, it is expected that ionizing radiation transiently mobilizes (replication) cellular factors promoting parvoviral DNA amplification.

Conclusions

Using the oncosuppressive parvovirus H-1 as a selective agent, we have succeeded in identifying in human cells of different origins a negative regulator of parvovirus replication. This factor was identified as p53, a protein involved in the etiology of many, if not all, human cancers.

On the one hand, cells resistant to H-1 could be rendered susceptible by inactivation of endogenous wt p53 protein (through oligomerization) or by deletion of the gene. On the other hand, susceptible cells became resistant to parvovirus infection after the re-expression of a wt p53 protein. p53 is a tumour suppressor gene whose expression is associated with the correct functioning of certain cell cycle check points and possibly as a consequence, with control over genomic stability. Indeed, the resistance of normal human and heterologous mutant p53 Li-Fraumeni fibroblasts and of the p53 re-expressing K562 subclones correlates with their refractoriness to gene amplification (Yin et al., 1992, Cell 70, 937-948, and our results with the K562 subclones). Hence, p53 seems to determine cell resistance to both parvovirus replication and gene amplification, suggesting that these phenomena may be mechanistically related. It has been shown by others that genomic instability preceeds tumorigenesis *in vivo*. As a consequence, parvovirus replication may constitute an early marker of neoplastic transformation.

Publications and communications.

Telerman, A., M. Tuijnder, T. Dupressoir, B. Robaye, F. Sigaux, E. Shaulian, M. Oren, J. Rommelaere and R. Amson. (1993). A model for tumor suppression using H-1 parvovirus.
Proc.Natl. Acad. Sci. USA. 90, 8702-8706.

Iotsova, I., Z. Kherrouche, J. Rommelaere and J. Cornelis. MVMp parvovirus early promoter is inhibited by the p53 antioncogene. p53 in Growth control and Neoplasia, Zürich, Switzerland, March 24-27, 1993.

Baldauf, A., J. Rommelaere, and K. Willwand. NS-1 abhängige Replikation von Minute Virus of Mice DNA *in vitro*. Frühjahrstagung der Gesellschaft für Virologie. Giessen, Germany, March 13-18, 1995.

Tuijnder, M., M.A. Tainsky, J. Rommelaere and J. Cornelis. Correlation between the

expression of wild-type p53 and restrictions to H-1 replication and gene amplification. VI Parvovirus Workshop, Montpellier, France, Sept. 10-14, 1995.

Baldauf, A., K. Willwand, and J. Rommelaere. Distinct steps of MVM DNA replication reproduced in an *in vitro* system. VI Parvovirus Workshop, Montpellier, France, Sept. 10-14, 1995.

Head of project 5: Dr. Bertazzoni

II. Objectives for the reporting period

Cellular and genetic characterization of DNA repair mutants (F. Nuzzo and M. Stefanini):

Cellular and genetic characterization of tricothiodistrophy (TTD), xeroderma pigmentosum (XP) and Cockayne syndrome (CS) patients. Chromosomal instability in homozygous and heterozygous carriers of XP mutations. Cellular and genetic characterization of mutagen-sensitive rodent mutants .

Analysis of poly ADP-ribosylation process (U. Bertazzoni and A.I.Scovassi):

Identification of ADP-ribosylated proteins in human cells treated with mutagens; analysis of expression and stability of mRNA for poly(ADP-ribose)polymerase (ADPRP); study of the ADP-ribosylation during programmed cell death; study of the distribution of antibodies to ADPRP in autoimmune diseases.

III. Progress achieved including publications

Cellular and genetic characterization of DNA repair mutants

DNA repair defects associated with TTD, XP and CS phenotypes
        The analysis of the cellular response to UV irradiation in TTD patients from different countries showed that TTD is frequently associated (25 out of 33 cases) with defects in nucleotide-excision repair (NER). By complementation studies, we demonstrated that the same genetic defect responsible for XP group D is present in the majority of TTD patients (22 out of 25). These results indicate that the association between TTD and XP-D cannot be considered fortuitous, and they suggest some kind of causal connection between XPD gene alterations and TTD features. The presence of the genetic defect responsible for XP group D, was also demonstrated by complementation analysis in two genetically unrelated patients showing clinical features of XP and CS. The recent finding that the XPD protein is a subunit of the basal transcription factor TFIIH, which is involved in DNA repair, transcription and cell cycle regulation, suggests that mutations in different functional domains of the XPD gene might give rise to different physiological phenotypes. Beside the XP-D defect, alterations in two other NER genes have been identified associated with TTD. A new gene, designated TTDA, appeared to be

defective in the patient TTD1BR whereas the XP-B gene, already described as responsible for XP/CS pathological phenotypes, was found to be defective in two related French patients.

Chromosomal instability in homozygous and heterozygous carriers of XP mutations

Chromosome analysis in cultured fibroblast strains from unaffected skin of XP patients and their relatives demonstrated the presence of clonal chromosome rearrangements in subjects carrying the XPC mutation (both homozygotes and heterozygotes) and in XP-D patients. This results suggested that cells at an early stage of transformation were present in the cell populations. To test this hypothesis, anchorage independent (AI) growth, a characteristic strictly linked to cellular transformation, was analyzed in one XP-C strain (XP9PV). In XP9PV the frequency of AI clones was about 100x higher than in the control population confirming the genomic instability of this strain. Fourty-one AI clones were isolated and specific chromosomes anomalies, in particular telomeric associations, were detected in several of them. In one clone (XP9UV25) we could detect in about 20% of mitoses a specific telomeric association between 5p and 16q as the sole chromosome anomaly. This association not only was maintained during successive passages (from the 5th to the 13th) but also underwent rearrangements generating (5p;16q) dicentrics with intercentromeric region with deletions or duplications of variable sizes, (5;5) or (16;16) homodicentrics and 5p+ or 16 q+ monocentric derivatives. The analysis of the structure of the rearranged chromosomes by two color FISH with painting probes for chromosomes 5 and 16 confirmed their origin from the (5p;16q) dicentric throughout breakage events within the intercentromeric region followed by reunion or healing of the broken ends. The breakage events could occur in any site of the intercentromeric region, however a preferential break point was the 16q heterochromatic (16qh) region. These findings document the evolution, in a fibroblast clone, of a diploid karyotype to an unbalanced one starting from a telomeric association and can represent a model of the generation of unbalanced karyotypes in transformed cells.

Cellular and genetic characterization of mutagen-sensitive rodent mutants

Genetic characterization of mutagen-sensitive clones isolated from rodent cell lines led to the identification of a new complementation group of UV-sensitive rodent cell lines, the eleventh group. By complementation analysis we demonstrated that the repair defect in the mutant UVS1 (isolated from the Chinese hamster cell line CHO9 and previously found to complement the UV sensitivity of mutants representative of groups 1 to 7) was genetically different from those present in mutants belonging to groups 8, 9 and 10.

Analysis of poly ADP-ribosylation process

Identification of ADP-ribosylated proteins in human cells

ADP-ribosylation, which is catalyzed by the enzyme poly(ADP-ribose) polymerase (ADPRP), represents a post-translational modification of several nuclear

proteins. Main acceptors of ADP-ribose are histones, ADPRP itself and DNA topoisomerase I. We addressed the characterization of the non-histone proteins ADP-ribosylated in human cells. The analysis has been performed by using different experimental procedures which allowed the specific labeling of modified species and their immunological recognition by highly specific antibodies. The experiments were essentially based on the separation of ADP-ribosylated proteins from intact or permeabilized cells or isolated nuclei. We have focused our attention on a 170 kDa peptide, possibly corresponding to DNA topoisomerase II. To prove this hypothesis, we have immunoprecipitated the enzyme from HeLa cell nuclei incubated with 32P-NAD. Our results demonstrated that a 170 kDa protein identified as topoisomerase II, is ADP-ribosylated in physiological conditions. To verify if the post-translational modification of this protein is modulated during DNA repair, we have treated HeLa cells with the alkylating agent dimethylsulfate. The results obtained indicated that the modification of topoisomerase II is not affected by the damage to DNA.

Analysis of expression and stability of mRNA for poly(ADP-ribose)polymerase

We have studied the regulation of the expression of the ADPRP gene in HeLa cells and quiescent and mitogen-stimulated human lymphocytes. The analysis consisted of the quantitation of mRNA molecules by means of a new technique based on PCR and involves co-amplification of a competitive target template by using the same primers as those of the cDNA target obtained by reverse transcription of the mRNA species. The results obtained comparing quiescent and proliferating lymphocytes or HeLa cells indicate that the proliferation state induces a notable increase in the expression of the enzyme. To determine the stability of mRNA for ADPRP, a new PCR amplification system was developed, using non-competitive conditions. We observed that in quiescent cells the half-life of ADPRP mRNA is about 1 h, whereas in proliferating cell cultures it was calculated to be about 4-5 fold higher.

Study of the ADP-ribosylation during programmed cell death

The mechanism leading to programmed cell death has been described in malignant cells treated with antitumoral drugs acting as inhibitors of DNA topoisomerase II. We have analysed the properties of the ADP-ribosylation process to elucidated if regulation of this reaction occurs during the death of apoptotic type. We have evaluated ADP-ribosylating activity by different specific assays (activity gel, boronate chromatography, ADP-ribose synthesis) and we have observed that in extracts from HeLa cells exposed to VP-16, the autoribosylated form of ADPRP is highly increased. Time-course experiments indicated that enzyme activation occurs immediately after internucleosomal DNA cleavage typically visible in apoptotic cells. Since ADP-ribosylation is dependent on the presence of DNA strand breaks or free ends, we have investigated if apoptotic DNA fragments could be able to stimulate enzyme activity. To assess our hypothesis, we have treated HeLa cells with VP-16 in the presence of $Zn2+$, a known inhibitor of nuclease(s) responsible for internucleosomal DNA fragmentation. In these conditions, the activation of ADPRP is prevented, supporting the idea that the activation of ADPRP is regulated by the appearance of small-sized DNA fragments occurring during cell death of

apoptotic type induced in HeLa cells by VP-16. Our observations have been extended to other malignant human cells treated with various topoisomerase II-poisons.

Study of the distribution of antibodies to ADPRP naturally occurring in autoimmune diseases

Autoimmune diseases are characterized by the development of antibodies against DNA and nuclear proteins. We have searched for the presence of autoantibodies to ADPRP in sera from patients affected by several autoimmune diseases. Our results strongly supported that poly(ADP-ribose)polymerase has to be considered as a new target of autoimmunity. Recently, experiments have been performed to correlate the distribution of ADPRP-antibodies with various pathological parameters. Preliminary data could suggest that the presence of specific autoantibodies could be correlated to the pulmonary involvement of some diseases.

PUBLICATIONS

Astaldi Ricotti G.C.B., Facchini A., Montecucco C.M., Negri C. and Scovassi A.I. - New targets of autoantibodies. Advances in Allergy and Immunology 1:187-194 (1992).

Bertazzoni U. and Scovassi A.I. - Correlation of poly(ADP-ribose)polymerase ctivity with cellular defense mechanism In: "Aging and cellular defense mechanisms" (Franceschi C., Crepaldi G., Cristofalo V. and Vijg I. eds.), Annals of the New York Academy of Sciences 663: 215-219 (1992).

Riboni R., Botta E., Stefanini M., Numata M. and Yasui A. - Identification of the 11th complementation group of UV-sensitive excision repair-defective rodent mutants. Cancer Res. 52: 6690-6691 (1992).

Scovassi A.I., Negri C., Negroni M., Dal V., Borzì, R.M., Meliconi R., Facchini A., Montecucco C.M. and Astaldi RIcotti G.C.B. - Detection of circulating autoantibodies to poly (ADP-ribose)polymerase in autoimmune diseases. In: "Aging and cellular defense mechanisms" (Franceschi C., Crepaldi G., Cristofalo V. and Vijg I. eds.), Annals of the New York Academy of Sciences 663: 508-509 (1992).

Scovassi A.I., Negroni M., Mariani C., Clerici L., Negri C. and Bertazzoni U. - ADP-ribosylation of topoisomerase II in physiological conditions. In: "ADP-ribosylation reactions" (Poirier G. and Moreau P. eds.), Springer-Verlag, N.Y., pp. 269-275 (1992).

Stefanini M. - DNA repair defects and cancer proneness in xeroderma pigmentosum. Medicine Biologie Environment 20: 3-11 (1992).

Negri C., Bernardi R., Braghetti A., Astaldi Ricotti GC.B. and Scovassi A.I. - Effect of chemotherapeutic drug VP-16 on poly(ADP-ribosylation) in apoptotic HeLa cells. Carcinogenesis 14: 2559-2564 (1993).

Negroni M. and Bertazzoni U. - Differential expression and stability of poly(ADP-ribose)polymerase mRNA in human cells. Biochim. Biophys. Acta 1173: 133-140 (1993).

Scovassi A.I., Mariani C., Negroni M., Negri C. and Bertazzoni U.- ADP-ribosylation of non-histone proteins in HeLa cells: modification of DNA topoisomerase II. Experimental Cell Res. 206: 177-181 (1993).

Guano F., Bernardi R., Negri C., Donzelli M., Prosperi E., Astaldi Ricotti G. and Scovassi A.I. - Dose-dependent zinc inhibition of DNA ladder in apoptotic HeLa cells regulates the activity of poly(ADP-ribose)polymerase and does not protect from death induced by VP-16. Cell Death and Differentiation 1: 101-107 (1994).

Bernardi R., Negri C., Donzelli M., Guano F., Torti M., Prosperi E. and Scovassi A.I. - Activation of poly(ADP-ribose)polymerase in apoptotic human cells. Biochimie 77: 378-384 (1995).

Mondello C., Casati A., Riboni R. and Nuzzo F. - Structural instability of a transmissible end-to-end dicentric chromosome in a xeroderma pigmentosum fibroblast clone. Cancer Genet. Cytogenet. 79: 41-48 (1995)

SHORT COMMUNICATIONS

Scovassi A.I., Negri C., Bernardi R. and Astaldi Ricotti G.C.B. - Analisi dell'effetto di inibitori della DNA Topoisomerasi II sull'ADP-ribosilazione. Convegno Scientifico "I processi di ADP-Ribosilazione", Ancona, Italy (1992).

Stefanini M., Vermeulen W., Giliani S., Nardo T., Sarasin A., Lehmann A.R. and Hoeijmakers J.H.J. - Identification of patients affected by trichothiodystrophy showing DNA repair defects different from that present in xeroderma pigmentosum complementation group D. UKEMS/DNA REPAIR NETWORK Joint Meeting, Swansea, U.K. (1992).

Stefanini M., Giliani S., Lagomarsini P., Nardo T., Sarasin A., Lehmann A.R., Vermeulen W. and Hoeijmakers J.H.J. - Genetic heterogeneity of DNA repair defects in trichothiodystrophy. 11th International Congress on Photobiology, Kyoto, Japan, S12-3, p. 159 (1992).

Bernardi R., Negri C., Braghetti A., Guano F., Astaldi Ricotti G.C.B. and Scovassi A.I. - Il trattamento di cellule HeLa con VP-16 induce apoptosi e provoca attivazione della poli(ADP-ribosio)polimerasi. VI ConvegnoScientifico "I processi di ADP-ribosilazione", Verona, Italy (1993).

Bernardi R., Negri C., Guano F., Donzelli M., Astaldi Ricotti G.C.B. and Scovassi A.I. - Appearance of apoptotic features in HeLa cell treated with VP-16. International Congress: "Molecular and cellular biochemistry of oxidative stress",

Urbino, Italy (1993).

Bernardi R., Negri C., Guano F., Donzelli M., Astaldi Ricotti G.C.B. and Scovassi A.I. - Analisi del processo di ADP-ribosilazione in cellule HeLa rese apoptotiche da trattamento con VP-16. Atti XXX Convegno SIBBM, Gubbio, Italy (1993).

Bernardi R., Negri C., Guano F., Prosperi E., Donzelli M., Astaldi Ricotti G.C.B. and Scovassi A.I. - Analisi del processo di ADP-ribosilazione in cellule HeLa rese apoptotiche da trattamento con VP-16. "1=B0 Incontro di studi sulla Morte cellulare", Roma, Italy (1993).

Guano F., Negri C., Facchini A., Montecucco C.M., Meliconi R., Astaldi Ricotti G.C.B. and Scovassi A.I. - Evidence for the enzyme poly(ADP-ribose) polymerase as a target of autoimmunity. Biotech RIA, Firenze, Italy (1993).

Mondello C., Casati A. and Nuzzo F. - High frequency of a dicentric chromosome involving 5p and 16q in a clone isolated from an XP fibroblast strain. Atti AGI, 39, 175 (1993).

Mondello C., Casati A. and Nuzzo F. - Anchorage independent growth of a xeroderma pigmentosum cell strain. Atti AGI, 39, 177 (1993).

Negri C., Bernardi R., Guano F., Astaldi Ricotti G.C.B. and Scovassi A.I. - Effect of cellular apoptosis induced by VP-16 on poly ADP-ribosylation process. "X Riunione Nazionale di Citometria", Orvieto, Italy (1993).

Negri C., Guano F., Bernardi R., Donzelli M. and Scovassi A.I. - Effetto dello zinco sul processo di apoptosi indotto da VP-16 in cellule HeLa. VI Convegno Scientifico "I processi di ADP-ribosilazione", Verona, Italy (1993).

Stefanini M., Vermeulen W., Giliani S., Kraemer K.H., Lehmann A.R. and Hoeijmakers J.H.J. - Detection of xeroderma pigmentosum (XP) group D and G defects in patients showing the clinical symptoms of XP and Cockayne's syndrome. BSCB/DNA Repair Network Conference on Cell cycle checkpoints, DNA repair and DNA replication strategies. St. John's College, Cambridge, UK, A164, (1993).

Bernardi R., Negri C., Guano F., Donzelli M., Prosperi E. and Scovassi A.I. - Regolazione dell'attivita' della poli(ADP-ribosio)polimerasi da parte dei frammenti internucleosomici di DNA originati in cellule apoptotiche. VII Convegno Nazionale: "I processi di ADP-ribosilazione", Sorrento, Italy (1994).

Bernardi R., Negri C., Donzelli M., Guano F., Prosperi E. and Scovassi A.I. - Activation of poly(ADP-ribose)polymerase in apoptotic human cells. 11th International Symposium on ADP-ribosylation, Strasbourg, France (1994).

Botta E., Broughton B.C., Weber C.A., Lehmann A.R. and Stefanini M. - Genetic

and molecular analysis of the DNA repair defect associated with trichothiodistrophy in Italian patients. Atti AGI 40 (1994).

Ghibelli L., Marini M. and Scovassi A.I. - Apoptosi e ADP-ribosilazione: analisi di alcuni punti-chiave risultanti dal confronto di sistemi diversi. VII Convegno Nazionale: "I processi di ADP-ribosilazione", Sorrento, Italy (1994).

Mondello C., Casati A., Riboni R., Ranzani G.N. and Nuzzo F. - Chromosome anomalies in anchorage independent clones from an XP-C strain. Symposiumon: "Molecular Genetics of Cancer", Cold Spring Harbor Laboratory, New York, USA (1994).

Riboni R., Casati A., Nardo T., Nuzzo F. and Mondello C. - Rearranged chromosomes deriving from a dicentric: structural analysis by "chromosome painting". III Congresso Nazionale SIMA, Viterbo, Italy (1994).

Donzelli M., Negri C., Bernardi R. e Scovassi A.I. - Risposta dell'enzima poli(ADP-ribosio)polimerasi alla formazione di frammenti di DNA durante il processo di apoptosi. VIII Convegno Nazionale "I processi di ADP-ribosilazione", Bologna, Italy (1995).

Scovassi A.I., Negri C., Donzelli M. and Bernardi R. - Post-translational modifications occurring during cell death. International Conference Cell Death in Human Pathology, Lecce, Italy (1995).

Scovassi A.I., Negri C., Bernardi R., Donzelli M., Prosperi E. and Guano F. - Regulation of poly(ADP-ribose)polymerase activity by the appearance of internucleosomal apoptotic DNA fragments. Keystone Symposium on Apoptosis, Colorado, USA (1995).

Head of project 6: Dr. Thomou-Politi

Objectives for the reporting period:

1. The modulation of CD2 antigen expression in X-irradiated CHO cells transfected with δH3 vector carrying the human CD2-cDNA, has been investigated. We have studied the effect of very low doses of X-irradiation on the level of CD2 protein expression.

2. The effects of low dose ionizing radiation on the CD2 gene and protein expression in normal human T lymphocytes has been investigated.

III.   Progress achieved including publications

Introduction

Ionizing radiation induces a variety of responses in mammalian cells. As it is well known such responses include activation of expression of genes coding for transcription factors, growth factors, proteases and other proteins.

Recently there seems to be a shift in interest towards the effects of low dose radiation on immune response of T cells to antigenic or mitogenic stimulation after exposure to low dose ionizing radiation.

The human CD2 gene encodes a cell surface T cell specific antigen that appears early in thymic ontogeny and is involved in cell-cell adhesion, signal transduction, T cell activation, differentiation and immune response. This Ag is expressed in thymocytes, T lymphocytes and NK cells and also is the receptor of sheep red blood cells (SRBC). Therefore we have investigated the effects of low dose ionizing radiation on the CD2 gene and protein expression in $CD2^+$ CHO cells and in normal human T lymphocytes in order to be clarified if the low dose ionizing radiation has a stimulatory and/or enhancing effect on immune response.

Results

1) Effects of X-irradiation on the CD2 protein expression in CD2$^+$ CHO cells

Thioguanine resistant CHO cells were stably cotransfected with πH3-CD2 and pSV2-gpt vectors. The resulting cotransfected CHO clones are HAT resistant and constitutively express the human cell surface CD2 antigen as was verified by their ability to form rosettes with sheep red blood cells (SRBC). Moreover when CD2$^+$ CHO clones were incubated with anti-CD2 mAb (OKT11), stained with FITC and analyzed by flow cytometry revealed a pattern of fluorescence intensity similar to that of peripheral T lymphocytes. One clone namely CL13, the most enriched in rosette positively cells, was chosen for further study.

Southern blot analysis of genomic DNA cleaved with various restriction endonucleases revealed that the CD2$^+$ CL13 clone contains only one copy of πH3-CD2 vector integrated in the CHO genome.

The CL13 cells were further tested by titrating their bioresponse to low doses of radiation affecting the quantitative expression of the CD2 antigen. It was found that very low doses of X-ray (2-6 cGy) did not affect the level of CD2 antigen compared to unirradiated control as was verified by rosette assay and flow cytometric anaysis. In contrast, the irradiated CL13 cells seemed to be very sensitive at 10-50 cGy showing decreased levels of fluorescence which could be attributed to the fact that around 50% of the cells have lost the CD2$^+$ phenotype and/or the CD2 expression was reduced in all CD2$^+$ cells.

Southern blot analysis of genomic DNAs from CL13 cells given 0-10 cGy of X-irradiation showed that no extra or missing bands and no amplification have occurred compared to unirradiated control.

Although the explanation for the mechanism involved in the loss of CD2$^+$ phenotype is obscure a number of possibilities may be considered. It is known that cell membrane and receptors may act as primary target for low doses of irradiation. So, the partial inhibition of erythrocyte rosette formation that we report may be attributed to the fact that free radicals produced by ionising radiation may affect the conformation of the CD2 receptor leading to a partial loss of CD2$^+$ phenotype in CL13 cells. Alternatively, a tentative hypothesis is to consider that low doses of X-irradiation trigger a trans-activating signal which switches off CD2 expression.

2. Effects of ionizing radiation on the CD2 gene and protein expression in resting and PHA activated normal human T lymphocytes.

Human peripheral blood mononuclear cells (PBMC) were ficoll separated, irradiated at doses from 0 to 200 cGy and cultured for 24 and 48 hours with or without suboptimal concentration of PHA (2 ìg/ml of culture medium) that as it is known stimulated human T lymphocytes. At the end of the culture cells were analyzed: a) for their ability to form spontaneous rosettes with sheep red blood cells (SRBC) and b) by flow cytometry using anti-CD2 (OKT11), anti-CD4 (OKT4) and anti-CD8 (OKT8) mAbs.

The results have shown that resting and PHA activated T lymphocytes irradiated at doses from 0 to 50 cGy bind more SRBC on their cell surface so the percentage of multi-layer rosettes forming cells (a T-lymphocyte that binds more than 15 SRBC, Fig. 1) is increased reaching a maximum at 50 cGy. In contrast at doses from 100 to 200

cGy the percentage of multi-layer rosettes is reduced almost to the unirradiated control (Fig. 2). Furthermore the FACS profiles produced, using anti-CD2 mAb (OKT11) by an EPICS analyzer, reveal a transposition to higher levels of fluorescence intensity at doses up to 50 cGy of X-irradiation while at 100 cGy the profile is almost identical to the unirradiated control (Fig. 3). Both 24 and 48 hours cultures with or without PHA gave similar FACS profiles but the differences in transposition of fluorescence intensity in irradiated and simtulated with PHA for 24 hours culture were more striking. The results have shown that there might be a stimulatory and/or enhancing effect of low dose ionizing radiation: a) on the CD2 protein expression and b) on the response of T cells to mitogenic stimulation. It is of interest to note that the enhaNcing effect of ionizing radiation on the response of T cells is demonstrable only within a narrow radiation dose range.

In contrast the FACS profiles produced, using anti-CD4 mAb(OKT4) or anti CD8 mAb (OKT8) by an EPICS analyser, are almost identical at doses from 0-100 cGy in 24 or 48 hours cultures with or without PHA (Fig. 4a,b) supporting the aspect that low doses of ionizing radiation does not affect the CD4 and CD8 surface proteins expression. Moreover, the ratio of $CD4^+$ (helper/inducer) to $CD8^+$ (cytotoxic/ suppressor) T cells in 24 and 48 hours cultures with or without PHA remains unchanged at all doses used, a fact which is in agreement with the observation of Nakamura et al., 1990 that the radiosensitivities of these cells are very similar at doses from 0-500 cGy of X-rays.

In order to asses if the changes observed in the expression of the CD2 antigen after X-irradiation, are the consequence of stimulation of CD2 gene transcription we performed Northern blot analysis, in irradiated lymphocytes at doses from 0 to 100 cGy cultured for 24 hours with or without PHA, using digoxigenin-11-dUTP labelled CD2-cDNA as a probe.

The results indicate that the level of CD2 mRNAs is significantly increased in irradiated T lymphocytes compared to unirradiated control and moreover remains elevated even at a dose of 100 cGy (Fig. 5a,b).

In order to determine whether the accumulation of CD2 mRNAs is the consequence of either stimulation of transcription and/or stabilization of performed mRNAs we stimulated PBMC with PHA for 12 hours to induce maximal levels of CD2 message. Actinomycin-D was then added to block further message production, the cells were irradiated at doses from 0 to 100 cGy, cultured without PHA for 2 and 4 hours given that the half life of the CD2 message is approximately 45 min. Finally, the cells were harvested for Northern blot analysis.

The results show that there was no extension of the life-span of 1.7 and 1.3 kb transcription products at all doses used supporting the aspect that the accumulation of CD2 mRNAs after X-irradiation is due mainly to stimulation of transcription and not to stabilization of preformed mRNAs (Fig. 6a,b).

From the results presented we conclude that *de novo* RNA synthesis is required for the up regulation of the CD2 antigen expression on the cell surface.

The fact that at 100 cGy the percentage of multilayer rosette forming cells is reduced while the CD2 mRNAs level remains elevated could be attributed mainly to conformational changes of the CD2 membrane receptor caused by free radicals produced by ionizing radiation. This radioinduced modulation of the CD2 receptor is

dose dependent and leads to partial inhibition of the T cells ability to form multilayer rosettes and to bind anti-CD2 mAb (OKT11). This aspect is also supported by Nishida et al. 1981 and Ojeda et al., 1991 who have demonstrated that free radicals produced by hypoxanthine plus xanthine oxidase system or by ionizing radiation have effects on the lymphocyte membrane receptors.

Our results as well as those of other investigators suggest that there might be a stimulatory and/or an enhancing effect of low dose ionizing radiation on the immune response of T lymphocytes.

Thus, stimulation of CD2 gene transcription as well as enhancement of the CD2 antigen expression and increased response of T cell to mitogenic stimulation after exposure to low-doses of X-irradiation could be considered as a putative adaptive response of cells exposed to genotoxic stresses. It is of interest to note that the enhancing effect on the immune response is demonstrable only within a narrow radiation dose range.

Publications and References

Kitsiou P., Sambani C. and H. Thomou (1993). Effects of low-doses of X-irradiation on the expression of human cell surface CD2 antigen in $CD2^+$ CHO cells. Int. J. Radiat. Biol. 64:621-626.

Pantelias G.E., Iliakis G.E., Sambani C. and G. Politis (1993). Biological dosimetry of absorbed radiation by C-banding of interphase chromosomes in peripheral blood lymphocytes. Int. J. Radiat. Biol., 63:349-354.

Th. Siatra-Papastaikoudi, A. Tsotinis, C.P. Raptopoulou, C. Sambani and H. Thomou, (1995). "Synthesis of new alkylamino-alkyl thiosemicarba-zones of 3-acetylindole and their effect of DNA synthesis and all cell proliferation", Eur. J. of Med. Chemistry 30:107-114.

Kitsiou, P.C. Sambani and H. Thomou (1994). "Effects of low doses of X-irradiation on the CD2 gene expression in normal human T lymphocytes" in 1st Mediterranean Congress on Radiation Protection, p. 100, 5-7 April, 1994, Athens.

Kitsiou P., Sambani C. and H. Thomou. "Stimulatory effect of low dose X-irradiation on the expression of the human T lymphocyte CD2 surface antigen", submitted to Int. J. Radiat. Bi

Nakamura N., Kusunoki, Y. and Akiyama, M. (1990). Radiosensitivity of CD4 and CD8 positive human T lymphocytes by an in vitro colony formation assay. Radiation Research, 123:224-227.

Nishida, Y., Tanimoto, K. and Akaoka, I. (1981). Effect of free radicals on lymphocyte response to mitrogen and rosette formation. Clinical Immunology and Immunopathology 19:319-324.

Ojeda, F., Andrade, J., Maldonado, C., Guarda, M.I. and Folch, H. (1991).

Radiation-induced surface IgG modulation; protein kinase C involvement. International Journal of Radiation Biology 59:53-58.

Fig. 1

Fig. 2

Fig. 4

Fig. 3

a

1　2　3

1.7
1.3

Fig. 5

b

1　2　3　4

1.7 —
1.3 —

Fig. 5

a

1　2　3

1.7
1.3

2h

b

1　2　3

1.7
1.3

4h
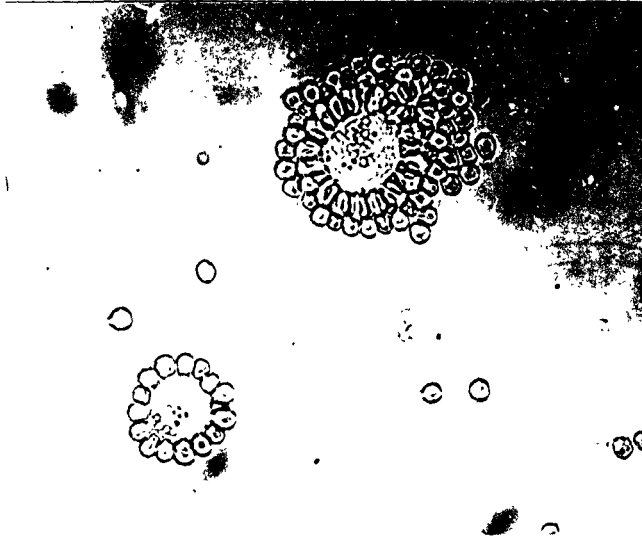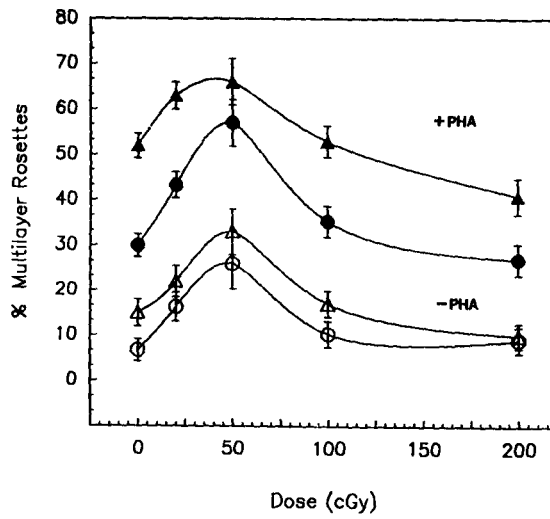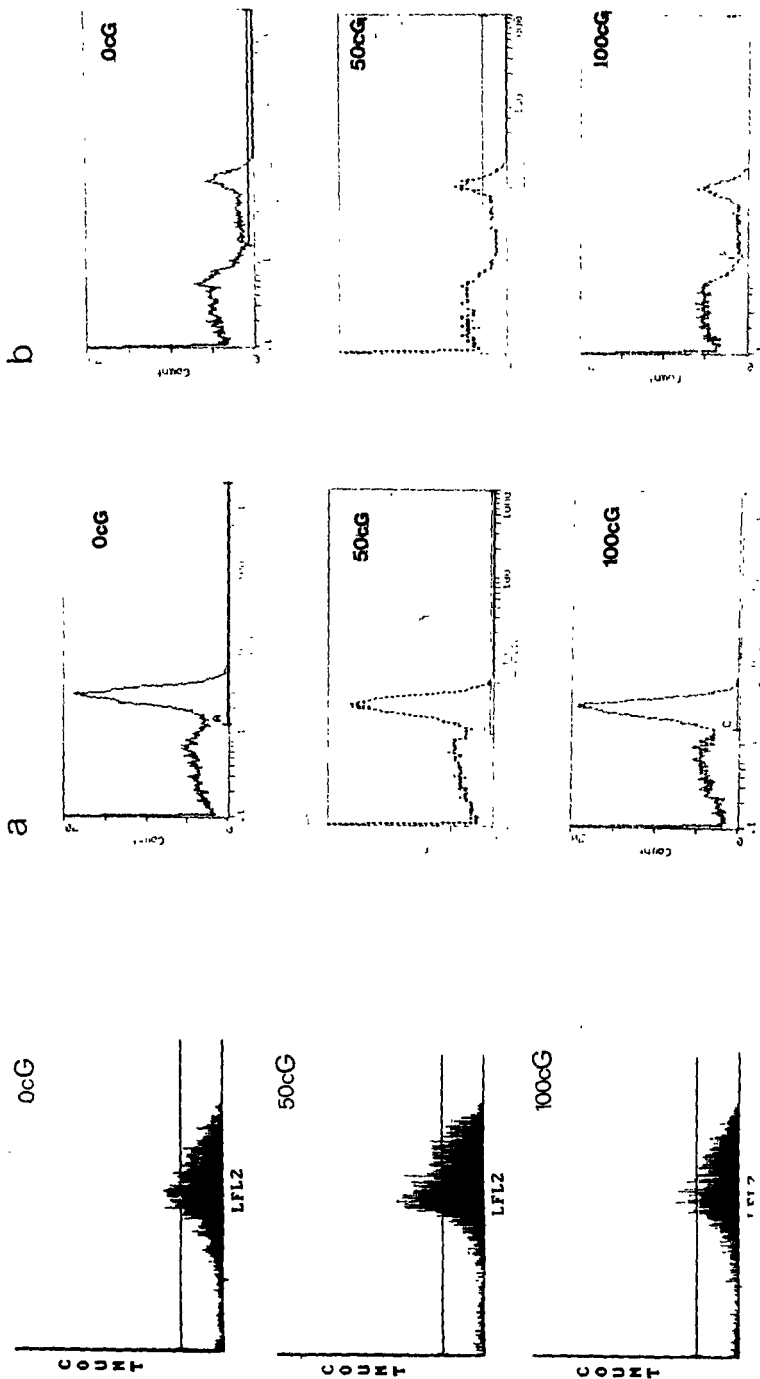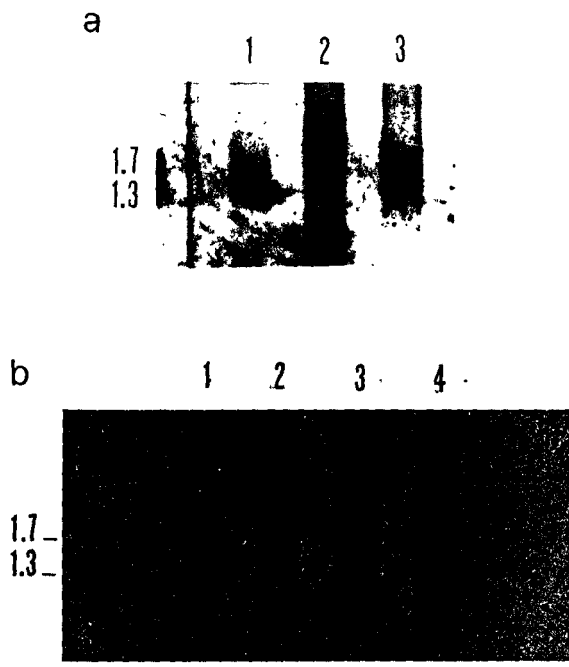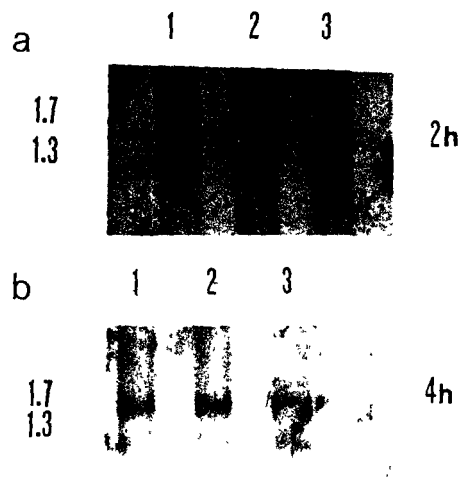
Fig. 6

Legends

Figure 1. Multi and single layer E rosettes formation by human stimulated T lymphocytes.

Figure 2. Effect of X-ray dose on the ability of resting and PHA stimulated human T lymphocytes to form multilayer rosettes with SRBC (o_o, Δ_Δ) resting T cells cultured for 24 and 48 hours respectively.
(●_●__Δ_Δ) T cells stimulated with PHA for 24 and 48 hours respectively.

Figure 3. Expression of CD2 Ag by T lymphocytes cultured for 24 hours with PHA. Immunofluorescence profiles are shown: (upper), unirradiated T cells; (middle), T cells given 50 cGy; and (lower), T cells given 100 cGy irradiation.

Figure 4. Expression of a) CD4 Ag and b) CD8 Ag by T lymphocytes cultured for 24 hours without PHA. Immunofluorescence profiles are shown: (upper), unirradiated T cells; (middle), T cells given 50 cGy; and (lower), T cells given 100 cGy irradiation.

Figure 5. Effect of X-irradiation on the CD2 mRNA accumulation in normal human T lymphocytes. Northern blot analysis of CD2 related RNA transcripts. Twenty micrograms of total RNA was loaded on each slot of 1% agarose-formaldehyde gel electrophoresed, transferred on nylon membrane and hybridized with a CD2-cDNA probe. RNA sources were as follows:
a) lane 1, unirradiated T cells cultured for 24 hours, lane 2-3, T cells given 50 and 100 cGy of X-irradiation respectively and cultured for 24 hours.
b) lane 1, resting T cells from peripheral blood; lane 2, unirradiated T cells stimulated with PHA for 24 hours; lane 3-4, T cells given 50 and 100 cGy of X-irradiation respectively and stimulated with PHA for 24 hours.

Figure 6. Effect of X-rays on the degradation rate of CD2 mRNAs species. Northern blot anlaysis of total RNA from PBMC stimulated for 12 h with PHA before the addition of actinomycin-D, irradiated and cultured for a) 2 hours and b) 4 hours. lane 1, unirradiated cells; lane 2-3; cells given 50 and 100 cGy of X-irradiation respectively.

Head of project 7: Prof. Herrlich

II. Objectives for the reporting period

Various radiation qualities such as ultraviolet irradiation (UVC), X-rays or alpha rays and DNA-damaging chemicals such as MNNG, mytomycin C, 4-nitroquinoline oxide, and hydrogen peroxide induce similar cellular reactions, e.g. DNA repair, cell cycle arrest, mutagenesis or apoptosis. In the reporting period we concentrated on the reactions of cells on UVC-irradiation and compared them to reactions induced by other non-physiological agents, such as X-rays and hydrogen peroxide. Most, if not all, cellular reactions to short wavelength ultraviolet irradiation depend on proteins whose synthesis or activity are modulated by UV irradiation. Affected proteins include the transcription factors c-Fos, c-Jun, Jun B, CREB and p53. One major question to be answered was to which extent the UVC-induced signal transduction chain to responsive genes is controlled by UVC-induced DNA damage and by the activation of membranal growth factor receptors. In addition, we started experiments aimed at understanding the mechanism(s) of radiation-induced p53 stabilization and we isolated an Ataxia cell clone which was partly complemented in its cell cycle parameters after transfection of a human cDNA library.

III. Progress achieved including publications

A. Involvement of UV-induced DNA damage and cellular membranes in the mammalian UV response

Irradiation of various cell types in culture with short wavelength UV (254 nm, UVC) induces the transcription of various genes. The doses employed induce an amount of DNA damage which is induced if a cell culture is exposed to sunlight for two hours at 2000 m altitude. Immediate early genes are activated in minutes after UV irradiation by the activation of transcription factors which control these genes. Examples are the transcriptional activation of the c-fos gene (which is controlled after UV by p62/TCF-SRF, the transcription factor CREB, and a factor binding to the +18/+38 element) and of the c-Jun gene (which is controlled by the transcription factors c-Jun and AFT-2). The HIV-1 long terminal repeat is transcriptionally induced by UV in the time frame of several hours through the release of the cytoplasmic transcription factor NFκB from its inhibitor and its translocation into the nucleus. These early processes occur also in the absence of protein synthesis (and thus must be

mediated by preexisting cellular proteins) and are in fact inducible by treatment of cells with inhibitors of protein synthesis. Other genes (such as the collagenase and the metallothionein IIA gene) are induced at late time points after UV irradiation, and their transcriptional induction depends on ongoing protein synthesis.

At least, three pathways seem to contribute to UVC-induced gene transcription, whose possible interactions and interdependencies have not yet been determined:

1. UV induced DNA damage. Involvement of UV-induced DNA damage in UV-induced gene transcription follows from the following observations:

- in Xeroderma pigmentosum cells, which cannot repair UV-induced DNA damage, much lower doses of UV induce maximal gene transcription as compared to wild type cells, as shown for collagenase I, MTIIA, and HIV-1. This suggests that persistent DNA damage plays a role. Since the repair of DNA damage takes hours, the same approach cannot be used to determine the dependence of early cellular reactions on DNA damage.

- Injection or transfection of UV-damaged DNA into cells activates NFκB-dependent transcription.

- The action spectrum of UV-induced early and late cellular reactions follows the absorption spectrum of DNA.

- T4 endonuclease V which destroys UV-induced pyrimidine dimers inhibits, upon introduction into cells, UV-induced NFκB-dependent transcription and UV-induced translocation of NFκB into the cells nucleus.

- Cell mutants with a defect in the activation of DNA-dependent protein kinase are inhibited with respect to UVC-induced c-Jun gene activation.

2. Membranal growth factor receptors. The UVC-induced activation of transcription factors is mediated via obligatory cytoplasmic signal transduction involving Src, Ras, Raf, mitogen-activated kinases and Jun-kinases. The UVC response is inhibited (I) by prior down-modulation of growth factor receptor signalling upon prestimulating the cells with growth factors, (II) by suramin, an inhibitor of receptor activation, or (III) by expression of a dominant-negative epidermal growth factor (EGF) receptor mutant. These data suggest the involvement of several growth factor receptors in the UVC response. Indeed, UVC induces the suramin-inhibitable immediate tyrosine phosphorylation of several growth factor receptors, such as the EGFR, the EGFR-relative erb B-2, and the platelet-derived growth factor receptor, and the association of EGFR with the bridging protein shc. UV (and EGF)-induced tyrosine phosphorylation of the EGFR is inhibited rapidly and specifically by the tyrosine kinase inhibitor AG1478. In the presence of this inhibitor UVC-irradiated cells show a slower loss of phosphates from tyrosine residues as compared to EGF-treated cells, suggesting that the mechanisms of EGF and UV-induced phosporylation of the EGFR differ.

3. UVC-induced CREB phosphorylation does not involve the EGF receptor. The criteria found for the UVC-induced activation of mitogen-activated protein kinases and the transcription factor TCF do not apply to phosphorylation and activation of the transcription factor CREB (cAMP responsive element-binding protein), which is involved in the transcriptional activation of the c-fos gene by UVC: Suramin and the EGFR-specific inhibitor AG1478 do not inhibit, and CREB phosphorylation is inducible by UV in cells pretreated with several growth factors (in contrast to MAP kinase). CREB phosphorylation depends on a UV-induced protein kinase (MW 108 kd) different from PKA and several Ca^{2+} dependent protein kinases.

As stated above it is not known whether and how the three pathways interact and whether DNA damage and membrane-dependent reactions are part of a single or of several signal transduction chains.

B. Comparison of UV-induced transciption with transcription induced by X-rays, H_2O_2 and MNNG

In our hands and in HeLa cells, if adjusted to equal-toxic doses, UV irradiation compared to other noxes, is the most efficient inducer of gene transcription. X-rays, for instance, have to be applied at a dose of 50 Gy in order to obtain a measurable induction of c-jun or c-fos transcription. Similar to the situation with UV, the transcription of the c-fos at the c-jun gene is seen early after X-ray irradiation, while induction of the collagenase gene is observed only late. In murine 3T3 cells, X-rays seem to be a more efficient inducer of gene transcription as compared to Hela cells, suggesting species or cell type specific regulation. MAP-kinase is activated after X-ray irradiation in human SV40 transformed fibroblast (GM637) at doses between 5 and 50 Gy, albeit with kinetics which differ from UV-induced MAP-kinase activation in Hela cells: while MAP-kinase is activated immediately after UV irradiation, peaks at 10 minutes and then declines again, MAP-kinase activation after X-rays is delayed and increases up to two hours after irradiation. This suggests inducer or cell type specific differences in signal transduction mechanisms. Also Jun-kinase is weakly activated upon irradiation with X-rays. However, in contrast to UV, we could not detect any phosphorylation of the EGF receptor at tyrosine residues (at doses up to 50 Gy), suggesting that X-rays do not address this membranal protein.

Also MNNG, MMS and H_2O_2-induced gene transcription is seen only at doses which are highly toxic. MMS induces a strong Jun-kinase activation but with kinetics which are delayed as compared to UV-induced Jun-kinase activation. H_2O_2 at a dose of 1 mM is a very efficient inducer of EGFR tyrosine phosphorylation. Similar to UV, it inhibits dephosphorylation of the EGFR in the presence of AG1478, suggesting that it either affects the conformation of the EGFR so that phosphatases cannot work on the receptor, or that it inhibits tyrosine phosphatases.

C. Radiation-induced stabilization of the tumor suppressor protein p53

Radiation-induced activation of p53 may follow different routes than radiation-induced activation of the transcription factors of the AP-1 family. This follows from the finding

that in contrast to AP-1, p53 is not activated by treatment of cells with growth factors. Thus, radiation-induced growth factor-dependent pathways may not play a role in p53 activation. Consistently, and in contrast to the findings with AP-1, suramin (see above) does not interfere with radiation-induced p53 activation. Upon irradiation of cells with either X-rays or UVC, the level of p53 is increased, presumably, as there is no change in RNA levels, by stabilization of the protein. In human lymphoblastoid cells derived from a normal donor, in a pulse chase experiment we determined a half life for p53 of around 2 hours which was increased to 4 hours upon irradiation of the cells with 5 Gy gamma rays. In murine 3T3 cells the half life of the p53 protein was around 20 min.

All human cells examined with wild type p53 react to UV and X-ray irradiation with p53 stabilization. Reacting cells include Ataxia telangiectasia cells which have been claimed to be deficient in the response to X-irradiation. After UV the dose dependency of induction depends on the repair of damage in the transcribed genes, suggesting that this damage delivers the inducing signal.

D. A partially complemented Ataxia telangiectasia cell clone displays enhanced survival and G1 block, but no inhibition of DNA synthesis after ionizing radiation

Cells from the recessive disorder Ataxia telangiectasia (AT) are characterized by their sensitivity against ionizing radiation (IR) and lack of radiation-induced G1 and DNA synthesis block. In an attempt to complement SV40 immortalized cells derived from AT complementation group D by stably transfecting a cDNA library derived from human wild type cells, we rescued one transfectant (clone 514) which had integrated several copies of cDNA and which was more resistant to ionizing radiation than parental AT cells. 514 cells showed the cell cycle parameters of wild type cells and were partially blocked, like wild type cells, in the G1 phase of the cell cycle after IR. They showed, however, like AT cells, no inhibition of DNA synthesis after IR. Our results demonstrate that the IR-induced G1 block is not sufficient for the IR-induced inhibition of DNA synthesis.

Publications

H.-P. Auer, H. König, M. Litfin, B. Stein, and H.J. Rahmsdorf. 1994. Ultraviolet irradiation, although it activates the transcription factor AP-1 in F9 teratocarcinoma stem cells, does not induce the full complement of differentiation associated genes. *Exp. Cell Res.* 213:131-138.

C. Blattner, A. Knebel, A. Radler-Pohl, C. Sachsenmaier, P. Herrlich, and H.J. Rahmsdorf. 1994. DNA damaging agents and growth factors induce changes in the program of expressed gene products through common routes. *Environ. Mol. Mutagenesis* 24:3-10.

E. Fritz, H.J. Rahmsdorf, and P. Herrlich. 1995. A partially complemented Ataxia-telangiectasia cell clone displays enhanced survival and G1 block, but no inhibition of DNA synthesis after ionizing radiation. *Rad. Res.*:in press.

P. Herrlich, H. Ponta, and H.J. Rahmsdorf. 1992. DNA damage-induced gene expression: signal transduction and relation to growth factor signaling. *Rev. of Physiol. Biochem. Pharmacol.* 119:187-223..

P. Herrlich, and H.J. Rahmsdorf. 1994. Transcriptional and post-transcriptional responses to DNA-damaging agents. *Curr. Opinion Cell Biol.* 6:425-431.

P. Herrlich, C. Sachsenmaier, A. Radler-Pohl, S. Gebel, C. Blattner, and H.J. Rahmsdorf. 1994. The mammalian UV response (Mechanism of DNA damage induced gene expression). *In: "Advances in enzyme regulation". Weber, G. (Ed.), Pergamon Press, Oxford, Vol. 34, pp. 381-395.*

A. Knebel, M. Iordanov, H.J. Rahmsdorf, and P. Herrlich. 1995. An oxidant sensor at the plasma membrane. *In: Proceedings, Conference: Biological Reactive Intermediates V*:submitted.

M. Krämer, C. Sachsenmaier, P. Herrlich, and H.J. Rahmsdorf. 1993. UV-irradiation-induced interleukin-1 and basic fibroblast growth factor synthesis and release mediate part of the UV response. *J. Biol. Chem.* 268:6734-6741.

A. Radler-Pohl, C. Sachsenmaier, S. Gebel, H.-P. Auer, J.T. Bruder, U. Rapp, P. Angel, H.J. Rahmsdorf, and P. Herrlich. 1993. UV-induced activation of AP-1 involves obligatory extranuclear steps including Raf-1 kinase. *EMBO J.* 12:1005-1012.

H.J. Rahmsdorf, S. Gebel, M. Krämer, H. König, C. Lücke-Huhle, A. Radler-Pohl, C. Sachsenmaier, B. Stein, H.-P. Auer, M. Vanetti, and P. Herrlich. 1992. Ultraviolet irradiation and phorbol esters induce gene transcription by different mechanisms. *In:"Induced effects of genotoxic agents in eukaryotic cells" Rossman, T.G. (ed), Hemisphere Publishing Corporation, Washington, Philadelphia, London, pp 141-161.*

H.J. Rahmsdorf. 1994. Modulation of Fos and Jun in response to adverse environmental agents. *In* The Fos and Jun families of transcription factors. P. Angel and P. Herrlich, editors. CRC-press, Boca Raton. in press.

H.J. Rahmsdorf, C. Sachsenmaier, A. Radler-Pohl, C. Blattner, H. van Dam, and P. Herrlich. 1995. Radiation-induced signal transduction. *Rad. Res.* 141:108-123.

C. Sachsenmaier, A. Radler-Pohl, R. Zinck, A. Nordheim, P. Herrlich, and H.J. Rahmsdorf. 1994. Involvement of growth factor receptors in the mammalian UVC response. *Cell* 78:963-972.

C. Sachsenmaier, A. Radler-Pohl, A. Müller, P. Herrlich, and H.J. Rahmsdorf. 1994. Damage to DNA by UV light and activation of transcription factors. *Biochem. Pharmacol.* 47:129-136.

S. van den Berg, H.J. Rahmsdorf, P. Herrlich, and B. Kaina. 1993. Overexpression

of c-fos increases recombination frequency in human osteosarcoma cells. *Carcinogenesis* 14:925-928.

Head of project 8: Dr. Simons

II. Objectives fo the reporting period

This project was undertaken because of our finding with mouse lymphoma cells that chemically induced DNA damage, next to the direct induction of mutations and chromosome aberrations, leads to an infidelity of DNA replication in the progeny of treated cells which can result in untargeted mutations.
The first objective was to establish whether ionizing radiation can induce a similar response and whether this response could be due to the induction of a stress response in the cells.
As moreover we had observed that carcinogen-induced immortalization of SHE (Syrian hamster embryo) cells was also due to the induction of an indirectly induced process, it was hypothesized that stress induced genetic instability could be a driving force in immortalization.
Therefore the second objective was to develop the means to test this hypothesis by establishing three assay systems (for: stress response, genetic instability and immortalization) in one and the same primary cell.

III. Progress achieved including publications

Induction of genetic instability in mammalian cells by ionizing radiation
The assay for the determination of genetic instability is based on the fluctuation analysis which allows to discriminate between directly induced mutations and delayed mutations which take place inthe progeny of treated cells. Ten fluctuation analyses were performed with GRSL mouse lymphoma cells with altogether over 8000 parallel cultures. All radiations were with 6 Gy. The directly induced mutant frequencies in the ten experiments were rather similar. The mean induction per Gy was $0.73 \times 10_{-5}$. In contrast with our findings with chemicals, a striking heterogeneity was observed among the ten experiments in the induction ofgenetic instability: the delayed mutant frequencies varied from zero to 6.1×10^{-6}. About half of the experiments displayed a strong indirectly induced mutational response which could persist up to the 10th generation after treatment. In that latter case the delayed mutations contribute to 10% in the induced mutational response.

A possible explanation for the heterogeneity in delayed mutational response was indicated by a correlation of this response with the cell density of the cultures used for irradiation ($+0.63$ $P=0.07$). This suggested that stationary cells might be more

sensitive for the induction of genetic instability. This was investigated by the comparison of the x-ray induced genetic instability in growing and stationary cells, both derived from one parental population. The cells which were kept stationary for 4 days befrore irradiation did not show an induction of genetic instability and the same was found for the cells which had been logarithmicaly growing for 10 days before irradiation. The remaining possiblity is that cells which are in a transition stage between cycling and G_0 are more sensitive to the induction of genetic instability.
In conclusion ionizing radiation like chemicals induced genetic instability but in contrast to chemicals the induction appears to require specific culture conditions.

Induction of genetic instability by stress response

Carcinogens induce, apart from the DNA damage, the transcription of a large number of genes, known as stress response. In order to investigate whether the induction of genetic instability is due to the induction of a stress response the effect of a stress response was studied in the absence of induced DNA damage. This was possible because a part of the UV-induced stress response consists in the secretion of "Extracellular-Protein-synthesis-Inducing-Factors" (EPIF) which are able to turn on part of exactly the same response in non-irradiated cells. For the production of EPIF growing or stationary GRSL mouse lymphoma cells were irradiated with 15 J/m^2 UV and incubated for 2 days. Medium from irradiated cells (EPIF medium) was collected and transferred to either growing or stationary cells. After 1 day incubation in EPIF medium, aliquots of 25000 viable cells were expanded to about 10^8 cells in normal medium and the mutation rate was determined. When the data from 48 determinations were taken together, EPIF was found to significantly enhance the mutation rate 1.8-fold (P=0.008). EPIF only enhanced the mutation rate when the EPIF producing cells and the EPIF treated cells were in the same condition, either both growing or both stationary. This indicates that the EPIF from growing and stationary cells is different and that the growing and stationary cells differ in their sensitivity to the excreted factors. As both the spontaneous and the EPIF induced mutation rate could be influenced by factors in the serum, EPIF was also produced in serum-free medium supplemented with BSA. Stationary cells were used both as producer cells and target cells. The overall effect in 13 experiments showed a 2.8 fold enhancement of the mutation rate after treatment with EPIF (P<0.002).
The mutation rate after EPIF treatment was further analysed with fluctuation tests to determine at which generation after seeding the mutational events take place. Five fluctuation tests were performed with EPIF produced in serum-free medium. As in the mass cultures an enhancement of the mutation rate after EPIF treatment was found. For each mutational event it was determined how many cell generations occurred between seeding after treatment and the mutational event. The resulting histograms showed that the distribution of the occurrence of the mutational events was different for EPIF and control cultures. In the EPIF treated group more mutational events were found from the first to the fifth generation after treatment compared to the control group (P<0.02). The mutation rate for the generations one to five after treatment was 10-fold higher in the EPIF treated group.

The same experiments also revealed that EPIF medium induced cell growth during the 24 h treatment period. A significant linear correlation between mutation rate and cell growth response was found for EPIF treated cultures (R = +0.59; P<0.002).

In conclusion the data obtained with the EPIF experiments indeed suggest that the induction of a stress response leads to an enhanced mutation rate.

Cytokines in EPIF-medium

In an attempt to identify secreted cytokines in EPIF medium, the amounts of Il-1, Il-2, Il-6 and TNF $\propto$ were determined in EPIF and control medium. The level of these cytokines appeared the same in the two media.

Variation in the spontaneous mutation rate

A stress response induced enhancement of the mutation rate could be either due to i)induction of a fixed amount of replication errors or ii) to an enhancement of the pre-existing error rate or iii) to induction of genetic instability in only those cultures with a low pre-existing error rate.

To discriminate between these possibilities the data obtained on the induction of genetic instability with UV-induced serum-free EPIF were further analysed. When the 13 experiments were divided into three groups according to the level of the spontaneous mutation rate it was found that in the first group the enhancement was from 1.3 ± 0.2 x10^{-7} to 3.3 ± 1.2 x10^{-7} (2.5-fold), in the second group from 2.4 ± 0.4 x10^{-7} to 8.7 ± 4.8 x10^{-7} (3.7-fold), and in the third group from 7.2 ± 5.8 x10^{-7} to 26.1 ± 24.8 x 10^{-7} (3,5-fold). The differences between the three groups indegree of enhancement are small and not significant indicating that the induction of replication infidelity by EPIF does not lead to a fixed amount of replication errors, but to an enhancement of the pre-existing error rate.
These data also suggest that the spontaneous mutation rate can vary very much from experiment to experiment. This led us to test whether a mutation rate is constant during the growth of these cells in the course of an experiment. Using approximately 8000 parallel cultures 271 mutational events were observed and it was determined at which time after seeding these mutations occurred. It was found that the spontaneous mutation rate decreases with time from 20x10^{-7} to about 2x10^{-7}/cell/generation.
A factor involved in influencing replication fidelity appeared to be cell density as maintaing cells at high density during growth resulted in a spontaneous mutation rate of 0.7x10^{-7} while maintaining the the cells at an extremely low cell density resulted in an enhanced mutation rate of 7.7x10^{-7}.

Thus altogether the spontaneous mutation rate can vary from 0.7x10^{-7} to at least 20x10^{-7} (approximately 30-fold); the data obtained with EPIF suggest that this figure could be een substantially higher.

Establishment of assay systems for stress response, immortalization and genetic instability in primary mouse keratinocytes

Stress response

Induction of a stress response in mammalian cells in vivo has a role in phenomena like inflammation and wound healing. For keratinocytes this has led to the concept of the "activation". The activated keratinocyte has a phenotype which differs fundamentally from that of the ususal phenotype: hyperproliferation, alterations in the cytoskeleton, migration, remodeling of the extracellular matrix etc, which all have a function in tissue repair after wounding. When keratinocytes are cultivated in vitro

they acquire characteristics of activated cells. We have used this phenomenon in the development of an assay system. It was found that favourable conditions for growth also promote cell migration. Numerous experiments have been performed to optimalize the conditions (e.g. media-constituents, pH, CO_2, substrates etc. Under the best conditions migrating cells even change their cytoskeleton completely and obtain a spindle morphology. These changes can be enhanced by several growth factors, by the tumor promoter TPA and by EPIF, secreted by UV-irradiated GRSL mouse lymphoma cells. By taking small epithelial fields as starting point the assay has been made quantitative: the increase in surface area by cell migration is measured. In figure 1 an example is given of an experiment in which induction of migration was found by treatment with EGF and IGF + EGF while inhibition of migration was found by treatment with hydrocortison or newborn calf serum. The assay is being developed and further and will be used soon to test the effect of tumor promoters and antipromoters.

Immortalization

According to the literature immortalization of primary mouse keratinocytes can be selection of TDR-(terminal differentiation defective)-foci from cells which have been treated with carcinogens. This selection is based on a gradual increase of the Ca concentration which induces differentiation in these cells. Cells from such foci can give rise to immortal cell lines. Also according to the literature spontaneous TDR-foci can be obtained from untreated cells by just culturing the cells at a high cell density and without elevating the Ca concentration. The resultant immortal cell lines appeared mutated in codon 61 of the Ha-ras gene. The latter procedure is being followed.
When the cells are seeded at a high density they enter a crisis after 2 to 4 weeks depending on culture conditions. During crisis foci can become visible; this can be as early as 13 days after seeding. The assay system is still in development as still improvements are found in obtaining these foci. Preliminary evidence suggests that focus formation is preceded by focal growth of stem cells which can be observed within 5 days after seeding. The assay system is still very variable but the effect of individual factors on the frequency of focus formation can be studied within an experiment. The foci can give rise to immortal cell lines but probably the cells have not been immortalized fully right from the beginning: a fraction of the foci were found to regress and the the cells from the foci which do give rise to immortal cell lines are difficult to handle initially.

Genetic instability

With respect to the role of genetic instability in immortalization no data are at present available. The frequency of focus formation can be as high as 10^{-5} per seeded cell. If the foci indeed originate from foci of growing stem cells the frequency could be as high as 10^{-3}. As the frequency of spontaneous point mutations in codon 61 of Ha-ras is expected to be lower than 10^{-8} it is strongly suggested that the foci do not arise from point mutations in this gene. The present experience with the cultivation of the cells from these foci allows to study the chromosomal stability shortly after the foci have arisen. At present it is also possible to test whether and when mutation in Ha-ras takes place during immortlization. Preliminary evidence suggest that the cells from early foci are still sensitive to the differentiation inducing effect of elevated Ca^{++} levels and thus are probably not yet mutated in Ha-ras.

Publications.

Boesen, J.J.B., N. Dieteren, E. Bal, P.H.M. Lohman and J.W.I.M. Simons. A possible factor in genetic instability of cancer cells: stress-induced secreted proteins lead to decrease in replication fidelity. Carcinogenesis 13 2407-2413 1992.

Simons, J.W.I.M. and M.J. Niericker. Induction of genetic instability in mammalian cells by ionizing radiation. In: K.H. Chadwick, R. Cox, H.P. Leenhout and J> Thacker (eds) "Molecular mechanisms in radiation mutagenesis and carcinogenesis." ECSC-EC-EAEC, Brussels pp 101-106 1994.

Boesen, J.J.B., M.J. Niericker, N. Dieteren and J.W.I.M. Simons. How variable is a spontaneous mutation rate in cultured mammalian cells? Mutation Res. 307 121-129 1994.
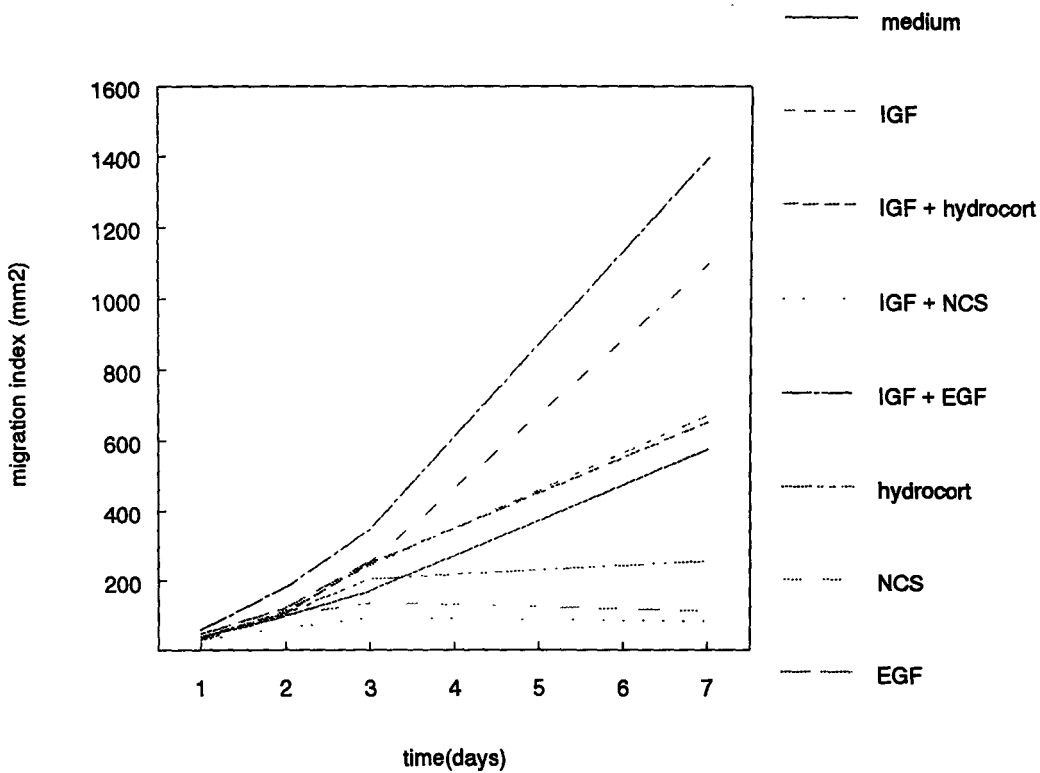
Figure 1.
Area of migration of cells from small epithelial fields stimulated by IGF-b (100 ng/ml), hydrocortsison (0.5 µg/ml), EGF (5 ng//ml) or 15% NCS (newborn calf serum).

Head of project 9: Dr. Russev

II. Objectives for the reporting period

1. Effect of low doses ionising radiation on DNA synthesis in eukaryotic cells

The objective of this investigation is to study on molecular level the processes leading to inhibition of DNA synthesis by ionising radiation in different mammalian cell lines. More specifically, the effect of γ-rays on the rate of replicon initiation is investigated by a specially designed experimental procedure permitting the separate analysis of the two major components of DNA synthesis - replicon initiation and chain elongation.

III. Progress achieved including publications

1. Effect of γ-rays on replicon initiation.
         Cells traverse cell cycle at uneven pace. To be able to change their speed and to choose sites of stopovers, cells have developed complex control mechanisms, which respond to different endogenous and exogenous signals. The best studied cases are the G1-arrest typical for mammalian cells, and the G2-arrest typical for yeast cells. Many less well characterised "check points" have been identified both in G1 and G2 phases, and even in mitosis, while no such point has been identified in the S-phase so far. This has led to the conclusion, that once in S-phase, cells are bound to complete it, the rate of DNA synthesis being constant and not a subject of control.
During the work on the project we were able to demonstrate that mammalian cells possess specific regulatory mechanism for controlling the rate of DNA synthesis in the S-phase. It is activated by a variety of agents such as X- and γ-rays and inhibitors of topoisomerase II, and leads to a temporary slow-down of the rate of replicon initiation. We studied the effect of several citostatic agents on the initiation and elongation steps of DNA synthesis. While many of them inhibit DNA synthesis by creating obstacles such as breaks, adducts or crosslinks in DNA, only few of them can change the rate of replicon initiation.

2. Molecular nature of the signal for slow-down of replicon initiation
         Both γ-radiation and inhibitors of topoisomerase II decrease the rate of replicon initiation in EAT and Friend cells to about 50% of the control value. The two agents differ profoundly in their nature and the fact that they have identical effect on DNA synthesis could be only attributed to their common ability to introduce double-strand breaks in DNA. To check the hypothesis that the double-strand breaks are the signal for activation of the regulatory pathway controlling replicon initiation in the S-phase, we carried out two sets of

experiments. In the first set of experiments cells were treated with VP-16 and 30 min later were irradiated with 5 Gy of γ-rays. One hour later cells were crosslinked with trioxsalen, labelled with ^{3}H-thymidine and DNA was isolated, denatured and electrophoresed. The combined treatment inhibited the initiation of DNA synthesis to the same extent as any one of the agents separately, i.e. their effect was cumulative. This result showed that both agents inhibit the initiation of DNA synthesis via the same mechanism. In the second set of experiments we studied the combined effect of γ-radiation and cis-DDP (cis-diamminedichloroplatinum (II)) on replicon initiation rates. Cis-DDP is a potent inhibitor of DNA synthesis. It is known to create bridges between purine moieties at the same strand, but is not generally known to introduce double-strand breaks in DNA. 5Gy of ^{60}Co γ-rays reduced the rate of initiation of DNA synthesis by 40% to 50%, and the same holds true for 2.5 μM VP-16. Further increase of the radiation dose and of VP-16 concentration does not cause any significant further decrease in the replicon initiation rate. On the other hand 2μM cis-DDP decreased the rate of replicon initiation only negligibly. Increasing of the cis-DDP concentration cause further proportional decrease in the initiation rate, which showed that in this case inhibition of replicon initiation is concentration dependent and is most probably an effect of the modified DNA structure, rather than of activation of specific control mechanism. When cis-DDP was combined with 5Gy, or 2.5μM VP-16 the effect was additive. This result shows that cis-DDP, a powerful DNA inhibitor, does not activate the specific control pathway for down-regulation of replicon initiation and confirms our previous conclusion, that the immediate signal for activation of this pathway are double-strand breaks in DNA. In addition, it could be speculated that this mechanism is quite sensitive, since doses of 1 to 5 Gy, which cause only a very limited number of double-strand breaks per genome, can activate it.

3. Biochemical pathways for transmission of the signal for slow-down of replicon initiation

Although the experiments described in the previous paragraph showed that the signal for activation of the down-regulatory pathway of replicon initiation is the introduction of double-strand breaks in DNA, they don't shed any light on the molecular mechanism of this down-regulation. Recently it has been suggested that it is mediated by specific protein factors. In order to check this possibility we performed the following experiments. Cells were treated with cycloheximide for 30 min and then irradiated with γ-rays. In control experiments cells were treated with cycloheximide, or with γ-rays only. One hour later cells were crosslinked with trioxsalen, labelled with ^{3}H-thymidine and chromosomal DNA was isolated, denatured and electrophoresed. We hypothesised, that if the γ-rays induced replicon initiation slow-down were mediated by de novo synthesis of certain protein factors, these factors would have not been synthesised in the presence of cycloheximide which would abolish the effect of the radiation. The experimental results showed that both γ-rays and cycloheximide reduce the replicon initiation rates to about 50 to 60 % of the control value. However the combined action of

the two agents did not restore the initial figure, but cause a cumulative decrease in the rate of replicon initiation, which was a clear indication that the two agents affect different metabolic pathways.

On the other hand, a considerable body of evidence has accumulated during the recent years, indicating that the common way for transmission of different signals in the cytoplasm and the nucleus is by phosphorylation and dephosphorylation, with different cellular kinases playing central role in these processes. There are also some data, that staurosporin, a broad spectre tyrosine kinase inhibitor, inhibits DNA synthesis as well. To check whether the signal for down-regulation of the replicon initiation was transmitted by phosphorylation, 1 hour prior irradiation with 5Gy γ-rays, cells were treated with staurosporin. 1μM staurosporin inhibits both initiation and total DNA synthesis to between 40 and 50% of the control value. The results of the simultaneous treatment of cells with γ-rays and staurosporin showed that the effect was not cumulative, i.e., no additional inhibition of replicon initiation was observed when cells were treated with the second agent over the value already reached by the treatment with the first agent. This result clearly indicates that both γ-rays and staurosporin affect the same metabolic pathway. The obvious conclusion to be drawn from these experiments was that induction of even a small amount of double-strand breaks in genomic DNA is immediately recognised by the cell and a signal is transmitted by a series of phosphorylation/dephosphorylation reactions to the site of initiation of DNA replication. As a result, the rate of replicon initiation is reversibly reduced down to roughly one half of the normal rate.

The last compound whose effect on DNA replication was studied in this series was 3-aminobenzamide (3-AB), an inhibitor of poly(ADP-ribosyl)synthetase. Poly(ADP-rybosil)synthetase can synthesise huge branched polymers built out of ADP-ribosyl moieties and attached to different proteins including poly(ADP-ribosyl) synthetase itself. It is known that DNA breaks and especially double-strand DNA breaks can activate the enzyme which leads to intensive poly(ADP-ribosyl)ation of chromatin in the vicinity of the breaks. The biological role of this process is not clear, although there are some speculations that it can play a role in the process of DNA repair. Friend cells were treated with 3-AB and 30 min later crosslinked with trioxsalen. DNA was isolated, denatured and electrophoresed and the analysis of the nascent DNA fragments synthesised between crosslinks showed that the drug did not cause any decrease in the rate of replicon initiation. As a matter of fact slight but consistent increase to about 120% of the rate of replicon initiation was observed in this case. When cells were treated with 3-AB and then with 5 Gy γ-rays, again no decrease of the rate of initiation of DNA synthesis was observed, i.e. 3-AB fully abolished the inhibitory effect of γ-rays.

Conclusions
Different physical and chemical agents, which introduce double-strand breaks in DNA molecules, activate a regulatory pathway, which leads to a temporary slow-down of replicon initiation during the S-phase. As a first step the

double-strand breaks are recognised by poly(ADP-ribosyl)synthesase, which poly(ADP-ribosyl)ates the chromatin proteins in the immediate vicinity of the break thus causing a relaxation of the chromatin structure in the region. Then a double-strand break specific protein, we presume that this could be protein Ku, binds to the generated DNA ends, rendered accessible by the modification, which activates the "350 kD" tyrosine kinase. Via unknown number of phosphorylation steps a replication initiation factor, we presume that it could be RPA, or equivalent, is phosphorylated. This inactivates the initiation complex and leads to a decrease of the rate of replicon initiation.

The biological role of this pathway is obvious. It is designed to help cells in S-phase, which have suffered double-strand breaks to repair their DNA, before being replicated, since replication of DNA with double-strand breaks could lead to genomic instability.

Publications

1. Lallev, A. and Russev, G., Effect of different agents causing double-strand breaks on DNA synthesis. Compt rend de l'Acad. bulg. Sci. 46 (1993)95-99.

2. Lallev, A. Effect of ionizing radiation on DNA synthesis in two different mouse cells. Compt. rend. de l'Acad. bulg. Sci. 46 (1993)100-103.

3. Lallev, A., Anachkova, B. and Russev, G. Effect of ionizing radiation and topoisomerase II inhibitors on DNA synthesis in mammalian cells. Eur. J. Biochem. 216, 177-181.

4. Tsvetkov, L. and Russev, G. Control of the initiation of DNA replication in mammalian cells. Eur. J. Biochem. (submitted)

5. Tsvetkov, L. and Russev, G. Poly(ADP-ribosyl) synthetase inhibitor abolishes the effect of γ-rays on replicon initiation. FEBS Letters (submitted).

Title: Studies on radiation-induced chromosome aberrations in mammalian cells. 2) Applied aspects.

1)   Olivieri   Univ. Roma "La Sapienza"
2)   Cortés-Benavides   Univ. Sevilla
4)   Palitti   Univ. Viterbo
5)   Savage   MRC
6)   Kalina   Univ. Safarikis

I. Summary of Project Global Objectives and Achievements

Objectives

A)   Validation of the adpative response (AR)

B)   Validation of the G_2 phase chromosomal radiosensitive assay in order to identify radiosensitive and cancer prone individuals

C)   Achievement of a meaningful score of chromatid-type aberrations that can be used for radiation-induced cytogenetic damage.

Achievements

A)   Cortés-Benavides et al. (Univ. Sevilla) reported the use of the cytokinesis-block micronucleus method to evaluate the AR as a good alternative to the single fixation method and scoring of chromosomal aberrations at metaphase for the study of the AR in human lymphocyes. With this method they observed a significant decrease in the yield of micronuclei in binucleate cells conditioned with various doses of peroxide and irradiated with either 1.5 or 3.0 Gy of X-rays later on. They also show a clear AR in binucleated cells conditioned with H_2O_2, while for low dose-irradiated cells the adaptation observed seems to depend upon the dose rate and never reached the extent observed in cells pretreated with peroxide.

However in human lymphocytes, where most of the studies on AR to ionizing radiation have been carried out, the interaction between the conditioning and the challenge treatment gives variable results. This variability may be partly due to the donor and to the type of protocol used; however the causes of this variability can only be understood if the mechanisms underlying the AR are grasped. In particular it is necessary to understand whether the conditioning treatment directly induces the repair enzymes or whether it acts by producing other changes in the cell which indirectly modify the effects of the challenge treatment. Of great importance in this connection are the changes that conditioning treatment

can produce in cell progression or in mitotic delay induced by the challenge dose. For this reason, at the Univ. of Rome, esperiments were carried out with human lymphocytes to test the effect of low-dosage X-ray irradiation (2 cGy) on cell-cycle kinetics and on the mitotic delay induced by a subsequent challenge treatment.

Taken as a whole, the results of these experiments show that even such a low dose of X-rays as 2 cGy induces significant variations in cell progression and can change, at least in some donor, the mitotic delay induced in G_2 by X-ray; thus these data indicate that the conditioning pretreatment can regulate two different cell cycle check-points: the G_1-S and the G_2-M transitions. It is not possible for the moment to relate these data to the adaptive response in human lymphocytes and to the variability observed in human lymphocytes at variance with positive results obtained in other test systems and with different end points.

On this respect Dr. Kalina (Univ. Safarikis) followed adpative response in lymphocytes of patients with Down syndrome and in homozygous and heterozygous ataxia telangiectasia patients.

The data obtained show an AR in lymphcytes of 3 normal subjects and do not indicate any significant AR in any of the five blood donors with Down syndrome. AR was found in control cells, when radiation and BLM were applied, and in AT heterozygotes after pretreatment with a low concentration of BLM, but not after a low dose of gamma rays. In AT homozygotes no AR was found either after a low dose of gamma rays or after a low dose of BLM.

B)   A first objective of the project was to investigate the relationship between repair processes that take place during G_2 phase of the cell cycle and the chromosome damage induced by fission neutrons by employing post-radiation treatment with inhibitors of DNA synthesis/repair such as caffeine, hydroxyurea (HU) and cytosine arabinoside (ara-C);

Whole blood cultures of human lymphocytes were exposed to various doses of fission neutrons or X-rays and treated post-irradiation during the last 2.45 h before harvesting with 5 mM caffeine, 5 mM Hu and 0.05 mM ara-C.

The presence of caffeine and HU strongly potentiate the yield of chromatid-type aberrations induced by both neutrons and X-rays. No potentiating effect, except at the highest dose of neutrons, was observed when irradiated cells were subsequently treated with ara-C. Since ara-C strongly potentiated the frequency of chromatid aberrations induced in G_2 lymphocytes by X-rays, the results obtained indicate that fission neutrons produce a smaller proportion of lesions, the repair of which can be inhibited by ara-C compared with the number produced by X-rays.

Furthermore the relationship between the repair processes occurring in G_1 phase of the cell cycle and the cytogenetic damage in ataxia telagiectasia (AT) cells was studied.

Lymphoblastoid cells derived from normal, heterozygote AT (HzAt) and three AT patients were exposed to X-rays or fission neutrons and post-treated with inhibitors of DNA synthesis/repair, such as inhibitors of DNA polymerases a, d and 3 (cytosine arabinoside, ara-C; aphidicolin, APC; buthyl-phenylenguanine, BuPdG) or ribonucleotide reductase (hydroxyurea, HU).

A strong increase of radiation-induced chromosomal aberrations was observed in normal and HzAT cells post-treated with ara-C, APC and HU, but not in the presence of BuPdG. No enhancing effect was observed in cells derived from AT patients, except for HU post-irradiation treatment.

These results suggest that the enzymes that can be inhibited by these agents are not directly involved in the repair of radiation damage induced in G_2 cells from AT patients, indicating that probably the AT cells used lack the capability to transform the primary DNA lesions into reparable products, or that AT cells might contain a mutated form of DNA polymerase resistant to the inhibitors.

C)   The initial proposals under this contract (by Dr. J. Savage at MRC) involved an investigation of the quantification of chromatid-type aberrations. These are produced during the later stages of cell-cycle transit (S and G_2) when the target cell population is very heterogeneous with respect to radiosentivity and therefore, the observed frequency is subject to modification by mitotic delay and perturbation. There is never a unique yield to set against a given dose.

Three approaches were used:

a)   The use of BrdU cell marking techniques which enable to pin-point the position of a cell at the time of radiation, and also to classify the kinds of aberrations present with increased accuracy.

b)   The mitigation of induced mitotic delay by chemicals, like Caffeine, and so to isolate and assess its effect upon observed yield.

c)   Computer modelling of cell cycle perturbation effects on observed aberration yield.

All three approaches were successful. The first, however, revealed a further, unanticipated, problem, having an important bearing upon observed yield. A high proportion of the exchange aberrations ordinary classed as simple two-break events with conventional solid staining, proved to be Complex, involving the interaction of 3, or more, breaks. It was clear that the actual amount of damage was being underestimated, and this has serious implications for dose-response curve profile, and the theoretical interferences usually drawn from them.

The newly introduced technique for chromosome painting (FISH) was showing up also for chromosome-type exchanges anomalous patterns which were readily interpretable as resulting from Complex exchanges; the frequency of such complex exchanges was very much higher than had been realised. Damage underestimation is occurring at doses generally used for radiation cytogenetics.

Hampered by lack of a detailed understanding of Complex exchange formation, Dr. Savage et al developed a new classification scheme ("the CAB system"), and expanded all the possible break interaction possibilities for up to 5 breaks in 5 chromosomes, and the painting patterns that will be derived from them. This data base has gained International recognition, and has already proved invaluable for modelling and predicting several facets of aberration theory.

Head of project 1: Prof. Olivieri

II. Objectives for the reporting period

To study of circumstances in which it is possible to obtain different types of interaction (i.e. synergistic response or adaptive response) between low dose irradiation and subsequent mutagenic treatment in G_2 phase human lymphocytes.

To ascertain whether conditioning pretreatment alone modified the cell proliferation of different donors, given the great importance of cell progression and of the mitotic delay induced in G_2 in the definition of cytogenetic damage.

III. Progress achieved including publications

Experiments were carried out using cultures of blood from donors who had previously displayed an adaptive response or not (Olivieri et al. 1989), to ascertain whether conditioning pretreatment alone modified the cell proliferation and the duration of radiation - induced arrest in G_2.

The donors were male, non-smokers, in apparently good health and about the same age (51-54 years).

Whole blood (0.5 ml) was added to 4.5 ml of RPMI 1640 medium without serum, 2 mM glutamine, 100 units/ml penicillin, 100 μg/ml strep-tomycin and 2% phytohemagglutinin M (Welcome).

Irradiation was carried out with 200 kVp X-rays (Gilardoni MGL 200/8D, 0.2 mm Cu added filtration, 6 mA, 0.20 Gy/min). 90 to 120 minutes before fixation, 0.1 ml of colcemid (final concentration 2×10^{-7} M) was added to each culture. Fixation was performed in accordance with standard cytological practice. Two parallel cultures were set up for each point examined.

Brd Urd (20 μM final concentration) was added to the cultures from 24 h until fixation so that the number of times a cell divided in culture could be determined in harlequin-stained preparations. In some experiments [^{3}H]dThd (3.7 x 10^3 Bq/ml; sp. act. 2.5 x 10^{11} Bq/mmol) was added immediately after irradiation with X-rays until fixation, and autoradiograms of the slides were prepared by standard methods.

Cell proliferation was studied by examining both mitotic indices (MI) and the number of times the cells had divided at various stages in the culture. In this case a replication index (RI) can be calculated by means of the formula RI = $(M_1 + 2M_2 + 3M_3)/100$. No variation in RI was observed. However the pooled data of ten experiments indicate variations in MI after irradiation with 2 cGy of X-rays between 11.00 and 23.00 after stimulation with PHA and fixation at varying times after this treatment. The MI in the different donors varies according to the time elapsing between treatment with 2cCy and fixation. Significant fluctuations in MI were observed compared with controls. These fluctuations did not occur at the same times in the different donors.

We also investigated the progress of S cells at the time of challenge into mitosis. The data of 8 experiments indicate that at least in some donor the number of mitoses labelled at various times during exposition to [^{3}H]dThd is significantly lower in 2cGy treated cultures. After irradiation with 30cGy the same difference is found between the different donors: here too some donor

displays a significantly lower labelled mitosis frequency in the pre-irradiated cultures.

Overall the data indicate that conditioning treatment (2 cGy) induces the following changes in the lymphocytes: a) progression of lymphocyte population after treatment is no longer in step with controls; b) in some donors conditioning treatment alone induces an extension of both G_2 and of the time taken by cells in S at the time of challenge to reach mitosis.

We do not know whether these effects are related to AR, on the other hand they could explaine a number of "exceptions" observed in human lymphocytes at variance with positive results obtained in other test systems and with different end points.

Publications under this contract

OLIVIERI, G., BOSI, A., GRILLO, R., SALONE, B., 1992, Interaction of low dose irradiation with subsequent mutagenic treatment. Studies with human lymphocytes, in Proceedings of the International Conference on Low Dose Radiation and Biological Defense Mechanism, Elsevier Sci. Publ. 279-282.

OLIVIERI, G., BOSI, A., GRILLO, R., SALONE, B., 1993, Synergism and adaptive response in the interaction of low dose irradiation with subsequent mutagenic treatment in G_2 phase human lymphocytes. In Obe G., Natarajan AT (eds.) "Chromosomal aberrations: Origin and significance", p. 150-159.

SALONE, B., GRILLO, R., BOSI, A., OLIVIERI, G., 1995, Effects of low-dose (2 cGy) X-ray on cell-cycle kinetics and on induced mitotic delay in human lymphocyte Mut. Res. (in press).

OLIVIERI, G., SALONE, B., AILLAUD, M., BOSI, A., 1955, Low-dose irradiation and cell cycle checkpoints in Obe G. Natarajan A.T. (eds.) Third International Symposium on Chromosome Aberrations (in press).

Contract number F13P-CT920031

Title of the Project: *Studies on radiation-induced chromosome aberrations in mammalian cells. 2) Applied aspects.*

Head of Project 2: Prof. Cortés-Benavides

Objectives for the whole period.-

As compared with higher dose of ionizing radiation, the cellular and genetic effects of low doses are, in general, poorly understood. In the recent years, however, there has been a general agreement in that this aspect of radiobiology is of paramount importance, since organisms are more likely exposed to very low doses and dose rates than to accidental high-dose exposures.

One interesting widespread phenomenon associated with low doses is the so-called adaptive response (AR), by which cells that have been given a exposure to low doses of DNA-damaging agents (conditioning treatment) develop an increased resistance to a subsequent exposure to a higher dose.

Since Samson and Cairns (1977) pioneer work on the AR of bacteria to alkylating agents via the induction of the DNA repair system, many attempts have been made to demonstrate AR in mammalian cells for various alkylating agents (Samson and Schwartz, 1980; Kaina, 1982) and in response to tritiated thymidine (^{3}H-TdR) or ionizing radiation (Olivieri et al., 1984; Wiencke et al., 1986; Shadley and Wolff, 1987; Wolff et al., 1988; Sankaranarayanan et al., 1989; Fan et al., 1990).

On the other hand, adaptation to oxidative damage has also been reported in both bacteria (Demple and Halbrook, 1983) and cultured mammalian cells (Wolff et al., 1989; Cortés et al., 1990a; Domínguez et al., 1993).

In human lymphocytes, while most of the studies on AR to ionizing radiation have been carried out in stimulated cells, only a few reports have dealt with the possible protection provided by a conditioning treatment given before stimulation (G0), and the results are controversial (Sanderson and Morley, 1986; Shadley et al., 1987; Cai and Liu, 1990; Wang et al., 1991). Some authors have not observed a protective effect of pre-exposure to low doses of X-rays against cytogenetic damage (Shadley et al., 1987; Wang et al., 1991), while others have reported evidence for an adaptive response (Sanderson and Morley, 1986; Cai and Liu, 1990).

We have reported the use of the cytokinesis-block micronucleus method (Fenech and Morley, 1985) to evaluate the AR as a good alternative to the single fixation method and scoring of chromosomal aberrations at metaphase for the study of the AR in human lymphocytes (Domínguez et al., 1993). In good agreement with previous results on the induction of adaptation to ionizing radiation-induced damage detected as chromosomal aberrations in metaphase in human lymphocytes conditioned with H_2O_2 (Wolff et al., 1989; Cortés et al., 1990a), we observed a significant decrease in the yield of micronuclei in binucleate cells conditioned with various doses of peroxide and irradiated with either 1.5 or 3.0 Gy of X-rays later on (Domínguez et al., 1993).

The objectives for this period were to carry out experiments on the AR in human lymphocytes when they are conditioned in G0 with either H_2O_2 given at different times before stimulation or a low-dose of X-rays given at different dose rates before irradiation with a challenge higher dose of X-rays. Taken as a whole, our results show a clear AR in binucleated cells conditioned with H_2O_2, while for low dose-irradiated cells the adaptation observed seems to depend upon the dose rate and never reached the extent observed in cells pretreated with peroxide.

Experiments and Progress achieved.-

Cell culture

Whole blood (0.5 ml) from four healthy donors was added to 4.5 ml of RPMI 1640 medium containing 10% fetal calf serum, 2 mM L-glutamine, 100 U/ml penicillin, 100 μg/ml streptomycin and, after conditionig treatment with either H_2O_2 or low dose X-rays, 2% phytohemagglutinin (PHA) to stimulate G0 lymphocytes.

Conditioning treatments

Conditioning treatments consisted of either 30 min pulses with 250 μM H_2O_2, given at different times (6.5, 3.5 or 0.5h) before stimulation or, alternatively, cells were given a low dose of 2 cGy of X-rays delivered at different dose rates (1, 10 or 20 cGy/min) from a Philips SL 75-20 linear accelerator, 8 MeV.

The cells treated with H_2O_2 were centrifuged and the medium was changed. The same manipulations, except the addition of H_2O_2, were carried out with the cells receiving the high dose of radiation alone later on.

Challenge treatment and cytokinesis block

Challenge treatment was at 30h after PHA stimulation, and consisted of an exposure to 1.5 Gy of X-rays delivered at a dose rate of 2.0 Gy/min.

Inmediately after irradiation, cytochalasin B (Cyt B, Sigma) diluted with PBS (from a stock solution in DMSO at 2.0 mg/ml and stored at -80°C) was added to the cell cultures at a final concentration of 6.0 μg/ml. After recovery in Cyt B for 24-30h, fixation was performed by the standard cytological procedure, i.e., cells exposed briefly to a 0.075 M KCl cold solution were then fixed in a methanol-acetic solution (3:1). Cytological preparations were made by dropping cells onto wet slides and staining with Giemsa.

Two thousand binucleated cells were scored blind for micronucleus frequency in each treatment by two different observers. A one-tailed t-test was used to determine if the number of micronuclei observed in cells conditioned before irradiation with 1.5 Gy of X-rays was significantly lower than the expected, i.e., they showed the adaptive response.

RESULTS

Conditioning with hydrogen peroxide

Previous experiments carried out in our laboratory showed that conditioning stimulated human lymphocytes with low doses of H_2O_2 results in a protection against chromosome damage induced by X-rays delivered later on (Cortés et al., 1990a; Domínguez et al., 1993). According to this, we chose a dose of 250 μM H_2O_2 as a suitable conditioning treatment in order to try to elicit the AR also in unstimulated (G0) lymphocytes from three donors.
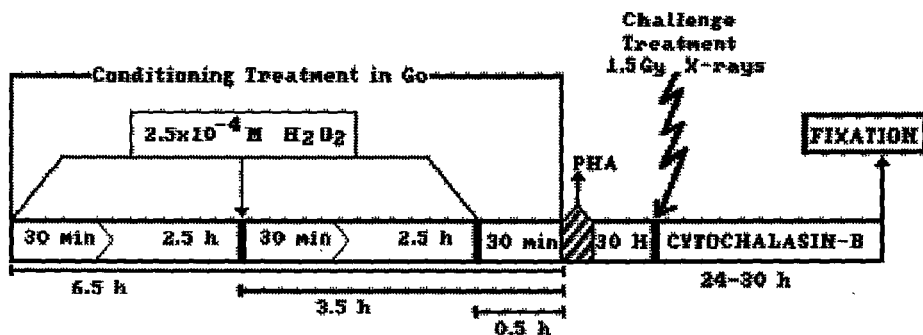
As shown in Fig. 1, cells were pulse-treated for 30 min with H_2O_2 at different times (6.5, 3.5 or 0.5h) as a conditioning treatment before the addition of PHA and irradiated 30h later with 1.5 Gy of X-rays. After a recovery of 24-30h in Cyt B, micronuclei were scored in binucleated cells.

TABLE 1.
ADAPTIVE RESPONSE IN G0 LYMPHOCYTES CONDITIONED WITH 2.5 x 10⁻⁴ M H_2O_2 AT DIFFERENT TIMES BEFORE STIMULATION.

Donor	Conditioning pretreatment (H_2O_2)	Challenge treatment (X-rays)	Number of micronuclei		Expected[a]	N° of cells scored
			Observed			
			N°	‰	‰	
A	-	-	21	10.5	-	2000
	6.5h	-	17	8.5	-	2000
	3.5h	-	20	10.0	-	2000
	0.5h	-	35	17.5	-	2000
	-	1.5 Gy	293	146.5	-	2000
	6.5h	1.5 Gy	218	126.5	144.5[c]	1723
	3.5h	1.5 Gy	152	85.7	146[b]	1772
	0.5h	1.5 Gy	140	70.0	153.5[b]	2000
B	-	-	24	12.0	-	2000
	6.5h	-	12	6.0	-	2000
	3.5h	-	12	6.0	-	2000
	0.5h	-	15	7.5	-	2000
	-	1.5 Gy	528	264.0	-	2000
	6.5h	1.5 Gy	308	154.0	258[b]	2000
	3.5h	1.5 Gy	351	175.5	258[b]	2000
	0.5h	1.5 Gy	327	163.5	259.5[b]	2000
C	-	-	21	10.5	-	2000
	6.5h	-	25	12.5	-	2000
	3.5h	-	17	8.5	-	2000
	0.5h	-	15	7.5	-	2000
	-	1.5 Gy	607	303.5	-	2000
	6.5h	1.5 Gy	404	202.0	305.5[b]	2000
	3.5h	1.5 Gy	406	203.0	301.5[b]	2000
	0.5h	1.5 Gy	434	217.0	300.5[b]	2000

a. Sum of the two individual treatments minus the control.
b. Observed frequency significantly lower than expected (P<0.01) (one-tailed t-test).
c. Observed frequency significantly lower than expected (P<0.05).

As can be seen in Table 1, in the combined treatments (conditioning and challenge), the difference between the expected and observed frequencies of micronuclei was, in all cases, statistically significant, i.e., they showed the AR, with reductions in the yield of micronuclei that reached values of about 30 percent for the three donors analyzed.

On the other hand, our results show that the time of treatment with H_2O_2 before stimulation seems not to be a major factor that influences the induction of the adaptation, for a similar AR was observed regardless of the time elapsed between the conditioning treatment and the stimulation of lymphocytes (Table 1).

Conditioning with low-dose X-rays

In Table 2 are shown the frequencies of micronuclei observed when G0 lymphocytes were conditioned with a low dose of 2 cGy of X-rays given at different dose rates (1, 10 or 20 cGy/min) inmediately before stimulation, and irradiated with a higher dose of 1.5 Gy as described above. Only when cells were pre-exposed to 2 cGy of X-rays delivered at a dose rate of 1 cGy/min they showed a statistically significant reduction in the yield of micronuclei as compared with those receiving the higher dose of X-rays alone, though of less magnitude than that observed in our previous study with conditioning doses of H_2O_2. For the other dose rates tested, on the other hand, the differences were not significant (Table 2).

TABLE 2.
ADAPTIVE RESPONSE IN G0 LYMPHOCYTES CONDITIONED WITH 2 cGy OF X-RAYS AT DIFFERENT DOSE RATES BEFORE STIMULATION.

Donor	Conditioning pretreatment (X-rays)	Challenge treatment (X-rays)	Number of micronuclei			N° of cells scored
			Observed		Expected[a]	
			N°	‰	‰	
A	-	-	10	5.0	-	2000
	1 cGy/min	-	17	8.5	-	2000
	10 cGy/min	-	21	10.5	-	2000
	20 cGy/min	-	23	11.5	-	2000
	-	1.5 Gy	546	273.0	-	2000
	1 cGy/min	1.5 Gy	483	241.5	276.5[b]	2000
	10 cGy/min	1.5 Gy	530	265.0	278.5[ns]	2000
	20 cGy/min	1.5 Gy	502	251.0	279.5[b]	2000
B	-	-	10	5.0	-	2000
	1 cGy/min	-	17	8.5	-	2000
	10 cGy/min	-	11	5.5	-	2000
	20 cGy/min	-	9	4.5	-	2000
	-	1.5 Gy	579	289.5	-	2000
	1 cGy/min	1.5 Gy	515	257.5	293.0[b]	2000
	10 cGy/min	1.5 Gy	644	322.0	290.0[ns]	2000
	20 cGy/min	1.5 Gy	545	272.5	289.0[ns]	2000
D	-	-	15	7.5	-	2000
	1 cGy/min	-	17	8.5	-	2000
	10 cGy/min	-	27	13.5	-	2000
	20 cGy/min	-	14	7.0	-	2000
	-	1.5 Gy	467	233.5	-	2000
	1 cGy/min	1.5 Gy	379	189.5	234.5[b]	2000
	10 cGy/min	1.5 Gy	533	266.5	239.5[ns]	2000
	20 cGy/min	1.5 Gy	500	250.0	233.0[ns]	2000

a. Sum of the two individual treatments minus the control.
b. Observed frequency significantly lower than expected (P<0.01) (one-tailed t-test).
ns. Observed frequency not significantly lower than expected.

DISCUSSION

Support for the existence of an adaptive response has been provided by Wolff and colleagues (Olivieri et al., 1984; Wiencke et al., 1986; Shadley and Wolff, 1987; Wolff et al., 1988, 1989) and by others (Sankaranarayanan et al., 1989; Cortés et al., 1990b; Cai and Liu, 1990).

Concerning the possible adaptation of unstimulated (G0) lymphocytes, Tuschl et al. (1983) observed an increase in unscheduled DNA synthesis and reduced sister chromatid exchange in UV-treated lymphocytes from radiation-exposed workers, while Moquet et al. (1987) did not found evidence to support that irradiated G0 lymphocytes become resistant to mitomycin C (MMC). Also negative results have been reported by Shadley et al. (1987) and Wang et al. (1991) on chromosome damage in G0 human lymphocytes primed with low dose of X-rays (between 1 and 5 cGy) and subsequently exposed to 1.5 or 3.0 Gy. Nevertheless, contrasting with this, the induction of an adaptive response in unstimulated human lymphocytes has been reported for chromosomal aberrations (Cai and Liu, 1990) as well as for cell survival and mutagenesis as end-points (Sanderson and Morley,1986).

X-ray damage is partly attributed to the production of free radicals which are also produced by H_2O_2 (Sobels, 1956). Boreham and Mitchell (1991) by comparing the relative efficiency of low and high LET radiation, have concluded that DNA single-strand breaks (ssb), as those efficiently induced by hydroxyl radicals, may be important lesions that signal the induction of the recombinational repair system, that is believed to be the major mechanism that confers resistance to ionizing radiation in yeast.

We have found that conditioning G0 human lymphocytes with H_2O_2, in agreement with our earlier results on adaptive response in stimulated cells (Wolff et al., 1989; Cortés et al., 1990a; Domínguez et al., 1993), seems to protect them from radiation damage detected as micronuclei in binucleated cells.

When conditioning in G0 was carried out in a similar fashion to that previously reported (Sanderson and Morley, 1986; Shadley et al., 1987; Cai and Liu, 1990; Wang et al., 1991), i.e. with low-dose X-rays, we have found a moderate adaptation only in cells that were given the irradiation at the lowest dose rate (1 cGy/min), while for higher dose rates (10 or 20 cGy/min) no protective effect was observed.

An explanation for the contradictory results reported by differents authors (see above) is not at hand. Focusing on chromosome damage, it is noteworthy that Cai and Liu (1990) observed an adaptive response in human and rabbit lymphocytes conditioned in G0 at a dose rate of 1 cGy/min, in good agreement with our own results, while in those investigations in which no adaptive response in G0 lymphocytes was reported (Shadley et al., 1987; Wang et al., 1991) higher dose rates were employed.

It has been argued (Shadley et al., 1987) that the lack of adaptive response in G0 lymphocytes as compared to that observed after stimulation should be in good agreement with reports showing that stimulated lymphocytes have a higher repair capacity than do unstimulated lymphocytes (Spiegler and Norman, 1969; Scudiero et al., 1976; Hamlet et al., 1982). Nevertheless, we have observed a clear adaptation when G0 lymphocytes were conditioned with H_2O_2, while a weaker but consistent response was induced by low-dose X-rays, depending upon the dose rate (only for low dose rate).

In yeast, it has been proposed that DNA single-strand breaks (ssb), as those almost exclusively induced by H_2O_2, should be much more efficient than DNA double-strand breaks (dsb) for the induction of radioresistance (Boreham and Mitchell, 1991). Our results on the efficiency of a conditioning in G0 with H_2O_2, in good agreement with our previous reports on the adaptive response induced by peroxide in stimulated lymphocytes (Wolff et al., 1989; Cortés et al., 1990a; Domínguez et al., 1993), seem to support the relative importance of ssb for the induction of a repair mechanism acting on subsequent radiation damage.

The use of the cytokinesis-block method in the present investigation to score micronuclei in binucleated cells, as compared with the scoring of chromosomal aberrations at metaphase to study the possible adaptation in G0 lymphocytes employed in previous investigations (Shadley et al., 1987; Cai and Liu, 1990; Wang et al., 1991), offers the advantage of being able to harvest the cells exposed to the challenge high dose of X-rays at different stages of the cell cycle and allow them to undergo any delay needed to repair before entering mitosis and showing up as binucleated cells.

REFERENCES

Boreham, D.R., and R.E.J. Mitchel (1991) DNA lesions that signal the induction of radioresistance and DNA repair in yeast, Radiat. Res., 128, 19-28.

Cai, L. and S.-Z. Liu (1990) Induction of cytogenetic adaptive response of somatic and germ cells *in vivo* and *in vitro* by low-dose X-irradiation, Int. J. Radiat. Biol., 58, 187-194.

Cortés, F., I. Domínguez, J. Piñero and J.C. Mateos (1990a) Adaptive response in human lymphocytes conditioned with hydrogen peroxide before irradiation with X-rays, Mutagenesis, 5, 555-557.

Cortés, F., I. Domínguez, S. Mateos, J. Piñero and J.C. Mateos (1990b) Evidence for an adaptive response to radiation damage in plant cells conditioned with X-rays or incorporated tritium, Int. J. Radiat. Biol., 57, 537-541.

Demple, B., and J. Halbrook (1983) Inducible repair of oxidative DNA damage in *Escherichia coli*, Nature, 304, 466-468.

Domínguez, I., N. Panneerselvam, P. Escalza, A.T. Natarajan and F. Cortés (1993) Adaptive response to radiation damage in human lymphocytes conditioned with hydrogen peroxide as measured by the cytokinesis- block micronucleus technique, Mutation Res., 301, 135-141.

Fan, S., G. Vijayalaxami, G. Mindek and W. Burkart (1990) Adaptive response to two low doses of X-rays in human blood lymphocytes, Mutation Res., 243, 53-56.

Fenech, M., and A.A. Morley (1985) Measurement of micronuclei in lymphocytes, Mutation Res., 147, 29-36.

Hamlet, S.M., M.F. Lavin and P.A. Jennings (1982) Increased rate of repair of ultraviolet-induced DNA strand breaks in mitogen stimulated lymphocytes, Int. J. Radiat. Biol., 41, 483-491.

Kaina, B. (1982) Enhanced survival and reduced mutation and aberration frequencies in V79 Chinese hamster cells pre-exposed to low levels of methylating agents, Mutation Res., 93, 195-211.

Moquet, J.E., D.C. Lloyd, J.S. Prosser and A.A. Edwards (1987) Sister-chromatid exchanges induced by mitomycin C after exposure of human lymphocytes in G0 to a low dose of X-radiation, Mutation Res., 176, 143-146.

Olivieri, G., J. Bodycote and S. Wolff (1984) Adaptive response of human lymphocytes to low concentrations of radioactive thymidine, Science, 223, 594-597.

Samson, L., and J. Cairns (1977) A new pathway for DNA repair in *Escherichia coli*, Nature, 267, 281-283.

Samson, L., and J.L. Schwartz (1980) Evidence for an adaptive DNA repair pathway in CHO and human skin fibroblast cell lines, Nature, 287, 861-863.

Sanderson, B.J.S., and A.A. Morley (1986) Exposure of human lymphocytes to ionizing radiation reduces mutagenesis by subsequent ionizing radiation, Mutation Res., 164, 347-351.

Sankaranarayanan, K., A.V. Duyn, M.J. Loos and A.T. Natarajan (1989) Adaptive response of human lymphocytes to low-level radiation from radioisotopes or X-rays, Mutation Res., 211, 7-12.

Scudiero, D., A. Norin, P. Karran and B. Strauss (1976) DNA excision-repair deficiency of human peripheral blood lymphocytes treated with chemical carcinogens, Cancer Res., 36, 1397-1403.

Shadley, J.D., V.Afzal and S. Wolff (1987) Characterization of the adaptive response to ionizing radiation induced by low doses of X-rays to human lymphocytes, Radiat. Res., 111, 511-517.

Shadley, J.D., and S. Wolff (1987) Very low doses of X-rays can cause human lymphocytes to become less susceptible to ionizing radiation, Mutagenesis, 2, 95-96.

Sobels, F.H. (1956) Organic peroxides and mutagenic effects in Drosophila, Nature, 177, 979-980.

Spiegler, P., and A. Norman (1969) Kinetics of unscheduled DNA synthesis induced by ionizing in human lymphocytes, Radiat. Res., 39, 400-412.

Tuschl, H., R. Kovac and H. Altmann (1983) UDS and SCE in lymphocytes of persons occupationally exposed to low levels of ionizing radiation, Health Phys., 45, 1-7.

Wang, Z.-Q., S. Saigusa and M.S. Sasaki (1991) Adaptive response to chromosome damage in cultured human lymphocytes primed with low doses of X-rays, Mutation Res., 246, 179-186.

Wiencke, J.K., V. Afzal, G. Olivieri and S. Wolff (1986) Evidence that the [^{3}H]thymidine-induced adaptive response of human lymphocytes exposed to subsequent doses of X-rays involves the induction of a chromosomal repair mechanism, Mutagenesis, 1, 375-380.

Wolff, S., V. Afzal, J.K. Wiencke, G. Olivieri and A. Michaeli (1988) Human lymphocytes exposed to low doses of ionizing radiations become refractory to high doses of radiation as well as to chemical mutagens that induce double-strand breaks in DNA, Int. J. Radiat. Biol., 53, 39-48.

Wolff, S., J.K. Wiencke, V. Afzal, J. Youngblom and F. Cortés (1989) The adaptive response of human lymphocytes to very low doses of ionizing radiation: A case of induced chromosomal repair with the induction of specific proteins, in: K.F. Baverstock and J.W. Stather (Eds.), Low Dose Radiation, Biological Bases of Risk Assessment, Taylor and Francis, London, pp. 446-454.

Publications under this Contract

Cortés,F., I.Domínguez, M.J. Flores, J.Piñero, J.C. Mateos (1994) Differences in the adaptive response to radiation damage in Go human lymphocytes conditioned with hydrogen peroxide or low-dose X-rays. Mutation Research, 311,157-163.

Cortés,F, I.Domínguez, B.Sandström (1994) Exogenous catalase introduced in CHO cells by electroporation does not protect against chromosome damage induced by ionizing radiation. Cell Biology International, 18,959-965.

Head of project 4:Dr.Palitti

II. Objectives for the reporting period.

To achieve new informations for radioprotection and radiotherapy as well as for identification of cancer prone individuals the influence of inhibitors of DNA synthesis or repair on the yield of radiation induced aberrations has been studied , particularly with the aim to understand the G2 radiosensitivity and the inter-individual variability in human subjects for response to the induction of chromosomal aberrations by ionizing radiation.

III Progress achieved including publications

A first objective of this project was to investigate the relationship between repair processes that take place during G2 phase of the cell cycle and the chromosome damage induced by fission neutrons by employing post-radiation treatment with inhibitors of DNA synthesis/repair such as caffeine,hydroxyurea (HU) and cytosine arabinoside (ara-C):
Whole blood cultures of human lymphocytes were exposed to various doses of fission neutrons or x-rays and treated post-irradiation during the last 2.45 h before harvesting with 5 mM caffeine,5 mM Hu and 0.05 mM ara-C.
The presence of caffeine and HU strongly potentiate the yield of chromatid-type aberrartions induced by both neutrons and x-rays. No potentiating effect,except at the highest dose of neutrons,was observed when irradiated cells were subsequently treated with ara-C (fig1). Since ara-C strongly potentiated the frequency of chromatid aberrations induced in G2 lymphocytes by x-rays,the results obtained indicate that fission neutrons produce a smaller proportion of lesions,the repair of which can be inhibited by ara-C,compared with the number produced by x-rays.

Futhermore the relationship between the repair processes occuring in G2 phase of the cell cycle and the cytogenetic damage in ataxia telagiectasia (AT) cells was studied.
Lymphoblastoid cells derived from normal,heterozygote AT (HzAt) and three AT patients were exposed to x-rays or fission neutrons and post-treated with inhibitors of DNA synthesis/repair,such us inhibitors of DNA polymerases a, d and 3 (cytosine arabinoside,ara-C;aphidicolin,APC;buthyl-phenylen-guanine,BuPdG) or ribonucleotide reductase (hydroxyurea,HU).
A strong increase of radiation-induced chromosomal aberrations was observed in normal and HzAT cells post-trated with ara-C,APC and HU,but not in the presence of BuPdG. No enhancing effect was observed in cells derived from AT patients,except for HU post-irradiation treatment (fig 2 for x-irradiation and fig 3 for fission neutrons)
These results suggest that the enzymes that can be inhibited by these agents are not directly involved in the repair of radiation damage induced in Ge cells from AT patients,indicating that probably the AT cells that we use lack the capability to trasform the primary DNA lesions into reparable products,or that AT cells might contain a mutated form of dNA polymerase resistant to the inhibitors
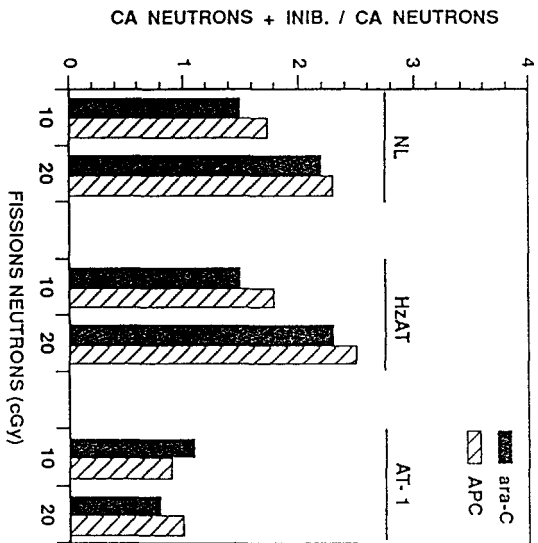
Figure 3. Effect of G2 post-irradiation treatments with ara-C and APC on chromatid aberrations induced in NL, HzAT and AT-1 cells by fission neutrons. CA, chromosomal aberrations.
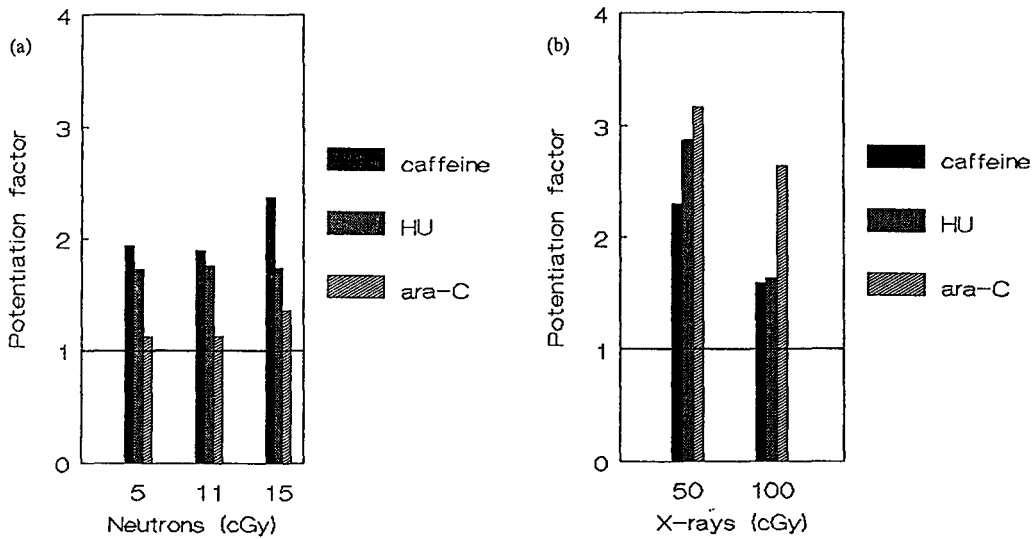
Figure 1. Potentiation factor. The lines indicate no potentiating effect
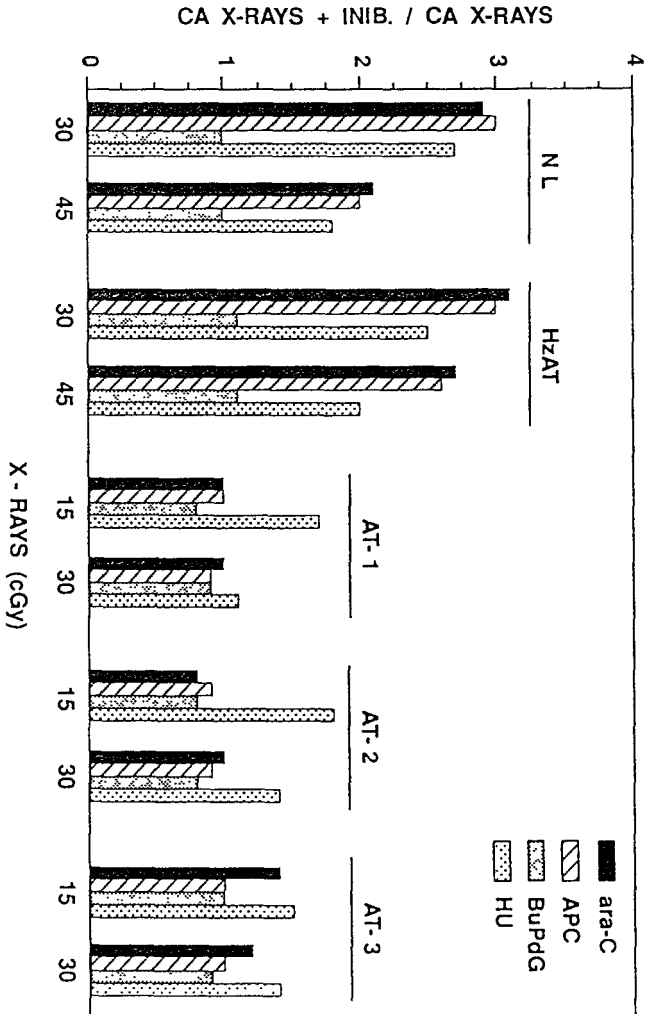
Figure 2. Effect of G2 post-irradiation treatments with ara-C, APC, BuPdG and HU on chromatid aberrations induced in NL, HzAT and AT cells by X-rays. CA, chromosomal aberrations.

Publications

Antoccia,A.,F.Palitti,T.Raggi,C.Catena and C.Tanzarella,1992,The yield of fission neutron-induced chromatid aberrations in G2-stage human lymphocytes:effect of caffeine,hydroxyurea and cytosine arabinoside post-irradiation.Int.J.Radiat. Biol 62:563-570.

Antoccia,A.,.F.Palitti,.T.Raggi,C.Catena and C.Tanzarella,1994,Study on the chromosomal damage induced by x-rays in ataxia telangiectasia lymphoblastoid cells:effect of inhibitors of DNA synthesis and repair. Physica Medica vol..X: 65-66.

Antoccia,A.,F.Palitti,T.Raggi,C.Catena and C.Tanzarella,1994, Lack of effect of inhibitors of DNA synthesis/repair on the ionizing radiation-induced chromosomal damage in G2 stage of ataxia telangiectasia cells.Int.J.Radiat. Biol. 66:309-317.

CONTRACT NO,   F13P-CT920031
TITLE OF PROJECT: Studies in radiation-induced chromosome aberrations
                   in mammalian cells.   2: Applied Aspects.
                   (Coordinator: Prof. G. Olivieri)
Project 5:   Team Leader: Dr John RK Savage   (MRC, Chilton, UK)

INTRODUCTION - SUMMARY OF OBJECTIVES FOR PROJECT 5

Numerical scores of chromosomal aberrations, following exposure of cells to ionizing radiation, have always formed, and continue to form, a very important end-point in radiobiology.

This is true both for the pragmatic approaches, like lymphocyte biological dosimetry in cases of accidental or environmental exposure (eg Chernobyl, Radon in homes), and for the more mechanistic experimental approaches, seeking to understand the responses of cells to detection and repair of damage after a radiation insult. They are also an important component in the study of long-term radiation effects like induced cancers and chromosome instability.

The sophisticated mathematical analyses of dose effects now available, and the interpretations derived from them, presuppose reliable numerical scores, and will be of no avail if the true frequencies are modified, or curves distorted.

The recognition of this problem was the basis for the initial proposals under this contract. Whilst in certain systems (for example, unstimulated G_0 human lymphocytes) it was fairly clear that the irradiated population was homogeneous with respect to radiosensitivity, so that observed scores of *chromosome-type* aberrations were independent of sampling time, and response curves unwarped, this was not true for the S/G_2 *chromatid-type* aberration systems. Here, both observed yield, and variation in the yield-time profile are affected greatly by any mitotic perturbation and delay introduced by the clastogen. As such perturbation will itself vary with dose (and with any additional experimental treatments given) it is obvious that dose-response curve shapes can be very unreliable.

Since *chromatid-type* aberrations are widely used, we felt it important to investigate effects of kinetic perturbations on yield. Three approaches were used
   a)   Use of BrdU cell marking techniques,
   b)   Use of chemicals to mitigate delay (eg Caffeine).
   c)   Computer modelling of cell-cycle perturbation effects.
Results are discussed in more detail in later sections.

During the course of these studies, it became clear that there was another set of underlying problems, also having an important bearing on aberration yield, and which we had not appreciated. Irradiation of BrdU potential "harlequin" chromosomes allowed us to classify, in much greater detail, the structure and origin of the *chromatid* exchange aberrations. These had, with conventional solid staining, always be considered as simple, two-lesion (2-break) interaction events. To our surprise, we found that a lot of them were, in fact, "Complex", involving the interaction of 3, or more, lesions. The frequency of such

multi-lesion events was LET-dependent, and probably dose-dependent. From these findings, it became obvious that we had been under-estimating the actual amount of chromosome damage induced by radiation, making even more uncertain the validity of observed aberration yields.

About this time, the technique of FISH chromosome "painting" was becoming popular, and was being applied increasingly to quantitative estimates of *chromosome-type* exchanges, because of its ability to detect, efficiently, the usually unseen reciprocal translocations. This exchange type is transmissible, and therefore of considerable significance for retrospective accident dosimetry, and other radiation protection problems. Workers using this technique began to report a fair frequency of unexpected, anomalous painting patterns, which we saw immediately, from our *chromatid* experiences, were obviously the result of multi-lesion interactions. Complex exchanges are therefore also a regular feature of *chromosome-type* exchanges, and consequent under-estimation of radiation-induced damage, together with the possibility of warped dose-response curves must be present in a system hitherto considered relatively simple and straight-forward.

Since such a conclusion has far reaching consequences, we transferred our efforts in the latter part of the contract to a thorough study, theoretical and practical, of the classification and quantitative consequences of Complex *chromosome-type* exchanges, and results to date are summarised in section **d** below.

RESULTS AND DISCUSSION

a) Using BrdU marking techniques to study *chromatid-type* aberrations.

Under previous contracts, we have developed a number of BrdU cell-marking techniques to study, and overcome, the scoring problems introduced by mitotic cycle perturbation. Basically, we have tried to answer the question, "Where was that cell I am scoring at the time of irradiation ?"

For more detailed study of the aberrations themselves, we irradiated cells in second division cycle following BrdU addition (ie. potentially "harlequin"). Immediately after irradiation, the BrdU medium was removed, and replaced by one containing thymidine. This allows us to distinguish cells that were in G_2 (pure harlequin with FPG staining) from those in S-phase (visible TT patches) at the time of radiation [3]. The sister-chromatid differentiation provides a much more detailed classification of aberration types, particularly *intra-arm intrachanges*. Always we adopted a multi-sampling time protocol, and studied the aberration types and frequencies in V79 cells during the transit of G_2 and S-phase.

A number of unexpected findings emerged:

i) A proportion of all chromatid breaks was accompanied by a colour-jump ($\equiv$ SCE) at the site of breakage. This proportion was <u>constant</u>, irrespective of dose and, moreover, remained the <u>same</u> for spontaneous breaks in the unirradiated control samples [9].

ii) Colour-jump breaks were also seen participating in *interchanges* either singly, or in pairs. We termed such interchanges "mixed" [9].

iii) The overall frequency of colour-jump breaks and mixed exchanges was greater when a high LET radiation (^{238}Pu α-particles) was used [1].

iv)   There was no evidence for BrdU radio-sensitization of chromatin for either breaks, *achromatic lesions*, or *intra-arm intrachanges*. The ratio of light to dark chromatid participation (either in a BB/TB or a TB/TT protocol) was 1.0 at all doses. In marked contrast, there was strong evidence of sensitization for those lesions participating in *interchanges*, with always a preference for light chromatids.

Colour-jump breaks and mixed exchanges with similar characteristics have since been seen in irradiated human fibroblasts, Syrian hamster cells, and JU56 Wallaby cells (unpublished observations). They indicate a) that a fixed proportion of all breaks are, as Revell originally suggested, incomplete type-1 intrachanges. Since some forms of other intrachanges are also seen, and these do not result in colour-jumps, it is a fair inference that additional fixed proportions of breaks are derived from these also, together with a contribution to the mixed interchange category. b) Many of the *interchanges* which we score as "simple" two-break events actually involve 3, or more, ie they are in reality, Complex exchanges.

These findings alert us to the facts that the formation of aberrations is more complicated than we usually assume, and that we are under-estimating the amount of chromatid damage that has actually occurred as the result of radiation.

In an attempt to simplify the situation, we have begun some work using restriction endonucleases to produce chromatid aberrations [5]. These will be derived from "clean", defined dsb, in contrast to the rather messy mix of damage resulting from radiation, and may help to clarify the origin of the colour-jump breaks.

b) The use of chemicals to mitigate the effects of mitotic delay.

Since mitotic delay and perturbation have a profound effect on the chromatid aberration frequency, its removal might help to establish a more reliable numerical value.

Caffeine is a substance which has been shown to mitigate delay after irradiation and, at the same time, produce a higher frequency of aberrations. The usual explanation is that ordinarily, delay allows time for repair, but, in its absence, cells continue progression to division, and arrive with relatively more unrepaired damage. Conversely, one could argue that the increased aberration frequency observed is purely the result of cancelling the perturbation and a consequent different mix of cells being present for sampling. Such an effect is readily demonstrable in the theoretical populations discussed in section c, below.

A multi-sampling time experiment was performed with V79 cells using the BrdU protocol mentioned above. The cells were exposed to 1.5Gy hard X-rays, and some cultures were then given 400μg/ml Caffeine.   As anticipated, mitotic delay was largely cancelled, but there was a negligible, non-significant effect upon aberration yield (all types). Colour-jump breaks, mixed exchanges and BrdU sensitization were all unaffected by the presence of caffeine [4].

It is evident from these results, that the enhanced aberration yield often observed after post-irradiation caffeine treatment is not necessarily causally related to the mitigation of delay. Also, in this instance, removal of cell perturbation has not had a major effect on observed frequencies.

c) Computer modelling of cell cycle perturbation effects.

It is an established fact that in heterogeneous cell populations, the underline observed underline aberration frequency is dependent upon the mixture of cells, from different cycle positions, present in the sample scored. This mixture changes, not only with sample time after exposure, but also as a consequence of all forms of treatment/dose produced delay and perturbation. Thus, any simple relationship between the intrinsic sensitivity pattern within a phase transit, and the scored yield-time aberration profile, is severed by these kinetic complexities.

In an attempt to understand these effects, and to assess their importance, we have developed a Monte-carlo simulation of a cycling cell population. This can be adjusted for any plausible phase transit time parameters and distributions, and each phase can be given an intrinsic sensitivity pattern for the production of aberrations. With this, we can generate an aberration yield-time profile.

Concentrating on the G_2P phase, we have added the facility to superimpose various models of mitotic delay in order to investigate effects on the yield-time aberration curve.

Three models have been considered; a) generalized delay - a cell is delayed according to its developmental position at the time of irradiation. b) Barrier delay (time) - a specific "Transition-point" for maximal delay is placed at a fixed time-before-metaphase, disregarding the developmental stage of each cell. c) Barrier delay (position) - the transition point is defined for a precise developmental position, and will therefore occur at a different time-before-metaphase for each cell.

The results [10] confirm our previous findings, worked out with much simpler population models. Using the same, simple, intrinsic sensitivity pattern for the production of aberrations in G_2P, a wide variety of different yield-time profiles results, depending upon the model of delay chosen. These profiles frequently display a fine structure (peaks, troughs) quite different from the known phase sensitivity pattern, indicating the danger of drawing inferences about sensitivity changes as a cell transits G_2 from aberration yields. The maximum peak height, or the integrated area under the profile are underline not underline valid measures of average sensitivity, and are therefore not reliable for use in constructing dose-response curves.

d) FISH painting and Complex *chromosome-type* exchanges.

With the advent of FISH chromosome "painting" applied to radiation-induced *chromosome-type* exchanges, it soon became apparent that the frequent anomalous patterns being reported were arising from Complex exchanges (those arising from 3, or more, breaks in 2, or more chromosomes) and that these must be occurring with a frequency much higher than we had hitherto suspected. It seemed clear that some parallelism was present with our unexpected *chromatid* aberration findings.

Because of their presumed rarity, no one had ever undertaken a serious theoretical analysis or classification of possible multi-break interactions, nor the likely outcomes when such configurations are painted. Such an analysis seemed to us a desirable and necessary pre-requisite for progress, and we concentrated our efforts here for the later period of the contract.

The number of possible arrangements of 3, 4,... breaks within and between chromosomes is quite large. We proposed that one approach would be to assign break combinations to families, based on the number of *Chromosomes*, the number of *Arms*, and

the number of *Breaks* (The **CAB** system [11]). 26 such families exist from the simplest *2/2/3* up to *5/5/5*. We have now completed the analysis of all 26 families.

Each family generates a large number of exchanges. If free interaction is allowed between break-ends, and *restitution* is a valid option, then the 26 families can produce a total of 15,060 exchange possibilities.

If <u>one</u> participating chromosome is painted, each configuration can yield several patterns, depending on the number of chromosomes involved. It turns out that in most cases, a set of <u>different</u> patterns can arise from one exchange, and often, one, or more, of these patterns will <u>appear</u> (and so be scored as) a "simple" dicentric (**2A**) or reciprocal translocation (**2B**). Thus, some of the **2A** and **2B** seen after irradiation are Complex-derived, and can contain hidden changes [8, 11, 12] - we term these *pseudosimples* [13, 14, 15] . Their presence means that, using painting, there will be more Complex exchanges present than we record, and unless we make a correction for this hidden component, actual damage will be under-estimated [13].

41,895 patterns are produced by the 26 families. All have been examined, resulting in 203 distinctive patterns which have been classified for scoring purposes (only those up to *CAB 4/4/4* have been published [11]).

The numerical relationships are being analysed to provide ratios and factors which may be used to correct experimental data for pseudosimples etc. with a view to obtaining a more accurate assessment of the true damage level.

In concert with these theoretical studies, radiation and painting studies have been done using human fibroblasts. These have confirmed that the frequencies of Complex exchanges are much higher than has been anticipated, recorded levels being of sufficient magnitude to influence dose-response curve shapes.

With low LET hard X-rays, the relative frequency in a random sample of exchanges is dose dependent; being very low below 2.0Gy, and ~ 20-25% at 4.0Gy. With high LET (^{238}Pu α-particles) relative frequency is higher (~ 40-45% [2]) and appears to be dose-independent. Currently, other qualities of radiation are being investigated.

Analysis above *CAB 5/5/5* is not contemplated (6 breaks generate 10,395 combinations of ends, and there are 29 *C/A/6* families !). However, Complex exchanges involving 6, 7, and even higher numbers have been observed at 4.0Gy x-rays and above. This raises a number of very fundamental questions with regard to our concepts of rejoining distance, site sizes, numbers and distribution of dsb, and the processes by which exchanges form [6, 7]. Put together with our *chromatid* findings, it is clear that we still have a lot to learn about the mechanisms of aberration formation.

PUBLICATIONS UNDER THIS CONTRACT.

1) Griffin CS, Harvey AN, Savage JRK (1994) Chromatid damage induced by ^{238}Pu α-particles in G_2 and S phase Chinese hamster V79 cells *Int.J.Radiat Biol.* **66**: 85-98

2) Griffin CS, Marsden SJ, Stevens DL, Simpson PJ, Savage JRK (1995) Frequencies of complex chromosome exchange aberrations induced by ^{238}Pu α-particles and detected by fluorescence *in situ* hybridization using single chromosome-specific probes *Int.J Radiat.Biol* **67**: 431-439

3)   Harvey AN, Savage JRK (1992):   Simple cell-cycle analysis in second-division cells. *Clin.Cytogenet.Bull.* **2**: 94-96.

4)   Harvey AN, Savage JRK (1994):   A case of caffeine-mediated cancellation of mitotic delay without enhanced breakage in V79 cells. *Mutation Res.* **304**: 203-209

5)   Harvey AN, Costa ND, Savage JRK (1994):   Electroporation and Streptolysin-O : A comparison of poration techniques. *Mutation Res.* **315**: 17-23.

6)   Savage JRK (1993): Update on target theory as applied to Chromosomal Aberrations *Environmental and Molecular Mutagenesis.* **22**: 198-207. Wiley-Liss Inc

7)   Savage JRK (1993):   Interchange and Intranuclear Architecture *Environmental and Molecular Mutagenesis.* **22**: 234-244. Wiley-Liss Inc.

8)   Savage JRK   (1994): FISH painting and Complex chromosome-type exchanges. *Clin.Cytogenet.Bull.* **2**: 81-84.

9)   Savage JRK, Harvey AN (1994):   Investigations of aberration origins using BrdU. In *"Chromosomal Alterations; Origin and Significance".* (Obe G, Natarajan AT, (Eds) ; pp 76-91   Springer-Verlag, Berlin.

10)   Savage JRK, Papworth DG (1994):   Review Article: Mitotic perturbation and G2 cell chromatid aberrations. *Rev.Brasil.Genet.* **17 (1)**: 121-125.

11)   Savage JRK, Simpson P (1994):   "FISH "painting" patterns resulting from Complex Exchanges"   *Mutation Res.* **312**: 51-60.

12)   Savage JRK, Simpson P (1994):   On the scoring of FISH-"painted" chromosome-type exchange aberrations.   *Mutation Res.* **307**: 345-353.

13)   Simpson PJ, Savage JRK (1994):   Identification of X-ray-induced Complex chromosome exchanges using fluorescence *in situ* hybridization: A comparison at two doses. *Int.J.Radat.Biol.* **66**: 629-632.

14)   Simpson PJ, Savage JRK (1995):   Estimating the true frequency of x-ray-induced Complex chromosome exchanges using fluorescence *in situ* hybridization. *Int.J.Radat.Biol.* **67**: 37-45

15)   Simpson PJ, Savage JRK (1995):   Detecting "hidden" exchange events within X-ray-induced aberrations using multicolour chromosome paints. *Chromosome Research.* **3**: 69-72

Head of project 6: Dr. Kalina

II. Objectives for the reporting period

     The objectives for the reporting period where to study the
heterogeneity of adaptive response to low dose of irradiation
and bleomycin in normal human pheripheral lymphocytes and in
patients with genetic diseases.
     In the first series of experiments we followed AR in
lymphocytes of patients with   DS and in homozygous and
heterozygous ataxia telangiectasia patients.
     The second series of experiments were devoted to study of
heterogeneity AR in normal persons on the basis of evaluation
of AR in lymphocytes of monozygotic twins.

III. Progress achieved including publications

     In experiments on the AR in persons with aneuploid
karyotype lyphocytes 5 patients   with DS were applied.
Duplicate whole blood cultures were set up in 5ml of RPMI
medium supplemented with 20% calf serum, antibiotics and 2%
PHA. Gama rays at a dose of 0.01 Gy (dose rate 2 cGy/min)
were applied 32h after stimulation, and a higher dose of
1.5Gy of gamma rays was delivered at the 48th hour off culture
(protokol Shadley et al. 1987). The amount of 0.1ml of
Colcemid (final concentration $2x10^{-7}M$) was added each culture
2h before fixation. The frequencies of chromatid and
isochromatid breaks, as well as occasional chromatid and
isochromatid exhcanges were recorded in at least 200 cells in
the following 4 groups in each experiment: control, adaptive
dose (0.01 Gy) only, challenge dose (1.50 Gy) only, and
adaptive dose plus challenge dose. The statistical
significance of reduction of the frequency of chromosome
aberrations was determined using Student´s t-test. The
expected value was calculated as a sum of individual doses
minus the control value.

Table 1 shows the results that indicate the effects of low dose gamma rays on the induction of AR in lymphocytes of 3 normal subjects. It can be seen that the freuency of chromosome aberrations was decreased by 34 - 54%. These results are in good agreement with data of other authors. The results of experiments carried out to study the AR in lymphocytes with trisomy are summarized in table 2. The presented data do not indicate any significant AR in any of the five blood donors with DS.

We suppose that the genetic mechanism (if any) resulting in the inability do induce an adaptive repair in normal and trisomic lymphocytes may be the same, but it is more likely that in lymphocytes with trisomy 21 also other factors, e.g. the cell cycle kinetics which is rather different in comparison with normal diploid cultured lymphocytes (Leonard and Mertz, 1983, Konečná et al., 1988), might play a role. However, to confirm such an assumption, further experiments aimed at studying the cell cycle dependence of the AR in trisomy 21 lymphocytes must be performed.

The results on the AR in patients with ataxia telangiectasia are presented in Table 3 and 4. Radiosensitivity of the lymphocytes in AT homozygotes was 5-6 times, and in AT heterozygotes twice as high as in the control cells (Table 3). In this respect our results differ from those published by Bender et al. (1985) who reported two times, and Humphreys et al. (1989) who recorded even 7-11 times higher sensitivity to X-rays in AT homozygotes as compared to control cells. These discrepancies in radiosensitivity of cells in AT patients might be explained by their different clinical and genetic features (Bundey, 1994). In our experiments, cell sensitivity in AT patients to BLM was two times higher as compared to control cells. This results is similar to that published by Scott and Zampetti-Basseler (1985).

As to the ability to induce AR, it was found in control cells, when radiation and BLM were applied, and in AT heterozygotes after pretreament with a low concentration of BLM, but not after a low dose of gamma rays. A similar variation in AR was observed also in lymphocytes of healthy donors exposed to different treatments (Sankaranarayanan et al., 1989). In AT homozygotes no AR was found either after a

Tab. 1. The effect of preirradiation on the frequency of
chromosomal aberrations in health donors´ lymphocytes

Donor	Treatment group	Number of cells scored	Observed No.	aberrat. %	Expec- ted %	Decre- ase %
	control	200	3	1.50	–	–
D₁	0.01 Gy	200	4	2.00	–	–
19 yr	1.50 Gy	198	53	26.80	–	–
46,XX	0.01+1.5 Gy	200	35	17.50	27.3	35,9*
	control	200	1	0.50	–	–
D₂	0.01 Gy	200	4	2,00	–	–
20 yr	1.50 Gy	200	42	21.00	–	–
46,XX	0.01+1.5 Gy	200	30	15.00	22.5	33,3*
	control	194	2	1.03	–	–
D₃	0.01 Gy	200	3	1.50	–	–
20 yr	1.50 Gy	195	56	28.70	–	–
46,XY	0.01+1.5 Gy	200	24	12.00	29,2	58.9**

* P < 0.05

** P < 0.01

Tab. 2 The effect of preirradiation on the frequency of chromosomal aberrations in DS lymphocytes

Donor	Treatment group	Number of cells scored	Observed aberrat.		Expected %	Decrease %
			No.	%		
DS1 8 yr 47,XX,+21	control	200	4	2.0	-	-
	0.01 Gy	200	4	2.0	-	-
	1.50 Gy	184	40	21.7	-	-
	0.01+1.5 Gy	200	37	18.5	21.7	14,7
DS2 14 yr 47,XX,+21	control	200	4	2.0	-	-
	0.01 Gy	200	2	1.0	-	-
	1.50 Gy	200	53	26.5	-	-
	0.01+1.5 Gy	196	40	20.4	25.5	20.0
DS3 11 yr 47,XY,+21	control	188	3	1.6	-	-
	0.01 Gy	200	1	0.5	-	-
	1.50 Gy	200	47	23.5	-	-
	0.01+1.5 Gy	190	46	24.2	22.4	*
DS4 7 yr 47,XX+21	control	200	2	1.0	-	-
	0.01	200	3	1.5	-	-
	1.50	200	8	24.0	-	-
	0.01+1.50 Gy	200	41	20.5	24.5	16,3
DS5 11 yr 47,XY+21	control	200	1	0.5	-	-
	0.01	200	3	1.5	-	-
	1.50	200	55	27.5	-	-
	0.01+1.50 Gy	200	53	26.5	28.5	7.0

* 8,0 % enhancement

Tab. 3. The effect of preirradiation on the frequency of chromosomal aberrations in healthy donors and in donors with ataxia telangiectasia

Donor	Treatment group	Number of cells scored	Observed aberrations		Expected value	Decrease %
			total	per cell		
Hlth cont.	control	594	6	0,010		
	0,05 Gy	600	11	0,018		
	1,50 Gy	593	151	0,255		
	0,05+1,50 Gy	600	89	0,148	0,263	43,70*
AT aa1	control	200	16	0,080		
	0,05 Gy	200	21	0,105		
	1,50 Gy	200	262	1,310		
	0,05+1,50 Gy	186	257	1,381	1,335	–
AT aa2	control	200	24	0,120		
	0,05 Gy	200	27	0,135		
	1,50 Gy	194	295	1,520		
	0,05+1,50 Gy	180	273	1,517	1,535	8,50
AT Aa1	control	200	9	0,045		
	0,05 Gy	185	15	0,081		
	1,50 Gy	200	112	0,560		
	0,05+1,50 Gy	193	102	0,528	0,596	11,40
AT Aa2	control	200	8	0,040		
	0,05 Gy	200	17	0,085		
	1,50 Gy	200	96	0,480		
	0,05+1,50 Gy	187	89	0,475	0,525	10,00

* P < 0,01

Tab. 4. The effect of pretreatment with BLM on the frequency
of chromosomal aberrations in healthy donors and in donors
with ataxia telangiectasia

Donor	Treatment group	Number of cells scored	Observed aberrations		Expected value	Decrease %
			total	per cell		
Hlth cont.	control	600	9	0,015		
	0,05 μgml^{-1}	600	8	0,013		
	1,50 μgml^{-1}	600	234	0,390		
	0,05+1,50 μgml^{-1}	591	157	0,266	0,388	31,60*
AT aa$_1$	control	200	18	0,090		
	0,05 μgml^{-1}	191	16	0,083		
	1,50 μgml^{-1}	200	156	0,780		
	0,05+1,50 Gy	188	129	0,686	0,773	11,30
AT aa$_2$	control	200	24	0,120		
	0,05 μgml^{-1}	200	21	0,105		
	1,50 μgml^{-1}	200	194	0,970		
	0,05+1,50 μgml^{-1}	190	173	0,911	0,955	4,70
AT Aa$_1$	control	200	6	0,030		
	0,05 μgml^{-1}	200	8	0,040		
	1,50 μgml^{-1}	200	82	0,410		
	0,05+1,50 μgml^{-1}	200	59	0,295	0,420	29,80*
AT Aa$_2$	control	200	4	0,020		
	0,05 μgml^{-1}	200	5	0,025		
	1,50 μgml^{-1}	200	94	0,470		
	0,05+1,50 μgml^{-1}	200	75	0,375	0,475	21,10*

* $P < 0,05$

low dose of gamma rays (Table 3) or after a lowa dose of BLM
(Table 4). In contrast to our findings, Shadley et al. (1987)
observed AR in the cells of AT patients when a low dose of
X-rays was used. These results indicate that the adaptive
ability of the lymphocytes is a variable trait also among AT
donors, similarly to that found in healthy donors (Bosi and
Olivieri, 1989) as a result of genetic heterogeneity. The
variability of AR in AT patients might be influenced also by
psysiological conditions during in vitro cultivation of cells
(Wojewodska   et al., 1994; Wojczik   1995. Moreover, cell
hypersensitivity in AT patients might play an important role
in AR induction.

In the study of heterogeneity AR in normal lymphocytes we
used 5 pairs of monozygotic twins. The AR was evaluated
according to Shadley et al. protocol. Preliminary results
indicate lower differencies of AR between MZ twins than amoung
genetic non - relative persons. These results are in
preparation for publication.

Publications:

- I. Kalina, H. Konečná, G. Némethová, N. Račeková: Adaptive
  response to ionizing radiation in normal and aneuploid
  human lymphocytes. Folia Biol. 40, 119-123, 1994.
- G. Némethová, I. Kalina, H. Konečná, N. Račeková: The
  adaptive response of peripheral lymhocytes to low doses
  of mutagenic agents in persons with genetic disorders.
  24th Annual meeting EEMS, August 31ts-September 3rd,
  1994, Poznaň, Poland.
- G. Némethová, I. Kalina, N. Račeková: The adaptive response
  of peripheral blood lymphocytes to low doses of mutagenic
  agents in patients with ataxia telangiectasia. Mutat.
  Res. (in press).

Title: Carcinogenic effects of low radiation doses and underlying mechanisms.

1)   Davelaar   Univ. Leiden
2)   Coppola   ENEA
3)   Bentvelzen   TNO - Delft
4)   Masse   CEA - Paris
5)   Chmelevsky   GSF
6)   Zurcher   TNO - Delft

I. Summary of Project Global Objectives and Achievements

Tumour induction in-vivo is the result of energy deposition and subsequent of biophysical and biochemical processes. This joint project embraces studies of the carcinogenic effects of low radiation doses in different animal models and the underlying molecular biological mechanisms. The influence of various exposure or host conditions on the probability of cancer development have been studied. The project involves the analysis of data from recently accomplished experiments, the completion of on-going experimental studies, and the performance of a limited selections of new series. Mechanistic studies of radiation induced neoplasia using animal models have been confined to thymic lymphoma, myeloid leukaemia, osteosarcoma and mammary carcinomas in rodents.

The progress achieved by the various participants can be summarized as follows:

1. AZL: The computer programs LifePrep and LifeStat have been developed to serve as a standard tool for the analysis of dose-effect relationships in animal models and are available to other groups working on in-vivo carcinogenesis. The program has been applied to tumour induction data in WAG-Rij rats after fractionated irradiation in order to study mammary carcinogenesis in view of radiation protection questions in general or the risk for tumour induction in large scale breast screening programs in particular.

2. ENEA: Studies on the induction of epithelial tumours in mice after irradiation with fission neutrons did not reveal any marked influence of the time regimen of neutron irradiation on survival and tumour induction at low doses. This agrees with the results of an experiment on the effect of dose fractionation of fission neutrons on neoplastic transformation of exponentially cells. Concerning the genetic predisposition to carcinogenesis the restriction length polymorphism of telomere-like sequences appear to be different in the CBA/Cne and CBA/H mouse colonies. In addition an experimental approach has been followed consisting of a bi-directional selective breeding for susceptibility and resistance to two-stage carcinogenesis, initiated by DMBA and promoted with TPA.

3. ITRI-TNO: The study on mammary cancer induction in rats after single dose and fractionated gamma irradiation with and without hormone administration has been completed as far as the collection of tumours is concerned. In females, which were not given oestrogens, a single dose of 1 Gy did not result in a strikingly elevated risk, irrespective of the age of exposure. When the animals are irradiated at 64 weeks of age, the relative risks are remarkably low. It was found that 3 of 25 radiation-induced mammary tumours contained a mutation in codon 12 of the K-ras oncogene and 1 in codon 13 of that gene. No ras oncogene mutations were found in any of the spontaneous mammary tumours.

4. CEA: The aim of the work is to identify the potential co-carcinogenic effect of combined exposure to irradiation and various occupational and/or environmental inhaled airborne pollutants. The effort was focused mainly on ozone in rats after pulmonary irradiation, either globally by fission neutrons or locally after inhalation of radon 222 and its short lived decay products. The role of cytochrome P450 1A1 (CYP 1A1) was investigated during co-carcinogenesis produced by inducers of this enzyme. Different groups of rats were treated by intramuscular injections of various chemical compounds to induce soft tissue tumours, mainly rhabdomyosarcomas and fibrosarcomas, at the site of injection to constitute a bank of neoplastic and pre-neoplastic lesions. The results suggest that CYP 1A1 expression alone in some particular cell type could be a primeval step of a co-carcinogenic process induced after local lung irradiation by inhalation of radon and its daughters.

5. GSF: The analysis methods for tumour induction in animals are performed in subsequent steps, notably the Kaplan-Meier estimators, the Cox regression for a joint analysis and the use of analytical functions. The applicability of the mathematical methods is illustrated on a lifetime experiment with Spraque-Dawley rats on the induction of carcinomas and sarcomas after irradiation with gamma rays and fission neutrons. This experiment confirms that for these two classes of neoplasms there are differences in radiation sensitivity, which lead to different dose response and different RBE values.

6. IVVO-TNO: Since the activities of the department of pathology have been terminated, the histopathological classification of lesions arising in rats after different radiation treatments has been performed at the Center for Radiological Protection and Dosimetry TNO at Rijswijk. The histopathological examinations of mammary tumours in rats treated with radiation and hormones have been completed. In addition to the benign (fibroadenomas) and malignant tumours (carcinomas), other neoplastic lesions have been observed.

Head of project 1: Dr. J. Davelaar

II. Objectives for the reporting period

With the finalization of the programs LifePrep and LifeStat the means were provided to analyze tumour induction data from different experiments. Main emphasis was placed on the analysis of the earlier and current studies on - mammary carcinogenesis after fractionated irradiation. In the present contract period more specific attention has been directed to the error propagation in the different steps of mathematical fitting.

III. Progress achieved including publications

The crude incidence data are initially corrected for loss of animals due to other reasons than the endpoints to be studied i.e. carcinogenesis. Subsequently different models e.g. Weibull distributions are applied. The statistical variation of the different steps are the following:

The fraction of animals surviving without evidence of failures, $S(t)$, in course of time can be estimated by the Kaplan and Meier (1958) method. An estimate, $\hat{S}(t)$, of the cumulative survival function, $S(t)$, is calculated with the product limit method by:

$$\hat{S}(t_n) = \prod_{i=1}^{n}\left(1 - \frac{F_i}{N_i}\right)$$

where: $\hat{S}(t_n)$ - probability of surviving t_n (failure time at sequence n) without evidence of a failure,
i - an index, running from 1 to n,
N(i) - the numbers still at risk at failure time t_i,
F(i) - number of failures, observed at failure time t_i.

With known values for $S(t_n)$, the standard error in $\hat{S}(t_n)$, $\sigma_S(t_n)$, is calculated for the product limit by:

$$\sigma_{\hat{S}}(t_n) = \hat{S}(t_n)\sqrt{\sum_{i=1}^{n}\frac{F_i}{N_i(N_i - F_i)}}$$

The subsequent step in the analysis is the application of an analytical function to the Kaplan-Meier data. A parametric Weibull function is often applied as a model for the surviving fraction, $S(t)$. This function is defined by:

$$S(t) = e^{-((t-\gamma)/\alpha)^{\beta}}$$

Where: α - the time-scale parameter,
                 β - the shape parameter,
                 γ - the time-shift parameter.

      Two independent mathematical tools, notably chi-square fitting and maximum likelihood optimization, are compared in the current study on error propagation. The error propagation is performed for both methods through the variance-covariance matrices of the parameters (see the LifeStat manual for details).
      After the completion of a joint Weibull function fit, the hazards of each datasets are proportional to each other. The relative hazard, η, calculated relative to the reference (or control) dataset, will be calculated by:

$$\eta = \frac{H_g(t)}{H_0(t)} = \left(\frac{\alpha_0}{\alpha_g}\right)^{\beta} , \qquad H(t) = \left(\frac{t-\gamma}{\alpha}\right)^{\beta}$$

Where: 0 - subscript for the reference (or control) dataset,
                 g - subscript for any other dataset.
In case of the joint fit, the time-shape parameters are equal ($\beta_0 = \beta_g$).

The variance in the relative hazard will be calculated according to:

$$v_{\eta} = v_{\beta\beta}\left(\frac{\delta\Lambda}{\delta\beta}\right)^2 + v_{\alpha_0\alpha_0}\left(\frac{\delta\Lambda}{\delta\alpha_0}\right)^2 + v_{\alpha_g\alpha_g}\left(\frac{\delta\Lambda}{\delta\alpha_g}\right)^2 + 2v_{\beta\alpha_0}\left(\frac{\delta\Lambda}{\delta\beta}\cdot\frac{\delta\Lambda}{\delta\alpha_0}\right)$$

$$+ 2v_{\beta\alpha_g}\left(\frac{\delta\Lambda}{\delta\beta}\cdot\frac{\delta\Lambda}{\delta\alpha_g}\right) + 2v_{\alpha_0\alpha_g}\left(\frac{\delta\Lambda}{\delta\alpha_0}\cdot\frac{\delta\Lambda}{\delta\alpha_g}\right)$$

      It turns out that the standard deviation in the chi-square fitting procedure is smaller than in the case of maximum likelihood optimization. An example of the analysis of the datasets of WagRij rats irradiated at 8 weeks, 17 weeks and 120 fractions respectively, according to both methods is given in table I. As is apparent from the table the standard deviations are about a factor of two smaller for the chi-square fitting. This difference is presently under investigation, since it may have significant implications for the derived relative hazards of a single dose in comparison with fractionated irradiation and consequently for the risks derived at low doses.

Table I. Standard errors in relative hazard as derived from different methods

Dose	Dataset	Max. Likelihood Rel.Hazard	S.E.	Chi-square Rel.Hazard	S.E.
0	controls	1.00		1.00	
0.3	8 weeks	0.36	0.31	0.74	0.2
0.3	17 weeks	0.50	0.35	0.52	0.21
0.3	120 fractions	1.22	0.71	0.99	0.44
1.2	8 weeks	3.70	1.78	2.99	1.0
1.2	17 weeks	1.64	0.85	1.48	0.55
1.2	120 fractions	1.42	0.8	1.41	0.5

Head of project 2: Prof. Coppola

II. Objectives for the reporting period

- Carcinogenic effect of fractionated doses of fission neutrons on $BC3F_1$ male mice.
- Induction of myeloid leukaemia in CBA/Cne male and female mice after irradiation with X rays and fission neutrons.
- Selection of two mouse populations with high or low susceptibility to two-stage skin tumour induction to be used for studies of genetic predisposition to skin carcinogenesis.
- Study of ovarian tumour induction, in respect to hormonal imbalance, by partial body irradiation of $BC3F_1$ female mice.
- Transformation assays of human cells.

III. Progress achieved including publications

The contribution of the ENEA Casaccia group was initially focused mainly on the study of the influence of dose, dose rate, and radiation quality on the induction of malignant transformation in different strains of mice of both sexes and various ages, with particular attention to low dose exposures. It involved the analysis of the results of recent experimental series, the completion of on-going experiments, and the performance of a limited selection of new series. In particular, it included the study of the effect of dose fractionation on the induction of tumors in $BC3F_1$ male mice by fission neutrons, as well as of the susceptibility to induction of myeloid leukemia and solid tumors in CBA/Cne mice of both sexes irradiated with fission neutrons.

In the course of the contractual period new attention was progressively growing with respect to the problem of genetic predisposition to oncogenesis. Therefore, towards the end of the contractual period some efforts have been directed to the preparation of experiments aiming to investigate this problem.

In the recent past, fractionation or protraction of high-LET radiation doses has been reported to result in an enhancement of tumour induction in several in vivo experiments on rodents in comparison to acutely given doses. As this may have important implications for radiation risks assessment, our

group was fostered to further investigate the influence of the temporal regime of irradiation on the effectiveness of low neutron dose exposures. To this aim, the results of our experimental studies of carcinogenesis in long-living BC3F$_1$ male mice after acute and fractionated doses of fission neutrons were analysed. For this, we considered about 950 BC3F$_1$ male mice, subdivided in controls plus 8 groups which had received five equal daily dose fractions of fission neutrons from the RSV-TAPIRO reactor, corresponding to cumulative doses of 0.025 to 0.71 Gy. A comparison was made with data relative to BC3F$_1$ mice acutely exposed to comparable doses of fission spectrum neutrons, for critical endpoints. Data treatment included the correction for competitive risks and the analysis in terms of cumulative mortality, death-rates for specific causes, and trend. The results of tumour induction in the lung are shown in Figure 1. They do not reveal any appreciable effect of neutron irradiation at doses up to 0.1 Gy, and do not indicate any difference in effectiveness between single and repeated exposures in the low neutron dose region.
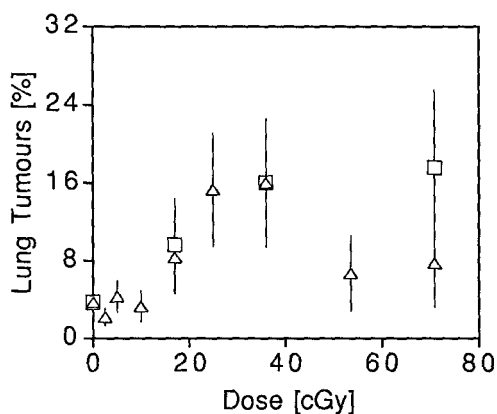
Fig. 1. Percent incidence of lung tumours in BC3F$_1$ male mice whole-body irradiated with fractionated (△) or acute (□) fission spectrum neutron doses. Bars are SE.

Myeloid leukemia was absent in the control group. For the irradiated animals, a positive significant trend was proved in the dose ranges 0-0.17 Gy and larger. We have also analysed the dose dependence of the complex of induced epithelial tumours. The percentage of mice bearing an epithelial tumour is plotted in Figure 2. As for the lung, epithelial tumour incidence does not appear to be modified by doses below 0.17 Gy. This type of data pooling may have shortcomings from a mechanistic point of view, but at the same time has the advantage of providing a straightforward and simple index of a major radiation risk. Another favourable aspect of this procedure of collating data is its ability to yield intrinsic robust results, as the frequency of events taken into account can be relatively high even when the sample size is limited.

The results of Figure 2 also show that the risk of induction of epithelial tumors in BC3F$_1$ male mice by fission neutrons from the TAPIRO reactor is similar in the same range of doses for both temporal modalities of neutron irradiation. In order to perform an easy comparison between the effect of fractionated and acute neutron doses, the dose responses between zero and 0.71 Gy were fitted with a simple second order polynomial (R=0.95 and R=0.99 for fractionated and acute neutron doses, respectively). The linear coefficients,

describing grossly the ability of radiation per Gy (±SE) to induce an epithelial tumour, were 87 (±34) for five daily doses of fission neutrons, and 64 (±40) for acute doses of neutrons, with a ratio of 1.36 (±1.00). The difference between the two linear terms is, however, not significant (Student's t=0.67, DF=9, P=0.5). In addition, due to the larger negative quadratic term in the case of dose fractionation compared to acute exposure, the overall enhancing effect appears to be absent.
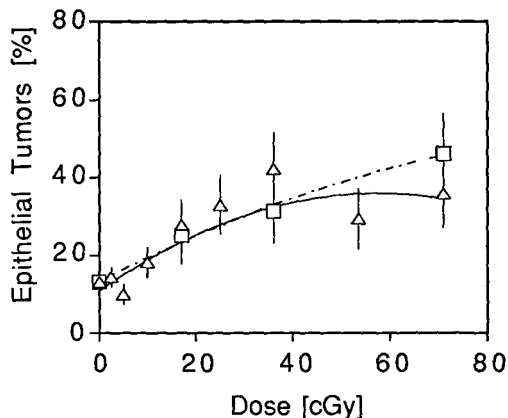
Fig. 2. Variations of epithelial tumour percent incidences in BC3F₁ male mice whole-body irradiated with fractionated (△) or acute (□) doses of fission spectrum neutrons. Bars are SE. Solid and dotted lines are for fractionated and acute irradiations, respectively.

Thus, the analysis of the results of our in vivo experiments indicates no significant effect of dose fractionation on tumour induction at low doses. However, for the lung, as for solid tumours in other organs the incidence at a dose of 0.71 Gy appears consistently lower for fractionated neutron doses than for acute exposures. The case of acute myeloid leukaemia remains somewhat ambiguous, however, this disease is very rare in our hybrid mice.

Due to the above findings, a new experimental series was carried out on CBA/Cne male and female mice to provide further data on the induction of acute myeloid leukaemia (AML) and malignant lymphoma by X rays or fission neutrons. Myeloid leukemia was not observed in the untreated controls, as in all our experiments, but was also practically absent in irradiated females (1 case over 602 diagnosed females). Conversely, a dose-effect curve could clearly be identified in irradiated males and appeared highly curvilinear for both radiation qualities. Malignant lymphoma was also expressed by irradiated male mice. The incidence of these systemic lesions after X rays was fitted with the expression

$$I(D) = (c+aD^2)e^{-bD}$$

where the coefficient c was put to zero for myeloid leukaemia. The results are shown in Figure 3.

These experiments have also provided material for studies of the genetic sensitivity to AML in rodents. There is, in fact, growing evidence that a proportion of spontaneously arising malignancies is strongly influenced by germ line mutations to tumour suppressor and protooncogenes and that for

some cancers there is a significant impact of these mutations in the human population. Therefore, in view of what observed in the CBA/H mice, an experiment was first carried out to determine the restriction length polymorphism of telomeric-like sequences in the CBA/Cne mouse colony to see whether a comparable distribution was present in the two colonies, that could be associated with AML susceptibility. To this aim, a total of about 50 spleens from young adult male mice were frozen immediately after excision and sent on dry ice for this type of analysis to Dr. M. Janowski (VITO, Mol, contract FI3P-CT92-0011). The results of this experiment indicated the presence of a polymorphism of the telomere-like repeats in the CBA/Cne colony that was different from that observed in CBA/H mice.
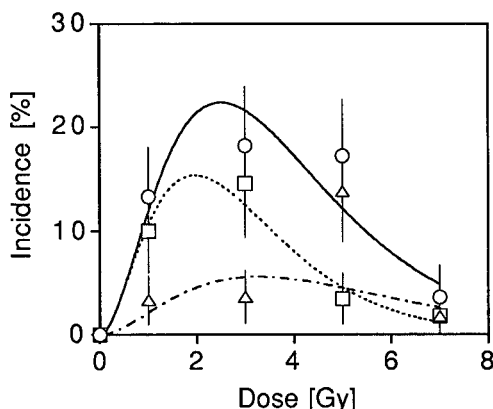
Fig. 3. Dose-effect relationships for myeloid leukemia (□), malignant lymphoma (Δ), and combined systemic lesions (○) in CBA/Cne male mice irradiated with scalar acute doses of X rays. Bars are SE.

In addition to studies of genetic factors influencing the susceptibility to oncogenesis in inbred mouse strains, it was considered very important to investigate the possibility of regulation by a number of genes of the susceptibility to tumour induction in a heterogeneous experimental population, as this may also have direct implication for the human case. To this aim, an experimental approach has been followed consisting of a bi-directional selective breeding for susceptibility and resistance to two-stage skin carcinogenesis, initiated by DMBA and promoted with TPA. The character chosen for the assortive mating is the number of papillomas at the end of a promotion period of about 50 days. The selection was started from a highly genetically polymorphic mouse population, produced by inter-crossing of eight inbred strains of mice. An increasing difference in the frequency of skin tumours was observed between the resistant (Car-R) and the susceptible (Car-S) lines through successive generations, which confirms the polygenic regulation of these characters, though some genes may have a dominating role. The change of susceptibility to skin tumours from generation F0 to F11 is seen in Figure 4.

Selection experiments are being continued to increase the interline separation, to obtain mice homozygous for all loci regulating the investigated character. When this is obtained, new experimental work is scheduled to investigate if the same genes controlling the selected characters might have also affected the spontaneous incidence and the radiation-induced tumours

(not only skin tumours) in the resistant and the susceptible lines of mice
irradiated either locally or whole-body.
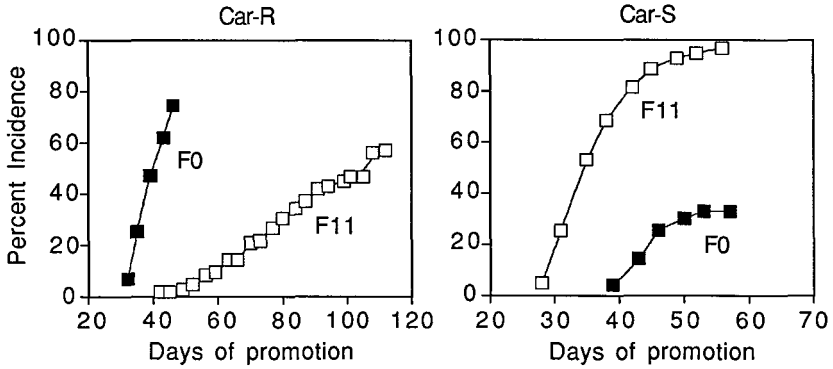
Fig. 4. Tumour incidence as a function of the promotion length in the two
selection populations.

Meanwhile, a preliminary experiment was carried out on Car mice of
the 10th generation to measure the life span of mice unirradiated or whole-body
irradiated with 3 Gy of 250-kVp X rays. The results are shown in Figure 5 and
suggest that the life span of unirradiated and irradiated Car mice is strongly
influenced by the selection for both sexes, but the radiosensitivity, in terms of
life-span shortening, appears to be grossly unaffected by the selection.
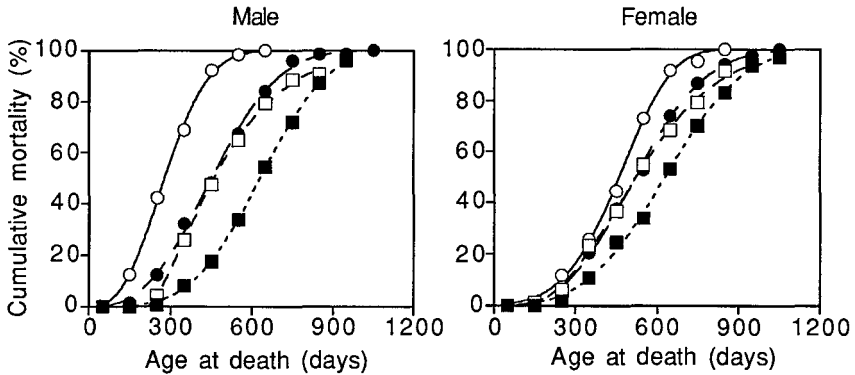
Fig. 5. Percent cumulative mortality in male and female Car mice within 1100
days after birth. Car-S (circles), Car-R (squares), Controls (full symbols), X-ray
irradiated (open symbols). Curves are best fits with the expression

$$100\left[1-\left(\exp-\left(\lambda(\tau-t)\right)^{\gamma}\right)\right]$$

An experimental study had also been planned on ovarian tumour
induction with irradiation of only one ovary, in order to investigate the
influence of hormonal imbalance caused by irradiation on the induction of

tumours in the unirradiated ovary. However, due to the large involvement of the group in the other research topics described here, only limited efforts have been concentrated on this problem and preliminary tests only were carried out during the contractual period, so that no results are reported.

In vitro studies of radiation induced neoplastic transformation in human derived cell lines from various epithelial tissues have been carried out by the same research team in collaboration with another coordinated project (contract FI3P-CT92-0043). The assessment of *in vitro* transformation of human cells requires the identification of malignant phenotypes that are progressively expressed during the process of neoplastic transformation. Altered cell morphology and multicellular organisation in foci, growth to elevated cellular density level and ability to growth without substrate anchorage are considered to be *bona fide* markers of cell transformation. However, the results of our preliminary experiments indicate the impossibility to unambiguously identify a correlation between the above end points and malignant cell transformation, which makes the use of this system for quantitative study of radiation induced neoplastic transformation not feasible at present. Experimental details are described in the progress report of the collaborating project.

Finally, in order to extend the utilisation of the TAPIRO reactor, a new irradiation facility has been prepared. Since the knowledge of the microscopic distribution of energy deposition is of a primary importance for the interpretation of radiobiological experiments, the microdosimetric characterisation of the radiation field in the available irradiation facilities has been carried out in collaboration with the University of Saar group. In addition, a dosimetric study in various irradiation configurations has been completed.

Publications

1. Coppola, M. How to model radiation carcinogenesis? In: Biophysical Modelling of Radiation Effects (K.H. Chadwick, G. Moschini, M.N. Varma eds.), pp 339-342. Adam Hilger, Bristol, 1992.

2. Coppola, M., Covelli, V. Experimental models for ionizing radiation carcinogenesis. In: Recent advances in human radiobiology, pp. 73-83. ENEA Serie Simposi, Roma, 1992.

3. Coppola, M. Modelli matematici in radiobiologia. In: Effetti biologici in radioterapia, pp 21-39. ENEA Serie Simposi, Roma, 1992.

4. Di Majo, V., Rebessi, S., Coppola, M., Saran, A., Pazzaglia, S., Covelli, V. Are somatic effects of low neutron doses detectable in vivo? In: Low Dose Irradiation and Biological Defense Mechanisms (T. Sugahara, L.A. Sagan, T. Aoyama, eds.), pp. 199-202. Elsevier Science Publishers B.V., 1992.

5. Di Majo, V., Rebessi, S., Coppola, M., Covelli, V. Induction of tumors in hybrid mice (BC3F1) after multifractionated neutron doses. 40th Annual Meeting of the Radiation Research Society, Salt Lake City, 1992.

6. Saran, A., Pazzaglia, S., Pariset, L., Coppola, M., Di Majo, V., Rebessi, S. and Covelli, V. Dose fractionation dependence of C3H10T1/2 cell transformation by fission spectrum neutrons. 40th Annual Meeting of the Radiation Research Society, Salt Lake City, 1992.

7. Coppola, M. Specification of fast neutron radiation quality from cell transformation data. Radiat. Prot. Dosim. 46, 211-212, 1993.

8. Saran, A., Pazzaglia, S., Pariset, L., Rebessi, S., Coppola, M., Di Majo, V., Covelli, V. Cell-cycle dependence of C3H10T1/2 cell transformation by fission spectrum neutrons. 41th Congress of the Radiation Research Society, Dallas, 1993.

9. Saran, A., Broerse, J.J., Zoetelief, H., Pazzaglia, S., Pariset, L., Coppola, M., Di Majo, V., Rebessi, S., Covelli, V. C3H10T1/2 cell transformation after fractionated doses of neutrons of different energies. Physica Medica, X, Suppl. 1, 80-81, 1994.

10. Rebessi, S., Di Majo, V., Coppola, M., Saran, A., Pazzaglia, S., Pariset, L., Covelli, V. Somatic effects of low neutron doses. Physica Medica, X, Suppl. 1, 82-83, 1994.

11. Saran, A., Pazzaglia, S., Pariset, L., Rebessi, S., Broerse, J.J., Zoetelief, J., Di Majo, V., Coppola, M., Covelli, V. Neoplastic transformation of C3H10T1/2 cells: a study of fractionated doses of monoenergetic neutrons. Radiat. Res. 138, 246-251, 1994.

12. Di Majo, V., Coppola, M., Rebessi, S., Saran, A., Pazzaglia, S., Pariset, L., Covelli, V. Neutron induced tumors in BC3F1 mice: effects of dose fractionation. Radiat. Res. 138, 252-259, 1994.

13. Pihet, P., Coppola, M., Loncol, T., Di Majo, V., Menzel, H.G. Microdosimetry study of radiobiological facilities at the RSV-TAPIRO reactor. Eleventh Symposium on Microdosimetry. Gatlinburg, 1992. Radiat. Prot. Dosim. 52, 1/4, 409-414, 1994.

14. Di Majo, V., Coppola, M., Covelli, V., Rebessi, S., Saran, A., Pazzaglia, S., Doria, G., Pioli C., Mouton, D., Biozzi, G. Life span of mice genetically selected for sensitivity and resistance to skin carcinogenesis. VII Convegno SIRR, Pisa, 1994.

15. Pazzaglia, S., Saran, A., Pariset, L., Rebessi, S., Di Majo, V., Coppola, M., Covelli, V. Trasformazione neoplastica radioindotta di cellule C3H10T1/2 in funzione delle fasi del ciclo cellulare. VII Convegno SIRR, Pisa, 1994.

16. Pazzaglia, S., Saran, A., Pariset, L., Rebessi, S., Di Majo, V., Coppola, M., Covelli, V. Sensitivity of C3H10T1/2 cells to radiation-induced killing and neoplastic transformation as a function of cell cycle. Submitted, 1995.

17. Saran, A., Di Majo, V., Coppola, M., Covelli, V., Rebessi, S., Pazzaglia, S., Doria, G., Pioli C., Mouton, D., Biozzi, G. Development of murine lines sunsitive and resistant to skin carcinogenesis. 43rd Congress of the Radiation Research Society, San José, 1995.

18. Pazzaglia, S., Saran, A., Pariset, L., Rebessi, S., Di Majo, V., Coppola, M., Covelli, V. Radiation induced neoplastic transformation of C3H 10T1/2 cells as a function of the cell cycle phases. 43rd Congress of the Radiation Research Society, San José, 1995.

19. Di Majo, V., Coppola, M., Covelli, V., Rebessi, S., Saran, A., Pazzaglia, S., Doria, G., Pioli C., Mouton, D., Biozzi, G. Car-R and Car-S mice sensitivity to radiation beams of different quality. 10th ICRR, Würzburg, 1995.

20. Pazzaglia, S., Saran, A., Pariset, L., Rebessi, S., Di Majo, V., Coppola, M., Covelli, V. Variation of radiosensitivity through the cell cycle for cell lethality and neoplastic transformation in C3H10T1/2 cells. 10th ICRR, Würzburg, 1995.

OBJECTIVES

A. To study the effects of multiple low dose fractions of X-rays (2.5 mGy) on the induction of mammary tumours in rats; the influence of the length of the interval between fractions, the effect of age at single dose exposure and the impact of oestrogen administration on mammary radiation carcinogenesis.
B. To study molecular changes (mutation-activation of oncogenes; deletion of tumour suppressor genes) in radiation induced mammary tumours of rats.
C. To study the genetics of susceptibility of rats to the radiation-induction of mammary tumours.

Progress achieved including publications

A. *Modifying factors involved in the induction of mammary cancer by radiation in the rat*

a. *Fractionation*
Female WA/Rij rats to which oestradiol-17ß has been administered, were subjected to fractionated exposure to Cs-137 gamma rays with fraction sizes of 2.5 mGy, 10 mGy and 40 mGy up to cumulated doses of 1 and 2 Gy. The relative risks of mammary tumours (after an observation period of 3 years) in comparison to unirradiated controls are presented in Table 1.

Table 1: Relative risks of mammary tumours in irradiated WAG/Rij rats to which oestradiol-17ß has been administered.

total dose		2.5 mGy	10 mGy40 mGy
0 Gy	1	1	1
1 Gy	1.4 ± 0.5	1.3 ± 0.5	3.3 ± 1.3
2 Gy	3.3 ± 1.1	2.2 ± 0.8	4.5 ± 1.8

At an accumulated dose of 1 Gy the fraction sizes of 2.5 and 10 mGy do not produce a significantly increased relative risk, while 40 mGy per fraction results in an elevated increased risk comparable to the risk obtained with a single dose of 1 Gy. At an accumulated dose of 2 Gy the inhibitory effect of fractionation on mammary tumour development is less evident, although the relative risks obtained with 2.5 and 10 mGy are substantially lower than obtained with a single dose of 2 Gy (see Table 4). A completely different picture with regard to the effect of fractionation was found in animals not treated with oestrogens (Table 2).

Table 2: Relative risks of mammary tumours in irradiated WAG/Rij rats to which no oestrodiol-17ß has been administered.

total dose	fraction size	
	2.5 mGy	10 mGy
0 Gy	1	1
1 Gy	3.04 ± 0.76	2.39 ± 0.69
2 Gy	2.18 ± 0.63	2.55 ± 0.64

The fraction sizes of 2.5 and 10 mGy produce in otherwise untreated females an elevated relative risk of mammary tumours as compared to unirradiated controls. The relative risks obtained with single dose irradiation (see Table 5) are not that much higher. Fractionation does not seem to have a striking inhibitory effect on mammary tumour development as ob-

served with oestrogen-treated animals. This has led us to the hypothesis that the low relative risk obtained with single doses in females, which were not supplied with oestrogens, is due to impairment of the endogenous hormone production by a single dose of radiation.

b. *Age*

Animals were implanted with pellets containing oestradiol-17ß at different ages and not irradiated. As can be concluded from Table 3 the administration of oestrogens at all ages strongly enhances the development of mammary tumours. The relative risk of the group given hormone treatment beginning at week 36 is surprisingly high.

Table 3. Relative risks of mammary tumours in WAG/Rij rats in which oestradiol-17ß pellets have been implanted at different ages.

age at treatment (weeks)	relative risk
8	19 ± 6
22	12 ± 4
36	80 ± 20
64	14 ± 3

When single doses of gamma rays are given to hormone-treated animals it was observed that in the age-range 8-15 weeks there is a strongly elevated risk of mammary tumour development as compared to hormone-treated but unirradiated controls. However, at the age of 36 to 64 weeks the relative risks are remarkably low (Table 4).

Table 4. Relative risks of mammary tumours in WAG/Rij rats, to which oestradiol-17ß has been administered, and irradiated with single doses at different ages.

age at exposure (weeks)	relative risk	
	1 Gy	2 Gy
8	5.91 ± 1.32	9.07 ± 1.72
10	6.61 ± 1.50	10.85 ± 1.96
12	10.38 ± 1.97	5.28 ± 0.97
15	10.42 ± 2.15	9.75 ± 1.99
22	1.60 ± 0.39	4.56 ± 0.87
36	0.56 ± 0.12	0.99 ± 0.18
64	0.47 ± 0.11	0.49 ± 0.11

Table 5: Relative risks of mammary tumours in WAG/Rij rats, to which oestradiol-17ß has not been administered, and irradiated with single doses at different ages.

age at exposure (weeks)	relative risk	
	1 Gy	2 Gy
8	1.67 ± 0.53	2.76 ± 0.84
12	2.97 ± 0.85	5.07 ± 1.47
16	1.57 ± 0.47	2.86 ± 0.86
22	1.34 ± 0.47	4.22 ± 0.97
36	2.66 ± 0.66	2.73 ± 0.76
64	0.27 ± 0.13	0.68 ± 0.24

In females, which were not given oetrogens, a single dose of 1 Gy did not result in a strinkingly elevated relative risk, irrespective of the age at exposure (Table 5). The effect of 2 Gy on mammary tumour development is greater. As has been found with hormone-treated animals when the animals are irradiated at 64 weeks of age, the relative risks are remarkably low. It is hypothesized that irradiation of postmenopausal female rats may lead to destruction of "spontaneously" transformed mammary cells, either directly or by stimulation of the immune system.

B. *Molecular changes in radiation-induced mammary carcinoma is rats*

a. *Oncogene mutations*

Twenty-five mammary carcinomas were selected from those groups of irradiated rats which showed a clearly elevated relative risk of mammary tumours (see former chapter). In addition, eight "spontaneous" mammary tumours were taken from the control groups. DNA was isolated from each tumour and tested for activating mutations in either the H-, K- or N-ras oncognes. For this test the first and second exons of either oncogene was amplified in each DNA sample by means of the polymerase chain reaction (PCR), using intronspecific primers. These primers were used in order to avoid amplification of pseudo-gene sequences. The PCR products were then transferred to nylon membrane filters and subjected to dot-blot hybridization with so-called allele-specific oligonucleotides (ASO). These ASO's contained 20 nucleotides and were selected according to anticipated mis-sense (activating) mutations for a given codon. The hybridization products were then subjected to a critical wash procedure. Only in the case of a perfect match between ASO and the PCR product, the hybridization product would be retained on the filter. With this procedure it was found that 3 of 25 radiation-induced mammary tumours contained a mutation in codon 12 of the K-ras oncogene and 1 in codon 13 of that gene. No ras oncogene mutations were found in any of the spontaneous mammary tumours. It is concluded that ras oncogene mutation is not a major pathway in mammary radiation carcinogenesis.

b. *Tumour suppressor deletion*

A subtraction hybridization-sequence independent PCR technique has been developed by us in order to detect homozygous deletions in rat tumour lines. DNA was isolated from a cell line derived from a WAG/Rij rat lung tumour, resulting from Ir-192 implantation. This DNA was then photobiotinylated. This modified tumour DNA was then hybridized with normal WAG/Rij rat liver DNA, digested by the restriction enzyme Sau3A. After hybridization the biotinylated DNA was removed with the use of avidin. The hybridization procedure and removal of biotinylated DNA was repeated twice. The remaining DNA was then fitted with a synthetic adaptor containing nucleotide sequences, which can interact with the sticky ends of Sau3A digested DNA. These oligonucleotides were also used as a primer for the PCR reaction. The PCR resulted in six different products: the largest had a size of 1.2 kb. The largest product was used as a probe in fluorescent *in situ* hybridization on metaphases of normal WAG/Rij rat fibroblast cultures. The probe reacted with 10 of 21 rat chromosomes, indicating that this probe harbours a moderate repeat sequence. In Southern blot hybridization experiments it was found with this probe that tumour DNA lacks several bands, hybridizing with this probe, in comparison to normal rat DNA. Four other cell lines from rat radiation-induced lung tumour lines lack a common sequence of 4 Kb size as detected with this probe in normal rat DNA. This homozygous deletion was also found in an radiation-inducecd rat rhabdomyosarcoma, but not in ten radiation-induced mammary tumours of WAG/Rij rats (arisen in the project described in the former chapter).

This subtraction hybridization-sequence independent PCR procedure has been applied to three mammary tumours of the WAG/Rij strain. It was attempted to get a sample contain-ing only tumour cells by differential centrifugation. In no case did we obtain any PCR product, presumably because normal cellular DNA was contaminating the tumour DNA samples. The procedure as developed by us can only be used for cultured tumour cell lines. So far we failed, despite vigorous efforts, to develop cell lines of radiation-induced rat mammary tumours.

c. *Radiation-induced stress response proteins*

We have once reported that many rats irradiated with single doses of either X-rays or neutrons have antibodies in their serum which react with an antigen in various tumour cell lines, including mammary tumour lines, but not in normal fibroblasts or mammary epithelial cells (P. Bentvelzen et al., Eur. J. Cancer 19, 1255, 1983). The majority of rats subjected to fractionated radiation with gamma rays (cumulated dose 1 Gy) has similar antibodies. These antibodies persist for more than a year. In none of twenty unirradiated controls such antibodies have been found.

By means of immunoprecipation with serum of an irradiated rat from the antigen has been isolated from a radiation-induced rat rhabdomyosarcoma as well as a rat pulmonary tumur line. Both tumour lines contain the mutated tumour suppressor gene product p53 in their cytoplasm. The protein reacting with sera form irradiated rats is not p53, however. It is a 40 kd protein, whose appearance can be induced *in vitro* in normal rat or mouse fibroblast by irradiation (2 Gy) within 16 hours. The antigen can also be induced by treatment with 3.5 per cent ethanol. This stress response protein did not prove to be complexed with other cellular proteins in tumour cell lines. We assume that the constitutive expression of this (radiation-inducible) stress response protein in various tumour cell lines plays a role in the neoplastic process.

C. *Genetics of susceptibility to mammary radiation carcinogenesis in rats*

Various lines of the SD rat stock are extremely susceptible to the development of mammary tumours; either spontaneously or after treatment with dimethylbenzantracene or ionizing radiation. The inbred SD/Rij rat strain, kept in our laboratory, was the least susceptible SD line, but considerably more prone to mammary tumour development than the BN or WAG/Rij rat strains. Recently, the SD/Rij strain has changed to an extreme susceptible strain, comparable to the Sprague Dawley rats used in the Brookhaven National Laboratory, New York. For instance, in 1990, 2 Gy of X-rays (2 Gy) would result in a 100 per cent tumour incidence at two years of age. At present, nearly all animals will have a tumour within a year after radiation.

A crossing programme has been carried out by us in 1992 with the at that time moderately susceptible SD/Rij strain and the relatively resistant BN strain (25% mammary tumours after 2 years; 2 Gy X-rays). The F_1 hybrid of these strain gets 75 per cent tumours at two years with this dose of X-rays. The F_1 was slightly less susceptible than the parental SD line. In the backcross generation to BN only 40 of 107 animals developed a mammary tumour at that age. In the backcross to SD 62 of 82 females got a tumour. These results do not contradict the hypothesis that a single SD gene controls the susceptibility to mammary tumours. The SD/Rij strain differs from the BN strain in the following coat colour genes: albino (c), Black (B), hooded (H) and kinky (k). In both backcrosses no association was found between any of these coat colour genes and tumour susceptibility. DNA was isolated from the tail tip of all individuals in both backcrosses. The DNA samples were subjected to Sourthern blotting after Hae III digestion with the minisatellite core probe 33.15 of Jeffreys. The SD/Rij strain differs considerably from the BN strain with regards to the Southern blot pattern with this probe. No association could be found, however, in the backcross generations between a single SD-specific band and mammary tumour development.

In 1994 a crossing programme has been caried out between the SD/Rij rat strain, which had changed to extreme mammary tumour susceptibility and the relative resistant WAG/Rij strain. Not only backcrosses to SD/Rij and WAG/Rij have been produced, but also an F_2 generation. The animals have been irradiated with X-rays (2 Gy). The experiment is still not completed, but many tumours have appeared before one year of age in all three groups, particularly in the backcross to SD.

D. *Publications*

- Broerse, J.J. and Van Bekkum, D.W.: Radiation carcinogenesis studies in animals. Advantages, limitations and caveats. In: Advances in Radiation Biology 1992, 16: 199-213.
- Broerse, J.J., Davelaar, J., Weeda, J., Bartstra, R.W. and Van Bekkum, D.W.: Mammary carcinogenesis in the rat after low-dose irradiation. In: Low dose Irradiation and Biological Defense Mechanisms (eds. Sugahara, T., Sagan, L.A. and Aoyama, T). Excerpta Medica 1992, pp. 211-214.

- Van Klaveren, P., De Bruyne, J., Van Winden, H., Kal, H.B. and Bentvelzen, P.: A common deletion in two gamma rays induced rat pulmonary tumor cell lines. Anticancer Res., 1994, 14: 565-570.
- Bentvelzen, P., Van Klaveren, P., De Bruyne, J., Van Winden, H., Kal, H.B. and Broerse, J.J.: Search for genetic changes in rat tumours induced by ionizing radiation. In: Molecular Mechanisms in Radiation Mutagenesis and Carcinogenesis (eds. Chadwick, K.H., Cox, R., Leenhouts, H.P., Thacker, J.). European Commission, 1994, pp. 229-232.

Final Report
1992-1995

Contract : FI3PCT920042

Head of project 4: initially Dr. R. Masse, Dr. G. Monchaux since 1994

II. Objectives for the reporting period (1992-1995)

1 - determination of tumour incidence after exposure to a global irradiation by neutrons from 252Cf at low dose and low dose rate,

2 - identification of the potential co-carcinogenic effect of combined exposure to irradiation and various occupational and/or environmental inhaled airborne pollutants.
The effort was focused mainly on the identification of the potential co-carcinogenic effect of ozone in rats after pulmonary irradiation either by global irradiation by fission neutrons or by local pulmonary irradiation after inhalation of radon 222 and its short lived decay products.

2 - constitution of a bank of tumours and the initiation of genetic studies to characterize mutations in tumour cells according to carcinogenic or cocarcinogenic treatment,

3 - determination of the role of cytochrome P450 1A1 (CYP 1A1) during cocarcinogenesis produced by inducers of this enzyme administered after exposure to radon and its progeny.

III. Progress achieved including publications

1) Irradiation by neutrons from 252Cf:

Four groups of Sprague-Dawley male rats were randomly selected.Two groups of rats were exposed to neutrons from 252-Cf during 30 hours at a dose of 0.025 Gy at different ages, 3 months and 15 months respectively. Two other groups of rats were exposed to neutron irradiation from the age of 3 months for a period of 1 year at doses of 0.025 and 0.053 Gy respectively. Then, the rats were housed in the same animal house and allowed to live until they died or killed when they were moribund according to the *Health Care and Use of Laboratory Animals from the European Legislature*. A full necropsy was conducted on all animals and tissue samples were kept systematically. This samples were embedded in paraffin and 5 mm thin sections were cut and stained for examined microscopic examination. The incidence of tumours and survival times of rats in the different experimental groups were compared with those of 500 contemporary unexposed control rats.

Preliminary results are summarized in table 1. No differences were statistically observed between the different groups considering the mean lifespan and the histological types of cancers. However, the survival time of rats exposed to neutrons from Cf-252 at a dose of 0.025 Gy at low dose rate was identical to that of controls. By contrast, the survival times of rats exposed to neutrons from Cf-252 at the dose of 0.025 Gy at high dose-rate and 0.053 Gy at low dose-rate were lower than that of controls.

Table 1

	Number of rats	Age (days)	Dose (cGy)	Dose rate (µGy/h)	Mean survival time (days)	Non Gland. Cancers	All Cancers
Controls	501				753	20.8%	34.2%
Group 1	152	100	2.5	950	725	30.9%	40.1%
Group 2	255	420	2.5	758	720	28.2%	42.7%
Group 3	249	135	2.5	3.58	758	33%	43.8%
Group 4	50	135	5.3	7.72	730	20%	32%

The results of this study will be submitted for publication in the course of the year 1996.

2 - Co-carcinogenic effects of ozone in rats:

The aim of this work was to estimate in rats the potential carcinogenic or co-carcinogenic risk of ozone, acting either alone as a complete carcinogen, or as a promoter after pulmonary irradiation either by global irradiation by fission neutrons or by local pulmonary irradiation after inhalation of radon 222 and its short lived decay products.

Experimental protocols

Different types of protocole were used:

1- Inhalation of ozone alone or after global irradiation by fission neutrons.

Five groups of animals were used:

- Group 1 : 50 rats exposed first to global irradiation by fission neutrons in the Silene reactor at a dose of 0.6 Gy which have been previously demonstrated to induce a lung cancer incidence of 10%
- Group 2 : 36 rats exposed to global irradiation by fission neutrons, and 1 month after irradiation, to continuous ozone exposure 0,8 ppm (at least 23 hours a day). Continuous ozone exposure was used to avoid the process of lesions mechanisms repair which occur in the hours following the end of exposure to develop.
- Group 3 : 36 rats were continuously exposed to ozone 0.8 ppm alone, as Group 2.
- Group 4 : 36 rats were exposed first to global irradiation by fission neutrons in the Silene reactor (fission neutrons: 0,6 Gy; gamma : 0.13 Gy) and 1 month after irradiation to ozone 0.4 ppm, 6 hours a day, 5 days a week, for 2 months.
- Group 5 : 36 rats were exposed to ozone 0.4 ppm alone, 6 hours a day, 5 days a week, for 2 months.

2- Inhalation of ozone alone or after exposure to radon and its daughters.

Four groups of animals were used:

- Group 1: 50 rats were exposed to radon at a cumulative exposure of 100 WLM which have been shown previously to induce a lung cancer incidence of about 20 to 22% .
- Group 2: 50 rats were exposed first to radon 1000 WLM, and one month after the end of exposure to ozone 0,2 ppm, 6 hours a day, 5 days a week, for 6 months.
- Group 3: 50 rats were exposed to ozone 0.2 ppm alone, 6 hours a day, 5 days a week, for 6 months.
- Group 4: 50 rats were exposed first to radon 1000 WLM, and 1 month after the end of radon exposure, to ozone by inhalation. Ozone inhalation was performed at a concentration of 2 ppm during 3 sessions of 5 hours each and at a monthly interval between 2 sessions.
It has been shown in previous studies that exposure to ozone 0.2 ppm induced cell proliferation at the level of the bronchioloalveolar epithelium from which the majority of rat pulmonary tumours are originating. The amplification of this cell population might contribute to a significant decrease of the latency period of such induced tumours.

Results

At the present time, the majority of these studies are still in progress. All the exposures, irradiation by fission neutrons, exposures to radon and progeny and ozone exposures by inhalation are finished in all groups. During all the experiments, the rats were kept according to the Guidelines for Care and Use of Laboratory Animals established by the European Communities. After exposure, animals were kept until they died or were moribund and then killed. A full necropsy was carried out on all animals. Whole lungs were fixed by intratracheal instillation of Baker formalin fixing solution, embedded in paraffin and sectioned serially in the frontal plane. Large 20 μm thick sections were prepared without staining and screened for lesions. When suspicious lesions were encountered, 5 μm thick sections were cut, stained with hemalun-eosin-saffron and examined microscopically. The majority of animals are now died or have been killed and the histopathological study is in progress

However, the results of the study of combined exposure to radon and ozone 0.2 ppm have been exploited and have been accepted for publication.

The incidence of lung cancer was 20% in Group 1, exposed to radon alone, 26% in Group 2 exposed to radon and ozone combined and 10% in Group 3, exposed to ozone alone, as compared with 0.8% in controls. Lung carcinomas induced by ozone alone showed a trend toward a preferential differentiation pattern to the squamous cell type. These results show a carcinogenic effect of ozone in rats for levels of exposure in the same range as those observed during peak levels of urban airborne pollution and suggest a potential cocarcinogenic effect of combined exposure to radon and ozone.

The preferential differentiation of lung cancers induced by ozone exposure to the squamous cell pattern has to be emphasized. Such findings have been previously reported in rats exposed to both radon and cigarette smoke. A synergistic effect was also reported by using the same exposure to radon plus 5-6 benzoflavone, known to be an inducer of cytochrome P-450 1A1. In this experimental model, target cells are confined to the bronchiolo-alveolar junctions. The hyperplasia observed at the same sites after ozone exposure might indicate that the same target cells are involved in the co-carcinogenic process.

Under the experimental conditions used, the co-carcinogenic effect of radon which has been observed, using high-level exposure, cannot be extrapolated to humans who are usually never exposed to such high levels. Further studies are needed to determine the effect of combined exposure to radon and ozone for lower radon exposure levels in the range of domestic or environmental exposures.

By contrast, the carcinogenic and co-carcinogenic effects of ozone appear to occur at environmental levels such as those encountered in photochemical smog. Thus, ozone, and perhaps other oxidizing pollutants such as NO_X, might be regarded as potential environmental carcinogens. Because very few experimental and epidemiological data have been reported, further studies are needed.

3 - Constitution of a bank of soft tissue tumours:

The aim of this study was to constitute a bank of tissue samples for further characterization of the mutations induced in tumour cells according to different carcinogenic treatments. Different groups of rats were treated by intramuscular injections of various chemical compounds to induce soft tissue tumours, mainly rhabdomyosarcomas and fibrosarcomas, at the site of injection to constitute a bank of neoplastic and preneoplastic lesions. Different groups of 20 Sprague-Dawley male rats received at the age of 3 months a single intramuscular injection of either rare earths compounds, stable Cerium, Lanthane, Lutetium and Gadolinium, or Cadmium or methylcholanthrene. Rare earths compounds were injected under the form of buffered hydroxyde at doses of 2, 10 and 50 mg/kg respectively. Cadmium was also injected under the form of hydroxyde at doses of 10 and 50 mg/kg. Methylcholanthrene was injected in corn oil solution at a concentration of 25 mg/kg.

About 100% of tumours occured at the site of injection in rats treated by methylcholanthrene within 6 months after injection. In rats treated by cadmium chloride, tumours occured after a latency period of about 1 year. In rats treated by rare earths compounds, few tumours occured after a latency period of about 18 months. Tumour tissue samples were taken on all animals bearing tumours and kept under the form of frozen or formalin fixed tissue samples for genetic studies. This study is still in progress. Tumour tissue samples were used for the development of specific immunochemical staining techniques for laser confocal microscopic examinations. Preliminary results are indicated in different student reports.

4 - Cocarcinogenic effect of cytochrome P450 1A1 inducers for squamous cell lung cancer induction in rats previously exposed to radon:

Association of radon exposure and inhalation of various occupational or environmental airborne pollutants may lead to synergistic effects for lung cancer induction. Experimentally, a co-carcinogenic effect results in increased tumour rates after combined administration of the potential carcinogens. A standardized protocol has been developped in rats to identify potential co-carcinogenic agents. This protocol consists in a 1000 WLM radon exposure, followed by exposure to the agent to be studied. The aim of this study was to characterize the cocarcinogenic effect of various cytochrome P450 1A1 (CYP 1A1) inducers in male Sprague-Dawley rats previously exposed to radon and radon daughters at a cumulative dose of 1000 Working-Level-Months (WLM). This was based on the hypothesis that polycyclic hydrocarbons are involved in the carcinogenic activity of several compounds, especially of tobacco smoke compounds. Three different CYP1A1 inducers were used: methylcholanthrene (MC), metabolized by CYP 1A1 into strong mutagenic compounds, 5,6-benzoflavone (βNF) metabolized into no-mutagenic compounds and 2,3,7,8 tetrachlorobenzo p-dioxin (TCDD) which is considered as

no-mutagenic and no-metabolized. These inducers were administered by 6 intramuscular injections of 25, 25 and 0.0013 mg/kg respectively at fortnightly intervals. Rats were studied 1 month or 4 months after the end of the treatments. Histopathological analysis showed the occurence of epidermoid nodules and/or squamous cell carcinomas in animals exposed to radon and each CYP 1A1 inducer. The latency period for the occurence of such lesions varied according to the inducer. For MC or βNF treated rats, these lesions were systematically observed 1 month after the end of treatment. Latency periods for about 100% tumour induction were about 100 days for MC and βNF but increased to 200 days for TCDD. Biochemical studies shown a similar global CYP 1A1 induction, measured by ethoxy resorufine O-deethylase (EROD) activity, an enzymatic activity associated with CYP 1A1. This induction was about 40 times the control value and exposure to radon alone did not modify the EROD activity. A similar induction of CYP 1A1 was observed in all treated groups whether rats were exposed to radon or not. Immuno-histo localization of CYP 1A1 has shown negligible expression of CYP 1A1 in controls and in rats exposed to radon only. Labelling was most confined to some unciliated bronchial cells. Treatments by the different chemicals induced similarly CYP 1A1 in endothelial, alveolar type II and unciliated bronchial cells whereas strong CYP 1A1 expression was observed after each chemical treatment in hyperplastic epithelial foci in all rats previously exposed to radon.

These results suggest that CYP 1A1 expression alone in some particular cell type could be a primeval step of a cocarcinogenic process induced after local lung irradiation by inhalation of radon and its daughters. Studies are in progress to warrant such hypothesis and to characterize the specific role of irradiation during the cocarcinogenic process.

Publications:

Poncy, J.L., Laroque, P., Fritsch, P., Monchaux, G., Chameaud, J. and Masse, R. (1993) An experimental two-stage rat model of lung carcinoma initiated by radon exposure. In: Twenty-Ninth Hanford Symposium on Health and the Environment "Indoor Radon and Lung Cancer: Reality or Myth? ", October 15-19, 1990, Richland, Washington, Part 2, Edited by F.T. Cross, Battelle Press, Columbus, Richland, pp.803-819.

Bisson, M., Richard, H., Altmeyer, S., Morlier, J.P., Monchaux, G. and Fritsch, P. (1993) Effect of radon inhalation on spontaneous and ozone induced proliferation of rat alveolar macrophages. Abstracts of the 25h Annual Meeting of the European Society for Radiation Biology, June 10-14, 1993, Stockholm, Sweden.

Monchaux, G., Morlier, J.P., Morin, M., Fritsch, P. and Masse, R. (1993) Identification du pouvoir cancérogène pulmonaire des polluants atmosphériques dans un modèle d'irradiation. Actes du Colloque "Pollution atmosphérique à l'échelle locale et régionale". Cachan - 7, 8, 9 décembre 1993, pp. 257.

Monchaux, G., Morlier, J.P., Morin, M. and Masse, R. (1994) Induction of lung cancer in rats by exposure to radon and radon daughters. Annales de la Société Belge de Radioprotection, **19**, (1-2), 27-60.

Trédaniel, J., Monchaux, G., Bisson, M., Morlier, J.P., Richard H., Lacroix, F., Fritsch, P., Morin, M., Masse, R. and Hirsch, A. (1994) Carcinogenic effect of ozone for induction of lung tumours in rats after exposure to radon and its daughters. Preliminary results. Annales de la Société Belge de Radioprotection, **19**, (1-2), 79-86.

Monchaux, G., Morlier, J.P., Morin, M., Chameaud, J., Lafuma, J. and Masse, R. (1994) Carcinogenic and cocarcinogenic effects of radon and radon daughters in rats. Environ. Health Perspect., **102**: 64-73.

Monchaux, G., Morlier, J.P., Morin, M., Fritsch, P., Trédaniel, J., and Masse, R. (1994) Etude des effets cancérogènes et cocancérogènes de l'ozone chez le rat. Pollution atmosphérique, **142**, 84-88.

Morin, M., Masse, R.and Lafuma, J. Etude expérimentale des différents types histologiques de cancers pulmonaires induits par l'irradiation. C.R. Acad. Sci. Paris, Sciences de la vie, **317**, 90-93.

Morin, M., Allin, F., Altmeyer, S. and Masse, R.(1994) Relations entre l'irradiation et l'apparition des tumeurs cérébrales chez le rat. C.R. Acad. Sci. Paris, Sciences de la vie, **317**, 277-281.

Morlier, J.P., Morin, M., Monchaux, G., Pineau, J.F., Chameaud, J., Lafuma, J. and Masse, R. (1994) Lung cancer incidence after exposure of rats to low doses of radon: influence of dose rate. Radiat. Protect. Dosimetry, **56,** 93-97.

Douriez, E., Kermanac'h, P., Fritsch, P., Bisson, M., Morlier, J.P., Monchaux, G., Morin, M. and Laurent, P. (1994) Cocarcinogenic effects of cytochrome P 450 1A1 (CYP 1A1) inducers for epidermoid lung tumor induction in rats previously exposed to radon. Radiat. Protect. Dosimetry, **56**, 105-108.

Monchaux, G. and Masse, R. (1994) Radon: occupational or domestic carcinogen? Radiat. Protect. Dosimetry, **56,** 81-88.

Monchaux, G., Morlier, J.P., Morin, M., Zalma, R., Pezerat, H. and Masse, R. (1994) Carcinogenic effects on rats of exposure to different minerals from metallic mine ores, radon and radon daughters. In: *Cellular and Molecular Effects of Mineral Dusts on Cells,* NATO ASI Series, Vol. H 85, Edited by J.M.G. Davis and M.C. Jaurand, pp. 159-164, Springer-Verlag, Berlin, Heidelberg.

Ogata, H. and Monchaux, G. (1994) Weibull distributions for radiation risk analysis in animal experiments. Jap. J. Risk Analysis, **6**, 74-78.

Monchaux, G., Morlier J.P., Chameaud, J., Debroche, M., Morin, M. and Masse, R. (1994) Carcinogenic effects on rats of exposure to mixtures of diesel exhausts, radon and radon daughters. Ann. Occup. Hyg, **38**, suppl. 1, 281-288.

Trédaniel, J., Bisson, M., Fritsch, P., Monchaux, G. and Masse, R. (1994) The increase of pulmonary alveolar macrophage (PAM) population after ozone inhalation: relative contribution of monocyte migration and PAM proliferation. Ann. Occup. Hyg, **38**, suppl. 1, 961-967.

Bisson, M., Fritsch, P., Trédaniel, J., Sabattié, P., Morlier J.P. and Monchaux, G. (1994) Cell proliferation in the adult lungs of controls and ozone exposed rats. In: Electron Microscopy 1994, Proceedings of the 13th International Congress of Electron Microscopy, Paris 17-22 July 1994, Volume 3B, Applications in Biological Sciences, pp. 1269-1270.

Monchaux, G. (1995) Evaluation du risque pour les populations exposées au radon: données épidémiologiques et expérimentales. In: "Toxicologie et Pollution de l'Air: Evaluation du Risque", Actes du Congrès, Dijon: 31 mars-1er avril 1995, pp. 167-183.

Monchaux, G., Morlier, J.P., Rochefort, P., Fritsch, P., Douriez, E., Morin, M. and Maximilien, R. (1995) Cocarcinogenic effects in rats of various agents following exposure to radon and radon daughters. Accepted for publication in Sci. Tot. Environment.

Monchaux G., Morlier, J.P., Trédaniel, J., Rochefort, P., Morin, M. and Maximilien, R. (1995) Cocarcinogenic effects in rats of combined exposure to radon and ozone. Accepted for publication in Sci. Tot. Environment.

D'Ortho, M.P., Harf, A., Fritsch, P., Monchaux, G. and Lafuma, C. (1995) Evolution of matrix metalloproteinase and elastase activities in ozone-induced acute lung edema in rats. Am. J. Physiology, in press.

Final Report

EEC contract F13P-CT92-0042

Carcinogenic effects of low radiation doses and underlying mechanisms

Laboratory: GSF

1   Introduction

Animal experiments used to be an essential tool in radiocarcinogenesis. They have been used to show that radiation can indeed produce a great variety of neoplasms if not all and later they were used to study the influence of a number of factors on the dose response, ranging from physical factors to biological characteristics such as sex, species or tissues.

Much has been said about the limitations of animal experiments, particularly about their main limitation that their results can not be applied to humans. Animal experiments are expensive and they have got more so with the need to investigate more refined questions and therefore to inflate the number of animals needed. Typical examples for expensive experiments are studies of the shape of the dose effect response at low doses. As with time animal experiments were getting more refined they were also getting more unpopular. The two factors price and unpopularity combined with the decrease of financial funding for research have contributed to practically stop animal experiments. Earlier results nevertheless remain, and moreover a very valuable effort is underway to assembe in a data bank results collected over the years in the laboratories of the European Communities.

These results should be used since, in spite of the limited applicability of animal experiments for risk extimates, they can help to decide on such issues where epidemiological data can not bring an answer. One may hope that one day fundamental research will have made enough progress towards elucidation of the mechanisms which from the initial injury bring about a neoplasm; in the mean time estimates of risk can not but result from a combined evaluation of observations in epidemiology, in animal experiments, and in radiobiology.

The concepts and methods used in the analysis of animal experiments are largely similar to those used in epidemiology. Animal experiments however tend as a rule to be simpler to analyse than epidemiological data since, with the latter, factors have to be considered which are absent in planned experiments. Such factors can be life style, sex, age at irradiation to name just a few While in epidemiology it is only exceptional that two individuals have the same characteristics, the analysis of animal data consists in the comparison of groups of animals which differ only by the treatment they received. For this reason it appears reasonable to use for such data specific programs. Such a software package has been prepared at Leiden [1] which consists of two different parts. One accepts raw data on indiviual animals and prepares a data set ready for analysis. The other one contains the various options for a more or less detailed analysis. Aim of our work was the description of the mathematical background for these analysis. We make use of a particular example as an illustration.

Doses (Gy)	number of animals	number of carcinomas	number of sarcomas
0	586	8	6
γ-rays			
1	505	20	33
3	120	11	6
fission neutrons			
0.02	300	10	18
0.08	158	10	18
0.4	150	14	15

Table 1: Synopsis of the experiment

2 The experiment

For the purpose of the present illustration data from a life-time experiment with Sprague-Dawleys rats were utilized [4]. Groups of rats were irradiated with γ-rays or fission neutrons. At death they were autopsied and a whole spectrum of malignant tumors recorded. Two groups of tumors have been selected for the analysis, a group of carcinomas and a group of sarcomas. The carcinomas are those of the digestive tract of the urinary tract, the sarcomas are those of the vasculary system. Table 1 gives basic information about the experiment.

Central to all analysis is the concept of the *tumor rate* $r(t)$ or *hazard function*. It is the probability per unit time that an animal develops a tumor at time t after irradiation. Related to the tumor rate are the *cumulative tumor rate* or *cumulative hazard* $R(t)$, and the *tumor incidence* $I(t)$:

$$R(t) = \int_0^t r(t')dt',$$ (1)

$$I(t) = 1 - \exp(-R(t)).$$ (2)

Another related function is frequently used instead of the tumor incidence, this is the probability that at time t after irradiation an animal is still tumor free,

$$S(t) = 1 - I(t) = \exp(-R(t)).$$ (3)

For nonparametric estimates of $S(t)$ we used the product-limit estimate. Our notation is to use N_i for the number of animals still in the experiment at time t_i after treatment and n_i for the number of tumors observed at time t_i (or in a time interval dt_i around t_i). The product-limit estimate of the probability $S(t)$ to be tumor free at time t and its standard deviation are given by

$$\hat{S}(t) = \prod_{i \in t_i \leq t} (1 - \frac{n_i}{N_i}) \quad \pm \hat{S}(t)\sqrt{\sum_{i \in t_i \leq t} \frac{n_i}{N_i(N_i - n_i)}}.$$ (4)

Figure 1 shows the product-limit estimate for each group.

3 Analysis

In Fig. 1 there seems to be no great difference between the sarcoma rates of rats exposed to 1 and 3 Gy of γ-rays. This impression was confirmed by the Mantel Haenzel test, which shows no significant difference.

It was beyond the scope of our work to perform a detailed analysis of an experiment chosen for illustrative purposes only. Nevertheless we see indications that for carcinomas the dose-effect

Dose (Gy)	Proportional hazards model		Weibull functions	
	carcinomas	sarcomas	carcinomas $\beta = 8.8 \pm 2.3$	sarcomas $\beta = 4.0 \pm 0.7$
	α	α	α (day^{-1})	α (day^{-1})
0	1	1	$(7.4 \pm 1.6) \cdot 10^{-4}$	$(4.0 \pm 1.2) \cdot 10^{-4}$
γ-rays				
1	5.5 ± 1.1	$9 3 \pm 1 9$	$(8.9 \pm 0.8)\ 10^{-4}$	$(6 8 \pm 1 0) \cdot 10^{-4}$
3	$20 2 \pm 4.8$	9.8 ± 3.4	$(10.3 \pm 1.6)\ 10^{-4}$	$(6 8 \pm 1 0) \cdot 10^{-4}$
fission neutrons				
0.02	2.5 ± 0.6	5.9 ± 1.3	$(8.2 \pm 0.8) \cdot 10^{-4}$	$(6.2 \pm 1.1) \cdot 10^{-4}$
0.08	12.4 ± 3.3	21.8 ± 5.1	$(9 8 \pm 0.8) \cdot 10^{-4}$	$(8.2 \pm 1 2) \cdot 10^{-4}$
0.4	$69.0 \pm 17 6$	35.9 ± 9.4	$(11.8 \pm 0.9) \cdot 10^{-4}$	$(9.3 \pm 1.6) \cdot 10^{-4}$

Table 2. Parameters of the proportional hazards model and the Weibull functions with their confidence intervals.

relation is linear, apart from RBE values slightly in excess of 10. For sarcomas the situation is less clear. If linearity is assumed at low doses values in excess of 30 would be deduced for the lowest neutron dose. This experiment confirms that for these two classes of neoplasms there are differences in radiation sensitivity which lead to different dose response and different RBE values. The results are however too limited to permit a numerical evaluaton of these differences.

The next step in the analysis consists in introducing analytical expressions to estimate the rates for each group of animals. For experiments where each group differs from the others by only one parameter, the proportional hazards model is particularly simple and reduces to

$$R_J(t) = \alpha_J R_0(t). \tag{5}$$

The index J designates the groups, $R_0(t)$ is the base-line function. The cumulative rates are proportional and the proportionality factors α_J reflect the influence of the exposure. The fits for the present data set are illustrated in Figure 2. The α coefficients normalized to the coefficient of the control group are given in Table 2 with their confidence intervals.

The proportional hazards model is not the only possibility. An attractive alternative is the Weibull model which agrees with the assumption that tumor induction is the result of a multistage process. It is a special case of an accelerated hazards model and of a proportional hazards model since its mathematical expression as a power function of time can be written as

$$R_J(t) = (\alpha_J t)^\beta. \tag{6}$$

The results of a fit of this model to the present data are depicted in Figure 3. The estimated parameters β and α_J are given also in Table 2.

4 Conclusions

A comparison between the sum-limit estimates of the cumulative rates and the rates derived with the Weibull function indicate some divergence and one may wish in a more systematic analysis to use functions that are closer to the data. Various possibilities have been discussed in the literature [6] and some could be implemented in the software PREP1. The Weibull model may nevertheless still fit the broadest range of data. It has the advantage to be easily modified to take into account extended irradiations which have not been considered here.

The use of analytical expressions to fit data does not imply any assumptions on the basic mechanisms of carcinogenesis. The fit of a function such as the Weibull function to a data set provides only a convienient tool to summarize an experiment, to compare results and to prepare

further experiments Basic questions of carcinogenesis are nevertheless raised by large animal experiments such as the one considered here for the illustration.

The analysis in terms of a proportional hazards model as well as with a Weibull function has confirmed the previous findings that the carcinomas and the sarcomas seem to follow different time patterns, the carcinomas appearing later in time after exposure than the sarcomas. The question arises then whether this characteristic difference applies generally to all carcinomas and to all sarcomas. A similar question as to the generality of the finding is raised by the difference in the dose relations, with a saturation effect for the sarcomas.

Because of samll numbers it would be impracticable to analyse the different tumor types separately Carcinomas and sarcomas being tumors of different types of tissues, differences in their radiation sensitivity are of interest with regard to their implications for risk estimation and also with regard to the mechanisms of carcinogenesis. In the experiment discussed here, although the sarcomas make up for approximately half of all tumors, few leukemias have been observed and their inclusion with the sarcomas of the valculary system would have left the results unchanged. In epidemiologic studies cohorts of humans exposed to radiation the bulk of tumors in excess consists of carcinomas labelled as solid tumors and of leukemias. Apart from leukemias, sarcomas are rare. In the Japanese bomb survivors study and in the British ankylosing spondilitis patients study differences have also been observed in the time patterns of appearance between leukemias and carcinomas. The excess leukemia rates appears as a wave a few years after irradiation and decay to normal values after 15 to 20 years. The excesses of solid tumors appear late after irradiation and in proportion to the age specific spontaneous rates .The only known exception are the bone sarcomas observed in a cohort of patiients treated with the α-emitter radium 224. The time pattern of these sarcomas is quite similar to the wave like shape observed with the radiation induced leukemias. The whole picture suggests that to the division between leukemias and solid tumors may indeed correspond a more fundamental division between carcinomas and sarcomas. This remains however to be ascertained.

Although results from animal experiments are not directly transferable to humans for purposes of radiation protection, they can participate in answering practical as well as more fundamental questions as hopefully this work has again demonstrated. In this regard one should note that more information may be in store in the material that has been collected in past animal experiments. We will try to go on analysing this material.

References

[1] Weeda J., Davelaar J., Broerse J.J. (1993): Lifestat 3.10 Users guide. Internal Report University Hospital Leiden.

[2] Gart J.J., Krewski D., Lee P.N., Tarone R.E., Wahrendorf J. (1986): The design and anlaysis of long-term animal experiments. Statistical Methods in Cancer Research Vol III, IARC Scientific publicationss N 79, Lyon.

[3] Chmelevski D., Morin M. (1991): Mathematical methods in the analysis of animal experiments. Radiat. Environ Biophys. 30, 253–257.

[4] Morin M., Masse R., Lafuma J. (1986): Life-span radiation effects studies in animals: what can they tell us. In: Proc. 22nd Handord Life Sciences Symposium (Thompson R., Mahaffey J.A. edt.) US Dept. of Energy CONF 830951,184.

[5] Lafuma J., Chmelevsky D., Chameaud J., Morin M., Masse R., Kellerer AM. (1989): Lung carcinomas in Sprague-Dawley rats after exposure to low doses of radon daughters, fission neutrons, or γ rays. Radiat. Res. 118.230–245.

[6] Cox D.R., Oakes D. (1984). Analysis of survival data. Chapman and Hall, London.
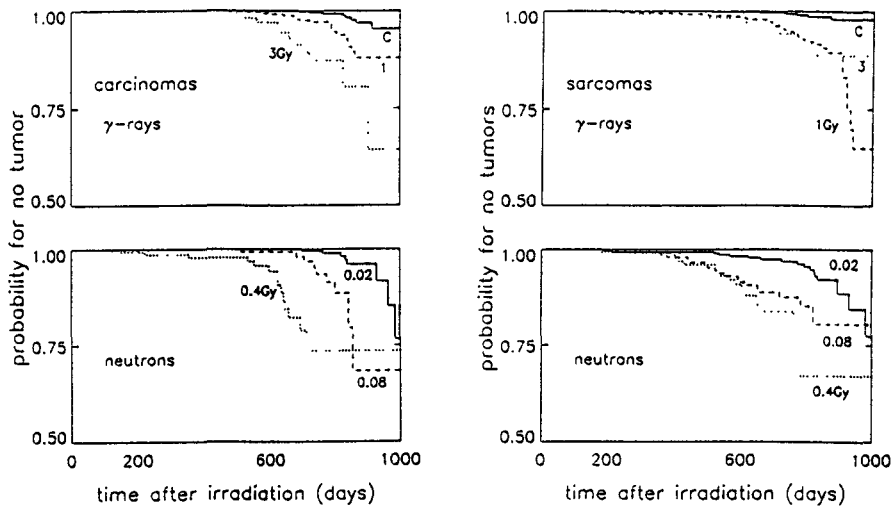
Figure 1 Product-limit estimate for the probability to be without sarcoma at the given time after exposure, see Eq. 4 For clarity the estimates are given without confidence intervals. The probability to be tumor free for the non-exposed group (C) is given in the upper panel with the two groups exposed to γ-rays.
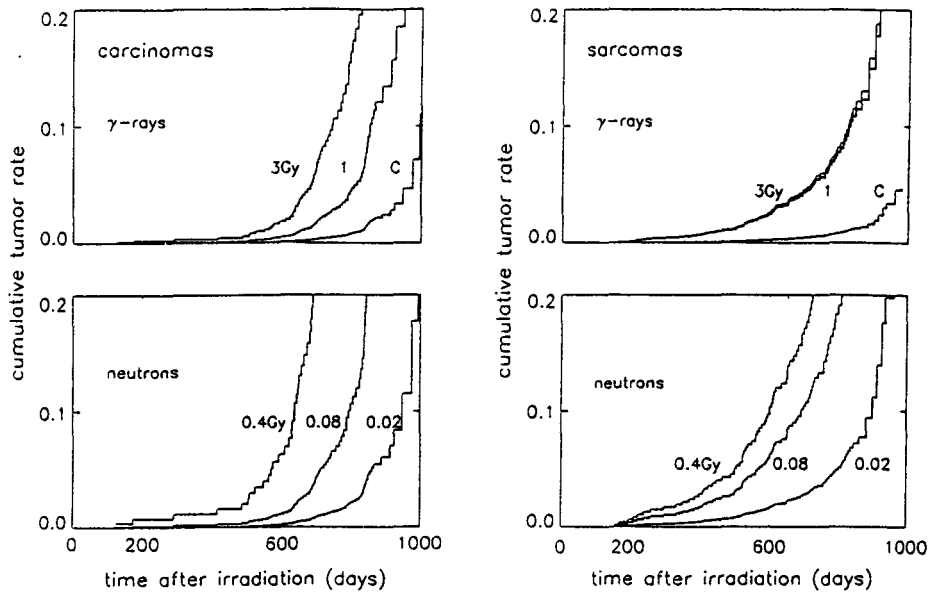
Figure 2: Cumulative tumor hazard rates according to the proportional hazards model, see Eq. 5. The curves are the maximum likelihood solution of a fit to the whole experiment.
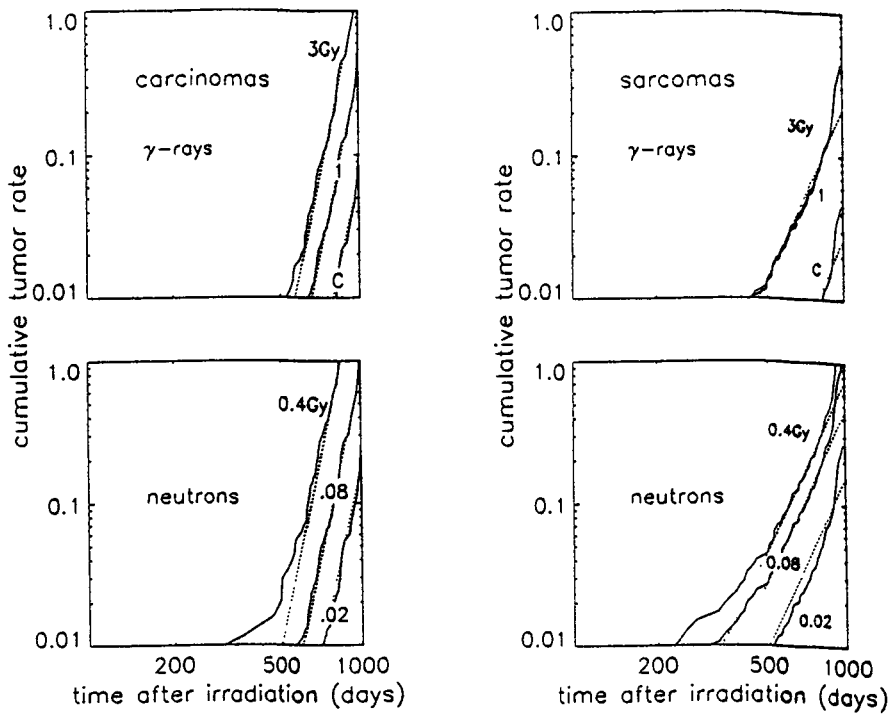
Figure 3: Cumulative tumor rates (dotted lines) resulting from a joint fit to Weibull functions see Eq. 6. The parameters are obtained by maximizing the likelihood of the whole experiment. The sum-limit estimates (full lines) are given for comparison.

II. Objectives for the reporting period

The histopathological classification of the lesions arisen in rats after different radiation treatments, with emphasis on mammary tumours.

III. Progress achieved including publications

The histopathological examination of mammary tumours appearing in rats treated with the hormone oestradiol 17ß, has been completed. The rats were given either single dose of gamma rays (Table 1) or fractionation scheme (Table 2). Each group consisted of 40 animals. With regard to single dose irradiation it is obvious that with a higher dose more malignant tumours are found. This is not observed, however, when the animals are irradiated at the relatively late age of 64 week of age.

The frequency of malignant tumours is considerably lower when the animals were subjected to fractionated radiation. It is not significant different from the results obtained with the unirradiated rats.

Table 1: Number of tumours, benign/malignant, for single dose irradiation

age at exposure (weeks)	0 Gy ben.	mal.	1 Gy ben.	mal	2 Gy ben.	mal
8	2	9	4	20	10	28
10	-	-	4	20	6	31
12	-	-	6	28	19	29
15	-	-	4	24	8	24
22	1	10	4	17	8	27
36	3	20	4	21	3	31
64	1	26	7	18	11	19

Table 2: Number of tumours, benign/malignant, fractionated irradiation

dose per fraction (mGy)	0 Gy ben	mal.	1 Gy ben	mal.	2 Gy ben.	mal
2.5	-	-	3	13	1	17
10	-	-	2	14	3	15
40	-	-	1	10	1	11

Histological classification of tumour types
Almost all of the tumours tabulated as "benign" were fibro-adenomas. Other benign tumours were classified as one fibroma, one was a papillary cystadenoma and one lipoma. The malignant tumours could be sub-divided into carcinomas (most cases) and carcinomas arising in fibro-adenomas. This last category comprised approximately 4 per cent of all malignant tumours in the single dose irradiated groups and approximately 1 per cent in the fractionation groups, whereas none has been found in the controls. Furthermore, one malignant mammary

tumour could be classified as sarcoma and one as adenosquamous carcinoma.
Non-mammary lesions have also been included in the study, but the histological slides have not been checked systematically, so quantitative information is not available at present. Qualitatively, the lesions that have been encountered are summarized in the following table.

Table 3: Non-mammary tumours: sites and types

site	benign	malignant
ovarium	folliculoma	
cervix		fibrosarcoma
uterus	leiomyoma	adenocarcinoma
	haemangioma	
adrenal cortex		carcinoma
small intestine		leiomyosarcoma
lung	haemangioma	
pituitary gland	adenoma	
liver	adenoma	
thyroid		carcinoma
spleen		fibrosarcoma

Final Report
1992-1995

Contract: F13PCT920043   **Duration: 1.9.92 to 30.6.95**   **Sector: B13**

Title: Measurement of oncogenic transformation of mammalian cells *in vitro* by low doses of ionizing radiation.

1)   Mill   Nuclear Electric
2)   Frankenberg   Univ. Göttingen
3)   Roberts   UKAEA
4)   Tallone Lombardi   Univ. Milano
5)   Kellerer   Univ. München
6)   Saran   ENEA

I. Summary of Project Global Objectives and Achievements

I.1   Global Objectives

This is a collaborative study of dose-response relationships for cell transformation *in vitro* at as low a dose as can be achieved. A realistic minimum dose at which to assess transformation frequency with adequate precision and achieve meaningful comparisons between participating laboratories is likely to be ~0.25 Gy. Close links are maintained with other laboratories working on cell transformation and with groups developing epithelial systems of human origin suitable for cell transformation *in vitro*.

Specific objectives include:

(a)   the preparation of a standard manual for cell transformation assays with the specific aim of standardising the protocol between participating laboratories; this will include precise criteria for scoring transformed foci and an explanation of the classification in terms of examples of transformed and non-transformed foci;

(b)   inter-comparison experiments at doses down to 0.25 Gy of X-radiation;

(c)   ultimately, by pooling data from each individual laboratory, the determination of dose-response relationships at as low a dose as is practical;

(d)   the eventual use of epithelial cell systems and assays that have an increased relevance to human risk estimation; and

(e)   the formation of individual subgroups for more specialised investigations: dose-rate effects with densely ionising radiations, the role of neighbouring entities of high ionisation density using ultra-soft X-rays and Auger-emitters, transformation frequency and the cell cycle and alternative transformation assays.

I.2   Global Achievements

I.2.1   Introduction

The principal risk from low doses of radiation is the induction of cancer. Currently the risks of developing cancer are predicted by various methods but these have not been validated at low radiation doses as routinely received during the operation of nuclear facilities and other sources of occupational exposure. Dose-response relationships for tumour induction can be studied using animal models but at low doses these can become expensive. An alternative is to use cell transformation *in vitro* for which a variety of systems are available. However only the C3H 10T½ mouse fibroblast system (Reznikoff *et. al.*, Cancer Research, 33, 3239-3249, 1973) and the CGL1 human hybrid system (Stanbridge *et al.*, Science, 215, 252-259, 1982; Redpath *et al.*, Radiation Research, 110, 468-472, 1987) provide the relatively high precision needed for work at low doses and dose-rates. These systems are used in a number of laboratories in Europe and the USA.

It is clear that, if reliable data at low doses are to be obtained, a large number of transformants must be scored to reduce the statistical variation. For one laboratory this may put a large strain on resources. For such an internationally important topic, this seems an ideal area for collaboration between laboratories and in June 1990 a collaborative project, partially supported by the CEC (contract Bi7-043 B13), was initiated with the following objectives.

(1)   To standardise the C3H 10T½ assay between participating laboratories.
(2)   To produce a standard code of practice for cell transformation in C3H 10T½ cells; so that other laboratories may have a standard for the comparison of results.
(3)   Ultimately, to establish the shape of the dose-response curve for cell transformation at low doses and dose-rates.
(4)   To extend these studies to more relevant cell transformation systems (*e.g.* human epithelial systems) as and when they become available.

The present contract is a continuation of contract Bi07-043 B13 which had broadly the same objectives. In this, the final report, collaborative inter-comparison experiments carried out between September 1992 and June 1995 and involving five of the six participating laboratories are described in sections I.2.3 to I.2.5 below. These collaborative experiments formed a central part of each laboratory's individual programme. This is followed by individual reports (sections II and III) from each participating laboratory.

I.2.2   Summary of Achievements prior to September 1992

The transformation assay, like many other biological assays, is susceptible to perturbations from a variety of influences. These perturbations do not normally hinder the comparison of results when made internally within each laboratory but often preclude the direct comparison of results between laboratories. Hence inter-comparison of results between laboratories is difficult unless steps are taken to minimise the effects of these influences. The initial phase of this project thus entailed the determination of the effect of various factors on plating efficiency, cell inactivation

and transformation frequency. It was found that one of the most critical for cell transformation is the convention used for scoring transformed foci and it became clear that scoring is an influential parameter in the C3H 10T½ transformation assay. Regular joint scoring inter-comparisons are necessary in order to maintain consistency between participating laboratories.

One of the first exercises carried out by the six collaborating groups was a focus-scoring inter-comparison. For this purpose each group circulated a number of flasks or petri dishes for scoring by the other groups. This was followed up by a joint scoring exercise during which a consensus score for each flask or dish was determined. Altogether four such exercises have now been completed. Initially, there was a relatively large discrepancy between some laboratories (up to a factor of 2), but the disagreement following the third scoring exercise was reduced to a maximum of about 20%. In Table 1 are shown the results of the statistical analysis after three inter-comparison and consensus scoring sessions. It is clear that scoring is an influential parameter in the 10T½ transformation assay and regular joint scoring inter-comparisons are necessary in order to maintain consistency between participating laboratories. An important goal was the production of a catalogue depicting various classes of foci and the score assigned to these foci. This will be a unique reference for scoring foci and will be an aid to other laboratories using the C3H 10T½ cell transformation assay to whom it will be made readily available.

TABLE I: Ratios and Standard Deviations of Individual Score to Consensus Score for Transformed Foci

Laboratory	Date of Focus Scoring Inter-comparison		
	July 1990	May 1991	October 1991
Berkeley	1.8 ± 0.6	0.7 ± 0.2	1.0 ± 0.2
Frankfurt	1 3 ± 0 3	0.8 ± 0.3	0.8 ± 0.2
Harwell	1.4 ± 0.2	1.3 ± 0.7	0.8 ± 0.3
Milan	0.8 ± 0.1	1.1 ± 0.3	1.0 ± 0.1
Munich	1.1 ± 0 3	1.1 ± 0.3	0.9 ± 0.1
Rome	--	1.2 ± 0.6	1.1 ± 0.2
OVERALL	1 31 ± 0.19	1.05 ± 0.49	0.95 ± 0.24

As a basis for scoring, the criteria of Reznikoff *et. al.* (Cancer Research, 33, 3239-3249, 1973) are used but with some modifications. No distinctions between type II and type III foci are made and the most important criterium is the presence of criss-crossing. Piling-up alone is insufficient to classify a focus as being malignantly transformed. A new type of focus, designated X, has been identified. These are characterised by long, fibrous sheaths of cells. Tumourigenicity studies have been carried out to verify the classification of transformed foci.

Other conclusions are (i) that the use of cells kept on ice for up to 72 hours does not compromise experiments, thus enabling the transportation of experimental cells

between laboratories; (ii) that serum batch, as long as this has been previously screened as suitable for transformation, is not critical; and (iii) that the use of seeding densities between 1 and 3 viable cells per square centimetre is a region of small variation in transformation frequency and should be used for all routine experiments. A summary of the data of the dependence of transformation frequency on seeding
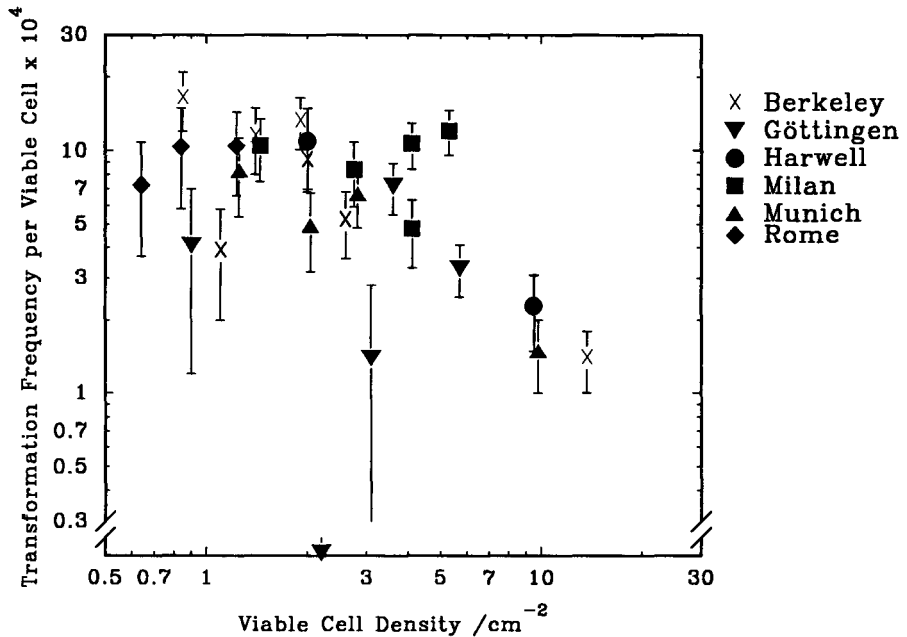
FIGURE 1   The Effect of Cell Seeding Density on Transformation Frequency: 5 Gy X-rays

density is shown in figure 1.

Inter-comparison measurements at doses down to 1 Gy have previously been reported. In this report further measurements are presented together with new measurements at doses down to 0.25 Gy. Further refinements to the protocol are also described.

I.2.3   Incubation Period

The standard assay for transformation in C3H 10T½ cells involves a total culture period of six weeks, including weekly medium changes after the two weeks. For the first three weeks cells are grown in medium containing 10% foetal calf serum (FCS), subsequently the medium contains 5% FCS. Further work has suggested the need to incubate cells for a fixed period of four weeks after confluence is reached rather than a fixed total period of six weeks. This four-week period of confluence is not normally achieved when cells are seeded at ~2 viable cells cm^{-2}. Irradiated cultures can take significantly longer than unirradiated cultures to reach confluence, particularly at high doses. Further investigations have shown that there are some differences in culture

conditions between the laboratories which result in a significant spread in the time taken for confluence to be reached. Results from two inter-comparison experiments in which the effect of incubation period was studied are shown in figure 2. Clearly there can be a large change in the measured transformation frequency between the standard period of six weeks and longer periods of eight or nine weeks. These results need to be interpreted in conjunction with growth-curve data for the same experiments which are shown in figure 3 and summarised in table II. Evident is the spread in the time taken to reach confluence which seems to depend on serum batch and other factors peculiar to each laboratory. When transformation frequencies are compared for incubation periods corresponding to four weeks at confluence the agreement between laboratories is significantly improved (see table III). There is a small increase in the spontaneous transformation for the longer incubation periods.
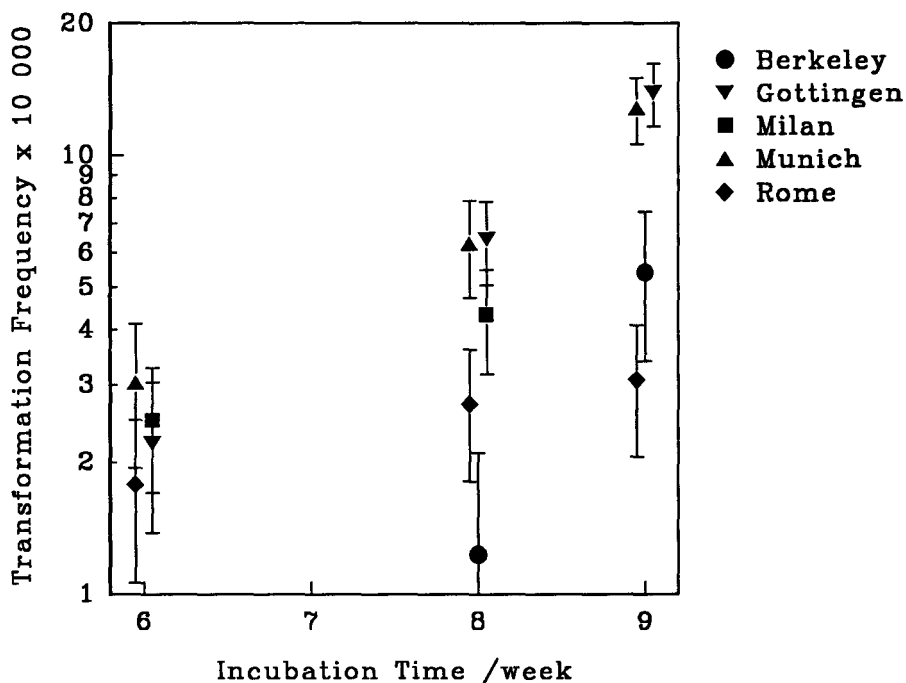
FIGURE 2   The Effect of Incubation Time on Transformation Frequency: 5 Gy X-rays

Following the results from these measurements all subsequent transformation experiments are incubated for a period of four weeks following the attainment of confluence.

TABLE II: Summary of Growth-Curve Data

Laboratory	Viable Cell Seeding Density /cm^{-2}		Approximate Cell Density at Confluence /10^4 cm^{-2}		Approximate Time to Reach Confluence /day	
	Control	5 Gy	Control	5 Gy	Control	5 Gy
Berkeley	1.6	1.3	3	2	18	28
Göttingen	1.7	1.5	6	4	17	21
Milan	2.7	2.7	5	4	15	18
Munich	2.3	1.7	5	4	17	21
Rome	2.0	2.4	4	4	17	19
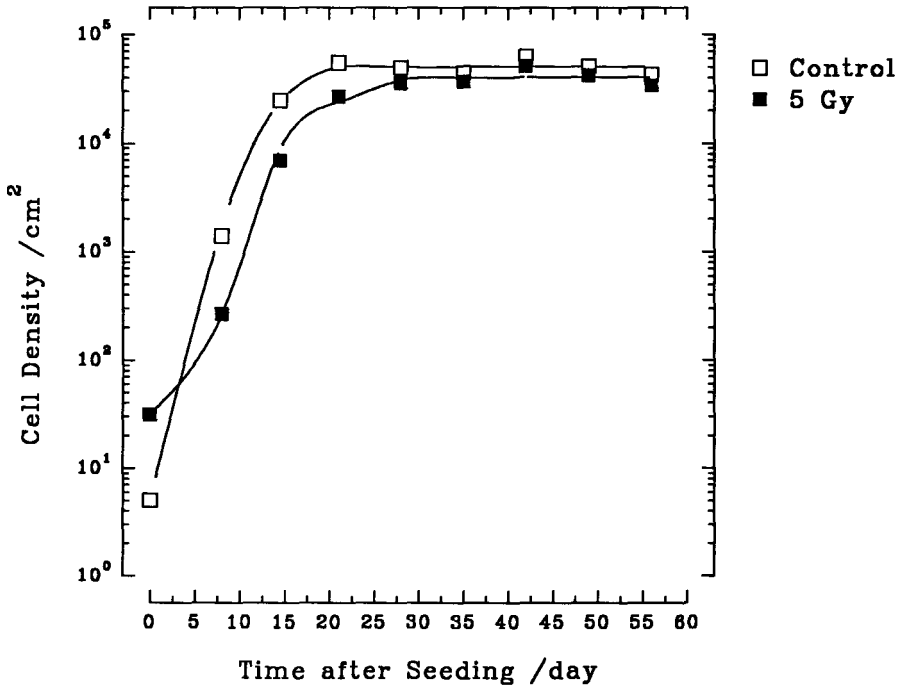
FIGURE 3   Combined Growth Curve Data from Five Laboratories: 0 and 5 Gy X-rays.

TABLE III: Transformation Frequencies for Incubation Period of Four Weeks Post-Confluence:
Dose = 5 Gy X-Rays (Data extracted from Figure 2 and Table II)

Laboratory	Transformation Frequency per Viable Cell x 10⁴
Berkeley	5.42 ± 2.02
Göttingen	6.45 ± 1.40
Milan	4.33 ± 1.16
Munich	6.29 ± 1.57
Rome	2.71 ± 0.90

I.2.4   Survival and Transformation Inter-comparison Experiments

Altogether nineteen inter-comparison experiments have been carried out during the period of this and the previous contract. The data presented in this section are from those covering all experiments. Initially, transformation experiments were carried out using the standard six-week protocol. Following the investigations on the time required to reach confluence (see section I.2.3), later experiments were incubated for a fixed time at confluence (4-weeks). Tables IV and V show the combined data from each laboratory. In general the transformation frequencies are the result of pooled data from at least three experiments.

In table VI the data from each laboratory have been combined to provide survival and transformation data. These combined values were obtained by weighting each
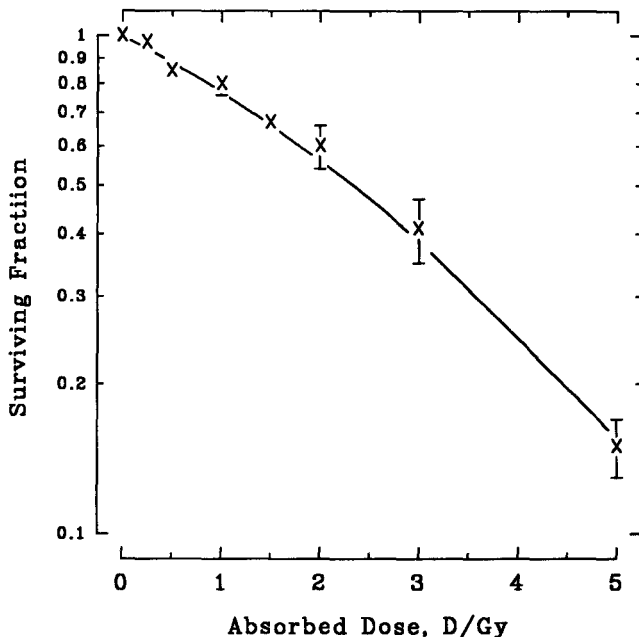
FIGURE 4   Survival Curve from Combined Data: 250 kVp X-rays

laboratory's individual data by the number of survivors (for transformation) and by the number of experiments (for surviving fraction). An alternative weighting of transformation frequency by total area produced combined transformation frequencies of similar value. Only data where the viable cell densities were less than ~4 cells cm^{-2} have been included in this analysis.

TABLE IV: Transformation Frequencies and Surviving Fractions: Experiments using Six-Week Protocol

Laboratory	Dose /Gy	Average Surviving Fraction	Total Number of Survivors	Total Growth Area /m^2	Total Number of Foci	Transformation Frequency per Surviving Cell x 10^4
Berkeley	0	1	120911	7.97	3	0.25 ± 0.14
	1	0.91	51296	3.99	11	2.19 ± 0.65
	2	0.71	54497	3.71	10	1.88 ± 0.59
	3	0.49	36334	3.26	8	2.25 ± 0.79
	5	0.25	51190	3.82	42	9.04 ± 1.33
Göttingen	0	1	63180	5.05	2	0.40 ± 0.20
	1	0.90	27400	2.14	1	0.37 ± 0.37
	2	0.37	14200	2.00	3	2.12 ± 1.20
	3	0.45	15800	1.32	2	1.27 ± 0.90
	5	0.19	65480	4.32	10	1.50 ± 0.47
Harwell	0	1	54674	4.00	5	0.92 ± 0.41
	1	0.75	46515	3.13	5	1.09 ± 0.48
	2	0.59	15981	0.83	0	<0.63
	3	0.36	25839	1.80	11	4.48 ± 1.32
Milan	0	1	160441	7.73	9	0.56 ± 0.19
	1	0.73	64779	6.22	11	1.70 ± 0.51
	2	0.61	59442	3.58	9	1.50 ± 0.50
	3	0.41	61116	3.56	15	2.50 ± 0.65
	5	0.16	52774	2.56	22	4.30 ± 0.90
Munich	0	1	151729	9.22	15	0.99 ± 0.26
	1	0.85	90955	6.68	22	2.44 ± 0.52
	2	0 60	45551	3.52	20	4.46 ± 1.00
	3	0.38	48372	3.54	17	3.56 ± 0.86
	5	0.13	77061	4.43	43	5.73 ± 0.88
Rome	0	1	95948	6.36	3	0.31 ± 0.18
	1	0.84	97826	6.56	3	0.31 ± 0.18
	2	0.63	63960	4.51	8	1.26 ± 0.44
	3	0.41	64880	4.46	8	1.24 ± 0.44
	5	0.12	51394	3.95	22	4.35 ± 0.92

TABLE V: Transformation Frequencies and Surviving Fractions: Experiments using Four-Week
Confluence Protocol

Laboratory	Dose /Gy	Average Surviving Fraction	Total Number of Survivors	Total Growth Area /m²	Total Number of Foci	Trans- formation Frequency per Surviving Cell x 10⁴
Berkeley	0	1	141877	7.54	11	0.79 ± 0.23
	¼	0.96 ± 0.03	258783	12.72	23	0.90 ± 0.19
	½	0.79 ± 0.08	78392	5.27	10	1.30 ± 0.41
	1	0.80 ± 0.01	52110	3.10	12	2.39 ± 0.68
	1½	0.75 ± 0.07	47920	2.70	15	3.29 ± 0.83
	3	0.59 ± 0.48	61885	2.12	12	2.04 ± 0.57
	5	0.17	13697	1.02	7	5.42 ± 1.99
Göttingen	0	1	188506	9.87	20	1.07 ± 0.24
	¼	0 97	242000	10.83	28	1.16 ± 0.22
	½	0.81	122667	6.50	13	1.07 ± 0.30
	1	0.67	63357	3.35	14	2.25 ± 0.60
	1½	0.66	61775	3.32	21	3.46 ± 0.76
	3	0.32	15600	1.00	8	5.30 ± 1.90
	5	0.17	31365	2.16	21	6.95 ± 1.50
Milan	0	1	191060	7.75	6	0.31 ± 0.13
	¼	0.90 ± 0.04	266580	11.50	8	0.30 ± 0.11
	½	0.88 ± 0.03	115654	5.90	4	0.35 ± 0.17
	1	0.67 ± 0.12	20979	1.60	1	0.48 ± 0.48
	1½	0.77 ± 0.07	28399	1.77	7	2.50 ± 0.34
	3	0.31 ± 0.02	32352	1.56	4	1.25 ± 0.60
	5	0.15 ± 0.05	33242	1.41	15	4.65 ± 1.20
Munich	0	1	195017	8.86	19	0.98 ± 0.23
	¼	0.92	168600	6.59	27	1.62 ± 0.30
	½	0.85	104523	4.90	23	2.23 ± 0.47
	1	0.87	53524	2.21	12	2.28 ± 0.66
	1½	0.60	57523	3.03	18	3.18 ± 0.75
	3	0.41	19400	1.20	13	6.91 ± 1.92
	5	0.095	26058	1.88	16	6.29 ± 1.57
Rome	0	1	134070	5.70	3	0.22 ± 0.13
	¼	1.11 ± 0.06	187712	7.66	2	0.11 ± 0.08
	½	0.91 ± 0.09	118957	5.24	6	0.51 ± 0.21
	1	0.76 ± 0.09	60654	2.73	0	<0.17
	1½	0.62 ± 0.10	54220	2.79	5	0.93 ± 0.41
	3	0.44 ± 0.06	23490	0.92	6	2.60 ± 1.05
	5	0.13 ± 0.04	33689	1.79	9	2.71 ± 0.90

TABLE VI: Transformation Frequencies and Surviving Fractions: Pooled Data from Collaborating Laboratories

Dose/ Gy	Surviving Fraction	Transformation Frequency per Surviving Cell x10 000		
		All Data Combined	6 Week Protocol	4 Week Confluence Protocol
0	1	0.65 ± 0.14	0.58 ± 0.17	0.70 ± 0.17
¼	0.97 ± 0.04	0.79 ± 0.26	-	0.79 ± 0.26
½	0.85 ± 0.02	1.05 ± 0.34	-	1.05 ± 0.34
1	0.80 ± 0.04	1.55 ± 0.40	1.41 ± 0.42	1.59 ± 0.52
1½	0.67 ± 0.03	2.71 ± 0.49	-	2.71 ± 0.49
2	0.60 ± 0.06	2.00 ± 0.51	2.00 ± 0.51	-
3	0.41 ± 0.06	2.63 ± 0.67	2.47 ± 0.74	2.91 ± 0.94
5	0.15 ± 0.02	4.85 ± 0.85	4.88 ± 1.20	5.09 ± 0.79
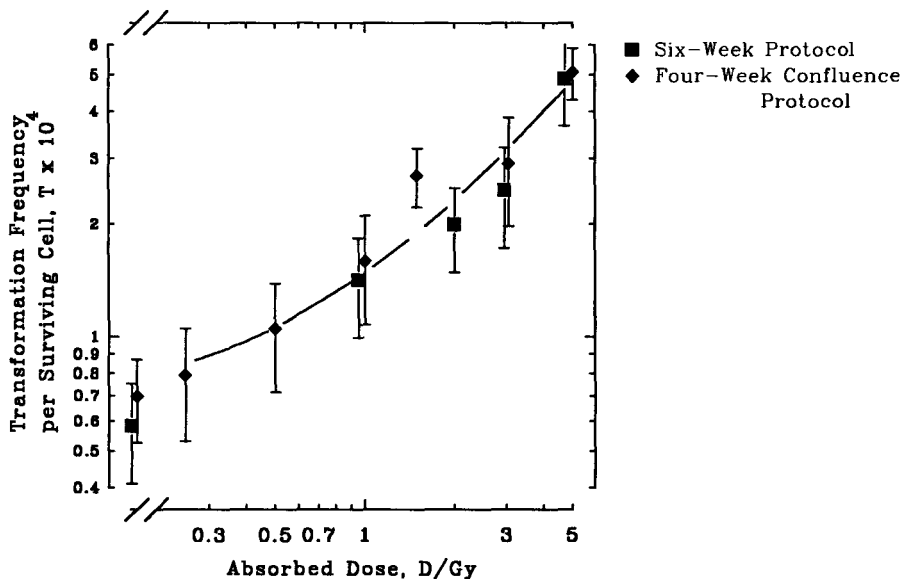
FIGURE 5   Transformation Frequencies from Combined Data: 250 kVp X-rays

Figures 4 and 5 show respectively the combined surviving fractions and combined transformation frequencies as a function of dose (data presented in Table VI). A linear-

quadratic fit to the survival curve produced the following relationship between surviving fraction (S) and absorbed dose (D) in gray:

$$S = \exp\{-(0.235 \pm 0.025).D - (0.0274 \pm 0.0076).D^2\}$$

Since the results in Figure 5 show there to be no significant difference in the transformation frequencies for the two different protocols for the doses used in these inter-comparisons, data at 1, 3 and 5 Gy and control values were combined in the final analysis of transformation frequency. A regression fit to the transformation data produced the following relationship between transformation frequency per surviving cell (TF) and absorbed dose (D) in gray:

$$TF = (0.829 \pm 0.084) \times 10^{-4}.D$$

A fit using a linear-quadratic relationship resulted in a non-significant value for the dose-squared term. The dose-response curve for the combined transformation frequencies from the two protocols and corrected for the spontaneous transformation frequency are shown in Figure 6.
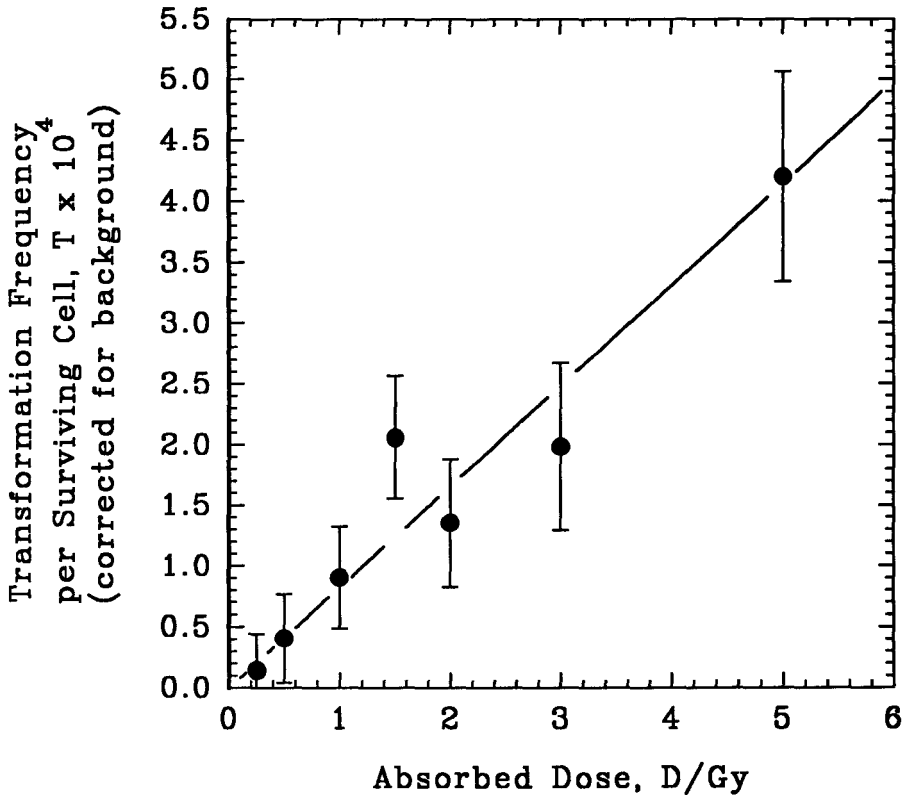
FIGURE 6   Radiation-Induced Transformation Frequencies from Combined Data: 250 kVp X-rays

I.2.5   Tumourigenicity Studies

In order to validate the amended scoring criteria for transformation, foci were isolated from cultures irradiated at Berkeley with a dose of 5 Gy of X-rays for subsequent assay *in vivo*. Cells were grown for two passages before being sent to St Andrews University where they were injected into athymic C3H mice. Mice were observed for eight months; in most instances where tumours did appear they did so at times much less than this. In many cases tumour cell lines were isolated and used for subsequent studies (see reports from projects 1 and 3 in section III). Prior to the tumourigenicity results being available the foci were scored, initially by Berkeley alone, and then by all laboratories. A comparison of consensus score (focus type) and tumour incidence is shown in table VII. It is difficult to identify non-positive foci prior to staining and hence fewer of these types of foci were available for tumourigenicity investigation. One possible reason why foci scored as non-positive may produce tumours is that the extra passaging of cells to provide sufficient for injection (~4 x 10^6 cells per mouse) may enable pre-malignant cells to progress to full malignancy. However, this explanation is currently being investigated by culturing non-tumourigenic focus cells for several passages prior to being re-tested for their tumourigenic potential. To date no late passage foci which failed to produce tumours at early passage have progressed to tumourigenicity.

TABLE VII: Results of Tumourigenicity Studies

Focus Type	Number of Foci Tested	Number of Tumour Producing Foci	Number of Mice Injected	Number of Tumour-Bearing Mice	Tumour Incidence	
					Fraction of Foci Producing Tumours	Fraction of Mice Developing Tumours
Control	-	-	19	0	0	0
-	5	2	32	23	0.40	0.72
+	16	9	97	67	0.56	0.69
X/+	4	2	21	16	0.50	0.76
X	2	1	9	4	0.50	0.44

I.2.6   Discussion and Summary

The C3H 10T½ cell transformation system has been widely used for a number of years to measure the malignant transformation by radiation and by chemicals. The radiosensitivity of this system is, however, rather low and experiments to determine the transformation frequency at low doses require a large number of samples in order to obtain significantly meaningful results. The exact details of the experimental protocol used can also significantly affect the measured transformation frequency. Evidence of this can be deduced from the scientific literature. For example Yang *et al.* (Radiation Research, 104, S-177-S-187, 1985) report on a series of experiments carried out over several years where the radiation-induced transformation frequencies were found to vary from ~1 to ~12 x 10^{-4} for a dose of 4 Gy of 225 kVp X-rays. The dose-response relationship was curvilinear. The values at the lower end

of this range are amongst the lowest radiation-induced transformation rates reported in the literature. In another publication, Borsa *et al.* (Radiation Research, 100, 96-103, 1984) report a transformation frequency of ~4 x 10^{-3} at a dose of 5 Gy of 250 kVp X-rays with an approximately linear relationship up to ~6 Gy: the highest transformation rate reported in the literature. There are a number of other publications in which transformation frequencies somewhere between these extremes of ~0.3 x 10^{-4} and ~7 x 10^{-4} Gy^{-1} are reported for similar radiation qualities. This variation, by over a factor of twenty between laboratories, makes an inter-comparison of results impossible.

The data from the collaborative experiments reported in section I.2.4 above are based on a large number of transformed foci (759 in total), far in excess of the numbers reported in any previous publication involving the C3H 10T½ cell transformation system. The total number of experimental samples was equivalent to over fifty-one thousand 55 cm^2 petri dishes. As such the results have a firm statistical basis. Moreover, experimental conditions which were found most likely to affect transformation frequencies were identified and well controlled as described in sections I.2.2 and I.2.3 and in the final report of the previous contract (Bi07-043 B13). The results presented in section I.2.5 indicate that the dose-response relationship as measured in the dose interval from 0.25 to 5 Gy is linear and directly proportional to dose. The sensitivity for 250 kVp X-rays was found to be (0.83 ± 0.08) x 10^{-4} transformants per gray, a value towards the lower end of the extreme values previously reported.

In summary the specific objectives (a) - (c) outlined in section I.1 have been achieved by this collaborative project:

(i)   The standard protocol on cell transformation *in vitro* using the C3H 10T½ mouse fibroblast system as recommended by the IARC working group (Kakunaga and Yamasaki, IARC Scientific Publication No. 67, 207-219, 1985) has been extended and further standardised by suitable inter-comparison experiments. A catalogue of transformed and non-transformed foci depicting several different morphologies has been produced. Additional recommendations that should be taken into account are:
- seeding density of cultures should be ~2 viable cells per square centimetre;
- cultures should be incubated for a fixed period of four weeks after confluence has been reached;
- regular consensus scoring is required;
- type II and type III (after Reznikoff *et. al.*) should be regarded as positively transformed clones, but with some modification to the scoring criteria;
- type X foci should be scored as positively transformed.

(ii)   Inter-comparison experiments and the results of pooling data from the participating laboratories has determined the dose response relationships for cell survival and cell transformation to a high precision.

Objectives (d) and (e) have been achieved through the individual laboratory programmes, the results of which are described in the sections III below.

Head of Project 1: Dr. Mill

II. Objectives for the reporting period

(a)   Participation in the standardisation of the C3H 10T½ cell transformation assay.

(b)   A study of dose-rate effects using 3.3 MeV α-particles.

(c)   Characterisation of transformed C3H 10T½ cells.

(d)   Radiation studies using the human colorectal cells.

III. Progress achieved including publications

1.   α-Particles - Dose-Rate Effects

The study of the effects of high-linear energy transfer (LET) α-particles is of importance for radiation protection as the human population is exposed to both natural and artificial alpha-emitting radionuclides in the environment. Of special relevance were the findings of Hill *et al.* (International Journal of Radiation Biology, 46, 11-16, 1984) on the greatly enhanced frequencies for oncogenic transformation in C3H 10T½ cells for very low dose-rates of fission neutrons. Data from our laboratory with neutrons and from elsewhere (Balcer-Kubiczek, *et al.*, International Journal of Radiation Biology, 59, 1477-1482, 1991) have not confirmed these initial findings. However, the controversy still exists as to whether irradiation by neutrons and α-particles at low dose-rates can be more effective than at high dose-rates. In particular, it has been suggested (Elkind, International Journal of Radiation Biology, 59, 1467-1475, 1991) that experimental artefact could explain why many laboratories do not observe enhanced transformation rates at low doses of high-LET radiation.

We have carried out experiments using α-particles from a ^{238}Pu source for exponentially growing (log phase) and plateau phase C3H 10T½ cells cultured on Hostaphan based dishes (2.5μm thick). The α-particle energy was 3.3 MeV and the LET 121 keV μm^{-1}. A dose of 0.36 Gy was chosen for the dose-rate comparison. The dose-rates used were 0.18 Gy min^{-1} (acute), 1.2 mGy min^{-1} and 0.13 mGy min^{-1} (chronic), the lower dose-rates extending over irradiation periods of either 5 or 45 hours. The temperatures of the samples were maintained at 37°C throughout the irradiation period.

Rather than an enhancement our results suggest that, for log-phase cultures, there is a reduction of ~30% in the transformation frequency for the chronic dose-rates compared with the acute dose-rate. This is contrast to results reported by Miller *et al.* (Radiation Research, 124, S62-S68, 1990). Our initial interpretation was that this difference could be explained by the different techniques used in delivering the dose; whereas Miller *et al.* used a fractionated regime, our experiments were carried out with continuous exposures resulting in a random sequence of events within the cell.

Subsequently we have compared fractionated and continuous irradiations at 1.2 mGy min^{-1} in order to confirm this hypothesis which would indirectly support the existence of a sensitive period for transformation in the cell-cycle. Our results, however, shown in table I, indicate no significance difference in the transformation frequency after continuous or fractionated

irradiation regimes and our data remain in conflict with those of Miller *et al.*.

Table I: Transformation frequency in C3H 10T½ cells after continuous or fractionated
exposure to 0.36 Gy of ^{238}Pu α-particles

Irradiation Regime	Surviving Fraction	Number of Cells at Risk	Number of 162 cm² Flasks		Transformation Frequency per Viable Cell x 10⁴
			Total	With Foci	
Control	-	48705	87	0	<0.21
Fractionated	0.61 ± 0.11	277020	434	29	1.1 ± 0.2
Continuous	0.67 ± 0.06	305065	423	37	1.3 ± 0.2

Because of a higher spontaneous transformation frequency for plateau-phase cultures no firm
conclusions about possible dose-rate effects in these cultures can be made, although high
factors (*i.e.* >3) for an enhanced response at chronic dose-rates are not compatible with the
observed data.

2. Tumourigenic and Growth Properties of Transformed Foci

Transformed foci of various types have been isolated from X- and α-particle irradiated
cultures of C3H 10T½ cells. These have been expanded for two or three passages and frozen
stocks established.
Various properties of
these transformed cells
have been measured,
including:
tumourigenicity,
growth properties (for
example doubling time,
saturation density and
length of the lag phase),
chromosome
complement and the
ability to reconstruct
the original focus, when
seeded onto monolayers
of untransformed cells.
The correlation between
focus classification and
tumourigenicity has
been presented in
section I above. The
growth characteristics
of tumours which
occurred from these
different types of foci
are shown in figure 1.
It would be useful to
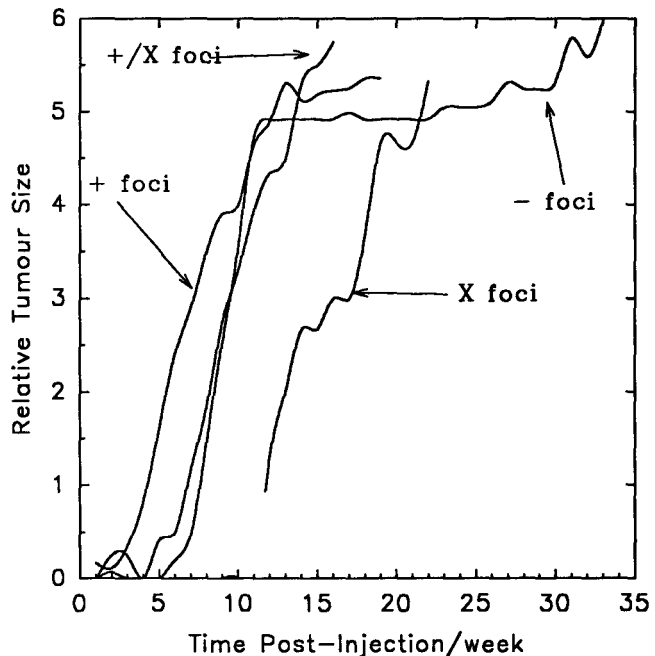
FIGURE 1: Growth Characteristics of Various Tumour Types

ascertain the reason why, in some instances, foci classified as negative, do produce tumours. Apart from the possibility of misclassification, one explanation may be that in the process of expansion to provide enough cells for injection a further (and final) step towards malignancy occurs. This is partially supported by the growth-curve data presented in figure 1 where it can be seen that there is an average lag of about five weeks compared with positively scored foci before tumours are observed. The curve for X foci is only for one focus. For +, +/X and - foci there were respectively eleven, two and three foci.

Cytogenetic analyses of various foci have shown a reduced chromosome number compared to the parent cell line with a further loss in the tumour cell lines isolated from the tumours induced in C3H mice by these foci. A number of the focus cell lines also show the presence of metacentric chromosomes (mouse chromosomes are normally acrocentric) which are also present, to a greater extent in the corresponding tumour cells and absent in unirradiated parent cells.

The focus cells or tumour cells were seeded onto confluent monolayers of unirradiated cells or seeded with an equivalent number of unirradiated cells in suspension, and the cultures examined for the appearance of foci, four weeks after confluence. The distribution patterns of reconstructed foci in the various focus categories is similar for the focus cells and their corresponding tumour cells. Focus and tumour cells (spontaneous and X-ray induced) reconstruct foci more efficiently when seeded onto confluent monolayers of unirradiated cells than when seeded using suspensions which contain equivalent numbers of unirradiated cells. Seeding of tumour cells resulted in a higher percentage of cultures with reconstructed foci. The (+) and (X) foci and their corresponding tumour cells form the same class of foci in the majority of the focus-containing cultures, regardless of the seeding conditions. The (X/+) foci and tumour cells form (+) foci in the majority of the focus-containing cultures

There was no significant differences between the foci and the control or tumour cells in the length of lag phase before exponential growth, the doubling time or plating efficiencies in either standard or reduced serum conditions. Transformed cells are reported to require fewer growth factors than untransformed to grow *in vitro*.

3.   Radiation Studies using the Human Colorectal Cells (AA/C1)

Colorectal cancer is an excellent, and well studied, example of the multi-step nature of cancer as described by Muto *et al.*(Cancer, 36, 2251-2270, 1975). It has also been observed that tumour progression in the adenoma-carcinoma sequence is accompanied by a series of characteristic genetic lesions which appear to occur in a preferred sequence. Although there is a preferred sequence of genetic lesions in this progression it appears that the order of events is not essential, rather it is the accumulated damage that determines tumourigenic potential. In addition the stomach, colon and the rectum are all radiologically significant tissues with high tissue weighting factors (w_T) and a suitable *in vitro* model of colon carcinogenesis is highly relevant for radiological protection purposes.

The adenoma derived PC/AA non-tumourigenic human cell line was isolated from the colon of a familial adenomatous polyposis coli patient (Paraskeva *et al*, International Journal of Cancer, 34, 49-56, 1984). From this non-clonogenic diploid cell line other cell distinct lines have been derived, *ie*, STX/AA and AA/C1. The STX/AA cell line arose as a spontaneous mutation and was found to be a mucinous carcinoma. The AA/C1 cell line is aneuploid, clonogenic and non-tumourigenic and is the one used for the radiation studies described here.

The progression from the non-tumourigenic AA/C1 cell line to the transformed adeno-carcinoma (AA/C1/SB/10M) cell line is accompanied by the acquisition of a number of characteristics. Amongst which is the loss of anchorage dependent growth.

Within the gut anchorage independence is typically a trait associated with well developed villous tumours, permitting cells within the tumour to break away from the primary tumour (a pre-requisite for metastasis). Although it is unclear which oncogenes or tumour suppressor genes are involved in this process it has remained a useful characteristic which has been used a number of times in the assessment of cellular transformation with both rodent and human cell lines. However, in some cases anchorage independent growth does not correlate well with malignant transformation in human cells and it is therefore necessary to isolate anchorage independent colonies and subsequent assay them for tumourigenic potential.

Surviving Fraction
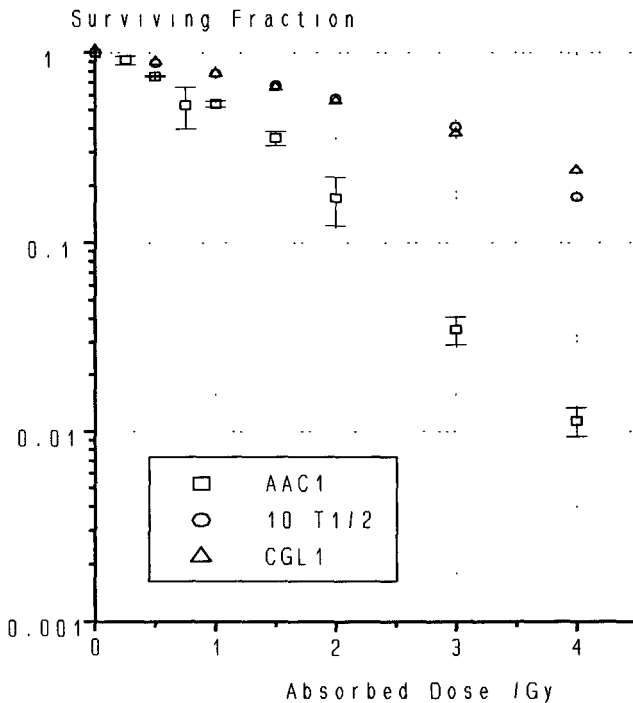
FIGURE 2: Survival characteristics of AA/C1 cells

The survival curve for AA/C1 cells after irradiation with 250 kVp X-rays is shown in figure 2. When compared with that for C3H 10T½ and CGL1 cells it suggests that AA/C1 cells are relatively radiosensitive. The AA/C1 cells have a relative surviving fraction at 2 Gy (SF$_2$) of 0.17 ± 0.05 compared with 0.58 and 0.56 for the C3H 10T½ and CGL1 cell lines respectively. The lack of any significant shoulder region could also be indicative of a poor capacity to repair radiation-induced sublethal damage. However, the results of split dose experiments (see table II) suggest that the AA/C1 cell may in fact be capable of a significant

degree of repair. These results are, however, not conclusive, since a proportion of the apparent repair may be due to cells arresting within S-phase where they are less sensitive to a subsequent second dose. The only way to deduce whether or not there is a significant degree of sublethal or potentially lethal damage repair is to follow damage induction and repair directly.

TABLE II: The results from split dose experiments with AA/C1 cells

Time between doses /h	Surviving Fraction for:	
	0.25 Gy followed by 2 Gy challenge dose	2 Gy followed by 2 Gy challenge dose
0¶	0.10 ± 0.006	0.021 ± 0.001
2	0.11 ± 0.015	0.059 ± 0.007
4	0.09 ± 0.007	0.041 ± 0.003
6	0.18 ± 0.011	0.024 ± 0.003

¶ Irradiated with a single 2.25 Gy dose or single 4.0 Gy dose
Control plating efficiency $= 0.95 \pm 0.05\%$
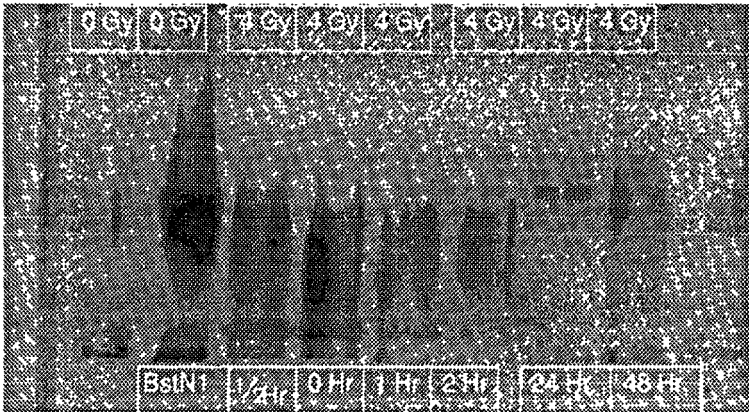
FIGURE 3: PFGE results for various times between irradiation and cell lysis. Samples were 5 x 10⁶ cells / ml.

Of the DNA lesions that radiation is known to induce, double strand breaks (dsb) are widely considered to be the most critical and have been shown to be related to radiation induced cell death and transformation. Furthermore it has recently been shown that cells defective in dsb

repair pathways are hypersensitive to radiation induced cell death (Ward, Progress in Nucleic Acid Research, 35, 95-125, 1988). Such cell lines, for example xrs-5, appear to share defects in genes normally involved in the repair of DNA double strand breaks, both induced exogenously and during the process of V(D)J recombination. A more recent discovery is that dsb repair is linked with V(D)J antibody component recombination and it has been shown that xrs-5 cells are also site specific recombination compromised. Such mutant studies are already beginning to provide new insights into DNA dsb repair pathways. The induction of dsb's has been reliably shown to be linearly induced with increasing radiation dose and levels of induced DNA dsb's decrease with post irradiation incubation time. Some workers have shown bi-phasic repair kinetics, with an initial rapid repair rate (half-time, $\tau_{\frac{1}{2}}$ of ~10-15 minutes) followed by a prolonged slower rate of repair ($\tau_{\frac{1}{2}}$ of ~40-200 minutes). Other workers, however, have only observed a linear repair rate. Of particular interest to the AA/C1 cell line Zaffaroni *et al.* (International Journal of Radiation Biology, 66, 279-285, 1994) have shown a correlation between poor repair rates and survival fractions where the most radiosensitive have the lowest repair kinetics. Pulse field gel electrophoresis (PFGE) was therefore employed to determine whether or not AA/C1 cells were deficient in DNA dsb repair. For dsb analysis PFGE is used as a molecular sieve in which DNA greater than approximately 2 Mb in size do not enter the gel, whereas smaller fragments, produced by dsb's, are slowly teased into the gel.From the preliminary results presented in figure 3 it can be seen that as time increases between irradiation and sample lysis so the degree of DNA smearing decreases. This indicates a decrease in the amount of fragmented chromosomal DNA, indicating that the AA/C1's are most likely capable of effective DNA dsb repair.

It has been proposed (Radford, International Journal of Radiation Biology 66, 557-560, 1994) that following irradiation there is a race between effective DNA repair and the onset of apoptosis It is conceivable that if the repair kinetics for the AA/C1 cells are poor then the "race" is won by the apoptic pathway rather than cell recovery. It is possible that following extensive sublethal injury and partial repair that AA/C1 cells may require other factors to prevent the onset of apoptosis. Alternatively the radiosensitivity of the AA/C1 cells may be indicative of their near "normality" in that they retain a higher degree of cellular integrity to survive sublethal damage compared to other cell lines; *i.e.* the AA/C1s' are "one step" closer to apoptosis than the other cell lines compared above.

Anchorage independent growth has frequently been used as a marker for *in vitro* transformation since it compares favourably with subsequent nude mouse tumourigenicity assays. It should be noted, however, that anchorage independent growth has been induced in normal human fibroblasts by high serum or hydrocortisone; hence, increased growth in agar may not represent anchorage independence but rather a growth factor requirement. Also it has been shown that anchorage independent growth can occur either early or late in the process of tumorigenesis. Hence there are still some question marks regarding the usefulness of agar growth as a marker of malignant transformation.

With most mutational assays a fixation period is required between mutagen exposure and the subsequent assay in order that a response may be observed. For AA/C1 cells the plating of agars following irradiation therefore took place either directly after irradiation, to see if there were any immediately inducible effects, or 7 or 21 days later. As with all mammalian non-tumourigenic cell lines the rate of background agar growth is very low, ~10^{-5} per surviving cell. Preliminary results have shown no significant increase in the number of agar colonies after X-ray doses up to 4 Gy when cells are plated at seven and twenty-one days after irradiation. The results when cells are plated immediately afer irradiation are shown in

figure 4. These data do suggest an increase in the proportion of surviving cells able to undergo anchorage independent growth. However, no significant effect is apparent below a dose of ~1-2 Gy. Further experiments are in progress using the AA/C1/SB cell line, a cell line established after sodium butyrate treatment of AA/C1 cells.
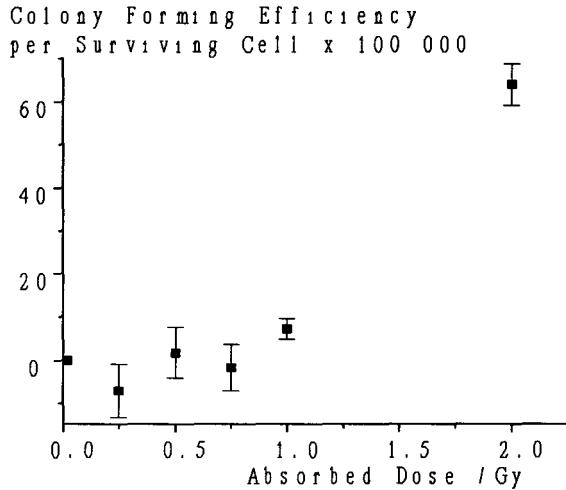
FIGURE 4: Dose-response for growth in agar for immediate plating after exposure to 250 kVp X-rays

Publications

1. The Effect of Dose-Rate on the Transformation Frequency of C3H 10T½ Cells Irradiated with 3.3 MeV Alpha-Particles. A.J. Mill, S.C. Hall, D.T. Goodhead, L.A. Allen, A. Butler, S. Marsden & D.L. Stevens.
    Paper presented at the Eleventh Symposium on Microdosimetry, Gatlinburg, Tennessee, U.S.A., 13-18 September 1992.

2. Dose-rate Effects for Transformation of C3H 10T½ Cells Irradiated with 3.3 Mev α-Particles. A.J. Mill, S.C. Hall, D.T. Goodhead, L.A. Allen, A. Butler, M.M. Lehane, S. Marsden and D.L. Stevens.
    International Journal of Radiation Biology, 65, 145, 1994. Paper presented at Radiation Research '93, Guildford, Surrey, U.K., 12-15 July 1993.

3. Factors likely to affect transformation frequency of C3H10T½ mouse fibroblasts.L.A. Allen, D. Bettega, A. Butler, P. Calzolari, D. Frankenberg, M. Frankenberg-Schwager, S. Futter, S.C. Hall, L. Hieber, M.M. Lehane, A.J. Mill, G.R. Morgan, L. Pariset, S. Pazzaglia, C.J. Roberts, and A. Saran.
    Paper presented at the International Symposium on Molecular Mechanisms of Radiation and Chemical Carcinogen-induced Cell Transformation, Mackinac Island, Michigan, U.S.A., 19-23 September 1993.

4. Characterisation of Foci Isolated from Irradiated C3H10T½ Cells. M.M. Lehane, A.J. Mill, S.C. Hall, L.A. Allen, A. Butler, A.C. Riches.
    Paper presented at the International Symposium on Molecular Mechanisms of Radiation and Chemical Carcinogen-induced Cell Transformation, Mackinac Island, Michigan, U.S.A., 19-23 September 1993.

5. Dose-Rate Effects for Transformation of C3H10T½ Cells Irradiated with 3.3 MeV Alpha-Particles. A.J. Mill, S.C. Hall, D.T. Goodhead, L.A. Allen, A. Butler, M.M. Lehane, S. Marsden, D.L. Stevens.
    Paper presented at the International Symposium on Molecular Mechanisms of Radiation and Chemical Carcinogen-induced Cell Transformation, Mackinac Island, Michigan, U.S.A., 19-23 September 1993.

6. Chromosome Changes in Spontaneous and Radiation Transformed C3H10T½ Mouse Embryo cells. M.M. Lehane, C.J. Roberts, A.J. Mill, L.A. Allen, A.C. Riches, P.E. Bryant, C.V. Briscoe, J. Melville. International Journal of Radiation Biology, 66, 426, 1994.
    Paper presented at the 18th L.H. Gray Conference, Radiation Damage in DNA: Physics, Chemistry and Molecular Biology, University of Bath, Avon, U.K., 10-14 April 1994.

7. Characterisation of Foci Isolated from Irradiated C3H10T½ Cells. M.M. Lehane, A.J. Mill, S.C. Hall, L.A. Allen, A. Butler, A.C. Riches, P.E. Bryant, C.V. Briscoe, J. Melville, C.J. Roberts.
    Paper presented at the joint meeting of the Association for Radiation Research and the Irish Radiation Research Society, University College, Dublin, Ireland, 23-26 June 1994.

8. A Standardised Protocol for the C3H 10T½ Cell Oncogenic Transformation Assay. D. Bettega, D. Frankenberg, L. Hieber, A.J. Mill, C.J. Roberts, A. Saran, L.A. Allen, P. Calzolari, M. Frankenberg-Schwager, M.M. Lehane, G.R. Morgan, L. Pariset and S. Pazzaglia.
    Paper presented at the joint meeting of the Association for Radiation Research and the Irish Radiation Research Society, University College, Dublin,Ireland, 23-26 June 1994.

9. Relationship between Morphology, Tumourigenicity, and other Characteristics of Spontaneous and Radiation Transformed cells. M.M. Lehane, A.J. Mill, L.A. Allen, A.C. Riches, P.E. Bryant, C.V. Briscoe, J. Melville.
    Paper presented at the meeting of the Association for Radiation Research, University of St. Andrews, Scotland, U.K., 5-8 April 1995.

10. Dose-Effect Relationships for Cell Transformation in a Human Epithelial Colorectal Cells. P.C. Clapham, A.J. Mill and C. Paraskeva.
    Paper presented at the meeting of the Association for Radiation Research, University of St. Andrews, Scotland, U.K., 5-8 April 1995.

11. The Effect of Low Doses on Cell Transformation in C3T 10T½ cells using a European Standardised Protocol. D. Bettega, D. Frankenberg, L. Hieber, A.J. Mill, G.R. Morgan, A. Saran, L.A. Allen, P. Calzolari, M. Frankenberg-Schwager, M.M. Lehane,

C.J. Roberts, L. Pariset and S. Pazzaglia.
Paper presented at the 10th International Congress of Radiation Research, Würzburg, Germany, 27 August - 1 September 1995.

12. Relationship between Morphology, Tumourigenicity, and other Characteristics of Spontaneously and Radiation transformed cells. M.M. Lehane, A.J. Mill, L.A. Allen, A.C. Riches, P.E. Bryant, C.V. Briscoe, J. Melville.
Paper presented at the 10th International Congress of Radiation Research, Würzburg, Germany, 27 August - 1 September 1995.

13. Determination of the Cell Transformation Efficiency of Hot Particles. P.J. Darley, M.W. Charles, A.J. Mill and L.A. Allen.
Paper presented at the 10th International Congress of Radiation Research, Würzburg, Germany, 27 August - 1 September 1995.

Head of Project 2: Prof. Dr. Frankenberg

II. Objectives for the reporting period

(a)   Participation in the standardization and intercomparison experiments for oncogenic transformation of C3H10T½ cells.

(b)   Experimental determination of the oncogenic transformation in C3H10T½ cells by carbon-K characteristic x-rays and by ^{60}Co gamma-rays as a reference radiation. Construction of an x-ray tube for the production of characteristic ultrasoft x-rays at high flux using electrons. This activity became necessary because the proton accelerator for the generation of ultrasoft x-rays is no longer available.

III. Progress achieved including publications

Oncogenic transformation of C3H10T½ cells by C_K characteristic x-rays

Characteristic carbon-K photons are an excellent tool for investigating the role of energy deposition patterns responsible for the induction of cancer, the principal risk from low doses of radiation. The photo-electron of a carbon-K photon (277 eV) has an energy of about 260 eV which generates 10 to 14 ionisations in a volume with a cord length of about 7 nm which is comparable with the diameter of the DNA double helix. Induction of DNA double strand breaks (dsb) by carbon-K photons is more effective by a factor of 3.8 compared with ^{60}Co gamma-rays (Frankenberg *et al.*, 1986). Similarly, the RBE of carbon-K photons at inducing chromosomal aberrations is approximately 3 (Virsik *et al.*, 1980, Thacker *et al.*, 1986). With this background, the RBE of carbon-K photons at inducing cell transformation was determined.

In this report we present all experimental data obtained on oncogenic transformation of C3H10T½ cells after exposure to characteristic ultrasoft x-rays and to ^{60}Co gamma-rays as a reference radiation. By bombarding an extremely pure graphite target with 520 keV protons a carbon-K photon beam was obtained which traverses a monolayer of C3H10T½ cells. The cell nucleus of these cells has a mean thickness of only 2.2 µm yielding a linear average dose, D, of 0.55 of the entrance dose. The cell survival as a function of the average dose, D, after exposure to carbon-K photons and ^{60}Co gamma-rays as a reference radiation together with RBE-values at different survival levels are shown in fig. 1. The curves represent linear-quadratic fits to the data. From the coefficients of the linear terms the RBE of 4.1 for C_K photons relative to ^{60}Co gamma-rays was calculated. At higher doses the RBE decreases to about 2 as depicted for definite survival levels in the inset of fig. 1.

Transformation frequencies after exposure to C_K photons and ^{60}Co gamma-rays are presented in fig. 2 as a function of the linear average dose. The solid lines in fig. 2 correspond to a linear-quadratic dose-relationship of the number T of transformants per 10^4 surviving cells. At low doses C_K photons are 4 times more efficient than ^{60}Co gamma-rays at inducing oncogenic cell transformation of C3H10T½ cells, as calculated from the coefficients representing the linear component of the fitted curves. The RBE is dose dependent and decreases with dose from 4.0 to about 2.0 at a transformation frequency of about 1 transformant per 10^4 survivors. The inset in fig. 2 shows RBEs of C_K photons at selected transformation frequencies.
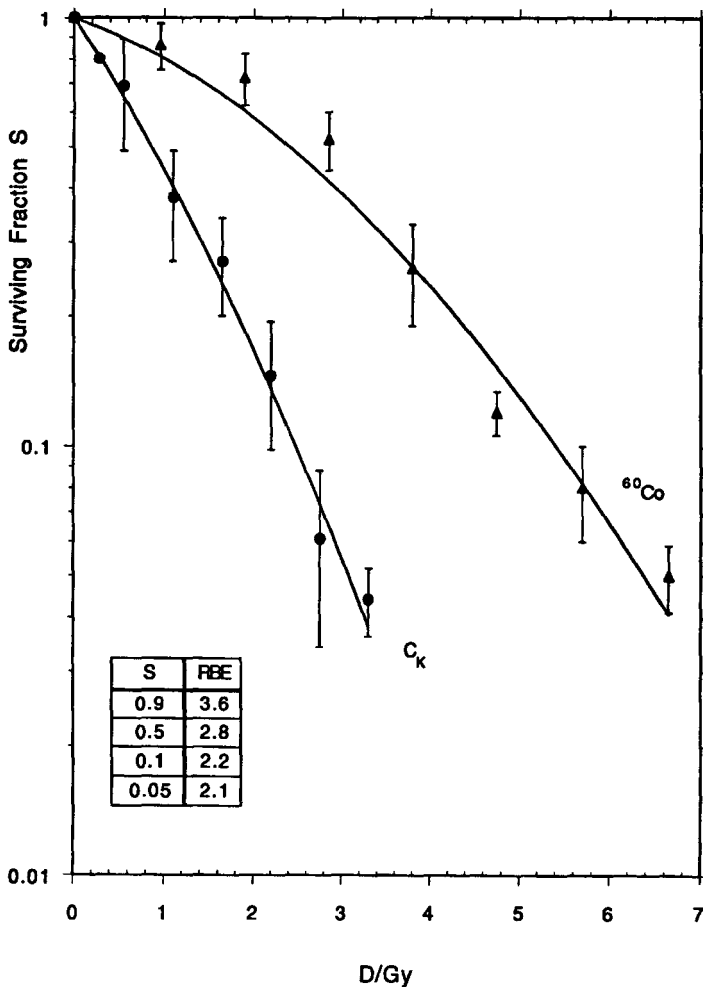
FIG. 1: C3H 10T½ survival after irradiation with C_K characteristic ultra-soft X-rays and ^{60}Co γ-rays. S: surviving fraction; D: dose.

The observation that at low doses C_K ultrasoft x-rays are 4 times more efficient than ^{60}Co gamma-rays at inducing oncogenic cell transformation of C3H10T½ cells means that clusters of 10 to 14 ionizations in volumes of less than 7 nm chord length corresponding to dE/dx-values of about 20 keV μm^{-1} on the average (ICRU 1970, Terrissol et al. 1978) are highly effective at inducing this endpoint. For particles with similar ionization density at the nanometer level along their tracks (approximately L_∞= 40 keV/μm) the linear component of the yield of transformants has an RBE of about 2 relative to orthovoltage X-rays (Yang and Tobias, 1980, Hei *et al.*, 1988). Based on the RBE of about 2 of orthovoltage X-rays relative to ^{60}Co gamma-rays for oncogenic transformation of C3H10T½ cells (Borek *et al.*, 1983), an RBE of about 4 of 40 keV μm^{-1} particles relative to ^{60}Co gamma-rays can be calculated. This value agrees with our RBE = 4.0 of C_K photons relative to ^{60}Co gamma-rays for the linear

component of the yield of C3H10T½ cell transformants. The agreement between the RBE-values of C_K X-rays and of particles of comparable LET determined for oncogenic transformation of C3H10T½ cells points to the importance of the ionization density at the nm-level as the parameter most relevant for oncogenic cell transformation rather than the *distribution* of such clusters which may be stochastic (as for C_K X-rays) or along a particle track.

$T/10^4$ viable cells	RBE
0.1	2.6
0.5	2.1
1.0	2.0
1.4	2.0
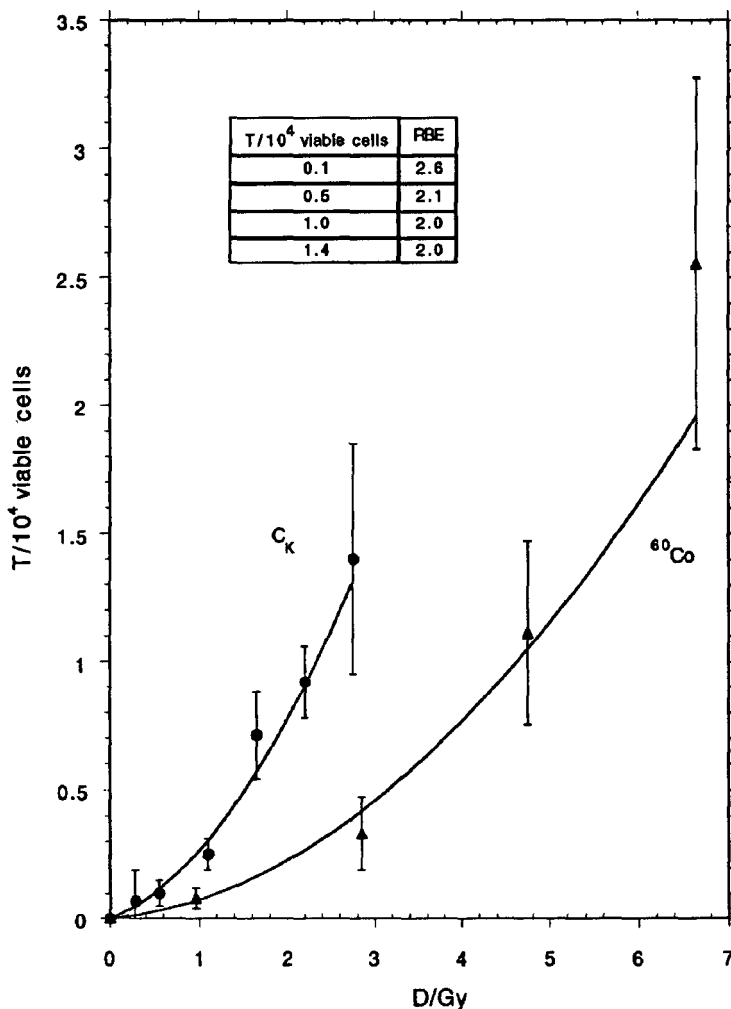
FIG. 2: Transformation of C3H 10T½ cells by C_K characteristic ultra-soft X-rays and ^{60}Co γ-rays. S: transformation; D: dose.

There is experimental evidence for oncogenic cell transformation being caused by (restriction enzyme mediated) dsb (Bryant and Riches, 1989, Borek *et al.*, 1991). The RBE of C_K characteristic X-rays relative to ^{60}Co gamma-rays at inducing dsb in yeast cells was found to be 3.8 (Frankenberg *et al.*, 1986) which is in accordance with the RBE = 4 for the linear

component of oncogenic cell transformation. This correlation supports the hypothesis that single radiation-induced dsb are DNA lesions which may be important for the induction of oncogenic cell transformation. A quadratic component for the yield of oncogenic cell transformation observed at higher doses of C_K X-rays implies that with decreasing mean distance between induced dsb cell transformation may also be caused by interacting dsb. This agreement of RBE-values supports the view that highly localized (7 nm) energy deposition events (277 eV) can efficiently induce dsb and chromosomal aberrations which may lead to oncogenic cell tranformation. Furthermore, by comparing the energy deposition patterns of carbon K photons and ^{60}Co gamma-rays it is the electron track ends (electrons with energies between about 100 eV and several hundred eV) which are responsible for oncogenic cell transformation after exposure to gamma-rays, x-rays or electrons.

X-ray tube for the production of characteristic ultrasoft x-rays at high flux using electrons

Since the 520 keV proton accelerator was no longer available an x-ray tube for the production of characteristic ultrasoft x-rays by electrons was constructed. The x-ray tube consists of a metal housing which is continuously pumped by a turbo-molecular pump (fig. 3). The cathode consists of five parallel tungsten wires 50mm in length and separated by 5 mm. The anode can be changed so that several characteristic x-ray energies are available (C_K: 277 eV, Cu_L: 923 eV, Al_K: 1487 eV, Ag_L: 2984 eV, Ti_K: 4511 eV, Fe_K: 6404 eV). The x-ray beam passes through the cathode filaments. High voltage and anode current are stabilized. For C_K and Cu_L radiation a 3.5 μm mylar foil with aluminium coating supported by a perforated aluminium plate with an aperture ratio of 47 % is used as a vacuum window. For Al_K radiation and all higher energies the window consists of a 7 μm aluminium foil and the same perforated plate. The foils have been optimized with respect to low absorption, low gas permeability and favourable filter characteristics for the photon beam. Additional filters improve the purity of the beam.

aperture for the exit of the photons
gas filling (hydrogen or helium)
air gap
guard ring
collector
high potential electrode
sector shutter
vacuum window
cathode
anode
vacuum
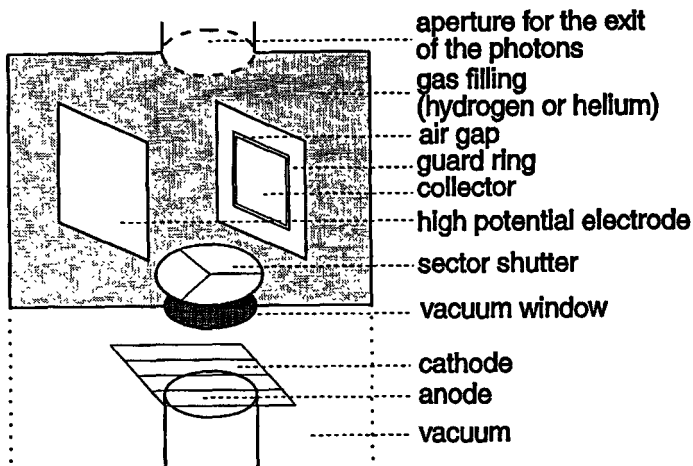
FIG. 3: X-ray tube with monitor chamber.

The photon beam can be stopped by a sector shutter just above the vacuum window. The beam passes a water cooled flight chamber continuously flushed with helium (hydrogen for C_K) in order to reduce the inhomogeneities of the photon beam and to monitor the dose during

the experiments. The monitor chamber consists of two parallel brass plates one of which is subdivided into an inner collector and a guard ring. The plates are positioned parallel to the beam axis and have a separation of 40 mm corresponding to the diameter of the collimated beam. A 1.5 µm mylar foil with an aluminium coating is used as the gas/air interface on top of the flight tube (fig. 3).

The absolute measurement of absorbed dose was made using an extrapolation chamber with a small volume ($\approx$0.4 - 4.0 x 10^{-7} m^3). The rear circular electrode is subdivided into an inner and outer graphite electrode like the monitor chamber. The high potential front electrode is a polycarbonate foil with a conductive aluminium coating. The potential of the chamber is kept at + 300 V independent of the distance of the electrodes, because the chamber reading has not yet been found to change with the distance at that potential.

For the calculation of absorbed dose three correction factors were taken into account. The density factor corrects for air density effects. Because of partial absorption of the characteristic x-rays within the chamber the entrance dose was calculated from measured values. The polarity factor was set to unity because measured values for positive and negative polarity were independent from the distance between the electrodes.

The dose rate depends linearly on the anode current and on the high potential U roughly following the rule: dose rate $\approx(U-U_0)^{1.9}$ with U_0: accelerating potential of the characteristic x-rays. The operating voltage and anode current are optimized with respect to the tungsten cathode evaporation and bremsstrahlung background. The x-ray tube yields dose rates of 53 Gy/min for Cu_L (operating voltage: 3 kV), 28 (100) Gy/min for Al_K (3 kV, 4.5 kV), 13 Gy/min for Ti_K (10 kV) and 8 Gy/min for Fe_K radiation (10 kV) at the entrance surface of cells in monolayer at the maximum anode current of 100 mA.

The dose uniformity within the area of cell dishes (ø 30 mm) is better than ± 3 % as measured with the extrapolation chamber using an aperture of 2 mm. Repeatability of dosimetry measurements during 2 h is about ± 1 %.

Spectrometry was performed using a Si(Li) detector. The bremsstrahlung background was estimated by a fit-program using least-square estimation. The ratio of bremsstrahlung-photons to Al_K-photons is 3 % (4 %) for 3 kV (4.5 kV). Because of the good filter properties of the 7 µm aluminium foil above the aluminium K edge, most of the bremsstrahlung has energies lower than the aluminium peak.

References

Borek, C., Ong, A., Morgan, W.F. and Cleaver, Z.E., 1991, Molecular Carcinogenesis, 4, 243-247

Borek, C.,Hall, E.J., and Zaider, M., 1983, Nature, 301, 156-158

Bryant, P.E. and Riches, A.C., 1989, British Journal of Cancer, 60, 852-854

Frankenberg, D., Goodhead D.T., Frankenberg-Schwager, M., Harbich, R., Bance, D.A., and Wilkinson, R.E., 1986, Int. J. Radiat. Biol. 50, 727-741.

Hei, T.K.,Komatsu, K., Hall, E.J., and Zaider, M., 1988, Carcinogenesis, 9, 747-750

International Commission on Radiation Units and Measurements, 1970, Report 16

Terrissol, M., Patau, J.P., and Eudaldo, T., 1978, 6th Symposium on Microdosimetry, edited by Booz, J. and Ebert, H.G. (Harwood Academic Publishers Ltd), pp. 169-178

Thacker, J., Wilkinson, R.E., and Goodhead, D.T., 1986, Int. J. Radiat. Biol. 49, 645-656.

Virsik, R.P., Schäfer, Ch., Harder, D., Goodhead, D.T., Cox, R., and Thacker, J., 1980, Int. J. Radiat. Biol. 38, 345-557.

Publications:

Frankenberg, D., Kühn, H., Frankenberg-Schwager, M., Lenhard, W., Beckonert, S.: Low energy (280 eV) electrons are 4.5 times more effective than gamma-rays to induce oncogenic cell transformation, 43rd Ann. Meeting Radiat. Res. Soc., San Jose/Cal., 1995, Abstract, p.167

Frankenberg, D., Kühn, H., Frankenberg-Schwager, M., Lenhard, W., Beckonert, S.: 0.3 keV carbon K ultrasoft x-rays are four times more effective than gamma-rays to induce oncogenic cell transformation at low doses, submitted to Int. J. Radiat. Biol.

Frankenberg, D.: DNA double-strand breaks as critical lesions for radiation induced cell transformation. Int. Symp. on Molecular Mechanisms of Radiation-Induced Cell Transformation, Mackinac Island, Michigan 1993, Abstract

Frankenberg, D., Kühn, H., Frankenberg-Schwager, M.: Onkogene Transformation von Säugerzellen durch ultraweiche charakteristische Röntgenstrahlen. Jahresbericht, GSF-Forschungszentrum für Umwelt und Gesundheit, 1992, 173-177

Michalik, V. and Frankenberg, D.: Simple and complex double-strand breaks induced by electrons, Int. J. Radiat. Biol. 66, 467-470

Michalik, V. and Frankenberg, D.: Two types of double-strand breaks in electron and photon tracks and their relation to exchange type chromosome aberrations, submitted to Radiat. Environm. Biophys.

Rassow, St.: Dosimetry for a 0.3 - 10 keV x-ray tube for cell irradiation, AAPM Meeting, Boston, Med. Phys., Vol. 22, 1995, 994, Abstract

Rassow, St., Kasten, G., Frankenberg, D.: An x-ray tube for characteristic x-rays between 277 eV and 6404 eV, 10th Internat. Congress of Radiation Research, Würzburg, 1995, Abstract

Rassow, St., Kasten, G., Frankenberg, D.: Characteristics of an x-ray tube for aluminium K_α x-rays (1487 eV), DGMP Tagung Würzburg (Röntgen-Gedächtnis Kongreß), 1995, Abstract

Head of Project 3: Mr. Roberts

II. Objectives for the reporting period

1.   Assessment of the rat tracheal epithelial cell (RTE) assay

2.   Use of transgenic mice for *in vivo* mutation measurements

3.   Mechanistic studies - cytogenetics and cell fusion

III. Progress achieved including publications

The risk of carcinogenesis is the major concern of radiological protection, especially at occupational or environmental doses. Animal or cellular models have an important role to play both in validating risk estimates and furthering our understanding of carcinogenesis. At present the contribution of such models is constrained by their limitations. In parallel with the main C3H 10T½ study, we have undertaken to evaluate other models of transformation or tumorigenesis to determine whether they have the potential to be used for quantitative measurements.

In vitro transformation assays need to be:

- Relevant - ideally based on primary cultures of epithelial cells that are likely targets *in vivo*
- Reproducible - based on objective criteria that can be equated directly to tumorigenicity
- Sensitive - the ability to measure the effect of small doses is crucial for radiological protection purposes

The project has three main parts:

1.   The rat tracheal epithelial cell (RTE) assay
2.   Use of transgenic mice for *in vivo* mutation measurements
3.   Mechanistic studies - cytogenetics and cell fusion

1.   RTE assay

The Rat Tracheal Epithelial Assay (RTE) has considerable potential as a 'bridging system' enabling tumorigenesis *in vivo* to be compared directly with transformation *in vitro*. It is has several attractive features:

I.   It uses primary epithelial cells of a relevant type, also found in man.
II.   Exposure can be *in vitro* or *in vivo*.
III.   Assays can be *in vivo* or *in vitro*.
IV.   Tumour types arising from *in vitro* exposures are similar to those occurring naturally.

The assay, as described by Thomassen and co-workers[1], claims to selectively isolate pre-neoplastic variants *via* their resistance to serum-induced differentiation. However, for the assay to be truly useful it must be reliable and sensitive. Initial investigations have focused

on the reproducibility of the technique and factors affecting transformation of the cells.

2. Transgenic mice

The availability of transgenic mice carrying a well-studied reporter gene (lacI - lacZ) allows mutations to be measured directly in vivo in any tissue. This approach is particularly attractive for radon studies since it allows comparative measurements in lung, bone marrow and other tissues, combined with regular sampling during lifetime exposure. However, it is important to establish the sensitivity of the method for low dose applications. The studies described here are based on the Stratagene Big Blue mouse. This animal contains approximately 40 copies of a lacI+lacZ shuttle vector per cell. Mutation in the lacI gene de-represses the lacZ gene allowing β-galactosidase to be expressed. Following recovery and packaging of the shuttle vector into *E. coli* mutant plaques appear blue, facilitating scoring.

3. Mechanistic studies

The mechanism of C3H 10T½ transformation is still uncertain. It has been suggested that it is a two step process, the first being a high frequency event occurring in nearly all the cells and the second a rare event occurring in only a small number of cells. Induction of chromosome instability has been proposed as the first event but this seems unlikely as it only happens in a relatively small number of cells. A better understanding of the mechanism may identify unequivocal markers of transformed cells, making the assay faster and more precise.

RESULTS

1. Bridging systems

A flow chart for the experimental procedure (fig.1) shows the principles involved.

Fig.1. Flow chart for isolation of rat tracheal epithilial cells
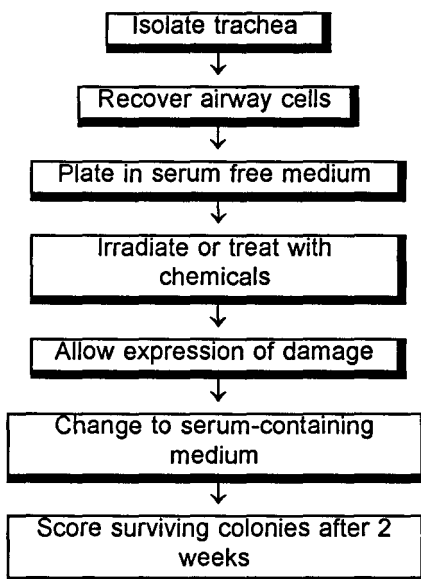
Initial experiments were carried out using the method of Thomassen et al[1]. However, it proved impossible to isolate viable cells using pronase treatment as described by the authors. Experimentation with the isolation procedure indicated that incubation of the tracheas for 90 min at 37^0C results released viable cells and this procedure was adopted for the experiments reported here. The number of cells isolated per trachea ranged from $1-5x10^5$, with a mode of $1.8x10^5$. Viability ranged from 74 and 95%. Overall, plating efficiency (PE) ranged from 0 - 10%, typical values being 0.8-2%. A number of factors were found to affect PE including age of donor animal, cell density and medium composition (fig. 2). Basal cells in the rat trachea preferentially bind the isolectin *Griffonia simplicifolia* I-B4 (GSI-B4)[2,3]. However, magnetic bead panning of the cell suspension prior to plating (Dynabead m450, 20:1 bead:cell ratio) did not increase the PE.

Morphological and immunocytochemical studies of the cultures indicated variable levels of contamination with endothelial and fibroblastic cells, which were capable of surviving prolonged exposure to serum-free medium. Given the low PE, contamination of the cell suspension with small (2-7 cells) clumps, possibly formed by clumping of the cells during plating, could not be completely excluded.

To investigate the sensitivity of the cells to radiation, cultures were irradiated with 2 Gy or 4 Gy ^{60}Co γ-rays and plated at different densities to accommodate the effect of cell density on PE (fig. 3). The cells appear radioresistant and the results suggest a shouldered survival curve. The actual survival values obtained were dependent on cell density, higher densities apparently leading to lower survival values. To try and overcome this problem feeder cells were added to normalise cell densities. Two types of feeder cell were used: NIH 3T3 fibroblasts (commonly used to support keratinocyte growth) and cells of RTE clones isolated from PE experiments. The 3T3 cells appeared to support growth of the RTE cells but did not give consistent plating efficiencies. The RTE clones either had no effect or were inhibitory.

2.   Transgenics

The methods for isolating and packaging the shuttle vector were as described by Stratagene. All products were obtained from them to ensure optimal recovery and expression of the shuttle vector. Isolation of high molecular weight DNA (>50kb) was checked by agarose gel electrophoresis prior to packaging.

In these initial experiments, Big Blue mice were obtained from Stratagene and exposed to whole-body doses of 2 Gy or 4 Gy from a ^{60}Co γ-ray source. Exposure time was approximately 10 minutes. Animals were either sacrificed immediately or were maintained under normal animal house conditions for various periods of time. On sacrifice, the lungs, thymus, spleen, bone marrow and GI tract were recovered, snap-frozen in liquid N_2 and stored at -80^0C. DNA was isolated using the recommended procedures.

Measurements have been obtained for stomach and lung mutation frequencies (see Table 1). Background mutation frequencies in this system appear to be tissue dependent, but may be in the order of $1x10^{-5}$. Mutations in both lung and stomach tissue were easily observed following irradiation with 2 Gy and 4 Gy. In the case of stomach, a greater than 15-fold increase over background was observed which was stable for over 2 months. Significantly increased mutation frequencies were also found in lung, but further work is needed to validate the apparent time dependence of mutation expression at different doses.

Fig. 2a. Effect of medium composition and plating density on PE of RTE cells
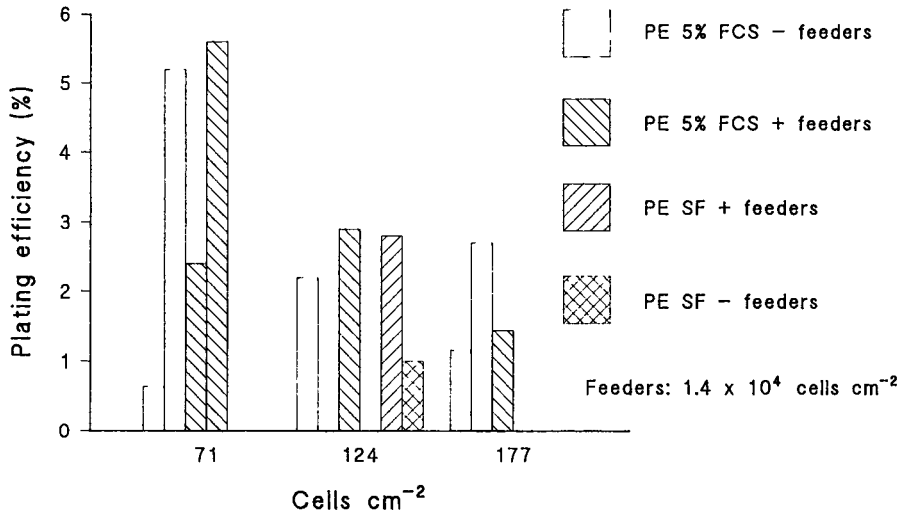
Fig. 2b. Effect of cell density and animal age on PE of RTE cells
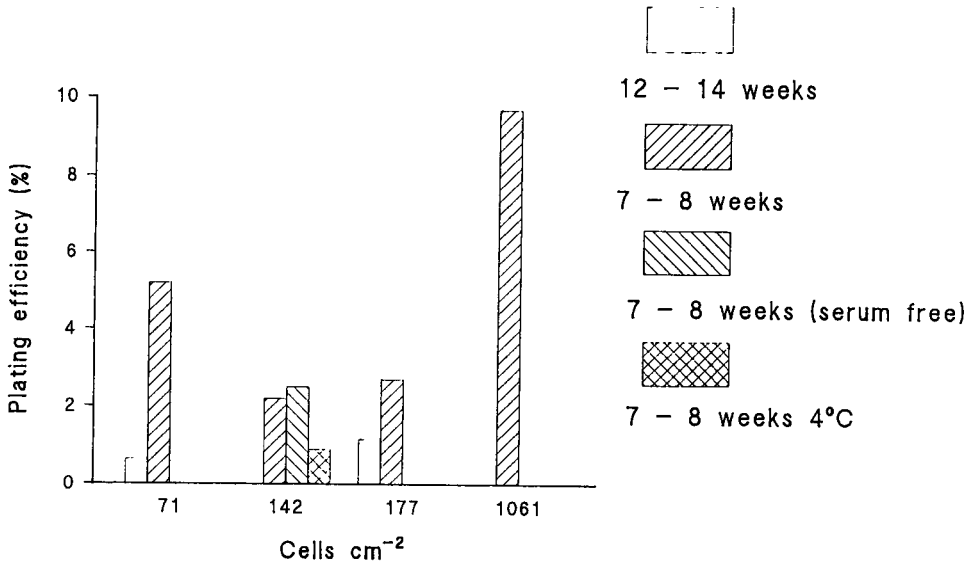
Fig. 3. Survival of RTE cells following irradiation
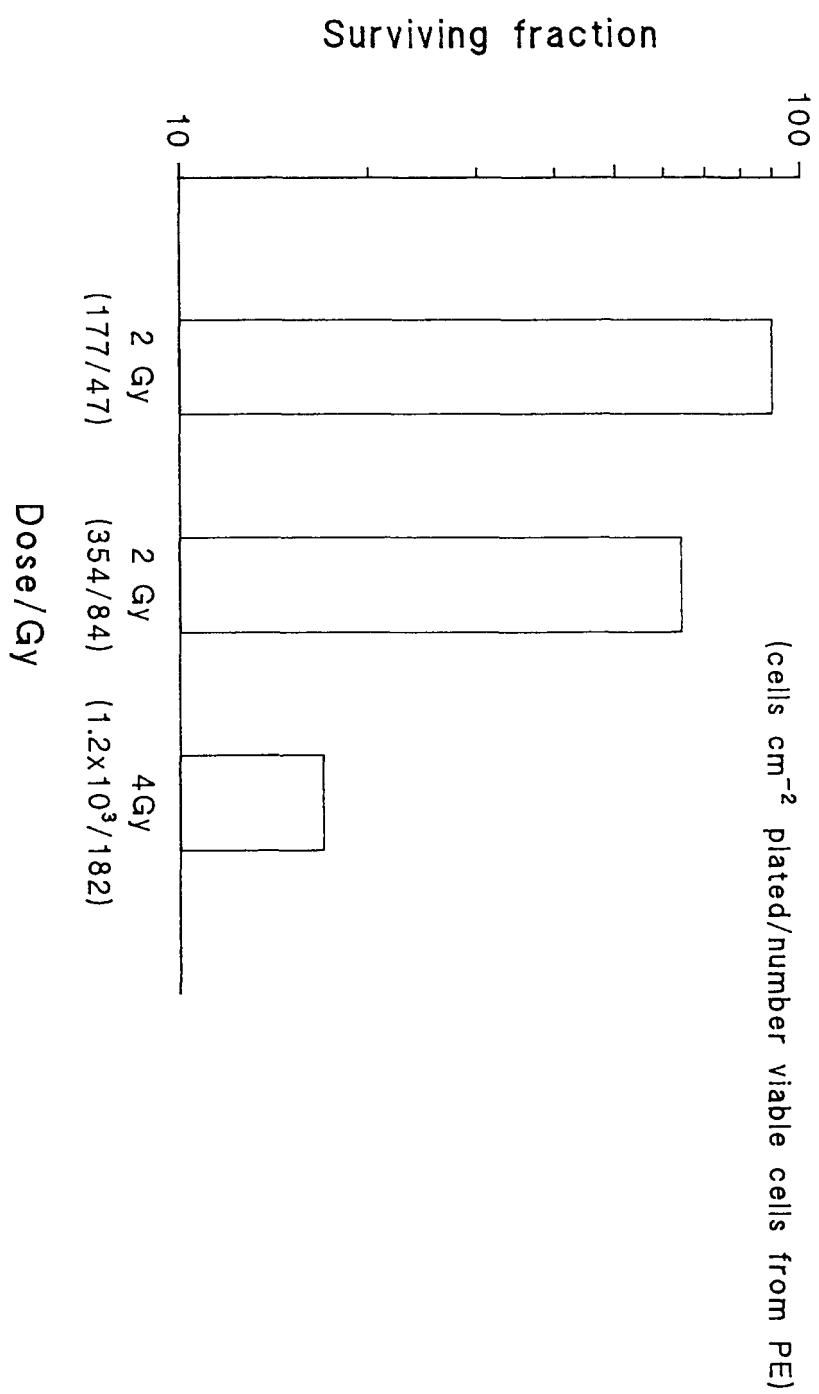
Table 1. Mutation frequencies in lung and stomach tissues of Big Blue mice after various times following whole body irradiation

Tissue (dose)	Time after exposure	Mutant plaques/ total plaques	Mutation frequency
Stomach (0 Gy)	29 days	4/302,000	1.32×10^{-5}
Stomach (4 Gy)	29 days	21/108,320	19.4×10^{-5}
Stomach (4 Gy)	69 days	65/282,191	23.0×10^{-5}
Lung (0 Gy)	0 hours	0/116,887	$< 1 \times 10^{-5}$
Lung (2 Gy)	24 hours	19/97,712	19.4×10^{-5}
Lung (4 Gy)	24 hours	7/212,307	3.3×10^{-5}
Lung (2 Gy)	48 hours	11/75,471	1.46×10^{-5}
Lung (4 Gy)	48 hours	48/112,528	42.7×10^{-5}

3. Mechanistic studies

3.1 Cytogenetics

Representative foci obtained from several transformation experiments carried out by Berkeley Technology Centre (BTC) were expanded in culture and inoculated into nu/nu mice for confirmation of tumorigenicity. Cell lines were established from the tumours and stored in liquid N_2 at sequential passages. Several foci and their corresponding tumour-derived cell lines have been examined and compared to the parent C3H 10T½ cells.

The parent line is hypo-tetraploid, as expected, with a modal number of 77 (fig. 4a.). Cell lines from a focus, before passage through an animal, show changes in chromosome number distribution but may or may not show changes in modal chromosome number. Any changes do not appear to correlate with tumour latency, although this has not yet been investigated in detail. In all cases examined so far, cell lines obtained from tumours show a reduction in the modal number of chromosomes, typically to 71 -73 (fig. 4b). In addition, these cell lines tend to have greater variation in chromosome numbers, ranging from <65 to >80, suggesting karyotypic instability.

3.2 Cell fusions

A series of cell fusion experiment were carried out between C3H 10T½ tumour cell lines to investigate possible complementation groups for tumorigenicity. In addtion, normal human fibroblast cells, HF27 (a kind gift of Dr. John Thacker, MRC Harwell), were fused with NIH 3T3 cells to investigate senescence.

3.2.1 HF27/3T3 hybrids
The HF27 cells had a very limited lifespan in culture, senescing after 5 - 9 subcultures. After fusion 49 mouse/human hybrid clones could be isolated with extended lifespans, suggesting that in many cases senescence could be overcome. These clones are being analysed for human and mouse chromosome complements in order to establish whether loss of senescence attributable to a specific effect or a non-specific phenomenon such as gene dosage.

Fig. 4a. Chromosome number in parent C3H10T½ cells
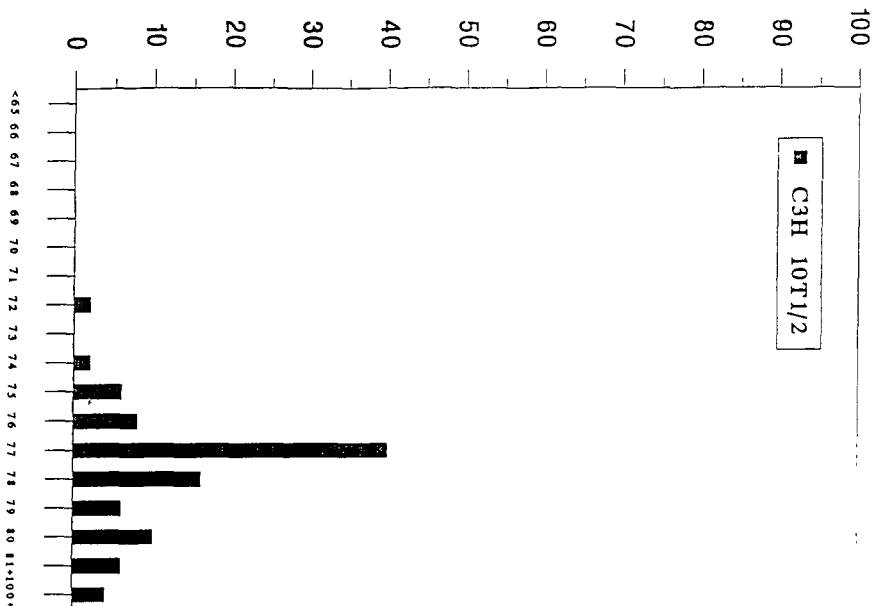
Fig. 4b. Chromosome numbers in three 10T½ tumour cell lines
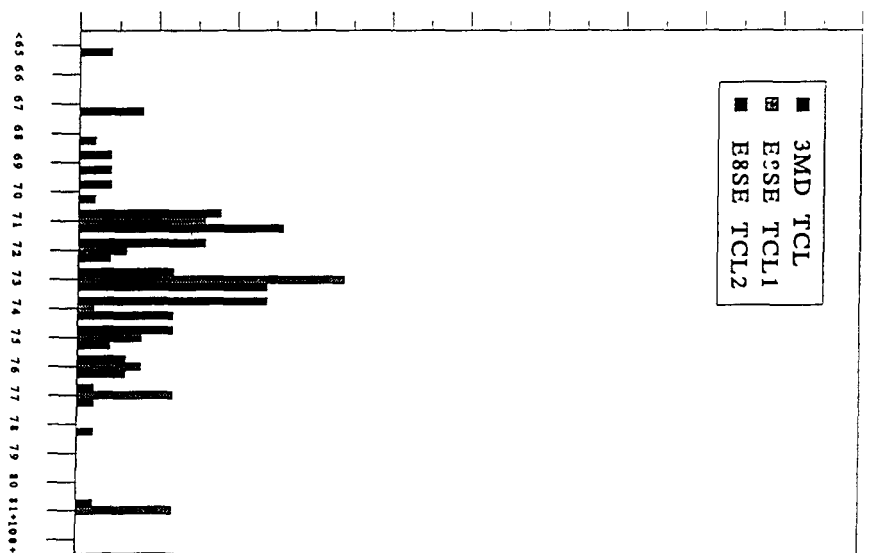
3.2.2 C3H 10T½ hybrids

Double selection methods needed to isolate fusion products from C3H 10T½ clones proved unsuccessful. The reason for this is not clear at present. Transfections with a plasmid vector and a retroviral vector conferring G418 and hygromycin resistance respectively were satisfactory but no doubly resistant clones could be isolated following fusion. Consequently this line of investigation was aborted.

DISCUSSION

1. Bridging systems - RTE assay and transgenics

Although there is a clear need for transformation assays which use human cells it is equally certain that animal-based transformation systems will be required to validate risk estimates. The clearly defined criteria of tumorigenicity is essential for validation of any approach intended to be used for radiological protection purposes and this can only be achieved in animals. The studies described here, carried out in parrallel with the group C3H 10T½ experiments, indicate the difficulty of reaching beyond those experiments to obtain reproducible data from primary cells.

The RTE assay remains an attractive proposition but further work is needed to overcome the low and variable PE which makes it difficult to obtain enough cells for useful experiments, particularly at low doses. An additional problem is that the cells which do grow may not be representative of the basal cell population as a whole and the implications of this are not clear at present.

The transgenic approach demonstrates that in vivo mutation frequencies can be measured relatively easily. This should yield valuable information about dose-response relationships in different tissues at different dose rates, and hence possible threshold effects, the persistance of muations and the modification of dose-response relationships by different agents.

2. Mechanistic studies

The mechanistic studies of ploidy changes following transformation of C3H 10T½ suggest that transformation is associated with loss of genes rather than activation of oncogenes. In addition, foci which are tumorigenic may appear little different to the non-transformed parent line, thus tumour cells in foci may be quite rare and misleading results could be obtained unless very specific, sensitive markers are used. Generally speaking, any population-based method may require its sensitivity to be carefully tested. Consequently, claims that increased tumorigenicity resulting from passage of cells through animals is due to genetic changes wrought by chromosomal instability, rather than selection of pre-existing variants may be premature.

REFERENCE

1. Thomassen, D.G., Saffiotti,U. and Kaighn, M.E. 1986, *Carcinogenesis,*7, 2033-2039

Head of Project 4: Prof. Tallone Lombardi

II. Objectives for the reporting period

1- participation in the standardisation of the C3H10T1/2 transformation assay and in the collaborative study of the dose-response relationship in cell survival and transformation after low doses of X-rays using the C3H10T1/2 system.

2- a systematic study of cell-cycle sensitivity variation of transformation frequencies and chromosome aberration in synchronised C3 H 10T1/2 cells exposed to 101 KeV/micron alpha particles. Extension of the study on transformation to CGL1 cells (Hela x skin fibroblast hybrid cells).

III. Progress achieved including publications

2a) Synchronisation techniques and radiobiological parameters of the CGL1 cells.

C3H10T1/2 cells
An essential requirement for the determination of cell cycle variation is to dispose of well synchronised cell populations which have the same characteristics of the exponential growing populations. Our first goal was then to test different synchronisation techniques to single out the most suitable in our experimental conditions.
The induction of cell cycle synchrony by means of chemical agents may result in a high background. Indeed, a value of 30×10^{-5} transformation/survivor was found in our laboratory in samples treated with 2×10^{-2} µg/ml colcemid, a concentration which was not cytotoxic. Two alternative techniques were therefore tested : one based on the release of cells from contact inhibition confluence and the second on mitotic collection of cells by shake-off. The two methods have been extensively described elsewere (Bettega et al. Radiat. Res.142, 1995) . The results can be so summarized:
Release from confluence. High cell yields were obtained about 2×10^6 cells/10 cm diameter dish. The progression of the population through the cell cycle was measured by flow cytometric analysis . At t = 0 h, 70-80% were G_1 cells but more than 50% were in G_1 over the full duration of the experiment (about 30 h). The first generation time of the population was longer than 25 h, compared with about 20 h in the asynchronous population.
Mitotic shake-off. . A total of 3.3×10^4 cells were collected per flask. Initial synchronization was high with both protocols: the initial mitotic index and percentage of paired G_1 cells after 2 h of incubation were both greater than 70% . Progression through the cell cycle was followed by measuring at various times, from 2 to 24 h from the collection, the mitotic index, fraction of labelled cells after tritiated thymidine incorporation and the relative number of cells. Our conclusions are that mitotic collection by shake-off produces populations with more than 70% of mitotic cells which progress in the cell cycle with doubling time and phase duration similar to asynchronous populations. A higher degree of synchrony after one generation time can be obtained by avoiding multiple collections and limiting cell maintenance in ice to under 40 minutes.

CGL1 cells
The Hela x skin fibroblast hybrid cell system, CGL1, was developed by Stanbridge et al (Science 215, 1982) and Redpath et al (Radiat. Res. 110, 1987) for in vitro transformation studies. In our experimental conditions plating efficiency of the asynchronous population was 67±8 %. No

significant difference was found when the cells were plated in the mylar dishes suitable for α irradiation for about 24 h (6 cells/ cm^2) and then replated at lower density in conventional Petri dishes. Generation time assessed from the slope of the growth curve in the time interval between 0 and 100 h was 20±2 h. A mean lethal dose of 0.57 ±0.06 Gy was found with 101 keV/μm α particles to be compared with the value of 0.6 Gy found in our laboratory and reported in the literature for C3H10 T1/2 cells.
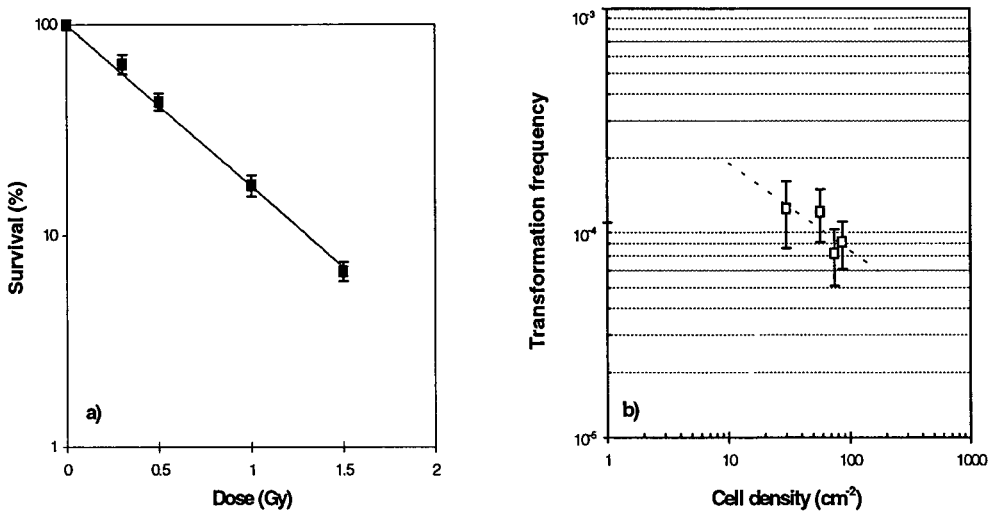
Figs.1 CGL1 cells: a) survival vs dose and b) transformation frequency vs viable cell density for cells exposed to 0.3 Gy of 101 KeV/μm α-particles. Bars are standard errors.

Fig. 1 a) shows survival vs dose in the interval 0.25 - 1.5 Gy. Fig 1 b) shows the trasformation frequency vs viable cell density. The data are well fitted by the function $Y = 4.86\ X^{-0.41}$ (where Y is transformation frequency (10^{-4}) and X viable cell density (cell/cm^2)). The slope is very similar to that found by Sun et al. with 7 Gy γ^{137}Cs (Radiat. Res. 114, 1988) in the density interval between 3 and 150 cell/cm^2. Following the convention adopted in the literature transformation frequency values were corrected using this cell density dependence and assuming a density of 50 cell/cm^2 as standard.

Cell populations were synchronized following a protocol similar to that we previously used with the C3H10T1/2 cells. A total of 8 x 10^6 cells / 150 cm^2 flask were plated about 24 h before collection (about 15 flasks per experiment) . One mitotic collection was performed after rinsing the flasks without serum . The collected suspension was mantained in ice throughout collection which took about 20 min. A total of 3x 10^5 cells were collected per flask. Initial mitotic index was 89±2 %. The harvested cells were plated in mylar dishes suitable for α irradiation . Progression through the cell cycle was followed by measuring the mitotic index,the fraction of labelled cells after tritiated thymidine incorporation and relative number of cells at various times between 2 and 24 h after the collection.

Figs. 2a) and 2b) show, as an example, the labelling and mitotic index distributions (upper part) and the growth curve (lower part) of one experiment performed with C3H10T1/2 and with CGL1 cells respectively.
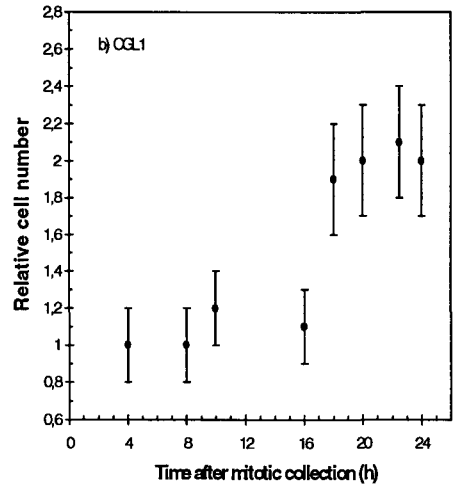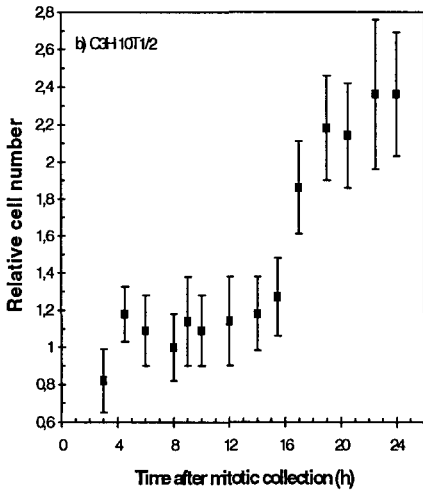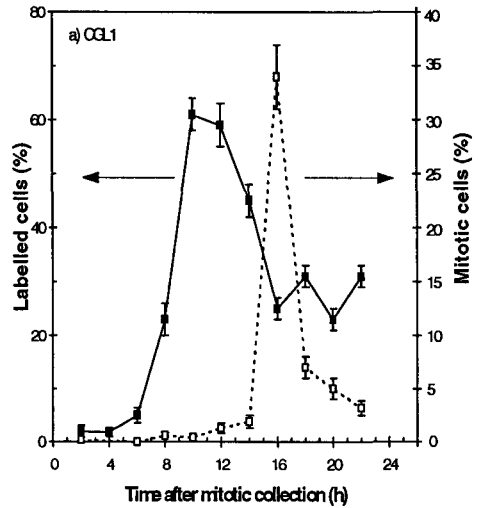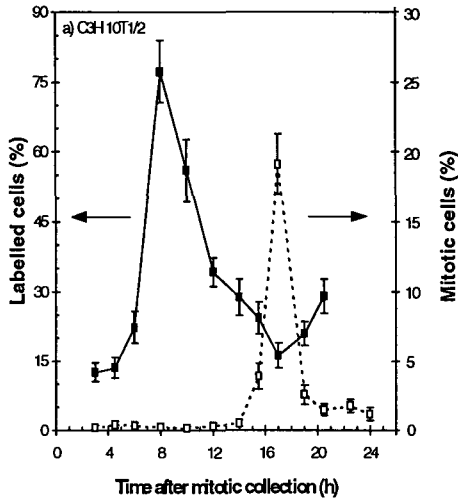
Figs. 2 a) and b). Labelling and mitotic index distribution (upper part) and the growt curve (lower part) of syncronised C3H10T1/2 and CGL1 cells.

2b) Transformation Frequencies

Cells synchronised by mitotic shake-off were irradiated with doses between 0.07 and 0.30 Gy of 4.3 MeV α-particles. For comparison, asynchronous populations were irradiated in parallel. 10T1/2 samples were treated using standard transformation assay technique.. CGL1 samples were treated using the protocol of Redpath et al (Radiat. Res. 110, 1987) and Sun et al (Radiat. Res. 114, 1988) with the Western blue based staining procedure. Briefly ,6 h after the irradiation the cells were removed by trypsinization and the immediately plated in 10 cm diameter dishes at cell concentration

such that the resulting number of viable cells was 50 /cm^2. The samples were incubated for 19 days with the growth medium changed once a week. The cultures were then fixed with 2% paraformaldehyde/PBS for 20 min , stained with Western blue and rinsed with PBS. Coloured foci 1 Figs 3 a) and b) show the results obtained with the C3H10T1/2 cells and CGL1 cells respectively.
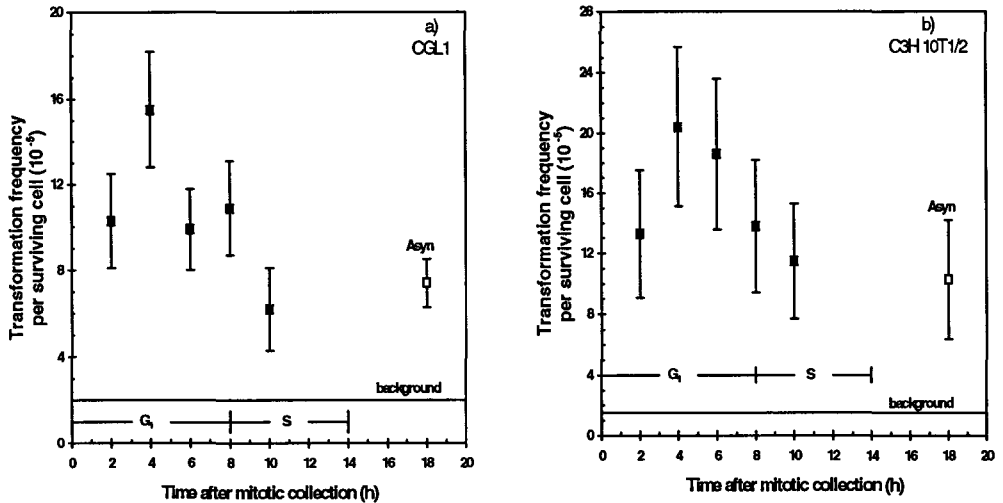
FIG. 3 ■ Transformation frequency vs time after mitotic collection in CGL1 cells (a) and C3H 10T1/2 cells (b) exposed to 0.3 Gy of 101 keV/μm α-particles. □ Value relative to the asynchronous population. Bars are standard errors.

With CGL1 the highest frequency value, $(15.5 \pm 2.7)\times10^{-5}$ transformation/survivor, occurs 4 h after mitotic collection, corresponding to mid G_1, and is a factor about 2 times higher than the value relative the asynchronous population $(7.4 \pm 1.1)\times10^{-5}$ transformation/survivor and the value relative to 10 h corresponding to early S $(6.2 \pm 1.9)\times10^{-5}$. The data seem to indicate that transformation frequency decreases when the cells progress from G_1 to the S-phase. The surviving fraction is constant throughout G_1 at a value of 0.63 ± 0.09. The results are very similar to those obtained with C3H 10T1/2 where the transformation frequency reaches its maximum between 4 and 6 h after mitotic collection and then decreases when the cells progress from G_1 to the S-phase. With C3H 10T1/2 errors are large so that no clear-cut conclusion can be drawn from the data per se. Nevertheless it should be noted that results using different cell systems from our laboratory are similar and similar results have also been obtained with different types of radiation by Miller et al. (Radiat. Res. 142, 1995) in C3H 10T1/2 cells exposed to monoenergetic neutrons and by Redpath et al. in HeLa x skin fibroblast exposed to fission spectrum neutrons (Radiat. Res. 141, 1995). All the data collected so far from different laboratories point to a region of increased sensitivity for transformation with high LET radiation as being located in G_1.

There have been different results with low LET radiation. Indeed, Miller et al. (Radiat. Res. 130,1992) found a 10-fold enhancement for cells in G_2 over cells irradiated in other phases with 3 Gy X rays. Cao et al. (Int. J. Radiat. Biol. 64, 1993) found a 5-fold enhancement in cells at mitosis over cells in the S-phase, with 3.5 Gy of ^{137}Cs γ rays. Redpath et al. (Radiat. Res. 121, 1990) found that G_2 and M cells are very sensitive compared to cells in mid-G_1 in HeLa x skin fibroblast exposed to ^{137}Cs γ rays. Cell cycle phase dependence of radiation transformation is different for high and low LET radiations, the common feature being the S-phase resistance.

2c)Chromosome aberration

Induction of chromosome aberrations were investigated in C3H10T1/2 cells irradiated with 3 Gy of X-rays and 0.6 Gy of alpha-particles. The two doses produce the same survival level of 37% in the asynchronous population. Cell-cycle phase at the time of irradiation was distinguished by using differential replication staining. X-irradiation induced more exchanges than deletions, whereas a predominance of isochromatid deletions was observed after alpha irradiation. This can be interpreted on the basis of the different patterns of energy deposition of densely- and sparsely-ionising radiation. Both X-rays and alpha-particles produced a significant increase in the frequency of Robertsonian translocations when cells are irradiated in G1 or S phase, but not in G2 phase.

Publications

1   D. Bettega, P. Calzolari, G. Noris Chiorda and L. Tallone Lombardi. Transformation of C3H10T1/2 cells with 4.3 MeV α-particles at low doses: single and fractionated dose effects. Radiat. Res. 131, 66-71, (1992)

2   D. Bettega, P. Calzolari, G. Noris Chiorda, A. Ottolenghi and L. Tallone Lombardi. Oncogenic transformation induced in C3H10T1/2 cells by high LET α-particles: fractionation effects. Joint Meeting of the Association for Radiation Research. Netherlands Radiobiology Society/ Swedish Radiobiology Society. St Andrews 1-4 April 1992

3   L. Tallone, D. Bettega, P. Calzolari, G. Noris Chiorda and A. Ottolenghi. A study of the transformation frequencies in C3H10T1/2 cells exposed to high LET radiation. Eleventh Symposium on Microdosimetry, Gatlimburg, USA, 13-18 sept. 1992, p. 101

4   A. Ottolenghi, D. Bettega, P. Calzolari, G. Noris Chiorda and L. Tallone Lombardi. Radiocarcinogenesis in vitro:"Inverse dose-rate effect". Il Nuovo Cimento 14D, 1191-1202 (1992)

5   D. Bettega, P. Calzolari, G. Noris Chiorda, A. Ottolenghi and L. Tallone Lombardi. Transformation frequencies and cell kinetic modifications in C3H10T1/2 cells exposed to single and fractionated doses of 4.3 MeV α particles. Proceedings of the VII Congresso Nazionale AIFB. Physica Medica IX, 12-15 (1993)

6   D. Bettega, P. Calzolari, A. Ottolenghi and L. Tallone Lombardi. Carcinogenesi da Radiazione: risultati in vitro. Relazione su invito. Atti del XVIII Congresso A.I.R.B. Napoli 21-23 Settembre (1989). Idelson 1993, pag. 137-147.

7   D. Bettega, P. Calzolari, G. Noris Chiorda, A. Ottolenghi and L. Tallone Lombardi. Cell cycle responces for oncogenic transformation in 10T1/2 cells exposed to α particles. International Symposium on Molecolar Mechanisms of Radiation and Chemical Carcinogen-Induced Cell Transformation. Michigan, USA September 19-24, 1993.

8   A. Ottolenghi, D. Bettega, P. Calzolari, C.K. Hill, G. Noris Chiorda and L.Tallone Transformation induced in C3H10T1/2 cells exposed to high LET radiations: an interpretation of the published data. Proceedings of the Eleventh Symposium on Microdosimetry . Gatlinburg, Tennessee . September, 13-18 1992. Radiat. Prot. Dosim. 52, 201-206, (1994)

9   D. Bettega, P. Calzolari, G. Noris Chiorda, A. Ottolenghi and L. Tallone Lombardi. Cell cycle dependence of 10T1/2 cell transformation. Proceedings of Radiation Research 1993, Guildford, UK, July 1993. Int. J. Radiat Res 65,145, 1994

10 M. Durante, G. Gialanella, G.F. Grossi, M. Nappo, M. Pugliese, D. Bettega, P. Calzolari, G. Noris Chiorda, A. Ottolenghi and L. Tallone Lombardi. Radiation-induced chromosomal aberrations in mouse 10T1/2 cells: dependence on the cell-cycle stage at the time of irradiation. Int. J. Radiat. Res, vol. 65, 437-447, 1994.

11 D. Bettega. Italian hadron radiobiology. Proceeding of the First International Symposium on Hadrontherapy, Como, Italy, Oct. 1993. Elsevier Science, U. Amaldi and B. Larsson Eds., 742-751 (1994)

12 D. Bettega, P. Calzolari, A. Costa, G. Noris Chiorda and L. Tallone. Oncogenic transformation of C3H10T1/2 cells exposed to α-particles: sensitivity through the cell-cycle. Radiat. Res. **142**, 276-280, 1995

13 S. Anziani, D. Bettega, P. Calzolari, G. Noris Chiorda, L. Tallone e L. Redpath. Is cellular sensitivity for radiation-induced transformation phase dependent?. VII Convegno Nazionale SIRR, Pisa, novembre 1994. Submitted to Physica Medica Dec. 94

Head of Project 5: Prof.Dr.Kellerer and Dr.Hieber

II. Objectives for the reporting period September 1992 to June 1995

(a)   Participation in the standardisation of the C3H 10T½ transformation assay to measure the transformation frequencies at low doses of sparsely and densely ionising radiation.

(b)   Investigation of cellular, cytogenetic, and molecular mechanisms underlying radiation-induced cell transformation and radiation carcinogenesis.

III. Progress achieved including publications

The aim of the project was to study the cellular, cytogenetic and molecular changes that occur during the multi-step process of neoplastic transformation induced by ionising radiation. The investigations should help to understand the mechanisms of radiation carcinogenesis. Syrian hamster embryo (SHE) cells were chosen as *in vitro* model system, since SHE cells can be transformed by various chemical carcinogenic agents and by the exposure to ionising radiation of different ionisation density. Cells of transformed phenotype induce tumors in nude mice after a short latency period, and tumor cell lines can be established. In addition, SHE cells do immortalize also spontaneously but at very low frequency. These spontaneously immortalized cell lines are non-tumorigenic, but they became neoplastically transformed if they were subcultured more than 40 times. Therefore, several stages in the transformation process can be studied.
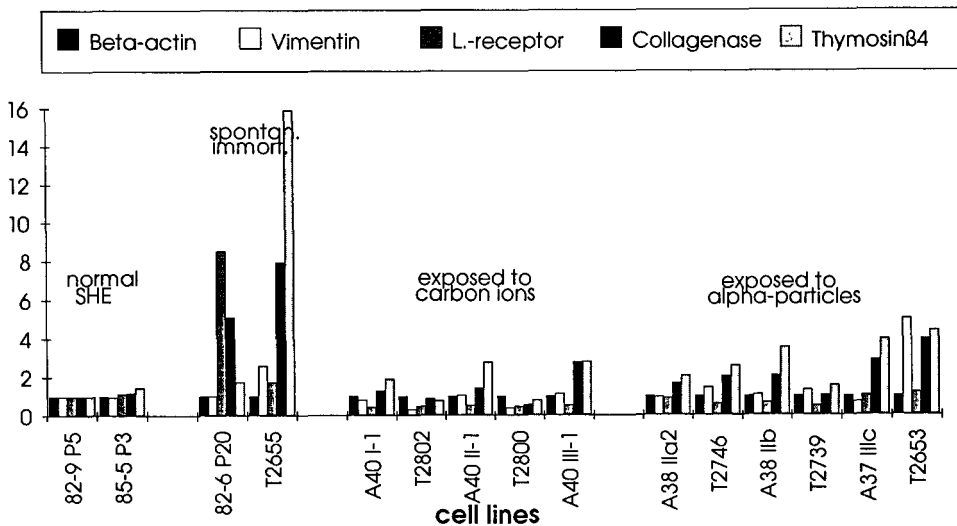
Figure 1: Expression pattern of different genes in spontaneously immortalized (82-6 P20), in radiation-transformed SHE cells(A####) and in tumor cell lines (T####) compared with normal SHE cells (82-9, 85-5). All data were normalized to ß-actin.

During the previous contract (No.BI7-0043), we have shown that the expression of several oncogenes is increased in radiation-transformed SHE cell lines. In addition, preliminary results on the deregulation of several other genes, that appear to be involved in neoplastic

transformation, has been investigated for one particular tumor cell line. During the present contract period, we have extended this analysis to a number of cell lines that have been immortalized and transformed either spontaneously or by alpha-particles or by 8 MeV/u carbon ions. The expression of the particular genes were studied by Northern Blot analysis. The up- or down-regulation of the vimentin gene, the laminin receptor gene, type IV collagenase gene, and of the thymosin ß4 gene is summarized in fig.1. Especially the laminin receptor gene, the type IV collagenase and thymosin ß4 are highly overexpressed in spontaneously immortalized SHE cells and in the tumor cell line T2655, established from a later on transformed cell line. But also radiation-transformed cell lines did show such over-expression, however only to a lower extent. The tumor cell lines exhibit only moderate changes in the expression of these genes. All the genes studied have been shown to be involved in animal or human carcinogenesis.

Table 1: **Cytogenetic Findings in a Spontaneously Transformed Syrian Hamster Cell Line A0 and the Corresponding Tumor-derived Cell Lines**

Passage Number	Tumor Cell Line	Modal Chromos. Number	Common Chromosome Abnomalities								Marker Chromosomes
4	-	44	-								
15	-	44	-								
18	-	44	2p- (76)								
25	-	44	2p- (93)								
43		44	2p- (100)								
	T-43.1	46/52	2p- (100)	3q+ (92)							
58		44	2p- (86)								
	T-58.1	44	2p- (92)								
	T-58.2	44	2p- (96)								
85		42/43	2p- (82)					-12 (91)	(-12,-12) (4)		+t(2q;12p) (100)
	T-85.1	45/46	2p- (84)	-5 (85)	5q+ (100)	-8 (80)	-12 (30)	(-12,-12) (70)	-Y (100)	+t(2q;12p) (92)
	T-85.2	45/46	2p- (96)				-12 (36)	(-12,-12) (64)		+t(2q;12p) (100)

+: gain of a whole chromosome
-: loss of a whole chromosome
p-: deletion in a short arm of a chromosome
q+: rearrangement of a long arm of a chromosome
q-: deletion in a long arm of a chromosome
t: translocation
( ): percentage of metaphases carrying a given chromosome aberration

Table 2: **Cytogenetic Findings in the Spontaneously Immortalized and Radiation-induced Immortalized Syrian Hamster Embryo (SHE) Cell Lines**

Cell line	Passage	Modal chr.No.	Common Chromosome Abnormalities							Markers		
C7	23	44, XY	-8 (100)	-16 (100)						+ rcp (8q; 16q) (100)		
C17	22	43, X0	-y (100)									
R I 5	30	44, XY	-3 (100)	-7 (100)	-15 (100)	16q- (97.4)	20q- (100)			+t (3p; 16q) (100)	+t (15q; 7q) (100)	+M (100)
R II 1	30	44, XY	3q+ (100)	6q+ (94.0)	9p+ (84 0)							
R II 5	23	44, XY	3q+ (100)	6q+ (94 0)								
R II 14	27	45/46, XY	3q+ (100)	6q+ (92.0)	+20 (94 0)	20p- (100)						
R II 17	25	44, XY										
R II 18*	29	79, XY	3q+ (100)	-6 (90.0)	-7 (85 0)	-8 (95 0)	-15 (90.0)	-X (100)	-Y (95.0)			

Table 3: **Cytogenetic Findings in the Spontaneously and Radiation-induced Morphologically Transformed Primary Syrian Hamster Embryo (SHE) Colonies that Became Immortal**

Primary colony	Modal chr.No.	Common Chromosome Abnormalities							Markers		
C7	44, XY	-8 (100)	-16 (100)						+rcp(8q; 16q) (98 0)		
C17	44, XY										
R I 5	44, XY	-3 (100)	-7 (100)	13p- (96.0)	-15 (100)	16q- (98.0)	20q- (88.0)	+t(3p; 16q) (96.0)	+t(15q; 7q) (100)	+M (100)
R II 1	44, XY	3q+ (100)	6q+ (98.6)								
R II 5	44, XY	3q+ (100)	6q+ (100)								
R II 14	44, XY	3q+ (100)	6q+ (100)								
R II 17	44, XY										
R II 18	44, XY	3q+ (98 0)	6q+ (100)								

*	:	deviation from teraploidy
-	:	loss of a whole chromosome
+	:	gain of a whole chromosome
q-	:	deletion in a long arm of a chromosome
q+	:	rearrangement in a long arm of a chromosome
p-	:	deletion in a short arm of a chromosome
p+	:	rearrangement in a short arm of a chromosome
+rcp	:	gain of a reciprocal translocation
+t	:	gain of a translocation
+M	:	gain of an unidentified marker chromosome
( )	:	percentage of metaphases carrying a given alteration

Based on the earlier data on cytogenetic changes in radiation-transformed and spontaneously immortalized SHE-cells, we extended the investigations of specific chromosome alterations in radiation-transformed SHE cells. The deletion in the short arm of chromosome #2 (2p-) that has been found in spontaneously immortalized cells is also present in several transformed cell lines that have been exposed to carbon ions. However, the data suggest that this deletion occurs spontaneously and it is not likely to be induced by radiation. The data are summarized in table 1.

In a further study we have analyzed a series of spontaneously and radiation-induced morphologically transformed SHE cell lines. The purpose of the study was to determine if specific chromosome changes occur which correlate with immortalization. In the non-irradiated culture, 18 morphologically transformed colonies were isolated, of which only 2 became immortal. In the culture, that has been exposed to 5 Gy γ-rays, 6 out of 18 transformed colonies isolated progressed to immortalization. Seven out of 8 immortalized cell lines exhibited either numerical and/or structural chromosome alterations (see table 2). Of 6 radiation-induced immortal lines, 4 lines (R II 1, R II 5, R II 14, and R II 18) showed rearrangements in the long arms of chromosome 3 (3q+) and chromosome 6 (6q+) nonrandomly. In all cases, both 3q+ and 6q+ occurred always as heterozygotes already in the primary morphologically transformed colonies (see table 3). Various other chromosome alterations were present in spontaneously transformed cells as well as in radiation-transformed cells (table 2 and 3). 3q+ and 6q+ were never found in the non-irradiated cultures, demonstrating that these chromosome changes are likely to be induced by irradiation. The data suggest that 3q+ and 6q+ might correlate with progression to immortality in SHE cells transformed by γ-irradiation.

In recent years, it became evident that mobile genetic elements are involved in mutagenesis and carcinogenesis. Long interspersed elements (LINEs) are such a class of repetitive elements of up to 6200 bp in length and about 100.000 copies of which most of them are truncated, but still they represent about 10% of the mammalian genome. Complete LINEs have 2 open reading frames (ORF) of which ORF2 codes for a reverse transcriptase. Similar to retroviruses complete LINEs are able to duplicative transposition. The mobility of these elements is usually strictly regulated that led to a species-specific distribution in the genome during evolution. However, DNA damage or cellular stress can initiate increased activation of transposition. These mutations lead to changes in the distribution of LINEs in the genome.

Differential hybridisation analysis of genomic DNA libraries from normal versus radiation-transformed cell lines revealed that preferentially clones which contain sequenzes homologous to LINEs were more frequently found in transformed cell lines than in primary cells. DNA sequence comparison showed homology of only about 70%, but there exist some highly conserved regions. Oligonucleotide primers constructed from the consensus sequences of highest conservation were used in PCR-amplification of genomic DNA, each of them generated a PCR-product pattern of high complexity when electrophoretically separated. Careful analyzed with the use of Southern hybridisation, these patterns exhibited distinct changes in length of a LINE-fragment, leading to a shift of the band in the gel (see figure 2) or showed a total loss of specified bands, when normal cells and neoplastically transformed cells of the same origin were compared (figure 3). These and similar changes can be used as markers for transformed SHE cells and tumor-cell lines established from nude mice tumors, that have been induced by subcutaneously injecting of transformed cells. In addition, we have evidence that the same primers (as contructed for SHE cells) can be used for PCR-

amplification of DNA from human tissues. This will now enable us to analyse also human tumor material in respect to tumor markers. Further studies of the mechanisms underlying the changes in the LINE-distribution will be of interest for the understanding of the carcinogenic processes.
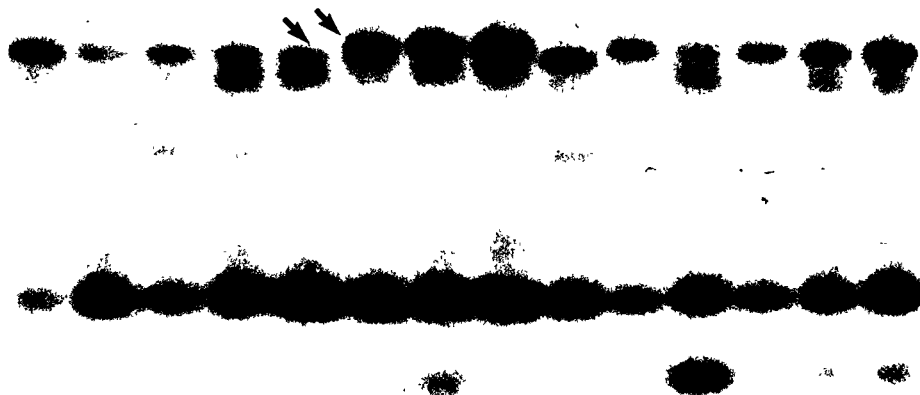
Figure 2: Southern Blot of Inter-LINE PCR-products from different SHE cell lines hybridised with a $(CA)_{10}$-Oligonucleotide. Arrows indicate a band shift to lower size in neoplastically transformed cells and tumor-cell lines. Lanes 1 to 5 (from left to right), different tumor-cell lines derived from primary stock cells at lane 6 and 7; lane 9 to 14; immortalized and/or spontaneously transformed cell lines derived from primary cell stock at lane 8.
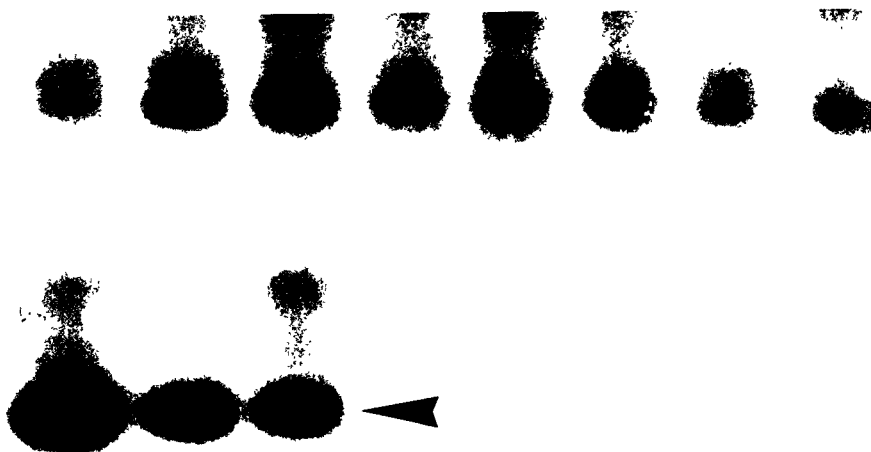
Figure 3: Southern Blot of Inter-LINE PCR-product pattern hybridised with a specific Inter-LINE probe, showing a loss of this fragment in 5 different tumor-cell lines Lane 1 (left), primary SHE cells; lane 2 and 3, spontaneously immortalized cells; lane 4 to 8, different tumor-cell lines.

Publications

L.Hieber, J.Smida, and A.M.Kellerer: Neoplastic transformation induced by heavy ions: Studies on transformation efficiencies and molecular mechanisms. In: Biological Effects and Physics of Solar and Galactic Cosmic Radiation (Eds: C.E.Swenberg et al.) New York: Plenum Publishing Corporation, 135-141 (1993)

R.C.Miller, G.Randers-Pehrson, L.Hieber, S.A. Marino, M.Richards, and E.J.Hall: The inverse dose-rate effect for oncogenic transformation by charged particles is dependent on linear energy transfer. Radiation Research, 133, 360-364 (1993)

L.Hieber, S.Endo, S.Leibhard, and J.Smida: Neoplastisch transformierte Säugetierzellen: Ein Modellsystem für molekularbiologische und zytogenetische Untersuchungen der Mechanismen der Strahlenkarzinogenese. In: Umweltradioaktivität Radioökologie Strahlenwirkungen (Hrsg.: M. Winter, A. Wicke) Köln: Verlag TÜV Rheinland, 835-840 (1993)

S.Endo, M.Metzler, and L.Hieber: Cytogenetic study of spontaneously transformed and radiation-transformed Syrian Hamster embryo cells. GSI Darmstadt: Scientific Report 92-1, 329 (1993)

J.Smida and L.Hieber: Gene expression studies in spontaneously transformed and radiation-transformed Syrian hamster embryo cells. GSI Darmstadt: Scientific Report 93-1, 227 (1994)

S.Endo, M.Metzler, and L.Hieber: Nonrandom karyotypic changes in a spontaneously immortalized and tumorigenic Syrian hamster embryo cell line. Carcinogenesis, 15, 2387-2390 (1994)

S.Endo and L.Hieber: Chromosome alterations that correlate with progression to immortality in Syrian hamster embryo cells transformed by g-irradiation. Int.J.Radiat.Biol., 67, 177-186 (1995)

S.Leibhard, J.Smida, and L.Hieber: Changes of Long Interspersed Element (LINE) pattern in radiation-transformed Syrian hamster embryo cells. GSI Darmstadt: Scientific Report 94-1, 210 (1995)

L.Hieber, S.Endo, S.Leibhard, and J.Smida: Neoplastische Transformation von Säugetierzellen: Modelle zum Studium der Strahlenkarzinogenese. Publikationen der Strahlenschutzkommision (SSK) der Bundesrepublik Deutschland, in press

Abstracts

J.Smida, L.Hieber, and A.M.Kellerer: Increased expression of a laminin-receptor gene in tumor cells derived from radiation-transformed Syrian Hamster embryo cells. Joint meeting of the Association for Radiation Research, The Netherlands Radiobiology Society and The Swedish Radiobiology Society, St. Andrews, UK, 1.-4.4.1992. Int.J.Radiat.Biol., 1992, 62, No.3, 378-379

A.J.Mill, S.C.Hall, D.Frankenberg, C.J.Roberts, D.Bettega, P.Calzolari, L.Hieber, and A.Saran: In vitro cell transformation at low doses of ionizing radiation: A collaborative European project. Joint meeting of the Association for Radiation Research, The Netherlands Radiobiology Society and The Swedish Radiobiology Society, St. Andrews, UK, 1.-4.4.1992

J.Smida und L.Hieber: Veränderte Genexpression in strahlentransformierten Embryo-Fibroblasten des Syrischen Hamsters. 2.Workshop 'Molekulare Strahlenbiologie' DNA Repair Network, Neuherberg, Germany, 11.-14.5.1992

J.Smida and L.Hieber: Radiation-transformed Syrian Hamster embryo cells exhibit altered expression of genes related to the extracellular matrix. 25th Annual Meeting of the ESRB, Stockholm, Sweden, 10.-14.6.1993.

S.Endo, M.Metzler, and L.Hieber: Chromosomal abnormalities in spontaneously immortalized and radiation-transformed Syrian Hamster embryo cells. Annual Meeting of the Association for Radiation Research, Guildford, UK, 12.-15.7.1993

S.Endo, J.Smida, S.Leibhard, and L.Hieber: Cytogenetic and molecular analysis of immortalized and neoplastically transformed Syrian hamster embryo cells. International Symposium on Molecular Mechanisms of Radiation and Chemical-induced Cell Transformation, Mackinac Island, USA, 19.-23.9 1993

L.Allen, D.Bettega, A.Butler, P.Calzolari, D.Frankenberg, M.Frankenberg-Schwager, S.Futter, S.C.Hall, L.Hieber, M.Lehane, A.J.Mill, G.R.Morgan, L.Pariset, S.Pazzaglia, C.L.Roberts, and A.Saran: Factors likely to affect transformation frequency of C3H10T1/2 mouse fibroblasts. International Symposium on Molecular Mechanisms of Radiation and Chemical-induced Cell Transformation, Mackinac Island, USA, 19.-23.9 1993

J.Smida, S.Leibhard und L.Hieber: Mittelrepetitive Sequenzen (LINE-L1) als genomische Marker für strahleninduzierte DNA-Rearrangements: Tagung 'DNA Schäden und ihre Reparatur', Göttingen, Germany, 1.-4.3.1994

L.Hieber: Strahlenkarzinogenese: Zelltransformation *in vitro*. 75.Deutscher Röntgenkongress, Wiesbaden, Germany, 11.-14.5.1994

J.Smida, S.Leibhard, and L.Hieber: Molecular changes in retrotransposonal elelement (LINE) clusters related to radiation-induced neoplastic transformation. Würzburg, Germany, Herbsttagung der Gesellschaft für Biologische Chemie, 19.-21.9.1994

J.Smida, L.Lehmann, A.M.Kellerer, L.Hieber, E.Lengfelder, F.Spelsberg, E.P.Demidchik, and H.Zitzelsberger: Analysis of p53 mutations and p53 expression in thyroid carcinomas of children from Belarus after the Chernobyl accident and of secondary thyroid tumors after radiotherapy. Würzburg, Germany, 10th International Congress of Radiation Research, 27.8.-1.9.1995

S.Leibhard, J.Smida, and L.Hieber: Inter-LINE-PCR: A novel method for analysis of genomic rearrangements. Würzburg, Germany, 10th International Congress of Radiation Research, 27.8.-1.9.1995

D.Bettega, D.Frankenberg, L.Hieber, A.J.Mill, C.J.Roberts, A.Saran, L.A.Allen, P.Calzolari, M.Frankenberg-Schwager, M.M.Lehane, G.R.Morgan, L.Pariset, and S.Pazzaglia: The effect of low doses on cell transformation in C3H 10T1/2 cells using a European standardised protocol. Würzburg, Germany, 10th International Congress of Radiation Research, 27.8.-1.9.1995

Head of project 6: Dr. Saran

II. Objectives for the reporting period

(a) To bring to completion the standardisation procedure of C3H10T1/2 cell transformation assay to measure the transformation frequency at low doses of X-rays in collaboration with the other participating laboratories.

(b) Study of neoplastic transformation induced by fission neutrons and monoenergetic neutrons of different energies.

(c) Study of synchronised populations of C3H10T1/2 cells exposed to either low or high LET radiation, to accurately investigate cell cycle-dependent sensitivity to cell killing and neoplastic transformation.

(d) To study two different cell systems of human origin: the RHEK-1 epithelial cell line and the CGL1 human hybrid cell line.

III. Progress achieved including publications

(a) Standardisation of Transformation Assay

Progress in determining the relevance of certain parameters for different results in various laboratories and thus in the standardisation of the transformation assay has been made. Intercomparison experiments at doses down to 0.25 Gy of X-rays have been performed and the data from each individual laboratory have been pooled in order to determine the dose-response relationship at doses less than 0.25 Gy. This part is described in details in section I of this report.

(b) Neoplastic Transformation by fission neutrons and monoenergetic neutrons

The study of the effects of fractionation of monoenergetic neutrons on neoplastic transformation of the C3H10T1/2 cell system has been completed and published. No significant difference between acute and fractionated irradiation was found for both cell inactivation and neoplastic transformation at all energies tested, although our experimental conditions were chosen in order to maximise the probability of any enhancement of transformation frequency by dose fractionation, according to biophysical models recently proposed. The data relative to neoplastic transformation are shown in Figure 1. The results of this study are in qualitative agreement with our data for fractionated irradiation carried out with fission-spectrum neutrons from the RSV-TAPIRO reactor (Table I). Our conclusion from this and from previous work, which included measurements with various radiation qualities, doses and fractionation schemes, is that although it might be important to understand the mechanistic nature of the inverse dose-rate effect of high-LET radiation on neoplastic transformation, the small magnitude of the effect and the dependency of its occurrence on a number of specific conditions, as reported recently (Miller et al., 1993), would limit its relevance in radiation protection.

TABLE I. **Survival and Transformation of C3H10T1/2 Cells Irradiated with Monoenergetic Neutrons**

No. fractions and dose per fraction (cGy)	Total dose (cGy)	Surviving fraction	No. of dishes	Total No. foci	No. of dishes without foci	Avg. No. of foci per dish $(\lambda)^a$	Transformation frequency per 10^4 surviving cells ($\pm$ SE)
Monoenergetic Neutrons							
Controls	0	1	1125	6	1119	0.0054	0.181 ($\pm$0.074)
0.5 MeV							
1 x 25	25	0.536	447	8	441	0.0135	0.917 ($\pm$0.373)
5 x 5	25	0.618	445	8	437	0.0181	0.780 ($\pm$0.275)
1 x 50	50	0.422	368	15	356	0.0332	1.827 ($\pm$0.523)
5 x 10	50	0.388	278	9	269	0.0329	1.710 ($\pm$0.564)
1 MeV							
1 x 25	25	0.680	583	16	570	0.0226	0.794 ($\pm$0.219)
5 x 5	25	0.761	589	17	578	0.0189	1.060 ($\pm$0.318)
1 x 50	50	0.551	425	19	406	0.0457	1.162 ($\pm$0.263)
5 x 10	50	0.593	462	24	443	0.0420	1.262 ($\pm$0.286)
6 MeV							
1 x 25	25	0.801	634	9	625	0.0143	0.363 ($\pm$0.121)
5 x 5	25	0.753	643	8	651	0.0124	0.393 ($\pm$0.138)
1 x 50	50	0.663	677	16	661	0.0239	0.694 ($\pm$0.172)
5 x 10	50	0.674	551	13	538	0.0239	0.707 ($\pm$0.195)
Fission Neutrons							
Controls	0	1	1063	4	1059	0.0038	0.156 ($\pm$0.078)
1 x 25	25	0.462	879	10	869	0.0114	0.640 ($\pm$0.202)
5 x 5	25	0.544	665	9	656	0.0136	0.602 ($\pm$0.199)
10 x 2.5	25	0.591	674	7	667	0.0104	0.504 ($\pm$0.190)
1 x 10.8	10.8	0.849	261	3	258	0.0115	0.483 ($\pm$0.278)
1 x 27	27	0.655	371	11	363	0.0296	0.913 ($\pm$0.321)
1 x 54	54	0.410	651	29	623	0.0445	1.570 ($\pm$0.294)
1 x 108	108	0.139	478	48	433	0.1004	3.523 ($\pm$0.512)
5 x 2.16	10.8	0.843	178	2	176	0.0113	0.534 ($\pm$0.376)
5 x 5.4	27	0.646	146	3	143	0.0207	1.140 ($\pm$0.652)
5 x 10.8	54	0.402	244	11	233	0.0461	1.510 ($\pm$0.451)
5 x 21.6	108	0.140	173	26	149	0.1490	3.930 ($\pm$0.774)
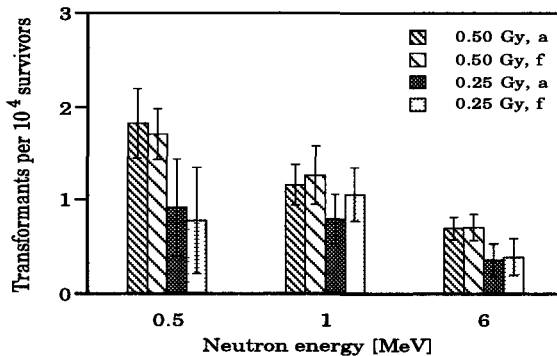
Fig. 1. Transformation frequencies of C3H10T1/2 cells after acute (a) or fractionated (f) doses of monoenergetic neutrons.

(c) Influence of the cell cycle on radiation induced cell transformation and killing

The participing laboratory has also completed the investigation of cell cycle-dependent sensitivity to both killing and neoplastic transformation of C3H10T1/2 cells exposed to low and high LET radiation, and the data are summarised in Table II.

Mitotic suspensions, collected using a mitotic shake-off procedure, were irradiated with 4 Gy of 250 kVp X-rays or 0.5 Gy of fission neutrons from the RSV-TAPIRO reactor at CR-Casaccia. For study of cell killing the mitotic-cell suspensions were either irradiated immediately after collection, or plated for subsequent irradiation, which was performed every hour, covering an interval of 17 hours. As shown in figure 2, the response pattern observed is similar after X-rays and neutron irradiation, but the magnitude of the variation through the cell cycle is smaller in the case of neutrons (1.3-fold compared to 5-fold).

For study of neoplastic transformation induction, the irradiation was performed immediately after collection, i.e. in M phase, or at later times corresponding to mid-G1, G1/S and G2 phases. The sensitivity of the G2/M phase was examined by irradiating the cells with 4 Gy of X-rays while still attached to the flask bottom, and dislodging them after 25 minutes. Similarly to cell survival, the transformation frequency shows a small variation after neutron irradiation (1.4-fold compared to 3.1-fold) for the phases examined (Fig.2).

TABLE II. Survival and Neoplastic Transformation of Asynchronous and Synchronous C3H10T1/2 Cells Exposed to Fission Neutrons or 250kVp X rays

	Dose (Gy)	Time relative to mitosis	Surviving fraction	No of viable cells per dish	No of dishes Tot	No of dishes with foci[a]	Tr F[b] / 10^4 surv. cells	SE[c]
Control								
Asynchronous cells	0	-	1	264	800	2	0,095	0,067
Synchronous cells	0	0	1	232	991	1	0,044	0,044
Neutrons								
Asynchronous cells	0,5	-	0,431	257	1034	16	0,606	0,151
Synchronous cells	0,5	0	0,422	262	1255	16	0,489	0,122
	0,5	4h	0.381	307	681	13	0.628	0 173
	0,5	9h	0.402	330	695	11	0.483	0 145
	0,5	15h	0.513	319	1033	15	0.459	0.118
X-Rays								
Asynchronous cells	4,0	-	0,282	218	945	9	0,440	0,150
Synchronous cells	4,0	0	0.264	248	925	12	0.526	0.152
	4,0	4h	0.302	220	660	10	0.694	0.219
	4,0	9h	0.369	337	664	5	0.224	0.100
	4,0	15h	0.410	359	804	9	0.313	0.104
	4,0	-25 mm	0.189	173	339	2	0.342	0.241

[a] Total No of Types II and III transformed foci.

[b] Transformation Frequency $/10^4$ survivants calculated combining the data from all experiments.
Tr F= λ average n_o of viable cells per dish, with $\lambda = -\ln (n_o$ of dishes without foci / Tot n_o of dishes)

[c] Standard errors = $\left(\sqrt{\lambda}/\sqrt{\text{Tot n.of dishes}}\right)/$Average n. of viable cells per dish.
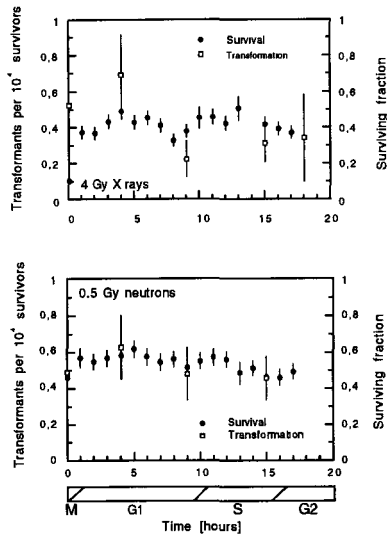
Fig. 2. Survival and transformation frequencies as a function of time after mitotic collection of C3H10T1/2 cells.

(d) Radiation induced transformation on cell lines of human origin

For the study of radiation-induced transformation on cells of human origin, we have tested the RHEK-1 epithelial line (Rhim et al., 1985) for its attitude to be developed into an assay system with which quantitative data for radiation-induced neoplastic transformation can be obtained. The survival of RHEK-1 cells after 250-kVp X ray or fission neutron irradiation is shown in Fig. 3.
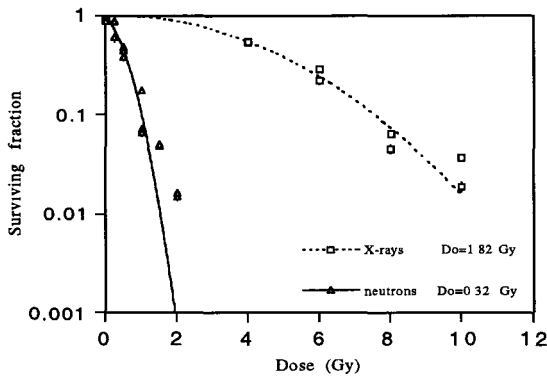
Fig. 3. Survival of RHEK-1 cells after irradiation with X rays (square) or fission neutrons (triangle).

The assessment of in vitro transformation in human cells requires the identification of malignant phenotypes that are progressively expressed during the process of neoplastic transformation. There are certain phenotypes that are considered to be *bona fide* markers of cell transformation such as: (i) altered cell morphology and multicellular organisation in foci, (ii) growth to elevated cellular density levels, (iii) ability to grow without substrate anchorage.

(i) -The morphological analysis of the monolayer has shown that after the treated cells have reached confluence they present alterations, exhibit the tendency to overlap and begin to pile up in focal areas. Unfortunately similar changes were also manifested by the unirradiated cells although the number and dimension of such focal areas were markedly reduced.

(ii) -As far as the gain of anchorage independent growth, each treated population exhibited some degree of growth in soft-agar that was greater than that observed in the control population.

(iii) -The growth potential in vitro was monitored by the exam of saturation density; the results are presented in figure 4 and do not show any increase in the saturation density of irradiated cells compared to control cells.
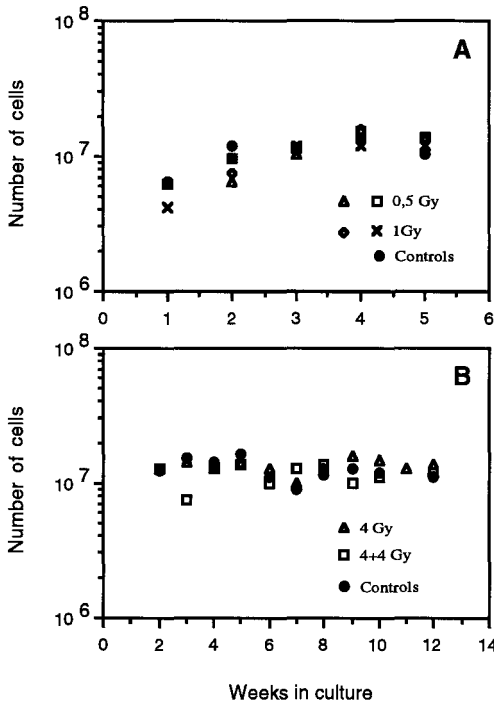
Fig. 4. Maximum number of RHEK-1 cells obtained after initial plating with 5 x10^3 cells per cm^2 irradiated either with fission neutrons (panel A) or with X-rays (panel B) followed by incubation at 37°C.

The impossibility to identify for this cell line criteria which are unambigously correlated with malignant cell transformation makes the use of this system for quantitative study of radiation-induced neoplastic transformation not feasible at present.

The human system CGL1 (Redpath et al., 1987), consisting of hybrids between HeLa cells and human fibroblasts has been obtained, along with the other participant laboratories, from Dr. J.L. Redpath. Preliminary studies have been performed on this system in our laboratory , including survival to X rays and fission neutrons. The results are shown in figure 5.
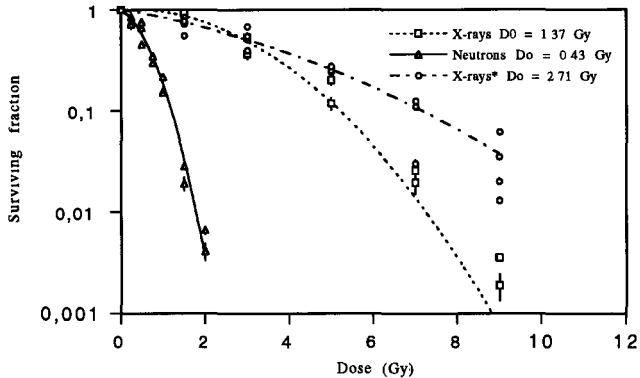
Fig. 5. Survival of CGL1 cells seeded: (i) immediately after irradiation with X-rays (square); (ii) following 6h incubation at 37 °C after irradiation with X-rays (circle); (iii) after irradiation with fission neutrons (triangle).

Neoplastic transformation frequencies are dependent upon the density of viable cells plated and in figure 6 the data from experiments carried out to measure the variation of the transformation frequency as a function of the density of viable cells plated post irradiation are shown graphically. The line through the data represents a computer-generated best fit, and this cell density dependency can be used to correct the transformation frequencies in our data for any cell density effect.
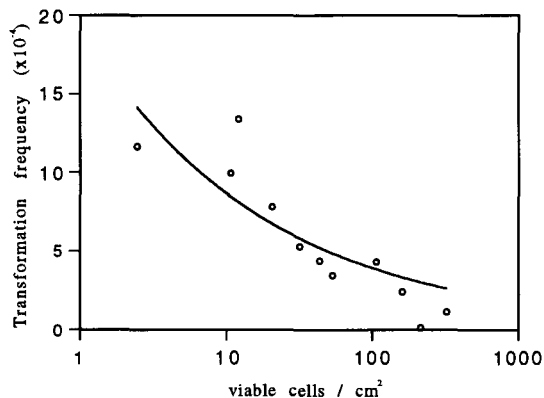
Fig. 6. Transformation frequency as a function of the density of viable cells plated 6 h postirradiation (7 Gy).

Table III summarise the data relative to neoplastic transformation as a function of dose of radiation. The data are also shown graphically in figure 7.

TABLE III. Transformation Frequency of CGL1 Cells Exposed to Fission Neutrons or 250 kVp X rays.

Dose (Gy)	Tot No. of T-75 flasks	No of foci per flask	Tot.No of viable cells	No of foci	Tr F/10^4 surv. cells	Tr F/10^4 surv. cells (corr)*
0	78	0.115	277740	9	0.32±0.11	0.33±0.11
0.25	24	1.291	86850	31	3.57±0.64	3.61±0.65
0.50	61	1.082	206775	66	3.19±0.39	3.31±0.41
0.75	22	2.363	93270	52	5.58±0.77	5.34±0.74
1.00	22	2.636	53145	58	10.91±1.43	12.711.67
1.50	34	0.294	139890	10	0.72±0.23	0.69±0.22
3.00	35	0.543	228563	19	0.83±0.19	0 69±0.16
5.00	34	1.294	140400	44	3.13±0.47	3.03±0.46
7.00	92	1.659	408188	156	3.82±0.31	3.60±0.29

* Transformation frequency corrected for cell density
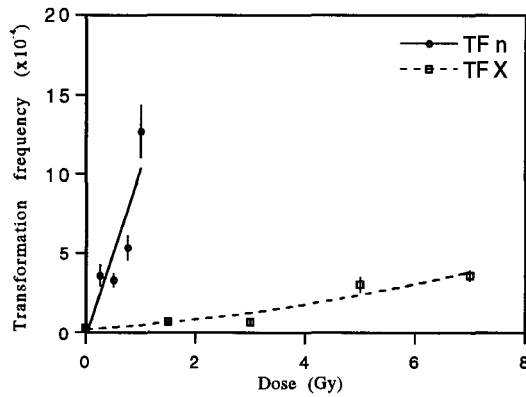
Fig. 7. Transformation frequency as a function of dose for CGL-1 cells after X-rays (square) or fission neutrons (circle) irradiation.

References

1. A. Saran, S. Pazzaglia, L. Pariset, S. Rebessi, M. Coppola, V. Di Majo, and V. Covelli. Cell-cycle dependence of C3H10T1/2 cell transformation by fission spectrum neutrons and X rays. Proceedings of the 41st Annual Meeting of Radiation Research Society, Dallas, March 1993. Abstract P-17-4, p. 84.

2. S. Pazzaglia, L. Pariset, A. Saran, S. Rebessi, M. Coppola, V. Di Majo, J.J. Boerse, J. Zoetelief, and V. Covelli. Neutron induced neoplastic transformation of C3H10T1/2 cells. Proceedings of the International Symposium on "Molecular mechanisms of radiation and chemical carcinogen-induced cell transformation", Mackinak (USA), September 1993.

3. A. Saran, J.J. Broerse, J. Zoetelief, S. Pazzaglia, L. Pariset, M. Coppola, V. Di Majo, S. Rebessi, V. Covelli. C3H10T1/2 cell transformation after fractionated doses of neutrons of different energies. Atti VI Convegno SIRR, Capri, October 1992. *Phisica Medica* 10 S1, 80-81 (1994).

4. S. Rebessi, V. Di Majo, M. Coppola, A. Saran, S. Pazzaglia, L. Pariset, V. Covelli. Somatic effects of low neutrons doses. Atti VI Convegno SIRR, Capri, October 1992. *Phisica Medica* 10 S1, 82-83 (1994).

5. A. Saran, S. Pazzaglia, L. Pariset, S. Rebessi, J.J. Broerse, J. Zoetelief, V. Di Majo, M. Coppola, V. Covelli. Neoplastic transformation of C3H10T1/2 cells: a study with fractionated doses of monoenergetic neutrons. *Radiation Research* 138, 246-251 (1994) .

6. V. Di Majo, M. Coppola, S. Rebessi, A. Saran, S. Pazzaglia, L. Pariset, V.Covelli. Neutron induced tumors in BC3F1 mice: effects of dose-fractionation. *Radiation Research* 138, 252-259 (1994).

7. D. Bettega, D. Frankenberg, L. Hieber, A.J. Mill, C.J. Roberts, A. Saran, L. A. Allen, P. Calzolari, M. Frankenberg-Schwager, M.M. Lehane, G. R. Morgan, L. Pariset, S. Pazzaglia. Joint meeting of the Association for RadiationResearch and the Irish Radiation Research Society, Dublin June 23rd-26th 1994.

8. S. Pazzaglia, A. Saran, L. Pariset, S. Rebessi, V. Di Majo, M. Coppola, V. Covelli. Radiation induced neoplastic transformation of C3H 10T1/2 cells as a function of the cell cycle phases. Proceedings of the 43rd Annual Scientific Meeting of the Radiation Research Society, San Jose (USA), April 1995, Abstract P-16-231.

Title: Molecular and cellular effectiveness of charged particles (light and heavy ions) and neutrons.

1)   Cherubini   INFN - Legnaro
2)   Michael   Hosp. Mount Vernon
3)   Goodhead   MRC
4)   Belli   ISS
5)   Sideris   NCSR "Demokritos"
6)   Kiefer   Univ. Giessen
7)   Reist   PSI - Villigen (CH) (EFTA partner)

I. Summary of Project Global Objectives and Achievements

Studies on the biological effects caused by radiations of different types and energies are necessary for identifying the physical characteristics of radiation that explain their actions on biological targets; in particular they are necessary to predict the biological effectiveness of any radiation, to give a better knowledge about the molecular lesions leading to cellular effects and to develop mechanistic models of radiation action, i.e. models based on biophysical considerations.

Global objectives of the present project can be summarized briefly as follow:

1) to perform direct comparison of the effectiveness of radiations of different types and energies in inducing significant biological effects in order to identify the physical characteristics of the radiation that are relevant to their biological action;

2) to gather a set of radiobiological data which could be used as a consolidated data-base to test models of radiation action used in radiation protection for a practical assessment of human risk;

3) to start investigation of the extreme low-dose effects by irradiating cells individually with exact numbers of particles, exploiting the experimental opportunity provided by the microbeam facilities;

4) to make comparative experiments using differentiated and non-differentiated human cells to study the influence of DNA conformation on the induction of radiation damage and on its repair;

5) to develop and establish assays to investigate DNA damage, in particular to detect the distribution of lesions within clustered damage sites, in order to provide new experimental data to validate biophysical models of radiation action;

6) to achieve technical developments suitable for novel radiobiological research;

7) to develop theoretical approaches for interpretation of experimental results.

    Comparison of the effectiveness of different charged particles. (Obj. 1 and 2)

Cell inactivation experiments on V79 cells

Measurements of the biological effectiveness of low-energy singly and doubly charged particles have been carried out by the Legnaro (LNL) and ISS groups, in collaboration between them, and by the Gray Laboratory group. Systematic comparative experiments on V79 cell inactivation by deuterons (in the LET range 13-57 keV/μm; partly carried out in the previous CEC contract), ^{3}He^{++}, ^{4}He^{++} (in the LET range 40-150 keV/μm) have been done by the LNL-ISS groups in view of comparison with the proton data previously obtained by the same groups; protons and deuterons (in the LET range 10-50 keV/μm) and ^{3}He^{++} (LETs from 59 to 105 keV/μm) have been utilized by the Gray Lab. group.

Experimental results of the Italian groups confirm a significant difference between ^{3}He^{++} and ^{4}He^{++} as regards to their biological effectiveness, paralleling the unexpected differences previously observed by the same groups between protons and deuterons. Unlike these

conclusions the Gray Laboratory group finds no difference between protons and deuterons with the same LET. No difference in RBE between protons and deuterons is detected by either group at an LET value of about 30 keV/μm while differences are reported by the LNL-ISS groups for LET values lower than this. The two groups are endeavouring to reconcile these differences by undertaking a dosimetric intercomparison; ionization measurements using the Gray Laboratory dosimetric equipment have been made at LNL and no discrepancies were observed to explain the differences observed in the biological results. Differences in the irradiation protocol followed by the two laboratories, (e.g. dose-rate, dose-range, cell conditions during irradiation) must be taken into account, even if, in direct (in house) comparison, they should play the same role for both the considered particles, i.e. protons and deuterons. Other differences between the two groups concern with data analysis. The LNL-ISS groups express RBE as linear coefficient ratio, α/α_x, so that RBE is strongly dependent on the initial part of the survival curves, while the Gray Laboratory group calculates the RBE at 10% survival, near the final part of the curve. However, the evaluation of RBE at 10% survival by LNL-ISS groups reduces but not reconciles the observed proton-deuteron differences.

Careful independent verification of the dosimetry of the particles beams as used at Legnaro has been performed by MRC and LNL groups. CR-39 discs have been irradiated at Legnaro with a selection of proton and deuteron beams to compare with the dose rates and doses that the local team prescribed using totally independent dosimetric methods (silicon surface barrier detector, SSBD). The CR-39 exposures in the position of biological samples also allowed evaluation of the uniformity of fluence across individual sample dishes and visualization of symmetry and size-uniformity of etched pits of individual tracks. Reproducibility of numbers of pits per area between discs irradiated with a given beam was good, with variation lying within the expectations of Poisson statistics. Considering the limitations of such comparisons, e.g. the need for low fluences for the accurate counting of pits and hence limitations on the counting statistics of the scattered-particle monitor, no significant discrepancy between expected and measured fluences (i.e. pit densities) could be found.

Mutation induction

The LNL-ISS groups have carried out extensive experimental work on mutation induction at the HPRT *locus* in V-79 cells irradiated with deuterons, in the LET range 18-57 keV/μm, and with $^3He^{++}$ and $^4He^{++}$ ions of 51 keV/μm. For all the charged particles considered, linear dose-response relationships have been obtained. Even for this biological end-point experimental evidence supports a difference in the biological effectiveness between protons and deuterons. On the other hand preliminary mutation experiments did not show any significant difference between $^3He^{++}$ and $^4He^{++}$ ions with the same LET.

The MRC group reports a dose-response relationship apparently linear for mutation induction on V79 cells after 121 keV/μm α-particles irradiation, with a mutation frequency of about $(1.04\pm0.30) \times 10^{-4}$ Gy $^{-1}$.

The extensive experimental work carried out by the Giessen group has resulted in the establishment of a large set of cross-sections for mutation induction, relative in particular to heavy ions with LET ranging from about 10 to 10^4 keV/μm. The overall picture (for details see Giessen report) confirms that also for these particles LET is not a unifying parameter and highlights the crucial importance of track structure when particles with comparable LET but different charge and velocity are used. The same group also started the molecular analysis of hprt⁻ mutants by multiplex polymerase chain reaction (PCR). Their findings, although preliminary, seem still to reveal a substantial fraction of "wild type" mutants, even with very high LET.

DNA double strand break induction

The Gray Laboratory group has devoted particular attention to the study of the relationship between radiation effectiveness and the role of clustered damage to DNA. Complex lesions are believed to be critical for radiation action and a consideration of their induction, repair and chemical modification is important for understanding their role. The group has studied the reaction kinetics of the chemical repair of radical precursors of ssb and dsb by thiols both in a model DNA system and in intact mammalian cells. Further studies have measured chemical

repair kinetics of both ssb and dsb with increasing LET, using pulsed protons and deuterons. Experimental evidence has also been collected about the fixation reactions which compete with chemical repair prior to damage being expressed in the DNA after irradiation. As part of their mechanistic work on DNA damage induction, the Gray Laboratory group reports further measurements of the critical energies requires to induce ssb and dsb, this year including the effects of hydration. These studies are designed to provide basic data to assist the development of Monte Carlo models (see below).

The ISS group has completed the experiments on the production of initial damage, by using the low speed sedimentation technique, and the analysis of the rejoining time course of DNA dsb induced in V79 cells after proton irradiation at the LNL. Dose-response curves for the initial damage induced by 41 and 58 keV/μm helium-3 ions have also been obtained. Gamma rays from ^{60}Co source have always been used as the reference. As far as dsb induction is concerned it has been confirmed that the RBE is quite independent of LET and it is not significantly higher than unity for all particles investigated (protons or He-ions). As regard to rejoining experiments significant differences in the rejoining kinetics can be recognized between γ-rays and protons of various LET, suggesting that dsb induced by different radiations are not homogeneous with respect to repair and that changing from sparsely to densely ionizing radiation and increasing the LET a more "complex" type of damage is induced.

The Giessen group has studied the induction of DNA double-strand breaks (dsb) in yeast after exposure to X-rays, α-particles and heavy ions, comparing the pulsed field gel electrophoresis technique with the neutral sedimentation technique, used in previous investigations. Dsb induction and inactivation cross-sections were calculated and, contrary to mammalian cells, in diploid yeast a linear relationship between these parameters was found. The RBE for dsb induction in yeast is clearly higher than unity for LET values around 100 keV/μm and clearly lower than unity in the LET range 10^3-10^4 keV/μm.

Comparison of the effectiveness of high and low dose rate irradiation with α-source

The investigation of a possible role of the dose-rate of high LET radiations on biological response is of actual interest to get insight the basic mechanisms of the interaction of ionizing radiations with living matter. Alpha-particles for high dose-rate irradiations (1 to tens of Gy/min) are obtained at LNL radiobiological facility set-up; for irradiations at low dose-rate (in the range 0.005-0.01 Gy/min) a ^{244}Cm alpha-emitter source based irradiator has been designed and constructed at LNL. Spatial and dosimetric characterization measurements of accelerated alpha beams and of ^{244}Cm alpha particles have been carried out by using a SSBD.

Biological effectiveness of fast neutrons

Experiments runs have been carried out at the LNL 7 MV Van de Graaff CN accelerator aimed at the physical and dosimetric characterization of the neutron beam (neutron energy distribution, flux, spatial homogeneity at the biological sample). Monoenergetic fast neutrons have been produced through the ^{7}Li (p,n)^{7}Be reactions, by using 0.500 - 0.700 mg/cm^2 ^{7}LiF production targets. Irradiation conditions for V79 cell inactivation studies are being optimized.

Low-dose irradiation; microbeam facilities (Obj. 3)

At the low dose levels generally encountered in environmental and occupational exposure to high-LET radiations, only a very small fraction of the cells at risk are traversed by a particle and a much smaller fraction by two or more particles. To approach these conditions in experimental investigations, construction, technical developments and optimization of charged-particles microbeam facilities have engaged LNL as well as Gray Laboratory, Giessen and PSI groups.

The LNL accelerator technical staff have developed the LPM "microbeam facility" at the 2 MV AN2000 Van de Graaff accelerator. They have carried out work on the focusing and controlling their beam systems, in order to increase performance, and for the optimization of a detector complex for single ion hits and of a fast beam switching system aimed to be used in the "single event" experiments.

Optimization of the charged-particle microbeam have been performed by the Gray Laboratory group, during the present contract period and the system is now in routine experimental use.

They developed several prototypes of particles collimators, based on silicon technology or consisting on fine-bore glass capillary, achieving 5 microns or 2.3 microns spatial resolution respectively. At the same time the development of detectors to register the passage of individual particles through each cell exposed to the microbeam has continued. The micronucleus assay has been used for relating chromosome damage to low doses and a full dose-effect curve showing a linear induction of micronuclei per binucleate cell with increasing mean particle traversal number, has been obtained. Adaptation of single-cell comet assay as well as of a clonogenic assay is in progress for use with the microbeam.

The Giessen group has set up and tested a microbeam device based on an ^{241}Am alpha emitter, with a beam collimator with 1 µm hole in a mica plate, for the investigation of single ion effects on individual cells.

An original technique for low dose irradiation, the so-called "palladium island technique", has been developed by PSI group in collaboration with Uppsala University, Sweden. The method enables the irradiation of more than a thousand cells simultaneously and the contemporary localization of the particle tracks. Test experiments with V79 cells confirmed the feasibility of the technique to perform low dose experiments such as single particle irradiations.

Use of human cellular system (Obj. 4)

Inactivation curves of human TK6 lymphoblasts and K562 pro-erythroblasts irradiated with X-rays have been obtained by ISS group. Preliminary experiments with protons of 11 keV/µm on suspension growing K562 cells have also been performed, but a modification of the irradiation device in order to increase the efficiency of cell recovery from the filters appears necessary.

DNA damage detection (Obj. 5)

The Gray Laboratory group have studied the role of higher-order repeating structure of the DNA in determining the fragmentation patterns, after irradiation with low and high LET radiation. Using conventional and pulsed-field electrophoresis systems they have compared the molecular weight distributions for DNA from cells irradiated with X-rays or 3 MeV α-particles (110 keV/µm). Experimental results show an enhancement of fragments in the 0.2-10 kbp region in DNA from cells irradiated with α-particles in comparison to X-rays, particularly around 500 bp. The Gray Laboratory group has set up the single cell gel electrophoresis technique ("comet" assay) for use in conjunction with their counted charged-particle microbeam. Initial results have distinguished DNA damage levels in hit and non-hit cells exposed to a low fluence of α-particle.

The Pulsed Field Gel Electrophoresis (PFGE) technique has been set up at ISS laboratory and used in DNA dsb induction experiments after irradiation with X-rays and protons of 31 keV/µm. The PFGE dose-response curves obtained in the dose range 10-60 Gy shows no difference between X-rays and protons in dsb induction, confirming the results obtained with the low speed sedimentation technique.

Experiments with the microgel single cell electrophoresis ("comet") technique have been carried out at the ISS on V79 cells irradiated with X-rays, in view of its possible application to the study of DNA damage induced by charged particles, including application with the microbeam at LNL for single-particle, single cell studies.

Also the Giessen group has been engaged in the development of the "comet assay"; after careful analysis technique sensitivity seem too low to unequivocally detect the action of individual light ions.

A complementary approach to the problem of DNA damage evaluation, has been followed by the "Demokritos" group, performing the measurement of thermal transition A $_{260}$ changes and dielectric-condutivity changes induced on mammalian macromolecular DNA after irradiation with gamma rays and with alpha particles. Data from Thermal Transition Spectrophotometry revealed a dual dose dependence response of the helix to coil transition temperature, measured by the changes of A_{260}, i.e. the hydrogen bond disruption for buffered solutions of macromolecular DNA, after irradiation with gamma-rays or alpha-particles: in the low dose region, i.e. 0-10 Gy, a DNA helix stability seems to be present; at higher doses a gradually decreasing mode of helix stability is observed.

Dependence of the transition temperature on dose has also been studied measuring the changes in conductivity, i.e. changes that proceed the hydrogen bond disruption. As a function of the dose, the parameter T_C, representing Thermal Conductivity Transition, follows a course qualitatively similar to the sigmoidal functions observed with A_{260} changes.

The observed conductivity changes and thermal transition changes support the recent theories of a dual phase DNA helix to coil transition where the disruption of the hydrogen bonds results from the preceding gradual disruption of the hydrophobic bonds between the successive nucleotides on the same DNA chain. The observed higher stability of the DNA molecules after gamma rays or alpha particles irradiation might be attributed to the formation of cross links between adjacent parts of DNA molecules which leads to the formation of molecules of higher thermodynamic stability. As far as RBE of different ionizing radiation is concerned, the large differences at the induced survival level observed between gamma and alpha radiations are not present when DNA helix to coil transition is used as the criterion.

Further investigation have been devoted to the effect of two organic free radical scavengers of the kind used for the comparison between the frequencies of single strand breaks and double strand breaks; the obtained results shows that their effects as free radical scavengers are confounded with a strong effect on the stability of the DNA molecules (for details see "Demokritos" report). These effects of free radical scavengers on the stability of irradiated DNA molecules might seriously affect the interpretation of experimental work of other laboratories, using the same scavengers, which contributed to the formulation of the cluster theories of radiation induced breaks.

Technical developments (Obj. 6)

Reports on this topic have been included in the appropriate sections, in order to give a more complete picture of the work carried out by each group to achieve its own objectives. Yet, as they constitute specific objectives of the present contract activities, it has to be mentioned the beam line for cell irradiation with heavy ions set up at LNL and the vertical beam line for irradiation with protons and α-particles set up at PSI.

A dedicated irradiation facility for heavy ions (in the mass range 6-40) has been installed at the +60° beam pipe of the LNL 16 MV XTU-Tandem accelerator. Test runs have been performed by using ^{58}Ni (174 MeV) beam. Radiobiological experiments are being carried out with ^{6}Li, ^{7}Li and heavier ions.

At PSI a beam line was set up with a 90°-magnet that bends the beam upwards to the target. It enables to expose the cells horizontally to protons or α-particles of 5-10 MeV up to 72 MeV energy and at an intensity from 10^4-10^6 particles/(sec cm^2). A circular beam spot of 3 cm in diameter at the cells exposed has been achieved.

PSI group has also been engaged in the optimization of the confocal laser scanning microscope image acquisition process in order to perform reliable calculation of the intersection length of a particle through a cell nucleus.

Theoretical developments (Obj. 7)

Particular effort have been devoted by MRC group in the analysis of Monte-Carlo simulated tracks of protons, deuterons and α-particles, in the region 20-30 keV/μm, for seeking microscopic features that may be responsible for their observed biological effectiveness. New high-accuracy data for particle (p, d, α) track-scoring statistics have been obtained but no simple property has been identified that simultaneously correlates well with the observed RBEs of both p and d or p and α.

"Demokritos" group has also been engaged, by Monte Carlo computer simulation, in the investigation of the physical and chemical processes (energy transport and deposition, ionisation distributions and the production of primary chemical species) connected with the interaction of charged particles (especially α) with water molecules. As result of this work, the group was able to develop accurate analytical LET-Energy and Range-Energy relations microdosimetric calculations for α-particles valid between 100 keV-10 MeV energy range.

Improved particle tracking methods, by elaboration of data libraries of reaction cross sections of photons and electrons, are being developed by the PSI group in order to permit tracking of the particles in the nm range and modelling of radical formation, diffusion and fate in water.

Head of project 1:   Dr. R. Cherubini

II.   Objectives for the reporting period

1 - Comparative experiments on V79 cell inactivation and hprt mutation induction using ^{3}He and ^{4}He beams with different LET values and direct (in-house) comparison with our previous proton and deuteron data.

2 - Execution of dosimetric and radiobiological intercomparisons with partners (MRC and Gray Lab.) of the present co-ordinated group.

3 - Execution of comparative experiments with low energy α-particles radionuclide source.

4 - Study of the biological effectiveness of a representative set of low-energy heavy ions for V79 cells inactivation.

5 - Single particles irradiation of V79 cells using protons and alphas at the microbeam facility.

6 - Study of the biological effectiveness on V79 cells of fast neutrons.

III.   Progress achieved including publications
   (In collaboration with ISS group)

In our early works we have shown, giving the first experimental evidence, that low-energy protons (in the LET range 7 - 38 keV/μm) are more effective than alpha particles at the same LET for inactivation and *hprt* mutation induction in V79-753B Chinese hamster cells [4,5]. Such results have subsequently been confirmed and extended by independent experiments carried out at the CRC Gray Laboratorary and at the MRC Harwell Laboratory. Parallel experiments on the induction of DNA damage in terms of single- and double-strand breaks not gave, in contrast, any indication of difference in effectiveness for the different radiation considered (X- , gamma-rays, protons, alpha particles).

Subsequently, in order to extend the investigated proton LET range, we have performed investigation with deuteron beams (in the LET range 13 - 57 keV/μm), that possess twice the range of protons with the same LET and the same velocity.

The direct comparison of the biological effectiveness of protons and deuterons for both the considered endpoints, in the same LET range, has shown, as an unexpected result, that deuterons appear less effective than protons in inducing both the considered biological endpoints, i.e. inactivation and *hprt* mutation induction (see Table I).

Table I:	RBE(expressed as α/α_X) values for inactivation and hprt mutatiom induction on V79 cells				
	PROTONS			DEUTERONS	
LET (keV/μm) at the cell midplane (3 μm)	Inactivation $\alpha/\alpha_X \pm$ s.e.	Mutation $\alpha/\alpha_X \pm$ s.e.	LET (keV/μm) at the cell midplane (3 μm)	Inactivation $\alpha/\alpha_X \pm$ s.e.	Mutation $\alpha/\alpha_X \pm$ s.e.
7.7	2.4 ± 0.3	2.6 ± 0.4	13.4	1.9 ± 0.3	
11.0	2.9 ± 0.4	3.5 ± 0.5	18.4	2.2 ± 0.4	2.6 ± 0.4
20.0	3.7 ± 0.4	4.3 ± 0.7	26.3	4.1 ± 0.4	
30.5	5.8 ± 0.6	5.9 ± 0.9	30.8	5.1 ± 0.5	4.2 ± 0.7
34.6	5.1 ± 0.5		39.5	5.8 ± 0.6	4.6 ± 0.8
37.8	4.4 ± 0.4		48.0	6.4 ± 0.7	
			57.0	7.3 ± 0.7	9.2 ± 1.6

For X-ray: $\alpha_X = 0.129\pm0.012$, for inactivation; $\alpha_X = (0.60\pm0.09) \times 10^{-5}$, for hprt mutation.

In order to extrapolate our upto date findings further to other heavier ions, and, in particular, to follow the anomalies already observed by using the hydrogen isotopes, more recently we have carried out extensive systematic and comparative experiments by using ^{3}He (in the LET range 38 - 200 keV/μm) and ^{4}He ions (in the LET range 50 - 150 keV/μm). Moreover, such a kind of investigation allow us to perform direct (in-house) intercomparison of the biological effectiveness of the different accelerated charged particles considered, by using the same cell line as well as the same physical and biological experimental conditions and protocolls.

Table II reports the RBE values for cell inactivation for ^{3}He and ^{4}He ions evaluated as α/α_X ratio. Figure 1 shows the RBE-LET relationship for the inactivation of V79 cells irradiated with ^{3}He and ^{4}He ions as a function of the LET. Each data point is representative of 2-5 (for helium-3) and 4-8 (for helium-4) independent experiments and the error bars denote one standard error of the mean. All individual dose-response curves have been fitted by the linear function S=exp(-αD).

Table II:	RBE(expressed as α/α_X) values for cell inactivation		
HELIUM-3		HELIUM-4	
LET (keV/μm)	$\alpha/\alpha_X \pm$ s.e.	LET (keV/μm)	$\alpha/\alpha_X \pm$ s.e.
41.4	4.34±0.48	51.5	4.70±0.50
45.5	4.43±0.48	56.8	4.68±0.49
51.1	5.98±0.60	70.0	4.76±0.50
58.4	5.55±0.65	104.2	6.31±0.63
73.9	6.16±0.65	150.5	3.26±0.35
87.5	5.26±0.51		
107.3	4.62±0.47		
139.4	2.52±0.32		

For X-ray: $\alpha_X = 0.129\pm0.012$
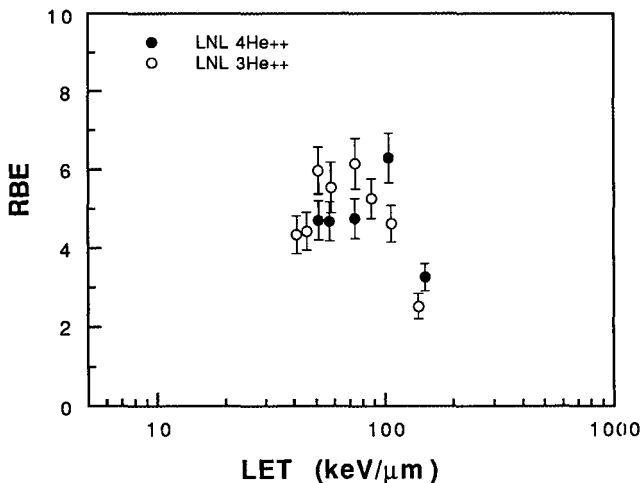
Fig. 1 : RBE-LET relationship for V79 cell inactivation induced by helium-3 and helium-4 ions (see Table II).

From Figure 1 it can be seen that the RBEs for ^{4}He rise as LET increase up to 104 keV/μm and then decrease, showing a maximum around 104 keV/μm, in agreement with well established literature data (Barendsen et al.; Goodhead et al.), while, the RBEs for ^{3}He rise as LET increase up to 87 keV/μm and then decrease, showing a maximum around 87 keV/μm. The RBEs for ^{4}He are lower than those obtained by us for ^{3}He in the LET range 50-90 keV/μm. These findings parallel the unexpected differences found in the intercomparison of our deuteron and proton RBE data indicating that careful and more sophisticated particle track structure description would be necessary for a better understanding of the radiation action in biological matter and for the definition of a more adequate parameter representative of the "radiation quality".

In order to extend the ^{3}He and ^{4}He ion effectiveness studies, very recently, we are carrying out systematic and comparative experiments on the hprt mutation induction in V79. Such an investigation will allows us to perform direct (in-house) comparison with proton and deuteron hprt mutation results, where a different effectiveness has also been found.
Preliminary dose-response curves for hprt mutation induction are presented in Figure 2 for 3He and 4He of the same LET value (51 keV/μm). Such preliminary mutation experiments did not show any significant difference between ^{3}He and ^{4}He ions for the LET value investigated. Further comparative experiments using helium ions with different LET values are planned.
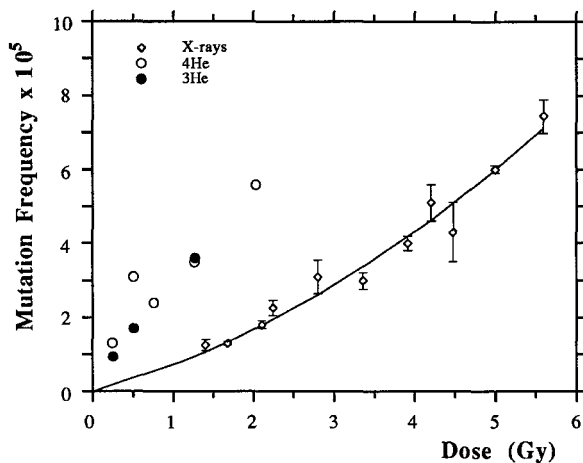
Fig. 2 - Preliminary hprt mutation curves obtained with ^{3}He (51.1 keV/μm) and ^{4}He (51.5 keV/μm) ions compared with the X-ray curve.

In order to confirm our observations on differences in biological effectiveness between protons and deuterons as well as between ^{3}He and ^{4}He and to solve the discrepancies between such our findings and the results obtained by the Gray Lab. group not showing, in contrast, any difference between proton and deuteron inactivation data, we have carried out experimental co-operative work with both the MRC and the Gray Lab. groups mainly intended to independent verification and intercomparison of the irradiation conditions with particular emphasis for particle beam dosimetry (and radiobiological procedures) used in the different Laboratories.

Up to date, intercomparative dosimetric experiments have been pursuit with the MRC group (see also the MRC report). Verification of the physical and dosimetric characterization of particle beams as used in our radiobiological experiments, usually accomplished by silicon surface barrier detectors (SSBD) and by CR39 solid state nuclear track detectors (SSNTDs), has been performed by irradiating the MRC CR39 SSNT detectors with a selected set of proton, deuteron, ^{3}He and ^{4}He beam energies and fluences at the same irradiation conditions (dose-rate, energies and geometry) as used at LNL for radiobiological experiments. Energy distribution, spatial particle uniformity, fluence/dose reproducibility at the same position of biological sample have been measured and compared. From the MRC CR39 results no significant differences between LNL and MRC dosimetric measurements could be found (see also the MRC report).

Intercomparative dosimetric experiments have also been performed at the LNL radiobiological facility with the CRC Gray Lab group. Verification of the physical and dosimetric characterization of the particle beams used in LNL radiobiological experiments has been carried

out by the usual Gray Lab dosimetric apparatus (ionization chamber) and by a SSB detector. Energy distribution, spatial particle uniformity (beam profile) fluence/dose reproducibility at the same position of biological samples have been measured by the Gray Lab group and compared with the LNL physical and dosimetric measurements. No significant differences were observed that could explain the discrepancies observed in the proton and deuteron biological data (see also the Gray Lab. report). Beside, for a careful comparison of the biological data gathered at the LNL and Gray Lab., differences in the irradiation protocol followed by the two laboratories (like dose-rate, dose range, cell conditions during irradiation, data analysis) must also be taken into account.

In order to complete the LNL-Gray Lab. physical and dosimetric intercomparison, a visit of the LNL group at the Gray Lab radiobiological facility is planned.

The investigation of a possible role of the dose-rate of high-LET radiations on biological response is of crucial importance, in particular, in the field of radiation protection for a better risk assessment. To contribute to such an investigation, comparative experiments at high and low dose-rate have been planned.

Alpha-particles (Helium-4 ions) for high dose-rate irradiations (1 to tens of Gy/min) are obtained at our own radiobiological facility set-up at the LNL 7 MV Van de Graaff CN accelerator. For low dose-rate (in the range of 0.005-0.01 Gy/min) irradiations a ^{244}Cm alpha-emitter source based irradiator has been designed and constructed at LNL Efforts have been spent to technical developments aimed to define the proper conditions for cell irradiation with the irradiator as well as precise spatial and dosimetric characterization measurements of ^{244}Cm alpha particles at the same position of the biological sample.

Particular efforts have been spent to design, built and test suitable stainless-steel Petri dishes, mounting a thin mylar foil as bottom and fitting the geometry of the ^{244}Cm alpha particles in air. Test experiments have been carried out . Routine experiments are being started.

In order to extend our study on lethal and mutagenic effects of light ions (protons, deuterons and helium ions) to other charged particles, such as heavy ions (in the mass range 6 - 40), a dedicated irradiation facility has been designed, constructed and installed at the +60° beam pipe of the LNL 16 MV XTU-Tandem accelerator. During the execution of test runs, we have performed, by using ^{58}Ni (174 MeV) beam, the beam line-irradiation apparatus alignment and some physical measurements for ion beam characterization. After the first test runs, during wich the aluminized mylar foil used as exit window for the extraction of heavy ion beams in air was broken, we have been involved in an hard technical development of our own heavy ion facility aimed to equip the heavy ion irradiation facility with an appropriate vacuum safety system mainly consisting of an ultra-fast vacuum valve, proper diaphragms, in addition to independent vacuum pumping systems, and proper vacuum gauges driving standard and ultra-fast vacuum valves. Time consuming irradiation facility on-beam alignement experiments and test runs have

recently been carried out using Ni, S and Li ion beams. V79 cell inactivation experiments have been started by using ^{7}Li and ^{6}Li. Very preliminary dose-response curves for V79 cell inactivation induced by 68 keV/μm ^{7}Li are reported in Figure 3.

Further ^{7}Li and ^{6}Li as well as heavier ions cell inactivation experiments are planned.
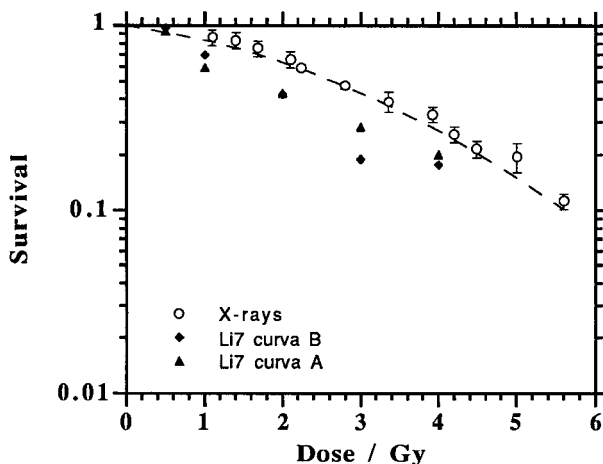
Fig. 3 - Very preliminary dose-response curves for V79 cell inactivation induced by 68 keV/μm ^{7}Li ions

Development of the LPM "microbeam facility" at the LNL 2 MV AN2000 Van de Graaff accelerator has continued. The accelerator technical staff and the LPM researchers have pursuit work on the focusing and controlling beam systems in order to increase its performances as well as in developing and testing the detector complex for detection of single ion hits and a fast beam switching system aimed to be used in the "single event" experiments. Our own contribution in this field has been focused to define proper "single cell" irradiation conditions. These concern, in particular, with the definition of protocol for the biological sample preparation, including the development of a suitable biostak, and the biological sample positioning system on the particle beam. The impinging charged particle position will be recorded by a solid state nuclear track detector. Appropriate cell and track detector image analyses will allow us to correlate the "biological effects" to traversals. The positioning of the sample will be accomplished by using an optical microscope connected to an especially designed computer controlled table housing the sample holder. The establishments of the most favourable configurations for all the above require special care and are under optimization. An adequate image analysis system together with the necessary software as well as a dedicated optical microscope have been purchased.

Experiments aimed to study the fast neutron biological effectiveness on V79 cells are being started. Test runs have been carried out at the LNL 7 MV Van de Graaff CN accelerator mainly aimed to physical and dosimetric characterization of the neutron beams (neutron energy distribution, flux, spatial homogeneity at the biological sample position, etc.). Monoenergetic fast neutrons have been produced trough the $^7Li(p,n)^7Be$ reactions, by using 0.500-0.700 mg/cm^2 ^7LiF production targets.

Sets of CR39 track detectors and TLDs have been irradiated at the same position of biological samples in order to verify fluences, spatial and energy distributions of the impinging neutrons on the T25 flask surface, foreseen to be used in the biological experiments. Routine biological experiments are planned.

Publications

Journals

- F.CERA, R. CHERUBINI, A.M.I. HAQUE, G. MOSCHINI, P. TIVERON, M.BELLI, F. IANZINI, , O. SAPORA, M.A. TABOCCHINI and G. SIMONE
  Radiobiology and radiotherapy projects with accelerated charged particles at the INFN-Laboratori Nazionali di Legnaro: present status and future perspectives
  Physica Medica, vol. IX(1),(1993)161-165

- M.BELLI, F.CERA, R. CHERUBINI, A.M.I. HAQUE, F. IANZINI. G. MOSCHINI, O. SAPORA, G. SIMONE, M.A. TABOCCHINI, P. TIVERON
  Inactivation and mutation induction in V79 cells by low energy protons: re-evaluation of the results at the LNL facility
  Int. J. Radiat. Biol.63(1993) 331-337

- A.WAHEED, A.MAJEED, F.CERA, P.TIVERON, R. CHERUBINI, G. MOSCHINI and E.U. KHAN
  Use of track detectors in biomedical sciences
  Nucl. Tracks Radiat. Meas. 22(1993)889-892

- D. BOLLINI, F. CERVELLERA, G.P. EGENI, P. MAZZOLDI, G MOSCHINI, P. ROSSI, V. RUDELLO.
  The microbeam facility at AN-2000 accelerator of Laboratori Nazionali di Legnaro.
  Nucl. Instr. and Meth. A328, 173-176 (1993)

- M.BELLI, F.CERA, R. CHERUBINI, D.T. GOODHEAD, A.M.I. HAQUE, F. IANZINI, G. MOSCHINI, O. SAPORA, G. SIMONE, D.L. STEVENS, M.A. TABOCCHINI, P. TIVERON
  Inactivation induced by deuterons of various LET in V79 cells
  Radiat. Prot. Dosim.52(1994) 305-310

- M. BELLI, F. CERA, R. CHERUBINI, A.M.I. HAQUE, F. IANZINI, G. MOSCHINI, O. SAPORA, G. SIMONE, M.A. TABOCCHINI and P. TIVERON
  Inactivation induced by low energy deuterons in V79 cells.
  Physica Medica, vol. X(1),(1994) 75-76

- F. CERA, R. CHERUBINI, A.M.I. HAQUE, G. MOSCHINI, P. TIVERON, F. CALZAVARA, L. TOMIO, M.G. TROVÒ, P.L. ZORAT and G. KRAFT

Application of charged particle beam for radiotheraphy
Physica Medica, vol. X(1),(1994)100-104

- M. BELLI, F. CERA, R. CHERUBINI, A.M.I. HAQUE, F. IANZINI, G. MOSCHINI, O. SAPORA, G. SIMONE, M.A. TABOCCHINI and P. TIVERON
DNA double strand breaks induced by low energy protons in V79 cells
Int. J. Radiat. Biol., 65, n.5, 511-522 (1994)

- M.A. TABOCCHINI, M. BELLI, F. IANZINI, L.LEVATI, E. PAGANI, O. SAPORA, G. SIMONE, F. CERA, R. CHERUBINI, A.M.I. HAQUE, G. MOSCHINI and P. TIVERON
Mutation induced by low energy protons in V79 cells
Advances in Space Research, in press

- M. BELLI, F. IANZINI, O. SAPORA, M.A. TABOCCHINI, G. SIMONE, F. CERA, R. CHERUBINI, A.M.I. HAQUE, G. MOSCHINI and P. TIVERON
DNA double strand breaks production and repair in V79 cells irradiated with light ions
Advances in Space Research, in press

Confecence Proceedings

- M.BELLI, F.CERA, R.CHERUBINI, A.M.I.HAQUE, F.IANZINI, G.MOSCHINI, O.SAPORA, G.SIMONE, M.A.TABOCCHINI, and P.TIVERON
The RBE of protons for cell inactivation: the experience with V79 cells
in: "Hadrontherapy in Oncology", Excepta Medica, International Congress Series 1077, Elsevier Science B.V., U.Amandi, B.Larsson Eds., 1994, pp. 702-705.
Proc. of the Intern. Symposium on Hadron Therapy, Como, Italy, Oct. 18-21, 1993

- R. CHERUBINI, F. CERA, F. CERVELLERA, A. DAINELLI, A.M.I. HAQUE, G. MOSCHINI, M. NIGRO, P. TIVERON, C. BISANTIS, F. CALZAVARA, E. MIDENA, L. TOMIO, M.G. TROVÒ, P.L. ZORAT AND G. KRAFT
Biomedical activities and radiotherapy projects with accelerated charged particles at the INFN-Laboratori Nazionali di Legnaro: present status and future perspectives
in: "Hadrontherapy in Oncology", Excepta Medica, International Congress Series 1077, Elsevier Science B.V., U.Amandi, B.Larsson Eds., 1994, pp. 400-405.
Proc. of the Intern. Symposium on Hadron Theraphy, Como, Italy, Oct. 18 - 21, 1993

- P. BOCCACCIO, D. BOLLINI, F. CERVELLERA, G.P. EGENI, S. FAZINIC, S. GALASSINI, A.M.I. HAQUE, G. MOSCHINI, P. ROSSI, V. RUDELLO.
The Legnaro proton microprobe: a general purpose facility for spatial elemental analysis and single particle irradiation.
4th L.H. Gray Workshop on Microbeam Probes of Cellular Radiation Response. Northwood, U.K., July 8 - 10, 1993

- R. CHERUBINI, F. CERA, M. DALLA VECCHIA, A.M.I. HAQUE. G. MOSCHINI, P. TIVERON, M. BELLI, F. IANZINI, O. SAPORA, M.A. TABOCCHINI AND G. SIMONE
Biological effectiveness of low-energy accelerated light ions
Presented at the 5th Annual Space Radiation Health Investigators Workshop USRA, April 26-28, 1994, Houston, TX, USA

- F. CERA, R. CHERUBINI, M. DALLA VECCHIA, A.M.I. HAQUE, P. TIVERON, G. MOSCHINI, M. BELLI, F. IANZINI, M.A. TABOCCHINI, O. SAPORA, G. SIMONE
Inactivation in V79 cells induced by high LET helium ions

Proc. of the "I Congresso Nazionale Congiunto SIRR-GIR: Radiazioni: dalla teoria alle applicazioni multidisciplinari". Pisa, November 24-26, 1994. In press

- M.BELLI, F.IANZINI, M.A.TABOCCHINI, O.SAPORA, F.CERA, R.CHERUBINI, DALLA VECCHIA, A.M.I.HAQUE, G.MOSCHINI, P.TIVERON, G.SIMONE
The induction and rejoining of DNA dsb in V79 cells exposed to low energy protons
Proc. of the "I Congresso Nazionale Congiunto SIRR-GIR: Radiazioni: dalla teoria alle applicazioni multidisciplinari". Pisa, November 24-26, 1994. In press

- R. CHERUBINI, F. CERA, M. DALLA VECCHIA, A.M.I. HAQUE. G. MOSCHINI, P. TIVERON, M. BELLI, F. IANZINI, O. SAPORA, M.A. TABOCCHINI AND G. SIMONE
Biological effectiveness of light ions for cell inactivation and mutation induction on V79 cells
Proc. of the "5th Workshop on Heavy Charged Particles in Biology and Medicine", GSI, Darmstadt, Germany, August 23-25, 1995. GSI-Report-95-10, August 1995, ISSN 0171-4556. pp.73-76

- G.SIMONE, M.BELLI, F.IANZINI, O.SAPORA, M.A. TABOCCHINI, F. CERA, R. CHERUBINI, M. DALLA VECCHIA, A.M.I. HAQUE, G. MOSCHINI, P. TIVERON.
Light Ions Induction and Rejoining of DNA dsb in V79 Cells
Proc. of the 10th International Congress of Radiation Research, Wurzburg, Germany, August 27-September 1, 1995. In press

Abstracts

- R. CHERUBINI, F. CERA, A.M.I. HAQUE, P. TIVERON, G. MOSCHINI, G. SIMONE, M. BELLI, F. IANZINI, O. SAPORA and M. A. TABOCCHINI
Mutation induction of low energy deuterons in V79 cells
Presented at the Radiation Research Society, 41st Annual Meeting, North American Hyperthermia Society 13th Annual Meeting, Dallas, TX, USA, March 20-25, 1993

- M. BELLI, F. CERA, R. CHERUBINI, A.M.I. HAQUE, F. IANZINI, G. MOSCHINI, O. SAPORA, G. SIMONE, M.A. TABOCCHINI and P. TIVERON
Comparison between protons and deuterons with the same LET in inducing mutation in V79 cells
Presented at the 25th Annual Meeting of the European Society for Radiation Biology, Stockholm, Sweden, June 10-14, 1993

- F. CERA, R. CHERUBINI, G.GALEAZZI, A.M.I. HAQUE, G. MOSCHINI, P. TIVERON
Caratterizzazione di fasci di particelle alfa per l'irraggiamento di cellule di mammifero
Presented at the "LXXIX Congresso Nazionale SIF", Udine, Italy, Sept. 22 - Oct. 2, 1993

- R. CHERUBINI
RBE values of stopping protons, alphas and deuterons in the range 20 - 40 keV/μm
Invited talk
Presented at the Proton Theraphy Co-Operative Group - PTCOG XIX, Oct. 31 - Nov. 2, 1993, Cambridge, Boston, USA

- M. BELLI, F. CERA, R. CHERUBINI, F. IANZINI, G. MOSCHINI, O. SAPORA, G. SIMONE, M.A. TABOCCHINI AND P. TIVERON
Initial production of DNA dsb does not parallel inactivation and mutation induction in V79 cells irradiated with low energy protons

Presented at the 18th L.H. Gray Conference - Radiation Damage in DNA: Physics, Chemistry and Molecular Biology, April 10-14, 1994, Bath, UK

- R. CHERUBINI, F. CERA, A.M.I. HAQUE, P. TIVERON, M. DALLA VECCHIA, G. MOSCHINI, G. SIMONE, M. BELLI, F. IANZINI, O. SAPORA AND M.A. TABOCCHINI
Direct comparison of RBE of low-energy accelerated light ions
Presented at the Radiation Research Society - 42st Annual Meeting, North American Hyperthermia Society 14th Annual Meeting, 29 April - 4 May 1994 Nashwille, TN, USA

- M. BELLI, F. IANZINI, O. SAPORA, M.A. TABOCCHINI, G. SIMONE, F. CERA, R. CHERUBINI, A.M.I. HAQUE, P. TIVERON and G. MOSCHINI
Effectiveness of deuterons and helium-3 ions with LET ranging from 40 to 60 keV/μm in inducing lethality in V79 cells.
Presented at the 26th European Society for Radiation Biology and European Society for Hyperthermic Oncology, 1-4 June 1994, Amsterdam, Netherlands

- R. CHERUBINI, F. CERA, A.M.I. HAQUE, G. MOSCHINI, P. TIVERON, M. BELLI, F. IANZINI, O. SAPORA, M.A. TABOCCHINI, G. SIMONE,
Light ion radiobiological facility at the Laboratori nazionali di legnaro: Irradiation protocols and inactivation induced by low energy protons
Presented at the 30th COSPAR Scientific Assembly, 11-21 July 1994, Hamburg, Germany

- F.IANZINI, M.BELLI, O.SAPORA, M.A.TABOCCHINI, G.SIMONE, F.CERA, R.CHERUBINI, A.M.I.HAQUE, G.MOSCHINI, P.TIVERON
DNA double strand breaks production and rejoining in V79 cells after irradiation with low energy protons
Presented at the 1995 Keystone Symposia, Taos, N M, USA, March 23-29, 1995

- M.BELLI, F. CERA, R. CHERUBINI, A.M.I. HAQUE, F. IANZINI, G. MOSCHINI, O. SAPORA, G. SIMONE, M.A. TABOCCHINI, and P. TIVERON
Biological effectiveness of low energy protons: DNA dsb production and rejoining in V79 cells
Presented at the Association for Radiation Research Meeting, St Andrews University, Scotland,UK, April 5-8, 1995

- F. CERA, R. CHERUBINI, M. DALLA VECCHIA , A.M.I. HAQUE, G. MOSCHINI, P. TIVERON, M. BELLI, F. IANZINI, O. SAPORA, M.A. TABOCCHINI, G. SIMONE.
Cell inactivation and mutation induction in V79 Cells Irradaited with Helium-3 and Helium-4 Ions
Presented at the 10th International Congress of Radiation Research, Wurzburg, Germany, August 27-September 1, 1995

- F. CERA, R. CHERUBINI, M. DALLA VECCHIA, S. FAVARETTO, G. GALEAZZI, A.M.I. HAQUE, G. MOSCHINI, P. TIVERON,
Accelerated charged particle radiobiological facilities at the INFN-Laboratori Nazionali di Legnaro
Presented at the 4th European Conference on Accelerators in Applied Research and Technology, Aug. 29 -Sept.2, 1995, Zürich, Switzerland

I. Partner: Cancer Research Campaign Gray Laboratory

Head of Project: Dr. B.D. Michael

II. Objectives of the Reporting Period

We have used the new irradiation arrangement reported last year to make further comparisons of the relative biological effectiveness (RBE) of singly and doubly charged ions in the LET range up to ~100 keV μm^{-1}. These studies provide information relating to the radial features of energy deposition around charged particle tracks that determine effectiveness; they also provide constraints for biophysical modelling of RBE as a function of radiation quality. This work is carried out using conventional "broad-field" irradiation techniques, i.e. with many charged particles passing through each cell at random. With these techniques, the doses are inevitably much higher than those directly relevant to radiation protection. Our charged-particle microbeam has been brought into routine use during the year and this has been developed to allow effectiveness to be determined down to the extreme low dose levels that apply in most environmental and occupational exposures to medium- to high-LET radiations, that of a single particle traversal of the cell nucleus. We report preliminary data on DNA damage and on micronucleus induction. This facility will also allow us to study in detail effects that are transmitted between hit and non-hit cells, such as have been indicated in several recent studies using conventional irradiation techniques. There is considerable evidence, including from our own laboratory, that radiation effectiveness depends strongly on clustering of lesions on DNA and we report studies relevant to this topic. We have carried out several investigations into the chemical stage of radiation effect directed at understanding and quantifying the reactions of the initial clustered radical sites on DNA and the pathways by which they go on to become clusters of stable lesions. These studies have used our fast kinetics techniques, employing pulsed low- and high-LET radiations, to characterize the processes. Whereas our earlier fast kinetics studies have mainly been on strand break prevention due to chemical repair by thiols, particularly the major naturally occurring thiol, glutathione, work this year has concentrated on the competing fixation reactions by which radical sites are converted into breaks. This work has shown further kinetic evidence for clustering at its most basic level, a 2-radical precursor of dsb induced by low-LET radiation, and is also the pilot study for experiments using medium- to high-LET radiations to investigate the degree of DNA radical clustering that is associated with their track structure. The complexity of radiation-induced DNA lesions derives from the distributions of energy depositions on a nanometer scale around charged particle tracks and partners in this and other consortia have modelled these processes using Monte Carlo simulations. While the distributions of energy deposition can be modelled with a fair degree of certainty, little is known about the relationships between the magnitudes of the energy depositions and the DNA damages that result. Our studies using low-energy electrons and photons with plasmid DNA are directed at quantifying these relationships in the important energy range from about 5 to several 100's of eV in which most of the energy transfer from high-energy particle tracks occurs. Our initial work was with dry DNA samples, and this year we have been able to examine the effects of hydration on strand breakage induction by synchrotron photons. As observed previously with dry DNA, we again find the unexpected result that photons with energies down to ~8 eV induce dsb efficiently. Modelling studies in the literature have indicated a substantially higher threshold energy for dsb induction and our further work on this topic will be directed at understanding and resolving the apparent difference and relating it to the processes that occur with high-energy particle tracks.

III. Progress Achieved During Reporting Period

Biological Effectiveness of Singly- and Doubly-Charged Particles

Using our new arrangement for irradiating V79 mammalian cells with low-energy particles, we have consolidated our measurements of the biological effectiveness of low-energy protons and deuterons. We now have data for the lethality of these particles in the LET range 10 keV/μm to 50 keV/μm (see Figure 1). In addition, we have acquired data for the RBE of ^{3}He^{++}
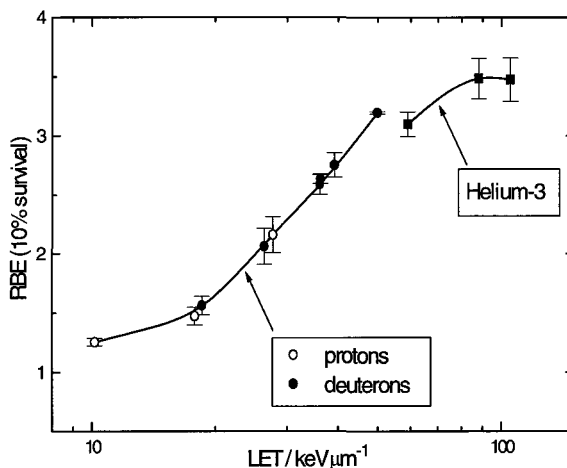
Figure 1. Effectiveness of low-energy singly- and doubly-charged particles.

ions with LET's from 59 to 105 keV/μm. Where the singly- and doubly-charged particle data approach each other (50-60 keV/μm), we find that protons and deuterons are more effective than ^{3}He^{++} ions of the same LET. This result confirms our conclusions reported previously, and is in agreement with the data of another group within our consortium (Belli and colleagues). There is disparity however regarding the relative effectiveness of protons and deuterons with the same LET. Unlike the studies undertaken at the LNL facility at Legnaro, we find no difference in the RBE's of protons and deuterons with the same LET. We are endeavouring to reconcile these differences by undertaking a dosimetric intercomparison between the Gray Laboratory and the LNL facility. Measurements using the Gray Laboratory dosimetric equipment have been made at LNL. The technique used by the Gray Laboratory is to measure ionization using a thin-window extrapolation chamber. This was compared with the LNL method (based on measurements of fluence and energy) and was found to be in reasonable agreement. Some anomalies were observed regarding measurements of energy using Gray Laboratory and LNL spectroscopy equipment, however lack of time did not permit these observations to be resolved. A visit by the LNL team to the Gray Laboratory is anticipated.

The Charged-Particle Microbeam

The charged-particle microbeam has been in routine use for performing radiobiological experiments since the beginning of 1995. Prior to this, we installed an arrangement for collimating the charged-particles that uses devices based on silicon technology. A range of collimators have been fabricated by a microengineering company that consist of microchannel 'V'-grooves etched into the surface of 2 mm by 2 mm by 1 mm thick silicon wafer pieces. In

use, each collimator is paired with an un-etched piece of the same size (to form a three-sided hole) using a gimballed jaw assembly mounted at the end of the beamline. The engineering company were unable to meet our specified minimum width for the 'V'-grooves (1 micron), however we do have a number of devices as small as 3 microns wide by 2 mm long, and these have been used for the majority of experiments. A big advantage of this type of collimator is that, if necessary, they can be disassembled, cleaned and re-used. In tandem with this approach, we are continuing to develop fine-bore glass capillary collimators as these may ultimately provide us with the best spatial resolution. So far, we have achieved good performance down to about 5 microns with the silicon devices. Preliminary evaluation of 1.5-micron bore capillaries that have been manufactured to our specification show that they will provide 2.3-micron resolution. We are currently negotiating for the manufacture of 0.5- to 1-micron bore capillary.

The development of detectors to register the passage of individual particles through each cell exposed to the microbeam has continued. A prototype transmission detector, comprising a thin scintillator, coupled via fine optical fibres to a pair of photomultiplier (PM) tubes has been assembled and evaluated. Although tests indicate that it is efficient (99%), it is currently too fragile to use in conjunction with cell irradiation experiments. Therefore, a more robust system has been developed, retaining the transmission detection principle. We have recently implemented an arrangement that uses a miniature photomultiplier tube (Hamamatsu R5600U-06) installed just above the cell dish, to detect the light from a transmission scintillator (5- to 10-micron thick anthracene) mounted at the collimator exit. Initial tests have proved highly satisfactory and this arrangement has recently been brought into routine use.

To accommodate the PM tube (and for other reasons), the cell dishes have been re-designed. The new design is made from medical-grade stainless steel in two parts, and uses a silicone rubber gasket to trap and stretch a thin film that forms the dish base. We now use 4 micron thick polypropylene, instead of Mylar for this purpose as it is optically cleaner, both in visible and UV light.
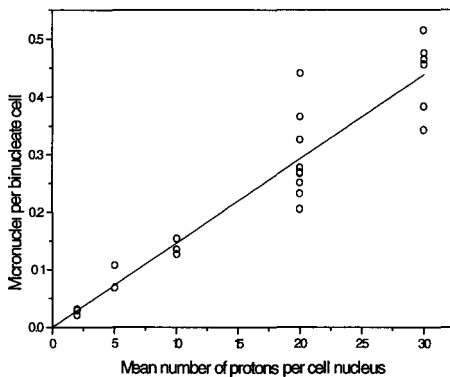
Figure 2. Induction of micronuclei in V79 cells as a function of the mean number of nuclear traversals by protons.

For relating chromosome damage to low doses we are using the micronucleus assay. By scoring acentric fragments *in situ* we have been successful in detecting an effect after traversals by just two (average number) 3.2 MeV protons. A full dose-effect curve (see Figure 2) shows a linear induction of micronuclei per binucleate cell with increasing mean particle traversal number. Our ongoing work is to score this endpoint in relation to counted particle traversals.

We wish to ascertain whether the apparent ability of a cell to survive a single traversal can arise because the DNA has not been hit. To do this, we have implemented the single-cell comet assay as a measure of DNA damage, such that it can be used with attached cells. Trials using broad-field α-particles show that it is possible to detect comet-tail migration after doses as low as 0.5 Gy. We have also adapted the clonogenic assay for use with the microbeam to measure cell lethality as a function of the number of particle traversals.

Clustered Damage to DNA

A major emphasis of our research is understanding the role of radiation damage to DNA in relation to biological effectiveness. In particular, we have examined the relationship between lesion complexity and effectiveness with studies to determine the role of clustered damage to DNA. This occurs as a consequence of single tracks of radiation crossing the DNA and inducing multiple events locally within it, reflecting the clustering of ionisations along the track itself. A simple manifestation of a complex lesion is the double strand break, considered important in radiation effect, but more complex associations of breaks and other damages are predicted from modelling studies. These lesions are believed to be critical for radiation action and a consideration of their induction, repair and chemical modification is important for understanding their role. Our interest is in two areas; firstly, we are developing molecular assays for complex lesions principally using end-labelling techniques to detect clusters of breaks and the association of other lesions such as base damage with these breaks. This involves the polynucleotide-mediated exchange reaction in a model plasmid DNA system and comparing the fragmentation patterns after low- or high-LET irradiation.

Secondly, investigation of clustered damage at the molecular level must *a priori* lead to a consideration of clustering of the initial free-radical sites. We have previously shown that even with low-LET radiation a DNA dsb can be considered a complex lesion originating from a biradical precursor, i.e. one radical on either strand of the DNA. This was done by following the reaction kinetics of the chemical repair of the radical precursors of ssb and dsb by thiols both in a model DNA system and in intact mammalian cells. Further studies have measured chemical repair kinetics of both ssb and dsb with increasing LET, using pulsed protons and deuterons, and have shown behaviour consistent with increased clustering of radicals.

Our recent studies have concentrated on the fixation reactions which compete with chemical repair prior to damage being expressed in the DNA after irradiation. In plasmid DNA we have observed chemical fixation of both ssb and dsb free radical precursors *in the absence of oxygen.* This has utilised our gas explosion system, where we can irradiate DNA with a short pulse of electrons (5 nS) and allow H_2S gas at high pressure to be added to the system at preset times to chemically rescue damage which has not been fixed, either in the presence or the absence of oxygen. The hypoxic fixation process we have observed is relatively slow with the half-life of the radicals being ~35 ms for ssb and 70 ms for dsb. This is an important observation as it provides a mechanism for the decrease in oxygen enhancement ratio with increasing LET on the basis of an increase in radical multiplicity. If one considers that the number of radicals associated with a dsb increases with LET, the probability that, even under hypoxia, at least one will be fixed by these processes and produce a strand break will increase. This provides an alternative hypothesis for the OER/LET effect to those of the oxygen-in-the-track and interacting-radical mechanisms which have previously been proposed. We have recently measured a similar process an *E. coli* strain 7 which is highly deficient in GSH, so the process is of importance in cellular systems. The first-order rate of the hypoxic fixation reaction of lethal lesions in *E. coli* was 45 s^{-1} in comparison to 10 s^{-1} and 20 s^{-1} measured for ssb and dsb respectively in pBR322 DNA. By the addition of various concentrations of oxygen during measurement of the fixation process the rate of

oxygen fixation has been determined in these systems. For pBR322 DNA the second-order rate constants were 1×10^8 $M^{-1}s^{-1}$ for dsb and 2.4×10^8 $M^{-1}s^{-1}$ for ssb free radical precursors. These approximately two-fold differences in fixation rate between ssb and dsb are consistent with our previous results showing that the precursors of a dsb is a biradical. For both radicals of the dsb to be chemically fixed either by oxygen or by the hypoxic mechanism a two-step process is required which would appear slower overall in comparison to the fixation of a single-radical ssb precursor. In *E. coli* strain 7, preliminary studies indicate that the rate for fixation of the oxygen-dependent precursors of lethality is ~4×10^7 $M^{-1}s^{-1}$. Interestingly, this is lower than the values measured in pBR322 DNA and may be a consequence of a higher viscosity in the cellular system influencing the oxygen diffusion and reaction rates.

Cellular Studies Measuring the Role of Higher-Order Structure

As well as clustering of damage at sites on DNA in the order of a few base pairs, when high LET tracks cross DNA, the unique higher-order repeating structure of the DNA may lead to defined fragmentation patterns. For example, tracks which cross the 30 nm fibre may lead to an enhancement of fragments in the 1-2 kb size range. Using conventional and pulsed-field electrophoresis systems we have compared the molecular weight distributions for DNA from cells irradiated with X-rays or 3 MeV α-particles (110 keV/μm). In the high molecular weight region in the dose range normally used for dsb determination (1-50 Gy) the distribution of fragmentation sizes appears random (0.2-10 Mbp). A similar observation is observed monitoring the fragmentation pattern in the range of 8-50 kbp. Using conventional electrophoresis we have followed the fragmentation patterns of DNA from cells irradiated with X-rays or α-particles in the 0.2-10 kbp region. We have observed an enhancement of fragments in this region in DNA from cells irradiated with α-particles in comparison to X-rays, particularly around 500 bp. Further studies have now begun to probe the role of chromatin structure on these differences, by modulating chromatin compaction in isolated nuclei. We will also probe smaller fragmentation patterns by using end-labelling protocols similar to those we are developing in plasmid DNA systems. One prediction is that at the level of the nucleosome we should see enhancement of fragments in the 80 bp region with both low- and high-LET radiations. Clustering occurs with low-LET tracks but to a lesser extent, principally via spur processes, but these may lead to enhanced energy depositions over the volume of the nucleosome and a greater opportunity for fragments of around 80 bp.

Low-Dose Studies on Single Cells.

As part of our microbeam project, we have modified the comet assay for the detection of ssb in individual cells to work *in situ* for attached cells. As part of the calibration of this technique, we have studied the induction of ssb by low doses of broad-field α-particles equivalent to an average of one α-particle traversal per cell. At this dose we observe two populations of comet tails. Some which have tail lengths equivalent to control cells and some which have damaged DNA leading to greater tail migration. In this study, where the average α-particle dose is 0.23 Gy, those cells that exhibit damage show an amount equivalent to that induced by 0.5 Gy of X-rays, suggesting an RBE for ssb induction greater than 1.0, i.e. higher than the values generally obtained using gross assays for ssb. The data also indicate that a single α-particle traversal can produces around 500 breaks. Further work will be carried out using counted particles to see how the induction of ssb relates to the actual number of traversals and whether there is a fraction of cells that have had their nuclei traversed but do not show ssb.

Critical Energies for the Induction of DNA Damage

We have previously reported measurement of the relationships between energy deposited in plasmid DNA by low-energy electrons and photons. The aims of these studies are to provide data to contribute to the development of biophysical models of the induction of DNA damage by high-energy radiations and to obtain mechanistic information about the pathways by which the damage is induced. The most frequent energy depositions by high-energy radiations are in the region of 25 eV and our earlier work showed important differences between the effects of electrons and photons at this energy. It also showed that ssb and dsb induced by photons in the range 7 to 25 eV appear to derive from a common precursor species.

All of our previous work has been with dry plasmids exposed under high vacuum which provides a model for the direct effects of radiation on DNA. This year we have developed a system which enables hydrated samples to be exposed to synchrotron photons. Initial results have been obtained in the energy range 8 to 11 eV and show a 2- to 4-fold increase in ssb and dsb induction attributable to additional indirect effect damage from water radicals produced in the hydration layer around the DNA. The increase is uniform across this energy range suggesting that hydration does not have a strong effect on the threshold energies for induction of ssb and dsb or on their action spectra; however, further measurements will need to be carried out above and below these energies.

Further work has been carried out with low-energy electrons. Improvements have been made in the sample preparation techniques and a new vacuum system has been developed to minimize surface contamination of the samples.

IV. Publications (1994-1995)

1. Folkard, M., Prise, K.M., Brocklehurst, B., Hopkirk, A., Munro, I.H. and Michael, B.D. DNA damage by low-energy photons and electrons. In: *"Proceedings of 10th International Congress of Radiation Research, Würzburg, Germany, 1995"* (submitted).

2. Folkard, M., Prise, K.M. and Michael, B.D. Conventional and microbeam studies using low-energy charged particles relevant to risk assessment and the mechanisms of radiation action. *Radiat Prot Dosim* (in press).

3. Makrigiorgos, G.M., Folkard, M., Huang, C., Bump, E., Baranowska-Kutylewicz, J., Sahu, S.K., Michael, B.D. and Kassis, A.I. (1994). Registration of radiation-induced hydroxyl radicals within nucleohistones using a molecular fluorescent detector. *Radiat Res.*, **138**, 177-183.

4. Michael, B.D., Folkard, M. and Prise, K.M. (1994). Microbeam probes of cellular radiation response. *Int J Radiat Biol*, **65**, 503-508.

5. Michael, B.D., Prise, K.M., Folkard, M. and Vojnovic, B. (1994). An investigation of clustered radiation-induced lesions in DNA. *Radiat Prot Dosim*, **52**, 277-281.

6. Michael, B.D., Prise, K.M., Folkard, M., Vojnovic, B., Brocklehurst, B., Munro, I.H. and Hopkirk, A. (1994). Action spectra for ssb and dsb induction in plasmid DNA: Studies using synchrotron radiation. *Int J Radiat Biol.*, **66**, 569-572.

7. Michael, B.D., Prise, K.M., Folkard, M., Vojnovic, B., Brocklehurst, B., Munro, I.H. and Hopkirk, A. (1995). Critical energies for SSB and DSB induction in plasmid DNA: studies using synchrotron radiation. In *Radiation Damage in DNA: Structure/function Relationships in Early Times.* Edited by: A.F. Fuciarelli and J.D. Zimbrick (Battelle Press, Columbus) pp. 251-258.

8. Michael, B.D., Prise, K.M., Gillies, N.E. and Folkard, M. Mechanistic studies of clustered radiation-induced damage to DNA. In: *"Proceedings of 10th International Congress of Radiation Research, Würzburg, Germany, 1995"* (submitted).

9. O'Neill, P., McMillan, T.J., Nikjoo, H. and Prise, K.M. (Associate Editors) (1994). Proceedings of the 18th L.H. Gray Conference, University of Bath, U.K. 10-14 April 1994. *Int J Radiat Biol.*, **66**, 419-653.

10. Prise, K.M. (1994). The use of radiation quality as a probe for DNA lesion complexity. *Int J Radiat Biol*, **65**, 43-48.

11. Prise, K.M., Folkard, M. and Michael, B.D. (1995). A comparison of the fast kinetics of radiation-induced DNA lesions from low- and high-LET radiations: clustered damage and dependence on OER. In *Radiation Damage in DNA: Structure/function Relationships in Early Times.* Edited by: A.F. Fuciarelli and J.D. Zimbrick (Battelle Press, Columbus) pp. 185-190.

12. Prise, K.M., Folkard, M., Newman, H.C. and Michael, B.D. (1994). The effect of radiation quality on lesion complexity in cellular DNA. *Int J Radiat Biol.*, **66**, 537-542.

13. Prise, K.M. Gillies, N.E., Fahey, R.C., Whelan, A., Newton, G.L. and Michael, B.D. (1995). The role of charge in the radioprotection of *E. coli* by thiols. *Int J Radiat Biol.*, **67**, 393-401.

14. Prise, K.M., Gillies, N.E. and Michael, B.D. A comparison of chemical fixation and repair reactions of ssb and dsb in plasmid DNA: LET and the role of oxygen. In: *"Proceedings of 10th International Congress of Radiation Research, Würzburg, Germany, 1995"* (submitted).

Head of project 3:   D.T. Goodhead

II.   Objectives for the reporting period

1.   Track structure analysis of proton, deuteron and α-particle beams and comparison of their energy deposition patterns in nanometre volumes with their relative biological effectiveness, with particular emphasis on the region of 20-30 keV μm⁻¹ and extensive track statistics.

2.   Comparison of dosimetric methods for charged particle irradiations at Legnaro and MRC, with small-volume ionization chambers and CR39 track detectors.

3.   Measurement of HPRT⁻ mutation frequencies in V79 cells by slow α-particles (100-130 keV μm⁻¹) for comparison with results of partners.

III.   Progress achieved, including publications

Previous work by members of this coordinated contract has shown that the relative biological effectiveness (RBE) of protons for cell inactivation and *hprt* mutation of cultured fibroblasts rises rapidly as LET increases from 20-30 keV μm⁻¹ [1]. Hence the RBEs are significantly higher and rise more rapidly than do the RBEs of α-particles of the same LETs. Neither these raised RBEs nor the differences between protons and α-particles are reflected in initial yields of double strand breaks (dsb), the total yields of dsb generally being similar, or slightly less than, those from equal doses of X- or γ-rays, even for high-LET α-particles of 120 keV μm⁻¹ of nearly maximum cellular effectiveness. These observations have been confirmed by various independent experiments within and without the coordinated contract.

These comparisons highlight the crucial role of microscopic features of the radiation tracks in determining biological effectiveness, presumably at the nanometre level in view of the very narrow tracks of the low velocity protons. They suggest also that some aspect(s) of 'clustered' damage are prime determinants of cellular effectiveness and that the severity spectrum of the initial molecular damage, including perhaps dsb or varying complexity with associated damage, is relevant via differential repairability [2,3]. Precise quantitative data on the differences in biological effectiveness of similar radiations, such as is being obtained by other members of this coordinated group should provide valuable analytic information to probe the biologically critical features of the radiation tracks and the biologically-relevant initial molecular damage.

There have also been observations by the Legnaro group of differences in RBE between protons and deuterons of the same LET, and most recently also between Helium -3 and Helium -4 ions. If confirmed, these would raise serious and fundamental questions regarding current concepts of track structure. It is currently assumed that particles of the same charge and velocity should have identical differential track structure; thus there should be differences only in proportional energy loss, noticeable only over relatively large distances.

Our own limited contributions to this coordinated contract have been in the three areas listed as objectives above.

Firstly, to seek track properties that may correlate with the experimentally observed differences in RBE between protons and α-particles, we simulated many segments of tracks of these particles, using Monte Carlo code MOCA14 of Wilson and Paretzke, of LETs covering the range from about 20 to 40 keV μm^{-1} and also α-particles of higher LET up to more than 100 keV μm^{-1}. These were each scored for absolute frequencies of energy deposition, versus magnitude of energy deposition, in cylinders of diameters 2, 10 and 25 nm (and lenths ½ to 8 times the diameter) thrown randomly into the volumes containing all parts of each track. Comparisons of any of these frequencies, as well as traditional parameters such as $\bar{z}_F$ and $\bar{z}_D$, has not readily revealed any property that simultaneously correlates well with the experimentally observed RBEs for both particles [4]. Although we could readily define parameters whose values for α-particles lay systematically below those of protons, the relative rise in α-particle values over the LET range 20-50 keV μm^{-1} had a general tendency to mimic the corresponding rise of the protons. This is unlike the observed RBE dependences (see reports by other partners in the coordinated group). However, this search for biologically relevant properties of the tracks was complicated by three factors: Firstly, there is not yet full experimental agreement between laboratories on the shape of the RBE-LET curve for protons particularly at the higher LETs and on where the RBE may maximize. Secondly, the experimentally reported difference between protons and deuterons is *a priori* clearly beyond any property within the simulated tracks. Thirdly, the scored frequencies for α-particles at the lower LETs were remarkably unstable. Although we scored total track lengths, total numbers of ionizations and numbers of scoring cylinders similar to those that have given statistically stable results for other radiations these did not appear to be adequate for the α-particles [4]. Consequently, we needed to increase the already large statistics and undertake repeat determinations on different samples of tracks to ensure stability of the results.

Radial distributions of ionizations around protons and α-particles of selected energies have also been evaluated from the simulated tracks and made available in tabular form [5]. These radially-averaged quantities are not suitable for comparing ionization numbers in nanometre-sized targets because such numbers will in reality be dominated by secondary-electron stochastics. However, they may provide some indication of probabilities of correlated effects over larger distances.

For all the above new data our scoring statistics exceeded the minimum criteria (total number of track interactions, volume scoring ratios, number of target hits) that we had previously judged satisfactory (Charlton *et al.*, Radiat. Prot. Dosim. *13*, 123 (1985)). However, it appeared from the scatter of α-particle data points (versus LET) that fluctuations were considerably greater than might be expected from simple statistics of numbers of interactions or target hits, no matter how thoroughly the track volumes were scored. Apparently even 10 μm of total simulated track length of say 30 keV μm^{-1} α-particles (total ~3 x 10^4 interactions) is insufficient to represent adequately the stochastics of such α-particles. Further scoring at this energy was therefore carried out on a series of 9 separate samples each of 20 μm total track, to determine the fluctuations, and on 175 μm combined. For typical parameters presented previously [4] significant improvement is apparent by increase to a 20 μm track length, and very high accuracy is achieved by 200 μm. For example, for the parameters $\bar{z}_F$, $\bar{z}_D$ and f(>200) in nucleosome-like 10 nm diameter and 5 nm length target cyclinders for 5.46 MeV α-particles, the values are now shifted by 8%, 6% and 6%, respectively, from previously. The latter value of 6% compares with an expected standard deviation of <2% from the earlier hit-statistics. The effect of track-length statistics become even more pronounced for larger target volumes and larger energy thresholds.

With our new high-accuracy data for particles (p, d, α) in the region 20-30 keV μm^{-1} we are now able to reconsider the diagrams and conclusions presented previously [4]. The α-particle parameter versus LET curves now become smooth, and the p and d curves remain so. For example, Figs. 1 and 2 show plots of $\bar{z}_F$ and f(>200 eV) as published in ref [4] (figs. 5 and 8) but now using only the new high-accuracy data in the case of α-particles of 20-30 keV μm^{-1}. The general conclusions, however, remain essentially unchanged for the many parameters considered: no simple property has been identified that simultaneously correlates well with the observed RBEs of both p and d; parameters can readily be defined for which values for p are systematically greater than for α, but then they tend to rise in similar fashion in the range 20-50 keV μm^{-1}. We have eliminated the previous uncertainty in relation to α-particle track-scoring statistics, but the other uncertainties to meaningful track analysis in the present project remain: agreement between laboratories on the detailed shape and maximum of the experimental RBE-LET relationship for protons so that matching properties of the tracks can be sought; and verification of the reported differences between p and d (also ^{3}He and ^{4}He) that are clearly beyond the scope of any current track-structure simulations. Real differences in biological effectiveness between quite similar particle tracks should provide valuable basic data for identification of biologically critical microscopic properties of radiation tracks.

The second objective was aimed at alternative methods and comparisons of aspects of the dosimetry of the particle beams as used at Legnaro for the cellular irradiations that have been showing the differences in effectiveness between protons and deuterons (and other particles). Initially, in a limited comparison we applied our small-volume ionization chamber methods and CR39 track-etch detectors to a selection of proton and deuteron beams at Legnaro to compare with the dose rates and doses that the local team prescribed using totally independent dosimetric methods. The CR39 exposures in the position of biological samples also allowed evaluation of the uniformity of fluence across individual sample dishes and visualization of symmetry and size-uniformity of etched pits of individual tracks. The limited selection of beams tested accorded well with expectations on these criteria. Total fluence measurements on post-etched CR39 disks should be able to provide a reliable and independent method for evaluating absolute doses and comparing those from proton and deuteron beams both in calibration tests and during routine biological experiments. Our 0.1 cm^3 thin-windowed ionization chamber also performed satisfactorily in these tests and can be used directly on line for comparative measurements of dose-rate and prescribed dose of proton and deuteron beams. Conversion to absolute doses would require local calibration checks of the picocoulomb meter in conjunction with the lengthy cables leading from the end of the beam line to the instrument position. Such detailed methods could be warranted to support specific findings of the CR39 comparisons.

We next supplied Legnaro with CR39 discs and a request list of desirable beams for measurement to match into their experimental schedules as appropriate. These were for irradiation to prescribed doses (or fluences) of CR39 discs in place of the biological samples, to allow measurement verification of the expected fluences, as well as uniformity across the sample area, and estimation of particle uniformity (charge/energy) from sizes of individual pits. We consequently received irradiated discs as follows and samples of these have been etched and analysed. Unetched samples remain available for future comparative processing and analysis as required.

Table 1: CR-39 track detector disc irradiations at LNL, Legnaro. (Fluence calibrations 10 June 1994; disc irradiations 13 June 1994.)

Beam		At cell/CR39 entrance		Prescribed fluence	Number of CR39
Particle	Energy (MeV)	Energy (MeV)	LET (keV/μm)	x 10^{-6} (cm −2)	discs
Proton	6.00	5.0	7.7	1.5	10
	4.50	3.2	10.8	1.6	5
	3.30	1.5	19 1	1 4	5
Deuteron	6.50	4.9	13.3	2.2	10
	5.20	3.2	18.1	3 4	5
Helium^{-3}	11.00	7.9	50.0	1.5	10
	10.00	6.6	56.9	1.5	10
Helium^{-4}	13.50	10.3	51.0	2.2	10
	12.50	9 1	55.7	1.7	10

Table 2 shows data from the first set of CR39 discs analysed. Reproducibility of numbers of pits per area between discs irradiated with a given beam was good, with variation lying within the expectations of Poisson statistics. The measured fluences (i.e. pit densities) tended to be systematically lower than the prescribed fluences for all beams, but least so for the proton beams. One of the limitations to such comparisons is the need for low fluences for accurate counting of pits, with minimal overlap, and hence limitations on the counting statistics of the scattered-particle monitor in the vacuum line that is used to determine the prescribed dose. Such short exposures may also tend to exaggerate stop/start non-linearities if any exist. The last column in Table 2 shows the proportion of clearly oversized pits in central areas of the discs, from particles of lower velocity (or greater charge). This provides low-resolution estimates of the purity of the beams at the exact position of the biological samples. The larger pits are likely due to lower velocity (lower energy) scattered particles of the primary beam (as can be seen in large numbers very close to the field edges). Generally the large pits were observed to be circular, indicating incidence approximately perpendicular to the disc and therefore that the scatter occurred a long way from the sample position.

Our third objective was aimed at a comparative point of *hprt* mutagenesis in V79 cells by high-LET α-particles to link our mutagenesis work with that of other partners. We have confirmed that the dose-response is apparently linear with a mutation frequency of about (1.04 ± 0.30) x 10^{-4} Gy^{-1} at an LET of 121 keV μm^{-1} at the incidence surface of the cell monolayer. This frequency is the average of eighteen determinations, consisting of four repeats at a dose of 0.36 Gy and two at 0.70 Gy and expression times of 5, 7 and 9 days in each case. The result compares with a frequency of 0.86 x 10^{-4} Gy^{-1} reported earlier by Thacker *et al.* (Radiat. Res., *92*, 343 (1982)) using similar methods and the same cell line.

Fig.2: Pit Density Measurements for CR-39 discs irradiated at LNL, Legnaro. June 10, June 13,1994

Beam	Energy (MeV)	LET at cell entrance (keV μm⁻¹)	Counts on 1st monitor	Disc No	Pits per area	± SEM	Pit density cm⁻²	± error	Fluence Legnaro cm⁻²	error (poisson on 1st mon)	Fluence/ Pit density	± error	Large pits (%)
Multiplication Factor							1.00E+06	1.00E+06	1.00E+06				
Proton	6	7.7	100	53	80.5	±4.0	1.18	±0.060	1.5	±0.15			
	4.5	10.8	500	61	75.7	±2.4	1.11	±0.037	1.6	±0.07	1.36	±0.09	1.0
	3.3	19.1	2500	59	67.6	±1.6	0.99	±0.026					
				60	74.2	±2.7	1.09	±0.041					
					mean		1.06	±0.020	1.4	±0.03	1.32	±0.04	2.3
Deuteron	6.5	13.3	100	68	151.8	±3.8	2.23	±0.060	2.2	±0.22	0.99	±0.10	
	5.2	18.1	500	63	176.1	±4.0	2.58	±0.064					
				65	187.5	±3.7	2.75	±0.061					
				66	187.1	±4.9	2.74	±0.077					
					mean		2.69	±0.039	3.4	±0.15	1.26	±0.06	1.1
Helium-3	11	50	200	28	105.3	±2.6	1.54	±0.041	1.5	±0.11	0.97	±0.07	0.3
	10	56.9	300	42	98.8	±2.6	1.45	±0.041	1.5	±0.09	1.04	±0.07	0.2
Helium-4	13.5	51	100	4	165.8	±3.6	2.43	±0.058					
				12	154.8	±3.6	2.27	±0.058					
				6	157.5	±3.6	2.31	±0.058					
					mean		2.34	±0.033	2.2	±0.22	0.94	±0.10	0.1
	12.5	55.7	100	16	105	±2.8	1.54	±0.044					
				20	103.5	±2.8	1.52	±0.044					
				22	98.6	±2.2	1.45	±0.036					
					mean		1.50	±0.024	1.7	±0.17	1.13	±0.11	0.2
Measured Area	6.82E-05	±7.0E-07 cm²											

Publications

[1]   M. Belli, F. Cera, R. Cherubini, D.T. Goodhead, A.M. Haque, F. Ianzini, G. Moschini,
        O. Sapora, G. Simone, M.A. Tabocchini and P. Tiveron. "The importance of track
        structure of different charged particles having the same LET for biophysical
        modelling." In: Low Dose Irradiation and Biological Defence Mechanisms, eds.
        T. Sugahara *et al.* (Elsevier Science) pp. 445-448 (1992).

[2]   D.T. Goodhead, J. Thacker and R. Cox. "Effects of radiations of different qualities on
        cells: molecular mechanisms of damage and repair." Int. J. Radiat. Biol. *63*, 543-556
        (1993).

[3]   D.T. Goodhead. "Initial events in the cellular effecs of ionizing radiations: clustered
        damage in DNA." Int. J. Radiat. Biol. *65*, 7-17 (1994).

[4]   M. Belli, F. Cera, R. Cherubini, D.T. Goodhead, A.M.I. Hague, F. Ianzini, G.
        Moschini, H. Nikjoo, O. Sapora, G. Simone, D.L. Stevens, M.A. Tabocchini and P.
        Tiverin. "Inactivation induced by deuterons of various LET in V79 cells." Radiat.
        Prot. Dosim. *52*, 305-310 (1994).

[5]   H. Nikjoo. "The calculation of ionization distributions around charged particle
        tracks." MRC Monograph 93/1, MRC Radiobiology Unit, Chilton, Didcot (1993).
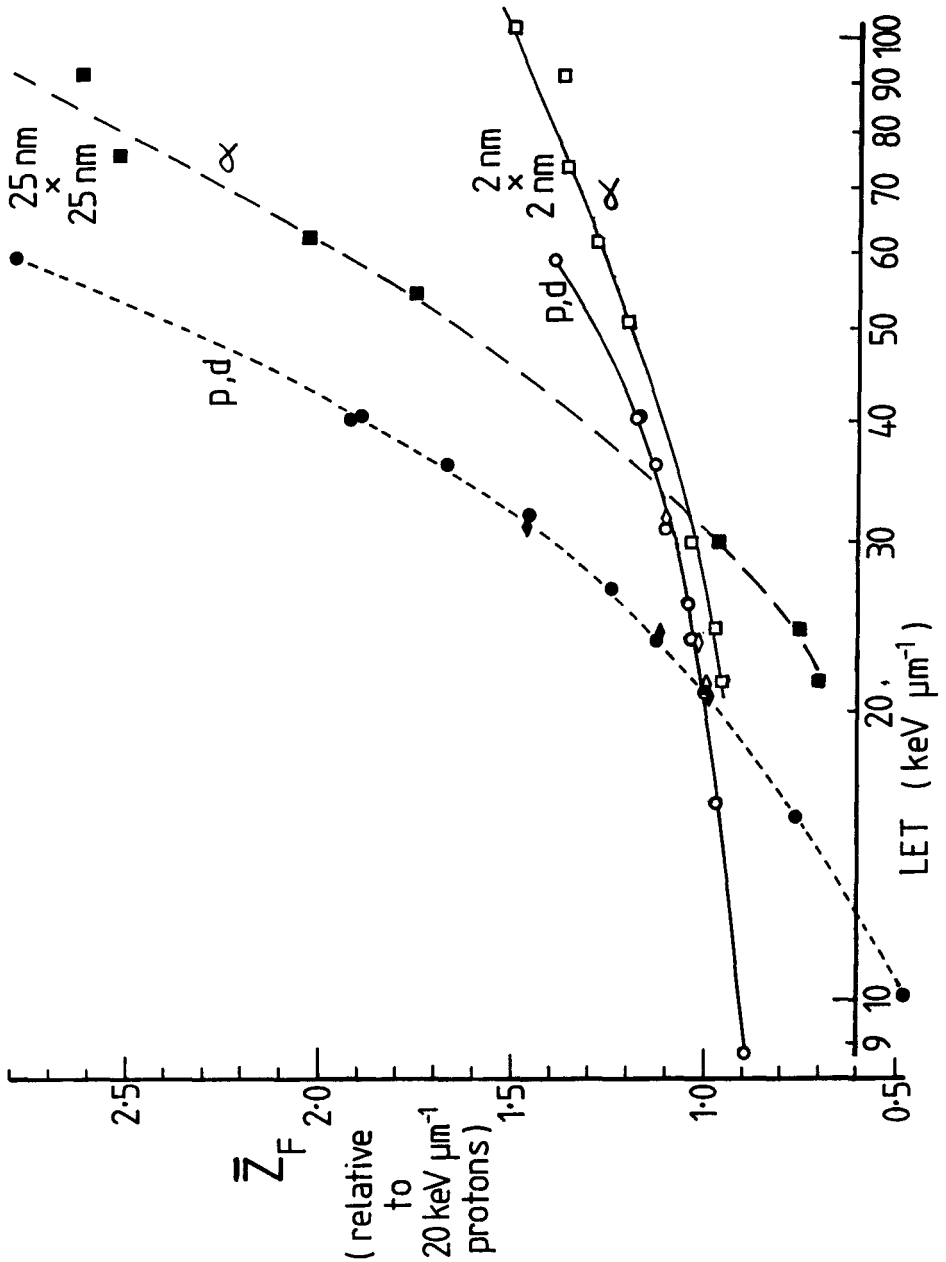
Fig. 1: Frequency mean specific energies ($\bar{z}_F$) in unit aspect ratio cylinders D = L = 2 nm or 25 nm randomly positioned in water uniformly irradiated with monoenergetic track segments of protons (circles), deuterons (diamonds) or α-particles (squares). All values of $\bar{z}_F$ are expressed relative to protons of 20 keV μm^{-1}.
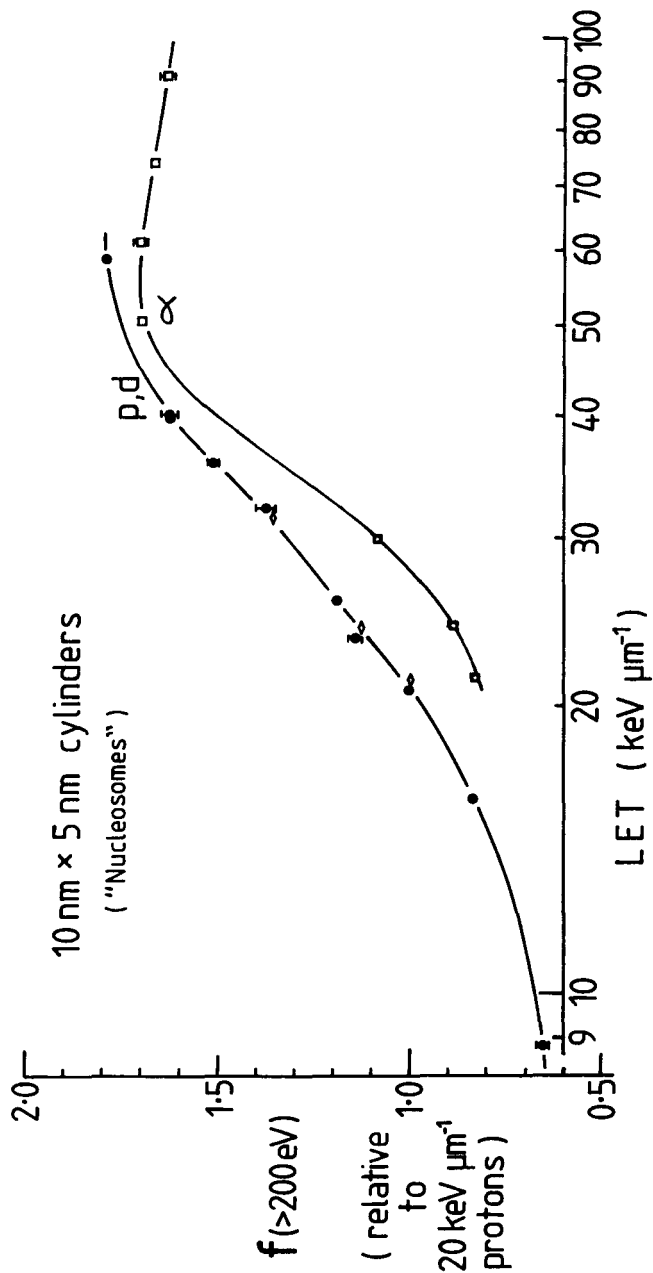
Fig. 2: Frequency of deposition of 200 eV threshold energy, f(>200 eV), in D = 10 nm by L = 5 nm cylinders ('nucleosomes') for protons (closed circles), deuterons (open diamonds) and α-particles (open squares), all expressed relative to protons of 20 keV μm⁻¹. Error bars are standard deviations of the number of events scored, assuming Poisson statistics. When not shown they are smaller than the symbol.

Head of project 4: Dr. M. Belli

II. Objectives for the reporting period.

1) Repair of molecular lesions.

2) Use of human cellular systems.

III. Progress achieved including publications.

(in collaboration with the LNL group)

1) In recent years, in the framework of a collaboration between the ISS and LNL groups, we have shown that the relative biological effectiveness (RBE) of protons for cell inactivation and mutation induction of V79 cells is higher than that observed for heavier charged particles in the LET range 10-30 keV/μm. These studies gave the first evidence that the RBE-LET relationships obtained with light ions may depend on the type of particle considered. These results were subsequently confirmed and extended by independent experiments carried out at the Gray Laboratory and at the MRC-Radiobiology Unit using the VEC facility at Harwell. More recently, in the attempt to relate changes in cellular functions to production of DNA damage, we have shown that the initial yield of double strand breaks (dsb) induced by X-rays, protons of various LET and He-4 ions, as measured by the neutral sucrose gradient technique, is quite insensitive to radiation type and LET. This finding supports the current opinion that the increased biological effectiveness for densely ionizing radiations can be due to clustering of ionization involving clustering of initial damage that, in turn, can affect repair processes. Clustered energy deposition and clustered damage are studied by other partners. In particular, model studies based on track structure are used for seeking properties that may correlate with experimental observations. Production of experimental data on damage repairability is therefore essential for establishing such correlations. To this aim we investigated the repair kinetics of the damage introduced in cellular DNA by charged particles of different qualities.

In the last year, we have completed the analysis of the rejoining time course of DNA dsb induced in V79 cells by protons of 11 and 31 keV/μm obtained at the LNL facility using the low-speed sedimentation technique. Gamma rays from a ^{60}Co source have been used as a reference. Experiments on the production of initial damage have been carried out in parallel with the rejoining experiments in order to gain information, on the same cell population, for both initial and unrejoined damage. Dose-response curves for dsb induction after irradiation with 41 and 58 keV/μm He-3 ions have also been obtained in view of forthcoming rejoining experiments for a comparison with the results already obtained for protons.

The dsb induction dose-response curves for protons (Fig. 1, Table 1) are in good agreement with those previously published (Belli et al. Int. J. Radiat. Biol., 1994, 65, 529-536). We confirmed that the RBE is not significantly higher than unity even when γ-rays are used as reference radiation instead that X-rays. The 3-helium results extend up to 60 keV/μm our previous finding that RBE for dsb induction is quite independent on LET and particle type (protons or He-ions) (Fig. 2).

For the rejoining experiments we used doses of 108, 111 and 144 Gy for γ-rays, 11 and 31 keV/μm protons, respectively. Even if they produce similar amounts of initial damage, namely about 7 dsb per 10^{12}u, there are significant differences in the rejoining kinetics, being those relative to γ-rays faster than those relative to protons. Moreover, the fraction of dsb left unrejoined after 120 min incubation is higher for protons than for γ-rays. These differences increase on increasing proton LET (Fig. 3).
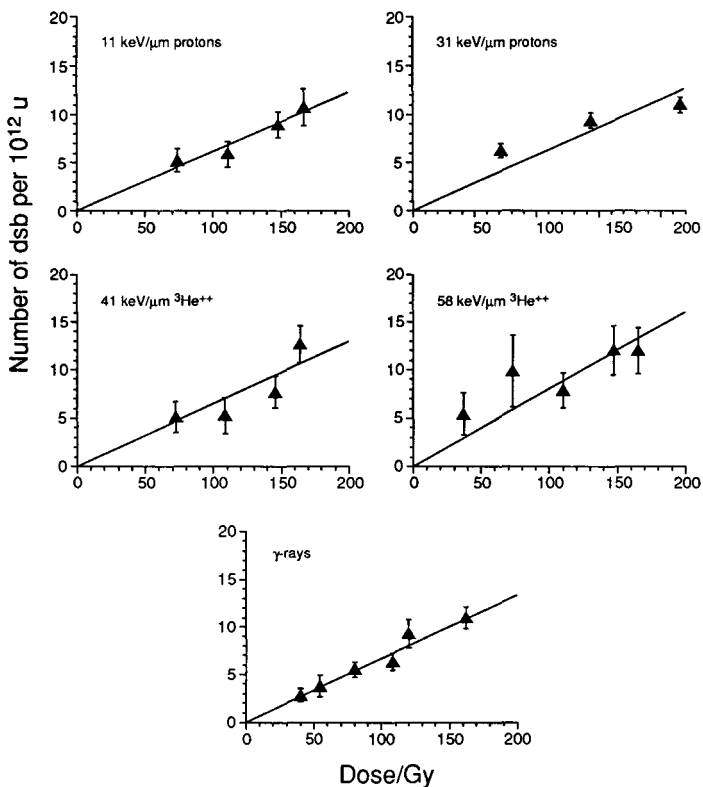
Figure1 - Dose-response curves for the initial number of dsb as measured by the sedimentation assay after irradiation of V79 cells with protons and He ions of various LET. Data for γ-rays are also shown for comparison.

TABLE 1: Best fit parameters and RBE values for dsb production

Radiation	Energy (MeV)	LET at 3 μm	α_{dsb} $(10^{-11} u^{-1} Gy^{-1})$	RBE $(\alpha_{dsb}/\alpha_{dsb,\gamma})$
γ-rays	-	-	0.67±0.01	-
Protons	3.24	11 keV/μm	0.62±0.05	0.93±0.17
	0.88	31 keV/μm	0.58±0.03	0.86±0.15
$^3He^{++}$	13.0	41 keV/μm	0.66±0.07	0.98±0.19
	10.0	58 keV/μm	0.81±0.09	1.21±0.24
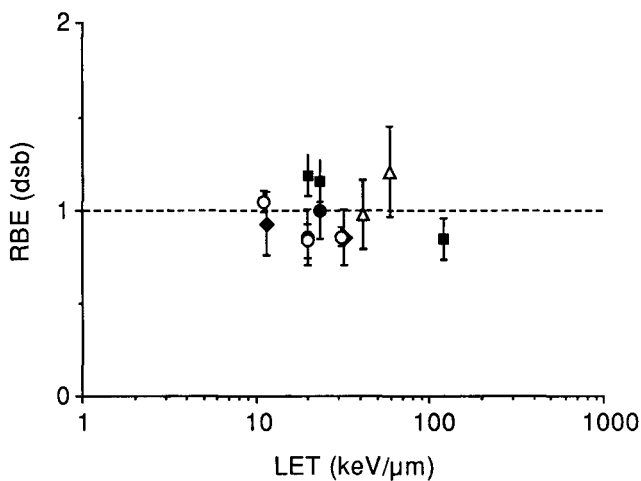
Figure 2 - $a_{dsb}/a_{dsb,g}$ as a function of the LET for protons (○: Belli et al., Int. J. Radiat. Biol., 65, 529-536, 1994, ●: Jenner et al., Int. J. Radiat. Biol., 61, 631-637, 1992) and alpha particles (■: Belli et al., Int. J. Radiat. Biol., 65, 529-536, 1994 and Jenner et al., Int. J. Radiat. Biol., 64, 265-273, 1993). Protons (◆) and He-3 (△), this paper.
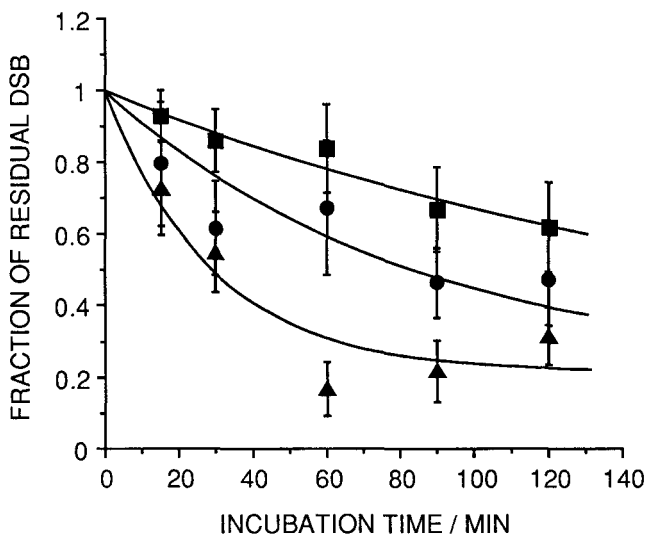
Figure 3 - Rejoning kinetics of DNA dsb induced after irradiation with, 31 (■), 10 keV/μm (●) protons and γ-rays (▲).

These experiments represent a first step in the analysis of the repair processes and clearly indicate that dsb induced by different radiations are not homogeneous with respect to repair. They suggest that changing from sparsely to densely ionizing radiation and increasing the LET, a more "complex" type of damage is induced, according to the hypothesis that clustered DNA lesions determine the severity of the effect. Our results suggest, therefore, that low energy protons produce a relatively higher proportion of this kind of damage with a consequent decrease in its repairability. This, in turn, could explain the higher RBE found for inactivation and mutation induction compared to that found for dsb.

The sedimentation technique we have used for this study gives a direct measurement of DNA molecular weight and as a consequence of DNA dsb. However, it has intrinsic limitation in sensitivity and is quite time consuming, so that we decided to set up the Pulsed Field Gel Electrophoresis (PFGE). With this techinque it is possible to perform the experiments here described at doses which better compare with those usually used for cell inactivation experiments. Moreover, the use of this technique allows an easier comparison (the plugs can be easly shipped from one laboratory to another) with the results eventually produced by other partners of this Coordinated CEC Contract. The PFGE dose-response curves obtained for dsb induction by X-rays and protons of 31 keV/μm in the dose range 10-60 Gy are shown in Fig. 4. It appears that the initial yield of DNA dsb is similar for both X-rays and protons, confirming the results obtained with the low speed sedimentation technique. Experiments are in progress on the short and long term (up to 24 h incubation) rejoining of dsb with protons and other light ions.

Furthermore, preliminary experiments on the evaluation of DNA damage by the microgel single cell electrophoresis ("comet") assay have been performed at the ISS on V79 cells irradiated with X-rays, in view of the possible application of the tecnique to the study of DNA damage induced by charged particles. This feasibility study has shown that it will be necessary to implement the instrumentation already present at LNL (microscope and CCD camera) for fluorescence and specific image analysis. The development of this technique will be very useful when applied in association with the microbeam at LNL for the single-particle, single-cell study.
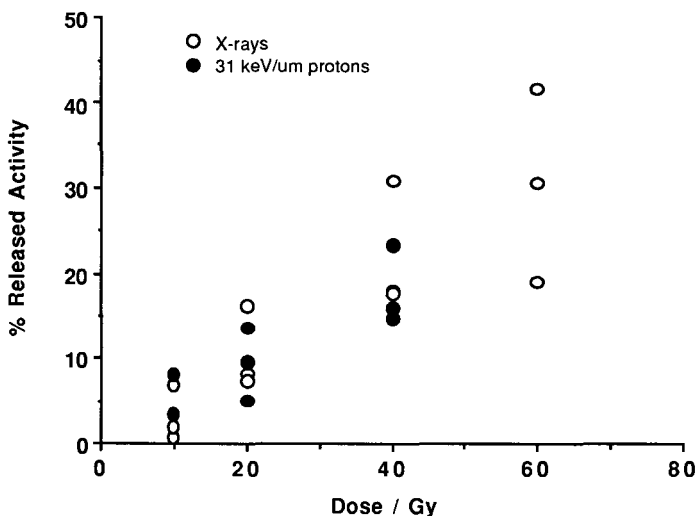
Figure 4 - Percentage of labeled DNA released from the PFGE plugs as a function of the dose for protons (closed symbols) and X-rays (open symbols).

2) Irradiation experiments on "in vitro" human cell culture can give more relevant information than that obtained with murine cells for developing biophysical models of radiation effects useful for risk assessment. The use of actively proliferating cells will help to establish the correlation between cell lethality and DNA damage after exposure to protons, deuterons and alpha particles in the same LET range. A comparison between differentiated and actively proliferating cells, that own a different structural organization of the genome, allows to study the influence of DNA conformation on the radiation induced damage and repair. Thus, in the framework of the collaboration with the LNL group, we put some efforts in beginning studies on human cell lines, namely TK6 and K562 (the latter able to undergo "in vitro" differentiation) showing different sensitivities. to X-rays.

So far we have performed few irradiation experiments of K562 human cells, growing as suspension culture, with protons of 11 keV/μm using the special filter based device shown in Fig. 5. Unfortunately, we have found difficulties in rescuing cells from the filter after irradiation and this fact prompted us to further modify the irradiation device in order to increase the efficiency of such rescue.
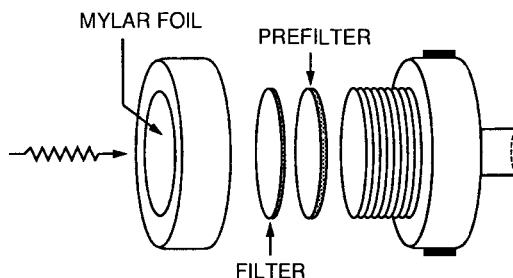
Figure 5 - Irradiation device for cells growing as a suspension colture.

It is worhtwhile to note that the licencing difficulties for the Cu-244 alpha source, whose set-up was planned for the preceeding period of the Contract, are now overcome. At present, the alpha source is at ISS and the irradiator is being assembled so that the planned experiments will start after the accomplishement of dosimetry calibration and the preliminary tests.

Previuos studies on cell inactivation induced by deuterons have shown that these particles are more effective than protons with the same LET. This result, unexpected because of the similarity in track structure between these two particles, has been confirmed also for mutation induction at the *hprt* locus and suggested that there should be other feature of the track structure until now overlooked, which are relevant for the biological effects of charged particles.
To get more insight on this point, in collaboration with the LNL group, we extended our investigation to other types of light ions with the same charge and different mass. In particular, we have carried out experiments on cell inactivation with He-3 and He-4 ions in the LET range 40-150 keV/μm. The results so far obtained show that there is a significant difference between these two particles, thus paralleling the results obtained for deuterons and protons. At present, we are carring out mutation induction experiments in the same LET range as that used for cell inactivation (see LNL report for further details).

Publications:

- "Biological Effectiveness of Light Ions for Cell Inactivation and Mutation Induction on V79 Cells ".
R. Cherubini, F. Cera, M. Dalla Vecchia , A. M. I. Haque, G. Moschini, P. Tiveron, M. Belli, F. Ianzini, O. Sapora, M. A. Tabocchini, G.Simone.
GSI-Report 95-10, ISSN 0171-4546, 73-76, August 1995.

- "Problems ans Perspectives in Proton Radiobiology".
M. Belli.
GSI-Report 95-10, ISSN 0171-4546, 73-76, August 1995.

- "Mutation Induced by Low Energy Protons in V79 Cells".
M. A. Tabocchini, M. Belli, F. Ianzini, L. Levati, E. Pagani, O. Sapora, G. Simone, F. Cera, R. Cherubini, A. M. I. Haque, G. Moschini, P. Tiveron.
Advances in Space Research, in press.

- "DNA Double Strand Breaks Production and Rejoining in V79 Cells Irradiated with Light Ions".
M. Belli, F. Ianzini, O. Sapora, M. A. Tabocchini, G. Simone, F. Cera, R. Cherubini, A. M. I. Haque, G. Moschini, P. Tiveron.
Advances in Space Research, in press.

- "Inactivation in V79 Cells Induced by High LET Helium Ions".
F. Cera, R. Cherubini, M. Dalla Vecchia , A. M. I. Haque, P. Tiveron, G. Moschini, M. Belli, F. Ianzini, M. A. Tabocchini, O. Sapora, G.Simone.
Proceedings SIRR 94 (Pisa), in press.

- "The Induction and Rejoining of DNA dsb in V79 Cells Exposed to Low Energy Protons".
F. Ianzini, M. Belli, M. A. Tabocchini, O. Sapora, F. Cera, R. Cherubini, M. Dalla Vecchia, A. M. I. Haque, G. Moschini, P. Tiveron, G.Simone.
Proceedings SIRR 94 (Pisa), in press.

- "Comparative analysis of the mutation spectra induced by protons and X-rays at the *hprt* locus in V79 cells".
L.Levati, E.Sorrentino, M.A.Tabocchini, E.Pagani.
Proceedings SIRR'94 (Pisa), in press.

- "Light Ions Induction and Rejoining of DNA dsb in V79 Cells".
G.Simone, M. Belli, F. Ianzini, O. Sapora, M. A. Tabocchini, F. Cera, R. Cherubini, M. Dalla Vecchia, A. M. I. Haque, G. Moschini, P. Tiveron.
Proceedings 10th International Congress of Radiation Research, 1995 (Wurzburg), in press.

- "Radiation quality and the effects of protons at the cellular and molecular levels".
M.A.Tabocchini .
Proceedings 10th International Congress of Radiation Research, 1995 (Wurzburg), in press.

Abstracts

- "Inattivazione di Cellule V79 Indotta da Ioni Elio di Alto LET".
F. Cera, R. Cherubini, M. Dalla Vecchia , A. M. I. Haque, P. Tiveron, G. Moschini, M. Belli, F. Ianzini, M. A. Tabocchini, O. Sapora, G.Simone.
"VII National Meeting of the Italian Society for Radiation Research and IX National Meeting of Research Activities in Radiochemistry, Chemistry of Radiation, Nuclear Chemistry and of the Radioelements".
Pisa, Italy, November 24-26, 1994.

- "Produzione Iniziale di Doppie Rotture sul DNA di Cellule V79 e Cinetica di "Rejoining" dopo Irraggiamento con Protoni di Bassa Energia".
M. Belli, F. Ianzini, M. A. Tabocchini, O. Sapora, F. Cera, R. Cherubini, M. Dalla Vecchia, A. M. I. Haque, G. Moschini, P. Tiveron, G.Simone.
"VII National Meeting of the Italian Society for Radiation Research and IX National Meeting of Research Activities in Radiochemistry, Chemistry of Radiation, Nuclear Chemistry and of the Radioelements".
Pisa, Italy, November 24-26, 1994.

- "Analisi Comparativa del DNA di Mutanti HPRT ⁻ Indotti da Fasci di Protoni e Raggi-X".
L. Levati E. Sorrentino, M.A. Tabocchini, E. Pagani.
"VII National Meeting of the Italian Society for Radiation Research and IX National Meeting of Research Activities in Radiochemistry, Chemistry of Radiation, Nuclear Chemistry and of the Radioelements".
Pisa, Italy, November 24-26, 1994.

- "DNA Double Strand Breaks Production and Rejoining in V79 Cells after Irradiation with Low Energy Protons".
F. Ianzini, M. Belli, O. Sapora, M. A. Tabocchini, G.Simone, F. Cera, R. Cherubini, A. M. I. Haque, G. Moschini, P. Tiveron.
"1995 Keystone Symposia - Repair and Processing of DNA Damage".
Taos, New Mexico, USA, March 23-29, 1995.

- "DNA Double Strand Breaks Production and Rejoining in V79 Cells after Irradiation with Low Energy Protons".
F. Ianzini, M. Belli, O. Sapora, M. A. Tabocchini, G.Simone, F. Cera, R. Cherubini, A. M. I. Haque, G. Moschini, P. Tiveron.
"43rd Annual Scientific Meeting of the radiation Research Society and 15th Annual Meeting of the North American Hyperthermia Society".
San Jose, California, USA, April 1-6, 1995.

- "Biological Effectiveness of Low Energy Protons: DNA dsb Production and Rejoining in V79 cells".
M. Belli, F. Cera, R. Cherubini, A. M. I. Haque, F. Ianzini, G. Moschini, O. Sapora, G.Simone, M. A. Tabocchini, P. Tiveron.
"Association for Radiation Research Meeting - DNA Damage, Recognition and Control, Genetic Instability, Mechanisms of Oncogenesis".
St. Andrews, Scotland, UK, April 5-8, 1995.

- "Influence of Chromatin Structure on DNA Damage and Repair in a Human Cellular Ssystem Capable to Undergo "in vitro" Differentiation".
F.Belleudi, B.Maione, V.Maresca, S.Pazzaglia, O.Sapora, M.A.Tabocchini
"Association for Radiation Research Meeting - DNA Damage, Recognition and Control, Genetic Instability, Mechanisms of Oncogenesis".
St. Andrews, Scotland, UK, April 5-8, 1995.

- "Biological Effectiveness of Light Ions for Cell Inactivation and Mutation Induction on V79 Cells ".
R. Cherubini, F. Cera, M. Dalla Vecchia , A. M. I. Haque, G. Moschini, P. Tiveron, M. Belli, F. Ianzini, O. Sapora, M. A. Tabocchini, G.Simone.
"5th Workshop on Heavy Charged Particles in Biology and Medicine".
Darmstadt, Germany, August 23-25, 73-76,1995.

- "Problems ans Perspectives in Proton Radiobiology".
M. Belli.
"5th Workshop on Heavy Charged Particles in Biology and Medicine".
Darmstadt, Germany, August 23-25, 73-76,1995.

- "Inactivation and Mutation Induction in V79 Cells Irradaited with Helium-3 and Helium-4 Ions".
F. Cera, R. Cherubini, M. Dalla Vecchia , A. M. I. Haque,   G. Moschini, P. Tiveron, M. Belli, F. Ianzini, O. Sapora, M. A. Tabocchini, G.Simone.
"10th International Congress of Radiation Research".
Wurzburg, Germany, August 27-September 1, 1995.

- "Light Ions Induction and Rejoining of DNA dsb in V79 Cells".
G.Simone, M. Belli, F. Ianzini, O. Sapora, M. A. Tabocchini, F. Cera, R. Cherubini, M. Dalla Vecchia, A. M. I. Haque, G. Moschini, P. Tiveron.
"10th International Congress of Radiation Research".
Wurzburg, Germany, August 27-September 1, 1995.

- "Radiation Quality and the Effects of Protons at the Cellular and Molecular Level".
M. A. Tabocchini
"10th International Congress of Radiation Research".
Wurzburg, Germany, August 27-September 1, 1995.

I. **Head of project: Dr. E.G. Sideris**

II. **Objectives for the reporting period**

Emphasis was given on the further development of our Monte Carlo computer simulation of the interactions of charged particles and especially of α-irradiation with water molecules and on measurements on thermal transition A_{260} changes and dielectric-conductivity changes induced on mammalian macromolecular DNA following exposure to γ-irradiation and α-irradiation.

III. **Progress achieved including publication**

The investigation of the physical and chemical processes (energy transport and deposition, ionisation distributions and the production of primary chemical species) at the initial stages of interaction of α-particles radiation with water medium, has been one of the major objectives in this study.

For purposes of α-particles microdosimetric calculations, simple but accurate analytical LET-Energy and Range-Energy relations were developed [1,2]. These expressions are valid in the 100 keV-10 MeV energy range for both vapour and liquid phases of water and the analysis was based on the available experimental data. The results showed that phase effects in water are of some importance, leading to lower LET values in the condensed phase, although the variation of this effect with energy is smooth. The maximum value (~ 1.1) of the vapour/liquid ratio occurs at about 0.5 MeV while for both phases the Bragg peak is found at about 0.7 MeV.

Our analytical Monte Carlo computer code simulates - event by event - the interactions of charged particles (protons and α-particles in the 1-10 MeV energy range) in a water vapour medium scaled to the density of liquid water. This code is also taking into account the interactions of the secondary ejected electrons (δ-rays) spectrum. The simulation is based on our semi-empirical approximation for the determination of the single differential ionisation cross section for the interaction of protons, α-particles and electrons with water [3]. This model combines the classical binary encounter approximation (BEA) with the Bethe theory and is consistent with experimental data for both differential and total ionisation cross-sections. As this approximation provides the relative contribution of each subshell of water to the ionisation interaction, the initial yields of the chemical species formed (H_2O^+, OH^+, H^+, etc.) can be estimated.

The ionisation and energy deposition distributions as a function of particle's energy (and/or path length) were calculated with this code for α-particles interactions with water [4]. It was found that the number of ionisations produced by the α-particles alone (primary ionisations) is about equal to the one produced by the ejected secondary electrons. The ratio primary/secondary ionisations decreases slowly from about 0.9 to 0.8 as the energy increases from 2 to 10 MeV. The result of this small deviation is that the differential w-value for the α-particles was estimated to be constant in the examined energy interval and equal to 32.0 (eV/ion pair) .

The percentages of the chemical species formed were found to be about 75% H_2O^+, 15% OH^+, 10% H^+ independent of the α-particles energy.

For the α-particles of the liquid samples, an experimental apparatus was designed and constructed. The radioactive source is placed inside a plexiglas housing, on the top of several removable plexiglas spacers, so that the source-to-exit window distance can be easily modified, providing a variety of dose rates at the exit window. An [241]Am α-particles surface source (Amersham) of 25 MBq nominal activity is used. The source has an active area of 3 cm diameter and the radioisotope is contained between a backing of silver, 0.2mm thick, and a front covering of gold alloy, 0.003mm thick. An exit window of 2 cm diameter is provided for irradiation. Several rings of internal diameter 2 cm are constructed from plexiglas, to serve as exposure wells. Mylar foils are stretched over the one face of the rings, taking care to avoid wrinkling. The liquid samples are placed on the Mylar foil. For each irradiation, the exposure well is firmly attached on the exit window, with the help of a plexiglas holder and an o-ring. The area inside the cylinder is evacuated to a pressure of about 0.1 Torr, which remains constant during the irradiation as it was indicated by the connected manometer. Due to pressure difference, the expected concave shape of the Mylar foil was observed and its sagitta did not exceed 2 mm. A lens-like piece of plexiglas with the same curvature as the Mylar was constructed, the liquid sample being sandwiched in between. The time of the irradiation is controlled by a shutter mechanism.

The energy spectra of the α-particles were measured with a passivated implanted planar (PIPS) Silicon detector (SPD 50-15-100, Canberra Industries, Inc.) which has an active area of $50mm^2$ and a resolution of 15 keV FWHM for 5.48 MeV α-particles. The spectra were recorded on a 2024 channels analyser (CATO, Silena S.p.A. Milano). A multipeak α-reference source (AMR.43, Amersham) was used for the detector and the electronics system calibration. The measured response of the system was 35 keV FWHM at 5.48 MeV. Live-time correction within the multichannel analyser was used to compensate the dead time.

The particle fluence homogeneity over the area of exit window, was investigated through measurements with the use of CR-39 plastic detectors. The exposed plastic detectors were etched and the etched tracks were recorded by a semi-automatic system which was developed in the frame of the "Energy Amplifier" project at CERN); the enlarged image from an optical microscope is automatically captured by a CCD camera, transferred to a PC and analysed by a special program that recognises and counts the number of pits. The pits were counted in frames of $0.16 \ mm^2$ area. analysis of the low). In order to have reliable estimation of the fluence, we measured the CR-39 response for both the energies of the α-particles and the geometry involved in this work, since the efficiency is closely related in the critical angle of incidence .

The irradiation with γ-rays is performed with the ^{60}Co-Gammacell 220 high intensity irradiator (Atomic Energy of Canada Ltd). Since we are interested in relatively low doses, a calibrated batch of Lithium Fluoride TLD chips (TLD100, Harshaw Co.) from parallel project of our group (Sakellariou *et al.* 1995 *Radiat. Prot. Dosim.* 60 in press) was used for dosimetry. The liquid sample contained in a small plastic tube, mounted on

a plexiglas support, is properly located on the irradiation chamber along with four TLD chips. The dose rate at the irradiation position was found to be (7.9 ± 0.2) cGy/s, in good agreement with both the values stated by the manufacturer and the routine calibration of the Unit. The minimum dose which can be delivered by a sample corresponds to a simple lowering and immediate raising of the sample drawer and was measured as (46.5 ± 6.0) cGy.

The small amount (7λ) of the DNA solution used for α- and γ-irradiation could influence significantly energy deposition calculations, if the energy transport by electrons is neglected. For the α-energies considered in this work, the mean energy of the ejected electrons is less than 50 eV as it is discussed in a previous publication of our group [Zarris *et al.* 1992 *IAEA Nuclear Data Section INDC 2*]. Thus, for the geometry used, the continuous-slowing-down-approximation (CSDA) is adequate for α-dosimetry. For γ-dosimetry, however, kerma approximation is not valid in the build-up region of bounded media. We by-passed the problem by designing the appropriate plexiglas support (see before) based on our analytical Monte Carlo simulation of the geometry involved [Sakelliou *et al.* 1992 *Physics Med. Biol.* 37:1859-1872]

On the basis of the above we calculate the LET and range distributions of the a-particles in the Mylar-liquid interface. The LET spectrum has a mean value of 128 keV/μm with 26 keV/μm FWHM , while the mean range of the particles in liquid water is 18.0 μm with 7.5 μm FWHM.

Our data from Thermal Transition Spectrophotometry reveal a dual dose dependence response of the helix to coil transition temperature, T_m, when samples of DNA are exposed to γ-irradiation or α-irradiation. This dual dose dependence response is present at the low dose region of 0 to 10 Gy. A tendency of DNA helix stability in this radiobiologically important region seems to be present. This tendency is present in samples exposed to γ-irradiation as well to α-irradiation. At this region no significant differences at the DNA helix stability were observed between samples exposed to γ-irradiation or to α-irradiation. At higher doses, above the 10 Gy, we observed the well known, from work with γ-irradiation, gradually decreasing mode of helix stability. Interestingly enough the turning point to the gradually decreasing mode at the higher doses appears to be at ~ 4 Gy for γ-irradiation and at ~ 16 Gy for α- irradiation.

This tendency of a dual dose dependence response was verified through experimental work with two independent methods that of Conductivity-Dielectric Measurements and Perturbed γ-γ Angular Correlation Studies.

Conductivity measurements, as are conducted in our laboratory, with dedicated instrumentation, permit the study conductivity changes evolving at the temperature region of the DNA helix to coil transition. They are carried out with Hewlett Packard Low Frequency Impedance Analyzer, Type 4192A. The gradual changes in the temperature are effected with the use of a dedicated thermostatic oven (Ando, Type TO-49) The observed changes in conductivity follow a sigmoidal function towards the temperature qualitatively similar to the sigmoidal functions observed with A_{260} changes. T_c be able to parametrize our results in a way permitting direct comparison with the results form Thermal Transition Spectrophotometry we developed
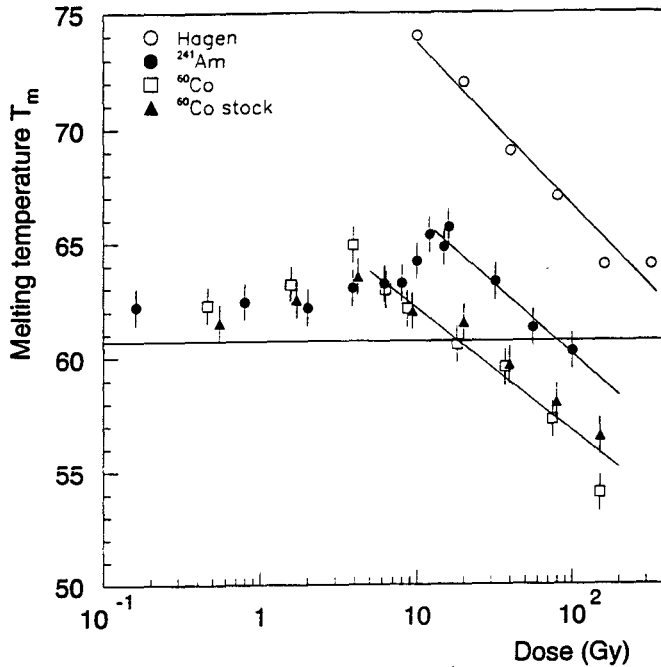
The dose dependence of helix-to-coil transition temperature, T_m, measured by the changes of A_{260}, i.e. the hydrogen bond disruption for buffered solutions of macromolecular DNA exposed to γ-irradiation and α-irradiation.
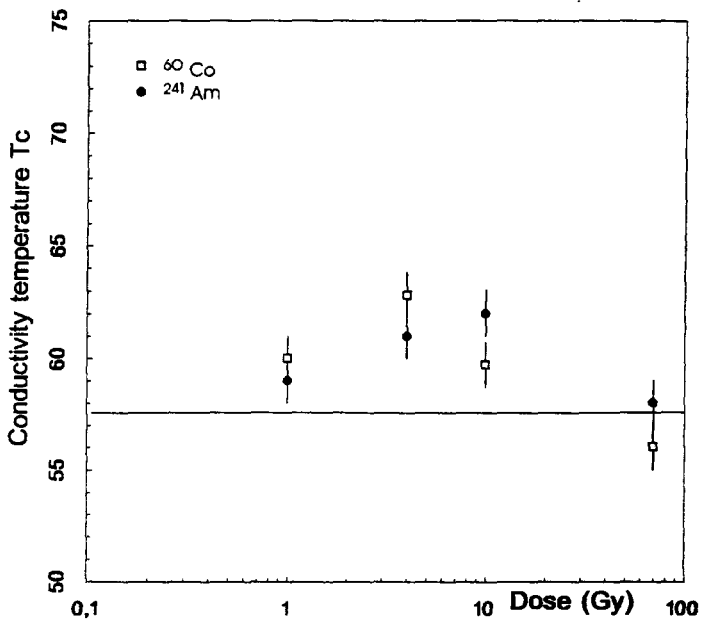
The dose dependence of helix-to-coil transition temperature, T_c, measured by the changes in conductivity, i.e. changes that proceed the hydrogen bond disruption for buffered solutions of macromolecular DNA exposed to γ-irradiation and α-irradiation.

the Thermal Conductivity Transition parameter, T_c. T_c is calculated from the first derivative of the original conductivity changes vs temperature, that is in the same way the well known T_m parameter of the Thermal Transition A_{260} changes is calculated. When the T_c parameter is plotted as a function of the dose the results verify our work with Thermal Transition A_{260}.

Conductivity changes precede those of Thermal Transition changes in the irradiated as well the non-irradiated samples. The tendency of a dual dose dependence response was also present at the radiobiologically important region of 0-10 Gy and the turning points to the gradually decreasing mode of the higher doses were at the same doses as those located with Thermal Transition A_{260}.

The observed precedence by 2 - 4 ^{0}C of conductivity changes vs A_{260} changes supports with evidence coming from macromolecular mammalian DNA the recent theories of a dual phase DNA helix to coil transition where the disruption of the hydrogen bonds, measured by the A_{260} changes results from the preceding gradual disruption of the hydrophobic bonds between the successive nucleotides on the same DNA chain. It is suggested that the known temperature dependency of the ion mobility facilitates the energy dependent disruption of the hydrophobic bonds and thus, the observed conductivity changes that precede those of A_{260} changes.

According to the results reported here the relationship between radiation dose and DNA helix to coil phase transition is not a simple one at least at the region of low doses of 0-10 Gy which is of interest for the purposes of Radiation Biology and Radiation Protection. The observed higher stability of the DNA macromolecules towards γ-irradiation as well as towards α-irradiation, verified by independent techniques, might be attributed to the formation of cross links between adjacent parts of DNA molecules which leads to the formation of molecules of higher thermodynamic stability. Cross linking has been observed in vitro as an intra- and inter- molecular process. Though no evidence has been reported, possible development of DNA cross links in the cell environment could of importance in estimating the effects of ionising radiations in living cells [Goodhead D *et al* 1993 *Intern. J. Rad. Biol.* 63:543-556, von Sonntag C 1994 *Intern. J. Rad. Biol.* 65:19-26]. Formation of cross links, at low doses of ionising radiation would facilitated by the expected preponderance of the frequency of single strand breaks over that of the frequency of double strand breaks.

Comparison between our results on γ-irradiation and α-irradiation leads to the conclusion that the large differences observed between these two types of ionising radiation, at the survival level, are not present when DNA helix to coil transition is used as a criterion. This verifies, by an independent technique, previous observations, where the frequency of radiation induced double strand breaks was used as the critical parameter for comparison between the effects of γ-irradiation and α-irradiation [Jenner *et al* 1994 *Radiat. Prot. Dosim.* 52:289-293].

When we tried to differentiate between the effects of γ-irradiation and those of α-irradiation, on the parameters used in this work, through the use of organic radical scavengers of the kind used for the comparison between the frequencies of single strand breaks and double strand breaks [e.g.
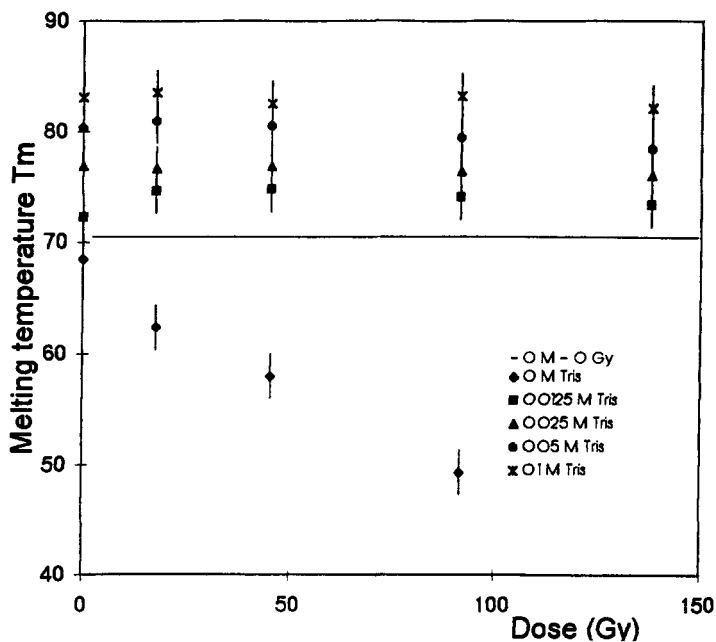
The dose dependence of helix-to-coil transition temperatures, T_m, measured by changes of A_{260}, i.e. the hydrogen bond disruption for buffered solutions of macromolecular DNA exposed to γ-irradiation and α-irradiation in the presence of the OH free radical scavenger Tris.
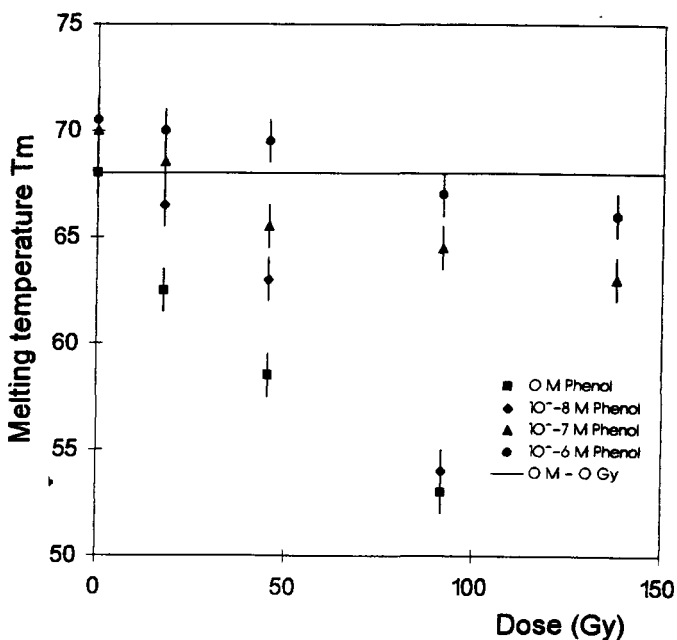
The dose dependence of helix-to-coil transition temperatures, T_m, measured by changes of A_{260}, i.e. the hydrogen bond disruption for buffered solutions of macromolecular DNA exposed to γ-irradiation and α-irradiation in the presence of the H free radical scavenger Phenol.

Krisch R *et al* 1991 Rad*iat. Res.* 126:251-259] we found out that these radical scavengers exhibit a strong effect on the stability of the DNA macromolecule. Tris (hydroxymethyl) aminomethane, Tris, was used as hydroxyl free radical scavenger] and Phenol was used as hydrogen free radical scavenger in irradiated aqueous solutions of DNA.

Our present work shows that both these free radical scavengers alter the T_m, the helix to coil thermal transition temperature of the DNA molecules exposed to γ-irradiation. The H˙ radical scavenger exerts a minor effect on the helix to coil transition temperature of the non irradiated DNA but exhibits a relatively strong effect on preventing the radiation induced decrease of this temperature, though the reaction constant k of the H˙ towards the DNA molecule is rather low. In opposite, in the case of the OH˙ scavenger, which strongly increases the helix to coil transition temperature of the non irradiated DNA molecules, exposure to gamma rays resulted in a moderate decrease of the radiation induced effect. This observation leads to the conclusion that a considerable part of the effect of this radical scavenger on the radiosensitivity of the DNA might be attributed not to the scavenging properties for OH. free radicals but to the effected increase on the stability of the DNA macromolecule.

From the effects of these two chemicals on non irradiated as well as irradiated DNA solutions it can be concluded that when considering their effect on DNA molecules exposed to ionising radiation it should be taken into account not only their properties as water free radical scavengers [e.g. Krisch R et al 1991 *Radiat. Res.* 126:251-259] but also their effect on increasing the thermostability of the DNA molecule as it is evident from their effect in non irradiated DNA samples. Thus, their effect on the DNA molecule as it is measured by the effected increase on the T_m temperature of the irradiated DNA, that is the helix to coil transition temperature, might be attributed to two factors: their free radical scavenging properties, as it has been known up to now and their effect in stabilising the DNA macromolecule as it was shown in this work.

This former effect seems to play a more important role in the case of Phenol, a Hydrogen free radical scavenger. As it was mentioned above, Phenol, at least in the concentrations used in this work, exhibits a minor effect on the helix to coil transition of the non irradiated DNA. In parallel the low reaction constant, k, of the H˙ towards the DNA molecule is in agreement with its low contribution to the radiation induced damage to this macromolecule [Kiefer J *Biological Radiation Effects* Springer Verlag 1990]. In spite of that, Phenol, a H˙ scavenger, exhibits a relatively strong effect on preventing the radiation induced decrease of the helix to coil transition temperature.

In opposite, in the case of Tris, which strongly increases the helix to coil transition temperature, the T_m, of the non irradiated DNA molecules, exposure to gamma rays resulted in a moderate decrease of the radiation induced effect on this parameter. This observation leads to the conclusion that a considerable part of the previously reported effect of this chemical on the radiosensitivity of the DNA might be attributed not to scavenging properties for OH free radicals as it has been hypothesised up to now but to the increased stability of the DNA macromolecule when in solution in the presence of Tris as it has been shown in this work.

On the basis of these results conclusions based on the use of organic free radical scavengers for studying radiation chemical mechanisms and especially the relative involvement of mechanisms related to the induction of single strand breaks and double strand breaks: two hit DSB's, one hit DSB's from single OH⁻ , one hit DSB's from several nearby OH⁻ and one hit DSB's from direct DNA hit [e.g. Krisch R. *et al* 1991 *Radiat. Res.* 126:251-259, Siddiqui M *et al* 1987 *Radiat. Res.* 112:449-463] should be, partially at least, reconsidered.

Conclusions A simple but accurate analytical LET-Energy and Range-Energy relations microdosimetric calculations for α-particles valid between 100 keV-10MeV energy range were developed. An analytical Monte-Carlo code simulates event-by-event interactions of charged particles in water vapour scaled to the density of liquid water. On the basis of these theoretical analysis the absorbed dose in DNA solution in the form of thin films was calculated. Our results, from work *in vitro*, indicate, that at the low dose region of 0.5 - 10.0 Gy, which is of interest for Radiation Biology and Radiation Protection, the presence of thermodynamically resistant regions of DNA molecules which are attributed to the formation of cross links between adjacent molecules. This might be of interest when considering the high local concentration of DNA molecules *in situ*. Our work with two organic free radical scavengers, which have been used in the past in support of the current theories of DNA double strand breaks *vs* single strand breaks, shows that their effects as free radical scavengers are confounded with a strong effect on the stability of the DNA molecules. Thus, conclusions referred to the formation of DNA breaks induced by ionising radiation and based on their action as free radical scavengers should be reconsidered.

Publications

E.G. SIDERIS, G. ZARRIS, A. ANAGNOSTOPOULOU-KONSTA, A.G. GEORGAKILAS and C.A. KALFAS, 1993, DNA-Water free radicals interaction and the thermostability of the DNA molecule. *Conference Proceedings S.I.F.* 43:239-242.

A. ANAGNOSTOPOULOU-KONSTA, P. PISSIS and E.G. SIDERIS 1993, Investigation of the water-biomolecules interaction using dielectric techniques. *Conference Proceedings S.I.F.* **43**: 219-222

G. ZARRIS, A. ANAGNOSTOPOULOS, A. PERRIS, L. SAKELLIOU and E.G. SIDERIS 1993, Dosimetric calculations of α particles incident on water. *Phys. Med. Biol.* 38:643-649

C.A. KALFAS, E.G.SIDERIS, G. LOUKAKIS and A. ANAGNOSTO-POULOU-KONSTA 1994, Rotational Correlation Times in irradiated DNA. *J. of Non-Crystalline Solids.* 172-174:1121-1124

E.G. SIDERIS, A.G. GEORGAKILAS, C.A. KALFAS and A. ANAGNOSTOPOULOU-KONSTA, 1994, Thermally stimulated electric changes during the helix to coil transition of irradiated DNA. *IEEE Dielectr. and Electr. Insul. Society ISE* 8:857-862.

Presentations in International Meetings

C.A. KALFAS, E.G.SIDERIS, G. LOUKAKIS and A. ANAGNOSTOPOULOU-KONSTA 1993, Rotational Correlation Times in irradiated DNA. *2nd International Discussion Meeting on Relaxations in Complex Systems*. Alicante, Spain.

G. ZARRIS, A ANGELOPOULOS, A PERRIS, L. SAKELILIOU and E.G. SIDERIS, 1994, High LET irradiation of aqueous DNA solutions: I. Dosimetry. *1st Mediterranean Congress in Radiation Protection*. Athens.

A.G. GEORGAKILAS, G. ZARRIS, E.G. SIDERIS, A. PERRIS and L. SAKELLIOU, 1994, High LET irradiation of aqueous DNA solutions: II. Experimental results. *1st Mediterranean Congress in Radiation Protection*. Athens.

K.S. HAVELES, A.G. GEORGAKILAS, TH. KATSORCHIS and E.G. SIDERIS, 1994, Free radical scavengers effects on the helix to coil transition of mammalian Deoxyribonucleic Acid exposed to gamma rays. *3d Joint Meeting on Chemistry of Biological Systems and Molecular Chemical Engineering*. Ioannina

Theses

Κ. ΧΑΒΕΛΕΣ 1994 "Επίδραση οργανικών χημικών ενώσεων επί της θερμικής μεταπτώσεως ακτινοβοληθμένου DNA". *Πανεπιστήμιον Αθηνών.*

M. KEKCHIDIS 1995 "Effects of Tris on the thermostability of the calf thymous DNA exposed to gamma rays" *Tbilisi State University.*

N. KEKCHIDIS 1995 "Effects of Phenol on the thermostability of the calf thymous DNA exposed to gamma rays" *Tbilisi State University.*

Project No. 6: Prof Dr. J. Kiefer

I. Objectives

The aims of the present study were

1. to obtain a data set for DNA double-strand break induction by charged particles including protons
2. to establish a data basis on mutation induction in mammalian cells induced by charged particles including protons
3. to characterise radiation induced mutants at the molecular level with the help of the multiplex polymerase chain reaction
4 to further develop approaches to study the action of single ions on indiviual cells

II. Progress achieved

INTRODUCTION

Our group is engaged in the investigation of molecular and cellular responses of charged particles to establish a data base which may be used for theoretical modelling and can thus ultimately lead to a well-founded rational basis for radiation protection. In order to contribute to reaching this goal a variety of radiation sources and a number of experimental methods are used The work of the last years has resulted in the establishment of a large set of action cross-sections over a wide LET range for DNA double-strand break induction, cell inactivation and mutation induction Mutants at the HPRT-locus were also analysed in regard to their molecular nature by multiplex polymerase chain reaction (PCR) The overall result is that no unique dependence of any of the parameters measured on LET exists but that track structure plays a very important role

MATERIALS AND METHODS

Cells: For double-strand break induction the diploid yeast strain 211*B was used, which was also employed in previous experiments The main mammalian cell line was V79 Chinese hamster although a few preliminary investigations were also carried out with the human MGH-U1 cell line. Culture conditions and assays for inactivation and mutation induction followed standard protocols

Irradiation sources Control experiments were performed with 80 kV (yeast) or 300 kV X-rays. The alpha source was an uncollimated ^{241}Am foil Accelerated protons were produced by a 2 MeV tandem accelerator (Nuclear Physics Department, Giessen) The exit window consisted of a small slit covered with a 2 μm Mylar foil Samples were moved along it on a sledge driven by a computer-controlled stepping motor Heavy ions were provided either by the UNILAC (up to 20 MeV/u) or the SIS accelerator at GSI, Darmstadt.
X-ray doses were measured by standard ferrous sulphate dosimetry, ion fluences determined by counting etch pits in suitable foils or glass plates placed at the site of the biological samples.

Investigated endpoints: DNA double-strand breaks (DSB) were measured in yeast by pulsed-field gel electrophoresis at "physiological" doses and high surviving fractions. For multiplex PCR of 6-thioguanine resistant mutants DNA was isolated and amplified in two assays, one for exons 1 and 4, the other for 2-3 and 5-9. The products were separated by constant gel electrophoresis
Details of all methods can be found in the publications listed at the end of this report

RESULTS

DNA double-strand break induction: Data for induction cross-sections obtained are listed in table I together with relevant ion parameters and inactivation cross-sections for comparison. It has to be pointed out that both, DSB induction and inactivation, were not only measured in the same experiment but in aliquots of the same sample which allows the comparison in a more direct way than in mammalian cells and demonstrates also the sensitivity of the technique. Contrary to mammalian cells in diploid yeast a linear relationship is found between inactivation cross-section (obtained from the final slope of the survival curve) and DSB induction cross-section (fig. 1)
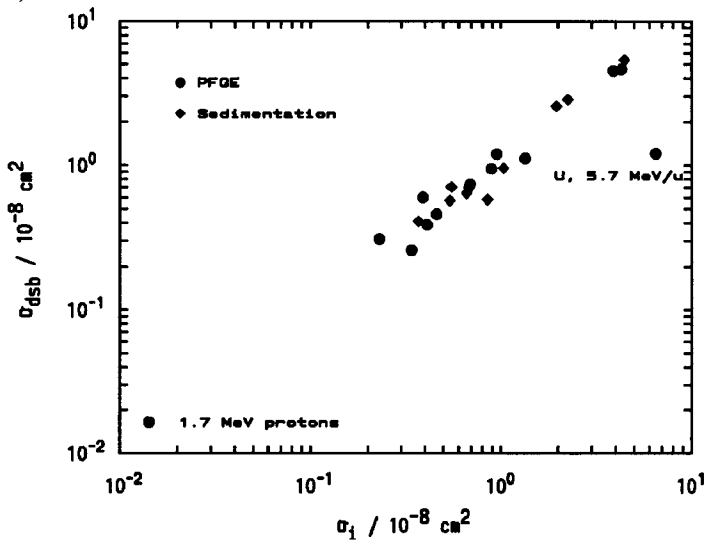
Fig. 1: DNA double-strand break induction cross-section versus the cross-section for cell inactivation
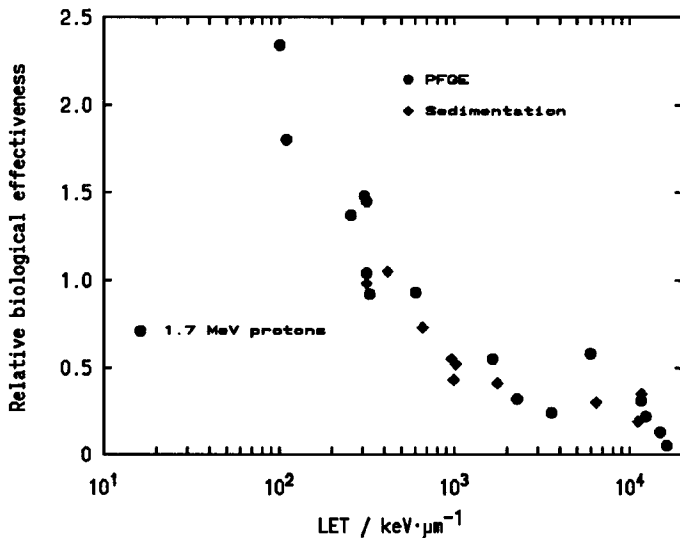
Fig. 2: RBE for DNA double-strand break induction versus LET

RBE-values are plotted in fig. 2: With protons we find a value of 0.71 (similarly as others in mammalian cells, see below) but a clear and significant elevation above unity in the range 100-200 keV/µm. For more densely ionising particles RBE decreases steadily. The scatter seen in the data do not represent experimental variations but have mainly to be attributed to differences in track structure when particles with comparable LET but different charge and velocity are used.

Table I: Summary of data for DNA double-strand break induction normalised to a DNA mass of 10^9 g/mol. As reference 80 keV X-rays were used with an LET of 6.3 keV/µm. The corresponding cross-sections are

$$\sigma_{dsb} = (2.26 \pm 0.12)\cdot 10^{-12}\ cm^2 \quad and \quad \sigma_i = (1.37 \pm 0.05)\cdot 10^{-12}\ cm^2$$

* Data obtained by the sedimentation technique by Akpa *et al.* (1992).

Ion	Energy [MeV/u]	LET [keV/µm]	σ_{dsb} [10^{-8} cm²]	σ_i [10^{-8} cm²]	r_p [µm]	RBE_{dsb}	Z^2_{eff}/β^2
p	1 7	16.2	0.0165±0.0010	0.0142±0.0005	0.15	0.71	275
α	0.88	110	0.26±0.01	0.34±0.05	0.05	1.80	1680
C	3.4	329	0.39±0.01	0.41±0.04	0.49	0.92	4349
C	18 0	101	0.31±0 01	0.23±0.01	8.39	2.34	958
O	2.9	604	0 74±0 01	0.69±0 03	0.38	0 93	8293
O	8 0	316	0 43±0.02	---	2.11	1 04	3473
O	10.7	257	0.46±0.01	0.46±0.01	3.46	1 37	2663
Ar	5.7	1654	1 20±0.01	0 95±0.03	1.19	0 55	19415
Ar*	5.0	1762	0 96±0.22	1.03±0.28	0.95	0.41	21287
Ar*	12.9	1020	0 70±0.14	0.68±0.01	4.76	0 52	10245
Ar*	13.4	994	0.57±0.05	0.54±0.03	5 08	0 43	9920
Ar*	14.0	966	0.71±0 12	0.55±0.04	5.47	0 55	9559
Ne*	4.9	661	0 64±0.11	0.66±0.01	0 92	0 73	8023
Ne*	9.8	418	0.58±0.09	0.85±0.08	2.98	1.05	4413
Ne*	14 4	316	0.41±0.08	0 37±0.02	5.74	0.98	3108
Ne	14 4	316	0 60±0.01	0.39±0.01	5 74	1.45	3108
Ne	15 0	306	0.69±0 09	---	6.15	1 48	2996
Ni	12.1	2283	0 95±0.04	0.89±0.02	4 27	0 32	2319
Kr	11.2	3586	1.12±0.07	1.34±0.14	3.74	0.24	36929
Xe*	11.8	6427	2.57±0.33	1.96±0.14	4.09	0.30	65572
Xe	14.0	5975	4 52±0.29	3.89±0.18	5.47	0 58	59145
Au*	9 1	11649	5.37±1.69	4 44±0.10	2.63	0.35	124649
Au	9.3	12309	3.83±1.00	---	2.73	0.22	123491
Au	9.3	11585	4.63±0 06	4.28±0.09	2.73	0.31	123491
Au	11 7	10863	---	3 96±0 06	4 03	---	111002
Pb*	12 7	11125	2 85±0 70	2 25±0 30	4 63	0.19	112026
U	5 7	16174	1 21±0 19	6 47±0 32	1 19	0.052	178540
U	9.3	14856	2 78±0 27	6 17±0.24	2.73	0.13	149173

Mutation induction in mammalian cells: A summary of data for mutation induction at the HPRT-locus and killing in V79 Chinese hamster cells is given in table II. It is also clear with these endpoints that LET is not a unifying parameter, and differences due to track structure are even more obvious, e. g. in the appearance of the so-called "hooks". Particularly with very heavy ions cross-sections decrease with increasing LET, since with lower ion energies penumbra extensions shrink, leading to a reduction in effectivity. The influence of penumbra electrons is less pronounced with lighter ions although they are still present.

RBE versus LET is plotted both for killing and mutation induction in fig. 3. For comparison the relationship for DSB induction (taken from fig. 2) is also included. Since in the field of radiation protection one is mainly interested in the action of low doses, calculations were made on the basis of the linear components of the mutation (fitted for X-rays to a linear-quadratic formula) and survival curves (for X-rays fitted to an α/β-expression). It is evident that RBE values rank in the order mutation>inactivation>DSB induction. Highest values sometimes exceed 20, the highest radiation weighting factor suggested by the ICRP.

Relative biological effectiveness
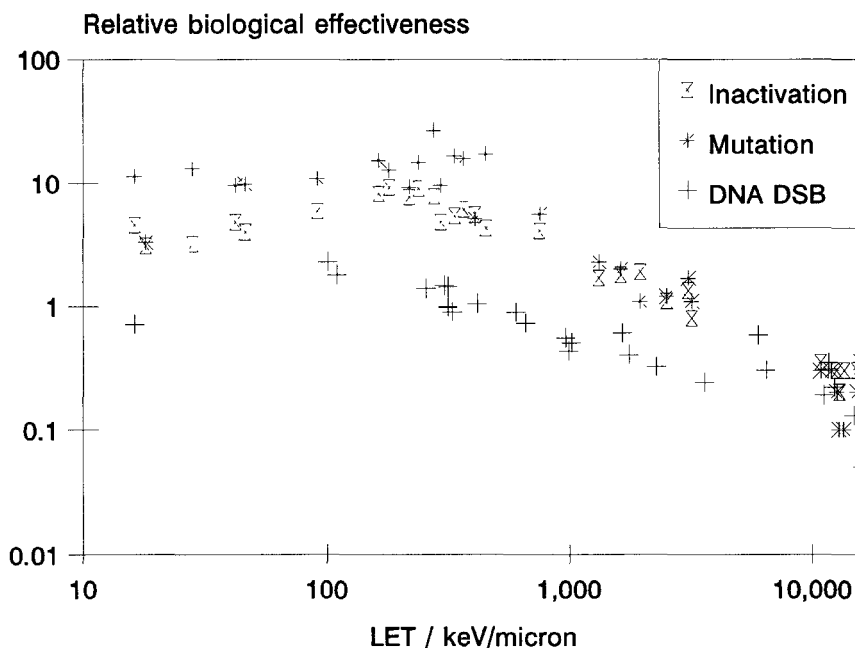
Fig. 3: RBE for cell killing and mutation induction versus LET Data for DSB induction are taken from fig 2 for comparison

Molecular analysis of mutations: Mutants induced by charged particles were picked, grown from separate clones and the DNA prepared for multiplex PCR of the HPRT gene. The exons were amplified in two runs, and the products analysed by gel electrophoresis. The work is not yet completed so that only preliminary results can be reported. The most extensive investigation was performed so far for alpha particles, heavy ion results suffer from the fact that the number of clones was relatively small (at least 12 per point) Results are summarised in fig 4, details of ion parameters are given in the legend. In spite of the preliminary character of our findings, the following seems to be clear. Even with very high LET there is still a substantial

Ion	E/M at cell surface (MeV/u)	LET (H_2O) ($keV/\mu m$)	Z^{*2}/β^2	rp (μm)	σ_ι (μm^2)	σ_m ($10^{-4}\mu m^2$)	σ_m/σ_ι (10^{-5})
p	1.7	16.2	275	0.15	1.7±1	0.5±0.1	2.94 ± 1.6
^{241}Am α	1.0	163	1699	0.06	31±3	6.8±2	2.2±0.7
O	1.9	754	11455	0.18	71.2±4.7	11.4±0.6	1.6±0.2
	* 8.8	276	3182	2.5	50±4	20.0±4.0	4.0± 0.8
	10.7	238	2663	3.5	49.5±2.7	9.5 ±1.1	1.91±0.2
	88	46	387	125	4.3±0.2	1.22±0.12	2.88±0.4
	396.0	18	126	1606	1.3±0.1	0.17±0.01	1.3±0.2
Ne	8.0	452	5293	2.11	45±4	21.3±3.0	4.75±1.1
	10.7	366	4070	3.5	52±4	15.7±5.0	3.03±1.2
	* 12.0	335	3666	4.2	42±3	15.0±5.5	3.5 ±1.3
	14.3	294	3127	5.7	33±4	7.7±2	2.32±0.9
	65	91	792	74	12.5±1	2.7±0.5	2.18±0.5
	191	42	321	465	4.7±0.2	1.1±0.1	2.26±0.3
	395	28	197	1599	2.1±0.2	1.0±0.1	4.73±0.7
Ni	6.0	3190	37205	1.3	61±6	9.1±0.8	1.5±0.3
	* 9.5	2517	27580	2.8	65±2	8.3±1.2	1.3±0.18
	* 14.3	1961	20535	5.7	87±5	5.7±1.8	0.65±0.05
	136	407	3285	261	52±2	5.6±1.1	1.1±0.2
	387	218	1565	1544	39±3	5.5±0.5	1.4±0.32
	630	180	1225	3536	38.5±1	6.2±0.6	1.6±0.2
Pb	11.6	11948	116633	4.0		8.7±0.6	
	* 15.2	10800	102501	6.3	88±8	9.2±2.6	1.1±0.33
	150	3090	23064	308	97±5	14.5±2.5	1.5±0.38
	500	1630	11489	2387	68±3	8.9±1.3	0.9±0.2
	980	1325	8829	7493	52±5	8.3±1.2	1.2±0.23
Au	2.2	12895	193900	0.24	57±2	4.1±0.7	0.7±0.2
	8.7	12568	126411	2.44	90±6	8.3±2.1	0.9±0.3
	9.3	12321	123491	2.73	80±15	12±3	1.5±0.6
U	* 3.9	15817	195911	0.62	71±5	15.0±2.0	2.1±0.37
	* 10.8	15220	139202	3.5	105±10	8.5±1.5	0.8±0.16
	* 12.7	13468	129809	4.6	90±9	4.5±2.0	0.5±0.20
X-ray	300 kV						1.7±0.4

Table II: Physical parameters and biological results from the various heavy ion exposures. (* : Data from Kranert et al. 1990).

fraction of mutants appearing as "wild type", i. e. either carrying point mutations or deletions which can not be resolved by the technique Their relative proportion decreases, however, with ionisation density while at the same time the fraction of total deletions increases The available data do not allow to discuss the influence of track structure which is hoped to be possible at a later stage when the analysis of the presently stored clones is completed.
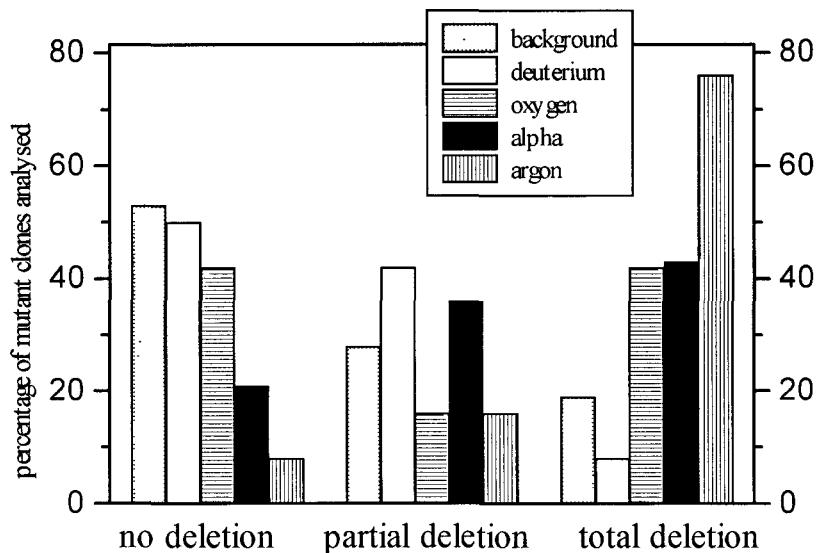
Fig. 4: Results of the PCR-analysis of HPRT-mutants with the following ion parameters: Deuterium: E/m 3.6 MeV/u, LET 10 keV/µm; Oxygen· E/m 88MeV/u, LET 52 keV/µm, Argon. E/m 5.6 MeV/u, LET 1611 keV/µm, [241]Am-alpha: E/m 1 MeV/u, LET 163 keV/µm.

Technical developments:

Microbeam apparatus: Our group has been engaged for quite some time in the investigation of single ion effects on individual cells These experiments were performed by identifying particle traversals on nuclear detector foils. In order to extend these studies, a microbeam device was constructed which is based on an [241]Am alpha emitter and beam collimation through a 1 µm hole in a mica plate The spatial resolution achieved so far is about 3 µm, biological experiments are in progress
Comet assay: The applicability of the comet assay for the detection of single ion effects on individual cells was investigated The "comets" are made visible by propidium iodide staining and are registered with the help of a computer-coupled CCD camera and evaluated by specially developped software Careful analysis revealed that the outcome is highly variable even under very well standardised experimental conditions. Also, the sensitivity appears too low to unequivocally detect the action of individual light ions. It appears thus doubtful whether the "comet assay" is a suitable means for the study of single ion action.

SUMMARY AND CONCLUSIONS

During the reporting period it was possible to collect a substantial set of data concerning the induction of DNA double-strand breaks in yeast and mutations in mammalian cells by charged particles. Our results with protons complement and confirm those by other participating groups: The RBE for DSB induction by 1.7 MeV protons (LET = 16.2 keV/μm) was found to be 0.71, which compares well with the value of 0.84 for 20 keV/μm protons by Belli *et al.* (1994). Our RBE value for inactivation of Chinese hamster cells (4.53 based on the comparison of initial slopes) is also close to that of Belli *et al.* (1989), who found for 17.8 keV/μm protons a RBE of 4.6 while our RBE for mutation induction (10.9) is larger by about a factor of 2 than that of the Italian group (5.4, Belli *et al.*, 1991). Whether this difference is real can only be decided by further experimentation. It is clear, however, that protons show unexpectedly high RBE values which may be significant for radiation protection purposes.

A detailed analysis of the heavy ion data, which cannot be described here because of space limtations, shows that LET is not a unifying parameter for any of the effects measured. There is a tendency, which is most pronounced with very heavy ions, that ions with higher specific energies lead to higher action cross-sections with a particular LET This points to the importance of penumbra electrons It is hoped that the data provided may be used for track structure models relating biological radiation action to the spatial distribution of energy deposition. It can also be stated that the main goals of the project - to establish a comprehensive data base for a variety of experimental endpoints - could be achieved. Further progress may also come from the molecular analysis of radiation induced mutants. The still preliminary results given above suggest that the density of primary ionisations is also reflected in the deletion pattern as revealed by the polymerase chain reaction.

References:

T. C. Akpa, K.-J. Weber, E. Schneider, J Kiefer, M. Frankenberg-Schwager, R Harbich, D. Frankenberg
Heavy ion-induced DNA double-strand breaks in yeast
Int. J. Rad. Biol. **62**, 279-287 (1992)

M. Belli, F. Cera, R. Cherubini, F Ianzini, G. Moschini, O. Sapora, G. Simone, M. A. Tabocchini, P. Tiveron
DNA double-strand breaks induced by low energy protons in V79 cells
Int. J Radiat Biol **65**, 529-536 (1994)

M. Belli, R. Cherubini, S Finotto, G Moschini, O Sapora, G Simone, M A Tabocchini
RBE-LET relationship for the survival of V79 cells irradiated with low energy protons
Int. J Radiat. Biol. **55**, 93-104 (1989)

M. Belli, F. Cera, R. Cherubini, F. Ianzini, G. Moschini, O. Sapora, G. Simone, M. A. Tabocchini, P Tiveron
Mutation induction and RBE-LET relationship of low energy protons in V79 cells
Int J Radiat. Biol. **59**, 459-465 (1991)

T. Kranert, E Schneider, J. Kiefer
Mutation induction in V79 Chinese hamster cells by very heavy ions
Int J Radiat. Biol **58**, 975-987 (1990)

III. Publications during the reporting period

Publications

1. J. Kiefer, M. Löbrich
   The repair-fixation model: General aspects and the influence of radiation quality
   in. *Biophysical modelling of radiation effects*
   (K. H. Chadwick, G Moschini, M M. Varma, eds)
   Adam Hilger Bristol-Philadelphia-New York, 211-218 (1992)

2. J. Kiefer
   Heavy ion effects on cells: chromosomal aberrations, mutations and neoplastic transformations
   Rad. Env. Biophys **31**, 279-288 (1992)

3. T. C Akpa, K -J Weber, E Schneider, J Kiefer, M. Frankenberg-Schwager, R. Harbich, D Frankenberg
   Heavy ion-induced DNA double strand breaks in yeast
   Int. J. Rad. Biol **62**, 279-287 (1992)

4. M. Löbrich, S. Ikpeme, J. Kiefer
   Analysis of the inversion effect in pulsed-field gel electrophoresis by a two-dimensional contour clamped homogeneous electric field system
   Analyt Biochem , **208**, 65-73 (1993)

5. J. Kiefer
   Problems, pitfalls, perspectives and potentials of quantitative theoretical models for cellular radiation action
   Mutation Research **289**, 27-37 (1993)

6. M. Löbrich, S Ikpeme, P. Haub, K.-J. Weber, J. Kiefer
   DNA double-strand break induction in yeast by X-rays and α-particles measured by pulsed-field gel electrophoresis
   Int. J. Radiat. Biol **64**, 539-546 (1993)

7. J. Kiefer, S Ikpeme, T C Akpa, K -J Weber
   DNA double strand break induction by very heavy ions Dependence on physical parameters
   Radiat Protection Dosimetry **52**, 295-298 (1994)

8. M. Löbrich, S. Ikpeme, J. Kiefer
   Measurement of DNA double-strand breaks in mammalian cells by pulsed-field gel electrophoresis: a new approach using rarely cutting restriction enzymes
   Rad. Res **138**, 186-192 (1994)

9 J Kiefer, U Stoll, E Schneider
   Mutation induction by heavy ions
   Adv. Space Res **14** (10), 257-265 (1994)

10. J. Kiefer
    Issues and problems for radiobiological research in space
    Adv. Space Res. **14** (10), 979-988 (1994)

11 M. Löbrich, S Ikpeme, J. Kiefer
   DNA double-strand break measurement in mammalian cells by pulsed-field gel
   electrophoresis an approach using restriction enzymes and gene probing
   Int. J. Rad. Biol , **65**, 623-630 (1994)

12. M. Kost, C. Russmann, J. Kiefer
    The cellular inactivation capability of accelerated heavy ions
    Proc. 5th Symp "Life Sciences Res. in Space", 205-208 (1994)

13. U. Stoll, E. Schneider, T. Kranert, J Kiefer
    Induction of HPRT-mutants in Chinese hamster V79 cells after heavy ion exposure
    Radiat. Env Biophys **34,** 91-94 (1995)

14. S. E Ikpeme, M Löbrich, T C. Akpa, E Schneider, J. Kiefer
    Heavy ion induced DNA double-strand breaks with yeast as a model system
    Radiat. Env. Biophys **34**, 95-101 (1995)

15 U. Stoll, A Schmidt, E Schneider, J. Kiefer
   Killing and Mutation of V79 Chinese Hamster Cells exposed to accelerated O- and Ne-
   Ions
   Radiat Res **142**, 288-294 (1995)

16. J. Kiefer, U. Stoll, M. Brend'amour
    Heavy ion action on biological systems
    Nucl. Instr. Meth. B, in the press

17. J. Kiefer, M. Kost, K. Schenk-Meuser
    Radiation Biology
    in: *Biological and medical research in space*
    Springer-Verlag, in the press

18. J Kiefer, S Ikpeme, M Brend'amour
    DNA double-strand break induction by heavy ions
    Proceedings 10th International Congress of Radiation Research
    Würzburg 1995, in the press

Objectives for the reporting period: (1. January 1994 - 30. June 1995)

Institute for Medical Radiobiology, CH-5232 Villigen PSI, Switzerland

Study of low dose radiation damage by reconstructing single tracks through single cells

The aim of the IMR-PSI group was to develop and evaluate a new irradiation technique which would permit to gather data to test models of carcinogenic potential of radiation used in radiation protection for a practical assessment of human risk. That is:

(i) a method which combines the possibility of irradiating more than a thousand cells simultaneously with an efficient colony-forming ability and the capability to localise a particle passage through a cell nucleus by measuring the track position in an attached detector.

(ii) realise a vertical beam line which permits to expose the cells horizontally to protons or α-particles, an irradiation chamber and a cell chamber which provide the cells with proper conditions.

(iii) establish library files to calculate energy spectra of δ-electrons and methods which permit particle tracking in the nanometer range. Comparison of the experimental results with microdosimetric models in terms of track structure to strive for an improved understanding of the biological consequences of low doses.

(iv) set up the experimental technique to investigate low dose effects and establish data analysis including means of defining the surface contours of cell nuclei to get intersection length of a traversing particle to determine its energy deposition; begin with first irradiations.

Progress achieved including publications:

Beam line

A beam line was set up with a 90o-magnet that bends the beam upwards to the target. It enables to expose the cells horizontally to protons or α-particles of 5-10 MeV up to 72 MeV energy and at an intensity from 10^4-10^6 particles/ (sec cm^2). A circular beam spot of 3 cm in diameter at the cells exposed is achieved by adjusting the setting of the quadrupol triplet. The position of the beam is controlled by (x,y)-profile monitors and its intensity is measured by a 1 mm thick scintillator counter which is exactly above the cell chamber [1].

A new method for low dose irradiations with measured track positions

The technique combines the possibility of irradiating more than a thousand cells simultaneously with an efficient colony-forming ability and the capability to localise the particle track through a cell nucleus. It consists on the one side of a cell chamber with palladium islands on an agarose layer, a method by which cells can be confined to restricted areas, and on the other side of a technique by which a particle passage through the cell nucleus can be accurately localised by measuring the track position in the attached detector. With the "palladium island technique", which was developed in collaboration with the Department of Radiation Sciences of the University of Uppsala, Sweden, cells are seeded on palladium islands with a cell suspension which is diluted to a very low cell concentration (1.5 x 10^3 cells/ml medium) so that cells will attach and grow on each palladium island as given by Poisson statistics, namely ~30% of the islands will have none, ~50% of the islands will be occupied by one and ~20 % two or more cells. Investigation of the spatial sensitivity of cells is enabled by dividing the localised particle passages into groups of events, whose track positions are close together relative to the cell contours.
To trace the particle passage through the cell nucleus on basis of the measured track in the detector, the relative position of cell chamber and detector has to be defined reproducibly at high accuracy. This is accomplished by three marks. They define two reference systems and give a way to control and adjust the relative position or to correct the displacement. The marks have a well defined circular aperture. The centres are determined optically by fitting circles into the apertures. The apertures of two corresponding marks overlap in the projection

such that the positions can be determined by simply adjusting the focus on the confocal laser microscope [2].

The following systematic errors were examined: (i) microscope stage, (ii) fluctuations due to temperature variation, (iii) mechanical deformations, (iv) relaxation of the mylar foils which make up the bottoms of cell chamber and detector and were stretched over rings out of steel, (v) changes due to absorption/desorption of humidity by the mylar foil or emulsion, (vi) local detachment of the emulsion by processing the film and (vii) reduction of the accuracy due to scatters in the set up.

(i)   The reproducibility of the systematic errors of the microscope stage made a correction by software feasible. The scales of the x- and y-axes were calibrated by laser interferometry, while the straightness and rectangularity of the axes were determined with help of an electronic calliper and of a certified standard cube which was mounted on the microscope stage. The room temperature is regulated by an air conditioner to avoid differences due to thermal expansion, and the cell chamber assembly can be repositioned on the microscope stage within 30 µm. The achieved accuracy of the microscope stage after applying the corrections was found to be of the order of 0.2 µm.
(ii) With the detector ring out of stainless steel, the observed extension is according to the coefficient of thermal expansion, with Invar (a steel with a very low coefficient of thermal expansion of the order of $10^{-6}/\,^{\circ}C$) tracks do not move back reproducibly to their initial positions, with deviations of up to 3 µm after cooling, probably due to a to big difference of the coefficients of thermal expansion of mylar foil and of Invar ring. This effect is being further investigated.
(iii) Mechanical tension between cell chamber and detector can cause deformations which results in deviations of up to 2 µm. It was avoided by proper design of the way the detector is fixed to the cell chamber.
(iv) No relaxation of the mylar foil was observed over the whole test period of up to six days.
(v)   There were no changes observed due to absorption/desorption of humidity by the mylar foil. Analogous changes of the emulsion are further examined.
(vi) Local detachment of the emulsion is widely avoided by pretreatment of the mylar foil with chrome alum gelatine to provide good adhesive surface between mylar foil and emulsion. Possible decrease of the correlation accuracy by processing the film is further investigated.
(vii) Calculations established minor error due to scatters. It is of the order of 0.1 to 0.3 µm depending on the particle energy and the thickness of mylar foils of 1.5 and 5 µm, respectively and showed that the LET distributions in the cell nuclei would be very narrow. [3,4].

To test the accuracy of the method, control measurements were performed with an assembly of two stacked detectors so that the distances between related tracks could be measured. Including all experiments performed, the overall average of measured differences between two related tracks is in x and y = (5 ± 2) µm. The achieved accuracy at the present state is mainly determined by rather large differences between different experiments. It has to be further improved.
As far, the detection efficiency of the track detector was determined for 62 and 30 MeV protons to be 90.6 % and 97.4 %, respectively. These measurements have to be confirmed and be extended to the lower energies used.

Software development for data analysis:

Particle tracks in the detector are identified after processing the image by applying logical operations on the binarised image to eliminate background, and object recognition software is used to determine the tracks. Since background is mostly at the surfaces of the mylar foil, further reduction of background is achieved by using sets of confocal images through the photo emulsion.
Macros were developed for an automated measurement of the apertures and to calculate the centres of the reference markers, in order to define the relative position of cell chamber and detector. Further a computer programme was set up which moves the microscope stage automatically to the positions of the cells and accomplishes an overlay of the image with the cells with that of the particle tracks in order to identify hit cells. Also the course of the cell proliferation is easily investigated using this programme. During one hour approximately 500 palladium islands may be examined.

Reconstruction of confocal laser scanning microscope (CLSM) images: quantitative assessment of cell contours

A reliable calculation of the intersection length of a particle through a biological object demands the exact determination of the contours of the cell nucleus. Laser scanning microscopy provides a set of confocal sections through a living cell in real time; however, each optical section of a three-dimensional fluorescent cell has many details obscured by blurred light from parts of the cell that are out of focus. The image acquisition process in confocal laser scanning microscopy has to be investigated in order to restore the observed images. The three-dimensional optical blurring of the microscope is characterised by its continuos point spread function (PSF), the image of a point-like light source. Considering the microscope as a linear and shift-invariant system, the observed image can be expressed mathematically as the 3-D convolution of the original fluorescent image and the PSF. The PSF of an imaging system can be used to improve the estimate of the object structure provided by the observed image.

The PSF was measured for three objectives of a Zeiss confocal laser scanning microscope using subresolution fluorescent beads. These PSFs were then used in the investigation of four different restoration algorithms. It was seen that linear restoration techniques, such as Wiener-filters, perform well at large signal to noise ratio. At high noise level, however, it has become clear that non-linear restoration techniques can be used to give superior results to those achievable by linear filters. Investigating the non-linear methods, reconstructions by constrained iterative deconvolution were carried out, a deterministic algorithm which is a modification to the Jansson-van Cittert method of successive deconvolution. This method has a good performance even in the presence of high noise level. The second implemented non-linear method originally developed by Gold converges about five times faster than the Jansson-van Cittert method but it doesn't work well on noisy images. One can observe that there is a trade-off between noise level and computational time. Figure 1 compares the three methods. A different approach is being investigated, based on a conjugate gradient algorithm proposed by Carrington, which permits image restoration on a higher resolution.

There are other aberrations to compensate for, caused by mismatches of refractive indices of the immersion oil and the aqueous medium. This mismatch yields an image that is scaled in the axial direction and has a drop of the intensity of up to 40% every 10 µm. These effects can mostly be avoided using water-immersion objectives [5,6].
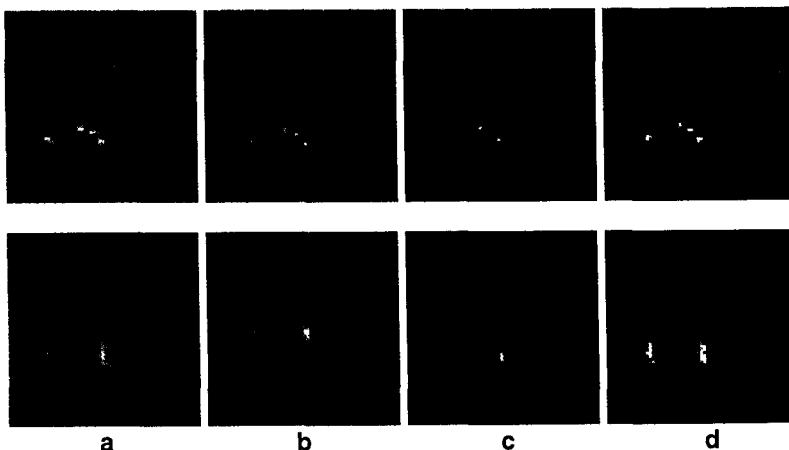
*Figure 1: Restoration examples of different algorithms. The 3-D data of fluorescent beads shown in **a** was restored with following methods: Wiener-filter **(b)**, Jansson-van Cittert **(c)** and Gold **(d)**. **Top row** : x-y slices, **bottom row** : x-z slices.*

Segmentation of the cell nucleus:
In order to determine the contour of the cell nucleus flexible Fourier surface models are used. The principle of these models is the following: The parametrical description of the surface of a simply connected 3-D object is defined by the coordinate functions $x(\phi,\theta)$, $y(\phi,\theta)$ and $z(\phi,\theta)$.

The two parameters φ and θ run over a spherical surface, i.e. $\phi=0...2\pi$ and $\theta=0...\pi$. The coordinate functions of the surface are then developed into a series of orthonormal basis functions. The surface is given by the coefficients of that series. A surface energy function is then defined which has its maximum if the surface lies on the contour of an object. Using a quasi-Newton algorithm, the surface energy function is maximised until the parametrised surface perfectly fits the contour of the cell nucleus. As cell nuclei are ellipsoid-like objects, the optimisation process can be initialised with an ellipsoid. Figure 2 shows an example with the parameters of the initial ellipsoid set manually. The aim is a fully automated segmentation of the cell images, thus a method is being developed based on the wave-equation that will enable to find the position of the initial ellipsoid. The basic idea is to start a wave propagation from the defined edge of the object. By means of the propagation speed and the number of iterations needed until the wave reaches the centre of the object, the dimensions of the object can be calculated. Since the axial resolution of images in confocal laser scanning microscopy is poorer than the ones in lateral direction, an anisotropic Laplacian is used to overcome the problem of different sampling distances in x-, y- and z-directions and permits to detect even flat cells as shown in Figure 3.
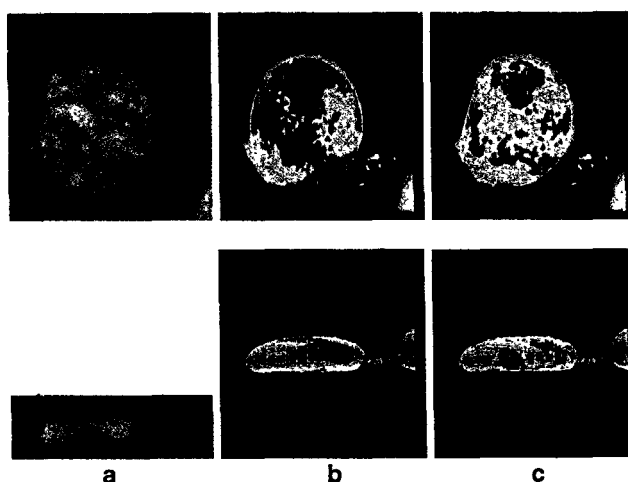
Figure 2: Segmentation example of a V79 cell nucleus. The images show x-y and x-z sections of the original 3-D data set (a), x-y and x-z projections of the initial placement of the ellipsoid (b) and the final segmentation result (c).

Nuclear data for particle track simulation in the nanometer range

Improved particle tracking methods are being developed which permit tracking of the particles in the nm range and modelling of radical formation, diffusion and their fate in water. Important prerequisites are reliable data of scattering, excitation and ionisation cross sections for photons, electrons, protons and alpha particles down to very low energies, that means down to 1 eV. The Lawrence Livermore National Laboratory distributed evaluated data libraries of reaction cross sections of photons and electrons, which cover a broad energy range from 10 eV up to 100 GeV and include all elements. At the Institute for Medical Radiobiology in Villigen PSI (IMR-PSI) these data library files were implemented in the Monte Carlo code GEANT, that was developed at CERN, Geneva, Switzerland and extended to particle tracking at low energies at IMR-PSI.
However, meaningful particle tracking requires further improvement of these data library files. For example, cross section data for photo excitation which are essential at low energies have to be included. Also Delbrück scattering and photon-nucleon scattering which become important at energies from 1 MeV upwards as well as photon absorption in light nuclei are

not yet taken into account. Further, the electron data library contains integrated cross sections for energies above 1 keV only, and for lower energies the cross sections have to be logarithmically extrapolated. Beside it, excitations by electrons are merely approximately calculated by assuming that all excitations arise from distant collisions at the outermost subshell.
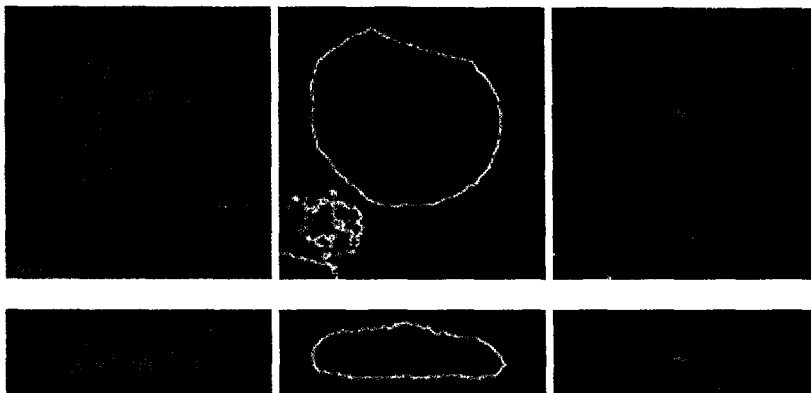
Figure 3: Detection of the centre of a cell nucleus (type v79). **On the left:** original gray-value images, **in the middle:** edge detection, **on the right:** wave propagation after 70 iterations. **Top row:** x-y sections, **bottom row:** x-z sections.

Therefore, improvements to the electron data library are being developed at IMR-PSI to establish cross sections of impact-ionisation by electrons using the Weizäcker-Williams method, taking into account close and distant collisions separately. A comparison of calculated cross sections with measured data indicates a good agreement for light as well as for heavy elements. Moreover, elastic scattering cross sections and scattering function for electrons are being extended from 1 keV down to 1 eV for light atoms and for water [10]. These improvements include solutions of Dirac's and Schrödinger's equations on the basis of results of the partial wave method.

Also, a data library for protons and alpha particles is being assessed. Thereby elastic scattering is set up using integrated cross sections and the scattering function on the basis of Moliere's formula. Improvements of the cross sections of impact-ionisation and excitations by protons and alpha particles include a separate treatment of the close and distant collisions, and integrated cross sections together with the energy spectra of ejected electrons are established using the Weizäcker-Williams method that was improved by Seltzer.

Fundamental for particle tracking in biological objects are reaction cross sections of secondary electrons at low energies in water. However, until recently there were hardly experimental data available to verify calculations. Most experiments were performed in hydrogen. To establish a data library of electron cross section in water, elastic scattering data at energies below 20 eV are supported on experimental data measured by Michaud and Sanche in amorphous ice, and for higher energies elastic scattering is calculated using Moliere's formula with modified screening parameters which were fitted to experimental data. Bremsstrahlung is included using cross sections on relevant nuclides, and impact-ionisation is determined taking into account close and distant collisions separately for each atomic subshell by applying the Weizäcker-Williams method. Excitation cross sections at energies below 20 eV are again supported on experimental data measured by Michaud and Sanche in amorphous ice. At energies between 20 eV and 10 keV excitation cross sections can be derived from data of Paretzke and at higher energies by partitioning using cross section for nuclides.

The calculated reaction cross sections are compared to and tested with available experimental data. (see Figure 4)
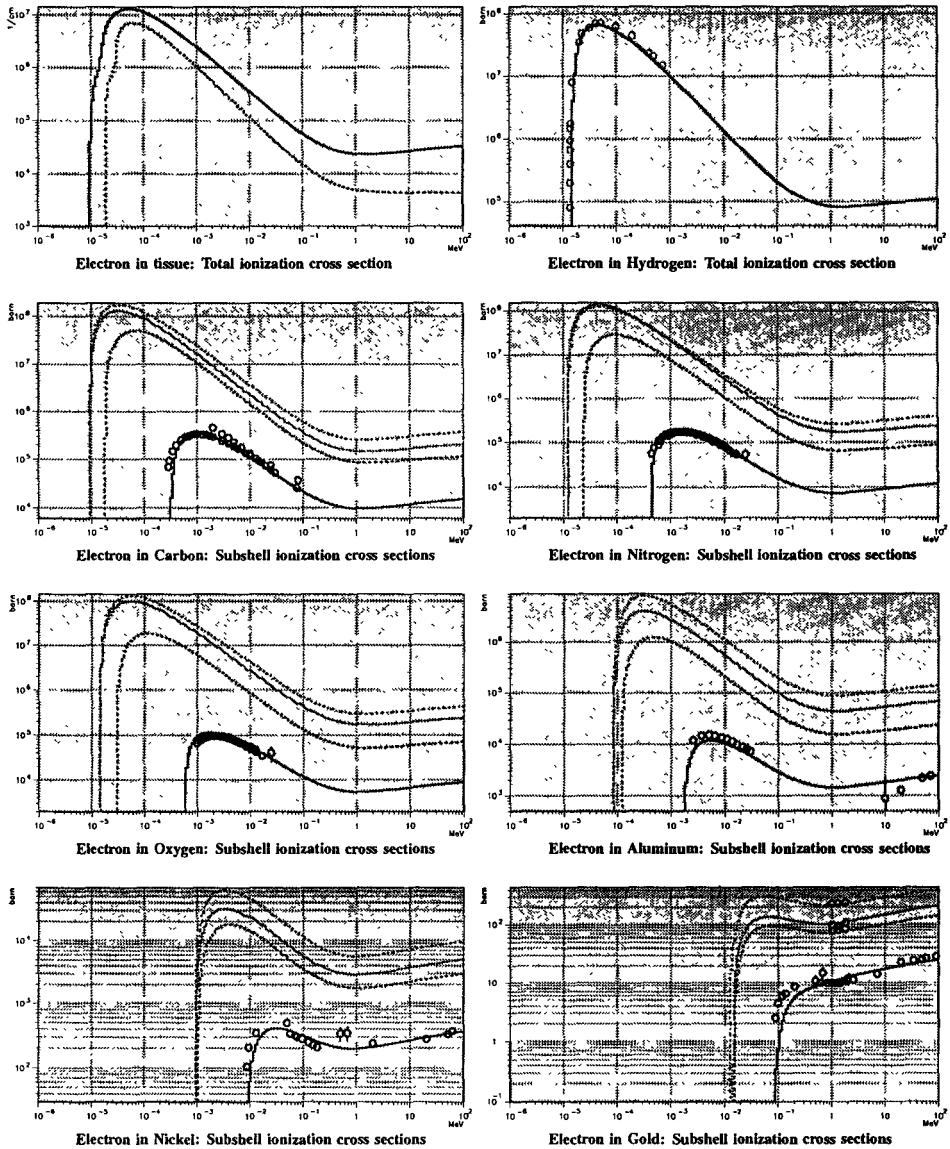
Figure 4: Cross sections for impact-ionisation by electron; In the first picture the new total ionisation cross sections (full lines) are compared with original GEANT values based on Møller's theory (dashed lines). In the other pictures the new subshell ionisation cross sections are compared with experimental values. Experimental data for Hydrogen are taken from L.J. Kieffer,"Low energy electron-collision cross-section data, Part I: Ionization, Dissociation, Vibrational Excitation", Atomic Data 1, p.19 (1969), and for other nuclides from X.Long et al, "Cross sections for K-shell ionization by electron impact", Atomic Data and Nuclear Tables, 45, p.353 (1990).

Biological test systems: V79 hamster fibroblasts

Material and methods:

Cells:
V79 Chinese hamster fibroblasts were cultured in minimal essential medium (Eagle's MEM with Glutamax-I, Gibco BRL) supplemented with 10% fetal calf serum, 50 U/dm^3 penicillin, 0.05 g/ dm^3 streptomycin at 37° C and 5% CO_2. These conditions provide a doubling time of 12 h (M. Belli et al., 1989). The plating efficiency was 80-90 per cent. Cells were cultured in special petri-dishes having a mylar foil instead of a common polystyrene bottom as culture surface (Petriperm, Hereaus AG). In order to expose the cells to an uniform dose they were confined to the central area of the petri-dish by seeding them in a centred ring made of stainless steel with 25 mm in diameter. The cells were seeded (7-$8x10^3$ cells per dish) three days before irradiation, and the ring was removed the following day. During irradiation cells were kept at 37° C and supplied with 5% CO_2. Twenty-four hours after irradiation, the cells were trypsinised, counted and reseeded in appropriate concentrations for assessment of the colony forming ability.

Conventional irradiations with 10 MeV protons:
To get familiar with the irradiation technique conventional low dose irradiations were performed with 10 MeV protons, and the observed cell survival was compared with the that obtained with X-irradiation. This is interesting to perform, getting a link between conventional irradiations with those by single particles.

Test experiments for irradiations with measured track positions:
On the basis of previous experiments with MCF7 human breast adenocarcinoma cells, a procedure for culturing V79 cells in the cell chamber was established. By applying a detailed washing protocol to all parts of the chambers, it was possible to eliminate toxic side effects in the V79 cell-system. This is an important prerequisite for investigation of the biological effect of single particle irradiations. Twenty-four hours before irradiation $1.5x10^4$ cells per cell chamber ($1.5x10^3$ cells/ml medium) were seeded to enable sedimentation and to permit the cells to attach to the palladium islands. Non-attached cells are removed by replacing the culture medium. Immediately before irradiation, the relative position of cell chamber and track detector was determined. The fate of individual cells is easily followed up to one week p.i. with the help of the computer controlled microscope stage.

Results and discussion:
Preliminary dose-response curves of conventional irradiations with 10 MeV protons and X-rays (80 kV) are shown in Fig. 5. These results have to be confirmed and completed by repeating the experiments with 10 MeV protons. There is indication of reduced cell survival after irradiations with X-rays at doses below 1 Gy, which is not present with proton irradiations. Test experiments confirmed the feasibility of the cell chamber to perform low dose experiment such as single particle irradiations. Toxic side effects were eliminated, and the experimental technique for single particle irradiations is established.

In-vitro mouse embryo genesis

Materials and methods

Embryos
Four to six females of B6C3F1 mice (Charles River Wiga GmbH, Sulzfeld, Germany) were brought together with a single male between 7:00 and 8:00 a.m. After one hour the females were removed. Those having a vaginal plug were separated and the embryos harvested the next day between 8:00 and 12:00 a.m. following the method of Hogan et al.
Modified Whitten medium prepared monthly and stored at 4°C was used in all experiments. At least thirty minutes before use, the medium was put in the incubator (37°C, 10% CO_2, 100% humidity) to adjust temperature and pH.

Culture dishes and fibrin glue
Commonly embryos were cultured in *in vitro* fertilisation culture dishes (Costar) with a centre well of approximately 1.5 cm in diameter. However, for irradiation with 20 and 10 MeV

protons hydrophilic Petriperm culture dishes (Heraeus) of 5.5 cm diameter with a 25µm thick foil as bottom were used. In order to keep the embryos in the centre of the dish (minimal beam diameter 2.5 cm) and also considering localisation of a particle passage through a nucleus of a blsatomere, they were embedded in a small drop of fibrin glue (Tissucol, Immuno AG, Switzerland).
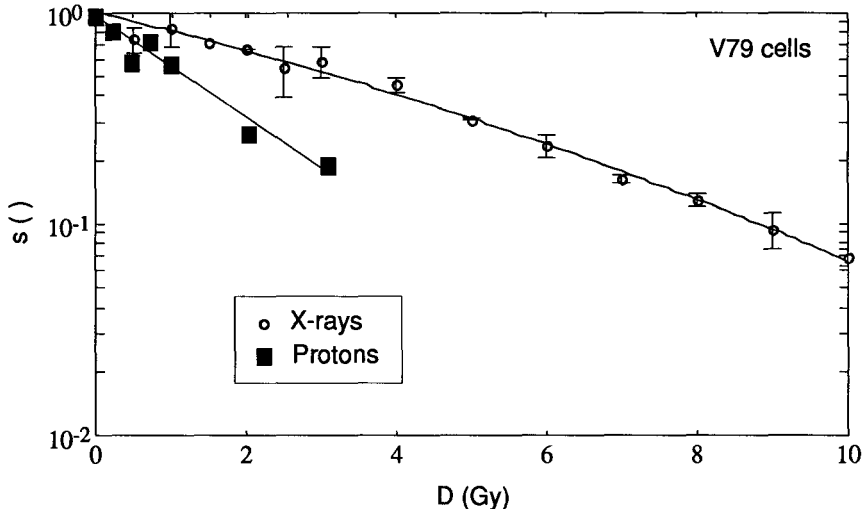
Figure 5: Survival curves for V79 cells irradiated with X-rays (80 kV) and protons (10 MeV).

The two components (Tissucol and thrombin solution) of the glue were prepared according to the instruction manual and separately diluted with medium (1 part glue with 19 parts medium). Embryos were placed in a drop of diluted Tissucol as small as possible and allowed to sink to the bottom. Thrombin solution was then gently layered around and on top of the Tissucol drop and the dish put back into the incubator. After the glue had hardened, medium was added.

Irradiation:
Irradiations were performed with protons of 45, 20 and 10 MeV energy. Culture dishes were brought to the target station by means of a preheated box. The irradiation chamber was kept at 37° and supplied with 10% CO_2 in bottled air which was let through an air washing bottle with distilled and sterilised water. The embryos were left on the target station according to the desired dose (0.1 - 1 Gy) from 3 to 25 minutes.

Endpoints:
Blastocyst formation (BCF) and hatching rate (HR) were examined as endpoints for dose response curves. Embryonic development was monitored up to six days p.i. with an inverted microscope and the number of embryos in a predefined development stage recorded daily. Samples were taken from a pool of embryos of 10 to 20 mice.
In a second experiment occurrence and duration of the three cell stage was investigated, using time lapse video microscopy. Duration of the three cell stage was defined as the end of cleavage of the first blastomere to appearance of a cleavage furrow in the second blastomere. Embryos collected within less than half an hour from only one to three mice were used in each of these experiments.

Time lapse video microscopy:
Time lapse recording of the embryonic development was accomplished using an Olympus inverted microscope (IMT-2) that was equipped with a commercially available Plexiglas

incubator. A specially designed inner chamber (7x12x2 cm; copper) housing the culture dish, was fitted at the microscope stage.

The circulating air in the incubator was preheated and temperature controlled by a sensor to maintain the temperature at 37°C. Bottled air containing 10% CO_2 was let into the inner chamber at a rate of 1 ml/s after it passed a gas-washing bottle, which was maintained at 37°C. To enhance humidity further, two small petri-dishes containing distilled and sterilised water were placed within the inner chamber.

Every minute the embryos were illuminated with red light (bright field illumination) for 3 seconds to record two half pictures by a Kappa CF 15/2 video camera and a Panasonic AG-6730 time lapse recorder.

Results of conventional irradiations (45, 20 and 10 MeV):

Samples of ten to twenty embryos were irradiated with doses varying from 0.1 to 1 Gy with protons of different energy (45, 20 and 10 MeV). Most of the experiments were repeated twice, however, some could be carried out only once as far.

With 45 MeV protons there was a clear dose response of the hatching rate observed which fits to the linear quadratic model (alpha = -0.28, beta = 1.64; Fig. 6). Data taken with 10 and 20 MeV protons are very preliminary and do not permit to draw any conclusion.

Hatching rate of mouse embryos irradiated *in vitro* with protons at late 2-cell stage
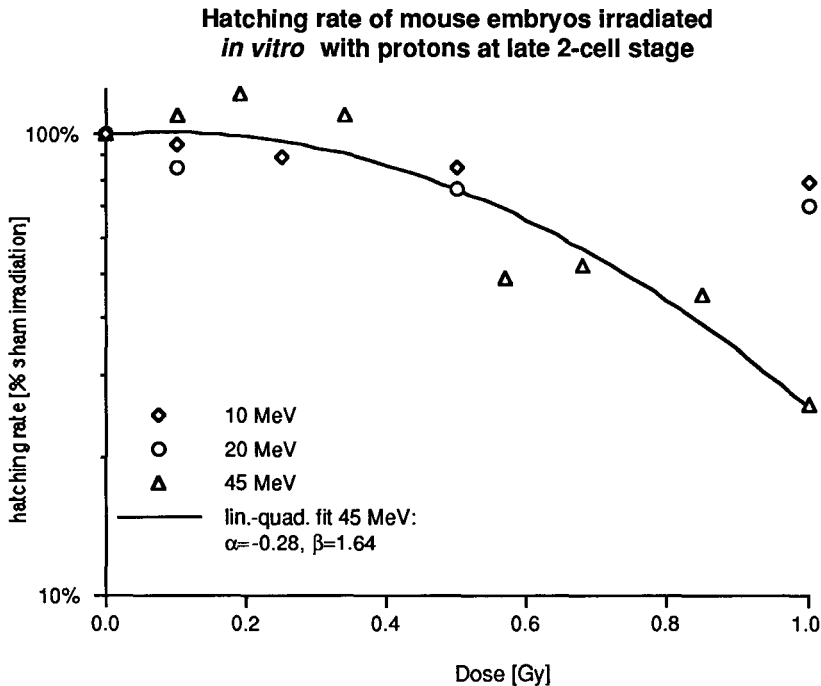
Figure 6: Hatching rate of preimplantation embryos after irradiation in the late 2-cell stage with 10, 20 and 45 MeV protons. Values are percentages of that of sham irradiations.

Results of three cell stage experiments:

Irradiations were performed with 10 MeV protons at 0.1 Gy and accompanied with two control experiments. Out of a total of fifty five embryos (36 controls, 19 irradiated) only in three cases (control) the two blastomeres divided synchronously, in all other embryos a distinct three cell stage was observed which lasted (2:02±2:35) hr's in irradiated embryos and (1:57±1:43) hr's in the controls. Three embryos in the first experiment showed a retarded second mitosis with a prolonged three cell stage compared to the others in that sample.

However this finding could not be verified by the second experiment, where the distribution was much more uniform.

After all nine embryos of the first control experiment had reached the four cell stage, they were removed from the microscope and allowed to develop in an incubator. Seven of the nine embryos hatched.

References

1. H.W. Reist, P. Doria, E. Heimgartner, D. Knespl, M. Kohler, B. Larsson, C. Markovits, C. Michel and J. Stepanek. *Study of low-dose radiation damage by reconstructing single tracks through single cells.* PSI Life Sciences Newsletter, 93 (1993) and Proceedings of SGSM-SGBT, Nov. 4-5, (1993), CH-5232 Villigen PSI, Switzerland, pp. 211-215.

2. H.W. Reist, W. Burkard, D. Calabrese, P. Doria, E. Heimgartner, D. Knespl, M. Kohler, B. Larsson, R. Leemann, C. Markovits, C. Michel, J. Stepanek, S. Teichmann and S. Tuor, *A new method to study low-dose radiation damage,* Jour. Radiat. Prot. Dosimetry (1995).

3. J. Stepanek and H.W. Reist, *Design calculations for single-cell experiments at the Inst. Med. Radiobiology,* PSI-Report TM-29-92-1, Paul Scherrer Inst., CH-5232 Villigen PSI, Switzerland (1992).

4. J. Stepanek and H.W. Reist, *Calculations of low dose irradiation damage with measured track position: distribution of LET's and of energy transfers to cell nuclei by low energy protons and α-particles,* PSI-Report TM-29-95-1, Paul Scherrer Inst., CH-5232 Villigen PSI, Switzerland (1995).

5. S. Tuor, H.W. Reist and P. Doria, *Track reconstruction to investigate cell damage by single particles,* PSI Life Sciences Newsletter 92, (1993), CH-5232 Villigen PSI, Switzerland

6. S. Tuor, *Extraktion geometrischer Primitiven aus digitalen Grauwertbildern durch effiziente Suche im Parameterraum,* Dissertation ETHZ-Nr. 10954, Federal Institute of Technology, Zurich, Switzerland (1995)

7. D. Knespl, H.W. Reist and J. Stepanek, *Particle track simulation in nanometer range for radiotherapy and radiation protection,* Proceedings of SGSMP-SGBT, Nov. 4-5 (1993), CH-5232 Villigen PSI, Switzerland, pp. 241-246.

8. J. Stepanek, *Advanced method to determine the radiation spectra due to a single atomic-subshell ionisation by particles or due to decay of radionuclides,* Proceedings of SGSMP-SGBT, Nov. 4-5, (1993), CH-5232 Villigen PSI, Switzerland, pp 223-228.

9. J. Stepanek, *Atomic interaction cross sections of positrons, protons and α–particles,* to be published.

10. M. Kohler, P. Binz, D. Bohrer, P. Doria, F. Dürr, E. Heimgartner, R.C. Leemann, H.W. Reist, S. Tuor and C. Michel, *"Coaching" the preimplantation mouse embryo in vitro to fulfil the needs of a sinlge particle irradiation,* PSI Life Sciences Newsletter, 92 (1994), CH-5232 Villigen PSI, Switzerland

11. M. Kohler, A. Kündig, H.W. Reist and C. Michel, *Modification of the in vitro mouse embryogenesis by X-rays and fluorochromes,* Radiat. Environ. Biophys. 33, 341 (1994)

12. M. Kohler, E. Raznikiewicz, T. Leemann, V. Guggiana, H. Walt, H.W. Reist and C. Michel, *3D-analysis of the mouse embryonic growth patterns in vitro by confocal laser scanning microscopy (CLSM).* PSI Life Sciences Newsletter, 104, (1992), CH-5232 Villigen PSI, Switzerland

Final Report
1992 - 1994

Contract: F13PCT920063   Duration: 1.9.92 to 30.6.95

Title: New technologies in the automated detection of radiation-induced
cytometric effects.

1)   Aten   Univ. Amsterdam
2)   Nüsse   GSF
3)   Bauchinger   GSF
4)   Green   MRC

I. Summary of Project Global Objectives and Achievements

The global aim of this project was to develop and evaluate new methods for the
analysis of radiation-induced cytogenetic changes in metaphase and in
interphase cells. The main criteria we formulated were that the development
should be toward automated methods that would provide quantitative data on
various types of aberrations and that these automated methods should yield
information that could be related to results obtained with cytogenetic
techniques based on visual microscopic analysis.

The background for this project is the still pressing need for sensitive
techniques to quantify the exposure of a person to ionising radiation. These
new techniques being developed should help to satisfy the medical need for
dose assessment on large populations in case of an accidental irradiation, and
be less time consuming than the conventional cytogenetic procedures used so
far. At the time of the start of this project the visual assessment of dicentrics in
human lymphocytes using transmission microscopy was still the most sensitive
technique to quantify an individual's exposure to radiation. Provided a
sufficient number of cells was evaluated in the first metaphases following the
irradiation, equivalent whole-body doses of 50-100 mSv of sparsely ionising
radiation could be detected. However, this technique alone could not satisfy
the need for dose assessments on large populations as has become evident after
several serious nuclear accidents in the years behind us. Moreover, the
precision of dose-estimations of old exposures is limited with this method. With

chromosome painting (Bauchinger, Green)

- To establish methods for the isolation of chromosomes and micronuclei that yield suspensions of particles with optimally preserved morphology. To evaluate a variety of methods for attaching fluorescent markers for specific chromosomal regions to these chromosomes and to micronuclei in suspension (Nüsse, Aten)

- To establish, by microscopic scoring, representative dose-effect curves for translocations highlighted by FISH. Radiation qualities and dose rates relevant for radiation protection purposes were used. The investigations also focused on the precise discrimination between stable and unstable aberrations (Bauchinger)

- To investigate of the organisation of chromosomes in interphase nuclei. Double strand breaks can result in chromosome exchanges at those sites in the nucleus , only,where chromatin fibres from adjacent chromosomes can interact. The observed dynamical organisation of the chromatin may facilitate this process (Aten)

- To further increase the sensitivity of the micronucleus assay using visual and flow cytometry methods for an improved biological dosimetry in humans (Nüsse)

- To create a fluorescence microscope image processing system for finding metaphase spreads, detecting labelled chromosomes at high resolution and for producing an analysis in terms of radiation dose (Green).

- To establish an automated technique for detecting karyotype abnormalities in large numbers of cells using slit-scanning of fluorescent chromosomes in suspensions prepared from irradiated cells (Aten).

The project, in general, was divided in two broadly overlapping phases. The first phase, lasting about 2 years, was focused on the development of the new methodologies mentioned above, taking place at the MRC (Green), GSF(Nüsse), and Amsterdam (Aten). As with most technical research projects, this phase of the investigations proved to be quite laborious and many obstacles had to be overcome. During this period of development an extensive reference data set on aberrations was being generated, at the GSF (Bauchinger), by visual scoring using FISH labelling of metaphase spreads. Interaction between the participants, in this phase of the project, centred on meetings, between one and two times per year, in which the participants systematically analysed the advances and problems connected with the different technical approaches. Predominant in all cases appeared to be the influence, on the performance of the different automated detection systems, of the biological variation, between individual chromosomes or micronuclei within one sample, and between different samples.

increasing time after exposure the frequency of cells containing such unstable aberrations gradually decreases. In fact, a more reliable procedure for estimating doses of previous radiation exposures would be the scoring of symmetrical translocations that have no selective disadvantage. For that purpose, however, a banding analysis using conventional staining and visual analysis techniques proved to laborious.

Our approach during the period of the project has been to adapt, and where necessary to develop new, advanced molecular cytogenetic detection techniques for radiation-induced chromosome changes and to introduce sensitive optical methods for the visualisation of the available optical information and intelligent, fast, image analysis procedures for the evaluation of the registered images. We aimed to demonstrate the potential of the new sample preparation methods, in combination with the automation of analysis systems, for the quantitative cytogenetic analysis of the chromosomal processes involved in the induction of aberrations by the following programme of investigations.

At the beginning of the project period various ways for the automated analysis of the expression of radiation-induced genomic damage as chromosomal aberrations were open. As none of the possible methods had been investigated in sufficient depth, we chose to pursue the problem from different sides by developing, in parallel, a number of promising methods. This approach required the input from a multi-disciplinary group of highly specialised investigators that could not be found combined in a single institute. By joining the effort of experienced scientists of several institutes from different E.U. member states we expected to advance sufficiently fast to allow a comparison of the merits of the different techniques developed through our common effort before the end of the project period.

The techniques selected for further development were:
- The detection of chromosome damage with automated microscopy and fluorescence in situ hybridisation (FISH) (Green)
- The analysis of micronuclei using flow cytometry and FISH (Nüsse)
- The slit-scanning analysis of dicentric chromosomes by flow cytometry (Aten)
- Investigation by confocal microscopy of the nuclear organisation in relation to radiation sensitivity (Aten).

The development of these techniques for the investigation of radiation-induced cytogenetic effects involved methods:
- To establish reliable, reproducible in situ hybridisation protocols with fluorescent probes for centromeres, telomere marking and for whole

The transition to the second phase, occurring for the different technologies at different periods of the project, was marked by a strongly increased interaction between the participants, as data started being generated by the different automated systems that could used to evaluate their performance (Nüsse - Bauchinger, Green - Bauchinger). Moreover, during the period covered by the second phase of the project, the exchange of samples between the participating groups became an integral part of several of the measurement programmes (Green - Bauchinger, Nüsse - Green). Nüsse and Aten collaborated on the tough problem of centromere labelling of micronuclei and chromosomes in suspension.

At the end of the project the feasibility of the different approaches had been demonstrated in principle. Although it is difficult to predict, at this stage of the development, which of the new techniques will prove to be ultimately the method of choice, it is evident that the data obtained by visual assessment of FISH labelled samples (Bauchinger), yield a wealth of quantitative aberration data as well as providing valuable information on the chromosomal processes involved. The quantitative microscopy method (Green) promises to provide the same type of information but faster which make it an attractive choice. The micronucleus test is by far the most rapid procedure of all the methods that we investigated but here the background can be problematic. The slit-scanning data (Aten) also can be obtained at a high rate but the system sofar has a limited sensitivity because of background problems. The dynamic organisation of chromosomes in interphase (Aten) is relevant for the understanding of mechanisms involved in the induction of aberrations.

Head of project 1: Dr. Aten

II. Objectives for the reporting period

The project was aimed at the development of two methods for the automated analysis of radiation-induced effects on chromosomes.

The aim of the first part of this project was to make available the method for the automated method, developed in our laboratory for the analysis of chromosomes by slit-scanning flow cytometry, for the detection of dicentric chromosomes isolated from irradiated cells.
Specific objectives:
The method should be made applicable to chromosomes isolated from human cells.
To increase the sensitivity of the detection of the fluorescence profiles of the chromosomes a highly light-efficient detection system should be developed. This should allow the slit-scanning technique to be applied to the analysis of chromosomes highlighted with centromere-specifc fluorescence labels.
The method for slit-scanning of dicentric chromosomes should be made suitable for standard cell sorter systems.

The aim of the second part of this project was to study the organization of interphase chromosomes in relation to the induction of aberrations.
Specific objectives:
The objective was to analyze factors involved with the rejoining of DNA-breaks resulting in new chromosome combinations. To this end we worked on the development of methods for the investigation of the mobility of chromatin inside its chromosome nuclear domain.

III. Progress achieved including publications

Slit-scanning analysis of chromosome aberrations

Stochastic chromosome changes such as radiation-induced aberrations result in chromosomes of variable size and DNA-content. Some of these aberrations, like dicentric chromosomes, can be recognized using flow cytometry if the morphology of chromosomes is introduced as an additional parameter. When chromosomes are analysed by slit-scan flow cytometry, the scanning of the fluorescence distribution of a DNA-specific fluorochrome along a chromosome yields a DNA profile in which the centromere is recognizable as a dip [1-5]. Introduction of centromere counting can render slit-scan flow karyotyping suitable for the detection of dicentric chromosomes Data on dicentric chromosomes obtained by centromere counting in slit-scan flow cytometry profiles had been reported recently [6]. These authors, however, did not

combine their slit-scanning analysis with a visual analysis of the suspected dicentrics. As they were not able to sort the relevant chromosomes their results are difficult to verify.

The application of slit-scan flow cytometry for analysis of dicentric chromosomes is hampered by the occurrence of false-positive signals caused mainly by aggregates of chromosomes that, like dicentrics, can result in trimodal profiles, i.e. profiles with two dips. To correct for these false-positive signals, it is necessary to evaluate profile characteristics that distinguish profiles generated by artefacts from profiles generated by dicentric chromosomes. Correction for false-positive signals will increase the reliability of the slit-scan flow cytometry method for the detection of dicentric chromosomes. In this study, trimodal profiles were examined in relation to the morphology of the associated chromosomes. We inspected these chromosomes that generated trimodal profiles by sorting them individually on slides. This involved the development of a module for on-line profile recognition to be used for dicentrics sorting and the development of a procedure for stretching and stabilization of chromosomes.

Until recently, centromere detection with a standard cell sorter system was restricted to the larger human chromosomes or Chinese hamster chromosomes [7,8]. The medium-sized and smaller human chromosomes were difficult to discriminate using the slit-scan method. Our aim was to develop a method for slit-scanning analysis and sorting of normal and dicentric chromosomes, including the smaller ones, that can be realized using standard cell sorter equipment without major additional investments. We evaluated the influence of the optical resolution of the instrument and of the length of chromosomes. These parameters, together with the orientation of the chromosomes during scanning, determine the efficiency of the slit-scan flow cytometer for the detection of centromeres.

Sensitive immuno- and in situ-labelling techniques can be used for highlighting specific regions of chromosomes. Labelling with fluorescent markers, of chromosome centromeres, in particular, can be extremely useful for the detection of dicentric chromosomes. The advantage of these cyto-chemical techniques is their specificity for the selected areas of chromosomes. The resulting labelling patterns show a high degree of contrast but the intensities of the fluorescence signals are too low for detection by slit-scanning flow cytometry methods described earlier. To overcome this problem, we have designed a new type of detector with a much higher sensitivity. The detector is based on the method of Time-Delayed-Integration (TDI).

Slit-Scan Flow Karyotyping

Slit-scan analysis was performed with 3 types of cell sorter systems: 1) a standard Ortho System 50 Cytofluorograph (Becton Dickinson, Mountain View, CA), 2) an improved Ortho System 50 Cytofluorograph and 3) a modified FACStar PLUS cell sorter (Becton Dickinson, Mountain View, CA). All cell sorters were equipped with a Spectra Physics 2000 Argon Ion Laser (Mountain View, CA). Particles were scanned by the laser beam in UV mode (400 mW), focussed into a ribbon shaped spot.

Sensitive slit-scanning detector based on TDI

Fig. 1 shows a schematic representation of the TDI slit-scanning detector for low light intensity detection. During the scanning, a strongly enlarged image of the chromosome is projected on the surface of the detector. The detector contains a number of parallel segments. Each segment consists of optical fiber that transports the fluorescence light to a light-sensitive sensor. This sensor transforms the light signal into an electrical pulse. During a scan, the fluorescence image of the chromosome moves across the front ends of the optical fibers mounted in the detector surface. Each detector segment 'sees' the complete image in time as a light pulse representing the fluorescence profile, but there is a time shift between the pulses registered by different detector segments. The output signal from each segment is delayed to synchronise it and then added to the output signal of the next segment. The detector thus functions as a 'conveyor belt' moving in synchrony with the fluorescence image that is projected on it. In this way an electrical 'image' of the fluorescence profile is accumulated on the conveyor belt.

Profile-Dip-Counter (PDC) module for on-line analysis of slit-scan profiles

We designed an analog module, the Profile-Dip Counter (PDC), to recognize dips "on-line", during the registration of the slit-scan profiles. The 'PDC' module is interfaced with the cell sorter. Dips or minima in a profile correspond to zero crossings in the time derivative. The 'PDC' was designed to interpret a crossing of the derivative with a count level as a profile dip. This count level was adjusted just below the zero level of the derivative. Counting of dips is started when the slit-scan signal first rises above a preset trigger level. Counting of dips is stopped after a time interval of 25 µs. The time interval corresponds to a particle length of 45 µm, taking into account a flow velocity of 1.8 m/s. The value of the output signal of the PDC module is proportional to the number of dips in the fluorescence profile. This signal is presented to the multiparameter processor 'MPP' of the cell sorter for about 5µs.

To synchronize the PDC signal and the direct fluorescence signal, processed by the "MPP", the processed fluorescence signal is held by activating a sample-hold circuit, which is a standard feature of the "MPP". The interval between input and output signals of the 'PDC' module should not exceed 70 µs, i.e., the maximum sample-hold time in the "MPP".

Counting dips generated by noise had to be avoided. The cut off frequency of the 'PDC' module is 4 MHz (3 dB point); this value lies within the frequency domain of the high frequency noise. The high frequency background, due to electronic and fluorescence noise, is, therefore, reduced by adjusting the filtering characteristics of the preamplifier to a cut off frequency of 2 Mhz. This cut off frequency separates the high frequency noise from the maximum signal frequency of 0.7 MHz defined by the optical resolution (2.5µm) and the flow velocity (1.8 m/s) of the slit-scanning system.

Cell Culture and Chromosome Isolation

The influence of the chromosome length and of the optical resolution of the laser focussing optics on the quality of slit-scan flow karyotypes was investigated using chromosomes isolated from NBCH and V79 Chinese hamster cells. The smallest Chinese hamster chromosome is about the size of human chromosome 19. The three largest Chinese hamster chromosomes are larger than the human chromosome 1. Chromosomes isolated from the human skin fibroblast cell line HSF7 were used to

investigate the performance of the slit-scan flow cytometer, after improvement of the spatial resolution and of the chromosome preparation technique. The cells were cultured according to standard procedures, chromosome isolation and stabilization was performed using the propidium iodide method [9]. To obtain homogeneous cell populations and to induce chromosome aberrations expressed in metaphase, cultures were irradiated in plateau-phase

Chromosome preparation for slit-scan analysis

For the detection of dicentric chromosomes by recognizing centromere dips in slit-scan profiles, the dips have to show up clearly. To increase the efficiency for centromere detection, we decided to increase the length of chromosomes by adding trypsin. After about 30 s of incubation at room temperature, trypsinization was stopped by adding trypsin inhibitor. To preserve the morphology of chromosomes during the sorting procedure, glutaraldehyde was added to a concentration of 0.1%. Finally glycerol was added to a concentration of 30%. Suspensions of chromosomes prepared in this way can be stored for up to 4 days (-12 C). After this period chromosomes started to swell. For the centromere labelling of human chromosomes in suspension we used several CREST anti-sera, isolated from the blood of patient suffering from the scleroderma syndrome, cf Fig. 2. In these experiments, we used directly labelled antibodies. The labelling procedure was performed in collaboration with the Edinburgh group [10].

Slit-scanning analysis and dicentric sorting

To determine which types of profiles correspond to actual dicentrics and which to artefacts, the sorter module was activated every time a trimodal profile was detected by the 'PDC' module. The chromosomes were sorted individually on separate slides or at separate locations on the same slide and then examined by FISH and fluorescence microscopy. This was performed in collaboration with the Munich group. The method of depositing chromosomes at separate and well documented positions on a slide enabled us to match the morphology of the sorted chromosomes with the shape of its slit-scan profiles. Over 500 profiles were analysed in relation to the type of particle, i.e. dicentric or artefact, that they represent. We applied several tests to these profiles, but we could find no criteria with which dicentric chromosomes can be identified unambiguously. We, however, did find cf. Fig. 3, that: (1) the value of the relative difference, D/D, between the nadir values of the two dips and (2) the value of the largest relative difference, H/H, between the heights of the three tops of a trimodal profile, were useful parameters for the analysis of these slit-scan profiles. Using D/D and H/H as parameters, we constructed two bivariate distributions, one for the set of trimodal profiles corresponding to dicentric chromosomes, cf. Fig. 4a, and one for the set of trimodal profiles corresponding to artefacts, cf. Fig. 4b. Each point in the bivariate distributions represents a single trimodal profile. The bivariate distribution graphs in Fig. 4a and Fig. 4b were segmented into zones, cf Fig 5a.. The fractions of dicentric chromosomes decreases from 0.7 for zone 'a' to 0 for zone 'f', cf Fig 5b.
Sofar no reliable dose-effect relation has been determined based on the slit-scan sorting technique. When a module for the on-line analysis of slit-scan signals using the additional shape criteria described above will be implemented, the frequency of 'false positive' signals will be reduced. Visual inspection of the chromosomes sorted

corresponding to these criteria should then overcome the problem of the remaining 'false positives', the high analysis rate allowing the evaluation of a large number of chromosomes.

Organization of chromosomes in the cell nucleus in relation to the induction of aberrations

Damage to mammalian cells is generally thought to result from changes in DNA. The cellular responses of these changes will depend on their nature and severity and on the effectiveness of their repair. In addition it can be suggested that the fate of DNA changes and the cellular responses may depend on their spatial location and their relation to the 3-D organisation of the cell nucleus, in particular the structural organisation of the chromosomes and their distribution in the nucleus [11]. The latter aspect has not been studied extensively as experimental techniques to analyse the arrangement of the nuclear chromatin have been very limited.

The aim of the project was to investigate the relation between nuclear structure and the induction of reciprocal translocations and dicentrics. Models describing the process of translocation induction at the molecular level assume the presence of two, or at least one, double-strand breaks (dsb) at the translocation site. Evidently, DNA-damage can result in new chromosome combinations at sites where DNA strands originating from separate chromosomes are in close proximity, e.g. within 30 nm of each other, only, i.e., at the boundary between two chromosomes. These aspects require further consideration.

The efficiency of doses of the order of 1-3 Gy of X-rays for the formation of chromosome translocations, in the order of 1 translocation per 40 dsb's, has interesting implications for the possible influence of the organization of chromosomes in the interphase nucleus. It has been well established by chromosome painting that individual chromosomes are located in separate domains in the cell nucleus. Much less is known about the shape of these domains and about the organization of chromosomes inside their domains. When it is assumed that the domains are organized as static units and that these have simple cigar-like shapes with smooth surfaces, and that breaks are not preferentially formed at the borders of chromosome domains, the upper-limit for the probability for translocation induction can be estimated to be considerably lower than cytogenetic data indicate.

This has led us to the following three questions: A) How are the chromosome domains organized at their boundaries? Are interfaces between domains well defined or is there a diffuse region where chromatin loops of neighbouring chromosome domains intertwine? No data have been published that clarify this problem. B) Are nuclei organized in a static manner or is there chromatin movement with respect to the boundaries, within the chromosome domains? This is a controversial subject; indirect evidence exists supporting both points of view. C) How are sites of DNA-repair, and of dsb's in particular, distributed over the chromosomal domain and its boundary? It is evident that these nuclear and chromosomal characteristics may vary

between cell types. In addition, they could depend on the proliferative status of the cells and other conditions

We have started the investigation of the first two questions. In these experiments we will apply DNA-replication and chromosome painting techniques.
A) The shape of chromosomal domains is being investigated using painting techniques.With chromosome painting individual chromosome domains can be visualized. Moreover, differently labelled paints for various chromosomes can be applied simultaneously. This provides us with a tool to study interaction at the boundary between chromosome domains.
B) To study time-dependent changes in the spatial distribution of the labeled DNA within individual chromosome domains pulse-chase replication labeling with two independent DNA labels will be used in combination with chromosome painting
For these experiments we have developed confocal methods for the 3-D investigation of nuclei labeled with three fluorochromes.
The results obtained by the investigation of the nuclear organization will be compared with chromosome painting data on the induction of dicentrics and reciprocal translocations.

For the complex image analysis of the spatial distribution of compartments in cell nuclei we are developing semi-automated 3-D image segmentation and analysis procedures. These procedures can be applied to 3-D images containing multiple isotropic and anisotropic domains. In addition to positional information on the domains, other qualities such as intensity and morphology features can be made available by using these procedures.
We have applied the procedures developped in our laboratory to study DNA-replication patterns. Fluorescence distributions in nuclei from cells labelled with two replication markers were analysed to determine how DNA-replication patterns change within short time intervals. 3-D image analysis techniques in combination with statistical methods allowed us to detect an avarage distance between differently labelled domains of a value of 0.08 um. A linear dependency was observed of the distance between the differently labelled domains on the time interval between the application of the two labels, cf Fig. 6. The data indicate that chromatin moves relative to the domain where replication takes place with a velocity of 0.5 um/h. Movement with respect to the boundaries of the chromosomal domains is now be investigated by combining chromosome paints with two independent replication markers. During the last period of the project, we worked out the staining techniques for the complex three colour experiment. We are now continuing the work on the segmentation and other analysis aspects of these three colour / 3D images.

REFERENCES

1. Lucas JN, Gray JW, Peters D, VanDilla MA. Centromeric index measurement by slit-scan flowcytometry. Cytometry 4:109-116, 1983.
2. Weier HU, Eisert WG. Two-parameter data acquisition system for rapid slit-scan analysis of mammalian chromosomes. Cytometry 8.83-90, 1987.
3. Bartholdi MF, Meyne J, Johnston RG, Cram LS: Chromosome banding analysis by slit-scan flow cytometry. Cytometry 10:124-133, 1989.

4. Oven CH van, Aten JA. Instruments for real-time pulse-shape analysis of slit-scan flow cytometry signals. Cytometry 11:630-635, 1990.

5. Zuse P, Hauser R, Männer R, Hausmann M, Cremer C. Real-time multiprocessing of slit-scan chromosome profiles. Comput. Biol. Med. 20 (6):465-476, 1990.

6. Lucas JN, Mullikin JC, Gray JW. Dicentric chromosome frequency analysis using slit-scan flow cytometry. Cytometry 12:316-322, 1991.

7. Lucas JN, Gray JW. Centromeric index versus DNA content flow karyotypes of human chromosomes measured by means of slit-scan flow cytometry. Cytometry 8:273-279, 1987.

8. Boschman GA, Rens W, Manders EMM, Oven CH van, Barendsen GW, Aten JA: On-line sorting of human chromosomes by centromeric index, and identification of sorted populations by GTG-banding and fluorescent in situ hybridization. Hum Genet 85:41-48, 1990.

9. Aten JA, Buys CHCM, Veen AY van der, Mesa JR, Yu LC, Gray JW, Osinga J, Stap J: Stabilization of chromosomes by DNA intercalators for flow karyotyping and identification by banding of isolated chromosomes. Histochemistry 87:359-366, 1987.

10. Fantes JA, Green DK, Palloy P, Summer AT. Flow cytometry measurements of human chromosome kinetochore labelling. Cytometry 10.134-142, 1989.

11. Cremer T, Kurz A, Zirbel R, Dietzel S, Rinke B, Schrock E, Speicher MR, Mathieu U, Jauch A, Emmerich P, Schertzhan H, Ried T, Cremer C, Lichter P. Role of chromosome territories in the functional compartimentalization of the cell nucleus. Cold Spring Harbor Symposia on Quantitative Biology, 58: 777-792, 1993

PAPERS PUBLISHED

Manders EMM, Stap J, Brakenhoff GJ, van Driel R, and Aten JA (1992) Dynamics of three-dimensional replication patterns during the S-phase, analyzed by double labelling of DNA and confocal microscopy. J. Cell Sci., 103: 857-862.

Aten JA, Bakker PJM, Stap J. Boschman GA, Veenhof CHN (1992) DNA-double labelling with IdUrd and CldUrd for spatial and temporal analysis of cell proliferation and DNA replication Histochem J. 24: 251-259.

Heilig R, Hausmann M, Rens W, Aten JA, Cremer C (1993) Time optimized analysis of slit-scan profiles on a general purpose personal computer. Comp. Appl. Biosc. 9: 381-385.

Rens W, van Oven CH, Stap J, Aten JA (1993) Effectiveness of pulse-shape criteria for the selection of dicentric chromosomes by slit-scan flow cytometry and sorting. Anal. Cell. Pathol. 5: 147-159

Manders EEM, Verbeek FJ, Aten JA (1993) Measurement of co-localization of objects in dual colour confocal images. J. Microsc. 169: 375-382.

Rens W, van Oven CH, Stap J, Jakobs ME, Aten JA (1994) A slit-scanning technique using standard cell sorter instruments for analyzing and sorting non-acrocentric human chromosomes, including the small ones. Cytometry 16:

Rens W, Boschman GA, Hoovers JMN, Manders EMM, Slater RM, Stap J, Aten JA (1994) Flow cytometric detection of chromosome abnormalities by measuring centromeric index, DNA content, and DNA base composition. Anl. Cell. Pathol. 6: 359-375.

Manders EMM, Hoebe R, Strackee J, Vossepoel, Aten JA (1995) Measurement of distances in three-dimensional dual-colour confocal images. Zool. Studies 34: 19-20.

Manders EMM, Strackee J, Aten JA. The largest contour segmentation; a tool for the localization of spots in confocal images. Cytometry (in press)

Image Plane
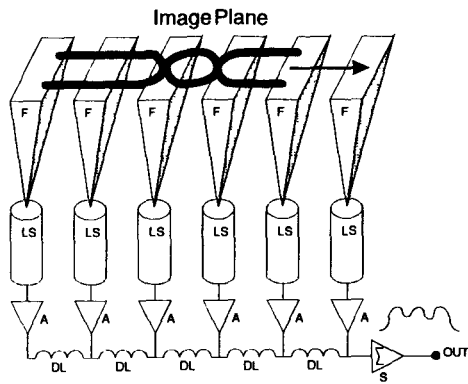
Schematic representation of the "Time Delayed Intergration" detector for the sensitive detection of slit-scanning signals. A: amplifier, DL: delay line, S: summation of signals, LS: light sensor, F: optical fiber.

Fig. 1
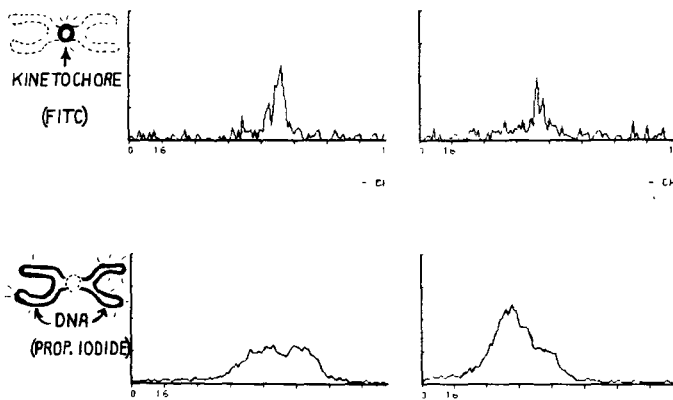
Two-colour slit-scanning flow cytometry analysis of crest-labelled human chromosomes

Fig. 2

TIME
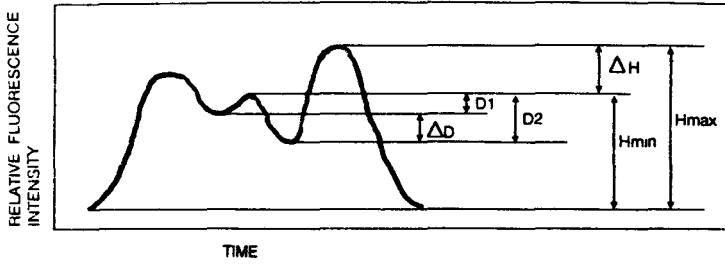
The two pulse-shape parameters that were used to characterize the slit-scan profiles. The first parameter is $\Delta H/\Sigma H$ with $\Delta H = H_{max} - H_{min}$ and $\Sigma H = H_{max} + H_{min}$. In latter expressions H_{max} is the largest top height and H_{min} is the smallest top height of the profile. The second parameter is $\Delta D/\Sigma D$ with $\Delta D = D_1 - D_2$, $\Sigma D = D_1 + D_2$; in latter expressions D_1 is the depth of the first dip, D_2 is the depth of the second one.

Fig. 3
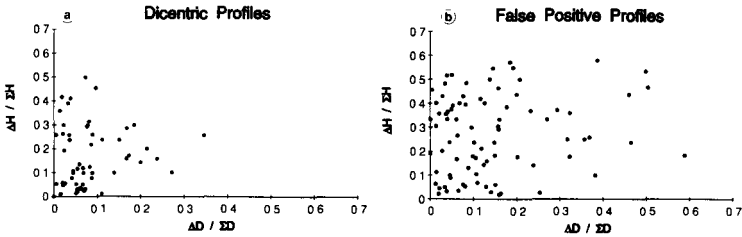
(a) The values of the parameters $\Delta H/\Sigma H$ and $\Delta D/\Sigma D$ calculated for trimodal slit-scan profiles corresponding to dicentric chromosomes, plotted in a bivariate distribution as a function of the two parameters presented in Fig. 6 (b) The values of the parameters $\Delta H/\Sigma H$ and $\Delta D/\Sigma D$ calculated for trimodal slit-scan profiles corresponding to aggregated chromosomes or monocentric chromosomes, plotted in a bivariate distribution presented in Fig. 6.

Fig. 4
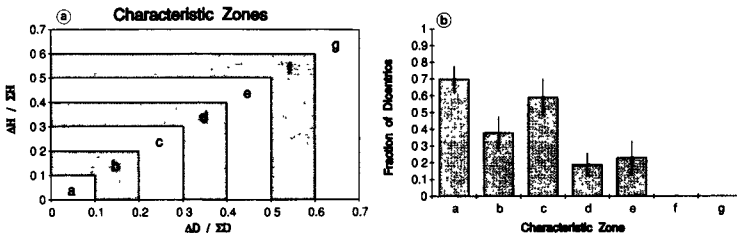
(a) Zones in the $\Delta H/\Sigma H$ versus $\Delta D/\Sigma D$ plane in which the number of dicentric profiles as well as the number of artefact profiles were counted. (b) Number of dicentric chromosomes relative to the total number of chromosomes detected in the zones presented in (a) S.E. indicated by error bars.

Fig. 5
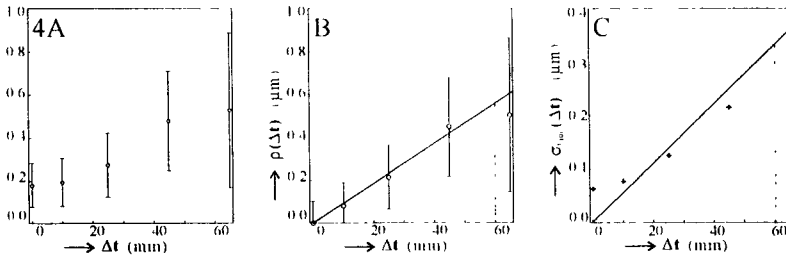
The measured distance $r(\Delta t)$ between domains of nascent and newborn DNA in a pair as a function of the time interval between the addition of the labels Δt (A) (error bars express the SD of $r(\Delta t)$) This figure is based on the measurement of 18 late S-phase nuclei. From this figure the error of measurement (σ_m = 80 nm) was estimated. Knowing this value σ_m and the measured distance r_{av} (Δt), the estimation of the distance between paired domains $\rho(\Delta t)$ was calculated (B) (error bars (standard error of the mean) in are too small to be plotted.). The biological standard deviation σ_{biol} (Δt) of the distance between paired domains was calculated (C). The fitted straight lines in (B) and (C) illustrate the linear time dependency of the estimated distance $\rho(\Delta t)$ and the biological standard deviation σ_{biol} (Δt). The factors v and m expressing the velocity of newborn DNA relative to the domains of replication and its variance are: v=0 55 µm/h and m=0.33 µm/h

Fig. 6

Head of project 2: Dr. Nüsse

II. Objectives for the reporting period

The primary goal of our investigations was the establishment of new flow cytometric micronucleus assays for the measurement of radiation-induced micronuclei (MN) in human lymphocytes with high precision for a possible application of this technique to detect low doses in humans exposed to ionising radiation. For this purpose a preparation technique had to be developed to obtain a suspension of nuclei and MN stained with fluorescent dyes for measurement of MN frequency and DNA distribution of MN in a flow cytometer. A clear cut discrimination between MN and unspecific particles had to be achieved to obtain a precise measurement of MN frequency. Data obtained with the new automated method were compared with data obtained by microscopic scoring using the cytochalasin B-technique. In addition, factors influencing the DNA distribution of MN were analysed using flow cytometry and image analysis in combination with several immunofluorescent methods using antibodies and DNA probes against telomeric and centromeric regions of chromosomes as well as chromosome-specific painting probes. Radiation sensitivity of various human cell lines was studied with these combined techniques

III. Progress achieved including publications

1. Flow cytometric analysis of micronuclei in cell cultures and human lymphocytes

Scoring of micronuclei (MN) provides a quantitative measurement for the degree of cytogenetic damage in cells and is, therefore, increasingly used to quantify cytogenetic damage in the human population for biomonitoring studies and for the dose estimation of humans exposed to ionising radiation. Although the conventional MN test using the cytochalasin B - technique is an established method, it cannot yet provide the capacity to screen larger human populations if more than the usual number of 1000 binucleated cells have to be analysed, especially in persons exposed to very low doses of ionising radiation We have therefore developed an automated flow cytometric technique for scoring MN in cultured cells and human lymphocytes (Schreiber et al , 1992 a,b)
A careful and easy preparation of a suspension of nuclei and MN was developed using a modification of a two-step method published earlier (Nüsse et al 1992 a) The DNA containing particles were stained with the fluorescent dyes ethidium bromide (EB) and HOECHST 33258 (HO) The dyes were excited with two lasers (488 nm and UV) and forward scatter intensity (FSC), EB-fluorescence (EB^{488}), HO-fluorescence (HO^{360}) and EB-fluorescence excited by the HO-fluorescence via energy transfer (EB^{HO}) were measured simultaneously in MN, nuclei and unspecific debris (Fig 1) MN could be separated from debris using FSC as verified by sorting of the respective particles For an even better separation of MN and debris, especially in the region of low DNA-fluorescence, ratios of the three fluorescences were calculated for all particles Only those particles were considered to be MN that showed the same two ratios of the fluorescence signals as compared to the fluorescence ratios of nuclei MN were counted between 0.5% and 10% of the DNA content of G_1-phase nuclei Using this technique the dose response relationships for radiation-induced MN were measured in mouse Ehrlich ascites tumour cells growing in suspension and in mouse NIH-3T3 cells (Fig. 2) Both dose response curves agreed well with independent measurements by microscopic scoring

Since MN are expressed in cells that have divided at least once, cell cycle progression after irradiation (i.e. the G_2-block) plays an important role in the analysis of radiation-induced MN. Especially in human lymphocytes the fraction of cells that have divided once has to be measured additionally. This could be achieved by using the flow cytometric BrdUrd/HO/EB-quenching technique (Schreiber et al., 1992 b). Fig. 3 shows as an example the frequency of MN in human lymphocytes irradiated in vitro as a function of dose. The insert shows a measurement of the fraction of cells in the second cell cycle using the BrdUrd/HO/EB method.
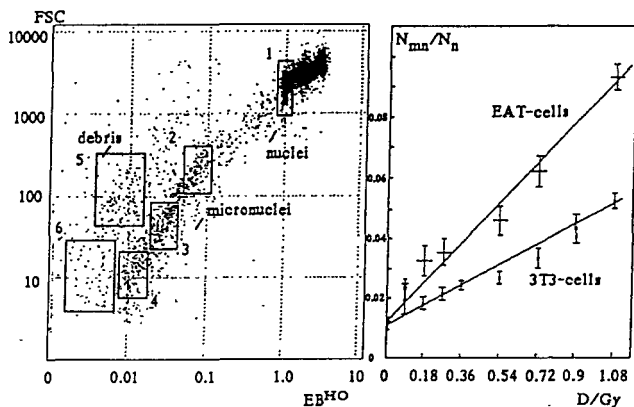
Fig. 1: Flow cytometric measurement of a suspension of MN and nuclei showing the position of G1-phase nuclei (1). MN (2,3,4) and debris (5,6) as verified by sorting

Fig. 2: Frequency of MN N_{mn} per nuclei N_n, N_{mn}/N_n, as a function of the dose for irradiated Ehrlich ascites tumour cells and mouse NIH 3T3 cells.
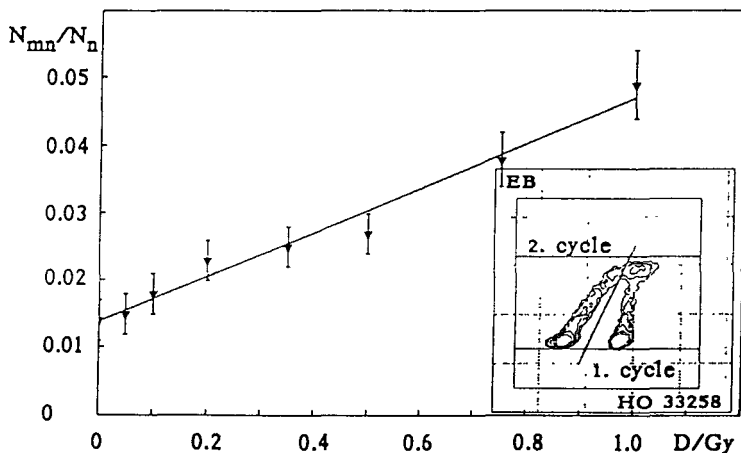
Fig. 3: N_{mn}/N_n as a function of dose in human lymphocytes irradiated in vitro. The insert shows a EB/HO distribution of lymphocytes treated with BrdUrd for 55 h. From such measurements the fraction of cells in the 2. cell cycle is calculated to correct the frequency of MN measured by flow cytometry.

2. Improvement of the flow cytometric technique for micronucleus scoring in human lymphocytes.

In cultured cells a good discrimination between MN and unspecific debris was possible and microscopic and flow cytometric data were usually found to agree very well. In human lymphocytes, however, this was not always the case. Comparison of flow cytometric data with microscopic measurements showed that the flow cytometric results were usually higher compared to results obtained by microscopic scoring. This effect was found to be caused by unspecific, DNA containing particles that can overlap MN during flow cytometric measurement. These particles were produced by dying cells in the population of lymphocytes during cultivation in vitro necessary to express MN.

An improvement of the original flow cytometric technique was therefore developed to bypass this problem. With magnetic beads (Dynabeads, DYNAL INTERNATIONAL, Oslo, Norway) conjugated to antibodies against the CD2-antigen expressed on T-cells it was possible to select intact T-lymphocytes from cellular debris using magnetic separation (Viaggi et al., 1995). With this improved technique lymphocytes from several donors were irradiated in vitro, cultivated for 60 h, and MN frequency was measured with the flow cytometric technique in a suspension of nuclei and MN prepared from magnetically separated intact T-lymphocytes. These data were compared with results obtained from microscopic scoring in the same blood samples using the cytochalasin B (CB)-technique. Fig. 4 shows flow cytometric measurements of EB-fluorescence (DNA) and forward scatter of a suspension of MN and nuclei from the same donor without (a) and with (b) magnetic separation. The position of MN, nuclei and debris is indicated. Comparison of Fig 4 a and b shows that most of the cellular debris overlapping the MN in the histogram (a) was removed by magnetic separation of intact lymphocytes (b).

To compare the results obtained with this improved flow cytometric technique with results obtained by the conventional CB-method, 21 unirradiated blood samples from 12 different donors were analysed in parallel. A significant higher mean value of the frequency of MN in divided cells was found with the flow cytometric method, $N_{mn}/N_d = 0 023 \pm 0.002$, compared with the CB-technique, $N_{mn}/N_d = 0.0066 \pm 0.0005$ (t-test, p < 0.001). This lack of correlation was probably due to the presence of DNA containing particles from fragmented cell nuclei that were not removed by the magnetic separation.

To analyse the sensitivity of the new technique in evaluating the MN frequency in human lymphocytes exposed to γ-irradiation and to compare these data with data obtained by microscopic scoring 9 blood samples of 6 donors were irradiated with doses ranged between 0 and 2 Gy and measured by flow cytometry (Fig. 5 a) and by microscopic scoring (Fig. 5 b). With increasing dose a clear correlation between the two techniques was found. The pooled data from 9 dose-response curves (Fig. 6) analysed by flow cytometry (1) and the CB-technique (2) showed a linear-quadratic dose dependence with comparable α- and β-coefficients

$$\alpha = (0 019 \pm 0.006) \text{ Gy}^{-1} \text{ (CB)}, \qquad \alpha = (0.035 \pm 0 01) \text{ Gy}^{-1} \text{ (flow)}$$
$$\beta = (0.036 \pm 0 005) \text{ Gy}^{-2} \text{ (CB)}, \qquad \beta = (0.0328 \pm 0.0069) \text{ Gy}^{-2} \text{ (flow)}$$

The constant term c was again found to be significantly higher in the flow cytometric data:

$$c = 0.0069 \pm 0 001 \quad \text{(CB)} \qquad c = 0.0272 \pm 0.002 \text{ (flow)}$$

due mainly to cells containing fragmented nuclei, as mentioned above.

For control samples or for doses < 0 2 Gy, the flow cytometric measurements showed a larger variability than the data from the CB-method It is therefore expected that a dose estimation of

men exposed to low doses of ionising radiation can at present not be improved by a flow cytometric analysis of MN in human lymphocytes. For doses > 0.5 Gy a tendency of correlation of the varying individual MN frequencies was found between the two techniques, implying that individual radiation sensitivities can be detected by flow cytometric analysis. A good agreement exists between the shapes of the dose-response curves (α- and β-coefficients) established from the mean MN frequencies of a group of donors. This indicates a similar precision of the two techniques in the detection of radiation-induced MN, when applied to pooled or averaged data from human collectives or groups. Thus, for cytogenetic analyses of collectives that can contribute to the solutions of epidemiological questions, flow cytometry could reduce an amount of time needed for microscopic scoring of MN, especially if the high degree of automation is considered as discussed by Schreiber et al. (1992 b).
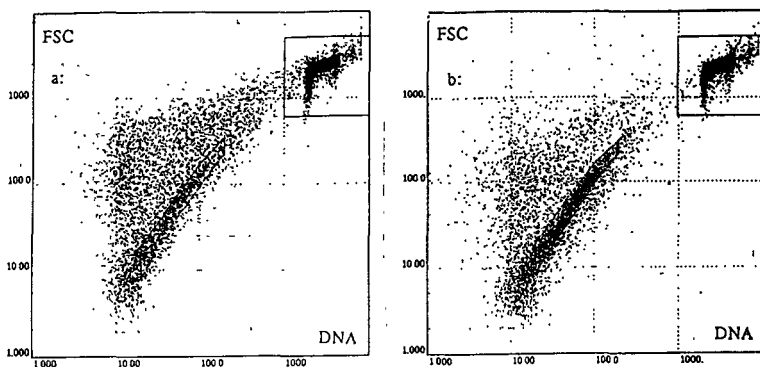
Fig. 4: Dotplots of suspensions of MN and nuclei from human lymphocytes irradiated with 2 Gy (^{60}Co γ-irradiation) and cultivated for 60 h. Forward scatter (FSC) against EB-fluorescence (DNA).
a: old technique (Schreiber et al., 1992 b),
b: after magnetic separation of T-lymphocytes using antibodies conjugated to magnetic beads.
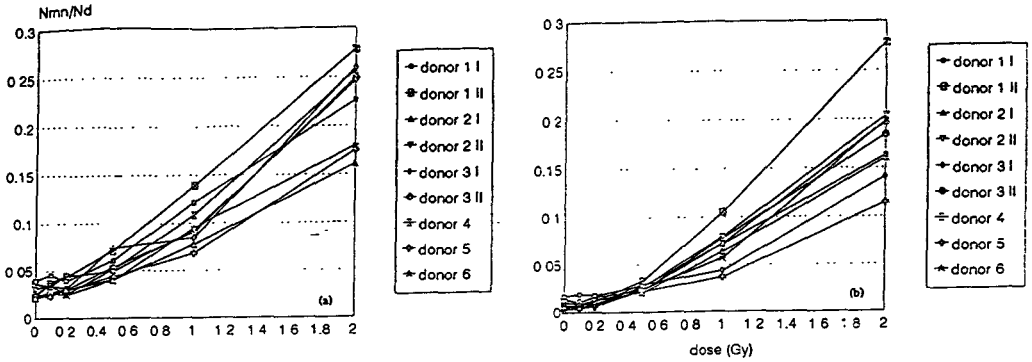
Fig. 5: Dose response curves for radiation-induced MN in lymphocytes from six donors, irradiated in vitro. a: Flow cytometric technique
b: CB-technique. N_{mn}/N_d = number of MN (N_{mn}) per divided cell (N_d).
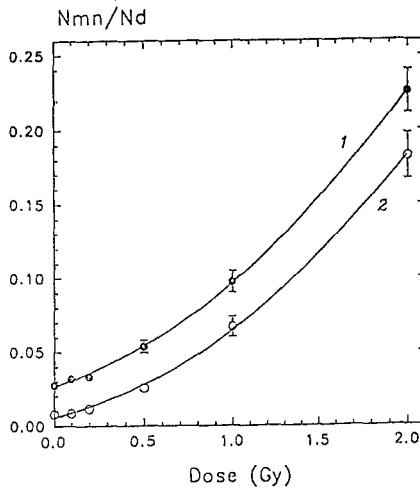
Fig. 6: Linear-quadratic fit of the pooled data derived from the nine independent analyses shown in Fig. 5 a and b 1 Flow cytometry and 1· CB-technique
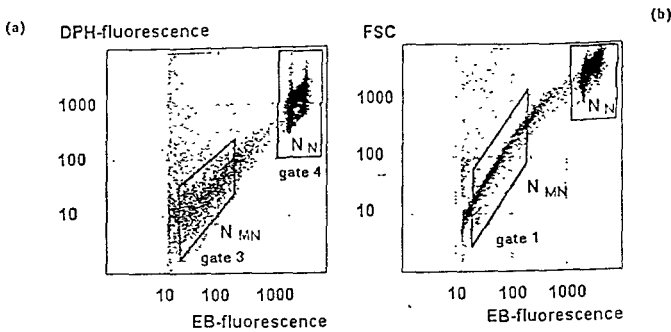
Fig. 7: Flow cytometric measurement of a suspension of MN and nuclei stained with DPH and EB. DPH-fluorescence intensity (a) and FSC (b) are shown as a function of EB-fluorescence intensity.

3. Flow cytometric analysis of micronuclei using membrane-specific dyes

As an alternative for the use of two DNA-specific dyes a second, new staining technique for flow cytometric analysis of MN was developed using membrane-specific fluorescent dyes in addition to the DNA dye especially for those cell types were a large amount of unspecific debris was found after the preparation of a suspension of nuclei and MN. For staining of membranes of nuclei, MN as well as membrane particles in the unspecific debris the lipophilic dyes 2-hydroxyethyl-7,12,17-tris(methoxyethyl)porphycene (HEPn) and 1,6-diphenyl-1,3,5-hexatriene (DPH) were used. These fluorescent dyes are located within the regions of the hydro-carbon bondings of membranes of cells. Due to their lipophilic character they have to be dissolved in organic solvents or in the lipid phase of liposomes depending on the sensibility of the targets to organic solvents. Compared to the earlier techniques this new technique has the advantage that two independent fluorescent signals (DNA and membranes) are obtained from nuclei, MN and debris in addition to the light scattering properties thus enabling an easier and more obvious separation of MN and debris (Wessels and Nüsse, 1995).

Both membrane-specific dyes can be excited by the UV-multilines of an argon ion laser. The spectroscopic properties of the membrane-specific dyes determines the optimal choice of the dye used for the staining of DNA. Therefore, several combinations of the membrane-specific dyes and the DNA dyes ethidium bromide (EB), HOECHST 33258 (HO) and proflavine (PF) were studied for the analysis of MN.

Fig. 7 shows as an example dot plots of DPH-fluorescence (a) and forward scatter intensity (FSC, b) as a function of EB-fluorescence together with the gates used to calculate the frequency of MN, N_{mn}/N_n. Using both gates (FSC/EB and DPH/EB) simultaneously it is possible to separate debris particles from MN according to their higher DPH-fluorescence and their higher FSC. Similar results were obtained using HEPn as membrane-specific dye in combination with proflavin as DNA dye. Fig. 8 shows the MN frequency in Chinese hamster cell cultures illuminated with UV-B light from a sun simulator as a function of the energy density, measured with three staining techniques: EB alone, DPH/EB and HEPn/PF. The results agree well, mainly also due to the fact that in these cells a low amount of debris was usually obtained This new staining technique will be used in future for an improved analysis of MN induction in human lymphocytes

a
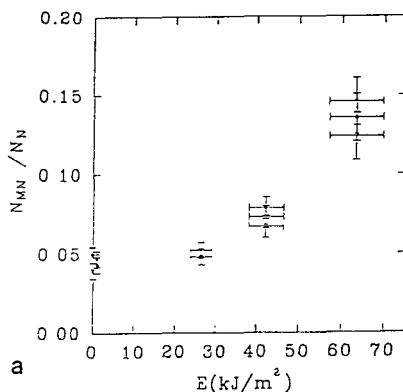
Fig. 8: Frequency of MN as a function of energy density in Chinese hamster cells after illumination in a sun simulator with a white spectrum extending from 296 nm to 2500 nm. Results of three different staining techniques are compared Open triangles: EB alone; solid triangles: HEPn/PF; circles: DPH/EB.

3. Analysis of the DNA distribution of radiation-induced micronuclei

We have shown recently (Nüsse et al., 1992 b) that the DNA content of radiation-induced MN is influenced by several factors: 1. DNA distribution of the chromosomes, 2. DNA synthesis in MN during S-phase and 3. by the presence of acentric fragments and whole chromosomes in MN. These three factors were studies in detail to quantitatively understand the shape of the DNA distribution of radiation-induced MN measured by flow cytometry:

1. With cell lines of different origin (Chinese hamster cells, Syrian hamster cells, mouse NIH 3T3 cells) showing various DNA distributions of chromosomes the effect of the chromosome distributions on the shape of the MN distribution could be demonstrated and simulated by a random breakage model of chromosomes to calculate the DNA distribution of MN (Nüsse et al., 1992 b).

2. DNA synthesis in MN could directly be observed using anti-BrdUrd antibodies (Kramer et al., 1990). With synchronised cells, irradiated during G1-phase and analysed after the first and the second division, the effect of DNA synthesis on the shape of the radiation-induced MN could be demonstrated (Nüsse et al , 1992 b) In addition, image analysis was used to study DNA synthesis in MN of human lymphocytes. DNA content and area of nuclei and MN induced by ionising irradiation and the aneugen carbendazim were measured on Feulgen-stained cells sorted from the second G_1-phase and the second G_2-phase after treatment using a Magiscan (Applied Imaging) image analyser (van Hummelen et al., 1995). For sorting of these cells the BrdUrd/HOECHST/EB-quenching technique was used. The DNA content distribution of radiation-induced and carbendazim-induced MN in the various phases of the cell cycle revealed that MN increased their DNA content in phase with the cell cycle. The mean DNA content of MN in G_2-phase was by a factor of two larger than in G_1-phase cells. In addition, it could be shown that the mean DNA content of carbendazim-induced MN in G_1- or G_2-phase cells was by a factor of nearly two larger compared to radiation-induced MN. These effects could, however, not be observed clearly, when the area of MN was analysed alone. These results demonstrate also that by measurement of DNA content of MN using image analysis it is possible to discriminate between clastogenic and aneugenic action of agents only if the cell cycle stage is taken into account.

3 The chromosomal composition of MN induced by ionising radiation was studied in mouse 3T3 cells for a quantitative understanding of the DNA distribution of MN. Using a combination of centromere- and telomere-specific DNA probes and fluorescence in situ hybridisation (FISH) the frequency of radiation-induced MN in mouse NIH 3T3 cells (Miller et al., 1992) or of MN induced by the tear gas CS (2-chlorobenzylidene malonitrile) as an aneugen showing one or several fragments and one or several chromosomes was measured in fixed samples (Miller and Nüsse, 1993). Fig. 9 shows the results of these studies Using the data from Fig 9 we were able to simulate the DNA distribution of radiation- and CS-induced MN measured by flow cytometry using random breakage of chromosomes and random combination of fragments and whole chromosomes (Nüsse et al., 1992 b, Miller and Nüsse, 1993). Fig. 10 shows as an example a comparison of the measured and the calculated DNA distribution of radiation-induced MN.

For a further verification of our model, MN with different DNA contents were sorted on slides, fixed and hybridised to a murine centromere-specific gamma-satellite DNA probe. A clear correlation between DNA content of MN and number of centromere hybridisation signals was obtained. Fig. 11 shows a comparison of the measured and the calculated fraction of radiation-induced MN containing fragments only and of MN containing whole chromosomes as a function of their DNA content. It can be seen that most MN contain fragments, as expected,

and that with increasing DNA content the fraction of MN containing fragments decreases, whereas the fraction of MN containing whole chromosomes increases. Similar data were obtained for CS-induced MN, in contrary to radiation-induced MN, however, most CS-induced MN contained whole chromosomes (Miller and Nüsse, 1993).
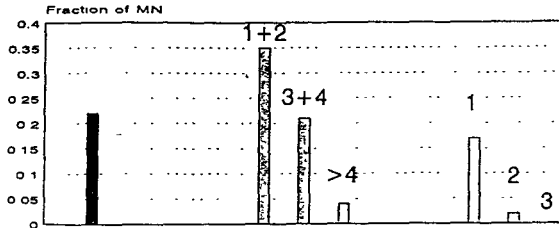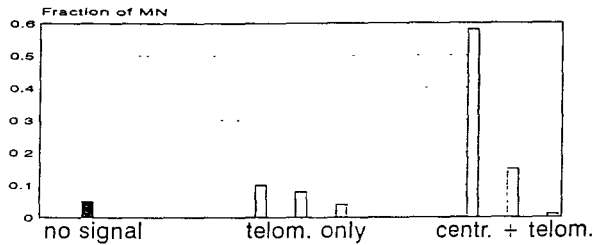
Fig. 9: Fraction of radiation- or CS-induced MN showing no hybridisation signals, telomeric signals only (representing 1, 2 or > 2 fragments per MN) and centromeric and telomeric signals simultaneously (representing 1, 2 or 3 chromosomes per MN)
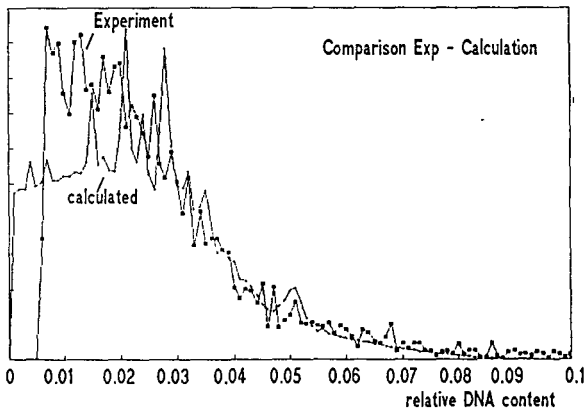
Fig. 10: Comparison between measured and simulated DNA distribution of radiation-induced MN in mouse NIH 3T3 cells. The simulated MN distribution was calculated using data from the FISH experiments shown in Fig. 9.
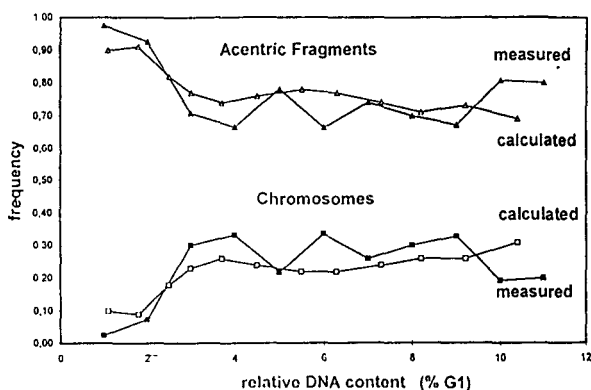
Fig. 11: Fraction of MN containing acentric fragments and whole chromosomes as a function of their DNA content. Sorted MN with different DNA contents were analysed with the FISH-technique using a centromeric DNA probe. Comparison of measured data with data obtained using the simulation model (Fig. 10).

4. Micronucleus induction in human cell lines with different radiation sensitivity

Flow cytometry was also used to analyse MN induction in several human cell lines obtained from patients with different syndromes: aniridia (JEOLI, normal karyotype), breast cancer (TEMAR, $21q^+$), ataxia telangiectasia (CV56, normal karyotype) and a chromosome instability syndrome (ANDMA, abnormal chromosome 8, 11, 21). (Slavotinek et al., 1995). Fig. 12 shows the MN frequency as a function of dose in these four cell lines. ANDMA was found to be the most radiation sensitive line, JEOLI the most resistant line. Similar results were obtained by microscopic scoring using the CB-technique (not shown).

We have also analysed sorted MN with chromosome-specific painting probes to study the nature of radiation-induced cytogenetic damage in various human cell lines including the radiation-sensitive AT cell line CV 56. Using painting probes for four different chromosomes (no. 1, 7, 11 and 14) it could be demonstrated that MN containing parts of chromosome no. 7 were underrepresented in all three cell lines studied as compared to the frequency expected on the basis of DNA proportionality (Slavotinek et al., submitted). If it is assumed that the chromosomal content of MN is an accurate reflection of the radiation-induced damage, then these results support a non-random model of radiation-induced cytogenetic damage for the chromosomes and cell lines studied so far.
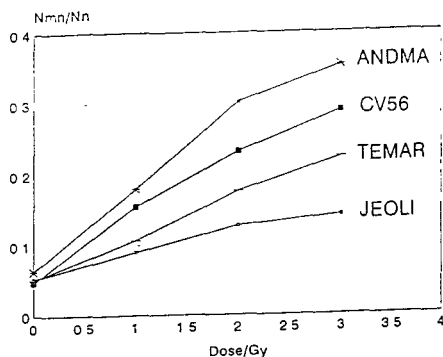
Fig. 12: MN frequency as a function of dose in four human cell lines with different radiation sensitivity.

List of publications:

van Hummelen, P., Nüsse, M., Castelain, Ph., Kirsch-Volders, M. (1995) Aneugen-induced micronuclei (MN) in human lymphocytes may be discerned using image analysis techniques when cell-cycle stage is taken into account. Environm. Molec. Mutagen. 25, 269-278.

Kramer, J., Schaich-Walch, G., Nüsse, M. (1990) DNA synthesis in radiation-induced MN studied by bromodeoxyuridine (BrdUrd) labelling and anti-BrdUrd antibodies. Mutagenesis 5, 491-495.

Miller, B.M., Werner, T., Weier, H.-U., Nüsse, M. (1992) Analysis of radiation-induced micronuclei by fluorescence in situ hybridisation (FISH) simultaneously using telomeric and centromeric DNA probes. Radiat. Res. 131, 177-185.

Miller, B.M., Nüsse, M. (1993) Analysis of micronuclei induced by 2-chlorobenzylidene malonitrile (CS) using fluorescence in situ hybridisation with telomeric and centromeric DNA probes, and flow cytometry. Mutagenesis 8, 35-41.

Nüsse, M., Recknagel, S., Beisker, W. (1992 a) Micronuclei induced by 2-chlorobenzylidene malonitrile contain single chromosomes as demonstrated by the combined use of flow cytometry and immunofluorescent staining with anti-kinetochore antibodies. Mutagenesis 7, 57-67.

Nüsse, M., Kramer, J., Miller, B.M. (1992 b) Factors influencing the DNA content of radiation-induced micronuclei. Int. J. Radiat. Res. 62, 587-602.

Schreiber, G.A., Beisker, W., Bauchinger, M., Nüsse, M. (1992 a) Multiparametric flow cytometric analysis of radiation-induced micronuclei in mammalian cell cultures. Cytometry 13, 90-102.

Schreiber, G.A., Beisker, W., Braselmann, H., Bauchinger, M., Bögl, K.W., Nüsse, M. (1992 b) Technical Report: An automated flow cytometric micronucleus assay for human lymphocytes. Int. J. Radiat. Biol 62, 695-709.

Slavotinek, A., Miller, E., Taylor, G.M , Nüsse, M., van Heyningen, V. (1995) Micronucleus frequencies in lymphoblastoid cell lines measured with the cytokinesis-block technique and flow cytometry. Mutagenesis, in press.

Slavotinek, A., Sauer-Nehls, S , Braselmann, H., Taylor, G.M., Nüsse, M. (1995) Chromosome painting of radiation-induced micronuclei. Submitted.

Viaggi, S., Braselmann, H., Nüsse, M. (1995) Flow cytometric analysis of micronuclei in the $CD2^-$-subpopulation of human lymphocytes enriched by magnetic separation. Int. J. Radiat. Biol. 67, 193-202.

Wessels, J.M., Nüsse, M. (1995) Flow cytometric detection of micronuclei by combined staining of DNA and membranes. Cytometry 19, 201-208.

Scoring of translocations using FISH

I. Summary of Project Global Objectives and Achievements

Analysis of radiation-induced symmetrical translocations by fluorescence in situ hybridisation (FISH, Pinkel et al. 1986) using painting DNA probes simultaneously with a pancentromeric α-satellite DNA probes for centromere detection was performed in metaphase preparations of human lymphocytes. After in vitro exposure of the cells, dose effect curves were established for X- and γ-rays using a cocktail of chromosome probes 1, 4 and 12. Further triple combinations of chromosome specific DNA probes (2, 7, 9; 3, 6, 10 and 8, 14, X) were used after irradiation with 3 Gy of 220 kV X-rays to examine whether a possible variability in the sensitivity of particular chromosomes or combinations to be involved in translocations and dicentrics exists. The data show that a DNA-proportional distribution of aberrations cannot be generally assumed. In reactor personnel and liquidators exposed at the Chernobyl accident FISH measurements of translocations were carried out for retrospective dose reconstruction using the generated calibration curve. Dose estimates obtained with FISH and conventional scoring (Qdr method) were found to be well in line. Serial examinations of exposed persons showed that translocation frequencies remained fairly constant for many years after exposure allowing the assessment of comparable doses at various sampling times. In case of a high contribution of clonal aberrations affecting target chromosomes to total translocation frequencies, an adequate correction has to be performed in order to obtain reliable estimates. A major objective of the present work was to provide reliable data from visual analysis of radiation-induced chromosome aberrations for a comparison and evaluation of results obtained with automated fluorescence microscope image processing systems and flow cytometry methods.

II. Objectives for the reporting period

- To establish a reliable and reproducible protocol for FISH/chromosome painting cocktail of chromosomes 1, 4 and 12) simultaneously with a pancentromeric probe.
- Analysis of the dose response relationship for translocations and generation of a calibration curve for translocations induced by γ-rays.
- Analysis of the DNA-proportional distribution of induced translocations and dicentrics in various triple combinations of painting probes.
- Retrospective dose estimation of subjects exposed at the Chernobyl accident.
- Analysis of the temporal behaviour of stable translocations.
- Comparative aberration measurements with automated fluorescence microscopy and flow cytometry.

III. Progress achieved

1. Analysis of dose-response relationship

In a first experiment with 220 kV X-rays a dose effect curve for symmetrical translocations based on about 17 000 cells (7 doses between 0 to 3.0 Gy) was generated (Schmid et al. 1992). Composite whole chromosome-specific DNA probes (painting probes) labelled with biotin were used for a combination of chromosomes 1, 4 and 12 (DNA content about 20% of the genome). Bound biotinylated probes were detected with streptavidin FITC conjugate. Propidium iodide was used as a counterstain.
Translocations could be efficiently detected by FISH. Their frequencies were 1.8-fold higher than the frequencies for dicentrics at a given dose. The dose-response curves for translocations and dicentrics were linear quadratic with a significant higher quadratic component for translocations (Table 1, Figure 1).
The finding of an excess of translocations compared to dicentrics rose the question whether in the FISH assay misscoring of dicentrics in favour of translocations is a sufficient explanation for the observed differences. It had to be further cleared up whether scoring of stable translocations in unstable cells can influence a FISH-based quantification of translocation data.

In a further experiment with 0 to 6.0 Gy of ^{137}Cs γ-rays (Bauchinger et al. 1993) translocations were measured by FISH with the biotin-labelled chromosome cocktail 1, 4, 12 (probe detection with streptavidin FITC conjugate) now simultaneously with a digoxigenin-labelled degenerate α-satellite pancentromeric DNA probe which was detected by sequential incubation with mouse anti-digoxigenin antibody, rat anti-mouse IgG and mouse anti-rat IgG, both labelled with AMCA according to Weier et al. (1991). Propidium iodide was used for counterstaining.
The background frequency of symmetrical translocations was 1.6×10^{-3} (11 411 cells from 11 individuals). Despite subtracting this value from induced frequencies at the various doses, similar as in the X-ray experiment, about 1.3 to 1.8-fold more translocations were found than dicentrics. Since the two-colour FISH provides a precise centromere detection in the painted chromosomes, the observation of higher translocation than dicentric frequencies cannot be explained by misscoring.
Again based on about 17 000 cells, a linear quadratic dose effect curve resulted for translocations. Similar to dose-response data obtained from conventional scoring of

dicentrics, γ-rays were less effective in producing translocations than X-rays (Table 1, Figure 1).

With increasing dose, the number of cells containing both, symmetrical and asymmetrical translocations in painted chromosomes is also increasing. In addition, dicentrics and acentrics are also present in the propidium iodide fluorescing part of the genome. As a consequence, a certain proportion of stable aberrations will be scored in unstable cells which have a selective disadvantage during cell proliferation. Whereas conventional dicentric scoring can be performed under cell cycle-controlled conditions, FISH analysis is not restricted exclusively to first division metaphases. This may influence the quantification of FISH-based translocation analyses. Using a pancentromeric probe, the analysed cells could be adequately classified into stable and unstable cells. Translocation frequencies determined only in stable cells were not found to be substantially different to total translocation frequencies, determined also in cells containing additional unstable chromosomal changes. Thus, for quantitative analyses, scoring of translocations must not be restricted to stable cells only.

2. Analysis of DNA-proportional distribution of aberrations

Triple combinations of painting probes usually cover about 12-22% of the total genomic DNA content. One specific objective of the project was to test whether a possible variability in the sensitivity of particular chromosomes and various combinations to be involved in translocations and dicentrics exists. Five triple chromosome combinations have been selected according to published results on the involvement of single chromosomes in radiation-induced or spontaneous breakage events obtained with banding. Although data on the breakpoint distribution per chromosome vary considerably, chromosomes 2,7,9 and 8,14,X were found to be over represented, whereas 3, 6 and 10 were found to be involved in fewer rearrangements.

Using chromosome specific DNA-probes 1,4,12; 2,7,9; 2,7,9$_{dig}$; 3,6,10$_{dig}$ and 8,14,X$_{dig}$, translocation and dicentric frequencies induced by 3 Gy of 220 kV X-rays were examined (Knehr et al. 1994). For unequivocal discrimination of translocations and dicentrics, a degenerate α-satellite pancentromeric DNA-probe, produced by in vitro amplification using a polymerase chain reaction (PCR) was used simultaneously with the painting probes. DNA of chromosome specific libraries of chromosomes 1-4, 6-9, 12 and 14 was biotinylated by nick-translation. Chromosome 9, 10 and X indicated by "dig" were labelled with digoxigenin, providing a chromosome-specific analysis even of morphologically similar target chromosomes by differential staining.

The analysis for DNA-proportional distribution of the observed aberration frequencies was performed using the formula of Lucas et al. (1992)

$$Y_i = 2.05 f_i (1-f_i) F_G \qquad (1)$$

relating the translocation or dicentric frequency Y_i measured by FISH for the i th combination to the respective genomic translocation frequency F_G (f_i is the labelled genomic fraction). The formula is based on the theoretical assumption that the participation of a chromosome in a symmetrical or asymmetrical translocation is proportional to its DNA content and that there is no preference for exchanges between particular chromosomes.

The χ^2-goodness-of-fit test was used to test the validity of a DNA-proportional distribution of the aberrations. An analysis of the total symmetrical translocations observed in the five chromosome combinations revealed a significant difference between the observed and predicted distribution. In Figure 2 the translocation and dicentric frequencies observed in the various chromosome combinations are plotted versus the DNA-content. In addition, the fit of equation (1) to these data is presented. The figure shows that the result can be attributed to the observed excess of translocations in the combination 8,14,X_{dig}. A similar analysis for the total dicentrics in the five combinations revealed, however, no significant differences.

An analysis with respect to single chromosomes revealed a significant difference between the observed and predicted distribution of symmetrical translocations. Figure 3 shows the observed and predicted (according to equation 1) frequencies of symmetrical translocations and dicentrics of the various chromosomes. The insufficient goodness of fit for equation (1) can be explained by the observation of a relative higher involvement of chromosomes with a lower DNA-content (X-14) in symmetrical translocations compared to the other chromosomes except chromosome 4 For chromosome 2 a remarkably lower translocation frequency than predicted from the DNA content by equation (1) became apparent.
There was also no indication for a DNA-proportional distribution of total dicentrics. Chromosomes 9,10,12 were considerably more frequently involved in dicentrics than predicted by equation (1) (Figure 3). The dicentric frequencies observed for these chromosomes were higher than that observed for all other chromosomes with a higher DNA content except for chromosome 3.
Although a 1:1 ratio of symmetrical translocations to dicentrics should be expected in theory, FISH-based measurements are contradictory irrespectively whether a centromeric labelling was used simultaneously or not. In our previous studies an excess of translocations was found after X-and γ-irradiation. In this study, an excess of symmetrical translocations was found for the combinations, 1,4,12; 2,7,9_{dig} and 8,14,X_{dig}. and for chromosomes 1,4,6,7,8 and X.
The observation of a lower frequency of symmetrical translocations than predicted in chromosome 2 and of an excess of dicentrics in chromosomes 9, 10 and 12 are not directly reflected in the results obtained for the combinations containing these chromosomes. Obviously excesses and deficits are balanced within most combinations. For the combination 8,14,X_{dig}, exhibiting an excess of symmetrical translocations, the observed deviation of the aberration frequency from a DNA-proportional distribution is significant and not consistent with the assumptions of equation (1). Thus the equation in its present form cannot be used to scale up to equal the full genome which is required to compare FISH measurements of translocations obtained with various randomly selected chromosome combinations. We therefore recommend further experiments, extending the present studies with selected chromosome combinations on different individuals. if similar deviations can be proved, it will be necessary to determine appropriate weighting factors which can be included in equation (1) or to use a contingency table analysis to take into account also the random process of rejoining.

3. Retrospective dose estimation

For retrospective dose estimation chromosome analyses were carried out in peripheral blood lymphocytes from 15 persons exposed to ionising radiation from the Chernobyl nuclear power plant (Salassidis et al. 1994). Nine subjects were

exposed as working personnel within or nearby the reactor immediately after the accident and three as members of teams of technicians participating in rescue and clean-up operations (so-called liquidators). For all, a history of acute radiation syndrome is reported. Blood samples were obtained between September 1991 and March 1992 on admission of the patients at the Department of Dermatology, University Clinic, Munich for symptoms of the delayed stage of the cutaneous radiation syndrome.

Biological dose estimates were determined, either by measuring the frequency of dicentric and ring chromosomes in first division unstable cells from conventional preparations (Qdr-method, Sasaki, 1983) or by measuring the frequency of stable translocations using FISH with painting probes for the chromosome combination 1, 4, 12 and a pancentromeric DNA probe. Qdr values are dose-dependent but independent of the time after exposure as well as of the inhomogeneity of the lymphocyte population and provided that a sufficient number of unstable cells is available allow a retrospective dose estimation. For a dose estimation based on translocation frequencies determined by chromosome painting, the γ-ray calibration curve described in section 1 was used.

Fig. 4 shows that with both methods comparable individual dose estimates between 1.1 to 5.8 Gy were obtained within acceptable confidence limits for the majority of investigated cases. Only in two cases (no. 7 and 9) significantly higher estimates were derived with Q_{dr} than by FISH. For three individuals (no. 5, 12, 15) consistently no elevated aberration frequencies were found with neither of the two methods. Unlike the other patients they were reportedly not been exposed during the accident, but as members of liquidation teams arriving at the accident site a few days later For comparative analysis with automated fluorescence microscopy slides with metaphase preparations from seven patients were distributed to MRC, Edinburgh.

4. Analysis of the persistence of stable translocations

Using the same FISH methodology as described in the previous sections, periodical follow-up measurements of translocations were carried out for the 12 highly irradiated cases demonstrated in section 3 (Salassidis et al. 1995). The results are demonstrated in Figure 5 which shows the frequencies of symmetrical translocations, detected by FISH for the chromosome combination 1,4,12, at different sampling times (I-VI) between September 1991 and July 1994. Applying a multivariate X^2-Poisson-homogeneity test for the complete data set excluding case no.1, it could be demonstrated that the observed variations of the translocation frequencies are not statistically significant (p>0.05, X^2=43.5, df=31). This is in accordance with the general assumption that symmetrical translocations represent fairly stable structural chromosomal rearrangements, which may persist even for decades after radiation exposure.

Since, however, the first chromosome analyses were performed not until about 5.5 years after the accident, one may ask whether these findings are representative for translocation frequencies present at the time of exposure. In our previous study we performed FISH measurements of translocations and conventional scoring of unstable chromosome aberrations using the time-independent Qdr method (Salassidis et al.1994). Since comparable dose estimates resulted from both methods for the majority of cases, we concluded that translocation frequencies actually reflect the initial chromosome damage. Beyond this, data from the present follow-up study provide evidence for a further persistence of symmetrical translocations allowing the estimation of similar doses at various times distant from

exposure. Case no.1 is considered as exceptional since the translocation frequencies observed at the two sampling times differ more than two-fold (difference test, p<0,0002). Whether the lower translocation frequency reflects a true decline cannot be decided, since unfortunately the patient could be examined only twice.

The present data show also that chromosome painting by FISH can be also efficiently used to study the occurrence of clonal symmetrical translocations. During follow-up examinations of patient no.9, a consistent derivative chromosome 1, der(1), was noted as the single abnormality in 5.5 to 9% of the cells analysed. Obviously a D-group chromosome (no. 13, 14 or 15) was involved in this particular structural rearrangement. Due to its high contribution to the total translocation frequency (between 16.5 and 23.5%), a clonal origin was postulated. For a precise characterisation of the potential clone, slides which had been first hybridised with the chromosome cocktail 1, 4 and 12, were processed for a second hybridization with either of the combinations 1,13, 1,14 or 1,15. After relocation of the registered cells containing the der(1), a complete reciprocal symmetrical translocation t(1q;13q) was identified. A G-banding analysis in 30 randomly selected metaphases eventually revealed the breakpoints 1q25 and 13q14.

The observed clone may be the result of an outgrowth of a particular lymphocyte population, which occurred already prior to the beginning of our measurements. During the observation time the fraction of clonal cells showed only insignificant variations (Poisson homogeneity-test, $x^2=3.63$, df=4, p>0.05) indicating that no further clonal expansion occurred.

For a reliable dose estimation, the contribution of such clonal aberrations to the total frequency of translocations has to be taken into account. The frequencies of total symmetrical translocations, measured at five examinations during two years of observation, ranged from 0.33-0.39 (F_p-value). These correspond to whole body equivalent dose estimates between 4.3 and 4.6 Gy obtained from our ^{137}Cs γ-ray calibration curve (Bauchinger et al. 1993). After correction for the contribution of the clone to the total translocation frequencies, F_p^*-values ranged from 0.28-0.34 corresponding to dose estimates between 3.9 and 4.3 Gy.

A correction for the contribution of clonal translocations to the total translocation frequency F_p is mandatory if F_p is about three standard deviations higher than F_p^*.

Due to the well-known fact that clonal chromosome abnormalities play an important role in the development and progression of malignant neoplasms, translocation analysis by chromosome painting may be also useful for an early detection of such stable chromosomal changes. As shown here, it may be used to screen for particularly affected chromosomes the specific breakpoints of which can be subsequently determined by banding analysis.

5. References

Lucas, J.N., A. Awa, T. Straume, M. Poggensee, Y. Kodama, M. Nakano, K. Ohtaki, H.U. Weier, D. Pinkel, J. Gray and G. Littlefield (1992) Rapid translocation frequency analysis in human decades after exposure to ionizing radiation, Int. J. Radiat. Biol., 62, 53-63.

Pinkel, D., T. Straume and J.W. Gray (1986) Cytogenetic analysis using quantitative, high-sensitivity, fluorescence hybridization. Proc. Natl. Acad. Sci. (USA), 83, 2934-2938.

Sasaki, M.S. (1983) Use of lymphocyte chromosome aberrations in biological dosimetry: Possibilities and limitations, in: T. Ishihara and M.S. Sasaki (Eds.) Radiation-induced chromosome damage in man, Alan R. Liss, New York, 585-604.

Weier, H.-U.G., Lucas, j.N., Poggensee, M. Segraves, R., Pinkel, D. and Gray, J.W., 1991, Two-color hybridization with high complexity chromosome-specific probes and a degenerate alpha-satellite probe DNA allows unambiguous discrimination between syymetrical and asymmetrical translocations. Chromosomea 100, 371-376.

6. List of publications

Schmid, E., H. Zitzelsberger, H. Braselmann, J.W. Gray and M. Bauchinger (1992) Radiation-induced chromosome aberrations analysed by fluorescence in situ hybridization with a triple combination of composite whole chromosome-specific DNA probes. Int. J. Radiat. Biol., 62, 673-678.

Bauchinger, M., E. Schmid, H. Zitzelsberger, H. Braselmann and U. Nahrstedt (1993) Radiation induced chromosome aberrations analysed by two-colour fluorescence in situ hybridization with composite whole chromosome-specific DNA probes and a pancentromeric DNA probe. Int. J. Radiat. Biol., 62, 673-678.

Knehr, S., H. Zitzelsberger, H. Braselmann and M. Bauchinger (1994) Analysis for DNA-proportional distribution of radiation-induced chromosome aberrations in various triple combinations of human chromosomes using fluorescence in situ hybridization, Int. J. Radiat. Biol. Int. J. Radiat. Biol. 65, 683-690.

Salassidis, K. ,E. Schmid, R.U. Peter, H. Braselmann and M. Bauchinger (1995) Dicentric and translocation analysis for retrospective dose estimation in humans exposed to ionising radiation during the Chernobyl nuclear power plant accident. Mutation Res. 311, 39-48.

Salassidis, K., V. Georgiadou-Schumacher, H. Braselmann, P. Müller, R.U. Peter and M. Bauchinger (1995) Chromosome painting in highly irradiated Chernobyl victims: a follow-up study to evaluate the stability of symmetrical translocations and the influence of clonal aberrations for retrospective dose estimation. Int. J. Radiat. Biol., in press.

Table 1: Curve fitting using the linear quadratic model $Y = c + \alpha D + \beta D^2$ for frequencies of translocations and dicentrics in chromosomes 1, 4 and 12

Radiation quality	Aberration type	$c \pm SE$ $\times 10^{-4}$	$\alpha \pm SE$ $\times 10^{-1} Gy^{-1}$	$\beta \pm SE$ $\times 10^{-2} Gy^{-2}$
137-Cs γ	translocation	17 0 $\pm$ 3.5	0.059 $\pm$ 0.043	1.67 $\pm$ 0.13
137-Cs γ	dicentric	0.9 $\pm$ 0 0	0.038 $\pm$ 0 021	1 32 $\pm$ 0.09
220 kV X-rays	translocation	22 6 $\pm$ 5.3	0.094 $\pm$ 0.047	2.86 $\pm$ 0 30
220 kV X-rays	dicentric	-	0.103 $\pm$ 0.029	1.24 $\pm$ 0 21
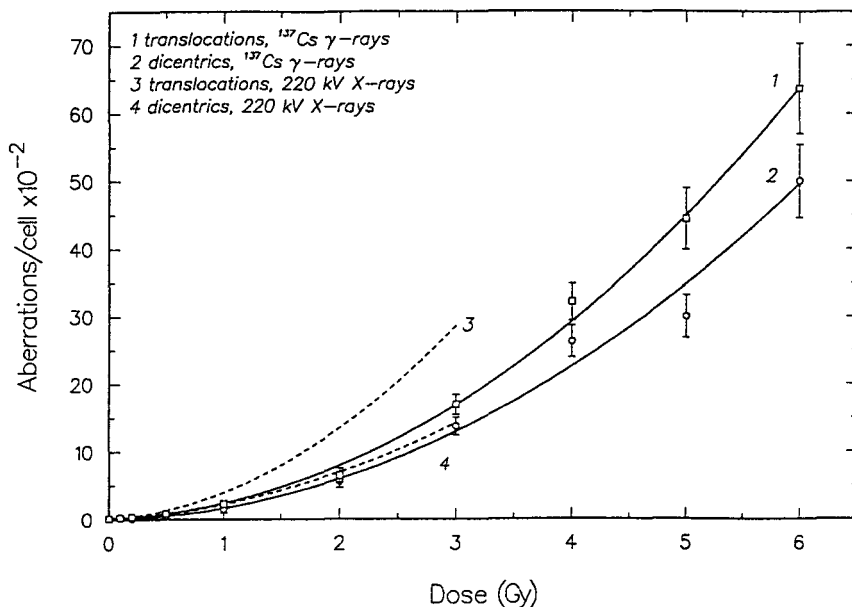
Figure 1: Dose-response curves for translocations and dicentrics involving painted chromosomes 1, 4 and 12 Data for curves 1 and 2 were obtained by simultaneous use of a pancentromeric DNA probe
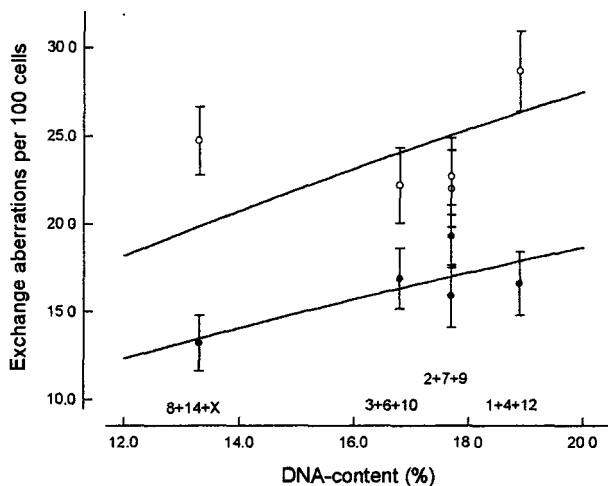
Figure 2: Frequencies of symmetrical translocations (°) and dicentrics (•) in various chromosome combinations measured by FISH versus DNA content. The curve represents the fit of equation (1) to the measurements. Error bars show the standard deviations of the means.
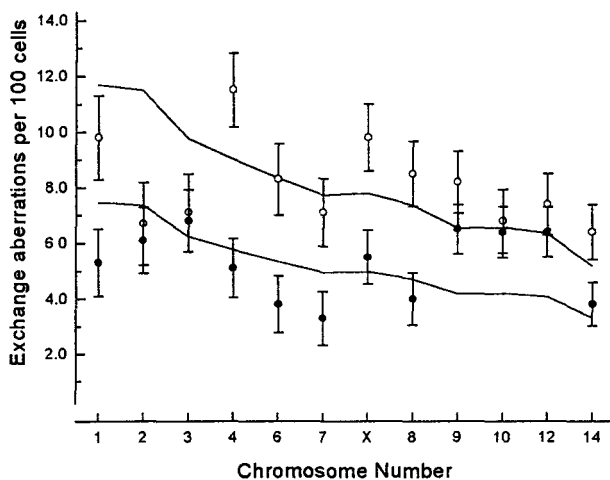
Figure 3: Frequencies of observed and predicted (according to equation (1)) symmetrical translocations (°) and dicentrics (•) measured by FISH. Predicted values are connected by straight lines. Error bars show standard deviation.
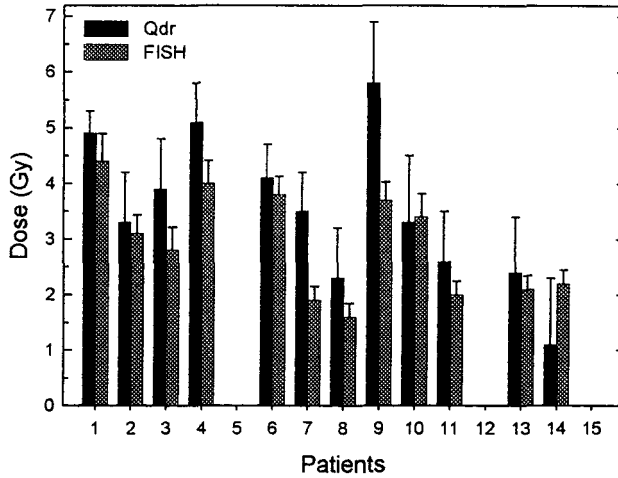
Figure 4: Individual dose estimates obtained from conventional chromosome analysis (Qdr method) and translocation scoring (FISH). Error bars represent the upper part of 90% confidence intervals.
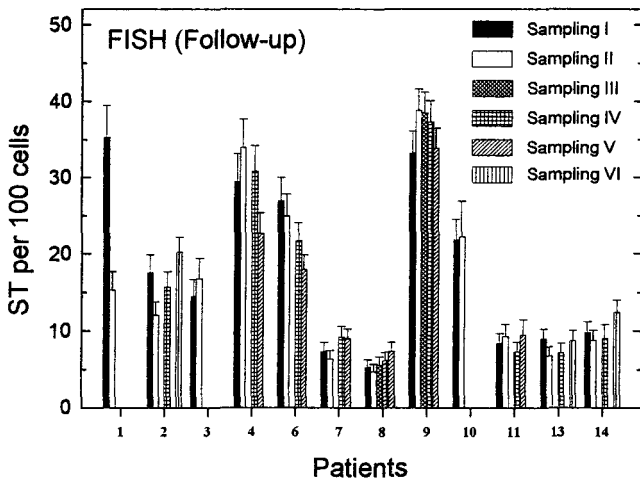
Figure 5: Follow-up measurements of symmetrical translocations (ST), carried out biannually (I-VI) between September 1991 and July 1994, in 12 highly irradiated Chernobyl victims. Symmetrical translocations were dected by FISH with the chromosome combination 1, 4 and 12 and a pancentromeric α-satellite DNA probe.

Head of project 4: Dr. Green
II Objectives for the reporting period

1. To design, build and assemble a semi-automatic system for the analysis of radiation induced damage to human chromosomes following fluorescence *in situ* hybridisation with chromosome paints.
2. To assemble a user-friendly software package for reviewing results.
3. To establish a large data base of chromosome aberration data containing manual and automatic scoring results which could be used to measure the performance of the automatic system.
4. To use this data to generate a calibration curve covering the range of 0-2.0 Gy exposure to X-irradiation.
5. To test the system with slides from individuals exposed at the Chernobyl accident, whose exposed dose had been estimated at GSF.

III Progress achieved including publications

During the period of the grant a semi-automatic system, capable of detecting abnormal cells, together with a review package, was brought into use. A large data base of 9000 cells was used to measure the performance, and X-ray calibration curves using several different parameters were established.This work was presented at several conferences and has been accepted for publication. A preprint is enclosed. Finally we collaborated with Prof. Bauchinger at GSF, Munich to test the system on a series of slides from Chernobyl workers.

Publications
FANTES, J.A, GREEN, D.K., HILL, W., STARK, M.H., GORDON, J.M. and PIPER, J. 1995, Application of automation to the detection of radiation damage using FISH technology. Int. J. Radiat. Biol. (In press)

Introduction
The feasibility of highlighting chromosome translocations using fluorescence *in situ* hybridisation (FISH) of whole chromosome painting probes has been established in several laboratories (Pinkel *et al.* 1988, Cremer *et al.* 1990). Extending this approach to scoring radiation damage in peripheral blood lymphocytes has been validated in several recent publications (Natarajan *et al.* 1992, Gray *et al.* 1992, Lucas *et al.* 1992, Schmid *et al.* 1992, Tucker *et al*, 1993).Stable reciprocal translocations, which are difficult to score even in banded preparations can be scored with ease. However only a fraction of the damaged chromosomes is detected, depending on how much of the genome is painted. The proportion of the total amount of damage detected is $2.05p(1-p)$, from the relation derived by Lucas *et al* (1992), where p is the proportion of DNA painted. If chromosomes 1 and 2 are both painted p is 0.18 and 27% of the damage can be detected. Thus in order to obtain a particular standard error on the total estimated frequency of abnormal metaphases or aberrations, correspondingly more metaphases must be analysed than would be required had all the damage been visible. Although analysis of painted metaphases can be extremely fast (Pipet *et al.* 1994) we aimed to increase further the speed of analysis by presenting the cytogeneticist with an enriched set of metaphases believed to be abnormal, an approach used previously for detection of dicentric chromosomes (Bayley *et al.* 1991).

METHODS

Slide Preparation

Peripheral blood lymphocytes from a healthy 42 year old male were irradiated with doses of 0.5, 1.0 and 2.0 Gy of 250kVp X-rays. Unexposed blood was used as a control. Short term blood cultures were set up for 48 hours, with the colcemid added for the final 1-3 hours. Standard methods were used to prepare slides, and these were hybridised with paints directly labelled with SpectrumOrange (Vysis) for chromosomes 1 and 2. Most hybridisations also included a probe for the heterochromatic region of chromosome 1 which was directly labelled with Spectrum Orange by nick translation. The slides were counterstained with DAPI.

Hardware System

The basic components were a Metasystems motorized fluorescence microscope, a Xillix Technologies Microimager-1400 CCD camera and a Sun Microsystems Unix workstation.

Analysis Procedure

This has been divided into four steps
- automatic metaphase finding
- automatic high resolution image capture
- automatic analysis for abnormal cells
- manual review

A small amount of manual interaction was required to load stage with slides, check focus, switch objectives and to centre and focus the first metaphase for high resolution capture.

Automatic Metaphase Finding

Metaphases were located with a x10, 0.5 NA objective using the DAPI counterstain. Focus and exposure time were determined automatically during the scan. Digitised fields were scanned for clusters of small above threshold image components, and a simple classifier was used to determine if the cluster was a metaphase (Piper *et al.* 1994). Finally the location of the cluster was filed. A slide could be scanned in ~20 minutes.

High resolution digitisation of metaphases

All the located metaphases were digitised using a x63 1.40 NA objective, together with the appropriate Leitz epi-illumination filter blocks and emission filters in front of the camera. Once the first metaphase was found manually and focused, cell recall, focus, exposure time and block and filter changes were all under automatic control. Pixel shift, which normally occurs when capturing images using different filter blocks, was calibrated during the manual set up and remained stable. Both DAPI and SpectrumOrange images were digitised. The DAPI image was thresholded to separate chromosomes from background, below background material was discarded, and this DAPI mask was applied to the Spectrum Orange image before both images were filed. High resolution digitisation took ~1 minute per cell.

Manual Scoring

In the original study to establish a data base and a calibration curve, every digitised cell was scored by a cytogeneticist using a system designed with a Motif

(OSF/MOTIF) Graphical User Interface which runs on any Sun SPARC station 10. The main design criteria were that it should be simple and fast and have a high resolution screen with clear display windows to enable the cytogeneticist to make a rapid decision on each metaphase. Digitised cells were read from the file and the SpectrumOrange paint and DAPI counterstain displayed in two windows. The cytogeneticist classified the cell as normal, abnormal or reject; a cell was classified as abnormal if it contained chromosome aberrations (dicentrics, translocations, insertions, inversions, fragments) involving painted chromosomes. Further facilities included merging paint and DAPI images, changing the colour look up table, zoom an printing. Any difficult cells could be recalled for analysis on the microscope. At low doses cells could be scored at ~300 metaphases an hour; this dropped to ~200 metaphases an hour when scoring images enriched for abnormal cells.

Automatic analysis for abnormal cells
In a normal metaphase painting of chromosomes 1 and 2 will result in 4 painted image components with a size distribution determined by the chromosome relative sizes. If any of the most common radiation aberrations (translocation, dicentric + fragment) involving a painted chromosome occurs, the result will be bi-colour chromosomes, an increase in the number of painted components and/or a change in the size distribution of the expected number of painted components. Automatic analysis was aimed at detecting the number and size distribution of painted chromosome components as this was more likely to lead to a reliable system than searching for bi-coloured chromosomes.
The strategy used for automatic analysis involved an initial automatic segmentation of the thresholded DAPI image to identify chromosomes. Spectrum Orange painted areas within the DAPI mask were then identified; weakly painted chromosomes tended to produce fragmented images and these were forced to merge if they might plausibly belong to the same chromosome. The number of painted objects was counted, and the area of each compared to the total chromosomal material. A cell was scored as abnormal if the count of painted objects was greater than 4, or if there was a clear imbalance in component sizes. The criteria for rejecting a cell were similar to those used by a cytogeneticist (incomplete or multiple cells, poor hybridisation, stain debris, prophase chromosomes). There were additional reasons for rejecting a cell for machine analysis such as difficulty in segmentation or poor thresholding.
Automatic analysis typically takes less than a minute per cell.

RESULTS AND DISCUSSION
The data set
A total of 9000 composite threshold images were collected and stored on disc. All of these cells were scored blind by a cytogeneticist as normal, abnormal or reject. The actual type and number of aberrations within each abnormal cell was also recorded. Data was collected at 1.0 and 2.0 Gy until 60 abnormal metaphases had been scored. At 0 and 0.5 Gy data from at least 2000 analysable metaphases was accumulated.
All of these images were also scored by the automatic analysis program as normal, abnormal or reject.

Manual analysis

The percentage of abnormal cells at each dose found by visual analysis of the digitised images (and occasional confirmation with the microscope) is shown in Figure 1.

A complete breakdown of aberrations found is shown in Table 1. The background frequency of symmetrical translocations is 5 times than that of dicentrics, slightly lower than that reported by Bauchinger (1993), though this may well depend on the age and medical history of the donor. The overall ratio of symmetrical translocations to dicentrics, after correcting for background, is 1.88:1. This agrees with the results of other studies using manual scoring techniques (Schmid *et al.* 1992, Bauchinger *et al.* 1993, Knehr *et al.* 1994), including those where pancentromeric probes were used to enhance the recognition of dicentric chromosomes.

Automatic analysis

The correlation between the automatic and manual scores at each radiation dose is shown in Table 2. From this table it can be calculated that the automatic analysis system on average classified 60, 59 and 73% of the normal, abnormal and rejected images correctly.

Clearly the automatic analysis strategy produced a relatively high number of false positives, often a result of paint debris or artefacts, or the incorrect inclusion of nuclei as chromosomes. It has been assumed that the abnormal images detected by the automatic scoring system would be reviewed by a skilled cytogeneticist and categorised as normal, abnormal or reject. Had this been the case in these experiments, the abnormal count at each radiation dose would be the true number of abnormals following review. In fact in this data set all images were visually scored. Those images deemed normal or reject in the review process were added to the respective totals of normal or rejected cells. The final results are the scores shown in Table 3.

Visual review after automatic analysis

Files of several hundred images scored as abnormal by the automatic analysis program were reviewed independently by two cytogeneticists. A 90% correspondence between scores was recorded; this is comparable to that recorded in a similar experiment scoring absorption stained metaphases for dicentric chromosomes (Bayley *et al.* 1991).

Dose calibration

Calibration points were generated both from the manual analysis and automatic analysis scores from Table 3. Both are shown graphically in Figure 1. These curves could be used for dose estimates of recent exposure to ionising radiation.

Figure 1 Calibration curve for manual scoring of data (upper line) and automatic analysis
followed by visual review (lower line).
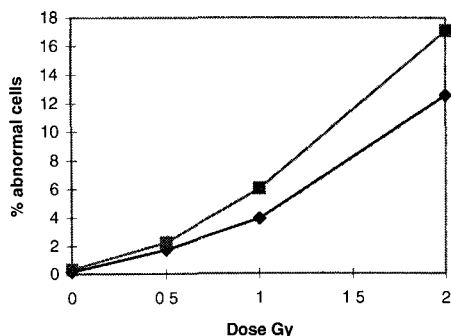
Image processing performance

As a detailed description of each abnormal cell was recorded during the manual
scoring, it was possible to determine those abnormalities which the automatic
approach could detect (for example an increase in the number of painted objects)
and those which cause neither a change in the number of painted objects (for
example the loss of a painted fragment) nor any asymmetry in painted area
distribution. Table 4 shows how 140 abnormal cells (scored as abnormal both by
manual and automatic analysis) were distributed in terms of expected and actual
automatic classification. Three out of every four abnormal metaphases which were
expected to be classified abnormal were detected. Those not expected to be
classified abnormal were equally distributed between normal and abnormal.

Timing and enrichment

Following automatic analysis the abnormal cells presented for review are on average
enriched three-fold in abnormal cells. Automatic metaphase finding greatly increases
the throughput of cells (Piper *et al.* 1994) and rapid scoring of abnomal cells is
obviously possible using the visual review system described here. The results at 1.0
Gy clearly illustrate this. At 1.0 Gy, manual analysis of 1000 cells painted with
chromosomes 1 and 2 would yield ~60 abnormal metaphase cells where breaks in
the painted chromosomes had occurred. This would take 5 hours of analysis, at a
typical rate of 200 cells/hour. Using the automatic system, more cells must be
analysed as only 65% of captured images are analysable and the false negative rate
is 40%. 2500 cells must be found and captured to ensure that 60 cells are presented
for review. These cells would be distributed amongst an enriched set of 400
metaphases which would require 1.3 hours of review at a rate of 300 cells/hour.
Table 5 shows similar calculations for all the doses considered here and clearly
demonstrates the speed advantage achieved at low doses.

Chernobyl cases

Through the CEC Radiation Protection Programme we had access to slides
prepared from peripheral blood cultures of individuals exposed to ionising radiation
after the Chernobyl nuclear accident in 1986. Dose estimates had been made
previously at GSF using paints for chromosomes 1,4 and 12, together with a
degenerate α-satellite pancentromeric probe, from a calibration curve for stable

translocations induced by ^{137}Cs γ-rays. The proportion (p) of the diploid DNA content painted by this combination of chromosomes paints is 0.193.

At MRC HGU the slides were painted with chromosomes 1 and 2 (p is 0.18), and without any prior knowledge of dose, put through the automatic analysis procedure. Slides were scanned for metaphases, these were digitised and the images analysed automatically for abnormal cells. Any abnormal cells were visually reviewed as described above, and the type and number of aberrations noted.

Problems arose both in metaphase finding and automatic analysis. Metaphases on the GSF slides were more compact than those on MRC slides and were initially missed by the metaphase finder. Adjustments were made and more metaphases were found. However these were then rejected by the automatic analysis program as segmentation of tight clusters of chromosomes was often difficult. In some cases the total number of abnormal and normal cells analysed was small, despite scanning four or five slides.

The MRC calibration curve was based on the % of abnormal cells, 48 hours after exposure to 0.5, 1.0 and 2.0 Gy of 250kVp X-rays. However the abnormal cells contained unstable aberrations (dicentrics) as well as stable aberrations (translocations), and so this was not a valid dose response curve to use for dose estimates 8 years after exposure to ionising radiation. Data on the number of translocations found in the abnormal cells was available and a new dose response curve was fitted. This was corrected for use with γ-radiation from data in Bauchinger *et al* (1993), as γ-rays have a lower RBE. Dose estimates of the Chernobyl cases were made from the frequency of translocations after visual review; these data are shown in Table 6 together with dose estimates from GSF; 95% limits are shown for both estimates. Details of the statistical analysis can be found in Silva et al. (1994). There are four potential sources of error in the data which arise from

1. the small number of cells scored for each individual case
2. random variation in the calibration curve
3. inaccuracy in the figure used in conversion to a γ-radiation calibration curve
4. lack of data above 2 Gy.

In 5 of the 8 cases where both dose estimates were available our estimates were higher than those of GSF, in two cases they were lower, and in 1 case they were equal. However in the 5 cases where 95% confidence intervals were also available, the intervals overlapped.

CONCLUDING REMARKS

We have demonstrated the potential of an automated system for analysis of radiation damage to human chromosomes following *in situ* hybridisation with whole chromosome painting probes. Further improvements in performance were envisaged but with the end of the grant, the retiral of Dr. D.K. Green and Dr.J. Piper leaving MRC HGU these could not be implemented. Although the system was originally designed to be used for detection of abnormal cells at low exposures, results from the Chernobyl slides were promising, but there were several discrepancies in the dose estimates. More accurate dose estimates would result from the availability of a calibration curve from γ-irradiated cells extending above 2 Gy, and more cells being scored from each case.

REFERENCES

BAUCHINGER, M., SCHMID, E., ZITZELBERGER, H., BRASELMAN, H. and NAHRSTEDT, U., 1993, Radiation-induced chromosome aberrations analysed by two-colour fluorescence

in situ hybridisation with composite whole-chromosome specific DNA probes and a pancentromeric DNA probe. Int. J. Radiat. Biol., 64, 179-184.

BAYLEY, R., CAROTHERS, A., CHEN, X., FARROW, S., GORDON, J., JI, L., PIPER, J., RUTOWITZ, D., STARK, M. and WALD, N., 1991, Radiation dosimetry by automatic image analysis of dicentric chromosomes. Mutat. Res., 253, 223-235.

CREMER, T., POPP, S., EMMERICH, P., LICHTER, P. and CREMER, C., 1990, Rapid metaphase and interphase detection of radiation-induced chromosome aberrations inhuman lymphocytes by chromosomal suppression *in situ* hybridization. Cytometry, 11, 110-118.

GRAY, J.W., LUCAS, J.N., PINKEL, D. and AWA, A., 1992, Structural chromosome analysis by whole chromosome painting for assessment of radiation-induced genetic damage. J. Radiat. Res., 33, 80-86.

KNEHR, S., ZITZELBERGER, H., BRASELMAN, H. and BAUCHINGER, M., 1994, Analysis for DNA-proportional distribution of radiation-induced chromosome aberrations in various triple combinations of human chromosomes using fluorescence *in situ* hybridization. Int. J. Radiat. Biol., 65, 683-690.

LUCAS, J. N., AWA, A., STRAUME, T., POGGENSEE, M., KODAMA, Y., NAKANO, M., OHTAKI, K., WEIER, H.-U., PINKEL, D., GRAY, J. and LITTLEFIELD, G. 1992, Rapid translocation frequency analysis in humans decades after exposure to ionising radiation. Int. J. Radiat. Biol., 62, 53-63.

NATARAJAN, A.T., VYAS, R.C., DARROUDI, F., and VERMEULEN, S., 1992, Frequency of X-ray induced chromosome translocations in human peripheral lymphocytes as detected by *in situ* hybridization using chromosome specific DNA libraries. Int. J. Radiat. Biol., 61, 199-203.

PINKEL, D., LANDEGENT, J., COLLINS, C., FUSCOE, J., SEGRAVES, R., LUCAS, J. and GRAY, J., 1988, Fluorescence *in situ* hybridization with human chromosome specific libraries: Detection of trisomy 21 and translocations of chromosome 4. P.N.A.S. USA, 85,9138-9142.

PIPER, J., POGGENSEE, M., HILL, W., JENSEN, R., JI, L., POOLE, I., STARK, M. and SUDAR, D., 1994, An automatic fluorescence metaphase finder speeds translocation scoring in FISH painted chromosomes. Cytometry, 16, 7-16.

SCHMID, E., ZITZELBERGER, H., BRASELMAN, H., GRAY, J.W., and BAUCHINGER, M., 1992, Radiation-induced chromosome aberrations analysed by *in situ* hybridisation with a triple combination of composite whole chromosome-specific DNA probes. Int. J. Radiat. Biol. 62, 673-678.

SILVA, M.J., CAROTHERS, A., DIAS, A., LUIS, J.H., PIPER, J. and BOAVIDA, M.G., 1994, Dose dependence of radiation-induced micronuclei in cytokinesis-blocked human lymphocytes. Mutat. Res. 322,117-128.

TUCKER, J.D., RAMSEY, M.J., LEE, D.A. and MINKLER, J.L., 1993, Validation of chromosome painting as a biodosimeter in human peripheral lymphocytes following acute exposure to ionising radiation *in vitro*. Int. J. Radiat. Biol. 64, 27-37.

Table 1 Chromosome aberrations identified by FISH in chromosomes 1 and 2 following manual analysis of visually acceptable metaphase images.

| | | | | | No aberrations per 100 cells | | | | |
| | | | | | ST | | | | |
Dose Gy	No cells	Ace	Dic	CR	C	IC	Inv	Ins	Total trans
0	2454	0.04	0.04	0	0.12	0.08	0.04	0	0.24
0.5	2180	0.37	0.60	0.09	0.60	0.60	0.05	0	1.24
1.0	998	1.10	1.61	0.40	2.30	1.10	0	0.10	3.51
2.0	392	3.06	6.12	1.28	8.93	2.81	0.26	0.26	12.24

Ace, acentric; Dic, dicentric; CR, centric ring; ST, symmetrical translocation; C, complete; IC, incomplete; Inv, inversion; Ins, insertion; trans, translocation

Table 2 Confusion matrices of manual versus automatic counts of normal, abnormal and rejected cells following *in vitro* radiation doses of 0, 0.5, 1.0 and 2.0 Gy. Columns give the manual analysis counts and rows give the automatic analysis counts. Bold figures show true correspondence between the two sets.

		Normal	Abnormal	Reject	Total
(a)	0 Gy				
	Normal	**1451**	4	326	1781
	Abnormal	368	**3**	163	534
	Reject	594	0	**1087**	1681
	Total	2413	7	1576	3996
(b)	0.5 Gy				
	Normal	**1239**	6	146	1391
	Abnormal	249	**29**	99	377
	Reject	529	12	**858**	1399
	Total	2017	47	1103	3167
(c)	1.0 Gy				
	Normal	**549**	12	100	661
	Abnormal	125	**32**	43	200
	Reject	251	14	**372**	637
	Total	925	58	515	1498
(d)	2.0 Gy				
	Normal	**179**	16	21	216
	Abnormal	48	**38**	16	102
	Reject	90	11	**122**	223
	Total	317	65	159	541

Table 3 shows the results after automatic analysis followed by hypothetical manual review, of all images scored as abnormal by the system. The final number of normal cells was the sum of those images scored as normal by the automatic analysis program and images judged to be normal following visual review.

Dose Gy	No normal cells	No abnormal cells	% abnormal cells	No reject cells
0	2143	3	0.14	1838
0.5	1640	29	1.73	1496
1.0	786	32	3.91	680
2.0	264	38	12.58	239

Table 4 Classification of 140 abnormal metaphase images by automatic analysis. The expected classification was based entirely on the criteria of additional painted areas or gross asymmetry of the distribution of painted areas.

Actual automatic classification	Expected automatic classification	
	Abnormal	Normal
Abnormal	**91**	11
Normal	26	**12**

Table 5 The number of metaphase cells that must be found and analysed, both manually and automatically to ensure that at least 60 abnormal cells involving aberrations of chromosomes 1 and 2 are visually reviewed by a cytogeneticist. The number of cells required for manual analysis using a fluorescence microscope alone is shown in the first column for each dose. The equivalent number of cells required to be captured and analysed automatically is shown in the second column, and the resulting number of cells to be reviewed shown in the third column. The estimated time spent by a reviewing cytogeneticist is shown in parenthesis in hours against the cell numbers.

Dose Gy	Manual analysis	Automatic analysis	
		Captured	Reviewed
0.5	3000 (15)	7500	1200 (4.0)
1.0	1000 (5.0)	2500	400 (1.3)
2.0	300 (1.5)	750	120 (0.4)

Table 6. Data from Chernobyl cases. The second column shows the total of abnormal and normal cells after automatic analysis and visual review; the third column contains the number of translocations in those cells scored as abnormal after visual review. Estimated doses from MRC calibration curve and GSF in final two columns.

Case	No abnormal + normal cells	No translocations	Estimated dose Gy (95%limits)	Estimated dose Gy (95%CI)
3297	103	8	2.7 (1.6-3.8)	1.6 (1.1-2.3)
3417	231	25	3.2 (2.5-4.0)	2.5 (2.0-3.0)
3418	129	14	3.3 (2.3-4.2)	2.8 (2.4-3.2)
3419	271	37	3.7 (3.0-4.3)	4.4 (3.9-4.9)
3455	87	1	0.9 (0.0-2.0)	0
3468	48	2	1.9 (0.3-3.5)	1.9 (1.4-2.4)
3469	90	12	3.6 (2.5-4.8)	2.1 (1.6-2.7)
3638	185	7	1.8 (1.0-2.6)	2.1
3713	178	17	3.0 (2.2 -3.8)	
3714	78	4	2.1 (0.9-3.4)	
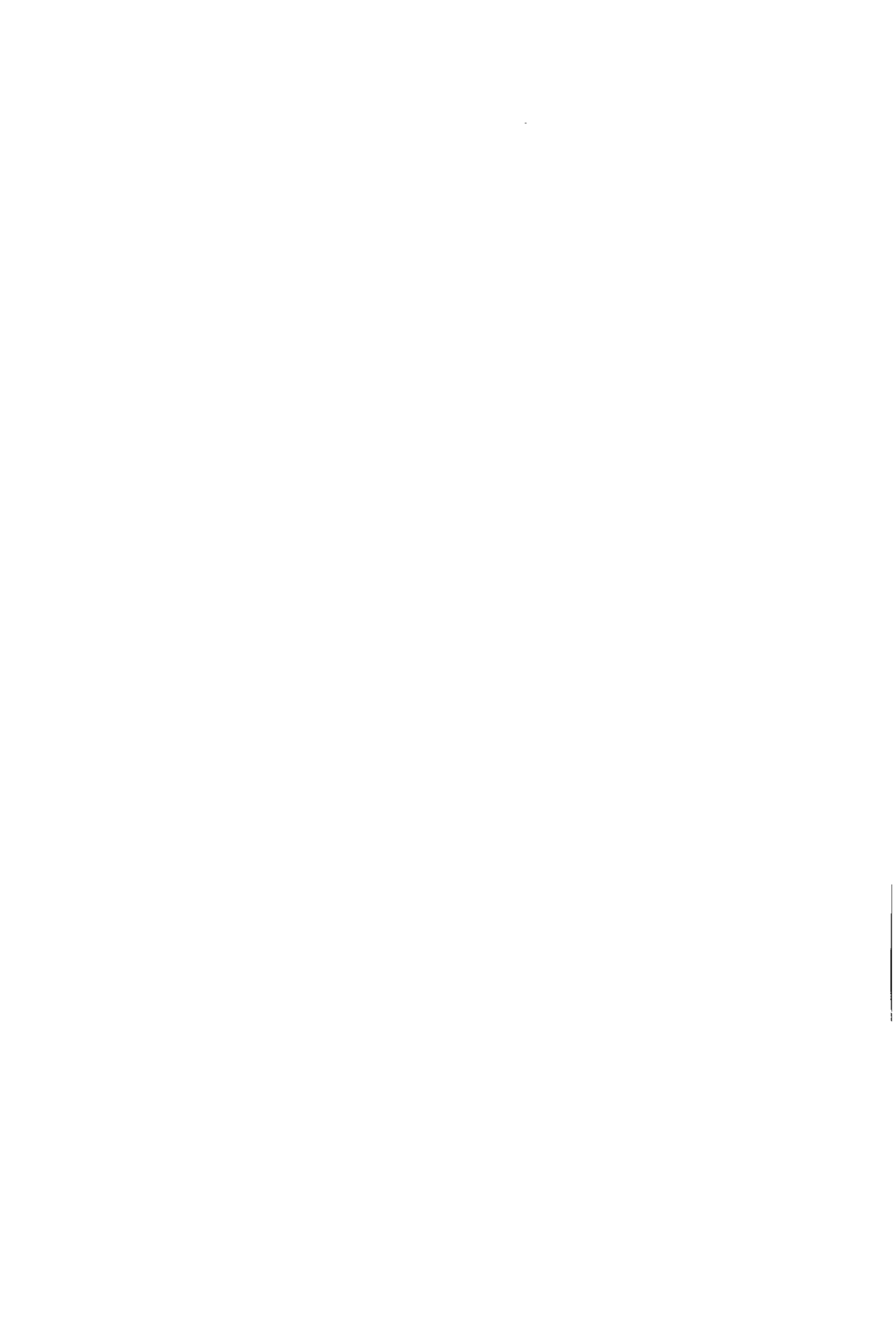
Final Report
1992-1994

Contract: F13PCT920064i Duration: 1.1.93 to 30.6.95   **Sector B13**

Title: The induction of chromosomal changes in human and rodent cells by accelerated charged
particles: early and late radiation effects

1)   Edwards   NRPB
2)   Natarajan   Univ. Leiden
3)   Bimbot   CNRS
4)   Dutrillaux   CIR
5)   Kraft   GSI

I.   Summary of Project Global Objectives and Achievements

The induction of chromosomal aberrations is used as one of the basic experimental data bases for
judgements made in radiological protection. It contributes to the judgements of radiation quality and to
the extrapolation of risk to low doses and low dose rates. Chromosomal change can be one of the early
steps in the long sequence of events which subsequently lead to neoplastic transformation of cells and
eventually to cancer. This contract aims to provide more detailed information on the radiation quality
dependence of aberration production and a better understanding of the production of chromosomal
aberrations both in the first cell cycle and after many cell divisions.

The first two projects used human lymphocytes irradiated in G_o. The aberration yield was
measured immediately following irradiation as well as at later times by the technique of premature
chromosomal condensation (PCC) and later at the first metaphase. It is the variation of these effects with
radiation quality that is the subject of this report. Particles of approximately constant LET are provided
by the accelerator, GANIL, in France. The third project provides the ion beam and measurements of dose
for particular irradiations.

The fourth and fifth projects concern the formation of unstable chromosomal aberrations in the
first and in subsequent cell cycles following irradiation. Again it was the variation of these effects with
radiation quality that formed the basis of these investigations. One group used Chinese hamster ovary cells
and a hamster-human hybrid cell line (hamster cells containing a single copy of human chromosome 2).
The other group used human fibroblasts. Both of these groups obtained their irradiations from the
accelerators at GSI Darmstadt.

The collaboration between the first three contractors has been very good. Three visits to the
GANIL accelerator were undertaken during the contract period. Had it not been for the unforseen
shutdown of the accelerator for modification then four visits would have taken place by the end of the
contract period. The fourth visit will now take place at the end of September 1995.

The workers under project 3 of this contract arranged and provided the charged particle beams of
oxygen and carbon ions. The three different particle beams of 996 and 1480 MeV oxygen ions and 425
MeV carbon ions concentrated measurements in the LET range 50-70 $keV.\mu m^{-1}$ which corresponds to the
radiation quality that has been predicted to be of maximum effectiveness for the production of
chromosomal aberrations in human lymphocytes irradiated in G_o and assayed at the first metaphase. For
these experiments, the two tandem cyclotrons at GANIL have produced particles of 95 MeV u^{-1} and their

energy has been reduced by the use of absorbers. The beam uniformity has been controlled by using a scattering foil and uniformity to within 20% over the 3 cm diameter of the biological target has been achieved. Although attempts have been made to use ionisation chambers to measure the dose rate in the beam, the most reliable estimates of dose have resulted from a measurement of particle fluence at the position of the cells and a knowledge of LET. It was only on the third visit that good agreement between the doses inferred from the ionisation chamber readings and those inferred from fluence measurement with plastic foils was achieved.

A misfortune on the second visit which used 92 MeV u^{-1} oxygen ions in which the plastic track etch detectors showed the existence of two ions was unexpected. The extra ion detected in the beam was thought to be caused by the break-up of the oxygen-16 ion to produce protons or helium-4 ions which were not stopped by the shutter or the beam-defining slit used in the exposures. By calculation from the measured fluence ratios it was estimated that the contribution to dose of these lower LET particles was about 30% on average contributing about 10% to the yield of aberrations in lymphocytes. The contribution to the measurement of PCC fragments could be as high as 30% because there is little evidence of an RBE for PCC fragment production much greater than 1. The yield of PCC fragments for this experiment are therefore probably overestimated.

The results from the two laboratories under projects 1 and 2 seem to give a coherent message since dicentric yields measured at the first metaphase agree. The group under project 2 also measured translocations using florescence in situ hybridisation (FISH) technique. For oxygen-16 ions a linear increase of translocation yield with dose was found and, when compared with dicentrics, the frequency was higher by a factor of 2 to 3. PCC fragments measured immediately after exposure, which means after about 45–60 mins of repair, appear linear with dose for all radiation qualities and the RBE values are not much greater than 1. The highest RBE seen is 2 for the 92 MeV u^{-1} oxygen ions and the yield is believed to be high for the reasons stated above. For x-rays the yield is about 3 PCC breaks per cell per gray.

With the PCC techniques (project 2) the kinetics of repair of heavy ion induced chromosome damage was also studied. Following irradiation of lymphocytes with 1480 MeV oxygen and 425 MeV carbon ions and imposing recovery times of 2 and 4 hours, the yield of PCC fragments decreased by 20-40% compared with 50-70% for x-rays. However when the DNA repair inhibitor ARA-a was added to the cells immediately after irradiation and maintained during fusion, the PCC yield increased by a factor of 2 which is similar to the increase obtained after x-irradiation. The RBE for 1480 MeV oxygen ions was about 2 which might be a small overestimate because of the beam contamination mentioned earlier.

A similar set of observations was obtained from project 5 using a CHO-K1 cell line and its DNA repair deficient counterpart, xrs-5. Both cell types were irradiated in G_1 and all chromosomal and chromatid aberrations were scored and pooled to provide the reported results. The chromosome aberrations scored were dicentrics, centric rings and excess acentric fragments while chromatid aberrations included breaks and exchanges.

For the production of all aberrations following x-irradiation, the repair deficient cell line was an order of magnitude more sensitive than the wild type cells. Following irradiation with highly energetic gold ions (780 MeV u^{-1} , LET = 1150 keV μm^1) the repair deficient line was only a factor of 2 more sensitive than the wild type line. All dose effect relationships appeared linear with dose which contrasts with the highly curved responses for human lymphocytes obtained at low LET. Converting the fluences for gold ions to dose, results in RBE values of about 2.5 for the wild type cells and 0.5 for the repair deficient mutant. The conversion assumes a nuclear area of about $100\mu m^2$ so that 10^6 particles cm^{-2} corresponds to 1 particle per cell nucleus.

An interesting feature of these experiments is the observation that for high LET and not low LET, chromatid breaks and exchanges were produced despite irradiation in G_1. This effect has not generally

been observed in human lymphocytes irradiated in G_o although some data in Sabatier et al (1990) suggests this might occur.

The principal implications of these experiments for mechanisms by which radiation induces aberrations in cells is that DNA repair is a very important factor. A current hypothesis is that radiation produces a large number of double strand breaks which are induced linearly with dose. Most double strand breaks restitute but a few either form an exchange with each other or exchange with an undamaged part of the same or another chromosome. Other work seems to indicate the yield of double strand breaks in the two cell lines is the same so there must be at least two types of repair, one that restitutes breaks rapidly and the other which forms exchanges or restitution on a rather longer time scale. The x-ray sensitive strain is then deficient in only the first of these repair systems and high LET radiation produces types of double strand breaks which are naturally resistant to the first form of repair.

The linearity of aberration yield with dose for x-rays for the Chinese hamster cell lines is open to question because the lowest dose used was 2 Gy but if the yield is linear with dose, this implies either that exchange between two double strand breaks is not important for this cell line or that inter-track action is a small or non-existent component. These arguments do not apply to the human lymphocyte system.

The observation of unstable aberrations in subsequent cell cycles has been investigated further under projects 4 and 5 and these two laboratories have collaborated well. During the contract period, the Dutrillaux group visited GSI seven times. Both cyclotrons (UNILAC and SIS) were used and the beam and dosimetry has been provided by the Kraft group. The important features of the results obtained from project 5 are as follows. The observations of chromosomal aberrations after many cell cycles following irradiation depends upon how the cells are grown. CHO cells propagated as mass cultures showed no sign of cell instability in later generations. However, when these cells were cloned individually, instability was seen in some of the colonies. The fraction of cells in each colony which contain aberrations is variable ranging from 5% (which is normal) to 50%. A possible reason for the failure to see cell instability in cells grown in mass culture is that normal cells grow faster than the few aberrant cells and thus dominate the cytogenetic picture.

Further experiments were done with UV24C2-3 cells, a human-hamster hybrid cell line containing one copy of human chromosome 2. The important results here are that x rays as well as neon ions (25 MeV u^{-1}, 183 keVμm^{-1}) produce chromosomal instability and there appears to be no marked dose dependence in the range studied. For the charged particle irradiations at the lowest dose, every cell is intersected by at least one particle so that in all these experiments every cell was irradiated.

By contrast, the work under project 4 has concentrated on the nature of aberrations seen in those cells showing instability. Using human fibroblasts irradiated with heavy ions the main feature is that the aberrations seen after about 25 passages involve the telomeric regions of particular chromosome arms; 1p, 13p, 13q, 16p and 16q are implicated. In this system the group has failed to observe such chromosomal instability following x-irradiation.

Overall the evidence on the mechanism by which chromosomal instability occurs is still not clear. The work presented here indicates that several cell types show the effect. The work from Dutrillaux (project 4) strongly implicates the telomeric regions of chromosomes and appears to be related only to high LET radiation. The results from Kraft (project 5) clearly show that x-rays as well as high LET particles can produce the instability effect so that it is not a specific high LET phenomenon. The necessity to use single cell cloning methods indicated by the Kraft group to express the instability effect contrasts with the cell culturing techniques used by the Dutrillaux group who found that some chromosomally abnormal cells exhibited growth advantage and eventually invaded the cultures.

Workers under projects 2, 4 and 5 have pointed out that cell type might explain these phenomena. The Kraft group have used immortalised cell lines which are transformed and which grow rapidly so that clones of undamaged cells will normally invade the whole colony. This makes unstable cells difficult, if not impossible, to see. Single cell clones can however show instability. The Dutrillaux group work with primary human fibroblasts which after about 45 to 50 passages become senescent. The reason for this is thought to be that the enzyme telomerase which maintains telomeric sequences is inactive in these primary cells. The result is that with continued cell proliferation the telomeres gradually shorten and lead to chromosomal instability characterised by end to end chromosomal associations. This process subsequently leads to cell senescence. However, this argument does not apply to the immortalised CHO cells because in these telomerase is active.

One the basis that different mechanisms may underly radiation induced genomic instability in mortal human fibroblasts and immortal CHO cells it is perhaps not surprising that these cell types exhibit differences in the LET-dependence of induction of the instability phenotype.

References

Sabatier, L, Al Achkar, W and Dutrillaux, B. (1990). Increasing complexity of chromosomal rearrangements after heavy ion bombardment of increasing LETs. Proc. 21st meeting of the European Society of Radiation Biology, Tel Aviv, 1988.

Head of Project 1:   **Mr A A Edwards**

II   Objectives for the reporting period

The objectives for this contract were to obtain dose-effect relationships for the induction of chromosomal aberrations in human lymphocytes for several charged particle irradiations. The cells were to be irradiated in G_o and aberrations scored at the first metaphase. The charged particles were to be obtained from GANIL at Caen in France and the irradiations were of the track segment type, that is at constant LET. The LET values of interest were from about 20 to 150 keV μm^{-1} which covers the range of maximal effect previously inferred from neutron irradiations. The more specific objectives to achieve the main aim, were to attend GANIL, irradiate and culture the cells, score the aberrations and fit appropriate dose effect relationships. Results for three separate ions have been obtained. The irradiations for one ion were done prior to the start of the contract but scoring and curve fitting was done during the contract period. A fourth ion will be used to irradiate blood in September 1995.

III   Progress achieved including publications

Previous work in this laboratory has aimed at measuring dose effect relationships for the induction of chromosomal aberrations in human lymphocytes by radiations of many different qualities. The dicentric aberration has received greatest attention because it is relatively easy and reliable to score and it has a low spontaneous frequency. Analysis of dose effect curves has consistently demonstrated that the yield curve

$$Y = C + \alpha D + \beta D^2$$

fits the observed data well. For research aimed at radiation protection, it has been the variation of the coefficient α with radiation quality which has received greatest attention. Previous work from just 5 neutron energy spectra from a fission spectrum to 14 MeV neutrons produced a hypothesis concerning the variation of α with LET. This hypothesised curve is shown in Fig. 1. The objective of using charged particles of nearly constant LET to irradiate lymphocytes has been to verify or revise these curves. Data for α-particles (120 keV μm^{-1}), 23 MeV helium-3 ions (22 keV μm^{-1}) and 190 MeV neon-20 ions (460 keV μm^{-1}) have all fallen close to this curve. Data for 9 MeV protons (5 keV μm^{-1}) lie about a factor 2 below the curve.

Data sufficient to derive dose effect relationships have been produced during this contract. The scoring data for 996 MeV and 1480 MeV oxygen ions and 425 MeV carbon ions are shown in Tables 1, 2 and 3. Dicentric distribution data are also shown. The methods of dosimetry for the three particle beams are described under project 3 of this contract. In brief, an ionisation chamber was used to calibrate the monitor current. To measure fluence, CR39 track etch devices were placed on the wheel which held the blood samples for irradiation. For the 996 MeV oxygen ion beam there was a discrepancy between the dose measured by the ionisation chamber and that measured by the track etch devices. This was attributed to incomplete collection of the ionisation current and so dosimetry was based on measured fluences.

For the 1480 MeV oxygen ion beam the track etch devices showed the existence of two distinct ions. Eventually the two ions were attributed to the main oxygen-16 ions and to break-up products of the oxygen ion, probably helium-4 or protons. Measurements of the fluences of these two particles showed that the disintegration products were variable whereas the oxygen beam fluence correlated well with beam monitor current. On average the ratio of fluence was about 1:1 but because the disintegration products had a lower LET than the oxygen beam the extra dose caused by the products was probably no more than 30%. The lower LET particles also had a lower biological effect so that it was likely that no more than 10% of the aberration yield was caused by the disintegration products. The quoted doses in Table 2 are those derived from the oxygen-16 fluence measurements and ignored the contribution by the lower LET
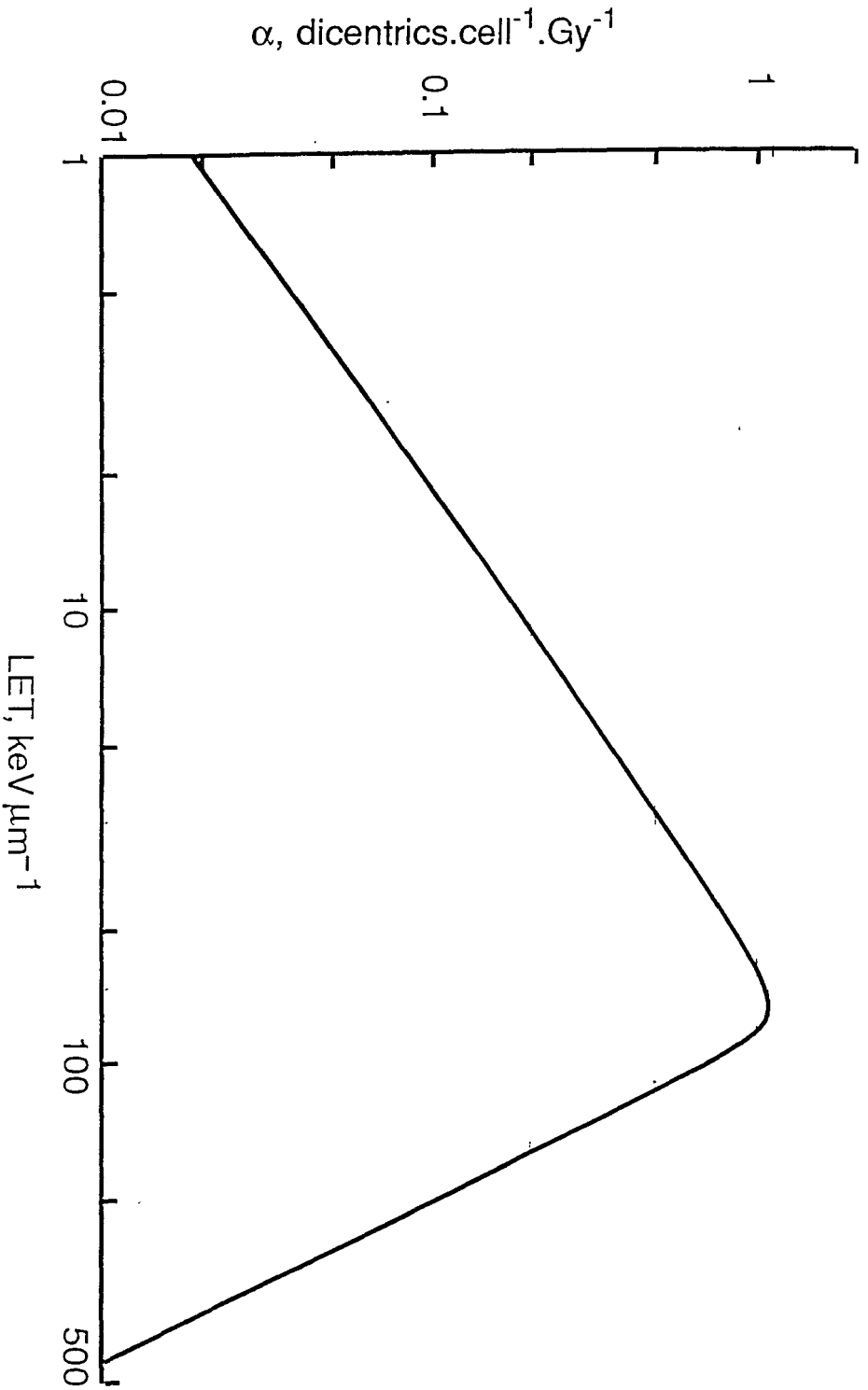
Fig. 1. A suggested variation of α with LET for dicentrics induced in human lymphocytes

Dose Gy	Cells scored	Aberrations seen			Dicentrics distribution						σ²/y	u
		dicentrics	centric rings	excess acentrics	0	1	2	3	4	5		
0	2000	1	0	4	1999	1					-	-
.077	575	9	0	16	566	9					0.99 ± .06	-0.3
.163	629	33	0	27	598	29	2				1.07 ± .06	1.3
.312	702	100	2	105	622	63	14	3			1.32 ± .05	6.0
.464	310	42	2	44	276	26	8	3			1.25 ± .08	3.1
.740	275	100	7	90	203	50	18	3	0		1.38 ± .09	4.5
1.11	234	101	7	81	158	54	20	1	1		1.15 ± .09	1.6
1.47	194	100	1	99	120	53	17	3	1		1.13 ± .10	1.3
2.22	45	37	0	45	19	18	5	3		1	0.96 ± .21	-0.2

Table 1

Measured aberration yields for 996 MeV oxygen ions of LET$_\infty$ = 67 keV μm^{-1}

Dose Gy	Cells scored	Aberrations seen			Dicentrics distribution								σ²/y	u
		dicentrics	centric rings	excess acentrics	0	1	2	3	4	5	6	7		
0	2000	1	0	4	1999	1							-	-
.092	753	16	0	35	737	16							0.98 ± .05	-0.4
.12	1500	71	5	75	1438	55	5	2					1.26 ± .04	7.3
.205	1420	138	8	112	1300	104	14	2					1.19 ± .04	5.2
.300	560	106	3	66	471	73	15	1					1.15 ± .06	2.6
.405	520	103	5	60	437	66	15	1	1				1.27 ± .06	4.4
.60	631	204	6	187	473	119	34	3	2				1.22 ± .06	3.9
.82	413	253	7	155	253	99	38	17	5	0	0	1	1.50 ± .07	7.2
1.20	190	163	3	138	92	55	27	11	4	1			1.30 ± .10	2.9
1.60	173	160	3	146	80	49	26	13	5				1.27 ± .11	2.5

Table 2

Measured aberration yields for 1480 MeV oxygen ions of LET$_\infty$ = 49 keV µm^{-1}

Dose Gy	Cells scored	Aberrations seen			Dicentrics distribution							σ^2/y	u
		dicentrics	centric rings	excess acentrics	0	1	2	3	4	5	6		
0	2000	1	0	4	1999	1						-	-
.048	1000	19	0	18	981	19						0.98 ± .04	-0.4
.097	2000	82	1	56	1924	71	4	1				1.13 ± .05	4.1
.19	1500	166	8	108	1361	114	23	2				1.24 ± .04	6.6
.30	588	141	8	83	479	83	22	2	2			1.33 ± .06	5.7
.46	442	141	4	105	332	85	20	4	1			1.22 ± .07	3.3
.72	236	138	7	102	134	75	18	9	1			1.07 ± .09	0.8
.95	213	158	8	97	105	70	27	10	1			1.06 ± .10	0.6
1.47	136	154	9	105	49	40	33	10	3	0	1	1.12 ± .12	1.0

Table 3

Measured aberration yields for 425 MeV carbon ions of $LET_\infty = 59$ keV μm^{-1}

disintegration products. For the 425 MeV carbon ions (Table 3) the agreement between the measurements from the ionisation chamber and the track etch devices was very good.

Inspection of Tables 1 to 3 shows that the number of radiation induced excess acentrics are on average about 20% lower than the number of radiation induced dicentrics. The number of centric rings is about 4% of the dicentrics which is perhaps marginally lower than the 5 to 10% which comes from previous experience. Overall there does not appear to be any important variation in the ratio of the aberrations scored with radiation quality. Similar ratios have been obtained following photon and neutron irradiation.

An analysis of the distribution of dicentrics amongst cells shown in Tables 1-3 shows clear signs of a dispersion greater than would be expected on the Poisson distribution. For curve fitting purposes an average ratio of variance to mean was selected and applied to all dose points for each ion. Values of 1.3, 1.25 and 1.2 were chosen for the data in Tables 1-3 respectively. The results of curve fitting to equation (1) and to the simpler linear form, are shown in Table 4.

Radiation	LET kev/μm	Dicentric yield coefficients		χ^2	DF	P
		α Gy^{-1}	β Gy^{-2}			
Oxygen ions 996 MeV	67	0.38 ± .03	-	14.0	7	0.05
		0.39 ± .05	0-.005 ± .049	13.9	6	0.03
1480 MeV	49	0.57 ± .04	-	48.5	8	<.0001
		0.45 ± .07	0.17 ± .09	32.3	7	<.0001
Carbon ions 425 MeV	59	0.67 ± .05	-	36.0	7	<.0001
		0.55 ± .07	0.23 ± .10	21.4	6	0.002

Table 4

Fitted values of α and β for radiation induced dicentrics for several ions

The probabilities of fit to these equations show some inconsistency in yields between doses for the same ion. According to Fig. 1 the α coefficients for 49, 59 and 67 keV μm^{-1} should be respectively about 0.85, 0.95 and 1.05 dicentrics per cell per Gy to be consistent with our previous experiments with neutron radiations. However, the ions used within this contract are more energetic than the 200-350 keV protons which have similar LET and which contributed to the curve in Fig. 1. The δ-rays (electrons) produced by the low energy protons have an energy no more than 1 keV so that all energy is deposited within 100nm of the proton track. For the energetic ions the δ-rays have much higher energy. The maximum energies of the 966 MeV oxygen ions, the 1480 MeV oxygen ions and the 425 MeV carbon ions are about 120, 180 and 70 keV respectively. These electrons have continuous slowing down ranges of about 200, 350 and 70 μm in tissue respectively and they all deposit some of their energy far from the path of the ion. Because these distances are large compared with the distance over which initial chromosome breaks are believed to interact, the ions behave biologically as if they had a lower LET. It is therefore possible to reconcile qualitatively the lower measurements of the α coefficients in Table 4 compared with those expected from Fig. 1.

An interesting feature of the results in Table 4 is that for the 49 and 59 keV μm^{-1} beams there appears to be a β coefficient which is just significantly positive. The best fit values shown in Table 4 are

about a factor of 3 or 4 higher than the β coefficient previously obtained for x and γ-rays but the uncertainties are large. From the report of project 3 there is some suggestion that larger doses may be underestimated because of non-linearity between the beam monitor current and the ionisation chamber current and this at least in part could account for the observed β coefficient with the 425 MeV carbon ions. The results shown here confirm the difficulty of detecting a small β-term in the presence of a large α term.

Publications

Edwards, AA, Finnon, P, Moquet, JE, Lloyd, DC, Darroudi, F and Natarajan, AT. The Effectiveness of High Energy Neon Ions in Producing Chromosomal Aberrations in Human Lymphocytes. Radiation Protection Dosimetry 52, 299-303 (1994).

Edwards, AA. The formation of chromosomal aberrations in human lymphocytes by radiations of different quality. Atelier sur les Programmes de Recherche Biomédicale en cours au GANIL. Caen, October 1993. GANIL Report RI 94 01 (1994).

Head of project 2: Prof. Natarajan

II. Objective for the reporting period

The aim of the project was to use the accelerators at LINAC (GSI, Darmstadt) and GANIL (Caen) to irradiate human peripheral blood lymphocytes with ions of nearly constant LET (in the range of 10-200 keV/μm), and to investigate;
(1) The initial frequency of chromosomal damages observed by using the Premature Chromosome Condensation (PCC) technique.
(2) The RBE values obtained in comparison to X-ray-induced chromosome damages immediately following irradiation.
(3) The kinetics of repair processes following high LET irradiation and their relation to those following low LET irradiation.
(4) Induction of chromosomal aberrations (unstable and stable) at the first mitosis following exposure.
(5) The modulating effect of DNA repair inhibitors (i.e. ara-A) on high LET radiations induced chromosomal aberrations.

III. Progress achieved including publications

Exposure to low doses of high LET radiation has been seriously considered as a potential human health hazard and the induction of chromosomal aberrations is used as one of the basic experimental data for judgements made in radiological protection.

For the first set of experiments the neon beam was obtained from the linear accelerator LINAC at GSI (Darmstadt). The energy of beam was about 180 MeV giving an average LET of 460 keV/μm. The induction of chromosomal aberrations immediately after irradiation was studied using PCC method. All other experiments using oxygen-16 and carbon-12 ions were performed at GANIL (Caen). For the second experiment, human lymphocytes were irradiated with Oxygen-16 ions of 65.77 MeV corresponding to a LET value approaching 70 keV/μm. The induction of chromosomal damage and repair after irradiation using the technique of PCC were performed. For the third and fourth experiments lymphocytes were irradiated with oxygen-16 ions of about 92 MeV and carbon-12 ions of about 40 MeV, corresponding to LET values approaching 49 and 59 keV/μm, respectively. We investigated the induction of chromosomal aberrations and kinetics of repair after irradiation with these heavy ions in the presence and absence of DNA repair inhibitor (i.e. adenine arabino-furanoside, ara-A), immediately after irradiation (using the PCC technique) and later on at the first mitosis by analysing unstable as well as stable aberrations in Giemsa stained preparations and following fluorescence in situ hybridization (chromosome-painting assay), respectively.

For the PCC assay, human lymphocytes were isolated using LeucoPREP™, cell separation tube (Becton Dickinson Labware). The resulting mononuclear cells were irradiated with heavy ions (i.e. Neon-20, oxygen-16 and cabon-12). The dosimetry has was done by Drs. Edwards (NRPB) and Freeman (CRN). The lymphocytes were injected into sample holders (about 1×10^6 cells/sample holder). For each dose point 4-5 sample holders were irradiated successively. Following irradiation lymphocytes were pooled and fused with mitotic Chinese hamster ovary (CHO) cells in the presence of polyethylene glycol (MW = 1450, 55% w/v) as fusing agent, which lead to condensation of lymphocytes nuclei prematurely. The mitotic CHO cells prelabeled with 5-Bromodeoxyuridine (BrdUrd) for at least 2 cell cycles, were obtaioned by mitotic shake off. Therefore, following Giemsa staining mitotic CHO cells could be differentiated from human interphase cells based on the Giemsa staining property of BrdUrd substituted chromosomes. Following one hr incubation at 37°C, the routine fixation protocol was used and air dried preparations were made and stained according to Fluorescence plus Giemsa technique and mounted in Depex.

For the metaphase analysis, after irradiation, the cells were removed from each trough by flushing with culture medium, lymphocytes were pooled and cultured for 48 hours. Colcemid was added 3 hrs before harvesting to accumulate mitotic cells. 5-Bromodeoxyuridine was added to the culture medium and following fixation and FPG-staining only first division cells were scored for dicentrics, centric rings and excess of fragments.

For chromosome painting assay, chromosome specific DNA libraries and fluorescence in situ hybridization (FISH) were applied to detect stable aberrations (i.e. translocations).

Bluescribe DNA libraries specific for chromosomes 1, 2, 3, 4, 10 and X (representing about 40% of human genome) were labeled with biotin-16 dUTP by nick translation and immunofluorescence staining was used according to the standard protocols.

Neon-20 ions (460 keV/μm):
Induction of chromosome aberrations by Neon-20 ions in interphase cells (immediately after irradiation):

Human lymphocytes were irradiated with Neon-20 (LET of 460 keV/μm) and immeidately fused with mitotic CHO cells. A linear dose response curve was observed (Table 1). One interesting observation was the distribution of PCCs, no scattering of PCCs for different doses was found, for example, for 4.4 Gy about 60% of cells were without excess of fragments and among others between 17 and 22 extra breaks per cells were found (Table 1). These cells with such a high frequency of aberrations obviously will die and never come to mitosis in routine culturing protocol for chromosome analysis. If we assumed that cells in irradiated samples with no excess PCCs were missed by particles and those hit did not die and had visible damage, the frequency of PCCs can be calculated based on the excess of PCC per damage cells, the RBE was found to be 1.5-1.9 compared with low LET (X-rays). When induced PCCs were estimated on the basis of excess of fragments in total number of cells analysed a value for the slope α of 2.1 $\pm$ 0.2 excess PCCs per Gy was found, and RBE of about 0.7 was found. These observations indicate that high interphase death and mitotic delay specially at high doses operating with Neon-20 irradiation (at LET of 460 keV/μm), however, they had no signifcant effect on PCC analysis.

Oxygen-16-ions:
Induction and repair kinetics of oxygen-16-ions induced chromosomal aberrations in interphase and metapahse cells:

Oxygen-16 ions with two different energy were generated and used (LET of 70 and 49 keV/μm).

PCC experiments:

The distributions of PCC fragments following irradiation with different doses of oxygen ions (Tables 2-4) indicate that lymphocytes were uniformly irradiated. A linear dose response curve was observed. From PCC data the RBE at 0 time with respect to X-rays is estimated to be in the range of 1.5-1.9 and 2-3 for 70 and 49 keV/μm, respectively. However, following irradiation of lymphocytes with oxygen-16 ions (LET of 49 keV/μm), in addition to PCCs fragments (scorable) rather high numbers (15-20%) of pulverized chromosomes (unscorable) were observed irrespective of the dose of irradiation and treatment regimens (Table 3 and 4), possibly due to contamination of other ions (i.e. protons or helium ions). These data were not included in the estimation of the frequency of breaks per cell for each dose of oxygen-16-ions.

In order to assess the kinetic of repair following irradiation of human lymphocytes with oxygen-ions of different energy. Following irradiation a recovery time of 2 or 4 hr was given in the presence and absence of inhibitors of DNA double strand break repair (ara-A). The results indicate that the rate of recovery following oxygen-16-ions is about 20-25% less than the value obtained with X-rays (Table 2-4). However, when ara-A was added immediately following irradiation and kept during one hour fusion time, PCC fragments increased about 70% in comparison to the regimen without ara-A (Table 5). A very similar enhancement was found when ara-A was used in combination with X-rays in human lymphocytes. These data indicate that though breaks caused by high LET radiation might repair rather slowly than those caused by low LET raidation the recovery of fast repair component of DNA double strand breaks is similar between low and high LET radiations.

Modulating effects of ara-A on oxygen-16-ions induced unstable and stable aberrations in human lymphocytes:

Two major classes of aberrations induced by low LET radiation in G_0 cells, namely stable (translocations) and unstable (dicentrics). It has been reported that frequency of translocations following low LET radiation is about 1.5-2 times more than the frequencies of dicentrics induced by a given dose of X-rays. We have investigated the induction of stable and unstable aberrations and the influence of DNA repair inhibitors (i.e. ara-A) following oxygen-16-ions (LET of 49 keV/μm) irradiation. A linear dose response curve was found for dicentrics and translocations, and increased frequency of translocations was about 2-3-fold higher than dicentrics (Fig. 1). When human blood lymphocytes were irradiated in the presence and post-incubated with ara-A which modifies the structure of chromatin and inhibits rejoining of DNA DSBs, an up to two-fold increase in the frequencies of induced dicentrics and translocations is encountered. Similar observation was made following X-irradiation, however, when ara-C or 3-aminobenzamide employed to study their influence on the frequencies of X-ray-induced aberrations, no effect in the frequencies of induced translocations was found, while the frequencioes of dicentrics increased.

Carbon-12 ions (LET of 59 keV/μm):

Following treatment of human lymphocytes with carbon-12-ions a linear dose response for induction of aberrations was observed. From PCC data the RBE at 0 time with respect

to X-rays is estimated to be in the range of 1.2-1.4 (Fig. 2). Following 4 hr recovery time, the frequency of breaks decreased by about 35-40% (Fig. 2) The rate of recovery following carbon-12-ions exposure is 15-20% less than the values obtained with X-rays.

Generally, these data indicate that there is a slight qualitative difference in the initial chromosome lesions induced by low and high-LET radiations. The repair processes following high LET radiation might be slower than following low LET radiation and/or more non-rejoining breaks are produced by heavy ions than by X-rays.
For the metapahse analysis, the crucial factor at high LET is the probability that a single particle crossing a cell nucleus will kill the cell. If the probability is large, RBE values will be small and vice versa (if this porbability is small, RBE values could be large). Of course higher values of RBE would be obtained if aberrations could be seen in the lymphocytes that suffer interphase death, in this respect the PCC technique with FISH (using centromeres and chromosome specific DNA libraries) offers the potentials for obtaining these data. In addition, it can shed some light to the mechansim of formation of unstable and stable aberrations following low and high LET irrdiations. Further experiments are in progress. In fact, the fourth visit to GANIL that will take place at the end of September 1995 during which, experiments to investigate further the correlations between high LET induced DNA lesions and observed biological effects at interphase and metaphase cells will be done.

Publications:

Edwards, A.A., Finnon, P., Moquet, J.E., Lloyd, D.C., Darroudi, F. and Natarajan, A.T. (1994). The effectiveness of high energy neon ions in producing chromosomal aberrations in human lymphocytes. Radiation Protection Dosimetry, 52, 299-303.
Darroudi, F. and Natarajan, A.T. (1994). Induction and repair of chromosomal damage by heavy ions in human lymphocytes, as detected by the technique of premature chromosome condensation. ESRP and ESHO Meeting, Amsterdam (The Netherlands), 117.
Darroudi, F., Natarajan, A.T. and Edwards, A.A. (1995) Induction and repair of chromosome damage following high LET irradiation of human lymphocytes, in interphase cells (manuscript).
Darroudi, F., Vermeulen, S. and Natarajan, A.T. (1995) Modulating effects of inhibitors of DNA repair on low and high LET irradiation-induced chromosomal damage in human lymphocytes (manuscript).

Table 1:
Induction of PCCs in human peripheral blood lymphocytes following irradiation with ^{20}Ne beam of 460 KeV/μm (fusion immediately after irradiation)

Dose (Gy)	cells scored	Distribution of PCCs													Excess/ PCCs	Damaged cells(%)	Mean PCCs/ damaged cell	Mean PCCs/ cell
		46	50	51	53	54	57	58	59	60	63	64	66	68				
0	60	60													0	0	0	0
1.3	55	25	5	20	4	1									156	55	5.2	2.8
2.2	48	28					1	9	8	2					251	42	12.6	5.2
4.4	35	20									1	2	10	2	297	43	19.8	8.5

Table 2:
Induction of PCCs in human lymphocytes following treatment with ^{16}O beam of 65.77 MeV

Dose (Gy)	Fusion time (hr)	No. of cells scored	Distribution of PCCs															Breaks per cell
			46	47	48	49	50	51	52	53	54	55	56	57	58	59	60	
0	0	50	50															0
0.5	0	52	6	11	11	8	7	3	5	1								2.3
1.0	0	40	0	0	1	4	11	5	5	7	2	2	1	1				5.8
1.5	0	40	0	0	0	2	4	5	4	6	9	2	3	1	2	2		8.4
0	0	50	50															0
1.5	2	45	0	0	0	5	8	7	7	5	6							5.7

Table 3:
Induction of PCCs in human peripheral blood lymphocytes following irradiation with ^{16}O beam of 49 KeV/μm (fusion immediately after irradiation)

Dose (Gy)	cells scored	Distribution of PCCs																								Breaks/Cell	I.F. Br./C.	Pul. (%)
		46	47	48	49	50	51	52	53	54	55	56	57	58	59	60	61	62	63	64	65	66	69	70	72	73			
0	50	50	0	0	0	0	0	0	0	0	0	0	0	0	0	0	0	0	0	0	0	0	0	0	0	0	46.0	0	0
0.2	44	15	0	4	4	8	4	5	2	0	1	1	0	0	0	0	0	0	0	0	0	0	0	0	0	0	49.1	3.1	10
0.4	50	9	3	4	3	4	5	8	4	2	4	0	2	1	0	0	0	0	0	0	1	0	0	0	0	0	51.0	5.0	12
0.8	46	6	0	2	3	0	3	0	4	0	7	4	1	4	1	4	1	2	0	1	0	1	0	0	1	1	53.8	7.8	12
1.6	45	3	0	0	0	0	0	2	2	0	2	2	2	4	4	6	2	2	2	3	5	4	2	1	1	1	60.8	14.8	15

Table 4:
Repair kinetics of PCCs in human peripheral blood lymphocytes following irradiation with ^{16}O beam of 49 KeV/μm (lymphocytes were fused with mitotic CHO cells 4 hours after irradiation)

Dose (Gy)	cells scored	Distribution of PCCs																								Breaks/Cell	Ind.Fre. Breaks/Cell	Pul. (%)
		46	47	48	49	50	51	52	53	54	55	56	57	58	59	60	61	62	63	64	65	66	69	70	72	73			
0	50	50	0	0	0	0	0	0	0	0	0	0	0	0	0	0	0	0	0	0	0	0	0	0	0	0	46	0	0
0.2	40	20	1	4	6	4	2	1	1	1	0	0	0	0	0	0	0	0	0	0	0	0	0	0	0	0	47.8	1.8	8
0.4	43	15	1	5	5	6	2	4	2	0	2	0	0	0	1	0	0	0	0	0	0	0	0	0	0	0	49.0	3.0	10
0.8	42	11	0	0	4	2	6	1	3	2	3	4	1	2	2	0	1	2	0	0	0	0	0	0	0	0	52.0	6.0	12
1.6	47	5	0	0	0	2	0	3	1	1	9	6	5	4	2	2	1	3	1	2	1	2	1	1	1	2	56.1	10.1	12

I.F. = Induced Frequency
Br./C. = Breaks/Cell
Pul. = Frequency (%) of cells with pulverized chromosomes.

Table 5:

Table 5

Induction of chromosomal aberrations in human lymphocytes following treatment with 92 MeV, O^{16} ions, and its modulation with inhibitors of DNA repair (i.e. ara-A)

Dose (Gy)	ara-A		Induced PCCs/ cell
	1 hr incubation-time	4 hr recovery-time	
0	-	0	-
0	+	4+	0.1
0.8	-	0	7.8
0.8	+	0	13.9
0.8	-	4-	6.0
0.8	+	4+	14.3
1.6	-	0	14.8
1.6	+	0	26.6
1.6	-	4-	10.1
1.6	-	4+	27.1

O16-ions-induced chromosomal aberrations in the presence & absence of ara-A

Chromosomal aberrations / 100 cells

—o— Dic - ara-A

—●— Dic + ara-A

—□— Tra. - ara-A

—■— Tra. + ara-A
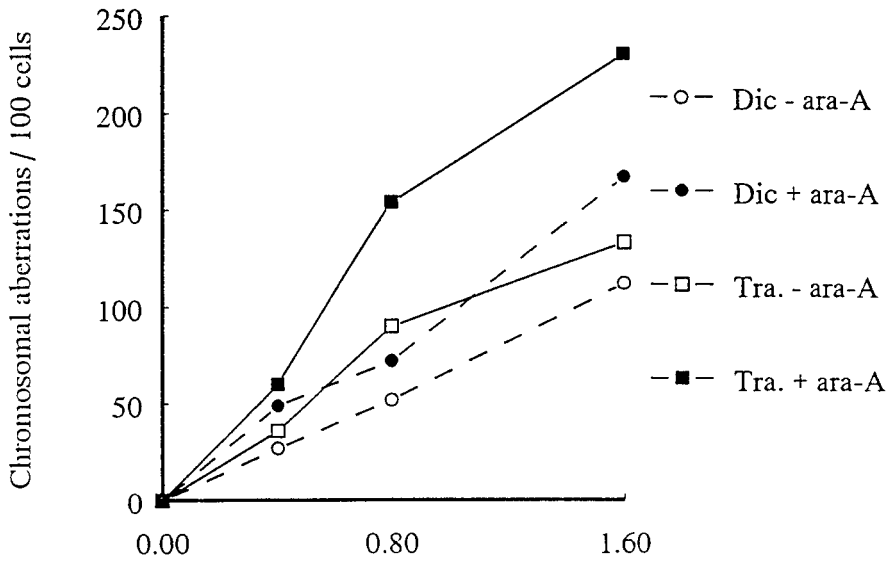
Fig. 1. Oxygen-16 dose (Gy)(49keV/um)

Induction and repair kinetic of C12-ions induced PCCs in human lymphocytes

Induced PCCs / cell

—o— No recovery

—●— 4 hr recovery
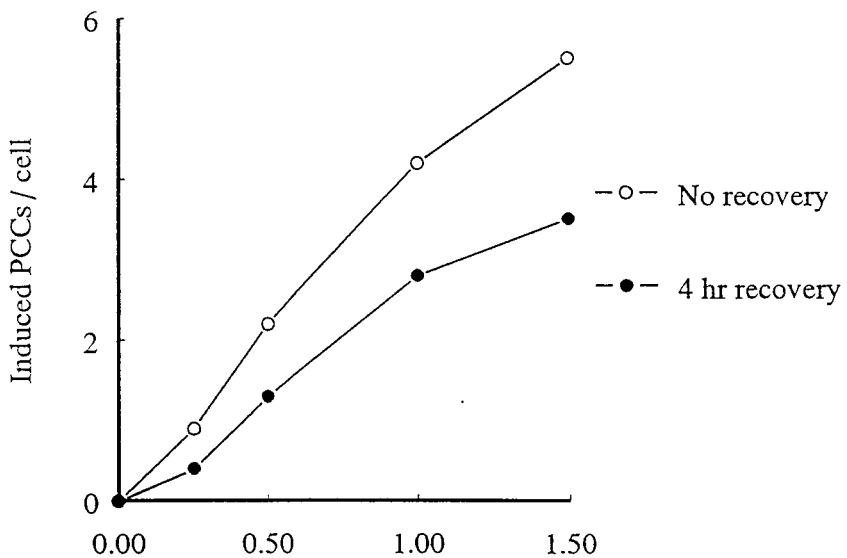
Fig. 2. Carbon-12 dose (Gy)(59keV/um)

Head of Project 3: Dr. Bimbot

II   Objectives for the reporting period

a)   Provide an accelerator beam line at GANIL to deliver beams of suitable uniformity and intensity to satisfy the requirements of biological experiments.

b)   Measure the uniformity and the fluence of these beams with precision.

c)   Provide the necessary support in equipment and manpower in order that biologists can carry out their irradiations at a nuclear physics facility.

d)   Carry out several sets of irradiations for the NRPB and the Leiden groups under different beam and energy conditions. Their results are reported under projects 1 and 2 of this report.

III   Progress achieved during Reporting Period

a)   Beam line

A beam line for the biological experiments has been set up in the target room G4 at GANIL. The beam conditions which are required for biology are very different from most other experiments carried out at GANIL in respect to the form of the beam and the way it is shared with other users. Intensities of the order of 10^5 particles/cm^2.s are required and in cases where the surface of the samples to be exposed are not too great this has been achieved by spreading out the beam by multiple scattering in a tantalum foil 6m upstream from the exit window of the beam line. This has been the method used for the irradiations by the NRPB and Leiden where the samples are only 3 cm wide. Another method uses the X-Y sweeping system which is available in the room G4 and is capable of spreading the beam over an area of 40 cm x 3 cm.

The pilot user at GANIL has the right to 90 % of the beam time with 10 % shared with a second user (a typical time structure would be 90s for the pilot and 10s for the others). Even though the biology experiments run at a duty cycle of about 10 % (the duration of an irradiation is of the order of a minute or two but the time necessary for changes between irradiations is of the order of 10-15 minutes) we have always operated as the pilot user for the NRPB irradiations since a constant beam is demanded for the entire period of the exposure. Some other experiments have been carried out as the second user. This has proved difficult but possible.

At the highest bombarding energies extra shielding had to be installed behind the site of the irradiations in the G4 target area for safety reasons.

b)   Measurement of the uniformity and fluence of the beam

In cases where the surface to be irradiated is relatively limited, i.e. for the NRPB exposures, the uniformity of the incident beam was observed directly in a gas profile monitor which was mounted after the beam exit window along the beam axis. The beam intensity departed slightly from a constant value presenting a convex shape over the exposed region but was considered to be acceptably uniform for the present application. The X-Y sweeping system is designed to spread out the beam in the horizontal plane by as much as 40 cm. This method has been used in some test runs and other biological experiments. To test the quality of the beam in this situation thermoluminescent detectors were positioned to determine the

relative dose in the horizontal and depth dimensions. When these were processed it was found that the dose as a function of depth showed the expected Bragg curve but in the horizontal plane the dose and thus the fluence showed serious departures from a constant value over the 20 cm width of the detectors. This must be looked into before using this method in future irradiations.

The beam intensities are too low to measure the fluence (or dose) by charge integration of the incident primary particles but two other methods are currently employed. The first is an active method where the fluence is inferred from the integrated current collected in an ionisation chamber. Typically a single incident ion traversing the chamber will create 10^4 new ions effectively amplifying the beam current to readable values. The second is a passive method where plastic foils are exposed to the beam. These serve as nuclear track detectors which, after etching, reveal the passage of the incident ions. The thermoluminescent detectors mentioned above are also passive devices but were not normalized for determining absolute fluences or doses. They were employed to measure the relative doses as a function of,position and depth.

The procedure adopted during the NRPB and Leiden irradiations was as follows. An ionisation chamber was placed after the exit window of the beam line and the currents recorded in this chamber were compared with those from a secondary electron monitor mounted before the exit window. Once the constant of normalization between the two currents was determined for a range of beam intensities the ionisation chamber was removed and replaced by the samples to be irradiated. The fluence was then inferred from the integrated current from the secondary electron monitor. Plastic track etch detectors were irradiated during the series of exposures and later on were etched and counted as a verification of the fluence values.

At the beginning it was found that there was poor agreement between the fluences inferred from the secondary electron monitor currents and those observed visually on the plastics. In a first experiment the track detectors yielded fluences which were 40 % higher. A number of parameters involving the ionisation chamber enter into the determination of the fluence which could be potential sources of error but incomplete ion collection was suspected to be the main reason for the deficit. The reference ionisation chamber of the NRPB was designed for X-ray dosimetry where the ion pairs are created at more scattered sites than in heavy ion bombardment. For heavy ions the ion pairs are densely clustered along the path of the incident particles. As a result ion collection is a more severe problem in the case of heavy ion radiation. The ionisation chamber was subsequently overhauled and in particular the depth reduced by a factor of two to improve the ion collection. The revised chamber was then tested under heavy ion beam conditions and compared with the GANIL ionisation chamber. The results of these tests were found to be very satisfactory. Any residual discrepancy between the dose readings was plausibly due to a systematic error in the nominal depth (5.6 and 3.2 mm for the NRPB and GANIL chambers respectively) of either or both chambers. In the last series of irradiations at GANIL good agreement was achieved between the fluence measured in the plastic track detectors and that inferred from the ionisation chamber. A precision of the order of 10 % for the dosimetry appears to have been attained.

When it was found that there were discrepancies between the fluence values of the two methods the results of the track detectors were retained as they were considered to be the more reliable. With the reservation that only low fluences can be counted accurately on the track detectors the determination of the number of holes per cm^2 in a plastic is subject to less systematic error than a fluence deduced indirectly from the charge collection in an ionisation chamber. Two other advantages of the track detectors have been appreciated. Firstly the presence of secondary particles in the primary beam (revealed by differences in the track diameters) showed up on the plastics for the irradiations at the highest bombarding energies allowing corrections to the dose to be made. Secondly they can provide further checks on the uniformity of the fluence.

c)   ***Support for biologists.***

A laboratory close to the target room G4 at GANIL where the irradiations are carried out has been made available to the biologists. Much of the equipment in this laboratory has recently been repatriated to its owners at GSI Darmstadt. Replacements have been made during the period of the contract.

Most of the work involved in setting up the experiments and conducting a suitable beam to the irradiation site has been done by the in-house scientists and technicians at GANIL. Nuclear physicists from several laboratories, IPN Orsay, the University and Centre A. Lacassagne Nice, and CRN Strasbourg have assisted the biologists with the irradiations and have assured the dosimetry where necessary.

d)   ***Irradiations for the NRPB.***

The NRPB project was to carry out a series of irradiations to observe the formation of chromosomal aberrations in human lymphocytes under a variety of conditions of beams, bombarding energies and doses. Two parameters of the irradiation field are involved; the linear energy transfer (LET) and the nuclear charge of the incident ions Z. For conditions relevant to the present programme the value of the LET decreases with increasing incident energy and increases with Z. The role of the LET value is evident as it is directly related to the density of damage inflicted on the biological medium. The dependence on Z arises since although two ions with the same LET will deposit the same energy per unit length along the ion path this energy will be distributed differently in the vicinity of the track for different values of Z of the incident ion. To date three sets of irradiation have been performed at GANIL for the NRPB and the Leiden groups. A list of the primary beam energies irradiations with their approximate LET values is given below.

BIO04 Aug., 1992	^{16}O 65.8 MeV/A	70 keV/μm
BIO07 Oct., 1993	^{16}O 95 MeV/A	50 keV/μm
BIO09 Apr., 1994	^{12}C 40 MeV/A	60 keV/μm

Two different beams, ^{12}C and ^{16}O, have been used but it is desirable to extend the range of LET values. With this aim the NRPB group has been programmed on two occasions for irradiations at 40 MeV/A ^{16}O for which the LET value is approximately twice those of the above list. On both occasions the irradiations were postponed for reasons beyond our control. On the last occasion beam time had been programmed for the month of June before the end of the present contract. A failure in the safety system was detected on the accelerator site and the experimental programme was interrupted pending a solution to this problem. Authorization has now been given to resume the experimental programme and these irradiations should be carried out before the end of September.

Publications

Protons, ions lourds, faisceaux radioactifs: de nouvelles voies pour la radiothérapie.
R.Bimbot, Bull. Soc. Phys., 90 (1993) 22.

Les lignes de faisceau GANIL et leurs équipements disponibles pour les applications médicales.
R.Anne, Atelier sur les Programmes de Recherche Biomédicale en cours au GANIL, Caen, Octobre 1993
GANIL Report RI 94 01 (1994).

The formation of chromosomal aberrations in human lymphocytes by radiations of different quality.

A.A.Edwards, Atelier sur les Programmes de Recherche Biomédicale en cours au GANIL, Caen, Octobre 1993 Report RI 94 01 (1994).

Les activités biologiques au GANIL.

R.Bimbot, Conf. sur le Rayonnement Synchrotron et les Spectrocopies Complémentaires en Science du Vivant et en Sciences des Matériaux, Orléans, Mars 1994.

Head of project 4 : Dr B. Dutrillaux

SPECIFIC CHROMOSOME INSTABILITY DETECTED IN HUMAN FIBROBLASTS AFTER HEAVY ION IRRADIATION

Laure SABATIER, Isabelle TESTARD, Jérôme LEBEAU, Michelle RICOUL, Luis MARTINS and Bernard DUTRILLAUX

The project aims at understanding immediate and long term consequences of heavy ion induced chromosome damages, chromosomal instability and clone formation, in relation with cellular transformation.

Objectives :

1) to study qualitatively the multiple chromosome aberrations induced by high LET particles;

2) to follow the transmission of these anomalies in human fibroblasts (primary cultures);

3) to search for the molecular origin of the radiation induced chromosomal instability;

4) to characterize the apparition and the specificity of chromosomal instability occurring several cell divisions after irradiation of fibroblasts from different donors.

Introduction

Although many set of data, the biological consequences of heavy ion irradiation remain poorly undertood (Tobias, 1985; Lett et al, 1986). Immediate consequences as DNA damages, chromosome damages have been described and heavy ions are very potent in inducing both. Heavy ions are also been demonstrated to be more efficient than low LET radiations in inducing cell death and cell transformation. Up to now, the events occuring between initial radiolesions and neoplastic transformation are poorly understood.

Over the years, studies with irradiated mammalian cells have shown that although a lot of DNA damages are immediate, some biological effects can be delayed and carried by surviving progeny of irradiated cells over many cell cycles i.e delayed reproductive death, gene mutations (Chang and Little, 1991; 1992; Seymour et al, 1986). Now, different set of data have shown that genomic instability can manifest several generations after cellular exposure to irradiation (Kadhim et al, 1992; Sabatier et al, 1992; Holmberg et al, 1993; Marder and Morgan 1993). Genomic instability would be a rare event that heavy ions would be very potent to induce. But does it mean that genomic instability is specifically induced by irradiation? Or does irradiation permit the early appearence of a naturally occuring phenomena? Discussion is open.

The delayed genomic instability, generally observed as a chromosomal instability can directly affect some genetic changes that permit to make up some of the progressive steps leading to cancer cell (figure 1).

The aim of this project was to study the long term effects of heavy ion irradiations of primary cultures of human fibroblasts.

IRRADIATION γ / heavy ions

DNA STRAND BREAKS
DOUBLE
SINGLE
CHROMOSOMAL DAMAGES
MUTATIONS

CELL DEATH

CELL TRANSFORMATION
TUMOUR

RADIATION-INDUCED CHROMOSOMAL INSTABILITY

Cancer cells :
clonal evolution from a single cell
chromosome imbalances
chromosome rearrangements
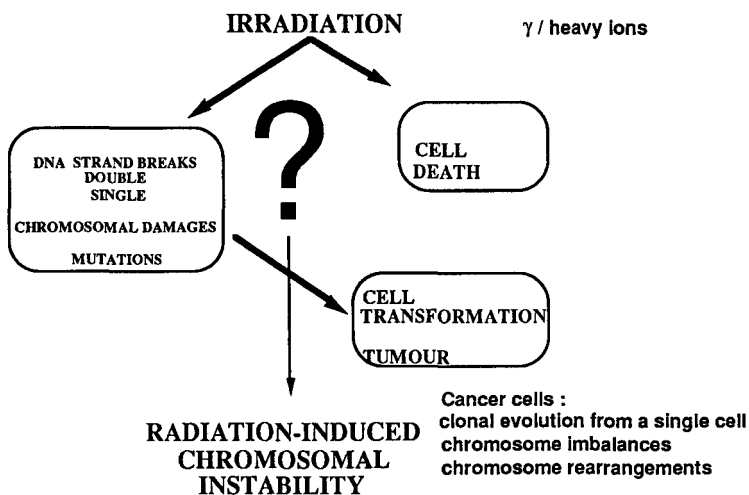
Figure 1 : Chromosomal instability : key step in cell transformation

The unusual characteristics of chromosome lesions induced by high LET radiations was recently demonstrated. These lesions are more complex than those induced by X or γ rays and their complexity increases with the LET (Sabatier et al, 1987; 1990). The behaviour of the cells carrying these lesions was followed in vitro. In recent years, evidence has been provided to suggest that chromosomal instability can manifest several cell generations after exposure to radiations. Chromosome damage can be one of the first steps in the sequence of events which led to the neoplastic transformation of cells.

Recently Kadhim et al (1992) demonstrated that irradiation by α particles of Pu-238 (LET=120keV/μm) induce a transmissible instability in mouse hematopoietic cells. Working with human dermis fibroblasts irradiated by heavy ions in a large range of LET (386-13600 keV/μm) we also showed that an instability (end to end associations) could also be acquired by human cells and that particular chromosomes were recurrently involved. We found that this instability led to specific chromosome imbalances and in particular monosomy (Sabatier et al, 1992; Martins et al, 1993). The specific involvement of telomeric regions may correspond to lesions of telomeric repeats, in particular deletions, as described in senescent and transformed cells (Greider, 1990).

Results and discussion

1) *to study qualitatively the multiple chromosome aberrations induced by high LET particles;*

The chromosomal damages induced by heavy ions in human lymphocytes differ quantitatively and qualitatively from those induced by low LET radiations in particular the induction of complex rearrangements (rearrangements involving at least three chromosome breakpoints). We have observed the induction of complex rearrangements by cell traversal of a single particle of Neon LET=75 keV/μm but not after Neon LET=31keV/μm indicating a LET dependence of the ability of a single particle to induce complex rearrangements.

The future use of oxygen ion for heavy ion radiotherapy leads us to focus on the biological effects of heavy ions with LET around 20-50keV/μm. We perform experiments with oxygen ions of 3 different energies. Blood from healthy donors was irradiated on SIS cyclotron (GSI,

Germany) with Oxygen ions (E= 80, 225 and 325 MeV/u). Lymphocytes show a decrease of mitotic index linked to a block of cell cycle before mitosis or cell death. There is also a delay in cell cycle progression in surviving cells as the fluence becomes greater. These phenomena increase with increasing LETs' of particles and fluences.

We observed that a high rate of dicentric and ring chromosomes are induced by Oxygen ion. Their number increases with the fluence of particles (2.10^6, 4.10^6, 10^7, 4.10^7 and 10^8 particles/cm^2), and is greater 52 hours than 72 hours after irradiation. This rate also increases when the LET of irradiation is higher (225 MeV/u <=> 26.8 keV/μm compared to 325 MeV/u <=> 21.6 keV/μm). But this tendency was not observed after 80 MeV/u irradiation despite its higher LET (55.4 keV/μm). The number of aberrations is in fact higher for both irradiations with lowest LETs (26.6 and 21.6 keV/μm). Cells seem to bear better a high rate of anomalies when the LET is low. This points out that not only the number of rearrangements but also their quality must be considered.

As previously shown (Al Achkar et al., 1988), aberrations with few breakpoints are transmitted better than complex rearrangements with several break points which lead to cell cycle delay or cell death. This statement is strengthen by the delay of cell cycle enhanced for 80 MeV/u irradiation since lowest fluences. After 52 hour culture, most of the mitoses are in their first mitosis post-irradiation, the percentage of abnormal cells observed after FISH painting of chromosome 1 on lymphocytes irradiated at 80 MeV/u also confirm results of dic and r scoring. The number of cells having chromosome(s) 1 rearranged increases with fluences up to 10^7 particles/cm^2 and then decreases (figure 2). Rearrangements induced by fluences above 10^7 part./cm^2 (0.89 Gy) are probably too complex to permit cell survival.

FLUENCE (particles/cm ^{2})
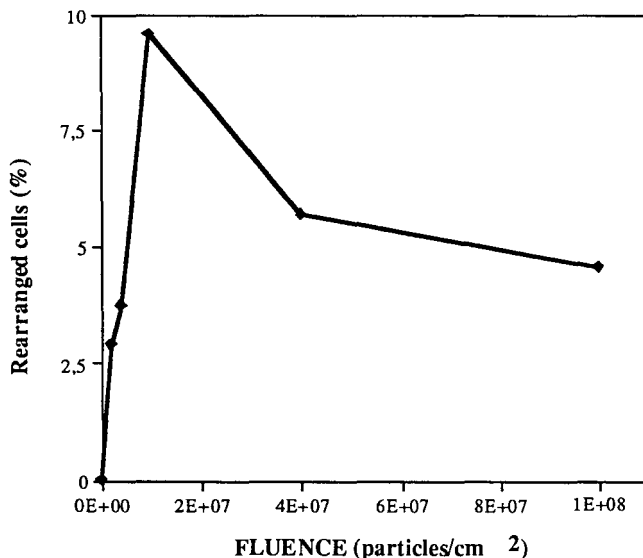
Figure 2 : Percentage of lymphocytes having at least one rearranged chromosome 1 after oxygen irradiation at energy of 80 MeV/u (LET=55.4keV/μm)

FISH painting on Oxygen irradiated lymphocytes at energies of 225 and 325 MeV/u displays that the number of cells having rearranged chromosomes is enhanced when the LET increases, but several particles are needed to induce complex aberrations. All these results obtained from FISH painting of chromosomes are in accordance with observations made after conventional cytogenetic analysis of lymphocytes irradiated with other ions (Sabatier et al, 1987; 1990).

Figure 3 chart — % of rearranged chromosome 1 (0–100), with legend:
- ☐ 1 break
- ▣ 2 breaks
- ◥ 3 breaks
- ■ 4 breaks

Bar values by fluence group:
- 2E+06: 66, 24, 10, 0
- 4E+06: 82, 18, 0, 0
- 1E+07: 53, 39, 6, 3
- 4E+07: 55, 27, 18, 0
- 1E+08: 58, 21, 21, 0

FLUENCE (part./cm2)	2E+06	4E+06	1E+07	4E+07	1E+08
DOSE (Gy)	0.18	0.36	0.89	3.56	8.9
Mean number of ions/nucleus	0.5	1	2.5	10	25
Number of cells analyzed	1267	427	365	333	381
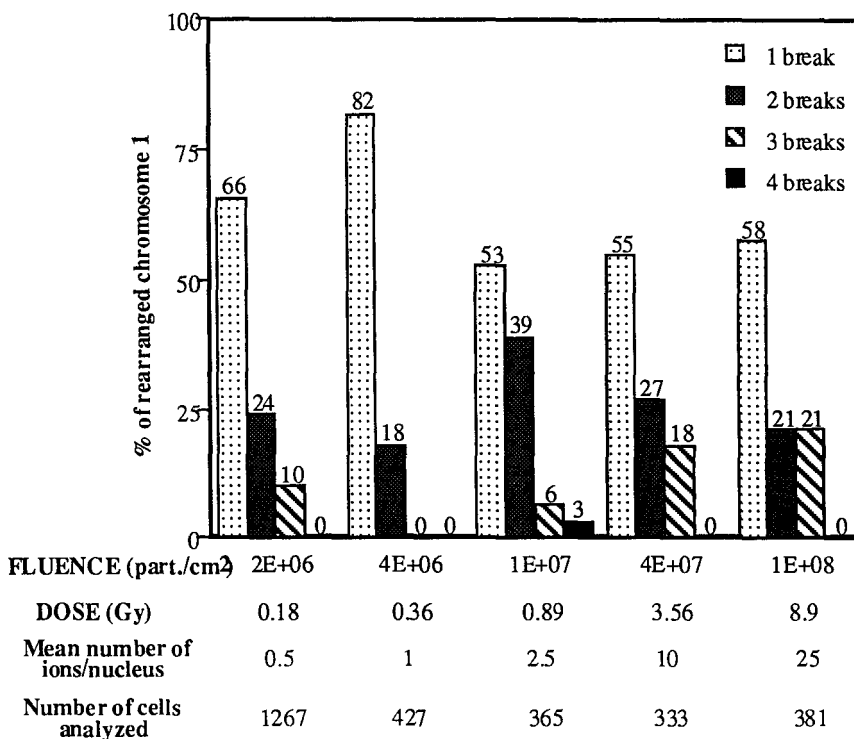
Figure 3 : Percentage of chromosome 1 having 1 to 4 breaks in human lymphocytes irradiated with 80 MeV/u Oxygen ions

Analysis of breaks among rearranged chromosomes 1 (after 80 MeV/u irradiation) shows that number of complex aberrations (more than 2 chromosome breaks) is increased with the fluence but appeared since lowest fluences (low doses < 0.2 Gy) (Figure 3) proving that only one particle of Oxygen LET= 55.4keV/μm is able to induce complex rearrangements. This point out the higher efficiency of heavy ions, compared to other kind of radiations, to induce such complex rearrangements. To clearly show this phenomenon, compared R-banding and painting analysis of chromosomes rearrangements in Oxygen irradiated lymphocytes are still in progress.

2) to follow the transmission of these anomalies in human fibroblasts (primary cultures);

We have observed that heavy ions are very potent in inducing chromosome damages, especially complex rearrangements. These complex rearrangements are poorly transmitted through cell divisions (a decrease of 30% of mitoses carrying such rearrangements at each cell division has been observed, Al Achkar et al, 1988). This could explain the good efficiency of heavy ions in inducing cell death. But we know that heavy ions are also very potent in inducing cell transformation (Suzuki et al, 1989) and our first hypothesis was that among all the radiation-induced chromosome rearrangements, one would confer a proliferative advantage to the cells and they would invade the culture as clones. To our surprise, we observe the appearence of de novo chromosomal instability several generations after cell irradiations. This instability leads to chromosome rearrangements invading cultures as clones. Thus the majority of the rearrangements observed several cell generations after irradiation have not been directly radiation-induced.

The first set of experiments has been performed with fibroblasts from the same human donor (TP).

The study of the 7 cultures irradiated at GSI by Neon ions (E=10.74 MeV/u, LET=386 keV/μm, fluences of 10^6, 2.10^6 and 4.10^6 particles/cm^2), Argon ions (E=10.52 MeV/u, LET=1207 keV/μm, fluences of 10^6, 2.10^6 and 4.10^6 particles/cm^2) and Lead ions (E=9.5 MeV/u, LET=13600 keV/μm, fluence of 2.10^6 particles/cm^2) shows identical results and permits to propose the following scheme :

     -irradiation by heavy ions induce multiple chromosomal alterations proportionally to fluence of the particles,
     -many cells directly affected by the track of one (or more) particles either die or do not give rise to viable descendants (majority of normal karyotypes in metaphases around the 5 - 10th passages)
     -a transmissible chromosome instability is observed in descendant cells,
     - this instability affects preferentially particular chromosomes(figure 4)
     - Specific structures are involved : telomeric regions of chromosome 1p, 13p, 13q, 16p and 16q arms,
     - some clones, characterized by chromosome rearrangements and imbalances, progresssively develop and invade all the cultures around passage 25 after irradiation (Sabatier et al., 1992; Martins et al., 1993).

While the cell cultures were carried on, the lifespan of the irradiated cells was increased. Control cultures have been prolonged up to 45 passages before death whereas the irradiated cells described before have died at 47, 54, 53, 49, 56, 45 and 50 passages for the various conditions described above, respectively.
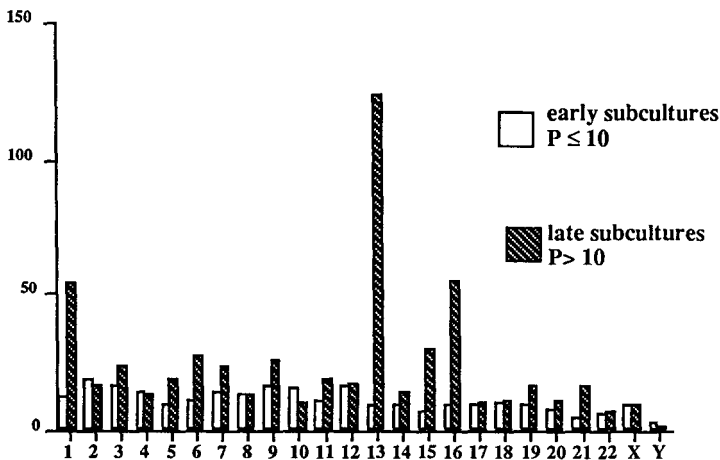
Figure 4 : Chromosomes involved in chromosome rearrangements detected after heavy ion irradiation of TP fibroblasts

We focus on the involvement of specific telomeres. After R-banding, the Giemsa staining of the p arm of chr13 is not the same for the two chromosomes. Thus, we can distinghish, a "light" and a dark chromosome. We observed the overinvolvement of the four telomeres but overall, the telomere of the light chromosome is overinvolved. We can postulate that the chromosome instability is linked to the length of the telomeric repeats of each chromosome.

3) *to search for the molecular origin of the radiation induced chromosomal instability.*

A specific involvement of telomeric regions may correspond to lesions of telomeric repeats, in particular deletions, as described in senescent and transformed cells. The same observations were done with ions of increasing fluences and LET. We wish to determine whether telomeres are shortened when the chromosomal instability appears.Two approachs are developed : a quantitative one (analyses of the mean length of telomeric sequences by Southern blotting) and a qualitative one (Fluorescence in situ hybridization).

We have compared the results obtained by the two techniques. Nine immortalized fibroblastic cell lines were used : DHS Cl2, DHS Cl4, HELOri⁻, HEL Cl1, CHSV3, CHSV4, W13A, WI98, LNSV. By Southern blot we can observed an important heterogeneity in the intensity and the size of the signal of each cell lines. The first results obtained by in situ hybridization show a good correlation with the results by Southern blot. The cell lines displaying an important mean length of telomeric sequences also show intense FISH signal.

In irradiated fibroblasts
- Our preliminary results show no shortening of the mean length of all telomeres. We try to precise the relations between the mean length of the telomeric repeats and the cell proliferation since irradiation. We decide to focus on the behaviour of the telomeric sequences of one chromosome (with subtelomeric probes, and cell sorting, work is in progress).

- We have now developped in situ hybridizations to look for a possible alteration of the telomeres of chromosomes specifically involved in instability. The characterization of the type of chromosome instability is focused on the distinction betwen telomeric associations (telomeric sequences are involved in the rearrangement) or dicentrics (telomeric sequences have been lost). Thus we need methods permitting the detection of telomeric sequences (Moyzis et al., 1989). We have adapted the methods of telomere in situ hybridization to our needings and obtain around 95% of chromosomes stained on both chromatids per cell. By in situ hybridization of the (TTAGGG) sequence we focus on telomeric regions of chromosomes specifically involved in instability. Although dicentric formation probably arose from telomeric fusions, no telomeric sequences were detectable by FISH at the junction of end-to-end dicentric. Thus, in irradiated human fibroblasts we can assume that chromosomal instability is correlated to telomere shortening. Now, we focus on the behaviour of telomeric regions of chromosomes 13, 16 and 1 prior the appearence of the instability for this donor.

4) *to characterize the apparition and the specificity of chromosomal instability occurring several cell divisions after irradiation in different donors;*

The specificity of chromosomal instability (25% of dicentrics involved chromosome 13) is questionnable because we have used fibroblasts of a single donor. Our previous experiments concerning a single donor, the specificity of the chromosome instability detected in his fibroblasts could be a characteristic of the three chromosomes involved, or vary from donor to donor.

Four additionnal experiments have been perform at GSI with Gold 9.4 and 800 MeV/u, Nickel 400 MeV/u and Oxygen 11.2 MeV/u. Primary cultures of human fibroblastes from 3 new donors have been irradiated. The cell cultures were carried on and karyoptypes established each five passages after irradiation. The work is in progress.

We present here data obtain after irradiation of human fibroblasts issued from another normal donor (FOU). The irradiation has been performed at GSI (SIS) with gold ions E= 800MeV/u. Five passages after irradiation, most of the caryotypes of the cells are abnormal. Each rearrangement differs from others. We detect one cell with a translocation between the chromosomes 3 and 5 : t(3;5). Ten passages after irradiation a chromosomal instability appears with dicentrics, endoreduplication leading to polyploïd cells and one clone is mostly

scored, cells with t(3;6). Passages after passages, we observed an accumulation of instability and then chromosomal rearrangements in cells. The caryotype of the major clone detected at the 17th passage show ten rearranged chromosomes. This clone invades progressively the cell culture through a clonal evolution similar to those observed in human cancer cells. The clonal evolution is presented in figure 5. We can observed the accumulation of chromosome rearrangements in the t(3;5) clone. This clone presents a proliferative advantage (against those with t(3;6)) as well in diploid than in tetraploid formula (endoreduplication is indicated by a cross in a circle). This donor presents an overinvolvement of the chromosome 3 in the chromosomal instability appearing long time after heavy ion irradiation.
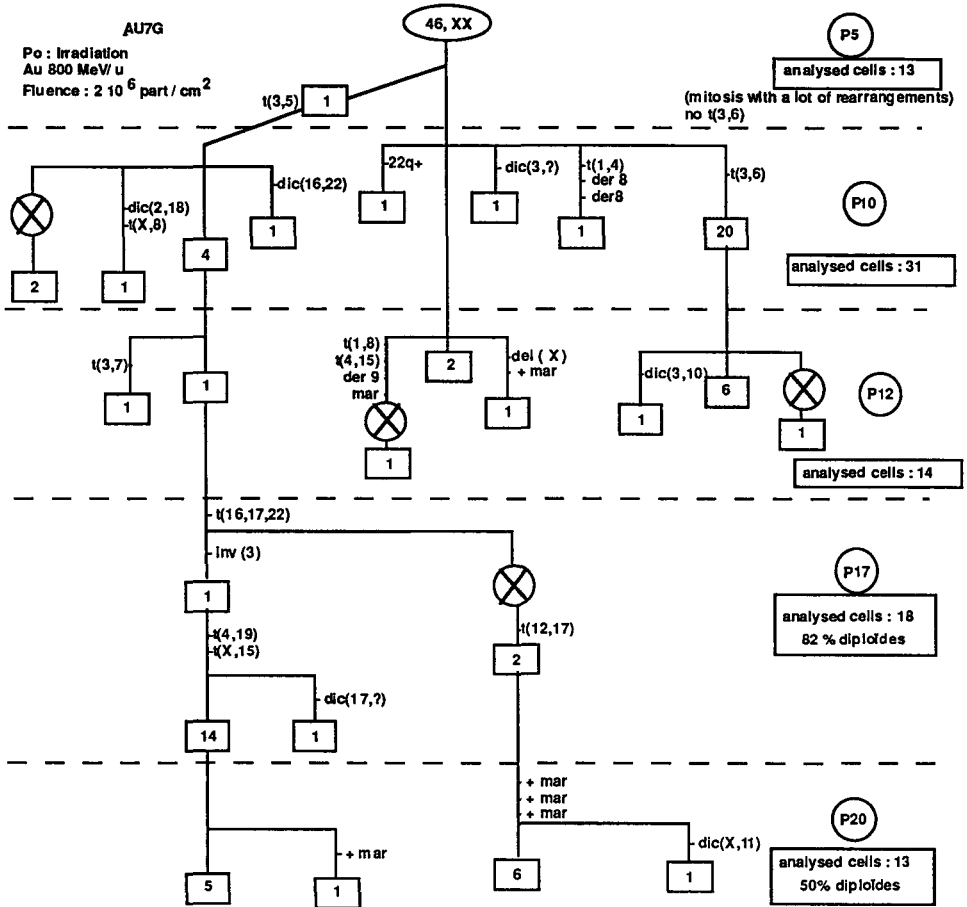
Figure 3 : Chromosome instability, accumulation of chromosome rearrangements and clonal evolution in heavy ion irradiated FOU fibroblasts

The induction of a clonal evolution of the caryotype after irradiation of human fibroblasts has never been detected in γ ray irradiated fibroblasts of this donor.
Thus we confirm our previous data on the chromosomal instability induced by heavy ions. The specificity of the chromosomes involved in the instability seems different for each donor.

Conclusion

During this project period, we have confirm that heavy ions are very potent in inducing complex rearrangements. The rate of complex rearrangements is function of fluences, LET, Particles. But few generations after irradiation most of the cells presents normal caryotypes or caryotypes with transmissible rearrangements (translocations, inversions). We have demonstrated that several cell generations after heavy ions irradiations (but not after γ rays irradiations) chromosomal instability can be detected, characterized by dicentrics, translocations, endoreduplications... The lifespan of the cells is increased but we failed to observe cell immortalisation (figure 6). The same kind of instability is observed just before senescence block in fibroblasts from the same donor.

Normal human fibroblasts have a proliferative capacity restricted to a finite number of cell divisions. The radiation-induced immortalization of human fibroblasts is poorly reported (Namba et al, 1985). Some data present a prolonged lifespan in X-irradiated human fibroblasts but they observed the escape of cultures from the commitment of early senescence in only 2 cases from 96 experiments (Kano and Little, 1985). We have reported one case of chromosomal instability in long term cultures of γ rays irradiation of human biopsies (Martins et al, 1994).
Ater heavy ion irradiations (8 experiments, 2 donors) we observed in each case the induction of a prolonged lifespan and chromosomal instability and we failed to observe such phenomena after γ irradiation of the same fibroblasts.

Increased life span and chromosomal instability would be rare events that heavy ions would be very potent to induce in primary human fibroblasts.
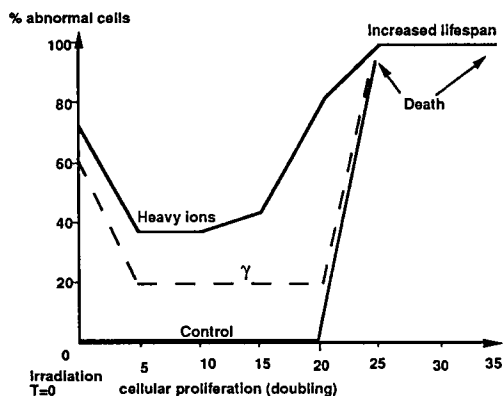
<u>Figure 6</u>: De novo chromosomal instability detected several cell generations after heavy ion irradiation

In Tp fibroblasts, we have found that radiation-induced chromosomal instability led to specific chromosome imbalances and monosomy (Sabatier et al, 1992; Martins et al, 1993). The same specific overinvolvement of chromosome 13 is also observed in senescent cells of this donor. We failed to observed in situ hybridization signal at the fusion of the end to end dicentrics (Sabatier et al, 1994). The end to end associations observed may be due to telomere shortening. This donor would present a large heterogeneity of telomeric repeat sequence lengths of his chromosomes 13p light would be the shortest. To test this hypothesis we will follow the chronology of appearence of chromosomal instability after SV40 transfection, before crisis, when telomeres shorten.
Many hypotheses could emerge, that we would like to test.
- could end to end association be due to minisatellite instability?

-Has irradiation directly eroded telomere ends and increased the telomere shortening?
- Has irradiation induced mutator genes which would have mutated cell cycle chekpoint genes which would permit the escape to senescence process and the early appearence of a naturally occuring phenomena : chromosomal instability observed in senescent cells (Benn, 1976)? In this idea, as the cells present and increased lifespan, the chromosomal instability lasts for several cell generations and clones can emerge.

Thus our major aim will be now to focus on the mechanisms of chromosomal instability. Is the chromosomal instability function of the donor, the type of cells or of the stress inflicted? We want improve our results with several other donors to focus at individual variations in the rate and the kind (telomeric associations, translocations, endoreduplication...) of chromosomal instability detected after heavy ion irradiations.
The characterization of the quality of chromosomal instability could be also of great interest because chromosomal instability is mainly detected after high LET radiations when we have studied primary human cells. But this phenomena can be induce as well after low than high LET in immortalized cell lines. Genomic and chromosomal instability can be observed in different stages of cell transformation and tumor progression. Different mechanisms could be involved depending of the characteristics of the cells beyond others, telomere dynamics and telomerase activity (Murnane et al, 1994).

In human solid tumors, chromosomal instability and jumping rearrangements are generally observed in premalignant or low grade malignancies (Pathak et al, 1988; Aledo et al, 1988). Clonal rearrangements leading to typical imbalances are detected in more advanced malignant tumors. We have seen that different donors present different de novo chromosomal instability. If human solid tumors are characterized by specific chromosomes imbalances, can we link specific chromosomal instability to cancer predisposition (Sabatier et al, 1995)?

References

AL ACHKAR W., SABATIER L., and DUTRILLAUX B. (1988) Transmission of radiation-induced rearrangements through cell divisions, Mutation Res., 198, 191-198.
ALEDO R., F.AVRIL M.F., DUTRILLAUX B. and AURIAS A. (1988) Jumping translocations of chromosome 14 in skin squamous cell carcinoma from a xeroderma pigmentosum, Cancer Genet Cytogenet., 33, 29-33.
BENN P.A. (1976) Specific chromosome aberrations in senescent fibroblast cell lines derived from human embryos, Am. J. Hum. Genet., 28, 465-473.
CHANG W.P. and LITTLE J.P. (1991) Delayed reproductive death in X-irradiated Chinese hamster ovary cells, Int. J. Radiat. Biol., 60, 483-496.
CHANG W.P. and LITTLE J.P. (1992) Evidence that DNA Double strand breaks initiate the phenotype of delayed reproductive death in Chinese hamster ovary cells, Radiation Res., 131, 53-59.
GREIDER, C.W. 1990, Telomeres, telomerase and senescence, BioEssays, 12, 363-369.
HOLMBERG K., FALT S., JOHANSSON A. and LAMBERT B. (1993) Chromosome aberrations and genomic instability in X-irradiated human T-lymphocyte cultures, Mutation Res., 286, 321-330.
KADHIM,M.A ,MACDONALD,D.A. GOODHEAD, D.T. LORIMORE, S.A.MARDSEN, SJ. and WRIGHT, E.G. (1992) Transmission of chromosomal instability after plutonium a-partticle irradiation, Nature, 355, 738-740.
KADHIM M.A., LORIMORE S.A., TOWNSENDK.M.S., GOODHEAD D.T., BUCKLE V.J. and WRIGHT E.G. (1994) Radiation-induced genomic instability : delayed cytogenetic aberrations and apoptosis in primary human bone marrow cells, Int. J. Radiat. Biol., 67, 287-293.
KANO Y. and LITTLE J.B. (1985) Mechanisms of human cell neoplastic transformation : relationship of specific abnormal clone formation to prolonged lifespan in X-irradiated human diploid fibroblasts, Int. J. Cancer, 36, 407-413.
LETT J.T., COX A.B. and BERGTOLD D.S. (1986) Cellular and tissue responses to heavy ions : basic considerations, Radiat. Environ. Biophys., 25, 1-12.

MARDER B.A., and MORGAN W.F. (1993) Delayed chromosomal instability induced by DNA damage. Mol. Cell. Biol., 13, 6667-6677.

MARTINS, M.B. SABATIER, L. RICOUL, M. PINTON, A. and DUTRILLAUX, B., (1993) Specific chromosomes instability induced by heavy ions : a step towards transformation of human fibroblasts, Mutation Research, 285, 229-237.

MARTINS M.B., SABATIER L., RICOUL M., GERBAULT-SEUREAU M. and DUTRILLAUX B. (1994) Clonal rearrangements in human irradiated fibroblasts, Mutation Res., 308, 169-175.

MOYSIS R.K., BUCKINGHAM J.M., CRAM L.S., DANI M., DEAVEN L.L.,JONES M.D., MEYNE J. RATLIFF R.L. and WU J.R. (1989) A highly conserved repetitive DNA sequence, (TTAGGG)n, present at the telomeres of human chromosomes. PNAS, 85, 6622-6626.

MURNANE J.P., SABATIER L., MARDER B.A. and MORGAN W.F. (1994) Telomere dynamics in an immortal human cell line EMBO J., 13 (20) 4953-4963.

NAMBA M., NISHITANI K., HYODOH F., FUKUSHIMA F.and KIMOTO T. (1985) Neoplastic transformation of human diploid fibroblasts (KMST-6) by treatment with ^{60}Co γ-rays, Int. J. Cancer, 35, 275-280.

PATAK S., WANG Z., DHALIWAL M.K. and SAKS P.C. (1988) Telomeric association : another characteristic of cancer chromosomes? Cytogenet. Cell Genet., 47, 227-229.

RITTER S., KRAFT-WEYRATHER W., SCHOLZ M. and KRAFT G. (1992) Induction of chromosome aberrations in mammalian cell after heavy ion exposure, Advances in Space Res., 12, 119-125.

SABATIER L. AL ACHKAR W., HOFFSCHIR F., LUCCIONI C. and DUTRILLAUX B. (1987), Qualitative study of chromosomal lesions indduced by neutrons and neon ions in human lymphocytes at Go phase, Mutation Research, 178,91-97.

SABATIER L., AL ACHKAR W. and DUTRILLAUX B.(1990) Increasing complexity of chromosomal rearrangements after heavy ion bombardment of increasing LET's. In frontiers in radiation Biology, Ed. E. Riklis, VCH, 287-294.

SABATIER, L. DUTRILLAUX B.and MARTINS B (1992) Specific radiation-induced chromosomal instability, Nature (London), 357, 548.

SABATIER L., LEBEAU J. and DUTRILLAUX B. (1994), Chromosomal instability and alterations of telomeric repeats in irradiated human fibroblasts. International Journal of Radiation Biology, 66 (5) 611-613.

SABATIER L., LEBEAU J. and DUTRILLAUX B. (1995) Radiation induced cancerogenesis : individual sensitivity and genomic instability. Radiation and Environmental Biophysics, in press.

SEYMOUR C.B., MOTHERSILL C. and ALPER T. (1986) High yields of lethal mutations in somatic mammalian cells that survive ionizing radiation, Int. J. Radiat. Biol., 50, 167-179.

SUZUKI M., WATANABE M., SUZUKI K., NAKANO K. and KANEKO I. (1989) Neoplastic cell transformation by heavy ions, Radiation Res., 12, 468-476.

TOBIAS C.A. (1985) The future of heavy ion science in biology and medecine, Radiation Res., 103, 1-33.

Head of project: 5:

Prof. G. Kraft

II.   Objectives of project:

Heavy ion beams in an energy range of 10 to 800 MeV/u were used to study early and late radiation effects in rodent cell lines. As a measure of early radiation effects the quantity and the quality of chromosomal damage were determined in first postirradiation metaphases stained with the Fluorescence-plus-Giemsa technique. For the evaluation of late radiation effects the de novo occurrence of chromosome aberrations in the progeny of irradiated cells was investigated by two different experimental protocols. In the first protocol, the exposed cells were propagated as mass cultures; in the second protocol cell clones derived from a single parent cell were established. Chromosome analysis was performed up to 40 population doublings postirradiation by means of conventional cytogenetic techniques and by fluorescence in situ hybridization.

III.   Progress achieved:

One important endpoint for the assessment of genetic risks resulting from radiation exposure is the measurement of chromosomal damage. Structural chromosome aberrations are a sensitive indicator of genetic damage and there is substantial evidence that the formation of aberrations is related to radiation induced carcinogenesis[1] and cell killing[2]. The general approach has been to analyze chromosome alterations in the first postirradiation mitosis, because only in these cells can structural aberrations be observed in their entirety. The number of cells carrying unstable aberrations such as dicentrics or rings decreases drastically with time after exposure, while cells with stable aberrations like reciprocal translocations are thought to survive and transmit these aberrations to their progeny.

In recent years evidence has accumulated to suggest that radiation exposure can also result in delayed effects manifested after several cell generations[3,4,5,6]. Obviously some cells which survive the initial radiation exposure transmit a latent chromosomal instability to their progeny that led to a de novo occurrence of aberrations many replication cycles later. Chromosome changes like imbalances and rearrangements that emerge in the offspring of irradiated cells are also observed in transformed and malignant cells indicating that the delayed expression of radiation damage may be an important factor in the development of cancer. Furthermore, there is evidence that radiation induced genetic instability depends on the genetic characteristics of the cell[4,7].

Yet, little information exists, so far, on the magnitude of this effect and its dependence on radiation quality. While in some cellular systems chromosomal instability was only observed after particle exposure[3], in other systems chromosomal instability occurred after x-ray and γ-ray exposure[5,6]. It was the aim of our study to investigate the specific effects of densely ionizing radiation on chromosomal level covering the induction of damage in first cycle cells as well as the delayed occurrence of aberrations many cell cycles later.

Material and Methods

1. Analysis of chromosome aberrations in first postirradiation metaphases

Investigations concerning the induction of early chromosomal damage were performed with CHO-K1 cells, a repair-proficient Chinese hamster cell line and xrs-5 cells, their repair-deficient counterpart, which shows a defect in the rejoining of DNA double strand breaks[8]. Because radiosensitivity depends strongly on cellular age[9], all experiments were performed with synchronous cells

Both cell lines were synchronized by mitotic shake off, seeded in cell culture dishes and allowed to attach and spread. The purity of the sample was controlled by the analysis of the DNA content in a flow cytometer and by the measurement of the cell size using a coulter counter. About two hours after seeding, when the majority of cells had reached mid G_1-phase, cells were irradiated at the SIS (GSI, Darmstadt) with 780 MeV/u Au ions (LET: 1150 keV/μm) under track segment conditions. For comparison x-ray experiments were performed. Because recent experiments have shown that the yield of chromosomal damage varies with sampling time[10,11], the number of aberrant cells and aberrations were determined at serial, multiple harvesting times postirradiation as described in detail elsewhere[11,12]. By the use of the Fluorescence-plus-Giemsa technique[13] it was assured that the analysis of chromosomal damage was restricted to first postirradiation metaphases. In addition, the induction of early chromosome damage by 196 MeV/u O ions (LET: 26 keV/μm) was investigated in CHO-K1 cells. Furthermore, CHO cells which survived the exposure to either 4 x 10^7 or 8 x 10^7 O ions cm^2 were propagated as mass cultures and investigated for a delayed expression of chromosomal damage as described below.

2. Examination of the delayed expression of chromosomal damage

Experiments concerning the de novo occurrence of chromosome aberrations in the descendants of cells, which survived the initial radiation exposure were mainly performed with CHO-K1 cells. Cells were exposed to C and O ions in the energy range of 10 to 270 MeV/u and the delayed expression of chromosomal damage was examined by two different protocols. The first protocol consisted of the regular subcultivation of cells up to 40 population doublings postirradiation. For each passage the exact number of cell divisions was recorded, the plating efficiency was determined and chromosome analysis was performed. The second protocol involved the analysis of chromosomal damage in the clonal descendants of a single parent cell, ie. directly after exposure cells were trypsinized and seeded in 96 well dishes to form single cell colonies. After 7 to 10 days colonies were expanded to get a sufficient amount of cells for chromosomal analysis. Aberrations were scored after classical Giemsa staining.

The second experimental protocol was also applied to UV24C2-3 cells, a hamster-human hybrid cell line. A hybrid line was chosen, because in these cells in addition to breaks, dicentric and ring chromosomes also chromosomal rearrangements involving the human chromosome (ie. reciprocal translocations, insertions) can be easily detected by fluorescence in situ hybridization[14, 15]. UV24 cells contain a single copy of the human chromosome 2 in a background of 20 to 21 hamster chromosomes. The human chromosome represents 5% of the total DNA of the hybrid cells and, as previously shown by the premature chromosome condensation (PCC) technique, the induction and the repair of chromatin breaks in the human chromosome follows a normal dose response curve[14]. Cells were exposed to either Ne ions (LET: 183 keV/μm) or x-rays and aberrations occurring in the hamster chromosomes as well as in the human chromosome were recorded. Additionally, some samples were analyzed after classical Giemsa-staining. Details for cell culture conditions are given in reference[14]. In all experiments concerning delayed radiation effects particle fluences were applied, which correspond at least to a mean number of 3 particle traversals per cell nucleus.

Results and Discussion

1.   Early radiation effects

Investigations of radiation induced damage in mutant strains of mammalian cells, which show a defect in the rejoining of DNA double strand breaks, provide an unique opportunity to examine the role of double strand breaks and the mechanisms of double strand break rejoining in the production of chromosome aberrations. This is particularly important, because there is increasing evidence that the DNA double strand break is the major lesion responsible for the formation of chromosome aberrations. Furthermore experiments of Chang and Little suggest that the induction of DNA double strand breaks initiates the delayed expression of radiation damage[16]. In order to gain more insight into the mechanisms leading to the formation of chromosome aberrations directly after radiation exposure, the induction of chromosome aberrations by x-rays and 780 MeV/u Au ions was investigated in xrs-5 cells, which show a defect in the rejoining of double strand breaks, and their wild-type parent CHO-K1.
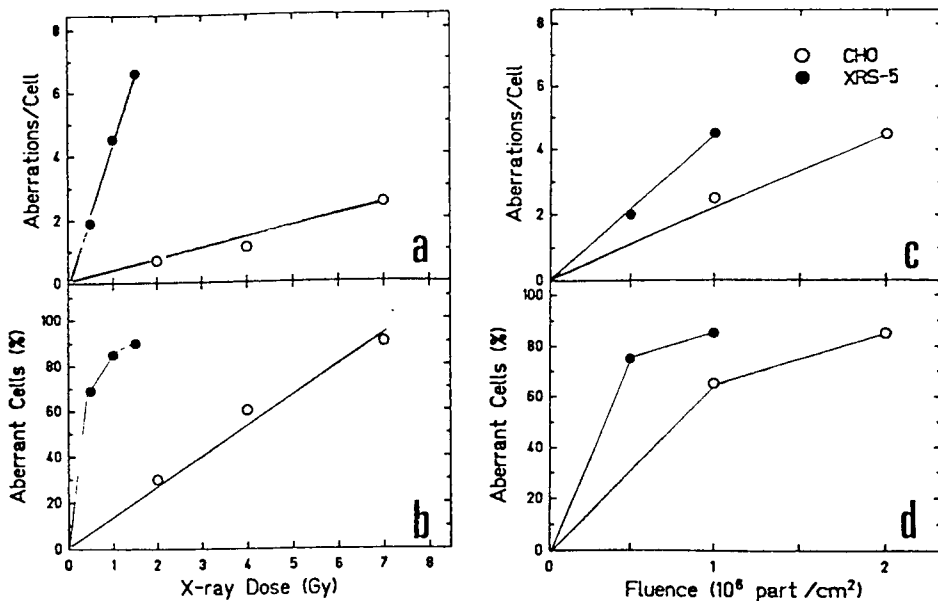
Figure 1: Frequency of aberrant cells and aberrations/cell induced in 1st generation CHO-K1 (open symbols) and xrs-5 cells (closed symbols) by x-rays and 780 MeV/u Au ions. Cells were exposed in G_1-phase and chromosomal damage was investigated at several postirradiation sampling times. Because radiation induced cell cycle perturbations and mitotic delay strongly interfere with the expression of chromosomal damage the contribution of each sample to the overall damage was considered (for details see references 11 and 12) and the compiled data were plotted.

After x-ray exposure a pronounced difference in the yield of chromosomal damage was found for xrs-5 and CHO cells: xrs-5 cells showed a five fold excess of aberrant cells and a twelve fold excess of aberrations/cell compared to CHO cells (fig. 1a,b). After high LET radiation however, these differences between both cell lines were diminished: the number of aberrant cells was only slightly higher in xrs-5 cells

(fig. 1d) and the aberration frequency/cell was only 2 times higher in the mutant strain compared to the wild-type parent (fig. 1c). Based on these observations as well as on other studies investigating the rejoining kinetics of radiation induced DNA strand breaks[14,17] it is evident that x-ray induced lesions are repaired with a high efficiency in wild-type CHO cells and only a small amount of these lesions appears cytogenetically as aberrations. In xrs-5 cells however, comparable doses of x-rays result in a much higher number of aberrant cells and aberrations per cell as shown in fig. 1 indicating that unrepaired DNA double strand breaks are causal in the production of chromosome aberrations. Furthermore, our finding that high LET radiation induces nearly the same amount of chromosomal damage in CHO and xrs-5 cells further supports the assumption that high LET induced lesions are more severe and less rejoinable than those induced by sparsely ionizing radiation - even for repair-proficient cells.

Furthermore, the comparison of the aberration types induced by densely and sparsely ionizing radiation in both cell lines revealed that the spectrum of aberration types changes as LET increases. When the aberration types are classified as chromosomal breaks (chromosome and chromatid breaks) and exchange-type aberrations for both cell lines an increase in the frequency of chromosomal breaks among the total number of aberrations with LET was found (fig. 2). However, in the mutant line the proportion of chromosomal breaks was generally higher than in the wild type parent. A shift in the spectrum of aberration types was also observed after the exposure of CHO cells to O ions (fig. 2), in V79 cells after irradiation with Ne, Ar and Kr ions (fig. 2) and in 10T1/2 cells after α-irradiation[9]. The occurrence of chromatid breaks in heavy ion irradiation samples despite exposure in G_1-phase indicates that these aberrations are not directly induced by DNA double strand breaks. They result probably from alkali-labile sites or single strand breaks which stayed unrepaired throughout G_1-phase and were converted into double strand breaks during S-phase. In the subsequent mitosis these double strand breaks can be expressed as chromatid aberrations as discussed in more detail in reference 11. Thus, the observed alterations in the spectrum of aberration types are a further indication that high LET induced lesions are qualitative different from low LET damage. A more detailed analysis of these chromosome experiments will be presented in a forthcoming paper.
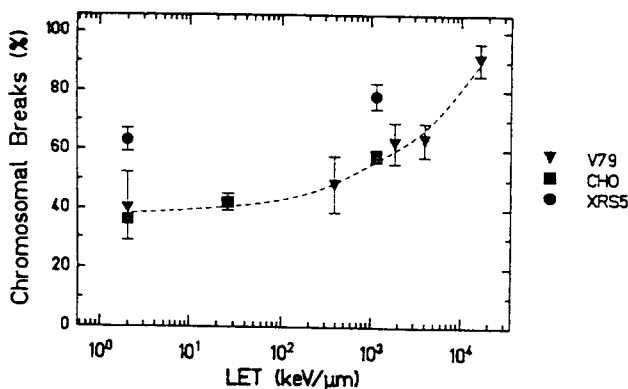
Figure 2: Proportion of chromosomal breaks (chromosome and chromatid breaks) among the total number of aberrations as a function of LET for repair-proficient and repair-deficient Chinese hamster cell lines. V79 and CHO cells belong to the category of repair-proficient cell lines, xrs-5 cells represent repair-deficient cell line. Cells were exposed in G_1-phase to charged particles or x-rays and chromosomal aberrations were analyzed as described in detail in references[11,12].

2.   Late radiation effects

Investigation of the de novo occurrence of chromosomal damage in cells surviving the acute exposure to ionizing radiation revealed that the applied protocol, ie. propagation of irradiated cells as mass cultures or single cell clones, has a strong influence on the experimental result. In the progeny of CHO cells irradiated with O ions of different energies and LET values and propagated as mass cultures, there was no indication of a delayed expression of chromosomal damage up to 40 population doublings postirradiation. As shown in figure 3 for 10.7 MeV/u O ions a high number of aberrant cells was only observed directly after exposure, ie. in first cycle cells. Then, this number declined with successive cell divisions and reached control level after about 8 population doublings. In parallel, the plating efficiency increased and at the time, when the number of aberrant cells reached the control value, the plating efficiency of irradiated cells reached control level as well.

In contrast, when cells were cultured according to the second protocol, chromosomal instability was detected. For example, in CHO-K1 clones derived from single cells after the exposure to 270 MeV/u C ions chromosomal instability was observed in 5 out of 20 (25%) cell clones 25 population doublings postirradiation. In the aberrant clones up to 50% of metaphases displayed chromosome aberrations, mainly dicentric chromosomes and chromatid breaks. These aberrations are probably not a direct consequence of the initial radiation exposure, because unstable aberrations are considered not transmissible over time. Investigation of chromosome damage 35 generations beyond the initial exposure showed that chromosomal destabilization persisted in the affected cell clones and emerged in further clones yielding a total frequency of 50% aberrant clones. Most clones which displayed a high number of aberrant cells showed a reduced plating efficiency as well as pointing to the role of aberrations in cytotoxicity. Data obtained for 3 of the clones are shown in figure 4 as examples.

Similar results were obtained, when the same protocol was applied for UV24C2-3 cells, a hamster human hybrid line. In 20% of cell clones derived from cells surviving 2, 3.5 and 5 Gy Ne-irradiation an enhanced frequency of aberrations were observed 20 to 25 population doublings postirradiation (table 1). In the majority of these aberrant cell clones indications for a delayed chromosomal destabilization were observed manifested as an increase in the number of unstable aberrations and the occurrence of various kinds of re-arrangements between the human and the hamster chromosomes. In a few aberrant cell clones chromosomal instability could not be detected. In these clones 30-100% of metaphases showed identical stable aberrations (translocations between the human and one or two hamster chromosomes) indicating that these aberrations were formed immediately after irradiation or during the first cell divisions and transmitted to daughter cells. Further experiments in which the occurrence of aberrations was investigated in UV24 cell after X-irradiation showed that x-rays were about three times more effective in the induction of aberrant cell clones than Ne ions: karyotype abnormalities were observed in approximately 70% of X-irradiated clones derived from cells surviving X-ray doses of 1.5, 3.5 and 8 Gy (table 1). In most of these aberrant clones indications for chromosomal destabilization were found as observed after Ne-exposure. Analysis of the number of breaks which occurred in the human chromosome indicate that it is involved in the formation of aberrations as expected from its relative size and the background frequency in control cells.

Taken together our experiments clearly show that densely ionizing radiation can lead to a delayed destabilization of the genome. Although marked differences were observed in the quantity and the quality of chromosomal damage induced by particles with different energies and LET values in first mitoses (figure 1 and reference 11) chromosomal instability manifested in all experiments with single cell clones as an increase in the number of cells with unstable aberrations. Moreover, our data indicate that this effect does not depend on applied dose or particle fluence (see table 1). Obviously the passage of one particle through a cell nucleus can trigger processes which finally lead to a delayed destabilization of the genome.
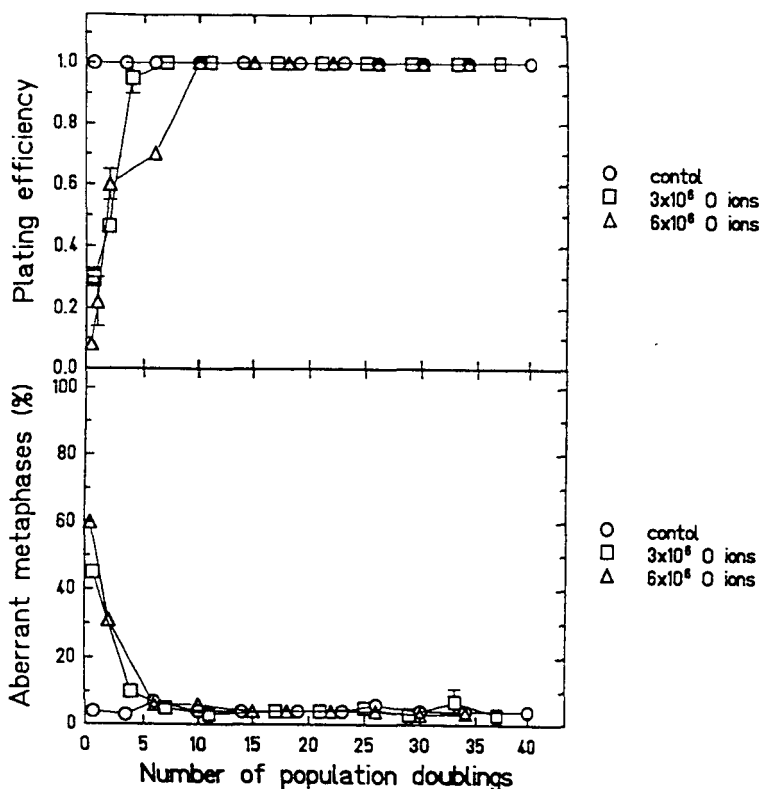
Figure 3: Frequency of aberrant metaphases and plating efficiency in CHO-K1 mass cultures analyzed at different population doublings after the exposure to 3 x 10⁶ and 6 x 10⁶ O ions/cm² (energy: 10.7 MeV/u, LET: 244 keV/µm). Results are mean of 3 separate experiments.
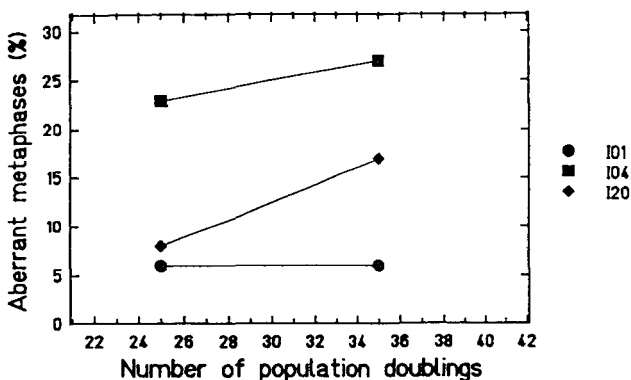
Figure 4: Delayed occurrence of chromosome damage in CHO-K1 clones derived from single parent cells after exposure to 270 MeV/u C ions with a corresponding LET value of 14 keV/µm. In this experiment 20 cell clones were generated and analyzed for chromosomal damage about 25 to 35 population doublings postirradiation. The number of aberrant cells observed at these two occasions is exemplarily shown for 3 clones.

The reason, why chromosomal instability was not detected in CHO cells propagated as mass cultures are not well understood. One possible explanation is that subpopulation which express radiation damage could not contribute substantially to the subcultured population. Due to their slower growth (data not shown) they are diluted progressively by normal growing progeny which do not show chromosomal damage.

Our data however, obtained in experiments with single cell clones of CHO and UV24 cells are consistent with those of Marder and Morgen, who observed chromosomal instability in a hamster-human hybrid cell line carrying the human chromosome 4 after 5 and 10 Gy x-ray exposure[1]. Chromosomal instability also occurred in X-irradiated human T-lymphocytes after clonal growth for 14 to 21 days[2], in primary human skin fibroblasts 15 passages after the exposure to low energy particles[3] and in murine haemopoietic stem cells 10 cell generations after irradiation with α-particles[4].

Meanwhile, there is increasing evidence that the length of telomeric sequences plays an important role for the integrity of chromosomes. In fact, the shortening of telomere length as observed in senescent fibroblasts, in tumour cells and in yeast est1 mutants is associated with an elevated amount of chromosome aberrations[18,19 and references therein]. Particularly, most of the aberrations observed in senescent fibroblasts[20] and tumour cells[18] are dicentric chromosomes. A similar phenomenon was found in our study as well as by others[4] several replication cycles postirradiation. By the use of R-banding Martins et al[4] could clearly demonstrate that indeed the telomeric regions of chromosomes were preferentially involved in the formation of dicentrics. Furthermore, for each cell line, ie. each donor, particular chromosomes were more often involved than others indicating that the delayed expression of chromosomal damage depends strongly on the genetic constitution of the cells.

These delayed effects on chromosomal level represent however, only one particular feature of radiation induced destabilization of the genome. Other examples are delayed reproductive cell death[21] and delayed mutations[22,23]. Identification of underlying cause and the mechanisms by which ionizing radiation induces a delayed destabilization of the genome as well as the assessment of possible health consequences are important challenges for future studies.

Exposure	Number of clones (cells) analyzed	Number of clones with	
		normal	abnormal
Control	25 (3300)	24	1 (4.0%)
1.5 Gy x-rays	6 (600)	1	5 (83.0%)
3.5 Gy x-rays	9 (1050)	3	6 (67.0%)
8.0 Gy x-rays	5 (750)	3	2 (40.0%)
2.0 Gy Ne ions	16 (2200)	14	2 (12.5%)
3.5 Gy Ne ions	6 (1100)	4	2 (33.3%)
5.0 Gy Ne ions	20 (3100)	16	4 (20.0%)

Table 1: Karyotypes in UV cell clones determined 20 to 25 cell divisions after the initial radiation exposure. Cell clones were classified as normal, when 2% aberrant metaphases were found at most. The neon ions had an energy of about 25 MeV/u with an LET 183 keV/μm

References

1   E Solomon et al, Chromosome aberrations and cancer. Science **254**, 1153-1160 (1991).

2   W C Dewey et al, Chromosomal aberrations and mortality of X-irradiated mammalian cells: Emphasis on repair. Proc. Natl. Acad. Sci. **66**, 667-671 (1971).

3   M A Kadhim et al, Transmission of chromosomal instability after plutonium α-irradiation. Nature **355**, 748-740 (1992).

4   M B Martins et al, Specific chromosome instability induced by heavy ions: a step towards transformation of human fibroblasts? Mutat. Res. **285**, 229-237 (1993).

5   K Holmberg et al, Clonal chromosome aberrations and genomic instability in X-irradiated human T-lymphocyte cultures. Mutat. Res. **286**, 321-330 (1993).

6   B A Marder and W F Morgan, Delayed chromosomal instability induced by DNA damage. Mol. Cell. Biol. **13**, 6667-6677 (1993).

7   L Sabatier et al, Chromosome instability and telomeric alterations detected in irradiated human fibroblasts, Proceedings of the 10th International Congress of Radiation Research, 27.8-1.9.1995, Würzburg, Germany, Volume 1, p. 38 (1995).

8   L M Kemp et al, x-ray sensitive mutants of Chinese hamster ovary cells defective in double strand break rejoining. Mut. Res. **132**, 189-1996 (1984).

9   M Durante et al, Radiation-induced chromosomal aberrations in mouse 10T1/2 cells: dependence on the cell-cycle stage at the time of irradiation. Int. J. Radiat. Biol. **65**, 437-447 (1994).

10   S Ritter et al, The kinetics of the expression of chromosomal damage depends strongly on radiation quality. Int. J. Radiat. Biol., **66**, 625-628 (1994).

11   S Ritter et al, Comparison of chromosomal damage induced by sparsely and densely ionizing radiation. Submitted to Int. J. Radiat. Biol. (1995).

12   S Ritter et al, A new approach to determine the total amount of radiation induced chromosomal damage. GSI Scientific Report 94-01, p. 229 (1994).

13   P Perry and S Wolff, New Giemsa method for the differential staining of sister chromatids. Nature **251**, 156-158 (1974).

14   E Goodwin, The LET dependence of interphase chromosome breakage and rejoining in two mammalian cell lines. PhD thesis, University of California, Berkeley (1988).

15   K Fussel: In situ Hybridisierung zur Untersuchung strahleninduzierter Chromosomenschäden. Diploma thesis, TH Darmstadt, FRG, GSI Report 94-07 (1994).

16   W P Chang and J B Little, Evidence that DNA double strand breaks initiate the phenotype of delayed reproductive death in Chinese hamster ovary. Radiat. Res. **131**, 53-59 (1992).

17   J Heilmann et al, DNA strand break induction and rejoining and cellular recovery in mammalian cells after heavy ion irradiation. Radiat. Res. **135**, 46-55 (1993).

18   S Pathak et al, Telomeric association: another characteristic of cancer chromosomes. Cytogenet. Cell Genet. **47**, 227-229 (1988).

19   C W Greider, Telomeres, telomerase and senescence. BioAssays **12**, 363-369 (1990),.

20   P A Benn, Specific chromosome aberrations in senescent fibroblasts cell lines derived from human embryos. Am. J. Hum. Genet. **28**, 465-473 (1976).

21   W P Chang and J B Little, Delayed reproductive death in X-irradiated Chinese hamster ovary cells. Int. J. Radiat. Biol. **60**, 483-496 (1991).

22   W P Chang and J B Little, Persistently elevated frequency of spontaneous mutations in progeny of CHO cells surviving X-irradiation: association with delayed reproductive death phenotype. Mutat. Res. **270**, 191-199 (1992).

23   T Stomato et al, Delayed mutation in Chinese hamster cells. Somat. Cell Molec. Genet. **13**, 57-66 (1987).

List of publications

S Ritter, E Nasonova, W Kraft-Weyrather and G Kraft: The kinetics of the expression of chromosomal damage depends strongly on radiation quality. Int. J. Radiat. Biol., **66**, 625-628 (1994).

K Füssel: In situ Hybridisierung zur Untersuchung strahleninduzierter Chromosomenschäden, Diploma thesis, TH Darmstadt, FRG, GSI Report 94-07 (1994).

S Ritter, E Nasonova, K Fussel and G Kraft: A new approach to determine the total amount of radiation induced chromosomal damage, GSI Scientific Report 94-01, p. 229 (1994).

S Ritter, K Fussel, H Strehl, G Kraft, E Nasonova, T Fomenkova: Radiation induced initial and delayed chromosomal damage, GSI Scientific Report 95-01, p. 206 (1995).

S Ritter, E Nasonova, M Scholz, W Kraft-Weyrather and G Kraft: Comparison of chromosomal damage induced by sparsely and densely ionizing radiation, submitted to Int. J. Radiat. Biol. (1995).

Conference contributions

S Ritter, E Nasonova, W Kraft-Weyrather, T Fomenkova und G Kraft: Induktion von Chromosomenaberrationen in CHO-K1 Zellen und reparaturdefizienten xrs-5 Zellen nach Hoch-LET Bestrahlung, DNA Schäden und ire Reparatur, 1.4.3. 1994, Gottingen, Germany.

S Ritter, E Blakely and G Kraft; Genetic instability induced by high and low LET radiation, Symposium on Genetic Instability and Cancer, 17-19.10. 1994, München, Germany.

S Ritter, E Nasonova and G Kraft: Differences in the induction of chromosomal damage after the exposure of cells to charged particles or x-rays, Third Symposium on Swift Heavy Ions in Matter, 15-19.5 1995, Caen, France.

E Nasonova, S Ritter, M Scholz and G Kraft: Influence of radiation quality on the induction of chromosomal damage, Fifth Workshop on Charged Particles in Biology and Medicine, 23-25.8.1995, Darmstadt, Germany.

E Nasonova, S Ritter, M Scholz, W Kraft-Weyrather and G Kraft: Comparison of chromosomal damage induced by high and low LET radiation, 10th International Congress of Radiation Research, 27.8-1.9.1995, Würzburg, Deutschland (invited talk).

S Ritter, G Kraft and E A Blakely: Delayed chromosomal instability by high and low LET radiation, 10th International Congress of Radiation Research. 27.8-1.9.1995, Würzburg, Deutschland (invited talk).

Final Report
1993-1995

Contract: F13PCT930067   Duration: 1.1.93 to 30.6.95   Sector B13

Title: Development and investigation of systems for the quantification of radiation
induced carcinogenesis in humans.

1) Mothersill   Inst of Technology - Dublin
2) Riches   Univ. St. Andrews
5) Luccioni   CEA - Paris
6) Martin   CEA - IPSN
7) Arrand   Univ. Brunel
8) Franek   IMG - DFC

Summary of Project Global Objectives and Achievements

The objective was to develop a system to quantify the risk of radiation-induced cancer
in humans. When the project was submitted the only in vitro system in use for
quantitative radiation studies was the C3H 10T1/2 mouse prostate cell line. Human
cell lines had just become available due to development of new culture techniques
and transfection vectors. The potential of these lines for quantitative studies had not
been investigated. Most of the available human lines had been transfected with human
or monkey viruses to immortalise them for study. This called their relevance into
question since the initial events in human carcinogenesis unlike rodent carcinogenesis
are rare and are prevented from occurring by a very complex and efficient system of
barriers. This makes them difficult to achieve in vitro and even more difficult to
validate due to the multistep nature of the process. However these are the events
which really require quantification and elucidation in radiation protection. The project
therefore pursued two parallel lines of investigation:
a. Evaluation of the existing human transfected or otherwise immortalised systems to
see whether they could yield quantitative data, whether these data made sense in the
context of known radiobiological responses and mechanisms and whether
comparative risks could be determined for dose rates and radiation qualities using
human cells from radiosensitive target organs: Quantitative data consistent with
radiobiological predictions could be obtained for a human thyroid cell line.
b. Development of new systems for investigating early events in non immortalised
cells: Animal and human tissues or primary cultures were irradiated and expression of
mutations or abnormalities in signal transduction or tumour suppresser genes was
quantified. In the human cultures p53 dependent apoptosis was found to be an
important mechanism removing damaged cells from the population and considerable
individual variation in p53 stabilisation was noted. Mutations in the p53 gene were
induced against a background of stabilised p53 protein at 0.5Gy in two primary
human systems. Animal studies showed long-term changes in the early response
genes cfos and cjun as well as similar stabilisation of p53. These systems also allowed
bridging from in vitro to in vivo
**The major conclusions from the study are that quantitative data on tumour
frequency can be obtained for limited lines of human cells which have already
been immortalised. These lines are useful for evaluating radiation risks for
smokers, patients with HPV 16 lesions and others with environmental
carcinogen exposure and for studying mechanisms or relative effects. The
primary human systems can give quantitative information on frequency of
relevant early events and inter-individual variation. An approach integrating
data from both types of system offers a real alternative to animal models.**

Recommendations are listed at the end of this concensus statement.

Background

Cancer induction remains the single most worrying effect of human exposure to low doses of ionising radiation. The challenge of this project was to find a way of measuring the risk to human target cells without having to rely on extrapolation from animal models or uncertain epidemiological studies. The group initially combined cell culturists, molecular biologists and radiobiologists. Later additions were an apoptosis expert and an in vivo/in vitro group. The strategy of the project management was to conduct related investigations using established human immortalised cells, primary human and animal tissues and animals. In this way it was hoped to obtain quantitative data and cross validate to human primary tissues and to animal in vivo systems.

Methods and cell systems used

When the proposal was originally approved several new human epithelial cell lines had just become available. These represented a potential increase in relevance over the existing C3H 10T1/2 system exclusively in use for quantitative work at the time. The lines had not been investigated by radiobiologists and the cause of their immortalisation was not known although virus transfection was a common immortalising agent. The cell lines tested during this project were HT ori cells (SV 40 immortalised human thyroid), HPV G cells (human keratinocytes transfected with HPV 16), L132 (Human bronchial epithelium unknown cause of immortalisation), S-HUC (human urothelial cells immortalised with SV 40), HaCAT cells (human skin from a melanoma patient with abnormal p53). Partners 1,2 and 7 were involved with this part of the project. Even at the start of the project it was accepted that the ideal cells for these studies would be primary normal cultures, although the chance of obtaining all the steps in multistage carcinogenesis in culture from low dose radiation exposure was remote. Therefore the second part of the project done in all the laboratories used human and animal tissues and concentrated on detection of mutations or early changes expression of growth control, apoptosis and signal transduction genes. Tissues from human adult and paediatric bladder, skin, oral cavity and gut and from pig skin and rat foetal brain were used. The animal tissues were irradiated in vivo or in vitro, the human tissues were irradiated as tissue explants as soon as possible after removal from the body. The endpoints used for identification of early events and for mechanistic investigations of cells and tumours from irradiated cell lines were
1. Mutations in the p53 gene and p53 protein expression and distribution,
2. Growth potential, including extended life-span,
3. Expression of signal transduction genes, *cfos, cjun* and p^{21ras} and EGFr proteins,
4. Induction of apoptosis and changes in the expression of bcl-2 and cmyc proteins.

Synthesis of results:

There follows a short summary of overall advances in the areas listed above. Full details of specific partner contributions may be found in the individual reports which follow this and in the listed publications.

1. The relevance of p53: When the project started two years ago, the results obtained by these and other groups were very confusing and seemed contradictory. The group used a complimentary approach to try to define the role of the detected changes in p53 in radiation carcinogenesis. The situation has now clarified considerably and is summarised as follows

a. p53 protein expression was detected by the Dublin and Saclay group following very low dose exposure (0.1-0.5Gy). The expression was widespread and at least in human cells, cytoplasmic. It persisted for several days post irradiation and was not the

same as the early wild type response which declines after a few hours.. Investigations by the Dublin, Brunel and Saclay groups, showed that the cells did not appear at this stage to have p53 gene mutations. The effect was therefore considered to be stable but post-translational. Since the stabilised protein remained in the cytoplasm in adult human cells, it was presumed that the net effect of the change would be to abrogate p53 function in the affected cells. The Saclay group found stabilisation of the protein in the nucleus in the foetal rat lung. This was associated with radiosensitivity and increased function. This contrasted with their observations in adult human cells and may equally well be explained by species or age differences

b. When human cultures were maintained until the senescence crisis, small foci were seen to develop in the Dublin group system (normal human epithelium), these were analysed in Brunel and later in Dublin and showed evidence of multiple instabilities in the p53 gene in focal cells. Surrounding cells although p53 protein positive were p53 mutation negative.

c. The St. Andrews and Brunel groups working with SV 40 transfected HTori cells (high levels of inactivated T antigen complexed p53 but no mutations) and extended lifespan L132 cells (which have high expression of stable p53 protein but no gene mutations also found high levels of induction of multiple instabilities in the hot spot exons of the p53 gene post low dose and dose rate irradiation.

Taken together these data suggest two distinct effects of radiation on the p53 system; first a common non mutational stabilisation of the protein. This effect requires further study, but obviously marks a reduced ability of irradiated cells to fine-tune their response to cellular signals controlled by p53 mediated pathways. The second effect is mutational. Mutations occur at a high frequency in the p53 gene in circumstances where p53 is post translationally stabilised. Two questions arise which require further study; first, what is the mechanism underlying the initial stabilisation of p53 and second, is the level of mutations in p53 indicative of the level of mutations through out the genome? Given the current data emerging from this project and other work world-wide on radiation induced genetic instability and the occurrence of new lethal and non lethal mutations in distant progeny of irradiated cells it could be suggested that the deregulation of p53-mediated surveillance by radiation makes genetic mutations anywhere in the genome of descendants of irradiated cells more probable. If these occur in a critical tumour suppresser gene, cancer initiation occurs. In this context the wide variation in the p53 stabilisation response seen by the Dublin laboratory in different patients, is relevant to design of radiation protection programmes based on identification of "at risk" sub-populations.

Conclusion: Low dose irradiation causes a generalised stabilisation of p53 protein in the cytoplasm of exposed human cells and their progeny preventing it's surveillance role. This may allow the observed high rate of mutations which occur in the descendants of irradiated cells.

2. Induction of p53 and other "early response genes " by very low doses and/or dose rates of radiation:
The groups in the project using radiation, included very low doses (< 0.5Gy) in their studies. All found these doses to be effective at inducing a whole group of proteins involved in signalling damage and orchestrating response. Apoptosis could also be detected at these low doses. Low dose rates (region 0.2-0.5Gy / hour) used by the Paris (rat glial cells) and Brunel (human bronchial cells) groups proved at least as effective as and often more effective than higher doses in inducing responses. The evidence from Brunel would suggest that the lowest dose rate was most effective in inducing p53 mutations. The Dublin group (human urothelial cells) has evidence of induction of p53 protein stabilisation after only 0.1Gy and this result has been confirmed in Dr Lechner's laboratory in the US using normal human bronchial epithelium. Induction of signal transduction

proteins cfos and cjun by the Saclay group and of epidermal growth factor receptor and $p^{21\ ras}$ by the Dublin group at these low doses points to a sustained cellular response to damage which may be associated with enhanced proliferation of irradiated cells. cfos and cjun and ras are transcription factors, EGFr stimulates cellular proliferation by increasing cellular EGF levels. Taken with the deregulation of p53 and the increase in bcl-2, the long-term change brought about in the majority of cells by these doses of radiation would appear to be one facilitating, as a priority, growth and repopulation, since the surveillance system appears to be disarmed. Experiments with low dose rates also showed induction of these proteins. These doses are in the occupational exposure range and are frequently encountered during medical exposures including mammography.

Conclusion: Low doses and dose rates of gamma and x-rays in the range of interest in radiation protection induce long-term expression of genes involved in cell growth.

3. Quantification of transformation frequency using human and other cells: The clearly unrealistic, goal of radiation transformation research is to irradiate a known number of normal human cells and determine how many of the survivors form a tumour in a compatible host. This would allow risk estimate to be based on actual data from cells of human target organs. This has now been shown by this project and by many other workers in the field to be a biologically unsound approach because of i. the complex multistep nature of the transformation process, ii. the likelihood that radiation can act at several points during this process and iii. the interactions which are now known to occur between different cell types during carcinogenesis in tissues. The group took a multifaceted approach to this problem; a. it was recognised that the new human culture systems had not been evaluated for their potential use, or defined in relation to their position along the carcinogenesis pathway. Each group in the project therefore obtained some of the lines and set up dose response experiments. The survivors from irradiation were injected into nude mice at St Andrews. These experiments quickly showed that the different lines had widely different capacities to transform (as defined by nude mouse tumour formation). All cells of the HPV G line formed tumours whether irradiated or not, as did the L132 bronchial cell line even though these cells had not been immortalised by transfection and had a limited lifespan in culture. The SV 40 transfected HUC line formed very few tumours and was extremely resistant to transformation by radiation. The group also became concerned about the uncertain staging of these cells. Finally the group concentrated on two lines; HTori 3 cells because they derived from human thyroid and gave meaningful dose quality data and the HaCat line, because these cells could be cultured as organotypic human skin and because the mutation leading to immortalisation was known to be in p53. Traditional transformation experiments were performed in St Andrews and yielded dose quality data suggesting a factor of four for transformation of HTori cells exposed to alpha versus gamma irradiation. The compromise of the p53 pathway by SV 40 in these cells should not detract from the results because as has been shown by the Dublin group, p53 function is affected by smoking and by exposure to nitrosamines in the environment. Analysis of transformation needs therefore to be done under various conditions of p53 function/dysfunction. The critical factor is to know the status of p53 and interpret results in this light.

b. The HaCaT cells were used in Saclay to look at the influence of mesenchyme on the radiation response of skin epithelial cells. The results suggested that in spite of the presence of p53 mutations in this line, it behaved like normal skin epithelium following irradiation and induced p53 in a wild-type manner. The mesenchyme was concluded to be exerting a major influence in this organotypic model. The line was used without mesenchyme in Dublin but no traditional transformants were obtained at the doses used.

c. An animal system (the rat foetal glial cell model) was used to try to validate in vitro results with reference to iv vivo experience. This longterm study required development of culture systems for rat glial cells and only very preliminary data was produced.

Conclusions: HTori cells can yield useful quantitative data, and are worth characterising in more detail. HaCaT cells in organotypic culture can provide useful mechanistic data on the influence of mesenchyme on epithelial cell transformation and on the role of p53. In general if cell lines are used for these studies they should be used only after characterisation of the status of key tumour suppresser genes, or to obtain relative data eg. effects of different dose rates or radiation qualities. They could also be useful in predicting risk for smokers and people with HPV virus infections who have cells with compromised p53.

4. Apoptosis following irradiation;measurement, role and control: During the course of this contract, it became apparent from the literature and the project work, that apoptosis was a major determinant of the frequency of initiating mutations. Apoptotic mechanisms induced following DNA damage, trigger programmed cell death in cells with unrepaired damage, preventing them from contributing to the reproductive population. A dead cell cannot ever form a cancer, but a live but damaged cell which avoids apoptosis is a key candidate. The measurement of apoptosis in relation to dose, dose rate and cell type was therefore regarded as a key objective. The PECO programme allowed the Prague Institute of Molecular Genetics who have wide experience of apoptosis measurement, to become involved for a short period in the project. This group compared methods and collaborated with Dublin to assess the levels of apoptosis in HPV-G cells. The results suggested that light microscopy or the TUNEL assay were most useful, a finding shared by other apoptosis laboratories. The Dublin laboratory finally decided to use morphology and the bcl-2/cmyc immunocytochemical staining pattern to quantify apoptosis in bladder cultures irradiated to 0.1-5Gy obtained from 22 patients. The main results from this study were that apoptotic death predominated at low rather than high doses in most patient cultures. The apoptosis seemed to be prevented by bcl-2 induction which occurred above a threshold dose in the 0.3-0.7Gy range and varied from patient to patient. A sub-group of about 30% of patients did not show induced resistance in this region and their pattern of bcl-2, cmyc and p53 induction post irradiation was clearly different.

Conclusions: Apoptosis is induced at low doses of radiation but prevented by bcl-2 protein induction at higher doses. Significant patient variation in response at the quantitative and qualitative level was seen and may be important for understanding the basis of individual radiosensitivity and cancer predisposition.

Overall recommendations

1. The **use of human in vitro systems** for carcinogenesis studies **must continue** in parallel with rodent studies **because the differences in rates of induction of initial carcinogenic steps in human and rodent systems point to mechanistic differences** as well as quantitative effects which need to be understood for risk assessment. The argument that p53 compromised cell lines are not relevant to human carcinogenesis no longer acceptable given the high proportion of the general population which our project has identified as having compromised p53 due to smoking or other environmental carcinogenic exposure..

2. The project has shown that **inter-individual variation in initial response to radiation** occurs, that the initial response can lead to abrogation of apoptotic cell death and loss of p53 surveillence. The type of initial response can be detected using

simple tests on biopsy material. If it can be demonstrated that these test predict for in vivo response it could help **identify radiosensitive sub-groups** before they are exposed to occupational or medical radiation.

3. The results from three different laboratories in the project using different systems clearly support a theory which is emerging world-wide that the "first event" in **radiation** carcinogenesis is is epigenetic and not mutational. It **predisposes all or most** of the **cells and their progeny** in an exposed tissue **to mutations** and seems in this project and other research to be associated with stabilisation of p53 or prevention of apoptosis by other means. This fundamentally alters the basis on which radiation risk assessment is determined. It is recommended **that research in this area be initiated urgently,** to determine the dose, dose rate and radiation quality relationships of this effect.

Head of Project 1: Dr Mothersill

II. Objectives for the Reporting period

1. To use primary human epithelial cells to identify and quantify the early pre immortalisation steps in radiation carcinogenesis.

2. In collaboration with Brunel University, to identify and quantify mutations in the human p53 tumour suppresser gene following exposure to low doses of radiation.

3. To identify, quantify and assess the relevance to carcinogenesis, of cell loss in the near and distant progeny of irradiated cells which have already undergone the immortalisation step.

4. In collaboration with Inst Molecular genetics, Prague, to identify the mechanism of cell death and it's control.

5. In collaboration with St Andrew's university, to screen surviving progeny of irradiated primary and immortalised human cells for ability to produce tumours in nude mice.

6. In collaboration with CEA Saclay to analyse media samples for presence of early response oncogene products in cultures of irradiated cells.

7. To analyse individual variation in post irradiation early responses in patients likely to be at high risk of cancer development.

III. Progress achieved including publications

1. The use of primary human epithelial cells to identify and quantify the early pre immortalisation steps in radiation carcinogenesis.

Considerable progress was made in the identification of early pre-immortalisation steps in human radiation carcinogenesis. The approach used was to obtain absolutely normal tissue, culture it using organotypic methods, expose the culture and assess the extent of development of clinically established, pre-neoplastic morphological features and cancer predisposing genetic changes. Four tissues were investigated; bladder (173 patients), skin (8 patients), cervix (126 patients) and oral mucosa (104 patients). Organotypic cultures were established in Clonetics medium without serum. Some cultures were exposed initially and followed for as long as possible, to allow post irradiation growth and development of pre-neoplastic hyperplasia, with associated loss of growth and apoptosis control. Others were exposed and fixed at different time periods to permit the study of initial responses to radiation in cultures which had grown and established differentiated structures which could be relevant to response in vivo (mucous coating, stem or basal cell stratification etc.). Endpoints for preneoplastic change included, i. conformational change in p53 with and without genetic mutation, ii. over expression of signal transduction proteins, p^{21ras}, or epidermal growth factor receptor, iii. loss of apoptosis control, including over expression of bcl-2, alterations in cmyc expression, presence of morphologically abnormal cells in cultures, hyperplasia and focus formation and cytoplasmic p53 expression. iv. Loss of gap junctional protein expression v. loss of senescence control, including extended culture life span and absence of senescence morphology. In all cases clinically defined and characterised tumours and preneoplastic lesions from the relevant tissues were used as positive controls. The main mean results for induction by radiation of growth control and signal transduction genes in the normal bladder are shown in table 1. Results for the other tissues were similar and are not shown. Details will be found in the theses presented by R. el-Gehani, H. Lambkin and M. Sheridan.

Table 1

Growth, Apoptosis and Protein expression following carcinogen exposure of human urothelium. Mean±S.E. of 156 patients for growth and protein expression measured on day 14 post irradiation and 15 patients for apoptosis measurements measured 4 hours after exposure.

Treatment	0	0.5Gy	5Gy	NNAL	N+0.5Gy	N+5Gy
%Cont Growth	100±4.3	39±12.6	65±15.5	105±8.9	98.6±4.4	92.1±6.4
% apop cells	1.2±0.2	21.4±18.8	4.3±4.1	1.1±0.3	1.6±0.5	1.2±0.4
% p53 +	12.6±8.1	76.3±24.8	54.8±21.1	45.2±6.1	58.6±31.4	65.1±6.4
% bcl-2 +	1.8±2.4	42.7±26.8	78.5±10.6	96.5±12.4	95.1±5.3	89.5±4.4
%cmyc +	24.3±17.6	30.9±16.5	50.9±5.8	73.8±12.9	74.1±13.4	66.3±13.8
% EGFr +	44.3±31.1	59.1±32.4	68.3±21.1	88.4±12.6	81.2±6.9	76.5±7.3
% ras +	0.8±0.4	68.4±22.3	89.7±21.5	59.1±26.7	88.5±7.9	99.6±6.2

NNAL is a specific nitrosamine derivative suspected of causing bladder cancer, found in urine from smokers. The active conc. used here is 5ng / ml. It was used here to try to augment the changes induced by radiation through it's sustained effect on gap junction intercellular communication, (see publ. 14)

The important results in this table are that radiation causes a sustained increase in expression of proteins which are associated with carcinogenesis. Expression patterns for p53 and bcl-2 in particular are very favourable to the progression of cells towards neoplasia. All these proteins are overexpressed in the positive control neoplastic and preneoplastic tissues and cultures examined (see publications 6, 9, M.Dent Sci. thesis from R. el Gehani and PhD theses from M. Sheridan and H. Lambkin).

The most pronounced reduction in growth potential of the cultures and highest amounts of apoptosis occurred after low dose exposure. The higher dose of 5Gy caused less apoptosis, (measured immediately) and less growth reduction after 14 days. Full grow back curves for twenty two patients meaned in Table 2 confirm this and show a consistent change in response of patients cultures to radiation occurring in the 0.3-0.7 dose range. This effect was published for the first nine patients earlier this year (publ 6). Electron microscopy clearly shows that apoptosis is a major response to 0.5Gy irradiation but is not found to the same extent after 5.0Gy or if nitrosamines are present (see publs 6, 12 and Ph D thesis from F.Lyng). The pattern of bcl-2 expression also changes from being very variable at 0.5Gy to being over-expressed in virtually all cells after 5Gy.

Gap junction intercellular communication (GJIC)was also investigated since it is important in maintaining normal growth control and damage response signalling. The results showed that gap junction connexins 43 and 26 had normal protein expression and mRNA activity (assessed using RT-PCR) following irradiation (0.5 or 5Gy) although GJIC was temporarily reduced for up to 1h. post exposure.

All these results taken together support an emerging hypothesis that the earliest carcinogenic steps occur in many cells following irradiation, are pre- immortalisation events and involve deregulation of apoptotic death and loss of growth control. Thus progeny of irradiated cells are predisposed to accumulation of further preneoplastic and later, neoplastic changes. It seems likely, given the hypersensitivity noted at low doses, that some mechanisms may operate differently in the low dose region and that the mechanisms designed to maintain tissue integrity (repair, repopulation) may require a threshold dose before becoming operational. It is not yet clear whether these

mechanisms reduce or increase the risk of radiation induced carcinogenic initiation but it is clearly very important to investigate this.

Table 2

Percent of control growth detected after 14 days in cultures from 22 patients exposed to gamma radiation doses in the 0.1-5 Gy range.

Dose (Gy)	% control survival measured on day14
control	100
0.1	55.5±8.5
0.2	35.1±13
0.3	46.8±8.2
0.4	35.1±30.1
0.5	70±13.1
0.7	65.9±10.3
1.0	70.1±11.2
2.0	68.6±10.8
3.0	67.9±10.5
5.0	48.8±10.3

2. Identification and quantification of mutations in the human p53 tumour suppresser gene following exposure to low doses of radiation.

Mutations in the p53 gene occur in over 50% of human cancers. Many others with viral (HPV or E1A) aetiology also have complexed or destroyed p53 protein even though a mutation may not be present. The easiest, some say only way to immortalise human cells in culture, involves mutating the p53 gene or otherwise complexing their p53 protein. The importance of the protein in human carcinogenesis particularly in preventing the early, pre-immortalisation steps, cannot now be doubted. In these experiments, p53 protein expression was found to be strongly increased by irradiation, in all the normal tissues examined(see publs 1, 2). Expression in control unirradiated tumours and preneoplastic lesion was similar as was expression in normal unirradiated oral and cystoscopic tissue biopsy cultures from smokers (publs 5,7,8,9,10). The pattern of cytoplasmic expression detected using the p53-240 antibody over two weeks post exposure to radiation, is highly suggestive of the presence of p53 mutations. However the wide spread distribution of the "mutant" protein and the implausibility of induction of widespread mutations in several cells in several patients by low doses of radiation, makes a post-translational mechanism more likely. To look at this, tissue cultures were maintained post-irradiation for as long as possible, then the DNA was extracted and analysed using PCR-SSCPE in collaboration with Brunel University. Only cultures from non smokers were used since other work in the laboratory had shown a statistically significant high level of SSCP gel mobility shifts in the p53 gene (exons 5-8) in bladder and oral biopsy cultures from smokers. The results for a representative sample of 5 individual bladder cultures from non smokers are shown in Table 3. Similar results were obtained for the other tissues but space precludes their inclusion. Immunocytochemistry data for these patients is also shown on the table. There are several interesting points from these results;

1. They clearly show that expression of the conformationally stable form of the protein does not mean that the gene is mutated. It does however mean that the protein is not functional since it is accumulating in the cytoplasm and is not present in the nucleus, the site of it's cell cycle control functions.

2. They show that p53 mutations do occur in these irradiated cultures but i. they are a late effect of radiation and they only occur in piled up foci which are not contact inhibited and show no differentiated characteristics, ii. They occur in the foci from both 0.5 and 5Gy irradiated cultures.

3. there is a suggestion that bcl-2 may be important since the patient with high bcl-2 pre- exposure had the greatest number of induced mutations (note that even for this patient the surrounding cells were negative for p53 mutations).

It is concluded from this section that the carcinogenic effects of radiation may involve stabilisation of p53 protein which in turn makes mutations in this and other genes more likely to occur. The possibility that factors other than radiation can induce the actual carcinogenic mutations in a radiation induced unstable population of cells cannot be ruled out and in fact seems the logical conclusion to draw from these data. It is important to investigate this further in more longterm cultures so that the instability effect and the mutation effect can be clearly separated and the role of radiation in each process defined for humans.

Table 3:

SSCPE-PCR mobility shifts [MS] post exposure , %bcl 2 and p53 immunocytochemical data pre- and post-exposure to irradiation for 5 normal urothelial cultures from non smoking patients.

Patient No.	1	2	3	4	5
MS 0Gy	0	0	0	0	0
MS 0.5Gy	0	0	0	0	0
MS 5Gy	0	0	0	0	0
MS 0.5Gy Foci	1	3	16	1	1
MS 5Gy Foci	1	?1	1	1	0
MS N+0.5Gy Foci	0	0	3	1	0
MS N+5Gy Foci	1	0	0	0	3
% post 0.5GY p53	64.3	84.8	68.8	53.9	51.1
%post 0.5Gy bcl-2	1.7	19.4	97.8	6.8	5.6
% control bcl-2+	0	1.2	99.3	0	0
% control p53+	0	0	0	0	0

3. Identification, quantification and assessment of the relevance to carcinogenesis, of cell loss in the near and distant progeny of irradiated cells which have already undergone the immortalisation step.

The work in this section was aimed at understanding the contribution of late post irradiation cell loss (lethal mutation, heritable lethal defects, de novo induction of lethal chromosomal aberrations), to the carcinogenic process in humans. Lethal mutations have been found post irradiation, by several investigators, in every repair competent cell system studied and have been detected in vivo in rodents. They do not occur in repair deficient cells or cells which have their ATP producing system inhibited. They occur for at least 70 cell divisions post irradiation and result in significant reductions in observed yield of cells over the expected yield if all cells had the same division potential as their unirradiated controls. They are obviously important to the quantification of transformation since they represent significant cell loss after the measurement of cell survival is usually made. Given the recent acceptance that initiation of carcinogenesis in humans, is a multi stage process, it is obvious that any process which remove cells from the exposed pool of progeny will

influence the ultimate probability of initiation. In addition there is the interesting problem of whether lethal mutations represent one end of a spectrum of mutations some of which may be carcinogenic (this would support the idea of irradiated cells providing a population of cells more at risk for mutation), or whether lethal mutations are a programmed cell death mechanism designed to rid populations of irradiated survivors of potentially carcinogenic cells. The major results of these studies are contained in publs 3, 12 and 13 and in the Ph D theses presented by S. O'Reilly and F. Lyng.

In summary they show:

1. Lethal mutations occur at a constant rate per cell division at all doses above a threshold which is at 2Gy for human immortalised keratinocytes (HPV-G cells). The dose induction curve for other cells has not yet been determined but other data would suggest the threshold may be lower in primary cells. The cell loss in HPV-G cells accounts for approximately 15% reduction in yield per cell division, i.e. 15% less cells than expected result from each division of the post irradiation population. An example of the cumulative effect of this on an expanded population of keratinocytes is to reduce to expanded population from the control value of 10^{13} cells per cell to 10^6 per cell after 2Gy and 50 population doublings post exposure. Doses below 2Gy yielded no lethal mutations in these cells. The slopes and intercepts of growth curves post irradiation which demonstrate this point are shown in table 4 . These results suggest that "lethal mutations" are a true mutation produced during the previous cell division and do not represent a "weeding out" of damaged cells. They could of course still be a mechanism for dealing with the products of instability, induced initially by irradiation.

2. Expression of lethal mutations is reduced in circumstances associated with progression of carcinogenesis. Three situations were investigated; ras transfection, incubation with the chemical carcinogen, nitrosamine and the use of transformed versus normal cells. In each case the yield of lethal mutations is reduced in the more neoplastic cells and eliminated altogether in fully malignant cells. In these latter cells, radiation led to increased cell division and greater division success. It is of great importance to assess the chromosomal stability and mutational load of these cells. preliminary results produced in association with E. Wright, suggest that yields of lethal chromosomal defects are quantitatively similar to lethal mutation loads in cell populations post irradiation. This may indicate that inhibition of lethal mutations is a major mechanism in progression towards a more malignant phenotype, but information on the non lethal chromosomal aberrations or mutations in these cells and the frequency on these in relation to lethal mutations is critical in any attempt to assess relevance to carcinogenesis in humans.

Table 4
Intercepts and slopes for the exponential portion (days 6-12 inclusive) of the post-irradiation growth curves for HPV transfected human keratinocytes

Dose (Gy)	y-axis intercepts of exponential regions of growth curves	slopes of exponential regions of growth curves
0	1.813	0.369
1	1.653	0.366
2	1.716	0.320
3	0.397	0.269
4	0.204	0.352
5	0.204	0.307
6	0.301	0.317

4. Identification the mechanism of delayed cell death and it's control.

This task involved an attempt to determine the mode of death of cells post irradiation and in particular the type of death undergone by late lethally mutated cells. Experiments performed in Prague and Dublin using electron microscopy and DNA fragmentation techniques suggested that lethal mutations occurred by apoptosis. At very high doses (5Gy and higher) necrosis was also a feature of distant clonal progeny of irradiated survivors.

The importance of apoptosis in the mechanism is confirmed by analysis of the anti-apoptosis protein bcl-2. This protein is induced in human primary cultures 2-4 hours following irradiation but declines with each cell division to low levels. It is likely that the presence of the protein initially overrules the apoptotic pathway after irradiation, but this pathway may re-emerge as the bcl-2 level falls. The persistence of bcl-2 in many tumours and neoplastic cell lines may support a key role for bcl-2 in facilitating an unstable, mutation prone state post irradiation. bcl-2 was not found to be induced in immortalised p53 compromised cells (HPV or HaCAT human keratinocytes). The mechanisms underlying control of bcl-2 induction and the relationship to p53 status need further investigation.

5. Screening of surviving progeny of irradiated primary and immortalised human cells for ability to produce tumours in nude mice:

This work aimed at assessing the tumourigenicity of abnormal cells identified in culture was performed in collaboration with Dr A Riches. The results were disappointing. All the HPV transfected human keratinocyte produced tumours in nude mice whether irradiated or not. Sections of these tumours were sent to Dr DiPaolo in NIH Bethesda, who developed the line and states the cells are not tumourigenic. The consensus of opinion is now that the "tumours" produced by controls are epidermal cysts and not malignant, since no invasion could be seen. When sections were scored blind at NIH, it was possible to identify tumours from irradiated cells as morphologically more anaplastic and there was evidence of invasion into the muscle (a very rare finding using nude mice). These results make the interpretation of results using these cells very difficult since it would be necessary to use markers of invasion and metastasis on sections to verify a radiation effect. Clearly quantitative data would be impossible to get with this system although it may prove useful later to determine the ability of radiation to convert from the non-invasive to invasive stage in multi-stage carcinogenesis. A full account of the work summarised here may be found in Dr O'Reilly's Ph D thesis. Nude mouse experiments were also performed using the foci which developed from primary urothelial and oral cultures. These foci failed to grow even though they had confirmed mutations in the p53 gene. Presumably further stages of malignant progression are required before cells will grow in nude mice.

It is concluded from these results that

i. Human cells immortalised by viral transfection are not useful for quantifying very early initial events in carcinogenesis since they have already undergone an undefined number of changes. They could however be very good for assessing radiation risk in people with HPV infection or in smokers(see section 7)! Knock out lines such as those developed by Cathy Reznikoff which have E6 or E7 proteins specifically transfected in to block p53 or Rb may be more useful for general mechanistic studies.

ii. Initial events caused by radiation (eg p53 conformational changes, genomic instability induction of anti apoptotic genes), which may ultimately lead to carcinogenesis need to be identified and quantified separately from the later or final events (eg nude mouse tumour production, acquisition of invasive or metastatic

potential). Strategies must be developed for identifying and characterising the early events in humans where barriers to carcinogenesis are so strong.

6. Analysis of media samples for presence of early response oncogene products in cultures of irradiated cells.

Media from representative experiments was collected but time and shortage of funds did not permit CEA to analyse the samples. Samples were therefore used in Dublin to look at early response proteins (mainly heat shock protein HSP 70 and LDH) and aerobic / anaerobic metabolism. Results are only preliminary but interesting enough to suggest further work would be worth while. HSP 70 was detected following any exposure to radiation (dose range 0.1-5Gy). LDH was also released into the medium but only at doses above 0.5Gy for human urothelium and 0.7Gy for oral mucosa. Analysis of LDH isoenzyme pattern in the cultured cells showed a shift from the aerobic to the anaerobic form post irradiation with the same tissue specific dose response pattern. This would be consistent with the induction of anti-apoptosis mechanisms at these doses which are thought to involve reduction of oxidative species. Analysis of lactate and glucose levels in media samples also supports this since much higher lactate production occurred in cultures from irradiated tissues (% of glucose used which was converted to lactate was 96 ± 0.8 for 5Gy irradiated cells compared to $46\pm16\%$ for 0.3Gy irradiated cells and $42\pm3.6\%$ for the controls.

7. To analyse individual variation in post irradiation early responses to identify patients likely to be at high risk of cancer development.

Prediction of radiosensitive people or those at increased risk of developing cancer from radiation is a major goal of this project and of radiation protection. The approach used to look at individual variation was to culture tissue from as many normal people and tissue types as possible and to look at the variation in response. Indicators of response were chosen on the basis of evidence that the gene product or process is implicated in initiation of carcinogenesis and that the expression of the endpoint varied in individuals. Endpoints finally chosen were post irradiation growth response, pre- and post- irradiation incidence of cytoplasmic p53, pre- and post - irradiation frequency of bcl-2 + cells, ratio of bcl-2 to cmyc positive cells. Information was also accumulated for EGFr and $p^{21\,ras}$ but these proteins were universally induced and so could not be relevant to individual response. The results of these studies are presented in publs 6 and 9 for urothelium and M Dent Sci thesis from R. el Gehani for oral mucosa. The major results and conclusions are summarised below:

a. Four groups of individuals could be identified on the basis of their p53 response measured 14 days post exposure;

Group 1 (approx. 24%) cytoplasmic p53 expressed on culture alone
Group 2 (approx. 26%) cytoplasmic p53 induced by radiation (range 0.1-0.5Gy)
Group 3 (approx. 20%) cytoplasmic p53 induced by radiation (10Gy) + Nitrosamine
Group 4 (approx. 30%) cytoplasmic p53 never detected.

The patients in group 1 were later shown to be smokers and a blind study done on both oral mucosa and bladder confirmed that smokers have cytoplasmic p53 protein expression and significantly more p53 mutations than non smokers matched for age, alcohol consumption and sex.

The patients in group 4 are curious. They had no evidence of HPV virus which could have explained their lack of inducible p53 and two were babies. They may represent a truly stable subgroup of the population.

Assuming that expression of cytoplasmic p53 expression points to deregulation of a major system which protects the genome from carcinogenic and other mutations, then the critical group from the radiation protection viewpoint would seem to be group 2 That is non smokers who readily induce cytoplasmic p53 expression following low test dose exposure. It is unlikely that the population would be exposed to, or survive, radiation doses delivered to group 3. Group 2 people have been identified from culture and exposure of small cold cut biopsy specimens. Therefore the test is both practical and relevant.

b. Induction of bcl-2 and the ratio of bcl-2 and cmyc;

Both bcl-2 and cmyc were induced to very variable extents by radiation. Neither protein correlated well with radiosensitivity as judged by the extent of growth of cells post irradiation. However since in normal human cells cmyc can induce apoptosis following DNA damage while bcl-2 prevents apoptosis, it was decided to look at the balance of these two proteins in cultures and correlate the balance or ratio of the two proteins with growth post irradiation. The summary table (5) shows a significant correlation between post irradiation growth and this ratio. This was confirmed for normal oral mucosa and for oral and bladder tumours. When the individual results for bladder mucosa are examined (fig1), the radiosensitive group are predominant in the lower left quadrant while the radioresistant group are in the upper right quadrant. a highly radioresistant subgroup appear with abnormally low ratios of bcl-2 to cmyc (lower right quadrant of graph.). When the p53 expression was cross correlated for these patients, this group were all adults in the group with no p53 induction post irradiation. This further suggests that this group of patients are radioresistant. It is significant that for this subgroup, radioresistance does not involve induction of bcl-2 since the instability associated with inhibiting the apoptotic mechanism might be thought of as radioresistance at the cost of genomic integrity. The results are fully presented in publ. 11

Table 5

Correlation between bcl-2 / cmyc ratio and % reduction in control growth

	% control growth	bcl-2 / cmyc ratio
Ratio < 1 (n=15)	30.3±7.5	0.59±0.07
Ratio > 1 (n=22)	67.1±12.8	5.4±1.5
paired t-test	p< 0.05	p< 0.05

c. Growth post irradiation

Growth post irradiation was highly variable. Patients could be broadly grouped into two groups on the basis of their response in the low dose region. Group one were radioresistant if exposed to doses above 0.4-0.7Gy. They showed a non-monotone response with an apparent threshold occurring in this dose region. Group two were radiosensitive with a monotone response. The expression of p53, bcl-2 and cmyc was highly correlated with the radiation response for these two groups. The preliminary data is presented for nine patients in publ.6. This has now been confirmed for 22 patients.

It is concluded from these studies that the variation in response to radiation between individual patients is very large. This can be detected as variation in growth potential post exposure or in levels of induction or expression of growth, cell cycle or apoptosis gene products. Clearly these processes are intimately involved in determining the ultimate fate of the irradiated cell since a dead cell cannot ever give rise to a cancer. It is of great concern to determine which individuals have sensitive and which have resistant responses to low dose irradiation. It is also important to understand whether

resistant responders are more or less likely to develop cancer, given that repair of damage or bcl-2 facilitated escape from apoptosis may in fact allow a damaged cell to persist long enough to get a first or further carcinogenic mutation.

Figure 1

Correlation between % control growth and bcl-2/cmyc ratio

% of control growth
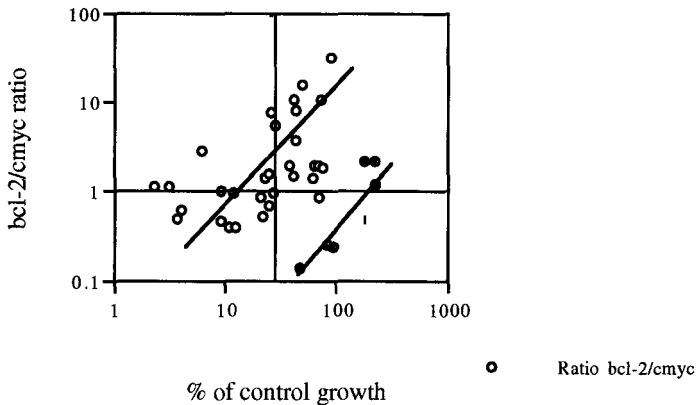
Note: The vertical line marks the mean reduction in growth for the entire group of patients (42.8%), the horizontal line marks the level where the bcl 2/cmyc ratio is one. (o) = p53 induced, (●) = no induction of p53.

Publications and theses from the contract:

Publications

1. Mothersill, C., Seymour, C.B., Harney, J., and Hennessy, T., High levels of stable p53 protein and of cmyc in cultured Human Epithelial tissue after radiation. Radiat. Res., 137, 317-322, **1994.**

2. Mothersill, C., Harney, J., and Seymour, C.B., Induction of Stable p53 and of cmyc over-expression in cultured normal human urothelium by radiation and n-nitrosodiethanolamine. Radiation Research, 138, 93-98, **1994.**

3. O'Reilly, S., Mothersill, C., and Seymour, C.B., Lethal mutations occur at a constant rate in human keratinocytes following carcinogen treatment, Internat. J. Radiat. Biol., 76 134-142. **1994.**

4. Lambkin H., Mothersill C., Kelehan P., Immunohistochemical detection of p53 in cervical tissues. J. Pathol. 172 13-18 **1994**

5. Harney, J., Murphy, D., Jones. M., and Mothersill, C., p53 Expression in urothelial tissue cultures from normal patients and those with transitional cell carcinoma. British Journal of Cancer, 71 25-29 January **1995**

6. Mothersill, C., Harney, J., Lyng, F., Cottell, D., and Seymour, C.B., Primary Explants of Normal Human Uroepithelium show an unusual Response to Low Doses of Cobalt 60 Gamma Rays. Radiat. Res. 142 177-183.**1995**

7. Mothersill, C., Harney, J., and Seymour, C., A Cancer sensitivity test based on expression of mutant p53 in cultured human cells. ECB 6 Proc. 6th European Cong. ed Alberrghina, Frontali and Sensi, 403-406 **1994**

8. Sheridan, M., Reid, I., Hennessy, T., and Mothersill, C. , Establishment of cultures of normal oesophageal mucosa from clinical biopsy material. In Vitro Cell and Developmental Biology, **June 1995**

9. Harney, J.,Seymour, C.B., Murphy, D., and Mothersill C., Variation in the expression of p53,bcl-2 and cmyc Oncoproteins in individual patient cultures of normal urothelium exposed to cobalt 60 gamma rays and n-nitrosoethanolamine. Cancer Epidemiology, Biomarkers and Prevention, **September 1995**

10. Sheridan, M., Reid, I., Mothersill, C., and Seymour, C.B., A predictive assay for individual patient response of oesophageal carcinoma to Chemoradiotherapy, J. Exp. and Clin. Cancer Res., 14, 74-75 **1995**.

11. C. Mothersill, J. Harney, F. Lyng, K. Parsons, T. Lynch, H. Gallagher, DM. Murphy, and C. Seymour, Overexpression of bcl 2 and cmyc and the post irradiation growth of human uroepithelial cells , Brit. J. Cancer, **under revision**

12. F.Lyng, Mothersill, C., O'Reilly, S., Cottell, C., and Seymour, C., Morphological Abnormalities in the distant progeny of irradiated cells. Rad. and Environ. Biophys. **Submitted**.

13. Mothersill, C.,Lyng,F., O'Reilly, S., Harney, J., and Seymour, C., Expression of Lethal Mutations occurs by apoptosis and is supressed in transformed cells and following carcinogen treatment of normal cells. Radiation Research, **under review**

14. Lyng, F., de Feijter-Rupp, H., Hayashi, T., Mothersill, C., Harney, J., Murphy, D., Cottell, D., And Trosko, J., Nitrosamines, including one found in the urine of tobacco smokers, block intercellular communication in human urothelial cells, Toxicology, **submitted**

Theses

Sandra O'Reilly Lethal mutations and transformation in a human immortalised cell line
Ph D University of Dublin, Trinity College July 1995

Fiona Lyng Ultrastructural effects of radiation and environmental carcinogens on human epithelial cells
Ph D University College Dublin July 1995

Rafa El Gehani p53, bcl-2 and ras oncoprotein expression in human oral mucosal cells
M. Dent. Sci University of Dublin, Trinity College, August 1995

Mary Sheridan Development of a predictive assay for radiosensitivity of human oral and oesophageal cells to radiation Ph D University of Dublin , Trinity College, September 1995

Helen Lambkin Molecular markers of carcinogenesis in tissues and cultured cells from the human cervix. Ph D University of Dublin, Trinity College, October 1995

Head of project 2:   Dr. Riches

II Objectives for the reporting period.

The primary objective for this project was to develop a suitable in vitro model of radiation-induced carcinogenesis using human epithelial cells.

1. To compare the transformation responses of human urothelial cell lines, a human keratinocyte cell line and a human bronchial cell line.

2. To compare the transformation response of a human thyroid epithelial cell line exposed to low LET (gamma) and high LET (alpha) radiation.

3. To estimate the RBE for oncogenic transformation by alpha particles using a human epithelial system.

4. To screen the radiation-induced human thyroid tumour cell lines developed in this project, for ras and p53 mutations using PCR methods.

III. Progress acheived including publications

Much of the information on the carcinogenic effects of ionising radiations has been established from animal experiments, in vitro studies using murine cell lines and epidemiological studies on man. The primary objective of the current proposal was to develop and investigate suitable human cell systems which would enable mechanisms of radiation carcinogenesis to be investigated and both focus and improve our understanding of radiation carcinogenesis in man.

Transformation studies using human epithelial cells have been carried out by Dr. Andrew Riches and Dr. Peter Bryant at the School of Biological & Medical Sciences, University of St. Andrews
As carcinomas are the commonest cancers in man, we have focussed on human epithelial cell systems for studies on radiation induced transformation. While human epithelial cells have been transformed by chemicals in vitro, it has previously proved difficult to develop suitable human epithelial cell systems which can be transformed with radiation. We have used a number of human epithelial cell lines to investigate this problem.

1.   Human urothelial cell lines

A number of urothelial cell lines (SV-HUC-1, BC16 and NT11) which had been immortalised following SV40 transfection were kindly provided by Catherine Reznikoff (Department of Human Oncology, Wisconsin, U.S.A.). These cells grow as epithelial sheets in vitro and are reported to be nontumorigenic in athymic nude mice. The lines stained positively for human cytokeratins and for large T antigen and also contained stabilised wild-type p53 antigen. Cells were exposed to gamma irradiation in vitro and passaged following irradiation to maintain the cells in a proliferative state. Following culture for a further 6 to 8 weeks the cells were harvested and transplanted to athymic nude mice. Foci were observed in the nude mice. These cells stained positively with human cytokeratin antibodies but were difficult to rederive as cell lines. Further groups of cultures were irradiated a number of times and following irradiation and passaging were then maintained as a confluent culture. Following periods in excess of 6 to 8 weeks following culture, foci appeared in the culture flasks in the form of papillomas. These have been transplanted to nude mice and have not produced tumours to date. Further groups were treated with methylcholanthrane and exhibited a similar morphological change. The cloning efficiency of cells following irradiation and following chemical carcinogen treatment was increased compared to the untreated cells.

While the urothelial cell lines have shown some promising results , it seems that these cells are extremely resistant to transformation by ionising radiations.

2. Human keratinocyte lines.

A human keratinocyte line immortalised by transfection with a human papilloma virus 16 recombinant plasmid construct was used (kindly supplied by Dr.DiPaolo). These cells were irradiated in Dr. Mothersill's laboratory in Dublin and following passaging were transplanted to athymic nude mice at St.Andrews. The cells formed tumours in the mice. However, control unirradiated cells in our hands were also tumorigenic. The growth and morphological characteristics of these tumours derived from irradiated and unirradiated cells are being compared.

While there are some encouraging differences in the tumours derived from irradiated cells and controls, this does not look to be a suitable sytem to exploit for radiation-induced transformation studies.

3. Human bronchial cell line.

A further human cell line was investigated. This bronchial epithelial cell line (L132) was studied in collaboration with Professor Janet Arrand at Brunel. However, control unirradiated cells were found

to be tumorigenic in the nude mouse assay and thus this system was not suitable for further transformation studies.

4.   Human thyroid epithelial cells

The human epithelial thyroid cell line (HTori-3) used was generated following transfection with a plasmid containing the origin defective SV40 genome. The cells were derived from normal thyroid follicular epithelium obtained from a lobectomy specimen from a female patient aged 35 years.

The human epithelial cells were exposed to a single or 3 equal fractionated doses of gamma irradiation. Following the last exposure the cells were passaged for 4-6 weeks. Tumorigenicity was tested following transplantation to athymic nude mice. Following a single exposure, 22 independent tumours were observed in 45 recipients and following three equal fractions, 18 independent tumours were observed in 31 recipients. Tumours were observed at all doses studied in the range 0.5 to 4 Gy. The latent period for appearance of tumours varied between 7/8 weeks upto 22 weeks after transplantation and thus screening takes a long time. It is thus necessary to screen for 4-6 months. The growth curves for the primary tumours were similar with volume doubling times of 10-20 days. The tumours consisted predominantly of areas of poorly differentiated cells with occasional evidence of small follicular areas. There was no evidence of local invasion or metastasis. The tumours were classified as undifferentiated, anaplastic carcinomas.

Cell lines were derived from the primary tumours. These cell lines are tumorigenic following transplantation to nude mice. The cells stain positively for human cytokeratins , do not express mutant p53 as measured by Western blotting and have a human karyotype. In vitro growth rate of these cells is increased compared to the control line. DNA fingerprinting has been used to check that the transformed lines were derived from the parent normal thyroid line.

In studies with cell lines, the possibility that cell sub-populations are being selected from the cell line following treatment must be excluded. The radiosensitivity of a number of derived tumour cell lines was compared to that of the parent cell line and shown in each case to be more sensitive than the parent line. Thus this supports the view that de novo transformation has been induced by gamma radiation (Fig.1).

Fig.1. Survival curves of the parent human thyroid epithelial cell line and derived tumour cell lines.
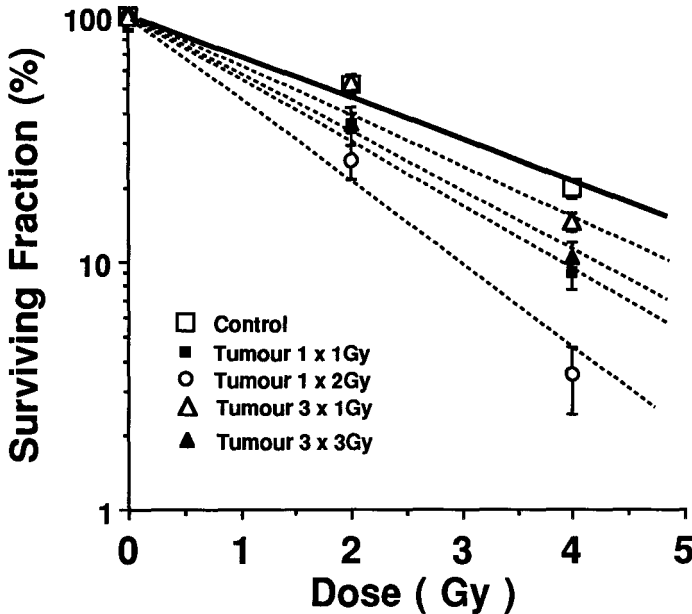
Following single doses of gamma irradiation, tumours were induced at doses as low as 0.5 Gy. Using multiple doses of gamma irradiation, the tumour incidence increases then decreases at the high accumulated doses giving a bell-shaped dose response curve.

Further experiments were undertaken to evaluate whether single doses of alpha irradiation could transform human epithelial cells. These experiments were undertaken in collaboration with Dr. Goodhead's group at Harwell using a plutonium 238 irradiator.

The human thyroid epithelial cells were seeded onto thin Hostaphan based chambers for irradiation. The topography of the cell monolayer was examined with a confocal laser microscope to establish that good track-segment irradiation conditions could be achieved, with the alpha particles losing only a small fraction of their energy in traversing a single cell. Following a single exposure to alpha irradiation, the cells were passaged then tested for tumorigenicity in nude mice. No tumours were observed following the transplantation of unirradiated control cells but 27 independent tumours were detected in 42 recipients receiving irradiated cells. Tumours were observed at all radiation doses in the 0.125 to 1.5 Gy range studied. G-test analysis showed a significant difference between the number of tumours in groups receiving cells irradiated with a dose of 0.5 Gy of alpha

particles compared to unirradiated controls (G = 22.1, df = 1, P < 0.001).

From colony survival data, the RBE at 10% survival was estimated to be 4.8 and from ratios of D_0's to be 3.9. As cells were passaged independently following irradiation, a comparison of tumour incidence following a single exposure to caesium 137 gamma irradiation and plutonium 238 alpha irradiation could be made (Fig.2.). The ratio of the peak incidence gives an RBE of 4 for transformation.

Fig.2. Tumour incidence following transplantation of irradiated human thyroid epithelial cells.
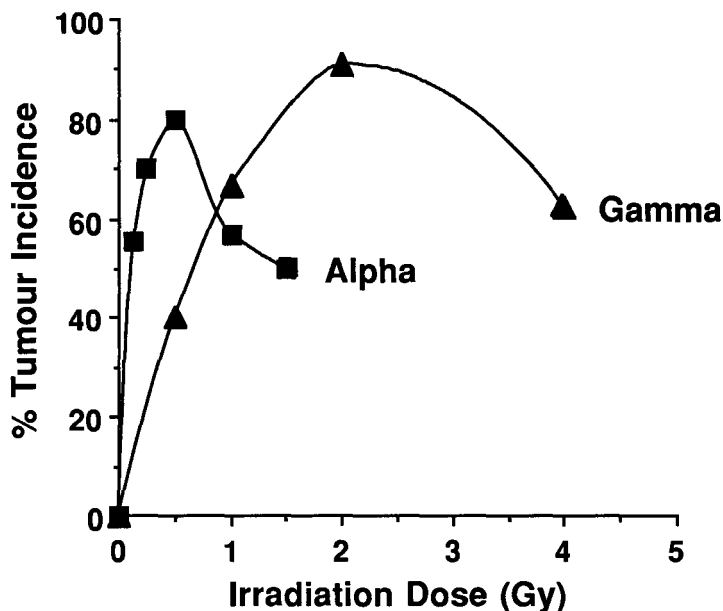
The parent Htori-3 cell line and 23 tumour cell lines produced following exposure to ionising radiation were screened for ras mutations. Following restriction endonuclease digestion of PCR amplified DNA, mutations were detected at H-ras codon 12 , K-ras codons 12 and 13 in the positive control cell lines (T24 and SW480). No mutations were detected in the human thyroid tumour cell lines.

Studies of p53 mutations using PCR-SSCP analysis of exons 5 - 8, in collaboration with Professor Janet Arrand and Dr. Simon Gamble at Brunel, revealed evidence of mutations in exons 5, 7 and 8 but not in exon 6.

In summary, we have shown that single doses of gamma or alpha irradiation and fractionated doses of gamma irradiation in vitro can induce malignant transformation of human thyroid epithelial cells. Estimates of RBE values have been obtained for transformation with alpha particles. Cell lines have been derived from these tumours also. This promises to be a useful model to investigate the molecular mechanisms of radiation carcinogenesis in human thyroid epithelial cells.

Publications.

O'Reilly, S., Mothersill, M., Seymour, C. Riches, A. & Bryant, P
    International Symposium on Molecular Mechanisms of Radiation and
    Carcinogen Induced Cell Transformation (1993).
    " An assessment of an HPV-16 transformed keratinocyte cell line for
    radiation transformation studies. "

Lehane, M., Mill, A., Hall, S., Allen, L., Butler, A. & Riches,A.
    International Symposium on Molecular Mechanisms of Radiation and
    Carcinogen Induced Cell Transformation (1993).
    " Characterisation of foci isolated from irradiated C3H10T1/2 cells. "

Mothersill, C., Seymour, C., O'Reilly, S., Harney, J., Bryant, P. & Riches, A.
    International Symposium on Molecular Mechanisms of Radiation and
    Carcinogen Induced Cell Transformation (1993).
    " Radiation induced changes associated with transformation of normal and
    immortalised epithelial cells in culture. "

Herceg,Z. Bryant,P. & Riches,A.
    Int.J.Radiat.Biol. 65 : 145 (1994)
    " Radiation-induced transformation of an immortalised human thyroid
    epithelial cell line. "

O'Reilly, S., Mothersill, M., Seymour, C. Riches, A. & Bryant, P.
    Int.J.Radiat.Biol. 65 : 146 (1994)
    " Determination of the number of surviving cells available for transformation
    following irradiation. "

Riches, A., Herceg, Z., Bryant., Wynford-Thomas, D., Stevens, D. & Goodhead, D.
    Int.J.Radiat.Biol. (in press)
    " Radiation-induced transformation of a human thyroid cell line after
    exposure to alpha particle or gamma irradiation."

Lehane, M., Mill, A., Hall, S., Allen, L., Butler, A., Riches, A., Bryant, P., Briscoe, C.,
Melville, J. & Roberts, C.
    Int.J.Radiat. Biol. (in press)
    " Characterisation of foci isolated from irradiated C3H10T1/2 cells."

Riches, A., Herceg, Z., Bryant, P. & Wynford-Thomas, D.
    Int.J.Radiat.Biol. 66 : 757 (1994)
    " Radiation-induced transformation of SV40 immortalised human hyroid
    epithelial cells by single and fractionated exposure to gamma irradiation in

vitro."

Gamble, S., Riches, A., Herceg, Z., Briscoe, T., Bryant, P., Colucci, S. & Arrand, J.
Int. J.Radiat. Biol. (in press)
Incidence of p53 mutation in low dose and low dose-rate irradiated human
epithelial cell lines. "

Riches, A., Herceg, Z. & Bryant, P.
Int.J.Radiat.Res. (in press)
" Investigation of ras mutation and expression time in radiation-induced
oncogenesis using a human thyroid epithelial cell line. "

Riches, A., Herceg, Z., Bryant, P., Wynford-Thomas, D., Stevens, D. & Goodhead, D.
10th International Congress of Radiation Research (1995)
" Transformation of a human thyroid cell line following exposure to alpha
particle or gamma irradiation. "

COMPARISON OF *EX VIVO* TRANSFORMATION OF RAT FETAL GLIAL CELLS INDUCED BY RADIATION OR CHEMICALS

Objectives for the reporting period:
-Establish transformed (immortalized) cell lines;
-Characterize the changes occuring during cell transformation to precise the chronology of events;
-Compare transformation processes with 2 different agents: chemical and γ radiation.

Results achieved:

Study of glial cell transformation
Two series of experiments were performed. The results from the first experiment lead us to raise the hypothesis that the mortality occuring when putting cells in culture (isolation and first days in culture) could have influenced the following events by selecting non "initiated" cells. So, characterization of cells was interrupted and a second experiment was performed using improved methods.

Animal treatment
For the first serie, pregnant Sprague-Dawley rats were either treated with ethylnitrosourea (ENU, 50mg.kg^{-1}) on day 18 of gestation or irradiated from day 14 to day 21 of gestation (cobalt 60, 3.5Gy at 0.5 Gy day^{-1}). For the second one, rats were treated with ENU, irradiated in the same conditions or sham irradiated.

Cell culture
Cell culture was performed under Dr H. Coffigny's supervision. In the first serie, fetal rat cortex were sampled on day 21 of gestation and glial cells were put in culture after mechanical dissociation. In the second experiment, fetal rat cortex were sampled at the same age and glial cells were put in culture after a milder cell dissociation procedure combining enzymatic and mechanical treatment. The culture medium was DMEM 10%FCS, with 4.5g.l^{-1}glucose instead of MEM previously. The immediate mortality was lower than in the first experiment, so we obtained a mixte population of different types of glial cells. In these conditions, neurons die rapidly
Culture medium was changed at least twice a week and cells were subcultured when they reached confluency (on the average every 2 weeks). Some were treated with phorbol myristate acetate (TPA) and other with the solvent (acetone) only. Those from the first experiment were maintained in culture for about 50 passages (some cultures were maintained for up to 70 passages) and the cells from the second one now reach about passage 20 (about 300 days of culture), they will be maintained until multiple chromosome rearrangements occur.

Morphology
Type I astrocytes were at early passages rather large cells, their size was much smaller at late passages. In the first experiment, after few months in culture, "foci" appeared on cell layers.
In the second experiment, along with consecutive passages, type I or type II astrocytes tend to predominate in cell cultures. In some cultures, presence of bipolar cells evokes progenitors cells.

Immunohistochemistry
Experiments were performed by Dr H. Coffigny with different markers: vimentin, MAP2, GFAP, A2B5, CNPase and galactocerebroside. Cells in culture were neither neurones (MAP2-) nor oligodendrocytes (CNPase- and galactocerebroside-), but astrocytes (GFAP+); during the first experiment, we could only obtain type 1 astrocytes and in the second, a mixte population with essentially astrocytes type 1 and 2. Few cells were A2B5+, they could be at the origin of the astrocytes II population.

Cell proliferation

Increase in proliferation occurs at about passage 20 for all cell cultures, independently of the treatment.

Colony forming ability

Clonogenic potential was estimated by seeding at 10^5, 2.10^5 or 4.10^5 on semisolid agar (collaboration with Dr D. Lefrançois).

Type 2 astrocytes give colonies even at early subcultures (P.7), but no colony was observed for culture with type 1 astrocytes even at the 21th subculture. If not due to an experimental bias, this result could be in relation with the fact that most progenitors of type I would not have been exposed, because they begin to differentiate during the last days of gestation. Conversely, type II astrocytes develop mainly after birth, therefore during exposure they were principally as progenitors.

Cytogenetics

Cytogenetic study was performed after R-banding technics. About 10 metaphases were analyzed by 2 observers for each subculture studied.

-Non treated glial cells: at P.4, most caryotypes were normal, 2/10 had non clonal aberrations. At P.18 (14 passages in presence of TPA), the six caryotypes studied were hyperploid (51-61 chromosomes), with an excess of chromosome 4 and structural rearrangements. At P.21 (17 passages in presence of TPA) of another experiment, all karyotypes were rearranged, with alterations delineating several clones.

-Cells from irradiated animals: at P.2, P.4 and P.7, most karyotypes were normal. At P.19, the cells were near diploïd, carrying a clonal rearragement. At P.21 from the first experiment, karyotypes were either hyperploid or polyploid (59 to 128 chromosomes). Some structural rearragements delineated small clones.

-Cells from animals treated by ENU, then acetone: at P.4, P.6 and P.9, all karyotypes were normal. At P.21, a majority of cells was near tetraploid. At P.27, besides diploid cells, hypotetraploid karyotypes were observed. At P.49, all were hyperploid (54-64 chromosomes) with structural aberrations. Some of these aberrations were clonal. The same characteristics were observed at passage 54. At P.65 and 70, beside hyperploid (49-63 chromosomes), highly polyploid karyotypes (up to226 chromosomes) were observed. Structural aberrations were distributed, defining various clones.

-Cells from animals treated by ENU, then TPA: at P.2, 5, 17 and 20, most karyotypes were normal, rare non clonal aneuploidies being observed. At P.23, all karyotypes were hypotetraploid (74-80 chromosomes), with non clonal aberrations. At P.35, cells were hyperploid (64-73 chromosomes) and carried identical clonal aberrations. At P.40 and 42, the hyperploidy was less marked (59-70 chromosomes). The same clonal rearrangements were observed, and additional ones were acquired. This corresponds to an usual evolution of cell transformation with monoclonality: diploidy ------> tetraploidy -----> chromosomes losses -----> hyperploidy and acquisition of clonal rearragements.

In conclusion, all cells in culture tend to acquire chromosomes aberrations aroud the 20th passage. These aberrations were either non clonal, monoclonal or multiclonal. The karyotypes the most suggestives of cell transformation were observed in ENU+TPA treated cells which underwent both endoreplications, chromosomes losses and rearrangements.

Results obtained on cells from the second experiment have confirmed the previous one: karyotypes were normal during the first passages and chromosome aberrations appeared at about the same time, when cell proliferation changes and therefore seem in relation with cell transformation. Actually, cells from the second experiment just arrived at the critical time of transformation. Within the next months, we will perform simultaneous comparative study of proliferation and clonogenicity on glial cells (as shown below for another cell type).

In parallel, while establishing the glial cell lines, we have set in culture cells from rat lung either irradiated or not in order to compare the transformation of cells originating from 2 different tissues.

Study of lung cell transformation

Animal treatment

Pregnant rats were irradiated (I) from day 21 to 5 days after birth (cobalt 60, 3.5Gy at 0.5 Gy day^{-1}) or sham irradiated (C).

Cell culture

Cell cultures (I or C) were established by explant technics from lungs of young rats either irradiated or not. Culture medium was changed at least twice a week and cells were subcultured when they reached confluency. They were maintained in culture for about 50 passages (i.e. about 2 years). Attempts were made first to try to induce cell differentiation and second to use β–naphtoflavone (BNF) as cocarcinogen (protocol followed for *in vivo* experiments performed in the Department). Due to lack of time and manpower, these assays were not completed.

Morphology

At first passages cells were large, polymorphic and rather pavementous. In the late passages, cultures consisted of an homogeneous population of small cells with spindle shape.

Immunohistochemistry

Experiments were performed by Dr J. L. Poncy with different markers: vimentin, cytokeratins. Results need to be confirmed

Cell proliferation

Maximum density at confluency changed from about 4.10^6 cells per $25cm^2$ flask at early passages (P.7 for instance) to reach 10 to 13.10^6 at the last passages studied of I cells.

Cell proliferation rate was assessed at the same time for different passages in culture: P.6, P.14, P.25, P.36 and P.49 for C cells and P.5, P.14, P.27, P.39 and P.53 for I cells. The method used was based on neutral red incorporation (absorbance at 540nm is proportionnal to the cell number). The rate was estimated for 4 different seeding densities. The results obtained for I and C cells at one density are shown below. For I cells, the decrease observed for the last measurement was due to intense lactic acid production.

Lung cells from irradiated rats
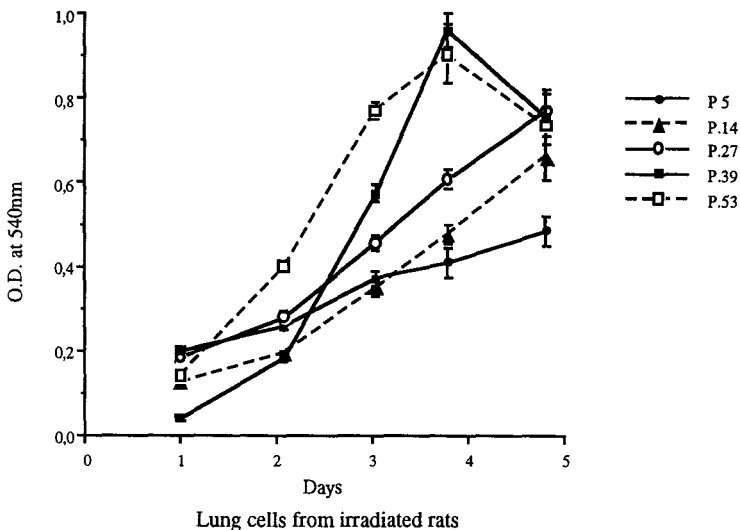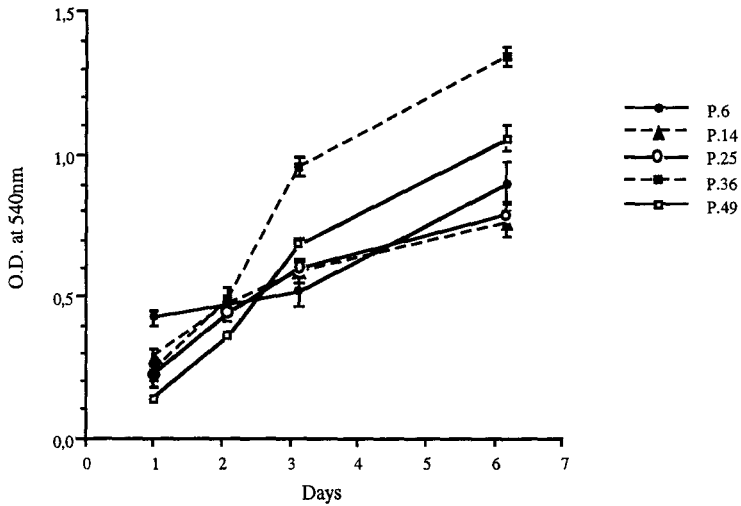
Lung cells from non irradiated rats

The increase in slope of the proliferation curves with increasing passages is shown below:

	I Cells					C Cells				
N° of passages	5	14	27	39	53	6	14	25	36	49
Slope (/day)	0.08	0.20	0.18	0.33	0.45	0.10	0.14	0.18	0.34	0.26

Colony forming ability
Clonogenic potential was estimated by 2 different technics:
-seeding cells in 3,5cm Petri dishes at low density: 1000, 500, 250, 125, 62 or 30 cells.cm^{-2}
with 2% FCS medium;
-seeding at 10^5, 2.10^5 or 3.10^5 on semisolid agar (collaboration with Dr D. Lefrançois).
On Petri dishes, colonies were observed even at the lowest density for I cells at P.39 and P.53.
The results obtained for I and C cells are schematized below (shaded areas indicating that colonies could not be counted).
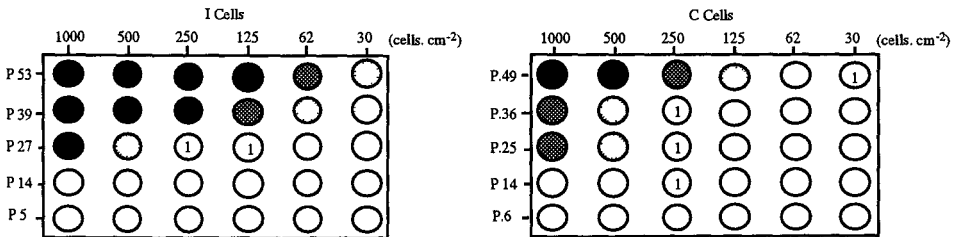
Test of colony forming ability for I and C cells

- ● High confluency
- ◍ Confluency
- ◯ Very high density
- ◯ High density colony
- ① One colony
- ◯ No colony
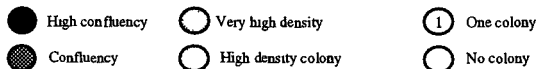
On semisolid agar, no colony was observed for C cells at P.15 or I cells at P.14. At 10^5, small colonies were observed at P.50 and large ones for I cells.

Cytogenetics
Cytogenetic study was performed on these cells at different passages in the same conditions as for glial cells. For I cells, karyotypes were performed at passages 21, 27, 29 and 49; for C cells, karyotypes were performed at passages 30 and 39.
For control lung cells, at P.30, the karyotype was diploid normal; at P.39, most karyotypes remained normal, but 3/12 cells had non clonal aberrations.
For irradiated lung cells, at P.21, 12/12 karyotypes were normal. At P.27 and P.29, most karyotypes were normal, but rare non clonal aberrations were observed. At P.49, all karyotypes were near diploid (11/13) or near tetraploid (2/13). Clonal aberrations were observed; they involved chromosome 13 and large markers, possibly hsr (homogeneously staining regions) carrying chromosomes, were observed in all cells. The presence of hsr suggests the cells have undergone a step towards transformation.
Cytogenetic study has been later performed, for both I and C cells, on the same passages as proliferation and clonogenicity evaluations. These karyotypes are not yet completely analyzed.

Electron microscopy
Experiments were performed in collaboration with Dr Y. Neveux (Hopital du Val de Grâce, Paris) in order to try to identify the cell type and check if we could observe the same morphologic changes (altered mitochondries) as for fibroblasts and chondrocytes at different passages during SV40 immortalization. Ultrastructural analysis is not yet achieved.

Further studies will consist in:
-maintaining cells in culture to follow evolution;
-testing tumorigenicity on nude mice;
-characterizing genetic changes in collaboration with other teams (CGH, in situ hybridization,...);
-studying oncogene expression.

In conclusion, so far some similarities appear concerning cytogenetic results, karyotypes are normal during early passages (up to about 20 for glial cells and at least 30 for lung ones) and chromosome rearrangements occur at about the same time as changes in proliferation and therefore seem related with transformation process and not with the previous treatment: chemical agent or irradiation.

Early steps of cell transformation : induction of transcription factors by ionizing radiation in skin cells.

Michèle Martin, Denis Biard, Laboratoire de Radiobiologie Appliquée, CEA, DSV, DRR, C.E.N. Saclay, 91191, Gif sur Yvette, cedex, France. Tél. (33 1) 39 56 29 15-Fax (33 1) 39 56 04 93

I. Introduction.

Radiation-induced neoplastic transformation is thought to occur as a multistage process. Ionizing radiation would cause an initial common event, followed by long term modifications of the cell which permit second rare events, and progression towards transformation. The initial common event is though to be related to DNA damage. However, the molecular processes leading to the secondary events, such as tumor promotion and progression, are presently poorly understood. Recent studies suggest that the early induction of stress proteins by various carcinogens like UV, TPA and ionizing radiation could be involved in these secondary events. By playing a role in processes like DNA repair, cell cycle arrest, or induction of mutations and genetic instability, early gene induction might contribute to carcinogenesis.

These inducible genes can be divided in four major groups: protein kinases, transcription factors, repair genes, and growth factors. Among the various proteins which can be induced by radiation, transcription factors are important because they regulate gene transcription by binding to specific promoter sequences which ultimately results in specific biological responses. Egr-1, NF-kB, c-myc, AP-1 and p53 are among the transcription factors which have been shown to be inducible by radiation.

The AP-1 genes
The proto-oncogenes *jun* and *fos* are the components of AP-1, which is a major transcription factor of the mammalian cell. AP-1 has the ability to control the transcription of several genes inducible by DNA damage such as UV and by tumor promoters like TPA. AP-1 is a dimer composed of various Jun and Fos proteins, whose dimerization occurs through their leucine zipper region. The c-Jun protein can dimerize with itself, and then bind as a homodimer to DNA. However, the heterodimer Fos/Jun has an increased affinity for AP-1 sites and is the most active form of AP-1. The various combinations between the various members of the Jun family (c-Jun, Jun-B, Jun-D) and of the Fos family (c-Fos, Fos-B, Fra-1, Fra-2) probably determine the functions of AP-1 and the genes which it regulates. The Fos proteins are not able to bind DNA on their own, thus their activity as transcription factors require binding to other regulatory proteins.

The p53 protein
The p53 protein is involved in the control of cell cycle, cell differentiation and proliferation. p53 belongs to the signalling pathway by which cells regulate the G1 - S transition of the cell cycle following genotoxic insult. Moreover, it plays a key role in apoptosis and DNA repair.

Wild-type p53 protein levels rise dramatically after exposure to ionizing radiation and various DNA - damaging agents, especially in hematopoietic cells. This rise results from as yet undefined changes in the post-transcriptional modifications undergone by the p53 protein such as phosphorylation, binding to other proteins, or oligomerization. At subsequent endpoints of DNA damage, a prolonged half-life was observed as well as increased DNA binding activity of p53 protein and enhanced transcriptional transactivation activity driven by this protein.

This DNA damage - induced stabilization of the p53 protein is thought to switch off replication in cells until DNA damage is repaired. But if such repair fails, p53 may trigger cell suicide by apoptosis in certain cell lines, including hematopoietic cell lines and human colon tumor-derived cell lines. This fine tuning of the balance between DNA repair and apoptosis may be mediated by the DNA binding properties of the p53 protein and by its transactivation of gene transcription.

Objectives of the study

The immediate early gene response to low doses of ionizing radiation is very poorly understood. Our study aimed at investigating such a response in skin cells, which has never yet been studied. For this purpose, we examined the expression of *fos* and *jun* AP-1 proto-oncogenes and p53 anti-oncogene in two skin models : the normal pig skin irradiated *in vivo*, and the reconstituted skin irradiated *in vitro*.

The early response of skin cells to low dose irradiation was assessed using the following endpoints :

- activation of the AP-1 transcription factor in the pig skin irradiated in vivo
- activation of the AP-1 transcription factor in human skin cells cultured in the reconstituted skin model
- activation of the p53 transcription factor in human skin cells cultured in the reconstituted skin model

II. Methods

Large White pigs were gamma irradiated. The pig was chosen as an experimental model because it is the reference in radiobiological studies of the skin. A cylindrical collimated ^{192}Iridium sealed source was set in a 2 cm in diameter annular collimator and applied to the skin surface of the flank. Doses ranging from 5 cGy to 16 Gy were delivered to the flank of the animals, with a dose rate of 0.6 Gy/min. The irradiated skin samples were removed at 2 hours, 6 hours, 15 hours, and 24 hours after irradiation and frozen. Control skin samples were taken from the non irradiated flank of each animal. The samples were directly frozen in liquid nitrogen.

The reconstituted skin is composed of an epidermal sheet (human or pig keratinocytes) which stretches on a dermal matrix (fibroblasts). This model accounts for the epidermal maturation (proliferation and differentiation) program of human keratinocytes, which is regulated by stromal cells. The irradiation was carried out using a ^{60}Co source at a dose rate of 0.2 Gy /min. At different times post-irradiation (3 h, 1 day, 1 week), samples were snap-frozen in liquid-nitrogen.

Maturation of the epithelium was characterized by differentiation products specific for keratinocytes (keratins, involucrin, filagrin), for mesenchymal cells (vimentin), or for basal membrane (collagen type IV, laminin).

III. Results

1) In vivo activation of the AP-1 transcription factor in pig skin cells

. Induction of AP-1 gene transcription
The expression of c-*fos and* c-*jun* messenger RNA was studied by Northern blotting. C-*fos* was constitutively expressed in normal epidermis and not expressed in normal dermis. Gamma irradiation induced a dramatic expression of c-fos mRNA in the pig skin cells. This induction was transient. It started 2 hours post radiation and was maximal at 6 hours. By 15 and 24 hours, the amount of c-*fos* mRNA had returned to basal level.
The threshold dose was not determined, as the lowest dose used (5cGy) already induced strongly the c-fos RNA. The maximum of induction was around 50 cGy, and most of the response was lost at 2 Gy.
C-*jun* and *jun*B mRNA were constitutively expressed in normal control skin cells. At 6 hours, the rise in c-*jun* and *jun*B inductions was very limited. The kinetics of expression were similar to that of c-*fos*, and exhibited a down regulation by 15 hours.

Moderate doses of gamma rays (ranging from 2 to 8 Gy) did not induce the AP-1 gene response.

. Induction of the AP-1 proteins : The proteins were studied by western blotting.
At 6 hours after irradiation, the induction of c-Fos, c-Jun and JunD proteins could be detected, with a peak occuring around 50 cGy.

. Increase of the DNA binding : The activity of the proteins was studied by gel
retardation assay. Nuclear proteins were isolated from the irradiated skin at 6 hours after irradiation, and incubated with an oligonucleotide coding for the AP-1 site of the collagenase promoteur. The binding was significantly increased after 5, 50 cGy and 2 Gy.

. Composition of the AP-1 dimer : This endpoint was investigated by gel
retardation assay using competition with specific antibodies. A dose as low as 5 cGy induced in skin cells AP-1 homodimers composed of c-Jun, JunD andJunB. No heterodimers with c-Fos were found.

We propose that low doses of gamma rays induce specific active AP-1 dimers because they control specific target gene cascades. The activation of AP-1 after low doses may take part of an adaptative response to gamma radiation.

2) In vitro induction of AP-1 genes in human skin cells

In vitro experiments were performed to address the cellular source of the AP-1 activity after low doses and the role of cell differentiation.
Human fibroblasts and keratinocytes were cultivated either as monolayers or in the model of the reconstituted skin. Thus the immediate early response was studied in different conditions, ranging from the *in vivo* conditions to a gradual loss of cell

differentiation. Cultured cells were treated by TPA (100 ng/ml) or gamma rays (Cobalt ^{60}, 0.2 Gy/min)

In the reconstituted skin, we found by northern blot that cells exhibited 3 hours after low dose irradiation a high induced c-*fos* expression. Moreover, both keratinocytes and fibroblasts took part in this radiation response. However, a gradual loss of the intensity of the response was observed according to the loss of cell differentiation in the various culture conditions. This effect was very significant for the fibroblasts in monolayers, which still responded to TPA but had lost the response to gamma radiation.

3) Discussion

In summary, we demonstrated that the activation of the AP-1 transcription factors are involved in the response of skin cells to low doses of gamma radiation.

Gene activation by radiation resulted in increase in protein amounts and activity after doses as low as 5 cGy. The collagenase gene is a possible target gene of the transcrition factor after low doses. Both keratinocytes and fibroblasts participated in this cell response. However, our results stress the importance of cell differentiation to obtain such a response.

One important question connected with these results is the following: what are the target genes that these transcription factors are supposed to regulate? Two types of irradiation effects are possible. Firstly, the consequences of inducing early genes by ionizing radiation may be DNA fragmentation and cell death, a larger number of mutations and chromosomal anomalies, or malignant transformation by a persistent rise in the formation of a proto-oncogene product.

Secondly, the consequences might be cell protection and repair. Several authors propose that the stress response induces or activates proteins that protect the cell against external insults. Interleukine-1 might be one of these genes, as it was found to be induced by neutron irradiation in SHE cells. This cytokine may act as a radioprotector.

In this context, the mechanism of AP-1 activation, and the cascade of genes that it subsequently activates, might be specific to low doses and take part of an adaptative response to gamma radiation.

4) Induction of the p53 protein in human skin cells

Normal human keratinocytes in the reconstituted skin model:
Normal keratinocytes allow to study the early steps of cell transformation in cells expressing a normal p53 gene. Thus, normal human epidermal keratinocytes were isolated from human mammary skin (mammoplasty procedure) or from human abdominal skin obtained after surgical excisions.

As evidenced by immunofluorescence stainings, we observed an early (3 h post-irradiation) and transient induction of p53 expression, likely due to an enhanced stabilization of the protein. Studies at the mRNA level were performed and they showed little variations of the *p53* mRNA level in keratinocytes and no modification in the fibroblasts.

Human immortalized keratinocyte cell lines HaCaT

Immortalized, non tumorigenic keratinocyte cell lines may allow to study the last steps of cell transformation after γ irradiation. We wanted to define the morphology, proliferation, genetic stability and gene expression for oncogene markers of HaCaT cell line. These human cells have been isolated from the normal skin of a cancer patient. They became "spontaneously" immortalized but remained non tumorigenic (Boukamp et al 1988). The status of the p53 gene has recently described as abnormal, as HaCaT cells have mutations for both p53 alleles.

HaCaT in monolayer:
In monolayer, HaCaT cells retained an epithelial morphology. Surprisingly, irradiation of HaCaT in monolayer resulted in a dose-dependent increase in the *p53* mRNA level 3 h post-irradiation, with graded doses of γ–rays up to 8 Gy. We have also performed immunoprecipitation procedure against p53 protein (with the pAb122 hybridome supernatant). A sustained stabilization of the protein was observed 3 h post-irradiation at 2 Gy.

HaCaT in the reconstituted skin model:
This cell line was cytogenetically characterized in collaboration with C. Luccioni (CEA). These cells were near tetraploid, exhibited numerous chromosome anomalies and were genetically unstable in culture. However, in the reconstituted skin, the HaCaT were still able to develop an epithelium.
HaCaT cells exhibited an abnormal *p53* gene expression. A high expression was demonstrated both at the transcriptional level with cDNA probes for *p53* and at the protein level using immunoprecipitation and immunofluorescence on histological slides in the skin model. A cytoplasmic localization of the p53 in HaCaT cells could be ascribed to the mutational pattern of the p53 gene, which was also revealed by its electrophoretic pattern after immunoprecipitation (appearance of Hsp70 - p53 complexes).
Following our strategy, we have irradiated the skin equivalent model (HaCaT cells and normal human fibroblasts) 3 weeks after gelling, when epithelium was stratified. We observed a high induction of p53 protein at doses as low as 0.5 Gy. This induction remained stable for 7 days following irradiation. We found no increase in *p53* mRNA level up to 2 Gy, but a strong induction of *p53* mRNA level with higher doses (8 Gy).

Conclusion

Most experiments published on p53 and the cellular response to gamma radiations concerned immortalized cells belonging to the hematopoietic lineage. We have developed two cellular models which allow to study the radiation response of the skin. Normal keratinocytes and fibroblasts allow to study the early steps of cell transformation in cells expressing a normal p53 gene. The radiation response can be studied in poor differentiation (monolayer) and high differentiation (reconstituted skin) culture conditions. In these cells, gamma rays induce the p53 protein with a post-transcriptional regulation.

In HaCaT cells, which have p53 mutations, the endogeneous p53 expression was high and abnormal. Furthemore, the induction by the gamma rays exhibited uncommon regulations, particularly an induction at the transcriptional level, which has never been described for cells belonging to the hematopoietic lineage. As certain p53 mutants loose their antiproliferative activities and acquire oncogenic properties, then this sustained induction of the p53 protein might be one of the key requirements for transition towards neoplasia. In conclusion, HaCaT cells might be a good model to study the last steps of transformation in cells with an abnormal *p53* gene.

In conclusion, the p53 gene was clearly involved in the response of human skin cells to low and moderate doses of gamma rays. Doses of 0.5 Gy already induced the protein. For normal keratinocytes, stabilization of the protein is the main regulation step. However, for abnormal keratinocytes, both transcription and protein stabilization might be regulation steps of p53.

p53 gene cascade is now partly discovered. Low dose radiation might activate the control that p53 exerts on the cell cycle. But other activities of p53, like involvement in transcriptional control and DNA repair, might occur after such doses.

IV. Publications

- Martin M., Pinton P., Crechet F., Lefaix J-L. Ionizing radiation regulates expression of c-jun protooncogene and TGFb1 growth factor gene in normal skin. **The Journal of Investigative Dermatology, 1992**, International Conference on the Molecular Pharmacology of the Skin, Berlin, vol 98, n°5, p 820.

- Martin M., Pinton P, Crechet F., Lefaix J-L., and Daburon F. Preferential induction of c-*fos* versus c-*jun* proto-oncogene during the immediate early response of pig skin to gamma rays. **Cancer Research, 1993**, 53, 1-4.

- Martin M. Early induction of transcription factors by ionizing radiation: example of the skin radiation response. In: **Molecular mechanisms in radiation mutagenesis and carcinogenesis, 1994**, K. H. Chadwick, R. Cox, H.Leenhouts, J. Thacker, (eds), European Commission, Brussels, pp233-238.

- M. Martin, F. Crechet, B. Ramounet and J-L Lefaix. Activation of c-*fos* by low dose radiation: a mechanism of the adaptative response in skin cells ? **Radiation Research, 1995**, 141, 118-119.

Congress presentations

- Martin M., Crechet F., Pinton P., Lefaix J-L., **1992**. Preferential activation of the c-fos protooncogene during skin radiation response.24th Annual Meeting of the European Society for Radiation Biology, **Erfurt** (D) 10-1992.

- M. Martin, P. Pinton, F. Crechet, J-L Lefaix, and F. Daburon, **1993**. Differential early upregulations of the c-*fos* and c-*jun* proto-oncogenes during skin radiation response. Colloque International: DNA replication, recombination and repair in the genesis of human cancer. **Paris**, 26-29 may 1993.

- D. Biard, and M. Martin, **1993**. Induction of the *p53* gene in normal human keratinocytes irradiated in the skin equivalent model. Congress of the ETCS, **Rennes**, 07 1993.

- M. Martin and D. Biard, **1993**. Early upregulation of the *p53* tumor suppressor gene in human epithelial cells irradiated in the skin equivalent model. International symposium: The molecular mechanisms of radiation and chemical carcinogen-induced cell transformation, **Mackinac Island**, USA, 09 1993.

- Arrand J., Biard D., Joiner M., and Martin M., **1993**. Assessment of potential markers for low dose radiation response in mammalian cells. International symposium: The molecular mechanisms of radiation and chemical carcinogen-induced cell transformation, **Mackinac Island**, USA, 09 1993.

- M. Martin, F. Crechet, D. Biard, B. Ramounet, J-L Lefaix. C-fos, a new marker of low dose irradiation in skin cells. Annual Meeting of the ESRB, **Amsterdam**, Holland, 06 1994.

- M. Martin, D. Biard, F. Crechet, B. Ramounet, and J-L Lefaix. Activation of c-fos by low dose radiation : a mechanism of adaptative response in skin cells ? International Meeting on gene induction and adaptative responses in irradiated cells : mechanisms and clinical implications. **Montréal**, Canada, 06 1994.

- D. Biard, M.C. Vozenin, M. Maratrat, M. Martin, and F. Daburon. **1995**Etude de l'expression des gènes dans la peau reconstituée in vitro par cytométrie à balayage laser. Cellules et tissus humains. Avantages et limites, problèmes éthiques. Colloque de la S.P.T.C, Paris, 16-17 mars 1995.

- M. Martin, N. Gault, F. Crechet, D. Biard, J-L Lefaix and F. Daburon, **1995**Alterations of AP-1 gene activities in irradiated skin cells. Radiation Research Congress, **Würzburg**, 28 08- 01 09 1995.

Head of project 7: Prof. J.E. Arrand

i) Objectives for the reporting period

1.   To assess p53 gene status in human lung (L132), thyroid (HTori 3) and urothelial epithelial cell lines (both irradiated and unirradiated, normal and tumour) used by the participating groups.

2.   Determination of effect of low dose/dose-rate ionising irradiation (γ rays 0.01-0.1Gy/hour) on p53 status and cell growth/colony morphology in L132 cells.

3.   Determination of p53 status in nude mouse tumour-derived cell lines, resulting from inoculation of γ and α irradiated HTori 3 cells (L132 cells were not feasible for this experiment due to the background levels of tumour formation with unirradiated cells)

4.   Characterisation of novel markers in low dose/dose-rate irradiation responses by 2D protein electrophoresis and differential cDNA library screening.

5.   Determination of relationship of transformation frequency in HTori 3 cells to p53 status and LET of irradiation.

ii) Progress achieved

        Having previously successfully set up SSCP analysis of p53 exons 5 to 8 inclusive, whereby known p53 mutations in cell lines were reliably detected in comparison to genetically normal cells, the technique has since been applied to human lung epithelial cells (L132), urothelial normal and tumour cell lines (with Dr Morthersill's group), and nude mouse tumour cells derived from HTori 3 cells irradiated pre-injection with either γ and α rays (supplied by Dr Riches group).   Initial studies with unirradiated samples revealed no unusual bands in any cell lines used in subsequent experiments, when compared to a normal human primary cell line (MCJ); the p53 status of the cell lines L132 and HTori 3 may therefore be regarded as genetically normal.

        Following this result, the SSCP technique was applied to samples which had been irradiated with either low dose or low dose/dose-rate ionising irradiation. HTori 3 cells were irradiated with varying doses of γ or α irradiation, then injected into nude mice. DNA was successfully extracted from small numbers of HTori 3-derived tumour cells, and SSCP analysis carried out. Electrophoretic mobility shifts were identified in PCR amplified exons from 5 out of 10 tumours isolated. Of these 5 possible mutations, 2 were in exon 5, none were in exon 6, 1 was in exon 7 and 2 were in exon 8. Results were observed as appearance of one or more secondary bands, not present in unirradiated samples, rather than a simple band shift, possibly due to the presence of mixed cell populations in the derived tumour.   In order to test this hypothesis, clonal cell lines were derived from the original

tumour line by Dr Riches' group and subjected to further analysis. Determination of p53 status in 3 clones of a line with suspected p53 mutations were carried out (Figure 1). Of the clonal lines investigated with suspected mutations in exon 7, single mobility shifts were detected in different clones, confirming a mixed population in the original tumour line.

In total, therefore, an increase of at least 50% in detectable mobility shifts has occurred following exposure to γ and α irradiation and subsequent nude mouse tumour end-point analysis.

Human lung epithelial cells were exposed to a cumulative dose of 0.5 Gray at dose rates of 0.1, 0.04 and 0.01 Gy/hour. These cells and corresponding sham-irradiated controls were maintained in conditions designed to reduce cell division but maintain viability for a maximum period of 18 weeks. After several weeks in these conditions, dense clusters of cells were seen to form in both irradiated and unirradiated flasks. However in the unirradiated flask these clusters soon lifted from the culture surface and would not re-seed to fresh flasks. Of the clusters observed in irradiated flasks, the majority survived and were capable of re-seeding fresh flasks if removed from the original flask. Especially at 0.04 Gy/hour dose rate, there was a tendency for formation of groups of cells exhibiting unusual morphology. These cells, along with cells from dense clusters and also apparently normal cells, were analysed for p53 mutations alongside samples from sham-irradiated. Cells, 47 samples in total, were analysed, the results are summarised in Table 1.

From Table 1 it can be seen that an increased level of mobility shift was detected in the irradiated samples when compared to unirradiated samples. A general spread of mobility shifts in amplified p53 exons was detected throughout the four exons studied (chosen for their predominance in p53-mutation mediated carcinogenesis), with no particular exon showing dominance over others. In addition, cell colony morphology did not appear to relate to either dose/dose-rate received or detectable mobility shifts in the samples analysed. Of great interest though is the predominance of detectable shifts in exons amplified from cells irradiated with 0.01 Gy/hour (85% of tested samples showing 1 or more mobility shifts, against 46, 44 and 0%, for 0.04, 0.1 and 0 Gy/hour respectively). In total an approximate 51% increase in detectable mobility shifts was observed in exons 5 to 8 of the p53 genes of low dose-rate irradiated L132 cells.

The identification of novel molecular markers responding to low dose ionising irradiation has resulted, by comparitive 2D protein electrophoresis in the detection of several up or down regulated or post-translationally modified protein species , including RPA subunits, XRCC1 and a heat shock protein identified by microsequencing and/or Western blotting. In addition we have recently cloned a low-dose down-regulated gene whose product shows homology to proteins involved in the heat-shock response.

Table 1, Incidence of detectable electrophoretic mobility shifts in PCR products (SSCP analysis) from exons 5 to 8 of the p53 gene in low dose/dose rate irradiated L132 cells

a) Relationship between dose-rate, mutation frequency and location of mutations along p53 gene

Exon	Dose rate (Gy/hour)				
	0	0.01	0.04	0.1	Total
5	0	4	1	3	8
6	0	5	1	3	9
7	0	2	2	2	6
8	0	3	3	3	9
total mutations	0	14	7	11	-
total +ve samples*	0	11	6	7	24
Total samples	5	13	13	16	47
%	0	85	46	44	51

b) Relationship between colony morphology and detectable p53 mutation

colony form	% with detectable mobility shifts		
	0.01Gy/hour	0.04Gy/Hour	0.1Gy/hour
Dense clumps/ unusual morphology	66	50	66
Visibly normal	66	43	60

* Samples scored as showing mobility shifts in one or more exons
Where total number of mutations scored is greater than total number of samples, this is due to shifts detected in more than one exon of some samples.

The relationship between linear energy of transmission (LET) and cell transformation was not apparent when correlated with p53 mutation in nude mouse tumour-derived cells. Numbers of p53 mutations were not significantly different between samples irradiated with either α or γ irradiation. Given that no appreciable difference between α or γ irradiation was observed, it is possible that differences in LET is not a significant factor in determining levels of damage by ionising radiation-mediated DNA damage, or that both types of radiation produce similar levels of DNA damage via different mechanisms or similar levels of side reactions.

iii) Conclusions.

1)   Approximately 50% of nude mouse derived tumours resulting from low dose irradiated HTori 3 cells showed abnormal p53 gene sequences.

2)   LET did not correlate with incidence of p53 mutation in low dose irradiated HTori 3 cells.

3)   Low dose/dose-rate irradiation of L132 cells resulted in approximately 50% increase of p53 gene mutation above control levels, in all samples tested.

4)   Dose-rate, cell morphology and exon-specific mutation did not appear to correlate with frequency of detectable p53 mutations in low dose-rate irradiated L132 cells, although a dose rate of 0.01Gy/hour gave a high mutation frequency

5)   In general, irradiation of human epithelial cell lines with low dose or low dose/dose-rate ionising irradiation appears to result in increased frequency (approximately 50%) of mutation in exons 5 to 8 of the p53 gene, known to be involved in between 50 and 80% of known human cancers.

6)   Novel gene and protein markers have been identified which appear to be responsive to low doses of ionising radiation in L132 cells.

Publications resulting from this work

Figure 1, SSCP analysis of exon 7 of the p53 gene of cloned cells from HTori 3 cells irradiated with low dose γ irradiation

N H1, H2, H3, U

N, normal, unirradiated cells,
H1,2,3, cloned HTori 3 cells from nude-mouse tumours,
U, undenatured control sample
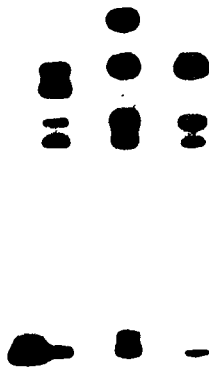
FINAL REPORT

F. FRANĚK, PRAGUE

1. Objectives

The objective of this part of the project was to analyze the levels of apoptosis in human cells and cell lines subjected to radiation or to carcinogenic chemicals. To conform with this objective, major emphasis has been put on the repertoire of assays and methods able to assess specifically and quantitatively the presence of the apoptotic process, and to distinguish it from necrosis.

Three methodical approaches were envisaged. The highest emphasis was put on the quantitative analysis of the status of DNA and chromatin. As an alternative approach the quantitation of apoptotic bodies, defined by their chemical resistance, was suggested. Finally, selective morphological methods were intended to be studied that would enable the quantitation of apoptotic cells on the single cell level.

The research on apoptosis belongs to fastest developing areas of animal cell biology. The repertoir of reliable methods for apoptosis assessment grew substantially larger since the time when this part of the project was designed (middle of 1993), and a variety of commercial reagents and kits became available. Therefore, the solution of the problem took into consideration the most recent methods, the critical survey of which follows.

2. Current methods of apoptosis assessment

2.1 Analysis of isolated DNA

The original methods that made it possible to identify the apoptotic mode of cell death were based on the analysis of the status of DNA, the "ladder" of oligonucleosomal fragments, demonstrated in agarose gel electrophoresis, being the most prominent example. However, the recent investigations have shown, that in some kinds of cells, e.g. in cell lines of epithelial origin, the cleavage of chromatin stops at large fragments, 50kb or 300 kb. Thus the absence of oligonucleosomal fragments does not necessarily indicate an absence of apoptotic process. The detection of large fragments is not possible by simple agarose gel electrophoresis, but only with field-inversion gel electrophoresis. The electrophoretic examination of DNA fragments requires $\sim 10^6$ cells. When labelled with radioactive thymidine, the cell number

required is by one order of magnitude lower.

Our contribution to the quantitative determination of large DNA fragments is the development of an alternative assay, namely gel chromatography according to our previous publication (Vomastek,T. and Franěk, F.(1993) Immunol. Lett.35: 19-24). The isolation procedure of DNA has to be extraordinary mild, e.g. an enzymic degradation of proteins and RNA avoiding the phenol extraction step (Neiman, P E. et. al. (1991) Proc. Natl. Acad. Sci. USA 88: 5857-5861). **The potential of this method to quantitate exactly intact DNA, large fragments and oligonucleosomes in a single step is unsurpassable by other known methods. The method required ~10^7 cells. The present effort is aimed at reducing the required number to ~10^6 cells. (Publication in preparation).**

2.2 Apoptotic bodies

While the morphological distinction of apoptotic bodies from damaged cells or from cell debris might be sometimes ambiguous, the treatment of the cell population under examination with 6M solution of guanidinium hydrochloride improves substantially the selectivity (Vomastek, T. and Franěk, F. (1993) Immunol. Lett. 35: 19-24). The cell number required for reliable counting of total cells/particles and of insoluble particles is, according to our experience, in the order of 10^3 cells.

2.3 Examination of DNA in cells

Some experiments are difficult to be carried out at the scale of tens or hunderds of millions of cells. Therefore, the availability of methods requiring lower cell numbers, or even single cells, opens new horizons for solving subtle problems of cell biology. The Cell Death Detection ELISA kit (Boehringer Mannheim) is based on immunoassay of fragmented chromatin using a monoclonal antibody to histones and another monoclonal antibody to DNA. Samples of the size of 1,000 cells are subjected to lysis and subsequent separation of intact and fragmented chromatin by centrifugation. According to our experience this immuoassay is very sensitive and reasonably reproducible.

Apoptotic cells may be distinguished by the morphology of the nucleus. The progress in the evaluation of the morphology of DNA or chromatin in single apoptotic cells has been enabled by introduction of various fluorescent stains. The classical staining of chromatin by acridine orange may be supplemented by more specific ethidium bromide or bisbenzimide H 33342. Apoptotic cells are distinguished by intense fluorescence of condensed chromatin and/or fragmented nuclei.

The fragmented DNA may be demonstrated by the In Situ Cell Death Detection Kit, Fluorescein (Boehringer Mannheim) that is based on theTdT-mediated dUTP nick end labelling technique (TUNEL). It labels the free ends of DNA and stains apoptotic cells with distinctly higher intensity than intact nuclei of viable cells.

Single cell visualization of chromatin fragments is possible by the single-cell gel electrophoresis, the so called comet assay (Rosselli, F., et al. (1995) Oncogene 10: 9-

17). The cells embedded in an agarose gel are fixed, permeabilized, and subjected to an electrical field for a couple of minutes. While intact chromatin does not move out of the cells, fragmented chromatin forms a comet-like pattern outside the cell when chromatin DNA is stained with ethidium bromide or with another suitable DNA stain. The apoptotic and non-apoptotic cells are inspected in fluorescence microscope and counted.

Flow cytometric analysis of the percentage of apoptotic cells has become reliable by introduction of the fluorescent labelling of DNA breaks in single cells in conjution with conventional cell cycle analysis (Gorczyca, E.W., et al. (1993) Leukemia 7: 659-670)

3. Progress achieved

3 1 Cell line

The human transformed keratinocyte line HPV-G was selected as a model cell line in the testing and comparison of quantitative methods for assessment of apoptosis induced by radiation. This cell line grows as an adherent layer both in plastic tissue culture vessels and in glass vessels, as well as on microscopic slides. The line requires only serum for growth and attachment.

Apoptotic HPV-G cells develop spontaneously during subculturing of the line·
(i) Upon trypsinization and subculturing not all cells attach to the substrate. They change their morphology and die by apoptosis within two to three days.
(ii) Cells divide even after reaching confluence. The suspension of dead cells beyond the layer of adherent living cells displays markers of apoptosis.

Priming for apoptosis can be carried out when cells detached by mild trypsinization are transferred to new serum-containing medium and the suspension is placed in bacteriological polystyrene Petri dishes, the surface of which does not allow attachment. HPV-G cells are round-shaped under these conditions , and remain viable as single cells or as small aggregates for 1-2 days. The suspension culture of HPV-G cells was used for induction of apoptosis by chemicals or by radiation .

3.2 Methods applied for apoptosis assessment
a) Spontaneous apoptosis

For spontaneously apoptotic HPV-G cells adherent viable cells served as a control. DNA was prepared both from control and from apoptotic cells using the mild

enzymatic method of Neiman (Proc. Natl. Acad. Sci. USA (1991) 88: 5857-5861) circumventing the conventional phenol extraction step. The DNA preparations from ~10^7 cells were analyzed by agarose gel electrophoresis and by gel chromatography. The agarose gel electrophoresis has shown that dead cell DNA is partly cleaved to large fragments. This finding is in agreement with the notion that the chromatin fragmentation in cells of epithelial origin does not proceed to oligonucleosomal fragments. The existence of large, but not of oligonucleosomal fragments, was clearly visualized in elution profiles of gel chromatographic analysis on Sephacryl S-1000 (Pharmacia) equilibrated in 1 M ammonium acetate (Fig1). *Paper reporting on the new method of DNA chromatography and on its analytical potentials is in preparation.*

Morphological examination in light microscope, using as the criterion of apoptosis the shrunken shape of the cells, works relatively specifically with trained ey. To eliminate entirely the subjective factor, counting of apoptotic bodies insoluble in guanidinium solution was introduced. The apoptotic index, i.e. the percentage of apoptotic cells/bodies relative to total cell count, obtained by counting shrunken cells, is always higher than the index obtained by counting insoluble apoptotic bodies, Various cells of haematopoietic origin, examined earlier in our laboratory, or by other investigators, displayed values of the converting factor between 3 and 10. The converting factor obtained with HPV-G cells was 2.1. This indicates a presence of a highly active tranglutaminase. The finding is conceivable, because non-transformed keratinocytes undergo terminal differentiation in which transglutaminase plays an important role. The cross-linking of cell proteins in the line HPV-G was thus found intense enough to serve as a marker of the degree of apoptosis.

b) Induced apoptosis

Apoptosis was found to be induced in HPV-G suspension cells by addition of ethanol or dimethylsulfoxide at 1 to 5% concenration Within 24 h upon addition of the inducer a major fraction of cells acquired apoptotic morphology.

The changes of chromatin, i.e.condensation and dissipation of condensed chromatin particles, were observed using four staining methods:

(i) Acridine orange. The chromatin is yellow, cytoplasm is green and RNA particles, obviously polyribosomes, are orange.
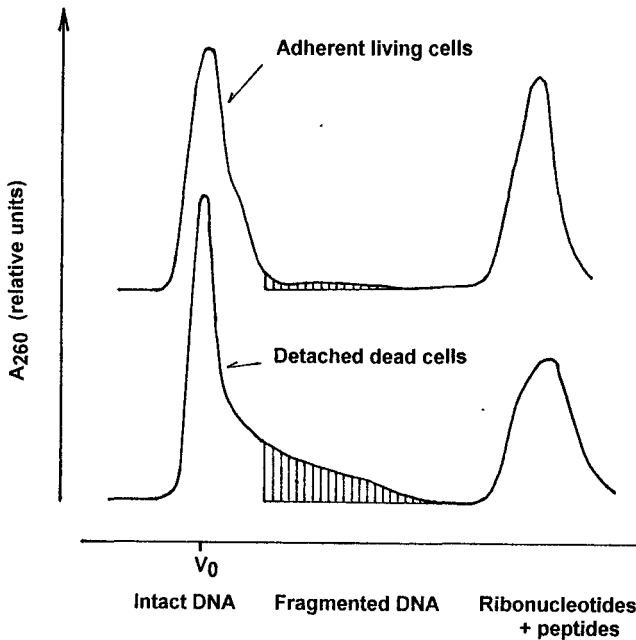
Fig.1 Chromatography profile of DNA isolated from viable and apoptotic HPV-G cells

(ii) Acridine orange plus ethidium bromide. In addition to characteristic staining of subcellular structures by acridine orange, an intense orange colour of DNA develops in cellls the membrane of which became permeable. This method allows to distinguish early apoptotic stage and late apoptosis, that has in some cells the features of secondary necrosis.

(iii) Bisbenzimide H33342. This stain is applied without fixation. The nucleus of a living cell is faintly blue. Apoptotic nucleus displays structures of condensed chromatin emitting intense blue fluorescence This staining method is specific for DNA, the background fluorescence of the cytoplasm is virtually non-existent.

(iv) TUNEL staining, fluorescein variant. The apoptotic nuclei are characterized by fluorescence exceeding markedly the background, and by intranuclear structures.This staining is extraordinary in its selectivity. Viable cells do not display any fluorescence (Fig.2)
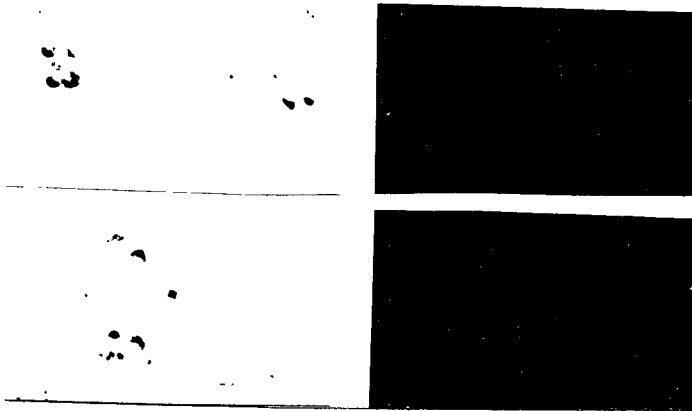
Fig. 2. TUNEL staining of HPV-G cells. *Upper row:* Viable cells immediately after detachment by trypsinization. *Lower row:* Cells 24 h after irradiation. *Left::* Light microscopy. *Right:* Fluorescence.

Single-cell electrophoresis is based on the visualization, by ethidium bromide, of DNA fragments that permeate through the impaired plasma membrane of a fixed cell, and move in the electric field. Comet-like pattern characterizes cells with fragmented DNA. The methods allows also to monitor DNA damage caused by radiation and the course of DNA repair. This method yields very specific information on the state of DNA in individual cells, and is applicable to cell populations counting only several hunderds of cells. Because the preparation of the sample comprises application of strong detergent solution immediately after embedding the cells into the gel, the stage of the apoptotic process becomes quicky frozen. Therefore, the method is applicable to monitoring kinetics of processes proceeding for several hours.

The *Cell Death Detection ELISA immunoassay* was shown to monitor with high sensitivity the fragmentation of chromatin caused either by spontaneous cell detachment or by apoptosis inducers, such as dimethylsulfoxide or irradiation.

The variety of above reported methods could be applied to HPV-G cells in the suspension state. The development of the short-term suspension culture of HPV-G cells in untreated plasticware opened numerous experimental approaches.

The HPV-G cells grown in a monolayer on tissue culture plastic or on glass were found to be rather resistant to irradiation by X-ray up to 10 Gy. The supension culture is more flexible and allows to adjust the medium during and after irradiation to reach radiosensitivty at lower doses. In pilot experiments the suspension culture was found to be easily applicable to flow cytometry.

Contract: F13PCT930081   Duration: 1.10.93 to 30.6.95   Sector: B13

Title: Development and validation of an image analysis system for automated detection of micronuclei in cytokinesis-blocked lymphocytes. A tool for biological dosimetry in individuals or populations occupationally or accidentally exposed to ionizing radiation

1)   Tates   Univ. Leiden
2)   Thierens   Univ. Gent
3)   De Ridder   Univ. Gent

I. Summary of Project Global Objectives and Achievements

Introduction

As indicated in the title, the project was initially directed exclusively towards development and validation of an image analysis system for automated detection of micronuclei in cytokinesis-blocked lymphocytes. However, when the project was granted, participants in the project were requested by the Commission to explore possibilities for automated detection of stable chromosomal aberrations such as translocations. Therefore, this final Progress Report will contain information on automated detection of micronuclei and translocations in human lymphocytes.

A. Automated scoring of micronuclei in cytokinesis-blocked binucleated lymphocytes.

All three participants were actively engaged in this part of the project and the experiments were performed in a highly integrated fashion. One of the tasks of Participant 1 was to assist in the validation of the "Discovery" image analysis program developed jointly by Participant 2 and Becton-Dickinson. Initially, the plan was to run this program not only on the "Discovery" in Gent (Participant 2) but also on the "Discovery" in Leiden. However, soon after the start of the project, the "Discovery" in Leiden was replaced by the more sophisticated "Fluorbance" of Becton-Dickinson. Unfortunately, the software for the "Discovery" could not be used for the "Fluorbance". For a variety of reasons, Becton-Dickinson did not adapt the "Discovery" software for use on the "Fluorbance". Consequently, Participant 1 was unable to contribute to the development of procedures for automated detection of 1) micronuclei in binucleated lymphocytes and 2) centromeres within micronuclei using fluorescence in situ hybridization (FISH). At a late stage of the project, Participant 1 was able to install "Discovery" software in the "Discovery" of the Erasmus University in Rotterdam. On the latter machine we performed automated measurements of micronuclei in lymphocytes from a single donor that were exposed *in vitro* to different doses of ionizing radiation. Microscope slides used for these measurements were also analyzed automaticallly on the "Discovery" of Participant 2 in Gent so that the effect of differences in operators could be studied.

Participant 1 also performed manual analysis of slides to construct dose-effect curves for radiation-induced micronuclei in lymphocytes from five healthy donors. These results could be compared with results of automated measurements collected by Participant 2 and

with results of manual scoring of irradiated lymphocytes of three healthy donors performed by Participant 3. Results of this thorough and integrated interlaboratory validation of automated and manual micronucleus scoring procedures indicated that the differences between the two procedures and between manual scoring in different laboratories are of the same magnitude. It is also concluded that frequencies of micronuclei after low dose exposures can be scored automatically and manually with the same accuracy.

The development and evaluation of image analysis algorithms for automated selection of cytokinesis-blocked binucleated lymphocytes with/without micronuclei was the main task of Participant 2. Technical details concerning the various image analysis procedures that ultimately result in selection of binucleated cells with/without micronuclei are given in in the progress report of Participant 2. In so far as it concerns the selection of binucleated lymphocytes with or without micronuclei, it can be concluded that the localization of such cells on slides - and their storage in the computer for retrospective visual inspection on the TV screen - can take place fully automatically. Upon visual inspection, more than 60% of the selected objects are indeed binucleated cells and 96.5 % of the binucleated objects without micronuclei were correctly classified. With the present state of the art, the automated selection must be followed by a quick and simple manual operation to remove false positive cells. Although the existing software can still be improved, the major stumbling block for large scale application of the automated detection procedure is a lack of financial resources for buying additional equipment such as a slide feeder and computer storage capacity that will allow unattended operation of the "Discovery" for long periods of time.

Participant 3 contributed substantially to the success of the automation procedure by developing appropriate fixation and staining procedures for suitable slide preparations. A particularly useful modification of the traditional preparation techniques involved the production of binucleated cells with touching or slightly overlapping nuclei. This is essential for the detection algorithm for binucleated cells which makes use of "electronic" construction of a centroid around the touching nuclei and which eliminates the time consuming segmentation steps for the cytoplasm around the nuclei. Micronuclei in such cells can then effectively be detected by screening for micronuclei in a circular imaginary cytoplasm with a dimension that is 10% larger than that of the centroid around the touching nuclei (for details see Verhaegen et al., 1994).

Another important activity of Participant 3 concerned the development of staining procedures for centromeres within micronuclei. It has long been known that the use of micronucleus frequencies for biological dosimetry purposes is severely hampered by the fact that there are large interindividual differences in spontaneous frequencies of micronuclei. Thus, when pre-exposure spontaneous micronucleus frequencies of irradiated subjects are unknown, it is difficult to calculate the radiation dose received with a large degree of confidence. This is particularly true for radiation doses below 1 Gy.

In the context of this project, Participant 3 developed an " absorption" in situ hybridization method for centromere detection in micronuclei. Subsequently, this method was used to determine the ratio of centromere positive/centromere negative micronuclei in 12 healthy subjects. Only a very small percentage of the micronuclei were centromere negative, while a high and variable percentage of the micronuclei was centromere positive (65-86%). This observation suggests the aneuploid nature of most spontaneous micronuclei. An additional finding was that the spontaneous frequency of centromere positive micronuclei increased with age whereas the frequency of centromere negative micronuclei remained constant with age. This supports the previous conclusion concerning

the aneuploid nature of most spontaneous micronuclei.

Furthermore, Participant 3 studied centromeres and micronuclei in lymphocytes irradiated with X-ray doses in the range 0.1-1 Gy. In this dose-range centromere positive micronuclei were not induced, whereas there was a dose-dependent induction of centromere negative micronuclei. The observation that spontaneous micronuclei are predominantly centromere positive whereas radiation-induced are mostly centromere negative offers interesting possibilities for increasing the sensitivity of the micronucleus technique for biological dosimetry purposes. For the one donor investigated the detection limit was 0.25 Gy for the conventional micronucleus assay whereas the detection limit decreased to 0.08 Gy when only centromere negative micronuclei are scored. These results are very promising and require further substantiation with more donors.

At the moment we are not in the position to measure centromeres within micronuclei automatically. This will only be possible when staining procedures have been modified in such a way that the same slide can subsequently be used for automated selection of - micronucleated cells and for detection of centromeres within the micronuclei of selected cells.

B.
Automated scoring of chromosomal translocations using single- and multi-colour fluorescence in situ hybridization (FISH) for biological dosimetry.
(Participant 1)

Accurate measurement of effects of radiation exposure is important for 1) detection of occupational and environmental exposure, 2) evaluation and guidance of medical treatment in cases of accidental exposure or 3) for measurement of radiosensitivity of tumours and normal tissue to optimize cancer therapy. By the mid 1960's it had been established that the frequency of chromosomal aberrations in peripheral blood lmphocytes can serve as an indicator of radiation exposure. This frequency can be measured by counting dicentrics, fragments and ring chromosomes in metaphase spreads. The background frequency of dicentrics is about 0.5-1 per 1000 cells in normal individuals, and its sensitivity is high, as an increase of dicentric chromosomes can be detected for relatively low radiation doses (0.2 Gy of X-rays). In order to detect exposure to low radiation doses, a large number of metaphases must be analyzed, which is a very time-consuming task to perform manually. Several attempts have been made to fully automate the aberration scoring on uniformly stained metaphase spreads. This was approached as a two step procedure in which the metaphase spreads were first located and subsequently analyzed for the presence of dicentric chromosomes. However, so far full automation of the scoring of dicentric chromosomes has not been achieved reliably due to the complex image analysis problems involved.

With the aid of *in situ* hybridization techniques it has now become possible to use the number of translocations as an indicator for biological dosimetry. An additional advantage is that translocations, unlike dicentrics, are stable aberrations so that the analysis can take place a long time after irradiation. The detection of translocations can be accomplished by using whole chromosome painting probes in combination with a counterstain for total chromosomal DNA. Translocations can then be scored by counting the number of chromosomes containing parts of the painting probes in relation to the original number of painted chromosomes. Within the present automation project a system is being developed for the automated scoring of radiation-induced translocations using single- and multiple colour fluorescence in situ hybridization. These studies were performed by Drs. Darroudi,

Natarajan and Tates from the Dept. of Radiation Genetics and Chemical Mutagenesis in Leiden in collaboration with Drs. Tanke, Vrolijk and Sloos from the Dept. of Cytochemistry and Cytometry in Leiden.

A critical first step in these activities involved development of an automated system that can automatically screen for metaphases in lymphocyte preparations using DAPI as counterstain. This system consists of a Macintosh IIfx computer, and an automated Ergolux microscope with a fluorescence illuminator, scanning stage, focus motor drive, computer controlled objective rotor and an automated filter wheel. As an image sensor, a Sony black and white CCD camera was used with capabilities for on-chip integration. Using this combination of equipment it was possible to automatically screen a single microscope slide for metaphases in a time span of about 70 minutes including a time period of 25 minutes for autofocussing. The false positive rate for metaphase finding was 7% whereas about 13% of metaphases were missed. These percentages correspond quite well with results from commercially available metaphase finders which mostly operate on Giemsa-stained slide preparations.

An important aspect of our metaphase finding system is that slides used for metaphase screening can subsequently be used for automated scoring of painted chromosomes and thus for translocation detection. The translocation detection starts with a relocation of preselected stored metaphases at high magnification using a dual band by-pass filter for FITC and DAPI. Initially single colour FISH was performed using a paint probe specific for chromosome 4. This procedure was used to screen for translocations induced in lymphocytes that were given an *in vitro* exposure of 4 Gy of X-rays. In this pilot study 120 metaphases were screened manually and automatically for induced translocations. The result was that the automated device correctly identified translocations in 90% of the metaphases selected. In more recent experiments, dual colour FISH was employed using paint probes for chromosomes 4 and 8 labelled with spectrum green and spectrum orange respectively. In this case cells from three healthy donors were exposed to 0.1, 0.25, 0.5, 1.0 and 2.0 Gy so that dose-effect curves can be constructed both manuallly and automatically. Results from the manual analysis are already available and thousands of automatically selected metaphases have been stored in the computer for future automated detection of translocations. Future comparison of manual and automated findings will allow us to validate the success of the automated screening procedure.

In the mean time, a new detection system with improved efficiency and sensitivity is being tested. This promising system consists of a DM-XRA microscope, a Power Macintosh computer and a Xilix camera. This powerful combination of new equipment will increase the speed of image analysis by about 800%. At the moment, the development of software for the new equipment is almost completed. Apart from these technological improvements we have been able to work out a more sensitive staining procedure for translocation scoring. This procedure is called ratio-labelling. It essentially involves staining of a probe for an individual chromosome pair with either a particular fluorochrome (e.g. AMCA, FITC or TRITC) or with a combination of fluorochromes mixed in a well-defined ratio. In this way more colours can be obtained thereby making it possible to separate at least 6 differentially stained chromosome pairs within the same metaphase without taking any spatial information into account. Details about results obtained with the ratio-labeling procedure will soon be published.

Head of project 1: Dr. Tates

II. Objectives for the reporting period
A.
Automated detection of micronuclei with/without centromeres in binucleated human lymphocytes
- Contribution to validation of a "Discovery" (Becton Dickinson) image analysis program for automated detection of micronuclei in binucleated lymphocytes by using software (developed by Participant 2 and Becton Dickinson) and a "Discovery" located in the Netherlands.
- Adaptation of the above program for a second generation image analyser "Fluorbance" (Becton Dickinson) which replaced the "Discovery" in The Netherlands in 1994.
- Development of an "absorption" in situ hybridization (ISH) method which utilizes two stains with non-overlapping absorption spectra i.e. methylgreen for nuclei plus micronuclei plus alkaline phosphatase-CAS red for identification of centromeres in micronuclei. Use of this method for automated detection of centromeres in micronuclei identified by means of the "Fluorbance".
- Validation of this method by comparing results of manual and automated measurement of micronuclei in several normal subjects and in lymphocytes exposed in vitro to different doses of X-rays.
B.
Automated metaphase finding and detection of chromosomal translocations in mononucleated human lymphocytes
- Contribution to the development of hard/software for automated metaphase finding and scoring of chromosomal translocations visualized by fluorescence in situ hybridization (FISH).
- Validation and improvement of this system by combining ratio-labeling staining procedures with chromosome specific probes. This will allow detection of translocations between more pairs of chromosomes and among labelled chromosomes.

III. Progress achieved including publications

ad A.
Micronucleus studies
For the micronucleus studies in The Netherlands numerous difficulties were encountered which centered around the availability of operational image analysers. At the the beginning of the project, a "Discovery" image analyser was available at the Dept. of Cytochemistry and Cytometry in Leiden. Initially it was impossible to install the software for automated micronucleus detection developed jointly by Participant 2 and Becton Dickinson. When these problems were solved, the "Discovery" was sold to the Erasmus University in Rotterdam and replaced by the more advanced "Fluorbance" image analyser. Participant 1 had access to the "Fluorbance" but, unfortunately, the software developed for the "Discovery" was incompatible with the "Fluorbance". It was agreed that Becton Dickinson would adapt the "Discovery" software to the "Fluorbance" but this was never realized. In addition, the performance of the "Fluorbance" for our- and other research projects was so poor that the equipment was returned to the manufacturer.

In view of these unforeseen difficulties, it was impossible for Participant 1 to validate the automated procedure for detection of micronuclei in binucleated lymphocytes and to develop methodology for automated detection of centromeres within micronuclei. Nevertheless, through help of the Erasmus University in Rotterdam and with assistance of Drs. de Scheerder from the Standard Dosimetry Laboratory in Belgium, we were able to install software for automated micronucleus detection a short period of time in the "Discovery" of Rotterdam. During this period we performed an automated measurement of micronuclei in lymphocytes from a single donor whose lymphocytes had been exposed in vitro to X-ray doses of 0.1, 0.2, 0.5, 1 and 2 Gy. Results of these measurements will be compared with automated measurements performed by other operators on the same slide preparations on the "Discovery" in Belgium. These results will be included in a joint publication.

Finally, Participant 1 performed manual scoring for micronuclei in lymphocytes from five healthy donors whose lymphocytes were exposed *in vitro* to the X-ray doses mentioned above. These results are included in the final report of Participant 2.

ad B.
Development of a system for automated metaphase finding and scoring of chromosomal translocations visualized by fluorescence *in situ* hybridization.
In close collaboration with Dr. Vrolijk and Prof. Tanke of the Dept. of Cytochemistry and Cytometry and Drs. Darroudi, Natarajan of the Dept. of Radiation Genetics and Chemical Mutagenesis in Leiden in The Netherlands and Participant 1, an image analysis system has been developed that can detect metaphases on the basis of a fluorescent counterstain (DAPI). With the same system one can subsequently analyze the number of translocations within selected metaphase cells with the aid of whole chromosome paints using biotin-16-dUTP and in situ hybridization. The system consists of a Macintosh IIfx computer, an automated Ergolux microscope equipped with fluorescence illuminator, scanning stage, focus motor drive, computer controlled objective rotor and an automated filter wheel. As a image sensor, a Sony black & white CCD camera was used with capabilities for on-chip integration.

The analysis was carried out in two steps. First, the test slide was automatically screened for the presence of metaphases using DAPI as counterstain, then the relocated metaphases were manually focused and digitized using a 100x objective in combination with a dual band by-pass filter for FITC and DAPI. Automatic scoring of the painted chromosomes was based on contrast differences between the painted chromosomes and the counterstain. To test the metaphase finder, slides were prepared from phytohaemagglutinin stimulated peripheral blood lymphocytes. Slides were stained with DAPI using standard procedures. To detect radiation-induced translocations automatically, a pilot study was performed in which lymphocytes were exposed *in vitro* to a high dose of 4 Gy X-rays. A second set of experiments was designed to construct dose-response curves for X-ray induced translocations (doses of 0.1, 0.25, 0.5, 1 and 2 Gy) in lymphocytes from three healthy donors. Standard protocols were used for culturing and fixing of blood lymphocytes. Air-dried preparations were made under an infra-red lamp. For the pilot study a single colour FISH was performed with a whole painting probe for chromosome 4 labelled with FITC. For the second set of experiments we thusfar used dual colour FISH for chromosomes 4 and 8.

ad B1.

Results of the pilot study

In this study a complete analysis of a slide (8 cm^2) for the presence of metaphases could be carried out automatically in about 70 minutes, of which about 25 minutes were required for autofocussing. The false positive rate for metaphase detection was 7%, while 12.7 % of the metaphases were missed. These figures correspond rather well with figures reported for commercially available metaphase finding systems for Giemsa stained specimens. Apart from the metaphase finding aspects of the methodology, 120 metaphases were examined automatically for the presence of translocations involving chromosome 4. Results were compared with those obtained by manual scoring. A correct classification rate of circa 90 % was obtained. Results were published recently (Vrolijk et al., 1994).

ad B2.

New developments

To improve the efficiency and sensitivity of the automated screening method for translocation events, a new system is being developed and tested. It consists of a DM-RXA microscope, a Power Macintosh computer and a Xillix camera. This new microscope has a higher efficiency for epi-illumination compared to the previously used Ergolux microscope. This will shorten integration times when images are captured. Besides an automated stage, focus motor drive, objective rotor and filter wheel, also the filter blocks of the fluorescence illuminator can be controlled allowing the selection of different excitation wavelengths for the different fluorochromes without a visible pixel shift. In this way no registration problems will occur between the counterstain image and the images from the painted chromosomes. Conversion of the image processing software from the 680xx-based processors to the Power PC processor will give a speed increase of circa 800% for image analysis, so that the performance of the system will be mainly limited by the time it takes to capture images. In the new system, the Sony camera has been replaced by the Xillix camera. The latter camera is more sensitive and has a larger chipsize, so that larger images (for metaphase finding) can be processed more efficiently thereby shortening the time it takes to analyze a slide, while the higher sensitivity of the camera will lower the exposure times. At this moment most of the software developments for the new system have been completed.

During the pilot study no colour information was taken into account for counting the number of painted chromosome parts. Painted chromosomes or parts thereof were detected on the basis of contrast differences relative to the DAPI counterstain. This resulted in a number of false positive signals. In order to improve the performance, separate exposures will be taken for the counterstain and for the painted chromosomes. In order to optimize these algorithmes and to test the performance of the system, 500 metaphases have been digitized for each of 6 different radiation doses. Two painting probes labelled with spectrum green and spectrum orange were thereby applied: one for chromosome 4 and one for chromosome 8. From this data set 25 images per radiation dose will be used as a learning set for the new algorithms, while the remaining 475 metaphases (per dose) will serve as a test set to determine the performance of the system and to construct dose-response curves both manually (Table 1) and automatically (in progress).

ad B3.

Colour processing

The sensitivity of the existing methodology can be increased further by applying so-called ratio-labelling procedures for the painting of chromosomes. In this way more colours can be obtained as a combination of two or three fluorochromes, while also translocations between painted chromosomes can be distinguished. A pilot study has been carried out, in which nine different chromosomes were labelled with a combination of AMCA, FITC and TRITC (Table 2). The 3 different colour images of a number of metaphase spreads were digitized sequentially using a cooled Photometrics black & white CCD camera in combination with the proper excitation and emission filters. The images were flat-field corrected, while also the aspecific fluorescence was subtracted. Finally corrections due to filter overlap were made, after which the colour images were converted to the HSI (hue-saturation-intensity) domain. On the basis of clustering techniques in the HS-plane at least 6 different labelled chromosome pairs could be separated without taking any spatial information into account. Further developments will be carried out to increase the speed of these algorithms, so that they can be efficiently incorporated into the software package for translocation scoring.

ad B4.

Conclusions

The results of a pilot study suggest that automatic detection of translocations is possible. Although no colour information was applied, a 90% correct classification rate was obtained. The first step of the process, namely the automatic detection of metaphase spreads on the fluorescence counterstain, has been realized with a similar performance as commercially available metaphase finders for Giemsa stained slides. The newly developed system will have a higher efficiency and will allow the analysis of more than one painted chromosome based on colour processing. This latter aspect will increase the sensitivity for translocation scoring.

It is expected that the new system - composed of the DM-RXA microscope, the Xillix camera and the Power Macintosh computer - will be operational by the end of this year. It will then be possible to automatically detect metaphases on the DAPI counterstain, to relocate and autofocus the metaphases at high magnification (63x or 100x objective), to acquire the separate colour images for the counting of the painted chromosomes and to score the number of painted chromosomes, or chromosome parts, automatically. Further research will then continue to increase the number of painted chromosomes to more than two, so that the sensitivity for translocation scoring will be even further increased. This obviously will allow to study involvement of specific chromosomes in radiation induced translocations. Finally the new system will be extensively validated by comparing results of automated and manual scoring.

Publications:

Vrolijk, J., Sloos, W.C.R., Darroudi, F., Natarajan, A.T. and Tanke, H.J. (1994) A system for fluorescence metaphase finding and scoring of chromosomal translocations visualized by in situ hybridization. International Journal of Radiation Biology, 66, 287-295.

Three papers incorporating the various aspects of improved translocation image analysis are in preparation.

Table 1:

X-ray-induced translocations in human peripheral blood lymphocytes (manual scoring) using FISH technique

Dose (Gy)	Chromosome labeled	Cells scored	Abnormal cells	Translocations			Total (%)	Trisomy (%)
				TT	RT	IT		
0	4	1520	0	0	0	0	0	0
	8		0	0	0	0	0	0
0.1	4	1606	0	0	0	0	0	0
	8		0	0	0	0	0	0.06
0.25	4	1607	5	2	3	0	0.4	0.2
	8		7	4	3	0	0.4	0
0.5	4	921	6	3	3	0	0.7	0.2
	8		6	3	3	0	0.7	0
1	4	1089	26	14	12	0	2.4	0.2
	8		16	11	5	0	1.5	0.4
2	4	922	58	32	27	5	7.0	0.2
	8		48	22	30	5	6.2	0

Table 2:

Schematic representation of a triple hybridization

Labeled probe	Detection	Signal
Probe 1 fluorescein		Green
Probe 2 digoxigenin	anti dig-TRIRC	Red
Probe 3 biotin	avidin-AMCA	Blue

.

Head of project 2: Dr. Thierens

II. Objectives for the reporting period
The objectives were the development and evaluation of image analysis algorithms for selection of cytokinesis-blocked cells and micronuclei within them. This work involved the implementation of the necessary software on the "Discovery" image analysis system (Becton-Dickinson) and the evaluation of the reliability of the automated detection by comparison with results of manual scoring. To remove artefacts resulting in false-positive or false-negative micronuclei, preparation techniques were adapted in close collaboration with Part.3 of the project.

A thorough validation of the procedure for automated scoring was performed by relocation of selected objects followed by manual inspection on the "Discovery" and also by an extensive comparison of the number of micronuclei scored manually under the light microscope by Participants 1 and 3. For this validation a close collaboration between the three participants in the project was necessary.

III. Progress achieved including publications

A.
Development of the algorithm for automated detection of micronuclei in binucleated cells
After an interactive study between Participants 2 and 3 of the project, it was concluded that with modification of the preparation technique yielding binucleated cells with touching nuclei, the use of a circle as searching region for micronuclei gave better and faster results than the time consuming segmentation of the cytoplasm. An algorithm for automated detection of micronuclei based on detection of binucleated cells with touching nuclei was worked out.

The flow diagram of the algorithm is represented in Figure 1. The first part of the program uses the low magnification camera of the system allowing a large field (25x objective-supplementary reducing lens x0.5). In this field morphometric characteristics such as area, perimeter, contour ratio, skeleton parameters of the objects are determined and binucleated cells are selected by the use of selection gates for the characteristics

considered. In the second part of the program at high magnification (25x objective-supplementary magnifying lens x2) the selected cells are viewed one by one to count the micronuclei within a circular region centred at the centroid of the double nucleus. It was found empirically that the best equivalent to the real cytoplasm is obtained when the circle encompassing the double nucleus is expanded by 10%.

Within this circular region the search for micronuclei is performed in two steps: a search for micronuclei that lye loose in the cytoplasm followed by the detection of micronuclei touching the nuclei. An object is accepted as a loose lying micronucleus if area and contour ratio (test for roundness) are within predefined limits. Micronuclei touching the nuclei are searched by scanning the edge of the object with two different methods. With the first method, a vector with the distances from edge-points to the centroid of the object is constructed. With this method micronuclei appear as small local maxima in the edge-centroid distance. This procedure allows also an artefact rejection : vectors with more than two large maxima are polynuclear (three and more) cells while a large number of small maxima points indicates metaphase chromosomes. With the second method that searches for touching micronuclei, the local convexity of the edge is para-metrised using the following procedure: the centroid of each piece of the edge determined by a chord with a certain predefined length is calculated and the distance from this point to the chord serves as parameter. With this method micronuclei are found as a small convex zone, flanked by two slightly concave zones. In both methods the position of a micronucleus on the edge is stored. The number of touching micronuclei obtained by methods 1 and 2 are pooled and to avoid double counting the micronuclei obtained by both methods are subtracted. Finally the number of overlapping micronuclei is added to the number of loose-lying micronuclei to yield the total number in the analysed cell.

To reduce the number of artefacts an accurate setting of the selection gates for the morphometric characteristics is of crucial importance. These selection gates are deter-mined experimentally using 1000 known objects (binucleated cells, mononuclear and poly-nuclear cells, artefacts) on the slides as imput for the program. This is illustrated in Figure 2 where the selection gate for the contour ratio is plotted versus area and perimeter together with the data used for the determination of the gate.

The image analysis program runs as a Microsoft Windows application with software written in the C++ language. Cell features are stored in a database on a cell-by-cell basis. Cells are classified in three different classes: binucleated cells without micronuclei (class noMN), binucleated cells with one or more micronuclei (class MN) and artefacts. The system allows graphical presentation of the results in the form of histograms or two-dimensional scatterplots. Images of the cells obtained at high magnification can be retrieved from the harddisk where they were stored during measurement. Incorrectly classified cells can be moved to the correct class by a simple reassignment operation.

A first evaluation of the program was performed on slides of a blood sample irradiated *in vitro* with a dose of 1 Gy X-rays. The automated system scored about 6000 cells, which were evaluated manually afterwards one by one on the Discovery after relocation. This evaluation showed that after careful settings of the selection gates more than 98% of the objects classified in the noMN class are in the correct class. It was concluded that false-negatives are not a problem for the system. On the other hand, a significant number of false-positives, depending on the quality of the slide, are present in the MN class. It was not possible to reduce this number to an acceptable level by appropriate gate selection. Consequently for the MN class visual inspection with eventual reassignment to other

classes after the automated analysis is required to obtain correct results. It has to be mentioned that this procedure is not time-consuming on the "Discovery" in the case of low doses (< 2 Gy), which usually play a role in practical biological dosimetry.

In conclusion, as reliable procedure for scoring micronuclei with the "Discovery" system we propose a semi-automated approach, in which the objects in the MN class are inspected visually after the automated scoring and are eventually reassigned to other classes.

B.
Validation of the semi-automated scoring procedure

The validation of the semi-automated scoring procedure, described above, was based on slides obtained from blood samples of five donors after irradiation with 0.1, 0.2, 0.5, 1 and 2 Gy of X-rays. Also the spontaneous incidence of micronuclei was recorded. The slides were prepared following a modified protocol described by Participant 3. For these slides micronuclei were scored by the semi-automated procedure on the "Discovery" in Gent (procedure 1). As a first step in the validation each selected object was relocated afterwards, and visually inspected (procedure 2). As a second step in the validation, the same slides were scored manually under the light microscope in Leiden by Participant 1. To investigate interlaboratory differences, the slides of three donors were also scored manually in Gent by Participant 3. For each data point 2000 binucleated cells were considered. The results of this thorough validation are summarized in Figure 3. In this figure the dose-response data obtained by the proposed semi-automated procedure on the "Discovery" (procedure 1) are compared with the data after complete visual inspection on the "Discovery" (procedure 2) and the results of the manual scoring by Participants 1 and 3.

The first step of the validation, e.g. procedure 2 on the "Discovery" in comparison to the results of procedure 1, showed that 62 $\pm$ 4 (s.d.) % of the selected objects were binucleated cells. The remaining objects were mononuclear, polynuclear cells and artefacts. Consequently about 3000 objects have to be analysed to obtain 2000 binucleated cells. Another important conclusion is that 96.5 $\pm$ 0.8% of the objects in the noMN class are classified correctly, supporting the reliability of the proposed semi-automated approach. Reassignment to the correct class of the remaining 3.5% involves an increase of the micronucleus yield by 15.4 $\pm$ 2.9%. The size of this systematic underestimation by procedure 1 is of the order of the statistical uncertainty on the micronucleus yield in the low dose range, considered in present study.

Figure 3 shows that the interpretation of the comparison of the data obtained by computerized image analysis with the results of the manual scoring is more difficult. Taking into consideration the manual data collected by Participant 1 for all donors, the differences with the automated scoring are not systematic: i.e. differences of opposite sign/direction are almost equally present. Taking into account also the manual data of Participant 3 for donors 1-3, it is clear that the interlaboratory differences between the micronucleus yields scored manually are of the same size as the differences between the automated and manual scoring. On the basis of results obtained with the present validation study, it is concluded that micronucleus frequencies after low dose exposures can be scored automatically and manually with the same accuracy.

Conclusion

A reliable semi-automated scoring procedure for micronuclei in binucleated cells has been developed which is very useful for the dose range usually encountered in daily radio(bio)logical practice. This procedure consists of a fully automated localization of binucleated cells and counting of the micronuclei within these cells. The procedure is followed by a simple and fast manual operation by means of which the false positives are removed.

A thorough interlaboratory validation of automated and manual micronucleus scoring procedures has indicated that the differences between the two procedures and between manual scoring in two laboratories are of the same magnitude. It is also concluded that that frequencies of micronuclei in the low dose range can be determined with the same accuracy by automated image analysis procedures as by manual scoring.

Publications

Verhagen, F., A. Vral, J. Seuntjens, N.W. Schipper, L. de Ridder and H. Thierens (1994) Scoring of radiation induced micronuclei in cytokinesis blocked human lymphocytes by automated image analysis. Cytometry, 17, 119-127.

Vral, A., F. Verhaegen, H. Thierens and L. de Ridder (1994) The in vitro cytokinesis-block micronucleus assay: a detailed description of an improved slide preparation technique for the automated detection of micronuclei in human lymphocytes. Mutagenesis, 9, 439-443.

Participants of the project (1995/96) Validation and comparison of automated and manual procedures for detection of binucleated lymphocytes with/without micronuclei. In preparation.

LMAG

LMAG Grey Image

threshold in
intensity histogram

LMAG Binary Image

Selection of binucleate cells.
measurement of
Area, Perimeter, Contour Ratio
Skeleton Features

HMAG

Grey Image of Selected
Cell at HMAG

automatic threshold
in intensity histogram

HMAG Binary Image

adjusting circle
around centre object
(=double nucleus)

double nucleus and
MN in circular region

Counting loose-lying MN.
Criteria of acceptance.
ratio Mn-area/Cell-area
Contour Ratio MN

Number of
Loose-lying MN

Determining Edge
of double nucleus

Edge of double nucleus

Scanning the Edge
for touching MN

Method 1   Method 2

Combination of
the results of the
two methods

Number of
Touching MN

Figure 1: Flow chart of the algorithm
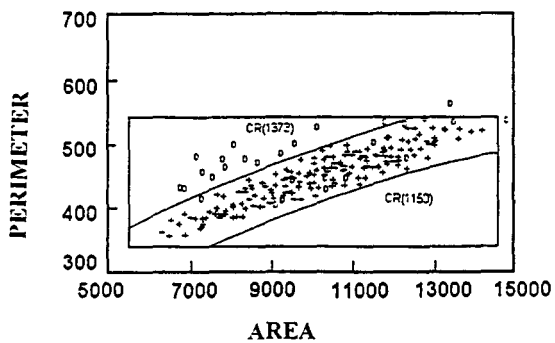
Figure 2: Selection gate for the contour ratio (full line) plotted versus area and perimeter together with the data used for the determination of the gate. The crosses represent binucleate cells, the circles are mostly polynucleate cells.
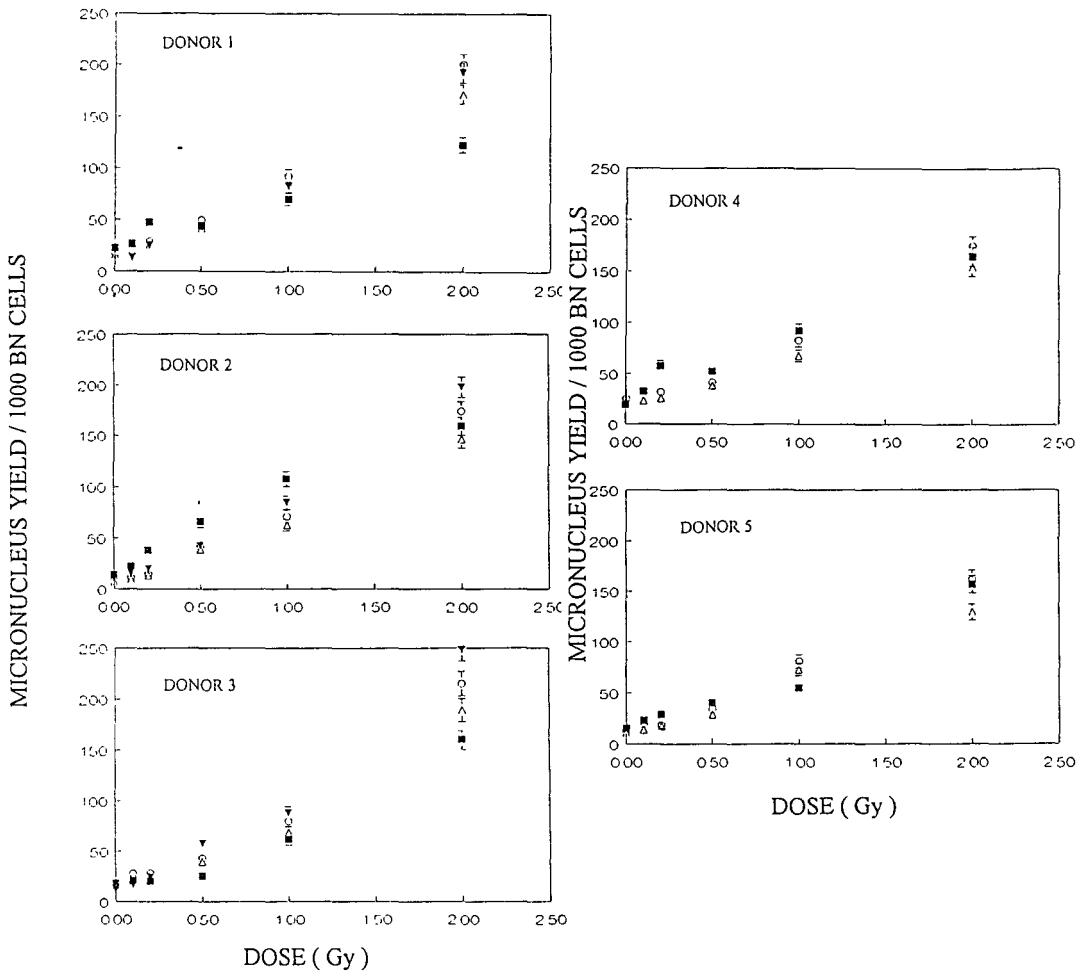
Figure 3: Comparison of micronucleus scoring with computerized image analysis and manual scoring by light microscopy

△ : micronucleus yield obtained by semi-automatic scoring with the Discovery analyser (procedure 1)

○ : micronucleus yield after complete manual evaluation with the Discovery system of the data obtained with procedure 1 (procedure 2)

▲ : micronucleus yield obtained by manual scoring by light microscopy in Gent

■ : micronucleus yield obtained by manual scoring by light microscopy in Leiden

Head of project 3: Prof. De Ridder

II. Objectives for the reporting period

A.

Development of a micronucleus-centromere assay to detect low doses of irradiation.
This implies:
1. further optimation of the "absorption" in situ hybridization (ISH) method which utilizes the peroxidase-diaminobenzidine (PO-DAB) reaction for the detection of the centromeres in micronuclei and the Romanowsky-Giemsa staining for the detection of nuclei and micronuclei.
2. investigation of spontaneous and radiation-induced MN for the presence of centromeres.

B.

Validation of the automated micronucleus scoring procedure by comparing the results of manual and automated micronucleus measurements in lymphocytes exposed to different doses of X-rays.
The automated measurements were performed by Participants 1 and 2 and the manual measurements by Participants 1 and 3.

C.

Development of an automated micronucleus-centromere scoring procedure.

III. Progress achieved including publications

ad A.

Development of a micronucleus-centromere assay to detect low doses of irradiation.
The detection of individual low dose exposures, in people with unknown pre-exposure spontaneous frequencies of micronuclei (MN), is impossible with the conventional MN assay because of the large interindividual differences in spontaneous frequencies of MN. To increase the sensitivity of the MN assay we optimized the ISH technique for centromere detection in MN. With this optimized MN-centromere technique, we investigated the origin of spontaneously occurring MN for 12 healthy donors. Radiation-induced MN were analysed for one donor in the dose range 0.1-1 Gy.

ad A1.

Optimization of ISH technique for centromere detection in micronuclei.
For optimization of the ISH technique we used the centromeric DNA probe 'p82H' (provided by A.R. Mitchell) which is a cloned alphoid sequence, present at the

centromeric heterochromatin of all human chromosomes (Mitchell et al., 1985). The probe was biotinylated by standard nick-translation. For the preparation of MN slides our automation protocol was used (Vral et al., 1994). This protocol uses a 25:1 methanol:acetic acid fixation of the cells, by means of which binucleated cells are obtained with touching nuclei. This enabled us to recognize binucleated cells because, during the ISH procedure, the cytoplasm of the binucleated cells was eliminated.

For the ISH procedure, slides were pretreated with RNase and pepsin followed by a postfixation in 4% paraformaldehyde. A probe concentration of 4 ng/μl (in 50% deionized formamide) was added to the slides. Probe and target DNA were denatured simultaneously (5 min, 80°C followed by overnight hybridization and postfixation washes. detection and visualization of the signal at the place of the centromere was achieved by immunoenzymatic absorption staining. As immuno-enzymatic absorption staining method we decided to use the indirect biotin-avidin method, whereby avidin was labeled with peroxidase. As substrate for peroxidase, diaminobenzidine (DAB) was used to get permanently stained slides. After this visualization method the nuclei were counter-stained with Romanowsky-Giemsa (4% in Hepes buffer) for 20 min., washed, air-dried and mounted. Centromere detection in MN was restricted to those binucleated cells where the DAB signals were also visible in the main nuclei. Besides MN slides, we also prepared metaphase spreads. In each experiment these metaphase spreads served as an internal control to prove that all centromeres were stained.

ad A2.
a. Centromere detection in spontaneous and radiation-induced micronuclei.
MN of 12 healthy donors were analyzed for the presence of centromeres to provide information about the origin of spontaneous micronucleus formation in human binucleated lymphocytes. We observed a large variation in the total frequency of spontaneous MN between the different donors (7-29/1000 BN cells). Only a very small percentage of these MN were centromere negative (CM$^-$, acentric fragment), while a high and variable percentage of these MN were centromere positive (CM$^+$; 65-86%, whole chromosome). When the donors were classified according to their age, we observed a linear increase in spontaneous MN with age. This increase was due to a comparabel increase in CM$^+$ MN, while the CM$^-$ MN remained constant with age (see Table I and Figure 1). Our finding of the high percentage of CM$^+$ spontaneous MN may point to the aneuploid nature of spontaneous MN. Because the linear increase in CM$^+$ MN is correlated with the overall increase in spontaneous MN with age, we tentatively conclude that aneuploidy is an age related process.

Analysis of MN for the presence of centromeres was also performed in lymphocytes of one donor whose lymphocytes were exposed to different doses of gamma rays. For the radiation-induced MN we observed that the increase in total MN number was due to an increase in CM$^-$ MN (see Table II). CM$^+$ MN were not induced with radiation doses ranging between 0.1-1 Gy. This demonstrates that for low doses of irradiation only breaks are induced and no chromosome laggards, pointing to the clastogenic action of ionizing radiation in this dose range. The increase in CM$^-$ MN with ionizing radiation further proves that the high yield of CM$^+$ spontaneous MN is not due to false positives.

b. The MN-centromere assay for detection of low irradiation doses.
In the framework of radiation protection, the low frequency of CM$^-$ spontaneous MN combined with the CM$^-$ character of radiation-induced MN will allow us to increase the

sensitivity of the MN assay for low irradiation doses by scoring only CM⁻ MN. For the one donor studied, we obtained a detection limit of 0.25 Gy with the conventional MN assay while the detection limit decreased to 0.08 Gy when only CM⁻ MN are scored (see Figure 2). This implies that for this donor the sensitivity of the MN assay was increased by a factor 3. These results are very promising and need further substantiation. In the context of this work dose-response curves for four additional donors will be constructed.

c. Comparison between centromere +/- MN and MN size.
From 50 CM⁻ MN and 50 CM⁺ MN the area was measured on the "Discovery" image analyzer. This was done by Participant 2 who also evaluated whether the MN area was correlated with the presence or absence of a centromere. The mean area for CM⁺ MN was $10.23 \mu m^2$ ($\pm 6.57 \mu m^2$) while the mean area for CM⁻ MN was $9.23 \mu m^2$ ($\pm 7.88 \mu m^2$). A Wilcoxon test showed no statistical significance for difference in the area of MN with or without centromeres. The study of MN size revealed that size of MN cannot be used as a criterium to distinguish between MN containing whole chromosomes or acentric fragments. Especially after higher doses of radiation the joining of several acentric fragments into one MN can be responsible for the occurrence of large radiation-induced MN. Also the difference in size of chromosomes may pose problems because a small chromosome can be smaller than an acentric fragment of a large chromosome.

ad B
The automated micronucleus assay.
a. Further optimization of the slides.
Pretreatment of cells with RNase instead of 5N HCl, prior to staining with Giemsa, resulted in a better and more reliable removal of cytoplasmic RNA. With the acid-catalysed hydrolysis (HCl) the cytoplasm often stained pink what posed problems for the software program.

b. Validation of the automated micronucleus scoring procedure.
For the validation of the automated MN scoring procedure, dose-response curves for 5 healthy donors were scored automatically as well as manually. Results are presented in the report of Participant 2 and in Figure 3 attached to that report. Results of this validation study will soon be written up for publication.

ad C.
Development of an automated procedure for simultaneous detection of micronuclei and centromeres within micronuclei.
At the moment we are testing the suitability of the MN slides stained with peroxidase-DAB for visualization of the centromeres combined with Romanowsky-Giemsa as nuclear stain for automated screening with the "Discovery". Because this work is still in an exploratory phase no conclusions can be drawn as yet.

Publications:
Verhagen, F., A. Vral, J. Seuntjens, N.W. Schipper, L. de Ridder and H. Thierens (1994) Scoring of radiation induced micronuclei in cytokinesis blocked human lymphocytes by automated image analysis. Cytometry, 17, 119-127.

Vral, A., F. Verhaegen, H. Thierens and L. de Ridder (1994) The in vitro cytokinesis-block micronucleus assay: a detailed description of an improved slide preparation

technique for the automated detection of micronuclei in human lymphocytes. Mutagenesis, 9, 439-443.

Vral, A., H. Thierens and L. de Ridder (1995/1996) Analysis of spontaneous micronuclei (MN) for the presence of centromeres to increase the sensitivity of the MN assay after irradiation. In preparation.

Vral, A. 1995. Ph.D. Thesis. " Evaluatie van stralingsgeïnduceerde chromosomale schade in human lymphocyten van het perifere bloed met behulp van de "cytokinesis-block' micronucleus methode" (Evaluation of radiation-induced chromosomal damage in human peripheral blood lymphocytes by means of the 'cytokinesis-block' micronucleus method).

Table I. Total no. of spontaneous MN and ratio CM+/- MN in binucleate cells cultured for 70h with 3.5µg/ml Cytochalasin B. Data for 12 donors.

donor age, sex	no. BN cells	total no. MN	CM+	CM-	MN/1000 BN cells total	CM+(%)	CM-(%)
1 (22y,f)	3000	22	16	6	7.3	72.7	27.3
2 (23y,f)	2000	34	22	12	17	64.7	35.3
3 (28y,f)	2000	29	19	10	14.5	65.5	34.5
4 (31y,f)	2000	41	33	8	20.5	80.5	19.5
5 (31y,m)	3500	75	57	18	21.4	76.0	24.0
6 (31y,m)	2000	46	37	9	23	80.4	19.6
7 (38y,f)	2000	44	35	9	22	79.5	20.5
8 (41y,m)	2000	54	39	15	27	72.2	27.8
9 (43y,m)	2000	38	29	9	19	76.3	23.7
10 (44y,f)	2000	57	49	8	28.5	86.0	14.0
11 (49y,f)	2000	42	31	11	21	73.8	26.2
12 (49y,m)	2000	29	23	6	14.5	79.3	20.7

Table II. Total no. of spontaneous and radiation induced MN and ratio CM+/- MN in binucleate cells cultured for 70h with 3.5µg/ml Cytochalasin B. Data for donor 12.

dose (Gy)	no. BN cells	total no. MN	CM+	CM-	MN/1000 BN cells total	CM+(%)	CM-(%)
0	2000	29	23	6	14.5	79.3	20.7
0.1	2500	52	23	29	20.8	44.2	55.8
0.25	1500	38	12	26	25.3	31.6	68.4
0.5	1000	53	12	41	53	22.6	77.4
1	1000	99	8	91	99	8.1	91.9
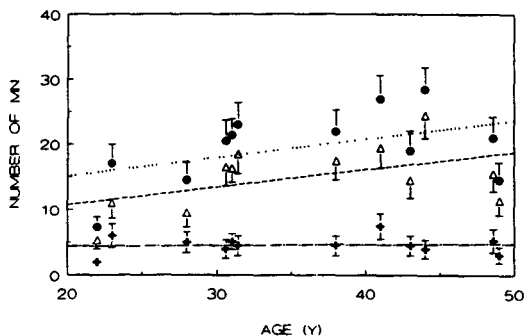
Fig. 1 : The spontaneous MN yield per 1000 CB lymphocytes as a function of age for cultured lymphocytes of 12 healthy donors. Besides the total number of spontaneous MN (●) also the number of CM+ MN (△) and CM- MN (+) are given together with the linear least squares fits, MN = a + bY, through the data (MN total ⸺⸺ , MN CM+ ---------, MN CM- ⸺·⸺·⸺). Error bars represent the statistical uncertainties (95% confidence limits) on the number of MN.
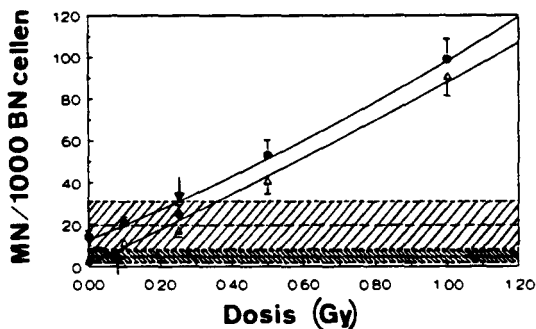
Fig. 2 : The MN number (MN total ● , MN CM- △) per 1000 CB lymphocytes as a function of γ-ray dose for cultured lymphocytes of one donor. The full lines represent the results of linear-quadratic fits, of the form $y = c + \alpha D + \beta D^2$, through the data. The 95% confidence bars for the mean number (based on the data of the 12 donors) of total spontaneous MN (▨) and CM-spontaneous MN (▨) are also given. The arrows indicate the lowest dose that can be detected for this donor with the conventional MN assay (↓) and the MN-centromere assay (↑).

Final Report
1992 - 1994

Contract: FI3PCT920005 Duration:1.9.92 to 30.6.95   Sector: B14

Title: Radiation-induced genetic effects in mammals and the
         estimation of genetic risks in man: a concerted
         approach using theoretical, epidemiological, cyto-
         genetic, biochemical and molecular methods

1) K. Sankaranarayanan   Univ. Leiden
2) C. Tease   MRC
3) P. Jacquet   CEN/SCK Mol
4) C. Streffer   Univ. Essen
5) A. E. Czeizel   NIH/WHO, Budapest

I. Summary of Project Global Objectives and Achievements

The global objective of this project is to strengthen the
scientific basis for the estimation of genetic risks associated
with the exposure of human populations to ionizing radiation and
to set the stage for further work in this area. To achieve this
objective, both theoretical and experimental studies were
undertaken as discussed below.

The *theoretical* studies included (1) an analysis of the impact
of concepts and findings emerging from advances in molecular
biology of human mendelian diseases on radiation risk estimation
for this class of diseases **(Sankaranarayanan)**; (2) an assess-
ment, through the use of specific genetic models, of the
consequences of the presence of germinal mutations in "cancer
predisposing genes" in the human genome to radiation cancer risks
in a population which consists of cancer-predisposed and non-
predisposed individuals **(Sankaranarayanan)**; (3) development of
mathematical models for the estimation of the radiation risk of
multifactorial diseases **(Sankaranarayanan)** and (4) an analysis
of detriment associated with cancers in a defined population in
order to make comparisons of detriment associated with cancers
and genetic diseases, both spontaneous and radiation-induced
(Czeizel).

On the *experimental* side, the work focused on (1) radiation-
induced aneuploidy and transmissible chromosomal aberrations in
germ cells of male and female mice using conventional cytogenetic
techniques, augumented by emerging molecular cytogenetic ones
(Tease); (2) the induction of congenital malformations (scored
in fetuses) by irradiation of male and female gametogenic
(especially immature oocyte) stages **(Streffer)**; (3) improving
methods for the in vitro culturing of oocytes of the guinea pig
in order to assess the extent to which oocytes of this species
can serve as a model for assessing chromosomal radiosensitivity
of human oocytes **(Jacquet)** and (4) molecular studies to define
the genetic basis of one common congenital abnormality in man,
namely cleft lip ± palate **(Sankaranarayanan)**.

A. *Theoretical studies*.
    1. Impact of advances in human molecular biology on radiation genetic risk estimates for mendelian diseases. In this part of the project, which is an extension of the work carried out earlier (Sankaranarayanan, K., Mutation Res. 258, 3-122, 1991), published data on the molecular nature of naturally-occurring mutations resulting in mendelian diseases, the distribution of mutational sites along the genes and mechanisms of origin of these mutations have been collated for a total of over 300 mendelian diseases. Overall, about 65% of mendelian diseases are due to point mutations (PMs), 22% are due to both PMs and length mutations (LMs; mostly deletions) and the remainder, due to LMs and microdeletion syndromes. In the majority of genes, the mutational sites of PMs are non-randomly distributed and this is also true of the distribution of breakpoints in LM-associated mutations. Further, accumulating evidence documents the existence of novel mechanisms in the origin of mendelian diseases (e.g., the expansion of trinucleotide repeat sequences in the coding or untranslated regions of the gene).
    The results of these and other analyses on the nature of radiation-induced mutations in experimental mammalain systems and comparison of mechanisms involved in the origin of spontaneous and radiation-induced mutations support the view advanced in 1991 that naturally-occurring mendelian diseases do not constitute an entirely adequate framework for radiation risk estimation and that current risk estimates for this class of diseases are conservative.

    2. Cancer predisposition, radiosensitivity and the risk of radiation-induced cancers. The fact that certain human mendelian diseases have one or another type of cancer as the principal phenotype and that cells from individuals with some of these disorders are more radiosensitive than those from "normal" individuals has long been known. The possibility that cancer-predisposed individuals may also be at an increased risk for radiation induced cancers has now come to the forefront of attention and has raised questions on the risk of radiation-induced cancers in a population consisting of both cancer-predisposed and "normal" individuals. This problem was investigated using a mendelian autosomal one-locus, two-allele model. The results show that when such heterogeneity with respect to cancer predisposition and radiosensitivity is present in the population, irradiation results in a greater increase in the frequency of induced cancers than when it is absent; this increase is detectable only when the proportion of cancers due to genetic predisposition is large and when the degree of predisposition is considerable. Application of the above model to the breast cancer data in A-bomb survivors in Japan (which suggest a relative risk of about 14 at 1 Gy for early onset breast cancers) shows that these results can be explained only if there are large differences in cancer predisposition (>1000-fold) and radiosensi-tivity (>100-fold) between predisposed and non-prediposed women.

    3. Estimation of the radiation risk of multifactorial diseases in man. So far, not very much progress has been made in the estimation of the radiation risk of multifactorial diseases. This is because of the lack of adequate theory, models and empirical

data. Work was therefore initiated to investigate the above problem within the framework of an ICRP Task Group on this subject.

In this work, the multifactorial threshold model (MTM) (which is commonly used to estimate recurrence risks to relatives from data on population prevalences on the basis of quantitative genetic principles) has been modified to answer the question of the effects of an increase in mutation rate on disease prevalence. The modifications include the incorporation of mutation (μ) and selection (s) and the assumption that the numbers of gene loci underlying these diseases are finite (2-20). The modified models enable one to estimate the "mutation component" (MC) of multifactorial diseases i.e., the proportion of disease incidence that is directly proportional to mutation rate. With arbitrarily chosen μ values of 10^{-6} to 10^{-5}, s coefficients of 1 and 0.5 and prevalences in the range from 1/1000 to 5/1000, under conditions of a permanent doubling of the spontaneous mutation rate, our models predict that the MC is of the order of 2-4% in the first 10 generations (and under 2% in the first two generations). This means that the expected increase in prevalence of multifactorial diseases under conditions of a fractional increase in mutation rate will be very small.

4. Estimates of detriment associated with cancers in a defined population. In earlier work, epidemiological and other data on mendelian and multifactorial diseases were analysed and estimates of detriment (i.e., the degree of harm, handicap or disability) associated with these at the individual and population levels were obtained. The present work extends this analysis to cancers thereby setting the stage for comparisons between genetic diseases and cancer, both naturally-occurring and radiation-induced. The basic data used in these analyses come from studies carried out in Hungary.

Twenty-eight different types of cancers were considered and four measures of detriment were used, namely, years of life lost, potentially impaired life, actually impaired life and economically impaired life. Considered overall, the average onset age for cancers is of the order of about 46 years; men get cancers about 5 years earlier than women, retire prematurely about 3 years later than women and die about 6 years earlier than women. In both sexes, early deaths (between 0 and 19 years) are predominantly due to lymphoid leukemia. Most cancers cause death in adulthood (i.e., between 20 and 69 years of age) and late death (< 70 years). Again in both sexes, adult deaths due to brain cancer and Hodgkin's disease account for over two-thirds of all cancer deaths. In males, deaths due to cancers of the upper respiratory tract account for more than 80% of all adult and late deaths whereas in females, the ratio of adult to late deaths is about 50:50.

At the individual level, in males, the average number of years of lost life years cover a range between about 6 to 19; in females, this ranges between 10 and 23 years. For potentially impaired life years, in males, the range is between 2 to 14 and in females, between 10 to 34. The estimates of actually impaired life years range from about 2 to about 10 in males and from about 10 to 25 in females. The economically impaired life years likewise encompass a range from 10 to 20 years in males and a similar range in females. Averaged over all cancers and both

sexes, the average number of years of lost life, potentially impaired life and actually impaired life and economically impaired life are about 14, 10, 15 and 12, respectively.

B. Experimental studies

1. <u>Radiation-induced sex-chromosomal aneuploidy in male germ cells of mice</u>. In one set of experiments, the potential of the technique of fluorescence in situ hybridization (FISH) to study radiation-induced sex-chromosome aneuploidy in germ cells of male mice was examined. Two repeat sequence DNA probes, one at the proximal end of the X chrmosome and the other for the long arm of the Y were used to measure aneuploidy in epididymal spermatozoa collected 6 or 30 days after X-irradiation (2 Gy) of the animals to sample germ cells which were spermatozoa and spermatocytes, respectively, at the time of irradiation. With the 30-day sample, the data point to increased proportions of cells with either no or 2 X-chromosome signals (relative to controls) suggesting induction of X-chromosomal aneuploidy. The Y chromosome probe gave diffuse signals in sperm heads making it difficult to identify cells with 2 Y chromosomes. Other probes examined (for the Y, chromosome 8 and telomeres and centromeres) did not show the sensitivity required for the detection of aneuploidy.

In other experiments, (i) the use of chromosome 8 probe mentioned above permitted a more precise localization of break-points of 3 chromosome rearrangements known to map to a similar position at the proximal end of the chromosome at the probe locus and (ii) chromosome-specific pools of DNA isolated through flow sorting (in collaborative work with Rabbits) were successfully used to confirm initial diagnosis of duplications of chromosome 1 and 12 and of breakpoints in a translocation between chromosomes 7 and 16, recovered from radiation experiments.

2. <u>Radiation-induced chromosomal anomalies in female mice</u>. In this part of the work, female mice were irradiated with 1 Gy, mated to unirradiated males and 14-day postimplantation stage embryos were analysed cytogenetically. The results showed that 14 of the 103 embryos carried structural chromosome anomalies (duplications, deletions and translocations); while some of these anomalies may be incompatible with livebirth, these data nonetheless suggest a high rate of induction of potentially transmissible chromosomal aberrations in immediately preovulatory oocytes of female mice.

3. <u>Guinea pig oocytes as a model system for the assessment of radiosensitivity of human oocytes</u>. Studies were conducted to develop and validate the use of guinea pig oocytes as a model for assessing the radiosensitivity of human immature oocytes, the principal stage at risk for genetic risks of radiation exposure of human females. The technical difficulties involved in the culturing of oocytes in vitro for cytogenetic studies have now been overcome. Well over 40% (and up to 80 to 90% if some precautions are taken) of the oocytes cultured with our prototcol yield analysable chromosome preparations at metaphase I of meiosis.

Histological studies showed that at birth, the ovaries of guinea pig females have predominantly "large" immature oocytes and small numbers of maturing oocytes. The nuclear morphology of

these large oocytes is that of a typical diplotene comparable to that of the human resting oocytes. In the guinea pig, the diplotene configuration, over a period of number of weeks, changes to the "contracted" configuration.

Two sets of experiments were carried out. In the first, the ovaries of newborn females were irradiated on the first 2 days after birth. A year later, the animals were killed on days 8-10 of an oestrous cycle (this is about 17 days in the guinea pig), meiotically competent oocytes were collected and cultured for analyses of chromosomal aberrations in metaphase I of meiosis. This age of females was chosen to sample immature oocytes which were of the large type at the time of irradiation. In the second, ovaries of adult females were irradiated on either day 3 (with collection and culturing of oocytes on day 10) or day 10 of the oestrous cycle (with collection and culturing of oocytes immediately after irradiation). These experiments were aimed at assessing radiosensitivity of oocytes in different stages of maturation. In both sets of experiments, the X-ray doses were 1 and 2 Gy.

The data clearly show that (i) all the oocyte stages studied respond with increased frequencies of chromosomal aberrations (translocations and chromatid breaks/fragments) and (ii) oocytes irradiated on day 10 of the oestrous cycle and cultured immediately, showed an enormous increase in the frequency of chromosmal aberrations (e.g., about 30-35% per Gy for transloc-ations) compared to those irradiated on day 3 (e.g., 2-3% per Gy for translocations) or to immature oocytes irradiated on days 1-2 after birth (about 1% per Gy).

A further set of experiments was prompted by the serendipitous finding that in oocytes of mature females irradiated on day 10 day of oestrous cycle (but collected and cultured one day after irradiation and processed for cytogenetic work), all oocytes were already in meiotic metaphase II. The suggestion was that irradiation by itself "stimulated" meiosis I in meiotically competent oocytes. This possibility was tested and confirmed in further experiments (irradiation of females on days 8-10 of the oestrous cycle, collection 18 h after and culturing; dose range studied: 0.25 to 4 Gy). The results showed that the stimulatory effect was dose-dependent with the lowest effective dose being between 0.25 and 0.5 Gy. The basis for this effect was investi-gated in additional studies (irradiation of females on day 8; collection and fixing of oocytes at different time intervals after irradiation). The data showed that all the "stimulated" oocytes had been eliminated by day 15 i.e., prior to ovulation and replaced by others that were contained in smaller follicles at the time of irradiation. In other words, there is evidence for an acceleration of growth and maturation of smaller follicles to compensate for the loss of large follicles in irradiated animals. These data thus provide a basis for future studies on the radiosensitivity of oocytes contained in the small follicles.

Comparison of the present results with those published for the mouse clearly suggest that there are important differences between mouse oocytes (the animal system thus far used as a surrogate for assessing the radiosensitivity of human females) and the guinea pig oocytes (which are more similar to human oocytes).

4. <u>Radiosensitivity of male and female gametogenic stages of the mouse to the induction of congenital malformations</u>. The choice of the HLG/Zte (Heiligenburger) strain for the present studies was dictated by the need to have a sensitive system for the assessment of these effects and by earlier findings that irradiation of various oogenic stages in mice of this strain resulted in significant induction of fetal malformations which were indistinguishable from those induced during organogenesis.

The responses of "immature" oocytes (γ-irradiation at day 19 of gestation and matings of the female mice so derived, 12 weeks after birth), "less mature" and "mature" oocytes (irradiation of adult females) and of various stages of spermatogenesis (irradiation of adult males) to the induction of malformations were studied. In all experiments, the uterine contents were exmained at day 19 of pregnancy. The results were the following: (i) irradiation of "immature" oocytes with 2.8 Gy (0.28 Gy/h) resulted in a significant increase in the frequency of malformed fetuses but this could not be demonstrated at the lower dose of 0.7 Gy; (ii) at a dose of 1.4 Gy ((0.011 Gy/h; this low dose rate permitted survival of "less mature" oocyte stages), these oocytes (sampled 29-49 days post-conception) responded with significant increases in malformation frequency; (iii) for irradiation of males (2.8 Gy), the overall picture is that all germ cell stages (post-meiotic, meiotic and pre-meiotic) were sensitive to the induction of malformations, the period of maximal sensitivity being around meiosis (conceptions occurring 22-28 days after irradiation) and (iv) the malformations recorded were almost exclusively gastroschisis.

One other interesting result emerged from this work: in experiments on irradiation of adult females, the contemporaneous controls which were 6 months old, had a higher spontaneous frequency (about 9%) of malformed fetuses (gastroschisis) relative to those which were half that age (about 2%). This finding thus points to a maternal age-effect for the origin of malformations.

5. <u>Molecular studies on the genetic basis of isolated cleft lip + palate (CL + P) in humans</u>. In this part of the work, a total of 21 multiplex, multigenerational families with isolated CL $\pm$ P identified through the records of the Hungarian Congenital malformation Registry was used. DNA was isolated from isolated nuclei of leukocytes and used in molecular studies. A total of 10 "candidate regions" on seven different chromosomes was screened for association or linkage of the trait using appropriate DNA probes.

The results exclude association or linkage to the TGFα locus on chromosome 2p originally claimed by Ardinger et al (Am. J. Hum. Genet 45, 348-353, 1991) and to the other candidate regions studied. Although not successful in the identification of genes involved in CL $\pm$ P, since dinucleotide repeat markers (CA_n) were used in the study (in addition to other markers), our data provide the first documentation on polymorphism of these markers in the Hungarian population.

Head of project 1: Dr. K. Sankaranarayanan

II. Objectives for the reporting period

1. Analysis of data on the molecular nature, distribution and mechanisms of origin of mutations underlying human mendelian diseases and assessment of their relevance for radiation genetic risk estimation for mendelian diseases.

2. Analysis of data on cancer predisposition and on radiosensitivity of cancer-predisposed genotypes to the induction of cancers; development of suitable genetic models for assessing the impact of heterogeneity in the population (with respect to the presence of cancer predisposition and enhanced sensitivity of such predisposed individuals) on the estimates of radiation cancer risks.

3. Review and analysis of current knowledge on multifactorial diseases in man; development of theory and mathematical models for the estimation of radiation risks of multifactorial diseases.

4. Molecular studies on the genetic basis of isolated cleft lip ± palate in man.

III. Progress achieved including publications

1. Impact of advances in human molecular biology on radiation genetic risk estimation.
   An earlier analysis (Sankaranarayanan, K., Mutation Res. 258, 3-122, 1991) of the available epidemiological, population genetic and molecular data on human mendelian diseases, the nature of radiation-induced mutations in mammalian experimental systems, and mechanisms of their origin and induction permitted three tentative conclusions: (i) many of the assumptions used in genetic risk estimation may not be valid; (ii) the risk estimates that have been made, if anything, are conservative i.e., on the high side and (iii) until a better framework is formulated it is prudent not to alter the risk estimates. The human data analysed then pertained to some 75 diseases. During the project period, this data-base has been expanded to include well over 300 mendelian diseases (K. Sankaranarayanan, unpublished). The analysis of these data confirms and extends the conclusions reached in 1991 and are discussed below.

   (a)   *Nature of spontaneous mutations underlying mendelian diseases.* Analysis of the molecular nature of mutations shows that of the 309 mendelian diseases analysed, 200 (65%) are predominantly due to point mutations (PMs), 69 (22%) are due to PMs and LMs [length mutations] and 40 (13%) are associated with LMs and microdeletion syndromes (MDS). If one considers autosomal dominant and X-linked diseases only, 89 out of 164 (54%) are due to PMs and the remainder, due LMs and MDS.

   (b)   *Mutational specificities.* Both the earlier and recent analyses of the distribution of PMs along the genes show that in

a small proportion of these, the mutational sites are distributed throughout the gene; however, in most, these sites are non-randomly distributed i.e., there are specificities. There is evidence that at least in part, this non-randomness is a reflection of the DNA sequence organization of the genes. Analyses of the distribution of breakpoints of deletions in LM-associated diseases likewise show the same phenomenon of non-randomness.

(c) *Mendelian diseases associated with expansion of trinucleo-tide repeat sequences.* Recent molecular studies have shown the operation of novel mechanisms in the origin of mendelian diseases. One of these concerns the expansion of trinucleotide repeat sequences (CAG, CTG, CGG and CCG) in the coding or untranslated regions of the gene. As of now, this mechanism has been found to be the cause of at least 8 mendelian diseases (Machado-Joseph disease, dentatorubral pallidoluysian atrophy, Huntington disease, myotonic dystrophy, spinocerebellar ataxia, fragile-X A, fragile-X E and spinal & bulbar muscular atrophy).

(d) *Molecular and clinical heterogeneities.* Data are rapidly accmulating which show that the basic concept of mutations in one gene causing one clinical disease may not always be tenable for all mendelian diseases. Likewise, there are instances where mutations in several different genes result in similar clinical phenotypes. The emerging picture of molecular and clinical heterogeneities poses a dilemma to clinicians and molecular geneticists and a challenge to risk estimators.

(e) *Radiation-induced mutations.* Currently available data on radiation-induced mutations in experimental systems permit three important conclusions: (i) most radiation-induced mutations are DNA deletions; (ii) there are not many mechanistic similarities between spontaneous and radiation-induced mutations, particularly for deletions (this is not entirely unexpected since ionizing radiation produces mutations by random deposition of energy in the cell whereas spontaneous mutations arise through specific mechanisms) and (iii) systems that have been used for the study of induced mutations have used genes which on average are more highly mutable enabling the investigator to maximize the chance of recovering induced mutations. In retrospect it is clear that, by and large, these are the genes with multiple mutational sites, point mutations or deletions at one or more of these sites giving rise to the phenotype under study.

(f) *Relevance for risk estimation.* The risk is estimated as a product of two quantities namely, prevalence (P) and 1/DD (DD = doubling dose) where $P = 10,000/10^6$ and $1/DD = 1/100$. With respect to P, two assumptions are important: (i) current prevalence represents a balance between mutation and selection and (ii) the genes for the diseases included in the estimate of P will all respond to induced mutation. On the first assumption, it is now clear that mutation-selection balance is probably applicable at best to about 15 to 20% of the $10,000/10^6$ and not for the remainder. On the second, since radiation induces predominantly deletions (and only about 50% of the mutations in human mendelian disease are due to deletions), even if we ignore specificities, it is obvious that the P estimate for risk

estimation purposes may need to be revised downwards.

Specificities however, cannot be ignored: if we take them into account, the P estimate will dwindle even further. Further, as is now known, diseases such as Huntington disease or myotonic dystrophy (which are included in the P estimate) arise by novel mechanisms mentioned earlier and are probably not inducible by radiation. It seems clear, therefore, that the prevalence estimate for risk calculations should be revised downwards. The consequence will be a lower estimate of risk.

Turning now to the doubling dose value of 1 Gy, this estimate is based on recessive mutations in the mouse for loci which have been pre-selected for high induced mutability, on average. It is well-known that, genes that sustain induced mutations to recessives have been observed to do so at a higher rate (lower DD; higher RMR) than those that sustain dominant mutations (higher DD; lower RMR). This suggests that if a DD based on *recessive* mutations is used for estimating the risk of *dominant diseases*, the risk will be overestimated.

Finally, implicit in the estimation of the DD is the assumption that genes which mutate at high rates spontaneously will also behave similarly after irradiation. This assumption is also open to doubt. A high spontaneous rate, depends, among other factors, on the size and sequence of the genes in question and on the types of mutational mechanisms involved. A high induction rate is more dependent on whether a random change in the gene can give rise to the phenotypes being studied.

It is thus clear that the probability of radiation inducing those specific mutations which underlie most of the known mendelian dominant diseases is likely to be small and that it is probably smaller than what one would infer from induced mutations in genes in the experimental systems, which have been pre-selected for high induced mutability. The message, therefore is that the concept that *all* naturally-occurring mendelian diseases can be used as a framework for risk estimation, may not be entirely correct. As far as radiation protection is concerned, the present estimates however do provide a margin of safety.

2. Cancer predisposition, radiosensitivity and the risk of radiation-induced cancers

(a) The state of the art. It is now recognized that at least 350 human mendelian diseases have cancer as a sole feature, a frequent concomitant or a rare complication. These diseases arise as a result of germinal mutations in "cancer predisposing genes". Further, there is evidence that individuals carrying mutations in at least some of these genes may be more sensitive to ionizing radiation-induced cancers at the individual level and, cell killing, chromosomal aberrations at the cellular level.

These two themes -- cancer predisposition and potentially increased sensitivity to radiation-induced cancers are now coming into sharper focus in both basic cancer biology and radiation carcinogenesis. There are at least three reasons for this:

1. The discoveries that mutations underlying these diseases are in tumor-suppressor genes and/or in those involved in the maintenance of genomic stability, cell cycle control and DNA repair have imparted a new dimension to our thinking about cancer predisposition; At least 21 such genes have now been cloned (including 9 tumor-suppressor genes, 11 DNA repair genes and 1 proto-oncogene).

2. A view that has gained currency in recent years is that, in addition to the rare mutant genes which confer a high cancer risk, there may be a much larger group which confers a lesser degree of risk without obvious familial clustering; the inference here that such inherited predisposition may contribute significantly more to the cancer incidence in the population than has been assumed.

3. As mentioned above, there is some evidence that cancer-predisposed individuals may also be more sensitive to radiation-induced cancers; should this prove to be true, the risk of radiation-induced cancers in a population in which these radio-sensitive subgroups exist may be higher than in a population which does not have these subgroups.

These reasons, therefore, provide a powerful rationale for modeling efforts and theoretical enquiries on the impact of cancer predisposition and of radiosensitivity on cancer risks in an irradiated population.

(b) Mathematical modeling. To study the above problem quantitatively, a mendelian, one-locus, two allele model was developed. This model assumes that one of the alleles is mutant and the genotypes carrying the mutant allele(s) are cancer predisposed and are more sensitive to radiation-induced cancers. Formal analytical predictions as well as numerical illustrations show that:

1. When such heterogeneity with respect to cancer predis-position *and* radiosensitivity is present in the population, irradiation results in a greater increase in the frequency of induced cancers than when it is absent.

2. This increase is detectable only when the proportion of cancers due to genetic predisposition is large and the degree of predisposition is considerable.

3. Even when the effect is small, most of the radiation-induced cancers will occur in predisposed individuals.

The above conclusions are valid for models of cancer when predisposition and radiosensitivity may be either dominant or recessive.

The published data on breast cancers in Japanese A-bomb survivors show that at 1 Sv, the radiation-related excess relative risk in women irradiated before age 20 is 13 compared to 2 for those irradiated at later ages. We examined the application of our model to the above data using two assumptions, namely, that the proportion of cancers due to genetic susceptibility at the BRCA1 locus (1/200) and the frequency of the mutant allele (0.0033) estimated for Western populations are valid for Japanese women. With our model, these results can be explained only if there are very large differences in cancer susceptibility (>1000-fold) and radiosensitivity (>100-fold) of the heterozygotes.

3. Multifactorial diseases: review, analysis and mathematical modeling for radiation risk estimation

Multifactorial diseases are those which are interpreted as resulting from a large number of causes, both genetic and environmental. Their clinical phenotypes are likely to represent final common pathways to which various etiological mechanisms including genetics have contributed. The common congenital abnormalities (e.g., neural tube defects, cardiovascular

malformations, pyloric stenosis, cleft lip ± palate etc) and many common conditions of adult onset (e.g., coronary heart disease, non-insulin dependent diabetes mellitus, essential hypertension, schizophrenia etc) are examples of multifactorial diseases. In terms of transmission characteristics, the majority do not fit mendelian expectations, but "run" in families. With the exception of coronary heart disease, at present, there are no data on the genes, their numbers and how they cause disease. During the program period, attention was focused on isolated common congenital abnormalities (CAs) which have a birth prevalence of about 6%.

   (a) Epidemiological features of congenital abnormalities. These include the following: (i) racial/ethnic, regional or seasonal differences in prevalence for some CAs; (ii) higher concordance rates in monozygotic twins than in dizygotic ones, but never 100%; (ii) the frequency of affected first degree relatives of a proband is many times (5 to 50) the prevalence in the general population and there is a sharp decrease in the proportion affected as one passes from first to second to third degree relatives; (iii) the relative increase in risk (i.e., relative to birth prevalence in the general population) is more marked with low birth frequency and (iv) the recurrence risks also depend on the number of affected family members, severity of the condition in the proband and whether one sex is more frequently affected than the other.

   (b) Multifactorial threshold model of disease liability.
   In 1961, Carter proposed the concepts of a hypothetical variable that underlies multifactorial conditions and of "threshold" to explain the inheritance of pyloric stenosis and applied these to interpret the observed differences in risks to relatives of affected males versus females. Subsequently, Falconer formalized these concepts quantitatively by advancing the multifactorial threshold model of disease liability (MTM).
   The assumptions of the simple version of MTM are: (i) all environmental and genetic causes can be combined into a single continuous variable called "liability" which, as such, is immeasurable; (ii) liability is determined by a combination of numerous genetic and environmental factors, acting additively without dominance or epistasis, each contributing a small amount of liability and therefore "normally" distributed and (iii) the affected individuals are those for whom the liability exceeds a certain threshold value.
   With MTM, it became possible to extend the usual methods of quantitative genetics developed for threshold characters to situations where the data, in the form of incidences, refer to an "all-or-none" classification. It enables the conversion of information on prevalence of a given multifactorial trait in the population (p) and in the relatives of those affected (q) into an estimate of correlation in liability between relatives from which heritability of liability (h^2) can be estimated.

   (c) Mathematical models for radiation risk estimation. As will be obvious, the MTM is a descriptive model and is not designed to answer questions about the impact of induced mutation on prevalence of multifactorial diseases. In order to answer these questions, mechanistic models i.e., those which can explain the

stability of prevalences of these need to be developed. Such models have long been used by quantitative geneticists for explaining dynamics and maintenance of variability in polygenic/quantitative traits, although not in the area of multifactorial diseases.

Our attempts at model building, therefore, focused on transforming the descriptive MTM into mechanistic ones using concepts derived from quantitative genetics, but with two important modifications, namely the following:

(i) assume that the stability of disease prevalences is a reflection of a balance betweeen the two opposing forces, mutation and selection and introduce mutation and selection as additional parameters in the MTM and,

(ii) assume that the numbers of genes involved are finite (in the range from 2 to 20). The use of this assumption is dictated by major findings that have emerged from biometric, biochemical and molecular genetic studies of coronary heart disease; they show that fewer loci with moderate effects can explain a large part of the variation in risks than is assumed by the classic biometric models which invoke a very large number of loci each with small additive effects.

The models that are being developed (within the framework of an ICRP Task Group on this subject of which the author is the Chairman) enable the assessment of the impact of a given increase in mutation rate on disease prevalence in the population. It also permits the estimation of mutation component (MC), an important quantity in the equation used for risk estimation (i.e., risk per unit dose = Prevalence x reciprocal of the doubling dose x mutation component).

To examine the properties of the model and their predictions, we used 3 and 4-locus models with arbitrarily chosen values of mutation rate (10^{-6} to 10^{-5}) and selection (1 and 0.5), values for thresholds and different hypothetical prevalences (1/1000 to 5/1000). For a permanent doubling (i.e., a 100% increase) in mutation rate, it has been found that: (i) the MC in the first 10 generations is of the order of 2-4%; (ii) although MC is a function of mutation rate, selection, threshold, environmental variance, recombination fequency and the factor by which the mutation rate is increased, its magnitude can be predicted from knowledge of heritability alone and (iii) for heritability of liability values >0.20, the MC for the first and second generations is less than 2%. The implication here is that for a fractional increase in mutation rate (1%, 10% etc), the MC will be very small and consequently the estimated risk will be very small indeed. The models have not yet been applied to empirical data.

4. Molecular studies on the genetic basis of isolated cleft lip ± palate (CL ± P) in man

This aspect of the work was focused on identifying gene loci, mutations at which underlie non-syndromic CL ± CP in humans. A total of 21 multiplex, multigenerational families with isolated CL ± CP was identified through the records of the Hungarian Congenital Malformation Registry (virtually complete ascertainment of multiply-affected CL ± CP families during the last 10 years in Hungary). DNA was extracted from isolated nuclei of leukocytes and used for molecular studies employing standard procedures. A total of ten "candidate gene regions" on seven

different chromosomes (1q32-q42, 2p13, 4p16.3-p16.1, 4q21-qter, 4q25-q34, 5q15-q23, 5q31.3-q33.3, 5q333-q35, 11p15.5 and 17q21) was screened for association or linkage of the trait under consideration using appropriate DNA probes. This choice was dictated by either linkage or association of these to CL ± CP in some of the published investigations or on inferences from mouse studies based on gene positions, tissue-specific expression and developmental timing.

The results of this study exclude association or linkage (i) to the TGFA locus on chromosome 2p originally claimed by Ardinger et al (Am. J. Hum. Genet. 45, 348-353, 1991); other published studies also did not confirm the Ardinger et al's findings, and (ii) to other candidate regions studied. Further work on genes involved in disturbances in the development of primary and secondary palate among those involved in transcriptional regulation (e.g., the homeobox and paired-box genes) may be fruitful. Although not successful in the identification of genes involved in CL ± CP, since dinucleotide repeat markers $(CA)_n$ (in addition to others) were used in this study, our data provide the first data on polymorphism of these markers in the Hungarian population.

PUBLICATIONS (1993-1995) and papers in press

Full papers
Sankaranarayanan, K (1993) Ionizing radiation, genetic risk estimation and molecular biology: impact and inferences. Trends Genet. 9, 79-84.

Sankaranarayanan. K (1993) Risk estimates for genetic effects of ionizing radiation including those for multifactorial diseases. Chinese J . Radiol. Med. and Protection 13 (6), 422-426.

Sankaranarayanan, K (1994) Estimation of genetic risks of exposure to chemical Mutagens: relevance of data on spontaneous mutations and of experience with ionizing radiation. Mutation Res 304, 139-158.

Sankaranarayanan, K., N. Yasuda, R. Chakraborty, G. Tusnady and A. E. Czeizel (1994) Ionizing radiation and genetic risks. V. Multifactorial diseases: a review of epidemiological and genetic aspects of congenital abnormalities in man and of models of maintenance of quantitative traits in populations. Mutation Res 317, 1-23.

Sankaranarayanan, K and R. Chakraborty (1995) Cancer predis-position, radiosensitivity and the risk of radiation-induced cancers. I. Background. Radiation Res. 143, 121-143.

Chakraborty, R and K. Sankaranarayanan (1995) Cancer predis-position, radiosensitivity and the risk of radiation-induced cancers. II. A mendelian single-locus model of cancer predisposition and radiosensitivity for predicting cancer risks in populations. Radiation Res. 143, 293-301.

Abstracts
Karcagi, V., L. Timar, K. Sankaranarayanan and E. Bakker (1993)

Linkage studies on Hungarian families with non-syndromic cleft lip and palate. (Abstract), Book of Abstracts, Proc. III Biennial Mammalian Developmental Genetics Workshop (8-12 Sept 1993), Bar Harbor, Maine.

Sankaranarayanan, K (1994) Hereditary diseases, genetic susceptiblity to ionizing radiation and radiation risks. (Abstract), Program and Abstract Book, European Society of Radiobiology Meeting, Amsterdam (June 1-4, 1994), p 78.

Sankaranarayanan, K (1995) Cancer predisposition, radiosensitivity and the risk of radiation-induced cancers. Book of Abstracts, UK. Env. Mutagen Society meeting (5-7 July 1995, Leicester, England), p 1.

Sankaranarayanan, K (1995) Re-evaluation of genetic radiation risks (Abstract), In: Radiation Research 1895-1995, Congress Proceedings, X Int. Cong. Rad. Res (Aug 27-Sept 1, 1995, Wurzburg, Germany), Vol 1 (U. Hagen, H. Jung and C. Streffer, Eds), p 35.

Papers in press or submitted for publication
Sankaranarayanan, K (1995) Re-evaluation of genetic radiation risks. Proc. X Int. Cong. Rad. Res, (Aug 27-Sept 1, 1995, Wurzburg, Germany), in press.

Karcagi, V., E. E. Bakker, L. Timar, A. E. Czeizel and K. Sankaranarayanan (1994). Non-syndromic cleft lip with or without cleft palate: exclusion of candidate loci in ten different regions of six chromosomes in Hungarian families (submitted).

Head of project 2: Dr. Tease

II. Objectives for the reporting period

1. To investigate radiation-induced sex chromosome aneuploidy in male mouse germ cells using fluorescence *in situ* hybridisation (FISH).

2. To investigate DNA probes of potential value for FISH analysis of radiation-induced chromosome damage in mouse germ cells.

3. To analyse post-implantation mouse embryos for radiation-induced chromosome damage.

4. To characterise heritable, radiation-induced chromosome anomalies using conventional cytogenetics and FISH.

III. Progress achieved including publications

1. Radiation-induced sex chromosome aneuploidy in spermatozoa

  The advances made in recent years in the technique of fluorescence *in situ* hybridisation (FISH) have made it feasible to screen human spermatozoa for numerical chromosome anomalies. Although in theory this technique is also applicable to the mouse, there is in fact a limitation in the current lack of DNA probes of a suitable nature for this type of study as few repeat sequence probes are as yet available. Nevertheless, the potential of the technique for mutation testing is such as to warrant preliminary studies in the laboratory mouse with those DNA probes presently available. The aims of this initial study were to determine whether an effect of X-irradiation on male germ cells could be detected.
  Young C3H/HeH x 101/H male mice were given 2Gy of acute X-rays and epididymal spermatozoa were collected 6 or 30 days after irradiation. Age matched, unirradiated males served as controls. The spermatozoa were washed twice in culture medium, fixed in 3:1 methanol-acetic acid and spread. Before use for *in situ* hybridisation, the cells were pre-treated with a mixture of trypsin and dithiothreitol (Joseph et al, 1984, Hum Genet 66:234). Two repeat sequence DNA probes were used, one for the *DXWas70* locus at the proximal end of the X chromosome, and the other for the long arm of the Y chromosome. The probes were used separately. Detection of X or Y chromosomes was carried out using the appropriate biotinylated probe and the standard avidin-FITC procedure. The results of this experiment are given in Table 1.
  In the control, unirradiated males, the proportions of cells with either an X or Y signal did not deviate significantly from the expected 50%. At the 6 day interval, both irradiated males had a slight excess of spermatozoa with a single X. However, even when the data from both males were combined, the excess was not significant ($\chi^2_1 = 1.69$, P > 0.05). The results for the Y chromosome were in agreement, with one male having a slight excess the other a small deficiency of cells with a single signal.
  At the 30 day interval, the irradiated male had a marked deficit of cells with either a single X or Y chromosome signal. Interestingly, the proportions of cells with 2 signals was elevated for both chromosomes although the effect was less marked for the Y. This apparent

discrepancy between the chromosomes is most likely an artefact resulting form the fact that the Y chromosome probe gave a somewhat diffuse signal in sperm heads compared with the X probe, and this made it more problematical to determine whether or not a cell had evidence of 2 Y chromosomes; only those cells which were unambiguous were included in this category, any ambiguous cells being assigned to the single signal group.

The apparent lack of any effect at the 6 day sampling interval is as expected as the cells would have been mature spermatozoa at the time of irradiation. At the 30 day

Table 1. The proportions of spermatozoa with an X or Y chromosome from unirradiated mice and from males given 2Gy of X-rays either 6 or 30 days before sampling.

Treatment group	Proportion of cells (%)			Total cells
	X	XX	-	
control	49.84	0.13	50.03	1583
2Gy/ 6 day	51.83	0.06	48.11	1588
	51.55	0.06	48.39	1610
control	49.78	0	50.22	1595
2Gy/ 30 day	47.33	1.29	51.29	1632
	Y	YY	-	
control	50.74	0	49.26	1624
2Gy/ 6 day	49.08	0	50.92	1628
	50.90	0	49.10	1605
control	49.51	0	50.49	1605
2Gy/ 30 day	48.52	0.46	50.78	1723

interval, however, the germ cells would have been at the primary spermatocyte stage and so could have scope for errors in chromosome disjunction to occur. The data point to increased proportions of cells with either no or 2 signals. Thus the treatment appeared to increase the risk of loss of a sex chromosome during meiosis. Cells with 2 signals could have arisen from either nondisjunction at anaphase II or failure of chromosome segregation at the cell level to produce a diploid cell. Tentatively, it was felt that the latter was the more likely explanation as in general cells with 2 signals appeared larger than neighbouring sperm with only one.

The observations made in this pilot experiment are in line with those reported earlier by Szemere and Chandley (1975, Mutat Res 33: 229) who found an elevated rate of triploidy in post-implantation foetuses after X-irradiation of pre-leptotene cells. The FISH approach to analysis of induced chromosome anomalies would therefore appear to be capable of identifying the same types of radiation-induced chromosome anomalies as conventional cytogenetic methods. The former method has the potential advantages, however, of screening a wider range of germ cells and their products and of examining the effects of a mutagenic treatment on specific chromosomes.

2. Investigation of DNA probes for use in FISH experiments.

Two principal problems were encountered in the radiation experiment described above in section 1. Firstly, the Y chromosome probe gave a large and somewhat diffuse signal in epididymal sperm heads which made it difficult to distinguish those instances where there were 2 signals present. Secondly, use of X and Y chromosome probes meant that detection of diploid sperm was also problematical. In an attempt to overcome these difficulties, various other probes were screened for their value in radiation experiments and for analysis of radiation-induced chromosome. anomalies.

(i) Y chromosome

The repeat sequence pSx1 (Capel et al, 1993, Nature Genet 5: 301) was found to give a small, but consistent signal when applied to chromosomes in metaphase I stage spermatocytes. However, when use in epididymal sperm preparations, the signal was less clear and occasionally difficult to distinguish from background signals produced by the detection protocol. In an attempt to strengthen the Y chromosome signal, a cocktail of DNA sequences for the Y chromosome short arm (kindly provided by Dr S. Laval) was used. Although the FISH signal on meiotic chromosomes did appear to be somewhat enhanced, overall the improvement was marginal as far as epididymal sperm preparations were concerned.

(ii) Chromosome 8

A 15.6kb repeat sequence probe that hybridises to the A4 band of chromosome 8 was described by Boyle and Ward (1991, Genomics 12: 517). This probe also gives a consistent signal when applied to meiotic chromosome and epididymal sperm preparations. On its own, however, it has limited value in detecting aneuploidy or diploidy in sperm. We have investigated the possibility of combining the chromosome 8 probe with another autosomal probe which would permit unambiguous discrimination of both chromosomally abnormal sperm. As no other repeat sequence autosomal probes have as yet become available, we have considered the use of YACs as these potentially should provide a strong, chromosome-specific signal (providing they are not chimeric). Using a YAC for a region at the distal end of mouse chromosome 2 (kindly provided by S. Ball), we have obtained a clear signal on meiotic chromosomes and a small signal of acceptable intensity on sperm preparations. To date, however, we have not succeeded in simultaneous hybridisation of the chromosome 8 repeat sequence probe and the chromosome 2 YAC.

(iii) Telomeres/centromere probes

A telomere repeat sequence probe, labelled with digoxigenin, was generated by PCR as described by Idjo et al (1991, NAR 19: 4780). On sperm preparations, the probe resulted in too many signals to make it of use for identifying aneuploid or diploid cells.

Probes for the major and minor satellite components of the centric heterochromatin of mouse chromosomes have been biotinylated using PCR. In sperm preparations, the former gave too intense and large a signal for use in identification of diploid cells. This was not the case for the minor satellite probe, however, and preliminary examination showed it to be of value for this purpose, but it was insufficiently sensitive to detect aneuploidy.

(iv) Development of chromosome paints

During the course of the grant, an opportunity arose to collaborate with a group interested in the isolation of chromosome-specific pools of DNA in the mouse using flow sorting. Such material can be used to produce chromosome paints; these have immense

potential for detection and characterisation of radiation-induced chromosome damage in mouse germ cells. The initial venture achieved sorting of all mouse chromosomes except numbers 10, 13 and 15 (Rabbitts et al, 1995), and subsequently, these chromosomes have been successfully isolated (Rabbitts et al, unpublished)

3. Chromosome anomalies in post-implantation foetuses

Recent work showed that some of the progeny of X-irradiated male mice carry visible chromosome anomalies (Cattanach et al, 1993, Nature Genet,) and a similar phenomenon was subsequently demonstrated following maternal irradiation (Tease and Fisher, submitted). Since the progeny chosen for cytological screening are those that show some adverse phenotype, it is possible that anomalies with little influence on the external appearance could be overlooked. In order further to investigate this possibility, it was decided to screen 14-day post-implantation stage embryos from females given an X-ray treatment, 1Gy of acute X-rays to immediately pre-ovulatory stage oocytes, known to cause heritable chromosome damage. The results of analysis of G-banded chromosome preparations from 103 foetuses are summarised in Table 2.

Overall, 14 embryos were found to have 1, and occasionally, 2 chromosome anomalies. The type of anomaly varied from deletion to presumptive duplications, inversions and unbalanced translocations. Two of the embryos were exencephalic, the remainder appeared morphologically normal.

Table 2.

Type of structural anomaly :			Embryos with structural anomalies	X0 embryos	Total embryos
duplication	deletion	translocation			
6	4	4	14	3	103

Previous observations on liveborn offspring of females given the same radiation treatment as here, have shown that some of the deleterious phenotypes occasionally present were associated with chromosome anomalies (Tease and Fisher, submitted). However, no systematic attempt was made to quantify the rate of transmissible chromosome anomalies as only selected animals were karyotyped. The data from the 14 day embryos thus provide some indication of potentially heritable chromosome anomalies. Given that 2 of the foetuses were clearly abnormal in being exencepahlic and almost certainly therefore not going to be viable, we are left with a rate of 11.6% of conceptuses with chromosome rearrangements that are potentially transmissible. Since the foetuses still had approximately 5 more days of gestation, it is possible that some of these anomalies would have been developmentally lethal. Nevertheless, we are still left with a surprisingly high rate of chromosome anomalies that may be transmitted to the next generation following X-irradiation of immediately preovulatory stage oocytes.

4. Analysis of radiation-induced chromosome anomalies using FISH

(i) Chromosome 8 rearrangements

The chromosome 8 probe described above in section 2 was used to analyse 3 chromosome rearrangements known to map to a similar position at the proximal end of the

chromosome as the probe locus. Two translocations, T(2;8)26H and T(2;8)2Wa, were found to have breakpoints on chromosome 8 slightly distal to the probe locus. A radiation-induced deletion, Del(8)7H, was shown to be distal to the probe locus (O'Keeffe and Tease, 1994).

(ii) Microchromosome

A radiation-induced, heritable microchromosome was recovered in one of the progeny of an X-irradiated female (Tease and Fisher, submitted). After hybridisation with the telomere probe, signals were seen at both ends of this small chromosomal element showing it to be a linear rather than a circular structure. The microchromosome was investigated further using various chromosome paints. To date, it has failed to show hybridisation with paints for chromosomes 1, 2, 4, 7, 10, 16, 19 and X (Tease and Fisher, in preparation).

(iii) Radiation-induced duplications

Two apparent duplications that arose in radiation experiments in which female mice were treated (Tease and Fisher, submitted) have been analysed to determine the accuracy of the preliminary characterisation. Both Dup(1) H and Dup(12) H hybridised successfully with paints for chromosomes 1 and 12 respectively, confirming the initial diagnosis.

(iv) Radiation-induced reciprocal translocation, T(7;16)67H.

A reciprocal translocation that was recovered following post-meiotic irradiation of a male, was shown by G-banding analysis to involve chromosomes 7 and 16 with the breakpoint on the latter in an extremely proximal position. Chromosome painting has confirmed the positions of the breakpoints, and a subsequent study was undertaken to analyse the influence of this radiation-induced chromosome rearrangement on the production of chromosomally imbalanced gametes. Through use of paints for chromosomes 7 and 16, it was possible to identify all the segregant products of the translocation multivalent in metaphase II spermatocytes and thereby to calculate the proportion of gametes that would be chromosomally imbalanced. The translocation had a high frequency of chain multivalents at metaphase I (approximately 80%) and this appeared to be correlated with a subsequent high rate of adjacent II orientation at anaphase I (Tease, submitted).

Publications

Tease C, Fisher G (1993) Cytogenetic detection of four new, visible deletions in the progeny of X-irradiated females. Mouse Genome 91, 855

O'Keeffe C, Tease C (1994) The relative chromosomal location of a repeat sequence probe and breakpoints of three chromosome 8 rearrangements using FISH. Mouse Genome 92, 352-353.

Rabbitts PH, Impey H, Heppell-Barton A, Langford C, Tease C, Lowe N, Bailey D, Ferguson-Smith MA, Carter N (1995) Chromosome specific paints from a high resolution flow karyotype of the mouse. Nature Genetics 9, 369-375

Tease C, Fisher G Cytogenetic and genetic studies of radiation-induced chromosome damage in mouse oocytes. I. Numerical and structural chromosome anomalies in metaphase II oocytes, pre- and post-implantation embryos. (submitted)

Tease C, Fisher G Cytogenetic and genetic studies of radiation-induced chromosome damage in mouse oocytes. II. Induced chromosome loss and dominant visible mutations. (submitted)

Tease C   Analysis using dual colour FISH of chromosome segregation in a mouse translocation heterozygote. (submitted)

Tease C, Fisher G   A heritable, radiation-induced microchromosome in the mouse. (in preparation)

Head of project 3 : Dr. Jacquet

II. Objectives for the reporting period

The extension of radiation studies to oocyte systems which are more comparable to the human one than the mouse oocyte, both in terms of sensitivity to killing and nuclear morphology, is strongly indicated. Investigations performed in our laboratory showed that the guinea-pig oocyte represents such a system. The aim of the present project was the development and validation of the female guinea-pig as a model for ascertaining the chromosomal radiosensitivity of human oocytes, with a particular emphasis on immature (or resting) oocytes, the main components of the female genetic pool. Our work consisted in three parts: (i) improvements of the techniques (developed earlier in our laboratory) to culture oocytes of this species and prepare them for cytogenetical analysis; (ii) investigating the radiosensitivity of the "large" immature oocyte which is present in the newborn animal; (iii) examining the influence of gestation hormones on the chromosomal radiosensitivity of the guinea-pig. Due to practical difficulties, this last aspect was, however, replaced by an extension of the part (ii), i.e. studies on the radiosensitivity of the guinea-pig oocyte at two different stages of its maturation.

III. Progress achieved including publications

1. <u>Improvements of the techniques to culture oocytes of the guinea-pig and prepare them for cytogenetic analysis.</u>

Performing cytogenetic studies on irradiated guinea-pigs presents some difficulties. First at all, hormonal stimulation of maturation and ovulation can not be obtained in this species, and the number of oocytes which are ovulated at each of the 17-day cycles is low (usually 2-5). The best way to obtain sufficient quantities of oocytes at metaphase I or metaphase II stages of meiosis is to culture them *in vitro* to the appropriate stage.
Jagiello (Chromosoma, 27, 95-101, 1969) gave some information on the cytology of meiotic chromosomes in the female guinea-pig but unfortunately, she gave no detail on the techniques that she used for isolation, culture and fixation of the oocytes. Later on, Yanagimachi (J. Reprod. Fertil., 38, 485-488, 1974) described a method of culturing guinea-pig oocytes, which yielded mature oocytes capable of fertilization. However, in that paper, no attempt was made to obtain analyzable chromosome preparations of either oocyte metaphase I or II . Everybody who is familiar with the technique of Tarkowski (Cytogenetics, 5, 394-400, 1966) for chromosome preparation of mouse oocytes or preimplantation embryos knows that complete metaphases with well stained and separated chromosomes are difficult to obtain, and that success partly depends on chance. One of the difficulties lies in the volume of the fixative used, which must be sufficient to allow a good spreading of chromosomes, while being small enough to quickly evaporate to avoid dispersion and artefactual loss of chromosomes. In the guinea-pig, additional problems are, 1) the difficulties of removing follicular cells which strongly adhere to the oocyte, 2) the necessity to remove the thick zona pellucida prior to the fixation in order to allow good spreading of the chromosomes, 3) the presence of numerous fat globules which may interfere with the quality of the preparations and 4) the high number of chromosomes (2n = 64), which makes the obtention of complete metaphases still more difficult than in the mouse (2n = 40)
During the first year of our this contract, we spent a lot of time to improve techniques

developed earlier in our laboratory to obtain good chromosome preparations from the guinea-pig oocytes. For relatively large scale investigations, such techniques had to be simplified to the maximum, while still providing with reproducible results. Attention was given not only to MI chromosomes, but also to MII chromosomes. Indeed, obtention of good chromosome preparations of MII oocytes should make possible to undertake, in a next future, studies on the induction of aneuploidy by radiation in the guinea-pig oocyte. In the following lines, complete details of our simplified method, now standardized, are given.

Animals

Dunkin-Hartley guinea-pigs from Bantin and Kingman Ltd (UK) are used for all our experiments. Animals are controlled daily for vaginal opening for at least two cycles before use. The day the vagina is open is designated day 0 of the oestrous cycle. Animals are sacrificed on days 8-10 of the oestrous cycle, when growing Graafian follicles are clearly visible at the surface of the ovaries

Chemicals

- Heat-inactivated foetal calf serum is used for collecting and culturing the oocytes.
- Hyaluronidase from ovine testes (Fluka) and pronase, B grade (Calbiochem), are used for removing cumulus cells and the zona pellucida at the end of the culture. The enzymatic solution is prepared each day by dissolving 15 mg hyaluronidase and 10 mg pronase in 10 ml Dulbecco's phosphate buffered saline (PBS) without calcium, magnesium and bicarbonate (Gibco, cat nr. 042-04200)
- Hypotonic treatment is performed in 1% sodium citrate containing 4 mg/ml bovine serum albumin (BSA).
- Fixation of the oocytes is made with a freshly prepared mixture of absolute ethanol- acetic acid (3:1), as recommended by Tarkowski.

Preparation of capillary pipettes

Two types of pipettes are selected for the manipulation of the oocytes: hand-pull Pasteur capillary pipettes with a sufficiently large aperture are used for any transfer of the oocytes, while pipettes with a smaller aperture, about equivalent to the diameter of the oocyte (80-90 μm) are useful for helping in removing the cumulus cells.
Another pipette, delivering about 10 μl drops, is used for the fixation.

Culture of oocytes and fixation of chromosomes

- Shortly before the sacrifice of the guinea-pigs, pronase and hyaluronidase are dissolved in PBS. The tube is closed and left at room temperature until use, later at the end of the culture. The culture medium consisting in 2 microdrops of 100 μl FCS covered with silicon or paraffin oil is prepared in Falcon dishes, one for each animal. Those culture dishes are kept at 37°c in an air-atmosphere. No difference was found between such culture system and the conventional culture in an atmosphere of 5% CO_2 in air.
- Guinea-pigs are sacrificed by CO_2 inhalation, and the ovaries are excised and placed in separate embryological watch glasses containing warm FCS. The ovaries are examined under incident light with a stereo-dissecting microscope. Relatively transparent areas on the ovarian

surface are punctured with disposable tuberculin syringe needles to release the content of the Graafian follicles Only healthy and large oocytes surrounded by dense layers of cumulus cells are kept for culture. They are generally dark due to the presence of many fat globules in their cytoplasm. Smaller and clear oocytes surrounded only by a few layers of cumulus cells, are deleted since they reveal unable to resume meiosis in culture. The meiotically competent oocytes are transferred to a microdrop of FCS in the culture dishes. Most often, 20-30 oocytes per female are collected, though this number may vary from a few to more than 50

- Oocytes are cultivated for 6-8 H in order to obtain MI preparations, and for 24 H if MII preparations are needed. In the guinea-pig, the disappearance of the germinal vesicle is difficult to detect because of the opacity of the cytoplasm. Examination of fixed oocytes reveals that this process and the formation of the MI spindle may occur as early as 3-5 H after the beginning of the culture. However it is very important to avoid fixation before 6 H, not only to maximize the number of oocytes that will reach the MI stage, but also to allow the migration of the spindle to the oocyte cortex. It is our experience that MI chromosomes which are fixed before the completion of this process are generally not analyzable. It probably results from the presence of the numerous fat globules that surround them in the cytoplasm and strongly interferes with their spreading . When migration of the spindle to the cortex has occurred, fat globules are preferentially accumulated at the pole opposite to that containing the MI spindle.

- Oocytes are picked up from the culture dish, and the tip of the pipette is carefully cleaned off with absorbing paper, to remove any traces of oil. Oocytes are transferred to an embryological watch glass containing PBS with pronase and hyaluronidase, at room temperature. In the guinea-pig, cumulus cells strongly adhere to the oocyte so that treatment with hyaluronidase has to be completed by repeating pipetting of oocytes, using a pipette with a small diameter aperture. The removal of most cumulus cells from the oocytes requires some time (2-5 min). When this is achieved, examination of the oocytes is continued at the highest magnification. Digestion of the zona pellucida by pronase is a very critical step, and needs particular attention. For this reason it is advised to work at room temperature with a rather low concentration of pronase (0.1%). It is our impression that higher concentration of pronase (i.e. 0.15 %) have a detrimental effect on the quality of the fixed chromosomes. The digestion of the zona pellucida is a slow initiated process suddenly accelerated. A space appears between oocytes and their zona pellucida, giving the impression that oocytes diminish in size. The outlines of the oocytes become somewhat irregular and gentle pipetting of one of them will cause it to deform, confirming that the digestion of the zona pellucida is nearly achieved. Then, all oocytes are very quickly removed from the medium and carefully gathered in the centre of an embryological watch glass containing the hypotonic solution. Usually the digestion of the zona pellucida will be completed in the hypotonic solution through the small quantity of pronase transferred with the oocytes. Hence, care is taken to avoid shaking the solution which would result in rapid dilution of the enzyme. However, if needed, removal of residual cumulus cells and of the zona pellucida can be completed at the end the hypotonic treatment through repeated pipetting. The presence in the hypotonic solution of protein (BSA) strongly reduces the weakness of the oocytes after removal of their zona pellucida, and avoids their loss during transfer on the slide. Loss of oocytes mostly happens with the use of unadapted capillary pipettes.

Hypotonic treatment is prolonged for at least 15 minutes before the beginning of the fixation. At that time, oocytes have recovered a perfectly spherical shape, and eventual small differences in their size are easily visible. Oocytes which are smaller than the majority of others are discarded, since they are meiotically incompetent and would invariably show a

diplotene nucleus after fixation.
- Fixation of the oocytes is another delicate process. A very small drop of hypotonic solution, containing a single oocyte, is placed in the centre of a small square engraved on the reverse side of a grease free slide. Then, the fixative (10 µl) is expelled on top of the oocyte. The fixative begins to spread on the slide and after a few seconds, the hypotonic microdrop containing the oocyte slightly reappears, enlarged by partial mixing with the fixative The microdrop usually moves slowly towards one edge of the slide, while the oocyte keeps its position. This phenomenon is accelerated by expelling a second drop of fixative at the microdrop edge.
This way, the aqueous microdrop is pushed to the edge of the slide by the spreading fixative. Immediately, the slide is placed vertically on a filter paper to help removing quickly the hypotonic solution and the excess fixative by absorption. A few seconds after, a third drop of fixative is quickly expelled just over the oocyte. Removal of the aqueous hypotonic solution reveals important for the success of the fixation since dilution of the fixative by water slows down its evaporation, facilitating artefactual loss of chromosomes during their spreading. This, together with the small volume of fixative used, reduces considerably that risk, while it also improves the quality of the fixation. Thus MI preparations, where one of the 32 chromosome pairs is missing, are rare and bivalents appear generally well separated, regularly cross-shaped. Loss of MII chromosomes occurs with a higher frequency than MI chromosomes. This could be due to the smaller weight of univalents compared to bivalents.
Using the labelling margin of the slide as a reference for the engraved square in which the oocyte was deposited, the relative oocyte position is pointed with a pencil.
All slide are stained with lacto-aceto orcein , one or two days after fixation.

The method above-described allows reproducible obtention of excellent chromosome preparations from M I guinea-pig oocytes About 40 % (178/460) oocytes cultured for 6-8 H and treated in this way yielded analyzable MI preparations. This percentage compares favourably with the 22% analyzable MI preparations obtained by Morrison et al. (Mutat. Res., 119, 169-175, 1983) for rabbit oocytes. Moreover, in our last series, and provided degenerated or remaining incompetent oocytes were discarded at the end of the hypotonic treatment, the proportion of those which yielded analyzable bivalent spreads frequently exceeded 50 % and reached sometimes as much as 80-90%. These values are roughly similar to those obtained by McGaughey and Chang (J. Exp. Zool., 1970, 397-409, 1969) (55%), but somewhat lower than those reported later by Kamiguchi et al. (Proc. Jpn. Acad., 52, 316-319, 1976) (84.2 %), for mouse oocytes This discrepancy partly results from the relatively high rate of guinea-pig oocytes which were already at MII after 6-8 H of culture. This rate did not depend on the duration of the culture. Indeed, second meiotic divisions were found at variable frequencies, either oocytes had been cultured for different short times, in the presence or absence of colchicin, or even they had been fixed directly after their collection. For example, we found as much as 53% MII oocytes in one series fixed without preliminary culture, while 10% were found in an other series cultured for 7 H. Second meiotic divisions were also reported by Edwards (Nature, 196, 446-450, 1962) in oocytes from other mammalian species including man, the mouse and the baboon, fixed directly after their collection. As pointed out by the author, it is clear that most if not all these MII oocytes had been stimulated in vivo, before removal of the ovaries. They had probably been liberated from atretic follicles. We assume that a similar phenomenon was responsible for the high proportion of MII which were frequently observed in preparations of guinea-pig oocytes fixed after short term cultures.

The technique described allows also obtention of good chromosome preparations from MII oocytes. All oocytes selected for fixation after 24 H culture revealed to be at MII, and 36 % of them (22/61) fulfilled the qualitative requirements for chromosome analysis. Most of them contained 64 univalents, representing both the chromosomes of the oocyte and of the first polar body.

In the mouse oocyte, the chromosomes of the first polar body, with their fuzzy-like appearance, differ markedly from the corkscrew-like twisted chromosomes of the oocyte. However, such difference was rarely seen in our guinea-pig preparations. In many cases (17/61), all the chromosomes appeared mixed in a single metaphase plate and their respective origin, oocyte or polar body, could not be ascertained. Less often (5/61), the chromosomes were separated in sets of 32 univalents. The high frequency of preparations containing 64 grouped univalents should clearly constitute a handicap for studies on the induction of aneuploidy by radiation or other mutagen. The proportion of MII oocytes available for such analysis can be improved by the mechanical removal of the first polar body, just before fixation, through careful and repeated pipetting.

Some advantages of our method are that oocytes are collected and cultured in the same simple biological medium, in an air-atmosphere. Culturing oocytes in an atmosphere of air represents a cheaper alternative to the conventional dioxide gas incubation. Furthermore, prior equilibration of the medium with gas, control and adjustment of its pH, are no longer required. Thus, oocytes can be cultured under less rigorous laboratory conditions. Other advantages are the excellent quality of the chromosome preparations usually obtained, and its reproducibility. This is essentially obtained by a careful control of the enzymatic treatment of oocytes at the end of the culture, by small modifications of the fixation procedure of Tarkowski, and by rigorous standardization of all manipulations. Unfortunately, these techniques will not be useful for the detection of numerical anomalies induced by radiation in the female germ cells of the guinea-pig.

2. Studies on the sensitivity of the guinea-pig oocytes to the induction of translocations by radiations.

2.1. *Radiosensitivity of the immature oocyte*

In an earlier work, we performed an histological study of oogenesis in control guinea-pigs. We found that ovaries of newborn animals (0-1 days) only contained immature oocytes of the "large" type and small numbers of maturing oocytes (Jacquet et al., Int. J Radiat. Biol., 65, 357-367, 1994). The nuclear morphology of the "large" oocyte is that of a typical diplotene, comparable to that of the human resting oocyte. In the guinea-pig, however, oogenesis continues for a number of weeks after birth, with the gradual evolution of diplotene oocytes from the "large" type to the "contracted" type. The time required for a large immature oocyte to undergo all the maturation process and reach ovulation is not determined for the guinea-pig. In the mouse, which has an estrous cycle of 4-5 days, the maturation period is at least 6 weeks (Oakberg, Mutat. Res , 59, 39-48, 1979). In order to ensure that all guinea-pig oocytes examined for cytogenetic damage were at the "large" immature stage at the time of irradiation, it was decided to irradiate ovaries of the newborn females during the two first days following delivery and to collect their meiotically competent oocytes one year after irradiation. The doses chosen for X-irradiation were 1 and 2 Gy.

An important remark to be made here is that this type of investigations is much time

consuming, due to.
1) the long estrous cycle of the guinea-pig (+/- 17 days) and, as a consequence, restricted possibilities of mating,
2) the long duration of pregnancy (+/- 68 days),
3) the restricted number of youngs produced (usually 3-3 5, or 1-1.5 female per successful pregnancy)
4) the time elapsing between irradiation of the newborn females and culture of their oocytes.

Collection and culture of the oocytes were performed on days 8-10 of the estrous cycle of the females, as described above. MI oocytes were examined for the presence of translocations and other chromosome anomalies. In case of doubt in the interpretation of a particular configuration, a second opinion was sought. Only "definite" translocations were considered in the results.

As shown in Table 1, no chromosome aberrations were found in MI oocytes from control animals, whereas small numbers of anomalies were found in those from animals irradiated with 1 or 2 Gy one year earlier. The anomalies consisted of chromosome fragments or chromatid breaks, as well as of translocations. The proportion of irradiated oocytes showing "definite" translocations was about 1 % Gy^{-1}.

Dose (Gy)	Oocytes examined	Number abnormal (%)	Number with transloc. (%)	Number with break/frag.(%)
0	74	0 (0)	0 (0)	0 (0)
1	202	4 (1 98)	2 (0.99)	2 (0.99)
2	151	5 (3.31)	4 (2.64)	1 (0 66)

TABLE I

Chromosome aberrations detected in metaphase I oocytes, after irradiation at the immature stage (examination one year after irradiation)

2.2. Radiosensitivity of the oocyte at different stages of its maturation

The following part of our work was devoted to the study of the radiosensitivity of the guinea-pig oocyte at two stages of its maturation.

In a first series of experiments, ovaries of adult females were X-irradiated with 1 or 2 Gy on day 3 of the 17-day estrous cycle. Their meiotically competent oocytes were punctured from the growing follicles on day 10, and they were cultured and fixed as described above.

In a second series of experiments, ovaries were irradiated with the same doses on day 10 of the estrous cycle. In this case, oocytes were collected and cultured immediately after irradiation.

As shown in Table 2, important differences were found in the yields of chromosome aberrations, according to the time of the estrous cycle at which irradiation had occurred. Irradiation at the beginning of the cycle induced low numbers of translocations and slightly

higher numbers of other aberrations. These effects were dose-dependent. The frequency of oocytes showing translocations was about 1 5 Gy^{-1}, i e a value comparable to that obtained after irradiation of the immature oocyte

When irradiation was delivered one week later, however, the frequencies of oocytes showing chromosome anomalies revealed much higher. This was true for translocations as well as for other types of chromosome aberrations. Multivalents implied variable numbers of chromosomes and in many cases the number of chromosomes implied could not be determined. These highly damaged metaphases were frequently associated with chromatid breaks The frequency of oocytes carrying translocations was 30-35 % Gy^{-1}.

Dose (Gy)	Day of irradiation	Oocytes examined	N^{ber} abnorm (%)	N^{ber} with transloc (%)	N^{ber} with break/frag. (%)
0	-	78	0 (0)	0 (0)	0 (0)
1	3	132	5 (3.78)	2 (1 51)	4 (3.03)
2	3	147	15 (10.20)	5 (3.40)	11 (7.48)
1	10	122	50 (40 98)	44 (36 06)	27 (22.13)
2	10	120	89 (74.16)	76 (63.33)	53 (44 16)

TABLE II

Chromosome aberrations detected in metaphase I oocytes irradiated on days 3 or 10 of the estrous cycle (examination 1 week or directly after irradiation).

2.3. Further studies on oocytes irradiated on day 10 of the estrous cycle

In some experiments, oocytes which had been irradiated on day 10 were collected and cultured 1 day after irradiation. Surprisingly, MI preparations revealed impossible to obtain: all fixed oocytes were already in MII. This phenomenon was studied more in details.

Thus, female guinea-pigs were irradiated on days 8-10 of the estrous cycle, with doses of X-rays ranging from 0.25 to 4 Gy, and their oocytes were punctured from the ovaries 18 hours thereafter. They were cultured *in vitro* for 6 hours and fixed according to our standardized method. In agreement with our preliminary results, all oocytes which had been irradiated with 4, 2 or 1 Gy revealed to be in MII. In addition, 60 % of those given 0.5 Gy had also reached this stage. For oocytes irradiated with 0.25 Gy, the difference against controls was not not significant (31 % against 25 %). Oocytes given 4 Gy were cultured for decreasing times, starting at 18 hours after irradiation. Collection and culture of the oocytes occurred in the presence of colchicin. Again, all fixed oocytes revealed to be in MII, whatever the duration of the culture. Furthermore, this was also true for oocytes fixed 18 hours after irradiation, without preliminary culture. Clearly, the oocytes had been stimulated *in vivo*, before removal of the ovaries. Oocytes irradiated with 2 and 1 Gy were also fixed 18 hours after irradiation, without being cultured : 71 % and 63 % of them, respectively, were at MII at that time. Finally, oocytes irradiated with 4 Gy were collected and cultured immediately after irradiation, for different times. The proportion of MII oocytes appeared not yet increased, 6 hours after

irradiation.

From these data, it can be concluded that

1) Irradiation is able to induce a very rapid stimulation of the first meiotic division in meiotically competent oocytes of the guinea-pig.

2) The importance as well as the rapidity of such effect are dose-dependent. The lowest effective dose seems to be located between 0.25 and 0.50 Gy. However, it may not be excluded that even lower doses be effective, the effect then requiring longer times than 24 hours to be expressed.

The stimulatory effect of radiation on the first meiotic division is probably due to a very rapid killing (atresia) or inactivation of follicular cells which normally exert an inhibitory effect on this process. As mentioned earlier in this report, atresia also occurs in "normal" conditions, and should be responsible for the relatively high frequency of MII figures observed in preparations of control oocytes fixed after short-term cultures.

The results reported here imply that all oocytes which were irradiated with 1 or 2 Gy on day 10, and which exhibited heavy chromosome damage when examined on the same day, would have evoluted quickly to the MII stage if they were remained in the ovaries.

Earlier, Oakberg and Clark (in "Effects of Radiation on the Reproductive System", Carlson & Gassner eds., Pergamon Press, 1964, pp.11-24) noted a marked decrease in the number of large oocytes, during the first ten days following irradiation of guinea-pig ovaries by 2 Gy. This suggests that oocytes could be eliminated from the ovaries soon after their radiation-induced meiotic division. On the other hand, an increase in the number of corpora lutea per female was noted by Cox and Lyon (Mutat. Res., 28, 421-436, 1975), in guinea-pigs irradiated with 4 Gy between days 6-12 of the cycle and mated at the first estrous post-treatment (i.e. 5-11 days after irradiation). This effect was attributed to the ovulation of abnormally high numbers of oocytes in irradiated animals ("superovulation effect"). Concommitantly, there was an apparent increase of the preimplantation loss in these animals. This suggests that a number of MII oocytes could remain in the ovaries for a number of days, before being ovulated and fertilized or shed from the ovaries as dead oocytes.

To examine this question, further experiments were undertaken in which females were irradiated on the ovaries on day 8, and their oocytes collected and fixed at various later time intervals following irradiation. The results showed that all stimulated oocytes had been eliminated from the ovaries by day 15, i.e. 2 days before ovulation, and been replaced by others that were contained in smaller follicles at the time of irradiation. Thus, the ovaries had apparently compensated for the loss of all large follicles by an acceleration of the maturation and growth of smaller oocytes, in order to allow a sufficient (or even larger, cfr. the study of Cox and Lyon) number of oocytes to be ovulated. The radiosensitivity of oocytes contained in these follicles is now under study. Thus, ovaries are still irradiated on day 10, and the surviving oocytes are punctured from the growing follicles on day 15, and cultured to the MI stage. Up to now, 31 MI preparations of oocytes which had been irradiated with 1 Gy and 57 others which had been irradiated with 2 Gy could be analyzed. In the 2 Gy group, 3 oocytes showed definite translocations and 3 others a chromosome or chromatid fragment.

2.4. Conclusions

A precise knowledge of the radiosensitivity of the guinea-pig oocyte will still require extended investigations. However, some important comments can already be made, in the light of the results obtained to date :

1) Recent results have shown that the mouse immature oocyte was sensitive to the induction of translocations and other chromosome aberrations by radiation (Griffin and Tease, Mutat. Res., 202, 209-213, 1988; Griffin et al., Mutat. Res., 231, 137-142, 1990; Straume et al., Mutat. Res , 248, 123-133, 1991). The results obtained in our laboratory allow to extend this conclusion to the immature oocyte of another mammalian species, which is closer to man in terms of nuclear morphology and sensitivity to killing by radiation.

Like those reported in the mouse, our results do not support the "near-zero" genetic risk for women, which was based on the previous inability to find genetic damage in mouse immature oocytes.

2) Due to differences in the types of radiation and/or experimental conditions used in the mouse and guinea-pig studies, a precise comparison of the radiosensitivities of immature oocytes of these two species is not yet possible. However, recent results of Straume et al. (Mutat. Res., 248, 123-133, 1991) suggest that the radiosensitivity of the mouse immature oocyte should be rather high. Our data indicated that the radiosensitivity of the guinea-pig immature oocyte is rather low.

3) Our data also evidenced a dramatic increase in the radiosensitivity of the guinea-pig oocyte during a time interval of only 1 week : oocytes irradiated at the beginning of the estrous cycle had a low frequency of chromosome aberrations, while those irradiated at the middle of the estrus cycle (when growing Graafian follicles are clearly visible at the surface of the ovaries) exhibited heavy chromosome damage. We found that such oocytes were evidently eliminated from the ovaries in a few days, after their evolution to the MII stage. The stimulation of the first meiotic division by radiation required less than 24 h after doses of 1 or 2 Gy and was probably due to a very rapid killing or inactivation of the follicle cells.

On the basis of these results, it can be concluded that the radiosensitivity of the nearly mature oocyte (1 week before ovulation) is clearly much higher than that of the corresponding stage in the mouse, both in term of sensitivity to killing and to induction of chromosome aberrations.

5) All together, our results suggest that important differences exist between the mouse and the guinea-pig, with regard to the radiosensitivity of their female germ cells. This underlines the necessity of performing studies in other mammalian species, in order to better define the genetic risks associated with an exposure of women to radiation.

3. Publications

Jacquet, P , J. Vankerkom and M. Lambiet-Collier (1994), The female guinea-pig, a useful model for the genetic hazard of radiation in man; preliminary results on germ cell radiosensitivity in foetal, neonatal and adult animals, *Int. J. Radiat. Biol., 65, 357-367.*

Jacquet, P., L. de Saint-Georges, L. Vankerkom and L. Baugnet-Mahieu (1995), A method for chromosome preparation of guinea-pig oocytes, *Mutation Res., 334, 309-316.*

P. Jacquet, L. de Saint-Georges, J. Vankerkom and L. Baugnet-Mahieu (1994), Stimulation of the first meiotic division of ovarian oocytes by low doses of radiation, *Cell Biol. Int., 18, 583 (abstr.).*

P. Jacquet, L. de Saint-Georges, J Buset, J. Vankerkom and L Baugnet-Mahieu (1995), Radiation-induced translocations in immature and mature oocytes of the guinea-pig, *10th Int. Cong. Radiat. Res , Würzburg (abstr).*

Head of project 4: Prof. Streffer

II. Objectives for the reporting period

1. Effect of gamma-rays (137Cs; dose rate = 0.011 Gy/h = 0.18 mGy/min; total doses = 0.7 and 1.4 Gy) on fetal damage (lethal effects and macroscopically visible malformations) after exposure of oogenesis stages.

2. Effect of gamma-rays (137Cs; dose rate = 0.28 Gy/h = 4.6 mGy/min; total dose = 2.8 Gy) on fetal damage (lethal effects and macroscopically visible malformations) after exposure of spermatogenesis stages.

3. Effect of gamma-rays (137Cs; dose rate = 0.28 Gy/h = 4.6 mGy/min; total dose = 2.8 Gy) on fetal damage (lethal effects and macroscopically visible malformations) after exposure of day 19 female fetuses.

4. Fertility of female mice half a year after exposure to low dose rate 137Cs gamma-rays.

III. Progress achieved including publications

INTRODUCTION

Usually, in the context of radiation induced "malformations" the attention is directed to an exposure during organogenesis, because it is well known from animal experiments and from a number of human studies that such effects are possible after exposure during this period. Previous experiments in our Institute, however, have shown that after exposure of various stages of oogenesis structural changes can be caused in mouse fetuses of the Heiligenberger strain (meanwhile HLG/Zte

strain) indistinguishable from malformations induced during organogenesis (see Final Report Bi6-077, 1992). Such an effect has considerable implications for risk estimates, because germ cells are at risk over the whole reproductive life time, whereas human organogenesis lasts for only about five to six weeks.

Therefore, we initiated extensive studies on a possible germ cell risk in the mouse strain mentioned above. The use of specific strains is crucial for such an analysis, because our preimplantation studies had revealed that the induction of malformations has a strong dependence on the mouse strain used.

Three different groups of mice were irradiated:

1. Adult female mice in order to study mature and less mature oocytes.

2. Adult male mice for the study of various stages of spermatogenesis.

3. Fetal female mice in order to analyse the response of immature oocytes.

METHODOLOGY

Fetal female mice (day 19 of gestation), adult female mice (12 weeks old), and adult male mice (12 weeks old) were irradiated with gamma-rays (137Cs; dose rate 0.28 Gy/h or 0.011 Gy/h) or sham-irradiated.

The adult mice were mated immediately after radiation exposure or, in some cases, after a delay of some weeks or half a year; those mice that had been exposed in the fetal stage were kept until an age of 12 weeks and then mated. Plug control was

carried out every morning and those females with a vaginal
plug (unequivocal sign of copulation) were singled out. 19
days after copulation (day of copulation = day 1), the mice
were killed by cervical dislocation and the uterine content
checked for early resorptions, late resorptions, late fetal
death, surviving fetuses, and fetuses with macroscopically
visible malformations.

RESULTS

Adult female mice

The major problem of studies on radiation effects on female
germ cells is the pronounced sensitivity of these cells with
regard to lethality. Previous experiments have shown that
using a low dose rate (0.28 Gy/h instead of 60 Gy/h) partly
overcomes this problem. Nevertheless, it had only been
possible to study oocytes exposed during an interval between 1
and 35 days before ovulation. All of less mature oocytes were
killed even at low total doses. Therefore, we examined a still
lower dose rate, i.e. 0.011 Gy/h.

As we had already shown that the most mature oocytes
(copulation 1-4 weeks after radiation exposure) did respond
with an increased frequency of malformed fetuses after
radiation exposure (irrespective of the dose rate), we started
mating in the fifth week after exposure in the experiments
with the dose rate of 0.011 Gy/h (=180 μGy/min).

With regard to lethality it turned out that the very low dose
rate used in the experiments indeed allows survival of some
less mature oocytes (weeks 5-7), but that starting with
week 8, no surviving oocytes were observed also under these
conditions.

Fig. 1 summarizes the results with regard to the teratogenic effects after exposure of the three groups (fetal and adult females, males) mentioned above. Unfortunately, one of the consequences of inbreeding our mouse strain was that the control level of malformations (almost exclusively gastroschises) raised markedly and the variability increased (colony-bred: about 1%, inbred: between 1 and 4%).

The variability, in particular, is a serious problem with regard to the detection of small effects. Therefore, a total dose of 0.7 Gy is not sufficient to show a statistically significant increase in the number of malformed fetuses in the population size examined (Fig. 1, Oogenesis (adult)). After a total dose of 1.4 Gy, however, a statistically significant increase in the number of malformed fetuses is observed for the rather immature oocytes that were exposed. (Note that the data summarize only weeks 5 to 7 before ovulation, whereas the somewhat higher dose rate of 0.28 Gy/h was applied to mice of weeks 1 to 5 before ovulation.)

An interesting question resulted from the fact that even at low dose rates female mice became sterile 8 weeks after radiation exposure: Was this sterility transient or permanent? Therefore, we exposed females to 1 Gy gamma-rays at 0.4 Gy/h and waited for about half a year before the first mating started. Out of 36 exposed females, 4 showed a plug, but none had an implantation on day 19 of gestation. Thus, sterility seems to be permanent. Another result of this study, however, was highly interesting: The spontaneous frequency of malformed fetuses in the controls was markedly higher than in young females. Whereas the spontaneous frequency in the contemporary controls was about 2%, when the females were around 12 weeks old, it increased for the half year old females to about 9%; all the malformations were gastroschises. This result further supports our hypothesis that gastroschisis induction has something to do with a labilization of the genome.

Adult male mice

Radiation-exposed male mice were mated for 8 weeks to
unirradiated females. With the exception of two weeks (number
5 and number 8) all stages of spermatogenesis showed a higher
frequency of lethal events after radiation exposure when
compared with control males. This difference was mainly due to
a higher frequency of preimplantation loss and early
resorptions.

Fig. 1 (Spermatogenesis) presents a summary of the results
with regard to the teratogenic effect. Obviously, radiation
exposure of male mice with 2.8 Gy at a dose rate of 0.28 Gy/h
enhances the number of malformed fetuses (almost exclusively
gastroschises) significantly. This result definitely rules out
the possibility that indirect radiation effects through the
mother are responsible for the observed increase in the number
of malformed fetuses.

Fig. 2 specifies the most sensitive periods of
spermatogenesis. The period with the highest sensitivity is
around meiosis. The most resistent stages seem to be the
spermatogonia. Those spermatogonia, which are damaged, are
obviously not able to develop to mature sperms.

Fetal female mice

No effects (neither with regard to lethality nor to
malformations) were observed after 0.7 Gy (dose rate:
0.28 Gy/h), when radiation exposure took place during
gestation (day 19) and those female mice exposed as fetuses
were mated about 12 weeks later. When, however, the total dose
amounted to 2.8 Gy, a statistically significant increase in
the number of malformations (gastroschises, exclusively) was
observed (see Fig. 1, Oogenesis (fetus)).

No increase in the frequency of early or late resorptions and fetal death occurred. Nevertheless, the number of implantations was about 20% lower in the exposed mice when compared to control mice. This reduction was most probably due to less ovulated oocytes; it cannot be ruled out, however, that preimplantation death was higher.

Summary

1. It is possible to increase the frequency of malformed fetuses (almost exclusively gastroschises) by exposing various stages of oo- and spermatogenesis of the HLG/Zte mouse strain to ionizing radiation.

2. The high sensitivity of immature stages of oogenesis with regard to lethal effects can be overcome to some extent by reducing the dose rate (from 60 Gy/h to 0.011 Gy/h). Those immature oocytes surviving radiation exposure under these conditions also show an increased teratogenic risk.

3. The spontaneous frequency of malformations increases markedly with increasing age of the mother.

4. The most probable explanation for the observed effects is a labilization of the genome by radiation exposure.

Publications:

W.-U. Müller, C. Streffer, S. Pampfer
The question of threshold doses for radiation damage:
malformations induced by radiation exposure of unicellular or
multicellular preimplantation stages of the mouse.
Radiat. Environ. Biophys. 33 (1994) 63-68

W.-U. Müller, H. Schotten
Induction of malformations by X-ray exposure of various stages
of the oogenesis of mice.
Mutation Research, in press

W.-U. Müller, C. Streffer, M. Knoelker
A genetic characterization of differences in the sensitivity
to radiation-induced malformation frequencies in the mouse
strains Heiligenberger, C57Bl, and Heiligenberger x C57Bl.
Radiat. Environ. Biophys., in press

Fig. 1: Malformations after Radiation Exposure of Various Stages of Oogenesis and Spermatogenesis
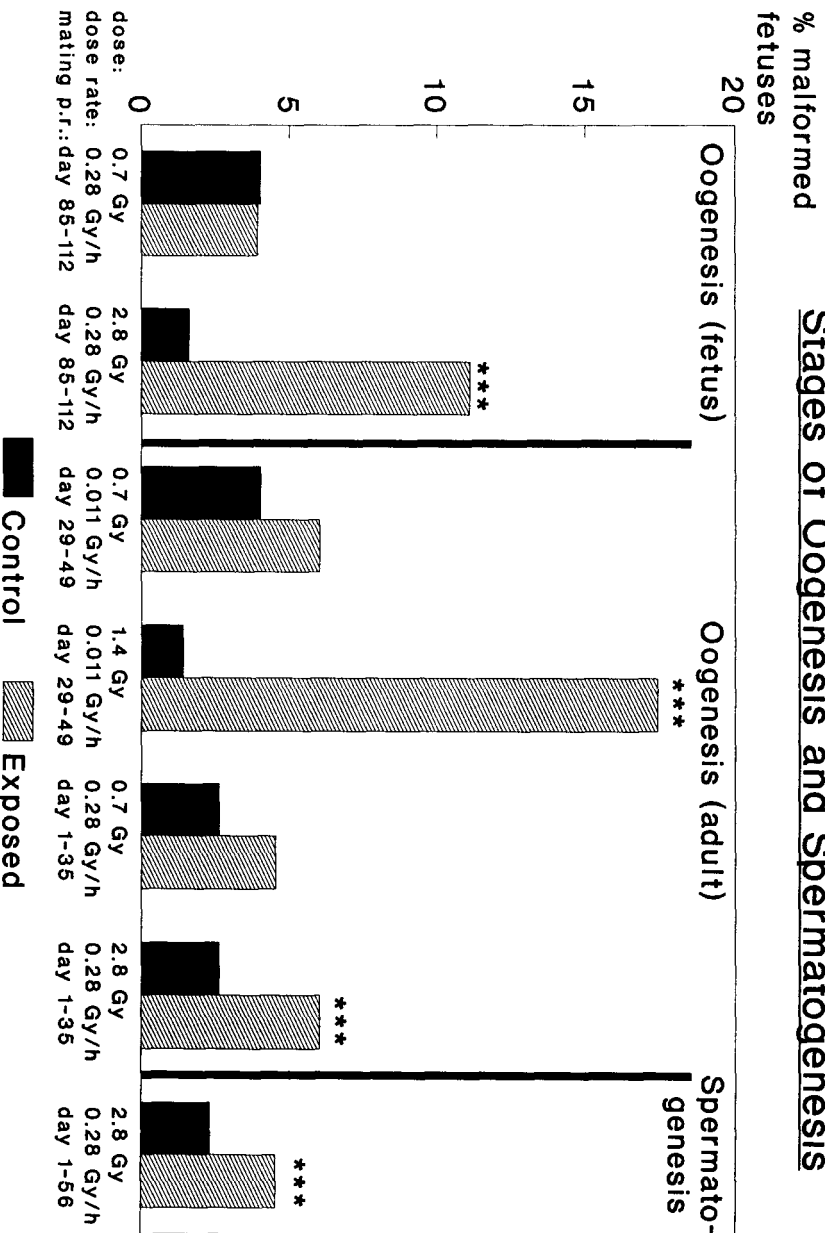
Significantly different from control at P<0.01 (***)

Fig. 2: Malformations after Radiation Exposure (2.8 Gy at 0.28 Gy/h) of Various Stages of Spermatogenesis
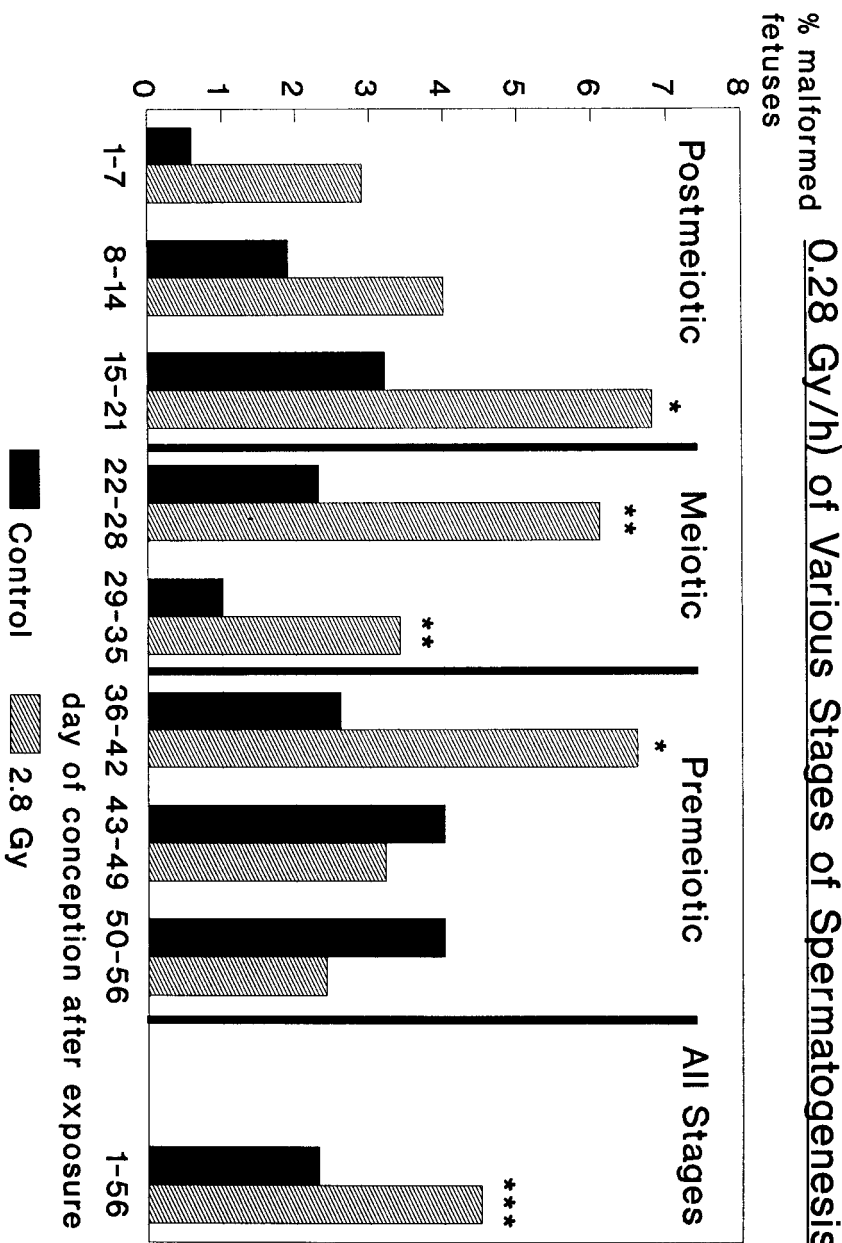
Significantly different from control at P<0.1 (*), 0.05 (**), 0.01 (***)

Head of project 5: Dr. A. E. Czeizel

II. Objectives for the reporting period

The main objective for the reporting period has been the compilation of epidemiological data (prevalence, mortality, morbidity etc) on 28 types of cancer in Hungary and, using these as a basis, estimate detriment associated with them employing four indicators, namely, years of lost life (YLL), potentially impaired life (PIL), actually impaired life (AIL) and economically impaired life (EIL).

III. Progress achieved including publications

(a) Baseline data. Baseline data on cancer mortality was compiled from the Annual records of the Central Statistical Office, Budapest. In these records, the data are broken down into age-groups of 5-year intervals ranging from age zero to a group older than 85 years of age. The years 1988 through 1992 were chosen for constructing mortality profiles. For the estimation of the onset ages, Korányi Institute for Lung Diseases provided the needed statistics while for all other cancers, data from the Hungarian Cancer Registry for 1988 and 1989 were used. Pertinent information on premature retirement was provided by the National Institute for Health Insurance.

(b) Indicators and methods used. The data compiled permitted computations of weighted averages for age at onset (ON), at death (AD) and at premature retirement (PR) for the different cancers.

Detriment at the individual level was estimated as follows, in terms of the average number of years of lost life (YLL), potentially impaired life (PIL), actually impaired life (AIL) and economically impaired life (EIL) :
  YLL = Average life expectancy [D] - average age at death [AD]
  PIL = Average age at death [AD] - average age of onset [ON]
  AIL = Average age at death [AD] - average age at premature
                                   retirement [PR]
  EIL = Age at normal retirement [NR] - average age at premature
                                   retirement [PR]

The ages at onset and at death were scaled in terms of ages from 0 to 64 and 0 to 74 for men and women respectively (In Hungary, the average life expectancies are 65 for men and 74 for women). However, the data on PR were scaled from age 20 to the

age of retirement, which is 55 for women and 60 for men (thus, by definition, the PR figures for men and women will not exceed the ages of 60 and 55 respectively).

(c) Mortality profiles. Data on mortality are presented in Table 1 and show the following:
1. Overall considered, the average age at onset for cancers is of the order of 46 years; men get cancers approximately five years later than women, retire prematurely about three years later than women and die about 6 years earlier than women.
2. In both sexes, early deaths (0-19 years) are predominantly due to lymphoid leukaemia; most cancers cause adult death (age range: 20-69 years) and late death (70+).
3. Again in both sexes, adult deaths due to brain cancer and Hodgkin's disease account for over two-thirds of all deaths due to these cancers and
4. In males, adult deaths due to cancers of the upper respiratory tract (mouth, lips, pharynx and oesophagus) account for more than 80% of adult and late deaths whereas in females, the ratio of adult to late deaths is about 50:50.

(d) Detriment estimates at the individual level. These are summarized in Table 2 and permit the following generalizations:
1. In males, estimates of the <u>average number of lost life years</u> cover a range between about 6 (for prostate cancer) to 19 years (for cancers of the brain, Hodgkin's disease and lymphoid leukaemia); in females, this range is between about 10 (cancers of the bladder, pancreas etc) to about 23 years (Hodgkin's disease, lymphatic leukaemia etc).
2. Comparable estimates for <u>potentially impaired life</u> in males range from about 2 (cancers of the oesophagus, myeloid and other leukaemia) to about 14 (cancers of lymphatic organs); in females, this range is from about 10 (cancers of mouth, lips and pharynx) to about 34 (leukemias other than myeloid and lymphatic and cancers of the kidneys).
3. The estimates for <u>actually impaired life</u> years range from about 2 (skin cancer) to about 10 (prostate cancer, lympho-sarcomas (cancers of the gall bladder and bile duct) in males. In females, this range is from about 10 (cancers of the lip, mouth and pharynx, colon and rectum, lymphosarcoma etc) to 25 (some forms of leukemia). Likewise the estimates of economically impaired life encompass a range from 10 to 20 years in males and a similar range in females.
4. Overall considered, the average number of years of lost life, potentially impaired life, actually impaired life and economically impaired life are, about 14, 10, 15 and 12, respectively (averaged over all cancers and both sexes).

We will use these estimates as a basis to (i) compute <u>detriment to the population</u> in terms of total number of years lost, potentially impaired life, actually impaired life and economically impaired life, taking into account the life expectancy, age at onset and age at premature retirement and (ii) compare these with those available for Mendelian diseases, congenital abnormalities and chronic multifactorial diseases.

Table 1.

The percentages of early, adult and late death

Cancer	Males			Females			Total		
	early	adult	late	early	adult	late	early	adult	late
Mouth, lips and pharynx	0.14	82.37	17.49	0.45	0.55	44.43	0.19	78.24	21.57
Oesophagus	0.00	80.92	19.08	0.00	0.56	44.13	0.00	77.79	22.21
Stomach	0.00	51.76	48.24	0.03	0.36	63.61	0.01	45.60	54.39
Colon	0.07	49.35	50.59	0.00	0.36	64.27	0.03	42.21	57.76
Rectum	0.02	50.66	49.32	0.03	0.41	59.08	0.02	46.34	53.64
Liver	0.40	56.99	42.61	0.39	0.45	55.03	0.40	51.97	47.63
Gall-bladder and bile-duct	0.00	47.39	52.61	0.00	0.38	61.71	0.00	40.58	59.42
Pancreas	0.03	60.63	39.34	0.00	0.42	57.54	0.01	52.00	47.99
Larynx	0.00	77.95	22.05	0.36	0.72	27.44	0.03	77.45	22.52
Lungs	0.01	69.92	30.07	0.01	0.58	41.57	0.01	67.45	32.54
Other thoracic organs	1.20	69.16	29.64	2.06	0.56	41.56	1.52	64.44	34.04
Skin	0.38	70.99	28.63	0.00	0.57	42.57	0.20	64.67	35.12
Breast	0.00	0.00	0.00	0.00	0.60	39.94	0.00	60.06	39.94
Cervix	0.00	0.00	0.00	0.03	0.67	32.60	0.03	67.37	32.60
Uterus	0.00	0.00	0.00	0.00	0.47	53.46	0.00	46.54	53.46
Ovaries	0.00	0.00	0.00	0.24	0.61	38.52	0.24	61.24	38.52
Prostate	0.02	24.69	75.30	0.00	0.00	0.00	0.02	24.69	75.30
Bladder	0.07	41.23	58.70	0.21	0.33	66.60	0.11	39.21	60.68
Kidnies	0.54	61.72	37.74	0.64	0.46	52.88	0.58	55.83	43.59
Brain	7.34	76.78	15.88	6.66	0.70	23.47	7.02	73.56	19.41
Lymphosarcoma	4.41	55.88	39.71	2.67	0.52	45.33	3.67	54.24	42.09
Hodgkin's disease	3.37	75.66	20.96	4.17	0.63	33.33	3.70	70.27	26.03
Other lymphatic organs	2.97	60.76	36.27	1.91	0.48	50.53	2.48	54.60	42.92
Myeloid leukaemia	0.19	63.50	36.31	0.16	0.50	49.69	0.17	56.26	43.57
Lymphatic leukaemia	9.17	47.04	43.80	8.21	0.35	56.59	8.76	41.99	49.26
Myeloid leukaemia	4.26	60.08	35.66	2.34	0.55	42.63	3.31	57.56	39.13
Other leukaemia	7.69	46.15	46.15	0.00	0.41	59.26	3.77	43.40	52.83
Unspecified leukaemia	3.95	44.74	51.32	4.08	0.47	48.98	4.01	45.75	50.24
Total	0.57	60.46	38.97	0.53	0.49	50.51	0.55	55.46	43.99

Table 2

The estimates of detriment in terms of life years lost (YLL), Potentially impaired life (PIL), actually impaired life (AIL) and economically impaired life (EIL)

Cancer	YLL			PIL			AIL			EIL		
	males	fem.	total	males	fem.	total	males	fem.	total	males	fem.	total
Mouth, lips and pharynx	12.83	17.46	15.59	3.86	9.96	6.22	4.06	10.45	6.55	11.89	8.91	10.14
Oesophagus	11.30	14.70	13.86	1.30	7.30	3.94	3.27	13.55	6.05	9.57	9.25	7.91
Stomach	9.58	11.93	10.77	5.77	16.74	10.74	6.74	16.18	11.43	11.32	9.11	10.20
Colon	9.54	11.03	10.38	4.90	16.56	9.98	6.81	16.90	11.32	11.35	9.11	10.52
Rectum	9.28	11.06	10.31	4.99	16.52	9.98	6.46	15.43	11.02	10.74	7.49	9.33
Liver	9.90	11.99	10.64	9.13	17.51	13.71	6.85	15.57	12.07	11.75	8.56	10.71
Gall-bladder and bile-duct	8.32	9.70	8.80	6.35	15.63	11.98	9.68	17.30	14.20	13.00	8.00	11.00
Pancreas	10.20	10.61	10.91	5.25	21.39	11.17	7.35	16.77	11.95	12.55	8.38	10.86
Larynx	10.90	18.20	13.59	3.45	13.80	6.15	5.28	9.45	7.84	11.18	8.65	9.43
Lungs	9.83	14.33	11.90	4.41	18.04	8.20	5.07	13.84	8.70	9.90	9.17	8.60
Other thoracic organs	14.52	17.49	15.93	-0.04	18.06	4.91	2.75	18.08	8.10	12.27	16.57	12.03
Skin	15.14	17.27	16.24	1.30	14.73	8.37	1.31	14.44	7.91	11.45	12.69	12.15
Breast	0.00	18.98	14.12	0.00	12.99	10.67	0.00	12.24	9.92	0.00	9.04	12.04
Cervix	0.00	11.45	17.41	0.00	14.70	12.27	0.00	12.61	10.18	0.00	12.59	15.59
Uterus	0.00	10.53	10.53	0.00	15.55	12.47	0.00	15.31	12.23	0.00	7.76	10.76
Ovaries	0.00	14.46	12.90	0.00	14.01	11.57	0.00	12.02	12.02	0.00	9.92	12.92
Prostate	6.33	0.00	6.96	0.00	0.00	7.62	9.10	0.00	13.47	10.43	0.00	8.43
Bladder	7.83	9.26	8.77	3.25	13.99	11.23	7.00	18.61	11.96	9.83	8.87	8.73
Kidnies	10.75	12.36	11.78	7.25	20.75	11.54	4.60	17.58	10.22	10.35	10.94	10.00
Brain	18.89	21.07	19.77	5.20	18.85	12.25	4.91	15.26	9.85	18.80	17.33	17.62
Lymphosarcoma	17.88	18.80	17.56	5.90	0.00	10.44	8.45	11.95	11.15	21.33	11.75	16.71
Hodgkin's disease	18.87	23.72	21.66	5.12	0.00	17.42	6.22	14.57	10.19	20.09	19.29	19.85
Other lymphatic organs	15.68	15.22	15.76	10.07	17.03	13.68	4.72	16.28	10.34	15.40	12.50	14.10
Myeloid leukaemia	9.87	10.97	10.10	13.57	17.49	16.81	5.40	19.78	12.90	10.27	11.75	11.00
Lymphatic leukaemia	22.36	20.87	21.38	8.13	12.70	11.79	-6.24	11.68	2.08	11.12	13.55	11.46
Myeloid leukaemia	18.24	17.98	18.15	-2.46	19.77	7.56	4.58	12.81	9.09	17.82	11.79	15.24
Other leukaemia	20.25	13.00	18.08	1.19	19.73	9.37	0.00	25.00	15.92	0.00	19.00	22.00
Unspecified leukaemia	19.16	15.97	17.16	2.75	34.00	12.27	-1.16	12.70	6.40	13.00	9.67	11.56
Total	11.28	14.12	13.96	5.17	16.31	9.96	6.30	15.22	9.92	12.58	10.34	11.88

Title: Genetic risks associated with exposure to ionizing radiation.

1)	Favor	GSF
2)	Van Buul	Univ. Leiden
3)	Cattanach	MRC
4)	de Rooij	Univ. Utrecht
5)	Miró Ametller	Univ. Barcelona - Autónoma
6)	Eeken	Univ. Leiden
7)	Hulten	EBHA

I. Summary of Project Global Objectives and Achievements

An adequate understanding of the genetic risks associated with radiation exposure as well as the mechanisms of mutation induction are essential for an informed action to protect mankind from the harmful effects of radiation. To this end our project has addressed the strategy of risk estimation based on experimental data in animals to determine factors important to the mechanisms of mutation induction by radiation exposure in germ cells. Experiments were conducted to improve risk extrapolation procedures as well as to determine the influences of DNA damage repair and cell killing on the levels of mutation induction by radiation. Genetic and molecular techniques have been employed to determine the region of the genome prone to radiation induced damage and to characterize the types of DNA damage resulting in transmitted mutational effects. The major achievements for the contract may be summarized as follows.

Comparative mutagenicity experiments were carried out in two mammalian species, the mouse (*Mus musculus*) and the hamster (*Mesocricetus auratus*). The radiation induced mutation rates to dominant cataract and enzyme activity alleles were determined in the various germ cell stages of both males and females. There do not appear to be differences in the observed mutation frequencies. These results do not contradict a major assumption required for the extrapolation of experimental animal radiation mutagenicity results to humans, i.e. no species differences in the sensitivity to radiation induced mutagenesis. In one respect, the mouse and hamster observations differ from humans: For both laboratory species there is an extremely high sensitivity to radiation induced cell killing in the immature oocytes. By contrast, the human immature oocyte is reported to be more radio-resistant to cell killing. Thus, the study of the female germ cell stages for extrapolation to the human situation employing laboratory mammals remains difficult. (GSF-Neuherberg)

The radiation doubling dose for the occurrence of enzyme activity mutations in spermatogonia of the mouse is estimated to be 1.5 Gy. This value is similar to the doubling dose

estimated for dominant cataract mutations and higher than the doubling dose estimated for recessive specific locus mutations. These observations emphasize the conclusion that estimations of human genetic risk should be based on animal experimental results for comparable genetic endpoints. (GSF-Neuherberg)

Related to the above finding, we have determined that radiation induced deletions are recovered as transmitted mutations expressing a mutant phenotype at a sub-set of the potential loci which when mutated may express a dominant phenotype in both the mouse and *Drosophila*. These responding loci are functionally haplo-insufficient, i.e. two functional gene copies are required for the development of the normal phenotype. This result clarifies a basic hypothesis in radiation genetics: Radiation induces mainly deletions, which result in loss of function mutations. It had been assumed that loss of function mutations lead to recessive mutant alleles, while dominant mutations are the result of gain of function mutational events. Our working hypothesis is that radiation induced dominant mutations are recovered at haplo-insufficient loci. These observations are important for the human situation, since we may predict that dominant mutations resulting from exposure to radiation would be expected to occur at haplo-insufficient loci.(GSF-Neuherberg, MRC-Harwell, Leiden)

In order to more intensely follow up on the study of haplo-insufficient loci in the mouse we have undertaken a mapping of dominant cataract mutations recovered in our mutagenicity experiments. These mutations would be expected to be haplo-insufficient. Mapping studies have proceeded following two protocols: In collaboration with M.F. Lyon (Harwell) visible markers have been employed. In addition, we have identified 42 microsatellite markers which screen in one cross the entire mouse genome. Results have identified previously known loci as well as unknown loci in the mouse, which when mutated result in a dominant cataract phenotype. Two of the loci involved, the *gamma-crystallin* gene cluster on mouse chromosome 1 and the *Small eye* gene on mouse chromosome 2 are interesting. The *gamma-crystallin* gene cluster is haplo-insufficient, which is surprising since genes encoding structural proteins were not expected to be haplo-insufficient. It is likely that the highly conserved clustered arrangement of the *gamma-crystallin* genes indicates a coordinated gene expression function. By deleting one or more of the *gamma-crystallin* genes within the cluster, the coordinated gene expression of the entire cluster is disrupted and results in a mutant phenotype. The second haplo-insufficient locus studied, *Small eye*, has been shown to be encoded by the *Pax6* gene and is important in the development of the CNS and the eye. Both genes studied have human homologues and these results from the mouse would predict that radiation induced mutations in humans at the homologous loci would result in dominantly expressed deleterious phenotypes. (GSF-Neuherberg, MRC-Harwell, Leiden)

A large group of multilocus deletions which express deleterious dominant phenotypes have been recovered in offspring of irradiated mice. The deletions have been localized to chromosomal regions and their distribution is non-random and

would suggest that certain regions of the genome are more prone to the occurrence of radiation induced large deletions. The homologous regions of humans should be of prime interest for both genetic and somatic effects of radiation. By contrast, a molecular analysis of mutations at the X-linked *Mottled* locus of the mouse revealed that mutant alleles recovered following parental irradiation were all intergenic alterations and not deletions. This observation suggests that radiation induced deletions on the X chromosome either do not occur or are not likely to survive or be transmitted. The situation appears similar to the radiation genetic results for haploid organisms (virus, bacteria, etc.) in which recovered radiation induced mutations are also mainly intergenic alterations. (MRC-Harwell)

A number of experimental procedures have been employed to study the heterogeneity of the mouse stem cell population, such as DNA repair inhibition with 3-aminobenzamide pretretment followed by irradiation, enrichment of the G1 phase by selected killing of S phase cells with hydroxyurea pretreatment or synchronization of the stem cell spermatogonia by stem cell depletion with triethylenemelamine pretreatment. A number of biological endpoints have been assayed, including spermatogonial cell killing, translocation, recessive specific locus, dominant cataract and enzyme activity mutations. In general, there is a correlation of the relative yields of the different radiation induced effects in the altered stem cell spermatogonial populations. Thus, the results would suggest a similar mechanism of radiation induced effect for the various endpoints. There are some exceptions, such as the present observation that mouse strain 101/H is apparently resistant to radiation induced translocation induction but sensitive to radiation induced specific locus mutations when radiation is applied as a single, acute dose. These findings emphasize differences observed in the relative frequencies of specific locus mutations and translocations following different radiation regimes (single or fractionated) and suggest that the specific locus and translocation mutational events may be induced in different sub-populations of the stem cell spermatogonia. The importance of the heterogeneity of the stem cell spermatogonia has also been emphasized by the dependence of radiation cell killing and translocation yields on the repair competence of the treated cell populations. (GSF-Neuherberg, MRC-Harwell, Leiden, Utrecht)

Three assumptions made in the model of Leenhouts and Chadwick for the induction of reciprocol translocations and point mutations by irradiation were tested: a) In the mouse testis, there are many more sensitive than resistant stem cells for the cell killing effect of irradiation; b) Radiosensitive stem cells have a high linear translocation-induction rate; c) Radioresistant stem cells have a low linear translocation-induction rate. Data from dose-response experiments for stem cell killing by X-irradiation and from cell counts of spermatogonia revealed that the numbers of resistant and sensitive stem cells are about similar. A dose-response experiment in which the seminiferous epithelium of 3H1 mice was synchronized, thus creating mice with abnormally high numbers

of either radiosensitive or radioresistant stem cells, revealed
no differences in the yield of translocations in these two
kinds of mice. These results cast doubt on the validity of the
three assumptions and attempts are now being made to develop an
alternative model. (Utrecht, MRC-Harwell, Leiden)

The most important question that remains is the relevance of
radiation genetic results from laboratory mammal species to the
human situation. To directly address this question experiments
with human germ cells have been undertaken. Employing the
human-hamster in vitro fertilization techniques a protocol to
screen for spontaneous and radiation induced micronuclei has
been established. (Radiation exposures were carried out on
mature spermatozoa in vitro.) The micronuclei observed have
been demonstrated to be from the human genome. Further, the
results for the micronucleus assay have been shown to parallel
the results for the more technically demanding chromosome assay
in the human-hamster experimental protocol. In a second series
of experiments, non-disjunction in human sperm has been
demonstrated with the FISH techniques. Aneuploidy frequencies
were shown to increase in men with histories of radiation
exposure, and the effect was shown to persist for as long as 10
years following radiation exposure. The mechanism for the long
term effects of radiation on increased frequency of aneuploidy
(induced primary non-disjunction or 3:1 meiotic segregation of
radiation-induced balanced translocations) is not yet known and
will be the subject of future studies. Again, a major
undertaking has been to develop and confirm simpler assay
methods. To this end, mutations at microsatellite loci have
been demonstrated and promise a more efficient screening
protocol in human populations. (Barcelona, Birmingham)

In summary, our project has critically addressed the
relevance of the laboratory mammal experimental results by
identifying the mechanisms leading to radiation induced
mutations which, should they occur in a human population, would
result in a deleterious phenotype, as well as a direct assay of
the human genome. As the comparative characterizations of the
mouse and human genomes continue we may anticipate an
identification of homologous chromosomal regions and homologous
genes which are prone to the effects of radiation and would
result in transmitted germ cell mutations with phenotypic
effects.

Head of project 1: Dr. Favor

II. Objectives for the reporting period

1) Radiation induced mutation rates to dominant cataract and enzyme activity alleles were compared in two laboratory mammals, *Mus musculus* and *Mesocricetus auratus*.

2) The sensitizing effect of 3-aminobenzamide in mouse spermatogonia on the radiation-induced mutation rate to dominant cataract and enzyme activity alleles was studied.

3) Recovered dominant cataract and enzyme activity mutations were genetically characterized.

III. Progress achieved including publications

1) An interspecific comparison of the radiation-induced mutation rates in germ cells of two laboratory mammals, the mouse (*Mus musculus*) and hamster (*Mesocricetus auratus*) has been carried out. Table 1 gives the observed mutation rates of dominant cataract and enzyme activity alleles in control or in offspring of radiation exposed parental generation mice (2+2 Gy gamma-irradiation, 0.375 Gy/min; 24 h interval between radiation exposures).

Table 1: Observed germ cell mutation frequencies (per locus, x 10^{-5}) in the mouse, *Mus musculus*, and the hamster, *Mesocricetus auratus*

Germ cell stage	Dominant Cataract		Enzyme Activity	
	Mouse	Hamster	Mouse	Hamster
Post-spermatogonia	–	3.0	7.6	10.8
Spermatogonia	1.1	1.1	1.8	–
Maturing oocytes	1.3	3.3	8.5	8.9
Immature oocytes	–	–	–	–

The observed mutation frequencies to dominant cataract or enzyme activity alleles are comparable in mouse and hamster for a particular germ cell stage of irradiation exposure, indicating no species differences in the sensitivity to mutation induction by irradiation in germ cells of the species studied. These results extend to a second species the observation in mice that 1) in males, post-spermatogonial stages are more sensitive to the induction of mutations by irradiation than are stem cell spermatogonia, 2) in females, the mutation rate observed in maturing oocytes following irradiation is comparable to the mutation rate observed in irradiated post-spermatogonial stages of males, 3) in hamsters as in the mouse, the immature oocytes are highly sensitive to radiation-induced cell killing such that litter size is greatly reduced and the resultant F_1 population sizes are too reduced to estimate a mutation frequency, 4) the per locus mutation rates to enzyme activity alleles are higher than the mutation frequencies to dominant cataract alleles. In summary, these results do not contradict the basic assumption required for an extrapolation from laboratory mammal experimental results to an estimation of human radiation genetic risk, i.e. no species differences in the sensitivity to mutation induction by radiation. However, both laboratory species exhibit high sensitivity to radiation-induced cell killing of immature oocytes, which differs from the human situation. Thus, for the study of the mutation process and an extrapolation of experimental results to humans for female germ cell stages, the two laboratory species studied are inappropriate. Further studies must deal with this problem.

2) Based on previous results from the participating laboratories of P. van Buul (Leiden) and B. Cattanach (Harwell), in which a demonstrated sensitizing effect of 3-aminobenzamide pre-treatment on radiation induced cell killing, chromosomal aberration and specific locus mutation frequencies, we undertook an experiment to confirm these results for the medically relevant genetic endpoints of transmitted mutations with dominantly expressed deleterious phenotypes. To this end, male mice were treated i.p. with 250 mg 3-aminobenzamide per kg body weight and 1 h following treatment exposed to 6 Gy gamma irradiation (0.375 Gy/min). Table 2 presents the results.

Table 2: Dominant cataract and enzyme activity mutation
frequencies in spermatogonia of the mouse following exposure to
radiation alone or radiation in combination with 250 mg 3-
aminobenzamide/kg body weight pre-treatment

Treatment	F_1 Offspring	Mutations	MR* x 10^{-5}
Dominant cataract			
6 Gy	11095	3	0.9
3-AB + 6 Gy	10371	10	3.2
Enzyme activity			
6 Gy	7539	1	1.1
3-AB + 6 Gy	9974	10	8.4

* MR = mutations per gamete per locus; For the dominant
cataract mutation results, 30 loci assumed; For the enzyme
activity mutation results, 12 loci screened.

For both genetic endpoints, the combined 3-aminobenzamide + 6
Gy treatment resulted in a higher observed mutation frequency
as that observed for radiation treatment alone. These results
extend the observed enhancing effect of 3-aminobenzamide pre-
treatment on the sensitivity to radiation induced mutagenesis
to a wider spectrum of genetic endpoints. Our original logic
for undertaking this experiment was the assumption that
radiation induces mainly deletions which result in "loss of
function" mutations. One may easily envisage such loss of
function mutations to result in recessive mutant alleles.
However, dominant mutant alleles have traditionally been
hypothesized to be due to "gain of function" mutational events
and not likely to be due to deletions. Our mutagenesis results
are in conflict with this hypothesis. Recently a large number
of genes in the mouse has been demonstrated for which loss of
function mutations result in a dominantly expressed mutant
allele. Such genes have been described as haploinsufficient,
i.e. two functional gene copies are required for the
development of the normal phenotype. Our present working
hypothesis is that a sub-set of the potential genes in the
mouse, which when mutated result in a dominant cataract
phenotype, are haploinsufficient. These haploinsufficient loci
are responding to radiation-induced mutagenesis, and it will be
important to genetically and molecularly identify the involved
genes.

3a) Two haploinsufficient dominant cataract genes have been
mapped in the mouse. In collaboration with M.F. Lyon (Harwell)
the large *Cat2* allelism group has been shown to be on mouse
chromsome 1, and represents mutations of one or more of the
genes in the gamma-crystallin gene cluster. This result is
surprising since genes which encode structural proteins are not
expected to be haploinsufficient. However, the clustered
association of the gamma-crystallin genes has likely been
conserved to facilitate coordinated gene expression. By

deleting one or more of the gamma-crystallin genes within the cluster, the coordinated expression pattern of the entire cluster would be disrupted and a mutant phenotype results.

The second haploinsufficient gene identified, which when mutated results in a dominant cataract phenotype is the mouse *Small eye* gene on chromsome 2. The mouse *Small eye* locus is encoded by the *Pax6* gene, which contains paired-like and homeobox domains, and is an important gene in the control of CNS and eye development.

3b) The above mentioned genes were mapped relative to conventional visible marker genes of the mouse. Unfortunately very few mouse facilities are able to maintain the marker gene stocks to allow a genome-wide screen of the entire mouse genome. Recently, the mouse genome has been characterized for location and size of short repetitive sequences (microsatellites), and they have been shown to be polymorphic among many of the standard inbred mouse strains. We have taken advantage of these findings, identified 42 microsatellite markers which allow segregation and linkage analyses of the entire mouse autosomal genome to map dominant cataract genes. The first radiation-induced dominant cataract mutation mapped with our new protocol was shown to be in the proximal region of chromosome 4 and is a previously unknown cataract gene. With the method now established, we will proceed to map our collection of dominant cataract mutations and will be able to identify in a relataively short time those loci which are responding to radiation-induced mutagenesis.

3c) Table 3 lists the dominant cataract and enzyme activity mutations recovered in the combined 3-aminobenzamide + 6 Gy mutation experiment. The mutations are characterized for phenotype, fertility and transmission of the mutant allele in an outcross of heterozygous mutant carriers to homozygous wildtype partners. For the group of 10 dominant cataract mutations, 4 mutations exhibited normal fertility and transmission; 5 mutations exhibited normal fertility and reduced transmission (which we interpret to be due to mutant alleles with reduced penetrance); 1 mutation was recovered with reduced fertility and reduced transmission. For the group of enzyme activity mutations, 4 mutations were recovered with normal fertility and normal transmission; 3 mutations exhibited normal fertility with reduced transmission; 2 mutations exhibited reduced fertility with normal transmission; 1 mutant phenotype was recovered with reduced fertility but the mutant phenotype has not been transmitted to the following generation. These groups of mutations represent the entire spectrum of possible mutant alleles when considering their effects on fertility and transmission and should be considered when discussing the potential genetic risks associated with radiation exposure in humans. Mutations with normal fertility and normal penetrance will persist in a population and offspring of a mutant carrier have a 50% risk of inheriting the genetic disease phenotype. Mutations with normal fertility but reduced penetrance will persist in the population but offspring

of a carrier of the mutation will have less than 50% risk of
developing the mutant phenotype. Offspring of mutant carriers
not expressing the mutant phenotype may also develop a mutant
phenotype. Thus, such mutations may be good animal models for
sporadic congenital diseases with a genetic component.
Mutations with reduced fertility will be quickly eliminated,
such that the major genetic risk consists of the first
generation offspring following radiation exposure.

Table 3: A characterization of dominant cataract and enzyme
activity mutations recovered in offspring of males treated with
3-aminobenzamide + 6 Gy gamma-irradiation

Mutant	Phenotype	Litter size	Transmission
ABX-10	Total opacity with iris anomaly	7.1	48
ABX-15	Nuclear opacity	8.9	44
ABX-16	Nuclear and zonular opacity	10.2	43
ABX-20	Nuclear opacity	7.7	22
ABX-22	Nuclear opacity	6.8	5
ABX-29	Polar-corneal opacity with iris anomaly	2.2	18
ABX-30	Suture-subcapsular opacity	7.2	5
ABX-32	Posterior suture opacity	7.0	24
ABX-34	Nuclear and zonular opacity	8.2	41
ABX-39	Nuclear opacity	6.3	26
2274	PGAM 160%	8.7	19
5447	GAPDH 50%	8.0	50
6958	GR 50%	7.0	49
7074	GR 50%	8.5	53
7384	MDH 50%	7.2	36
7426	GR 160%	8.0	23
7543	MDH 160%	1.8	0
7836	MDH 55%	6.6	46
8078	GR 55%	4.0	50
9698	GR 50%	2.0	50

Publications

Kratochvilova, J., and J. Favor (1992) Allelism tests of 15 dominant cataract mutations in mice. Genet. Res., Camb. 59, 199-203.

Merkle, S., and W. Pretsch (1993) Glucose-6-phosphate isomerase deficiency associated with nonspherocytic hemoloytic anemia in the mouse: An animal model for the human disease. Blood 81, 206-213.

Pretsch, W., S. Merkle, J. Favor and T. Werner (1993) A mutation affecting the lactate dehydrogenase locus Ldh-1 in the mouse. II. Mechanism of the LDH-A deficiency associated with hemolytic anemia. Genetics 135, 161-170.

Everett, C.A., P.H. Glenister, D.M. Taylor, M.F. Lyon, J. Kratochvilova-Loester and J. Favor (1994) Mapping of six dominant cataract genes in the mouse. Genomics 20, 429-434.

Favor, J. (1994) Spontaneous mutations in germ cells of the mouse: estimates of mutation frequencies and a molecular characterization of the mutagenic events. Mut. Res. 304, 107-118.

Favor, J., and A. Neuhäuser-Klaus (1994) Genetic mosaicism in the house mouse. Ann. Rev. Genet. 28, 27-47.

Pretsch, W., J. Favor, W. Lehmacher and A. Neuhäuser-Klaus (1994) Estimates of the radiation-induced mutation frequencies to recessive visible, dominant cataract and enzyme-activity alleles in germ cells of AKR, BALB/c, DBA/2 and (102xC3H)F1 mice. Mutagenesis 9, 289-294.

Sandulache, R., A. Neuhäuser-Klaus and J. Favor (1994) Genetic instability at the *agouti* locus of the mouse (*Mus musculus*). I. Increased reverse mutation frequency to the A^w allele in *A/a* heterozygotes. Genetics 137, 1079-1087.

Sandulache, R., W. Pretsch, B. Chatterjee, W. Gimbel, J. Graw and J. Favor (1994) Molecular analysis of four lactate dehydrogenase-A mutants in the mouse. Mammal. Genome 5, 777-780.

Stambolian, D., J. Favor, W. Silvers, P. Avner, V. Chapman and E. Zhou (1994) Mapping of the X-linked cataract (Xcat) mutation, the gene implicated in the Nance Horan Syndrome, on the mouse X chromosome. Genomics 22, 377-380.

Favor, J. (1995) Mutagenesis and human genetic disease: Dominant mutation frequencies and a characterization of mutational events in mice and humans. Env. Mol. Mutagen. 25, S26: 81-87.

Head of project 2: Dr. Van Buul

II. Objectives for the reporting period

Our work aimed at:
(a) Further characterization of the hyposensitivity of scid
     mice for radiation induced chromosomal translocations.
(b) More detailed analysis of chromosomal involvement in
     radiation induced translocation formation.
(c) Evaluation of transgenic mouse systems for studying
     mutations in spermatogonial stem cells.
(d) Correlation of radiation induced spermatogonial stem cell
     killing and translocation formation.

III. Progress achieved including publications

        In scid mice the effects of several factors known to
affect the sensitivity of normal mice to the induction of
translocations in spermatogonia were examined. These include
dose-fractionation with a 24 h interval, pretreatment with 3-
aminobenzamide (3-AB) or low dose-rate exposures. The data
obtained confirm the earlier reported hyposensitivity of scid
mouse spermatogonial stem cells for the recovery of induced
translocations. In addition, these results indicate that the
hyposensitivity is probably not due to certain characteristics
of the spermatogonial population in scid mice but probably
stems from the DNA-repair deficiency in scid mice, which in
turn may prevent the formation of stable chromosomal transloc-
ations. Studies on bone marrow cells of scid mice point in the
same direction and suggest strong elimination of translocation
carrying cells in scid mice during post-irradiation, cell pro-
liferation, possibly via falling apart of the translocation at
the original points of exchange or due to lethal damage at the
translocation break points.
        Using a composite DNA probe for mouse chromosomes 1, 11

and 13 in combination with FISH, the involvement of these three chromosomes in induced translocations recovered from irradiated spermatogonia was analyzed. Results from various post-irradiation sampling periods indicated similar over-representation of the painted chromosomes in translocation formation and no change with time. This suggests that clonal proliferation cannot be held responsible for the earlier observed non-randomness. Experiments with the DNA-repair inhibitor 3-AB showed loss of the recorded over-representation, indicating that probably the repair of lesions is causing this phenomenon rather than non-random induction.

Some experiments with a plasmid-based transgenic mouse mutagenicity model, allowing rescue and cloning of all types of mutations, including deletions, have been initiated. The first results show that treatment regimes producing very high frequencies of specific locus mutations in spermatogonia i.e. two times hydroxyurea (HU) followed by an acute X-ray exposure, likewise due for recovered lacZ mutations. At this moment we are checking whether this sensitization is specific for spermatogonial stem cells by analyzing spleen, liver and brain samples from the same mice. In later stages, sequencing of recovered mutations will take place.

One of the most important assumptions in the interpretation of experimental data about radiation induced genetic damage in spermatogonial stem cells of mammals is a strong correlation between cell killing and the induction of genetic changes in a heterogeneous cell population. In collaboration with de Rooij and Bootsma (Utrecht) we have studied both parameters after combined treatments with 3-AB, HU and X-rays. This resulted in a model for the spermatogonial radiation response which could explain nearly all experimental results obtained with fractionated X-ray exposures or with combined treatments of X-rays and all kinds of chemical agents such as cyclophosphamide, Adriamycin a.o. In this model accumulation of cells in the G_1 stage of the cell cycle due to induction of P53 plays a central role and at this moment we are further testing the model by suppressing P53 with caffein and using P53 'knock out' mice.

Publications

Buul, P.P.W. van, C.M.J. Seelen, K.H. Schöppink and D.G. de Rooij (1992) Induction of chromosomal aberrations in spermatogonial stem cells of steel and dominant spotting mice by single X-ray exposures, Int. J. Rad. Biol., 62, 376 (abstract).
Buul, P.P.W. van, H.J. Goudzwaard and C.M.J. Seelen (1992) Induction of chromosomal aberrations in mouse premeiotic germ cells following combined treatments with X-rays and chemical clastogens, Int. J. Rad. Biol., 62, 361 (abstract).
Buul, P.P.W. van, C.M.J. Seelen, K. Schöppink and J.H. Goudzwaard (1992) Absence of translocation induction in mouse stem cell spermatogonia by chemical mutagens probably due to selective elimination, Mutagenesis, 7, 271-275.
Buul, P.P.W. van, K. Schöppink, J.M. Zandman, A.S. Balajee, J. Vrolijk, H.J. Tanke and C.M.J. Seelen (1993) Induction and repair of X-ray induced DNA strand breaks in oocytes

and embryonic cell cultures of normal and *scid* mice, Int. J. Rad. Biol., 63, 797 (abstract).

Buul, P.P.W. van, K. Schöppink, D.G. de Rooij and C.M.J. Seelen (1994) Reduced recovery of translocations from X-irradiated spermatogonial stem cells of dominant spotting (W^v/+) and Steel (Sl^{con}/Sl^{con}) mice, Radiation Res., 137, 171-176.

Buul, P.P.W. van and A.L. Bootsma (1994) The induction of chromosomal damage and cell killing of mouse spermatogonial stem cells following combined treatments with hydroxyurea, 3-aminobenzamide and X-rays, Mutation Res., 311, 217-224.

Noz, K.C., M. Bauwens, P.P.W. van Buul, A.A. Schothorst, S. Pavel and B.J. Vermeer (1994) Comet assay demonstrates higher levels of UVB-induced DNA damage in dysplastic nevi compared to nevocellular nevi, The J. of Investigat. Dermatol., 102, 602 (abstract).

Buul, P.P.W. van, D.G. de Rooij, J.M. Zandman, M. Grigorova and A. van Duyn-Goedhart (1995) X-ray induced chromosomal aberrations and cell killing in somatic and germ cells of *scid* mice, Int. J. Radiat. Biol., 67, 549-555.

Buul, P.P.W. van, I.M. Zandman, M. Grigorova, J.J.W.A. Boei and A.T. Natarajan (1995) Mitotic and meiotic detection of radiation-induced translocations in mouse stem cell spermatogonia using fluorescence *in situ* hybridization, Chromosome Res., 3, 1-6.

Buul, P.P.W. van and A. van Duijn-Goedhart (1995) Lack of sensitization effects on X-ray induced translocations in spermatogonial stem cells of *scid* mice, submitted for publication.

Head of project 3: Dr. Cattanach

II. Objectives for the reporting period

1. To complete a specific locus mutation study upon strain 101/H.

2. To reinvestigate translocation induction by X-rays in 101/H spermatogonia.

3. To complete a specific locus mutation study with compound chemical - X-ray treatments.

4. To complete the characterisation of deletions, duplications and other categories of chromosome changes deriving from the specific locus mutation studies.

5. To complete a collaborative study upon the basis of the heterogeneity in radiosensitivity of spermatogonial stem cells (with Drs de Rooij and van Buul).

6. To continue molecular genetic analyses of the *Mo* locus and feasibility studies upon pulse field gel electrophoresis as a mutation screening system.

III. Progress achieved including publications

1. The 101/H specific locus mutation study has been completed. The key finding was that whereas the 101/H response to a 24h fractionated 3 + 3 Gy X-ray regime was similar to that of the "standard" F1 hybrid mouse, a significantly higher response was obtained with a single 6 Gy dose (χ^2 = 8.52; P = 0.0036). The latter finding is in complete contrast to the previously observed lower response when translocation was the genetic end-point used (Cattanach and Rasberry 1994). The result is surprising, if not remarkable, but is not totally novel insofar as the translocation and specific locus mutation responses in hybrid mice do not always correlate well with different treatment regimes (the single dose-response curve, the responses to 24h and longer interval fractionation regimes). It would seem that the two classes of mutation derive differentially from different components of the spermatogonial stem cell population.

2.   The above conclusion is at least in part dependent upon
the   reliability   of   the   earlier   translocation   studies
(Cattanach   and   Rasberry   1994).   Insofar   as   the   radiation
treatments severely damage the stem cell populations of the
101/H strain and translocation scoring becomes problematic,
and   perhaps   modified,   under   such   conditions,   it   seemed
essential to verify this component of the work.

     The translocation response following single 1, 3, 5 and 7
Gy X-ray exposures has therefore now been sought using a
modified cytogenetic technique.   At all but the lowest dose
the 101/H translocation yields were lower than those from the
hybrid.   Overall, the mean difference was 0.320 ± 0.084 which
is highly significant (F(1,63) = 14.2; P = 0.00030).   Clearly,
the   earlier   translocation   data   are   substantiated;   the
contrasting translocation-specific locus mutation responses
therefore appear real.

3.   Large doses of hydroxyurea kill cells in the S phase of
the cell cycle (Oud *et al* 1979).   Several treatments are
therefore   expected   to   enrich   the   G1   component   of   the
population.   We have previously shown (Cattanach *et al* 1989)
that when 2 doses of 500 mg/kg HU are given at 3h apart prior
to 6 Gy X-irradiation the specific locus mutation response of
spermatogonial stem cells is greatly enhanced, suggesting that
G1 is the most sensitive phase of the cell cycle to this class
of   genetic   damage.   We   have   now   utilised   the   combined
treatment to investigate whether stem cells surviving 24h
after population depletion are synchronised in one phase of
the cell cycle as inferred from certain fractionated X-ray or
compound chemical - X-ray treatments with translocation as the
genetic end-point, or could still be heterogeneous in their
radio-sensitivity (see Cattanach *et al 1989*).

     The   results   are   shown   in   Table   1.   When   the   HU
pretreatment was given 24h after population depletion by TEM,
the 6 Gy cell killing and specific locus mutation responses
were greatly enhanced over the concurrent TEM + X-ray control.
This might suggest that a significant level of heterogeneity

Table 1

Treatment	Median day of return to fertility	No F1 progeny scored	Specific locus mutation frequency per locus/gamete
TEM + X-rays	109 days	7036	8.29×10^{-5}
TEM + HU + X-rays	138 days	6184	23.10×10^{-5}
3AB + X-ray 1	79 days	7798	20.15×10^{-5}
TEM + 3AB + X-rays	120.5 days	8784	35.77×10^{-5}

3AB = 3 aminobenzamide, 1 ml of a 0.1M solution ½h prior to X-rays; X-rays, 6 Gy dose; TEM = triethylenemelamine, 2 mg/kg 24h prior to X-rays; HU = hydroxyurea, 2 x 500 mg/kg 3h and 6h prior to X-rays.

remains 24h after population depletion. However, this conclusion may be questioned in view of the very low control TEM + X-rays mutation response (8.29×10^{-5}) relative to the much higher response of 30.20×10^{-5} obtained in a earlier study (Cattanach et al 1989). In view of this uncertainty both components of this study are being repeated.

Work by van Buul et al (1990) has shown that pre-treatment of mouse spermatogonial stem cells with 3 aminobenzamide (3AB) prior to irradiation enhances the translocation yield. We have now investigated whether the specific locus mutation response is similarly enhanced both in normal undamaged spermatogonia and in cell populations 24h after population depletion. In the normal populations the levels of cell killing indicated by median day of return to fertility were enhanced (79 days) relative to historical control levels (69 days; Cattanach et al 1989), and the specific locus mutation frequency (20.15×10^{-5}) was also enhanced relative to historical control levels of about 13.00×10^{-5} (Cattanach et al, 1989; Russell, 1964). The sensitised, depleted population however gave a yet higher response (30.77×10^{-5})which was clearly well above that of the concurrent TEM + X-rays control (8.29×10^{-5}, Table 1); the level of cell killing also appeared to be slightly increased. However, interpretation is again foiled by the unexpectedly low TEM + X-rays yield. Final interpretation will await the findings of the repeat study indicated above.

4. Up until recently cytogenetically large deletions and duplications have been rarely found or described. However, by screening for intrauterine growth retardation combined with phenotypic anomalies we have shown that such chromosomal changes can readily be detected. Primarily from the specific locus studies described above we have detected a further 63 large deletions which are compatible with survival to breeding age and establishment in stocks. Each of the deletions has been cytogenetically characterised, and the viability, fertility and phenotypic effects assessed. Eighteen stocks of mice carrying cytogenetically visible duplications have similarly been generated and studied, together with 6 paracentric inversions. The phenotypic effects have ranged from such minor subtle changes as darker coats and white feet through to craniofacial and other skeletal abnormalities, and presumed neurological defects that lead to head bobbing, tremours and waltzing. Translocations and dominant mutations at known and as yet undefined loci have also been detected and characterised.

Many of the deletion and duplication stocks are now being employed in genetic studies upon gene dosage and gene regulation in various laboratories. Notable examples are 1. a duplication of distal Chr 16 encompassing the region of homology with the segment of human Chr 21, the additional dose of which leads to Down's syndrome, 2. a presumed deletion which shows an imprinting inheritance and which has now been mapped to an imprinting region of the genome, and 3. deletions of a proximal region of Chr 3 which leads to oligospermy and sterility in males.

Table 2

Strain and or treatment	Anomalies detected					Estimated frequency (x10^{-4})		Specific locus mutation frequency/locus/gamete x10^{-5} (excluding s)
	Del	Dp	In	s	Total	Del only	Del + s Total	
101/H, X-rays	4	–	–	8	12	3.7	11.0	16.8
3H1, X-rays	3	3	–	4	10	1.5	3.6	6.9
TEM + X-rays	7	4	3	14		9.9	14.2	7.1
TEM + HU + X-rays	9^d	3	–	5^c	17	14.6	22.6^c	10.8
3AB + X-rays	6	3^a	1	6^c	16	7.7	15.4^c	8.6
TEM + 3AB + X-rays	13^d	6	2^b	5^c	26	14.8	20.5^c	30.4

Del, deletion; Dp, duplication; In, inversion; s, s mutation (deletion). 3AB, HU, X-ray and TEM treatments are as given for Table 1. a. one is an insertion. b. one is an inverted duplication. c. not studied cytogenetically but all s mutations so far studied have been shown to be deletions. d. including a cluster of 2.

A key observation most evident with the deletions is the non-randomness of their distribution throughout the genome. Thus, of the 63, 14 have involved distal Chr 14 and span the *s* locus, 8 have involved distal Chr 10 and span the *Sl* locus, 9 have involved central Chr 1 and represent a series of overlapping deletions, and 6 have involved proximal Chr 3 and give rise to male sterility. Clearly these regions of the genome are effectively haplo-sufficient. By contrast no deletions have been detected in Chrs 11, 12, 15 and 19, and in some chromosomes, eg Chr 2, only small localised deletions have been found.

The incidences of these chromosomal changes in the 101/H and compound chemical-X-ray specific locus studies are shown in Table 2 and compared with the specific locus mutation frequencies. The two frequencies correlated reasonably well, suggesting the mechanisms of induction may be similar, and different from those leading to translocation.

5. The Harwell component of the collaborative study with Drs de Rooij and van Buul have now been completed. The object has been to synchronise the spermatogonial stem cell populations throughout the testis by rearing male mice on a vitamin A deficient diet and then at a selected time identified by bodyweight loss, providing the missing vitamin to allow spermatogenesis to proceed. The mice were then X-irradiated at one of two specified times post vitamin A treatment when the stem cells were deduced to be synchronised to stages of their cell cycles previously shown to be resistant or sensitive to killing. After recovery of the stem cell populations the mice were killed and the translocation frequencies estimated. A total of 127 mice given X-ray doses ranging from 1 Gy to 8 Gy together with 5 unirradiated controls have been studied. 200 cells from each male have been examined for the presence of translocations, total about 25,500 cells. The results are currently being collated.

6. A comprehensive search for the molecular basis of mutations at the X-linked *Mo* locus (corresponding to Mencke's in humans) has been undertaken. Fifteen independent mutations have been studied, these arising from radiation and chemical mutation studies conducted at Harwell, Neuherberg and elsewhere. As deletions form approximately 20% of the mutation spectrum at the homologous human (Mencke's) locus, we were surprised to find that none of the mouse mutations comprised deletions. Also surprising was the finding that half of the mutations from radiation studies were associated with restriction fragment length variants inherited from the non-irradiated parent. They were thus spontaneous in origin and it is therefore possible that those associated with irradiated chromosome were also spontaneous.

A further significant finding was that all the male viable Mo mutations were associated with RT-PCR products of normal size but that 3 additionally produced aberrantly spliced, smaller transcripts. Sequence analysis has shown that these aberrant transcripts are unusual in that they are not associated with cryptic sites or with mutations at the

concensus splice junctions at the intervening exon-intron boundaries.

A search for radiation-induced lesions at a series of X-linked loci by pulsed field gel electrophoresis (PFGE) has been undertaken. Fifteen F1 female offspring from crosses between PT tester stock females and irradiated 3H1 males were analysed. To date, no genomic rearrangements have been detected. As no deletions have been found in the vicinity of three X-linked mutations (Td, Li, Bhd), in addition to Mo, that arose in radiation mutagenesis experiments, it is possible that the mouse X chromosome is unusually refractory to carrying deletions. It will be of interest to repeat these experiments in autosomal regions known to be capable of tolerating deletion and rearrangement.

Publications

Burtenshaw, M.D., Evans, E.P., Woodward, A-M., Vizor, L. and Cattanach, B.M. Six new radiation-induced deletions. Mouse Genome, 93:422-424 (1995).

Evans, E.P., Burtenshaw, M.D., Cattanach, B.M., Woodward, A-M. and Vizor, L. Four further radiation-induced duplications. Mouse Genome, 93:424-426 (1995).

Burtenshaw, M.D., Cattanach, B.M., Evans, E.P., Woodward, A-M. and Vizor, L. Further deletions deriving from spermatogonial X-irradiation. Mouse Genome, 92:349-350 (1994).

Cattanach, B.M., Evans, E.P., Rasberry, C., Wood, M. and Glenister, P.H. Rescue of a male sterile mutation by in vitro fertilisation. Mouse Genome, 90(1):87-89 (1992).

Cattanach, B.M., Burtenshaw, M.D., Rasberry, C. and Evans, E.P. Large deletions and other gross forms of chromosome imbalance compatible with viability and fertility in the mouse. Nature Genetics, 3:56-61 (1993).

Cattanach, B.M., Rasberry, C., Burtenshaw, M. and Evans, E.P. A further mutation at the splotch locus. Mouse Genome 91(1):115-116 (1993).

Cattanach, B.M. and Rasberry, C. New mutations at the tabby locus. Mouse Genome 91(1):116 (1993).

Cattanach, B.M., Evans, E.P., Burtenshaw, M.D., Glenister, P.H., Vizor, L. and Woodward, A.-M. Radiation-induced deletions. Mouse Genome 91(4):853-854 (1993).

Cattanach, B.M. and Evans, E.P. Radiation-induced large deletions and other gross forms of chromosome imbalance in the mouse. In radiation protection: Molecular mechanisms in radiation mutagenesis and carcinogenesis. Eds. K H Chadwick, R Cox, H P Leenhouts and J Thacker. European Comm. pp. 93-100 (1994).

Cattanach, B.M., Evans, E.P., Burtenshaw, M.D., Rasberry, C., Woodward, A-M. and Vizor, L. Further radiation-induced deletions. Mouse Genome, 92:111-113 (1994).

Cattanach, B.M., Beechey, C., Rasberry, C. and Evans, E.P. Two further *Sp* mutations. Mouse Genome, 92:503-504 (1994).

Cattanach, B.M., Clements, S. and Evans, E.P. Two new chromosomal insertions. Mouse Genome 93 in press (1995).

Cattanach, B.M., Clements, S., Woodward, A-M. and Evans, E.P. Three further cytologically visible duplications. Mouse Genome, 93 in press (1995).

Evans, E.P., Burtenshaw, M.D., Cattanach, B.M., Vizor, L. and Woodward, A-M. Cytogenetic detection of visible duplication. Mouse Genome, 92:113-114 (1994).

Evans, E.P., Vizor, L., Woodward, A.-M., Rasberry, C. and Cattanach, B.M. Further detection of cytologically visible chromosome duplications. Mouse Genome 93:147-148 (1995).

Evans, E.P., Burtenshaw, M., Woodward, A-M., Vizor, L. and Cattanach, B.M. Eight further large chromosome deletions. Mouse Genome 93 in press (1995).

George, A.M., Reed, V., Chelly, J., Monaco, A.P., Tumer, Z., Horn, N. and Boyd, Y. Analysis of *Mnk*, the murine homologue of the locus for Menkes' disease in normal and mottled mice. Genomics 22:25-37 (1994).

Rasberry, C. and Cattanach, B.M. Three new mottled mutations. Mouse Genome 91(4):851-853 (1993).

Rasberry, C. and Cattanach, B.M. A new mutation at the *Ph* locus. Mouse Genome, 92:504-505 (1994).

Reed, V., George, A.M., Rasberry, C., Cattanach, B.M., Lyon, M.F. and Boyd, Y. Molecular analysis of a series of mutations at the mottled locus. Mouse Genome, 91:331-333 (1993).

Reed, V. and Boyd, Y. Mutations in mottled dappled are RFLVs. Nature Genetics 8:11-12 (1994).

Head of project 4: Dr. D.G. de Rooij

II. Objectives for the reporting period
1. Estimation of the numbers of spermatogonial stem cells per testis, resistant or sensitive to cell killing by radiation.
2. Comparison between the sensitivity of stem cells for the induction of reciprocal translocations, in stem cells resistant and stem cells sensitive towards cell killing by irradiation.
3. Determination of the sensitivity of stem cells for cell killing by a second dose of X-rays, 24 and 96 hr after the first dose.
4. Evaluation of the model of Leenhouts and Chadwick for the induction of reciprocal translocations and point mutations by irradiation.

III. Progress achieved including publications
1. Estimation of the numbers of spermatogonial stem cells per testis, resistant or sensitive to cell killing by radiation.
     As reported before, a first estimation of the numbers sensitive and resistant stem cells was done from the results of a dose-response experiment for X-rays and from the results of cell counts of spermatogonia throughout the epithelial cycle. From these results it was estimated that the numbers of resistant and sensitive stem cells are about similar (publications 1-3).
     To confirm this conclusion, the dose-response relationship for cell killing by 1 MeV fission neutron irradiation of mouse spermatogonial stem cells in various stages of the epithelial cycle has been studied. As reported before, it was found that the stem cells are most sensitive in stages VII and VIII when they are quiescent, showing a D_0 value of 0.27 Gy, and resistant in stages XII-VI showing a D_0 of on the average 0.60 Gy (Table 1). From the dose-response curves the extrapolation numbers on the Y-axis could be determined as no shoulder can be expected after fission neutron irradiation because of the lack of repair (Table 1). These extrapolation numbers represent the numbers of spermatogonia produced in 10 days by the spermatogonial stem cells after a dose of 0 Gy.
     The next step was to determine the size of the repopulating colonies in numbers of cells, 10 days after irradiation, formed by the surviving stem cells. In principle, division of the extrapolation numbers by the average number of cells per colony should render the number of stem cells present in a certain epithelial stage characterized by the D_0 value found in that stage.
MATERIALS AND METHODS: In an experiment in cooperation with Dr. R. Huiskamp (ECN, Petten) 3H1 hybrid mice received a dose of 1.5 Gy of 1 MeV fission neutrons. These were the same mice as used in the dose-response experiment. Ten days after irradiation the mice were killed, and the seminiferous tubules were processed to obtain tubular whole-mount preparations. The epithelium was scanned for spermatogonia, and 10 colonies per animal per stage or group of stages were studied. Six areas were defined on basis of the stages of the cycle of the seminiferous epithelium: stage XI (IX during irradiation, IX_{irr}), stage XII (X_{irr}), stage I (XI_{irr}), stages I-VI ($XII-III_{irr}$), stage VII-early IX (V-early VII_{irr}), and stage IX-X (stage late VII-early IX_{irr}). A distance criterion was used to distinguish separate colonies, based on previous work on

CPB-N mice. When a colony extended over several stages, the colony was considered to have its origin in, and thus belong to, the stage of the geographical midpoint.

RESULTS: The raw data indicated that the colony sizes, in number of spermatogonia, varied between 2 and 336 cells (Table 1). Mean size was 60 cells, with a median value of 47 cells per colony. Colony size varied with the stage of the epithelium, with colonies in areas $IX-XI_{irr}$ containing the most cells. Colonies in stages V-early VII_{irr} were the smallest, while colonies in both stages $XII-III_{irr}$ and late VII-early IX_{irr} had intermediate number of cells.

In CPB-N mice it was demonstrated that a large variation in colony sizes indicates the occurrence of spontaneous degeneration of cells in the colonies. Disregarding spontaneous degeneration, the maximum colony sizes indicate that 8.4 divisions had taken place during the 10 days post-irradiation, indicating a cell-cycle duration of about 28 hours. Taking spontaneous degeneration into account, estimates for the duration of the cell cycle vary between 20-30 hours. However, the cell cycle duration of the differentiating spermatogonia, which is generally shorter than that of the undifferentiated spermatogonia, is 29 hours. This makes it unlikely that the longer colonies have arisen from one stem cell. Therefore, we investigated the possibility that confluency between individual repopulating colonies had occurred. The frequency distribution of the colony sizes showed several peaks, up to colony sizes of over 200 cells. This is suggestive of confluency, and several theoretical studies were carried out, simulating colony growth and confluency. The colonies in area V-early VII_{irr} were the smallest, and thus are the most likely to be undisturbed by confluency. The data obtained on these colonies were in good agreement with data obtained previously on colonies in the CPB-N mouse: 27 ± 21 cells per colony in the 3H1 mouse in areas V-early VII_{irr}, 10 days after 1,5 Gy, and 28.5 ± 16 cells per colony in the CPB-N mouse in areas $IV-VII_{irr}$, 10 days after 0.75 Gy.

Table 1. Preliminary results of the determination of the numbers of spermatogonial stem cells in various stages of the cycle of the seminiferous epithelium with a specific radiosensitivity.

Epithelial stages at irradiation	Average colony size ± SEM	Range	N_0	D_0	Corrected number of stem cells with D_0	number of stem cells present
XI	85±32	6–258	268	0.67	10.5	9.6±0.4
XII–III	50±14	3–203	345	0.57	13.7	10.5±0.4
V–VII	27± 9	2– 91	257	0.47	10.6	14.4±0.7
VIII	44±23	2–137	283	0.27	10.7	13.0±0.6
IX	77±22	7–336	249	0.49	10.7	13.0±0.6
X	68±13	3–294	295	0.54	14.5	(11.3)

Based on the similarity between colonies in 3H1 and CPB-N mice in areas $IV-VII_{irr}$, we decided to model colony growth based on the characteristics determined for CPB-N mice. The number of divisions was set at 8 to 9, with each cell in each generation

having a 25% probability of spontaneous degeneration. In the biological material, only groups of 2 or more cells were considered to be colonies. A computer program was written to generate 1000 colonies according to these values. To simulate an x% confluency rate over 1000 colonies, x*10 random numbers were generated between 1 and 1000. A number y indicated that colony y confluenced with colony (y+1). Confluency rates were simulated from 5 to 100% per 5%. The resulting, simulated data were in good agreement with the actual data, but should be considered preliminary. The simulations upto now were partly based on results obtained in CPB-N mice. We would like to consider the effects of differences in stem cell kinetics between 3H1 and CPB-N mice before presenting final estimates of confluency.

CONCLUSIONS: Data obtained from a dose-response experiment with X-irradiation and from cell counts, indicate the number of radioresistant stem cells to be about similar to the number of sensitive stem cells. Detailed data from a dose-response experiment with fission neutron irradiation and from studying colony size at 10 days after irradiation will now be used to confirm this estimate. At the moment the data gathered, are further processed to ultimately render an estimation of the numbers of radioresistant and radiosensitive stem cells per testis.

2. Comparison between the sensitivity of stem cells for the induction of reciprocal translocations, in stem cells resistant and stem cells sensitive towards cell killing by irradiation.

The goal of this experiment was to test the assumption of Leenhouts and Chadwick, that radiosensitive stem cells have a high linear translocation-induction rate, and that radioresistant stem cells have a low linear translocation-induction rate. This experiment was done in a close cooperation between the groups in Utrecht (M.E.A.B. van Beek, Y. van der Meer, R.A.J. Tegelenbosch, D.G. de Rooij), Harwell (E.P. Evans, M. Burtenshaw, B.M. Cattanach) and Leiden (P.P.W. van Buul).

MATERIALS AND METHODS: The seminiferous epithelium of 3H1 was synchronized using the vitamin A-depletion and -repletion protocol. It was estimated that at respectively 40 and 45 days after repletion with vitamin A, the testes would be synchronized in stages VIII-X (45 days) or stages I-IV (40 days). This was confirmed prior to the experiment using some 'pilot' mice, and also concomitantly with the main experiment. Since spermatogonial stem cells in stages VIII-X have a D_0 value for X-rays, of 1.4 Gy, and in stages I-IV a D_0 value of 2.6 Gy, irradiation at 45 days after repletion with vitamin A would be aimed at a population of radiosensitive stem cells, while irradiation at 40 days after repletion with vitamin A would be aimed at a population with radioresistant stem cells. Measuring the length of the time-interval between irradiation and return of fertility gave us an indication whether the spermatogonial stem cell population in each individual mouse was indeed more 'sensitive' or 'resistant'.

RESULTS: The 3H1 mice appeared to be relatively resistant to the induction of vitamin A deficiency. This caused unexpected problems, which were solved in an intense contact between the Harwell and the Utrecht group. In spite of this problem, 2/3 to 3/4 of the mice showed a satisfactory synchronization of the seminiferous epithelium to a restricted number of stages (Table

Table 2. Degree of synchronization achieved in the seminiferous epithelium of 3H1 mice, subjected to the vitamin A-depletion and -repletion protocol

Mouse	days after vitamin A repletion	% of tubules showing restored spermatogenesis	part of cycle enriched	synchronization factor
M808	37	100	VIII-X	2.7
M809	37	100	IV-VIII	2.0
M815	37	100	VII-X	1.9
M839	40	100	XII-III	2.3
M840	40	100		1.0
M841	40	100	XII-VI	1.4
M811	42	100	III-VII	2.0
M812	42	90	II-VI	2.9
M813	42	99	IV-VIII	1.7
M825	45	70	VIII-IX	3.9
M826	45	85	VIII-X	2.6
M827	45	100		1.0
M845	45	100	VI-IX	1.9
M846	45	100	VIII-X	2.2
M847	45	100		1.0
M886	109	100	VIII-I	1.2
M887	109	100	VIII-I	1.2
M888	109	100	VII-I	1.1

2). The mice M886-888 were irradiated at day 40 (4Gy) but despite the long interval and the irradiation still some remnants of the synchronization were present.

The synchronization of the seminiferous epithelium was also reflected in the time interval between irradiation and return of fertility. In respectively, the 'sensitive' and 'resistant' groups this interval was 88 and 109 days after 6 Gy, and 164 and 229 days after 8 Gy. After 1 and 2 Gy no difference was observed, and after a dose of 4 Gy this interval was slightly shorter in the sensitive group compared to the resistant one (70 vs. 78 days).

However, the percentages of spermatocytes observed with multivalents was indistinguishable between the 2 groups (Figure 1A). When it was assumed that only 1 out of 4 mice were optimally synchronized, and we selected per dose in each group, the mice with the shortest ('resistant' group) or longest ('sensitive' group) interval to return to fertility after irradiation, still no difference at all was observed (Figure 1B). When we selected per dose in each group the mice with the lowest ('resistant' group) or highest ('sensitive' group) translocation induction rates we do see differences in induction rates, but in both groups we still see a 'hump' in the curve. However, different induction rates should explain the humped curve, and this hump should not appear when irradiating populations consisting of only sensitive or resistant stem cells.

Translocation Induction in Spermatogonial Stem Cells of 3H1 Mice Synchronized in Different Stages of the Seminiferous Epithelium
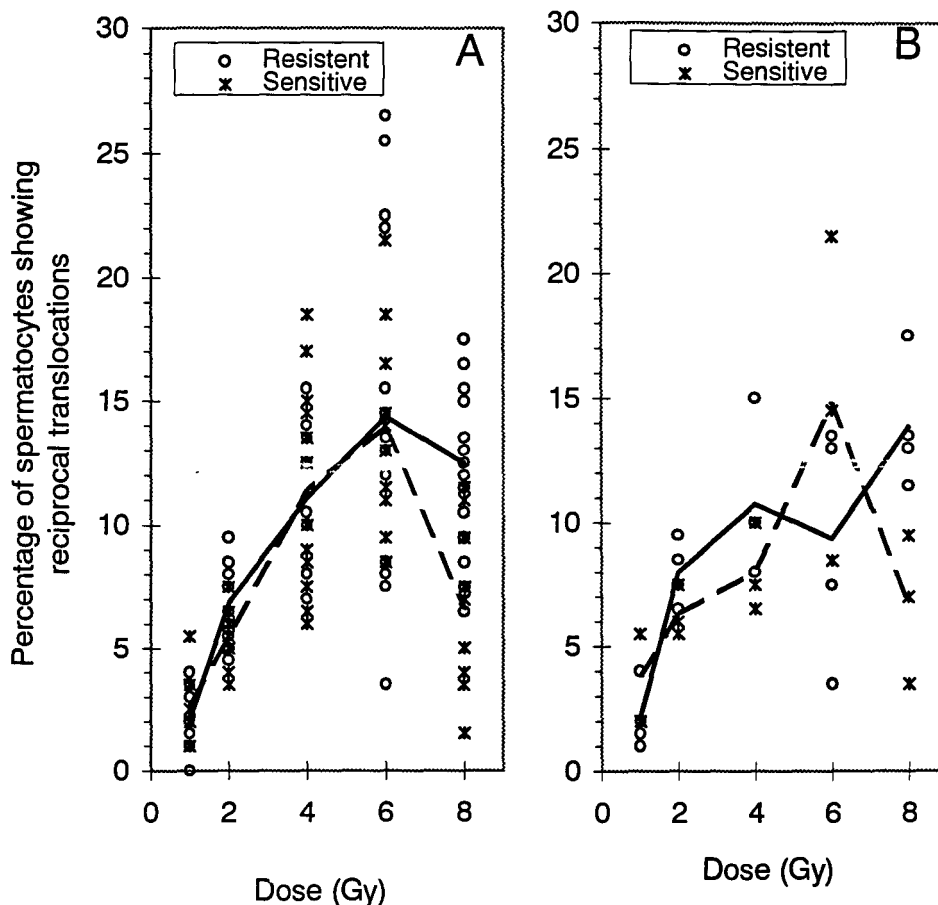
Figure 1: Translocation induction in spermatogonial stem cells in testes, synchronized by vitamin A-depletion and -repletion, of 3H1 hybrid mice.
A: all data per mouse are given. **Circles** : mice irradiated at 40 days after repletion with vitamin A, while the **solid line**connects the average values in this group, where the spermatogonial stem cells were radioresistant during irradiation. **Asterix:** mice irradiated at 45 days after repletion with vitamin A, while the **dashed** line connects the average values in this group, where the spermatogonial stem cells were radiosensitive during irradiation.
B: (Symbols as in A): Mice were selected according to a **short**interval between irradiation and return to fertility (resistant group), or a **long**interval (sensitive mice). Mean intervals for mice used in plot B (resistant, sensitive): after 1 Gy 43, 53.5 days.; after 2 Gy: 43.3, 59.3 days; after 4 Gy: 60.8, 87.3 days; after 6 Gy: 64.5, 166.7 days; after 8 Gy: 86.3, >365 days.

CONCLUSIONS: We conclude that this experiment failed to substantiate the assumptions of Leenhouts and Chadwick that radiosensitive stem cells have a high linear translocation-induction rate, and that radioresistant stem cells have a low linear translocation-induction rate. At the moment we are studying the data further to elaborate an alternative explanation for the occurrence of the 'hump' in the translocation induction curves vs. dose. A paper describing the experiment, results, and consequences is in preparation.

3. Determination of the sensitivity of stem cells for cell killing by a second dose of X-rays 24 and 96 hr after the first dose.

The pattern of mutation induction by split irradiation doses differs depending on the interval between the 2 doses. Since it is generally assumed that the radiosensitivity of a cell is an important factor determining its sensitivity to mutation induction, it was decided to measure the radiosensitivity of spermatogonial stem cells in different stages of the seminiferous epithelium at both 1 and 4 days after a first dose of 1 Gy of X-radiation. Sofar, only the 4 day interval experiment has been completed.

MATERIALS AND METHODS: 3H1 hybrid mice were given a dose of 1 Gy of X-rays. For the 4 day interval, after 4 days they were irradiated with graded doses of X-rays between 0.5 and 6 Gy of X-rays. On day 11 after the first irradiation, day 7 after the second dose, the mice were sacrificed and cross-sections of their testes were prepared. In these cross sections the stage, number of Sertoli cell nucleoli, and number of spermatogonia were recorded until a minimum of at least 250 tubules, containing at least 75 (60 of which were clearly in good condition) undifferentiated spermatogonia in at least 50 (40 of which contained spermatogonia in clearly good condition) different tubules. Numbers of spermatogonia were expressed per 1000 Sertoli cells. Stage II and IV, V and VI, and X and XI were summed together before analysis.

RESULTS: Similar to after an acute dose of radiation, variations were observed in the radiosensitivity of the spermatogonial stem cells, but to a lesser degree. While the lowest D_0 value found was comparable to the lowest D_0 during acute radiation, the highest D_0 value at 4 days after a first irradiation was medium compared to the D_0 values found at acute irradiation.

The D_0 values at 4 days varied with the stage of the seminiferous epithelium during the (second) irradiation in a similar manner as during the first irradiation: the radioresistance of the spermatogonial stem cells at the second irradiation is determined by the stage at the second irradiation, while the stage (and concomitant radiosensitivity) during the first irradiation did not seem to influence the radiosensitivity at 4 days after this first irradiation (Table 3).

The extrapolation number of the dose-response curves made 4 days after a first irradiation reflects the number of spermatogonial stem cells present at 4 days after a first irradiation. If, after the first irradiation, the regeneration parameters are the same in all stages, then these extrapolation numbers should reflect the number of stem cells that survived the first irradiation. A relatively high extrapolation number was found in areas where the stem cells were sensitive, or newly

radioresistant, while the extrapolation number was relatively low in areas where the stem cells had been radioresistant for a longer time. These data indicate that the regeneration parameters are not identical in all stages. The study of the colony formation should shed light on this phenomenon. However, it is interesting that in a previous study in CPB-N mice cells in colonies that derived from sensitive stem cells and from newly radioresistant stem cells, seemed to be less prone to spontaneous degeneration than cells in colonies derived from stem cells that had been radioresistant for a longer time, and that, in the CPB-N mouse, showed an intermediate D_0 value.

Table 3. Radiosensitivity of spermatogonial stem cells in various epithelial stages of 3H1 mice for acute X-irradiation and for fractionated irradiation, 4 days after a dose of 1 Gy of X-irradiation.

Stage at first dose	acute D_0 in stage	Stage at day 4	acute D_0 in stage	D_0 second irradiation at day 4
early I	2.5	VII	2.4	1.8 (1.6-2.0)
middle I		late VII	1.4	
late I-middle II	2.7	late VII-VIII		1.7 (1.5-1.9)
late II	2.4	late VIII	1.4	1.4 (1.3-1.7)
III	2.7	early IX		
early IV		middle IX	1.6	
late IV	2.7	late IX		
early V		early X		1.5 (1.3-1.7)
V-early VI		middle X	1.8	
late VI	2.4	XI	2.5	2.1 (1.6-2.6)
early VII		late XI-early XII		2.0 (1.8-2.4)
middle VII	1.4	middle XII	2.7	
early VIII		I	2.5	
late VIII	1.4	late I	2.8	
early IX		middle II		2.3 (2.0-2.6)
middle IX	1.6	late II	2.4	
late IX		III	2.7	
late IX-early X		late III		1.7 (1.6-1.8)
middle X-early XII	.8	IV		
early XI	2.5	V		
middle XI		VI		1.9 (1.7-2.2)
late XI-early XII		late VI	2.4	1.8 (1.6-2.0)
XII	2.7	VII		

CONCLUSIONS: The radiobiological characteristics of the spermatogonial stem cells at 4 days after a first irradiation with 1 Gy are in line with what could be expected based on a (rather) regular progress of the cycle of the seminiferous epithelium. It is expected that the interpretation of these results, especially the extrapolation numbers, can be more detailed when the study of the colony-formation (after fission neutron irradiation) has been completed. The results will be presented at the 10th ICRR in August 1995, in Würzburg, Germany (publ. 5)

4. Evaluation of the model of Leenhouts and Chadwick for the induction of reciprocal translocations and point mutations by irradiation.

The model of Leenhouts and Chadwick for the induction of reciprocal translocations and point mutations by irradiation, included the following assumptions:
1. In the normal mouse testis, there are many more sensitive than resistant stem cells for the cell killing effect of irradiation.
2. Radiosensitive stem cells have a high linear translocation-induction rate.
3. Radioresistant stem cells have a low linear translocation-induction rate.

In the dose-response experiment for cell killing by X-irradiation it was found that in 3H1 mice the spermatogonial stem cells were most sensitive in stage VIII where these cells are quiescent, showing a D_0 value of 1.4 Gy. The stem cells were most resistant in stages XI-V, when these cells are proliferating, showing a D_0 value of 2.6 Gy. Based on the D_0 values for sensitive and resistant stem cells and on the D_0 for the total population, a ratio of 45:55% of sensitive to resistant spermatogonial stem cells was estimated for cell killing. Cell counts of spermatogonia throughout the epithelial cycle indicated that the stem cells are actively dividing during half of the cycle. In view of the difference in radiosensitivity between quiescent and proliferating stem cells these data too, indicate that there are about as many sensitive as resistant stem cells. This notion will be substantiated by the results of the fission neutron experiment, the results will have to studied in further detail.

Anyhow, these data indicate that the first assumption mentioned above is not correct. A first attempt was made to improve the model by incorporating the new data on the ratio of resistant to sensitive cells and using various values for the translocation yield in sensitive and resistant stem cells. A good fit with the experimental data was found when the translocation yield (Y; in % abnormal cells) after a radiation dose D was described by $Y=e^{\tau D}$ with $\tau=1$ for the sensitive and $\tau=0.1$ for the resistant spermatogonial stem cells, with a maximal $e^{\tau D}$ of 100.

Unfortunately, as described above, the synchronization experiment did not reveal any confirmation of assumptions 2 and 3. The data will now be analyzed in further detail and an attempt will be made to develop an alternative model for the induction of reciprocal translocations and point mutations by irradiation.

CONCLUSIONS: The data obtained during this project do not confirm the validity of three important assumptions made in the model of Leenhouts and Chadwick for the induction of reciprocal translocations and point mutations by irradiation. An alternative model will be developed.

Publications
1. Van der Meer, Y. , Tegelenbosch, R.A.J., Cattanach, B.M., De Rooij, D.G. 1992. Proliferative activity and radiosensitivity of spermatogonial stem cells in C3H/101 F1 hybrid mice. Int. J. Radiat. Biol. 62, 361. Abstract.
2. Tegelenbosch, R.A.J., De Rooij, D.G. 1993. Quantitative study of spermatogonial kinetics in the C3H/101 F1 hybrid mouse. Mutation Res. 290, 193-200.

3. Van der Meer, Y., Cattanach, B.M., De Rooij, D.G. 1993. The radiosensitivity of spermatogonial stem cells in C3H/101 F1 hybrid mice. Mutation Res. 290, 201-210.
4. Tegelenbosch, R.A.J., Huiskamp, R., De Rooij, D.G. 1994. The effect of fast fission neutron irradiation on spermatogonial stem cells in C3H/101 F1 hybrid mice; a dose-response study. Joint meeting European Soc. Radiat. Biol. and European Soc. Hyperthermic Oncol., June 1994. Program Book Abstract nr. P116.
5. Van Beek, M.E.A.B. van, Cattanach, B.M., De Rooij, D.G. 1995. Radiosensitivity of spermatogonial stem cells at 1 and 4 days after 1 Gy of X-rays. Abstract Book Xth International Congress of Radiation Research, Würzburg.

4 articles are in preparation

Head of project 5: Dra. Miró Ametller

II. Objectives for the reporting period

The aim our project was the development of a method to assess radiation-induced chromosomal damage in human spermatozoa by the scoring of micronuclei in human-hamster embryos at the two-cell stage.

The specific objectives for the development of our project for this 3 year-period have been:

(1) The establishement of the technique to analyze micronuclei in two-cell human-hamster embryos and the establishement of criteria to score micronuclei.

(2) To acertain the human or hamster origin of micronuclei by FISH procedures using total human or hamster denatured DNA as probes.

(3) The establishement of a dose-effect curve for radiation-induced micronuclei.

(4) To evaluate whether scoring of micronuclei is useful for the quantification of chromosomal damage occurring in spermatozoa by comparing radiation induced human micronuclei with the induction of breaks and fragments in sperm derived chromosomes.

(5) To analyze in detail the chromosomal content of γ-rays induced micronuclei by FISH procedures using human centromeric and telomeric DNA probes.

III. Progress achieved including publications

1. **Establishment of the technique and criteria to score micronuclei.**
   The micronucleus assay can be incorporated to the human-hamster fertilization system as a test to assess radiation-induced chromosomal damage in human spermatozoa. This assay system has been established in our laboratory by culture of zona-free hamster eggs, fertilized by human spermatozoa, until the two-cell stage. Micronuclei are scored in human-hamster embryos at the two-cell-stage whenever blastomere nuclei, and eventually micronuclei are visualized under a phase-contrast microscope.

   For micronucleus assessment, only monospermic eggs can be taken into account, in order not to overestimate the frequency of micronuclei if polispermic eggs were analyzed. To eliminate unfertilized and polyspermic eggs, only those fertilized eggs with a second polar body and two pronuclei were chosen under an inverted microscope with Nomarski's interferential contrast (x250). Monospermic eggs were cultured in a 5% CO_2 incubator at 37ºC until they divided (approximately 20h after insemination).

In human-hamster hybrids at the two-cell stage, micronuclei appear as spherical bodies similar to, but smaller than, the main nucleus of the blastomere. In preliminary tests we established some criteria for the scoring of micronuclei: (a) Micronuclei are scored at the two-cell stage only when the main nucleus of each blastomere can be visualized, (b) the second polar body is so small that it may be mistaken for a micronucleus when the polar body overlays the blastomere; thus, to avoid confusion, only those fertilized eggs at the two-cell stage where the second polar body is visible are considered for the scoring of micronuclei, and (c) Micronuclei should not be linked to the main nucleus by any nucleoplasmic bridge.

2. Origin of micronuclei

The micronucleus assay has recently been used to investigate the induction of micronuclei in human-hamster two-cell embryos after in vitro fertilization of intact oocytes by γ-irradiated human spermatozoa (Kamiguchi et al. 1991 Mutat. Res. 252: 297-303). However, nobody had demostrated if micronuclei arising in 2-cell human-hamster embryos were of human or hamster origin. So, we incorporated FISH techniques with total human and hasmter DNA probes to our interspecific in vitro fertilization system, to determine whether micronuclei present in two-cell hybrids were of human origin.

Prior to hybridization of human or hamster genomic DNAs with embryo nuclei and micronuclei, slides containing separated first cleavage metaphases of human and hamster origin were used to discard cross-hybridization of the probes, demostrating that there is no more homology between human and hamster DNA than the overall interspecies homology neutralized by routine prehybridization with herring sperm DNA.

A total of 181 two-cell embryos obtained after fertilization of hamster eggs by human spermatozoa irradiated at 4Gy of γ-rays were subjected to FISH methodologies using denatured human or hamster genomic DNA as probes. With total human DNA, we analyzed 97 two-cell embryos. A total of 107 micronuclei were scored in these embryos (110.3%) (Table I). Using the FISH techniques with the human probe, we found that all but one of the 107 micronuclei analyzed (99.1%) showed the yellow dots of fluorescein. Thus, in situ hybridization of micronuclei with total human DNA revealed their human origin.

However, hybridization with only human DNA cannot exclude the possibility that micronuclei contain hamster DNA in addition to human DNA. Taking this into consideration, we also perfomed in situ hybridization with total hamster DNA. Using this probe, we analyzed 84 two-cell embryos. A total of 42 micronuclei were found in these embryos (50%) (Table I), and only one of them (2.3%) hybridized with the hamster probe, revealing the single human origin of most micronuclei (97.7%). These results are consistent with the low frequency of structural chromosome abnormalities (0,5-1,4%) found in hamster oocytes (Martin, 1984. Biol. Reprod. 31: 819-825).

Table I. Origin of micronuclei (Mn)

	Number of two-cell embryos analyzed	Total number of Mn	Number of Mn of human origin	% of Mn of human origin
FISH with **Human** genomic DNA	97	107	106	99.1%
FISH with **Hamster** genomic DNA	84	42	41	97.7%

Using the hamster DNA probe, the observed incidence of micronuclei per embryo was much lower than that found when hybridization was perfomed with human DNA (0,5 vs 1.1). This difference is probably due to the absence of fluorescent signal in micronuclei of human origin when hamster DNA is applied, which makes them undetectable even with DAPI staining. This results in an underestimation of the number of micronuclei of human origin. Thus, the margin of error to take into consideration must be very low, leading to the conclusion that the micronucleus test represents a good method to evaluate the genetic damage caused in human sperm not only by ionizing radiations but also by chemical mutagens.

3. Radiation induction of micronuclei: dose-effect relationship.

The efficiency of the micronucleus test to assess radiation induced chromosomal damage in human spermatozoa has been investigated. Micronuclei were scored in two cell human-hamster embryos, after exposure of human spermatozoa to 0, 0.10, 0.25, 0.50, 1.00, 2.00 and 4.00 Gy of γ-rays.

We have scored micronuclei of 101 two-cell embryos of one sperm donor at 0 Gy and a total of 598 two-cell embryos at different irradiation doses. The final data of the dose-response for the induction of micronuclei by exposition of human spermatozoa to gamma-rays are shown in table II. Two-cell embryos with 1 to 5 micronuclei were observed. However, 73.6% of micronucleated embryos had only one micronucleus.

Table II.   Micronucleus induction in two cell embryos after gamma-irradiation of human spermatozoa.

Dose (Gy)	Number of embryos examined	Number of micronuclei	Micronuclei per embryo	Embryos with micronuclei (%)
0.00	101	8	0.08	6.9
0.10	115	10	0.09	6.9
0.25	124	13	0.10	8.9
0.50	69	12	0.17	13.0
1.00	76	19	0.25	19:7
2.00	142	59	0.41	24.6
4.00	72	52	0.72	52.8

The dose-effect relationship for the frequency of micronuclei at the two-cell stage was statistically compatible with a linear fit [1], with Y as the mean number of micronuclei per two-cell embryo and D as the radiaton dose in Gy (p<0.0001; r^2= 0.994). In order to take overdispersion into account, each observation was weighted by the reciprocal sample mean variance (N/α 2) (Huber et al, 1994. Mutat. Res. 306: 135-141)

[1] Y= 0.07393 (± 0.004522) + 0.1661 (± 0.005406) D

When we attempted to fit the same data (frequency of micronuclei per two-cell embryo at the different doses) to a linear quadratic model, a small but negative β coefficient was obtained. The negative value of β could reflect a saturation effect that was only evident at the highest dose (4Gy). This saturation effect is probably due that at higher doses more than one aberration will be involved in a single micronucleus.

The dose-effect curve for the proportion of micronucleated embryos fitted to a linear equation [2]

[2] Y= 6.674 (± 1.1107) + 11.126 (± 0.6366) D

Equation [1] was obtained by means of the weighted least squares approximation and using the GLIM program (Baker and Nelder, 1985). For equation [2] a linear regression was performed. A representation of equations [1] and [2] is shown in figures 1 and 2.

Figure 1

Dose-effect curve for the production of micronuclei (mn) by gamma-irradiation of human spermatozoa

Figure 2

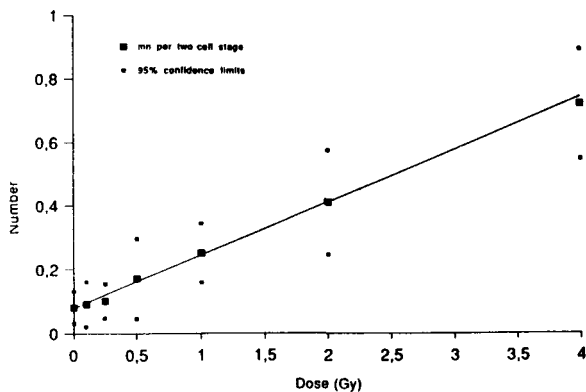Dose-effect curve for the percentage of two-cell stages with micronuclei (mn)
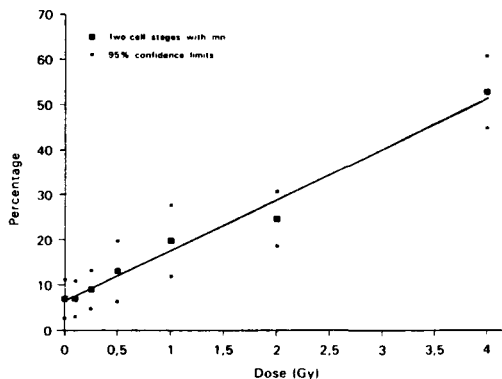
4. Comparison between micronuclei and chromosome analysis.

To evaluate whether scoring of micronuclei is useful for the quantification of chromosomal damage occurring in human spermatozoa, induced micronuclei at the different doses of sperm irradiation were compared to the induction of breaks and fragments in sperm derived chromosomes.

Chromosomal aberrations were scored by identifying chromosomal and chromatid breaks and acentric fragments, because among chromosome aberrations, symetric exchanges with complete repair are not the source of lagging chromosome segments. and do not contribute to the formation of micronuclei.

The number of micronuclei per embryo induced at different doses were modified according to the results found by FISH (objective 2) where 1.11 micronuclei in 100 two-cell embryos examined were found to be of hamster origin. So, taking into account this consideration, the number of micronuclei per embryo induced by different doses of gamma rays is shown in table III.

Table III. Comparison between micronuclei and chromosome aberrations.

Dose (Gy)	Two-cell stages with micronuclei (%)	Sperm complements with breaks and fragments (%)	Micronuclei per two-cell stage (corrected)	Breaks and fragments per sperm complement
0.00	6.9	5.5	0.07	0.07
0.25	8.9	6.7	0.09	0.07
0.50	13.0	11.0	0.16	0.12
1.00	19.7	21.7	0.24	0.25
2.00	24.6	39.5	0.40	0.45
4.00	52.8	58.6	0.71	0.81

As shown in table III, the percentages of micronucleated embryos were similar to those of sperm derived chromosome complements with breaks and fragments at the different doses (Rho=1, Spearman coefficient) (figure 3). A similar correlation was also found between the number of micronuclei per embryo and the number of breaks and fragments per spermatozoon (Rho= 0.986, Spearman coefficient) (figure 4).

Figure 3.   Figure 4.

Dose-response relationship of the percentage of two-cell stages with micronuclei (mn) and sperm complements with breaks and fragments (br/fra)
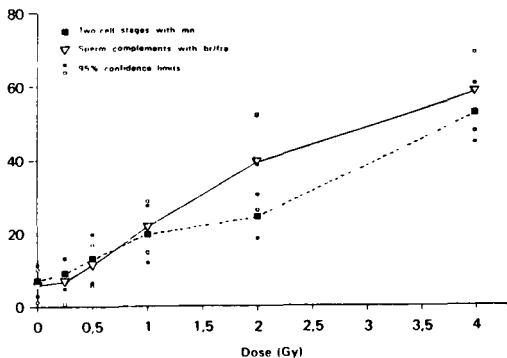
Dose-response relationship of the number of micronuclei (mn) per two-cell stage and the number of breaks and fragments (br/fra) per sperm complement

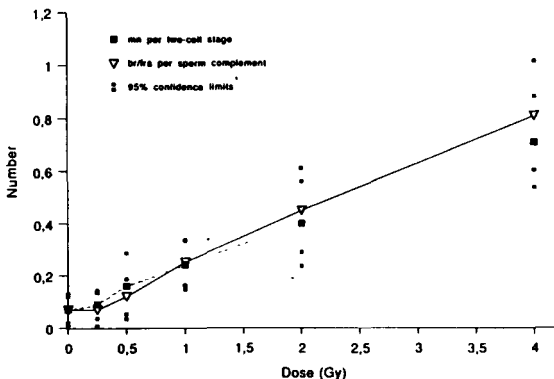It should be noted that at low dose ranges (0 - 0.5 Gy) the incidence of micronuclei was slightly higher than that of breaks and fragments (figures 3 and 4). Such differences, even though small, could be due to semistable aberrations such as dicentric chromosomes or to mitotic dysfunction such as chromosome lagging, that could give rise to micronuclei. Inversely, at high doses of gamma rays the yield of breaks and fragments was higher than the incidence of micronuclei. This different type of dose-dependent response is not surprising since at higher doses more than one aberration can be involved in a single micronucleus.

In conclusion, micronuclei induction coincide well with the induction of breaks and fragments, providing evidence that the micronucleus test is useful for the quantification of chromosomal damage in human spermatozoa. Our in vitro data can contribute to assess the genetic risks of in vivo exposure, and can be used for human biomonitoring in the case of occupational or accidental exposure to gamma rays.

5. Characterization of micronuclei

Ionizing radiation is thought to cause micronuclei mainly through the production of acentric fragments. Hoewever, it has been shown that it also induce centromere-containing micronuclei in peripheral lymphocytes (Eastmond and Tucker, 1989. Environ. Mol. Mutagen. 13: 34-43).

The aim of the investigations presented here was to analyze in detail the chromosomal content of γ-rays-induced micronuclei in two-cell human-hamster embryos by FISH using centromere-specific and telomeric DNA probes.

Prior to hybridization of embryo nuclei and micronuclei with DNA probes, the specificity of centromeric and telomeric DNA probes was determined by using first cleavage metaphases with separated human sperm and hamster egg chromosome complements. The centromeric DNA probe used by us (α-satellite DNA) hybridized to the centromeric regions of all human chromosomes, but not with hamster centromeric regions. Telomeric DNA probe was constituted by the highly conserved sequence $(TTAGGG)_n$ and hybridized with the telomeres of human and hamster chromosomes. This unspecificity of telomere probe does not interfere with our results because, as reported before (objective 2), most micronuclei in two-cell embryos were of human origin.

We analyzed a total of 641 two-cell embryos, 269 arising from non-irradiated spermatozoa, 244 after a dose of 2 Gy and 128 after 4 Gy. As expected, there was a dose-dependent induction of micronuclei (0.1 micronuclei per embryo for unirradiated sperm, 0.51 at a dose of 2 Gy and 0.73 at 4 Gy).

The relative frequencies of centromere-positive (C+) micronuclei (referred to the total number of micronuclei) were 33.3%, 21.6% and 23.7% for the groups of 0, 2 and 4 Gy respectively. This means that spontaneous micronuclei as well as radiation induced micronuclei originate basically from acentric fragments.

To consider whether γ-radiation induces aneuploidy (by anaphase lag) or has mainly a clastogenic effect, results must be evaluated in absolute frequencies of micronuclei (referred to the total number of embryos analyzed) (Table IV and figure 5). Thus, the absolute frequencies of centromere-negative (C-) micronuclei were 6.7% for spontaneously occurring micronuclei 40.2% for the 2 Gy dose and 55.5% for the 4 Gy dose. The increase of C- micronuclei is in concordance with the known clastogenic effect of γ-rays and the high number of acentric fragments known to be induced by γ-rays in spermatozoa. Absolute frequencies of C+ micronuclei also increase with radiation dose (3.3%, 11.1% and 17.2%). Since the number of radiation induced dicentric chromosomes in spermatozoa is low (Brandiff et al, 1988. Env. Mol. Mutagen. 12: 167-177), our results are consistent with previous reports that considerer ionizing radiation as an inducer, even if weak, of aneuploidy.

Table IV. Absolute frequencies of centromere-positive (C+) and centromere-negative (C-) micronuclei (Mn).

Dose (Gy)	Number of two-cell embryos analyzed	Total number of Mn	Number of C - Mn (absolute frequency)	Number of C + Mn (absolute frequency)
0	269	27	18 (6.7%)	9 (3.3%)
2	244	125	98 (40.2%)	27 (11.1%)
4	128	93	71 (55.5%)	22 (17.2%)

Figure 5

Induction of micronuclei (Mn) in two-cell embryos by gamma-rays
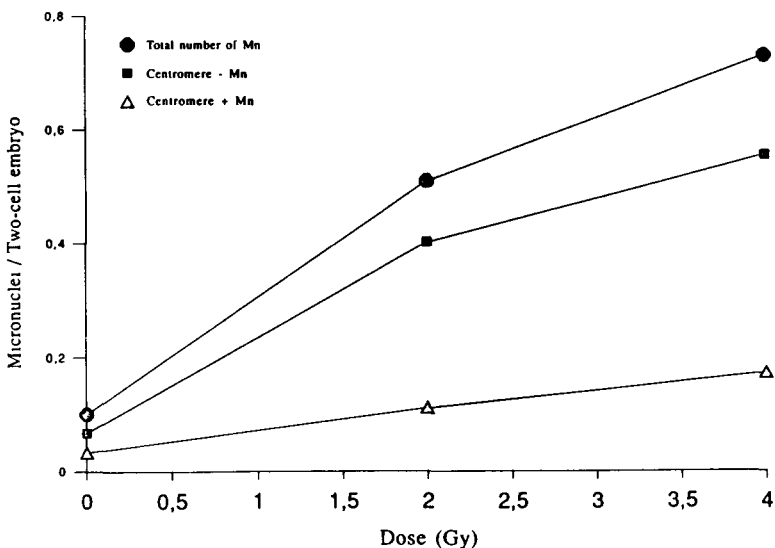
When characterization of micronuclei was perfomed by double FISH (Table V) we observed that all C- micronuclei showed telomeric signals. It could also be seen that, as expected if C-T+ micronuclei derive from acentric fragments, there is a strong increase in their absolute frequency with dose of radiation.

Table V. Characterization of micronuclei (Mn) by double FISH (absolute frequencies).

Dose (Gy)	Number of two-cell embryos analyzed	Total number of Mn	Number of C+/T+ Mn (absolute frequency)	Number of C+/T- Mn (absolute frequency)	Number of C-/T+ Mn (absolute frequency)
0	269	27	7 (2.6%)	2 (0.7%)	18 (6.7%)
2	156	81	14 (9.0%)	4 (2.6%)	63 (40.4%)
4	78	60	10 (12.8%)	4 (5.1%)	46 (59.0%)

C+ Centromere-positive, C-, Centromere-negative; T+ Telomere-positive; T-, Telomere-negative

Among those micronuclei showing centromeric signals, C+T+ micronuclei were much more frequent tham C+T- ones. From these results we can conclude that micronuclei which contain centromeric signals derive more frequently from dicentric chromosomes or from whole chromosomes suffering anaphase lag than from rings. Nevertheless, both types of C+ micronuclei increase with dose of radiation.

In conclusion, the micronucleus assay, as compared with the analysis of metaphases from sperm derived complements represents a real cost and time saving. Moreover, when FISH techniques are applied, it is also possible to characterize micronuclei to distinguish between aneugenic and clastogenic effect of mutagenic agents.

Publications

Tusell L, Alvarez R, Genescà A, Caballín MR, Miró R, Barrios L, Egozcue J (1995). **Human origin of micronuclei in human x hamster two-cell embryos.** Cytogenetics and Cell Genetics 70: 41-44.

Tusell L, Alvarez R, Caballín MR, Genescà A, Miró R, Ribas M, Egozcue J. **Induction of micronuclei in human sperm-hamster egg hybrids at the two-cell stage after in vitro gamma-irradiation of human spermatozoa.** Environmental Molecular Mutagenesis (in press).

Egozcue J, Tusell L, Alvarez R, Genescà A, Barrios L, Caballín MR, Miró R. **Interspecific micronucleus model for the study of induced chromosome aberrations in human male germ cells.** Chromosomes Today (in press).

Tusell L, Alvarez R, Genescà A, Caballín MR, Miró R, Egozcue J. **Characterization of spontaneous and radiation-induced micronuclei in two-cell human-hamster embryos by the use of centromere and telomere DNA probes**. (in preparation)

Invited lectures

Egozcue J. **Chromosome abnormalities in human sperm.** IX Annual Meeting of the European Society of Human Reproduction and Embryology. Thessaloniki, June 18-30, 1993.

Egozcue J. **Interspecific micronucleus model for the study of induced chromosome aberrations in human male germ cells.** Chromosome Conference Madrid, September 11-15, 1995.

Congress Communications

Tusell L, Alvarez R, Miró R, Caballín MR, Genescà A, Ribas M, Egozcue J. **Micronucleus test to assess chromosomal damage in human spermatozoa.** 23rd Annual Meeting of the European. Environmental Mutagen Society. Barcelona, September 27-October 2, 1993.

Tusell L, Alvarez R, Genescà A, Caballín MR, Miró R, Barrios L, Gómez D, Egozcue J. **Human origin of micronuclei in human-hamster two-cell embryos.** X Annual Meeting of the European Society of Human Reproduction and Embryology. Brussels, June 25-29, 1994.

Tusell L, ALvarez R, Caballín MR, Genescà A, Miró R, Ribas M, Egozcue J. **Micronucleus test as an indicator of sperm exposure to gamma rays.** 24th Annual Meeting of the European Environmental Mutagen Society. Poznan, August 31 - September 3, 1994.

Tusell L, Alvarez R, Genescà A, Caballín MR, Miró R, Egozcue J. **Centromere detection in radiation-induced micronuclei of two-cell human-hamster embryos.** 25th Annual Meeting of the Environmental Mutagen Society. Noordwijkerhout, June 18-23, 1995.

Head of project 6: Dr. Eeken

II. Objectives for the reporting period

General goal: The frequency and nature of X-ray induced
dominant mutations affecting morphology and/or viability and
livespan in Drosophila melanogaster

Objective reporting period: To complete the genetic and
cytogenetic analysis of the X-ray induced dominant mutations
and to examine a representative number of mutations at the
molecular level.

III. Progress achieved including publications

A. Dominant mutations affecting morphology.
   The dominant mutations used in this study are recovered
after irradiation of Drosophila males with a dose of 15-17 Gy.
The approximate number of scored irradiated spermatozoa,
spermatids and spermatogonial cells are, 300.000, 40.000 and
240.000 respectively. The data on dominant mutations can be
compared directly with data on recessive mutations as reported
in the literature (Eeken et al., 1994, Mutation Res. 307: 201;
Eeken et al., 1995a, in prep) since these were recovered
largely from the same experiments. The genetic and cytogenetic
analysis reported last year has been finalised.

   Genetic and cytogenetic analysis.
   The dominant mutations recovered were tested genetically to
allocate them to a particular chromosome and cytogenetically to
establish possible associated chromosomal rearrangements. The
mutations are listed in Table I.
All mutants found have been tentatively assigned to 22
complementation groups. Of these, 16 can be classified as

alleles of definite genes: Notch, Beadex, Bubble/Bag, miniature, Attenuated, Plexate, Delta, cubitus interuptis, Tegula, Antennapedia, Bithorax, Humeral patch, Stubble-like X-linked, Clipt, Pigmentless, brown. The remaining groups, Beadex/Beadex-like, "Small wings", Beaded, Wings curled upwards, Wings outstretched/Wings curved down, Tumerous-like are less well defined and may contain mutants of different genes. The group designated Wings outstretched/Wings curved down is heterogenous. The genetic chromosome mapping shows that about half maps to the II-chromosome whereas the other half maps to chromosome III (in two cases the mutation apparently mapped to both these chromosomes, and the cytological analysis revealed that these mutations were in fact accompagnied by a translocation between these two chromosomes). The cytological analysis shows that most of the mutations that mapped on chromosome II show some abnormality in region 36 of the chromosome. It appears most likely that these mutants are defect in the gene coding for the myosin heavy chain resulting in abnormalities most easily recognisable in the wings (these mutants also have impaired flying capability). In collaboration with the Department of Genetics of the University of Nijmegen (Netherlands) these mutants will be further characterised.

   Molecular analysis of X-ray induced intragenic dominant Notch mutations.
   From all the Notch mutations recovered in this study, eight were selected, that cytogenetically did not show any abnormality at the Notch locus and one that apparently was based on an inversion. Also included was a mutation from the Beadex-like group as a control. The Notch gene spans approximately 37 kb of genomic sequences and produces during development several alternatively spliced transcripts. Using digestions with several restriction enzymes and three probes nearly spanning the complete 37 kb, Southern blots gave the following results. (1) The mutation based on the inversion did not show any abberant bands in the Southern blots. It is concluded that it has a break upstream of the analysed region. The Beadex-like mutations shows a normal restriction pattern as expected. From the 8 intragenic Notch mutations, two show a clear internal deletion of approximately 2 and 6 kb. The remaining 6 mutants show a normal restriction pattern indicating that they are due to basepair changes or small deletions (100 bp maximum as the resolution limit of our analysis).

The following main conclusions can be drawn:
(1) Although the inherent variable nature of dominant mutations may influence the frequencies, it is obvious that, depending on the gene studied, they may differ with a factor of 10-50.
(2) In a number of cases null alleles of a gene will cause a dominant phenotype. The frequency of X-ray induced dominant mutations in these genes is highest. The nature of these mutations ranges from multilocus deletions to pointmutations. In these cases, the frequency is modulated by the presence of haplo-subvital loci. An example is formed by the Notch mutations. Similarly, Bubble/Bag, Plexate and Delta show relatively high frequencies of mutations and are based on a null allele (deletions/chromosome rearrangements). That the

frequency of dominant mutations at these loci is lower than at the Notch locus reflects the presence of neighbouring haplo-subvital loci. In principle the frequency and nature of dominant mutations at these type of loci resemble that of recessive visible mutations.

(3) In the majority of loci where in principle a mutation can lead to a dominant phenotype (approximately 150 in Drosophila), these appear to arise not from chromosomal rearrangements as multilocus deletions, inversions or translocations, but from intragenic lesions. The frequency of dominant mutations in these loci is lower with an order of magnitude compared to the Notch-type of loci.

(4) Due to trans-regulatory factors involved in the regulation of some of the Drosophila genes, all breakage phenomena in the vicinity of such a gene may lead to a dominant phenotype. An example of this type has been recorded in our experiments. All dominant brown eyecolor mutants recovered are based on inversions and translocations (not deletions). The frequency can be relatively high since the target of breakage appears to be relatively large.

(5) The molecular analysis of the intragenic Notch mutants shows that 2 out of 8 analysed are due to deletions in the size range of several kb's. The remaining 6 mutations are due to deletions smaller than 100 bp or basepair changes.

(6) The spectrum of lesions causing the Notch mutations appears similar in all three irradiated germline stages (Table II). Possibly the number of mutations based on chromosome breakage is slightly higher in irradiated spermatids. This would be in agreement with the observed higher frequency of induction.

B. Dominant mutations affecting viability and livespan.

The major class of X-ray induced mutations are multilocus deletions. All these multilocus deletions are recessive lethals. They can only be maintained in heterozygotes; homozygotes are not viable. In heterozygous condition only few show a visible effect (dominant) in those cases where a haplo insufficient (but not lethal) gene is included (for example Notch and Delta; see section A). However it has been shown that the majority of multilocus deletions have dominant effects on viability and livespan. In the longevity studies we identified a major factor affecting livespan in region 5/6 of the polytene chromosome map. This factor is not associated with a multilocus deletion but apparently with a gene-mutation. However multilocus deletions of this region are not available (possibly due to the fact that it harbours haplo-subvital loci; see section A). Indeed a first attempt to induced deletions in this region by selection of X-ray mutations uncovered by a recessive visible mutant (cx) located just distal of region 5/6 proved not successful (induced deletions could not be recovered). A similar experiment using a recessive visible mutant (m) located proximal to region 5/6 gave the same result; no deletions of the 5/6 region can be recovered. Whether the presence of haplo insufficient lethality genes in the 5/6 region are associated with the factor affecting livespan is at this moment still speculative.

An additional aspect of radiation induced damage was revealed in the last experiments. Due to a rearrangement in the

irradiated chromosome, the yellow locus was placed in close proximity of a block of heterochromatin. The induction of translocations involving the yellow locus in this chromosome was increased with a factor of 5-10 in comparison to the situation where there is no heterochromatin present. This situation may open possibilities to study the effect of heterochromatin on breakage phenomena induced by radiation.

Eeken, J.C.J., A.W.M. de Jong, M. Loos, C. Vreeken, R. Romeijn, A. Pastink and P.H.M. Lohman (1994) The nature of X-ray-induced mutations in mature sperm and spermatogonial cells of Drosophila melanogaster. Mutation Res., 307, 201-212.
Eeken, J.C.J., A.W.M. de Jong (1995a, in prep.) The nature of X-ray-induced mutations in the radiosensitive spermatid stage using Drosophila melanogaster.
Eeken, J.C.J., A.W.M. de Jong, M. Loos, B. van Veen and J. Zonneveld (1995b, in prep.) The nature of X-ray-induced dominant mutations in Drosophila melanogaster.

Table I

Classification of Dominant mutations based on genetic chromosome localisation and cytogenetic analysis

```
Notch (X-linked):
Notch recovered from irradiated spermatozoa:
M09-B13        XLRL, wN, F1 female sterile          Df(1)wN
M10-A26        XLRL, wN, F1 female sterile          Df(1)wN
M12-A12        XLRL, wN, F1 female sterile          Df(1)wN
M14-A21        XLRL, wN, F1 female sterile          Df(1)wN
M11-A23        XLRL, wN                             Df(1)3B-3E + In(1)1B;11B/C
M11-A22        XLRL, N, F1 female sterile
M14-A27        XLRL, N, F1 female sterile
M13-A6         XLRL, N                              Df(1)3C4-3C7
BA1-A4         XLRL, N^Co-like, covered by N^+Y     Df(1)3C7-3D/E + T(X;2L)tipX-HE;36C
M13-A2         XLRL, N                              In(1)1B;N + In(1)N;20      Mol.Analysis
M08-A2         XLRL, N                              normal X
M11-A24s       XLRL, N, covered by N^+Y             normal X                   Mol.Analysis
M12-A16s       XLRL, N, covered by N^+Y             normal X                   Mol.Analysis
M12-A28        XLRL, N, covered by N^+Y             normal X                   Mol.Analysis
M13-A9         XLRL, N                              normal X
M11-A6**       XLRL, w/wN                           Tp(X;3R)3C2-3E;93D
M15-A8**       XLRL, N                              T(X;2L)3F;21A -> F1, 3x N

Notch recovered from irradiated spermatids:
M31-C21        XLRL, wN, F1 female sterile          Df(1)wN
M35-C27        XLRL, wN, F1 female sterile          Df(1)wN
M32-C9         XLRL, wN, died                       Df(1)wN
M32-C15        XLRL, wN, died                       Df(1)wN
M33-C15        XLRL, wN, died                       Df(1)wN
M37-C18        XLRL, wN, died                       Df(1)wN
M33-C10        XLRL, wN                             Df(1)3A5-3D
M33-C25        XLRL, wN                             Df(1)3B-3D
M36-C3         XLRL, wN                             Df(1)3B-3D
M36-C13        XLRL, wN                             Df(1)3A5-3E/F
M41-C33        XLRL, wN                             Df(1)3A3-3C15
M32-C27        XLRL, N, F1 female sterile
M38-C4         XLRL, N, F1 female sterile
M39-C13        XLRL, N, F1 female sterile
M32-C30        XLRL, N, died
M33-C18        XLRL, N, died
M34-C17        XLRL, N                              Df(1)3C7-3D/E
M31-C16        XLRL, N                              T(X;3R)3C7;98D
M36-C20        XLRL, N, NOT covered by N^+Y         T(X;2L)3C7;22E + In(1)3C7;20
M39-C20        XLRL, N, covered by N^+Y             T(X;3R)3C7;87F
M39-C30        XLRL, N, covered by N^+Y             T(X;2L)3C7;33C/D
M41-C19        XLRL, N, covered by N^+Y             T(X;2L)3C7;30A
M34-C27        XLRL, N                              normal X
M35-C11*       XLRL, N, covered by N^+Y             normal X
M38-C16        XLRL, N                              normal X                   Mol.Analysis
M38-C28        XLRL, N                              normal 3C + T(X;2)13B;50B   Mol.Analysis
M41-C13        XLRL, N, covered by N^+Y             normal X                   Mol.Analysis
M37-C35**      XLRL, N, covered by N^+Y             T(X;2L)8F;40/41 -> F1, 3x N
M37-C13**      semi lethal                          probably Dp(1;1)N
M37-C35sub**   lethal                               probably Dp(1;1)N

Notch recovered from irradiated spermatogonial cells:
M18-E18        XLRL, wN, F1 female sterile          Df(1)wN
M19-E27        XLRL, wN, F1 female sterile          Df(1)wN
M20-E18        XLRL, wN                             Df(1)3A4-3E
M22-E4         XLRL, wN                             Df(1)3A8-3D
M25-E7         XLRL, wN                             Df(1)2F-3D5
M15-E3         XLRL, N, F1 female sterile
M11-E4         XLRL, N, covered by N^+Y             normal X                   Mol.Analysis
M17-E26        XLRL, N, covered by N^+Y             normal X                   Mol.Analysis
```

*M35-C11, x N^+Y --> covered males all strong Delta-like + RE.
** no Notch mutations in the strict sense, however comparable to Df's.

```
Beadex (X-linked):
M39-C21         X-linked, male viable                    T(X;3)17C;71B + In(3)63C;71B


Bubble/Bag (X-linked):
M10-A14         XLRL, not covered by N⁺Y                 Df(1)13C-14B3
M32-C13         XLRL, not covered by N⁺Y, variable       Df(1)13D-14C
M34-C1          XLRL, not covered by N⁺Y, variable       Df(1)13C-14C
M39-C31         XLRL, not covered by N⁺Y, variable       In(1)9B;13B (mottled Bg?)


Beadex or Beadex-like (X-linked):
M11-A12s        XLRL, not covered by N⁺Y                 normal X, LOST
M14-A22         XLRL, not covered by N⁺Y                 normal X                      Mol.Analysis
M13-E9          XLRL                                     normal X + effect lost, DISCARDED
M14-F13         XLRL, variable                           N/Bx regions normal + In(1)2B;6A LOST
BA05-A38s       X-linked, male viable                    normal X
BA13-A6s        XLRL, Nᶜᵒ-like, not covered by N⁺Y       normal X
BA13-A29s       XLRL, Nᶜᵒ-like, not covered by N⁺Y       normal X
BA13-A35        XLRL, not covered by N⁺Y, variable       normal X
M36-C12         XLRL                                     normal X, LOST
M39-C23         XLRL, not covered by N⁺Y, variable       normal X
M39-C34         XLRL, not covered by N⁺Y, variable       normal X


Miniature (X-linked):
M14-A21         XLRL                                     LOST
M34-C1          male viable + sterile                    normal X
                                                         + In(3L)64E;73B + In(3R)88F;98C
M38-C13         XLRL                                     Df(1)10B3-11A


"Small wings" (dominant vestigal-like) (X-linked):
BA12-A65s       X-linked                                 LOST
BA13-A13s       X-linked                                 LOST
BA12-A67s       X-linked, very slight effect,            LOST


Attenuated (X-linked):
M05-B4          XLRL forked                              Df(1)15F-16A4/5


Plexate (chrs.II):
M09-F14         chrs.II + l(3)                           In(2LR)22A;60B/C(Px)
BA04-A59s       chrs.II + l(3)                           Df(2R)60C6-Px-60E3
BA14-A11        chrs.II + l(3)                           Df(2R)60B12/14-Px-60D1


Beaded (97F) (Bd-like autosomal):
M10-A7          chrs.III, Bd-Ser-like                    In(3L)65B;78A, Bd region normal
M31-C20         chrs.II or III                           Df(2R)49C-50C
                (at 16/2/94 effect lost, DISCARDED)
M34-C35s        chrs.II, Bd-Ser-like, variable           In(2R)49E;52A/B
M38-C2          chrs.II or III                           LOST
M41-A20         chrs.II Bd-like                          all chrs. normal
```

```
Delta (chrs.III, 92A1/2):
M11-A18        chrs.III     rec. let.        Df(3R)92A1/2(=Dl)
M11-A20        chrs.III     rec. let.        Df(3R)91D;92B/C
M11-E26        chrs.III     rec. let.        Df(3R)91D;92B
BA01-A3        chrs.III     rec. let.        Df(3R)92A(Dl);92B5
BA03-A6s       chrs.III     rec. let.        Df(3R)91B5;92A4
BA03-A32s      chrs.III     rec. let.        Df(3R)91B5;92A8
BA10-A8        chrs.III     rec. let.        Df(3R)91C6/7;92A14
BA10-A45a      chrs.III     rec. let.        Df(3R)91E1;92B1/2
BA10-A45b      chrs.III     rec. let.        Df(3R)91E1;92B1/2
BA12-A20a      chrs.III     rec.let.         Df(3R)91C1;92A14
BA12-A35s      chrs.III     rec. let.        Df(3R)91C1;92A14
BA14-A4        chrs.III     rec. let.        Df(3R)91C;92A14
BA14-A22       chrs.III     rec. let.        Df(3R)91E/F;92A14
M34-C10        chrs.III     rec. let.        Df(3R)91D/E-92E + In(3R)80/81;91D/E
M39-C34s       chrs.III     rec. let.        Df(3R)91C;92A14
M41-C8         chrs.III     rec. let.        Df(3R)92A1;92C
M41-C27        chrs.III     rec. let.        Df(3R)91B;92A
M14-A27        chrs.III     rec. let.        In(3R)86E;92A1/2(Dl)
M38-C16s       chrs.III                      In(3R)86E;92A1/2(Dl)
M39-C29        chrs.II+III                   T(2;3)33E;92A1/2
M35-C22        chrs.III                      normal Dl + Df(3R)92F;93E
M36-C30s       chrs.II+III                   normal Dl + T(2;3)53E;97C
BA02-A26       chrs.III     viable           normal 3L, normal 3R
BA03-A20s      chrs.III     viable           normal 3L, normal 3R
BA04-A27       chrs.III     ?                normal Dl, normal Bd + Df(3R)98C;98D2
BA09-A41       chrs.III     rec. let.        normal Dl
BA10-A70       chrs.III                      normal 3L, normal 3R
BA11-A4        chrs.III                      normal 3L, normal 3R
BA12-A14       chrs.III                      normal 3L, normal 3R
BA12-A20b      chrs.III     viable ?         normal 3L, normal 3R
BA13-A3s       chrs.III     rec. let.        normal 3L, normal 3R
M34-C14s       chrs.III                      normal Dl
M38-C27        chrs.III     viable           normal Dl
M39-C8         chrs.III     viable           normal Dl
M33-C28        autosomal dom.      weak      normal Dl
M37-C20s       autosomal dom.      weak      normal Dl
M32-C14        very weak phenotype + low viability (DISCARDED)
M38-C28        autosomal dom. low viability, low fert (LOST)


Delta-like on IV:
M11-E4         chrs.IV                       In(4)101;102F


cubitis interuptis^Dom (chrs.IV):
M34-C10        chrs.IV
M34-C35        chrs.IV


Wings curled upwards (Cy-like):
BA10-A92s      chrs.III                      T(3;4)67D/E;102 ***
M04-A21        not on chrs.III               all chrs. normal

*** break close to haywire (ERCC3) tested for MMS-sensitivity, not sensitive!


Tegula (=decapentaplegic, chrsII, 22F):
M34-C21        chrs.II + III    viable?      T(2;3)22F(dpp);69F
```

Wings outstretched/Wings curved down + parts deformed (cell death?)
(MHc, Muscle myosin heavy chain, 36A/C - Mhc-c, 60E - Actin, 88F)

BA07-A18	chrs.II	In(2)35/36 ?
BA09-A80s	chrs.II	Df(2L)35E;36C ?
BA14-A3s	most likely on II	In(2)36A;36B ?
BA14-A9	probably on II	36A/B ?
BA14-A26	chrs.II	normal + "strange" 36A/C ?
M32-C17	chrs.II	normal + "strange" 36A/C ?
M33-C6	chrs.II + Antp-like (Ba?)	In(2R)40/41;60C + "strange" 36A/C ?
M36-C12	Os, autosomal dom.	LOST
M36-C16	chrs.II, Os/D + RE	In(2R)40/41;52D + "strange" 36A/C ?
M36-C25	Os, autosomal dom.	LOST
M37-C20	blistered-like chrs.II + III	T(2;3)30A;100B + "strange" 36A/C ?
M38-C19	Os + Px ?	In(2R)40/41;60C + "strange" 36A/C ?
M38-C21-1	Os, autosomal dom.	"strange" 36A/C ?
M39-C15	Os + Up chrs.II + III, viable	T(2;3)59A;75F + In(2R)40/41;59A
BA08-A47	chrs.II or III ?, viable ?	35/36 ? + normal 3L/3R
BA09-A48	chrs.III	normal 3L/3R
BA13-A8a	chrs.III viable	normal 3L/3R
BA13-A8b	chrs.III viable	LOST
M32-C27	chrs.III	Tp(2;3)48F-52D;80/81 + Tp(3;2)81F-87B;24C
M38-C21-2	chrs.III lethal	normal 3L/3R
M41-C10	chrs.III lethal	normal 3L/3R

Antennapedia (=ANTC, chrs.III, 84A/B):
M32-C1	Antp, males sterile	LOST
M33-C19	chrs.III	Tp(3;3)81F-84B(ANTC);96C
BA12-A34	chrs.III	In(3LR)67F;84A/B(ANTC)

phenotype eyes reduced/deformed (Deformed = ANTC: chrs.III, 84A/B):

Bithorax (=BXC, chrs.III, 89E):
BA01-A2	Cbx-like, chrs.III,	
	+ slight effect on eyes + antennae	In(3RL)89E(BXC);72B
M38-C23	X-linked, male viable	T(X;3)20;80/81 + In(3)89B(BXC);90A + normal X

phenotype split thorax + apparently X-linked due to additional Translocation

Hup (Humeral patch - 7C) "shoulders":
M41-C2	X-linked (variable) + SLRL	normal X

Stubble-like (X-linked)
M41-C4	XLRL	In(1)8A4;14B2/3

Stubble-like (most likely Cpt, 32 region):
M10-E18	chrs.II	In(2L)32E/F;35D/E

Pigmentless (Ps):
M34-C26	chrs.II	In(2R)43E(Ps);44D1

Tumerous-like (X-linked):
BA03-A20s	X-linked	no cyto, died 20/1/94

Eyecolor (brown Dominant: chrs.II, 59E):
M07-A20	bw	In(2R)59E(bw);40/41 + T(X;2L)9B;30C
M10-A2	bw	In(2R)59E(bw);40/41
M10-B24	bw, chrs.II = l(2)	In(2R)57D;40/41 + 59E normal
M11-A25	bw	In(2R)59E(bw);40/41
M21-E22	bw, chrs.II + III	T(2R;3)57D;80/81 + 59E normal
M28-E18	bw, chrs.II + III	T(2R;3R)59E(bw);81F
M31-C15	bw	T(2R;3R)59E(bw);97A
M35-C17	bw, chrs.II	T(2R;3R)59E(bw);81F
M38-C9	bw, chrs.II + III	In(2R)57B4;59E(bw) + In(2R)57B4;40/41
		+ T(2;3)40/41;80/81
M41-C3	bw, chrs.II	In(2R)40/41;59E(bw) + In(2L)32;40/41

Table II

Mutational spectrum of X-ray induced Notch in spermatozoa, spermatids and spermatogonial cells.

	total	not analysable	analysed	wN	mld	rearr	normal-X
spermatozoa	15	2	13	5(38%)	1(7%)	1(7%)	6(48%)
spermatids	27	5	22	12(57%)	1(5%)	5(24%)	4(14%)
spermatogonial cells	8	1	7	5(71%)	-	-	2(29%)

wN: multilocus deletions including the neighbouring genes white and Notch
mld: cytologically visible multilocus deletions
rearr: inversions/translocations
normal-X: no visible cytological abnormality

Head of project 7: Prof. Hulten

II. Objectives for the reporting period 1992-1995

Our aim for the reporting period has been to develop new technology
for the direct identification of radiation-induced genetic
abnormalities in the soma and germ-line of man. The investigations
include (i) a FISH assay for induced translocation rate in
lymphocytes, (ii) a FISH assay for aneuploidy rate in human sperm,
(iii) a DNA assay for assessment of mutation rates in human sperm,
and (iv) a FISH meiotic segregation analysis of translocations. We
have utilized a cell bank of lymphocytes and spermatozoa from men
exposed to ionising radiation as a result of (1) radiotherapy,
(2) accidental and (3) occupational exposure, as well as (4) normal
controls in our evaluation of this technology.

III. Progress achieved including publications

   PLEASE SEE ATTACHED REPORT

GENETIC RISKS ASSOCIATED WITH EXPOSURE TO IONISING RADIATION

Progress achieved including publications

(i)   FISH assay for induced translocation rate in lymphocytes

We have evaluated chromosome painting by FISH as an indicator of radiation induced damage in human lymphocytes in an in vitro study[1]. This has demonstrated that it is a sensitive technique for radiation dosimetry, comparing favourably with measurements of DNA strand breaks.

In a detailed FISH study using chromosome paints for chromosomes 1, 3 and 5 of radiotherapy-induced lymphocyte damage (10 years post treatment), we have shown that stable translocations persisted at a rate x 10 that found in normal controls[2,3,4]. The corresponding study of occupationally exposed men is ongoing. We have banked and are analysing blood lymphocytes from 10 workers and 10 matched controls using the FISH assay. The results of this study will be available in the Autumn, 1995.

(ii)   FISH assay for aneuploidy rate in human sperm

(a) Normal unexposed control data
In order to establish a reliable molecular cytogenetics assay for radiation-induced chromosome abnormalities in human sperm, data on a large control material has been collected and evaluated. We have used FISH with centromere-specific probes in dual colour analysis with the probes for chromosomes X, Y, 1 and 12. We have analysed a total of 110.000 sperm from 8 apparently normal, fertile men in the age range 20-45 years, who have no known accidental or occupational exposure to ionising radiation[5,6]. To our knowledge this is the largest control material investigated to-date. The hybridisation efficiency was high at 99.8-100.0% of individual spermatozoa. The diploidy rate was documented as 0.02%. The sex chromosome ratio was nearly 1:1, but with a slight increase in X sperm in relation to Y sperm. The rate of XY sperm, corresponding to first meiotic non-disjunction was approximately double (0.32%) to that of the second with XX at 0.11% and XY at 0.14%,

respectively. The aneuploidy rates for chromosomes 1 and 12 were established as 0.07% and 0.10%, respectively. However, there is an indication of some inter-individual variation between men. No age dependency in abnormality rate has so far been found.

(b) Data on radiotherapy and occupational exposure to ionising radiation

We have performed the same analysis on a total of 30,000 sperm from men exposed to ionising radiation by radiotherapy or as an occupational hazard[2-4]. The hybridisation efficiency using the centromere specific probes for chromosomes 1 and 12 in dual colour experimentation was 99.9-100.0%. No increase in aneuploidy rate in sperm in comparison to controls was found in men who had been exposed to low levels of ionising irradiation as an occupational hazard. An increase in aneuploidy rate at 2.5 times the normal was, however, found in sperm following radiotherapy more than 10 years previously. This is contrasted to the rates of translocations in blood lymphocytes, which were increased 5-10 times normal values.

It is important to note that the aneuploidy rate documented in sperm could be caused by either primary whole meiotic chromosome non-disjunction or alternatively be the result of first meiotic 3:1 secondary translocational non-disjunction. If the sperm aneuploidy rate detected represents simple primary non-disjunction, the genetic effect in offspring is by comparison relatively low. On the other hand, should the aneuploidy rate be caused by translocations induced in premeiotic spermatogonia, where we are identifying only one meiotic segregation product, the genetic impact in future generations could be high. In order to investigate this further, it is essential that the meiotic segregation patterns of translocations in human males is established. We have therefore used constitutional translocation carriers for meiotic segregation analysis by FISH. The results of these investigations are described below separately (iv). To get further insight into the genetic risks associated with exposure to ionising radiation we should wish to proceed to investigate chromosomal meiotic segregation in exposed men. This would be very valuable, as it would allow direct differentiation and estimation of the relative frequencies of radiation-induced primary and secondary, translocation, non-disjunction, the latter being associated with a higher risk for liveborn offspring with genetic disease.

We have found the FISH sperm assay to be a reliable technique, however, it is time consuming and labour intensive. We have therefore sought to utilize alternative DNA technologies for investigation of radiation induced germ-line damage.

(iii) DNA assay for assessment of mutation rates in human sperm

We have as an alternative sought to develop a DNA assay for radiation-induced mutation in human spermatozoa. We hope to automate this technology, using an ABI gene scanner[7]. The new approach involves lysis of sperm, serial dilution to give approximately 5-15 sperm per tube and either polyacrylamide gel electrophoresis (PHGA) or an analysis on the ABI gene scanner following PCR, using fluorescently labelled allele specific oligonucleotides (ASO's). We have used both Dinucleotide and Tetranucleotide repeat sequences for this mutation analysis.

(a) Dinucleotide assay
We initially used dinucleotide repeat sequences, as these are utilized in our routine service. A screening was undertaken on 3 normal sperm donor samples, using 2 ASO's. Approximately 1,000 sperm were analysed per control sample. The results indicated the mutation rate to be 1/500 sperm for one of the ASO's. However, we were unable to obtain any reliable results for the other ASO. Stutter bands were produced, which could be the result of DNA replication slippage, which is further increased by the high number of amplification cycles that were performed.

(b) Tetranucleotide assay
As an alternative to the dinucleotide we have progressed to develop a tetranucleotide assay. This involves using an ABI gene scanner. The potential for the analysis of a high number of sperm samples by automation using this technology makes this approach attractive. The preliminary results indicate that this is more feasible than the dinucleotide assay. We have found the normal rate of mutation in sperm to be very low, using the D21S11 probe. On the other hand there is a significant mutation rate in sperm from a patient exposed to radiotherapy.

The tetranucleotide analysis has the added advantage over conventional dinucleotide and PAGE analysis in that fewer cycles of PCR have to be used and hence less replication slippage will occur. Furthermore, tetranucleotides are more stable than dinucleotides, and therefore stutter bands are less likely to occur, easing the interpretation of the data. The gene scanner is also able to size the alleles and can determine how many bases have been deleted/added, when a mutation is found. Therefore a more detailed picture is obtained. Rapid results are obtainable, as one gel can be used a couple of times and this runs more quickly than conventional PAGE.

(iv)   Meiotic   segregation   of   translocations

In order to evaluate the relevance for future generations of aberrations detected by the sperm FISH assay, further information is required on the meiotic behaviour with respect to chiasma formation and first meiotic segregation of spermatogonial translocations. The development of FISH has allowed such information to be obtained in the human male for the first time. We have used FISH with whole chromosome libraries in combination with repeat sequence DNA probes, specific to certain autosomes, to investigate both the normal meiotic process and the meiotic segregation of translocations in human male carriers[8-12]. It has turned out that the 3:1 first meiotic translocation segregation is very rare by comparison to the 2:2 segregations. An increased rate of chiasma formation with specific hotspots within the interstitial segment, i.e. between the centromere and the translocation breakpoint, further complicates and distorts the gametic output. The detailed meiotic analysis performed on translocation carriers has allowed predictions to be made on chromosomal abnormality rate in sperm, which has been verified by FISH analysis.

Publications and Presentations

(1) <u>Plummer, S.M., Pheasant, A.E., Johnson, R., Faux, S.P., Chipman, J.K., Hultén, M.A.</u>: Evaluation of the relative sensitivity of chromosome painting (FISH) as an indicator of radiation-induced damage in human lymphocytes. Hereditas <u>121</u>,139-145, 1994.

(2) <u>Armstrong, S.J., Perring, S.A., Bundey, S., Hultén, M.A.</u>: The potential of FISH for evaluation of radiation-induced chromosome aberrations in the soma and the germ-line. Clinical Genetics Society, London, March, 1994.

(3) <u>Armstrong, S.J., Perring, S.A., Bubdey, S., Hultén, M.A.</u>: The potential of FISH for evaluation of radiation induced chromosome aberrations in the soma and the germ-line. 18th L.H. Gray conference, Bath, April, 1994.

(4) <u>Perring, S.A., Armstrong, S.J., Bundey, S.E., Hultén, M.A.</u>: The potential of FISH for evaluation of radiation induced chromosome aberrations in the soma and germ-line. Association of Clinical Cytogeneticists, Cardiff, July, 1994.

(5) <u>Goldman, A.S.H., Fomina, Z., Knights, P.A., Hill, C.J., Walker, A.P., Hultén, M.A.</u>: Analysis of the primary sex ratio, sex chromosome aneuploidy and diploidy in human sperm using dual colour fluorescence in situ hybridisation. Eur. J. Hum. Genet. <u>1</u>, 325-334, 1993.

(6) <u>Hultén, M.A. and Goldman, A.S.H.</u>: The potential of Multicolour FISH for Meiotic Chromosome Analysis. <u>In</u>: Chromosome Alterations, (Eds AT Natarajan and G, Obe), Springer Verlag, pp235-251, 1994.

(7) <u>Perring, S.A., Armstrong, S.J., Bundey, S.E., Hultén, M.A.</u>: Radiation-induced germ-line mutations. 10th International Congress of Radiation Research. Germany, 1994.

(8) <u>Goldman, A.S.H. and Hultén, M.A.</u>: Chromosome in situ suppression. hybridization in human male meiosis. J. Med. Genet. <u>29</u>, 98-102, 1992.

(9) <u>Armstrong, S.J., Kirkham, A.J. and Hultén, M.A.</u>: XY chromosome behaviour in the germ-line of the human male: A FISH analysis of spatial orientation, chromatin condensation and pairing. Chromosome Research <u>2</u>, 445-452, 1994.

(10) <u>Goldman, A.S.H. and Hultén, M.A.</u>: Analysis of chiasma frequency and first meiotic segregation in a human male reciprocal translocation heterozygote t(1;11)(p36.3;q13.1) using fluorescence in situ hybridisation. Cytogenet. Cell Genet. <u>63</u>, 16-23, 1993.

(11) <u>Goldman, A.S.H. and Hultén, M.A.</u>: Meiotic analysis by FISH of a human male 46,XY,t(15;20)(q11.2,q11.2) translocation heterozygote: quadrivalent configuration, orientation and first meiotic segregation. Chromosoma <u>102</u>, 102-111, 1993.

(12) <u>Armstrong, S.J., Goldman, A.S.H., Hultén, M.A.</u>: Analysis of meiotic chromosome configuration and segregation in a male carrier of the common reciprocal translocation t(11;22)(q23;q11); no evidence found for predisposition to 3:1 events. In Manuscript, 1995.

Final Report
1992 - 1995

Contract: **FI3PCT920021**   Duration : **01.09.92- 30.06.95**   Sector : **B15**

Title: Dose assessment, early cellular and late carcinogenic effects of exposure
to radon and its progeny.

1)   P. Fritsch (G. Monchaux, since 1994)   CEA - Paris
2)   C. Collier   UKAEA

I - Summary of Project Global Objectives and Achievements

The aim of this project was : to provide better characterization of the exposure conditions to radon and its progeny, to estimate doses delivered to the different lung compartments using biological indicators and to study early cellular and late carcinogenic effects after exposure to radon alone or combined exposure with other airborne pollutants. The main objectives were :

1 - to establish standard radon metrology between participant laboratories to ensure that the methods and equipment currently used in the metrology of radon and radon daughters by each of the participating laboratories during exposures yield comparable results.

2 - to study the effect of exposure conditions on the deposition of radon daughters in the respiratory tract. This was to enable more accurate estimates of radiation dose to the different regions of the rat lung to be made, to standardise the methods so that the results from each participating laboratories could be compared.

3 - to develop new assays for biological dosimetry in the different parts of the respiratory tract using cytological methods allowing to provide more accurate estimates of the dose delivered to different regions. This included the comparison of effects observed in animals exposed to radon and radon daughters with those observed in animals after homogeneous thoracic irradiation by external gamma rays from Co-60.

4 - to develop studies on the early subacute effects of radon exposure on the epithelial cells of the rat respiratory tract , using cell proliferation and nuclear aberrations incidences as indicators of radiation damage.

5 - to initiate further life-time carcinogenicity studies on the effect of dose and dose rate on radon lung tumour induction and combined effects with other airborne pollutants.

II. Objectives for the reporting period

The four main topics developed over the reporting period were :

1 - to complete biological dosimetry techniques in the rat respiratory tract on alveolar macrophages recovered by bronchoalveolar lavage after radon exposure,
2 - to develop new histo-cytological methods for dose-assessment in the different compartments of the respiratory tract dose
3 - to assess late carcinogenic effects by life-time studies to investigate dose-rate effects and effects induced by radon in combination with other environmental airborne pollutants.
4 - to carry out preliminary studies on lead deposition after exposure to thoron.

Most problems concerning topics 1 and 2 have been resolved. New histological assays have been developed which appears appropriate for dose estimate within the entire respiratory tract. Alterations of epithelial cell proliferation have been characterised under various experimental conditions but further studies are needed to know their biological significance. New carcinogenic and cocarcinogenic studies have been initiated and these studies are still in progress.

III. Progress achieved including publications

1) Biological dosimetry

The purpose of this study was :

1) to measure the deposition of radon progeny within the respiratory tract of rats by gamma spectrometry of ^{214}Pb under two different conditions of unattached fraction fp .
2) to correlate this deposition for a similar cumulative exposure with the incidence of nuclear aberrations in alveolar macrophages recovered by bronchoalveolar lavage.

Three-month old male Sprague-Dawley rats (OFA, Iffa-credo, France) were whole-body exposed to radon and progeny. Exposures under *static* conditons were performed without air renewal so that radon daughters were simply allowed to attach themselves on the natural ambient aerosol. Exposures under *dynamic* conditions were performed by continuous air recirculation by a closed loop system. Once the equilibrium between radon and its progeny had

been reached, rats were introduced into the inhalation chamber and exposed for 3 hours. After rapid removal from the chamber, they were anaesthetized and killed according to the directive of Care and Use of Laboratory animals from the European legislature.

The retention of ^{214}Pb was measured in the nasopharynx, the tracheobronchial region and the whole lungs by counting the γ ray emission at 0.609 MeV with a germanium detector (Ge HP type N, Intertechnique, France). For each sample, at least 3 measurements were performed at different moments of the decay to estimate the initial deposit. All these measurements were performed according to the recommendations of the European Late Effect Project (EULEP) which managed the collaboration between the European laboratories involved in animal studies on radon. Micronuclei and binucleated cells were scored in alveolar macrophages extracted by bronchoalveolar lavage in 2 groups of rats, 8 days after exposure under *static* or *dynamic* conditions at a similar cumulative dose. Cytospins of cell suspension were air-dried, fixed in ethanol-ether (1/1 v) and stained with Giemsa before light microscopic observation.

The measurements of exposure parameters under *static* conditions are shown in table 1. Equilibrium factor F was about 0.37 and *fp* near 10%. The ^{214}Pb retention was measured in 3 rats exposed during 3 different sessions. Parameters measured under *dynamic* conditions are shown in Table 2. Under these experimental conditions, *fp* was higher than 80%, with a nearly constant disequilibrium at about 0.17. The distribution of ^{214}Pb was measured in 2 rats during 2 successive sessions.

The same measurements were performed under the different conditions of exposure for a similar PAEC. The parameters measured during *static* exposure (107 rats inside the chamber) or *dynamic* exposure (only 3 rats exposed) are shown in table 3. Measurements of ^{214}Pb deposition were performed on 2 rats per group. Table 4 shows the percentage of micronucleated and binucleated alveolar macrophages recovered from the rats that were exposed during 8 hours under *static* or *dynamic* conditions and killed 8 days later. The controls corresponded to 5 unexposed rats killed at the same age.

Under *static* conditions, at about 25 mJ.m^{-3} (1200 WL), the aerosol characteristics in the Razès facility are, high F (0.37), low *fp* (10 %) and activity median diameter in the range of 0.1 to 0.3 µm (Masse, 1992). ^{214}Pb measurements showed that most of the radionuclide retained in the respiratory tract was located in lung tissues. Under *dynamic* conditions (F ≈ 0.17, *fp* > 80%), at about 400 WL, a large retention of ^{214}Pb was observed in the nasopharynx which was quantitatively similar to that measured in lungs. For a similar PAEC, at about 440 WL, similar ^{214}Pb lung retentions were measured but the retention in the nasopharynx was 5 times larger under *dynamic* than under *static* conditions.

Most of these ^{214}Pb retention values correspond to ^{218}Po deposition within the different compartments of the respiratory tract which readily form ^{214}Pb. These results indicate that *fp* variations mainly altered deposition of radon daughters in the nasopharynx but that, in fact, lung deposition was not changed. Assuming that alveolar macrophages are homogeneously distributed within the alveolar tissue, nuclear aberration scoring in these cells could allow us to compare doses delivered to the deep lung after *static* and *dynamic* exposure (Bisson, 1994). The similar percentage of micronucleated or multinucleated alveolar macrophages observed under these 2 exposure conditions seems to confirm that there is no difference due to an increased *fp* in the dose delivered to the bronchio-alveolar compartment. This is in agreement with our preliminary results obtained in female rats exposed to radon progeny under *dynamic* conditions which showed incidence of lung tumours similar to that measured after *static* exposure to the same cumulated dose. However, these results are conflicting with those previously reported after inhalation exposure experiments indicating an increased risk of lung cancer in rats with a rising degree of unattachment (Cross, 1984). Further studies are in progress to estimate radon daughter deposition, dose distribution in the different epithelial target cells of rats according to radon exposure conditions.

Table 1 : Inhalation parameters and ^{214}Pb retention in the respiratory tract of rats under *static* conditions in a long term exposure to radon and progeny (PAEC= 25 mJ.m^{-3}).

Aerosol parameters	Mean	±	SD	Units
Activity concentration of ^{222}Rn	12347	±	1987	kBq/m3
Activity concentration of ^{218}Po	5942	±	1261	kBq/m3
Activity concentration of ^{214}Pb	4450	±	1120	kBq/m3
Activity concentration of ^{214}Bi	4378	±	1742	kBq/m3
FA = Activity ^{218}Po / Activity ^{222}Rn	48	±	10	%
FB = Activity ^{214}Pb / Activity ^{222}Rn	36	±	9	%
FC = Activity ^{214}Bi / Activity ^{222}Rn	35	±	14	%
F = Equilibrium factor	0.37	±	0.11	
Potential Alpha Energy Concentration	25.2	±	8.1	mJ/m3
	1212	±	389	WL
fp = unattached fraction of PAEC	11	±	2	%
Distribution of ^{214}Pb activity in the respiratory tract (mean values ± SD in 3 rats)				
^{214}Pb activity in nasopharynx	2.7 ± 1.3 kBq			
^{214}Pb activity in trachea	0.3 ± 0.1 kBq			
^{214}Pb activity in lungs	9.7 ± 1.8 kBq/g			

Table 2 : Inhalation parameters and ^{214}Pb retention in the respiratory tract of rats under *dynamic* conditions in a long term exposure to radon and its progeny (PAEC $\approx$ 8 mJ/m^3).

Aerosol parameters	Mean	±	SD	Units
Activity concentration of ^{222}Rn	8924	±	1125	kBq/m3
Activity concentration of ^{218}Po	6330	±	812	kBq/m3
Activity concentration of ^{214}Pb	1319	±	221	kBq/m3
Activity concentration of ^{214}Bi	418	±	106	kBq/m3
FA = Activity ^{218}Po / Activity ^{222}Rn	71	±	9	%
FB = Activity ^{214}Pb / Activity ^{222}Rn	15	±	3	%
FC = Activity ^{214}Bi / Activity ^{222}Rn	5	±	1	%
F = Equilibrium factor	0.17	±	0.1	
Potential Alpha Energy Concentration	8.3	±	1.2	mJ/m3
	400	±	58	WL
fp = unattached fraction of PAEC	85	±	5	%
Distribution of ^{214}Pb activity in the respiratory tract (mean value ± SD in 2 rats)				
^{214}Pb activity in nasopharynx	9.5 ± 3.5 kBq			
^{214}Pb activity in trachea	0.4 ± 0.1 kBq			
^{214}Pb activity in lungs	7.5 ± 2.1 kBq/g			

Table 3 : Inhalation parameters and ^{214}Pb retention in the respiratory tract of rats under *static* or *dynamic* conditions for a similar PAEC (9 mJ/m^3).

Aerosol parameters	Static	Dynamic
Activity concentration of ^{222}Rn	4632 kBq/m3	9925 kBq/m3
Activity concentration of ^{218}Po	2408 kBq/m3	7146 kBq/m3
Activity concentration of ^{214}Pb	1713 kBq/m3	1488 kBq/m3
Activity concentration of ^{214}Bi	1667 kBq/m3	397 kBq/m3
FA = Activity ^{218}Po / Activity ^{222}Rn	52 %	72 %
FB = Activity ^{214}Pb / Activity ^{222}Rn	36 %	15 %
FC = Activity ^{214}Bi / Activity ^{222}Rn	37 %	4 %
F = Equilibrium factor	0.36	0.16
fp = unattached fraction of PAEC	12 %	87 %
Potential Alpha Energy Concentration	9.3 mJ/m3	8.9 mJ/m3
	450 WL	429 WL
Cumulative dose after 3 hours	27.9 mJ/m3.h	26.7 mJ/m3.h
of exposure	7.9 WLM	7.5 WLM
Distribution of ^{214}Pb activity in the respiratory tract (mean value ± SD in 2 rats).		
^{214}Pb activity in nasopharynx	1.9 ± 0.5 kBq	10.75 ± 3.9 kBq
^{214}Pb activity in trachea	0.2 ± 0.1 kBq	0.5 ± 0.5 kBq
^{214}Pb activity in lungs	5.0 ± 2.9 kBq/g	5.3 ± 3.2 kBq/g

Table 4 : Percentage of micronucleated and binucleated alveolar macrophages (AM) one week after exposure to 300 WLM under static or dynamic conditions (mean value ± SD in at least 3 rats).

	% of micronucleated AM	% of multinucleated AM
Controls	0.19 ± 0.10	1.34 ± 0.69
Static (fp = 12%)	1.22 ± 0.26	2.91 ± 0.74
Dynamic (fp = 87%)	1.47 ± 0.42	2.30 ± 0.78

<u>2) Dose assessment in the the different compartments of the lungs:</u>

Micronuclei scoring has been performed to estimate dose delivered to the lungs after heterogenous irradiation after exposure to radon and its progeny by inhalation. In a first step, these studies were limited to the deep lung after either extraction of alveolar macrophages (AM) by bronchoalveolar lavages. All theses studies have been performed in close colaboration with AEA/Harwell. Dose estimates were performed after comparison with micronuclei formation induced *in vitro* by irradiation with a particles. We have also shown that, after irradiation, micronuclei formation can be largely increased by an acute ozone exposure which transiently stimulates lung cell proliferation, mainly epithelial cells. By this way we have developed a more sensitive experimental procedure to score micronuclei in post replicative cells on lung thick sections by scanning confocal microscopy allowing to obtain high quality optical section images.

Male Sprague-Dawley rats (OFA/SD, Iffa-credo, France) were exposed at the age of 3 months. The whole-body exposure to radon and progeny was performed at a very high potential alpha energy concentration (PAEC) during 24 hours in the Razes facility at a cumulative dose of 1000 WLM. The equilibrium factor F was 0.8 and the unattached fraction of PAEC *fp* about 10% . One week after radon exposure, a single ozone exposure was whole-body performed during 5 hours at a concentration of 2 ppm. BrdU (5-bromo 2'-deoxyuridine) was administered 18 hours before pentobarbital anaesthesia. Thick cryostat sections (80 mm) of fixed tissue were stained to visualize labelled cells and observed by scanning confocal microscopy (Bisson, 1995).
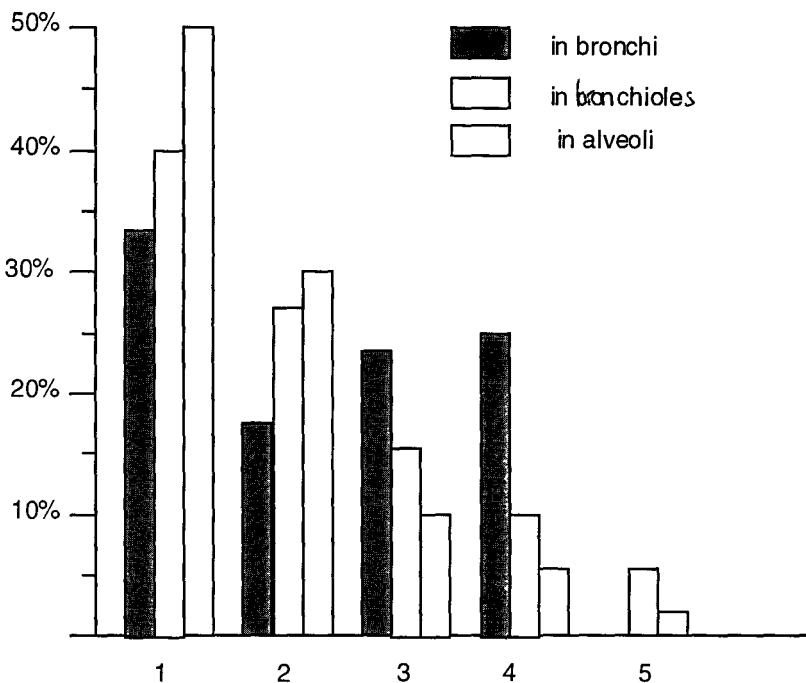
figure 1: percentage of micronucleated cells containing
1, 2, 3, 4 or 5 micronuclei in the different lung compartments of the rats.

Figure 1 shows that about 50% of micronucleated alveolar cells contained only one micronucleus whereas, in alveolar ducts and in bronchi, this population corresponded to 43% and 33% of the total micronucleated cells respectively. The percentage of cells containing 4 micronuclei was higher in bronchi than in bronchioles or in alveoli, 25%, 10% and 5% respectively.

This histological study using a new approach provides very interesting data for dose distribution within the different parts of lung tissues. These techniques have been improved and will be used in the very next future to provide more quantitative results on dose distribution in the different epithelial target cells.

Two different approaches have been performed: a study of nuclear aberrations in alveolar macrophages extracted by pulmonary lavage to estimate dose delivered to the deep lung compartment and an histological study using confocal microscopy to estimate micronuclei frequency in the different lung compartments. Micronuclei frequency in alveolar macrophages was measured from 1 to 5 weeks following irradiations. Dose effect relationships appear linear and 1 WLM correspond to about 7 mGy of gamma rays delivered homogeneously by external

was measured from 1 to 5 weeks following irradiations. Dose effect relationships appear linear and 1 WLM correspond to about 7 mGy of gamma rays delivered homogeneously by external irradiation with [60]Co. A more complete study as a function of time following irradiation is in progress which includes the effect of exposure to 2 ppm ozone during 5 hours from 48 to 72 hours before animal killing. This was performed to increase the spontaneous proliferation of alveolar macrophages. Preliminary results as concerned evolution of micronuclei frequency and maximal observed micronuclei frequency measured after 300 and 1000 WLM are similar to data reported at the Lovelace which have been recently published (Johnson and Newton, 1994). These authors conclude, after a comparison with micronuclei frequency induced by *in vitro* α irradiation that 1 WLM correspond to 10 mGy alpha. Because parameters of alveolar macrophage renewal might be quite different *in vivo* and *in vitro* such dose equivalence cannot be performed. In fact, from our results, taking an EBR value of 3 for induction of micronuclei, 1 WLM corresponds to about 2 mGy alpha a value which is in the range of those previously described but two to three times higher than that reported for deep lung fibroblasts of rats (Khan et al., 1994). We have also studied the effect of exposure conditions on nuclear aberrations. Two conditions were studied, "dynamic" exposure to 171 WLM with and equilibrium factor of 0.2 and 0.7 "unattached" fraction and "static" exposure to194 WLM with and equilibrium factor of 0.8 and 0.08 "unattached" fraction. Although, [214]Pb deposition was 7 times higher in the upper respiratory tract after "dynamic" than after "static" exposure, the lung deposition were similar as were similar the micronuclei frequency in alveolar macrophages .

We have previously proposed an histological method to estimate doses delivered to the different lung compartments. This corresponds to micronuclei measurement in post replicative cells after an appropriated stimulation of cell proliferation induced by acute ozone exposure. These post-replicative cells are visualized on 70 μm thick section by confocal microscopy after immuno-staining of bromodeoxyuridine incorporated into DNA. One week after irradiation, frequency of cells with micronuclei in bronchial epithelial cells appear similar after 7.5 Gy from ^{60}Co and 300 WLM and much higher after 1000 WLM. Preliminary results on the distribution of the number of micronuclei per cell in different lung compartments shown a gradual increase of doses delivered from the alveoli to the bronchial epithelium which is clearly visualized by a gradual modification of the distribution of the number of micronuclei per cell. Further studies are needed to provide quantitative results appropriate for dose estimate. Nevertheless, the results demonstrate that local dosimetry can be accurately performed by histological methods within acceptable time examination. Moreover, after optimal exposures to radon and its progeny or external γ irradiations, significant results can be obtained in few animals. Thus this method could be useful to characterize the delivered doses in different animal species under different exposure conditions taking into account each compartment of the respiratory tract.

3) Carcinogenic studies.

The first studies on the effect of dose rate on lung tumor induction after exposure of rats to low doses (25 to 100 WLM) are now achieved.

Studies on the co-carcinogenic effects of combined exposure to radon and ozone are still in progress.

However, it has ben shown that chronic ozone exposure at 0.2 ppm (6 hours a day, 5 days a week during 6 months) 1 month after the end of irradiation by inhalation of radon and its progeny, increases about twice the lung tumor incidence (40 %). Ozone exposure alone, at concentration which are often measured during episodes of photochemical urban airborne pollution, induces 6 % tumors compared with 0.9 % in controls (7-8). Histological analysis has to be completed to characterise a significant additive or synergic effect of ozone (See final report FI3P-C-920042).

Inducers of cytochrome P-450 1A1 (CYP 1A1) administered at least 1 month after radon exposure appear to be strong synergistic agents inducing distal lung epidermoid carcinomas within a few months. Effects appear similar for metabolised compounds such as methylcholanthrene an 5-6 benzoflavone which form mutagenic or non mutagenic metabolites whereas, tumour induction was deladed after 2,3,7,8 tetrachlorobenzo -p-dioxine treatment which is considered as an unmetabolized inducer. In all cases, immunohistological study has shown an overexpression of CYP 1A1 in target cells located at the bronchiolo-alveolar junction. A more complete kinetic study is still in progress.

4) Lead deposition studies

After inhalation of radon and its daughters, lead deposition in the respiratory tract is a complex phenomenon involving also polonium deposition. In the case of thoron, the half life of ^{216}Po is short enough so that deposition of lead could be more accurately characterised. For that purpose, a small facility has been developed to expose rats to thoron and its daughters. Thoron is formed from 2 Kg ^{228}ThO2 powder which was maintained at about 60 °C. Animals were exposed during 3 hours with or without cigarette smoke as aerosol carrier corresponding to an equilibrium factor of 2 and 27 % respectively. A significant ^{212}Pb deposition of 1000 Bq in lungs was only measured using cigarette smoke. Thus the facility developed appears appropriate to characterize lead deposition within the respiratory tract and its biological behaviour.

Overall Conclusions of the Project

Important developments have been performed during the progress of the project. This was due mainly to the fruitful collaboration established between the two partners involved.

Significant methodological improvements were performed on different topics:

- the metrology of radon and radon daughters in the inhalation chambers atmosphere has been improved and an effort has been undertaken to standardize methods between the two participating laboratories.

- measurements of deposition of radon progeny have lead to comparable results in both laboratories consistent with previous results obtained from *in vivo* studies performed in CEA.

- cellular proliferation and measurement of nuclear aberrations induced in the different compartments of the respiratory tract were performed in both groups.

- an histological method to estimate doses delivered to the different lung compartments has been developed in CEA using micronuclei measurement in post replicative cells after an appropriated stimulation of cell proliferation induced by acute ozone exposure by confocal microscopy.

The collaboration between the two groups should lead to further developments to assess the effect of dose-rate at low cumulative exposure, to compare the induction of lung cancers after exposure to radon and its progeny with that observed after γ rays or X-rays irradiation and to establish the extent to which early biological dosimetric such as nuclear aberrations and cell proliferation might be used to predict late effects from exposure to radon and its progeny.

Publications:

Bisson, M., Richard, H., Altmeyer, S., Morlier, J.P., Monchaux, G. and Fritsch, P. (1993) Effect of radon inhalation on spontaneous and ozone induced proliferation of rat alveolar macrophages. Abstracts of the 25h Annual Meeting of the European Society for Radiation Biology, June 10-14, 1993, Stockholm, Sweden.

Poncy, J.L., Laroque, P., Fritsch, P., Monchaux, G., Chameaud, J. and Masse, R. (1993) An experimental two-stage rat model of lung carcinoma initiated by radon exposure. In: Twenty-Ninth Hanford Symposium on Health and the Environment "Indoor Radon and Lung Cancer: Reality or Myth? ", October 15-19, 1990, Richland, Washington, Part 2, Edited by F.T. Cross, Battelle Press, Columbus, Richland, pp.803-819.

Bisson, M., Morlier J.P., Fritsch, P., Richard, H., Altmeyer, S. and Monchaux, G. (1994) Biological dosimetry in alveolar tisue and early 214-Pb retention in the respiratory tract of the rat after radon exposure under different physical conditions. Annales de la Société Belge de Radioprotection, **19**, n°1-2, 61-68.

Monchaux, G., Morlier, J.P., Morin, M., Chameaud, J., Lafuma, J. and Masse, R. (1994) Carcinogenic and cocarcinogenic effects of radon and radon daughters in rats. Environ. Health Perspect., **102**: 64-73.

Monchaux, G., Morlier, J.P., Morin, M. and Masse, R. (1994) Induction of lung cancer in rats by exposure to radon and radon daughters. Annales de la Société Belge de Radioprotection, **19**, (1-2),.27-60

Strong, J.C., Morlier, J.P., Monchaux, G., Barstra, R.W. and Groen, J.S. (1994) Intercomparison studies in radon exposure facilities for animals in Europe. Final report of a EULEP Task Group. EULEP Newsletter, **76**, 14-18.

Bisson, M., Poncy, J.L., Strong J.C., Baker, S., Monchaux, G. and Fritsch, P. (1994) Biological dosimetry in different compartments of the respiratory tract after inhalation of radon and its daughters. Radiat. Protect. Dosimetry, **56**, 89-92.

Douriez, E., Kermanac'h, P., Fritsch, P., Bisson, M., Morlier, J.P., Monchaux, G., Morin, M. and Laurent, P. (1994) Cocarcinogenic effects of cytochrome P 450 1A1 (CYP 1A1) inducers for epidermoid lung tumor induction in rats previously exposed to radon. Radiat. Protect. Dosimetry, **56**, 105-108.

Morlier, J.P., Morin, M., Monchaux, G., Pineau, J.F., Chameaud, J., Lafuma, J. and Masse, R. (1994) Lung cancer incidence after exposure of rats to low doses of radon: influence of dose rate. Radiat. Protect. Dosimetry, **56**, 93-97.

Monchaux, G. and Masse, R. (1994) Radon: occupational or domestic carcinogen? Radiat. Protect. Dosimetry, **56**, 81-88.

Trédaniel, J., Bisson, M., Fritsch, P., Monchaux, G. and Masse, R. (1994) The increase of pulmonary alveolar macrophage (PAM) population after ozone inhalation: relative contribution of monocyte migration and PAM proliferation. Ann. Occup. Hyg, **38,** suppl. 1, 961-967.

Bisson, M., Fritsch, P., Trédaniel, J., Sabattié, P., Morlier, J.P. and Monchaux, G. (1994) Cell proliferation in the adult lungs of controls and ozone exposed rats. In: *Electron Microscopy 1994*, Proceedings of the 13th International Congress of Electron Microscopy, Paris 17-22 July 1994, Volume 3B, Applications in Biological Sciences, pp. 1269-1270.

Morlier, J.P., Bisson, M., Janot, M., Fritsch, P., Pineau, J.F., Morin, M. and Monchaux, G. (1995) Deposition of 214Pb and nuclear aberrations in alveoli of rats after exposure to radon under different conditions. Accepted for publication in Sci. Tot. Environment.

Bisson, M., Fritsch, P., Morlier, J.P., Sabattié, P., Trédaniel, J., Richard-Le Naour, H. and Monchaux, G. (1995) Dose repartition in alveoli, alveolar ducts and bronchi cells of rats exposed to radon and its progeny. Accepted for publication in Sci. Tot. Environment.

Bisson, M., Fritsch, P., Trédaniel, J., Morlier, J.P., Monchaux, G. and Masse, R. (1995) Kinetics of spontaneous and ozone-induced nuclear aberrations in rat pulmonary alveolar macrophages after local irradiation. Submitted to Int. J. Radiation Biology.

Morlier, J.P., Fritsch, P., Janot, M., Pineau, J.F., Morin, M. and Monchaux, G. Compared deposition of radon 222 and radon 220 (thoron) progeny and nuclear aberrations in the respiratory tract of rats after exposure under different aerosol conditions. Sumitted to IRPA 96, Vienna.

Final Report
1992-1995

Contract: **FI3PCT920021**   Duration: **01.09.92-30.06.95**   Sector: **B15**

Title: **Dose assessment, early cellular and late carcinogenic effects of exposure to radon and its progeny**

1)   Fritsch   CEA Paris
2)   Collier   UKAEA

1.   SUMMARY OF PROJECT GLOBAL OBJECTIVES AND ACHIEVEMENTS

Head of Project 2: Dr C G Collier

II Objectives during reporting period:

1)   Standardisation of radon metrology, to ensure that results obtained by participating laboratories during exposures are directly comparable.

2)   Studies of the effect of exposure conditions on respiratory tract deposition of radon daughters in the rat.

3)   Studies of the early sub-acute effects of radon on the epithelial cells of the rat respiratory tract, using proliferation and nuclear aberrations incidences as indicators of radiation damage.

4)   Studies of the early sub-acute effects of radon exposure on respiratory tract cells using damage to DNA as and index of potential carcinogenicity

5)   Initiation of life-time carcinogenicity studies to investigate dose and dose rate effects on radon induced lung-tumour induction over a suitable range of dose levels.

III progress achieved including publications:

1) *Standardisation of radon metrology*

In order to effectively evaluate the radiation dose to the lung (normally in rats or mice) several radiological and aerosol parameters are required. These should include individual radon daughter concentrations (^{218}Po, ^{214}Pb and ^{214}Bi) together with a knowledge of the fraction of these nuclides which have not become attached to aerosol particles, normally termed the "unattached" fraction. Intercomparison exercises were therefore undertaken at the facilities of the two collaborators; at CEA in June 1992, and AEA in Sept. 1993. The measurements included comparisons of the techniques used to estimate radon progeny concentrations in air. Measurements were made with animals present in the chambers (36 rats at AEA and 200 rats at CEA). AEA made radon progeny concentration measurements in both facilities whereas CEA, due to the non-portability of their equipment, only made these measurements in their own facility. At AEA, air was recirculated through the chamber at 0.7 air changes an hour and carnauba wax aerosols were generated continuously, providing "unattached" PAEC fractions of the order 1 %. Measurements were also made with no added aerosol to provide 'unattached' fractions of 55%. Measurements were made in the CEA facility without ventilation and without aerosols being generated.

Before measurements were made on the chambers, sampling flowrates and ^{241}Am reference source activity was intercompared. It was concluded that in the case of flow measurements CEA were underestimating by about 10% for the rates normally used for sampling.

Grab sampling techniques followed by gross alpha counting of the filter during three time periods using the methods of Thomas (1971) were used by both groups to determine radon progeny concentrations, although different sampling flow rates and sampling/counting regimes were used. AEA also provided measurement data from their semi-continuous radon progeny measurement system (AEA-2) which employs alpha spectrometry, this system also supplies data on the 'unattached' fractions (Strong, 1990). This device was used at CEA and AEA and results obtained in this way agreed with those from the standard grab sampling method used by AEA to within ± 5%. The estimates of PAEC were in good agreement (mean ratio of AEA:CEA measurement 0.98 range 0.8-1.2), and estimates of individual daughter concentrations were also in agreement (mean ratios 1.03, 0.97 and 1.02 for ^{218}Po, ^{214}Pb and ^{214}Bi respectively).

'Unattached' fractions were measured by using screen/filter combination techniques and were only compared at the CEA facility. Both AEA and CEA compared the alpha activity on both the screen and the backing filter. Filters and screens were analysed in the same way as the plain filter samples for radon daughter concentration, using a three gross alpha count method (Thomas, 1971). Three measurements were made at the CEA facility at both low and high 'unattached' fractions. Very good agreement was seen at a high 'unattached' fraction (0.62:0.67 AEA:CEA). This was not so close with the two measurements at the low 'unattached' fraction (0.14:0.21 and 0.13:0.1 for AEA:CEA).

These intercomparison exercises resulted in improvements of the methods used by both groups, have shown that the groups are in reasonable agreement, especially in the case of PAEC, and have shown that the collaborating laboratories are able to produce exposure data comparable to each other.

2)   *Effect of exposure conditions on respiratory tract deposition of radon daughters in the rat*

Estimates of the radon progeny deposited in the lungs of animals exposed for short periods, between 3 and 4 hours, were made during the metrology intercomparisons. Only one rat was measured at CEA, whereas at AEA five different studies each with 3 rats were used. After exposure, the animals were removed from the chambers and killed by intraperitoneal injection of sodium penta barbitone. The lungs were excised and then counted by gamma ray spectrometry by both groups. CEA used a germanium detector while AEA used NaI detectors. CEA used reference sources, uranium ore and ^{226}Ra respectively, to calibrate their detectors, whereas AEA took a filter sample at the end of the exposure which was analysed by gross alpha counting (Thomas, 1971) and then gamma counted. The alpha counts provided an estimate of the individual radon progeny on the filter at the cessation of sampling from which the activity of ^{214}Pb and ^{214}Bi at the time of gamma counting could be calculated, thus two calibration factors for ^{214}Pb and ^{214}Bi were established for each exposure. To compare the validity of the AEA method with that used by CEA, the mean calibration factors (standard deviation of $\pm$ 7.7% for ^{214}Pb and 2.5% for ^{214}Bi) calculated from those obtained from the six exposures at AEA were used to estimate the activity of a ^{226}Ra source (1.998 kBq). The activities of ^{214}Pb and ^{214}Bi were found to be 1.67kBq and 1.75 kBq, thus AEA underestimate the activities of these nuclides by 16% and 12% respectively. Corrections for decay were made by CEA using a graphical technique to estimate the activity of ^{214}Pb and ^{214}Bi at the end of the exposure. AEA calculated these corrections using standard decay equations. The samples were also weighed so that lung deposition could be specified in terms of activity per wet weight of tissue (Bq g^{-1}). In the one rat measured at CEA, considerable discrepancies were found in the levels of ^{214}Bi between the two groups. A reassessment of the methods employed resulted in much closer agreement by the time of the second comparison conducted at AEA, the results for individual animals during this study are given in table 1.

| Test/ | Lung deposition, Bq gm^{-1} measured by AEA/CEA | | |
Nuclide	Rat-1	Rat-2	Rat-3
1 ^{214}Pb	600/400	560/300	400/450
^{214}Bi	830/650	860/450	550/650
2 ^{214}Pb	800/650	770/700	530/550
^{214}Bi	680/800	370/650	530/600
3 ^{214}Pb	2290/2050	1910/1900	1210/-
^{214}Bi	4330/4100	4070/4000	3210/-
4 ^{214}Pb	2080/1900	1750/1800	2150/2000
^{214}Bi	2890/3000	2410/1600	2560/2500
5 ^{214}Pb	3350/3400	2410/2500	2410/2700
^{214}Bi	4210/4400	3830/2600	3560/3500

Table 1
Deposition of ^{214}Pb and ^{214}Bi measured by both groups in the same animals

Deposition measurements have been made during all of the exposures conducted for the life-span studies. Animals (n=26) for the deposition measurements were normally exposed for a minimum of four hours to potential alpha energy concentrations in the range 600 to 1700 working levels (WL) at 'unattached' fractions of less than 0.015. After removal from the chamber the animals were killed by interperitoneal injection of sodium pentabarbitone. The lungs were excised, weighed and then counted using gamma ray spectrometry. The 218Po, 214Bi and 214Pb activities deposited were calculated in terms of Bq g-1 from the wet weight of the individual lungs. These data were plotted against the potential alpha energy (PAEC) in the chamber during the exposure for all three nuclides. A representative plot (in this case for 218Po deposition) is shown in Figure 1. Lines were fitted to each set of the three sets of data using a standard least squares linear regression technique, in this way it was possible to obtain the deposition rates shown in Table 2. The errors shown are the standard error values for the slope coefficients calculated from the least squares regression method.
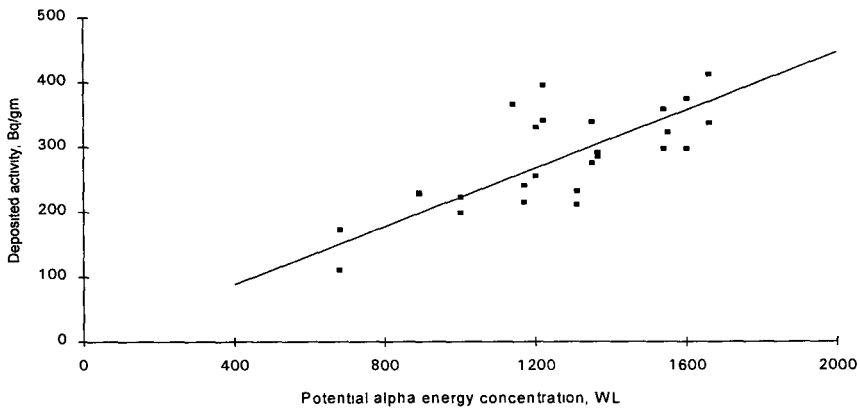
Figure 1
Deposition of ²¹⁸Po in rat lungs compared to the PAEC in the exposure chamber

Nuclide	Deposition, Bq g⁻¹ per WL
^{218}Po	0.22 ± 0.01
^{214}Pb	1.33 ± 0.04
^{214}Bi	1.80 ± 0.06

Table 2
Deposition rates of ²¹⁸Po, ²¹⁴Bi and ²¹⁴Pb in rat lung

Goodness of fit using both F and t statistics indicated that the slope coefficients were useful for predicting the deposition of ^{218}Po, ^{214}Bi and ^{214}Pb from the potential alpha energy concentration at the high attachment fractions used in this study. As the deposition rate of all three progeny in the lung during exposure had been found in terms of potential alpha energy concentration it was then possible to estimate the absorbed dose to the lung for unit exposure. Using the alpha particle energies of 6.0 and 7.68 MeV for ^{218}Po and ^{214}Po, respectively, the absorbed dose-rate to whole lung was found to be 2.4×10^{-9} Gy s⁻¹ per WL. Thus an integrated exposure of 1 Working Level Month (WLM) will result in an absorbed dose of 1.5 mGy to the rat lung. Studies by Bisson et al (1994) in which the incidence of micronuclei in alveolar macrophages following radon/radon daughter exposure was compared with that induced following thoracic irradiation using ^{60}Co gammas, indicated that 1 WLM induced about the same increase as 8-9 mGy of gamma. These two results are consistent if the biological effectiveness for alpha irradiation was in the region of 6 for micronucleus induction in alveolar macrophages.

3)   *Early sub acute-effects of radon on epithelial cells of the rat respiratory tract.*

In 1992, two studies were conducted in which the incidence of nuclear aberrations at various times after exposure were determined. In an earlier study, Sprague Dawley rats had been exposed in the CEA Razes facility to 4 levels of potential energy alpha concentrations (PAEC), ranging from 150 to 1000 WLM. The dose rate in these studies was constant at about 8 WLM/hr. In the first 1992 study (again exposed at Razes), Sprague Dawley rats were exposed to either 250 or 1000 WLM at dose rates of 10 and 40 WLM/hr respectively. In the second 1992 study, Sprague Dawley rats were exposed in the AEA facility at Harwell at a level of 880 WLM and dose rate of 10 WLM/hr. In all studies, groups of at least 3 rats were killed at various times after exposure. The lungs were lavaged and alveolar macrophages recovered. Analysis of cytospin preparations was performed at AEA to give the incidence of nuclear aberrations in the alveolar macrophages. The types of aberration observed were micronucleated cells, bi-nucleated cells and cells containing more than one type of aberration. For all the studies and types of aberration, the incidence of aberration was observed to peak at about 14-21 days after exposure and then return to control levels by about 70 days after exposure (Figure 2). The magnitude of the response was related to dose within any study, but there were variations in the extent of the response between studies.

Proliferative responses have been measured in the lung epithelium of the animals killed for early effects studies. Bromodeoxyuridine (an analogue of thymidine) is used to label cells which have undergone proliferation during the labelling period (4 hrs in these studies). The cells are visualised using immuno-histochemical staining techniques. In the first study, using animals exposed at the CEA facilities at Razes, proliferation was measured in four areas: alveolar, bronchiolar, bronchial and tracheal epithelium. Peak responses were observed between 14 and 21 days after exposure, with the alveolar response occurring slightly later than the bronchial. The highest response was observed in the bronchial epithelium, which is to be expected as this area probably receives the highest dose following radon daughter exposure. A linear dose response was observed in all regions (Taya et al 1994). Similar responses were observed in the two further studies.
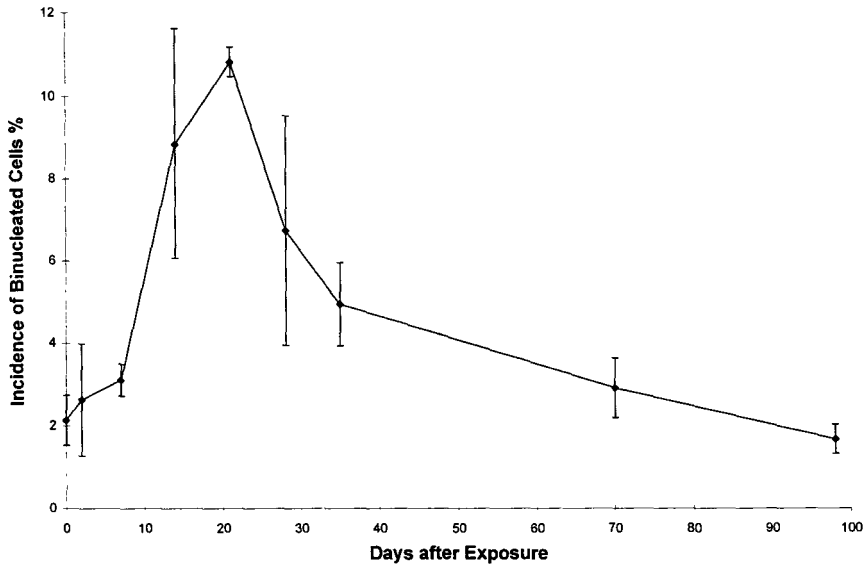
Figure 2
Time course of incidence of binucleated alveolar macrophages
following radon/radon daughter exposure (n<4 ± Std Err)

In 1993, a study was conducted to determine the effect of animal age at exposure on the early effects of radon/radon daughter exposure. Studies conducted by other groups (CEA and TNO) have shown considerable variation in the age of animals at exposure (4 weeks to 6 months). Prior to commencing life-span studies, knowledge of the effect of age on response to radon/radon daughters was required in order to determine the age of animals to be used for such studies. Cell proliferation at 14 days in the alveolar and bronchial epithelium was used as the marker for the early responses in these studies. Animals ranging in age from 4 to 40 weeks were exposed in the AEA facility over a period of one week to a total dose of 440 WLM. Animals were maintained for 14 days and then cellular proliferation was determined. The incidence of proliferating cells in the alveolar region is given in Figure 3 for both the control and exposed animals. The youngest animals showed the highest proliferation rates (at least 10 fold higher than the adult animals). In both exposed and un-exposed animals, the elevation above adult levels fell with age and by 12 weeks the levels were as for the adult animals. Exposure to radon/radon daughters resulted in an increase in proliferation of between 2 and 6 fold. The study demonstrated that the use of animals less than 12 weeks of age would not be appropriate in dosimetric studies and raised doubts about their suitability for life-span studies as the higher proliferation rates could result in higher cell death and therefore lower tumour incidences. As a result of the uncertainties over the use of young animals, it was decided that as a rule, only animals older than 12 weeks would be used to study radon exposure effects at AEA (Baker S T 1994: Collier et al 1995).
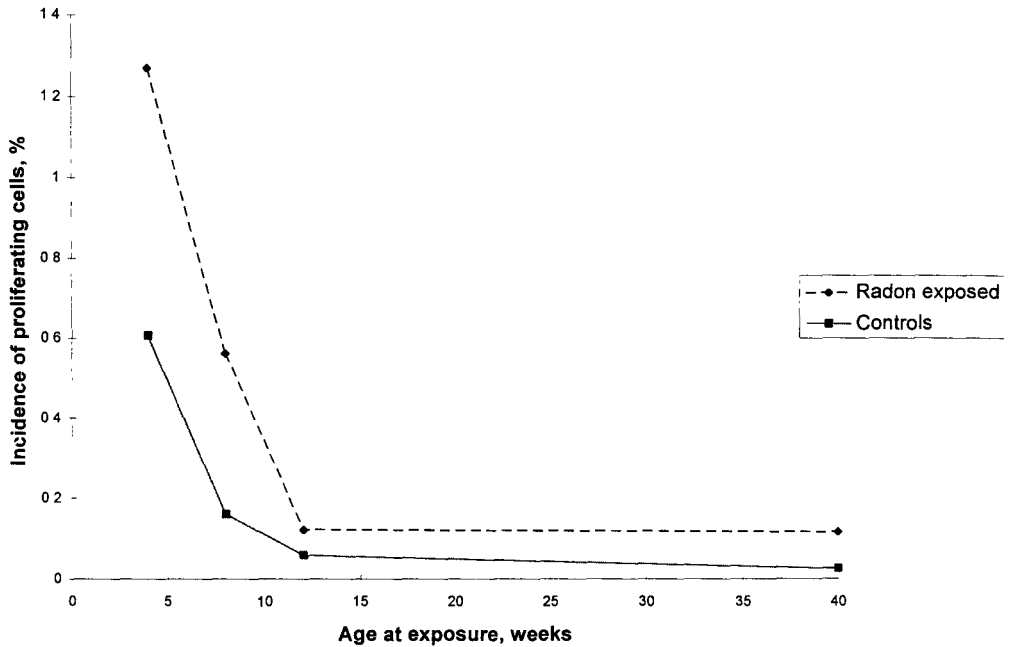
Figure 3
**Incidence of proliferation in animals of different ages**

In 1994, exposures for life-time studies on lung tumour induction commenced. Adult male Sprague Dawley rats were exposed in groups, to doses ranging from 200 to 3200 WLM at a dose rate of 1000 WL. From each exposure group, two animals were taken 14 days after exposure to assess early effects on nuclear aberrations and epithelial proliferation (n=28). The incidence of nuclear aberrations in the alveolar macrophages was determined on the cytospin preparations. The incidence of cells containing one or more micronucleus, two nuclei (binucleated cell) or multiple micronuclei (including fragmented nuclei) was determined. The incidence of micro nucleated cells increased with increasing exposure up to 1500 WLM. At the highest exposure level (3100 WLM) there was a decrease in the incidence of micro-nucleated cells compared with that at 800 WLM. For binucleated cells there was a dose dependant increase in incidence up to 800 WLM, which then levelled off. For cells containing multiple micronuclei (including fragmented nuclei), there was a dose dependent increase in incidence throughout the range of the doses studied. The decline in the incidence of binucleated and micro nucleated cells was directly related to the increase in the number of cells with multiple micro- or fragmented nuclei. The incidences of each form of aberration are shown in figure 4. Fragmentation of the nucleus is a characteristic of apoptotic cells and it is possible that apoptosis is responsible for the appearance of cells containing fragmented nuclei at the high dose levels. Further studies are planned to investigate this further.

Following page - **Figure 4. Incidences of nuclear aberrations in alveolar macrophages recovered at 14 days after exposure from animals exposed for life-span studies**
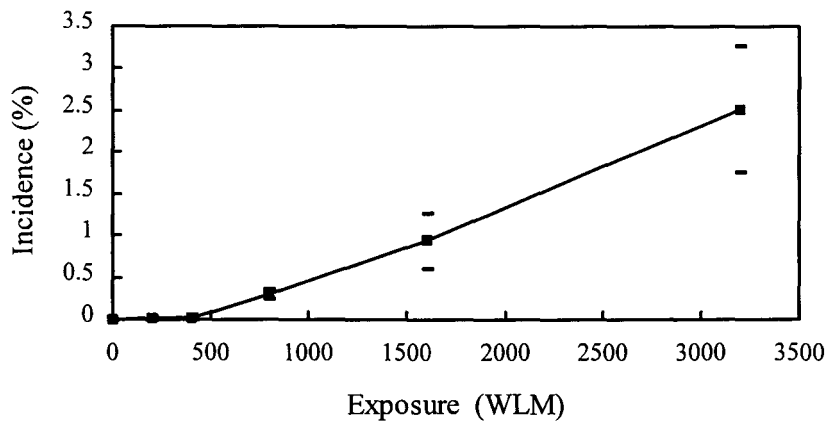
a) Binucleated Alveolar Macrophages
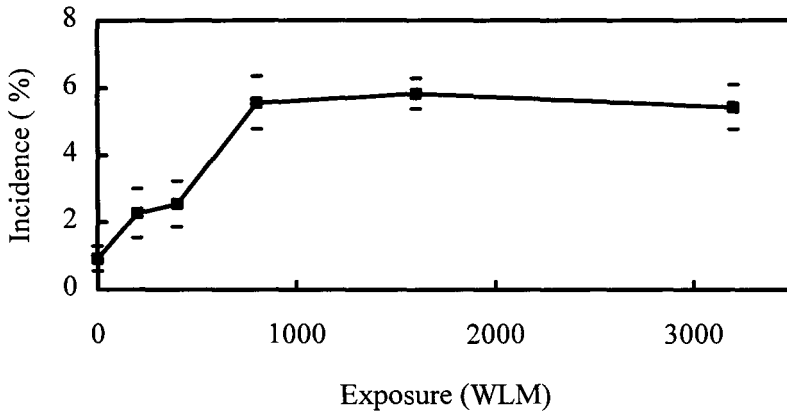
b) Micronucleated Alveolar Macrophages
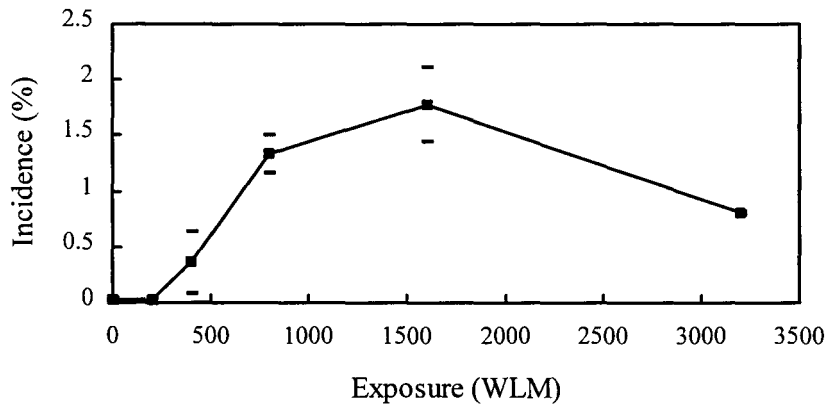
c) Multi micronucleated Alveolar Macrophages (including cells with fragmented nuclei)

Cell proliferation was measured in 2 animals from each exposure conducted for the life-span studies. These were the same 28 animals as used for nuclear aberrations effects measurements. All animals were killed at 14 days after exposure. In the alveolar region, proliferation rose to a peak at 800 WLM and then fell to levels below those of unexposed animals at exposures of 3200 WLM. In the bronchiolar region, proliferation peaked at between 200 and 400 WLM and again fell to levels below those of control animals at higher doses. The incidence of proliferating cells in the alveolar and bronchial regions are given in Figure 5. The highest response (control:peak response ratio) was observed in the alveolar region, with a five-fold increase in proliferation. The bronchial epithelium showed a response of a three-fold increase. In the earlier studies (Taya et al 1994) the bronchial epithelium had been the most sensitive. The fall in proliferation at the higher doses is probably due to cell killing. The proliferative response in the alveolar region had a peak at slightly lower doses than that of micronucleus induction in the alveolar macrophages (peak at 1600 WLM), but was similar to the level at which the maximal response for binucleated cells was first observed. The incidence of proliferation and nuclear aberrations will be related to lung tumour incidences at the end of the study to determine whether early effects markers can be used to determine late effects.

Both nuclear aberrations and cell proliferation indicated a dose-response to radon/radon daughter exposure at 14 days after exposure. The response is more clearly identifiable with the nuclear aberrations than with the proliferation, as even following radon exposure, the incidence of proliferating cells is very low in the respiratory tract. The validity of the use of early markers to predict late effects will not be known until the life-span study is complete.

4)   *Studies of the early sub-acute effects of radon exposure on respiratory tract cells using damage to DNA as and index of potential carcinogenicity*

In addition to the early effects being studied for dosimetry, changes in gene expression are being investigated both in animals killed immediately after exposure (deposition animals) and in the life-span animals. Initially, frozen sections were cut from lungs of animals used for deposition studies. These animals had only been exposed for a maximum of 5 hrs and hence had only received about 40 WLM. For animals in which carcinogenicity was being studied (doses 200-3100 WLM), which have died, wax sections were cut from the right apical lobes of the lungs following fixation in buffered formalin. Initially p53 (clone CM1) and PCNA (clone DO10) have been examined, with pan-cytokeratin as a control. No increased expression of either protein was observed in sections from the deposition study animals. Studies on the life-span animals are still in progress.

5) *Initiation of life-time carcinogenicity studies to investigate dose and dose rate effects on radon induced lung-tumour induction*

In 1994, approximately 700 rats were exposed in the first life-span study to be conducted using the AEA radon facility. This study is a dose-response study conducted at constant dose rate (~1000 WL), with total exposures ranging from 200 to 3100 WLM. The rats were the same age and strain as those used by CEA (France) in their life-span studies and one objective of this study is to demonstrate comparable results with those obtained by the CEA. The dose levels chosen were expected (from CEA results) to cover the peak lung tumour incidence (about 1000 WLM) and to extend into a region where incidence of lung tumours falls off due to cell killing.

a)   Proliferation in bronchiolar
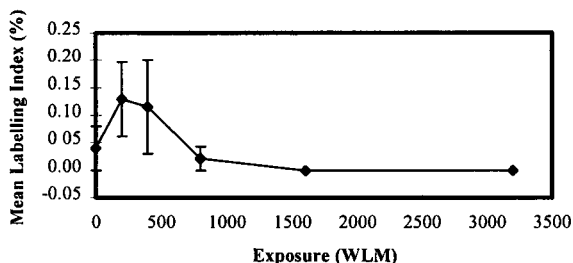
b) Proliferation in alveolar region
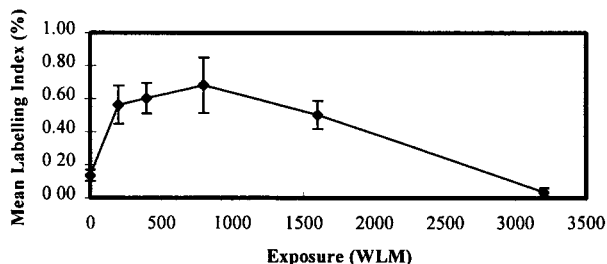
Figure 5
Proliferation in lung regions following exposure during life-span studies
(n=4, mean ± Std Err)

Five groups of adult male Sprague Dawley rats have been exposed at doses ranging from 200 to 3100 WLM. The dose rate in terms of PAEC for these exposures has been kept constant (approximately 1000 WL) and hence the doses received by each group have been determined by the exposure period (minimum 1.5 days, maximum 20 days). The animals were co-exposed to an aerosol of Carnauba wax (count median diameter 0.15 μm) which acted as a vector aerosol for the radon progeny and resulted in 'unattached' fractions for PAEC of 2%. The numbers of animals in each dose group are given in Table 4. Approximately thirty five animals were exposed simultaneously and hence multiple exposures were required for each dose group (total 14 exposures). Actual exposure levels (WLM) for each exposure are given in Table 4 along with the numbers of animals on life-span study, those taken for deposition measurements (see section 2) and those taken for early effects (see section 3) In addition, two groups of control animals are being maintained. One group has been exposed for 4 weeks to Carnauba wax aerosol only, the other group are cage controls. The majority of the animals are now being maintained for their life-span. There have been very few early deaths to date, indicating that the exposures are not causing acute effects. In addition, differential cell counts conducted on lavage fluid recovered from animals killed at 14 days after exposure showed no evidence of an inflammatory response at doses between 0 and 800 WLM. A slight increase in lymphocytes and neutrophils was observed at 1600 WLM, which was more pronounced at 3200 WLM. These two highest dose levels were predicted from studies at CEA to have lower lung tumour incidences than the peak incidence at about 1000 WLM, probably due to cell killing. The facts that a mild inflammatory response was seen in these animals; cell proliferation was decreased (see section 4); incidence of micronucleated and binucleated alveolar macrophages was decreased at the highest dose; and the indication that apoptosis may be occurring at the highest dose level in the alveolar macrophage (see section 4) all indicates that the doses chosen, cover the range of peak effect and up into doses where cell killing effects begin to occur to a significant extent.

Nominal exposure WL	Individual Exposure levels WL	Number exposed	Life span study	Deposition Study	Early effects study
200	174,195, 250,254	168	156	6	6
400	382, 383, 390	122	118	4	4
800	758, 795, 801	112	106	2	4
1600	1577, 1586, 1594	116	102	8	6
3200	3095	44	36	6	2
Sham	0	72	68	0	4
Cage controls	0	52	52	0	2

Table 4
Details of nominal exposure levels, actual exposure levels attained in individual exposures, number of animals exposed and numbers taken for life-span, deposition measurements and early effects studies in dose-response study I

Full post-mortem examinations will be conducted at death of the life-span animals. Techniques to identify the total number of tumours in the lungs of each animal at death using macroscopic techniques are being investigated. Full histopathological evaluation of all lesions will be conducted. It is anticipated that this study will continue for three further years. The dose response relationship for lung tumour induction will be compared with that obtained by the CEA.

Title: Induction of osteosarcoma and leukaemia by bone-seeking alpha-emitting
          radionuclides.

1)   Höfler   GSF
2)   Harrison   NRPB
3)   Wright   MRC
4)   Erfle   GSF
5)   Skou Pedersen   Univ. Århus
6)   Höfler.   Univ. München - Technische

I. Summary of Project Global Objectives and Achievements

I Summary of Project Global Objectives and Achievements

The objective of this project was the identification of the mechanisms of radiation-induced carcinogenesis. Two experimental strategies were defined that use as a model system the radiation-induced carcinogenesis of bone and bone marrow. The first series of experiments entailed the characterization of the metabolic pathways of alpha-emitting radionuclides, and subsequently identification of the cellular targets for radiation carcinogenesis. The second series of experiments were designed to identify the molecular events involved in radiation carcinogenesis in these tissues.

Introduction
Although the therapeutic application of alpha-emitting radionuclides has to a large extent ceased, both occupational and non-intentional exposures continue. Radiation protection strategies define acceptable limits of exposure based upon the increased probability of malignant growth following from irradiation. Assessment of the carcinogenic potential of low doses and low dose rates of radiation pose particular difficulties, as inferences must be made from both epidemiological and experimental data obtained at higher levels of exposure. A more precise elucidation of the carcinogenic process will allow identification of any molecular changes in tumor cells generated following radiation exposure. The application of any such molecular indices would permit more accurate quantification of the cellular effects of radiation exposure at low doses. Consequently direct assessment of dose-response effects would be possible on both a population and individual basis. Furthermore, understanding the molecular processes would have the additional benefit of identifying those individuals within the population particularly at risk from exposure to ionizing radiation.

The metabolic pathways of alpha-emitting radionuclides, and the cell populations undergoing carcinogenic transformation after exposure to alpha-radiation.
Observations in human populations exposed to bone-seeking alpha-emitting radionuclides have established that tumors of the haematopoietic and skeletogenic systems are the predominant radiation-induced malignancies. The clinical experience is closely mirrored by in vivo animal studies, which confirm the radiation-sensitivity of these tissues. However, little is known about the target cell population affected by the alpha-irradiation. The more precise delineation of this population is an essential step in unravelling the molecular events responsible for radiation carcinogenesis.

The osteoblast lineage is initiated by commitment and differentiation of mesenchymal stem cell population resident within the bone marrow. These cells give rise to the osteoblastic cells on bone surfaces, which in turn terminally differentiate to give the long-lived osteocyte cell population of mature bone. The process of cell generation is continual due to the ever present remodelling of adult bone. Theoretically the entire lineage may be at risk from radiation exposure, and give rise to tumors at any stage of development from marrow precursors to mature bone cells. Irradiation of the sensitive cells may take place in the bone itself, but also within the marrow. We have attempted to define the points at which interaction between bone cells and carcinogenic radiation takes place. In contrast the hematogenic bone marrow is relatively well defined, in both its lineages and location. The leukemiagenic potential of alpha-emitting radionuclides in the marrow was examined in part in collaboration with the CEC Radiation protection project CT920064.

Studies carried out by VITO have established an in vitro culture model of osteogenic differentiation from murine bone marrow precursors. The administration of Americium 241 to mice prior to analysis of marrow cell population induced a dramatic increase in the in vitro proliferation of the cells of the osteogenic lineage. The in vivo data from NRPB indicate that a significant proportion of administered

Americium 241 does indeed enter the marrow cell mass. Thus the osteogenic stem cell must be considered as a potential target of osteosarcomagenic radionuclides that otherwise are deposited in bone.

In vivo data from NRPB has also established that a number of other radionuclides are able to enter the skeleton, and ultimately irradiate osteogenic and hematopoietic marrow elements. In particular Polonium 210 contamination was shown to result in some 10% of the dose reaching the marrow. Polonium 210 was administered in vitro in the VITO cell culture system, and the effects upon skeletogenic precursor cells examined. Significantly, the addition of Polonium 210 to cultures of marrow derived cells potentiated the proliferation and osteogenic differentiation. The effect was not seen directly on the putative stem cell (CFU-F) population, but on cells derived from CFU-F derived precursors. One consequence of transformation of these mesenchymally derived precursor cells would be their potential to develop mixed-cell tumors, containing differentiated cells representing other mesenchymal lineages such as adipocytic, fibroblastic and myxoid. Indeed, reassessment of human data from alpha-particle contaminated subjects suggests a significant proportion of osteosarcoma tumors may indeed be admixtures of different differentiated cells (e.g. malignant fibrous histiocytoma). Other tumors are restricted to a pure osteoblastic lineage, and presumably arise from the more committed osteogenic cell precursors. The GSF-IMV has analyzed the effects of irradiation on a series of osteogenic cell lines established from murine chondylus tissues derived from transgenic animals. The expression of dominant oncogenes in these cells appears to provoke an increased proliferation of the osteogenic cell lineage, and these cells were subjected to in vitro irradiation. Whilst irradiation alone was able to induce cell transformation it was demonstrated that retroviral infection could potentiate the transforming effect. Thus, the sensitive cell population appears in this case to be a cell comitted to the osteoblastic lineage, sensitive to retroviral infection and the subversion of normal cell growth by the virus genome.

The radionuclide distribution studies of the NRPB have concentrated upon three bone-seeking radionuclides Plutonium 239 , Americium 241 and Uranium 233. The dose distribution studies show the majority of the injected radionuclide that is retained is deposited within the skeleton (85% of retained Plutonium 239, 88% of retained Americium 241 and 97% of retained Uranium 233). Differences in the skeletons ability to handle the various radionuclides were also established. All three radionuclides deposited on the endosteal surface of those bones having a large interface with the blood and marrow cavities. Plutonium appeared to also deposit on the periosteal surface of the bones. The remodelling of the murine skeleton is minimal during growth, and consequently redistribution of the radionuclides was not dramatic as the animals aged. There was an approximate correlation with the bone-deposited dose and the incidence of osteosarcomagenesis in these animals, where Plutonium 239 resulted in significantly more osteosarcoma incidence (18% vs 8% and 4% for Americium 241 and Uranium 233 respectively. This suggests that a sensitive cell population also resides within the endosteal region of those bones with a high surface area in contact with the marrow and blood spaces.

The deposition of radionuclides in the marrow may result in direct irradiation of hematogenic marrow cell elements, as well as that of the osteogenic lineage. Indeed NRPB studies have shown that the deposition of injected radionuclides Plutonium 239, Polonium 210 and Americium 241, and to a lesser extent Uranium 233, results in concentration at the marrow-bone interface. Thus marrow elements may also be indirectly irradiated. The frequent juxtaposition of proliferating marrow cell populations and the skeleton makes this a highly plausible mechanism. Studies by the MRC have shown that non-clonal genetic alterations (both chromosomal instability and the appearance of point mutations within a target gene) are increased in the daughters of progenitor cells exposed to alpha-irradiation. Whilst of significancefor the mechanistic insight, this data also suggest that the alteration in

the hematogenic marrow is the result of a mutation in the stem cell, transmitted to progeny, that affects the ability of the cell to retain the integrity of its genetic information. In vivo studies have been performed by the MRC that confirm the stem cell origin of the effect. Thus, the instability phenotype was retained for at least a year in animals reconstituted by irradiated bone marrow. The mechanistic basis of the instability appears to be generated as a consequence of irradiation damage, as the ability of the stem cell to survive a single alpha particle transit was demonstrated in vitro (see below).

Molecular events in alpha-particle induced radiation carcinogenesis

There is a hierarchical set of molecular events involved in radiation carcinogenesis, starting with alteration of the DNA, through disturbance of the function of individual genes and finally culminating in the alteration of cellular functions that result in loss of growth control and malignancy. Over the last decade there has been a rapid advance in understanding the molecular mechanisms involved in the carcinogenic process. The number of genes that are directly affected by mutations in tumor cells is limited, the majority of those identified exert regulatory control over the rates of cell proliferation, differentiation and apoptosis. Molecular analysis of the genetic events in radiation-induced carcinogenesis will focus upon identifying which mutational events take place.

The role of genetic factors in determining carcinogenic risk was firmly established by the experiments of the GSF-P. In a mouse model system they have introduced gene mutations into the male germ line by chemical mutagenesis. The offspring of these mutagenised parents were shown to be at a significantly increased risk of radiation-induced osteosarcoma, with a marked shortening of the tumor latency period. Thus we can conclude that heritable factors can influence susceptibility to radiation-induced malignancy. This observation makes it possible to define future studies to identify the genes responsible for determining susceptibility.

The methods available for the analysis of gene mutations has changed dramatically during the course of the project. A range of different alternatives has been tested by the TUM and their relevance to the detection of gene alterations in radiation induced tumors evaluated, in particular the possible mutation of the p53 tumor suppressor gene locus. These studies have demonstrated that immunohistochemical study of p53 mutations is prone to generate both false-postive and false-negative results. Single-stranded polymorphism conformational (SSCP) analysis proved highly effective in detecting single base alterations in the p53 sequence, but could not be recommended as the method of choice for analysis of large sample numbers as the frequency of such mutations appears low in the samples of radiation induced osteosarcomas studied (see below). Finally a reverse-transcription and polymerase chain reaction (RT-PCR) approach was adopted, and the PCR product sequenced completely. This approach was consequently employed by the GSF-P for the characterization of p53 mutations.

The p53 tumor suppressor gene is implicated in the regulation of DNA repair and genome stability. Thus, in cells subjected to DNA damage p53 mediates cell cycle transit to allow repair or to initiate cell suicide in severely damaged cells. Consequently loss of p53 function would be anticipated to have dramatic repercussions for the integrity of the genome in irradiated cells. In a collaboration between the GSF-P and the GSF-IMV it was established that p53 gene mutations were a frequent occurrence in radiation-induced osteosarcoma cell lines. The frequency of p53 mutations in these preliminary studies was close to 100%, suggesting that loss of p53 function may be a key event in radiation carcinogenesis, particularly in the skeleton. Efforts to repeat this observation in tumor tissue have met with only moderate success. In a series of 18 osteosarcomas generated by treating Balb/c and NMRI mice with the alpha emitter Thorium 227 p53 gene mutations were only detected in 5 cases (28%). Whilst 4/5 mutations were deletions, indicative of direct radiation-induced mutagenesis, the majority of tumors did not exhibit p53 mutation. Thus, it must be assumed that some of the mutations observed earlier in cultured cells

may arise during the culture period, or that single cells within the tumor containing such mutations possess a strong growth advantage in vitro. Nevertheless, p53 gene loss is certainly evident in a proportion of tumors arising after irradiation, and must certainly contribute to the carcinogenic process.

The activation of retroviral sequences, regarded as constitutive passive bystanders within the genome, may play a role in the etiology of the malignant cells generated by irradiation. Studies by the GSF-IMV and the IMB have continued to elucidate the mechanisms by which the activated retroviral genome can influence malignancy. Using transgenic mouse models the IMV has been able to show a strong cooperative effect between the tumorigenic Akv murine retrovirus and the c-myc and c-fos gene products, expressed from transgenes. In trangene bearing mice strains the presence of the c-fos or c-myc transgene alone was associated with a high rate of malignancy. The tumorigenesis was highly tissue selective, the c-fos trangenic mice developed primarily bone tumors, whilst c-myc transgenic mice developed mostly lymphomas. In both c-fos and c-myc transgenic mice the additional burden of infection with Akv retrovirus produced a shortening of the tumor latency period, and a net increase in tumor formation. No alteration in the type of target cell transformed during the carcinogenic process was seen after addition of virus, although some phenotypic differences in the tumors were noted. Thus a combination of dominant oncogene over-expression and viral infection serves to increase susceptibility to malignancy in specific cell populations. The IMB has developed a PCR based method for the analysis of retroviral integrations, and it is hoped this assay will shed light onto the number of viral reintegrations in radiation-induced cancers.

In vitro studies have also confirmed the importance of retroviral sequences in the oncogenic process following irradiation. Using osteogenic cells present within the murine mandibular chondyle the IMV has established that a combination of Radium 223 and infectious retrovirus can synergise in activating cell proliferation. The increased cell division is presumed to be the result of deregulated proliferative control associated with oncogenesis. Extraction of the irradiated and infected cells from the chondyle tissue confirmed that the proliferative activity was maintained in vitro during cell culture, and presumably indicates a direct interaction of irradiation and virus on the target cells. A search for the potential mediators of the enhanced cell proliferation was initiated by the IMV, and proved fruitful.Whilst the classical oncogenes c-fos, c-myc and c-jun were unaffected, the recently described T1 gene was significantly over-expressed.

The molecular mechanism(s) responsible for the carcinogenesis following irradiation are certainly transferred to progeny cells, either as active genetic alterations or by epigenetic mechanisms such as viral infection. The MRC study has revealed that radiation-induced alterations in the stability of the genome itself are transmitted during cell divisions. Thus, alpha-particle induced chromosomal aberrations are found in the colonies derived from irradiated murine bone marrow. Intriguingly, the frequency of aberration is strain dependent, with CBA/H showing a far greater incidence of chromosomal damage. This indicates strongly that there is a genetically determined component modifying the chromosomal damage by alpha-irradiation. The integrity of the genome is maintained by a number of processes, ranging from DNA proofreading and repair pathways to automatic suicide of cells containing irreparable DNA damage. Thus, the maintenance of the DNA lesions in succeeding generations implies a radiation-induced defect in the control of genome stability. In the case of retroviral elements within the genome this may result in the permanent activation of hitherto dormant proviral sequences.The studies by the IMB have shown that, for a selected model provirus integration site, the radiation-induced induction of viral transcription is in fact mediated by both positive and negative regulatory factors. Their analysis in vitro has implicated DNA methylation patterns as being the probable negative regulator of expression. Thus, any alteration in the cells capacity to maintain and replicate methylation patterns would result in activation of the quiescent locus. The IMB´s data suggest a causal link between irradiation and loss of methylation as a potential mechanism for activating hitherto inert proviruses.

Head of Project 1: Prof. H. Höfler

II Objectives for the reporting period

1) We have previously identified p53 gene mutations in cell lines established from radiation-induced murine osteosarcomas. Such mutations may be induced during the carcinogenic process, may be selected for in vitro, or may arise as spontaneous mutations during cell culture. Our objective is to directly screen tumor material for p53 gene mutations.

2) The genetic background may play a critical role in determining the susceptibility of an individual to carcinogenic influences of radiation. We have conducted an experiment to determine if radiation-induced osteosarcomagenesis is indeed influenced by heritable genetic factors.

III Progress achieved including publications

<u>The role of the p53 tumor suppressor gene in radiation-induced osteosarcomagenesis</u>

Characterization of the molecular changes taking place in malignancies induced by ionizing radiation will increase our understanding of the mechanisms underlying the carcinogenic process. Ultimately this knowledge may be used in establishing more accurate predictions of the carcinogenic risk following exposure to radiation. Over the last decade great advances have been made in the understanding of the molecular processes involved in carcinogenesis. A 53 kilodalton phosphorylated nuclear protein (p53) appears to play a central role in the carcinogenic process. Loss-of-function mutations of the p53 gene, or changes in cellular p53 protein content indicative of gene mutation, have been observed in over half of all human malignancies examined. Inactivation of the p53 gene locus by homologous recombination in mice, or the inheritance of a p53 gene mutation via the germ line in man are both associated with an increased incidence of malignancy. The studies by Partner 06 (TUM) have demonstrated very effectively that the screening method of choice should be the sequencing of PCR amplified p53 cDNA generated from reverse transcribed p53 mRNA.

Studies completed in collaboration with Partner 04 (GSF-IMV) during the previous contract (B17-0002C) revealed a high frequency of p53 gene alterations in cell lines established from alpha-particle-induced murine osteosarcoma. In 6/6 cell lines there was molecular evidence of a disruption of at least one allele of the p53 locus. However, spontaneous mutation of the p53 gene may have occurred during the establishment of the cell lines from the osteosarcoma tissue. Such a mutation would afford a growth advantage in vitro leading to selection for cells bearing mutated p53 alleles. It is necessary to confirm the p53 mutation events in tumor tissue, and to determine the frequency with which p53 is mutated in the tumors.

Osteosarcomas were induced by i.p. injection of thorium 227 (185 kBq/kg) in female Balb/c and NMRI mice. Portions of neoplastic growths arising in the skeleton were aseptically removed and passaged into isogenic recipient mice. The skeleton and the remaining tumor tissue was examined radiographically, and the pathological diagnosis confirmed after decalcification of the tumor tissue. Transplanted osteosarcomas were harvested after the initial passage, adherent tissues dissected away, and the tumor cryopreserved until required. RNA was isolated from the osteosarcoma tissue by homogenization of the frozen tissue in 6M Guanidinium isothiocyanate. After centrifugation to remove the mineralized matrix the RNA was isolated by cesium chloride gradient centrifugation. The resultant RNA was converted to single-stranded DNA template by reverse transcription and used as template in PCR amplifications. The p53 transcripts were amplified in the PCR reaction by using primers specific for the coding region of the p53 transcript (5´primer in Exon 1 and 3´primer in Exon 11). These

primers allow amplification of the expressed gene without amplification of the genomic pseudogene locus. The amplified PCR product from each tumor, spanning the coding region of the p53 gene, was further examined by a series of overlapping DNA sequencing reactions. A total of 18 thorium-induced osteosarcomas were examined by the RT-PCR methodology.

The p53 mRNA was also examined in liver tissue obtained from 10 control mice (5 Balb/c and 5 NMRI) to confirm that the RT-PCR methodology was stable, and that the rate of "spontaneous" p53 mutation in these strains was negligible. In addition, 7 osteosarcomas arising from experimental FBR-retrovirus infection of NMRI mice, and 1 NMRI mouse osteosarcoma induced by the injection of 75 kBq beta-emitting Zr95 were included in the study for control purposes.

Mutations of the p53 gene locus were detected in 5 of the 18 thorium-induced osteosarcomas. The nature of the mutations observed was remarkable, with 4 of them characteristic of intragenic deletions, and only one being a point mutation (See Table 1).

Table 1: Alterations in the p53 tumor suppressor gene locus detected in thorium-227 induced mouse osteosarcomas.

Deletion	Exons 6,7,8 and 9
Deletion	Exon 10 (6 bases)
Point mutation	Exon 8 (GGA-GTA)
Deletion	Exon 4 (from base 19), 5,6,7,8,and 9
Deletion	Exon 9

In the control (non-irradiated) tumors a silent point mutation was observed in one virus-induced osteosarcomas (Exon 4 ACC-ACT), but no other evidence of p53 mutation was noted. In the remaining control tumor, the Zr95-induced osteosarcoma, we detected a deletion (Exon 2 from base 80, 3,4,5,6,7,8 and exon 9 to base 66). In all cases the mutation was confirmed by a separate RT-PCR and sequencing.

Thus, in 28% of thorium-induced osteosarcomas we have observed a mutation affecting the p53 locus. This is a much lower frequency than observed in osteosarcoma cell lines established from alpha-emitter induced tumors. The differences may lie in the growth advantage of small cell populations bearing p53 mutations. However, in the osteosarcoma tissue we examined the proportion of p53 mutant cells must be below the sensitivity limit of the methodology (10%). These data suggest that p53 is not an initial event in radiation-induced osteosarcomagenesis, nor is loss of p53 gene function essential for malignant cell growth. The nature of the p53 mutations detected in both the Thorium 227 and Zirconium 95 treated animals is entirely consistent with a DNA-damaging effect of irradiation.

Genetic susceptibility to radiation-induced osteosarcoma

A number of heritable cancer syndromes are recognized, in which mutations at key genetic loci are passed via the germ line and predispose the offspring to cancer. With the increased sensitivity of genetic screening it is now apparent that non-mutated alleles present at similar loci influence the susceptibility of an individual to cancer, controlling primarily the latency period of tumor formation. Dependent upon the alleles inherited at these susceptibility loci, an individual may be at greater or lesser risk of developing a particular cancer. Our own empirical observations have shown that the susceptibility to radiation-induced osteosarcoma varies considerably between different inbred mouse strains. We consequently devised an experiment to demonstrate that genetic factors can indeed influence the susceptability of mice to radiation-induced osteosarcomagenesis.

The multigenerational transmission of cancer susceptibility has been established in cancer families, and in initial mouse experiments performed by Nomura. We designed an animal model of multigenerational carcinogenesis, in which we sought to increase overall radiation-susceptibility by exposure of the germ-line of the male parents to a chemical mutagen (Ethylnitrosourea-ENU). A dose of ENU was selected that has been shown to induce a high frequency of germ line mutations in the mouse specific locus test (coat color). The mutagenised offspring were then subjected to an osteosarcomagenic treatment with Thorium 227, and the latency period for osteosarcoma formation determined.

Eighty day old male mice of an F1 102 x C3H cross were treated with a mutagenic i.p. dose of 160mg/kg ENU. After a five month recovery period the mutagenised mice were crossed with T-stock females. The efficiency of the mutagenesis was confirmed by performing the specific locus test on the offspring. 5/955 mutations were seen in offspring form ENU-mutagenised mice, whilst 0/1057 mutations were seen in a control collective of offspring from non-mutagensised fathers (P= 0.024). The osteosarcomagenesis was carried out in female mice, and F1 offspring of both ENU-treated and control fathers were exposed to a single dose of 37 kBq/kg i.p. Thorium 227. The skeletal dose of 2 Gy has given an osteosarcoma incidence of around 20-30% in other mouse strains. In the control animals, no ENU treatment and no exposure to radioactivity, only a single spontaneous tumor was observed. No tumors were observed in the non-radiation exposed offspring of ENU-treated fathers. Thus the rate of spontaneous carcinogenesis was not influenced by ENU treatment.

The incidence of osteosarcoma in irradiated mice was slightly higher than anticipated, but treatment of the fathers with ENU did not influence the absolute incidence (see Table 2). However, the latency period for radiation-induced osteosarcoma formation was significantly shortened in the offspring of ENU-treated fathers. (see Table 2). Thus, although ENU mutagenesis did not influence the total incidence of osteosarcoma (which was high compared to pure inbred mouse strains), the introduction of mutations into the mouse by ENU-mutagenesis of the male germ line did shorten the latency period. This observation is a clear demonstration that genetic factors control the susceptibility of the mouse skeleton to radiation-induced osteosarcoma. This represents the first step in identifying susceptibility genes.

Table 2: Cumulative osteosarcoma incidence (corrected for competing risk) after incorporation of 36 kBq/kgThorium 227

	Father untreated	Father treated with ENU	Father untreated	Father treated with ENU
Time after injection (days)	No radiation	No radiation	Thorium 227	Thorium 227
1-300	0/69	0/69	0/65	2/65
301-600	0/65	1/66	3/63	11/61*
601-900	0/43	1/48	15/39	12/39
* P=0.019 (Fischer´s Exact test)				

Publications 1992-1995

Atkinson M.J., Dalke C., Hartmann E., Mitreiter K., Höfler H., Strauss P.G., Schmidt J., Erfle V., Luz A.   Mutations of the tumor suppressor gene p53 in murine osteosarcomas induced by alpha emitting radionuclides. in Health effects of internally

deposited radionuclides: Emphasis on radium and thorium , eds van Kaick G., Karaoglou A., Kellerer A.M. World Scientific Press, Singapore pp.389-392 1995.

Höfler H., Luz A., Atkinson M.J. Molecular biology of carcinogenesis: The unstable genome in Health effects of internally deposited radionuclides: Emphasis on radium and thorium, eds van Kaick G., Karaoglou A., KellererA.M. World Scientific Press, Singapore pp.385-388 1995.

Luz A., Neuhäuser-Klaus A., Linzner U., Müller W.A., Atkinson M.J., Höfler H. Genotoxic treatment of the paternal germline: Influence on bone tumor induction in the F1 generation by 227 Thorium in Health effects of internally deposited radionuclides: Emphasis on radium and thorium, eds van Kaick G., Karaoglou A., KellererA.M. World Scientific Press, Singapore pp.381-384 1995.

Luz A., Neuhaüser-Klaus A., Atkinson M.J., Linzner U., Müller W.A., Höfler H. Transgenerational carcinogenesis: Increased sensitivity for radiation-induced osteosarcoma after genotoxic treatment of the paternal germ line. 25th Annual Meeting of the European Society for Radiation Biology Book of Abstracts 1993; L14:09.

Mitreiter K., Atkinson M.J., Luz A., Höfler H. Charakterisierung von p53-Genveränderungen im strahleninduzierten Osteosarkom. Verh Dtsch Ges Path 1992; 76, 376.

Mitreiter K., Schmidt J., Luz A., Atkinson M.J., Höfler H., Erfle V., Strauss P.G. Disruption of the murine p53 gene by insertion of an endogenous retroviral-like element (ETn) in a cell line from a radiation induced osteosarcoma. Virology 200: 837-841 1994.

Mitreiter K., Strauss P. G., Schmidt J., Atkinson M.J., Luz A. Alteration of the murine p53 tumour suppressor locus in radiation-induced osteosarcoma. 24th Annual Meeting of the European Society for Radiation Biology Book of Abstracts 1992; Book of Abstracts, S. 100.

Spanner M., Müller W. A., Atkinson M.J. The role of ferritin in the intracellular uptake of radionuclides. 24th Annual Meeting of the European Society for Radiation Biology Book of Abstracts 1992; Book of Abstracts, S. 85.

Spanner M., Weber K., Lanske B., Ihbe A., Siggelkow H., Schütze H., Atkinson M.J. The iron-binding protein ferritin is expressed in cells of the osteoblastic lineage in vitro and in vivo. Bone (in press)

Strauss P.G., Mitreiter K., Luz A., Atkinson M.J., Höfler H., Schmidt J., Erfle V. Mutation of the p53 tumor suppressor in radiation-induced murine osteosarcomas in Molecular mechanisms in radiation mutagenesis and carcinogenesis, eds K.H. Chadwick, R. Cox, H.P. Leehnouts and J. Thacker, CEC Press Luxembourg pp 217-220 1994

Head of project 2: Dr. Harrison

II. Objectives for the period

1) To complete studies of the toxicity of the three bone-seeking radionuclides, ^{239}Pu, ^{241}Am and ^{233}U, in mice, comparing the incidence and distribution of osteosarcoma, the incidence of leukaemia and the distribution of dose.

2) To undertake studies to determine the distribution and retention of ^{210}Po in the skeleton of rats after administration of either of ^{210}Po or ^{210}Pb with the objective of assessing α-doses and leukaemic risk from these naturally-occurring nuclides. To compare the distribution of ^{238}Pu and ^{210}Po in marmoset bones.

III. Progress achieved including publications

Plutonium-239, americium-241, uranium-233 study

Following either occupational or environmental exposure of individuals to alpha-emitting isotopes of plutonium (Pu), americium (Am) or uranium (U), their entry into the bloodstream will result in long-term retention in bone and a consequent risk of osteosarcoma and leukaemia. The International Commission on Radiological Protection (ICRP) has recently adopted models for the behaviour of radionuclides in the skeleton which take account of the physiological processes of bone-remodelling and growth. The models treat plutonium and americium similarly, allowing for burial of surface deposits during mineral deposition and transfer to the marrow and release to the circulation during bone resorption. Uranium behaves more like calcium and the alkaline earth elements and the model assumes more rapid transfer from surfaces to bone volume. No change has been made, however, to the assumption that the sensitive cells for osteosarcoma induction are uniformly distributed on endosteal bone surfaces and those for leukaemia induction are uniformly distributed throughout red bone marrow. Furthermore, radionuclides are assumed to initially deposit uniformly on endosteal bone surfaces.

Previous studies of the distribution and retention of ^{239}Pu, ^{241}Am and ^{233}U in mice after systemic injection as the citrate complexes showed that the whole-body retention of ^{239}Pu and ^{241}Am were similar with values of about 80% and 70% respectively, after 1 day, falling to about 50% and 45% after 4 weeks and about 25% and 20% after 448 days. The total retention of ^{233}U was considerably lower, falling from about 15% after 1 day to about 5% after 4 weeks and about 3% after 448 days. For each nuclide, the skeleton was the major site of long-term retention. As a percentage of whole body activity, the skeleton initially accounted for 30%, 18% and 65% of retained ^{239}Pu, ^{241}Am and ^{233}U, respectively, increasing to 85%, 88% and 97% respectively, after 56 days; the corresponding values after 448 days were 86%, 94% and 99% respectively. On the basis of these data, it was estimated that the same average bone dose would be delivered by ^{239}Pu, ^{241}Am and ^{233}U over 448 days following administration at levels of activity in the ratio 1 : 1.05 : 5.25.

The induction of osteosarcoma and acute myeloid leukaemia (AML) was studied using groups of 50 - 100 mice given intraperitoneal injections of ^{239}Pu, ^{241}Am and ^{233}U as the citrate complexes. Each nuclide was administered to three groups of animals at levels of activity

estimated to give average bone doses, over 500 days, of 0.2, 0.6 and 1.2 Gy. To avoid chemical damage to the kidneys from U, the administration of each nuclide was fractionated over a 3 week period. The animals were kept until they became moribund or died. Osteosarcomas were identified by x-ray examination of the skeleton at death and the tumours confirmed by histological examination. Confirmation of AML was made from blood counts, analysis of blood smears for abnormal cells and passaging the spleen homogenate into untreated mice to look for myeloid leukaemia development. The alpha particle induction of AML in the CBA/H mouse is characterised by deletion and rearrangement at specific sites on chromosome 2. As an additional aid to diagnosis of AML a number of the leukaemias were karyotyped and have shown chromosome 2 rearrangements characteristic of AML.

A total of 35 suspected osteosarcomas have been identified to date by x-ray examination of the skeleton at death. Confirmation by histological examination is nearing completion; confirmation of diagnoses by a consultant pathologist will be completed by December 1995. The incidences of confirmed osteosarcomas in mice given ^{239}Pu are 2%, 8.3% and 18% for the 0.2, 0.6 and 1.2 Gy groups, respectively (see Table). Three animals in the 1.2 Gy group have 2 or 3 osteosarcomas present. The unconfirmed incidences for ^{241}Am are 2%, 4% and 8% and for ^{233}U are 1%, 3.3% and 4%. The control mice showed no osteosarcomas.

Twenty-four AMLs have been confirmed to date. The incidences of AML in mice given ^{239}Pu are 3%, 5% and 2% in the 0.2, 0.6 and 1.2 Gy groups, respectively. The incidences for ^{241}Am are 3%, 2.6% and 0 and for ^{233}U are 5%, 8.3% and 4%. No acute myeloid leukaemias were observed in control mice.

Preliminary statistical analysis of the results has shown that osteosarcoma incidence, fitted as a linear function of dose, showed significant differences (p = 0.03) between the nuclides with toxicity in the order ^{239}Pu > ^{241}Am > ^{233}U (Figure 1). The incidence of AML was best fitted as a linear-quadratic function of dose because of the observed reduction in leukaemia rate in the highest dose group for each nuclide (Figure 2). Differences between nuclides was less apparent than for osteosarcoma and are not significant. When the histological analyses are complete further statistical evaluation of the results will be undertaken.

Bone samples were taken from each mouse at post-mortem for radiochemical analysis to enable the average bone dose to death to be estimated separately for each animal. Figure 3 shows the estimated doses and time of death of all animals in each dose group, separately for each nuclide. These data will be used for further analysis of osteosarcoma and AML risk.

Studies to examine the distribution of ^{239}Pu, ^{241}Am and ^{233}U in the individual bones of the skeleton have been completed. The general pattern of distribution of the radionuclides was similar, with greater concentrations being seen in the thoracic, lumbar and sacral vertebrae and sternum and lower concentrations in the paw bones, radii, ulnae and clavicles. For ^{239}Pu, initial concentrations in the main body of the vertebrae were about four times greater than in the bones with lowest concentrations. Differences in concentration between bones were reduced with time. For ^{241}Am and ^{233}U, the initial differences in concentration and change with time were less than for ^{239}Pu.

The distribution of ^{239}Pu, ^{241}Am and ^{233}U within the skeleton has been studied using alpha-track autoradiographs of femur prepared using the plastic detector, CR39 (Figure 4). These studies have shown that ^{239}Pu was deposited fairly evenly on endosteal bone surfaces

and to a lesser extent on periosteal surfaces. At later times, some burial in the form of lines of activity was apparent as well as areas with more diffuse activity indicative of redeposition during bone remodelling. Progressive accumulation of ^{239}Pu in marrow was also observed. Americium-241 deposited more evenly on all bone surfaces and also in the internal surfaces of vascular canals in the cortical bone. With time, some burial occurred at the growth plate and some accumulation of americium in marrow macrophages was also seen but less than that observed for plutonium. Uranium-233 deposited on both periosteal and endosteal bone surfaces but not evenly, concentrating preferentially on some parts of the surface. Small amounts of diffuse activity were seen throughout the bone marrow and bone mineral. To quantify the distribution of alpha activity in bone, fission track autoradiographs of ^{239}Pu and ^{241}Am in femur sections have been produced. For ^{241}Am, distribution was determined by superimposing alpha-track autoradiographs and bone images produced by neutron activation. Track counts on random areas of sections have been used to make preliminary estimates of dose. Full account has not yet been taken of doses to bone surfaces and marrow from activity near but not on bone surfaces. However, initial calculations show averaged endosteal bone surface doses in the order ^{239}Pu > ^{241}Am > ^{233}U, consistent with the observed incidences of osteosarcoma. Further analysis will be undertaken of the regional distribution of dose and dose to different cell types on bone surfaces and of the distribution of dose in bone marrow relative to sensitive cells.

Lead-210, Polonium-210 studies

Uncertainties in red bone marrow doses and leukaemic risk from the natural alpha-emitter ^{210}Po as the daughter of ^{222}Rn and ^{210}Pb have recently been highlighted. One uncertainty has been the behaviour of ^{210}Po entering bone marrow from the circulation or produced from ^{210}Pb in mineral bone.

The tissue distribution and retention of ^{210}Po has been studied in rats after intravenous injection of either ^{210}Po citrate or ^{210}Pb citrate. In addition, a comparative study of the behaviour of ^{238}Pu and ^{210}Po in the marmoset has been completed.

The initial distribution of ^{210}Po after administration of ^{210}Po citrate showed that about 10% of the administered activity was deposited in the skeleton. Retention in the skeleton fell to about 1.5% of administered activity over 200 days, representing about 12% of the total body burden at this stage. Autoradiography showed that ^{210}Po in the skeleton was uniformly distributed throughout bone marrow. After administration of ^{210}Pb citrate, about 90% of ^{210}Po formed from ^{210}Pb in bone was retained in bone at times up to 400 days after administration. The distribution of the remaining 10% is consistent with release to the circulation and redistribution as ^{210}Po with uptake in liver, spleen and a small proportion (~10%) in bone marrow. Thus autoradiographs of bone show ^{210}Po very largely confined to mineral bone with low concentrations in marrow.

Four male marmosets were given intravenous injections of ^{239}Pu and ^{210}Po in citrate solution; 2 animals were killed at 1 week and 2 at 1 month. The results obtained for the distribution of ^{238}Pu in liver and bone were reasonably consistent with the current ICRP dosimetric model. Results for the tissue distribution of ^{210}Po at 1 week were similar to the values obtained for rats, with about 10% of the total activity retained in the skeleton. Autoradiographs prepared from the femurs of marmosets showed activity on bone surfaces, attributable to ^{239}Pu, and throughout the marrow, attributable to ^{210}Po.

The results obtained in these studies have contributed to changes in the ICRP biokinetic model for Po. Making specific allowance for the uptake of 10% of systemic ^{210}Po in red bone marrow increases the dose to this tissue by a factor of about six.

Publications

Ellender, M, Robbins, L, Bouffler, S D, and Harrison, J D. Induction of osteosarcoma and leukaemia by ^{239}Pu, ^{241}Am and ^{233}U in CBA/H mice. EULEP Newsletter, **67** 25-26 (1992).

Ellender M, Haines JW and Harrison JD. Bone dosimetry of ^{239}Pu, ^{241}Am and ^{233}U in a long term effects study using CBA/H mice. EULEP Newsletter **77** 13-14 (1994)

Ellender M, Haines J W and Harrison J D. The distribution and retention of plutonium, americium and uranium in CBA/H mice. Human and Experimental Toxicology **14** 38-48 (1995)

Robbins L and Ellender M. Husbandry procedures and health problems associated with a long-term mouse study. Animal Technology **44** 247-255 (1993)

Table. Incidence of osteosarcoma and myeloid leukaemia in CBA/H mice following the administration of ^{239}Pu, ^{241}Am and ^{233}U.

Average bone dose at 500 days (Gy)	0	0.2	0.6	1.2
^{239}Pu				
No of mice entered	100	100	60	50
No with acute myeloid leukaemia	0	3	3	1
No with osteosarcoma	0	2	5	9
^{241}Am				
No of mice entered	100	100	75	50
No with acute myeloid leukaemia	0	3	2	0
No with osteosarcoma	0	2	3	4
^{233}U				
No of mice entered	100	100	60	50
No with acute myeloid leukaemia	0	5	5	2
No with osteosarcoma	0	1	2	2
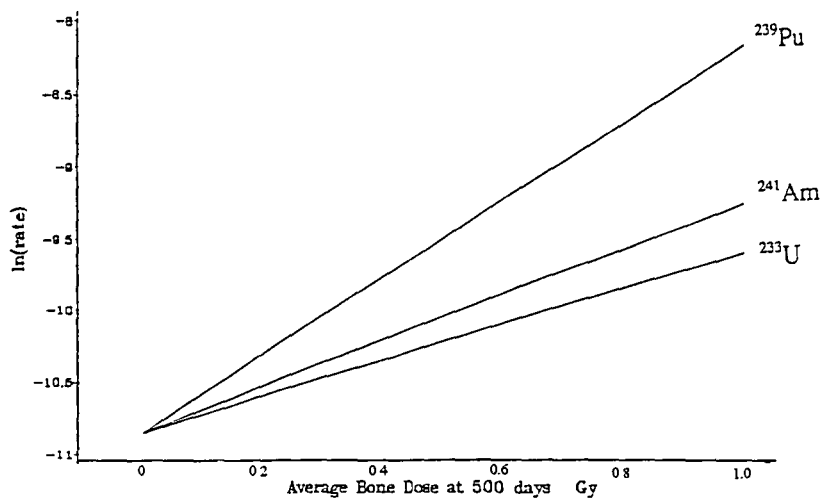
Figure 1. Model of osteosarcoma rate following administration of ^{239}Pu, ^{241}Am and ^{233}U.
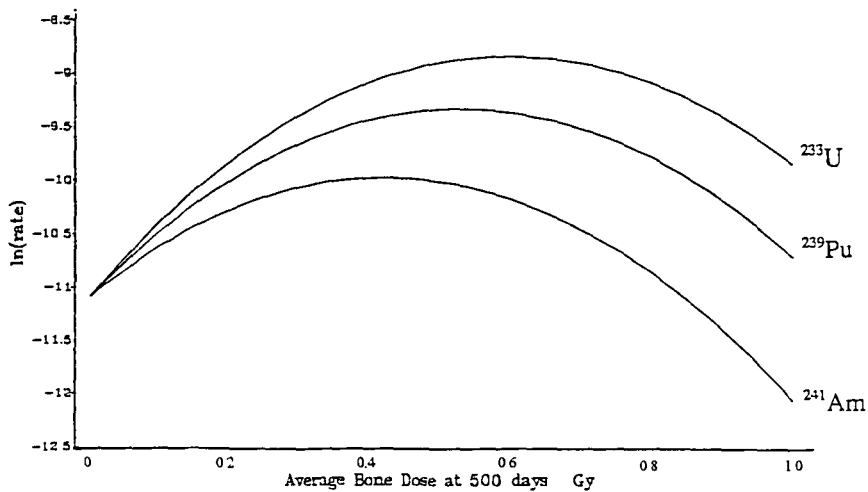
Figure 2. Model of myeloid leukaemia rate following administration of ^{239}Pu, ^{241}Am and ^{233}U.
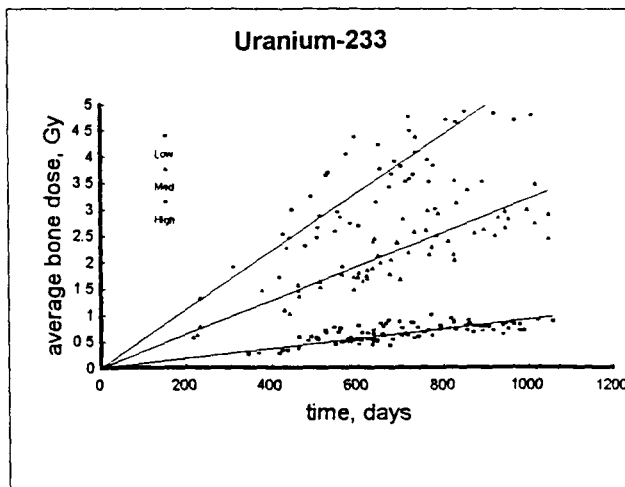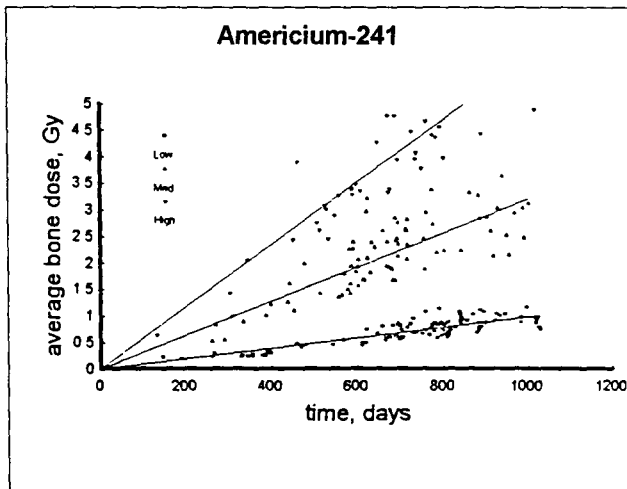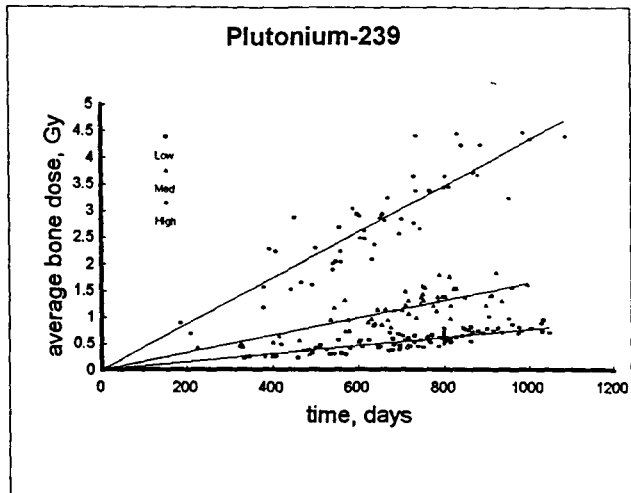
Figure 3. Estimates of average bone dose to death for individual mice in low, medium and high dose groups

Autoradiograph of mouse femur 1 day after injection of ^{239}Pu citrate showing an even deposition predominantly on endosteal bone surfaces with some accumulation on periosteal bone surfaces. There is also a low concentration of activity throughout the marrow.
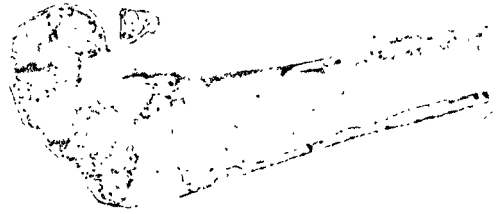
Autoradiograph of mouse femur 224 days after injection of ^{239}Pu citrate showing burial of activity, particularly in cortical bone, an accumulation of activity in the bone marrow and a region of new metaphyseal bone with low concentrations of ^{239}Pu.
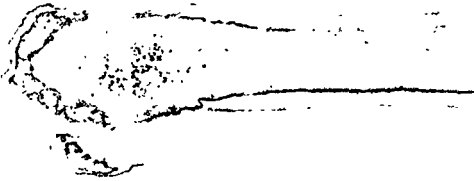
Autoradiograph of mouse femur 1 day after injection of ^{241}Am citrate showing an even deposition on all bone surfaces including those of vascular canals within the cortical bone.

Autoradiograph of mouse femur 224 days after injection of ^{241}Am citrate showing burial particularly in cortical bone, a region of new metaphyseal bone with low concentrations of ^{241}Am and some accumulation of activity in the bone marrow.
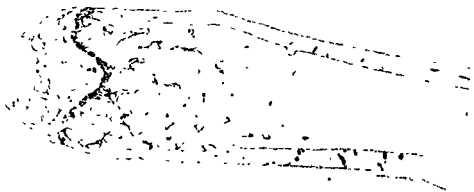
Autoradiograph of mouse femur 1 day after injection of ^{233}U citrate showing uneven distribution of activity, on bone surfaces and some diffuse activity throughout the bone.
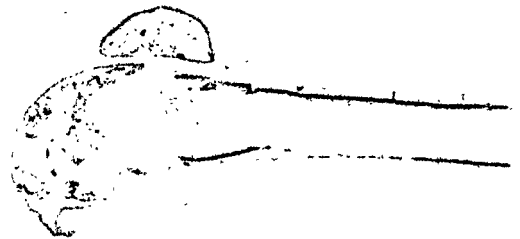
Autoradiograph of mouse femur 224 days after injection of ^{233}U citrate showing uneven lines of buried activity and small amounts of diffuse activity throughout the bone.

Figure 4. Autoradiographs of mouse femurs showing deposition of ^{239}Pu, ^{241}Am and ^{233}U.

Head of project 3: Dr. Wright

II. Objectives for the reporting period

The major objective was to develop *in vitro* techniques to investigate the effects of alpha particles on haemopoietic stem cells in order to provide a mechanistic link to our previous animal studies in which myeloid leukaemias had been induced by alpha-emitting radionuclides. In preliminary studies, we had observed a high frequency of non-clonal cytogenetic aberrations in clones of cells derived from murine haemopoietic stem cells surviving low doses of α-particle irradiation. These results suggested that a transmissible genetic instability can be induced in a stem cell, resulting in a diversity of aberrations in its clonal progeny many cell divisions later. Our objectives have been to investigate further this induced instability:-

- To confirm the induction of chromosomal instability by alpha-particle-irradiation

- To investigate further the probability of murine haemopoietic stem cells surviving a single alpha-particle track.

- To investigate the capacity of surviving stem cells to proliferate and express alpha-particle-induced genetic damage *in vitro*.

- To extend the cytogenetic study to the *in vivo* situation using bone marrow transplantation techniques.

- To develop techniques that will allow comparable studies of human cells.

- To explore genetic factors influencing induced instability by exploiting various inbred strains of mice.

III. Progress achieved including publications

The induction of chromosomal instability by alpha-particles

We have developed novel techniques for studying primary murine haempoietic stem cells irradiated with environmentally relevant doses of alpha-particles. Using a clonogenic culture system, a high frequency of non-clonal cytogenetic aberrations in clones of cells derived from CBA/H haemopoietic stem cells surviving low doses of α-particle irradiation (0.25. 0.5, 1 0 Gy) has been confirmed. Approximately 50% of clones (in which there have been approximately 10-15 cell divivions) express instability in up to 20% of the cells. The major aberration types are chromatid breaks, chromosome fragments and minutes and the ratio of chromatid-type aberrations to chromosome-type aberrations is ~ 3 : 1. The data are consistent with the aberrations arising *de novo* in the cell cycle immediately prior to cell harvesting and reflect a tansmissible induced chromosomal instability.

Kadhim, M.A., Macdonald, D.A., Goodhead, D.T., Lonmore, S.A. Marsden, S.J. & Wright, E.G. Transmission of chromosomal instability after plutonium α-particle irradiation. *Nature*, 355, 738-740, (1992).

Alpha-particle-induced delayed mutations

As there is every reason to believe that genetic instability will produce not only non-clonal chromosome aberrations but also mutational events not detected by cytogenetic methods, we have developed a system to detect single gene mutations in individual cells in the clonal descendants of haemopoietic stem cells. The approach is based on the autoradiographic method described to detect variant thioguanine-resistant lymphocytes due to mutations in the hypoxanthine guanine phosphoribosyl transferase (*hprt*) gene. Our studies have revealed an increased incidence of mutations in the clonal descendants of alpha-irradiated murine stem cells.

Harper, K., Lonmore, S.A. & Wright, E.G. Delayed appearance of radiation-induced mutations at the hprt locus in murine haemopoietic stem cells. Submitted for publication

Inactivation of murine haemopoietic stem cells by alpha-particles

Inactivation of murine stem cells assayed as spleen colony-forming units (CFU-S), has been determined after in vitro irradiation under well defined conditions with small numbers (≤ 3) of alpha-particles of incident energy 3.3 MeV (LET 121 keV mm^{-1}). he CFU-S compartment is age-structured with the earlier members (day 12 CFU-S) having greater self-replicative capacity than the later members. The later members measured as day 8 CFU-S are multipotential cells with negligible self-replicative capacity and are highly responsive to proliferation and differentiation stimuli.

Exponential survival curves were obtained with inactivation dose coefficients 1.833 ± 0.11 and 1.63 ± 1.22 Gy^{-1} for day 8 and day 12 CFU-S respectively, corresponding to inactivation cross sections of $35.6 + 2.1$ and 31.7 μm^2. The results indicate that that these radiosensitive stem cells have a probability of surviving the passage of a single alpha-particle track, estimated at 8 and 18% per particle passage, respectively, if the cells have a diamater of 7μm (the modal diameter determined by velocity sedimentation). These results suggest that those stem cells that survive a single alpha-particle traversal ($\simeq 0.5$ Gy) have a very high probability of transmitting chromosomal instability.

Lorimore, S.A., Goodhead, D.T. & Wright, E.G. Inactivation of haemopoietic stem cell by slow alpha-particles. *International Journal of Radiation Biology,* **63**, 655-660, (1993).

In vivo transmission of alpha-particle-induced chromosomal instability

The non-clonal cytogenetic aberrations in the clonal cultures are consistent with a transmissible chromosomal instability induced in a stem cell resulting in a diversity of aberrations in its differentiating progeny many cell divisions later. To determine whether this phenomenon is demonstrable *in vivo*, α-irradiated bone marrow cells obtained from male mice have been transplanted into female recipients. In the repopulated haemopoietic system, we have observed persisting chromosomal instability up to one year post-transplantation in the donor cells. Direct preparations of the bone

marrow were obtained at 3,6, 9 and 12 months post transplantation; these preparations contained, on average 10% aberrant cells (range 6-19%) with the major aberration types being chromatid breaks, chromosome fragments and minutes. The findings demonstrate a long-lived *in vivo* effect of the α-particle-induced lesion in the donor repopulating stem cells.

Watson, G.E., Lorimore, S.A. & Wright, E G Long-term in vivo transmission of alpha-particle-induced chromosomal instability in murine haemopoietic cells. Submitted for publication.

Alpha-particle-induced genomic instability in human bone marrow cells

Collaborative studies have led to the development of a quantitative clonogenic assay for human marrow cells comparable to the stem cell assay for murine cells operationally defined as a CFU-A assay.

Holyoake, T.L., Freshney, M.G., Konwalinka, G.,, Haun, M., Petzer, A., Fitzsimmons, E., Lucie, N P., Wright, E.G. & Pragnell, I.B. Mixed colony formation in vitro by the heterogeneous compartment of multipotential progenitors in human bone marrow. *Leukemia*, **7,** 207-213, (1993).

This development has allowed us to carry out studies of the effects of alpha-particle irradiation on human bone marrow comparable to those with murine stem cells. Similar results to our findings with murine stem cells have been demonstrated in studies of bone marrow cells from some human donors and the absence of chromosomal instability following α-particle irradiation of stem cells from other individuals in these studies has been attributed to a genetic component in the expression of radiation-induced chromosomal instability.

Ultrastructural analysis of colonies derived from CFU-A in marrow suspensions exposed to 0.5 Gy α-particles, revealed an increased incidence of apoptotic cells. These apoptotic cells appeared to occur randomly throughout the growing colony at

the time when cytogenetic aberrations were detected. As the apopotic cells are defined by morphological criteria on examination of ultrathin sections it was not possible to quantitate with great accuracy the incidence of apoptosis in the colonies but the cells were readily detected at an incidence of up to 5 per 100 cells on examination of random fields.   Delayed apoptosis might reflect DNA damage arising in the descendants of irradiated cells that is incompatible with cell survival and not expressed as a karyotypic abnormality.

Kadhim, M.A., Lorimore, S.A. Hepburn, M.D., Goodhead, D.T., Buckle, V.J & Wright, E.G. Alpha-particle-induced chromosomal instability in human bone marrow cells. *Lancet*, 344, 987-988, (1994).

Kadhim, M.A., Lorimore, S.A. Towmsend, K.M.S., Goodhead, D.T , Buckle, V.J. & Wright, E.G. Radiation-induced genomic instability: delayed cytogenetic aberrations and apoptosis in primary human bone marrow cells. International Journal of Radiation Biology, 67, 287-293, (1995).

Alpha-particle-induced chromosomal instability in human lymphoblastoid cells.

Experiments, to date, have concentrated on the use of primary cells to investigate alpha-particle effects in order to minimise any artefacts arising from potential abnormalities of cells in established cell lines. A major diffculty with this approach is that the assay systems for haemopoietic stem cells are differentiation driven and mature post-mitotic cells are rapidly generated in the cultures. As an alternative cellular system that is potentially more amenable to mechanistic studies we have chosen to investigate alpha-particle effects on lymphoblastoid cells from normal individuals and individuals with known mutations that predispose to the development of malignant diseases.

With cells from normal individuals, a marked inter-individual variation in the expression of chromosomal instability has been noted, similar to that observed with primary marrow cells. Cells from certain patients with chromosome instability syndromes express ongoing instability in culture but a highly significant increase in

instability can be induced by a-irradiation. Current investigations indicate that the genetic susceptibility component is distinct from the cancer predisposition in these particular individuals and are consistent with alpha-particle-induced chromosomal instability being independent of the p53 status. The p53 gene product functions in the regulation of the cell cycle, "sensing" some, as yet poorly defined, aspect of the DNA structure. If DNA is damaged *e.g.* by radiation, p53 protein accumulates and this is causally related to a cell cycle delay and/or induction of apoptosis.

Kadhim, M.M., Walker, C.A., Plumb, and Wright, E.G. Alpha-particle-induced chromosomal instability in human lymphoblastoid cells is p53-independent. Submitted for publication.

A genetic component to alpha-particle-induced chromosomal instability

Initial studies were carried out using bone marrow obtained from the CBA/H strain of laboratory mouse. More recent studies have investigated marrow from B6D2F1, C57Bl/6, 129 and DBA/2 strains. Using DBA/2 marrow, results directly comparable to the initial studies with CBA/H marrow have been obtained - the majority of stem cells that survive an alpha-particle traversal transmit chromosomal instability to many of their differentiating progeny. The situation with B6D2F, C57Bl/6 and 129 is qualitatively similar but the expression of instability, in terms of the number of stem cells transmitting the lesion and the number of progeny cells exhibiting chromosomal aberrations, is significantly less. The B6D2F1 strain results from a cross between C57Bl/6 and DBA/2 suggesting that expression of instability is genetically recessive and that a relatively small number of genes are involved. Potentially, these can be identified by the use of microsatellite mapping. Studies using a quantitative clonogenic assay for human haemopoietic stem cells has confirmed a marked inter-individual variation comparable to that observed between the mouse strains. These data are consistent with the expression of alpha-particle-induced chromosomal instability having a marked dependence on the genetic characteristics of the target cell.

Nuclear Fission Safety Program 1990-1994
FI3P-CT92-0051
Final report

Head of project 04: Prof. Dr. V. Erfle

Radiation-induced osteosarcomagenesis in vivo and in vitro: effects of low dose α-irradiation and radiation-activated retroviruses on differentiation pathways

Radiation induced osteosarcomas show several characteristic features including retrovirus activation and new integration into host DNA, alterations in the p53 gene, increased levels of p53 gene product, and amplifications of the c-myc gene. In addition to α-emitting bone-seeking radionuclides, both the c-fos and the v-fos genes are efficient inducers of osteosarcomas in mice. The frequent involvement of one ore more of the above genes in carcinogenesis suggests that mutations, rearrangements and/or aberrant transcription of protooncognes or tumour suppressor genes represent either causal events for the deveopment of neoplasia or may be generated during tumor development. Subsequently, transgenic mice as well as cell or tissue cultures from transgenic mice, carrying one or more of these mutated genes as a genetic trait, represent individuals, or harbor cells, in an advanced stage of neoplastic transformation. They served as model systems with increased sensitivity to the transforming activity of α-irradiation and retrovirus infection.

II. Objectives for the reporting period:

In vivo and *in vitro* studies on the role of radiation-activated retroviral genes in the initiation, fixation, enhancement and/or accelaration of radiation-induced genomic alterations and radiation-induced neoplasia

These objectives are implemented by

a) characterization of cooperating effects of radiation-activated retroviruses, α-irradiation and cellular genes associated with cell cycle control and tumorignesis in radiation-induced osteosarcoma

b) establishment of transgenic mice carrying genetic alterations which are identified in radiation-induced osteosarcomas and studies of their sensitivity to retrovirus infection

c) evaluation of the susceptibility of p53 transgenic mice to osteosarcomagenic doses of ^{223}Ra.

d) establishment of skeletal tissue cultures and cell lines from transgenic mice as sensitive in vitro models for radiation-osteosarcomagenesis, and

e) pathogenicity studies of in vitro treated tissues

III. Progress achieved including publications

ad a)   An important role for the p53 gene in osteogenic sarcomas has been imputed by identification of somatically acquired gene altertions in human osteosarcomas and by the development of osteosacomas in p53 transgenic mice. We detected in 18 out of 31 radiation-induced osteosarcomas and in 8 of 9 cell lines established therefrom, alterations in the p53 gene region or elevated levels of p53 RNA. Expression of the osteoblast marker gene osteocalcin was substantially reduced in tumors which sumultaneously showed high steady state levels of

p53 RNA and vice versa. These data suggest that p53, in addition to its function in cell cycle control and regulation of DNA synthesis, may be involved in the control of osteogenic differentiation in osteosarcomagenesis.

In one of the osteosarcoma cell lines we observed the insertion of a murine endogenous retrovirus-like ETn element into intron 4 of the p53 gene. This insertion resulted in a p53-ETn-p53 fusion mRNA, a novel form of p53 mutation. These findings suggest that activated endogenous retroviruses and retrovirus-like elements might pose an enhanced risk for individuals esposed to noxae which activate endogenous retroviruses.

ad b)   Transgenic mice carrying the transgenes c-fos, c-myc, c-fosxc-myc F1 hybrids, p53 transgenic and p53-null mice have been successfully bred in our laboratory.

To study possible interactions between retroviral genes and oncogenes we chose c-fos and c-myc transgenic mice as test strains. Due to deregulated oncogene expression c-fos transgenic mice are predisposed to aberrant bone formation and bone tumor development whereas c-myc transgenics show enhanced lymphoma incidence.

After infection of newborn c-fos transgenic mice with Akv, a prototype endogenous mouse retrovirus, tumor incidence was significantly increased and the latency period was shortened. The tumors of Akv-infected c-fos-transgenic mice differed from benign osteomas which developed in Akv-infected control mice and also from osteosarcomas which developed in non-infected c-fos transgenic mice. They contained bone together with fibrous tissue, they lacked invasive growth, but they were transplantable in syngeneic mice.

Infection of newborn c-myc-κ transgenic mice carrying different numbers of copies of the c-myc-κ transgene also enhanced tumor development and shortened the latent period. The tumors contained several copies of Akv and the proviruses were highly expressed. Common provirus integration sites as found in Moloney leukemia virus-induced lymphomas were no apparent targets for Akv insertion.

The data indicate a synergistic effect of endogenous retroviruses with activated oncogenes, as shown here for the c-fos and the c-myc transgenes, in tumor development. The resulting bone tumors in infected c-fos transgenic mice exhibit characteristical features of both, Akv-induced osteomas and c-fos-induced osteosarcomas suggesting a similar influence of both tumorigenic entities on the tumor phenotype. Moreover, the critical genes interacting with endogenous retroviruses seem to differ in bone tumorigenesis and in lymphomagenesis.

ad c)   To investigate the above findings in more detail, double transgenic mice were generated and the different mouse line successfully bred in our institute. In vivo experiments are progress to investigate the effect of α-(^{227}Th)irradiation on p53 transgenic mice which are either transgenic for a mutant p53 gene or double transgenic for mutant p53 and an endogenous retrovirus. The transgenic mice are characterized by an increased risk for tumorigenesis including development of osteosarcomas.

ad d)   A culture model of in vitro differentiating osteogenic tissue derived from mandibular condyles of neonatal mice was used to study ^{223}Ra effects on osteogenic tissue. Irradiation of mandibular condyles from neonatal mice with with doses ranging between 0.007 kBq/ml and 7.4 kBq/ml ^{224}Ra for 3.5, 7, 10.5, 14, and 21 days in the presence and in the absence of infectious retroviruses induced enhancement of proliferation together with increased osteogenic differentiation in irradiated tissues. These findings suggested that α-irradiation enhances the susceptibility of skeletal cells to proliferation-inducing effects of bone-pathogenic retroviruses. The enhancement of cell proliferation, which was observed in low dose-irradiated mandibular condyles, was not due to enhanced transcriptional activity or significant induction of the growth control genes c-fos, c-jun or c-myc.

Irradiated mandibular condyles showed enhanced RNA levels of the T1 gene. T1 is a gene stimulated by the oncogene Ha-ras and was isolated from Ha-ras transformed NIH3T3 cells. T1 expression was analysed by reverse transcription of total cellular RNA from irradiated condyles and sequence-specific amplification of a 400 bp sequence by PCR. In contrast to non-irradiated tissues, irradiated tissues showed expression of T1 at 2 hours after start of the

culture, suggesting that T1 is activated by ^{223}Ra. In situ hybridization analysis showed high T1 expression in the progenitor cell layer of the tissues, indicating that these cells are particularly sensitive to ^{223}Ra in skeletal tissue.

Irradiated and/or retrovirus infected mandibular condyles were dissociated by collagenase and single cell suspensions were used to establish monolayer cell lines. The highest cell proliferation was found in cell lines established from tissue which had been irradiated and infected, indicating a cooperative effect of α-iirradiation and retrovirus infection on skeletal cell growth.

Osteoblast-progenitor cell lines (KM) and clonal sublines (KMK) therefrom have been established from normal mice and from myc-transgenic, from p53 transgenic, from myc/p53 transgenic F1 mice as well as from p53 null mice lacking one or both functional p53 genes. Different cell lines from each of these genotypes varied significantly in their sensitivity to radiation-induced cell transformation. A maximal effective dose of 3 Gy was established for induction of cell transformation.

Cooperating effects of ↑ irradiation and retrovirus infection on cell transformation were observed in these osteoblast-progenitor cell lines. Whereas noninfeced KM2-cells were not transformed by irradiation, cell transformation was observed in retrovirus-infected cells and transformation frequency increased dose-dependently after irradiation.

ad e)   *In vitro* short term irradiation and/or retrovirus infection are not sufficient for the induction of neoplastic transformation of skeletal tissue. Osteoblast-progenitor cell lines are more sensitive for retrovirus and/or radiation-induced transformation than tissue cultures, however, subcutaneous transplantation of morphologically transformed cells does not consistently lead to tumorigenesis in syngeneic mice.

Publications

Goralczyk, R., Closs, E.I., Rüther, U., Wagner, E.F., Strauß, P.G., Erfle, V., Schmidt, J. Characterization of fos-induced osteogenic tumours and tumour-derived murine cell lines. Differentiation 44:122-131 1990.

Leib-Mösch, C., Brack-Werner, R., Salmons, B., Schmidt, J., Strauß, P.G., Hehlmann, R., Erfle, V. The significance of retroviruses in oncology. Onkologie 13:405-414 1990.

Pedersen, L., Strauss, P.G., Schmidt, J., Luz, A., Erfle, V., Jørgensen, P., Kjeldgaard, N.O., Pedersen, F.S. Pathogenicity of Balb/c-derived N-tropic murine leukemia viruses. Virology 179:931-935 1990.

Luz, A., Müller, W.A., Linzner, U., Strauss, P.G., Schmidt, J., Mülller, K., Atkinson, M., Murray, A.B., Gössner, W., Erfle, V., Höfler, H. Bone tumour induction after incorporation of short-lived radionuclides. Radiat. Environ. Biophys. 30:225-227 1991.

Aresu, O., Nicolo, G., Allavena, G., Melchiori, A., Schmidt, J., Kopp, J.B., d'Amore, E., Chader,-G., Albini, A. Invasive activity, spreading on and chemotactic response to laminin are proterties of high but not low metastatic mouse osteosarcoma cells. Invasion and Metastasis.11:2-13, 1991.

Hallberg, B., Schmidt, J., Luz, A., Pedersen, F.S., Grundström, T. SL3-3 Enhancer factor 1 transcriptional activators are required for tumor formation by SL3-3 murine leukemia virus. J. Virol. 65:4177-4181, 1991.

Pedersen, F.S., Paludan, K., Dai, H.Y., Duch, M., Jorgensen, P., Kjeldgard, N.O., Hallberg, B., Grundström, T., Schmidt, J., Luz, A. The murine leukemia virus LTR in oncogenesis: effect of point mutations and chromosomal integration. Radiat. Environ. Biophys. 30:195-197, 1991.

Luz, A., Erfle, V., Strauß, P.G., Müller, K., Schmidt, J., Müller, W.A., Linzner, U., Gössner, W., Höfler, H. The role of age and genetic background as cofactors in the pathogenesis of radiation-induced osteosarcomas. USDOE Report UCD-472, 136:30-33, 1991.

Pedersen, L., Behnisch, W., Schmidt, J., Luz, A., Pedersen, F.S., Erfle, V., Strauss, P.G. Molecular cloning of osteoma-inducing replication-competent murine leukemia viruses from the RFB osteoma virus stock. J. Virol. 66:6186-6190, 1992.

Strauss, P.G., Müller, K., Zitzelsberger, H., Luz, A., Schmidt, J., Erfle, V., Höfler, H. Elevated p53 RNA expression correlates with incomplete osteogenic differentiation of radiation-induced murine osteosarcomas. Int. J. Cancer 50:252-258, 1992.

Goralczyk, R., Luz, A., Erfle, V., Schmidt, J. Metastatic growth of v-fos-induced osteosarcoma following in vitro cultivation. Zentralbl. Pathol. 138:97-102 1992.

Goralczyk, R., Luz, A., Erfle, V., Schmidt, J. Metastatic growth of v-fos-induced osteosarcoma following in vitro cultivation. Zentralbl. Pathol. 138:97-102, 1992.

Strauss, P.G., Müller, K., Zitzelsberger, H., Luz, A., Schmidt, J., Erfle, V., Höfler, H. Elevated p53 RNA expression correlates with incomplete osteogenic differentiation of radiation-induced murine osteosarcomas. Int. J. Cancer 50:252-259, 1992.

Strauß, P.G., Schmidt, J., Luz, A., Erfle, V. Radiation-induced osteosarcoma: a model for evaluation of molecular pathway to transformation. In: Novak, J.F. and McMaster, J.H. (eds) Frontiers of Osteosarcoma Research. Hofgrefe & Huber Publishers, Seattle-Toronto-Göttingen-Bern, pp. 411-418, 1993.

Strauss, P.G., Mitreiter, K., Zitzelsberger, H., Luz, A., Schmidt, J., Erfle, V. Höfler, H. Inverse correlation of p53 and osteocalcin RNA expression in murine osteosarcomas. In: Novak, J.F. and McMaster, J.H. (eds) Frontiers of Osteosarcoma Research. Hofgrefe & Huber Publishers, Seattle-Toronto-Göttingen-Bern, pp. 289-292, 1993.

Strauss, P.G., Mitreiter, K., Luz, A., Atkinson, M.J., Höflier, H., Schmidt, J., Erfle, V. Mutation of the p53 tumor suppressor in radiaton-induced murine osteosarcomas. In: K.H. Chadwick, R. Cox, H.P. Leenhouts and J Thacker, (eds.) Molecular Mechanisms in Radiation Mutagenesis and Carcinogenesis, ECSC-EC-EAEC, Brussels, Luxembourg, pp.217-222, 1994.

Mitreiter, K., Schmidt, J., Luz, A., Höfler, H., Erfle, V., and Strauss, P.G. Disruption of the p53 Gene by Insertion of an Endogenous Retrovirus-like Element (ETn) in Radiation-induced Osteosarcoma. Virology 200:837-841, 1994.

Luz, A., Krump-Konvalinkova, Snell, G., Strauss, P.G., Höfler, H., Erfle, V., Schmidt, J. Murine leukemia virus Akv promotes bone tumor development in fos transgenic mice. Verh. Dt. Ges. Pathol. 78:265-269, 1994.

Schmidt, J., Linzner, U., Luz, A., Heermeier, K., Silbermann, M., Livne, E., Erfle, V. Irradiation of in-vitro differentiating skeletal tissue with osteosarcomagenic doses of [224]Radium: effects on proliferation and osteogenic differentiation. In: K.H. Chadwick, R.

Cox, H.P. Leenhouts and J Thacker, (eds.) Molecular Mechanisms in Radiation Mutagenesis and Carcinogenesis, ECSC-EC-EAEC, Brussels, Luxembourg, pp.209-216, 1994.

Schmidt, J., K. Heermeier, U. Linzner, A. Luz, M. Silbermann, E. Livne and V. Erfle Osteosarcomagenic doses of ^{224}Radium (^{224}Ra) and infectious endogenous retroviruses enhance proliferation and osteogenic differentiation of in vitro-differentiating skeletal tissue. Rad. Environ. Biophys.33:69-79, 1994.

Speth, C., Luz, A., Zeidler, R., Lipp, M., Wendel, S., Dorn, S.,Erfle, V., Strauss, P.G., and Schmidt, J. Akv murine leukemia virus enhances lymphomagenesis in myc-kappa transgenic and in wild-type mice. Virology 206:93-99, 1995.

Schmidt, J., Krump-Konvalinkova, V., Luz, A., Goralczyk, R., Snell, G., Wendel, S., Dorn, S., Pedersen, L., Strauss, P.G., Erfle, V. Akv murine leukemia virus enhances bone tumorigenesis in hMT-c-fos-LTR transgenic mice. Virology 206:86-92, 1995.

Werenskiold, A.K., Rößler, U., Löwel, M., Schmidt, J., Heermeier, K., Spanner, M., Strauss, P.G. Bone matrix deposition of T1, a homologue of interleukin-1 receptor. Cell Growth Diff. 6:171-177, 1995.

Gerstenfeld, L., Uporova, T., Huang, L.F., Schmidt, J., Strauss, P.G., Gundberg, C., Mizuno, S., Glowacki, J. Regulation of osteogenesis and gene expression: differences revealed by in vitro and in vivo studies with clonal osteosarcoma cells. Orthop. Trans. 1995.

Schmidt, J., Speth, C., Luz, A., Strauß, P.G., Lipp, M., Zeidler, R., Brem, G., Erfle, V. Tumor induction with α-emitting radionuclides: the provirus - oncogene connection. In: K.H. Chadwick, A. Karaoglou (eds.) Health effects of internally deposited radionuclides: special emphasis on radium and thorium, CEC Proceedings, pp. 393-396, 1995.

Atkinson, M., Dahlke, C., Hartmann, E., Mitreiter,K., Höfler, H., Strauss, P.G., Scmidt, J., Erfle, V., Luz, A. Mutation of the tumor suppressor gene p53 in murine osteosarcomas induced by alpha-emitting radionuclides. In: K.H. Chadwick, A. Karaoglou (eds.) Health effects of internally deposited radionuclides: special emphasis on radium and thorium, CEC Proceedings, pp. 389-392, 1995.

Head of project 5: Prof. Skou Pedersen

II. Objectives for the reporting period

Retroviral proviral elements may be carried in the germ line of birds and mammals and their expression may be repressed in somatic cells although the proviral transcriptional unit is fully functional. We have used endogenous proviruses as models for the analysis of factors affecting the activation of retrotransposon elements and for the possible pathogenic effects caused by activated elements. In a new development we use retroviral vectors to establish a cell culture model for the study of radio-sensitive sites in DNA.

Specific objectives were:

1) To analyze molecular mechanisms of radiation-activation of silent proviral genes.

2) To determine pathogenic sequences in proviral genes.

3) To construct and test retroviral vectors with telomere-like repeat DNA.

III. Progress achieved including publications

1) Activation of silent proviral genes.

The expression of endogenous ecotropic proviruses has been shown to vary considerably among inbred strains of mice. This variation, of importance for strain-dependent disease development, may be determined by *cis*-acting DNA elements within the proviral sequences as well as by the site of integration. The germ line of the low leukaemic Balb/c strain carries, at the locus *emv*-1, a single ecotropic provirus that is never expressed at high levels *in vivo* and rarely spontaneously activated in derived cell cultures. Similarly, integrated retroviral vector proviruses may be transcriptionally inactive when integrated at certain DNA sites. As models for activation of retrotransposon elements we have focussed on mechanisms of activation of the *emv*-1 provirus in Balb 3T3 cultures and on activation of silent Akv-neo and SL3-3-neo vector proviruses in L691 mouse lymphoma cells.
Actively dividing cultures of Balb 3T3 cells were exposed to a low dose of gamma-radiation (700 rads). Five days after the treatment, cells with an active provirus were identified by immunostaining using antibodies directed against the proviral Gag or Env proteins. Gamma-irradiation, which efficiently results in strand breaks, yields low frequencies of virus induction (10^{-3} - 10^{-4}).
Using the model of silent vector proviruses, rare cells with activated proviruses can be selected by growth in G418 containing medium. By subsequent growth in medium without G418, provirus expression falls back to zero, thereby demonstrating the reversibility of provirus activation.
Silencing of a provirus may result from the presence of an inhibitor or the absence of specific activating factors. A negative influence may come from DNA-methylation that has a role in the establishment of inert chromatin structures. Irradiation may reduce DNA-methylation as a result of specific damage of DNA at the locus or by a general effect on DNA synthesis and repair. Specific activating factors that may overcome the repression may appear as a result of biochemical changes after irradiation.
The work has focussed mainly on negative effects associated with methylation of DNA at the locus in the untreated cell. As previously seen for other proviruses we observed an increase in

frequencies of activation after irradiation in cell cultures treated with BrdUrd during DNA repair. We also found an increase of provirus activaton after 5-azacytidine treatment. It suggests that a modification by methylation of DNA double helix can influence endogenous provirus induction. The expression of the provirus may still be sensitive to the influences of chromatin structure, DNA modification and *cis*-acting control elements in the flanking host cell sequences.

We have used 5-azacytidine treatment of cells in culture to demethylate a large part of CpG dinucleotides. Southern blotting analysis shows that the region corresponding to the endogenous provirus sequence is highly methylated. A few specific sites in this sequence were found to be only partially methylated in a population of untreatred cells. By treatment with 5-azacytidine we have been able to activate proviruses in about 20% of the cells. In nuclear extracts we have detected proteins that bind to a methylated DNA-probe from the provirus promoter. A search for such proteins may be important to understand the mechanisms of repression and activation of provirus transcription.

Two strategies have been pursued to identify activated proviral genes in mammalian cells By the first strategy a provirus product is picked up by recombination with a defective retroviral vector carrying a selectable marker gene. In continuation of the work presented by Lund *et al.* (1993), we use vectors with a defective binding site for the tRNA primer. By the second approach, a provirus RNA product is detected by its ability to be selectively incorporated into retroviral particles. In the latter approach we have used cell lines engineered to produce retroviral proteins from RNA that is not in itself encapsidated

2) Pathogenicity of proviral genes.

The proviral LTR may regulate both retroviral and adjacent genes. Provirus reinsertions resulting from activation of an endogenous provirus may therefore be part of a cascade of radiation induced events leading to transformation. We have developed a hemi-specific polymerase chain reaction technique that allows the determination of DNA sequences adjacent to a provirus or to another piece of DNA of known sequence by a simple two-step procedure (Sørensen *et al.*, J. Virol. 1993) The technique uses partly degenerate primers with a defined pentanucleotide sequence in the 3' end. We have further expanded the potential of this technique by testing a number of new primers. The methodology has been applied to proviral integrations in tumours and in cell culture models as well as to analysis of other regions associated with genetic rearrangements.

We have continued our previous collaborative work with Institut für Molekulare Virologie, GSF, FRG, on a panel of molecular clones of endogenous proviruses or proviruses from radiation induced or non-radiation induced osteosarcomas and tumours of the haematopoietic system. Results are emerging from a long-term series of experiments of the pathogenic potency and tumorigenic specificity of specifically engineered mutated and recombinant viruses. As part of these studies tumour DNAs are analyzed for proviral integration sites and for alterations in LTR sequences that occur during tumourigenesis.

3) Retroviral vectors with telomere-like repeat DNA.

This project is directly linked to work carried out in the group of Dr. Roger Cox, National Radiological Protection Board, U.K., on radiation induced myeloid leukaemia and chromosome 2 fragility. Interstitital telomere-like repeat arrays on chromosome 2 may be linked to its sensitivity to radiaiton induced rearrangements and may have a role in radiation-induced myeloid leukaemia. To establish a cell culture model system that allows the study of the radiosensitivity of telomere-like repeat sequences inserted into various chromosomal locations, we have inserted DNA-

sequence elements with telomere-like arrays of biological or chemical origin into a retroviral vector. We have documented that retroviral vectors with shorter repeat arrays are transferred accurately and efficiently and begun studies of radiosensitivity of cell clones with telomere-like repeats inserted at various chromosomal locations.

Publications:

Sørensen, M.S., Duch, M., Paludan, K., Jørgensen, P., and Pedersen, F.S.: Measurement of hygromycin B phosphotransferase activity in mammalian cell extracts by a simple dot-assay. Gene 112, 257-260 (1992).

Pedersen, K., Lovmand, S., Jørgensen, E.C.B., Pedersen, F.S., and Jørgensen, P.: Efficient expression and replication of murine leukemia virus with major deletions in the enhancer region of U3. Virology 187, 821-824 (1992)

Jørgensen, E.C.B., Pedersen, F.S., and Jørgensen, P.: Matrix protein of Akv murine leukemia virus: Genetic mapping of regions essential for particle formation. J. Virol. 66, 4479-4487 (1992).

Nielsen, A.L., Pallisgaard, N., Pedersen, F.S., and Jørgensen, P.: Murine helix-loop-helix transcriptional activator proteins binding to the E-box motif of the Akv murine leukemia virus enhancer identified by cDNA cloning. Mol. Cell. Biol. 12, 3449-3459 (1992)

Pedersen, L., Behnisch, W., Schmidt, J., Luz, A., Pedersen, F.S., Erfle, V. and Strauss, P.G.: Molecular cloning of osteoma-inducing replication-competent murine leukemia viruses from the RFB osteoma virus stock. J. Virol. 66, 6186-6193 (1992).

Nørby, P.L., Pallisgaard, N., Pedersen, F S., and Jørgensen, P.: Determination of recognition sequences for DNA-binding proteins by a polymerase chain reaction assisted binding site selection method (BSS) using nitrocellulose immobilized DNA binding protein. Nucl. Acids Res. 20, 6317-6321 (1992).

Lund, A.H., Duch, M., Lovmand, J., Jørgensen, P. and Pedersen, F.S.: Mutated primer binding sites interacting with different tRNAs allow efficient murine leukemia virus replication J. Virol. 67, 7125-7130 (1993).

Sørensen, A.B., Duch, M., Jørgensen, P. and Pedersen, F.S.: Amplification and sequence analysis of DNA flanking integrated proviruses by a simple two-step polymerase chain reaction method. J. Virol. 67, 7118-7124 (1993).

Duch, M , Paludan, K., Lovmand, J., Pedersen, L., Jørgensen, P. and Pedersen, F.S.: A correlation between dexamethasone inducibility and basal expression levels of retroviral vector proviruses Nucl. Acids Res. 21, 4777-4782 (1993).

Pallisgaard, N., Nielsen, A L., Pedersen, F S., Birkelund. S. and Jørgensen, P.: A common poly-linker in a set of vectors for expression of eukaryotic genes in mammalian and insect cells and bacterial cells. Gene 138, 115-118 (1994).

Final Report
1992 - 1995

Contract: FI3PCT920008   **Duration: 1.9.92 to 30.6.95**   **Sector: B21**

Title: Research on the management of accidentally radiation exposed persons.

1)	Fliedner	Univ. Ulm
2)	Wagemaker	Univ. Rotterdam - Erasmus
3)	Covelli	ENEA
4)	Jammet	CIR

I. Summary of Project Global Objectives and Achievements

The working programme 1992-1995 on "Research on the Management of Accidentally Radiation Exposed Persons" conducted by the groups in Ulm (Prof. Fliedner), in Rotterdam (Prof. Wagemaker), in Rome (Prof. Covelli) and in Paris (Prof. Jammet) is outlined in table 1 (see page 5). From this table it can be seen that the objectives of the working programme were to contribute to four research areas:

- pathophysiology of radiation induced alterations of the immuno-hematopoietic system, the respiratory and the gastrointestinal systems and the central nervous system
- diagnosis of the radiation syndromes: preclinical and clinical approaches
- prevention of the radiation syndromes
- therapy of the radiation syndromes

Table 1 also indicates which group contributed in more detail to what research area. There is no doubt that all groups did more research work than could reasonably be expected in the frame of the given time and available resources. Two major symposia were held between the contributing scientists, one in Ulm (Germany) in May 1993 and one in Paris (France) in Jan./Feb. 1994. Beyond that many bi- or trilateral consultations were held so that the contributing scientists had the opportunity to discuss with each other important aspects resulting in an intensive approach of coordinated research in the given field.

As far as the <u>pathophysiology of radiation induced alterations of the immuno-hematopoietic system</u> is concerned, the <u>Group of Prof. Wagemaker</u> contributed extensively to the radiobiological characterization of hemopoietic stem and progenitor cells and their subsets analyzed by most advanced technology. They came to the conclusion that the short-term and most likely the long-term repopulating stem cells are confirmed to the small (0.05 of all bone marrow cells) $CD34^+/DR^{dull}$ fraction. The <u>Group of Prof. Fliedner</u> studied extensively the biological and molecular biology characterization of stem and progenitor cells with the goal of their purification which is a prerequisite for their characterization in terms of replication and differentiation. They succeeded to develop a novel approach resulting in a rapid isolation of pure (>99.5% purity by FACS analysis) $CD34^+LIN^-$ cells. This group also studied - using the reverse transcriptase polymerase chain reaction (RT-PCR) - the expression of antigens linked to differentiation in single $CD34^+$ cells from cord blood (CB), peripheral blood (PB) and multipotent cells from blasts cell colonies (BCCs).

The Group of Prof. Jammet (Dr H. Magdelenat) paid particular attention to the mechanisms and modulation of radiation induced apoptosis of human lymphocytes and established that radiation exposure of these cells induces not only nucleosomal degradation of chromatin but also the degradation of 28S ribosomal RNA (rRNA). Furthermore, there is evidence of a relationship between ubiquitin gene expression, ubiquitination of nuclear proteins and radiation mediated apoptosis in normal human peripheral blood lymphocytes suggesting that the polyubiquitin gene appears to be one of the "death" genes in γ-ray mediated apoptosis. The particular interest of the Group of Prof. Covelli in Rome in this research area concentrated on the pathophysiology of the immune system and on the interaction of cytokines to modify the radiation response.

In summary, the consortium has been quite successful in promoting the pathophysiological basis of therapeutic approaches to overcome the acute radiation syndrome in man, using the most advanced technologies available

In the research area "diagnosis of the radiation syndromes: preclinical and clinical approaches", all groups were able to make innovative contributions. The Rotterdam Group (Prof. Wagemaker) studied hemopoietic growth factors in vivo to assess and diagnose the residual capacity of the bone marrow after high dose exposure to radiation with special reference to growth factors that stimulate immature hemopoietic cells. The Ulm Group (Prof. Fliedner) advanced the possibilities to detect DNA damage after exposure doses of 0.3-1 cGy by means of single cell gel electrophoresis methods ("Comet Assay") and developed a new approach to detect residual damage in mononuclear blood cells by exposing them to a standard conditioning dose. With this approach residual damage was detected - for instance in children from the Chernobyl region, in liquidators and in patients after ^{131}I therapy. Thus, it appears that a tool is available that is less time-consuming but of equal value to chromosomal studies. The Ulm Group also advanced their "biomathematical granulocyte system model" to assess radiation damage to the stem cell pool in the marrow spaces by extrapolating from the granulocyte response pattern after irradiation, how many (virtual=calculated) stem cells must have been affected and to establish a threshold value for the need to treat bone marrow failure by stem cell transplantation. The Group in Paris (Prof. Jammet, Dr. E.D. Carosella) contributed to this area by studying the effects of total body irradiation (given for therapeutic reasons) in its effect on the various lymphocyte populations in their radiation response. They concluded that T and B subsets seem to be equally radiosensitive after in vivo TBI with the exception of one immature thymocyte subset. However, by comparison, the CD34^{+} progenitor/stem and natural killer (NK) cells seem to be more radioresistant. These findings are of importance for the pathophysiological evaluation of effects of radiation exposure. The Group in Paris (Dr. Magdelenat) contributed also interacting data on the plasma concentration of various cytokines during the first 24 hours after TBI in patients but concluded that more work has to be done in order to determine whether cytokines may be employed in the assessment of radiation injury.

Under term "prevention of the radiation syndromes", studies are summarized to investigate which means are available to modify the radiation syndromes in such a way that they would result in a diminished impairment of health. In this sense, the term "prevention" should be understood by refering to "secondary prevention". In this area, two major questions were addressed: in what way would the administration of cytokines be useful to accelerate hemopoietic recovery to avoid the need for

intensive care and in what way can one avoid graft rejection and graft-versus-host disease if an allogeneic stem cell transplantation has to be done to save the patients life. The Rotterdam Group (Prof. Wagemaker) completed and published a full study on the *in vivo* efficacy and side effects of IL-3, of IL-6 and tested the IL-6/IL-3 combination of growth factors *in vivo*. In addition, they completed a study of receptor distributions of IL-6, IL-3, GM-CSF and SCF. The Ulm Group (Prof. Fliedner) expanded the basic knowledge in this field by preclinical studies addressing two questions: Is growth factor treatment able to stimulate hemopoietic activity in protected marrow (after partial body irradiation) and will growth factor treatment accelerate repopulation of an irradiated bone marrow by stimulating the seeding of stem cells from protected marrow sites. It could be shown that the repopulation of damaged bone marrow sites can be accelerated by administration of two growth factors (rhG-CSF and rhGM-CSF). The Group in Paris (Prof. Jammet, Dr. A. Fischer) concentrated on the problem of avoiding graft rejection and graft-versus-host disease after haploid identical marrow transplantation by infusion of donor T cells devoid of alloreactivity towards a recipient. They showed that the infusion of anti-host-depleted T cells to haplo-compatible irradiated mice together with T depleted marrow syngeneic to the T cells led to significant protection against both GVHD and rejection and to increased survival. The Group in Rome (Prof. Covelli) studied improved technologies for a rapid and precise HLA typing in humans. This technique requires a small amount of cells for DNA extraction (5×10^6) a reasonable time (6 hours) and is at low cost (60 US $). Thus, it can be expected to improve the approaches to reduce or avoid immunological consequences after bone marrow transplantation.

The consortium also contributed extensively to the field of <u>therapy of the radiation syndromes</u> in a variety of means and ways. The Group in Rotterdam (Prof. Wagemaker) identified a "window" of about 7-10 Gy of TBI where hemopoietic stem cell transplantation should be considered and further developed as a life saving therapy for radiation accident victims, at least to abridge a period of 4-12 weeks of profound cytopenia. In this area, the transfusion of allogeneic CD34$^+$ positive cells to achieve transient engraftment as a means to facilitate the mangement of radiation accident victims was considered to be most relevant. A similar conclusion was reached by the Ulm Group (Prof. Fliedner). In cooperation with transplant teams of the Hematology Departments in Heidelberg, Ulm and Houston, Texas, the results of blood stem cell transfusions performed under autologous and allogeneic conditions to repopulate aplastic bone marrow were evaluated. It was conclusively demonstrated that the most appropriate indicator of stem cells in a transfusate are CD34$^+$ cells and that their number correlates with the granulocyte pattern of regeneration and is proportionate to the number of "virtual" stem cells calculated by means of biomathematical simulation. The Group in Paris (Prof. Jammet, Dr. Magdelenat, Dr. Carosella, Dr. Gluckman) used clinical opportunities to address several basic as well as applied questions. This group has a particular competence in the use of cord blood hemopoietic stem cells as an alternative source of stem cells. More than 50 cord blood transplants have shown that long-term engraftment can be achieved in patients with different diagnoses including both malignant and non-malignant disorders. However, the number of cells transplanted is low compared to blood or bone marrow derived stem cells. Therefore - at present - the time of hemopoietic recovery seen is relatively long. Therefore, a lot of research has been done to characterize the biological properties of cord blood cells by means of cell culture techniques. Also studies have been performed on the immunological properties of cord blood cells which is important for answering the question of the

induction of graft-versus-host disease using cord blood cells. In addition, extensive studies have been performed in Paris to show that it is possible and feasible to expand the number of progenitor cells in cord blood by the molecule CD31 mAb in the presence of growth factors like rhGM-CSF, rhCSF and erythropoietin. Thus, cord blood stem cells - especially after amplification - will have to be considered a very important alternative source of stem cells to reconstitute radiation induced hemopoietic failure.

It is also worth pointing out that data bases have been set up in Ulm and in Paris to collect case histories of patients given irradiation and appropriate treatment. Furthermore, registries are available for recruiting stem cell donors, including a European Cord Blood Bank.

In conclusion, there is no doubt that the Consortium of Scientists in Rotterdam, Paris, Rome and Ulm has very successfully contributed to the improvement of existing and the development of new approaches to manage accidentally radiation exposed persons.

Table 1:

		Prof. Jammet FRANCE	Dr. Wagemaker NETHERLANDS	Prof. Covelli ITALY	Prof. Fliedner GERMANY
1	Pathophysiology of radiation induced alterations of the	Radiation induced depression of different cell lines of blood cell formation with particular emphasis on interaction of stem cells and stroma cells	Reassessment of the radiation sensitivity of hemopoietic stem cells	The influence of ionizing radiation on functions of lymphocyte populations	Replication and differentiation of hemopoietic stem cells after total and partial body irradiation
1 1	Immuno-hematopoietic system	Kinetics of various categories of lymphocytes	Influence of intensive care on LD050 of bone marrow damage		Kinetics of hemopoietic reconstitution after total and partial body irradiation development of biomathematical models to simulate pathophysiological courses of events to assess the remaining and initiating stem cell pool
1 2	Respiratory and gastrointestinal system	Possibilities and limitations to tolerate single, repeated radiation exposures in relation to dose and dose rate			
1 3	Central nervous system	Development of radiation induced changes in the CNS neurological and psychic consequences, EEG changes			Assessment of radiation damage to the microenvironment of the bone marrow, the lung and the GI system
2	Diagnosis of the radiation syndromes pre-clinical and clinical approaches	Indicators of TBI and PBI Indicators of efficiency of growth factors, models relating biological indicators and physical dosimetry	Stimulation by hemopoietic growth factors as a test for the capacity of autochthonous regeneration	Biological indicators to evaluate the radiation induced damage of the immune sytem and to predict the pathological consequences	Blood cell deviation (quantity, quality) as prognostic indicators for or against stem cell transplantation (granulocytes, blood stem cells, platelets) Chromosomal and single cell DNA injury changes as indicators for hematopoietic cell system damage
3	Prevention of the radiation syndromes	Use of enzymes to prevent the development of fibrotic changes (lung, skin) and of vascular late effects	Hemopoietic growth factors as "radioprotectors"	Recombinant cytokines as "radioprotectors"	Prophylactic administration of growth factors to prevent radiation hemopoietic failure Research on the establishment of "stem cell banks" for persons "at risk"
4	Therapy of the radiation syndromes	Methods for inhibition of graft versus host disease (GvHD) including selective elimination of lymphocytes Improvement of stem cell transplantation (incompatible, purified stem cells, cord blood stem cells) Use of hematopoietic growth factors Improvement of radioactive decorporation in order to reduce the radiation effects on hematopoietic and immune system	Acceleration of autochthonous regeneration by hemopoietic growth factors Possibilities to replace conventional intensive supportive care by a specific combination of hemopoietic growth factors Transient engraftment of purified stem cells	Modulation of the immune response by recombinant cytokines Improvement of the rapidity in HLA typing for preparing for bone marrow transplantation Selection of bone marrow donors with appropriate immune responsiveness to prolong survival and reduce morbidity of radiation chimeras	Evaluation of drugs that enhance the endogenous production of hemopoietic growth factors Stem cell mobilization into the peripheral blood by drugs or by growth factors Improvement of approaches to use blood derived stem cells for bone marrow reconstitution

Head of project 1: Prof. Fliedner

II. Objectives for the reporting period

The Ulm Group under the directorship of Prof. Dr. T. M. Fliedner envisaged to contribute to the cooperative programme on "Research on the Management of Accidentally Radiation Exposed Persons" in the following areas:

In the field of "pathophysiology of radiation induced alterations of the immuno-hematopoietic system", the work concentrated on the replication and differentiation of hemopoietic stem cells and on the assessment of radiation damage to the microenvironment of the bone marrow and on the radiation response characteristics of stromal progenitor cells and their modulation by growth factors. In the field of improvement of diagnostic possibilities of radiation syndromes, it was the intention to analyze blood cell changes as an indicator to assess the need for stem cell transplantation. In addition, it was important to use a new tool - the comet assay - as an indicator for hematopoietic cell system changes. In the area of prevention of the radiation syndromes, the Ulm Group concentrated on the prophylactic administration of growth factors in the canine model and on the development of stem cell banks for "persons at risk". Finally, the Ulm Group contributed to the therapy of the radiation syndromes by improving approaches to use blood derived stem cells for bone marrow reconstitution and by the evaluation of drugs that enhance the endogenous production of hemopoietic growth factors.

III. Progress achieved including publications

1   Pathophysiology of radiation induced alterations of the immuno-hematopoietic system

1 1   Studies on the pathophysiological mechanisms of hemopoietic stem cell replication and differentiation as a basis to better understand the mechansims of radiation response

Hemopoiesis is sustained by a pool of hemopoietic stem cells (HSC) that are defined by their ability to self-renew and to differentiate into lineage(s)-committed progenitors. The progenitors in turn differentiate into morphologically recognizable precursors, which mature to terminal elements circulating in the peripheral blood (PB). Monoclonal antibodies (MoAbs) directed against the CD34 antigen recognize a heterogeneous population of progenitor cells, which represents approximately 1-2% of the mononuclear cells (MNC) present in human bone marrow (BM) and umbilical cord blood (CB). The $CD34^+$ population comprises largely progenitor cells committed to erythroid, granulomonocytic, megakaryocytic or B lymphoid lineage, but also multipotential progenitor cells and a small subset of repopulating stem cells. Based on cell-surface antigen expression the CD34 population can be divided into subsets with differing functional properties, as evaluated by *in vitro* colony assays, long-term culture systems, blast cell colony assays (CFU-B) and xenograft models such as immunodeficient mice and fetal sheep

Development of HSC/HPC purification strategies are essential for the investigation of radiaton effects on primitive hemopoietic stem cells. Several monoclonal antibody-based strategies such as immunoaffinity columns or immunomagnetic particles have been applied to purify CD34$^+$ cells and immature subsets thereof. For experimental purposes or for autologous stem cell transplantations positive/negative as well as negative/positive selection strategies have been reported to result in highly purified fractions of CD34$^+$Lin$^-$ cells or other immature CD34$^+$ subsets. Isolation of highly purified, complex CD34$^+$ subpopulations can be accomplished most reliably by flow cytometry cell sorting. This has been applied to isolate undifferentiated CD34$^+$ hemopoietic progenitor cells (HPC) from different stem cell sources such as those that were CD34$^+$CD33$^-$CD18$^-$, CD34$^+$CD33$^-$, CD34$^+$CD38$^-$, CD34$^+$CD45RA$^{-/low}$CD71$^{-/low}$, CD34$^+$HLA-DR$^-$c-kit$^{+/low}$, CD34$^+$Thy-1$^+$Lin$^-$.

Due to the low frequency of CD34$^+$ cells lengthy flow cytometry cell sorting times are necessary to obtain a sufficient number of highly purified cells. This difficulty may be overcome by enrichment of CD34$^+$ cells prior to sorting. However, CD34$^+$ enrichment protocols must be compatible with the subsequent cell sorting step, i.e., anti-CD34 as well as other color-conjugates MoAbs used for flow cytometry purification of enriched CD34$^+$ cells must specifically recognize their targets. CD34$^+$ cells can be rapidly isolated from different hemopoietic sources using MoAbs directed to CD34 and immunomagnetic beads. Subsequent flow cytometry cell sorting requires removal of beads from enriched CD34$^+$ cells, usually by enzymatic treatment with chymopapain. Further purification of enriched, chymopapain treated CD34$^+$ cells with primitive immunophenotype by cell sorting requires identification of chymopapain resistant key cell surface antigens.

Development of this two-step protocol has allowed the Ulm Group to isolate highly purified immature CD34$^+$ subsets which are then available for further functional and molecular characterization. Furthermore, an improved purification strategy for the rapid isolation of pure (>99,5% purity by FACS analysis) CD34$^+$LIN$^-$ cells has been recently developed by the Ulm Group (unpublished results). These early progenitors are highly enriched in LTC-ICs and CFU-Bs and thus comprise a considerable proportion of primitive HSCs/HPCS which are available for studies aimed to analyze the effects of ionizing irradiation at the molecular level. However, the mechanisms that control proliferation and differentiation of primitive HSCs/early HPCs under physiological conditions as well as after exposure to ionizing irradiation are still poorly understood. This is largely due to (i) the extreme rarity of early HPCs and HSCs in human CB, PB and BM, (ii) limitations of presently available protocols that do not allow the isolation of homogeneously purified CD34$^+$ subsets, and (iii) quantitative difficulties when only a few cells are available for analysis. Thus, single cell analysis by using highly sensitive techniques such as the RT-PCR may be applied to resolve these problems.

The Ulm Group has applied and refined the reverse transcriptase polymerase chain reaction (RT-PCR) technique to study expression of antigens linked to differentiation in single CD34$^+$ cells from cord blood (CB), peripheral blood (PB) and multipotent cells from blast cell colonies (BCCs). This strategy was used to investigate the mRNA phenotype of multipotent BCCs. Notably, the mRNA phenotype of BCCs revealed that BCCs are characterized by the expression of a unique differentiation marker profile, i.e., CD34$^+$CD33$^-$CD38$^-$Thy-1$^-$c-kit$^+$, and thus resemble primitive hemopoietic cells with stem cell-like phenotype. Furthermore, extensive studies on the mRNA phenotype of single cells derived from BCCs revealed that BCCs

represent a homogeneous population of cells. Thus BCC derived cells may represent a precious source of a homogeneous population of undifferentiated hemopoietic cells for further unicellular culture studies. Studies are now underway to investigate whether single cells from BCCs can be induced to unilineage differentiation and proliferation. This would allow us to investigate the cascade of gene expression that controls differentiation along a particular hemopoietic lineage.

The RT-PCR was also applied to investigate effects of chymopapain on epitopes of several key cell surface markers coexpressed with CD34. Antigen expression was comparatively analyzed by flow cytometry and the limiting dilution reverse transcription polymerase chain reaction (LD RT-PCR): LD RT-PCR allows to detect the expression of antigens degraded by chymopapain, which are not identified by flow cytometry. Monoclonal antibodies (MoAbs) that recognize chymopapain-resistant epitopes on several coexpressed cell surface markers were identified: these included MoAbs directed against CD11a, CD13, CD18, CD38, CD45R0, CD51, HLA-DR, Thy-1, c-kit, flt-3 and mdr-1. RT-PCR of single sorted $CD34^+CD18^-$, $CD34^+CD33^-$, $CD34^+CD38^-$, $CD34^+Thy-1^-$ and $CD34^+c-kit^-$ cells, as well as corresponding double-positive cells, demonstrated that their antigenic phenotype corresponded with their mRNA phenotype. The frequency (LD RT-PCR) of CD18, CD38, Thy-1 and c-kit RT-PCR signals on pure sorted $CD34^+CD18^-$, $CD34^+CD38^-$, $CD34^+Thy-1^-$ and $CD34^+c-kit^-$ cells, respectively, was similar in corresponding subsets treated ($chym^+$) or not ($chym^-$) with chymopapain.

Furthermore, by competitive RT-PCR we demonstrated downmodulation of the CD34 mRNA in single sibling $CD34^+$ cells induced to erythroid unilineage differentiation. Thus, RT-PCR allows semiquantitation of mRNA transcripts in individual cells. Our study on the phenotypic profile of CB $CD34^+$ cells shows that several key cell surface markers of hemopoietic progenitor cells are chymopapain resistant. More important, the results of the Ulm Group demonstrate that the RT-PCR can be applied to the analysis of multiple RNA species and their quantitation in single hemopoietic progenitor cells. This RT-PCR approach will be used in forthcoming studies to analyze and semiquantitate both markers linked to differentiation and genes that control proliferation and differentiation in early, intermediate and late HPCs and HSCs which have been exposed or not to ionizing irradiation. Furthermore, the Ulm Group has performed collaborative studies aimed to induce differentiation and proliferation of highly purified HSCs/HPCs along specific hemopoietic lineages. Notably, it could be demonstrated that highly purified HSCs/HPCs stimulated by the recently cloned growth factor thrombopoietin alone, proliferate and differentiate selectively along the megakaryocytic lineage. The establishment of cell culture conditions within the frame of this European project that allows unilineage differentiation of highly purified HSCs/HPCS along the megakaryocytic, erythroid, granulocytic and monocytic lineage will enable further studies on the effects of ionizing irradiation on different hemopoietic lineages.

Other studies of the Ulm Group have focussed on the effects of early acting hemopoietic growth factors (HGFs) on the repair of radiation induced damage to highly purified hemopoietic $CD34^+$ cells. After exposure of $CD34^+$ cells to different radiation doses (0-146 cGy) the effects of HGFs on the repair kinetic were investigated. Combinations of interleukin-3 (IL-3), IL-6 and c-kit ligand proved to be most effective with respect to radiation-induced damage as evaluated by clonogenetic assay and Comet-assay.

Currently, further studies are being performed in the Ulm laboratory aimed to investigate HGF requirement for the *ex vivo* expansion of radiation-exposed and non-exposed primitive hemopoietic stem/progenitor cells.

1.2   Assessment of radiation-induced DNA damage in canine bone marrow stromal cells and hemopoietic cells as measured by the comet assay

The progenitor cells of the stromal elements in canine bone marrow are much less radiosensitive than the hemopoietic progenitor cells as reflected by their respective D_0 values of ~ 2.5 Gy and in the range of 0.12 to 0.6 Gy. It was of interest to know whether such differences could be related at least in part to the amount or the nature of the initial damage to the genome.

To test for this possibility, the alkaline single-cell gel electrophoresis technique for the in situ quantitation of DNA strand breaks and alkali-labile sites was employed. Canine buffy coat cells from BM aspirates and cells harvested from CFU-F colonies or from mixed populations of adherent BM stroma cell layers were exposed to increasing doses of X-rays, embedded in agarose gel on slides, lysed with detergents and placed in an electric field. DNA migrating from single cells in the gel was made visible as "comets" by ethidium bromide staining. Immediate DNA damage was much lower in cultured stroma cells than in hemopoietic cells in BM aspirates. These results suggest that the observed differences in clonogenic survival could be partly due to differences in the type of the initial DNA damage between stromal cells and hemopoietic cells.

1.3   Characterization of radiation response characteristics of stromal progenitor cells (CFU-F) from canine bone marrow to *in vitro* irradiation and their modulation by hemopoietic growth factors

In these experiments, it was tested whether clonogenic survival of CFU-F after *in vitro* irradiation can be influenced by growth factors present in the incubation period after irradiation. The radiation dose response-curves obtained under standard conditions in the presence of 20% fetal calf serum (FCS) were characterized by a D_0 value of 2.5±0.5 Gy. The addition of basic fibroblast growth factor (b-FGF) increased the plating efficiency but caused no significant changes in the D_0 value. In contrast, the presence in the cultures of 10% serum obtained from total body irradiated dogs (~4 Gy) in the phase of bone marrow aplasia not only caused a similar increase in the plating efficiency but in addition was associated with a considerable increase in the radioresistance as reflected by the increased D_0 value of ~3.1±0.2 Gy. These results indicate that the proliferative capacity of stromal progenitor cells after irradiation is dependent on the presence of certain growth factors elaborated by the organism after radiation exposures. The nature of these factors is unclear.

2.   Diagnostic possibilities of radiation syndromes

2.1   Recognition of reversible and irreversible damage of the hemopoietic stem
        cell pool by bioengineering appraoches

In the management of accidentally radiation exposed persons, the key question for
the medical doctor is to answer the question whether or not a spontaneous recovery
of the hemopoietic system can be expected or not. in the reporting period of 1992-
1995, the Ulm Group refined its approaches to assess the damage to the stem cell
pool by homogeneous and inhomogeneous radiation exposure by means of
bioengineering modeling. Based on the earlier model of granulocytic cell renewal,
the pattern of granulocyte changes after total body exposure in different dose ranges
was used to simulate this pattern by the biomathematical model developed. This
allows one to associate a particular granulocytic response pattern with a particular
number of remaining intact and of latently injured hemopoietic stem cells. One has to
remember that the stem cells are distributed in the hemopoietic sites of marrow in
the appropriate skeletal units (bones) and are normally in a continuous exchange via
the migratory blood stem cell pool. After homogeneous penetrating radiation
exposure, all stem cell sites would be expected to be injured to the same extent.
However, in the real world, it is difficult to visualize such a homogeneous exposure
and it is most likely that some parts of the stem cell pool distributed throughout the
organism are injured more and others less. However, the question of a reversible or
an irreversible damage to the stem cell system depends not on the "exposure dose"
but on the number of intact remaining stem cells somewhere in the skeleton.
Therefore, the decisive value on which to base therapeutic strategies is not the
calculated "exposure dose" but the number of "virtual stem cells" remaining intact.
There are two clear cut granulocyte response patterns after radiation exposure. If
the blood granulocyte concentration increases during the first 12-36 hours and
decreases precipitously between days 4 and 6 after irradiation to values below 200-
300 per mm^3, this pattern is compatible with a dose to complete destruction of the
stem and progenitor cell pools. The number of remaining virtual stem cells
calculated by the biomathematical model used is much lower than 1% of normal.
Under these circumstances, the patient can only be saved by stem cell
transplantation. If, however, the granulocytes decrease more slowly during the days
4-6 after irradiation after a transient abortive rise, most likely to values of 300-800
per mm^3 at the most, this indicates some continued cell production in the
hemopoietic precursor compartment. The calculated fraction of remaining intact
virtual stem cells associated with such a granulocyte response pattern is in the order
of 1-5% of normal. Under these circumstances, the therapeutic approach will include
the use of antibiotics to combat possible infections, the use of platelets in case of
severe thrombocytopenia and - most importantly - the use of growth factors to
accelerate hemopoietic recovery which is expected to occur spontaneously under
these conditions. Details of this approach are found in the list of publications

2.2   The Comet Assay - A new biological indicator to assess genotoxic effects and
        the repair capacity in the hematopoietic cell system after irradiation

Techniques which permit a quick and easy detection of DNA damage in cells of
individuals accidently, environmentally or occupationally exposed to ionizing
radiation are essential. So far, an analysis of structural chromosomal aberrations in
mitogen-stimulated peripheral blood lymphocytes has had the greatest value in

radiation biomonitoring. Classic cytogenetic analysis as well as the micronucleus test are methods which measure an effect on cell systems in the human organism on the single cell level. The disadvantages of the cytogenetic methods are their limitation to proliferating cells as well as the time consuming preparation. Results can be expected only days or weeks after the actual exposure. Biochemical and molecular biological methods do not allow a statement about distribution of DNA damage (or repair) among individual cells. Furthermore, these test systems are not specific for radiation, require a large amount of cell material and are often not sensitve enough to detect low dose exposure.

Our studies evaluated the applicability of the comet assay as a new tool for the biomonitoring of radiation exposed individuals. This technique detects single- and double-strand breaks, alkaline-labile damage, as well as incomplete excision repair sites in the DNA of individual cells. The advantages of this technique include: (a) data are collected at the level of single cells, providing information on the intercellular distribution of damage and repair; (b) the assay is sensitive, simple, and cost effective; (c) the assay requires only few cells for analysis; (d) the ability to evaluate DNA damage in proliferating and non-proliferating cells; (e) any cell population (e.g. cells isolated via beads or FACSsorter) can be used.

In order to demonstrate the practicability of the comet assay for the detection of DNA damage caused by low doses of ionizing radiation, we exposed human peripheral blood cells to radiation (X-rays 2 - 300 cGy) *in vitro*. Our data showed that the extent of DNA damage was significantly increased above the control values even at 5 cGy and that it showed a clear dose-relationship. To investigate the repair kinetics for radiation-induced DNA damage following acute and chronic (fractionated) irradiation, we exposed periperal blood to 100 cGy and examined the tail moment at different time intervals. Most of the repair (approximately 50%) occurred within the first 15 minutes. This was followed by a period of slower repair. After incubation of 30 minutes, the median tail moment decreased by approximately 60-70%. The repair was essentially complete by the end of 2 hours. Of great interest is the effect of a fractionated irradiation. For that we exposed human blood cells several times to 100 cGy of X-rays, interrupted by a 2 hours period to permit repair. The DNA damage induced by one acute dose was repaired within 2 hours, whereas the effect of fractionated irradiation gave a totally different result. The tail moment of the initial damage increased indicating an accumulation of the damage and the repair activity clearly decreased.

To test whether these effects can also be observed *in vivo*, we analyzed the blood cells of 40 patients subjected to a radioiodine therapy, one liquidator and one child involved in a radiation accident and 22 children from the Chernobyl region.

First we assessed the intra-individual and inter-individual variability as well as the influence of age, sex and smoking habits in an unexposed control group of 100 healthy volunteers. The results show that there is only a small and therefore neglectable variation in the intra-individual variability as well as in the inter-individual variability. No significant differences could be observed in relation to age, sex and smoking habits. In the following, the data of the control group are compared to the data obtained in the blood of persons exposed to ionizing radiation:

Patients subjected to a radioiodine therapy. the average control value for the patients before therapy was the same as for a group of healthy volunteers. During

therapy with ^{131}I all of the patients showed a significant increase in DNA damage caused by ionizing radiation. One of the important outcomes of this study is the fact that very low doses of ionizing radiation *in vivo* lead to DNA damage. We could show significantly increased DNA damage for calculated blood doses (day of the max. damage) from 0.3 cGy to 41 cGy. Moreover, most of these patients showed repair within the observation time of 7-10 days. This study demonstrated that the comet assay is a sensitive biomarker for the measurement of genotoxic effects induced by low-doses of radiation.

Children from radioactively contaminated regions in the Western Ukraine: these children live in contaminated areas and are therefore exposed to a chronical external and internal irradiation. To see whether there is an initial DNA damage and/or an affected repair of DNA damage in the blood cells, we analyzed the peripheral blood prior and several times after an *in vitro* irradiation of 100 cGy. The results we obtained revealed a significantly increased number of damaged blood cells in these children. Furthermore, the leukocytes of the children showed a decreased repair capacity in comparison to an unexposed control group. The same effects could be observed in a child who was accidently exposed to an intermitted dose of 1.5-2 Gy. In this child the DNA repair capacity of the blood cells was affected to an even higher degree.

Chernobyl liquidator: the investigation of the Chernobyl worker also indicates that chronic radiation can lead to persisting DNA damage *in vivo*.

The results of these studies indicated that intermitted or chronical exposure to radiation *in vivo* leads to a decreased DNA repair capacity of blood cells as monitored with the comet assay.

In conclusion:
 On the one hand, we could show that the comet assay is an excellent indicator test capable of detecting DNA damage and repair following an acute exposure also to very low doses of ionizing radiation *in vitro* and *in vivo*. On the other hand, our results with the chronical or intermitted exposed persons pointed out that the DNA damage accumulates and that the repair capacity decreases. This shows that we are also able to detect chronic or intermitted radiation exposure even after a longer period of time and that we are able to recognize affected people by an impaired repair system. Thus, the comet assay is a good approach for the human biomonitoring of populations or single persons exposed to acute, intermitted or chronic ionizing radiation.

3.   Secondary Prevention and Treatment of the Radiation Syndromes

3.1   In the field of research directed to the handling of radiation syndromes both aspects, i.e., prevention and therapeutical approaches were studied in pre-clinical models on a common basis

The aim of the experimental work was to study in dogs the efficiency of short-term growth factor treatments in accelerating the hemopoietic recovery after partial body irradiation with a large single dose given to a major fraction of the total bone marrow mass. The studies were focussed on two major questions: 1.) Whether growth factor treatment is able to stimulate the hemopoietic activitiy in the protected marrow

and/or 2) whether growth factor treatment can accelerate the repopulation of the irradiated bone marrow by stimulating the seeding of stem cells from the protected marrow sites. In the literature this latter process is termed "mobilisation".

The two growth factors rhG-CSF (recombinant human granulocyte colony-stimulating factor) and rhGM-CSF (recombinant human granulocyte-macrophage colony-stimulating factor) were studied under strictly similar experimental conditions.

The dogs received irradiation of the upper body (UBI) with a single dose of 11.7 Gy, comprising ~72% of the total bone marrow mass. Treatment with both of the CSFs was employed for 7 days by daily injections of 30 μg/kg starting 24 hrs after UBI. The irradiated control animals showed a depression of the blood granulocytes to <30% of the initial values in the period from day 5 to day 10, followed by continuous recovery in the period from day 8 to day 15. In contrast, treatment with rhG-CSF caused much stronger effects, as reflected by two phases of granulocytosis and an early recovery to nearly normal levels at day 15 after UBI. Determinations of progenitor cells (GM-CFC and BFU-E) and absolute cell numbers in defined BM samples revealed that rhG-CSF accelerated the hemopoietic recovery in the irradiated sites within the first 21 days after UBI in comparison to the controls and the rhGM-CSF treated animals. Treatment with rhG-CSF, but not with rhGM-CSF, was associated with a strong supra-normal increase of progenitor cells in the blood within the first 8 days. Therefore, the enhanced repopulation in the irradiated bone marrow during and after treatment with rhG-CSF probably is due to enhanced seeding of stem cells from the protected marrow. In contrast, no clear effects of the treatment with rhG-CSF or rhGM-CSF could be detected in the protected (non-irradiated) marrow sites. The results indicate that under conditions of partial body irradiation the repopulation of extremely damaged bone marrow sites can be accelerated by treatment with the two growth factors tested. However, applied as short-term treatment, rhG-CSF proved to be superior to rhGM-CSF.

3.2   Evaluation of stem cell transplantation after myeloablative therapy of patients
        with hemopoietic malignancies

There is still a great deal of debate as far as the use of stem cell transplantation in the treatment of the acute radiation syndrome is concerned. The Ulm Group in the last four years utilized the opportunity to evaluate patients with hemopoietic malignancies that were treated by a myeloablative therapy followed by an autologous and allogeneic stem cell transplantation.

These studies serve to refine the pathophysiological thinking of the use of pluripotent hemopoietic stem cells to treat hemopoietic failure such as seen after lethal total body radiation exposure.

These studies were performed in close collaboration with the hematological groups in the Department of Medicine of the University of Ulm, in the Department of Medicine of the University of Heidelberg and in the Department of Medicine, Hematology and Oncology of the MD Anderson Hospital in Houston, Texas. Ten patients of the Heidelberg University Hospital suffering from acute myelocytic leukemia were given 14.4 Gy fractionated total body irradiation followed by an autologous blood stem cell transfusion. The hemopoietic progenitor cells were

collected by means of leukapheresis during the CFU-GM overshoot seen after cyclophosphamide administration.

As a comparison, five AML patients of the Medical Department of the University of Ulm were subjected to allogeneic bone marrow transplantation. Six comparison patients were treated with autologous bone marrow transplantation with cryopreserved stem cells. Both patient groups received cyclophosphamide and 12 Gy total body irradiation as a conditioning regimen.

Six patients of the MD Anderson Hospital in Houston were included. They suffered from multiple myeloma and were conditioned with cyclophosphamide as well as busulphan and thiotepa and received autologous blood stem cells. These patients received G-CSF after autologous stem cell transplantation until 3000 granulocytes per µl were reached.

In all these patients the granulocyte regeneration was observed and evaluated in relation to the number of stem or progenitor cells transfused.

The analysis of the granulocyte response pattern was done using the biomathematical granulocyte model that was refined from previous work by the scientists (Prof. Dr. E.P. Hofer and Dr. B. Tibken) from the Department of Measurement, Control and Microtechnology of the University of Ulm. This model allows one to relate the granulocyte response pattern to the number of transfused hemopoietic stem and/or progenitor cells.

The key question was whether the mathematical calculation of the virtual stem cells corresponded linearly to the number of biological stem and progenitor cells measured as colony-forming units or with the $CD34^+$ cells in the transfusate.

It was possible to simulate with the granulocyte model used the regeneration pattern of granulopoiesis after autologous and allogeneous bone marrow transplantation as well as after autologous blood stem cell transplantation in a total of 21 patients who did not receive cytokines after transplantation.

In the simulation studies of six cases who received after autologous blood stem cell transplantation G-CSF for enhancement of regeneration, there are regeneration patterns that require further study.

As far as the correlation between the calculated virtual stem cell number determined by the simulation model and the number of transfused stem and progenitor cells was of particular importance (Satz ist unvollständig!!). There is no doubt that there is an excellent correlation between the calculated number of stem and progenitor cells if the $CD34^+$ cells in the transfusate are used. There was not a convincing correlation between the calculated virtual stem cell number and the number of colony-forming units in the transfusate.

This led to the conclusion that most likely one has in the future to determine the number of $CD34^+$ cells in the transfusate as a reliable indicator of the presence of stem cells for the use in the treatment of radiation exposed persons.

Publications

Fliedner, T.M.: Knochenmarktransplantation und ihre Problematik bei Strahlenunfällen. In: Strahlenschutz in Forschung und Praxis, Band 33, S. 185-191. 1992.

Fliedner, T.M., Heinze, B. und U. Plappert: Biologische Indikatoren zur Evaluation der Beanspruchung des Organismus durch ionisierende Strahlen. In: B. Kreutz und C. Piekarski (Hrsg.): 32. Jahrestagung der Deutschen Gesellschaft für Arbeitsmedizin in Köln 1992, 395-399. Gentner, Stuttgart 1992.

Fliedner, T.M. und W. Nothdurft: Simulationsmodelle der Hämatopoese zur Abschätzung der Strahlenbeanspruchung bei fraktionierter oder chronischer Strahlenbelastung. In: B. Kreutz und C. Pierkarski (Hrsg.): 32. Jahrestagung der Deutschen Gesellschaft für Arbeitsmedizin in Köln 1992, 400-406. Gentner, Stuttgart 1992.

Kolb, H.J., Guether,W., Duell,T., Socie, G., Schaeffer, E., Holler, E., Schumm, M., Horowitz, M.M., Gale, R.P. and T.M. Fliedner: Cancer after bone marrow transplantation, IBMTR and EBMT/ EULEP Study Group on Late Effects. Bone Marrow Transplant. 10, Suppl. 1 135-138, 1992.

Nothdurft, W., Selig, C., Fliedner, T.M., Hintz-Obertreis, P., Kreja, L., Krumwieh, D, Kurrle, R., Seiler, F.R. et al.: Haematological effects of rhGM-CSF in dogs exposed to total body rrradiation with a dose of 2.4 Gy. Int. J. Radiation Biology, Vol. 61 4 , 519-531, 1992.

Petri, J.B., Thoma, S., Lamping, C., Fliedner, T.M., Peschle, C. and B.L. Ziegler: Retrovirus-mediated gene transfer into multipotent human hematopoietic progenitor cells. Blood 80:179a (705), 1992.

Szepesi, T., Fliedner, T.M. und D. Densow: Entscheidungskriterien der medizinischen Erstversorgung nach nuklearen Unfällen in Notfallambulanzen. Beitr. Anaesth. Intens. Notfallmed. 41:111- 122, 1992.

Weinsheimer, M., Rothenbacher, D., Heinze, B. and T.M. Fliedner: "Biologische Dosimetrie" am Beispiel der Srahlenexposition. In: Verh. der Deutschen Gesellschaft für Arbeitsmedizin, 31. Tagung in Berlin 1991, 461-463 Genter Verlag Stuttgart, 1992.

Ziegler, B.L., Lamping, C., Petri, J.B., Fliedner, T.M. and S. Thoma: Phenotype analysis of umbilical cord blood (CB) CD34$^+$ cell subpopulations. Blood 80:408a (1623), 1992.

Ziegler, B.L., Thoma, S., Petri, J.B., Thomas, C.A. and C. Lamping: Single cell RT-PCR: Immobilized DNase I efficiently removes genomic DNA contaminating total RNA prepared from a single cell. Blood 80:198a (783), 1992.

Ziegler, B.L., Lamping, C., Thoma, S., and C.A. Thomas: Single-cell cDNA-PCR: Removal of contaminating genomic DNA from total RNA using immobilized DNase I. Biotechniques 13:726-729, 1992.

Fliedner, T.M., Weiss, M., Hofer, E.P., Tibken, B. und Y. Fan: Blutzellveränderungen nach Strahleneinwirkung als Indikatoren für die ärztliche Versorgung von Strahlenunfallpatienten. In: F. Holeczke, Chr. Reiners, O. Messerschmidt: Strahlenexposition bei neuen diagnostischen Verfahren. Biologische Dosimetrie - 6 Jahre nach Tschernobyl. Strahlenschutz in Forschung und Praxis, Band 34, 137 - 154, Gustav Fischer Verlag Stuttgart, 1993.

Kreja, L., Thoma, S., Selig, C., Ziegler, B.L. and W. Nothdurft: The effect of recombinant human stem cell factor and basic fibroblast growth factor on the in vitro radiosensitivity of $CD34^+$ hematopoietic progenitors from human umbilical cord blood. Experimental Hematology 21:1436-1441, 1993.

Selig, C., Nothdurft, W. and T.M. Fliedner: Radioprotective effect of N-Acetylcysteine on granulocyte/macrophage colony-forming cells of human bone marrow. J. Cancer Res. Clin. Oncol., 119:346-349, 1993.

Ziegler, B.L., Thoma, S., Lamping, C., Gause, H., Werner, A.K. and T.M. Fliedner: Identification of $CD34^+$ cell subsets from cord blood by flow cytometry and cDNA-PCR. Experimental Hematology 21:1136, 1993.

Calvo, W., Alabi, R., Nothdurft, W. and T.M. Fliedner: Cytotoxic Immigration of gGranulocytes into megakaryocytes as a late consequence of irradition. Radiat. Res. 138:260-265, 1994.

Densow, D., Fliedner, T.M. and D. Arndt: Übersicht und Kategorisierung von Strahlenunfällen und -katastrophen als Grundlage medizinischer Maßnahmen.. In: Bundesminister für Umwelt, Naturschutz und Reaktorsicherheit (Hrsg.): Medizinische Maßnahmen bei Strahlenunfällen. Veröffentl. der Strahlenschutzkommission, Band 27, 9 - 50, Gustav Fischer, Stuttgart 1994.

Fliedner, T.M: Strahlenwirkungen bei externer Ganz- und Teilkörperbestrahlung. In: Bundesminister für Umwelt, Naturschutz und Reaktorsicherheit (Hrsg.): Medizinische Maßnahmen bei Strahlenunfällen. Veröffentl. der Strahlenschutzkommission, Band 27, 65 - 84, Gustav Fischer, Stuttgart 1994.

Fliedner, T.M.: Blutstammzelltransplantation. In: Bundesminister für Umwelt, Naturschutz und Reaktorsicherheit (Hrsg.): Medizinische Maßnahmen bei Strahlenunfällen. Veröffentl. der Strahlenschutzkommission, Band 27, 241- 250, Gustav Fischer, Stuttgart 1994.

Fliedner, T.M.: Überblick über medizinische Maßnahmen beim Strahlenunfall. In: Bundesminister für Umwelt, Naturschutz und Reaktorsicherheit (Hrsg.): Medizinische Maßnahmen bei Strahlenunfällen. Veröffentl. der Strahlenschutzkommission, Band 27, 251 - 264, Gustav Fischer, Stuttgart 1994.

Fliedner, T.M., Nothdurft, W., Tibken, B., Hofer, E., Weiss, M. and H. Kindler: Haemopoietic cell renewal in radiation fields. Adv. Space Res. Vol. 14, No. 10, (10)541-(10)554, 1994.

Körbling, M. and T.M. Fliedner: History of blood stem cell transplants. In: R.P. Gale, Ch. Juttner and P. Henon (Eds.): Blood stem cell transplants. Cambridge University Press, p. 9-19, Cambridge 1994.

Szepesi, T. and T.M. Fliedner: Evaluation of accidental acute irradiated persons with respect to therapeutic measures. Izotoptechnika, Diagnosztika, Vol. 37, Suppl., 5-15, 1994.

Thoma, S., Lamping, C. and B.L. Ziegler: Phenotype analysis of hematopoietic CD34$^+$ cell populations derived from human umbilical cord blood using flow cytometry and cDNA-polymerase chain reaction. Blood 83:2103-2114, 1994.

Ziegler, B.L., Lamping, C., Thoma, S., Peschle, C and T.M. Fliedner: Single-cell RT-PCR: Isolation of mRNA from single hemopoietic cells allows detection of multiple mRNA species. Blood 84 (suppl. 1):1272 (1074), 1994.

Ziegler, B.L., Thoma, S., Lamping, C., Peschle, C. and T.M. Fliedner: A panel of monoclonal antibodies identifies chymopapain-resistant epitopes of antigens coexpressed on CD34$^+$ hemopoietic progenitor cells. Blood 84 (suppl.1):272a (1075), 1994.

Fliedner, T.M., Cronkite, E.P. and V.P. Bond (Eds.): Assessment of radiation effects by molecular and cellular approaches. Stem Cells, Vol. 13, Suppl. 1, AlphaMed Press, Dayton, Ohio, 1995.

Fliedner, T.M.: The Need for an Expanded Protocol for the Medica Examination of Radiation-Exposed Persons. In: Fliedner, T.M., Cronkite, E.P. and V.P. Bond (Eds.): Assessment of Radiation Effects by Molecular and Cellular Approaches. Stem Cells, Vol. 13, Suppl. 1, AlphaMed Press, Dayton, Ohio, 1 - 6, 1995.

Fliedner, T.M., Wüstermann, P.-R., Tibken, B. and E.P. Hofer: Structure and function of the immune system under influence of ionizing radiation: New approaches of biomathematical modeling. In: Hagen, U., Jung, H.. and C. Streffer (Eds.): Radiation Research 1895-1995. Vol. 1: Congress Abstracts. Congress Proceedings of the 10th Intern. Congress of Radiation Research Würzburg, Germany, 75, 1995.

Fliedner, T.M.: Blood stem cell transplantation (from preclinical to clinical models). Stem Cells 13 (Suppl. 3), AlphaMed Press, Dyton, Ohio, 1995 (in press).

Frickhofen, N., Körbling, M. and T.M. Fliedner: Is blood a better source of allogeneic hematopoietic stem cells for use after radiation accidents? Bone Marrow Tranplantation 1995 (in press).

Guerriero, R., Testa, U., Gabbianelli, M., Mattia, G., Monteroso, E., Macioce, G., Pace, A., Ziegler, B.L., Hassan, H.J. and C. Peschle: Unilineage megakaryocytic proliferation and differentiation of purified hematopoietic progenitors in serum-free liquid culture. Blood 1995 (in press).

Hassan, H.J., Guerriero, R., Testa, U., Gabbianelli, N., Mattia, G., Nonteroso, E., Macioce, G., Pace, A., Ziegler, B.L. and C. Peschle: Megakaryocyte growth and maturation from purified peripheral blood progenitors in unilineage serum-free liquid culture. Haematologica 1995 (in press).

Heinze, B., Arnold, R., Rutzen-Loesevitz, L. and T.M. Fliedner: The role of stable chromosome aberrations as biological indicators of radiation effect: Studies in patients after total body irradiation and bone marrow transplantation. In: Fliedner, T.M., Cronkite, E.P. and V.P. Bond (Eds.): Assessment of radiation effects by molecular and cellular approaches. Stem Cells, Vol. 13, Suppl. 1, AlphaMed Press, Dayton, Ohio, 191 - 198, 1995.

Heinze, B., Bink, K., Bunjes, D., Rutzen-Loesevitz, L., Zick, L. and T.M. Fliedner: Stable chromosome aberrations: Involvement of special chromosomes or of specific chromosome break points? In: Hagen, U., Jung, H. and C. Streffer (Eds.): Radiation Research 1895-1995. Vol. 1: Congress Abstracts. Congress Proceedings of the 10th Intern. Congress of Radiation Research Würzburg, Germany 1995, 377, 1995.

Kreja, L., Selig, C., and W. Nothdurft:. Assessment of DNA damage in canine peripheral blood and bone marrow after total body irradiation using the single-cell gel electrophoresis technique. Mutation Research 1995 (in press).

Kreja, L., Plappert, U., Selig, C. and W. Nothdurft: Radiation-induced DNA damage in canine hemopoietic cells and stromal cells as measured by the comet assay. Environmental and Molecular Mutagenesis 1995 (accepted for publication).

Nothdurft, W., Fliedner, T.M., Fritz, T.E. and T.M. Seed: Response of hemopoiesis in dogs to continuous low dose rate total body irradiation. In: Fliedner, T.M., Cronkite, E.P. and V.P. Bond (Eds.): Assessment of tadiation rffects by molecular and vellular spproaches. Stem Cells, Vol. 13, Suppl. 1, AlphaMed Press, Dayton, Ohio, 261 - 267, 1995.

Nothdurft, W., Kreja, L. and C. Selig: Acceleration of heamopoietic recovery in dogs after extended field partial body irradiation by treatment with colony-stimulating factors (rhG-CSF and rhGM-CSF). British Journal of Haematology 1995 (submitted for publication)

Paul, W.: Die Analyse der Regeneration der Granulozytopoese nach Stammzelltransplantationen mit Hilfe eines biomathematischen Computermodells. Inauguraldissertation, Universität Ulm 1995.

Plappert, U., Raddatz, K., Molt, S., Rieth, W. and T.M. Fliedner: Der Comet Assay - ein neuer Indikatortest zum Nachweis genotoxischer Beanspruchung. Arbeitsmed. Sozialmed. Umweltmed. 30: 60-65, 1995.

Plappert, U., Raddatz, K., Rieth, W. and T.M. Fliedner: The comet assay - a biomarker for detection of genotoxicity induced by chemicals and radiation. Clinical Chemistry 1995 (in press).

Plappert, U., Raddatz, K., Roth, S. and T.M. Fliedner: DNA damage detection in man after radiation exposure - the comet assay - its possible application for human biomonitoring. In: Fliedner, T.M., Cronkite, E.P. and V.P. Bond (Eds.): Assessment of radiation effects by molecular and cellular approaches. Stem Cells, Vol. 13, Suppl. 1, AlphaMed Press, Dayton, Ohio, 215 - 222, 1995.

Plappert, U., Molt, S., Roth, S. and T.M. Fliedner: DNA damage detection in man after radioiodine therapy. In: Hagen, U., Jung, H.. and C. Streffer (Eds.): Radiation Research 1895-1995. Vol. 1: Congress Abstracts. Congress Proceedings of the 10th Intern. Congress of Radiation Research Würzburg, Germany 1995, 209, 1995.

Selig C, Kreja L. and W. Nothdurft: Investigation of megakaryopoiesis in myelosuppressed bone marrow using immunogold-silver staining (IGSS). European Journal of Haematology (submitted 1995).

Selig, C., Kreja, L., Fliedner, T.M. and W. Nothdurft: Influence of G-CSF and GM-CSF on cycling characteristics of hematopoietic cells at different sites of canine bone marrow after partial body irradiation. In: Hagen, U., Jung, H.. and C. Streffer (Eds.): Radiation Research 1895-1995. Vol. 1: Congress Abstracts. Congress Proceedings of the 10th Intern. Congress of Radiation Research Würzburg, Germany 1995, 235, 1995.

Wüstermann, P.R., Tibken, B., Brücher, S., Mehr, K., Fliedner, T.M. and E. Hofer: Biomathematical modeling of lymphocyte responses after whole body irradiatin to assess the degree of damage to the immune system. In: Hagen, U., Jung, H.. and C. Streffer (Eds.): Radiation Research 1895-1995. Vol. 1: Congress Abstracts. Congress Proceedings of the 10th Intern. Congress of Radiation Research Würzburg, Germany 1995, 265, 1995.

Ziegler, B.L, Lamping, C.P., Thoma, S.J. and T.M. Fliedner: Analysis of gGene rxpression in small numbers of purified hemopoietic progenitor cells by RT-PCR. In: Fliedner, T.M., Cronkite, E.P. and V.P. Bond (Eds.): Assessment of radiation effects by molecular and cellular approaches. Stem Cells, Vol. 13, Suppl. 1, AlphaMed Press, Dayton, Ohio, 106 - 116, 1995.

Ziegler, B.L., Weiss, M., Thoma, S., Lamping, C. and T.M. Fliedner: Biologic indicators of exposure: Are markers associated with oncogenesis useful as biologic markers of effect? In: Fliedner, T.M., Cronkite, E.P. and V.P. Bond (Eds.): Assessment of radiation effects by molecular and cellular approaches. Stem Cells, Vol. 13, Suppl. 1, AlphaMed Press, Dayton, Ohio, 326 - 338, 1995.

Ziegler, B.L, Lamping, C.P., Thoma, S.J., Thomas, C.A. and T.M. Fliedner: Single-cell cDNA-PCR. In: G. Sarkar (Ed.): Methods in Neurosciences. Vol. 26: PCR in Neuroscience, 62 - 74, Academic Press, San Diego 1995.

Head of project 2: Dr G. Wagemaker

II. Objectives for the reporting period

In the reporting period studies on the four subjects of research have been continued.

- Assessment of the radiation sensitivity of hemopoietic stem cell subsets which are relevant for both short-term and long-term hemopoietic regeneration is a key factor in the pathophysiology of radiation-induced alterations of the immunohemopoietic system. Priority has been given, therefore, to the identification of those subsets in both murine systems and rhesus monkeys as well as the development of vitro assays for immature hemopoietic cells.

- Studies on the *in vivo* of hemopoietic growth factors to assess and diagnose the residual capacity of the bone marrow after high dose exposure to radiation, with special reference to growth factors that stimulate immature hemopoietic cells. The studies were extended to circulating immature hemopoietic cells.

- The use of recombinant hemopoietic growth factors to enhance and accelerate immunohemopoietic reconstitution, with emphasis on those growth factors that accelerate the regeneration of immature, CD34 positive bone marrow cells; and, in conjunction:

- The search for an optimal combination of hemopoietic growth factors to shorten the duration of pancytopenia after high dose exposures, eventually followed by studies directed at a possible shift of the LD50/30d without supportive care. The use of allogeneic stem cell transplantation as a means to facilitate the management of high radiation victims is also studied in the rhesus monkey model.

III Progress achieved including publications

After establishment of a considerable heterogeneity of radiation sensitivity of stem cell subsets in mice, i.e., cells with long-term reconstitution being less radiosensitive than those responsible for short term recovery, and corroboration of these findings in rhesus monkeys in that supportive care alone allows for ultimate hemopoietic reconstitution which was not in agreement with the once assumed radiation sensitivity of hemopoietic stem cells characterized by a D_0 of 0.6 Gy, considerable attempts have been made to separate and characterize these subsets to determine the radiation sensitivity of purified stem cell populations. Using a murine competitive transplantation assay, the separation of short- and long-term reconstituting stem cell subsets became established, and specific limiting dilution type long-term bone marrow culture assays were developed. The frequency of the long-term reconstituting stem cells was estimated at 1-2 per 105 bone marrow cells and their pluripotential nature was demonstrated. In practice, this means that the properties, including the radiation sensitivity, of those cell populations can be directly studied. These results have been extrapolated to rhesus monkeys and humans. In rhesus monkeys, a limiting dilution long term bone marrow culture assay has been developed for stem cells subsets, which is being validated by flow cytometric phenotypic analysis and experiments directed at transplantation of subsets. The receptor distribution of immature CD34 positive cells of rhesus monkeys has been established for IL-6, IL-3, GM-CSF and SCF, which means that, in combination wit other surface markers such as RhLA-DR, a variety of stem cell subsets can be distinguished differing in stage of differentiation and/or maturation. The most immature stem cells have been tested for their *in vivo* properties using transplantation experiments. These results demonstrated that, in primates,the short-term and, most probably, also the long-term repopulating stem cells are confined to the small (0.05% of all bone marrow cells) CD34+/DR^{dull} fraction. This fraction has been studied in detail for growth factor receptor distribution *in vitro* and growth factor responses *in vivo*.

The use of growth factor treatment as a diagnostic tool after high dose exposure has been further investigated. Earlier, we reported a disappointing correlation between radiation dose, growth factor treatment and recovery of mature peripheral blood cells. For this reason, the studies were extended to immature CD34 positive cells in both bone marrow and blood. Bone marrow aspirates to determine the number of clonogenic CD34 positive cells were highly informative with respect to the effects of growth factor treatment, but not before the third and the fourth week after radiation exposure. However, immature CD34 positive cells appeared to start circulating soon after irradiation, reaching a first peak value in the first week. The number of circulating CD34 positive cells appeared to be well related to bone marrow CD34 positive cells and is proposed now as a marker for residual stem cell numbers.

The use of combinations of hemopoietic growth factors to accelerate hemopoietic reconstitution after total body irradiation was a central issue of research. Growth factors that stimulate the recovery of immature, CD34 positive bone marrow progenitor cells, such as IL-6, IL-3 and SCF are most likely required for optimal effectiveness of late acting growth factors such as erythropoietin, thrombopoietin and G-CSF, and on growth factors that stimulate the clinically important recovery of thrombocytes. With some 25 hemopoietic growth factors currently available, it is not feasible to test all possible permutations in an *in vivo* model. Therefore, this research is supported by the analysis of the receptor distribution of hemopoietic growth factors, which is thought to be related, be it in a complex way, to the *in vivo* responses to growth factors. We completed and published a full study on the *in vivo* efficacy and side effects of IL-3, completed a full study on IL-6, completed the receptor distributions of IL-6, IL-3, GM-CSF and SCF and tested the IL-6/IL-3 combination of growth factors *in vivo*. These growth factors did not appear to act in synergism if given simultaneously. The preclinical development of thrombopoietin (TPO) has now become an immediate priority. Pilot experiments demonstrated that TPO is highly effective in preventing thrombopenia at the midlethal dose of 5 Gy TBI but ineffective at a dose of 8 Gy TBI, which is similar to all other, both early and late acting, growth factors studied. This leaves a window of about 7 - 10 Gy TBI where hemopoietic stem cell transplantation should still be considered and further developed as a life-saving therapy for radiation accident victims, at least to abridge a period of 4 weeks to 3 months of profound cytopenia. The use of allogeneic CD34 positive cells to achieve transient engraftment as a means to facilitate the management of radiation accident victims will be further studied in conjunction with the analysis of CD34 positive stem cells subsets reported above.

Publications 1994 / 1995

Van Gils FCJM, Budel LM, Burger H, Van Leen RW, Löwenberg B, Wagemaker G. Interleukin-3 (IL-3) receptors on rhesus monkey bone marrow cells: species specificity of human IL-3, binding characteristics, and lack of competition with GM-CSF. Exp. Hemat. 1994, 22: 248-255.

Van den Bos C, Kieboom D, Van der Sluijs JP, Baert MRM, Ploemacher RE, Wagemaker G. Selective advantage of normal erythrocyte production after bone marrow transplantation of α-thalassemic mice. Exp. Hemat. 1994, 22: 441-446.

Van der Loo JCM, Van den Bos C, Baert MRM, Wagemaker G, Ploemacher RE. Stable multilineage hematopoietic chimerism in α-thalassemic mice induced by a bone marrow subpopulation that excludes the majority of day-12 spleen colony-forming units. Blood 1994, 83: 1769-1777.

Burger H, Mostert MC, Kok EM, Wagemaker G, Dorssers LCJ. Cloning and expression of interleukin-3 genes of chimpanzee and new world monkeys. Biochimica et Biophysica Acta 1994, 195-198.

Van Gils FCJM, Westerman Y, Visser TP, Burger H, Van Leen RW, Wagemaker *G*. Neutralizing antibodies during treatment of homologous nonglycosylated IL-3 in rhesus monkeys. Leukemia 1994, 8: 4, 648-651.

Wognum AW, Westerman Y, Visser TP, Wagemaker G. Distribution of receptors for granulocyte-macrophage colony-stimulating factor on immature CD34+ bone marrow cells, differentiating monomyeloid progenitors, and mature blood cell subsets. Blood 1994, 84: 3, 764-774.

Burger H, Wagemaker G, Leunissen JAM, Dorssers LCJ. Molecular evolution of Interleukin-3. J. Mol. Evol. 1994, 39: 255-267.

Poorthuis BJHM, Romme AE, Willemsen R, Wagemaker G. Bone marrow transplantation has a significant effect on enzyme levels and storage of glycosaminoglycans in tissues and in isolated hepatocytes of mucopolysaccharidosis type VII mice. Pediatric Research 1994, 36: 2, 187-193.

Dorssers LCJ, Burger H, Wagemaker G, Koning JP. Identification of functional domains of interleukin-3 by construction of primate interspecies chimera. Growth Factors 1994, 11: 93-104.

Wognum AW, Visser TP, De Jong MO, Egeland T, Wagemaker G. Differential expression of receptors for interleukin-3 on subsets of CD34 expressing hemopoietic cells of rhesus monkeys. Blood 1995, 86; 2: 581-591.

Van Gils FCJM, Van Teeffelen MEJM, Neelis KJ, Hendrikx J, Burger H, Van Leen RW, Knol E, Wagemaker G, Wognum AW. Interleukin-3 treatment of rhesus monkeys leads to increased production of histamine-releasing cells that express IL-3 receptors at high levels. Blood 1995, 86; 2: 592-597.

Wagemaker G, Neelis KJ, Wognum AW. Surface Markers and Growth Factor Receptors of Immature Hemopoietic Stem Cell Subsets. Stem Cells 1995; 13: 1, 165-171.

Wagemaker G. Heterogeneity of radiation sensitivity of hemopoietic stem cells subsets. Stem Cells 1995; 13: 1, 257-260.

De Jong MO, Wagemaker G, Wognum AW. Separation of myeloid and erythroid progenitors based on expression of CD34 and c-kit. Blood 1995; (in press)

Head of project 3: Dr. Covelli

II. Objectives for the reporting period

The project is focussed on radiation damage and recovery of the immune system, aimed at designing appropriate strategies for medical intervention in radiation accidents and radiotherapy.

The main objectives are:
1. Effects of IL-11 on the recovery of T and B lymphocytes in sublethally irradiated mice.

2. Technical improvements for rapid and precise HLA typing in humans.

Studies on mice. In our previous studies aiming at the design of appropriate strategies to accelerate recovery of the immune system after irradiation, we found that rmu IL-3, a T cell-derived cytokine, is able to induce differentiation and growth of thymocytes and splenic T and B lymphocytes in mice exposed to X-rays (200-500 cGy). The recovery, however, was complete at 7 days only after 200 cGy whereas full recovery was not achieved before 2, 3, and 4 weeks after 300, 400, and 500 cGy, respectively. These studies were extended to investigate the effects of rhu IL-11, a cytokine produced by bone marrow stromal cells, at 7 days after irradiation. It was found that rhu IL-11 is able to restore thymus and spleen cell number as well as T and B cell mitotic responsiveness in mice exposed to 200 cGy but not to higher doses (300 or 400 cGy).

The partial recovery obtained with IL-3 or IL-11 alone prompted us to investigate whether these cytokines given together could synergize and promote

recovery of lymphocytes in mice exposed to 300 cGy or higher radiation doses. IL-11 had, indeed, been shown to synergize with IL-3 in the formation of megakaryocyte colonies, in the maturation and/or activation of monocytes and monocyte progenitors, and in the erythroid differentiation.

Male and female C57BL/6 mice were total-body irradiated (300-700 cGy) and daily injected subcutaneously with 0.1 ml PBS alone or containing 1-15 μg rmu IL-3 and 1-8 μg rhu IL-11 for 5 days starting immediately after irradiation. Mice were sacrificed 7 days after irradiation and individually (4 mice/group) tested. Thymuses and spleens were aseptically removed and single cell suspensions prepared to assess cell number and function. Thymus cells were counted, analyzed by FACS for expression of CD4 and CD8 markers, and assayed for the mitotic response to Con A. Spleen cells were counted and assayed for mitotic responses to Con A and LPS.

Results show that 300 cGy decrease thymus cell count and mitotic response to Con A by about 75% at 7 days after irradiation. Injection of 5 μg IL-3 alone is unable to enhance these parameters significantly. However, if mice were also injected with 1-5 μg IL-11, thymus cell number and mitotic response were significantly increased, the most effective doses of IL-11 being 4 and 5 μg which yielded full recovery. Similar results were found by FACS analysis. Also spleen cell number and mitotic responses to Con A and LPS were decreased by 300 cGy but fully recovered if mice were injected with 5 μg IL-3 and 4 or 5 μg IL-11.

Mice exposed to 500 cGy and treated with 5 μg IL-3 and 4-8 μg IL-11 failed to recover T and B lymphocytes at 7 days after irradiation. However, mice exposed to 500 cGy and treated with 5 μg IL-11 and 4-8 μg IL-3 displayed full recovery of thymus and spleen cells if 5 μg IL-11 were combined with 7 or 8 μg IL-3.

Mice exposed to 700 cGy and treated with 5 μg IL-11 and 15 μg IL-3 showed complete recovery of thymus and spleen cell number and mitotic responses at 7 days after irradiation, whereas 15 μg IL-3 alone were ineffective. Similar results were obtained by FACS analysis of thymocytes.

In conclusion, the results illustrate that it is possible to counteract radiation-induced damage of thymus and spleen cells in mice exposed to lethal doses of X-rays. The recovery of T and B cell number and functions was complete as soon as 7 days after irradiation and could be achieved by injecting mice with a

combination of recombinant IL-11 and IL-3. The synergism of these cytokines was very efficient when a small dose (5 μg) of IL-11 was injected with higher doses of IL-3. It is a remarkable finding with possible clinical applications in radiation therapy.

Studies on humans. In humans, bone marrow transplantation after lethal radiation doses (big accident) must be done between HLA phenotypically identical individuals since the family of irradiated patients is often involved in the accident. The donor must be found in the International Registry and the HLA typing done with a DNA typing starting by a small amount of DNA amplified by polymerase chain reaction and subsequent hybridization by allele specific oligonucleotide probes or by direct sequence of HLA loci region, HLA-A, HLA-B, HLA-C for class I and HLA-DR, DQ, DP for class II.

Our laboratory has set up a typing with this last methodology and has already developed a class II antigen typing method by manual direct sequencing of DR, DQ and DP loci. This technique requires a small amount of cells for DNA extraction (5.000.000), as a reasonable time, 6 hours, to obtain DR, DQ, DP results, at a low cost of $ 60.0. At the moment, this method is being used to select bone marrow transplantation donors for leukemic patients for International Registries. Class II antigen typing performed in our laboratory with DNA techniques has increased patient survival from 8% - 70%.

Publications

1. Doria G., Pioli C., Saran A., Covelli V.
    Fattori immunogenetici nella insorgenza di tumori sperimentali.
    Annali Italiani di Medicina Interna, 8: 104, 1993.

2. Pioli C., Caroleo M.C., Nisticò G., Doria G.
    Melatonin increases antigen presentation and amplifies specific and non specific signals for T cell proliferation.
    Int. J. Immunopharmacol., 15: 463, 1993.

3. Doria G., Leter G., Mancini C., Frasca D.
    Effect of recombinant IL-3 on lymphocyte populations in irradiated mice.
    Stem Cells, 11(suppl. 2): 93, 1993.

4. Brunelli R., Frasca D., Fattorossi A., Pioli C., Zichella L., Doria G.
    Effects of hormone replacement therapy on PBL from menopausal women.
    II International Congress ISNIM, Paestum. Abstract, p. 184, 1993.

5. Brunelli R., Utsuyama M., Mancini C., Leter G., Zichella L., Hirokawa K., Doria G.
    Repopulation of recipient and grafted thymuses in gonadectomized old mice.
    II International Congress ISNIM, Paestum. Abstract, p. 285, 1993.

6. Frasca D., Leter G., Mancini C., Doria G.
    Injection of sublethally irradiated mice with recombinant IL-3 induces recovery of T and B cells.
    II International Congress ISNIM, Paestum. Abstract, p. 53, 1993.

7. Doria G., Frasca D.
    Regulation of cytokine production in aging mice.
    II International Congress ISNIM, Paestum. Abstract, p. 281, 1993.

8. Frasca D., Doria G.
    The synthetic thymic hormone THF g-2 enhances T cell functions in aging mice.
    II International Congress ISNIM, Paestum. Abstract, p. 282, 1993.

9. Baschieri S., Fattorossi A., Doria G.
    Meccanismi di induzione della tolleranza nel timo di topi adulti: le cellule Vß8+ a fenotipo maturo (CD4+8- e CD4-8+) sono eliminate dal superantigene SEB (Staphylococcal Enterotoxin B) con cinteiche diverse.

XXI Convegno Nazionale del GCI, Viterbo. Riassunto, p. 21, 1993.

10. Doria G.
An introduction to immunosuppression.
International Workshop on Advances and Perspectives in the Area of
Immunosuppression, Venezia, p. 83, 1993.

11. Pioli C., Saran A., Mouton D., Biozzi G., Covelli V., Doria G.
Dominanza incompleta della suscettibilità alla cancerogenesi chimica in
topi (Car-RxCar-S)F1.
Tumori, 79(suppl. 3): 133, 1993.

12. Pioli C., Saran A., Mouton D., Biozzi G., Covelli V., Doria G.
Insorgenza e progressione di tumori cutanei indotti in topi selezionati per
resistenza o sensibilità alla cancerogenesi chimica.
II Convegno Nazionale della S.I.M.A., Assisi. Riassunto, p. 37, 1993.

13. Frasca D., Spanò M., Leter G., Doria G.
T and B cell recovery induced by recombinant IL-3 in sublethally
irradiated mice.
Eur. J. Histochem., 37(suppl.): 18, 1993.

14. Baschieri S., Fattorossi A., Doria G.
Differential effects of the superantigen Staphylococcal Enterotoxin B
(SEB) on single positive thymocytes in adult mice.
Eur. J. Histochem., 37(suppl.): 17, 1993.

15. Caroleo M.C., Doria G., Pioli C., De Sarro G.B., Rotiroti D., Nisticò G.
Pineal regulation of immune response and cytokine actions on CNS.
In: Nitric Oxide: Brain and Immune System, S. Moncada, G. Nisticò,
E.A. Higgs (eds.), Portland Press, p. 19, 1993.

16. Pistillo M.P., Sun P.F., Mantero S., Ferrara G.B.
Shared epitopes of the HLA-DR10 molecules recognized by murine and
human mAbs.
Eur. J. Immunogen., 20: 111, 1993.

17. Obata F., Tsunoda M., Kaneko T., Ito K., Ito I., Masewicz S., Mickelson
E.M., Ollier W.E.R., Pawelec G., Cella M., Ferrara G.B., Kashiwagi N.
Human T-cell receptor TCRAV, TCRBV, and TCRAJ sequences newly
found in T-cell clones reactive with allogeneic HLA class II antigens.
Immunogenetics, 38: 67, 1993.

18. Colonna M., Brooks E.G., Falco M., Ferrara G.B., Strominger J.L.
Generation of allospecific natural killer cells by stimulation across a
polymorophism of HLA-C.

Science, 260: 1121, 1993.

19. Colonna M., Borsellino G., Falco M., Ferrara G.B., Strominger J.L.
    HLA-C is the inhibitory ligand that determines dominant resistance to
    lysis by NK1- and NK2-specific natural killer cells.
    Proc. Natl. Acad. Sci. 90: 12000, 1993.

20. Frasca D., Leter G., Doria G.
    Murine recombinant interleukin 3 induces recovery of T and B cells in
    irradiated mice.
    Blood, 83: 1563, 1994.

21. Di Majo V., Coppola M., Rebessi S., Saran A., Pazzaglia S., Pariset L.,
    Covelli V.
    Neutron induced tumors in BC3F1 mice: effects of dose-fractionation.
    Radiat. Res, 138: 252, 1994.

22. Saran A., Pazzaglia S., Pariset L., Rebessi S., Broerse J.J., Zoetelief J.,
    Di Majo V., Coppola M., Covelli V.
    Neoplastic transformation of C3H10T1/2 cells: a study with fractionated
    doses of monoenergetic neutrons.
    Radiat. Res., 138: 246, 1994.

23. Saran A., Broerse J.J., Zoetelief H., Pazzaglia S., Pariset L., Coppola M.,
    Di Majo V., Covelli V.
    C3H10T1/2 cell transformation after fractionated doses of neutrons of
    different energies.
    Physica Medica, 10(suppl.): 80, 1994.

24. Rebessi S., Di Majo V., Coppola M., Saran A., Pazzaglia S., Pariset L.,
    Covelli V.
    Somatic effects of low neutron doses.
    Physica Medica, 10(suppl.): 82, 1994.

25. Pistillo M.P., Cella M., Mantero S., Ferrara G.B.
    Proliferation and immunoglobulin secretion of lymphoblastoid cell lines
    are differently affected by soluble cytokines.
    Cell Prolif., 27: 293, 1994.

26. Doria G., Frasca D.
    Aging and genetic control of immune responsiveness.
    Immunol. Let., 40: 231, 1994.

27. Frasca D., Guidi L., Bartoloni C., Tricerri A., Vangeli M., Antico L.,
    Carbonin P., Errani A., Doria G.

Age-related modulation of cytokine production, IL-2R expression and function in a population of healthy subjects (22-97 years).
Aging, Immunology and Infectious Disease, 5: 3, 1994.

28. Pioli C., Saran A., Mouton D., Troiani C., Doria G., Covelli V., Neveu T., Biozzi G.
Genetics of chemical carcinogenesis. 2. Papilloma and malignant conversion in susceptible (Car-S) and resistant (Car-R) lines of mice produced by bidirectional selective breeding, and in their (Car-SxCar-R)F1 hybrids.
Carcinogenesis, 15: 2629, 1994.

29. Fattorossi A., Baschieri S., Biselli R., Doria G.
Three color flow cytometric analysis of Vb expressing thymocytes exposed to an exogenous superantigen "in vivo".
Cytometry, 7(suppl.): 317A, 1994.

30. Doria G., Frasca D.
Regulation of cytokine production in aging mice.
Ann. N.Y. Acad. Sci., 741: 299, 1994.

31. Pioli C., Saran A., Mouton D., Biozzi G., Covelli V., Doria G.
Controllo genico della induzione di papillomi cutanei e della loro trasformazione maligna.
Tumori, 80(suppl.): 21, 1994.

32. Doria G., Frasca D.
Ricerche sperimentali precliniche sugli effetti immunologici di peptidi timici sintetici durante l'invecchiamento.
Congresso sulle "Terapie Ormonali Sostitutive" dell'I.N.R.C.A. e l'Associazione Gerontechnology, Milano. Riassunto, p. 283, 1994.

33. Doria G.
Genetic control of immune responses and senescence.
XLVII Annual Scientific Meeting of the Gerontological Society of America, Atlanta. Abstract, p. 292, 1994.

34. Frumento G., De Totero D., Ferrara G.B., Chersi A., Pernis B.
Cellular mechanisms of exogenous peptide binding to HLA class II molecules in B cells.
Cell. Immunol., 155: 1, 1994.

35. Cella M., Longo A., Ferrara G.B., Strominger J., Colonna M.
NK3 specific natural killer cells are selectively inhibited by Bw4 positive HLA alleles with isoleucine 80.
J. Exp. Med., 180: 1235, 1994.

36. Frumento G., Molina F., Pernis B., Ferrara G.B.
    Characteristics of class I-bound-peptides.
    Human Immunol., 41: 87, 1994.

37. Ferrara G.B., Bini D., Cella M.
    HLA-class II sequence-based typing.
    Convegno Consorzio Interuniversitario Biotecnologie, Brescia, 1994.

38. Doria G., Mancini C., Leter G., Utsuyama M., Hirokawa K.
    Age-related propensity of Mls-1^a mice to develop Vb6$^+$ T cells after irradiation and syngeneic bone marrow transplantation.
    J. Cell. Biochem., 21A(suppl.): C2-522, 1995.

39. Bini D., Delfino L., Morabito M., Pera C., Ferrara G.B.
    Tipizzazione HLA di classe I (Locus A e Locus B) e di classe II (DRB1, DQA1, DQB1, DPB1) mediante sequenza diretta.
    Convegno "Synthetic Oligonucleotides and and Peptides in Biotechnology", Ferrara, 1995.

40. Bini D., Delfino L., Morabito M., Pera C., Ferrara G.B.
    HLA class I (Locus A and B) and class II sequence-based typing.
    EFB and BSHI Joint Meeting, Brighton, 1995.

41. Pioli C., Saran A., Mouton D., Covelli V., Biozzi G., Doria G.
    Susceptibility and resistance to chemical carcinogenesis in genetically selected mice.
    XIII Meeting of the European Association for Cancer Research, Berlin. Abstract, (in press).

42. Di Majo V., Coppola M., Covelli V., Doria G., Pioli C., Rebessi S., Saran A., Mouton D., Biozzi G.
    Sviluppi di linee murine sensibili e resistenti alla cancerogenesi cutanea.
    VII Convegno Nazionale della S.I.R.R., Pisa. Riassunto, (in press).

43. Saran A., Di Majo V., Coppola M., Covelli V., Pioli C., Doria G., Rebessi S., Mouton D., Biozzi G.
    Development of murine lines sensitive and resistant to skin carcinogenesis.
    R.R.S./N.A.H.S. Annual Meeting, Oak Brook(USA). Abstract, (in press).

44. Pazzaglia S., Saran A., Pariset L., Rebessi S., Di Majo V., Coppola M., Covelli V.
    Radiation-induced neoplastic transformation of C3H10T1/2 cells as a function of the cell cycle phases.
    R.R.S./N.A.H.S. Annual Meeting, Oak Brook(USA). Abstract, (in press).

45. Di Majo V., Coppola M., Covelli V., Rebessi S., Saran A., Pazzaglia S., Doria G., Pioli C., Mouton D., Biozzi G.
Life span of mice genetically selected for sensitivity and resistance to skin carcinogenesis.
I Convegno Nazionale sulle "Radiazioni: dalla teoria alle applicazioni multidisciplinari", Pisa, (in press).

46. Doria G., Pioli C., Mancini C., Arbitrio M., Frasca D.
Regulation of cytokine production in aging mice.
IX International Congress of Immunology, San Francisco. Abstract, (in press).

47. Frasca D., Pioli C., Leter G., Doria G.
Synergistic effects of IL-3 and IL-11 on the recovery of the immune system after irradiation.
IX International Congress of Immunology, San Francisco. Abstract, (in press).

48. Tricerri A., Vangeli M., Guidi L., Coppola R., Errani A.R., Canetta M., Frasca D., Doria G., Bartoloni C., Gasbarrini G.
Proliferative response to anti-CD3+anti-CD28 of lymphocytes from gastric vein and peripheral blood: preliminary results.
IX International Congress of Immunology, San Francisco. Abstract, (in press).

49. Guidi L., Errani A.R., Tricerri A., Vangeli M., Antico L., Menini E., Frasca D., Doria G., Bartoloni C..
Immunological profile of actue "academic" stress..
IX International Congress of Immunology, San Francisco. Abstract, (in press).

50. Arbitrio M., Frasca D., Pioli C., Doria G.
Modulazione della produzione di citochine in topi vecchi.
XXIII Convegno Nazionale del GCI, Viterbo. Riassunto, (in press).

51. Pioli C., Frasca D., Leter G., Guidi F., Doria G.
Effetto sinergico di IL-3 e IL-11 sul recupero del sistema immunitario dopo irraggiamento.
XXIII Convegno Nazionale del GCI, Viterbo. Riassunto, (in press).

52. Frasca D., Pioli C., Leter G., Doria G.
Use of cytokines to enhance recovery of the immune system after irradiation.
I European Congress of Pharmacology, Milan. Abstract, (in press).

53. Doria G., Frasca D.

Preclinical experimental research on the immunological effects of synthetic thymic peptides during aging.
Gerontechnology, (in press).

54. Doria G., Pioli C., Leter G., Frasca D.
Recovery of the immune system induced by cytokines in irradiated mice.
X International Congress of Radiation Research, Würzburg. Abstract, (in press).

55. Doria G.
I processi di difesa e l'evoluzione del sistema immunitario.
XXII Seminario sull'Evoluzione Biologica dell'Accademia Nazionale dei Lincei, Roma, (in press).

56. Covelli V., Coppola M., Di Majo V., Rebessi S., Saran A., Pazzaglia S., Pioli C., Mouton D., Bouthillier Y., Biozzi G., Doria G.
Life span and lymphoma incidence in high or low antibody responder mice from selection GS.
Aging, Immunology and Infectious Disease, (in press).

57. Frasca D., Pioli C., Leter G., Doria G.
Cytokine-induced recovery of the immune system in irradiated mice.
XI Congresso Nazionale dell'Associazione Italiana di Immuno-farmacologia, Taormina. Riassunto, (in press).

58. Brunelli R., Frasca D., Perrone G., Pioli C., Fattorossi A., Zichella L., Doria G.
Hormonal replacement therapy: short term effects on lymphocytes and granulocytes.
Obstet. Ginecol. Investigat., (in press).

59. Utsuyama M., Hirokawa K., Mancini C., Brunelli R., Leter G., Doria G.
Differential effects of gonadectomy on thymic stromal cells in promoting T cell differentiation in mice.
Mech. Ageing and Dev., (in press).

60. Tricerri A., Vangeli M., Guidi L., Coppola R., Errani A.R., Canetta M., Frasca D., Doria G., Bartoloni C., Gasbarrini G.
Functional study of gastric vein lymphocytes: preliminary results.
International Symposium on Clinical Immunology, San Francisco. Abstract, (in press).

61. Pazzaglia S., Saran A., Pariset L., Rebessi S., Di Majo V., Coppola M., Covelli V.
Sensitivity of C3H10T1/2 cells to radiation-induced killing and neoplastic transformation as a function of cell cycle

Int. J. Rad. Biol., (in press).

62. Tricerri A., Guidi L., Vangeli M., Frasca D., Riccioni M., Covacci A., Coppola R., Bartoloni C., Doria G., Gasbarrini G.
Lymphocyte proliferative response to Helicobacter pylori CagA protein in patients with duodenal ulcer or gastritis.
The Lancet, (submitted).

Centre International de Radiopathologie
Final Report
Contract F13P CT 920008
Dr. H. MAGDELENAT

I-Title of the Project

Experimental and Clinical Research on Management of Radiation Accident Casualties.

II General Objective

To provide experimental and clinical data related to the victims of radiations.

1.- Pathophysiology : mechanisms and modulation of radiation iduced apoptosis of human lymphocytes.

2.- Biological indicators : dose and time related alterations of cytokines (diagnosis and prognosis) and HLA expression (treatment) after TBI. Characterisation and Detection of haematopoietic stem cells by PCR.

3.- Therapy of radiation syndromes : methods for improving allogenic bone marrow transplantation (B.M.T.).

4.- Patient evaluation : establishment of a national data base, including patients treated according to various modalities of TBI.

III.- Progress achieved including publications

1.- Pathophysiology of radiation induced apoptosis of human lymphocytes (Institut Curie, Paris)

Experimental research :

The molecular basis of radiation induced intermitotic cell death of human lymphocytes was investigated :

• When irradiated *in vitro* at 5 to 10 Gy with γ-ray (^{60}Co) and maintained in culture for 24 hours, 70 to 85% of the total number of peripheral blood lymphocytes (PBL i.e. matureT and B cells) showed morphological changes characteristic of apoptosis (chromatin condensation, nucleosomal fragmentation and cell shrinkage).

A dose-effect relationship was observed between 0 and 5 Gy, higher doses leading to a plateau of efficacy. Individual variations were observed, with at present no other identified determining parameter than gender, females disclosing slightly higher radiosensitivity than males.

• We have established that irradiation of PBL, besides inducing nucleosomal degradation of chromatine, also induces the degradation of 28S ribosomal RNA (rRNA). A time course study of this process showed an initial (0 to 2 hours) increase of 28S rRNA synthesis, in accordance with the definition of apoptosis as a metabolically active process, followed by a consistent decrease and disappearance of 28S rRNA by 12 hours after irradiation (1). Sequential in situ hybridisation of 28S rRNA showed the progressive degradation of rRNA starting in the nucleoli then affecting endoplasmic rRNA.

• We have established several evidences of a relationship between ubiquitin gene expression, ubiquitination of nuclear proteins and radiation mediated apoptosis in normal human peripheral blood lymphocytes (2).
Following 5 Gy of γ-irradiation we observed that :
a) the ubiquitin mRNA level is increased as a consequence of the activation of the transcription of the polyubiquitin gene, UbB (4 to 5 fold as estimated by run-on assay), 15 to 90 min after iniatiation of apoptosis;
b) specifically in apoptotic, and not in all irradiated cells, nuclear proteins are highly ubiquitinated (immunoprecipitation and Western blotting, using monoclonal or polyclonal anti-ubiquitin antibody);
c) sequence-specific inhibition of ubiquitin expression by antisense oligonucleotides significantly decreased the proportion of cells disclosing the apoptotic death pattern (30 to 35% of apoptotic cells instead of 70 to 80% after 10 Gy).
d) antisensetreatment (to Ub mRNAs) provoked a decrease of ubiquitinated nuclear proteins, specially of a 40 kDa nuclear protein, as shown by immunoprecipitation and Western blot.

These results highly suggest that the polyubiquitin gene appears to be one of the "death" genes with induced transcriptional and functional activity in γ-ray mediated apoptosis and that, the ubiquitination of nuclear proteins is involved in the chromatin disorganization and the oligonucleosomal fragmentation, key features of apoptosis.
The physiological role of the ubiquitin pathway is multiple, protein ubiquitination being involved in ATP-dependent proteasomal proteolysis and in post traductional modifications of a number of regulatory proteins, we have searched for the role of protein ubiquitination in radiation induced apoptosis.

• We have obtained experimental evidence that radiation induced apoptosis is partly (30-40 %) inhibited by dipeptide competitors of the "N-end rule" ubiquitin tagging of proteins, the initial step to addressing protein to the 26S proteasome complex for degradation.
In addition, preliminary results have shown that the proteasome inhibitor MG12 enhances the efficacy of radiation induced apoptosis at non toxic concentrations (10^{-7}M).
These data strongly support the role of the ubiquitin dependent proteasomal proteolysis in radiation induced apoptosis and that modulation of this proteolytic pathway can alter the intensity of apoptotic cell death.

• Finally we have obtained preliminary data showing that the transcriptional activity of P53, a regulatory protein of the cell cycle which is also involved in the commitment to apoptosis of cells with heavy DNA damage, can be induced by hairpin oligonucleotide binding sequences (activation of transcription of wafl) without inducing apoptosis. We are now investigating further the role of post translational modifications of P53 in modulating radiation induced apoptosis (in collaboration with Pr D Lane, Dundee)

2- Biological indicators

2-1 Cytokines
The plasma concentrations of various cytokines (TNFa, IL1, IL6) have been studied in the first 24 hours following total body irradiation (TBI) of patients in remission prepared for bone marrow transplantation (10 Gy in 4 hrs or after a fraction of 2 Gy). Only IL6 disclosed elevated levels after radiation but transiently (0-6 hours) and only above 5 Gy, making IL6 an unreliable biological indicator of accidental overexposure (4).

2-2- Early assessment of irradiation by apoptotic committment of peripheral blood lymphocytes after TBI.

• We have developped an *in vitro* test for the early detection (< 24 heures) of the comitment of lymphocytes to apoptosis after total body irradiation (TBI). The test consists in maintaining PBL from irradiated donors for 24 hours in culture before observation of apoptotic cells. Initially the apoptotic fraction was measured by fluorescence microscopy examination. We have recently added a flow cytometry determination which give similar results with greater statistical significance.
We have obtained consistent results from this test (3), showing that *in vivo* committment to apoptosis of lymphocytes following 2 Gy TBI can be revelead from blood sample withdrawn immediately after irradiation (the tests require 24 hr of cell culture) or from a blood sample withdrawn 24 hr after irradiation (no cell culture required). These tests may prove useful as early biological indicators of accidental total (or partial) body irradiation.

2-3 *H L A:* :five patients treated by 10 Gy (4 hr) TBI for various hematological diseases were analyzed for the genomic expression of HLA Class II antigens using PCR amplification, in comparison with serological phenotyping (microlymphotoxicity).

Twenty four hours after TBI, PCR allowed Class II HLA typing whereas microlymphocytotoxicity was consistently negative (5, 6).

3.- Establishment of the National Registry of total Body Irradiation (Hôpital Tenon, Paris)

No complete database including both dosimetric and clinical data is at present available in France. The G.E.G.M.O. (Groupe d'Étude de Greffe de Moelle Osseuse allogénique) and F.A.G. (France Auto Greffe) registries are clinically oriented, whereas E.U.L.E.P. (European Late Effect Project) focuses on late effects follow up.

In order to study more precisely the consequences of high dose TBI (10 Gy) delivered in a limited number of fractions (1 to 10) over 2 to 4 days, which approaches the hypothetical conditions of accidental overexposure, a single Registry has been initiated, which will collect the dosimetric and clinical data from 26 French Radiotherapy Centers. As a specific feature of this prospective Registry, dosimetric data will be collected in real time (on line)

Publications

(1).- J. DELIC, M. COPPEY-MOISAN, H. MAGDELENAT, γ-ray induced transcription and apoptosis-associated loss of 28S rRNA in interphase human lymphocytes. Int. J. Radiat. Biol., 64 (1), 39-46, 1993.

(2).- J. DELIC, M. MORANGE, H. MAGDELENAT, Ubiquitin pathway involvement in human lymphocyte γ-irradiation-induced apoptosis. Molecular and Cellular Biology, 13 (8), 4875-4883, 1993.

(3).- J. DELIC, H. MAGDELENAT, C. BARBAROUX, M-P. CHAILLET, B. DUBRAY, E. GLUCKMAN, A. FOURQUET, T. GIRINSKY, J.-M. COSSET, In vivo induction of apoptosis in human lymphocytes by therapeutic fractionated total body irradiation (FTBI). Br. J Radiat. Biol., in press 1995.

(4).- T.A. GIRINSKY, M. PALLARDY, E. COMOY, T. BENASSI, R. ROGER, G. GANEM, J-M. COSSET, G. SOCIE, H. MAGDELENAT, Peripheral blood corticotropin-releasing factor, adrenocorticotropic hormone and cytokine (interleukin beta, interleukin 6, tumor necrosis factor alpha) levels after high- and low-dose total-body irradiation in humans. Radiat. Res., 139, 360-363, 1994.

(5).- J-M. COSSET, C. RAFFOUX, M-P. CHAILLET, G. SOCIE, E. BRIOT, J-Y. FOLLEZOU, E. GRIMAUD, B. DUBRAY, T. GIRINSKY, Class I and II HLA typing after a 10 Gy-4 hour therapeutic total body irradiation. Health Physics, 64(6), 667-670, 1993.

(6).- J-M. COSSET, C. RAFFOUX, M-P. CHAILLET, E. CHAPUIS, G. SOCIE, E. GLUCKMAN, T. GIRINSKY, Letter, Health Physics, 66(6), 709, 1994.

(7).- M. TEYSSIER, E. CAROSELLA, E. GLUCKMAN, M. KIRSZENBAUM.
PCR intracellulaire : nouvelle approche de diagnostic tissulaire et cytogénétique. Immunoanal. Biol. Spéc. (1994) 9, 159-164.

(8).- A. FISCHER, P. LANDAIS, W. FRIEDRICH et al.
Bone marrow transplantation (BMT) in Europe for primary immunodeficiencies other than severe combined immunodeficiency: A report from the European Group for BMT and the European Group for Immunodeficiency. Blood., 83 (4), 1149-1154, 1994.

(9).- M. CAVAZZANA-CALVO, S. SARNACKI, E. HADDAD et al.
Prevention of bone marrow and cardiac graft rejection in an H-2 haplotype disparate mouse combination by an anti-LFA-1 antibody, Transplantation, in press 1995.

Pr. A. FISCHER

CONTRAT F13P CT 92008

PREVENTION OF GRAFT REJECTION AND GRAFT VERSUS HOST DISEASE AFTER HAPLOIDENTICAL MARROW TRANSPLANTATION (BMT) BY INFUSION OF DONOR T CELLS DEVOID OF ALLOREACTIVITY TOWARDS RECIPIENT.

More than 70 % of potential marrow recipients lack a suitable HLA genetically matched donor. A matched unrelated donor can be found for another 20 % of them. Use of haploidentical marrow is hampered by the occurrence of several life threatening complications, i.e. graft versus host disease (GVHD), graft rejection (the occurrence of which being dramatically increased by marrow inoculum T cell depletion performed for prevention of GVHD), long lasting immunodeficiency and high incidence of relapses in patients with leukemia. Several strategies like increased host immunosuppression and marrow T cell depletion have been tested to reduce incidence and severity of some of these problems . Though some improvement in clinical results have been noticed, the procedure still failed in a majority of patients.

A possible approach to simultaneously counteract all of these problems consists in the add back of donor T cells that may reduce risks of graft rejection, of severe infections and of leukemia relapses. However, donor T cells contain a high proportion of alloreactive, potentially harmful cells.

In this setting, two strategies can be envizaged to avoid excessive donor anti-host alloreactivity :

1. to transfer a suicide gene in donor T cells and to kill them *in vivo* at a suitable time
2. to functionally deplete donor T cell population from most of anti-host T cell reactivity.We have chosen to test the latter approach which carries the advantage -if feasible- to enable donor T cells to exert positive effects over a longer period of time post BMT.

The method we have designed consists in *in vitro* activation of donor T cells by host mononuclear cells in a mixed leukocyte reaction. Following a 2-day incubation, donor T cells are treated with an immunotoxin specific for the α chain (p55-CD25) of the IL-2 receptor which is selectively expressed by activated T cells. We have previously shown that this procedure can kill about 98 % of proliferate and cytotoxic T cells specific for host (1) as shown by limiting dilution analysis. Reactivity to 3rd party alloantigens and to foreign antigens (such as EBV or (CMV) is preserved (2). Similar findings were made in a murine model (3).

Infusion of anti host-depleted T cells to haplo-compatible irradiated mice together with T-depleted marrow syngeneic to the T cells led to significant protection against both GVHD and rejection and to increased survival (3).

These results provide an experimental basis to set up a clinical procedure :

This will require the development of an immunotoxin usable for *ex vivo* treatment of donor lymphocytes prior to infusion to patients.

An immunotoxin (to CD25) is being prepared in collaboration with F. UCKUN (Minneapolis) and J. WIJDENES (DIACLONE, Besançon).

This new immunotoxin will be compared in *in vitro* experiments for efficacy and specificity of depletion of alloreactive T cells to the previously used Ricin-BB10 (anti-CD25) immunotoxin. Experiments will consist in LDA of CTL and proliferative responses towards haploidentical cells and third party cells.

Once satisfactory results achieved and optimal usage defined, a pilot clinical study will be proposed. It will be carried out in children undergoing haploidentical BMT because of high risk leukemia or lethal inherited disorders and who lack an HLA matched donor (either genetically or phenotypically).

Prevention of graft rejection after haploidentical marrow transplantation by treatment of the recipient with a monoclonal anti-LFA-1 antibody.

In a murine combination where marrow donor and recipient share only one H-2 haplotype, infusion of a low dose of T-cell depleted marrow ($\approx$ 2 x 10^6 cells) led to constant graft rejection in 9 Gy-irradiated host. We have demonstrated that infusion to the recipient of anti-LFA-1 monoclonal antibody -able to inhibit T and NK cell cytotoxic activity- partially prevents graft rejection and enables long-term survival of up to 50 % of mice with either full or mixed chimerism (4). Interestingly, in the latter setting, transplanted mice lymphocytes were found areactive to both donor and host MHC antigens *in vitro* (mixed leukocyte reaction and cytotoxic T-cell activity) whereas reactivity to 3rd party cells was preserved. *In vivo*, host or donor skin graft, but not 3rd party graft were accepted. These results show feasibility of this strategy which leads to competence of the immune system after transplantation with mutual tolerance between donor and host.

Further experiments will be performed in adequate transgenic antiH-2K^b mice transplanted with H-2K$^{b(+)}$ marrow to study tolerance mechanism.

These results further establish experimental background for human (ongoing) clinical studies assaying usage of anti-LFA-1 antibody in recipients of non HLA identical marrow.

1. CAVAZZANA-CALVO M, FROMONT C, LE DEIST F, DEROCQ JM, GEROTA I, GRISCELLI C, FISCHER A. Specific elimination of alloreactive T-cells by an anti-IL2 receptor β chain specific immunotoxin Transplantation 1990, 50, 1-7.

2. VALTEAU-COUANET D, CAVAZZANA-CALVO M, FROMONT C, FISCHER A. Functional study of residual T-lymphocytes after specific elimination of alloreactive T-cells by a specific anti-interleukin 2 receptor β chain immunotoxin. Transplantation 1993, 56, 737-38.

3. CAVAZZANA-CALVO M, STEPHAN JL, SARNACKI S, CHEVRET S, FROMONT C, DE COENE C, LE DEIST F, GUY-GRAND D, FISCHER A. Attenuation of graft-versus-host disease and graft rejection by ex vivo immunotoxin elimination of alloreactive T-cells in an H-2 haplotype disparate mouse combination. Blood 1994, 83, 288-93.

4. CAVAZZANA-CALVO M, SARNACKI S, HADDAD E, DE COENE C, CALISE D, YVON E, CERF-BENSUSSAN N, FISCHER A. Prevention of bone marrow and cardiac graft rejection in an H-2 haplotype disparate mouse combination by an anti-LFA-1 antibody. Transplantation, in press.

ceɔ -*E.D. CAROSELLA*

PROJECT SAINT-LOUIS HOPITAL

L.I.R.R. - C.E.A.

HEAD OF PROJECT : *Dr. E.D. CAROSELLA*

The SAINT-LOUIS Hôpital team of the European Working Grup supported by the EC contract n° F 13 P - CT 92-0008 have concentrated the activities during the period of September 1992 to July 1995 on 5 major areas :

1- MULTICOLOR FLOW CYTOMETRY ANALYSIS OF BLOOD CELL SUBSETS IN PATIENTS GIVEN TOTAL BODY IRRADIATION BEFORE BONE MARROW TRANSPLANTATION

2- IONIZING RADIATION EFFECTS ON THE KGla PRIMITIVE HEMATOPOIETIC CELL LINE

3- FUNCTIONAL ROLE OF PECAM-1/CD31 MOLECULE EXPRESSED ON HUMAN CORD BLOOD PROGENITORS

4- BY55 MONOCLONAL ANTIBODY DELINEATES WITHIN HUMAN CORD BLOOD AND BONE MARROW LYMPHOCYTES DISTINCT CELL SUBSETS MEDIATING CYTOTOXIC ACTIVITY

5- INTRACELLULAR PCR AND RT-PCR : NEW APPROACHES FOR DIAGNOSTICS

1- MULTICOLOR FLOW CYTOMETRY ANALYSIS OF BLOOD CELL SUBSETS IN PATIENTS GIVEN TOTAL BODY IRRADIATION BEFORE BONE MARROW TRANSPLANTATION

Although radiosensitivity of human blood cells has been extensively studied, *in vitro* and *vivo* results, although often conflicting, suggest that B lymphocytes and helper T cells are more sensitive to ionizing radiation than cytotoxic T lymphocytes However, the extrapolation of *in vitro* data to *in vivo* situations remains questionable. On the one hand, *in vitro* laboratory conditions may not accurately reflect *in vivo* conditions. On the other hand in most *in vivo* studies, radiation treatment is only given to a part of the hematopoietic and/or lymphoid system. Therefore, a redistribution and/or repopulation of lymphocytes from non irradiated areas might occur and forbid an accurate evaluation of the radiosensitivity of the blood cell subsets. We therefore, decided to take advantage of the TBI schedule to determine the radiosensitivity of different blood cell subsets, and try to pinpoint a particular radioresistant subset.

In our previous study we showed that at least 4 to 12 h are required after radiation treatment to adequately assess the decline in lymphocytes; this finding has been confirmed in the present work where the lymphocyte count drops from $1.064 \times 10^9/l$ before irradiation to 0.667 and $0.498 \times 10^9/l$ 6 h after 2 Gy and 12 h after 4 Gy of whole body irradiation, respectively. Single-color analysis of T and B lymphocytes (CD3+, CD4+, CD5+, CD8+, CD19+) also showed a decrease in all subsets, with the B lymphocytes (CD19+) being the most sensitive. In multicolor flow-cytometry analysis, major lymphocyte subsets sharing the helper/inducer phenotype (CD3+ & CD4+) and the suppressor/cytotoxic phenotype (CD3+ & CD8+) appeared equally sensitive to the *in vivo* whole body irradiation. These findings contradict other *in vivo* studies and might be due to the fact that in these former studies, irradiation was given to a part of the lympho-hematopoietic system thus, allowing lymphocyte redistribution from non irradiated areas. Furthermore, study of the T lymphocytes bearing the "naive" (CD3+4+45RA+) and "memory" (CD3+4+45RO+) phenotypes revealed that they were equally radiosensitive *in vivo*. This finding contradicts a recent *in vitro* study that suggested a higher radiosensitivity of the CD45RO+ T lymphocyte subset (as compared to CD45RO-).

This discrepancy may be due to *in vitro* conditions in this latter study where the authors used cell culture (including the use of growth factors) and dose range (0 to 10 Gy) that make comparisons of results between this study and our own *in vivo* study almost impossible. The finding that the CD34+ cell fraction remained relatively unchanged after the first two TBI fractions is of interest. It is now clear that the CD34+ bone marrow cell subset contains the pluripotent stem cells, as well as the precursors of each distinguishable hematopoietic lineage. Furthermore, the presence of circulating CD34+ cells in human peripheral blood has been demonstrated and there is an evolving role of peripheral stem cell transplantation in the therapy of human malignancies. Several methods to mobilize stem cells into the circulation have been described, but to date only two methods have been applied, namely chemotherapy or hematopoietic growth factor-induced mobilization. Thus, our findings suggest that this rare CD34+ cell subset seems to be less radiosensitive than the above mentioned B and T lymphocyte subsets. However, whether or not this post irradiation CD34+ population always contains cells from the progenitor/stem cell pool and retains its multipotential capacity is still unknown. Even if a large number of patients were included in this study, it is obvious that we can not completely rule out for the CD34+ subpopulation which represents a very low cell number in normal control individuals that the apparent radioresistance of this population is at the level of the background signal. One lymphocyte subset with a CD3-, 4+, 8- phenotype reached 63% of its initial value after 4 Gy TBI. This lymphocyte subset has been described in T cell differentiation as a thymocyte subset. Whether this 63% value is the expression of an intrinsic, although moderate, radioresistance of this rare T lymphocyte subset or is due to radiation-induced circulation of immature thymocytes within the blood flow, requires further investigation.

Multicolor flow-cytometry analysis of the natural killer (NK) cell subsets showed that the CD3-, 56+ cell subset decrease after irradiation was due to a sharp decrease in the CD3-, 56-, 16+ subset; a decrease in the CD3-, 56+, 16- subset with only a moderate decrease of the CD3-, 56+, 16+ double positive population (74% of its initial value after 4 Gy). This latter finding would have been missed in two-color cytometry analysis. The finding that the CD3-, 56+, 16+ NK subset seems to be relatively radioresistant in these *in vivo* conditions is of

interest. Resting host-derived NK cells appear capable of mediating resistance to both autologous and allogeneic bone marrow grafts and have been implicated in both the graft-vs.-leukemia and graft-vs.-host effects. Thus, this radioresistance of NK cells could be of clinical relevance in both allogeneic bone marrow transplantation and accidental radiation-induced aplasia. Although this radioresistance of NK cells has been described in the mouse model *in vivo* and in human *in vitro* experiments, so far, no such evidence after *in vivo* TBI in humans has been reported to our knowledge.

In conclusion, our study provides evidence that T and B cell subsets seem to be equally radiosensitive after *in vivo* TBI with the exception of one immature thymocyte subset. However, by comparison, the CD34+ progenitor/stem and NK cells seem to be more radioresistant. These latter results could provide clues to the understanding of the pathophysiogeny of either radiation-induced aplasia and the engrafment/rejection process following BMT.

2 - IONIZING RADIATION EFFECTS ON THE KGla PRIMITIVE HEMATOPOIETIC CELL LINE

The HSC must be capable of self-renewal to maintain a long-term supply of progeny and capable of differentiation into multiple hematopoietic lineages, including lymphocytes. The human HSC shares the CD34 antigen together with (Thy1, C-Kit) and without lineage specific antigens (CD33, CD38, CD71...). These phenotypically defined "HSCs" have been assayed *in vitro* (using LTC-IC, HPP-CFC assay) or *in vivo* (in the SCIDhu model) but correspond to very low numbers of cells accounting for less than 1% of bone marrow cells. This low frequency and the requirement for functional tests based on the differentiation of the HSC hamper direct studies of the radiobiological features of HSC. For this reason, we used the KGla cell line that shows an immature phenotype : KGla cells were found to be CD 34 positive, Thy1 (CDw90) low, CD 38 low, HLA-DR negative and lineage negative. KGla may thus be used as an experimental model for the study of the HSC radiosensitivity.

Northern blot analyses of irradiated KGla cells showed two sequential increases of *c-jun* transcripts. The first one, early and transient, corresponds to the classical cellular response to IR as previously observed in human myeloid leukemia and epithelial tumor cell lines. An unexpected second increase was observed later on, 24 and 48 hours following the irradiation. The origin of this late *c-jun* transcript augmentation is unknown. It might be due to a partial cell cycle synchronization following IR. Indeed, in U-937 cells, *c-jun* expression was shown to be restricted to G0/G1 phase. The timing of *c-jun* increase at 48 hours correlates with the exit from the G2/M block to the G1 phase. Thus, the increase of *c-jun* transcripts might be due to a cell synchronization in G1 phase.

A biphasic alteration of bcl-2 expression was also observed 30 minutes following IR, with a reduction of mRNA levels after 1 Gy and normalization at higher doses. Since bcl2 has been shown to inhibit apoptotic cell death in many cellular models, variations of bcl2 levels may have affected the mechanism of cell death. In fact, in KGla, minimal cell death by apoptosis occurred following irradiation whatever the irradiation dose. Thus, apoptosis is not the mechanism of death in KGla cells following IR exposure.

Other genes studied did not show expression or radiation-induced expression. These results may be due, firstly, to the relatively low sensitivity limit of the northern blot technique with total RNA, since we were able to detect *c-kit* mRNA in normal KG1a cells using a RT-PCR technique (data not shown). Secondly, the IR-response may be cell-type specific. This might be the case for genes such as IL-1 that displays an increased transcription in mouse spleen cells or alveolar macrophages after irradiation. Thirdly, irradiation effects may appear at the post-translational level as described for p53 or TGF genes. Finally, the therapeutic irradiation doses used in this study (1 to 3 Gy) were far below the doses (up to 20 Gy) at which TNF and IL1 gene transcription has been showed to be induced.

Cell cycle kinetic studies showed the absence of G1 phase arrest following irradiation in KG1a cells. The absence of detectable p53 transcripts, as observed by northern blot, might explain the deficit in G1 checkpoint integrity. A classical dose-dependent G2/M arrest was observed 24 h after irradiation. The percentage of cells in this phase decreased after 48 h. This may be due to a recovery of G2/M-arrested cells or to dilution by the non-arrested cells which continue to grow.

KG1a survival following IR, although well described by a linear-quadratic function of doses is consistent with an exponential relationship between the irradiation dose and the cell survival. A D_0 value of 1.75 Gy [1.67, 1.85] was derived. This value is higher than those previously reported in the literature for CFU-GEMM, CFU-GM or BFU-E colonies, which were in the 0.50-1.65 Gy range. Thus KG1a cells might be less radiosensitive than these human hematopoietic progenitors. However, one should note that this high D_0 value could be due to the absence of *p53* induction and subsequent apoptotic death.

Taken together, this data indicates that radiation-induced cell death of KG1a, a cell line that has relatively high D_0 value, does not seem to be the result of the apoptotic pathway but occurs subsequent to a G2/M phase arrest with a possible role for the *c-jun* gene.

3 -FUNCTIONAL ROLE OF PECAM-1/CD31 MOLECULE EXPRESSED ON HUMAN CORD BLOOD PROGENITORS

In an attempt to define subset-specific cell surface glycoproteins we produced mAbs by repeated immunization with functional IL2-dependent human T cell clones or with functional leukemic cell lines. In the present report we describe a novel CD31 mAb termed IP28A that was obtained by immunizing mice with PBL. The initial screening was done in order to select antibodies reacting with cord blood mononuclear cell subsets. Preliminary extensive indirect simple immunofluorescence staining performed with IP28A mAb revealed that different leukemic T cell lines including Jurkat were also reactive. We show that IP28A recognizes a 130-135 kDa cell membrane structure and as we found that it specifically reacted with L cells transfected with CD31, we could demonstrate that IP28A is a CD31 mAb recognizing a unique epitope. Analysis of cord blood mononuclear cells from different samples revealed that in most donors 20-30 % of gated lymphocytes were reactive with IP28A. Two color FACS analysis indicated that CD31 molecules were expressed by subpopulations of CD34+cells, CD8+cells, B-cells and NK cells derived from cord blood. These results are in agreement with those reported by others. Interestingly, we show that the CD31 molecule is expressed in high amounts on human CD34+ hematopoietic cells isolated from the cord blood. The expression of PECAM-1 on CD34+ cells suggests that this molecule may function as a heterotypic adhesion molecule and/or homotypic adhesion molecule and thus it may have an important role in directing both lineage commitment and trafficking of early hematopoietic progenitor cells. Similarly, it could be proposed that CD31 molecules might be involved in intrathymic compartmentalisation and maturation of early T-lymphocytes as they are highly expressed on thymocytes and on endothelial cells. We therefore studied whether IP28A mAb exhibited agonistic properties that could be measured by testing its effect on the growth of progenitors. It should be noted that it is well known that the interaction of a mAb with its epitote may mimic the interaction of the molecule with on of its ligands. The results presented in this work show that IP28A/CD31 molecule is implicated in the regulatory process of hematopoiesis. The addition of CD31 mAb to in vitro cultures of cord blood-derived mononuclear cells revealed that this mAb promotes significantly the growth potential of hematopoietic progenitors

forming CFU-GM and those forming BFU-E. It should be noted that not only the number of formed clusters and colonies was augmented but also a high growth capacity of the resulting myeloid colonies was observed in most cultures. These results indicate that differenciation of hematopoietic progenitors in cultures supplemented with CD31mAb could be related to its direct action on these cells. A stimulatory signal transduction would follow the binding of CD31mAb to its epitope with probable enhancement of growth factor receptor expression permitting on optimal proliferative response upon addition of growth factors. In addition, the release of GM-CSF and IL3 by the CD34+ cells upon CD31 molecule stimulation should be taken into consideration. However, it is worth emphasizing that an indirect effect of IP28A/CD31mAb should not be ruled out as accessory cells including T-cells, monocytes and NK cells exert an important modulating influence on hematopoiesis. Also, it has been reported that engagement of PECAM-1 modulates the adhesive functions of β1 integrins in T lymphocytes and β2 integrins in lymphokine-activated killer cells. The role of NK cells on hematopoiesis is contradictory, both stimulatory and inhibitory effects are described. With regard to the mechanism of hematopoietic inhibition, it has been suggested that interactions of NK lymphocytes with contaminating accessory cells, rather than progenitor cells themselves, could induce activation of NK cells with subsequent secretion of growth inhibitors such as TNF and IFNγ. On the other hand, NK cells produce hematopoietic growth factors such as IL3 and GM-CSF. To further determine whether IP28A mAb is directly active on stem cells, we performed CFU-GM cultures with highly enriched CD34+ cord blood cells. The results seem to indicate that IP28A mAb has a direct action on the hematopoietic progenitor. It has yet to be determined whether these effects are unique to the IP28A mAb-defining epitope or whether they can be reproduced by the mAbs that recognize other epitopes of the CD31 molecule.

In conclusion, we demonstrate that CD31mAb in the presence of growth factors like rhGM-CSF, rhSCF and erythropoietein can induce significant growth of cord blood progenitors. Cord blood is used successfully for pediatric hematopoietic stem cell transplant however, its application in adults remains limited by the amount of cord blood that can be collected. So, it is important to define the role of different cytokines in combination with other stimulatory signals provided by cell surface structures involved in cell-cell interaction, for achieving a considerable amplification of cord blood progenitors in order to sustain hematological reconstitution in adults.

4-BY55 MONOCLONAL ANTIBODY DELINEATES WITHIN HUMAN CORD BLOOD AND BONE MARROW LYMPHOCYTES DISTINCT CELL SUBSETS MEDIATING CYTOTOXIC ACTIVITY

In the present study we compared the cell surface phenotypes of the cell populations defined with the BY55 mAb in umbilical cord and bone marrow. Phenotypic studies of bone marrow mononuclear cells revealed that BY55+ lymphocytes were less abundant than in the peripheral blood from adults. However, they also consisted in a heterogeneous cell population containing $CD3^+CD8^+TCR\alpha\beta^+$, $CD3^+CD8^+TCR\gamma\delta^+$, and $CD3^-$ lymphocytes. Interestingly, and similar to the $BY55^+CD3^+CD8^{bright+}$lymphocytes (expressing $TCR\alpha\beta^+$) sorted from adult peripheral blood, the $CD8^+BY55^+$ isolated from bone marrow and bearing either the $TCR\alpha\beta$ or the $TCR\gamma\delta$ were functional CTL. The $BY55^+$ cell population in cord blood samples corresponded to 22-35 % of the lymphocytes that failed to express the CD19 molecule. In CBL, BY55 mAb reacted exclusively with a lymphocyte subset that lacked the CD3-TCR expression and differed from the CD56, CD16 or CD11b mAb-defined cell subset. Functional studies revealed that positively isolated $BY55^+$ circulating umbilical CBL exhibit highly efficient NK activity, whereas no killer activity was found with the sorted $BY55^-$ population. We do not know yet whether NK activity is due to each single $BY55^+$ cell or to the fraction coexpressing the CD56 molecule representing > 80 % of the total $BY55^+$ cells. More important was the finding that no CTL activity could be detected from the CD3-enriched $BY55^-$ cell population.

Taking together these results indicate that BY55 mAb identifies the cytotoxic lymphocytes that correspond to different cell subsets in the cord blood and in the bone marrow. This finding is of the utmost interest particularly because the cord blood and the bone marrow are both sources for hematopoietic stem cell transplantation. These different populations might exert different consequences on the occurrence of GVHD, which is the most serious complication of bone marrow transplantation. A preliminary analysis of the International Cord Blood Transplantation Registry has shown an absence of acute and chronic GVHD in children transplanted with an HLA identical or one HLA antigen mismatched sibling cord blood transplant. The same trend has been observed in children receiving matched unrelated or two/three antigen mismatched

related cord blood transplant. This difference with patients receiving bone marrow was attribued to the immune deficiency of newborn, to the young age of donor and recipient, to the presence of naive nonactived T cells in cord blood, and to the absence of exposure to previous cytomegalovirus or other virus infection. More clinical experience is needed to confirm this finding and also to demonstrate that the diminution of graft-versus-host will not be associated with an increased incidence of rejection and leukemic relapse. Therefore, several reports showing that the frequency of alloreactive CTLp were similar in adult blood and in cord blood are puzzling. Our observation showing the lack of functionally active CTL in cord blood and their presence in bone marrow therefore seems of the utmost interest. This could indicate that acute GVHD would be directly attributable to $CD3^+BY55^+$ cells, while less severe chronic GVHD would correspond to $CD3^+BY55^-$ CTLp. Alternatively, as the unique cytotoxic cell subset that was $CD3^-BY55^+$ in cord blood corresponded to NK cells, we cannot exclude the possibility that $BY55^+$ NK cells exert a suppressive effect on the generation of effector cells responsible for GVHD. Evidence in support of this last hypothesis comes from a murine bone marrow transplantation model in which NK cells were transferred with bone marrow cells into allogenic mice. No GVHD was noted in these recipients. Interestingly, we show here the presence of $BY55^+CD3^+CD8^+$ CTL in the bone marrow cells. In conclusion, understanding of the cellular mechanisms involved in the phenomenon whereby cord blood (in contrast to bone marrow) causes less GVHD should help us to understand the mechanism of the tolerance in transplantation. Further, the identification using BY55 mAb of a cell surface molecule only expressed by cells inducing or suppressing GVHD may open new therapeutic approaches for transplantation.

5 - INTRACELLULAR PCR AND RT-PCR : NEW APPROACHES FOR DIAGNOSTICS

The aim of this study was to improve the technique of *in situ* polymerase chain reaction (PCR) on glass slides in order to detect CD34 and c-kit genes on individual mononulcear cells (MNC). This method appears to increase the sensivity of ISH without loss of morphology; MNC were deposited on slides, fixed and permeabilized. After PCR *in situ*, hybridization was realised with a digoxigenin-d'UTP (DIG)-labelled probe. Detection is mediated by an anti-DIG antibody conjugate to alkaline phosphatase and the colour substrate of this enzyme. It is worthy to mention that some PCR products diffused out of the cells in which amplification occurs and can be detected by electrophoresis of the supernatant. This direct qualitative control approach leads to rapid visualisation of amplified products before subsequent ISH. The PCR positive cells were identified by a black-blue coloration, whereas with the same hybridization cells that underwert PCR without Taq polymerase stay uncoloured.

(M. TEYSSIER, E. CAROSELLA, E. GLUCKMAN, M. KIRSZENBAUM - PCR intracellulaire : nouvelle approche de diagnostic tissulaire et cytogénétique - *Immunoanal; biol. Spéc.* (1994) 9, 159-164).

In situ RT-PCR constitutes an important improvement of the *in situ* PCR technique that is able to amplify the mRNA in a single cell. We have worked out this method to detect the CD34 gene transcripts in KG1a cell line. KG1a cells were deposited on slides, fixed and permeabilized then the mRNA were transcribed into cDNA using MMLV Reverse Transcriptase. After this step PCR amplification, *in situ* hybridization and detection were performed as described above. We obtained a positive signal only in the cells when the Taq polymerase was present during PCR and all blanks were negative

For the période June 1994 - June 1995, we plan to study by using *in situ* RT-PCR, the effect of ionizing radiations on the expression of CD34 gene in KG1a cells after 1-8 Gy exposure.

ADVANTAGES OF USING FOETAL AND NEONATAL CELLS FOR TREATMENT OF HEMATOLOGICAL DISEASES IN HUMAN.

E.GLUCKMAN. Bone Marrow Transplant Unit. Hopital Saint Louis Paris France

I CORD BLOOD HEMATOPOIETIC STEM CELLS AS AN ALTERNATIVE SOURCE OF STEM CELLS.

Bone marrow transplantation (BMT) is now recognised as an effective treatment for an increasing number of hematological diseases including malignancies, aplastic anemia and hereditary disorders. Hematopoietic stem cells (HSC) used to reconstitute hematopoiesis after intensive myeloablative therapy are typically obtained from the bone marrow or more recently from peripheral blood after mobilisation by various growth factors.(1)(2)(3) Suitable marrow must be provided by an HLA-A, -B and -DR identical related or unrelated donor; unfortunately, such a donor is not always available because of the extreme polymorphism of the HLA system. Even when a donor is available, the inability of current methods of HLA typing techniques to determine all the potential mismatches means that recipients of unrelated bone marrow transplants are at extreme risk for graft versus host disease(GVHD)(4). Finding new and readily available sources of hematopoietic stem cells will broaden the availibility of this treatment and improve the outcome of the transplant. New sources of HSC currently under investigation are adult cytokine mobilised peripheral blood stem cells and placental blood collected at birth. The first has the advantage of containing a large number of CD34+ progenitor cells and is easily collected, it has the disadvantage of containing a large number of peripheral blood mature lymphocytes which are known to be the effectors of graft versus host disease. Cord blood has the advantage of being easily collected without any risk to the donor, and it contains immature HSC and lymphocytes. These properties should increase the probability of engraftment and diminish the risk of severe graft versus host disease, the disadvantage might be that the number of cells collected in a single cord blood might be insufficient for long term engraftment in the host.

Preliminary analysis of the results of more than 50 cord blood transplants performed throughout the world shows that long-term engraftment has been observed in patients with different diagnoses including both malignant and non malignant disorders(5)(6)(7)(8)(9). The number of cells infused was inferior to the number infused in bone marrow transplants or peripheral blood stem cell

transplants (PBSCT), but, despite this small number of cells, the incidence of graft failure was low. Furthermore, there was no correlation between the number of cells and the speed of engraftment, and the addition of in-vivo growth factors did not modify the speed of engraftment. This is probably due to the unique properties and growth factor-independence of hematopoietic stem cells from cord blood(10). It is likely that a limited number of primitive hematopoietic stem cells are sufficient to induce long term engraftment: the present limitation for standardising methods of quantification of HSC, as well as the absence of criteria to identify "stem cells" explain why the minimum number of HSC necessary for engraftment is unknown. It is estimated that long term engraftment can be obtained with 1 5 to $5x10^5$ LTC-IC from bone marrow and $2x10^4$ LTC-IC from cord blood.(11)

Another very important clinical finding is the observation that the incidence of acute and chronic graft versus host disease has been low in family or unrelated matched and mismatched cord blood transplants. To date, the follow-up is not sufficient to know if these cells are able to mount a graft- versus-leukemia (GVL) reactivity.

Cord blood is an abundant source of stem cells that are usually discarded and whose collection is entirely safe to the donor, as the blood is only removed from the placental side of the umbilicus post parturition and clamping. There exists a very large number of potential donors with a possibility of selecting donors according to rare HLA haplotypes. Frozen cells can be tested in advance and can be available at short notice, decreasing the length of the search for donors. Additionally, there is a low prevalence of infectious diseases at birth, particularly cytomegalovirus (CMV), which is a major cause of transplant-related mortality, and thus, cord blood transplants may be associated with lower incidence of post transplant infection.

This has led to an exponential increase in the interest in cord blood transplant and to the development of cord blood banks across the world. (12) (13).

II PROPERTIES OF CORD BLOOD HEMATOPOIETIC STEM CELLS.

It has been shown that foetal and cord blood hematopoietic stem cells are different from adult blood and marrow hematopoietic stem cells.(14) In vitro, clonogenic assays of hematopoietic stem cells from cord blood have demonstrated that colonies are larger and more enriched with immature progenitors.than those obtained from adult marrow and peripheral blood(15) Cord blood stem cells

show more potential growth in long-term culture and can be expanded.(16) (17). There are differences in cytokine requirement for growth in-vitro and for replating capacity, possibly due to autocrine or paracrine production in culture. (10). Stable and long-term engraftment has been observed in SCID mice without the need of additional growth factors(18). Ontogeny-related changes may be related to the decrease of telomeric length with age.(19)

The possible clinical applications of these properties include the use of cord blood hematopoietic stem cells for characterisation of primitive progenitors, selection of cell subsets, in-vivo expansion and use for gene transfer and gene therapy.

This could be particularly important for the treatment of genetic diseases where the diagnosis can be performed in-utero, and cord blood can be collected at birth, transfected, and transplanted immediately. On a larger scale, autologous cord blood collection and cryopreservation could be offered in families with an increased risk of cancer, autoimmune disease or infection.

III IMMUNOLOGICAL PROPERTIES OF CORD BLOOD CELLS

Graft-versus-host disease(GVHD) is the major barrier to successful allogeneic bone marrow transplantation. This can be overcome by T-cell depletion, use of immunosuppressive drugs or in-vivo monoclonal antibodies, but this is often associated with an unacceptable increase of the relapse rate, demonstrating the importance of the graft-versus-leukemia(GVL) activity associated with allogeneic BMT. Early results from unrelated cord blood transplants have provided evidence of lower incidence and severity of acute and chronic GVHD in the recipient than would have been predicted from adult volunteer donor bone marrow transplants. Several hypotheses can explain the decrease of GVHD, some are already known: the incidence of GVHD diminishes with donor and recipient age, with the absence of donor and recipient herpes virus species infections and with a low number of lymphocytes infused. All these requirements are met by cord blood but not necessarily by adult bone marrow or peripheral blood. Other explanations for thedecrease of GVHD can be found in the study of immune function of cord blood cells. It is known that cord blood lymphocytes are enriched in immature progenitors. Lymphoid subsets in cord blood differ from those of adult blood. Immature CD3- 8+ or 7+ cells are present; CD3+ cells have a naive, non activated phenotype (CD25-,DR-,CD45RA lo); and most CD3- cells are NK cells (CD16+, CD56+).

Immune deficiency of cord blood lymphocytes might also be explained by the presence of a small number of maternal cells.(20) In a previous study, we used the polymerase chain reaction amplification of 2 minisatellite sequences and found a maternal specific allele in one sample out of 42 cases tested.(22) Using PCR amplification of non-inherited HLA antigens, the New York cord blood bank group has been able to detect maternal cell contamination in 3 cases out of 3000 cord blood samples studied. Using fluorescent in-situ hybridisation, the Seattle group found maternal cells in 6/44 unfractionated cord blood samples at levels ranging from 1/2500 to 1/100. Finally, we used a highly sensitive, allele specific amplification method and have shown that maternal specific alleles were found, in 10 out of 10 samples studied, at a frequency of 10^{-4} to 10^{-5} of cord blood nucleated cells. The presence of maternal cells, at such a low level, in cord blood samples is probably insufficient to induce GVH after transplantation, but it may play a role in the establishment of the foeto-maternal tolerance and in the transmission of infection from the mother to the new-born.

The mechanism of cytotoxicity seems different in cord blood compared to adult peripheral blood. While most of the tests of proliferation and the study of CTL-p and HTL-p seem normal or slightly decreased when compared to adult subpopulations, the study of lymphoid subsets seems to show that there is an increase of CD 3- subsets mostly, of the NK subset. Cytotoxicity seems mostly dependent on the NK subsets as shown by the study of perforin expression and of the BY55 monoclonal antibody which recognises functional cytotoxic T or NK cells (21) (22)

It remains to be established that the decrease of GVH is an active phenomenon of suppression by these cell subsets.(23)

CONCLUSION

Cord blood banks have been established in several countries for use in family and unrelated transplants. In addition, cord blood cells are widely used for experimental purposes and for the development of cell and gene therapy. For this reason, it is mandatory to organise exchanges between these banks and to develop methods of standardisation of collection, cell separation, purification, quantification of HSC, methods of cryopreservation and thawing. The European Cord Blood Bank (ECBB) group has begun to work on these aspects as well as on the methods of detection of transmissible infectious or genetic diseases. A registry of cord blood transplants has been

established within the Immunology working party of the European Blood and Marrow Transplant Group.

REFERENCES

1 BENSINGER WI, WEAVER CH, APPELBAUM FR, ROWLEY S, DEMIRER T, SANDERS J, STORB R, BUCKNER CD. Transplantation of allogeneic peripheral blood stem cells mobilized by recombinant human granulocyte colony stimulating factor. Blood.1995;85:1655-1658.

2. KORBLING M, PRZEPIORKA D, HUH YO, ENGEL H, VAN BIESEN K, GIRALT S; ANDERSSON AB, KLEINE HD, SEONG D., DEISSEROTH AB, ANDREEFF M CHAMPLIN R. Allogeneic blood stem cell transplantation for refractory leukemia and lymphoma: potential advantage of blood over marrow allografts. Blood 1995; 85: 1659-1665.

3. SCHMITZ N, DREGER P. SUTTORP M, ROHWEDDER EB, HAFERLACH T, LOFFLER H, HUNTER A, RUSSELL NH. Primary transplantation of allogeneic peripheral blood progenitor cells mobilized by Filgrastim(Granulocyte colony stimulating factor). Blood 1995; 85: 1666-1672.

4. GOLDMAN JM for the WMDA executive committee. A special report :bone marrow transplants using volunteer donors- recommendations and requirements for a standardized practice throughout the world-1994 update. Blood.1994;84: 2833-2839.

5. GLUCKMAN E, BROXMEYER HE, AUERBACH AD et al. Hematopoietic reconstitution in a patient with Fanconi's anemia by means of umbilical cord blood from an HLA identical sibling . N. Engl. J. Med 1989; 321: 1174-1178.

6 VOWELS MR LAMPOTANG R, BERDOUKAS V, et al. Correction of X linked lymphoproliferative disease by transplantation of cord blood stem cells . N. Engl. J. Med 1993; 329: 1623-1625.

7 ISSARAGRISIL S; VISUTHISAKCHAI S, SUVATTE V, TANPHAICHITR VS, CHANDANAYINGYONG D, SCHREINER T, KANOKPONGSAKDI S, SIRITANARATKUL N, PIANKIJAGUM A. Brief report: transplantation of cord-blood stem cells into a patient with severe thalassemia . New Engl J of Med. 1995. 332:367-369.

8. WAGNER JE, KERNAN NA, BROXMEYER HE, GLUCKMAN E. Allogeneic umbilical cord blood transplantation: report of the results in 26 patients. Blood, 1993; 82, Sup 1: 86a.abstract

9.WAGNER JE , BROXMEYER HE, BYRD RL. et al. Transplantation of umbilical cord blood after myeloablative therapy. Analysis of engraftment. Blood. 1992; 79: 1155-1157.

10. SCHIBLER KR, LI Y, OHLSRK,et al. Possible mechanisms accounting for the growth factors independence of hematopoietic progenitors from umbilical cord blood. Blood.1994; 84: 3679- 3684.

11. TRAYCOFF C; KOSAK ST, GRIGSBY S, SROUR EF. Evaluation of ex-vivo expansion potential of cord blood and bone marrow hematopoietic progenitor cells using cell tracking and limiting dilution analysis. Blood. 1995; 85: 2059-2068.

12. RUBINSTEIN P, ROSENFELD RE, ADAMSON JW, STEVENS CE. Stored placental blood for unrelated bone marrow reconstitution. Blood. 1993; 81: 1679-1690.

13. E. GLUCKMAN. European organisation for cord blood banking. Blood Cells .20: 601-608. 1994.

14. BROXMEYER HE, DOUGLAS GW, HANGOC G et al . Human umbilical cord blood as a potential source of transplantable stem/progenitor cells. Proc. Natl Acad Sci USA.1989; 86: 3828-3832.

15. BROXMEYER HE, HANGOC G, COOPER S et al. Growth characteristics and expansion of human umbilical cord blood and estimation of its potential for transplantation in adults. Proc. Natl. Acad Sc USA. 1992; 89: 4109-4113.

16. MAYANI H, DRAGOWSKA W, LANSDORP PM. Cytokine-induced selective expansion and maturation of erythroid versus myeloid progenitors from purified cord blood precursor cells. Blood. 1992; 79: 2620- 2627.

17. MAYANI H, DRAGOWSKA W, LANSDORP PM. Characterization of functionally distinct subpopulations of CD34+ cord blood cells in serum-free long-term cultures supplemented with hematopoietic cytokines. Blood. 1993;82: 2664-2672.

18. VORMOOR J, LAPIDOT T, PFLUMIO F, RISDON G, PATERSON B, BROXMEYER et al Immature human cord blood progenitors engraft and proliferate to high levels in severe combined immunodeficient mice . Blood. 1994; 83: 2489- 2497.

19. VAZIRI H, DRAGOWSKA W, ALLSOPP RC, THOMAS TE, HALEY CB, LANSDORP PM. Evidence for a mitotic clock in human hematopoietic stem cells: loss of the telomeric DNA with age. Proc. Natl. Acad. Sci. USA. 1994; 91: 9857-9860.

20. SOCIE G, GLUCKMAN E, CAROSELLA E, BROSSARD Y, LAFON C, BRISON O. Search for maternal cells in human umbilical cord blood by polymerase chain reaction amplification of two minisatellite sequences. Blood. 1994; 83: 340-344.

21. BENSUSSAN A, GLUCKMAN E, EL MARSAFY S, et al. By55mAb delineates within human cord blood and bone marrow lymphocytes distinct cell subsets mediating cytotoxic activity. Proc. Natl. Acad. Sci USA, 1994; 91: 9136-9140.

22. BERTHOU C, LEGROSMAIDA S, SOULIER A, WARGNIER A, GUILLET J, RABIAN C, GLUCKMAN E, SASPORTES M. Cord blood lymphocytes lack constitutive perforin expression in contrast to adult peripheral blood T lymphocytes. Blood. 1995; 85: 1540-1546.

23. RISDON G, GADDY J, HORIE M, BROXMEYER HE. Alloantigen priming induces a state of unresponsiveness in human umbilical cord blood T cells. Proc. Natl. Acad. Sci. USA. 1995; 92: 2413-2417.

RESUME

UTILISATION DU SANG FOETAL ET NEONATAL POUR LE TRAITEMENT DES MALADIES HEMATOLOGIQUES CHEZ L'HOMME

La greffe de moelle osseuse allogénique est un traitement efficace d'un grand nombre de maladies hématologiques malignes ou non. De nouvelles sources de cellules souches hématopoïétiques sont actuellement à l'étude. Elles sont isolées soit, du sang après mobilisation par des cytokines chez l'adulte ou, du sang placentaire prélevé à la naissance. L'analyse des résultats de plus de cinquantaine de greffes de cellules souches hématopoïétiques du sang placentaire a montré une prise à long terme dans la majorité des cas, malgré le faible nombre de cellules injectées. Par ailleurs, l'incidence et la gravité de la réaction du greffon contre l'hôte a été faible même lorsque le donneur n'était pas totalement HLA compatible. Le recul est insuffisant pour savoir si la fonction graft versus leukemia est maintenue. La facilité d'obtention de ces cellules explique le développement de banques de sang placentaire.

Les propriétés des cellules souches hématopoiétiques du sang placentaire sont originales avec un enrichissement en cellules immatures et une plus grande capacité d'expansion in vivo et in vitro. Ceçi est particulièrement important pour la thérapie cellulaire et la thérapie génique.

Le déficit immunitaire du nouveau né est caractérisé par un accroissement de populations T immatures, un enrichissement en cellules NK et la présence de cellules naives non activées suppressives. L'ensemble de ces caractéristiques peut expliquer la diminution de la GVH et la possibilité de faire des greffes non strictement HLA identiques. Ceçi devrait aboutir à la diminution du pool de donneurs nécessaires pour traiter un plus grand nombre de patients.

Contract: F13P-CT 930069   **Sector: B1**

Title: Radiation effects and their treatment on the connective and vascular tissues in various organs.

Coordinator   CIR
       B.P. 34
       F-92260 FONTENAY-AUX-ROSES
       Tel. 33-146547266

1   Dr. H. Magdelénat   2   Prof. AJ. Van der Kogel
      CIR   Univ. Nijmegen
      B.P. 34   Institute of Radiotherapy
      F-92260 FONTENAY-AUX-ROSES   Postbus 9101
      Tel. 33-146547266   NL-6500 HB NIJMEGEN
      Laboratoire de Radiopathologie   Tel. 31-80615354
      Institut Curie
      F-75231 Paris Cedex 5

I. Summary of project and global objectives

The objective of the project was the development of new methods of diagnosis, prevention and treatment of radiation induced lesions to organs other than the hæmatopoietic system and skin, with special focus on the alterations of connective or supportive and vascular tissues following radiation overexposure. The development of such methods was based on an increased knowledge of physiopathological alterations and the introduction of modern investigative and therapeutical tools (physical devices and molecular or cellular biology) The organs considered were the muscles, lungs, and the central nervous system.

Previous results, mainly on radiation-induced skin fibrosis, prompted us to consider Superoxyde dismutase (SOD) as a potential therapeutical agent in the treatment of lesions resulting from acute irradiation of these organs. Although semeiological investigations could

be achieved following focal cranial irradiations, limited clinical trials with SOD could be undertaken in lung fibrosis. Accordingly, in vitro and animal models were developed and used for physiological, histopathological and pharmacological studies. The cooperation between CIR (Paris) and University of Nijmegen was particularly effective in histopathological investigations related to experimental material from both institutions.

II. Major achievements

Contribution of the CIR (Paris)

1 - Experimental sequential study of Magnetic Resonance Imaging (MRI) of irradiated skeletal muscles in relation with histopathological features.

Twenty two New-Zealand rabbits have been irradiated (Dr Lefaix, Jouy en Josas) at 120 Gy with a source of Iridium 192, then examined serially (twice a month) by 1.5 Tesla proton magnetic resonance imaging (MRI) (Dr Rahmouni, Créteil), and séquentially biopsied to study the histological evolution from early inflammatory reaction to installed fibrosis and the alterations of the prolin/hydroxyprolin ratio of fibrotic areas. At 8 weeks, a grade 1 fibrosis appeared, after a period characterized by the presence of inflammatory cells, increase of oedema in the dermis and microvascularization in the underlying muscular tissue. MRI (T1, T2 or Turbo-flash) was modified as soon as the second week after irradiation, indicating oedematous and vascular changes. Histological examination was performed at different times of the progression of fibrosis.

2 - Therapeutic approaches of radiation-induced fibrosis of the lung by Superoxyde Dismutase (SOD)

Clinical study. (Dr Campana, B. Perdereau, Institut Curie)
Lung fibrosis affects a number of patients exposed to accidental or therapeutical ionizing radiations on the chest. According to the beneficial effects of Superoxyde dismutase (SOD) observed in the patients treated for radiation induced skin fibrosis at the Institut Curie as well as results reported in the litterature, SOD was proposed for treatment of radiation induced lung fibrosis
A pilot study has been conducted on 9 patients presenting with symptomatic lung fibrosis which developped 5 to 9 months after radiotherapy. Bovine SOD was administered by inhalation (aerosols) : 35mg (125 000 units) 3 times a week (every second day) for 2 weeks (Total SOD required : 210mg). Based on an estimated aerosol deposition of 10% in the lung, the SOD delivered to the lung was approximately 75000 units.

Cough symptoms improved in 9/9 patients, breathing frequency in 8/9 with an average gain in peak flow of 34 % .Thorax X ray showed objective response in 6 patients. No toxicity was observed.

This clinical programme was interrupted due to legal restrictions on the use of bovine proteins for clinical investigations. It was recently resumed in collaboration with IMAS (Barcelona) These restrictions posed the issue of therapeutical approaches based on animal products for human use.

Two alternatives to the use of bovine SOD were considered :

SOD like compounds from non animal sources (SPD)

Human recombinant SOD (h rSOD)

As a prerequisite to clinical investigations, it was decided to develop a rat model of radiation induced lung fibrosis to be used for pharmacological and preclinical studies of anti fibrosis compounds . r-hSOD is now available for these investigations.

Experimental study. (Institut Curie, Fontenay aux Roses)

First, 40 Sprague-Daley male rats (age:7 weeks) were irradiated on one lung (right lung) with a ^{60}Co external source at CEN/Fontenay aux Roses (IPSN/DS, Dr Rannou), in order to define the optimal fibrogenic dose, the optimal geometry of irradiation fields, as well as the time course for the development of an assessable lung fibrosis.

The veterinary, qualitative histological morphology (microscopy and confocal microscopy, DPTE/DSV CEN/FAR, Dr P Fritsch) and morphometic analysis (Hopital Broussais, Pr Bruneval) data led to the following conclusions:

• the optimal weight of the animals at time of irradiation is 260-280 g
• the optimal ^{60}Co dose for animals irradiated in one single irradiation under mild anaesthesia is 25 Gy.
• the time required for an histologically assessable lung fibrosis is 16 weeks.

Second, the efficacy of the aerosol route of administration for therapeutic compounds was investigated, since it will be the one preferred for clinical applications.

The 40 irradiated rats inhaled ^{99}Tc labelled albumin in an experimental inhalation device for rodents (DPTE/DSV, Dr D Hoffschir) designed for the simultaneous treatment of 8 rats in controlled conditions (pressure, flow rate, volume, concentration). Thus a relatively homogenous deposition yield and distribution was obtained, close to that expected from reference data on organ deposition with various labelled compounds. A deposition yield at the bronchoalveolar level of 0.15 % of the total dose of macromolecular compounds may thus be reproducibly obtained in the rat. This is significantly lower that the expected delivery yield in humans but remains relevant for further pharmacological studies in the rat.

3 - Radiation effects on the central nervous system (Salpêtrière, Institut Curie)

The department of Neurology (Hopital de la Salpêtrière) and the Laboratory of Radiopathology (Institut Curie) are collaborating to study the effects of cerebral irradiation (RT) on cognitive functions.

Increased survival in some patients treated for a brain tumor explains that the risk of late cerebral damages due to RT is becoming an important issue. Radionecrosis is the best characterized but its incidence after conventional external RT has dropped since Sheline identified its main predisposing factors. On the other hand, an ill defined diffuse encephalopathy also called "diffuse cerebral radiation injury" or "RT-induced leukoencephalopathy" is becoming the most frequent complication of cerebral RT in long term survivors.

This entity differs from radionecrosis in clinical-radiological aspects as well as in pathology and neither its incidence, pathogenesis nor its predisposing factor are clear. To study this problem, we used a clinical, pathological and experimental approach.

Clinical studies

Several features are required for the diagnosis of RT-induced cognitive dysfunction :
1) A history of cerebral irradiation months to years before the onset of clinical symptoms.
2) Absence of recurrent tumor. 3) Absence of any other cause of cerebral dysfunction.

To better define the incidence and predisposing factors of the "diffuse cerebral radiation injury syndrome", we undertook two studies of cognitive functions in our long term survivors of gliomas.

In the first study (Sichez et al, submitted), a battery of psychologic tests was administered to 32 patients, aged from 26 to 61 years, who had survived 2 years or more after treatment with surgery and radiotherapy for supratentorial gliomas without evidence of recurrent tumor on MRI. Two groups were identified. A first group of 17 patients had neuropsychologic scores similar to estimated premorbid level (group I). A second group of 15 patients had abnormal neuropsychologic scores, lower that their estimated premorbid level (group II). In comparison with normal patients, those with abnormal neuropsychologic scores were older at the time of treatment (p = 0.001), had a lower post operative karnofski index (p = 0.008) and more often had left sided lesions (p = 0.001). Comparison of karnofski indexes between the post operative time point and the date of neuropsychological evaluation did not show a significant change over time in groups I and II. Nonetheless, 3/32 patients (9 %) developed a progressive decrease of their karnofski indexes.

This study suggests that vigorous treatment of gliomas with surgery, radiotherapy and sometimes chemotherapy does not induce a substantial cognitive dysfunction in a majority of long term survivors (53 %). When cognitive dysfunction is identified (47 %) of patients), our data suggest that it has generally been present since the post operative period.

Finally, a minority of elderly patients (9 %) develop the clinical picture of "diffuse cerebral radiation injury".

The second study was a 4 years prospective evaluation of cognitive functions in adults receiving conventional radiotherapy for a supratentorial glioma (Vigliani, Sichez, et al, submitted).

The study was performed in 17 patients who underwent conventional focal RT for a low-grade glioma or for a good prognosis anaplastic glioma. Results were compared with those of 14 "control" patients harboring low grade gliomas who did not receive radiotherapy. A transient significant decrease of performances for the Reaction Time and PM 38 tests was observed at the 6 months time-point in the irradiated group with return to baseline values 12 months post-RT.

Subsequently, no other significant changes were observed over a 48 months follow-up period in the irradiated and non irradiated groups. Nonetheless when the scores of each patients were considered over time instead of the mean values of the group, 1 irradiated patient (5.8 %) showed clear signs of progressive deterioration while 2 irrradiated patients (12 %) experienced long-lasting improvement. Individual changes did not occur in non irradiated patients. This study suggests that, apart from an early-delayed transient drop of neuropsychological performances at 6 months, focal conventional RT carries a low risk of long-term cognitive dysfunction in the first 4 years after irradiation, *but only when administered to young adults.*

To further progress in the understanding of predisposing factors for RT-induced cognitive dysfunction, we undertook a detailed study of the literature on this subject (Vigliani and Delattre, submitted). Since Sheline was able to identify important predisposing factors for radionecrosis with a careful study of the literature in the late seventies, we thought that this strategy could be useful for the "diffuse cerebral radiation injury syndrome". The following conclusions were drawn : 1) The risk of developing late dementia is affected by at least 3 predisposing factors including the age of the patient, the irradiation scheme (dose in neuret and volume of irradiation field) and the administration of concurrent chemotherapy. Thus, the risk of developing dementia which is 0 when radiation is administered focally with a dose < 1000 neuret and without concomitant chemotherapy in a patient aged less that 60 years increases to a 100 % risk when RT is administered to the whole brain with a dose > 1000 neuret concomitant chemotherapy in a patient aged more than 60 years (figure 1). 2) Clinical and radiological data as well as very few pathological studies all suggest that white matter is the main target for RT-induced cognitive damage (leukoencephalopathy) and that "classic radiation necrosis" is not involved.

Pathological studies

Because the pathological substratum of this radiation induced syndrome is so poorly known with only 4 detailed cases reported in the literature, we undertook a pathological study of 4 additional patients who died as a consequence of RT-induced dementia (Vigliani, Duyckaerts et al, manuscript in preparation). The grey matter and neurons were normal in all patients. Although a severe and diffuse white matter pallor, sparing the U fibers, was present in all cases, 2 types of lesions were identified : one patient who had received "neoadjuvant" chemotherapy with VM 26, 5 FU and CCNU before RT had a severe and isolated spongiosis of the white matter without axonomyelinic loss, gliosis, necrosis or vascular damage suggesting a state of chronic edema, possibly related to chronic damage to the blood-brain barrier. The other patients who had not received chemotherapy had a diffuse axonal and myelinic loss with gliosis in the white matter. In addition two of them had multiple minute or very small foci of necrosis (not exceeding a few millimeters) disseminated in the white matter. These minute foci of necrosis were quite different from "classic radionecrosis", mainly because of their very small size, dissemination, and absence of significant vascular lesions. The punched out foci of necrosis that we found are similar to the experimental observations made by Caveness after conventional cerebral RT in the monkeys. Thus the pathological substratum of RT-induced leukoencephalopathy with dementia is not homogenous with at least 2 different pathological pictures despite common clinical and radiological features ; one is suggestive of pure chronic edema and the other indicates severe axonal lesions with disseminated punched out microscopic foci of necrosis.

Experimental studies

I. A model of cognitive dysfunction after conventional cerebral radiotherapy in the old rat.

In order to better define the pathogenesis of the syndrome of RT-induced diffuse cognitive dysfunction, we developed an experimental model in the old rat (Lamproglou et al, 1995). A course of whole brain radiation therapy (30 Gy/10 fractions/12 days) was administered to 26 Wistar rats ages 16-27 months, while 26 control rats received sham irradiation.
Sequential behavioral studies including one-way avoidance, and a standard operant conditioning method (press lever avoidance) were undertaken. In addition, rats were studied in a water maze 7 months post radiation therapy.
Prior to radiation therapy, both groups were similar. No difference was found 1 and 3 months postradiation therapy. At 6-7 months postradiation therapy, irradiated rats had a much lower percentage of avoidance than controls for one-way avoidance (23 % vs 55 %, p<0.001) and two-way avoidance (18 % vs 40 %, p<0.01). Seven months postradiation therapy the reaction

time was increased (press-lever avoidance, 11.20 s vs 8.43 s, p<0.05) and the percentage of correct response was lower (water maze, 53 % vs 82 %) in irradiated rats compared with controls. In conclusion, behavioral dysfunction affecting mainly memory can be demonstrated following conventional radiation therapy in old rats.

Studies are currently being performed with the brains of the rats, including current pathology, electron microscopy, Golgi preparations, and immunohistochemistry for neurotransmitters analysis.

II. A model of acute cognitive dysfunction after whole body irradiation. possible effects of liposomal superoxide dismutase.

Acute encephalopathy is a well known complication of therapeutic or accidental whole body irradiation. Since one of our objectives is to identify radioprotective agents, both for acute and chronic neurological complications of RT, we developed a model of acute cognitive dysfunction after whole body irradiation. In a first step, we demonstrated that whole body irradiation with a single dose of 4.5 Gy induced a significant alteration of a learning task (one-way avoidance) for at least 2 weeks (Lamproglou et al, unpublished results).

In a second step, we studied the effects of liposomal bovine superoxide dismutase in this model (Lipsod, 0.5 mg/kg SC started one hour after irradiation for 14 days).

The preliminary results clearly suggest a protective effect of Lipsod. However, further experiments are needed to confirm these preliminary findings.

Conclusion

Substantial progress have been made in the clinical description, predisposing factors and patholological features of RT-induced late cognitive dysfunction after conventional cerebral RT. For the first time, an experimental model of this syndrome has been developed which should be useful to understand its pathogenesis.

An acute model of cognitive dysfunction after whole body irradiation has been developed which seems quite useful to test radioprotective agents. In the future we hope to try these radioprotective agents in the chronic model.

Publications

Lamproglou I, Qi Ming Chen, Boisserie G, Mazeron JJ, Poisson M, Baillet F, Le Poncin M, Delattre JY. Radiation-induced cognitive dysfunction : an experimental model in the old rat.(1995) Int J Radiation Oncology Biol. Phys. 31: 65-70

Sichez N, Chatellier G, Poisson M, Delattre JYEtude neurologique des survivants à long terme de gliomes (submitted)

Vigliani MC, Sichez N, Poisson M, Delattre JY. A prospective study of cognitive functions following conventional radiotherapy for supratentorial gliomas in young adults: 4 year follow-up (submitted)

Vigliani MC & Delattre JY Radiation-induced intellectual deterioration of adult: a review (submitted)

II Contribution of the University of Nijmegen, Institute of Radiotherapy

Objectives of the group

The contribution of the University of Nijmegen was :

In vitro studies : To study the effects of cytokines on the radiation response of various classes of glial cells (astrocytes, oligodendrocytes, glial progenitors). To initiate studies on the role of SOD and other potential modifiers of oxydative injury. To elucidate the role of different modes of cell death (mitotic and apoptotic) in specific glial cell populations.

In vivo studies : To study vascular perfusion and permeability in gliomas and the normal rat brain after irradiation. To compare quantitative morphology (image analysis of vascular architecture, perfusion, and permeability) with NMR spectroscopy and imaging (D^2O perfusion and ^1H / ^{31}P spectroscopy). To investigate the possible modifications in the development of radiation injury by SOD, ACE-inhibitors (Captopril) and inhibitors of polyamine synthesis (DFMO) in the rat spinal cord.

Clinical studies : NMR spectroscopy and imaging of brain tumor patients before and after treatment with nicotinamide combined with carbogen breathing and radiation.

Specific objectives for the last reporting period

To continue studies on the role of SOD and other potential modifiers of oxydative injury in glial cells in vitro. To investigate the role of apoptotic cell death in specific glial cell types, and in vivo at various times after irradiation of the spinal cord as a function of radiation dose and age of the animal.

To perform a detailed analysis of the vascular architecture of gliomas and normal rat brain after irradiation, and to study the role of concomitant anti-angiogenic drugs and retinoids. To continue the comparison of morphological vascular parameters with NMR spectroscopy and imaging (D^2O perfusion and ^1H / ^{31} P spectroscopy) of irradiated rat brain and implanted gliomas.

Clinical studies : NMR spectroscopy and functional imaging of normal brain and tumors in patients before and after treatment with nicotinamide combined with carbogen breathing and radiation will be continued.

Achievements of the group

In vitro studies. Studies on the role of various growth factors on the radiation response of glial cells and their progenitors were completed. A comparison was made of the clonogenic survival of glial progenitors plated on monolayers of freshly prepared astrocytes with purified O-2A progenitors and oligodendrocytes. A major problem has been that these cells did not adhere to the surface of culture dishes, and a large effort was made to improve the adherence and purification/enrichment of specific glial cell types, and finding an appropriate assay to test the effectiveness of growth factors. We have finally settled for a ^{3}H-thymidine incorporation assay as a screening procedure for various growth factors. In these studies, a large effect on proliferation of neonatal 0-2A progenitor cells obtained from the spinal cord was observed for bFGF and PDGF. Other growth factors tested were EGF, hCSF, hSCF, and NGF did not show any proliferative response. A combination of bFGF with radiation showed a small but significant survival enhancement, when present during the whole post-irradiation incubation period (2-3 days). These results agree with results obtained in other cell systems, notably the vascular endotheliium. All other factors tested did not modify the radiation response of glial progenitors, either measured by the ^{3}H-thymidine incorporation assay or the clonogenic assay.

Other responses. Studies on the effects of the polyamine inhibitor DFMO and the vasoactive substance nicotinamide were completed. DFMO showed a small protective effect on glial progenitor cells, while nicotinamide had no effect when tested in vitro. Nicotinamide and irradiation of the adult spinal cord, followed by excision assay and in vitro assessment of progenitor survival, showed a significant sensitization of progenitor cells. These latter experiments are currently repeated and a final publication will be submitted in 1995.
The angiotensin-converting enzyme (ACE) inhibitor captopril, which protects the kidney from radiation injury, was shown to be ineffective in the rat spinal cord. No modification of the radiation response was measured.
In the last reporting period, experiments with superoxyde dismutase (SOD) as a potential modifier of oxydative injury have been performed. In vitro survival of glial progenitor cells was not modified by SOD, while a control experiment in which the radical scavenging aminothiol-compound WR-1065 was added before irradiation showed a significant protective effect of the thiol compound. This work is submitted for publication.

Mechanisms of cell death. Studies of the induction of apoptosis as a mode of cell death of different populations of glial cells in the CNS have been carried out in this project. Apoptosis was measured by a in situ nick translation procedure (in situ end-labeling with the enzyme terminal transferase and biotin-dUTP as substrate). Experiments have been performed in vitro

in presence or absence of bFGF and PDGF, and in vivo after spinal cord irradiation. These experiments have not been concluded yet, but the present results do not indicate apoptosis to be a significant mode of cell death in radiation injury of the adult CNS.

In vivo studies of vascular perfusion and permeability in gliomas and the normal rat brain. In this project, a large effort has been spent to develop computerized image analysis of vascular architecture and function. Using fluorescent perfusion markers and specific markers of the vascular endothelium, quantitative image analysis of vascular perfusion and architecture can now be reliably carried out in complete tissue sections. The morphological parameters of vascular size, density and intercapillary distance have recently been expanded with analyses of perfused vascular domains, to correlate vascular morphology with vascular perfusion studies carried out with NMRSpectroscopy and dynamic MRI.

[31] P-MRS studies. The relationship between the bioenergetic status of human glioma xenografts in nude mice and morphological parameters of the perfused vascular architecture was analysed. Two tumour lines with a different perfused vascular architecture were used for this study. The relative perfused tumour area (RPTA) and the percentage of intercapillary distances larger than 200 µm (icd[200]), were related to the P_i/ATP ratio of the tumour. The mRPTA reflects the mean fraction of the convective transport area of 0_2 and nutrients. Intercapillary distances larger than 200 µm have been shown to be associated with low oxygen and glucose levels. The results confirmed the expectations : with increasing icd[200], the P_i/ATP ratio increases linearly, while an inverse relationship was found with the perfused tumor area.

[2]H_2O and Gd-DTPA kinetic studies. ^2H_2O kinetics were compared to dynamic Gd-DTPA studies using T1-weighted FLASH imaging of tumour slices (1.5 mm). The Gd-DTPA diffusion was fast in tumor regions with a high vascular density and short intercapillary distances as measured with quantitative analyses of the perfused vascular architecture in comparable tissue slices. The ^2H_2O curves took more time to reach the steady state due to tumour regions with large intercapillary distances (> 200 µm). The results of these studies suggest that the distribution of intercapillary distances may play an important role in the diffusion-limited part of the uptake curve.

Clinical studies. NMR spectroscopy and imaging of brain tumor patients before and after treatment with nicotinamide combined with carbogen breathing and radiation is now completed. A first publication is accepted and in press.

Nicotinamide administration and carbogen breathing induced a shift towards pH values. These results are now being prepared for publication.

Publications

van der Maazen RWM, Thijssen HOM, Kaanders JHAM, de Koster A, Keyser AJM, Prick
MJJ, Grotenhuis JA, Wesseling P, van der Kogel AJ. Conventional radiotherapy
combined with carbogen breathing and nicotinamide for malignant brain tumors.
Radiother. Oncol. in press, 1995.

Haustermans K, van der Kogel AJ, Vanacker B, van der Schueren E. Influence of combined
use of nicotinamide and carbogen on rat spinal cord tolerance. Radiother. Oncol. 31:
123-128, 1994.

Bernsen HJJA, Rijken PFJW, Oostendorp T, van der Kogel AJ. Vascularity and perfusion of
human gliomas xenografted in the athymic nude mouse. Br. J. Cancer. 71: 721-726,
1995.

Rijken PFJW, Bernsen HJJA, van der Kogel AJ. Application of an image analysis system for
the quantitationi of the tumor perfusion and vascularity in human glioma xenografts.
Microvascular Res., accepted 1995.

van der Sanden BPJ, Rijken PFJW, Heerschap A, van den Boogert HJ, Bernsen HJJA,
Hagemeier NEM, van der Kogel AJ. In vivo ^{31}P-magnetic resonance spectroscopy and
morphological analyses of the perfused vascular architecture of human glioma
xenografts in nude mice. Cancer Research, submitted for publication, 1995.

Bernsen HJJA, Rijken PFJW, Hagemeier NEM, van der Kogel AJ. Vascularization of
intracerebral and subcutaneously transplanted human glioma xenograft. Submitted to
Cancer Res., 1995.

Bernsen HJJA, Rijken PFJW, Hagemeier NEM, van Mujen G, van der Kogel AJ. The
monoclonal antibody 9F1 as a marker for mouse endothelium : a comlparison with the
marker for vascular basement membrane marker collagen IV for staining the
vasculature of human glioma xenografts. In preparation, 1995.

Overall Conclusion

The achievements of the project are multiple:

i) a contribution to the histopathological correlations with radiation induced
syndromes at the level of muscle, lung and brain tissues, with special emphasis on vascular
lesions   through a reinforced collaboration between neurologists from Paris and
radiobiologists from Nijmegen.

ii) the development of animal models for the evaluation of behavioural and cognitive alterations resulting from acute and chronic irradiation of the central nervous system.

iii) the development of animal models (essentially rodent) for pharmacological and preclinical studies as prerequisite of treament of acute irradiation syndromes in these organs, specially the lungs and the central nervous system.

iv) a clinical evaluation of radiation induced late effects on the cognitive functions after focal cranial irradiation in humans, and preliminary histological and histochemical correlations.

Investigations in all of these domain will continue, mainly oriented towards therapeutical approaches of lung and nervous system lesions.

<div align="center">

Final Report
1992 - 1994

</div>

Contract: F13PCT920064b   **Duration: 1.7.92 to 30.6.95**   **Sector :   B22**

Title: Reduction of risk of late effects from incorporated radionuclides

1)	Stradling	NRPB
2)	Volf	KfK
3)	Poncy	CEA - Bruyères-le-Châtel
4)	Archimbaud	CEA - Pierrelatte (IPSN)
5)	Burgada	ADFAC
6)	Rencova	CHZ

I. Summary of Project Global Objectives and Achievements

The overall aims of this project were to improve the efficacy of treatment for incorporated actinides by the administration of chelating agents and to provide guidance to those involved in the treatment of accidental overexposures.

The chelating agents recommended for enhancing the excretion of plutonium (Pu), americium (Am), thorium (Th) and neptunium (Np) from the human body are the trisodium calcium and -zinc salts of diethylenetriaminepenta-acetic acid (DTPA); the current agent of choice for uranium (U) is sodium bicarbonate. These substances are not completely effective and previous studies by the partners in collaboration with the University of California and Lawrence Berkeley Laboratory had shown that analogues of siderophores, notably the hydroxypyridonate code named 3,4,3-LI(1,2-HOPO) was appreciably more effective than DTPA after the inhalation and intravenous injection of Pu; the ligands were considered equally effective for Am under these conditions. Other, but preliminary, studies carried out under the previous contract indicated that 3,4,3-LI(1,2-HOPO) had an affinity for Th, that the administration of Zn DTPA in drinking water could be an effective method for reducing the body content of Pu and Am after the inhalation of transportable forms, and that certain phosphonic acid derivatives were more effective than bicarbonate for the decorporation of uranium. On the basis of these previous results, the studies carried out under this contract were designed to

-       investigate the comparative efficacies of 3,4,3-LI(1,2-HOPO) and DTPA for Pu and Am after simulated wound contamination as nitrate and the tributylphosphate (TBP) complex (1,2,3,5) and Pu after inhalation as TBP (3,5)

-       investigate the comparative efficacies of 3,4,3-LI(1,2-HOPO) for Th after inhalation and deposition at wound sites (1,5,6)

-       investigate the efficacy of 3,4,3-LI(1,2-HOPO) for the decorporation of uranium (4,5) and neptunium (3,5)

-       examine the toxicity of 3,4,3-LI(1,2-HOPO) (3,5)

-       consider improved methods of synthesis of 3,4,3-LI(1,2-HOPO) (5)

-       validate reports of significant developments with other siderophore analogues, eg. TREN-(Me-3,2-HOPO) (1)

- optimise the efficacy of orally administered DTPA (1,2)

- synthesise and test new phosphonic acid derivatives and other substances for removing uranium from the body (1,4,5)

During the course of the contract, the National Institute of Public Health, Prague (6) became attached to the contract under the PECO Agreement. The studies conducted on the decorporation of polonium (Po) and Th are included in this report.

All the above studies were conducted with rats, other than those on the toxicity of 3,4,3-LI(1,2-HOPO) for which non-human primates were used. The 3,4,3-LI(1,2-HOPO) was synthesised at ADFAC (5); other siderophore analogues were obtained as a gift from the Chemistry Department, University of California, Berkeley. For the studies on uranium decorporation, the phosphonic acid derivatives were synthesised at ADFAC (5) and the calixarenes at IPSN Pierrelatte (4). The diethyldithiocarbamate derivatives used for Po were synthesised at the Chemistry Department, Vanderbilt University, Nashville, Tennessee.

Comparative efficacies of 3,4,3-LI(1,2-HOPO) and DTPA for Pu and Am (NRPB, Kfk, CEA, ADFAC)

Of all the methods of intake investigated, the greatest differences between the efficacies of 3,4,3-LI(1,2HOPO) and DTPA occurred after simulated wound contamination. After an initial muscular deposit of 0.3 ng Pu and 1.6 ng Am (200 Bq each of ^{238}Pu and ^{241}Am) a single local administration of 30 μmol kg^{-1} body mass of 3,4,3-LI(1,2-HOPO) reduced the body contents by 7d to 0.9% and 0.8% respectively of those in untreated controls. The corresponding values after the local administration of 30 μmol kg^{-1} DTPA followed by intraperitoneal (ip) injections of 30 μmol kg^{-1} at 6h, 1d, 2d and 3d were 34 and 27 times higher respectively. The efficacy of 3,4,3-LI(1,2-HOPO) for Pu and Am was reduced when treatment commenced 6h after exposure (both 8% controls) or when the mass of Pu deposited was increased 600 fold (5% controls). However the corresponding values after DTPA administration were still 8 and 10 times higher.

After the intramuscular injection of ^{238}Pu-TBP (10 kBq, 16ng Pu), the local administration of 30 μmol kg^{-1} 3,4,3-LI(1,2-HOPO) reduced the amounts of ^{233}Pu retained in the wound site, skeleton and liver to 75%, 20% and 25% respectively of those in controls. DTPA had only a minimal effect on mobilising ^{238}Pu at the wound site though the skeletal content was reduced to about 60% of control values.

The ligand 3,4,3-LI(1,2-HOPO) has also been shown to be appreciably more effective than DTPA after the inhalation of Pu-TBP. When the initial lung deposit (ILD) was 80 Kbq ^{238}Pu, the amounts retained by the liver and skeleton by 7d after the repeated administration of 30 μmol kg^{-1} (iv 1h, im 24h, 48h) were 1.7% and 7.1% of those in controls; using the same protocol with DTPA the values were 4 times higher. Further studies showed that for an ILD of 7.5 Kbq, 3 μmol kg^{-1} 3,4,3-LI(1,2-HOPO) was as effective as 30 μmol kg-1. DTPA when the ligands were administered repeatedly by iv injection (1h, 1d, 2d). However, this advantage was lost when either the commencement of treatment was delayed for 1d or the ILD was increased 3-fold.

After the intravenous injection of ^{238}Pu and ^{241}Am, 3,4,3-LI(1,2-HOPO) was appreciably more effective than ZnDTPA when the ligands were administered either orally or by subcutaneous infusion. With a single oral administration of 30 μmol kg^{-1} 3,4,3-LI(1,2-HOPO) at 1h, the amounts of ^{238}Pu in the skeleton and liver by 7d were 12% and 6% of those in controls; the values with ZnDTPA were 6 and 7 times higher respectively. The retention of ^{238}Pu in the skeleton and liver after the infusion of 3 μmol kg^{-1} d^{-1} 3,4,3-LI(1,2-HOPO) for 14d, 4% and 2% of controls were 7 and 1.5 times less than when using a dosage of 30 μmol kg^{-1} d^{-1} ZnDTPA. For ^{241}Am the amounts retained in the skeleton and liver after the oral administration of 3,4,3LI(1,2-HOPO), 17% and 5% of controls, were 3 and 10 times less than with ZnDTPA; the amounts after infusion, 9% and 2% of controls, were 2 and 3 times less.

Comparative efficacies of 3,4,3-LI(1,2-HOPO) and DTPA for Th (NRPB, ADFAC, CHZ)

Studies performed under this contract have shown that the administration of DTPA is not an effective method of treatment for Th deposited in the lungs or at simulated wound sites. Whilst considerable improvements in decorporation have been effected with 3,4,3-LI(1,2-HOPO), the differences between the efficacies of the chelates are less than after Pu administration. At a mass concentration of Th in the rat lung simulating human exposure to 750 times the Annual Limit on Intake (ALI) for 228Th, the body content of Th was reduced by 7d to 17% of that in controls by repeated ip injection of 30 μmol kg^{-1} 3,4,3-LI(1,2-HOPO); the value after DTPA administration was 80%. For a simulated exposure to the ALI for [232]Th, the body contents after administration of these ligands were 69% and 91% of controls respectively. These data also demonstrate the effect of the mass of Th on the efficacy of treatment.

The superiority of 3,4,3-LI(1,2-HOPO) over DTPA has also been established after simulated wound contamination. For example, after the im injection of [228]Th, the amounts retained in the body at 7d after local and repeated ip injection of 30 μmol kg^{-1} 3,4,3-LI(1,2-HOPO), 14% controls, were 4 times less than after DTPA administration. A two-fold difference was observed (40% v 80% controls) when treatment was delayed for 1d. After the intramuscular injection of [234]Th, the repeated local administration of 3,4,3-LI(1,2-HOPO) commencing 1h after exposure reduced the skeletal content to 35% controls; under these conditions DTPA was ineffective and DFO-HOPO increased the skeletal content 1-4 fold.

Decorporation of U and Np with 3,4,3-LI(1,2-HOPO) (CEA, IPSN, ADFAC)

The ligand 3,4,3-LI(1,2-HOPO) also has an affinity for U and Np although its efficacy for these metals is substantially less than for the other actinides.

After either the im or iv injection of U, the immediate administration of 30 μmol kg^{-1} 3,4,3-LI(1,2-HOPO) by the same route reduced the kidney and skeletal contents by 1d to about 20% and 50% of those in controls. Under these conditions it was noteworthy that after the administration of 640 μmol kg^{-1} of NaHCO$_3$, the current agent of choice, these values were about 1.5 fold greater. However, 3,4,3-LI(1,2-HOPO) was appreciably less effective when treatment was delayed 30 min. Under these conditions the kidney and skeletal contents were reduced to only 50% and 80% of controls.

Studies have been carried out on the comparative efficacies of 3,4,3-LI(1,2-HOPO) and DTPA after the iv injection of [239]Np(IV) and [237]Np(V). After prompt administration (30 min) 3,4,3-LI(1,2-HOPO) reduced the body contents to 50% of controls by 1d after exposure; DTPA was ineffective. Neither ligand caused a significant reduction in the skeletal content. Supplementary biochemical studies have demonstrated the extreme difficulty of removing Np from the Np-transferrin complex with these ligands although greater success was achieved in the dissociation of its complexes with cytosolic proteins in the liver.

Toxicity of 3,4,3-LI(1,2-HOPO) (CEA, ADFAC)

Preliminary studies have been undertaken on the comparative toxicity of 3,4,3-LI(1,2-HOPO) and DTPA. After the repeated administration of 30 μmol kg^{-1} (iv day 0, ip days 3,6,9,16,20,23,26). For biochemical measurements on blood and urine, the samples were collected up to 180d after exposure. Kidney and liver biopsies were performed 8d and 180d after the termination of treatment. No significant differences were observed when the biochemical and histological data were compared with those for untreated animals. The administration of 3,4,3-LI(1,2-HOPO) to humans must await of course the results of comprehensive toxicity testing. This will require financial support from the nuclear industry.

Synthesis of 3,4,3-LI(1,2-HOPO) (ADFAC)

The synthesis of the substance by the published method is difficult and the chemical yield is low. Alternative methods are being investigated and it is hoped that considerable improvements can be made.

Comparative efficacies of 3,4,3-LI(1,2-HOPO) and other siderophore analogues (NRPB)

During the course of the contract the results of intravenous injection studies undertaken by the Lawrence Berkeley Laboratory in collaboration with the University of California suggested that a new siderophore analogue TREN-Me(3,2-HOPO) was as effective as 3,4,3-LI(1,2-HOPO) for the decorporation of Pu and possibly other actinides. The substance was reported as being easier to synthesise and of lower toxicity in mice than 3,4,3-LI(1,2-HOPO).

Subsequently studies were undertaken by the partners on the comparative efficacy of TREN-(Me-3,2-HOPO), 3,4,3-LI(1,2-HOPO) and another siderophore analogue 5-LI-(Me-3,2-HOPO) after the deposition of Pu, Am and Th in the lungs or at simulated wound sites. In all these cases 3,4,3-LI(1,2-HOPO) was easily the most effective ligand but significantly the other siderophore analogues were more effective than DTPA for ^{238}Pu and ^{241}Am after wound contamination (but not inhalation), and for ^{228}Th after inhalation or wound contamination.

Efficacy of ZnDTPA administered in drinking water (NRPB, Kfk)

In principle, the administration of ZnDTPA in drinking water could be of value for the treatment of inhaled forms of Pu and Am nitrate. In the experimental studies undertaken the masses of Pu and Am deposited in the rat lung simulated acute human exposure to 60 and 7200 times the ALIs for ^{239}Pu and ^{241}Am respectively. Of the various protocols investigated, the optimal effect was achieved with the continuous intake of 95 µmol kg^{-1} d^{-1}. When treatment began 1h after exposure and continued for 21d the amounts of Pu and Am retained in the body by 21d were 8% and 5% of those in controls respectively. When treatment was delayed 7d the corresponding values by 28d were 18% and 20% of controls. This method of administration was as effective as twice-weekly injections of 30 µmol kg^{-1} DTPA. Importantly, no detectable histopathological effects were observed in the liver, kidneys and gastrointestinal tract after oral administration.

Other studies were designed to assess the toxicity of orally administered ZnDTPA and the reduction of bone tumour risk. The ligand was administered to 50 day-old rats at a dosage of 100 µmol kg^{-1} d^{-1} from 4d or 30d after intravenous injection of 37 kBq kg^{-1} ^{239}Pu until death, at about 800d. This near lifetime exposure to ZnDTPA caused no obvious toxicity. After treatment the total number of osteosarcomas was reduced to about one-half of those in untreated animals, and commensurate with the reduction in skeletal content. Survival of the rats was only significantly increased when treatment started early and bone tumours were absent.

Decorporation of uranium with phosphonic acid derivatives and calixarenes (NRPB, IPSN, ADFAC)

Several phosphonic acid derivatives of different structural types and two calixarene derivatives have been evaluated after the administration of uranyl nitrate. Some of the phosphonates, eg. diethylenetriamine-pentamethylene phosphonic (DTPMP) acid and 1,2 diamino cyclohexyl tetramethylene tetraphosphonate (CDTT) were moderately effective after prompt administration of 300 µmol kg^{-1}; by 4d after exposure the kidney and total body contents were reduced to 10% and 30% of those in controls. However, the efficacy of these substances decreased rapidly with the delay in administration and after 30 min were largely ineffective. The calixarene derivatives tested so far have been ineffective and have exhibited toxic symptoms.

Decorporation of polonium (CHZ)

The current agents of choice dimercaptopropanol (BAL) and dimercaptosuccinic acid (DMSA) and dithiocarbamate (DDTC) are only partially effective. Recent studies have investigated the efficacies of bis-dithiocarbamates of which that code named HOETTTC has so far proved to be the most effective.

After the intravenous injection of ^{210}Po, the repeated subcutaneous injection of 0.4 mmol kg^{-1} commencing immediately or 1h after exposure, reduced the body content by 7d to 58% of controls; importantly ^{210}Po did not accumulate in the liver.

After the intramuscular injection of ^{210}Po, the local administration of DMPS at 2h post exposure followed by the repeated subcutaneous injection of HOETTTC reduced the body content to 30% of controls by 14d.

Meetings and Publications

The partners have met every autumn to present the results of the most recent research and discuss future directions of the work. Reports of these meetings have been published in the EULEP Newsletter. In addition, progress has also been reviewed during the course of the EULEP General Assembly in Reisensburg as well as through frequent personal contact.

The contract has generated an appreciable number of research papers which have either been published in the open scientific literature or in the proceedings of various international conferences.

Summary

The objectives of the contract have been fully met. The studies described have advanced our knowledge on the potential of new chelators, notably 3,4,3-LI(1,2-HOPO) for the decorporation of Pu, Am and Th. The work has also drawn attention to some of the limitations of those substances recommended currently and where alternative regimes may be at least as effective. The future use of 3,4,3-LI(1,2-HOPO) in humans will depend on the results of comprehensive toxicity testing and an improved method of synthesis. Some progress has been made on the decorporation of uranium, neptunium and polonium, but more effective regimens are still required.

Head of project 1: Dr. Stradling

II. Objectives for the reporting period

(1)   to investigate the comparative efficacies of 3,4,3-LI(1,2-HOPO) and DTPA for Pu and Am after simulated wound contamination

(2)   to investigate the comparative efficacies of 3,4,3-LI(1,2-HOPO) and DTPA after deposition of Th in the lungs and at simulated wound sites

(3)   to compare the efficacy of 3,4,3-LI(1,2-HOPO) with those of the more recently synthesised siderophore analogues TREN-(Me-3,2-HOPO) and 5-LI-(Me-3,2-HOPO)

(4)   to optimise treatment with orally administered DTPA for removing inhaled Pu and Am from the body after inhalation as nitrate

(5)   to test new phosphonic acid derivatives for the decorporation of uranium.

III. Progress achieved including publications

Decorporation of Pu and Am after simulated wound contamination

A likely route of accidental intake of Pu and Am by workers is from wound contamination. With DTPA as a comparison, 3,4,3-LIHOPO has been examined for its ability to remove ^{238}Pu and ^{241}Am from the rat after the subcutaneous and intramuscular injection of 200 Bq of each actinide (0.3 ng Pu, 1.6 ng Am) administered as nitrate. For the subcutaneous experiments ^{238}Pu and ^{241}Am were injected into the region immediately above the extensor cruris muscle of the hind-leg. Intramuscular injections were at a depth of 5 mm at the centre of the extensor cruris muscle block.

After the subcutaneous injection of ^{238}Pu and ^{241}Am, both ligands were more effective after local administration than after intraperitoneal injection, intravenous injection or continuous infusion using an implanted osmotic pump. Dosages of 3 μmol kg^{-1} of 3,4,3-LIHOPO were more effective than dosages of 30 μmol kg^{-1} DTPA after each mode of administration.

The most effective regimen of those investigated for subcutaneous ^{238}Pu and ^{241}Am involved the local administration of 30 μmol kg^{-1} of 3,4,3-LIHOPO 30 min after exposure followed by intraperitoneal injections of 30 μmol kg^{-1} at 6h, 1, 2 and 3d. By 7d, the amounts of ^{238}Pu and ^{241}Am in the body, ie. wound site and other tissues, were 2% and 7% of those in controls. When DTPA was administered under these conditions, the corresponding values were 20% and 26%.

The ligand 3,4,3-LIHOPO was even more effective for ^{238}Pu and ^{241}Am after their intramuscular injection. After a single local administration of 30 µmol kg^{-1} at 30 min, the amounts retained in the body by 7d were respectively 0.9% and 0.8% of those in controls. The corresponding values after the local and repeated intraperitoneal administration of 30 µmol kg^{-1} DTPA were 32% and 22%. The increased efficacy of 3,4,3-LIHOPO after intramuscular injection was attributed to the greater retention of ^{238}Pu and ^{241}Am at the wound site (98% v 67% of the initial deposit) at the commencement of treatment.

An important consideration is the delay between exposure and treatment. The efficacy of both ligands was reduced appreciably with time although 3,4,3-LIHOPO retained its superiority. For example when repeated treatment with 30 µmol kg^{-1} of 3,4,3-LIHOPO commenced 6h and 1d after the intramuscular injection of ^{238}Pu the amounts retained in the body 7d after exposure were respectively 8% and 19% of those in controls; the corresponding values using DTPA were 66% and 75%. The data for ^{241}Am were similar to those for ^{238}Pu. These results have implications for the treatment of humans with DTPA. If administration is delayed, until, for example, more information on the severity of the accident is available, treatment is likely to be only partially effective.

Another consideration is the effect of mass deposited at the wound site. When the amount of Pu (180 ng as ^{239}Pu) was increased 600 fold the efficacy of treatment decreased. After the local administration of 30 µmol kg^{-1} 3,4,3-LIHOPO at 30 min and intraperitoneal injections at 6h, 1, 2 and 3d after exposure the amounts of ^{239}Pu retained in the body 7d after subcutaneous and intramuscular injection were respectively 7% (cf 2%) and 5% (cf 0.9%) of control values. The corresponding amounts after DTPA administration were 33% and 47%.

The results above show that 3,4,3-LIHOPO represents potentially a most significant advance for the treatment of wounds contaminated by Pu and Am.

Comparative efficacies of siderophore analogues and DTPA for Pu and Am

The hydroxypyridinonates TREN-(Me-3,2-HOPO) and 5-LI-(Me-3,2-HOPO), together with DTPA, were examined for their ability to remove ^{238}Pu and ^{241}Am from the rat after inhalation or simulated wound contamination as nitrates. The data are compared with those obtained previously for 3,4,3-LI(1,2-HOPO).

After the inhalation of ^{238}Pu, the most effective ligand was 3,4,3-LI(1,2-HOPO). By 7d after exposure, the amount retained in the body after the repeated intraperitoneal injection of 30 µmol kg^{-1} at 30 min, 6h, 1d, 2d, 3d, 4.5% of untreated controls, was 5 times lower than with TREN-(Me-3,2-HOPO) and 5-LI-(Me-3,2-HOPO) and 3 times lower than with DTPA. For ^{241}Am, TREN-(Me-3,2-HOPO), 3,4,3-LI(1,2-HOPO) and DTPA were equally effective, the amount in the total body at 7d being 10% of those in controls.

In the subcutaneous injection experiments the most effective ligand for ^{238}Pu was again 3,4,3-LI(1,2-HOPO). By 7d, the body content after the local administration of 30 µmol kg^{-1} at 30 min followed by intraperitoneal injection of 30 µmol kg^{-1} at 6h, 1d, 2d, 3d was 2% of controls. The corresponding values for TREN-(Me-3,2-HOPO) and DTPA were 3.5 and 9 times higher respectively. For ^{241}Am, the efficacies of the three siderophore analogues were similar. The amounts retained in the body at 7d, 8% of controls were appreciably less than after DTPA administration, 20%. Due to its lower solubility, 5-LI-Me-3,2-HOPO could be injected locally at dosages of only 3 µmol kg^{-1}. Nevertheless, the reduction in the body content of ^{238}Pu and ^{241}Am using the regimen above was similar to that found for TREN-(Me-3,2-HOPO).

After the intramuscular injection of ^{238}Pu and ^{241}Am, the amounts retained in the body 7d after the local administration of 30 µmol kg^{-1} 3,4,3-LI(1,2-HOPO), 0.9% of controls, were respectively about 20 and 40 times less than after the administration of TREN-(Me-3,2-HOPO) and DTPA at this dosage.

After the local administration of 3 µmol kg^{-1} 3,4,3-LI(1,2-HOPO) and 5-LI-(Me-3,2-HOPO), the body contents of ^{238}Pu (6% v 10% controls) and ^{241}Am (9% v 7% controls) were similar.

At present, it is concluded that 3,4,3-LI(1,2-HOPO) remains the most effective ligand for the decorporation of Pu and Am. However, the data obtained for the other siderophore analogues are encouraging. Both are appreciably more effective than DTPA for removing these actinides from simulated wound sites. The ligand TREN-(Me-3,2-HOPO) is of such low acute toxicity that the efficacy of treatment should be improved further by the administration of higher dosages. The results obtained for 5-LI-(Me-3,2-HOPO) suggest that other linear hydroxypyridinonates could be prepared which are of similar potency to 3,4,3-LI(1,2-HOPO) yet far easier to synthesise.

Comparative efficacies of siderophore analogues and DTPA for Th

The comparative efficacies of 3,4,3-LI(1,2-HOPO) and DTPA for removing ^{228}Th from the rat were investigated after subcutaneous (sc) and intramuscular (im) injection. The commencement of treatment was delayed 30 min, 6h or 1d and the animals killed at 7d. In all cases 3,4,3-LI(1,2-HOPO) was appreciably more effective than DTPA although the efficacy of treatment and the relative effectiveness of the ligands decreased rapidly with their delay in administration. Optimal removal occurred when initial local administration at 30 min after exposure was followed by repeated ip injection at 6h, 1, 2 and 3d. Under these conditions the body content of ^{228}Th was reduced to 20% of controls after sc injection and 15% after im injection. The corresponding values using repeated DTPA administration were 80% and 54%.

The ligands TREN-(Me-3,2-HOPO), 5-LI-(Me-3,2-HOPO) and 3,4,3-LI(1,2-HOPO) were examined after the inhalation of $^{230+232}$Th as nitrate. The initial lung deposit of Th, 4.2 µg, was equivalent to that which would deposit in the alveolar-interstitial region of the human lung after acute exposure to the ALI for 'natural' Th. In control untreated animals, the amounts of Th in the lungs and total body 7d after exposure were 70% and 78% of the initial deposit. All three ligands were ineffective after a single intraperitoneal injection of 30 µmol kg^{-1} administered 30 min after exposure. By 7d, the amounts of Th in the lungs and total body with TREN-HOPO were 99% and 93% of controls; the corresponding values with LIMe-HOPO were 94% and 91% and with 3,4,3-LIHOPO 93% and 87%. The efficacy of 3,4,3-LIHOPO increased appreciably when the ligand was administered further at 6h, 1, 2 and 3d after exposure. In this case the lung and body contents were reduced to 73% and 69% of controls. The corresponding values after the repeated administration of 30 µmol kg^{-1} DTPA were 93% and 91%. The efficacies of 3,4,3-LIHOPO and DTPA after human equivalent intakes of 1 ALI of natural thorium are considerably less than for intakes of the nanogram level, which simulates exposure to about 10^3 times the ALI for ^{228}Th; in the latter case the body contents could be reduced to 17% and 78% respectively of controls after their repeated administration. These data demonstrate the influence of the mass of Th on the efficacy of treatment.

Studies have also been undertaken on the comparative efficacy of the three hydroxypyridinonates after the subcutaneous and intramuscular injection of Th nitrate (300 Bq ^{228}Th, 10 pg Th). After the subcutaneous injection of Th, the amounts retained at the wound site and in the total body of untreated rats 7d after exposure were 32% and 72% of the initial wound deposit. After the local subcutaneous administration of 30 µmol kg^{-1} TREN-HOPO these amounts were reduced to 14% and 17% of those in controls; the corresponding values after administration of 30 µmol kg^{-1} 3,4,3-LIHOPO were 7% and 14%. The local administration of 3 µmol kg^{-1} LIMeHOPO reduced the amounts retained at the wound site and total body to 31% and 41% of controls. After the intramuscular injection of Th, the amounts retained at the wound site and in the total body 7d after exposure were 46% and 62% of the initial deposit. These amounts were reduced to 26% and 33% respectively of those in controls after the local intramuscular administration of 30 µmol kg^{-1} TREN-HOPO and 7% and 19% when using the same treatment regimen with 3,4,3-LIHOPO. The corresponding values after the administration of 3 µmol kg^{-1} LIME-HOPO were 53% and 63%.

The first wound study above showed that 3,4,3-LIHOPO was substantially more effective than DTPA after subcutaneous and intramuscular injection of Th. The other results reported show that TREN-HOPO is inferior to 3,4,3-LIHOPO for removing Th from the body after simulated wound contamination, but superior than DTPA.

Oral administration of DTPA

The efficacy of ZnDTPA administered in drinking water was examined for removing ^{238}Pu and ^{241}Am from rats after their simultaneous inhalation as nitrates. The amounts of ^{238}Pu and ^{241}Am deposited in the lungs were equivalent to about 60 and 7200 times the mass concentrations calculated to be in the pulmonary region of human lungs after acute exposure to the annual limits on intake for ^{239}Pu and ^{241}Am.

All treatments using ZnDTPA commenced at 1h or 7d after exposure and continued for an interval of 21d using various treatment regimens. The dosages were 3600 μmol kg^{-1} d^{-1} (3 x 10^{-2}M administered every third day), 950 μmol kg^{-1} d^{-1} (10^{-2}M administered continuously or throughout alternate weeks) or 95 μmol kg^{-1} d^{-1} (10^{-3}M administered continuously). ZnDTPA was also administered by repeated intraperitoneal injection at dosages of 30 μmol kg^{-1} body weight.

All oral treatments were equally effective when treatment commenced at 1h. In all cases the amounts of Pu retained in the lungs and total body at 21d were 2% and 8% of controls respectively; the values for Am were 3% and 5%. Treatment was less effective when delayed for 7d, although all oral treatment regimens were again equally effective. In this case the amounts of Pu retained in the lungs and total body at 28d were 6% and 18% of controls respectively; the values for Am were 9% and 20%. Oral treatment proved as effective as the repeated injection of ZnDTPA at dosages of 30 μmol kg^{-1}. With the latter method of administration the total body contents of Pu and Am at 21d were 5% and 3% of controls; the corresponding values at 28d were 25% and 29%.

Histopathological studies on the liver, kidney and three regions of the gastrointestinal tract have indicated that there were no detectable effects on tissue structure. These results are consistent with previous studies undertaken at Kfk Karlsruhe when using the above treatment protocols.

Decorporation of uranium

Recent studies have shown that the stability of polyaminocarboxylate complexes with metal ions was improved when the chelates were sterically rigid. Since phosphonic acid derivatives are known to complex uranium, five analogous substances have been synthesised and their efficacy for decorporation examined in the rat. The substances were:- 1-2 diamino cyclohexyl tetramethylene tetraphosphonate (CDTT); 1-2 diamido cyclohexyl methane tetraphosphonate (CDMT); Benzo cyclopentene bisphosphonate (BCPBP); 1-2 phenylene dicarboxy diamido methane tetraphosphonate (DDMT); and 1-2 diamido cyclohexyl ethane tetraphosphonate (CDET).

In a preliminary screening experiment, uranium, as uranyl nitrate (300 Bq ^{233}U, 10 μg U) was administered by intraperitoneal injection and the phosphonic acid derivatives (300 μmol kg^{-1} body wt) at pH7 by the same route immediately afterwards.

The most effective substance was CDTT. By 4d after exposure, the uranium contents of the kidneys and total body were 0.88% and 10.3% respectively of that injected; the corresponding values for untreated rats were 9.2% and 28.8%. These values were similar to those obtained after the administration of dipropylenetriaminepentamethylenephosphonic (DTPMP) acid, examined previously. The uranium contents of the kidneys and total body after the administration of CDMT were 5.8% and 35.9% of the amounts injected; the corresponding values for BCPBP were 2.3% and 17.1% and for DDMT 3.3% and 18.8%. The administration of CDMT, BCPBP and DDMT resulted in enhanced retention of uranium in the liver, respectively 9.7%, 4.0% and 2.3% of the amount injected compared

with 0.25% in controls. The administration of CDET at 300 µmol kg^{-1} resulted in toxicological symptoms and its efficacy at this dosage was not investigated further.

At the lower dosage of 30 µmol kg^{-1}, CDTT and two other derivatives, cyclohexylamino-methylenebisphosphonic (CABP) and tetra-amino (tris ethyl) hexamethylenephosphonic acid (TTHP) were only partially effective and not considered further.

It is concluded that the development of more effective substances for removing uranium from the body remains an important requirement for radiological protection of the worker.

Publications

Stradling, G N, Gray, S A, Ellender, M, Pearce, M, Wilson, I, Moody, J C and Hodgson, A. Removal of inhaled plutonium and americium from the rat by administration of ZnDTPA in drinking water. Human Exp. Toxicol. 12 233-239 (1993).

Stradling, G N, Gray, S A, Moody, J C, Pearce, M J, Wilson, I, Burgada, R, Leroux, Y G P, Raymond, K N and Durbin, P W. The efficacies of 3,4,3-LIHOPO and DTPA for enhancing the excretion of plutonium and americium from the rat after simulated wound contamination as nitrates. Int. J. Radiat. Biol. 64 134-140 (1993).

Stradling, G N, Gray, S A, Moody, J C, Wilson, I, Pearce, M J, Burgada, R and Raymond, K N. Comparative efficacy of 3,4,3-LIHOPO and DTPA for plutonium (IV) and americium (III) after simulated wound contamination. In Proc. Symp. on Chelating Agents in Pharmacology, Toxicology and Therapeutics, pp55-57. Plzen Medical Report Supplement 68/1993.

Stradling, G N. Recent progress in the decorporation of plutonium, americium and thorium. Radiat. Prot. Dosim. 53 297-304 (1994).

Gray, S A, Stradling, G N, Pearce, M J, Wilson, I, Moody, J C, Burgada, R, Durbin, P W and Raymond, K N. Removal of plutonium and americium from the rat using 3,4,3-LIHOPO and DTPA after simulated wound contamination: effect of delayed administration and mass of plutonium. Radiat. Prot. Dosim. 53 319-322 (1994).

Stradling, G N, Gray, S A, Pearce, M J, Wilson, I, Moody, J C, Burgada, R, Durbin, P W and Raymond, K N. Decorporation of Th-228 from the rat by 3,4,3-LIHOPO and DTPA after simulated wound contamination. Hum. Exp. Toxicol. 14 165-169 (1995).

Stradling, G N (Ed). Task Group Report on Reduction of Risk of Late Effects from Incorporated Radionuclides. EULEP Newsletter 72 3-18 (1993).

Stradling, G N (Ed). CEC Association Agreement. Reduction of Risk of Late Effects from Incorporated Radionuclides. EULEP Newsletter 75 35-45 (1994).

Stradling, G N (Ed). Task Group Report on Evaluation of New Chelators. EULEP Newsletter 78 12-14 (1994).

Stradling, G N (Ed). CEC Association Agreement. Reduction of Risk of Late Effects from Incorporated Radionuclides. EULEP Newsletter 79 10-22 (1995).

Stradling, G N, Gray, S A, Pearce, M J, Wilson, I, Moody, J C and Hodgson, A. Efficacy of TREN-(Me-3,2-HOPO), 5-LI-(Me-3,2-HOPO) and DTPA for removing plutonium and americium from the rat after inhalation and wound contamination as nitrates: comparison with 3,4,3-LI(1,2-HOPO). NRPB Memorandum M-534 (1995).

Gray, S A, Pearce, M J, Stradling, G N, Wilson, I, Hodgson, A and Isaacs, K R. Optimising the removal of inhaled plutonium and americium from the rat by administration of ZnDTPA in drinking water. Hum. Expt. Toxicol. (in press).

Stradling, G N. Decorporation of plutonium, americium and thorium; a review of recent progress. In proc. 5th International Conference on Oral Chelation, Milan, Nov. 12th-13th 1993. Eds. K. Kontoghiorghes and V. Carnelli. Medical and Surgical Paediatrics (in press).

Stradling, G N. Reduction of risk of late effects from incorporated radionuclides. Annual Report to the CEC for the period September 1993-July 1994 (in press).

Bhattacharyya, M H, Breitenstein, B D, Metivier, H, Muggenburg, B A, Stradling, G N and Volf, V. Traitement de la Contamination Interne Accidentelle des Travailleurs. Eds. G.B. Gerber and R.G. Thomas. IPSN: Fontenay aux Roses, 1995.

Stradling, G N (Ed.) CEC Association Agreement: Reduction of Risk of Late Effects from Incorporated Radionuclides. EULEP Newsletter (in press).

Head of project 2: Prof. Volf

II. Objectives for the reporting period

(1)   To investigate the comparative efficacies of 3,4,3-LIHOPO, DFO-HOPO, DTPA-DX, DTPA and DFOA for Pu and Am after intravenous injection.

(2)   To investigate dose- and time-effect relationships of treatment with 3,4,3-LIHOPO and DFO-HOPO after intravenous injection of Pu and Am.

(3)   To investigate local and systemic chelation treatment of simulated wounds contaminated with Pu, Am and Th.

(4)   To reduce the risk due to incorporated Pu-239 by oral DTPA.

III. Progress achieved including publications
Decorporation of Pu and Am early after intravenous injection

The effectiveness of early single chelate injections (30 μmol kg^{-1} at 1h) on Pu-238 retention in tissues decreased in the order 3,4,3-LIHOPO > DFO-HOPO > DTPA > DTPA-DX and for Am-241 in the order 3,4,3-LIHOPO > DTPA-DX > DTPA >> DFO-HOPO. LIHOPO decreased the contents of Pu in bone and liver to 9% and 3% respectively of those in untreated controls. Corresponding values for Am-241 in bone and liver were 30% and 6% respectively. With both chelators a similar effect on Pu was achieved by prompt single oral treatment and by a single injection delayed for an hour, provided the oral dose exceeded about 3 times that given as injection. When LIHOPO was administered by continuous infusion, a superior effect was achieved with total chelate amount only slightly exceeding that given as single injection. The retention of Pu and Am was reduced to <5% and 10% of controls, respectively; the contents in the liver were <2% of controls.

Dose- and time-effect relationships with 3,4,3-LIHOPO and DFO-HOPO

At the lower dose-level, both after injection or oral chelate administration, the effect of LIHOPO on retention of Pu exceeds that of DFO-HOPO. With higher doses of both chelators a similar effect on Pu can be achieved. Whilst DFO-HOPO does not affect Am retention, a substantial reduction in Am retention can be achieved by LIHOPO. When comparing the relative removal effectiveness of injected LIHOPO on the two actinides, it is more pronounced with Pu, especially in

the bones and after low chelator doses. Orally administered low doses of LIHOPO, however, mobilize more Am than Pu, both from the liver and bone.

The effectiveness of a single injection of 30 μmol kg^{-1} LIHOPO decreases with increasing time after Pu administration, much more slowly than that of the same dose of DFO-HOPO. With DFO-HOPO the calculated half times for the mobilized fraction of Pu from bone and liver are 5h and 12h, respectively. The removal effect of LIHOPO on Pu decreases from the 3rd day in liver and kidneys with a half-time of 29d and 23d, respectively, and in the bones there is no loss of LIHOPO efficiency up to 10d post Pu injection. The removal effect of LIHOPO on Am in soft tissues decreases with time similar to that for Pu; in the bones, however, at 10d virtually no Am can be removed by a single LIHOPO injection.

Decorporation of Pu, Am and Th after simulated wound contamination

Contaminated wounds were simulated by intramuscular injections of actinides in 0.3M nitric acid into musculus quadriceps femoris. In a short-term experiment, the effect of Pu-mass on efficiency of LIHOPO was investigated. After injection of equal activities of Pu-238 and Pu-239 less of the latter was removed, obviously because its mass was about 300 times greater than that of Pu-238 and correspondingly the molar ratio of LIHOPO to Pu-239 much less favourable for chelation. Surprisingly, Am-241 which was injected simultaneously with Pu-239 was also less mobilized from the injection site than was Am-241 injected with Pu-238.

A simulated delayed protracted treatment of activity partly deposited in a contaminated wound and partly in the tissues was initiated at 4d or 30d after single injection of actinides; organ retention of activity was reduced to about 20% and 60% of control values, respectively. Whole body counting of Am-241 indicated that a substantial fraction can be removed, even if treatment started as late as 30d after injection of Am.

Two pilot experiments on treatment after wound contamination with Th-234 indicate that under identical conditions LIHOPO is more effective than any other chelator tested. However, effectiveness of this chelator with Th is less than previously observed with Pu and Am.

Detoxication of Pu-239 by oral DTPA

In the life-time experiment on reduction of bone tumour risk in rats after a single intravenous injection of 37 kBq kg^{-1} Pu-239, the chelator Zn-DTPA was added to drinking water at 10^{-3}M concentration, starting at 4d or 30d post Pu.

At present, histopathological data on osteosarcoma incidences are available. They indicate that after treatment the total number of osteosarcomas was reduced to about one half of that in untreated rats, irrespective of the delay in treatment. It thus seems possible to remove Pu from critical cell populations even if treatment is delayed. Indeed, evaluation of microautoradiographs of undecalcified bone sections indicate that radiation dose-rates in the 0-10 μm endosteal layer were substantially reduced (to less than 50% of those in untreated rats) both after early and delayed DTPA treatment).

On the other hand, survival of rats could be significantly increased only when treatment started early and only in animals without bone tumours. This indicates that it is also necessary to evaluate other reasons of death, including incidence of soft tissue tumours. This work is underway.

Publications

Volf, V, Burgada, R, Raymond, KN, Durbin, PW. Early chelation therapy for injected Pu-238 and Am-241 in the rat: comparison of 3,4,3-LIHOPO, DFO-HOPO, DTPA-DX, DTPA and DFOA. Int. J. Radiat. Biol. 63, 785-793 (1993).

Volf, V, Burgada, R, Rencova, J, Raymond, KN, Durbin, PW. Decorporation of Pu-238, Am-241 and Th-234 from rats by 3,4,3-LIHOPO. EULEP Newsletter 75, 40 (1994).

Volf, V, Luz, A, Sontag, W. Update on study on detoxification of Pu-239 in rat by oral DTPA. EULEP Newsletter 75, 37 (1994).

Head of project 3: Dr. Poncy, Dr. Paquet

II. Objectives for the reporting period

(1)   to investigate the comparative efficacies of 3,4,3-LI(1,2-HOPO) and DTPA for Pu-TBP after simulated wound contamination.

(2)   to investigate the comparative efficacies of 3,4,3-LI(1,2-HOPO) and DTPA after inhalation of Pu-TBP

(3)   to optimise treatment with LIHOPO after inhalation of ^{238}Pu as Pu-TBP complex

(4)   to investigate the efficacy of 3,4,3-LI(1,2-HOPO) for the decorporation of Np

(5)   to examine the toxicity of 3,4,3-LI(1,2-HOPO).

III. Progress achieved including publications

(1)   **The efficacy of 3,4,3-LI(1,2-HOPO) for enhancing the excretion of plutonium from the rat after simulated wound contamination as the tributyl-n-phosphate complex.**

Solvent extraction processing of plutonium in the nuclear industry is dominated by the Purex process which employs a solution of tributyl-n-phosphate (TBP) as extractant and HNO_3 as salting agent. The metabolism of plutonium, introduced into rats as the Pu-TBP complex, has been studied but no effective treatment for decorporation of the compound is currently available. The siderophore analogue 3,4,3-LI(1,2-HOPO) - referred to hereafter as LIHOPO - has been examined here for its ability to remove ^{238}Pu from rats after i.m. or s.c. contamination as the tributyl-n-phosphate (TBP) complex. 80 ng Pu kg^{-1} body mass were injected in rats and the chelating agents were administered 30 min after the contamination, at a dosage of 30 μmol kg^{-1}, either by i.v. or local injection. After i.m. contamination, LIHOPO was significantly superior to DTPA in removing translocated ^{238}Pu. Local (i.m.) administration of 30 μmol kg^{-1} of LIHOPO reduced the amounts of Pu in the skeleton, liver and kidneys to 20%, 25% and 45% respectively, of those in untreated animals, and lead to a reduction of the total translocated Pu by a factor 4.5. By contrast, DTPA had little action on the removal of Pu from these organs (65%, 85%, and 100% of the controls, respectively) and reduced the translocated ^{238}Pu by a factor 1.4. Similar results were obtained after i.v. injection of both ligands. After treatment with LIHOPO, ^{238}Pu was excreted predominantly in the faeces (14-18 times more than in untreated animals), whilst after DTPA administration, a large fraction of ^{238}Pu was eliminated via

the urine (13-18 times more than in control animals).

LIHOPO was more effective than DTPA in removing both translocated and wound ^{238}Pu, after s.c. contamination. It removed 55-65% of the total translocated ^{238}Pu, whereas DTPA removed at best 10-15%. The main effects were observed on the skeletal and the liver contents of the treated animal (35-40% and 20-40%, respectively, of the controls). At the wound site, LIHOPO removed 35-40% of the deposited ^{238}Pu while DTPA had no significant action (8-15% of deposited Pu). No significant difference was observed after local or i.v. injection of the ligands, neither on the translocated nor on the wound Pu. ^{238}Pu excretion was increased twice as much by LIHOPO than by DTPA. After LIHOPO administration, fifty percent of the injected ^{238}Pu was excreted by 7 d, whereas 12% was excreted by the untreated animals. With LIHOPO as treatment, the main route of excretion was fecal, whilst DTPA increased the urine excretion of ^{238}Pu by a factor 10.

For each experimental treatment, the results demonstrated that LIHOPO was more effective than DTPA in removing the whole body Pu. This was true for both routes of administration of Pu (i.m. or s.c.) and of the ligand (local or systemic injection). LIHOPO was significantly superior to DTPA for preventing organ deposition of the translocated Pu, and was equivalent or more efficient than DTPA in mobilizing Pu from the wound site.

(2) **Efficacy of LIHOPO for reducing the retention of ^{238}Pu in rat after inhalation of the tributyl phosphate complex.**

After inhalation of Pu-TBP, DTPA was demonstrated to be ineffective for enhancing the ^{238}Pu excretion. Nevertheless, the efficiency of the ligand depends both on the mass of radionuclide inhaled and on the dosage of the ligand. In this study we have compared the efficacy of DTPA and LIHOPO after inhalation of different masses of Pu-TBP and after different kinds of treatment regimens, which correspond to early, single or repeated injections and also delayed injection.

In four different exposures, the mean lung activities in the untreated animals were 869 ± 74 Bq (1.3 ng Pu); 4500 ± 800 Bq (6.7 ng Pu); 15 ± 2 kBq (22.4 ng Pu) and 37 ± 3 kBq (55.3 ng Pu) respectively. The first two groups correspond to a low or moderate level of internal contamination, the last two to a high level. The two chelating agents were injected at dosages of 30 μmol kg^{-1} body-weight. Three different treatment schedules for both chelators were used: (1) single: one i.v. injection, 1 h after exposure; (2) repeated: one i.v. injection 1 h after exposure, followed by two i.m. injections, respectively, 1 and 2 days later; (3) delayed: one i.p. injection 1 day after exposure.

The LIHOPO was shown to be more effective than DTPA for increasing the elimination of ^{238}Pu from the lungs and reducing the amounts deposited in the organs 7 days after exposure. At the lowest lung content (969 Bq) one i.v. injection of LIHOPO at 1 h after inhalation reduced the amount of Pu in liver and skeleton, by 7 days, to 6.0 and 11.7 %, respectively, of those in untreated rats. At the highest lung content (37 kBq), the corresponding value for lung, liver and skeleton were 57.4, 8.2 and 17.8 % respectively. In this case, lung retention was significantly reduced with LIHOPO, compared to DTPA treatment. With repeated treatment, the Pu content of the lung and other organs at 7 days were reduced appreciably by LIHOPO. For the lowest lung content, the ratio of lung activity in controls to lung activity in treated rat was 4.2 after repeated LIHOPO treatment compared with 2.7 for DTPA. The corresponding values were 2 and 1.6, respectively, for the highest lung deposit. After delayed treatment, the Pu contents in all measured organs were reduced less than after early treatment. In this case, 3,4,3-LIHOPO and DTPA were considered to be equally effective.

In conclusions, LIHOPO was more effective than DTPA after inhalation of PuTBP complex

(3) **Optimisation of treatment with LIHOPO**

In that case, lower amounts of LIHOPO (31 μmol kg^{-1}) were administered to rats, and the

efficacy of the ligand was assessed after both prompt and delayed treatment. The animals were contaminated by inhalation of an aerosol of ^{238}Pu-TBP. The initial lung deposit of ^{238}Pu were 7.5 kBq ± 1.1 kBq (11.7 ng Pu) or 25 kBq ± 2.8 kBq (39 ng Pu). In both cases, the duration of exposure was 60 min. Four groups of rats were used in each experiment (7.5 or 25 kBq of initial lung deposit of Pu-TBP): group 1: 4 rats exposed to Pu-TBP as untreated controls group 2: 8 rats exposed to Pu-TBP and treated with 3,4,3-LIHOPO at a dosage of 3 µmol kg^{-1} group 3: 8 rats exposed to Pu-TBP and treated with CaNa$_3$-DTPA at a dosage of 3 µmol kg^{-1} group 4: 8 rats exposed to Pu-TBP and treated with CaNa3-DTPA at a dosage of 30 µmol kg^{-1}. Then, groups 2,3 and 4 were divided into two groups each:

a)   **prompt and delayed treatment:** four rats were treated by one intravenous injection 1 h after contamination, followed by two intraperitoneal injection 1 and 2 d later

b)   **delayed treatment only:** four rats were treated by one intravenous injection 1 d after contamination, followed by two intraperitoneal injection 1 and 2 d later.

The values of total body content, expressed as percentage of controls at 7 d, show the efficacy of the 3 regimens employed. It is evident from the data that 3 mol.kg-1 of 3,4,3-LIHOPO were effective for increasing the elimination of the Pu inhaled. Nevertheless, the ligand seemed to be more effective for the lower lung Pu deposit (about 7.5 kBq) than with high concentrations. Seven days after inhalation, the total body content was about 30 to 60% less than that observed in untreated animals. The best results were obtained with prompt administration of 3,4,3-LIHOPO (1 h after contamination). Under those conditions, the body content was reduced to one third of that in untreated rats. At the lower lung deposit, the efficacy of 3 µmol.kg^{-1} of 3,4,3-LIHOPO was comparable to that of DTPA used at a dosage of 30 µmol kg^{-1}. However, when lung deposit was higher (25 kBq), DTPA was more effective. The significance of these observations remains unknown, since it is possible that the composition of the aerosol (excess of TBP and solvent) affect the ability of the ligand to approach and complex the Pu, more than the amount of the radionuclide, when only nanograms are present.

Each organ was affected by the decorporation processes. Treatment with 3,4,3 LIHOPO was more effective when animals were treated soon after contamination, especially for low lung deposit. The time interval before ligand injection was more important for 3,4,3-LIHOPO than for DTPA whatever the mass of plutonium deposited in the lungs. When the treatment was administered 1 d after contamination, the DTPA may have been somewhat effective although none of the differences were statistically significant. At lower lung deposit, plutonium retention was equivalent for the liver and lower for the skeleton and the kidneys after LIHOPO than after DTPA injected at low or high dosage. With high lung contamination, the efficiency of 3,4,3-LIHOPO was higher than DTPA 30 µmol kg^{-1} for the kidneys but was lower for lungs and skeleton. This observation confirms the efficiency of LIHOPO to decrease retention in the kidneys whatever was the initial lung deposit.

The results show that 3 µmol kg^{-1} of 3,4,3-LIHOPO can remove appreciable amounts of Pu from the body when inhaled as a tri-N-butylphosphate complex. The ligand was more effective than DTPA at the lower lung deposit of Pu. The reverse was observed at the higher lung content of Pu. The importance of a prompt treatment after contamination has been emphasised. We have previously demonstrated the importance of a repeated treatment. This study shows that rapid intervention could be important too.

(4)   **The efficacy of LIHOPO for enhancing the Np decorporation**

The efficacy of 3,4,3-LIHOPO and CaDTPA has been tested for removing neptunium in rat after systemic administration. Two methods were used, corresponding to investigations at either whole

organism or molecular level. In a first step, six rats were contaminated by intravenous injections with either 3.3 pg of ^{239}Np (IV) or 39 µg of ^{237}Np (V). These two isotopes were chosen because of the discrepancy in their abilities to complex with chelators. The two ligands 3,4,3-LIHOPO and CaDTPA were administered at a dosage of 30 µmol.kg^{-1} by i.v. injection 30 mn after the end of the contamination and the animals were sacrificed 24 h later. The results showed the inefficacy of the DTPA to remove the neptunium from the body whatever the isotope used. The 3,4,3-LIHOPO seemed to be more effective. We observed a reduction of the hepatic burden (54%) and of the skeletal burden (50%) after injection of ^{239}Np (IV) and ^{237}Np (V) respectively.

In order to understand the mechanisms involved in the neptunium decorporation, an attempt was made to identify the blood protein responsible for the radionuclide binding. Rats were injected intravenously with 3.3 pg of ^{239}Np (IV) or ^{239}Np (V) and blood was collected 30 mn after. The serum was separated and subjected to gel permeation and ion exchange chromatography. In these conditions, 98% and 91% of ^{239}Np (IV) and ^{239}Np (V) respectively were bound to blood transferrin, the iron binding protein. These results suggest that the injected Np (V) was reduced to Np (IV) at the physiological pH, since Np (V) has no affinity for any biological ligand.

The action of the two chelators, DTPA and 3,4,3-LIHOPO, on the dissociation of the complex neptunium-transferrin was then tested *in vitro,* by means of gel permeation chromatography and protein precipitations. In these conditions it was shown that DTPA was unable to remove neptunium from transferrin, even when used at high concentrations (40 mmol kg^{-1}). The action of 3,4,3-LIHOPO was better but remained limited since 5 mmol kg^{-1} were required to removed 45% of the neptunium bound to transferrin. The usual therapeutic dosage (i.e. 30 µmol kg^{-1}) removed less than 10% of the neptunium and seemed to be ineffective for the decorporation of the systemic compartment. The strength of the complex Np-Tf seemed to change depending on the initial valency state of the radionuclide injected. This resulted in a higher efficacy of both 3,4,3-LIHOPO and DTPA for removing neptunium when injected as Np(V), but without statistically significant difference.

Regarding the inefficacy of the ligands to dissociate the complex Np-Tf, an attempt was made to study the binding of the radionuclide with the cytosolic proteins of the hepatocytes. After contamination, the liver was homogenized and the soluble proteins were extracted after centrifugation (100,000 g, 45 mn) and gel permeation chromatography. The neptunium coeluted with three class of proteins, with molecular weights of 20, 130 and 450 kd respectively. A preliminary study showed that DTPA and 3,4,3-LIHOPO seemed to be more effective to remove Np from the cytosolic proteins than from the transferrin.

All the results showed that DTPA and 3,4,3-LIHOPO were few or not effective to remove neptunium after systemic contamination. This imply to undertake further investigations with new chelators and to focus specific attention on the speciation of the radionuclide in the organic matrix.

(5) Toxicity of LIHOPO

The potential toxicity of 3,4,3-LIHOPO was investigated in baboons with:

1)   clinical laboratory measurements used for humans

2)   observations of histological changes in biopsies of baboon kidneys and livers.

Table: Characteristics of baboons (Papio papio) used in this study

No. monkey (sex)	Date of birth	Treatment	Weight 3.6.92
1st experiment: Treatment June/July 1992			
523 (f)	22.7.88	control	4.6 kg
529 (m)	11.8.89	control	5.6 kg
534 (m)	26.7.90	control	3.7 kg
530 (m)	8.10.89	DTPA (30µmol./kg)	4.8 kg
531 (m)	20.12.89	DTPA (30µmol./kg)	4.7 kg
535 (m)	25.10.90	LIHOPO (30µmol./kg)	3.1 kg
2nd experiment: Treatment April/May 1993			**27.04.93**
529 (m)	11.8.89	DTPA (30µmol./kg)	8.3 kg
534 (m)	26.7.90	LIHOPO (3µmol./kg)	5.8 kg
536 (m)	4.3.91	LIHOPO (30µmol./kg)	3.6 kg

Chelating agents were injected at dosages of 30 or 3µmol kg^{-1}, intravenously on day 0 and intramusculary on days 3,6,9,13,16,20,23, and 26. Urines and blood samples have been collected just before, at the end and 6 months after the end of chelate treatments. Parameters which have been analysed, were in serum: glucose, nitrogen compounds, electrolytes, enzymes, total proteins and lipids, in urine: diuresis, glucose, nitrogen compounds and electrolytes. The different biochemical parameters observed early and latter after the end of 3,4,3-LIHOPO treatment did not shown significant changes which might traduce kidney and hepatic disturbances.

Biopsies of liver and kidneys were performed on each animal one week after the end of chelate administrations and others 6 months latter. Observations in light microscopy on semi-thin sections did not shown significant structure alterations in hepatic and renal tissues from treated animals by either 3,4,3-LIHOPO or DTPA. Only few vacuoles were observed in hepatic cells after LIHOPO administration. The electron microscopy study confirm the minor toxicity of 3,4,3-LIHOPO just after treatment which does not inhibit the recovery of the cells.

General conclusions:

It is evident from the studies described above that LIHOPO is the most effective compound for the decorporation of Pu yet tested. It is efficient for the different routes of administration tested and the mass of radionuclide administered. For these reasons it could be considered that LIHOPO will replace DTPA in the future, for some specific decorporation purposes. This means that future work should assess its toxicity on animals, define optimum therapeutic regimen in humans and find a new - and easier - way of synthesis, which is at present difficult. By contrast, LIHOPO was not efficient in removing neptunium after contamination and a special attention have to be given to this radionuclide.

Publications:

PONCY J.L.; RATEAU G., BURGADA R., BAILLY T., LEROUX Y., RAYMOND K.N., DURBIN P.W. and MASSE R., 1993, Efficacy of 3,4,3-LIHOPO for reducing the retention of ^{238}Pu in rat after inhalation of the tributyl phosphate complex. Int. J. Radiat. Biol., 64 (4): 431-436.

FRITSCH P., PAQUET F., LANTENOIS G., HOFFSCHIR D., PONCY J.L., 1993: Comparative toxicity of 3,4,3-LIHOPO and DTPA in baboons. Eulep Newsletter. 72: 7-8.

PAQUET F., PONCY J.L., FRITSCH P. MASSE R., 1994: Decorporation of plutonium-TBP in rats after 3,4,3-LIHOPO treatment. Eulep Newsletter, 75: 3940.

PAQUET F., PONCY J.L., RATEAU G., BURGADA R., BAILLY T., LEROUX Y., RAYMOND K.N., DURBIN P.W., MASSE R., 1994: Reduction of the retention of ^{238}Pu inhaled as the tributylphosphate complex in rats treated by 3,4,3-LIHOPO. Radiat. Protect. Dos., 53 (1-4): 323-326.

PAQUET F., PONCY J.L., METIVIER H., MASSE R., 1995. Neptunium decorporation: a new approach combining both *in vivo* and *in vitro* studies. EULEP News. 79 :16.

PAQUET F., GRILLON G., RATEAU G., PONCY J.L., FRITSCH P., BURGADA R., BAILLY T., RAYMOND K.N., DURBIN P.W., 1995. The efficacy of 3,4,3LIHOPO for enhancing the excretion of plutonium from the rat after simulating wound contamination as the tri-n-butyl phosphate complex. Internat. J. Radiat. Biol. (submitted).

PAQUET F., PONCY J.L., METIVIER H., 1995. The efficacy of 3,4,3-Li(1,2 HOPO) for enhancing the excretion of Pu-TBP from the rat after wound contamination. Eulep News.

PAQUET F., PONCY J.L., RAMOUNET B., METIVIER H., 1995. The effect of DTPA on the systemic and bone fraction of neptunium. Eulep News.

Head of project 4: Dr. Archimbaud

II. Objectives for the reporting period

The objectives of the reporting period were:

- to find a molecule for preventing the deposit of uranium in the body, and more specifically in the bones, and for enhancing its excretion after accidental contamination,

- to propose a methodology in order to characterise the more efficient decorporating molecule.

The tested molecules have been synthesized at the Laboratoire de Chimie des Organoéléments, Université Pierre et Marie Curie, Paris, in the laboratory of R.Burgada excepted the Calixarenes and the tripodes which have been synthetized in our laboratory in Pierrrelatte.

III. Progress achieved including publications

Experimental methods

Chemical studies

Synthesis of the Calixarenes
Sulfonate calix[6]arene (S6) and Sulfonate calix[8]arene (S8) were synthesized in the laboratory, and the purity of the synthesized molecules was controlled with R.M.N. and microanalysis.

Synthesis of Tripodes
Two tripodes have been synthetised in the laboratory of Pierrelatte: the tris(2-carboxyethyl)phosphine oxyde (1), and the tris(ethoxyethylphosphonic acid)nitril ammonium (2).

(1) $O = P(CH_2CH_2COOH)_3$

(2) $HN (CH_2CH_2OCH_2CH_2COOH)_3$
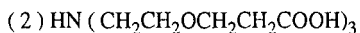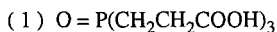
Stoechiometric studies
The stoechiometry of the chelate and the chelating constant of uranyl-ligand were determined using the displacement method and Job diagrams. On JOB diagrams, the maximum absorbance was found at a ratio equal to 0.5 and 0.66 for S6 and S8 respectively. The stochiometry of 1 uranyl ion chelated by 1 S6, and 2 uranyl ions chelated by 1 S8 was derived from these diagrams. The chelating constants were found equal to $(1.8\pm0.1)\times10^{19}$ and $(7.0\pm0.9)\times10^{40}$ respectively. The stability of the chelates as a function of pH was determined showing that S8 in particular forms a stable chelate at biological pH.

Biological studies

Products :
  a) Phosphonates:
  Three phosphonates molecules were screened *in vivo* :
  Trimethane Phosphonic Acid (T.P.A.),
  Ethylene Diamine Tetramethane Phosphonic Acid (E.D.T.P.)
  Cyclohexane Diamine Tetramethane Phosphonic Acid (C.D.T.P.A.).
  Solutions $4\ 10^{-4}$ M were prepared in saline with $CaCl_2$ (pH 7.2)
  b) Tripodes:
  The compound (1) has been tested *in vivo*. A solution $2\ 10^{-4}$ M was prepared in saline (pH 7.2).
  c) Calixarenes:
  Calixarene S6 and S8 have been tested *in vivo*. Solutions $0.1\ 10^{-4}$ M. were prepared in saline (pH 7.2).
  d) 3,4,3-LIHOPO:
  The 3,4,3-LIHOPO, is more correctly nammed 3,4,3-LI(1,2-HOPO). Solutions of 3,4,3-LIHOPO (12mM) were prepared in $0.14\ mol.l^{-1}$ NaCl (pH 7.2) ; The animals were injected with 3 or 30 $\mu mol.kg^{-1}$.
  e) Sodium bicarbonate
  Solution of sodium bicarbonate (1.33 %) was prepared in distilled water ;

Uranium
Stock solution of uranyl nitrate was prepared in saline (1,5 μM). The concentration of the solution was measured by fluorimetric assay . The injected solution was prepared extemporaneously such that 1 ml contained a dose of 0.84 $\mu mol.kg^{-1}$ (pH = 5).

Animals
Male Sprague Dawley rats Ico OFA-SD (IOPS-Caw) weighing about 250 g were housed individually in metabolism cages one week before the administration of uranium and the following 24 or 48 hours for collection of urine and faeces. Food and water was available ad libitum. All procedures involving the rats were carried out in accordance with the Animals (Scientific Procedures) Act 1986.

Administration of uranium and chelating treatment
Groups of five animals were each injected with uranium and then treated either with saline (controls), or sodium bicarbonate (640 $\mu mol.kg^{-1}$) or the compound to test.

Three different regimens were tested :
  i) uranium was injected intramuscularly in the right hind leg and the substances administered locally 5 minutes later; (for 3,4,3-LIHOPO and the tripode molecule)
  ii) uranium was injected intravenously into the saphenous vein and the substance (3,4,3-LIHOPO) administered immediately afterwards by the same route, the animals being previously anaesthetised with sodium pentobarbital (40 mg.kg^{-1}) (Sanofi).
  iii) uranium was injected intramuscularly and the substances administered intraperitoneally 30 minutes later ;(all compounds)

Samples
Twenty four hours after treatment, animals were killed by injection of a lethal dose of sodium pentobarbital (500 mg.kg^{-1}). The uranium content of urine, faeces, kidneys and femora was measured by fluorimetric assay.

Toxicity studies
In order to test the toxicity of calixarenes S6 and S8, the agents were injected intra-peritoneally. The weight of the animals and their blood parameters were controlled systematically during up to 35 days. The chelating agents were injected peritoneally with variable concentrations half an hour after intoxication.. For each chelating molecule and concentration, a control batch and a batch of animals injected with the decorporant were killed 6, 24 and 48 hours after intoxication. For each animal, uranium weight was analysed by fluorimetry in the kidney, the skull-bone and the urines.

Metabolism studies
In order to explain the toxicity of the Calixarene, a ^{14}C labelled compound has been synthetized in the laboratory and administered to Sprague Dawley rats. 10 animals were intraperitonealy injected with a solution of parasulfonic-calix[8]arene (6.1 10^2 mBq). Pairs of rats were killed 2, 4, 7, 14 or 31 days after intoxication and the activity was counted in urine, feces, kidneys, liver, spleen and cartilage (sternum).

Experimental results

<u>Calixarenes</u>

Decorporation results:
The results which could be obtained *in vivo* to gain information on the effectiveness of S6 and S8 after intoxication with uranyl nitrate are summarised in Table 1. A slight enhancement of uranium concentration is observed in the kidneys for the highest concentration of S6. Concerning the tests made with S8, the results are insufficient and not significant.
Toxicity
The toxicity tests were performed for S6, S8 and the monomere.The monomere exhibited no toxicity at any dose. Using a concentration of 13 mg kg^{-1} of S6, hepatic effects were observed confirmed by blood analysis. At 28 mg kg^{-1} of S6, a strong loss of weight was observed. The same effects were observed with S8, however less severe and induced at slightly higher concentrations.

Metabolism
The results show that after 4 days, 15 % of the injected activity are bound onto the kidneys. 31 days after intoxication, about 8 % of the injected activity are still remaining in the kidneys. This can explain why, in spite of a good *in vitro* complexation, no enhancement of urinary excretion was observed *in vitro*. Surprisingly, no specific binding was observed in the liver, though an hepatic toxicity was obtained after Calixarene injection.

<u>Tripode</u>
The tested compound was non effective for uranium decorporation.

<u>Phosphonates</u>
The results of uranium excretion in intoxicated animals after the different decorporating treatments are summarised in Table 1.

At low doses uranium intoxication, TPA and EDTP seemed to increase the excretion of uranium. However the quantity of uranium excreted remained lower with respect to controls at high dose of uranium (100-200 mg kg^{-1}). Diuresis and uranium excretion were found lower with respect to controls by applying EDTP and CDTPA at the same doses of uranium. Furthermore an uranium excretion similar to controls was observed by administrating simultaneously EDTP and a diuretic.

Table 1. Results of decorporation studies expresssd as uranium (U) weigh in different organs observed in animals treated with the different ligand and killed 48 h. after injection with uranyl nitrate.

Chelating agent	Uranium (μmol.kg^{-1})	Molar ratio L/U	Percentage Urine	relative to U in urine	untreated U in kidneys	animals U in bone
TPA	0.092	1	150	270[*]	71	95
	0.092	10	200	265[*]	130	87
	0.42	400	120	90	90	180
EDTP	0.092	1	90	132	106	100
	0.092	10	90	171[*]	72	127
	0.42	400	70	100	54	92
	0.84	100	50	67	50	125
EDTP + Dimazon	0.84	100	88	80	-	-
CDTPA	0.84	100	50	74[*]	35	130
S6	0.092	1	100	75	102	90
	0.092	13	100	104	105	84
	0.092	100	120	87	147	124
S8	0.092	50	-	74	-	-
	0.092	100	-	76	-	-
	0.17	76	113	77	-	-

$p < 0.05$ vs control (Mann-Whitney test)

The differences observed in uranium excretion in intoxicated animals were therefore attributed rather to variations of diuresis rather than chelating action. The lower uranium concentration observed in kidney cells was also attributed to the decreasing flow of uranium in the kidney rather than a protecting effect due to the action of phosphonates. In other respect the concentration of uranium in bone by treated animals was found similar or slightly higher compared with controls.

Table 2. Tissue retention and urinary excretion after intramuscular administration of 3,4,3-LIHOPO in rats following immediately intramuscular injection of uranyl nitrate (0.84 μmol.kg^{-1}).

Treatment immediate Group (N=5)	Uranium as % of control values after 24 hours		
	Kidney	Bone (femora)	Urine
LIHOPO 30 μmol.kg^{-1} i.m.	23 ± 3	46 ± 5	155 ± 18
NaHCO$_3$ 640 μmol.kg^{-1} i.m.	87 ± 15	67 ± 22	123 ± 8

All data are expressed as the mean + standard error.
Percentage of administered U for untreated animals in kidney 18.2 %, Femora 1.4 % and Urine 29.5%
$P < 0.05$ vs control (Mann-Whitney test) for LIHOPO.

Intramuscular contamination

The results show that 3,4,3-LIHOPO is effective in decreasing the tissue content of uranium after intramuscular contamination (Table 2).

A single injection of 30 μmol.kg^{-1} of 3,4,3-LIHOPO at the wound site immediately after the contamination lowered the uranium content in the kidneys by around 5 fold, and deposition in bone by a factor 2. This reduction in the content of uranium in target organ was accompanied by a significant increase of the urinary excretion of uranium.

Table 3. Tissue retention and urinary excretion after intraperitoneal administration of 3,4,3-LIHOPO, 30 minutes after an intramuscular injection of uranyl nitrate (0.84 μmol.kg^{-1}) in rats.

Treatment(30 mn) Group (N=5)	Uranium as % of control values after 24 hours		
	Kidney	Bone (femora)	Urine
LIHOPO 30 μmol.kg^{-1} i.p.	54 ± 9	82 ± 13	135 ± 18
NaHCO$_3$ 640 μmol.kg^{-1} i.p.	64 ± 13	114 ± 33	108 ± 15

All data are expressed as the mean ± standard error.
Percentage of administered U for untreated animals in kidney 15.5, Femora 1.25 % and Urine 22.5%
$P < 0.05$ vs control (Mann-Whitney test) for LIHOPO in kidney and urine.

Table 4. Tissue retention, urinary and faecal excretion after intravenous administration of 3,4,3-LIHOPO in rats following immediately an intravenous injection of uranyl nitrate (0.84 μmol. kg^{-1}).

Treatment immediate Group (N=5)	Uranium as % of control values after 24 hours			
	Kidney	Bone(femora)	Urine	Faeces
LIHOPO (a) 3 μmol.kg^{-1} i.v.	94 ± 13	97 ± 34	107 ± 13	115 ± 29
LIHOPO (b) 30 μmol.kg^{-1} i.v.	21 ± 4	61 ± 8	184 ± 10	120 ± 40
NaHCO$_3$ 640 μmol.kg^{-1} i.v.	76 ± 20	102 ± 25	129 ± 22	139 ± 50

All data are expressed as the mean ± standard error.
(a) Percentage of administered U for untreated animals in kidney 15.3 %, Femora 3 % and Urine 31.4%
(b) Percentage of administered U for untreated animals in kidney 15.3 % , Femora 2.2% and Urine 39 %
$P < 0.05$ vs control (Mann-Whitney test) for LIHOPO (30 μmol.kg^{-1}).

The treatment with 3,4,3-LIHOPO was less effective when administered intraperitonealy and 30 minutes later (Table 4). Indeed, in this case, the uranium content of the kidneys was only decreased by a factor 2 compared with controls. Again an appreciable increase in urinary excretion (30%) occured. In bone, the delayed treatment was ineffective in preventing deposition of uranium. The treatment with sodium bicarbonate reduced only uranium content in the kidneys (36%) and had no effect on urinary excretion.

These results demonstrate the very fast absorption and distribution of uranium and emphasize the necessity to implement a very early treatment.

Intravenous contamination

After intravenous contamination (Table 4), a single intravenous injection of 30 µmol.kg^{-1} of 3,4,3-LIHOPO immediately after the contamination reduced the uranium content of the kidneys by a factor 5 and deposition in bone by a factor 1.6.

At the same time, the amount of uranium excreted via the urine was increased by a factor 1.8, compared to untreated controls.

Effect of dose

The treatment regimen employed in this experiment (3 and 30 µmol.kg^{-1}) was similar to that described for plutonium decorporation studies.

No effect on uranium excretion and deposition in tissues was observed after intravenous administration of 3 µmol.kg^{-1} of 3,4,3-LIHOPO (Table 4), showing that this dose was too low with regards to the amount of injected uranium. At this concentration, the molar ratio between the ligand and uranium was only 3.5:1.

In contrast, efficiency of 3,4,3-LIHOPO for uranium was observed for a tenfold higher molar ratio obtained with the concentration of 30 µmol.kg^{-1}. It is possible that the efficiency of the treatment with 3,4,3-LIHOPO could be enhanced further by increasing the molar ratio between ligand and uranium. It is interesting to note that in the studies with plutonium, this ratio value was much higher since the amount of actinide deposited in the wound was only about 12.10^{-6} µmol. per animal , to compare with the 0.21 µmol. of uranium per animal administered in this study. It would be certainly possible in further work to optimize the treatment protocol by repeated injections of the chelate or in increasing the dose. Such a therapeutic approach raises the question of the toxicity of this compound but recently, a short study of the toxicity of 3,4,3-LIHOPO in baboons showed that the dosage of 30 µmol.kg^{-1} administered repeatedly during one month did not induce any physiological or histological alteration in kidney or liver.

Stability and excretion of the complex

Urinary excretion was strongly enhanced (about 85 % after intravenous treatment). Taking into account that it is the major route for elimination of uranium and that, without any treatment, about one half of the uranium content of the vascular compartment is cleared through the urine in 24 hours, this represents an important gain in terms of the amount of uranium excreted. The decrease of uranium in the kidneys and the concomitant enhancement of the urinary excretion after treatment with 3,4,3-LIHOPO suggests that the complex formed in the blood remains stable at the urine pH and does not dissociate during glomerular filtration. This prevents free uranyl ions from binding to protein of renal tubule cells, an effect which leads to nephrotoxicity. The stability of the complex as a function of the pH is one of the major parameters to be considered in the choice of a chelating agent. In this respect, 3,4,3-LIHOPO seems to be an attractive molecule.

In contrast, the fecal excretion of uranium was not enhanced by the administration of 3,4,3-LIHOPO (Table 4), unlike the results obtained after the treatment of plutonium or americium contamination. In the absence of any treatment, less than 1 % of hexavalent soluble uranium salt injected intravenously is excreted by feces. This value has to be compared with the mean of 30.6 % of intramuscularly injected uranium cleared in the same time through the urinary tract in these experiments.

Speciation and modelisation studies

Despite of interesting results already obtained, the decorporation therapy remains non completly satisfactory. Studies are still in progress in order to find a molecule able to chelate them *in vivo* and to enhance their excretion out of the body. We suggest here the specification conditions for guiding the work in order to obtain compounds appropriated to *in vivo* chelation. This specification takes into account the chemical behaviour of the compound, and specially the higher affinity of some atoms for complexation. It also takes into account the biological behaviour of the metal and of the complex: particularly, the complex has to remain stable at urine pH, and the interaction between the chelate and biological components has to be as low as possible.

The first stage will consist in speciation studies in the biological field. The determination of the physico-chemical characteristics of a contaminant will allowed to determine its biokinetics. On the other hand, the determination of the kind of interactions between the contaminant and the biological components and of the stability of the complex formed *in vivo* in the blood will lead the choice of chelate able to compete with.

In the second stage, structural studies of the contaminant will help to determine a potential chelate whose size and ionic properties will fit. This will allow to select families of complexing molecules which will be made hydrosoluble with appropriated groups.

The next step will consist in modelisation studies. The computer program « Hyperchem » is used in order to modelise the complexation of uranyl ion. This program calculates the energy of the system Uranium/Ligand. It is currently checked with the complex U/CO_3^{2-} which will make a reference.

If the geometric, electrostatic and quantic data are adequat, this will allow to validate the hypothesis and to select the most attractive compounds.

Conclusions

It may be concluded that 3,4,3-LIHOPO reduces appreciably the deposition of uranium in the kidneys when given immediatly after injection. This result is interesting as the kidney is the target organ after heavy contamination with soluble forms of uranium. Furthermore, the results, especially those obtained after intramuscular contamination, show that 3,4,3-LIHOPO is also able to reduce by two-fold the deposition of uranium in bone. Thus, the efficacy of 3,4,3-LIHOPO for removing uranium from the body represents a significant advance for prompt treatment of contamination with transportable form of this compound. After a single administration of 30 $\mu mol.kg^{-1}$ of 3,4,3-LIHOPO, the chelate was appreciably more effective than the agent currently used, bicarbonate, administered in the same conditions. It is however necessary to work futher about uranium decorporation to better these results which are not totaly satisfactory.

Publications

ARCHIMBAUD M., HENGE-NAPOLI M-H., LILIENBAUM D., DESLOGES M., MONTAGNE C. -1994- Application of Calixarenes for the decorporation of uranium: present limitations and further trends. Radiation Protection Dosimetry, 53,1-4, 327-330.

MONTAGNE-MARCELLIN C., ARCHIMBAUD M., ANSOBORLO E., CRISTAU H.J.- 1994 - Synthèse d'une série de Calix[8]arènes marqués au [14]Carbone. Journal of Labelled Compounds and Radiopharmaceuticals, 36, 3, 301-306.

HENGE-NAPOLI M-H., ARCHIMBAUD M., ANSOBORLO E., METIVIER H., GOURMELON P., 1995 - Efficacy of 3,4,3-LIHOPO for reducing the retention of uranium in rat after acute administration. International Journal of Radiation Biology, *In Press*.

Head of project 5: Dr. Burgada

II. Objectives for the reporting period

1) To synthezise for the Laboratories from the Community known substances for their activities if these are not available; this is to avoid any constraints of commercial or courtesy disposability. If that is the case the Laboratories can dispose of the product they have chosen, only on the basis of scientific criteria, they are also self governed in their choice and orientation. The decision was taken to Synthesise the siderophore analogue 3,4,3-LI(1,2-HOPO) so that its efficacy for removing Pu, Am and Th from experimental animals could be investigated by CEA, Kfk and NRPB. As a consequence of a good result obtained by the partners, our program must maintain permanently the availability of product for the members of the Group.

2) Our objectives were also to synthesise new phosphonic acid derivatives for use by the CEA and NRPB in studies designed to remove uranium from the body. The strategies in the choice of proposed substances take place on the results already obtained with a certain number of diphosphonates and on the structural analysis by X ray diffraction of metallic complexes from these diphosphonates.

3) Taking into account, the synthesis of the 3,4,3-LI(1,2-HOPO) by the published method is difficult and the chemical yield is low, it was decided, during our meeting of September 1994 in Paris, to search a better procedure of synthesis.

III. Progress achieved including publications

1) Six g. Of 3,4,3-LI(1,2-HOPO) was synthesized and distributed amongst the partners:
Drs. V. Wolf, N. Stradling, J.L. Poncy, F.Paquet and I. Rencova.

2) Fourteen phosphonates was also synthesized : BCPEP-T652, CDTT-T624, CDMT-T550, DDMT-T627, CDET-T650, DCET-T674, CTMP-T675, CABP-T679, TTHP-T695, HAMDP-T776, AMDP-T780, HEDP-T777, AEDP-T778. For the NRPB and the CEA.

3) Alternative synthesis of 3,4,3-LI(1,2-HOPO): After seven months of work we do not succeed but some results are promising. These results are presented hereafter.

List of publications:

I) Synthesis of new ligands for uranium decorporation T. Bailly[1], R. Burgada[1], G.N. Stradling[2] and S.A. Gray[2] [1]Universite Pierre et Marie Curie, CNRS, Paris, France and [2]NRPB, Chilton, UK

2) The efficacity of some new phosphonic acid derivatives for enhancing the excretion of uranium from the rat G.N. Stradling[1], S.A. Gray[1], J.C. Moody[1], J.M. Pearce[1] and R. Burgada[2] [1]NRPB, Chilton, UK and [2]Pierre et Marie Curie Universite, Paris, France

3) Removal of plutonium and americium from the rat using 3,4,3-LIHOPO and DTPA after simulated wound contamination: effect of delayed administration and mass of plutonium

S.A. Gray [1], G.N. Stradling [1], M.J. Pearce [1], I. Wilson [1], J.C. Moody [1], R. Burgada [2], P.W. Durbin [3] and K.N. Raymond [3]
1 National Radiological Protection Board, Chilton, Didcot, Oxon, OX11 ORQ, UK
2 Laboratoire de Chimie des Organoelements, Univ. P. et M. Curie, Paris F-75252, France
3 Dept of Chemistry and Lawrence Berkeley Lab., University of California, Berkeley, California, 94720, CA, USA

4)Decorporation of Pu-238, Am-241 and Th-232 from rats by 3,4,3-LIHOPO

V. Volf [1], R. Burgada [2], J. Rencova [3], K.N. Raymond [4] and P.W. Durbin [4]
1 Kernforschungszentrum, Institut fur Toxikologie, Karlsruhe, FGR
2 Laboratoire de Chimie des Organoelements, Universite Pierre et Marie Curie, Paris, France
3 National Institute of Public Health, Centre of Radiation Hygiene, Prague, Czech Republic
4 Dpt of Chemistry and Lawrence Berkeley Laboratory, Univ of California, Berkeley, USA

5) Comparative efficacies of 3,4,3-LIHOPO and DTPA for removal of THORIUM-228 from the rat after simulated wound contamination

G.N. Stradling [1], S.A. Gray [1], M.J. Pearce [1], I. Wilson [1], J.C. Moody [1], R. Burgada [2], P.W. Durbin [3] and K.N. Raymond [3]
1 National Radiological Protection Board, Chilton, Didcot, Oxon OX11 ORQ
2 Laboratoire de Chimie des Organoelements, University P. et M. Curie, 75252 Paris, France
3 Dpt of Chemistry and Lawrence Berkeley Laboratory, Univ of California, Ca 94720, USA

EULEP Newsletter, **75**, p. 38,40 and 41,1994.
6)   Chelation therapy of incorporated Pu-238 and Am-241. Comparison of 3,4,3-LiHOPO, DFO-HOPO, DTPA-DX-DTPA and DFOA in rats
       V. Volf, R. Burgada, K.N. Raymond, P.W. Durbin
       Int. J. Radiat. Biol., **1993**, <u>63</u>, 785-794
7)   The efficacies of 3,4,3-LIHOPO and DTPA for enhaucing the excretion of plutonium and americium from the rat after simulated wound contamination as nitrates
       G.N. Stradling, S.A. Gray, J.C. Moody, M.J. Pierce, I. Willson, R. Burgada, T. Bailly, Y. Leroux, K.N. Raymond, P.W. Durbin
       Int. J. Radiat. Biol., **1993**, <u>64</u>, 133-140
8)   Efficiency of 3,4,3-LiHOPO for reducing the retention of 238 Pu in rat after inhalation of tributyl phosphate complex
       J.L. Poncy, G. Rateau, R. Burgada, T. Bailly, Y. Leroux, K.N. Raymond, P.W. Durbin, R. Masse
       Int. J. Radiat. Biol., **1993**, <u>64</u>, 431-436
9)   Etude par RMN de l'addition des fonctions NH, OH et PH sur l'éthenylidène bis phosphonate de diéthyle. synthèse de gem bis phosphonates fonctionnalisés
       T. Bailly, R. Burgada
       Phosphorus sulfur and silicon, **1994**, <u>86</u>, 217-228
10)   Synthesis of new ligands for Uranium decorporation
       T.Bailly, R.Burgada, GN Stradling and SA Gray
       EULEP Newsletter, **1994**, <u>75</u>, 37.
11)   The efficacity of some new phosphonic acid derivatives for enhancing the excretion of Uranium from the rat.
       GN. Stradling, SA. Gray, JC. Moody, JM.Pearce and R.Burgada
       EULEP Newsletter, **1994**, <u>75</u>, 38.

Synthesis of 3,4,3-LI{1,2-HOPO}

The results presented in this report concern our last seven months of work centered on the improvement of the 3,4,3-LI{1,2-HOPO}'s synthetic procedure, with as main objective the improvement of the purity and the yield. It's so necessary to know or at last to formulate an hypothesis on the reasons why, in the original process, the yield is very low. (Scheme 1)
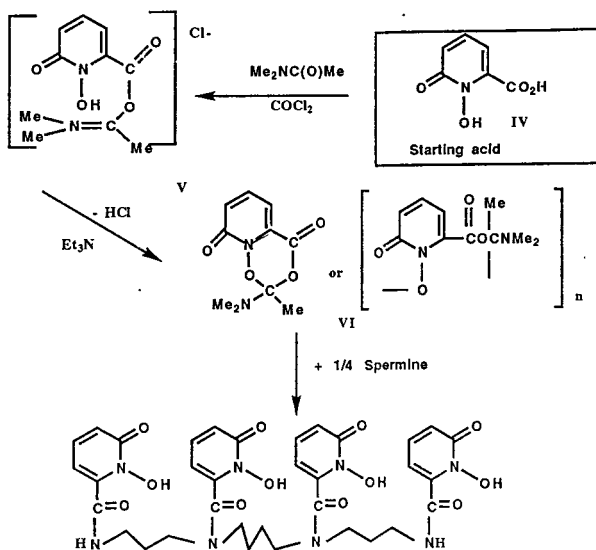
Scheme 1

The main reason, after Raymond and his associates, is due to the fact that spermine is firstly alkylated on the two primary nitrogen atoms. This lead to an intermediate in which the two secondary nitrogen atoms are deactivated by formation of an hydrogen bond between the acidic hydrogen of the amidic function and the nitrogen in position 5 and 10 so the resulting weak nucleophilicity of these nitrogen atoms must be counterbalanced by a greater reactivity of the activated reagent's carboxylic group. (scheme 2)
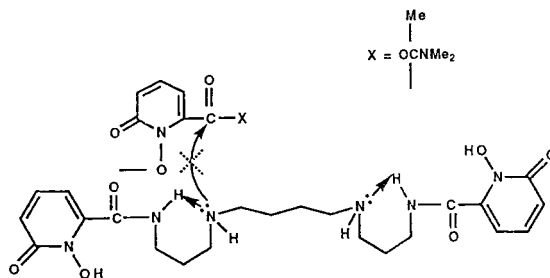
Intermediary step

Scheme 2

In other words X must be a better leaving group than the leaving group used in the published technique.

In our mind a second reason can explain the low yield of the classical synthesis:

The starting activated acid, existing under a more or less polymerised form, reacts with a polyamine of a relatively important size, it's well known that the interactions between the reactionnal sites are, in this case, not good, for steric crowding reasons.

Before writing about the strategies we have chosen to avoid these difficulties, it's interesting to consider a few instructive results previously published by a number of authors. The scheme 3
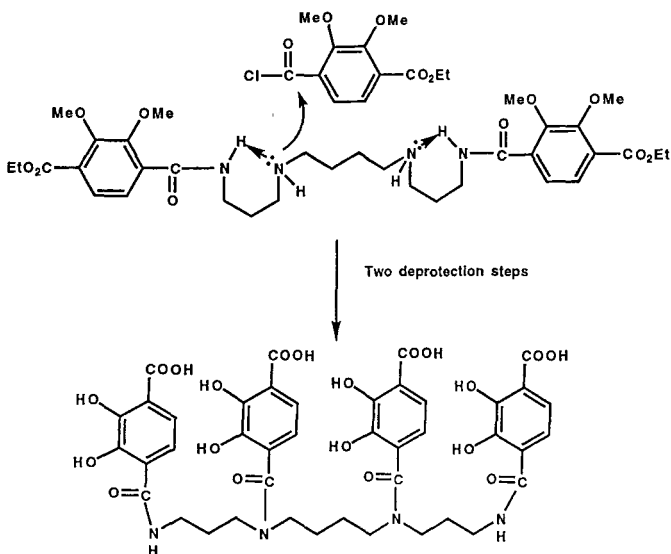
Scheme 3

show the synthesis of LICAM C obtained very pure with a good yield by reaction of 4 molecules of activated acid on a molecule of spermine. Nevertheless, we have also in this case the opportunity of an intramolecular H bond in the intermediate step. But contrarily to the 3,4,3-LI(1,2-HOPO)'s synthesis the acid function is activated as acid chloride, the best leaving group, moreover the reagent protected on all his other reactive functions is not a polymer. Another very instructive exemple is given by the synthesis of parabactin that uses the spermidine as polyamine backbone. (scheme 4)

In a first step the spermidine's primary nitrogen atoms have been protected by a carbobenzyloxy group. Note that here again the required conditions to establish an hydrogen bond are present.

Activation of the COOH group with:
PhO)₂P(O)Cl-Pyridine
EtOC(O)Cl -Pyridine
SOCl₂-DMF
(COCl)₂-Et₃N
Failed

Deprotection NH₂   52%   A

B   52%

83%

Parabactin
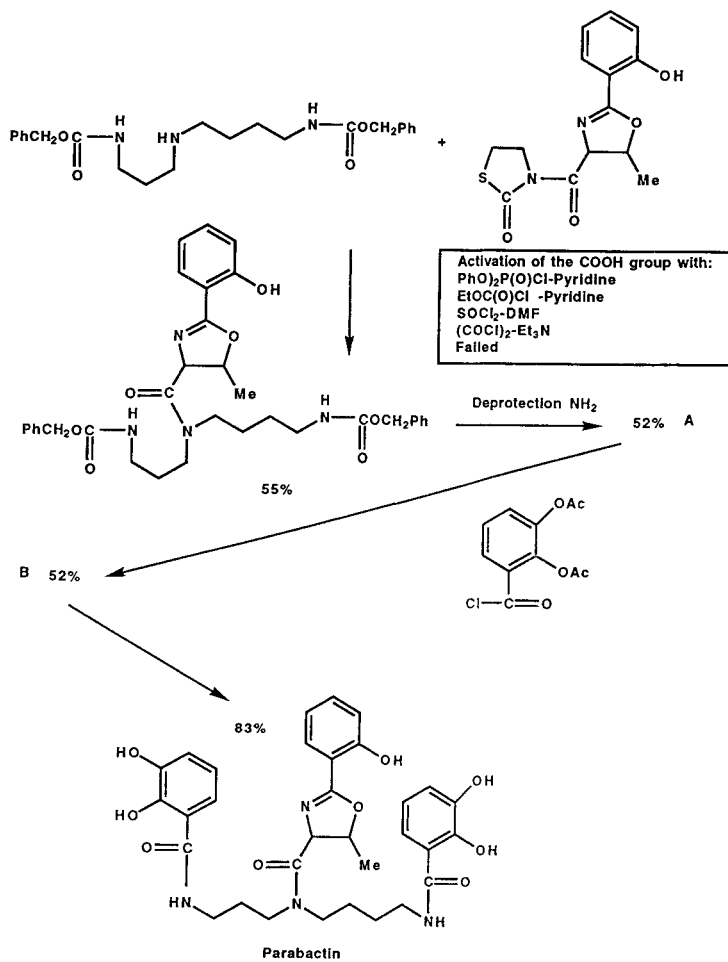
Y.Nagao and coll. J.Chem.Soc Perkin I 1984 p.183

Scheme 4

The scheme 4 shows all the activation procedures of the carboxylic group that have been unsuccessfully tested. The only one leaving group which leads to a modest coupling yield is a thiazolidine thione structure. Finally the parabactin is obtained with a 60% overall yield. Let's look at a last example on the synthesis of spermexatin that is always a spermidine derivative. In this case, the acidic function of the reagent, is activated with an hydroxysuccinimid moiety as leaving group and the complexing hydroxylamine function is protected with a benzyloxy group. In this synthesis, in spite of the H bond, the spermexatin is obtained with a 69% overall yield. Again the reagent is monomeric, protected on his reactive functions and activated with a good leaving group. These exemples show us clearly that the formation of an intramolecular hydrogen bond, wich weakened the secondary nitrogen atom reactivity can be offset by using a better activation process of the reagent's acid function.

83%

Spermexatin
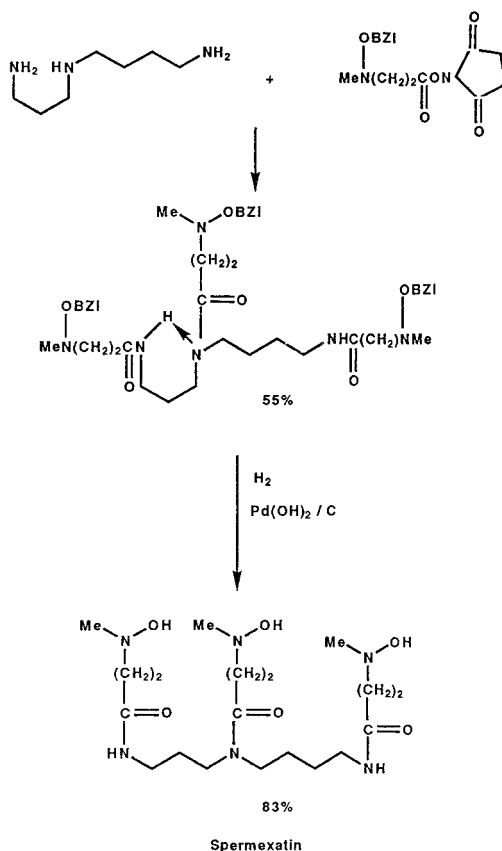
S K Sharma and coll. J Med.Chem 1989 32 357

Scheme 5

- 2649 -

Let's come back to the synthesis of 3,4,3-LI(1,2-HOPO). In order to go round the difficulties we have just presented we looked for other possibilities.

The first one is to use a completely different procedure of synthesis. There are of course in this direction a lot of ways (scheme 6). One of them is founded on a coupling reaction between a pyridine cycle, free of reactive functions, and the spermine. The complexing groups C=O and N-OH are generated only after that.

For example the bromopicolinic acid 1b is activated under acid chloride form, then condensed on spermine with formation of 1bsp which is oxidised in 2bsp after that the bromine atom is substituted with an OH group to give the final product 3sp that is the 3,4,3-LI(1,2-HOPO). The results in this direction, in spite of a great number of experiences, were not conclusive (see annex 1) so this strategy was no longer investigated.

At that time we decided to consider again the starting acid used in the Raymond's synthesis and to search a better activation process.
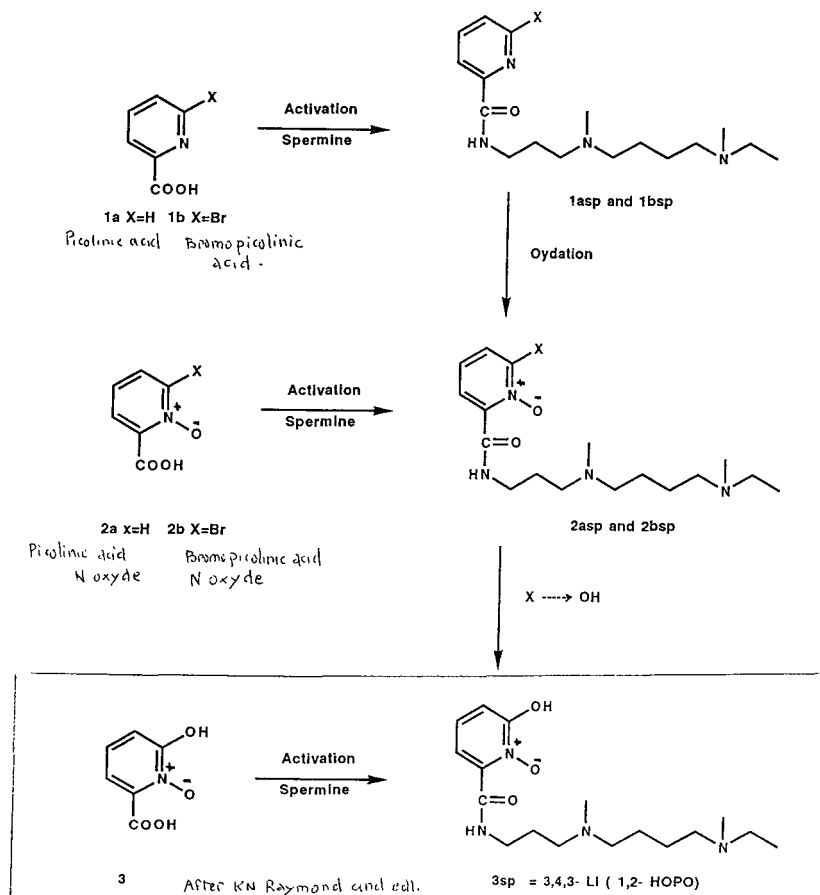
Scheme 6

The scheme 7 shows all the activation reactions that have been studied on the Raymond's starting acid. The compound VI, or his polymerised form, is used in the published synthesis of 3,4,3-LI(1,2-HOPO) with the results we know (5 % overall yield).
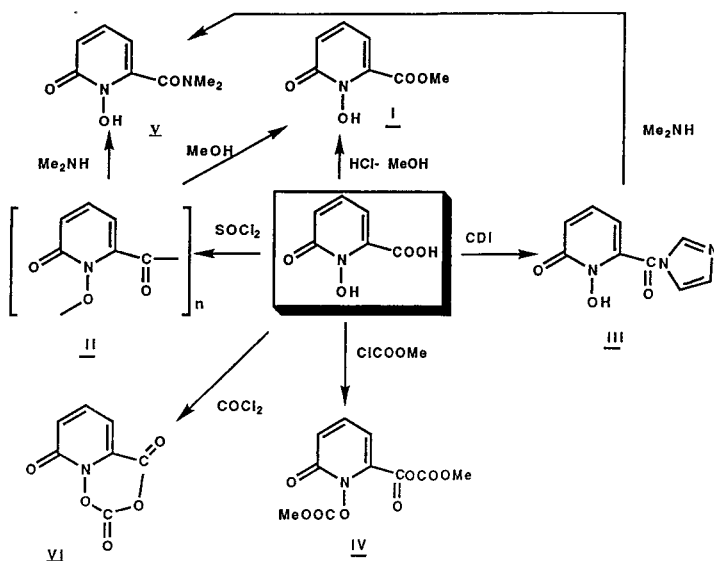
Scheme 7

The compound II, also described by Raymond and his associates, is an activated polymer which good reacts with a simple amine, for example to get the amide V with a good yield.

We have unfortunately seen that the synthesis of polymer II is very impredictable and needs an optimisation. In addition his reaction with a long chain polyamine, as the spermine leads to mediocre yield. We have repeated and checked all these reactions. We have also synthesised the activated structure III by a reaction with carbonyl diimidazole and the structure IV by reaction with methylchlorocarbonate. In these structures, the choice of the living group allows to get compounds which are not polymeric. Thus in the activated pyridone III, the OH function remains to be free.

The compound III also reacts with the dimethylamine, as test reagent, to give the amide V with a good yield. In the work currently in progress we have also noticed a good reactivity of compound III with the spermine. Let us now consider the intramolecular hydrogen bond mentioned at the beginning of this report.

The scheme 8 shows one of the four acidic activated units, by X, which must be fixed on the four nitrogen atoms of the spermine (compound A). The compound B represent the reaction step where the spermine has already been substituted on the two primary nitrogen atoms.

It's at that moment that the H bond is established, reducing the reactivity of the last two secondary nitrogen atoms. To get round this difficulty, with elimination of any possibilities of an H bond, two types of protection may be considered. The first one consist in using a spermine, in which the two primary nitrogen atoms are substituted by an electron donor group, for example a methyl group which led to a slightly different 3,4,3-LI(1,2-HOPO) from the authentic one. The second solution is to choose an easily removing benzyle group at the end of the reaction. In this last case, the dibenzyle spermine 1-14 must be used.

This compound has been prepared with a good yield.
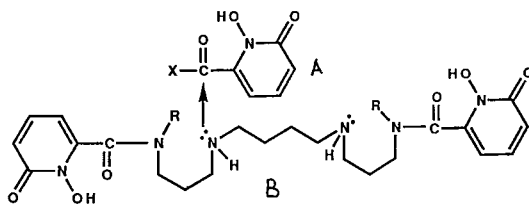
R = Me , PhCH$_2$

Scheme 8
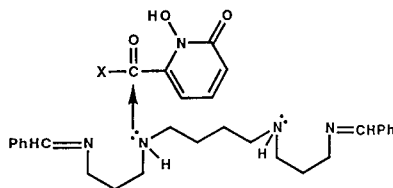
Scheme 9

In a second type of protection the two primary nitrogen atoms are, in a first step, selectively protected for example as imine.(scheme 9). In a second step the two secondary nitrogen atoms are alkylated. In the following step the protecting groups are hydrolysed and a second coupling reaction is done. This work is in progress.

In conclusion, to date, our attempt to synthesise the 3,4,3-LI(1,2-HOPO) by a new procedure was not successful.

However, the partial results obtained allow us to hope a success in the coming months.

Synthesis of LIHOPO after KN Raymond and col.

In order to synthesize the final product B, the coupling group of the intermediate A must be activated (for exemple as acide chloride). Unfortunatly the activated coupling group react immediately with the complexing group N-OH with the formation of a polymeric material.
Of course the polymer contain the link C(O)-ON-C(O) that is an activated form of the carboxylic fonction (it is an auto-activated form of the starting acid A and so should be reactive with an amine group)

Complexing groups   A   Coupling Group   B   Carrier(polyamine)
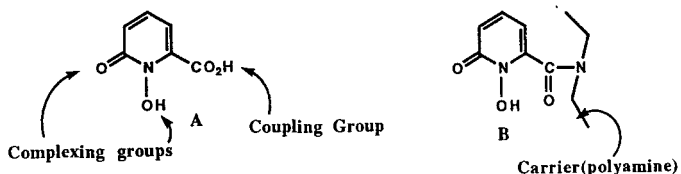
Alternative Synthesis of LIHOPO

This work has been based on two strategies A) and B) :

A) The alternative synthesis is founded on a coupling reaction between a pyridine cycle, free of reactive fonction, and the support (spermine). The complexing groups C=O and N-OH are generated only after that. We also include in this work a search of another reagent of activation (for exemple DCC, hydroxysuccinimide and so on...)
Exemple:
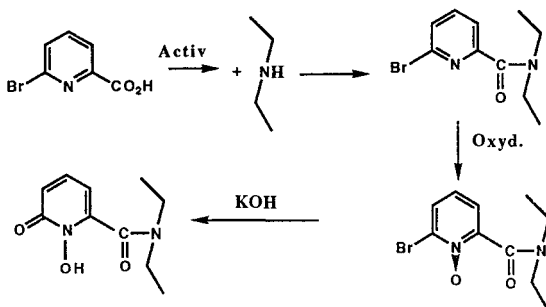
B) Another approch in the alternative synthesis is to seach from the acid A (starting product of the Raymond' procedure) another technique of activation with or without protection deprotection sequence.

Strategies used in the alternative synthesis

A

Theory:

On the base of preceeding argumentation, the next 4 pyridines cycles have been be tested
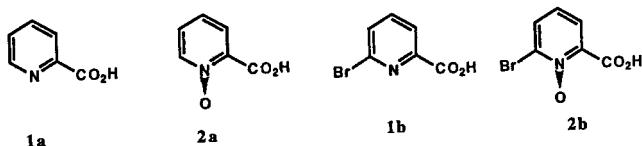
picolinic acid **1a** , picolinic acid N oxyde **2a**, bromopicolinic acid **1b**, bromopicolinic acid N oxyde **2b**

In every case the activation step is performed either by the standard procedure (COOH--- COCl) or by another route (for example DCC)

After the activation step, the pyridines' cycles are bound on the support. We choose in a first approach the ethylenediamine as test support.

Pyridines **1a, 1b, 2a, 2b** are now Pyridines **1aED, 1bED, 2aED, 2bED** (*ED* = Ethylene diamine)

The next steps are:

I) Pyridine **1aED** : Oxydation in position 1 and hydroxylation in position 6

II) Pyridine **2aED** : Hydroxylation in position 6

III) Pyridine **1bED** : Oxydation in position 1 and subtitution of Br with OH

IV) Pyridine **2bED** : subtitution of Br with OH

Results:

I) The compound **1aED** was obtained with a correct yield but the oxydation reaction in position 6 was not good.

(Type of activation of 1a used : acid chloride).

II) The activation of 2a as acide chloride is not conclusive.

The reaction **2a** + ED + DCC (as coupling reagent) --------> **2aED** is promising but there is some difficulties in the purification step.

III) The activation of **1b** as acid chloride is good but the condensation with **1b** fail probably due to the hight reactivity of the Br atom with the NH_2 fonction of **ED.**

IV) Taking into account that Br atom is more reactive in **2b** than in **1b** this experiment was not done.

Conclusion:

The principle of strategy A: Generation of complexing groups in the last steps on the pyridine ring already binded to the spermine was not retained.

I)Pyridine 1a

Theoretical scheme:
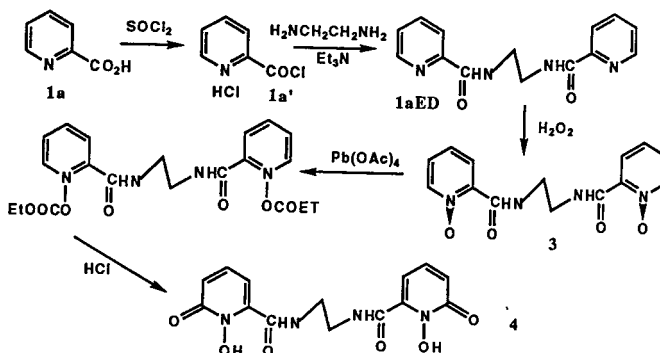
Experimental results

The compounds 1a and 1aED have been obtained with a correct yield

The oxidation of 1aED is not complete in spite of two successive oxidation procedure

Conclusion the way from pyridine 1a is no longer studied

II) Pyridine 2a

Theoretical scheme:
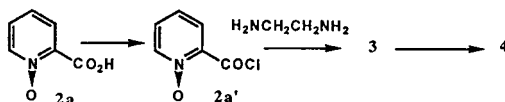
Experimental results

The compounds 2a' was not obtained with a good yield

Conclusion the way from pyridine 2a is no longer studied (another procedure of activation may be sudied).

III) Pyridine 1b

Theoretical scheme:
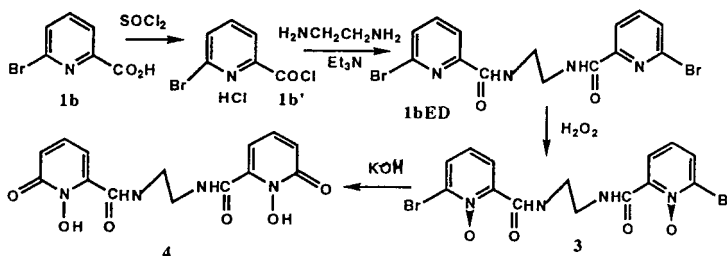
Experimental results

The compounds 1b' was obtained with a good yield but the compound 1bED was obtained with a poor yield ; probably due to a similar reactivity of the bromine atom and the carbonyle chloride function.

Conclusion This way was non longer investigated.

IV Pyridine 2b

Theoretical scheme:I
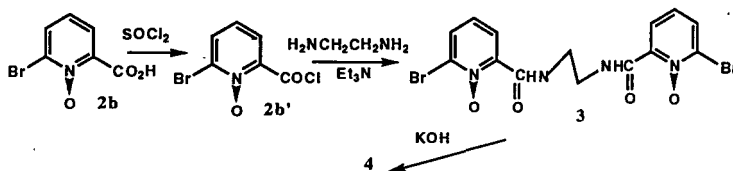
Taking into account that the bromine atom is more reactive in the structure 2b than in the structure 1b, it is not useful to investigate this way.

Head of project 6: Dr. Rencova

II. Objectives for the reporting period

A Polonium-210 decorporation

(1)   More detailed studies with bis-dithiocarbamates which in pilot experiments were effective in reducing retention of [210]Po : Relationship between the time at which treatment is initiated after exposure to [210]Po and the effectiveness of such treatment.

(2)   Investigation of the efficacy of DMSA and its monoester derivative.

(3)   Investigation into the effect of bis-thiocarbamates in combination with selected vicinal dithiols: role of the chelators as well as time schedule of their repeated administration.

(4)   Comparison of efficiency of treatment with bis-dithiocarbamates after different routes of polonium incorporation.

(5)   Reduction of subacute lethal toxicity of [210]Po by chelators.

B Thorium-234 decorporation

Efficacies of 3,4,3-LI(1,2-HOPO) and CaDTPA for [234]Th decorporation

III. Progress achieved including publications

Decorporation of intravenously injected [210]Po

The biokinetics of iv injected [210]Po was used as a model for the behaviour of [210]Po absorbed into the blood from any other site of entry into the body.

The effectiveness of bis-dithiocarbamates has been studied to reduce [210]Po in organs and tissues of rats as a function of time from the beginning of the repeated treatment. Here are formulas of the used chelators :
N,N'-dimethylethylenediamine-N,N'-biscarbodithioate (MeTTC),
N,N'-diethylethylenediamine-N,N'-biscarbodithioate (EtTTC),
N,N'-di(2-hydroxyethyl)ethylenediamine-N,N'-biscarbodithioate (HOEtTTC).

Only HOEtTTC was efficient in decreasing the total content of [210]Po in tissues substantially when the sc treatment (0.4 mmol kg^{-1} body weight for 5 consecutive days) was delayed for 1 h. In control rats, 57% of [210]Po was retained at 7d. [210]Po was decreased in all investigated tissues: blood, spleen, bone, liver, kidney, muscle, skin. MeTTC and EtTTC caused substantial decrease only in kidney, and kidney and blood, respectively. After EtTTC treatment an increase of [210]Po in liver was observed.

In a metabolic study the effect of HOEtTTC was compared with that of parent compound N,N'-diethylamine-N-carbodithioate (diethyldithiocarbamate, DDTC). Two dosages of DDTC (0.4 and 0.8 mmol kg^{-1} body weight) were used in repeated treatment started 1 h after injection of ^{210}Po. At the higher dosage DDTC was as efficient as was HOEtTTC 0.4 mmol kg^{-1} (30 % of ^{210}Po was excreted via faeces), but toxic effect of the former ligand was observed. The rats appeared to be ill, their body weight was 85% of the controls. DDTC caused transient accumulation of ^{210}Po in liver. When HOEtTTC was administered, the faecal excretion of ^{210}Po was increased from the very beginning of the treatment.

Further, the efficiency of two dithiols was studied : meso-2,3-dimercaptosuccinic acid (DMSA) and monoisoamyl-2,3 dimercaptosuccinate (MiADMS). After repeated sc treatment with MiADMS (0.4 mmol kg^{-1} body weight for 5 consecutive days) the enhanced excretion of ^{210}Po via faeces and urine was found. The main route of excretion was via faeces. At d 7 treated rats excreted 36% and 26% of injected activity when the treatment started immediately and with 1 h delay, respectively. Control rats excreted 12%. However, after treatment high accumulation of ^{210}Po in kidneys occurred. Therefore the balance of activity in all investigated tissues amounted to 66 % of controls. The efficiency of MiADMS was decreased when its first administration started 1 h later (84 % of control rats).

It was found that the effect of MiADMS is different from that of its parent compound DMSA which caused decrease of excretion of ^{210}Po via faeces. Therefore, with DMSA the total ^{210}Po in body tissues was slightly increased (115-119% of controls).

Decorporation of ^{210}Po after simulated wound contamination

Contaminated wounds were simulated in rats by intramuscular injection of ^{210}Po. The aim of the study was to determine the effectiveness of chelation treatment as a function of time, dosage, and route of chelate administration. Ten newly synthesized substances containing vicinal sulphydryl and carbodithioate groups were used and their effect was compared with that of chelators clinically applicable in man 2,3-dimercaptopropane-1-ol (BAL), 2,3-dimercaptopropropane-1-sulphonate (DMPS), DMSA and DDTC. Results indicated first that complete removal of ^{210}Po from the injection site was achieved by only two local injections of DMPS, beginning as late as 2 h after injection of ^{210}Po. Second, many substances mainly induced translocation of ^{210}Po from the injection site into other tissues. Third, a combined local treatment at the injection site with DMPS (two dosages, 0.5 mmol kg^{-1}) plus repeated systemic, sc, treatments with MeTTC, EtTTC and HOEtTTC (5 dosages, 0.5 mmol kg^{-1}) resulted after one week in the reduction of the estimated total body retention of ^{210}Po to about one half of that in untreated controls. When the administration of HOEtTTC was prolonged (10 dosages) the overall retention of ^{210}Po was reduced to one third of controls.

Comparison of efficiency of treatment with bis-dithiocarbamates after different routes of polonium incorporation

Comparison of experiments on decorporation after iv and im injected ^{210}Po has revealed the different efficiency of bis-dithiocarbamates. When their administration started 1 h after iv injection only HOEtTTC was substantially effective. On the other hand, all three bis-dithiocarbamates were efficient in reducing ^{210}Po in the body after im administration of ^{210}Po when combined treatment started 2 h later.

Reduction of subacute lethal toxicity of ^{210}Po

Preliminary experiment on the reduction of subacute lethal toxicity of ^{210}Po revealed good efficiency of HOEtTTC when the repeated sc treatment started immediately after iv injection of ^{210}Po. Whereas all control animals died till d 37, 90% of treated rats survived 5 months when they were sacrificed.

Wound contaminations were simulated by im injections of ^{234}Th. After the repeated im treatment with LIHOPO, CaDTPA and DFO-HOPO (30 µmol kg^{-1}) which started 1 h after administration of ^{234}Th 62%, 89% and 82% of ^{234}Th of controls were established in the whole body at d 7, respectively. Only LIHOPO decreased substantially the activity of ^{234}Th in skeleton to 35% of control values. CaDTPA was inefficient and DFO-HOPO increased ^{234}Th to 140% in this tissue.

Publications

J. Rencova, V. Volf, D. Bubenikova, M.M. Jones, P.K. Singh. Chelation of Po-210 in rats by derivatives of DDTC and DMSA. EULEP Newsletter 75, 35-36 (1994).

V. Volf, R. Burgada, J. Rencova, K.N. Raymond, P.W. Durbin. Decorporation of Pu-238, Am-241 and Th-234 from rats by 3,4,3-LIHOPO. EULEP Newsletter 75, 40-41 (1994).

J. Rencova, V. Volf, M.M. Jones, P.K. Singh. Decorporation of polonium from rats by new chelating agents. Radiat. Prot. Dosim. 53, 311-313 (1994).

J. Rencova, V. Volf, M.M. Jones, P.K. Singh. Efficiency of the derivative of DMSA for polonium-210 decorporation in rats. EULEP Newsletter 79, 10-11 (1995).

V. Volf, J. Rencova, M.M. Jones, P.K. Singh. Combined chelation treatment of simulated wounds contaminated with Po-210 in rats. EULEP Newsletter 79, 11 (1995).

J. Rencova, V. Volf, M.M. Jones, P.K. Singh, R. Filgas. Bis-dithiocarbamates : effective chelating agents for mobilization of polonium from rat. Int. J. Radiat. Biol. 67, 229-234 (1995).

V. Volf, J. Rencova, M.M. Jones, P.K. Singh. Combined chelation treatment for polonium after simulated wound contamination in rats. Submitted to Int. J. Radiat. Biol.

Final Report

Contract: **FI3P-CT920059**   **Sector: B23**

Title: Radiation effects and their treatment after local exposure of skin and sub-cutaneous tissues.

1) Masse   CEA-FAR
2) Hopewell   Univ. Oxford
3) Coggle   Hosp. St. Bartholomew
4) Di Carlo   IFO

GENERAL DESCRIPTION OF THE CONTRACT

The aim of the collaborative group was to bring together experimental and clinical researches, performed by the different participants, on diagnosis, prognosis, pathogeny and treatment of local radiation exposure of the skin and subcutaneous tissues.

Acute localized irradiation and external contamination are the most frequent accidental events in radiation protection hazards. Cases of over-exposure of skin and underlying tissues, including skeletal muscles, can occur in both medicine and industry. In a major accident situation, as indicated by experience from Chernobyl and Goiania, significant numbers of persons would be affected. The severity of a radiological damage depends on the energy deposited in the tissues, the dose-rate, the surface irradiated and the radiosensibility of the subjects. Early diagnosis and late effects prognosis are fundamental to evaluate the extent of the injuries and to manage the treatment.

Dose-effect curves have been established for the various endpoints (erythema, dry or moist desquamation, permanent ulcer or healing) from experiments in animal models and from observations in radiotherapy patients. These studies have provided a suitable basis for improving radiological protection criteria for the skin. The pathogenesis of different late

effects, including atrophy, fibrosis and sclerosis, observed after local exposure of skin and underlying tissues, has been assessed in the pig, the rabbit and the mouse in the first 18 months after exposure. Skin has been widely used in radiation carcinogenesis studies because of the accessibility and visibility of the tumors in this tissue. Both rat and mouse models have proved to be sensitive, reproducible systems to study the dose and time response of cancer induction following different mode and qualities of radiation exposure.

All these responses have been documented in human skin after accidental overexposure; the clinical studies on the Chernobyl and Goiania accidents victims made obvious combined injury, adding the effects of local and regional or total exposures. The problem of hot particles has been posed in these cases more acutely than as a hazard in the nuclear power plants.

At least some remarks would sum up the general objective of these joined contracts. Localized overexposure accidents are rather rare and generally due to industrial sources manipulation; their clinical evolutions are dramatic and surgical interventions are accepted rather bilatedly by the patients because of the extremely painful and hopeless nature of the pathological process in these injuries. Experience and knowledge supplied by both clinical following up of such lesions and experimental observations should be useful to give scientific basis for setting a common and well accepted management protocole of these radiological injuries. Studies on the pathogeny, the prevention and the treament of fibrosis, the pre-transformation of certain sort of skin cells, will be directly applicable to the management of the late effects of radiotherapy. Combining clinical and experimental researches worked out by the different contractants seem to be more efficient way to obtain rapidly practical methods for localized radiation injuries management.

I. Summary of Project

Dosimetry: Interaction between radioactive sources and living tissues may occur in two cases: accidental overexposures and radiotherapy treatment. In both situations it is important to evaluate the consequences of the absorbed dose upon physiological functions. NMR studies of the Fricke solution, formed with ammonium ferrous sulphate solution in acid environment represents an attractive dosimeter. The particularly of this study was that different dose rates and intensity gradient including high doses allowed us to represent accidental conditions. A linear relationship between absorbed doses and the NMR parameters was obtained (Saclay).

Diagnosis: the diagnosis of early (inflammatory reaction), subacute (thrombosis and ischemia) and late (necrosis and fibrosis) of radiation injuries of skin and underlying tissues was performed on rabbits using 67 Ga scintigraphy, NMR imaging of the skin and computed tomography, and in pigs, using NMR imagerie, spectoscopy and skin relief measurement (Saclay).

In man, thermography after cryostimulation was used to appreciate the severity of the late effects of radiation injuries in the hand and fingers (Roma).

The clinical evolution of the lesions was followed in pigs locally irradiated with β rays from 90Sr / 90Y and 170Tm sources applied on the skin, alone or combined with X rays (Oxford) or 60Co γ rays (Saclay). The time course development of late dermal thining was followed and compared with regards to irradiation protocol, β ray energy, combination with X or γ rays and dose rate (Oxford).

In man, an attempt of grading fibrosis by histological methods was undertaken in skin biopsies (Paris).

Pathogeny: The pathogeny of early and late effects was approached by measuring the expression of AP1 and p53 genes in irradiated pig skins (Saclay) with low and high doses; important results were obtained concerning the time course of the early response of these genes, related to the dose. After either β or γ ray irradiation, the prevalent role of TGFβ1 in the development of fibrosis was pointed out in pigs (Saclay) and mice (London); moreover, it was suspected in dermal tumors in mice (London).

An increase in adhesion molecule expression (ELAM-1) at the dermal endothelial cells level was reported in pigs after β ray irradiation (Oxford).

Pathophysiology: The pathophysiology of the irradiated skin in man was studied in biopsies at the cellular level, i.e. fibroblasts and keratinocytes, by appreciating the expression of TGFβ1, EGF and PDGF receptors, and α-actin, as a marker of myofibroblasts (Paris).

Treatment: In pigs, highly beneficial effects of liposomal bovine Cu/Zn-SOD given by a systemic way, was pointed out on skin and muscular tissue fibrosis: the volume of the fibrotic tissues in pigs treated 5-6 months after local exposure to 160 Gy (skin surface dose) decreased in 2 months by 70% (Saclay). A significant effect of oral administration of essential fatty acids, before and after irradiation, was reported in pigs after β exposure: the dose modification factor concerning the severity of the clinical lesions, i.e. erythema, moist desquamation and necrosis, ranged from 1.14 to 1.35.

In an experimantal animal model of crushed muscle, simulating radionecrosis, the use of thrombolytic agents (urokinase and actilyse) seemed beneficial in reducing the level of circulating CK consecutive to the muscle injury (Boucicaut Hosp. Paris).

In man, a long term follow up study of the first clinical trial using the liposomal bovine Cu/Zn-SOD by systemic way was published in 1994 (in collaboration with Saclay). In an other study, the beneficial effect of liposomal bovine Cu/Zn-SOD as topical application, was appreciated in skin biopsies from 44 patients, with regards to the decrease of the fibrosis grade (Paris). In the 132 patients treated by topical SOD for radiation-induced fibrosis for 90 days and followed by telethermography with cryostimulation for a period ranging from 18 to 72 months, 50% showed a continuous improvement of the fibrotic lesion, 30% a durable stabilisation and 20% a slight deterioration (Paris).

I. Head of project N°1: Dr. R. MASSE

CEA - Direction des Sciences du Vivant, - Département de Radiobiologie et de Radiopathologie, Laboratoire de Radiobiologie Appliquée, 91191 GIF SUR YVETTE cedex

1 - Dosimetry

Interaction between radioactive sources and living tissues may occur in two cases: accidental overexposures and radiotherapy treatment. In both situations it is important to evaluate the consequences of the absorbed dose upon physiological functions. NMR studies of the Fricke solution, formed with ammonium ferrous sulphate solution in acid environment represents an attractive dosimeter by NMR imaging.

As a preventive and therapeutic controls dosimetry may be necessary to evaluate the absorbed dose. It was shown by J.C. Gore et al. (1984) that a linear relationship exists between the absorbed dose in a Fricke solution through the amount of Fe3+ created and the (T1-1) rate which characterizes Nuclear Magnetic Resonance relaxation. L. E. Olsson (Olsson et al. 1990) has also developed the measurements of dose distributions in radiotherapy from this principle. The purpose of our work was to verify the dose-effect relationship and to extend more particulary this study to a dose range similar to an accidental condition involving a 60Cobalt and a 192Iridium γ rays.

The solution was incorporated in a gelling substance made with agarose. Exposed to γ rays an oxidation transforms ferrous to ferric ions. Both Fe2+ and Fe3+ ions are paramagnetic and the spin lattice relaxation process of protons is accelerated according to the amount of Fe2+ transformed into Fe3+ since dipolar interaction governs this process. Thus T1 weighted image contrast may be used to detect the formation of ferric ions. A linear relationship may be established between the amount of Fe3+ created and the spin-lattice relaxation rate of protons leading to a straightforward dose-effect relation.

We realized experiments with γ rays of 192Iridium and 60Cobalt. The doses were in the 0 to 100 Gy range. The concentrations of Fe2+ were 0.5, 1, 1.5 and 2 mM and these solutions were incorporated in a gelling substance of 4% agarose. The particularly of this study was that different dose rates and intensity gradient including high doses allowed us to represent accidental conditions.

It was observed in a first time that the concentration of agarose powder included in the sample has an influence in the diffusion of Fe3+ ions from irradiated area to nonirradiated area. To limit this perturbation of relaxation times measurements, we decided to use a compact

structure of the gelling substance ie agarose powder 4%. And to explore the possibilities of these dosimeter systems, we studied the influence of three parameters: the initial concentration of ferrous ions (0.5, 1, 1.5, 2 mM), the intensity of dose irradiation (0, 20, 40, 60, 80, 100 Gy) and the nature of the dose (60Cobalt and 192Iridium). In a second time we have shown that incorporation of Fe2+ and production of Fe3+ could change the characteristics of the protons longitudinal relaxation processes. One can notice an effective decrease of the longitudinal relaxation times according to the increase absorbed dose; neverthless this process is less efficient for the transverse relaxation time T2. Therefore the observed behavior correspond well to the T1 results.

1 - 1. Ferrous ions concentration

It was obseved that the evolution of the T1's values as a function of absorbed doses was influenced by Fe2+ concentration. For lower concentration (0.5 mM) the evolution is non linear. For [Fe2+]=1mM the linearity was obtained between 20 and 60 Gy only. For the most important doses a stabilization of T1's values was noticed. Above 1.5 mM a linear variation was obtained with a constant slope for the interval from 20 to 100 Gy : 1.13±0.05 ms Gy-1.

1 - 2. Absorbed dose

Our model presents a bi-evolution of the dose-effect relation : betwen 0 and 20 Gy with a slope equal 6.5±0.05 ms Gy-1. This can be attributed to the strong paramagnetics properties of Fe3+ ions with regard to Fe2+ions. On the other hand an absorbed dose of 100 Gy decreases the T1's value by a factor of 1.8 compared to a dose of 20 Gy in the favourable cases of [Fe2+]=1.5 to 2 mM. And the intervalle 20 - 100 Gy may represent the second domain mentioned before.

1 - 3. Source of irradiation

We have studied the influence of the source (60Co or 192Ir). The processes previously described are similar for the two cases. However the 60Co source gives a more well defined linearity and more coherent measurements of NMR intensities than the 192Ir source. This property can be attributed to the model for irradiation. In fact the 60Co source allows a complete and uniform irradiation of the sample compared to the 192Ir source which was less uniform. We have reported the dose-effect relation as the NMR intensity plotted against the absorbed dose for 60Co and 192Ir rays. NMR imaging experiments were performed with a T1-weighted spin echo sequence (TR=300 ms, TE=33 ms) allowing a more intense signal for the shortest T1's values.

(a)   (b)
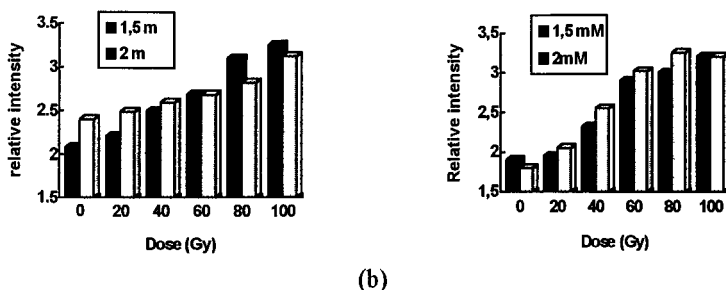
Figure 1: relative NMR intensity obtained for a 60Co (a) and 192Ir (b) source using a T1-weighted spin echo sequence (TR=300 ms, TE=33 ms).

1 - 4. Conclusion

The dosimetry method using nuclear magnetic resonance developed by L. E. Olsson with X rays and 60Co g rays and for absorbed doses contained betwen 0 and 60 Gy has been extended to the 60 - 100 Gy range. Thus we have been able to establish a full experimental linear relationship for doses delivred to the dosimeter phantoms in a range of frequents overexposure conditions (0 to 100 Gy). The study was performed with γ rays of 60Co and 192Ir sources which are frequently encountered in realistic accidentals conditions. Thus NMR appears as a performant and reproductible tool of dosimetric method. NMR techniques presents advantageous new possibilities of investigations like measurements of T1's values and NMR intensities signal.

2 - Diagnosis

2 - 1. Magnetic resonance micro-imaging of the skin

Our experimental model of acute localized irradiations has been developed in the rabbit with an industrial radiographic source (192Ir, Emg = 0.38 MeV). In this study, we irradiated rabbits on the back (Vth lumbar vertebra level) at a skin surface dose of 120 Gy. Healthy and irradiated skin biopsies were taken from rabbits and we examine the structure variations of irradiated skin, using magnetic resonance micro-imaging. Images were taken in the skin surface plane and high resolution images were obtained by transverse selection of 3 mm slices with a spatial resolution images of about 40 μm per pixel. T1, T2, diffusion weighting and magnetization transfer contrast (MTC) were performed in order to increase the image sensibility.

2 - 2. Normal skin

NMR imaging experiments were developed in order to improve mainly two kinds of parameters : the spatial resolution in the depth direction and image contrast. The first goal was realized by application of large intensity gradients. NMR contrasts are governed by relaxation processes (T1 and T2) and the choice of the sequences. Modifications of the relaxation times T1 and T2 induced by alteration of the skin and consecutively contrasts induced by T1, T2, diffusion weighting and magnetization transfer sequences, allowed to highlight effects of irradiation of the cutaneous tissue. To validate the high spatial resolution imaging method, images of pigs skin biopsies were realized especially in the depth direction, providing a good differentiation between skin layers (epidermis and dermis) and subcutaneous hypodermis layer. Spatial resolution (35 µm per pixel) allowed to differentiate epidermis, dermis with several of its appendages like hairs follicles canals and sebaceous glands.

2 - 3. Irradiated skin

Using identical conditions, images of irradiated skin of rabbits were performed for judicious periods of the evolution of tissues after irradiation. The different steps of pathological reactions of irradiated cutaneous tissue have been detected with a good reproducibility.

The observations performed between 48 and 72 hours after irradiation demonstrated that a modification of the tissue structure corresponding to a **transient erythema** could be detected by NMR imaging. These early effects could be attributed to a macromolecular disorganization that induces a loss of signal in the affected layers. Seven days after irradiation important modifications occured in the affected area and effects were more pronounced. Highly vascularized dermis presented an oedema generally one week after irradiation. All images of biopsies were characterized by a more intense signal which corresponded to an accumulation of fluid in the affected area. **Oedema** was also characterized by an increase of the dermis volume which can be delimited with a great accuracy with NMR imaging. Images performed two weeks after exposure to ionizing radiation indicated clearly the aggravation of the pathology. Indeed, this time corresponded to the transition period between oedematic and necrotic structures. Then we could observe the loss of signal corresponding to the "dry" structure of **necrosis**. Generally it appeared first in the superior layers of dermis and it progressively spread in the depth layers where a part of the oedema subsisted. On the third week, NMR imaging confirmed the development of necrosis by a whole loss of signal in the irradiated area in the skin structure which is clinicaly observed.

First steps in Nuclear **Magnetic Resonance Spectroscopy** of the irradiated pig skin allowed us to obtain spectras of irradiated and healthy skin, 24h and 3 weeks after irradiation.

It seemed also interesting to evaluate the importance of inflammation in acute early effects of irradiation, but also chronic inflammatory lesions in the skeletal muscle, which can accompany necrotic and late fibrotic process. **Inflammatory lesions can be visualized by scintigraphy with radionucleide Gallium-67.**

2 - 4. Scintigraphy

An uptake of the lesion was observed in the first week (day 3) and still last after a period of observation of 4 months with a ratio between 0.51 to 0.65. This uptake seemed to increase for 4 months and could be cutaneous, according to the results of biodistribution performed after 24, 48, 72h in 3 rabbits, sacrified at day 21, 28, 81 after irradiation. The values of skin lesion-to-safe skin ratio were respectively 6.7, 3.2 and 1.5.There was no difference of uptake between the left and right muscles in this biodistribution.

2 - 5. CT

A thickening of the skin appeared after four days post-irradiation (compared to the other side). The density of the skin lesion was higher than that of the safe skin (70-90 UH *vs* 25 UH). A modification of subcutaneous tissues was observed in the second week after irradiation: the fat disappeared and was replaced by a hypodense formation in comparison with the iliospinal muscle (40-45 UH *vs* 70 UH); its depth (3 mm) was relatively constant during a month. In the third week, a hypodensity appeared in the iliospinal muscle, located superficially, and spreaded for 4 months, time of observation. Fast, it was heterogeneous, with pseudo-liquid zones. In the fourth week, a hyperdensity was observed at the edge of the iliospinal muscle, with a density of 65 UH, which increased to 120 UH in the ninth week: it corresponded to a calcification in the lesion. The right iliospinalis muscle appeared to be thinner than the left in the eighth week.

2 - 6. Radiation-induced modifications of the skin microrelief

Studies of the early and late changes in skin following accidental or therapeutic irradiation have included observations of pigmentation, atrophy, fibrosis or telangiectasia. Telangiectasia has provided useful dose - response relationships when arbitrary scales have been aplied to its severity (Turesson, 1991). Irradiated skin often feels drier than normal, and it is a common clinical observation that sweating is reduced in irradiated skin. A pilot study in 28 irradiated patients, showed that 11 of them, with atrophy and telangiectasia, had no functional eccrine glands with a technique using silicone elastomer imprints of the skin (Morris et al., 1992).

However, the main characteristic of the skin surface is not the density of the eccrine glands but the existence of relief, which has been shown to exist for a very long time in the plantopalmar zones. It is only recently that it seemed interesting to analyze the other zones, and, although the skin relief vary from one zone to another, it presents many particular characteristics and varies under the influence of numerous parameters. These factors can be exterior (humidity, temperature, mechanical restrictions, chemical agents), UV radiation or interior (aging, drugs, or diseases). Exluding the palmoplantar zones, the relief of all the areas of the human body is composed of plateaus crossed by valleys. These valleys can be separated into very deep (~100mm) principal furrows that cover great distances and secondary furrows, more superficial and running through one or two plateaus and the replica technique is used to quantify the skin relief. The method consists of obtaining a silicone elastomer replica of the skin. This imprint reproduces the negative image of the surface to the smallest details. As a result of its insufficient hardness, it is necessary to make a second imprint of the replica using epoxy resin. It is therefore this second imprint that is then analyzed by the measuring instrument instead of the skin itself.

The most common method used to investigate skin topography is profilometry, generally consisting in a mechanical stylus, involving a direct contact between the positive second imprint and the tip of measurement or an optical profilometer based on a triangulation method, able to measure skin relief directly from first negative replica. Such an apparatus allows to quantify the skin surface either in 2 dimensions (2D) or in 3 dimensions (3D).

In a morphological analysis of a skin profile, classical filters such as RC filters or Gaussian filters cannot be used to separate the two families of furrows, but spectral or Fourier analysis of a skin profile is a possible method of filtering. The Fourier analysis of a skin surface profile allows the reconstruction of a simplified profile showing the presence of main furrows. The exact position of these furrows can then be detected, and the separation of all the furrows into two classes and their quantification become easy.

A preliminary study in the pig, of the irradiated skin topography showed a relative decrease of the vertical amplitude parameters (~15%) of the skin relief in three pigs irradiated with single doses of 90Sr-90Y β rays (32, 64 and 96 Gy under 7 mg.cm2; skin source distance: 2.6 cm) and one pig irradiated with a single dose of 92 Ir γ rays (160 Gy skin surface dose; skin source distance: 1.7 cm), 24 hours after irradiation whatever the dose.

This preliminary result has been reproduced **in a larger study group** of pigs irradiated with single doses of 90Sr-90Y β rays and a longer time period after irradiation, and showed similar results.
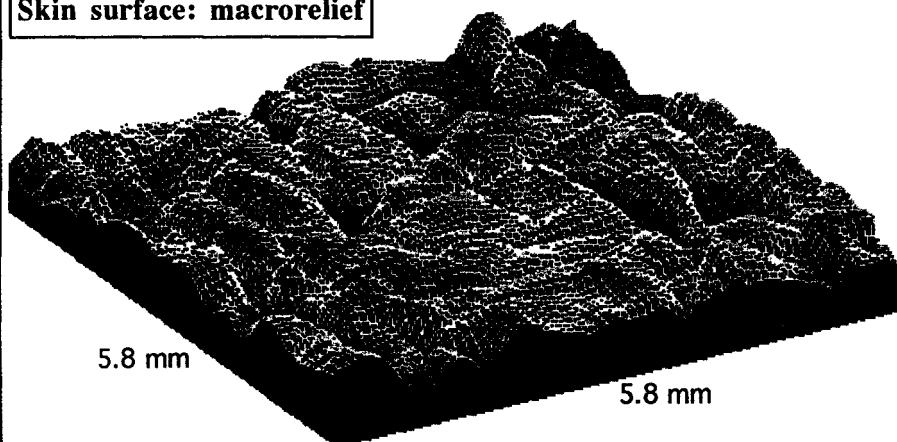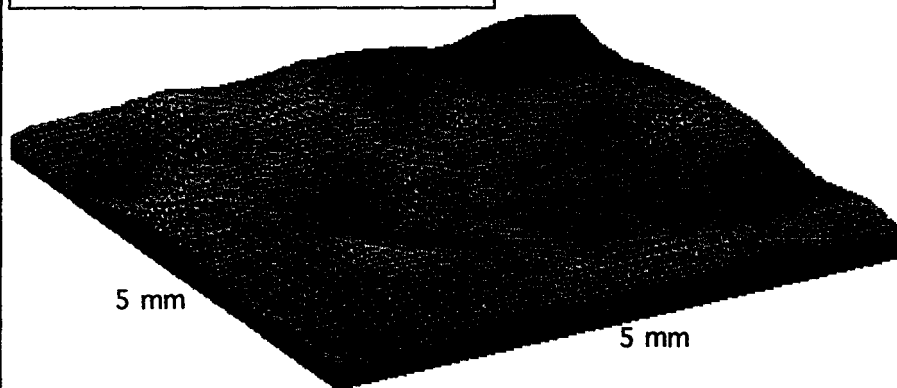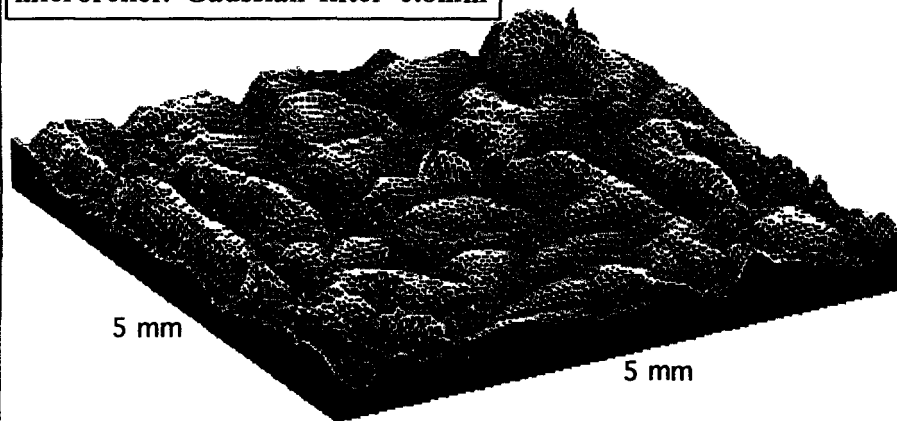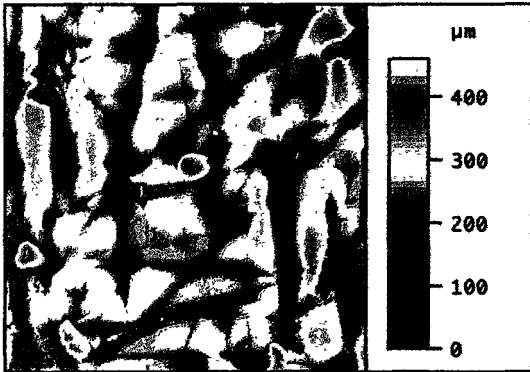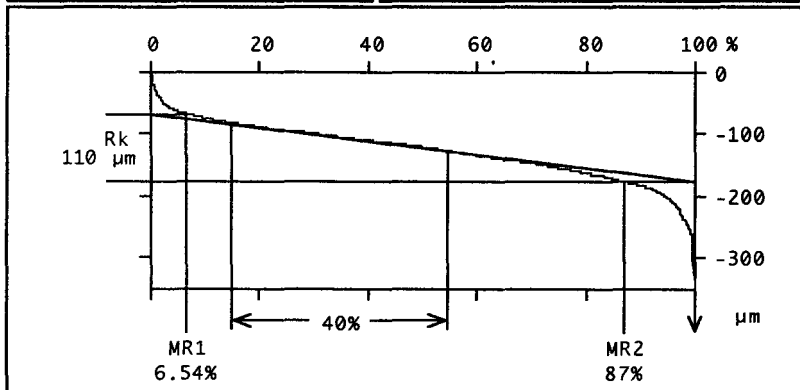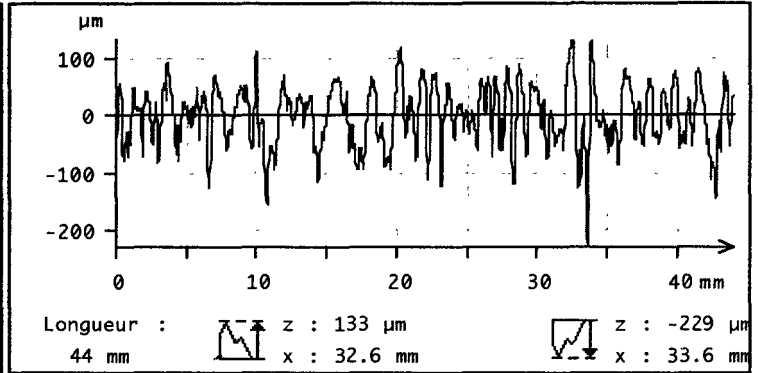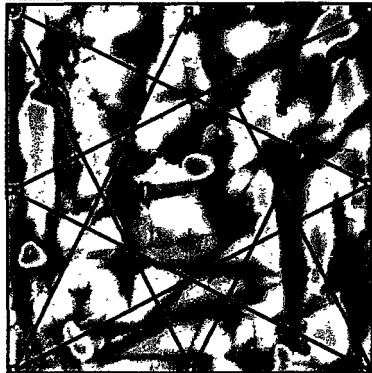
Pig skin microrelief 24 h after 64 Gy (β) irradiation

Pig skin microrelief roughness parameters

(Filter: 0.8 mm)

sRa	= 39.6	μm
sRv	= 246	μm
sRp	= 213	μm
sRt	= 458	μm
sRq	= 49.7	μm
sRsk	= -0.421	
sRku	= 3.39	

Longueur :   z : 133 μm   z : -229 μm
44 mm   x : 32.6 mm   x : 33.6 mm

Pig skin profile: roughness parameters

Ra	= 42.9	μm
Rv	= 229	μm
Rp	= 133	μm
Rt	= 362	μm
Rq	= 52.4	μm
Rsk	= -0.3	
Rku	= 3.01	
RSm	= 934	μm
RS	= 396	μm
Rpm	= 52.9	μm
Rtm	= 123	μm
Ry	= 361	μm

Rk
110 μm

MR1
6.54%

MR2
87%

40%

Roughness

R	= 59	μm
Rmax	= 261	μm
AR	= 378	μm
Pt	= 362	μm
Kr	= 0.312	

Ondulation

W	= 115	μm
Wmax	= 199	μm
AW	= 1405	μm
Wt	= 257	μm
Kw	= 0.164	

Pig skin profile: Rk parameters

Rk	= 110	μm
MR1	= 6.54	%
MR2	= 87	%
A1	= 108	μm
A2	= 380	μm
Rpk	= 32.9	μm
Rvk	= 58.4	μm
Rpk*	= 66.2	μm
Rvk*	= 173	μm

Pig skin microrelief 24 h after 64 Gy (β) irradiation

3 - Treatment

Pathophysiological evolution of a 192Ir γ-rays radio-induced muscular lesion was studied in experimental models developed in pigs and rabbits to simulate accidents which occured among humans. Cutaneous and muscular radionecrosis started from early epithelial, microvascular and vascular lesions, and late muscular and connective tissue lesions.

Our therapeutic studies in pigs have shown the interest of an early surgical treatment *a minima*. In rabbits, the association of non steroidal anti-inflammatory (flurbiprofène) and haemorheological agent (trimétazidine) among 10 other medical treatments, given for 8 weeks after an irradiation of 80 Gy single dose at the skin surface, involved a dose reduction factor of 2, with regards to the evolution of the skin injuries and the deep muscular fibronecrotic process.

Sub-cutaneous and muscular fibrosis are common and irreversible late effect of radiation on normal tissues. An experiment was designed in the pig to test the effectivness of superoxide dismutase in reducing late radiation-induced fibrosis. In this model, fibrosis appears in 4 to 5 months. The heterogenous sclerotic tissue is composed of stable fibrotic areas poorly cellularized and active areas with a high density of myofibroblasts and inflammatory perifibrotic part. Lipsod administration modalities were 6 intramuscular injections during 3 weeks (twice weekly) either 10 mg/inj (5 pigs) or of 100 mg/inj (5 pigs). A methodic evaluation by 2 examiners consisted in measures before and after treatment: sum of the 2 largest perpendicular measurable dimensions, cutaneous projected surface of palpated fibrotic block, ultrasound fibrosis deepness and extrapolated volume.

We conclude that Lipsod is the first drug ever described that reduces a radiation-induced fibrosis. Its efficacy in this model was highly significant, with a regression higher than 40% in size and 70% in surface and volume, 12 weeks after the end of treatment. This response was rapid, reproductible without dose-effect nor toxicity in the limits studied. This work confirms human results published recently in a long term follow up study.

4 - Mechanisms of late skin damage

1) The TGF-b1, a key cytokine

Although radiation-induced fibrosis has long been characterized by excess fibroblast proliferation and extracellular matrix deposition, the origin of cell activation in these late

effects of radiation accidents or radiotherapy is still controversial. Experiments were designed to test the hypothesis that an abnormal production of TGF-b 1 growth factor occured in irradiated tissues and resulted in continuous signals for tissue repair and long-term cell activation.

TGF-b1 growth factor gene expression was examined in a well-characterized pig model of radiation-induced fibrosis, using Northern-blot and indirect immunofluorecence. We found that the TGF-b mRNA level was increased at all stages of fibrosis development in this model, from the early erythematous phase 3 weeks after irradiation to the late phase when the wound healing process seems completed (Martin, 1993, 1).

TGF-ß expression
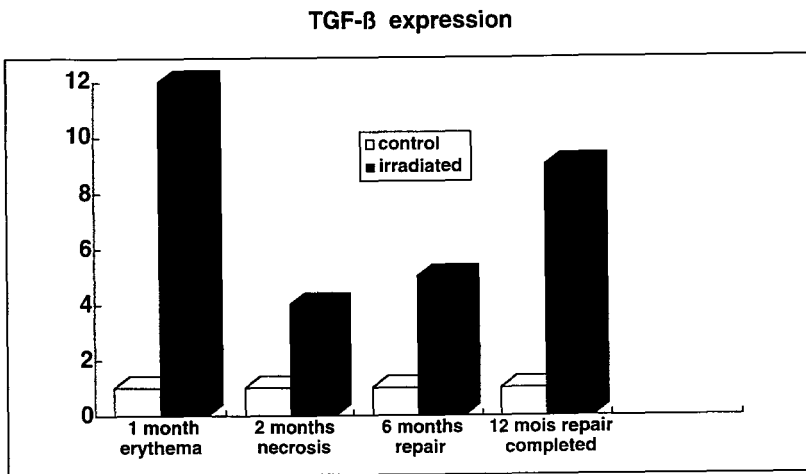
TGF-ß mRNA is overexpressed at all stages of fibrosis development

The cellular sources probably varied according to the time. The inflammatory cells might be the major source during the early erythema and later inflammatory phases. During the late phases of fibrosis development (6 months after irradiation to 2 years), we could demonstrate, using immunofluorescence, the presence of the protein in endothelial cells of capillaries, in myofibroblasts, and in the collagenous matrix of the fibrotic tissue. Cell culture was used to characterize the growth factor expression in myofibroblasts isolated from the fibrotic tissue. This allowed to show that this cell type is a major source of TGF-b. We postulate that autocrine loops of TGF-b activation might occur in fibrosis myofibroblasts.

Similar experiments were performed on human tissues of women treated with radiotherapy for breast cancer. Fibrosis was removed from 7 months to 4 years after irradiation. A concomitant increase gene expresion of TGF-b and collagen type I and III was observed in these fibrotic tissues (Delanian, 1992, 15).

2) Altered balance between proteases and protease inhibitors

We previously demonstrated that the abnormal deposition of the collagenous matrix in the fibrotic process was partly due to an enhanced synthesis of the matrix components by the myofibroblasts. The balance between synthesis and degradation was then investigated in the pig model of radiation fibrosis. Secretion of the major proteases and of their inhibitor, the TIMP (tissue metalloproteinase inhibitor), were studied in primary cultures of myofibroblasts. The results showed that an overall decrease in protease activity occured in the fibrotic cells, resulting both from transcriptional and post-transcriptional regulations. On the contrary, TIMP synthesis was significantly stimulated. In conclusion, the pathologic deposition of extracellular matrix results both from a decreased degradation of the matrix components and from an increased synthesis (Lafuma, 1994, 2).

3) Chromosomal anomalies

Cytogenetic studies were performed to further characterize the fibrotic cells (Sabatier, 1992, 18). It was found that most of the fibroblasts have structural chromosomal rearrangements. The rate and complexity of these rearrangements were higher than in any other pathological condition known, except in high-grade malignancies. However, no specific recurrent anomalies could be found. The fibroblasts constituting the fibrotic tissue then probably originated from irradiated cells. These results, in parallel with previous data on cell proliferation and differentiation, might suggest that the myofibroblasts from radiation-induced fibrosis are abnormal cells, which have carried out some of the early steps leading to cell transformation .

5 - Mechanisms of early events in irradiated skin

The results obtained on the TGF-b1 pointed out that the synthesis of this growth factor was upregulated during the first clinical phase of erythema, which occured 3 weeks after

irradiation of the pig thigh. In the literature, it was published meanwhile that ionizing radiation can induce a very early response in irradiated cells. This response was described as "the immediated early gene response". It occured within the first minutes and hours after irradiation and consisted in the activation of the transcription of genes involved in signal transduction and in the control of gene expression. A second wave of gene activation was described for growth factors like TNF. We first adressed the following question : does the TGF-b take part of a second wave of gene activation after irradiation in skin cells?

The possible induction of the growth factor was then investigated at various times after irradiation of the pig skin. It was found that both TGF-b1 and collagen type I mRNA were highly induced at 6 hours in the irradiated pig skin, during the first wave of gene response. These early inductions were found only after doses high enough to induce fibrotic lesions several months thereafter. These in vivo results suggest a role for the induction of early response genes in the pathophysiologic effetcs of ionizing radiation on skin (Martin, 1992, 3).

- Involvement of the AP-1 transcription factors

During the immediate early gene response to ionizing radiation, the activation of transcrition factors like AP-1, c-myc and NK-kB was recently demonstrated in cultured cells. As the TGF-b has an AP-1 motif in its promoters, we tried to answer the following question : is the AP-1 family of transcription factors involved in the early response of pig skin cells to gamma rays?

For that purpose, the induction of the c-fos and c-jun genes, which are major members of this AP-1 family, was studied by northern blot in skin samples irradiated in vivo. Following high radiation doses, 16 to 48 Gy, the two genes were concomitantly induced, although c-fos induction was preferential. Both inductions were time and dose dependent (Martin, 1993, 6; Martin, 1994, 1). Therefore; we could demonstrate that c-fos and c-jun inductions were part of the in vivo response of skin cells to high gamma doses. We postulated that these early activations played an important in inducing gene cascades initiating late tissue damage.

Publications

[1992 1] - Wegrowski J., Lefaix J-L , Lafuma C. Accumulation of glycosaminoglycans in radiation-induced muscular fibrosis. **International Journal of Radiation Biology, 1992, 61, 5, 685-693.**

[1992 2] - Delanian S., Martin M., Lefaix J-L. Expression des gènes TGFb1, collagène I et collagène III dans la fibrose cutanée humaine induite par une irradiation thérapeutique. **Bulletin du Cancer / Radiothérapie, 1992, 79, 613.**

[1992 3] - Martin M., Pinton P., Crechet F., Lefaix J-L. Ionizing radiation regulates expression of c-jun protooncogene and TGFb1 growth factor gene in normal skin **Journal of Investigative Dermatology, 1992, 98, 5, 820.**

[1992 4] - Lefaix J-L. (a). La radionécrose cérébrale. Méthodes d'étude en expérimentation animale. **S.T.A.L., 1992, 17, 135-143.**

[1992 5] - Lefaix J-L. (b). La radionécrose cérébrale. Limites et perspectives des modèles expérimentaux. **Radioprotection, 1992, 27, 3, 251-261.**

[1992 6] - Lefaix J-L. (c). Pathological features of cerebral radiation necrosis. Part I. Cerebral radiation necrosis in experimental animals. **Bulletin du Cancer / Radiothérapie, 79, 125-135.**

[1992 7] - Lefaix J-L. (d). Pathological features of cerebral radiation necrosis. Part II. Cerebral radiation necrosis in man. **Bulletin du Cancer / Radiothérapie, 1992, 79, 251-270.**

[1992 8] - Martin M., Lefaix J-L. Fibrose radio-induite: aspects cliniques, cellulaires et moléculaires. Introduction: la fibrose cicatricielle radio-induite. **Radioprotection, 1992, 27, 2, 174-180.**

[1992 9] - Martin M., Crechet F., Pinton P., Lefaix J-L., Daburon F. Expression du gène du TGFb dans un modèle expérimental de fibrose radio-induite. **Radioprotection, 1992, 27, 2, 186.**

[1992 10] - Lafuma C., El Nabout R., Hovnanian A., Martin M. Modification de l'expression des métalloprotéinases de la matrice extracellulaire (MPMs) et de leur inhibiteur tissulaire (TIMP) par les fibroblastes issus de fibrose porcine sous-cutanée post-radique. **Radioprotection, 1992, 27, 2, 187.**

[1992 11] - Sabatier L., Martin M., Crechet F., Dutrillaux B Fibrose cutanéo-musculaire radio-induite chez le porc approche cytogénétique. **Radioprotection, 1992, 27, 2, 188.**

[1992 12] - Lefaix J-L , Daburon F., Fayart G. Dosimetry study of an accidental overexposure to 192 Ir gamma rays. **Health Physics, 1992, 63, 6, 692-694.**

[1992 13] - Lefaix J-L., Daburon F., Tricaud Y.. Evolution radiopathologique spontanée et après traitement médical dans deux modèles d'accident d'irradiation localisée. **Bulletin du Cancer / Radiothérapie, 1992, 79, 189-198.**

[1992 14] - François-Joubert A.., Leviel J-L., Lefaix J-L., Lebail J-L. In vivo study of rabbit irradiated skeletal muscle by NMR imaging. **British Journal of Radiology, 1992, 65, congress supl., 67.**

[1992 15] - Delanian S., Martin M., Lefaix J-L. TGFb1 collagen I and III gene expression in human skin fibrosis induced by therapeutic irradiation. **British Journal of Radiology, 1992, 65, congress supl., 82-83.**

[1992 16] - Delanian S., Lefaix J-L., Martin M., Daburon F Efficacité thérapeutique majeure de la superoxyde dismutase liposomiale (Lipsod) dans la fibrose cutanéomusculaire. **Bulletin du Cancer / Radiothérapie, 1992, 79, 528.**

[1992 17] - Daburon F., Fayart G., Baradat M., Libotte S. Transfert du radiocésium présent dans du foin contaminé par les retombées de Tchernobyl à des brebis gestantes et à leurs produits à différents ages. **Radioprotection, 1992, 27, 4, 423-435.**

[1992 18] - Sabatier L., Martin M., Crechet F., Pinton P , Dutrillaux B. Chromosomal anomalies in radiation-induced fibrosis in the pig. **Mutation Research, 1992, 284, 257-263.**

[1993 1] - Martin M., Lefaix J-L., Pinton P , Crechet F., Daburon F. Temporal modulation of TGFb1 and b-actin genes expression in pig skin and muscular fibrosis after ionizing radiation. **Radiation Research, 1993, 134, 63-70.**

[1993 2] - Delanian S., Martin M.., Housset M.. La fibrose iatrogénique en cancerologie (I): aspects descriptifs et physiopathologiques. **Bulletin du Cancer , 1993, 80, 192-201.**

[1993 3] - Delanian S., Lefaix J-L., Housset M. La fibrose iatrogénique en cancerologie (II): principales étiologies et possibilités thérapeutiques. **Bulletin du Cancer , 1993, 80, 202-212.**

[1993 4] - Lefaix J-L., Delanian S., Tricaud Y., Martin M., Hoffschir D., Daburon F., Baillet F. La fibrose cutanéo-musculaire radio-induite (III)· efficacité thérapeutique majeure de la superoxyde dismutase Cu/Zn liposomiale. **Bulletin du Cancer , 1993, 80, 799-807.**

[1993 5] - Lefaix J-L., Martin M., Tricaud Y., Daburon F. Muscular fibrosis induced after pig skin irradiation with single doses of 192 Ir gamma rays. **British Journal of Radiology, 1993, 66, 537-544.**

[1993 6] - Martin M., Pinton P., Crechet F., Lefaix J-L., Daburon F Preferential induction of c-fos versus c-jun protooncogene during the immediate response of pig skin to gamma rays **Cancer Research, 1993, 53, 1-4.**

[1993 7] - Daburon F., Fayart G., Nublat F. Action des substances modifiant l'absorption du radiocésium et son excrétion par le lait chez les ovins. **Radioprotection, 1993, 28, 2, 163-172.**

[1993 8] - Chalansonnet A., El Kamouni N., Briguet A., Daburon F., Lefaix J-L. Mise en évidence des effets d'une irradiation aiguë localisée par imagerie de résonnance magnétique du tissu cutané. **Radioprotection, 1993, 28, 4, 411-421.**

[1994 1] - Martin M. Early induction of transcription factors by ionizing radiation· example of the skin radiation response. In Molecular mechanisms in radiation mutagenesis and carcinogenesis, 1994, K.H. Chadwick, R Cox, H. Leenhouts, J. Thacker, (eds.), European Commission, Brussels, pp. 233-238

[1994 2] - Lafuma C., Azzi El Nabout R., Crechet F , Hovnanian A., Martin M. Matrix metalloproteinases and tissue inhibitor of metalloproteinase expression in primary pig skin fibroblasts cultures derived from radiation-induced skin fibrosis. **Journal of Investigative Dermatology, 1994, 102, 945-950.**

[1994 3] - Biard D.S.F., Martin M., Le Rhun Y., Duthu A., Lefaix J-L., May E., May P. Concomitant p53 gene mutation and increased radiosensitivity in rat lung embryo epithelial cells during neoplastic development. **Cancer Research, 1994, 54, 3361-3364.**

[1994 4] - Delanian S., Bravard A., Luccioni C , Martin M., Lefaix J-L., Daburon F. Métabolisme anti-oxydant et fibrose cutanéo-musculaire radio-induite: modulation du phénotype fibroblastique par la superoxyde dismutase Cu/Zn bovine sous forme liposomiale (Lipsod) ? **Bulletin du Cancer , 1994, 81, 475.**

[1994 5] - Delanian S , Baillet F., Huart J., Lefaix J-L , Maulard C., Housset M. Successful treatment of radiation-induced fibrosis using liposomal Cu/Zn superoxide dismutase: clinical trial. **Radiotherapy and Oncology, 1994, 32, 12-20.**

[1994 6] - Lefaix J-L. Thèse d'Habilitation à Diriger des Recherches, Université Paris XI, 5 octobre 1994.

[1994 7] - Delanian S. Effet thérapeutique de la superoxyde dismutase Cu/Zn sous forme liposomiale dans la fibrose radio-induite cutanéo-musculaire· de la clinique à la biologie moléculaire. Thèse de Sciences, Université Paris V, 10 octobre 1994.

[1995 1] - Martin M., Crechet F., Ramounet B., Lefaix J-L. Activation of c-fos by low dose radiation. a mechanism of the adaptative response in skin cells? **Radiation Research, 1995, 141, 118-119.**

[1995 2] - Lefaix J-L., Mignot J. Modifications radio-induites du relief cutané: résultats préliminaires chez le porc; **Radioprotection, 1995, 30, 2, 221-233.**

[1995 3] Delanian S. & Lefaix J-L. Fibrose après radiothérapie· mécanisme, prédiction, possibilité thérapeutiques. **Revue de Presse et d'Oncologie Clinique, 4, 2, 1-4.**

[1995 3] Lefaix J-L & Daburon F. Diagnosis of acute localized irradiation. In *"Radiological Accident: The injured victims. logistic, Diagnostic and therapeutic approaches, in case of accidental irradiation and contamination".* April 1995, Grenoble, France.

[1995 4] Daburon F & Lefaix J-L. Treatment assays of acute localized irradiation. In *"Radiological Accident· The injured victims. logistic, Diagnostic and therapeutic approaches, in case of accidental irradiation and contamination".* April 1995, Grenoble, France.

[1995 5] Leviel J-L., François-Joubert A., Ibarrola D., Lefaix J-L. Suivi au long cours par RMN in vivo de l'irradiation localisée du muscle squelettique du lapin In *"Radiological Accident: The injured victims. logistic, Diagnostic and therapeutic approaches, in case of accidental irradiation and contamination".* April 1995, Grenoble, France.

[1995 6] - Chalansonnet A., Bonnat J-L., Fenet B., Briguet A., Lefaix J-L. Detection of early effects of a skin irradiation by NMR imaging and specroscopy. In *"International Conference on Radiation Protection and Medicine",* june 1995, Montpellier, France.

[1995 7] - Chalansonnet A., Bonnat J-L., Briguet A., Lefaix J-L. Dosimetry of irradiated agarose gels by NMR imaging. In *"International Conference on Radiation Protection and Medicine",* june 1995, Montpellier, France.

[1995 8] - Lefaix J-L., Rahmouni A., Dao T.H., Vasile N., Lafuma C. Nuclear magnetic resonance of acute irradiation induced fibrosis: experimental study in the rabbit. In *"International Conference on Radiation Protection and Medicine",* june 1995, Montpellier, France.

[1995 9] - Albérini J-L., Dazord L., Bourguet P., Lefaix J-L. Gallium-67 and X-rays computerized tomography imaging in acute irradiation lesions: experimental approach in the rabbit.. In *"International Conference on Radiation Protection and Medicine",* june 1995, Montpellier, France.

[1995 10] - Lefaix J-L & Daburon F. Accidental localized irradiation with γ or β rays: an experimental approach of the biological dosimetry. In *"International Conference on Radiation Protection and Medicine",* june 1995, Montpellier, France

[1995 11] Daburon F & Lefaix J-L. Acute localized γ irradiation· treatment assays in pigs and rabbits In *"International Conference on Radiation Protection and Medicine",* june 1995, Montpellier, France.

[1995 12] - Martin M. Thèse d'Habilitation à Diriger des Recherches, Université Paris XI, septembre 1995.

Cooperating scientist: H. Magdelénat
Laboratoire de Radiopathologie - Physiopathologie, Institut Curie, 26 rue d'Ulm, 75231 PARIS cedex 05

Objectives:

1 - Physiopathology of the irradiated skin (patients and experimental models)

> Histochemical/Immunohistochemical study
> Nuclear Magnetic Resonance Imaging (animal model)

2 -Treatment of localized radiation-induced fibrosis by Superoxyde dismutase (SOD)

> Pathological study and clinical follow up

Progress achieved including publications

1 - Physiopathology of the irradiated skin

1.1 -Human physiopathology

The immunohistochemical study of human skin biopsies from irradiated patients (20-40 Gy) demonstrated that dermal fibroblasts acquire an activated "myofibroblastic" phenotype, characterized by the expression of smooth muscle cells-a-actin cytoplasmic microfilaments, in particular at the dermal-epidermal junction. Desmin immunodetection was negative, as in normal skin.

Epidermal Growth Factor- Receptors (EGFR) were overexpressed by all the cellular layers of the epidermis, up to 10 years after irradiation. Since normal epidermis only faintly express EGFR in cells of the basal layer, overexpression of EGFR appears as a pathognomonic indicator of previous irradiation.

In biopsies of irradiated skin (30 samples), dermal fibroblasts and suprabasal layers of epidermal cells strongly expressed Transforming Growth Factor-b (TGF b1). The immunolocalisation was essentially intranuclear. Normal skin biopsies (10 samples) disclosed faint TGFß1 immunoreactivity, mainly in the intercellular matrix of the dermis and in the cytoplasm of keratinocytes.

No quantitave modification of the steady state TGFb mRNA expression could be detected by Northern Blot analysis of skin biopsies. The immunohistochemical detection, using two anti-TGFß1 polyclonal antibodies, demonstrated an irradiation-dependent expression of TGFß1 which appeared localized in the nucleus of fibroblastic cell cultures from explants of g-irradiated human skin. The immunolocalisation was also nuclear in cultured normal human skin fibroblasts after in vitro g-irradiation at 2, 4 and 6 Gy. Sequential analysis of TGFß immunolabelling of fibroblasts nuclei, 1, 3, 6, 12, 24, 48, 72 and 96 hours after irradiation in vitro, demonstrated that the nuclear localization appeared as early as 3 hours after g-irradiation and remained untill 48 hours. The labelling became diffuse at 72 hours and was mainly cytoplasmic at 96 hours.

The sequential ARN-Polymerase Chain Reaction (RT-PCR) analysis did not show a consistent variation of intrafibroblastic TGFß1 mRNA, at least for the time course studied.
These data suggest a role for TGFß in the regulation of gene expression in mesenchymal and epithelial cells, the alteration of this expression ultimately resulting in radiation induced skin fibrosis.

Platelet Derived Growth Factors (PDGFAA, BB and AB) are known to play a role in wound healing.An immunohistochemical study showed that PDGF Receptor-b are overexpressed in the dermal fibroblasts of biopsies of irradiated skin, compared to normal skin, both by the number of stained cells and the staining intensity.
These immunocytochemical observations were reproduced on normal fibroblasts grown and irradiated (2-6 Gy)*in vitro*.

In vitro irradiated dermal fibroblasts displayed membrane ruffling and actin circular formations (phalloidin labelling) 24 hour after irradiation (4 Gy) and serum deprivation.Ruffling increased when PDGF BB was added to the serum deprived medium. Membrane ruffling was induced in non-irradiated and in fibroblasts irradiated at 2 Gy only after incubation with PDGF BB. This type of actin reorganization is mediated by the PDGF Receptorß , through its protein-tyrosine kinase activity. Further investigations are necessary to understand the dose dependent PDGF receptivity of irradiated fibroblasts.

These data emphasize the role and the complex interactions of cytokines in the physiopathology of radiation induced skin fibrosis.

1.2 -Animal model

In 1993, 22 rabbits New-Zealand were irradiated at 120 Gy on the back, (skin surface dose; Dr J-L. Lefaix, CEA-DSV-Laboratoire de Radiobiologie Appliquée, 91191 Gif sur Yvette), then examined regularly (twice a month) by 1.5 Tesla proton nuclear magnetic resonance imaging (MRI; Dr Thua Dao & Dr A. Rahmouni, Département de Radiologie, Hopital Henri Mondor, Créteil). Eight of them were surgically biopsied to study the histological evolution from the early inflammatory reaction towards late fibrosis and the alterations of the prolin/hydroxyprolin ratio. Fibrosis was graded from 0 to 4 by Sirius Red staining and spectrophotometry.

NMR imaging was modified in the irradiated field as early as the 2d week after the irradiation, indicating oedematous and vascular changes, with a T2 hypersignal persisting with no modification until the 8th month, when contrast enhancement restricted only to the periphery of the lesion. At 8 weeks, grade 1 skin fibrosis appeared, after a period characterized by the presence of inflammatory cells, increase of oedema in the dermis and microvascularization in the underlying muscular tissue. Muscular grade 1 fibrosis (optical density/mm2 between 0.8 and 1, after Red Sirius stain) was observed 15 weeks after irradiation. Between 7 and 8 months, fibrosis increased and reached grade 2, replacing partially melted muscular fibers. The microvascular network was reduced.

This work is not completed.

2 -Topical treatment of localized radiation-induced fibrosis by (SOD)

2-1 Objective grading of fibrosis

The extent of fibrosis was graded on histological sections, using an histochemical staining of collagen fibers by Red picrosirius, described by Junqueira et al (1979). Briefly, this method stains collagen fibers in red on fixed paraffin embedded tissue sections and cryosections. The sections were eluted with NaOH 1N and Optical Density (O.D.) was measured with a spectrophotometer at $\lambda = 540$ nm. This permits an objective evaluation of the amount of collagens, and the dermal fibrosis was classified in 5 grades, from 0 (normal dermis) to 4 (deep fibrosis), according to the O.D. per mm2 of skin section (Table 1). Skin area was measured by microplanimetry.

Table 1: Sirius Red spectrophotometric grading

Grade	[OD 540/mm2]
0	< 0.0025
1	0.0025-0.01
2	0.011-0.020
3	0.021-0.030
4	> 0.031

2-2 Histological and immunohistochemical study

A controlled study, concerning 44 patients with cutaneous radiofibrosis following conservative breast cancer treatment, was conducted in 1992 to evaluate, in addition to clinical and physiological parameters, the histological and histochemical response to SOD treatment. Patients were treated with topical application of bovine SOD (3650 U/mg) incorporated in a polyethylene glycol oinment at a daily dose of 2 x 800 U for 90 days (total dose : 150 000 U or 40 mg SOD). Skin punch biopsies (3 mm diameter) were taken from 42 informed patients before and 3 months after completion of treatment. Skin fibrosis was graded on Haematoxylin-Eosin and picro-Sirius Red stained cryosections, quantified by the eluated O.D./mm2 (see above). The fibroblastic phenotype (vimentin, SMC a-actin) and the expression of TGF b or EGF receptor were studied by immunohistochemistry, using specific monoclonal or polyclonal antibodies and an avidin-biotin complex for the revelation of the labelling. The labelling was scored from 0 to 4, taking into account the percentage of stained cells and the staining intensity.

Before treatment, 41/42 (98%) patients presented with grade 2 to 4 dermal radiofibrosis and one with grade 1. Fibosis grade increased with time from irradiation.

Three months after completion of topical SOD treatment, fibrosis grade significantly decreased in 31/41 (74%) patients. The mean score dropped from 3.1 to 1.9 (-37%), with a mean change of 1.1 ($p<0.001$). Immunohistochemistry demonstrated no significative changes in vimentin or TGF b expression after treament with SOD, but an increase of the SMC a-actin positive fibroblastic phenotype, with a mean score increasing from 1.40 to 2.0 (+57%), and of the EGF-receptor score in epidermal cells, the mean score increasing from 1.6 to 2.4 (+54%). The mean scores increased by 0.6 ($p<0.001$) for SMC a-actin and by 0.8 ($p<0.001$) for EGFreceptors.

These results provide an objective histological support for the clinical efficacy of SOD in the treatment of late radiation-induced skin fibrosis

2-3 Long term clinical follow up of SOD treated patients

Till now, a total of 132 patients have been treated by topical SOD for radiation induced fibrosis (150 000 IU over 90 days) and are followed by numerical telethermography, dynamic cryostimulation and clinical evaluation. 77 with a follow up longer than 18 months (55 with follow up between 18 and 24 months, 19 between 30 and 36 months and 6 between 42 and 72 months) were evaluated. Compared to the response at 12 months, 50 % of these patients show a continuous improvement of the fibrotic lesions, 30 % a durable stabilisation and 20 % a slight deterioration. Thus, the effect of topical SOD appears durable after initial treatment.

Publications

Benyahia B , Magdelénat H. Immunohistochemical charaterization of human g-irradiated skin Bull Cancer/Radiother, 1993, 80,126-134

Perdereau B, Campana F, Vilcoq JR, de la Rochefordiere A, Barbaroux C, Fourquet A, Magdelénat H Superoxyde dismutase (Cu/Zn) en application cutanée dans le traitement des fibroses radio-induites. Bull Cancer, 1994, 81, 659-669

Benyahia B, Campana F, Perdereau B, Gez E, Fourquet A, Magdelénat H. The effects of superoxide dismutase topical treatment on human skin radiofibrosis: a pathological study. The Breast (in press 1995).

Benyahia B, Magdelenat H. Nuclear localization of transforming growth factor ß in fibroblasts and epidermal cells of human g-irradiated skin. (submitted)

Participating scientists

Benyahia B

Campana F

Dao T H

Lefaix J-L

Magdelénat H

Perdereau B

Rahmouni A

Head of Project 2:   **Dr. J.W. Hopewell**

II.   Objectives of the reporting period

The reported studies have been undertaken on pig skin, a species whose skin is the most similar to human skin. The principle objectives for the reporting period 1st September 1992 - 30 June 1995 have been as follows:-

- the time course of the development of late dermal thinning after ^{90}Sr/^{90}Y irradiation.
- the time course of the development of late dermal thinning after ^{170}Tm-irradiation.
- a comparison of data obtained from ^{170}Tm-irradiation with those obtained for ^{90}Sr/^{90}Y irradiation.
- a comparison of the effects of mixed ß and photon exposure with ß-irradiation alone.
- an evaluation of the effects of low-dose-rate radiation on the skin.
- a study of increased adhesion molecule expression on endothelial cells after irradiation.
- prevention of early and late radiation-induced skin lesions by essential fatty acids (EFAs).

III.   Progress achieved including publications

Development of late dermal thinning after ^{90}Sr/^{90}Y irradiation:

Time-related changes in skin thickness have been evaluated in the pig using a non-invasive ultrasound technique after exposure to a range of single doses of ß-rays from 22.5 mm diameter ^{90}Sr/^{90}Y plaques. A reduction in relative skin thickness developed in two distinct phases (Fig 1). The first phase was between 12 weeks and 20 weeks after irradiation. No further changes were then seen until 52 weeks after irradiation when a second phase of skin thinning was observed. This was complete after 76 weeks and no further changes in relative skin thickness were seen in the maximum follow up period of 129 weeks. The timing of these phases of damage was totally independent of the radiation dose. However, the severity of both phases of radiation-induced skin thinning was dose-related.
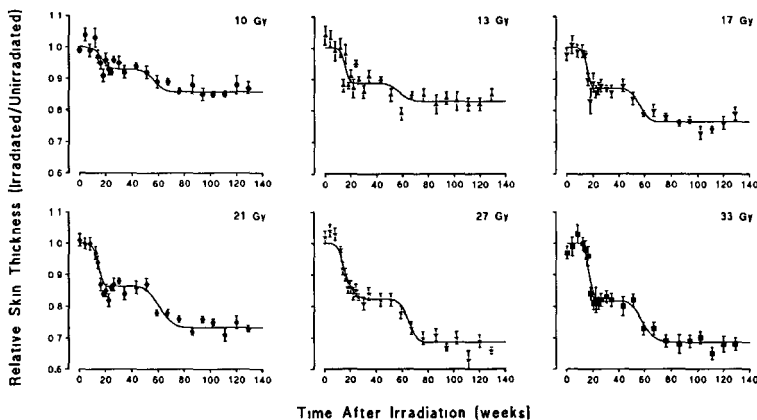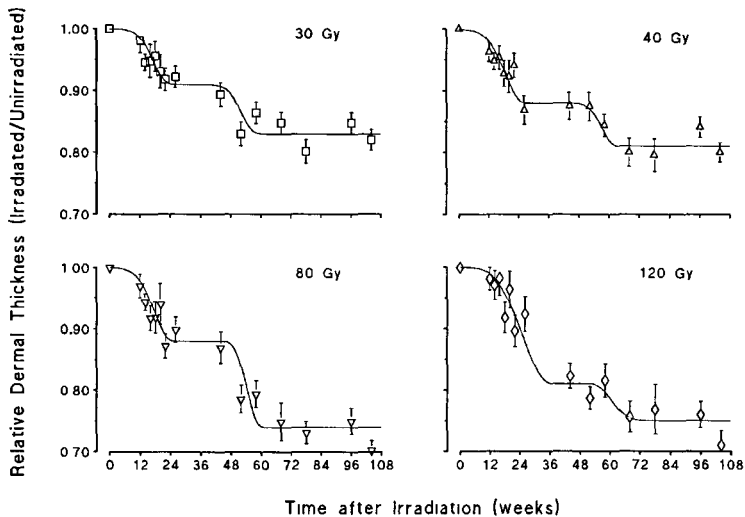

Figure 1: Time-related changes in the relative thickness of irradiated skin compared with adjacent areas of unirradiated skin of the pig after exposure to ^{90}Sr/^{90}Y ß-rays.

Development of late dermal thinning after ¹⁷⁰Tm irradiation:

Time-related changes skin thickness were also evaluated after exposure to a range of single doses of ß-rays from a 20 mm x 40 mm ¹⁷⁰Tm plaque. The same non-invasive ultrasound technique was used as for after ⁹⁰Sr/⁹⁰Y irradiation. The pattern of development of skin thinning was again biphasic and similar to that after irradiation with ⁹⁰Sr/⁹⁰Y plaques. The first phase of reduction in relative skin thickness developed between 12 and 20 weeks after irradiation. There were no further changes in the thickness of the irradiated skin until approximately 50 weeks after irradiation when the second wave of development of reduction in relative skin thickness was seen.

Figure 2: Time-related changes in the relative thickness of irradiated skin compared with adjacent areas of unirradiated skin of the pig after exposure to ¹⁷⁰Tm ß-rays.

Comparison of data obtained from ¹⁷⁰Tm-irradiation with those obtained for ⁹⁰Sr/⁹⁰Y irradiation:

The biphasic pattern of development of skin thinning was similar after both ⁹⁰Sr/⁹⁰Y and ¹⁷⁰Tm irradiation. However, the degree of skin thining after ⁹⁰Sr/⁹⁰Y was considerably greater than that after ¹⁷⁰Tm irradiation for the same skin surface dose. This was more evident when the average relative skin thickness measurements, obtained over the periods 20-51 weeks and 76-129 weeks after irradiation, were plotted against dose (Fig 3). Both phases of radiation-induced skin thinning were dose-dependent and had a steep initial portion to the dose-effect curve, which tended to become shallower at higher doses. The shape of the dose-effect curves were the same in both cases but the degree of dermal thinning was greater in the case of ⁹⁰Sr/⁹⁰Y irradiation compared with ¹⁷⁰Tm irradiation. This was due to the difference in depth dose characteristics of ⁹⁰Sr/⁹⁰Y and ¹⁷⁰Tm β-rays ⁹⁰Sr/⁹⁰Y emits 2.27 MeV ß-rays which are more penetrative than ß-particles of 0.97 MeV emitted from ¹⁷⁰Tm.

The iso-doses relative to the skin surface dose, for 2.27 MeV and 0.97 MeV ß-rays suggest that in case of ⁹⁰Sr/⁹⁰Y irradiation, about 95% of the skin surface dose reaches the papillary plexus and around 50% reaches the deep dermal plexus. After ¹⁷⁰Tm irradiation less than 10% of the surface dose is received by the dermal plexus.

However, when the skin thinning after $^{90}Sr/^{90}Y$ and ^{170}Tm irradiations were expressed in terms of dose at 900 mm depth, the mid-dermis depth, comparable results were obtained from both radiation qualities. This was true for both the early and late phases of dermal thinning (Fig. 4).
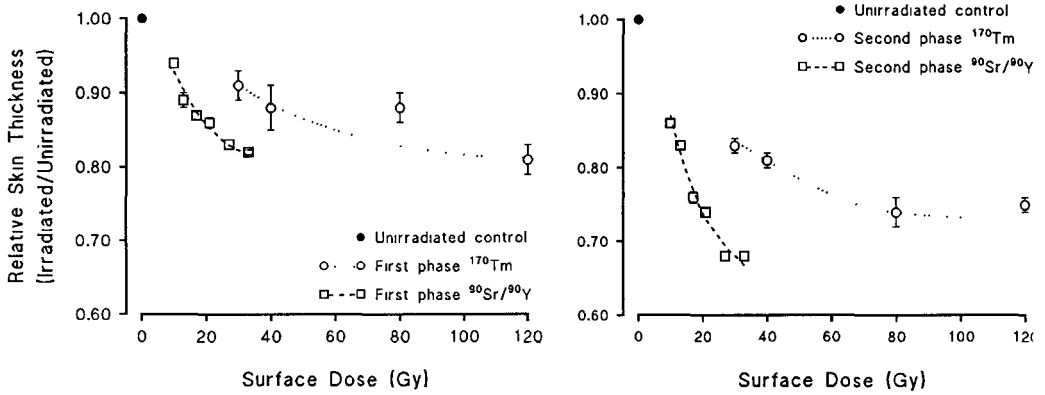

Figure 3: Relative skin thickness against skin surface dose after irradiation with $^{90}Sr/^{90}Y$ or ^{170}Tm ß-rays.
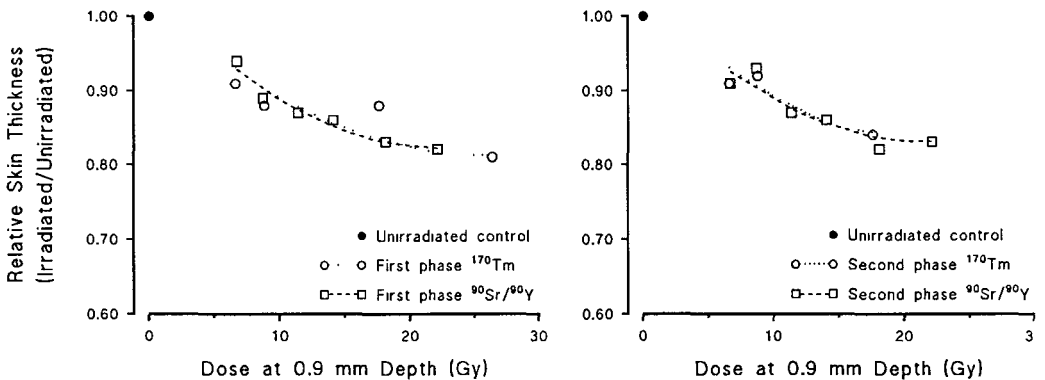

Figure 4: Relative skin thickness against dose at 900 mm depth of skin after irradiation with $^{90}Sr/^{90}Y$ or ^{170}Tm ß-rays.

This implies that the target cells responsible for both early and second phase of skin thinning in irradiated pig skin are located at around 900 mm depth. This corresponds to a layer in reticular dermis of pig skin. This also suggests that skin dose should be assessed at a depth in the skin, rather than the surface, to predict responses from ß-emitters of differing energy.

Comparison of the effects of mixed ß and photon exposure with ß-irradiation alone:

Exposures to mixed radiation qualities are a feature of many radiation accidents. In this study irradiation was with 5 mm or 2 mm diameter $^{90}Sr/^{90}Y$ plaques in a 4 cm x 4 cm field concurrently irradiated with a fixed dose of 10 Gy of 250 KV X-rays. Irradiation schedules, the incidence of moist desquamation and the mean latency period for the development of moist desquamation are shown in Tables 1 and 2.

Table 1: Incidence of moist desquamation and its mean latency in pig skin after irradiation with ß-rays from 5mm diameter $^{90}Sr/^{90}Y$ plaques or with ß-rays and X-rays.

| Dose (Gy) | | moist desquamation | Mean latency period |
ß-rays	X-rays		±SE (weeks)
25	10	0/12	N/A
35	0	4/12	6.0 ± 0.00
50	10	8/12	5.80 ± 0.22
60	0	6/12	6.40 ± 1.00
70	10	11/11	5.40 ± 0.25
80	0	9/12	5.06 ± 0.40
95	10	12/12	4.75 ± 0.22
105	0	12/12	4.90 ± 0.30

N/A   not applicable

Table 2: Incidence of moist desquamation and its mean latency in pig skin after irradiation with ß-rays from 2mm diameter $^{90}Sr/^{90}Y$ plaques or with ß-rays and X-rays.

| Dose (Gy) | | moist desquamation | Mean latency period |
ß-rays	X-rays		±SE (weeks)
110	10	6/12	5.75 ± 0.23
120	0	2/12	5.50 ± 0.00
155	10	9/12	4.55 ± 0.28
165	0	8/12	4.72 ± 0.26
185	10	11/12	4.36 ± 0.20
195	0	11/12	4.36 ± 0 24
230	10	12/12	3.79 ± 0.22
240	0	12/12	3.75 ± 0.27

There was no significant difference in the incidence of moist desquamation and latency period for moist desquamation between fields irradiated with ß-radiation alone and ß- plus X-rays to a larger area (Table 3).

Table 3. ED_{50} values (Gy $\pm$SE) for the incidence of moist desquamation after exposure of pig skin to ß-rays from $^{90}Sr/^{90}Y$ plaques of 5 mm and 2 mm diameter in 4 cm x 4 cm sites concurrently irradiated with 10 Gy of 250 kV X-rays.

Protocol	$^{90}Sr/^{90}Y$ source diameter	
	5 mm	2 mm
ß-rays	54.0 ± 10.0	151.8 ± 12.7
ß-rays + X-rays	57.3 ± 5.5	122.0 ± 45.9

Evaluation of the effects of low-dose-rate radiation on the skin:

Studies of early and late reactions to exposures from radiations of differing dose-rate were carried out, as such data is required for the continued improvement of radiological protection guidelines for the skin. Most of the experimental data presently available for deterministic effects relate to high dose-rate exposure, a high proportion of accidental industrial irradiations are the consequence of lower-dose-rate contamination.

In this study, irradiation was with standard 22.5 mm diameter $^{90}Sr/^{90}Y$ plaques, giving dose rates of 10.7 cGy/min, 5.2 cGy/min and 2.4 cGy/min to total doses which ranged from 18-100 Gy. The specific range was dependent on the dose-rate. This involved exposures lasting from 2.8 hr to 69.5 hr. These long exposures were carried out on un-anaesthetised pigs, the sources being held in a plastic holder that could be stitched to the skin surface. This procedure was carried out under full anaesthesia and the sources were fixed to the holders just prior to recovery. A brief anaesthetic was required to remove $^{90}Sr/^{90}Y$ sources   The dose-response relationships for the incidence of early moist desquamation and for late ($\geq$15 months) dermal thinning were compared with those for acute exposures i.e. ~300 cGy/min exposures.

The dose-related incidence of moist desquamation, noted within the first 10 week period after exposure, is shown in Figure 5. Clearly dose-rate has a marked effect on the dose-related incidence of this acute radiation reaction; doses of 30-40 Gy, usually associated with a very high incidence of desquamation after acute exposure showed an incidence of <20% after low dose-rate irradiation. The doses associated with a 10% (ED_{10}) or a 50% (ED_{50}) incidence of moist desquamation, for the different dose-rate exposures are listed in Table 4, both increase with the decrease in dose-rate.

Late changes in dermal thickness were assessed at 72 weeks after low dose-rate irradiation, a time point at which previous investigations (Rezvani *et al.*, 1994) have indicated that the ratio of the thickness of irradiated to unirradiated skin to be maximum, this not changing by further increasing the observation time to 130 weeks. Dermal thickness was measured in histological sections of tissue taken from the centre of irradiated sites. A comparison was always made with measurements from unirradiated skin sites on either side of the irradiated sample in order to minimise the effects of regional variations in dermal thickness on the flank of pigs.
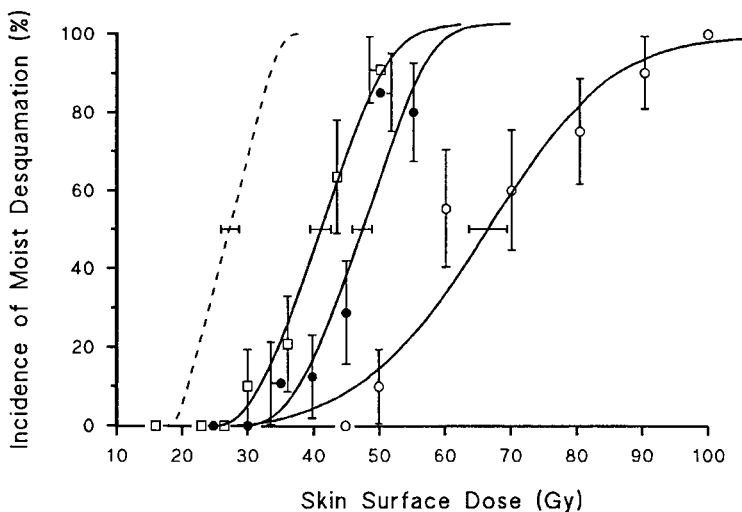
Figure 5. Dose-related changes in the percentage incidence of skin sites on pigs showing moist desquamation after irradiation with 22.5 mm diameter $^{90}Sr/^{90}Y$ plaques with dose rates of ~300 cGy/min (- - - -); 10.7 cGy/min ($\square$); 5.2 cGy/min ($\bullet$); or 2.4 cGy/min (O). Error bars indicate ±SE. The ED_{50} values (±SE) are indicated for each dose-rate.

Table 4. Variation in ED_{10} and ED_{50} values for moist desquamation after irradiation with 22.5 mm diameter $^{90}Sr/^{90}Y$ plaques of differing dose-rate.

Dose-rate	Iso-effective doses (Gy)	
(cGy/min)	ED_{10}	ED_{50}
300	21.1	27.3
10.7	31.9	41.1
5.2	37.8	47.0
2.4	46.8	66 5

The dose-related variations in relative dermal thickness are illustrated in Figure 6. The severity of late radiation damage was clearly reduced by the reduction in dose-rate from ~300 cGy/min to 5.2-10 7 cGy/min. A further marked reduction in the severity of the reaction was produced by the reduction in dose-rate to 2.4 cGy/min. These data were further assessed to determine the dose-related incidence of skin sites showing either a ≥20% or a ≥30% reduction in relative dermal thickness. From these dose-effect curves the dose associated with a 50% incidence of the specified response (ED_{50}) could be determined (Table 2). The ED_{50} values increase with the increase in levels of effect assessed and with the decrease in dose-rate.
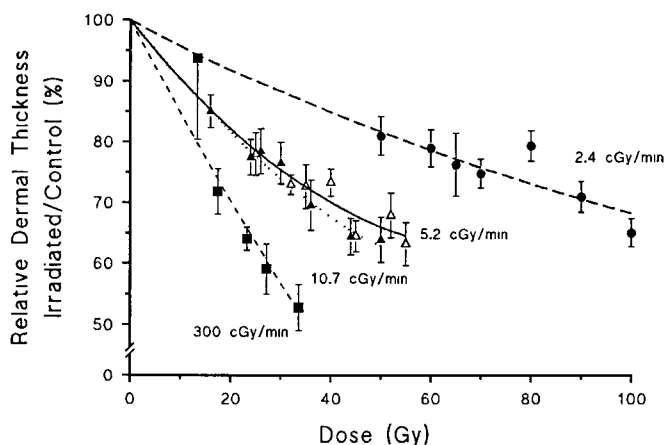
Figure 6. Dose-related changes in the relative dermal thickness (irradiated/unirradiated) of pig skin ≥72 weeks after irradiation with 22.5 mm diameter plaques of $^{90}Sr/^{90}Y$ of dose-rate ~300 cGy/min (■); 10.7 cGy/min (▲); 5.2 cGy/min (△) or 2.4 cGy/min (●). Error bars indicate ±SE.

Table 5. Variation in ED_{50} values for a ≥20% and a ≥30% reduction in relative dermal thickness in pig skin at ≥72 weeks after irradiation from 22.5 mm diameter $^{90}Sr/^{90}Y$ plaques of differing dose-rate.

| Dose-rate | ED_{50} ±SE (Gy) for dermal thinning | |
(cGy/min)	≥20%	≥30%
300	10.27 ± 1.73	17.13 ± 1 69
10.7	20.65 ± 2 34	37.84 ± 3.93
5.2	23.01 ± 2.92	39.72 ± 3.85
2.4	59.16 ± 6 55	100.69 ± 1.39

These iso-effective doses for both acute and late radiation-induced damage to pig skin, after exposure to different dose rate sources, have been used to calculate the dose reduction factors (DRFs) associated with the lower dose-rate irradiations. The relationships between the DRFs and dose-rate for the endpoints of early moist desquamation and late dermal thinning (at two levels of effect) is shown in Figure 7. There would appear to be a good linear relationship between the DRF and the log of the dose-rate for both the early and the late endpoint (correlation co-efficient ≥0.96). The relationship for late damage appeared to be independent of the level of effect used to evaluate damage With a reduction in dose-rate, late damage would appear to be spared more than early damage and hence early lesions become of greater concern in situations of low dose-rate contamination of the skin.
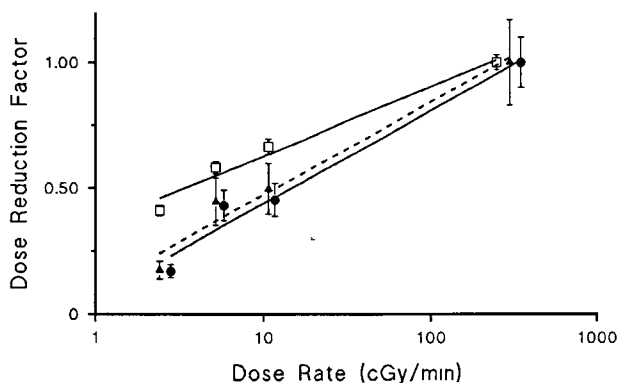
Figure 7. Variation in the dose reduction factor (relative to ~300 cGy/min) with dose-rate for early moist desquamation (□) or late dermal thinning (≥20% ▲; ≥30% ●) in pig skin. Error bars indicate ±SE.

Study of the role of increased adhesion molecules expression on endothelial cells in the pathogenesis of both early and late radiation damage to the skin:

An important component of an inflammatory response is the localisation of leukocytes at the sites of inflammatory lesions. Adhesive molecules, present on the surface of the endothelial cells and leukocytes, play a major role in endothelium-leukocyte interactions. Before leukocytes are attracted to the endothelium, they must first adhere to the vascular endothelium. It has been shown *in vivo* that the earliest changes noted following localised irradiation of the kidney appear to be leukocyte adhesion to the endothelial cells of the glomerular capillary loops.

In the study of early and late radiation-induced skin lesions, the expression of endothelial-leucocyte adhesion molecule (ELAM-1) was examined. Skin fields of 4 cm x 4 cm, on the flanks of pigs, were irradiated with 18Gy of X-rays. In this model 18 Gy of 250 kV X-rays is well tolerated. It causes no moist desquamtion or necrosis but bright red erythema was seen in about 45% of the cases Skin fields were removed surgically at intervals of 2, 4, 6, 8 and 10 weeks after iradiation. After excision of the irradiated field a 1.5 cm x 1.5 cm skin specimen was removed and processed for histochemical identification of ELAM-1 using a primary antibody to the adhesion molecules. Staining was with fast red in association with a secondary antibody (Dako-D651).

ELAM-1 expression was assessed by a light microscopy using an arbitrary score of 0 = none, 1 = minimal, 2 = moderate and 3 = strong expression. This scoring system takes into account the quality and quantity of red staining observed in histological sections.

The average score for ELAM-1 expression with respect to time after irradiation is shown in Figure 8. Irradiation induced ELAM-1 expression within 2 weeks after irradiation and reached its maximum at around 4 week after irradiation This had subsided around 10 weeks after irradiation. This time related expression of ELAM-1 corresponds very closely to the manifestation of radiation-induced skin erythema.
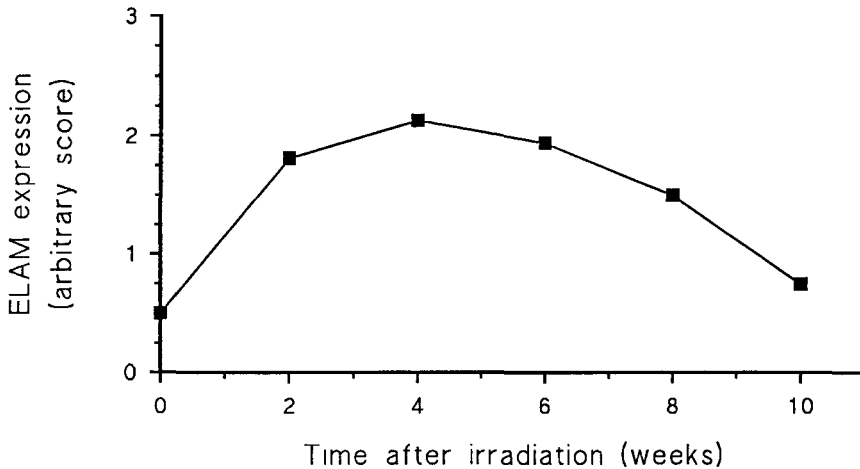
Figure 8: ELAM-1 expression in irradiated pig skin with time after irradiation.

Prevention of early and late radiation-induced sequelae in the skin: the potential beneficial effects of the use of essential fatty acids (EFAs):

To assess the ability of EFAs to ameliorate early and late radiation-induced injury to the skin the effects of two orally administered oils So-1100 [containing linoleic acid (LA) and GLA] and So-5407 [containing eicosapentaenoic acid (EPA) in addition to LA and GLA] were evaluated. Results were compared with animals receiving a 'placebo' oil, So-1129, which contained a similar amount of LA to the other two 'active' oils but no GLA or EPA. The oils were supplied by Scotia Pharmaceuticals Ltd. (Guildford, U.K.).

Groups of animals were allocated to receive the 'active' and 'placebo' oils according to the protocols in Table 6. The oils were given daily, orally both before and after irradiation with single doses of $^{90}Sr/^{90}Y$ ß-rays from 22 5mm diameter plaques at a dose-rate of ~3.0Gy/min, measured at 16mm depth. Skin sites, 16 per flank, were irradiated on each pig.

Following irradiation, the severity of the acute skin reaction was assessed at weekly intervals for 10 weeks. Sites were examined for the presence or absence of bright red erythema and/or moist desquamation. Late reactions were evaluated over the period 10-16 weeks after irradiation by assessing the presence or absence of dusky/mauve erythema and/or dermal necrosis. The data for each of these criteria were analysed using probit analysis and ED_{50} (±SE) values, the doses required to cause the effect in 50% of skin fields irradiated, were calculated. These values were used as a means of comparing different treatment schedules.

Table 6. Experimental design for studies involving the irradiation of pig skin with single doses of ^{90}Sr/^{90}Y ß-rays

Experimental Group	Oil	daily dose (ml)	Number of animals
A	So-1100	1.5	4
B	So-1100	3.0	6
C	So-1100	6.0	4
D	So-5407	3.0	2
E	So-1129	3.0	2
F	So-1129	6.0	4
G	So-1100	3.0	2[a]
H	So-1100	3.0	2[b]
I	So-1129	3.0	2[a]
J	So-1129	3.0	2[b]

[a]Oils only given for 4 weeks prior to irradiation
[b]Oils only given for 10 weeks after irradiation

The ED_{50} values (±SE) for the endpoints of bright red erythema and moist desquamation for pigs receiving various doses of the 'active' oil, So-1100, and the placebo oil, So-1129, are given in Table 7. In the largest series of animals which received 3.0ml of the oils daily, administration of So-1100 as compared with So-1129 for just 4 weeks prior to irradiation had no significant effect on the dose-effect relationship for either the incidence of bright red erythema or moist desquamation. This lack of effect was reinforced by a comparison with historical data for moist desquamation, where the ED_{50} (±SE) was 27.32 ± 0.52Gy, intermediate between the values of present 26.00 ± 1.87 Gy and 27.91 ± 1.15 Gy for So-1100 and So-1129, respectively.

Administration of 3.0ml of oils, daily, for 4 weeks prior to irradiation and over the time course of the acute skin reaction, produced a significant modulation (p<0.05) of the radiation response in animals receiving So-1100 as compared with So-1129. Dose modification factors (DMFs) of between 1.13 and 1 24 were obtained. There was also a suggestion of an effect produced by the 'placebo' oil, So-1129, since the ED_{50} values for both bright red erythema and moist desquamation, when this oil was given over the time course of the reaction, were higher than when this oil was just given prior to irradiation. For moist desquamation, where a comparison with historical control data from pigs receiving no oils is possible, a significant effect of the 'placebo' oil is suggested with DMFs of 1.1 ± 0.04 and 1.14 ± 0 04 when compared with the -4/+16 week and +10 week So-1129 groups, respectively. Further evidence for a 'placebo' effect were supported by the results obtained when pigs were given daily doses of 6 0 ml of each oil; the greater modulation produced by So-1100 relative to So-1129 was not seen. Administration of a lower dose of 1.5ml of So-1100 modified the expression of the inflammatory bright red erythema response but not the severity of moist desquamation.

Table 7. Variation in the ED_{50} values ($\pm$SE) observed following single doses of $^{90}Sr/^{90}Y$ ß irradiation for the acute skin reaction of bright red erythema and moist desquamation. Either So-1100 or So-1129 were administered daily for various treatment periods. Dose modification factors (DMFs) are quoted ($\pm$SE) when the difference between ED_{50} values for the two oils was significant.

Treatment Period (wks)	Oil Dose (ml)	$ED_{50} \pm SE$ So-1100	So-1129	DMF $\pm$SE)
i) Bright red erythema				
-4/+16	1.5	35.90 ± 1.2	-	-
-4	3.0	26.81 ± 1.15	29.68 ± 1.68	NS
-4/+16	3.0	39.23 ± 0.98	31.76 ± 1.39	1.24 ± 0.06
+10	3.0	41.16 ± 3.79	34.44 ± 2.35	1.20 ± 0.14
-4/+16	6.0	35.05 ± 1.12	38.71 ± 1.47	NS
ii) Moist desquamation[a]				
-4/+16	1.5	28.30 ± 0.93	-	-
-4	3.0	26.00 ± 1.87	27.91 ± 1.15	NS
-4/+16	3.0	33.81 ± 0.8	30.04 ± 1.18	1.13 ± 0.05
+10	3.0	31.74 ± 1.08	31.03 ± 1.42	NS
-4/+16	6 0	33.44 ± 0.95	31.22 ± 0.94	NS

[a]Historical control value, no oils, ED_{50} ($\pm$SE) 27.32 ± 0.52Gy

For the later dermal reactions of dusky/mauve type erythema and ischaemic dermal necrosis, daily doses of 3.0 ml of So-1100 also produced a significant modification in the radiation response when results were compared with those seen in the 'placebo' group (Table 8). However, the oil had to be given over the time course of the radiation response to be effective No significant effect was seen when So-1100 (3 ml/day) was only given prior to irradiation There was evidence, indicative of a 'placebo' effect, when So-1129 was given both before and after irradiation at a dose of 6.0 ml/day. The ED_{50} values were significantly higher than when the same oil was given at 3.0 ml/day and for historical data for pigs receiving no oil (p<0.001). At this higher dose of oil there was no significant additional gain obtained from the use of So-1100; DMFs were not significantly different from 1.0 (Table 8) For these later dermal vascular reactions, 1.5 ml/day of So-1100 produced a significant modulation of the expression of radiation damage when compared with the combined data for pigs receiving 3.0 ml/day of So-1129. The DMFs of 1.26 ± 0.09 and 1.16 ± 0.08 were not significantly different from those obtained using 3.0 ml/day of So-1100 both before and after irradiation (Table 8).

Studies involving the oil So-5407 were only carried out using 3.0 ml/day, given both before and after irradiation. The results of these investigations are given in Table 9. For the early endpoints there appears to be a modification in the response seen when compared with a 'placebo' group, however, the difference in ED_{50} values suggesting DMFs of 1.14 ± 0.08 and 1.15 ± 0.08, respectively, only approached statistical significance (p $<0.1>0.05$).

Significant modification of the later dermal reactions was seen after the administration of So-5407 over the time course of the reaction as compared with So-1129. These changes were consistent with DMFs of 1.32 ± 0.13 and 1.2 ± 0.12, for dusky/mauve erythema and ischaemic dermal necrosis, respectively.

The DMFs noted following irradiation with single doses of $^{90}Sr/^{90}Y$ ß-rays using the oil So-5407 were in the same range as those found using So-1100. Neither agent was found to act as a classical radioprotector but had to be given over the time scale of the expression of radiation damage and hence could be used in the prophylactic treatment of radiation accident victims. They have been administered to humans over periods up to 1 year without significant adverse side effects.

Table 8. Variation in the ED_{50} values ($\pm$SE) for the later dermal reactions of dusky/mauve erythema (DE) and ischaemic dermal necrosis (N) after the administration of either So-1100 or So-1129 for various time periods following irradiation with single doses of $^{90}Sr/^{90}Y$ ß rays. DMFs are quoted ($\pm$SE) when the difference between the ED_{50} values for one to two oils was significant.

Treatment Period (wks)	Oil Dose (ml)	$ED_{50} \pm SE$		DMF $\pm$SE)
		So-1100	So-1129	
i) Dusky/mauve erythema (DE)[b]				
-4/+16	1 5	32.96 ± 1.61	-	$1.26 \pm 0.09^{[a]}$
-4	3 0	$26.50 \pm 1 30$	27.50 ± 1.10	NS
-4/+16	3 0	$33.53 \pm 1 89$	$24.84 \pm 1 53$	1.35 ± 0.11
-4/+16	6.0	37.97 ± 1.82	38.44 ± 2.08	NS
ii) Dermal necrosis (N)[c]				
-4/+16	1.5	40.95 ± 2.12	-	$1.16 \pm 0.08^{[a]}$
-4	3 0	34.80 ± 1.40	35.00 ± 1.50	NS
-4/+16	3 0	40.64 ± 1.31	35.70 ± 1.55	1.14 ± 0.06
-4/+16	6 0	49.56 ± 3.01	51.93 ± 3.87	NS

[a]DMFs determined by a comparison with the combined data for 3.0ml of So-1129
[b]Historical control value, no oil, 25.56 ± 5.66Gy
[c]Historical control value, no oil, 35.34 ± 4.02Gy

Table 9. Variation in ED_{50} values ($\pm$SE) for the acute skin reactions of bright red erythema (C) and moist desquamation (MD) and the later dermal reactions of dusky/mauve erythema (DE) and necrosis (N) after single doses (SD) of $^{90}Sr/^{90}Y$ ß irradiation. DMFs are quoted for ($\pm$SE) for the comparison between So-5407 and So-1129.

| Reaction type | $ED_{50} \pm SE$ | | DMF $\pm$SE |
	So-5407	So-1129	
C	36.23 ± 1.97	31.76 ± 1.39	1.14 ± 0.08
MD	34.60 ± 1.85	30.04 ± 1.18[a]	1.15 ± 0.08
DE	32.88 ± 2.54	24.84 ± 1.53[b]	1.32 ± 0.13
N	42.74 ± 3.90	35.70 ± 1.55[c]	1.20 ± 0.12

[a]Historical control value, no oils 27.32 ± 0.52Gy
[b]Historical control value, no oil, 25.56 ± 5.66Gy
[c]Historical control value, no oil, 35.34 ± 4.02Gy

Publications

1992:

Rezvani, M., Nissan, M., Hopewell, J.W., van den Aardweg, G.J.M.J., Robbins, M.E.C. and Whitehouse, E.M. Prevention of X-ray-induced late dermal necrosis in the pig treated with monochromatic light. *Lasers Surg. Med.* **12**, 288-293, 1992.

Hopewell, J.W., Robbins, M.E.C. and Scott, C.A. The effects of So-1100 in reducing the severity of radiation-induced damage to pig skin. *In: Eicosanoids and other bioactive lipids in cancer, inflammation and radiation injury.* Eds. Nigam, S., Marnett, L.J., Honn, K.V. and Walden, T.L., Kluwer Academic Publishers (Boston) pp. 345-348, 1992.

1993:

Hopewell, J.W., Sieber, V.K., Heryet, J.C., Wells, J. and Charles, M.W. Dose and source-size related changes in the late response of pig skin to irradiation with single doses of ß-rays from sources of different energy. *Radiat. Res.* **133**, 303-311, 1993.

Rezvani, M., Robbins, M.E.C., Hopewell, J.W. and Whitehouse, E.M. Modification of late dermal necrosis in the pig by treatment with multi-wavelength light. *Brit. J. Radiol.* **66**, 145-149, 1993.

Valkovic, V., Jakscic, M., Watt, F., Grime, G.M., Wells, J. and Hopewell, J.W. Effects of ionising radiation on the trace element composition of hair. *Nucl. Instr. Meth. Phys. Res.* **B75**, 173-176.

Hopewell, J.W., Calvo, W., Jaenke, R., Reinhold, H S., Robbins, M.E.C. and Whitehouse, E.M. Microcirculation and radiation damage. *In: Acute and long-term side-effects of radiotherapy.* Eds. Hinkelbeim, W., Bruggmaser, G., Frommhold, H. and Wannemacher, M. *Rec. Res. Can. Res.* **130**, 1-16, 1993

Hopewell, J.W., Robbins, M.E.C., van den Aardweg, G.J.M.J., Morris, G.M., Ross, G.A., Whitehouse, E., Horrobin, D.F. and Scott, C.A. The modulation of radiation-induced damage to pig skin by essential fatty acids. *Brit. J. Cancer,* **68**, 1-5, 1993

1994.

Rezvani, M., Hamlet, R., Hopewell, J.W. and Sieber, V.K. (1994). Time and dose-related changes in the thickness of pig skin after irradiation with single doses of ^{90}Sr/^{90}Y ß-rays.
Int. J. Radiat. Biol. **65**, 497-502.

Hopewell, J W, van den Aardweg, G.J.M.J., Morris, G M., Rezvani, M. Robbins, M.E.C, Ross, G.A and Whitehouse, E.M, (1994): Unsaturated lipids as modulators of radiation damage in normal tissues. In: *New approaches to cancer therapy: unsaturated lipids and photodynamic therapy.* Ed. D.F Horrobin pp 88-108.

van den Aardweg, G.J M.J., Hopewell, J.W. and Whitehouse, E.M. (1995): The radiation response of the cervical spinal cord of the pig : effects of changing the irradiated volume. *Int. J. Radiat. Oncol. Biol. Phys.* **31**, 51-55.

1995

Morris, G.M., Hopewell, J.W., Ross, G.A., Whitehouse, E., Wilding, D. and Scott, C.A. (1995). Trophic effects of essential fatty acids in pig skin. *Cell Prolif.* **28,** 73-84.

Rezvani, M., Hopewell, J.W. and Robbins, M.E.C. (1995). Initiation of non-neoplastic late effects: the role of endothelium and connective tissue. *Stem Cells* 13 (Suppl.) 248-256.

II. Objectives of the reporting period:

to complete the histopathological analysis of the skin tumours induced by localised beta irradiation;

to analyses the levels of transforming growth factor beta-1 mRNA in these skin tumours;

to complete the immunohistochemical analysis of the transforming growth factor beta-1 protein in normal skin and skin tumours.

III. Progress achieved including publications.

During the reporting period from 1992-1995 it has been the aim of this project to investigate the expression of the transforming growth factor beta-1 with a view to establishing its role in the pathogenesis of radiation fibrosis and skin cancer induction after superficial beta irradiation. Two strains of mouse were used, the inbred agouti CBA/Ca mouse and the outbred, albino CD1 mouse. It has previously been demonstrated that these strains have a differing sensitivity to radiation induced skin cancer. The transforming growth factor beta-1(TGFβ1) is the most commonly occurring isoform of the transforming growth factor beta gene family. It is expressed to some degree in nearly all tissues. Its effects include autocrine and paracrine stimulation of cell proliferation via modulation of cell cycle progression, cell differentiation and cell migration, angiogenesis and control of extracellular matrix synthesis, deposition and degradation. Many of these processes find a crucial role in wound healing. Transforming growth factor beta-1 may have a pivotal role in both the acute desquamative phase and in the establishment of chronic dermal fibrosis seen in the skin after irradiation. Furthermore in previous studies of radiation carcinogenesis in mouse skin it has been found that the majority of tumours arising are of dermal, notably fibroblastic origin. Given the regulatory functions of TGFβ1 with respect to the extracellular matrix and the apparently inappropriate deposition of matrix constituents during fibrosis and the potentially mitogenic effect of this factor upon fibroblasts the study of this molecule may provide important insights into the molecular pathogenesis of radiation fibrosis and cancer induction.

The expression of TGFβ1 mRNA has been followed in both strains of mouse from a few hours after irradiation to fifteen months after irradiation. Time points encompassed the acute phase, the histological detection of fibrosis and the macroscopic detection of tumours. The expression of mRNA was followed using quantitative PCR and has been localised within the tissue using *in situ* hybridisation. The translation of the TGFβ1 transcripts was established by immunohistochemical localisation of the protein.

Histopathological characterisation of the radiation induced tumours has been performed together with an analysis of TGFβ1 mRNA expression within a selection of these tumours. Again immunohistochemistry has been used to establish the translation and localisation of the TGFβ1 protein within the tumour tissue.

The results of these studies are as follows. A localised dose of 50Gy strontium-90 betas was delivered form an 11mm diameter source to mouse flank skin. No reaction is visible for the first 3-4 days. The skin the exhibits increasing erythema and pigmentational changes followed by dry and moist desquamation. The reaction reaches a peak with total denudation of the area around day 14. This is followed by a rapid re-epithelialisation of the area from the hyperplastic edges of the epidermis. The epidermis is macroscopically normal in appearance by 30 days.

The percentage change in the expression of TGFβ1 during this acute period of the radiation response is shown in the figure below for both mouse strains. Also included on the graph are the mean skin scores for the acute reaction.
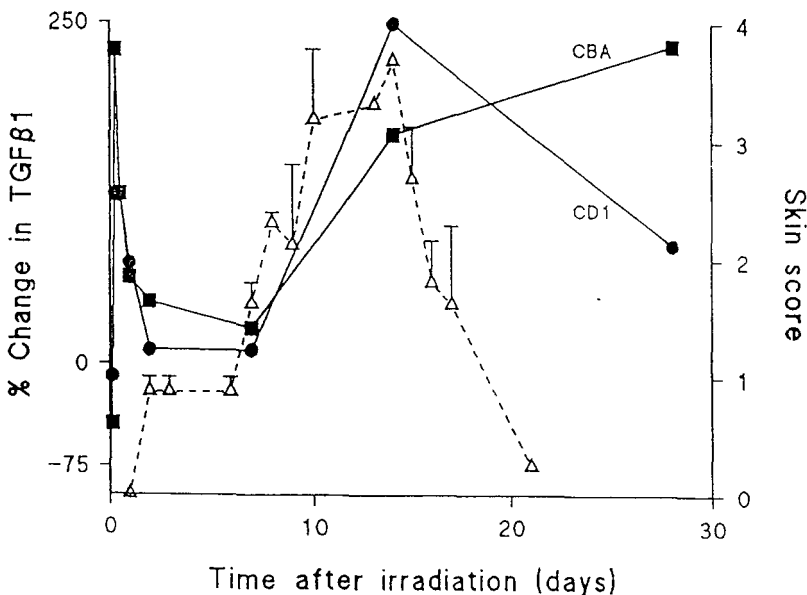

Both mouse strains showed similar fluctuations in TGFβ1 expression. A rapid but transitory rise was detected between 6 and 12 hours after irradiation. Subsequently values returned to near control levels at 7 days before rising again between 14 and 30 days. A dose response for TGFβ1 expression was also obtained at the fourteen day time point. The curve below shows values for percentage increase in TGFβ1 expression rising sharply before becoming asymptotic.
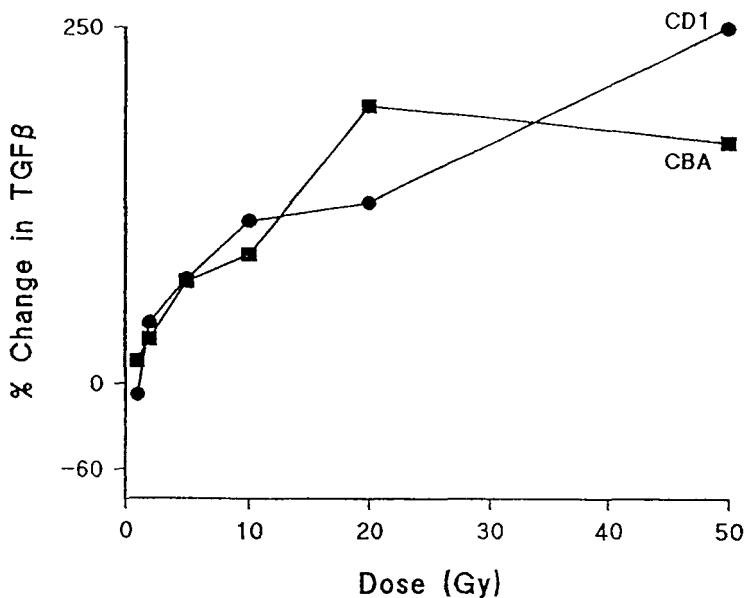
In situ and immunohistochemical studies of the TGFβ1 mRNA and protein revealed the mRNA to be localised in the basal layer and first 2-3 suprabasal layers of the hyperplastic epidermis at fourteen days. The localisation of the protein was confined to the suprabasal layers only.

The figure below illustrates the fluctuations in TGFβ1 expression for the remaining period of study from 2-15 months for both mouse strains.
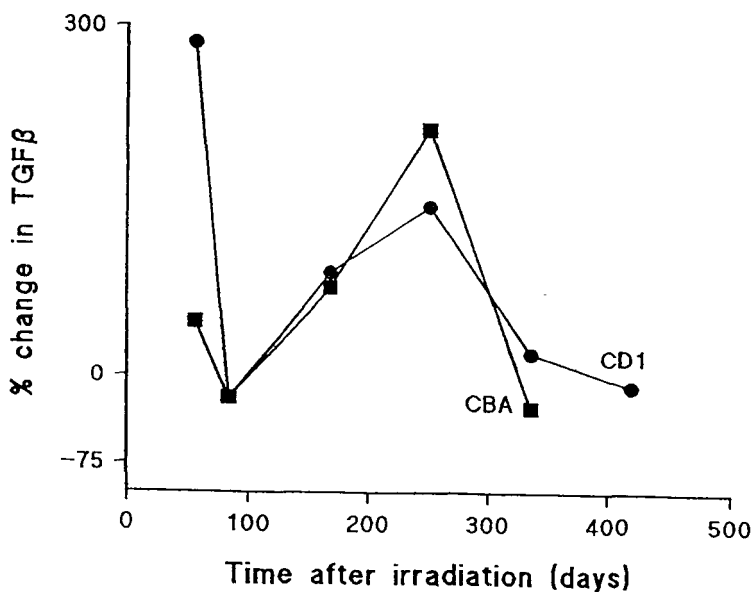
Again both strains show similar changes in expression of this period of study. After the macroscopic resolution of the acute response levels of TGFβ1 expression remain elevated within the irradiated area then decline to control levels around three months before expression is increased again between 6 and 9 months after irradiation. This period of elevated TGFβ1 expression coincides with the detection of chronic radiation fibrosis and is characterised by extensive dermal remodelling. Localisation of the TGFβ1 protein during this period indicated a switch from epidermal to dermal. Much of the protein being sequestered by elements of the extracellular matrix.

Tumours began to be detected from approximately 1 year after irradiation. CBA mice show zero tumour incidence in the unirradiated mice. Tumours were detected in irradiated mice with a cumulative tumour incidence of 54.3% ± 7.5 and a mean latent period of 86 ± 3 weeks after irradiation. The cumulative tumour incidence in control CD1 mice was 13.6% ± 5.3. Irradiation increased this incidence to 81.2% ± 16.5. Irradiation also decreased the mean latent period for tumour detection in CD1 mice from 89 ± 9 weeks to 70 ± 5 weeks.

Tumour incidence and the distribution of tumour histopathologies are illustrated in the graphs below for CBA irradiated mice and CD1 mice both irradiated and control.

| CD1 controls | 6/65 |
CD1 irradiated	23/62
CBA controls	0/62
CBA irradiated	46/143
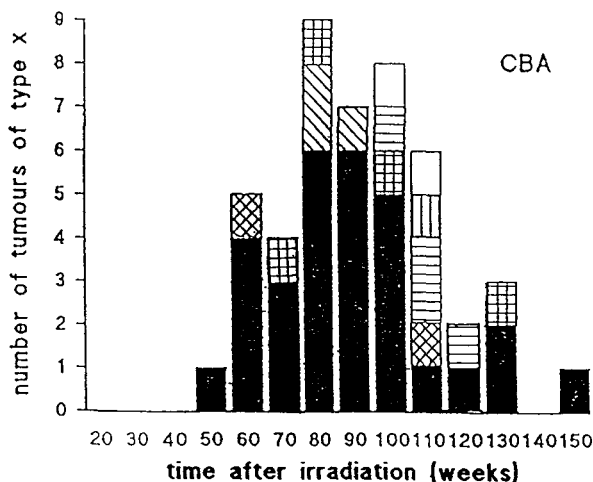
| ■ Malignant Fibrous Histiocytomas | ⧄ Fibrosarcoma |
▨ Leiomyosarcoma	⊞ Rhabdomyosarcoma
⧉ Squamous Cell Carcinoma	⊟ Papilloma/haemangioma
⊞ Fibroma/Fibromatosis	☐ Spindle Cell Sarcoma
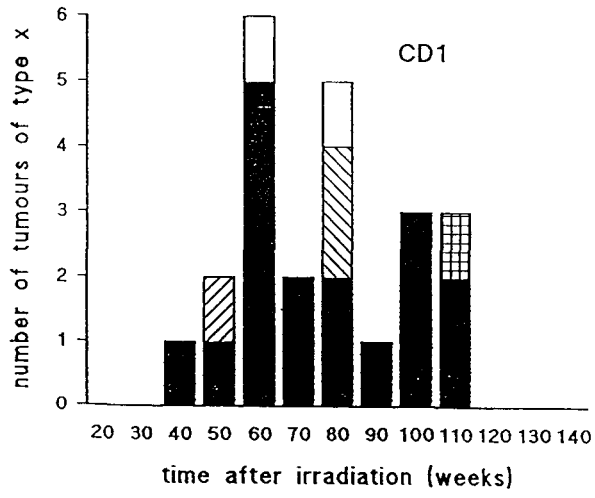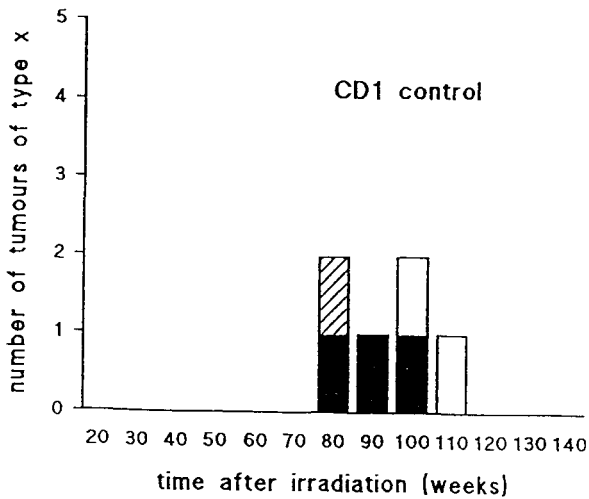
100% of tumours arising in CD1 mice, whether irradiated or not, were of dermal origin.
86.9% of tumours arising in CBA mice were of dermal origin. Of these tumours
malignant fibrous (MFH) were predominant as follows:

CD1 controls	6/6	50% MFH
CDI	17/23	73% MFH
CBA	30/40	65% MFH

After the initial detection of the tumours weekly vernier calliper measurements were made in three dimensions to estimate tumours volumes. Working with MFH tumours only statistical fitting of straight lines by least squares to tumour growth curves gave mean volume doubling times of 1.28 ± 0.09 weeks for MFH's from CD1 mice and of 1.56 ± 0.037 weeks for MFH's from CBA mice. Using the mean volume at the time of detection it was possible to estimate the number of volume doublings that may have occurred over the lifespan of the tumour from its inception as a single transformed tumour stem cell. The mean volume doubling time and the estimated number of volume doublings enabled an extrapolation back to a tentative time for initial clonal expansion. For CD1 MFH tumours this was estimated to be 39-40 weeks and in CBA mice it was estimated to be 48-50 weeks prior to tumour detection i.e. the mean latency period. Displayed graphically this places the period of initial clonal expansion of the "tumour stem cell" during the period of elevated TGFβ1 expression around 6-9 months after irradiation. This is shown below for both strains.
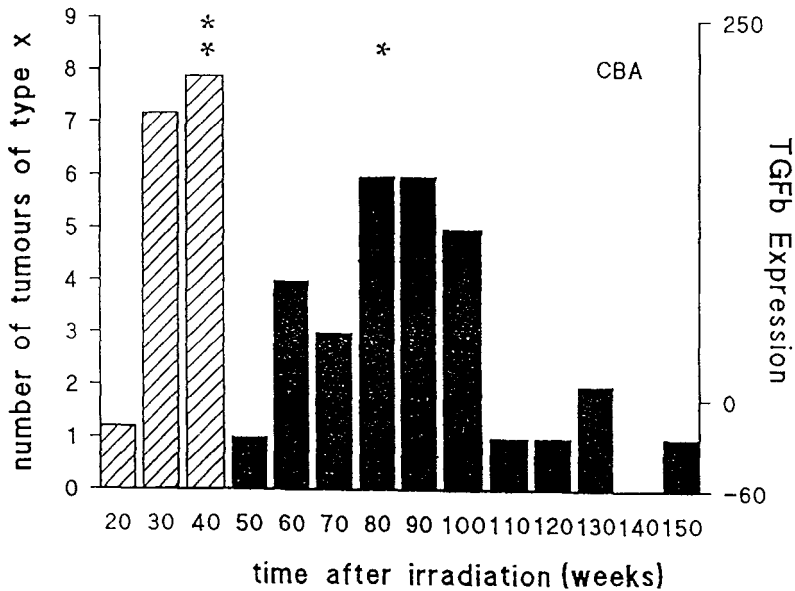
A graphic representation of the time for expansion of the initiated clone to a detectable size, extrapolating back from the mean time of detection. ///// Expression of TGFβ1 in irradiated skin; ▮ distribution of MFH tumour incidence. * Mean time for tumour detection; ** estimated time at which initiation events are still represented by a single cell. ** to * estimated mean time for promotional events leading to a palpable malignancy.
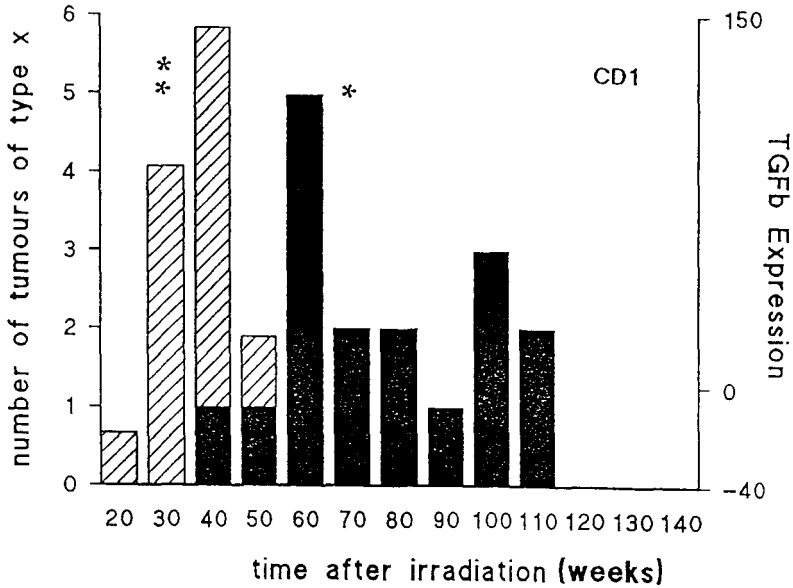
16 skin tumours were analysed for the expression of TGFβ1 mRNA. Elevated levels of expression were found in all tumours examined and ranged from 5-80 fold increases when compared to control skin in the respective tumour bearing mouse. On average a 9-10 fold increase in TGFβ1 mRNA expression was found in radiation induced dermal tumours. Immunohistochemical localisation of the TGFβ1 protein found it to be translated in all tumours. Distinctive patterns of localisation were detected in those tumour identified as malignant fibrous histiocytomas compared with other tumours of dermal origin. In all tumours examined there appeared to be a particular association between the TGFβ1 protein and stromal elements. The role of this factor in fibrogenic tumour proliferation is at present unclear but its contribution may largely be due to its control of stromal matrix and also the immunosuppressive capabilities of TGFβ1

Summary

The molecular mechanisms underlying the response of the skin to radiation remain unclear. Transforming growth factor-beta 1 is important in cell proliferation, differentiation, cell migration and the synthesis of extracellular matrix by fibroblasts. It should therefore be a significant cytokine in the radiobiological response of the skin. This study was designed to investigate the role of this factor at all stages of the radiobiological response observed in mouse skin.

Semi-quantitative PCR and immunohistochemical techniques were used to study the expression of TGFβ1 in mouse skin after localised exposure to Strontium-90 beta radiation 1-50Gy.

A transient 2-3 fold increase in TGFβ1 mRNA occurred within 6-12 hours post-irradiation. A sustained increase of 2-3 fold occurred over the 30 days of the acute injury period. High levels of the TGFβ1 protein were detected in the suprabasal cells of the epidermis but not in the basal cells. Over-expression of TGFβ1 continued long after the resolution of the acute epithelial injury, only returning to control levels ~90 days post-irradiation. Further increases in TGFβ1 expression were detected between 3 and 12 months post irradiation corresponding with the appearance of dermal fibrosis. Skin tumours appeared around 12 months after irradiation. The albino CD1 mice showed an increased tumour incidence of 25 % over the agouti CBA mice. The tumours in both strains were predominantly of dermal origin. Levels of TGFβ1 mRNA in the tumours were 5-80 times higher than those in control skin. In all cases the TGFβ1 mRNA was translated.

It is concluded that the results strongly support the initial idea that TGFβ1 is of importance in the molecular pathogenesis of radiation injury in skin.

Publications:

Randall k. Coggle JE. 1995 Expression of transforming growth factor-β in mouse skin during the acute phase of radiation damage. International Journal of Radiation Biology (in press).

ISTITUTO OSPITALIERO DERMOSIFILOPATICO DI S. MARIA E S. GALLICANO

ROMA

TELETHERMOGRAPHY WITH THERMOSTIMULATION IN THE MEDICAL SURVEILLANCE OF RADIATION WORKERS.

Di Carlo A.

S. Gallicano Dermatological Institute for Research and Care. Rome.

INTRODUCTION

The recent legislative decret 230/95, in adopting Euratom Directives on safety of plant and health protection of workers and the public against the dangers of ionizing radiations (1), establishes a requirement for preventive and periodic medical surveillance of radiation workers, that is of workers who, for occupational reasons, are liable to receive doses higher than those fixed for the general public (Art 6 Annex IV). This surveillance is entrusted to Authorized doctors registered, after passing a special examination, in the national list provided for by art 88 of the aforesaid decree, in the case of workers in category A (those liable to receive doses exceeding 6 mSv/year) and Competent Doctors, as defined by Legislative Decree 626/94, for workers in category B (those liable to receive doses exceeding 1 mSv/year but under 6 mSv/year). Six-monthly medical examinations are required for workers in Category A and annual ones for those in Category B. These examinations, which must be recorded on

a specific personal Health Document (DSP) conforming to the Ministry model and duly stamped by the competent Authority, must include the specialist and instrument tests considered necessary by the doctor. Among these tests complementary to the medical examination, non invasive methods to assess functionality of skin vessels are very important. Plethysmography and laser-doppler are indicators of severely radiodamaged tissues while capillaroscopy provides only morphological data, not suitable for biologic dose assessment; finally, TPO_2 technique works by heating the tissues under examination and thus alters the steady state of the microvessels.

Telethermography (TTG) can provide objective morpho-functional indications, quantifiable and repeateable, on the physiopathological condition of the peripheral microcirculation, in particular of the hands, which are the part of the body most exposed in some occupations, especially in the hospital environment (heart surgeons, endoscopists, dentists, hortopedicians etc.). Telethermography (TTG) gives a videoimaging of the skin temperature, which depends on its conductivity via blood vessels and perivascular tissues. By this technique, infrared radiation is detected at distance and visualized simultaneouly on the monitor as light/dark points (or colour isotherms) in a continuous pattern. The thermal picture is immediately provide, thus it is not necessary the plotting and mapping, as happens for other thermometric procedures. The efficiency of this technique for biologic dosimetric purposes after accidental irradiation in man has yet been demonstrated in previous studies, showing the precocious appearance of altered thermal gradients which gives a good indication of irradiated volumes. Nevertheless in chronic radiation exposure standard TTG is not always able to evaluate functionality of the

microvessels, particularly in cases of minimal damage. For this purpose, we applied a cold stress on the skin and recorded thermal recovery time (TRT) of stimulated area (telethermography assisted by thermostimulation, TTG/TS) (2). It was so possible to evidentiate minimal functional alterations of the blood supply, even in the absence of clinical lesions. Clinical picture and diagnostic problems in chronic occupational radiodermatitis. This is a classical chronic pathology of slow, gradual development, with a possible epithelioma evolution if not appropriately treated. It is caused today, as in the recent past, by exposure to subclinical doses (doses, that is, which do not provoke evident clinical signs and symptoms immediately after exposure) repeated over time for months and years. Specific dosimetric testing, to be adequate, must be performed with thermoluminescence dosemeters (TLD) incorporated in rings or brecelets, since for this purpose the data supplied by film badge dosemeters worn on the chest under a leaded coat are entirely insufficent and unreliable. This type of dosemeter check of radiation-exposed workers hands was only introduced in very recent years and even now is not in universal use in all health environments where there is a specific risk. There is also some resistence to its use by workers (in particular by surgeons) because it creates some problems in the finer use of the hands. In view of the above, it is still not entirely rare today to encounter occupational radiodermitis especially in those who have been operating for many years.

The clinical pictures, often unfocused and non-specific, are not easy for the diagnose, at least in the initial stage. The dorsal skin of the fingers and perhaps also the distal metacarpal part, becomes drier and shiny. The hair fall out and the nails se em more fragile with

incisions on the free edge, linear ridges and furrows in the proximal-distal direction on the surface. Other signs may include paresthesia, hypersensitivity to thermal stimulation, and slight alterations to the finer prehensile movemeʈs. The subsequent symptoms, symptoms, late in appearing and slow in their evolution, comprise gradual atrophy of the epidermis, appearance of teleangectasia and of achromic and hyperchromic areas (the so called coal marks)), fragility to trauma with small hemorrhagic suffusions, disappearance of the dermatoglyphs at the finger tips.

In the clinically evident phase there is a sclerosis of connective tissues, with tapering fingers, skin stuck to the deeper layers. The epidermis may preent areas of verrucose hyperkeratosis or islands of dyskeratosis, ragades and microulcerations in correspondence with the articular folds. The ungueal dystrophies become more severe, with cracks, esfoliations of the upper layers, pachyonychia, onycolysis and sometimes destruction of the layers with pterigium. On the lateral face of the finger and fingers tips most markedly in correspondence with the free edge and distal margin of the ungueal bed, there may be a marked hyperkeratosis with very painful horny formations. In some cases the ulcerated areas may involve deeper parts with necrotic phenomena of the tendinous layers. In this stage microbial complications, particular periungueal, are not rare.

Particularly in the subclinical phases, that is in the absence of clinical evident signs, and also in initial stages with slight and non-specific manifestation TTG/TS can make a useful contribution to early diagnosis and subsequent follow-up of the cases identified by it. Another important aim of the survey undertaken with this metod is the possible identification of a minimum threshold for response to

TTG/TS, that is in the correpondance of the accumulated doses from chronic or repeated exposure. In this regard it must be remembered that the threshold value for a positive response with TTG (without cryostimulaytion) after acute accidental irradiation was estimated by Gongora at about 2 Gy (220 rad) for gamma rays (3). This value is undoubtedly also reliable for other low LET electromagnetic or particulate radiation (X-rays, accelerated electrons).

MATERIALS AND METHODS

The equipment used was the AGEMA Thermovision, models 680 –880, that comprises basically an infrared camera to capture the image and a television set to display it. In the IR camera which is similar to an ordinary telecamera, the images are scanned into a great number of thermal points and focused on photo-sensitive crystals that transform them into corresponding electric signals. These are amplified and fed to the cathode of the TV-monitor type producing the videosignal and forming the image on the screen of the display unit. Thermal pictures have been documented on Polaroid film in black/white or colour-code isotherms (eight different colours, from the yellow to the blue, the black indicating gradients above and below the selected range); the instant photo were taken from the display, and in the 870 model, provided with computer software, from the colour video-terminal of the computer (15 colours, from the white to the blue, the black indicating the temperature below the selected range). Special functions of the software gave the possibility to image analysis, storage and video-recording in real time. It was possible, for example to

determine in an immediate manner the mean temperature of a cutaneous area "frozen" on the colour video-display, or follow on the screen the variations in time of one or more points of the thermal picture. A macrothermography was also possible, using special extension lens to obtain a vision as close as 20 cm.

By this technique performed at distance it is not possible to perfectely know the absolute temperature of a cutaneous area; this fact it is not important in the medical field, it being more important to obtain accurate temperature-differential measurements (thermal gradients) Neverthless the image of a cutaneous surface that appears on the monitor in normal conditions of measurement is a mosaic of hyper- and hypothermic areas that are the expression of local factors (circulatory, flogistic-metabolic etc.) and general ones. This fact results in great variability in findings from one patient to the next and also for the same subject observed at brief interval of time. The sensitivity of current equipment, which reaches $0,1^{o}C$, makes it not possible to detect gradients above this value, creating significant difficulties in both clinical and experimental work. Moreover in physiolgically "hot" skin areas such as the temporal region, axilla, neck, Scarpa's triangle etc. it is not easy to identify directly the pattern of specific skin lesions, such as malignat tumors (squamous cell carcinoma, melanoma). To overcome these difficulties it is decisive to adopt the "thermostimulation" procedure (4,5,6,7,8), consisting in a thermal stress exercised by contact on the skin to be examined. By this procedure it is possible to evaluate the thermogenic capacity of skin lesions against that of the skin in which they are seated, based on the different times of visualization on the screen. In particular the thermostimulation procedure is very useful in the

study of the function of the micro-vessels, since diffusion (convection) of heat through the vessels is a feature of the skin. Examining thermographically a skin area chronically exposed to ionizing radiations without relevant clinical findings, it is possible to observe on direct thermographic examination, performed in condition of optimal equilibrium of the body with the external ambient (eg 21ºC, 50% of humidity), the absence of any significant thermal gradient difference from the healty symmetrical skin, whilst by thermostimulation the vascular damage is expressed by a prolonged time of recovery. Rational use of thermostimulation has been made possible by utilization of a special equipment (thermostimulator) that can ensure standard parameters of temperature and contact time. The thermostimulator comprises a metal tank of 5 litres capacity containing a 50% alcohol-water solution kept at a constant temperature by a heating-cooling system; this can be set in the range of 1ºC to 50ºC by a variable-interval selector. A pump drives this liquid through a double rubber tube 1,5 m. long, at the end of which is a latex balloon of 250 ml of capacity wich is placed, when filled, on the area of the skin to be examined. A handle contains the pump starter button. The temperature of the liquid in the container and the time of aplication are displayed on monitors. The loss the temperature from the central tank through heath dispersion does not exceed 0,5ºC. In our study thermostimulation is applied at parameters of +5ºCx20 seconds (cold stimulation). This procedure let it possible to perform the thermographic examination without the waiting time of the climatization.

The investigated subjects during the last 7 years were subdivided into 4 groups, which were respectively: a I group (n=220) including normal subjects, without hyperthension, diabetes or systemic disease, not smokers, never professionally exposed to radiations; a II group (n=18) including chronic professional radioexposed workers with clinical signs of radiodermitis, as severe scleroatrophy and onicodistrophy; a III group (n=21) including chronic professional radioexposed workers (more than 20 years) with minimal clinical lesions (onicodistrophy); and, finally, a IV group including professional radioexposed workers without clinically evident lesions (n=146). In this study, carried out in cooperation with the health physicist, we tried to take into account when possible the main parameters concerning the dosimetry, physic characteristics of the source, and the geometry source-subject.

RESULTS

In the I group the values of thermal recovery time have been: 2-6 minutes +/-40 seconds in 193 subjects (87,7%), less than 1 minute in 4 subjects (1,5%), more than 6 minutes in 24 subjects (10,8%).
For the II group the affected fingers showed a TRT less than 30 seconds in 11 subjects (61,2%) and over 6 minutes in 7 subjects (38,8%).
In the III group the affected fingers gave the following results after thermostimulation: more than 6 minutes in 15 subjects (71,5%) and between 2-6 minutes in 6 subjects (28,5 %), no subject showed TRT less

than 2 minutes.

In the IV group the radioexposed fingers showed a TRT of 2-6 minutes in 104 workers (71,2%), a TRT less than 2 minutes in 6 cases (4,1%) and TRT more than 6 minutes in 36 cases (24,6%).

COMMENT

These results seem demonstrate first of all that in a normal population there is a great variability of responses to the thermal stress with central values between 2 and 6 minutes.

In subjects with severe radiodermitis this variability is greatly reduced, as only two polar responses were detected, namely a prolonged TRT and a very precocious one. In both cases the histological examination carried out (respectively in 3 and in 4 subjects) revealed a vascular damage (dilatation, thrombosis, endotelitis), besides the alterations of the epidermis, of the collagen and of the fibroblasts. These histological changes were more evident in cases with a precocious TRT.

In less severe radiodermitis (III group) the large percentage of prolonged TRT could demonstrate an impaired functionality of the skin vessels.

Finally, in chronically exposed workers (IV group) we observed a higher percentage (statistically significant) of prolonged TRT vs the controls. These workers are now submitted to periodical clinical-instrumental controls in order to verify possible modifications of this pattern.

The possibility of a rigorous evaluation of the parameters of the thermostimulation as well as of the thermal recovery times could constitute a great advantage in the diagnostic field, according to the purposes followed by other Authors.

Even if it is premature to deduce, from the data collected, a characteristic pattern of microcirculatory functional response from chronic exposure to radiation "noxa", we neverthless consider the study of the greatest interest and one which, when a larger number of cases and appropriate follow-up are available, will provide indication of value for the diagnosis and prognosis, complementary to the clinical examination and even in initial cases, precursors of the clinical signs which as already mentioned usually appear very late and almost always, initially, in a non-specific form.

REFERENCES

1) Cipollaro A, Crossland P. Rays and radium in the treatment of diseases of the skin. Lea and Febiger, Philadelphia 1967

2) Ippolito F, Di Carlo A. La metodica della criostimolazione nell'indagine termografica in dermatologia. Boll Ist Dermatol S. Gall 1980;10:165-184

3) Gongora R, Strambi E, et al. Thermographie et irradiation aiguë. Arch Scienze Lav 1989;5:41-46

4) Di Carlo A. Thermography in patients with systemic sclerosis. Thermology Osterreich 1994;4,18-24

5) Ippolito F, Di Carlo A. Impiego della termografia con criostimolo nella radioprotezione. Riv Med Lav Ig Ind ,1993;XVII,33-38

6) Di Carlo A. Telethermography in the diagnosis of cutaneous malignant melanoma. III Europ. Conf. on Engineering and Medicine Abstract p 402. Florence 1995

7) Di Carlo A, Strambi E, Ferrara FM. Telethermography with cryostimulation technique as a diagnostic tool in chonic localized irradiation: case contribution. Intern Conf on Radiation and Medicine. Oral presentation. Abstract n° 26 (*). Montpellier 1995

8) Di Carlo A. Thermography and the possibilities for its applications in clinical and experimental dermatology. Clinics in Dermatology, 1995, (in press).

* Supported by the concerning CEE project.

Final Report
1992 - 1994

Contract: FI3PCT930076   Duration: 1.1.93 to 30.6.95   Sector: B24

Title: Thyroid and its proximate tissues radiation dosimetry; stochastic and deterministic biological effects in humans and model systems.

1)	Lamy	Univ. Bruxelles (ULB)
2)	Malone	Hosp. Federated Dublin Voluntaries
3)	Smyth	Univ. Dublin - College
4)	Williams.	Univ. Cambridge

I. Summary of Project Global Objectives and Achievements

1) Human data base for dosimetry
Thyroid mass, iodine kinetics have been defined in pregnant women and neonatals as a basis for dosimetry in such subjects.

2) Dosimetry
a) Foetal and neonatal dosimetry · have been defined using phantoms
b) Thyroid dose maps : have been established for all European countries allowing to estimate doses for population in case of nuclear accident
c) Dosimetry · a new dosimetry unit has been proposed.

3) New models
a) 5 new models of transgenic mice expressing all types of thyroid tumors have been created
b) for radiation · human thyroid cell lines have been created but they dedifferentiated

4) Oncogenesis
a) proliferation pathways of the thyroid have been defined
b) proliferation mechanisms in tumors : first demonstration of the oncogenic transformation of a 7 transmembrane receptor (the TSH receptor) as the cause of 90% of hyperfunctioning adenomas and congenital hyperthyroidisms.

5) Oncogenes in experimental and human tumors
The patterns of expression of several oncogenes (ret, met) and of IGF1 have been defined in all types of human thyroid tumors and in murine tumors by immunohistochemistry and in situ hybridization

Head of project 1: Prof. Lamy

II. Objectives for the reporting period

.

The aims of the program of the Brussels group were to
1) develop new cell and animal models for the study of radiation carcinogenesis

2) develop our knowledge on proliferation mechanisms in normal and tumoral thyroid cells and to apply this knowledge to radiation induced thyroid cancers.

III. Progress achieved including publications

1) Development of new models

     a) Transgenic models
     In vitro cell transformation, spontaneous or induced by various agents (radiation mutagenetic agents), is strongly influenced by the biological activation of the cells (eg cell density, multiplication rate, pH, cell substrate, etc.). It is therefore quite likely that the carcinogenetic yield of a radiation dose may depend on the particular physiological framework of the target thyroid. Availability of different in vivo models would therefore be important in this regard. Unfortunately the only in vivo experimental model used now is the mice or rat treated with antithyroid drugs and irradiation, with the limitation that the frequency and time of onset of tumors is very variable. We have developed various models of transgenic mice.

     We had cloned before the thyroglobulin promoter. The thyroglobulin promoter has been placed upstream of chloramphenicol acetyl transferase cDNA. When injected into mouse oocytes with a pBR322 vector, this promoter has been shown to be able to target the expression of the gene specifically in the thyroid of injected mice and of their offspring. Depression of the thyroid by triiodothyronine treatment decreases, while stimulation by antithyroid drugs increases the expression of the gene.

We have developed models of thyroid tumors in transgenic mice :

1) Mice expressing the adenosine A2 receptor in the thyroid. Because most cells generate adenosine, this receptor behaves as a constitutive activitor of adenylate cyclase. Our in vitro work on thyroid cells in primary culture had shown that on periods of minutes to days such activation would lead to hyperfunction and growth. Indeed the A2 mice developed hyperthyroidism and goiter. Detailed studies demonstrated hypersecretion, high iodide uptake and high cell proliferation rate. These mice thus represent perfect models of hyperfunctioning adenoma, but in the mice the adenoma involves the whole gland.

2) Mice expressing the E7 oncogene from HPV16. This gene inhibits the function of the retinoblastoma protein. Its specific expression in thyroid leads to euthyroid goiter. There is an increased proliferation rate but the function of each thyroid cell is reduced. These mice represent good models of simple goiter.

3) Mice expressing a constitutive adrenergic alpha 1 receptor. These receptors activate constitutively, through to a small extent both the adenylate cyclase and the phospholipase C cascades. The mice present an euthyroid goiter but develop in time foci of papillary carcinoma.

4) Crosses of mice expressing the adenosine A2 receptor and the E7 oncogene. These mice develop a huge goiter, hyperthyroidism and invasive and metastasizing follicular carcinoma. These mice represent good models of follicular carcinomas.

5) Mice expression the viral oncogene SV40 LT. These mice develop huge goiters, hypothyroidism and invasive anaplastic tumors. They represent good -models of anaplastic carcinoma.

The influence of I^{131} irradiation and antithyroid treatment of the models are now studied. In all cases I^{131} (1 μCi at 15 days age) induces invasive tumors. In cases 4 and 5 these tumors appear much earlier than in control mice.

b) Human thyroid cell lines

Human cells have proven to be extremely refractory to ionizing radiation-induced neoplastic transformation. Since the transition from a normal to a malignant state is thought to involve several steps, it would seem reasonable to examine the effects of radiation at different points along this pathway. Furthermore, preneoplastic cells (eg. cells which possess many of the properties of neoplastic cells yet which are not tumorigenic) may be easier to neoplastically transform than normal cells. With the above points in mind, we think it is essential to develop immortalized human thyroid cell lines.

A subgenomic fragment of the tumorigenic HPV-16 has been cloned in the pML2 vector (derived from pBR322). The cDNA fragment containing the full sequences of the immortalizing genes E6-E7 is under the control of the powerful LTR promoter of Mo-Mu LV Several protocols have been tried. The final protocol is described hereafter. Human thyroid cells transfected by the lipofection method have been cultured for one week., trypsinized, plated again and treated with a general cyclic AMP enhancer (forskolin) for 3 weeks, then passaged again for another 2 weeks. While many cells degenerate and die, some foci of cells with epitheloid morphology appear. These cells have been passaged 19 times with alternative treatment with forskolin and TSH for 11 months after the transfection. These cells multiply

with a doubling time of 60-70 hrs in medium with 0.2 % serum. They exhibit a typical epitheloid morphology. They secrete thyroglobulin and this secretion is stimulated by a factor of 3 by thyrotropin (from 5 to 15 ng of Tg/pg DNA/ 48 hours). These results are similar to those obtained in primary cultures of human thyroid cells. Their cyclic AMP levels are enhanced by a factor of 3 in response to TSH 500 µU/ml from 0.4 to 1.3 pMole/µg DNA). However their growth was not stimulated by TSH or activation of the cyclic AMP cascade. Moreover after passage 40 the cell strain progressively lost its differentiation characteristics.

These experiments were pursued following different approaches
1) the same methodology were used on new human thyroid cell preparations. The parallel work of McCormick on the immortalization of human fibroblats by a similar technology shows that although success is very rare (2 in 5 years work) one is sufficient !

2) new protocols of transfection were used, eg. electroporation of cells in suspension which should give us much higher yields of transfection.

3) new protocols of selection with treatments of cells with various combinations of alternative treatments : a) without serum, to eliminate fibroblasts, with serum to promote growth; b) with TSH to select TSH responsive cells, without TSH to prevent desensitization; c) with forskolin (i.e. increased cAMP) to maintain differentiation, without forskolin to avoid selection of glucose transport mutants.

4) use of the HPV immortalizing genes E6 and E7 separately.

5) use of cells transfected with the constitutive adenylate cyclase activating adenosine A2 receptor which has been shown to stimulate proliferation of dog thyroid cells in primary culture and to generate hyperfunctioning adenomas involving the whole thyroid in transgenic mice.

Using these methodologies no cell line has been obtained yet. The ideal cell line should 1) retain its differentiation as judged by iodide trapping, cyclic AMP response to TSH, thyroglobulin, thyroperoxidase and TSH receptor gene expression (Northern blotting) and cell polarization in culture;

2) retain its proliferation characteristics; quiescence under basal conditions, triggering by TSH and forskolin (cyclic AMP), epidermal growth factor, serum and phorbol esters;

3) immortality.

Unfortunately these efforts have not yet produced such a cell line . It should be pointed out that this goal has not been reached by any of the other laboratories involved in such work, although many have tried.

2) Proliferation and tumorigenesis mechanisms

a) Normal mechanisms
Oncogenes causing the transformation of a cell type usually correspond to protooncogenes involved in the normal control of proliferation and differentiation in this cell. To analyze the oncogenic steps in thyroid cell carcinogenesis it is therefore important to

characterize the pathways inducing proliferation in these cells. Our strategy is to define pathways in the more easily available dog thyroid cell and to confirm the validity or correct conclusions for human thyroid cells. We have defined the pattern of proteins phosphorylated in response to the three major growth pathways of the dog thyroid: the TSH cAMP, the EGF serum protein tyrosine kinase and the phorbol ester protein kinase C pathways. We have defined the pattern of protooncogene expression and protein synthesis in the three mitogenic pathways. The TSH cAMP pathway which is both mitogenic and differentiating enhances cmyc, cfos, Jund and JunB expression but depresses cJun expression. The expression of cmyc is short lived. The pathway does not involve Ras or MAP kinase.

The growth factors (FGF, HGF) pathways and the protein kinase C pathway activated by phorbol esters are both mitogenic and dedifferentiating. They induce the expression of cmyc cfos, cjun Junb and Jund the first being long lived. The pathways involves Ras and Map kinase.
The patterns of cyclin and CDK expressions have been defined for all the mitogenic pathways. The main conclusion emerging from these studies is that while the pathways are almost completely distinct at the level of protein phosphorylation they converge at the level of early protooncogene expression and are similar at the level of the fundamental cell cycle machinery, i.e. at the level of cyclins and CDK phosphorylation and expression.

b) Proliferation mechanisms in tumors.
The work on mechanisms has suggeste·l that any constitutive activation of the proteins of the cyclic AMP pathway should lead to hyperfunctioning adenomas. Taking advantage of our first cloning of the TSH receptor we have searched for such mutations in this first element of the cascade. Mutations conferring constitutive activation to the receptor have now been found in 9 out of 13 hyperfunctioning adenomas, thus defining the pathogenetic mechanism of these tumors. Similar mutations have now been found in thyroid of patients with congenital hyperthyroidism We are now investigating the role of such mutations in cancer patients from the Chernobyl area.

Allgeier, A., S. Offermanns, J. Van Sande, K. Spicher, G. Schultz, and J.E. Dumont 1994 The human thyrotropin receptor activates G-proteins Gs and Gq/11. J. Biol. Chem., *269*:13733-13735.

Baptist, M., J.E. Dumont, and P.P. Roger 1992 Demonstration of cell cycle kinetics in thyroid primary culture by immunostaining of proliferating cell nuclear antigen: differences in cyclic AMP-dependent and -independent mitogenic stimulations. J. Cell Sci., *105*:69-80.

Baptist, M., J.E. Dumont, and P.P. Roger 1993 Demonstration of cell cycle kinetics in thyroid primary culture by immunostaining of proliferating cell nuclear antigen: differences in cyclic AMP-dependent and -independent mitogenic stimulations. J. Cell Sci., *105*:69-80.

Baptist, M., V. Pohl, J.E. Dumont, and P.P. Roger 1991 Various facets of the intracellular heterogeneity in thyroid primary culture. Thyroidology, *3*:109-113.

Brabant, G., C. Maenhaut, J. Kohrle, G. Scheumann, H. Dralle, C. Hoang Vu, R.D. Hesch, A. von zur Muhlen, G. Vassart, and J.E. Dumont 1991 Human thyrotropin receptor gene: expression in thyroid tumors and correlation to markers of thyroid differentiation and dedifferentiation. Mol. Cell Endocrinol., *82*:R7-12.

Breton, M.F., P.P. Roger, B. Omri, J.E. Dumont, and M. Pavlovic-Hournac 1989 Thyrotropin but not epidermal growth factor down-regulates the isozyme I (PKa I) of cyclic AMP-dependent protein kinases in dog thyroid cells in primary cultures.. Mol. Cell Endocrinol., *61*:49-55.

Coclet, J., F. Lamy, F. Rickaert, J.E. Dumont, and P.P. Roger 1991 Intermediate filaments in normal thyrocytes: modulation of vimentin expression in primary cultures. Mol. Cell Endocrinol., *76*:135-148.

Corvilain, B., E. Laurent, M. Lecomte, J. Van Sande, and J.E. Dumont 1994 Role of the cyclic adenosine 3',5'-monophosphate and the phosphatidylinositol-Ca2+ cascades in mediating the effects of thyrotropin and iodide on hormone synthesis and secretion in human thyroid slices. J. Clin. Endocrinol. Metab., *79*:152-159.

Corvilain, B., J. Van Sande, E. Laurent, and J.E. Dumont 1991 The H2O2-generating system modulates protein iodination and the activity of the pentose phosphate pathway in dog thyroid. Endocrinology, *128*:779-785.

De Maertelaer, V., G. Hoffman, M. Lemaire, and J. Mendlewicz 1987 Sleep spindle activity changes in patients with affective disorders. Sleep, *10*:443-451.

Dremier, S., J. Golstein, R. Mosselmans, J.E. Dumont, P. Galand, and B. Robaye 1994 Apoptosis in dog thyroid cells. Biochem. Biophys. Res. Commun., *200*:52-58.

Dremier, S., M. Taton, K. Coulonval, T. Nakamura, K. Matsumoto, and J.E. Dumont 1994 Mitogenic, dedifferentiating, and scattering effects of hepatocyte growth factor on dog thyroid cells. Endocrinology, *135*:135-140.

Dumont, J.E., F. Lamy, P. Roger, and C. Maenhaut 1992 Physiological and pathological regulation of thyroid cell proliferation and differentiation by thyrotropin and other factors. Physiol. Rev., *72*:667-697.

Dumont, J.E., C. Maenhaut, and F. Lamy 1992 Control of thyroid cell proliferation and goitrogenesis.. Trends in Endocrinol. Metab., *3*:12-17.

Duprez, L., J. Parma, J. Van Sande, A. Allgeier, J. Leclère, C. Schvartz, M.J. Delisle, M. Decoulx, J. Orgiazzi, J.E. Dumont, and G. Vassart 1994 Germline mutations in the thyrotropin receptor gene cause non-autoimmune autosomal dominant hyperthyroidism. Nature Genetics, *7*:396-401.

Kopp, P., J. Van Sande, J. Parma, L. Duprez, H. Gerber, E. Joss, J.L. Jameson, J.E. Dumont, and G. Vassart 1995 Congenital hyperthyroidism caused by a mutation in the thyrotropin-receptor gene. N. Engl. J. Med., *19*:150-154.

003059.
Lamy, F., F. Wilkin, M. Baptist, J. Posada, P.P. Roger, and J.E. Dumont 1992 Phosphorylation of mitogen-activated protein kinases is involved in the epidermal growth factor and phorbol ester, but not in the thyrotropin/cAMP, thyroid mitogenic pathway. J. Biol. Chem., *268*:8398-8401.

003107.
Ledent, C., J.E. Dumont, G. Vassart, and M. Parmentier 1991 Thyroid adenocarcinomas secondary to tissue-specific expression of Simian virus-40 large T-antigen in transgenic mice. Endocrinology, *129*:1391-1401.

002462.
Ledent, C., J.E. Dumont, G. Vassart, and M. Parmentier 1992 Thyroid expression of an A2 adenosine receptor transgene induces thyroid hyperplasia and hyperthyroidism. EMBO J., *11*:537-542.

Ledent, C., A. Marcotte, J.E. Dumont, G. Vassart, and M. Parmentier 1995 Differentiated carcinomas develop as a consequence of the thyroid specific expression of a thyroglobulin-human papillomavirus type 16 E7 transgene. Oncogene, *10*:1789-1797.

Ledent, C., M. Parmentier, G. Vassart, and J.E. Dumont 1994 Models of thyroid goiter and tumors in transgenic mice. Mol. Cell. Endocrinol., *100*:167-169.

Lejeune, C., J. Mockel, and J.E. Dumont 1994 Relative contribution of phosphoinositides and phosphatidylcholine hydrolysis to the actions of carbamylcholine, thyrotropin (TSH), and phorbol esters on dog thyroid slices: regulation of cytidine monophosphate-phosphatidic acid accumulation and phospholipase-D activity. I. Actions of carbamylcholine, calcium ionophores, and TSH. Endocrinology, *135*:2488-2496.

Maenhaut, C., G. Brabant, G. Vassart, and J.E. Dumont 1992 In vitro and in vivo regulation of thyrotropin receptor mRNA levels in dog and human thyroid cells. J. Biol. Chem., *267*:3000-3007.

Malone, J., J. Unger, F. Delange, R. Lagasse, and J.E. Dumont 1991 Thyroid consequences of Chernobyl accident in the countries of the European Community. J. Endocrinol. Invest., *14*:701-717.

Miot, F., F. Wilkin, S. Dremier, N. Uyttersprot, F. Lamy, J.E. Dumont, and C. Maenhaut 1994 Cloning of cDNA specifically involved in the thyroid cAMP mitogenic pathway. Horm. Res., *42*:27-30.

Mockel, J., C. Lejeune, and J.E. Dumont 1994 Relative contribution of phosphoinositides and phosphatidylcholine hydrolysis to the actions of carbamylcholine, thyrotropin, and phorbol esters on dog thyroid slices: regulation of cytidine monophosphate-phosphatidic acid accumulation and phospholipase-D activity. II. Actions of phorbol esters. Endocrinology, *135*:2497-2503.

Parma, J., L. Duprez, J. Van Sande, P. Cochaux, C. Gervy, J. Mockel, J.E. Dumont, and G. Vassart 1993 Somatic mutations in the thyrotropin receptor gene cause hyperfunctioning thyroid adenomas. Nature, *365*:649-651.

Parma, J., J. Van Sande, S. Swillens, M. Tonacchera, J.E. Dumont, and G. Vassart 1995 Somatic mutations causing constitutive activity of the thyrotropin receptor are the major cause of hyperfunctioning thyroid adenomas: identification of additional mutations activating both the cyclic adenosine 3',5'-monophosphate and inositol phosphate-Ca2+ cascades. Mol. Endocrinol., *9*:725-733.

Paschke, R., A. Metcalfe, L. Alcalde, G. Vassart, A. Weetman, and M. Ludgate 1994 Presence of nonfunctional thyrotropin receptor variant transcripts in retroocular and other tissues. J. Clin. Endocrinol. Metab., *79*:1234–1238.

Paschke, R., M. Parmentier, and G. Vassart 1994 Importance of the extracellular domain of the human thyrotropin receptor for activation of cyclic AMP production. J. Mol. Endocrinol., *13*:199–207.

Paschke, R., M. Tonacchera, J. Van Sande, J. Parma, and G. Vassart 1994 Identification and functional characterization of two new somatic mutations causing constitutive activation of the thyrotropin receptor in hyperfunctioning autonomous adenomas of the thyroid. J. Clin. Endocrinol. Metab., *79*:1785–1789.

Pirson, I., S. Reuse, and J.E. Dumont 1994 Regulation of the Max gene expression by different mitogenic pathways in dog primary thyrocytes. Exp. Cell Res., *210*:33–38.

Pohl, V., C. Maenhaut, C. Gerard, G. Vassart, and J.E. Dumont 1992 Differential regulation of thyrotropin receptor and thyroglobulin mRNA accumulation at the cellular level: an in situ hybridization study. Exp. Cell Res., *199*:392–397.

Raspe, E., S. Reuse, P.P. Roger, and J.E. Dumont 1992 Lack of correlation between the activation of the Ca(2+)-phosphatidylinositol cascade and the regulation of DNA synthesis in the dog thymocyte. Exp. Cell Res., *198*:17–26.

Raspé, E. and J.E. Dumont 1994 Control of the dog thyrocyte plasma membrane iodide permeability by the Ca2+-phosphatidylinositol and adenosine 3',5'-monophosphate cascades. Endocrinology, *135*:986–995.

Raspé, E. and J.E. Dumont 1995 Tonic modulation of dog thyrocyte H2O2 generation and I- uptake by thyrotropin through the cyclic adenosine 3',5'-monophosphate cascade. Endocrinology, *136*:965–973.

Robaye, B., A.P. Doskeland, N. Suarez-Huerta, S.O. Doskeland, and J.E. Dumont 1994 Apoptotic cell death analyzed at the molecular level by two-dimensional gel electrophoresis. Electrophoresis, *15*:503–510.

Roger, P.P., M. Baptist, and J.E. Dumont 1992 A mechanism generating heterogeneity in thyroid epithelial cells: suppression of the thyrotropin/cAMP-dependent mitogenic pathway after cell division induced by cAMP-independent factors. J. Cell Biol., *117*:383–393.

Roger, P.P. and J.E. Dumont 1995 Thyrotropin-dependent insulin-like growth factor I mRNA expression in thyroid cells. Eur. J. Endocrinol., *132*:601-602.

Taton, M., F. Lamy, P.P. Roger, and J.E. Dumont 1993 General inhibition by transforming growth factor beta1 of thyrotropin and cAMP responses in human thyroid cells in primary culture. Mol. Cell. Endocrinol., *95*:13-21.

Vassart, G. and J.E. Dumont 1992 The thyrotropin receptor and the regulation of thyrocyte function and growth. Endocrine Rev., *13*:596-611.

Vassart, G., J. Parma, J. Van Sande, and J.E. Dumont 1994 The thyrotropin receptor and the regulation of tyrocyte function and growth: update 1994. Endocrine Rev., *3*:77-80.

CEC Radiation Protection Research Action
Project : F13P - CT930076 (Thyroid)

Final Report From : Dr. J.F. Malone

The overall project objectives as outlined in the initial proposal are as follows :

- Advance fetal and neonatal thyroid dosimetry, and the dosimetry for sensitive target organs / tissues (e g. brain), liable to be irradiated by radionuclides contained in the fetal thyroid, or maternal organs

- Using newly available data on thyroid mass and iodine kinetics, provide country by country (or region) maps for the probable distribution of thyroid radiation dose throughout Europe.

- Derive a more scientific reliable and easier to measure unit than radiation dose against which risksk can be assessed in the thyroid.

Introduction

The report is discussed in three separate sections beginning with fetal thyroid dosimetry including phantom construction, experimental and theoretical results, and conclusions regarding fetal detriment from ^{131}I in the thyroid The next section discusses the status of iodine deficiency in Europe from a dosimetry point of view, incorporating published data for thyroid mass and uptake as well as estimated dose estimates from ^{131}I for each country The final section presents work on the current status of radiation units and their ability to reflect risk of detriment from radiation in the thyroid. The group suggest a new unit and examine it's usefulness for application with risk coefficients.

Progress Achieved including Publications :

• **Fetal Thyroid Dosimetry**

The accumulation of radioactive iodine, ^{131}I, in the fetal thyroid poses a risk of detriment to the thyroid as well as the developing proximal glands. A phantom was constructed to estimate the absorbed dose per unit cumulated activity to the fetal brain at four different stages of gestation, the results of which are presented below .

Absorbed Dose per Unit Cumulated Activity (μGY/MBq/sec)

	12 Weeks	24 Weeks	36 Weeks
Calculated	0.033	0.01	5e-4
Phantom	0.023	0.005	0.001

It was determined from these results that the risk of mental retardation threshold was only exceeded when therapeutic doses of ^{131}I were ingested by the mother. Further to this, work was continued to determine the risk of detriment for all tissue proximal to the thyroid.

Having reviewed many sources, it was felt that there was not enough comprehensive new fetal anatomical data to merit building a fetal phantom complete with organs and bone structure at different stages of gestation for the purposes of thyroid dosimetry. Instead, an approach was taken that circumvented the problems of locating the specific position of fetal organs proximal to the thyroid.

The fetal trunk and head were modelled as elliptical cylinders in perspex for 16, 24 and 36 weeks gestation. By assuming the thyroid occupies the position x = 0, y = 0, z = 0 at the top of the phantom, and by placing TLD's at known positions, it is possible to obtain a map of the doses at different points in the fetal head and trunk. The configuration is illustrated below :

Model of the Fetal Trunk
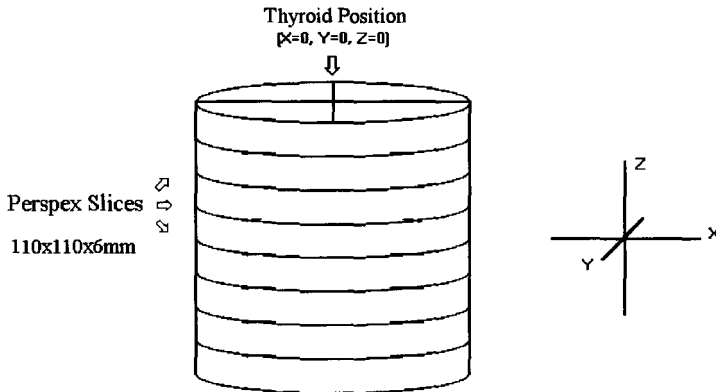
The dimensions of the fetal head and abdomen have been investigated and are well documented for different stages of gestation (Sanders, 1990). The fetal abdominal dimensions (anterior-posterior & transverse diameters) were curve-fitted with respect to gestational age. The results are presented below :

Fetal Abdomen Circumference

versus

Gestational Age
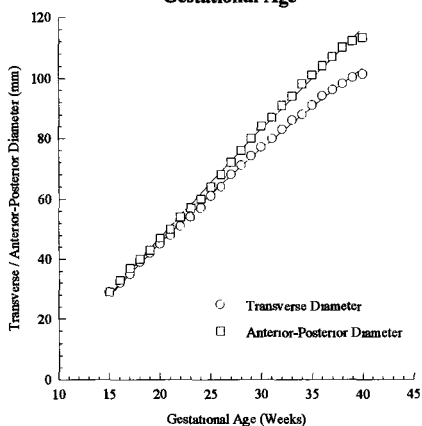
Regression Equations

Trans Diam   -0 024x² + 4 33x - 31.64, r² = 0.9988
A-P Diam   . -0 014x² + 4 26x - 32 53, r² = 0.9983

From these equations, ellipses were constructed using the diameters as a measure of the ellipse eccentricity for 16, 24 and 36 weeks respectively. However, it was found that for the early stages of gestation, the circumference of the fetal head was in fact larger than that of the fetal abdomen. Thus, for the 16 and 24 week phantom, the abdominal ellipses were replaced by ellipses corresponding to shape of the fetal head in order to make the phantom generic The eccentricity of these ellipses (biparietal diameter & frontal-occipital diameter) was derived from the formula (Chudleigh & Pearce, 1992):

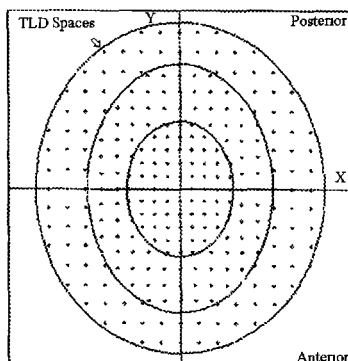$$HC = 1.62(BPD + OFD)$$

where   HC = Head Circumference (tabulated vs gestational age)
        BPD = Biparietal Diameter
        OFD = Occipital-Frontal Diameter

The three ellipses corresponding to the three different stages of gestation were superimposed on top of each other and TLD positions were calculated for each ellipse as illustrated below :

Fetal Phantom at 16, 24, 36 weeks

The volumes of ^{131}I to be used at each stage of gestation were determined from Evans (1967) and are tabulated below :

Gestational Age (Weeks)	Thyroid Volume (mls)	Thyroid - Crown Distance (mm)	Number of Perspex Slabs
16	0.05	56 0	10
24	0 31	89.0	15
36	1.04	137.0	23

The number of slabs used for each stage of gestation corresponds to the distance between the fetal thyroid and the top of the crown as this distance encompasses all proximal thyroid tissue. These values were taken from England (1983) and are tabulated above with the number of slabs required per phantom.

An estimate of the absorbed dose per unit cumulated activity, S, to each slab was made using the MIRD schema, for comparison with experimental findings, and is discussed below :
The MIRD schema assumes that absorbed dose may be represented as :
$$D = A x S$$
where D is the absorbed dose, A is the cumulated activity in the thyroid, and S represents the absorbed dose per unit cumulated activity The cumulated activity, A, is a product if the initial activity, Ao, of ^{131}I taken into the thyroid and the time it spends resident in the gland, the effective half-life. The initial activity may be represented by the uptake of the thyroid. The effective half-life varies with sex and age as well as the clinical state of the thyroid. The absorbed dose per unit cumulated activity, S or S-factor, is a function of thyroid mass and is calculated from

$$S = S_{ref} * \frac{M_{ref}}{M}$$

where S_{ref} = S for the thyroid of reference man (1.652µGy/MBq s)
M_{ref} = Reference man thyroid mass (19.63g)
M   = Population thyroid mass (g)

In conclusion, a phantom has been constructed to measure dose to the fetal brain from ^{131}I in the fetal thyroid Results indicate that therapeutic doses of ^{131}I must be ingested to initiate detriment. A generic phantom has also been constructed to simulate all fetal proximal tissue. TLD's have been calibrated and positioned to ensure maximum spatial resolution. Work is continuing to obtain dose estimates from this phantom for all proximal tissues

• **Thyroid Dose Maps**

Iodine deficiency manifests itself in a population in the form of elevated thyroid mass / volume and increased iodine uptake. In the presence of a nuclear accident, this would imply the elevated uptake of radioiodines and hence an increased dose to the thyroid.

In Europe, there is a marked variation in the dietary intake of iodine and hence the mass and uptake of the thyroid. The continent may be divided up into three categories of iodine deficiency as illustrated below.
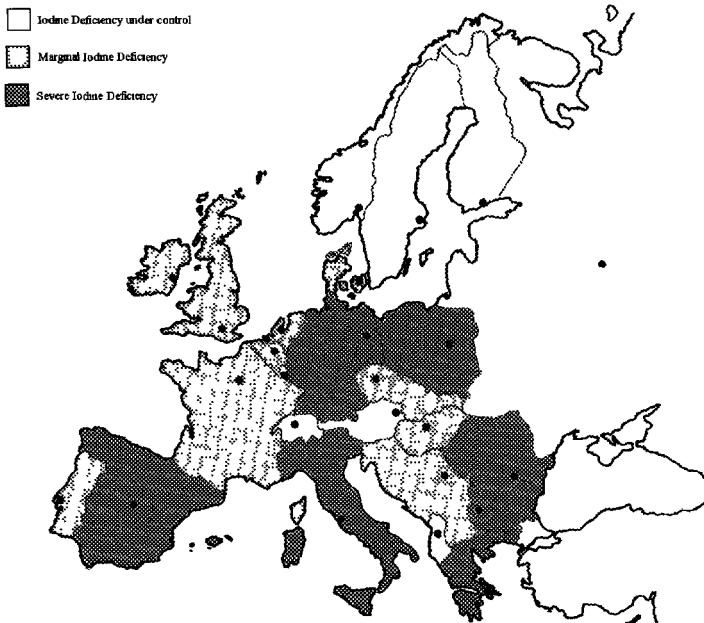
1   Iodine deficiency presently under control :
     Austria, Switzerland, Norway, Sweden, Finland.

2   Marginal iodine deficiency .
     Belgium, Czechoslovakia / Slovakia, Denmark, France, Hungary, Ireland, Portugal, Britain.

3. Moderate to severe iodine deficiency .
     Bulgaria, Germany, Greece, Italy, Poland, Romania, Spain.

Iodine deficiency has also recurred after transitory resolution in Croatia and Netherlands

From the point of view of thyroid dosimetry, the most important effects of ID are on the percentage iodine uptake by the gland and the mass of the gland. Illustrated below are the reported ranges of iodine uptake in the thyroid expressed as a percentage of the ingested iodine

Iodine Uptake in Europe - % Administered Dose

These ranges have been calculated from iodine excretion levels in Europe reported by Delange (1994) using the relationship formulated by Stanbury between urinary iodine excretion and iodine uptake as reported by Ermans (1993)

$$U = \frac{57.4}{57.4 + E}$$

where   U = Uptake as a % of the ingested iodine
         E = Urinary Iodine Excretion level (μg per 24 hrs)

Since the urinary iodine level is considered to be a good indicator of the dietary iodine intake, it is clear from the above relationship and illustrated values that those areas with iodine deficiency have a high uptake level. For example, Germany, a region of severe iodine deficiency has an uptake range of 45.1 - 75.2 %, whereas Sweden, an area of sufficient dietary iodine intake, has an uptake range of 14.8 - 27.7 %. This would infer that the Swedish population would recieve a lower dose from an ingestion of radioiodine than the German population. However, this neglects the effect of thyroid mass which may be shown to have a more significant effect on the absorbed dose.

Tabulated below are reported values for thyroid mass in the literature (quoted at end). Also tabulated are dose ranges based on these figures and the previously discussed uptake ranges, calculated using the MIRD method (see previous section) and assuming each population has ingested 1 MBq of [131]I. For the purposes of the dosimetry presented here, the effective half-life was assumed to take on a value of 7.3 days for adults, 7 0 days for schoolchildren, and 4.8 days for neonates as reported by ICRP 56 (1989) ·

Country	Sex	Age (Years)	Thyroid Mass (g)	Absorbed Dose Range (Gy/MBq)
Sweden	M	-	11 1	0.41 - 0.76 *
	F	-	7 7	0.59 - 1 10 *
Finland	-	-	10 4	0.47 *
Denmark	M	13-91	19.6	0.61 - 0.92 *
	F	13-91	17.5	0.68 - 1.03 *
Holland	M	-	14.7 *	0 55 - 0 76
	F	-	10.7 *	0 76 - 1 05
Belgium	N	-	0 84 *	11 98 - 13.09
	-	8-11	2.7 *	4.97 - 5 43
	-	>17	11.6 *	1.29 - 1.41
Ireland	M	-	15.6	0.48 - 0.96 *
	F	-	12.2	0.61 - 1.23 *
Britain	M	9-11	5 03 *	1.67 - 2 46
	F	9-11	5.87 *	1.43 - 2 11
Germany	M	-	26.9	0.51 - 0.85 *
	F	-	16.5	0.84 - 1.38 *
Poland	-	6-8	6.1, 4 8 *	1.36 - 3.37
	-	9-10	7.2, 5.7 *	0 5 - 0.65
	-	11-12	8.4, 6 6 *	
	-	13	9.1, 8.0 *	
	F (Pregnant)	27	27.8 *	
Slovakia	M	-	11.8	1.09 - 1.71 *
	F	-	10.6	1.21 - 1 9 *
Swiss	N	-	1.2 *	4.53 - 5 25
	-	11-20	11.6 *	0 7 - 0.81
	-	21-30	17 *	0.48 - 0 55
	-	61-70	28 *	0.29 - 0.34
Austria	-	6	2 55 *	1.18 - 2 98
	-	10	3.83 *	2.09
	-	14	3 23, 6 42 *	
	-	16	4.07 *	
Hungary	F	11	13 0 *	0 68 - 1 39
	-	6	3.5 *	0.84 - 5 15
	-	14	10.6 *	
Italy	-	6	2.7 *	1 33 - 8 65
	-	14	6.3 *	
Croatia	-	7-11	9.9 *	1.08
	M	12-15	11.6 *	0.92
	F	12-15	10.6 *	1.01
	-	13	10.2 *	1.05
Norway	-	-	Swedish Mass	0 52 - 1 10
France	-	-	Irish Mass	0.5 - 1 23
Portugal	-	-	Irish Mass	0.6 - 2.14
Spain	-	-	German Mass	0 39 - 1.22
Greece	-	-	German Mass	0.28 - 1.10
Romania	-	-	German Mass	0.35 - 1.10
Bulgaria	-	-	German Mass	0.56 - 1.38

The above results clearly demonstrate the dramatic effect of thyroid mass on the absorbed dose regardless of the high iodine uptake in iodine deficient areas. For example, the Swedish population receive a dose in the range 0 41 - 1 10 Gy/MBq ingested, while the severely iodine deficient region of Germany recieves a dose in the range 0.51 - 1.38 Gy/MBq ingested. Hence, the ratio of the highest doses received by the two populations is 1.25, i.e. the German dose is 1.25 times that of Sweden, which does not reflect the huge differences in iodine uptake between the two populations, 74.16% and 27.68% respectively This brings into question the use of the quantity absorbed dose as a suitable indicator for risk analysis. This argument has been raised by previous authors (Malone & Gilligan, 1990) and is addressed in the next section of the project.

The above dose estimates have been based on, in so far as was possible, recent data for each country However, in most cases, data regarding thyroid mass was not quoted in conjunction with urinary iodine excretion values and thus, for the purposes of dosimetry, this had to be assumed This assumption may be invalid for those countries where the state of iodine deficiency is regionally variable, such as Portugal which is considered to have mild deficiency although there are pockets of severe deficiency present. These populations will have a modified dose distribution compared to those areas of mild deficiency.

Similarly, iodine metabolism is highly age and sex dependent, with children presenting a higher turnover of thyroidal iodine and smaller gland masses than adults. This results in higher doses to children and neonates than for adults. It would be preferable to produce dose estimates for each population based on age, sex and region. However, in the vast majority of cases, results are presented for schoolchildren only. Furthermore, many authors quote the extent of goitre prevelance in their country and in some cases provide detailed maps of that prevelance, yet no determination of the prevailing thyroid mass may be made from this data.

Consequently, from the point of view of thyroid dosimetry, it is essential to examine a cross-section of the population of each country where both thyroid mass / volume and urinary iodine excretion levels are recorded in tandem, as well as the age and sex of the subjects.

In conclusion, thyroid dose estimates have been made for each European state based on data from the literature. The inadequacy of this data has been highlighted for a number of cases and suggestions have been made to improve the situation.

• **Radiation Dose Unit**

As previously discussed, absorbed dose has been demonstrated to provide an inaccurate reflection of the detriment to a gland due to it's dependency on mass. In a paper concerning this argument, Gilligan & Malone (1991) proposed that it was not unreasonable to assume that the probability of a cell undergoing initiation was a stochastic process with no threshold. Therefore, the number of cells undergoing initiation will increase linearly with the number of cells in which energy is deposited.

The aim of this study was to compare different types of proposed concepts that may give a better representation of the actual risk based on the above hypothesis. These were :

1. Absorbed Dose (joules per kilogram), D
2. Integral Absorbed Dose (joules), I
3. Biologically Effective Energy (joules), B

Absorbed dose is simply the product A x S as discussed previously. The integral absorbed dose is the product of the absorbed dose and the gland mass. The biologically effective energy is the energy imparted per cell summed over the total number of cells in the gland and may be written as .

$$B = F \sum_n E_n$$

where E_n = Energy imparted per cell
           F = Factor accounting for edge effects ($F = 1$ for this calculation)
           n = Total number of cells in the thyroid.

To obtain an estimate of n, eleven thyroids were examined for their epithelial cell content per gramme of thyroid. The results are summarised below ·

Thyroid Number	Epithelial Cells x 10^6 per gramme	Comments
1	31.3	*50g thyroid, Graves Disease, Hyperplastic*
2	25.0	*Multinodular Goitre*
3	28.0	*35g thyroid, Normal*
4	21 1	*Benign Colloid goitre*
5	23.4	*Colloid Nodule*
6	14.9	*Nodular Goitre*
7	31.3	*5g Thyroid, Granulomatous Thyroiditis with Fibrosis*
8	20.1	*30g Thyroid, Benign Colloid Nodule*
9	20.5	*No Report*
10	23.7	*Colloid Nodule*
11	25.0	*Normal*
Mean ± S.D.	24.03 ± 4.94	

From these results, three thyroid types, presented below, were chosen for dosimetry calculations ·

Thyroid Type	Epithelial Cells x 10^6 / g
Normal	25
Colloidal	21
Hyperplastic	31

In order to perform the dosimetry calculations it was assumed that 1 MBq of ^{131}I was ingested and the thyroid uptake was 30%. The effective half-life was taken to be 7 6 days (Henrichs, 1982). It was also assumed that the epithelial cells comprised 70% - 80% of the cellular content (Studer & Ramelli, 1982) and 30 % of the total thyroid mass (Malone et al., 1983). The number of mutations per cell per gray was taken to be 2.5 x 10^{-5} (Nakamura et al., 1989). The calculations are summarised below .

Thyroid	1	2	3
Tissue Type	Normal	Colloidal	Hyperplastc
Gland Mass (g)	20	20	20
Mutations / Cell / Gray		2.5×10^{-5}	
Cells x 10^6/ g	25	21	31
Absorbed Dose (Gy)	0.46	0.46	0.46
Integral Absorbed Dose (mJ)	9.2	9.2	9.2
Biologically Effective Energy (mJ)	9.2	9.2	9 2
No. of Mutations	5750	4830	7130

Each method of dose calculation gave similar results regardless of the number of cells contained in each thyroid This may be attributed to the mass dependency of each of the concepts and does not reflect the proposed increased risk in those thyroids with an elevated number of cells

However, this group proposes a different approach to this problem that reflects the hypothesis that there is an increased risk of mutation with an increased number of cells. The quantity to be measured is *Number of Cells per milli-Joules Energy* in the Thyroid. This is calculated by multiplying the number of cells per gramme by the thyroid mass and dividing by the incident energy. If we take the same parameters as before and assume 10mJ is deposited in the thyroid, then the calculation is as follows :

Tissue Type	Normal	Colloidal	Hyperplastc
Gland Mass (g)	20	20	20
Mutations / Cell / Gray		2.5×10^{-5}	
Cells x 10^6/ g	25	21	31
Energy (mJ)	10	10	10
Cells x 10^6 / mJ	50	42	62
No. of Mutations	5750	4830	7130

In this case, the cells / mJ values reflect the increased number of mutations in the hyperplastic thyroid and hence the increased risk of detriment. On examining the hyperplastic thyroid at different weights, similar results were found and are tabulated on the following page.

Tissue Type	Hyperplastic	Hyperplastic	Hyperplastc
Gland Mass (g)	20	30	40
Mutations / Cell / Gray	$2 5 \times 10^{-5}$		
Cells x 10^6/ g	25	21	31
Energy (mJ)	10	10	10
Cells x 10^6 / mJ	50	63	124
No. of Mutations	5750	10867	28520

Again, the quantity Cells / mJ reflects the increased risk in the larger thyroids, due to the increased number of cells Therefore, in the context of risk assessment, this group proposes the use of the quantity Cells / mJ for use with those organs where the number of cells per gramme may be estimated

In conclusion, three important areas of doimetry have been reviewed by this project. Fetal dosimetry has been reviewed and a generic phantom that incorporates all fetal proximal tissues has been constructed. Results from this phantom will prove to be very useful for estimating detriment to the fetus from ingestion of ^{131}I. Data for important thyroid parameters have been accumulated from many sources in the literature and dosimetry maps have been constructed for every European state. The inadequacy of the data for a number of countries has been highlighted and the group has suggested a number of solutions. Notwithstanding this, the maps will prove to be very useful for estimating population doses and detriment from ^{131}I should a nuclear accident occur. Finally, the group has highlighted the weakness of current doimetry methods in predicting radiation damage and the initiation of cancer cells in the thyroid gland. A new unit has been proposed and examined, and with further investigation, may prove to be an excellent indicator of radiatoin damage to all human organs

• **Publications**

Gilligan P. and Malone JF., 1991, Radiology of the Thyroid: Estimates of Consequences of Radiation Fallout, In Proceedings of EORTC Study Group, Dublin, 1992, (Berlin, Henning)

Malone JF., 1992, Consequences of Iodine fallout : Dosimetric and Radiobiological Considerations, In 'Iodine deficiency in Europe - A Continuing Concern', Ed. Delange et al , (New York, Plenum Press)

O'Hare NJ., Gilligan P , Murphy D., Malone JF., Estimation of Fetal Brain Dose from ^{131}I (in preparation).

- **References**

Aghini-Lombardi, 1993, Iodised Salt Prophylaxis of Endemic goitre : An Experience in Toscana, Italy, Acta Endocrinol , 1993, 129, 497 - 500

Ando et al., 1994, Endemic goitre in Calabria : Etiopathogenesis and Thyroid Function, J. Endorinol. Invest., 17, 329 - 333.

Berghout et al., 1987, Determinants of Thyroid Volume as Measured Directly by Ultrasonography in Healthy Adults in a Non-Iodine Deficient Area, Clin Endocrinol , 26, 273 - 280.

Berghout et al., 1988, The Value of Thyroid Volume Measured by Ultrasonography in the Diagnosis of Goitre, Clin. Endocrinol., 28, 409 - 414.

Chanoine et al., 1991, Determination of Thyroid Volume by Ultrasound from the Neonatal Period to Late Adolescence, Eur. J. Pediatrics, 150, 395 - 399.

Chudleigh & Pearce, 1992, Obstetric Ultrasound - How Why and When, 2nd Ed. (Church-Livingstone).

Delange, 1994, Iodine Deficiency in Europe, In 'Thyroid International', Ed. Hennemann et al., (Merck, Darmstadt).

Delange et al , 1986, Regional Variations of Iodine Nutrition and Thyroid Function during the Neonatal Period in Europe, Biol. Neonate, 49, 322 - 330.

England, 1983, A Colour Atlas of Life Before Birth, (Wolfe Press, London).

Ermans, 1993, Iodine Kinetics in Iodine Deficiency, In 'Iodine Deficiency in Europe - A Continuing Concern', Ed Delange et al., (Plenum Press, New York), 51 - 56.

Escobar Del Rey et al., 1981, A Survey of Schoolchildren from a Severe Endemic Goitre Area in Spain, Quarterly J. of Medicine, L., 198, 233 - 246.

Evans et al , 1967, Radioiodine Uptake Studies of the Human Fetal Thyroid, Journ. Nuc Med., 8, 157-165.

Gilligan, Fetal Brain Dose and Detriment from ^{131}I in the Fetal Thyroid, (Thesis).

Gutekunst et al., 1986, Goitre Epidemiology · Thyroid Volume, Iodine Excretion, Thyroglobulin and Thyrotropin in Germany and Sweden, Acta Endocrinologica, 112, 494 - 501.

Hegedus, 1990, Thyroid Size Determined by Ultrasound Influence of Physiological Factors and Non-Thyroidal Disease, Dan Med Bull, 37, 249 - 263.

ICRP 56, 1989, Age-Dependent Doses to Members of the Public from intake of Radionuclides · Part 1, 47 - 48, (Pergamon Press, New York).

Iodine Deficiency in Europe - A Continuing Concern, Ed. Delange et al., (Plenum Press, New York), 51 - 56.

ICCIDD Newsletters, 2 . 4 Nov. 1986, 3 : 4 Nov 1987, 4 : 2 May. 1988, 4 : 3 Aug. 1988, 4 . 4 Nov. 1988, 6 1 Feb. 1990, 8 · 1 7 . 3 Aug. 1991, 7 : 4 Nov. 1991, Feb. 1992 , 8 : 3 Aug. 1992, 8 : 4 Nov. 1992, 9 · 1 Feb. 1993, 11 : 1, Feb. 1995.

Langer et al., 1992, The Importance of Optimal Iodine Intake, the Present Status and Prespective in Slovakia, Vnitr. Lek., 38, (Abstract).

Lindberg et al , 1989, The Impact of 25 Years Iodine Prophylaxis on the Adult Thyroid Weight in Finland, J. Endocrinol. Invest., 12, 789 - 793.

Malone et al., 1983, Glandular Epithelium with Particular Reference to Thyroid, In 'Cytotxic Insult to Tissue', Ed. Potten & Hendry, (Churchill-Livingstone, Edinburgh), 186-187.

Malone & Gilligan, 1990, Problems in Dosimetry including Consideration of Special Groups   In Utero the Neonate Children and Adults, In 'Iodine Prophylaxis after Nuclear Accidents', Ed Rubery & Smales, (Pergamon Press, London), 65 - 79.

Nakamura et al., 1989, X-ray Induced Mutations in Cultured Human Thyroid cells, Radiation Research, 119, 123-133

Nauman & Wolff, 1993, Iodide Prophylaxis in Poland after the Chernobyl Reactor Accident : Benefits & Risks, American Journal of Medicine, 94, 524 - 532.

Nohr et al., 1994, Iodine Status in Neonates in Denmark - Regional Variations and Dependency on Maternal Iodine Supplementation, Acta Paediatrica, 83, 578 - 582.

Nygaard et al., 1993, Thyroid Volume and Morphology and Urinary Iodine Excretion in a Danish Municipality, Acta Endocrinol., 129, 496 - 500.

Oberhofer et al , 1992, Goitre Epidemiology in South Tyrol, 117, 1508 - 1512, (Abstract).

Oliveira et al., 1983, Bocio Endemico No Sul de Portugal, Soc of Medical Sciences, Lisbon, 1 - 6.

Oliveira et al., 1988, Bocio Endemico Em Potugal, Medicina & Cirurgia, 8, 475 - 489.

Sanders, 1991, Clinical Sonography - A Practical Guide, 2nd Ed., 505 - 535.

Yokoyama et al , 1986, Determination of the Volume of the Thyoid Gland by a High Resolutional Ultrasonic Scanner, Journ. Nuc. Med., 27, 1475 - 1479.

Head of project 3: Dr Smyth

II.   Objectives for the reporting period

1.   Establishment of baseline data for dietary iodine intake, thyroid volume and gross
     morphology in an area without endemic goitre, against which changes in iodine intake
     as a result of altered dietary habits or a programme of iodine prophylaxis could be
     measured. Incorporate findings into detriment determinations (Collaboration with
     Malone, Dublin)

2.   To initiate a study examining prospective changes in maternal renal handling of
     ingested iodine during the three trimesters of pregnancy and postpartum.

3.   To investigate the iodine content of breast milk from nursing mothers and to
     compare findings with other European studies.

4.   To establish the relationship between maternal and neonatal urinary iodine
     excretion in breast feeding and non-nursing mothers.

5.   To establish an experimental model whereby the effects of external irradiation on
     intercellular signalling systems in organ and cell cultures of animal and human
     thyroid can be determined.

6.   To investigate the presence of abnormal (non-TSH) stimulators of thyroid growth in
      patients with thyroid cancer and to study the intracellular signalling systems through
     which such ßstimulators act to promote growth processes in the human thyroid.

7.   To construct regional dosimetric maps incorporating data for thyroid volume and
     dietary iodine intake in Europe (Collaboration with Malone, Dublin)

.

III.   Progress achieved including publications

Thyroid Volume

Mean values ± SE for thyroid volume obtained in randomly selected patients (different subjects
in each group) during the three trimesters of pregnancy and at 6 and 15 to 24 weeks postpartum
compared to non pregnant controls shown in Fig. 1. Also shown are the mean values
obtained from 20 subjects studied sequentially during pregnancy (same subjects studied
throughout pregnancy and postpartum).
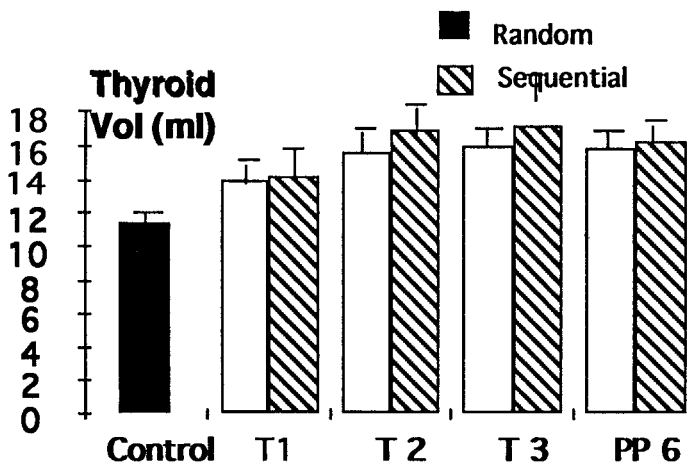
Fig. 1 Thyroid Volume (Mean±se ml) in Random v Sequentially studied Groups

It can be seen that in the random group, there was a significant increase in mean-thyroid volume compared to non-pregnant control values and this occurred as early as the first trimester and was maintained throughout the three trimesters of pregnancy. A maximum increase of 41.6% over control mean values was observed in the third trimester. An identical pattern was observed in the sequentially studied subjects with mean values being almost superimposable on the those obtained in the random group. A maximum increase in thyroid volume of 52.2% over the non-pregnant mean value was observed in the sequentially studied subjects. The percentage of individual patients in the various study groups having enlarged thyroid glands (i.e > 18.0 ml) are shown in Table 1. The numbers of enlarged thyroids increase reaching a maximum of 31.0% in the second trimester, which is maintained throughout pregnancy and even to 14 to 24 weeks postpartum.

Group	N	Mean±SE (Ml)	% Enlarged
Control	95	11.3±0.5	6.3
T1	41	13.9±0.8	19.5
T2	29	15.6±1.0	31.0
T3	45	16.0±0.7	30.2
PP 6	84	15.9±0.7	32.0
PP 14-24	28	15.6±1.0	32.1

Table I Mean Values±SE for thyroid volume measured by ultrasound and % of individual enlarged values (>18.0Ml) during pregnancy and postpartum.
T= Trimester 1,2,3. PP= Weeks postpartum.

Urinary Iodine Excretion in Pregnancy

An early report had shown that in contrast to findings in other European countries where iodine intake is low, urinary iodine excretion in the study in the study population increased during the three trimesters of pregnancy. Because this finding was at variance with other reports, the study was repeated in two parts :-

(a) retrospective: Random urine samples were obtained from groups of patients attending a maternity hospital during the first, second and third trimesters of pregnancy (T1, T2 and T3), at delivery+ 3 days and at 6 and 15 weeks postpartum (PP). Results were expressed as μg Iodine excreted /L of urine (μg/L) or as μg of I excreted / gram creatinine. As iodine excretion in Northern European countries demonstrates a seasonal variation, results were compared to a controlled non-pregnant female population (N=1063) sampled at different seasons over a two year period.

(b)Prospective: A group of 38 individual pregnant patients from within the retrospective group were available for follow up sequential studies during the three trimesters of pregnancy. Results for this group are shown in Fig.2. Iodine excretion in the Prospective group paralleled that observed in the retrospective group (not shown) rising as early as the 1st Trimester and remaining elevated throughout gestation. An interesting observation was the precipitous fall in UI at delivery returning to non-pregnant control values within 3 days. The same pattern was observed whether results were expressed as μg Iodine excreted /L of urine (μg/L) or as μg of I excreted / gram creatinine. These findings offering further confirmation that the increase in urinary iodine excretion observed during pregnancy was a real effect which reflected increased renal iodine loss during gestation.
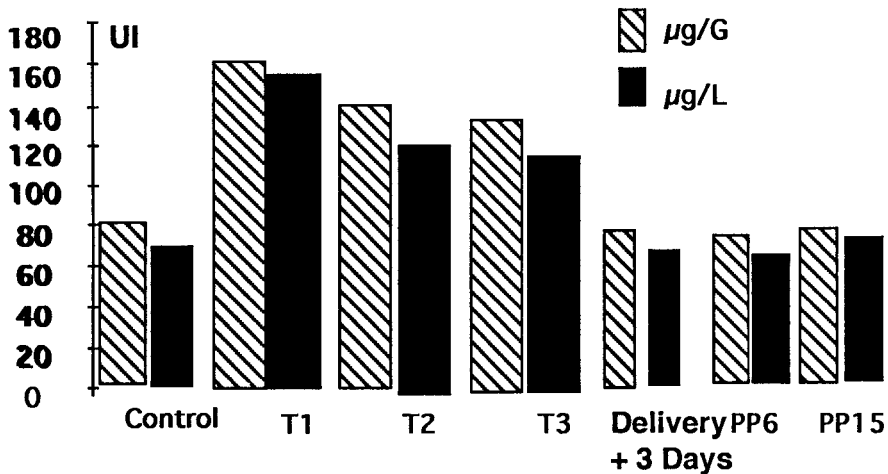
Fig.2 UI Excretion in the Sequential Group (N=38)
Median UI Values(ml)

In view of the discrepancy in UI excretion patterns in pregnancy between Ireland and those reported from other European countries, UI excretion was investigated in 2 further groups of pregnant women residing on either side of the Irish Sea . The regions selected were the North Eastern region of the Republic of Ireland (IRL-NE) and Cardiff, Wales (UK-Cardiff). As shown in Fig. 3 There was a dramatic increase in UI excretion during pregnancy compared to pregnant controls in both IRL - NE and UK- Cardiff populations confirming the earlier findings in the IRL Dublin population. This increase in levels of excretion was particularly evident in the IRL-NE population and was also apparent from the high levels of iodine excretion found in school-children from this region (Mean value 255±89 μgL :Median 272 μg/L). The iodine excretion patterns recorded in both pregnant mothers and schoolchildren were observed during the winter months and most probably reflected the seasonal increase in the iodine content of winter milk previously reported in Ireland and other Northern European countries.
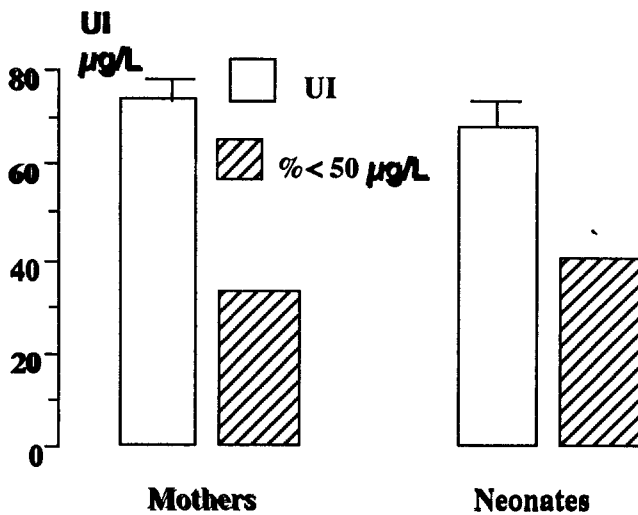
Fig.3 UI excretion during pregnancy in populations drawn from both sides of the Irish Sea.

Breast Milk Iodine (BMI)Studies: Samples of breast milk were taken
for iodine analysis at 3 days following delivery from 52 nursing mothers. Urine samples were
simultaneously obtained from both mother and neonates. The mean BMI value was 84 ± 7.4
μg/l (Median 74). There was a wide variation with values ranging from 20-300 μg/L. There
was a highly significant correlation between mothers BMI and UI excretion as measured in the
neonate. ($r = 0.81$ p<.001) thus demonstrating in infants the ability of UI excretion to
accurately reflect dietary iodine intake. BMI values were consistent with those from other
European countries with similar dietary iodine intakes.

Maternal and Neonatal Iodine Status: To investigate the effect of increased gestational UI on
neonatal iodine status, urinary iodine excretion (UI μg/L) was measured in casual urine
specimens obtained at 3 days following delivery from 108 mothers and their 3 day old infants.
Results are shown in the accompanying Figure 4.
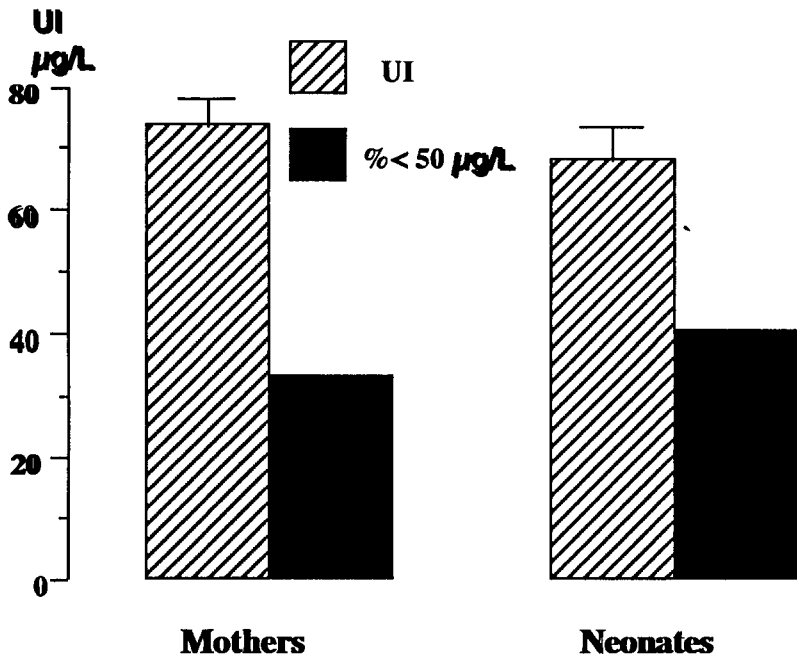
Fig. 5 UI Excretion in Mothetrs and Neonates

As shown in Fig.5 there was no significant difference in either mean UI between mothers and neonates (74.5±5.7μg/L and 68±4.6μg/L respectively) but this masked the fact that neonatal UI varied with the mode of intake. UI in 64 Breast -feeding mothers (76±5.6μg/L) was significantly lower than in their infants (100±6.8μg/L; p<0.01) . However as shown in Fig. 6, the corresponding UI mean in 44 bottle-fed infants (43±3.5 μg/L) was significantly lower than in the breast feeding group (p<0.01). In addition the % of individual values <50μg/L (6.25% in the breast feeding group) was ten times greater than that of 62.5% in bottle feeders (p<0.001).
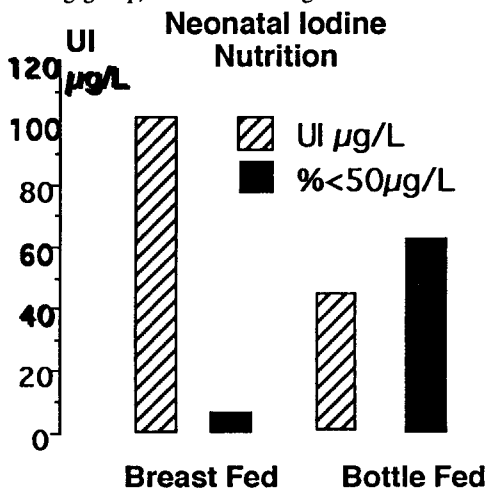
Fig. 6 UI excretion p[atterns in 3 day old neonates (Breast or Bottle Feeding).

UI in Breast -feeding mothers (76±5.6μg/L) was significantly lower than in their infants (100±6.8μg/L; p<0.01) and the percentage of low values (<50μg) was only 6.25% in neonates compared to 26.5% in mothers. The observed UI excretion in breast fed infants demonstrates that the iodine concentrating ability of the breast will maintain neonatal iodine intake and offer a degree of protection against deficiency even at the expense of the mother . Such protection is frequently absent in neonates of non-nursing mothers.

Thyroid Dosimetry

An experimental model has been established whereby organ cultures, frozen sections and cell cultures can be exposed to external irradiation. An X-ray source of 200KV with a filtration = 2.0mm aluminium has been set up to deliver from 1-10 Gy to thyroid specimens (organ or tissue cultures) at a distance of 43.0cm from the focus. Organ cultures of guinea pig thyroid were irradiated with X-rays to give a calculated dosage of 1,000 rads. Following irradiation the thyroid tissue was snap frozen at -70°C and 12μm sections cut on a cryostat. Irradiated and control tissues were assessed cytochemically for lysosomal naphthylamidase(LNase) activity, an index of lysosomal membrane permeability. No significant difference was observed in free LNase activity between irradiated and control sections. However, when tissues were exposed to acid labilisation using acetate buffer (pH 5.0) the irradiated tissue appeared to lose the ability to respond to acid labilisation as latent intralysosomal enzyme activity only increased by 6.6%. In contrast the increase in the latent enzyme activity was 54.1% in the control tissue.

Growth Stimulation in Thyroid Cancer

IgG concentrates prepared in serum from patients with Graves' disease or nontoxic goitre have been shown to exert growth stimulatory effects on human and guinea pig thyroid tissues. The presence of such stimulators, previously shown to separate Graves' disease from other goitrous conditions by their ability to stimulate cAMP production in thyroid follicular cells, was investigated in IgG's prepared in sera from 13 patients with thyroid carcinoma. Significant augmentation of glucose-6-phosphate dehydrogenase(G6PD) activity within thyroid follicular cells, an index of stimulation, was promoted by all 13 thyroid cancer IgG concentrates; mean 37.0 %, range 8.0- 71.0% (nongoitrous reference range < 8.0 %). This demonstrates the presence of a non-TSH thyroid stimulator, as all patients had suppressed TSH (< 0.1 mU/L). In an attempt to elucidate the mode of action of IgGs in thyroid cancer, human thyroid tissue was incubated with IgG in the presence of 3 cAMP inhibitors, potassium iodide, diflouromethylornithine (DFMO) and carbamylcholine as well as indomethacin, an inhibitor of cAMP independent stimulatory pathways. Thyroid cancer IgG stimulated G6PD activity in human thyroid tissue was significantly inhibited by all 3 cAMP inhibitors. In contrast, indomethacin had little effect in reducing G6PD stimulation. These finding demonstrate the presence of non-TSH dependent growth in thyroid cancer mediated via a cAMP dependent stimulatory pathway.

Dosimetric Maps

Appropriate data from the above findings as well as available data on thyroid mass and urinary iodine excretion were incorporated into map (in collaboration with Malone, Dublin).

Publications

Smyth, PPA. 'Status of iodine deficiency in Ireland.in Iodine deficiency in Europe. A continuing concern. Workshop, Brussels.(F. Delange, JT Dunn and D Glinoer eds). NATO ASI Series A ,Plenum Press, New York (1993) 317-322.

Smyth, P.P.A . " Thyroid Disease and Breast Cancer " Clinical Symposium: The Female Thyroid In Health and Disease Eds Glinoer,D and Martino E.Journal of Endocrinological Investigation, (1993)16: 396-401.

Lazarus, JH, Smyth, PPA, Parkes, A.B., Darke, C and N' Diaye, A.M. "Are immunological factors involved in the pathogenesis of endemic goitre in Senegal." Journal of Endocrinology (1993) 137: 208.

Long, H.A., O'Herlihy, C. and Smyth P.P.A. "Human chorionic gonadotrophin (hCG) as a thyroid growth stimulator in normal pregnancy." Journal of Endocrinology (1993) 137: 216

Long, H.A., Conway, D.J., Mercer, P.M., Murphy, D., Stokes, M., Sheahan, K., O'Higgins, N.J. and Smyth, P.P.A. "Glucose-6-phosphate dehydrogenase (G6PD) O_2 sensitivity : a cytochemical adjunct to the diagnosis of thyroid carcinoma." Journal of Endocrinology (1993)137: 20.

Martino E, Glinoer D and Smyth PPA (eds) "The Female Thyroid in Health and Disease". Journal of Endocrinological Investigation, (1993)16: 373-401

Long, H.A.,Hetherton AM, Ryan R,Radcliffe M, O'Herlihy, C. and Smyth P.P.A. "Studies on Pregnancy Goitre". Irish J Med Sci (1993) 162 (Suppl1): 16.

Bonar DB, Smith DF, Hetherton AM and Smyth PPA. " Hypothyroidism in Irish Women". Irish J Med Sci (1993) 162(Suppl1): 43. .

Doran, M., McDermott, E.W.M., Mercer, P.M., P.P.A. Smyth and O'Higgins, N.J. "Changing trends in thyroid carcinoma". Irish J Med Sci (1993) 162: 98..

Hetherton AM, Smyth PPA, Jones T, Ferriss BJ, O'Flynn W, O' Donnell J and Cunningham F."Regional dietary iodine intake in Ireland". Irish J Med Sci (1993) 162: 111.

Smyth PPA, O'Carroll D, Hetherton AM , Coveney E, Mc Alister V, Mc Dermott EWM , Murray MJ and O'Higgins NJ ."Thyroid Enlargement and Breast Cancer". Irish J Med Sci (1993) 162:100.

Doran, M., McDermott, E.W.M., Mercer, P.M., Smyth P.P.A.Cassidy M, Cross KS and O'Higgins, N.J. "Thyroid Carcinoma in a Dublin Hospital :Changing trends". Irish J Med Sci (1992) 161: 49..

Ahmed M, Cunningham FO Smyth PPA, Hetherton AM , Murray M and O'Higgins NJ "Comparison of thyroid volume in patients with breast cancer attending two different study centres".Irish J Med Sci (1993) 162: 237.

Mercer, P.M, Murphy, D., Stokes M, Long, H.A., Conway, D.J., Sheahan, K., O'Higgins, N.J. and Smyth, P.P.A. "Glucose-6-phosphate dehydrogenase (G6PD) O_2 activity : a metabolic index in the diagnosis of thyroid carcinoma." British J Surgery (1993) 80: 1208.

Lazarus JH, Phillips DIW, Parkes AB, Smyth PPA and Hall R. Status of iodine nutrition in the United Kingdom. in Iodine Deficiency in Europe - A Continuing Concern. F Delange, JT Dunn and D Glinoer eds. NATO ASI Series, Plenum Press (New York) 1993: 323.

Bonar BD, Hetherton AM, Smith DF, Darke C and Smyth PPA. Hypothyroidism in a Community : Prevalence and Pathogenesis. J Endocrinological Invest. (1993) 16:140.

Long HA, O'Herlihy C and Smyth PPA. Pathways for thyroid growth stimulation in normal pregnancy. J Endocrinological Invest. (1993) 16:149.

Long HA, Hetherton AM, Ryan R, Radcliff M, O'Herlihy C and Smyth PPA. Control of thyroid volume during pregnancy. Thyroid (1993)3:T-8, 16.

Smyth PPA., Long HA , Sheahan K, O'Higgins NJ. The "Glucose-6-phosphate dehydrogenase (G6PD) O_2 insensitivity phenomenon: A metabolic index in thyroid carcinoma. Thyroid (1993) 3:T-112,221.

Cusack YA, Riordain DO' , Mercer PM , O'Higgins NJ and Smyth,PPA. O2 insensitivity of G6PD activity in human breast carcinoma.
J. Endocrinology (1994) 140: OC13.

Conway DJ, Long HA , Mercer PM , Riordain D O', O'Higgins NJ and Smyth PPA . Thyroid stimulation in thyroid cancer. J. Endocrinology (1994) 140: P250.

Hetherton AM, Smith DF, Ryan R, O'Herlihy, C. and Smyth P.P.A. Neonatal iodine nutrition. Irish J Med Sci (1994) 163: 246.

Long HA , Conway DJ, Mercer PM , Murphy, D., Stokes M, Sheahan K, O'Higgins NJ and Smyth PPA. "Glucose-6-phosphate dehydrogenase (G6PD) O_2 activity as a metabolic marker in   thyroid carcinoma. Irish J Med Sci (1994) 163: 248.

Smyth PPA. Pregnancy and thyroid function. J. Endocrinology (1994) 140: S32.

Cusack YA, O'Riordain D, Mercer PM , O'Higgins NJ and Smyth PPA. Superoxide dismutase deficiency in breast cancer.   Irish J Med Sci (1994) 163: Supp13,34.

Smyth P.P.A., Smith DF, Hetherton AM, and O'Herlihy, C. Neonatal iodine intake: Breast v Bottle feeding. Irish J Med Sci (1994) 163: Supp13,37.

Thyroid Volume and Urinary Excretion during pregnancy and the Postpartum period: A prospective study. Smyth PPA, Smith DF, Hetherton AM, Radcliff M and O'Herlihy C. Journal of Endocrinological Investigation (1994) 17:P37

Barakat, M., Carson, D., Hetherton, A.M., Smyth, P.P.A. and Leslie, H. Hypothyroidism Secondary to Topical Iodine Treatment in Infants with Spina Bifida. Acta Paediat (1994) 83: 741-743.

M H Hassett, A Boyce , V. Greig, C O' Herlihy and PPA Smyth. Abnormal thyroid stimulators in pregnancy and hyperemesis gravidarum ? J Endocr. (1995) 144:P369.

PPA Smyth , DF Smith , EWM Mc Dermott & NJ O'Higgins. Thyroid peroxidase (TPO) autoantibodies in breast disease. J Endocr. (1995) 144:P40.

P P A Smyth, C Darke, A B Parkses, AM Hetherton, D F Smith, and J H Lazarus. Lack of HLA restriction in the pathogenesis of endemic goitre in an african population. J Endocr. (1995) 144:P170.

Conway DJ, TF Moran, DF Smith & PPA Smyth. Does intrathyroidal iodine content determine responsiveness to TSH stimulation ? J Endocr. (1995) 144: 169

Communications

"Are immunological factors involved in the pathogenesis
of endemic goitre in Senegal?
 12th Joint Meeting of British Endocrine Societies Liverpool, (March 1993).

Human chorionic gonadotrophin (hCG) as a thyroid growth stimulator
in normal pregnancy
12th Joint Meeting of British Endocrine Societies Liverpool,
(March 1993).

"Glucose-6-phosphate dehydrogenase (G6PD) O_2 sensitivity :
a cytochemical adjunct to the diagnosis of thyroid carcinoma. 12th Joint Meeting of British
Endocrine Societies Liverpool, (March 1993).

Studies on Pregnancy Goitre. National Scientific Medical Meeting, Dublin (March 1993)

Hypothyroidism in Irish Women. National Scientific Medical Meeting, Dublin (March 1993)

Hypothyroidism in a community: Prevalence and pathogenesis.
21st Annual Meeting of the European Thyroid Association,
Cardiff, July 1993.

Pathways for Thyroid growth stimulation in normal pregnancy.
21st Annual Meeting of the European Thyroid Association,
Cardiff, July 1993.

The Glucose-6-phosphate dehydrogenase(G6PD) O2 insensitivity phenomenon: a metabolic
index in thyroid carcinoma.
67th Meeting of the American Thyroid Association.
Tampa, November 1993

Control of thyroid volume during pregnancy.
67th Meeting of the American November 199 Thyroid Association.
Tampa, November 1993

Neonatal iodine nutrition.
18th Annual Meeting of The Irish Endocrine Society.
Cork, November 1993.

Glucose-6-phosphate dehydrogenase(G6PD) activity as a metabolic marker in thyroid
carcinoma.
18th Annual Meeting of The Irish Endocrine Society.
Cork, November 1993.

O2 Insensitivity of G6PD activity in human breast carcinoma.
13th Joint Meeting of British Endocrine Societies.
Bournemouth ,March 1994.

Thyroid stimulation in thyroid cancer.
13th Joint Meeting of British Endocrine Societies.

Bournemouth, March 1994.

Pregnancy and thyroid function.
13th Joint Meeting of British Endocrine Societies.
Bournemouth, March 1994.

Superoxide dismutase deficiency in breast cancer.
National Scientific Medical Meeting.
Dublin, April 1994.

Neonatal Iodine Intake: Breast versus bottle feeding.
National Scientific Medical Meeting.
Dublin, April 1994.

Thyroid volume and urinary iodine excretion during pregnancy and the postpartum period: a prospective study. 22nd Annual Meeting of theEuropean Thyroid Association.
Vienna, August 1994.

Abnormal Stimulators in Benign and Malignant Thyroid Disease19th Annual Meeting of The Irish Endocrine Society.
Galway November 1994.

Does intrathyroidal iodine content determine responsiveness to TSH stimulation ?
14th Joint Meeting of British Endocrine Societies.
Warwick.
March, 1995

Alterations in thyroid volume and iodine status in pregnancy:correlation with neonatal iodine intake . 27th British Congress of Obstetrics & Gynaecology.
Dublin, July 1995.

Head of Project 4: Prof Williams

II. Objectives for the reporting period

The aim of this study was to compare expression of certain key oncogenes, growth factors and their receptors in a variety of human thyroid tumours from patients exposed to previous radiation and from patients with no history of radiation exposure, correlate the pattern of expression of these factors with the morphology of the tumours studied and exposure to radiation. In addition, we studied the expression of the same factors in a number of tumours induced in animals by a regime of radiation and goitrogen administration. The regulation of thyroid growth is multifactorial and difficult to dissect in vivo. We therefore also studied a number of tumours induced by radiation administration in transgenic mice which constitutively express the pA2 receptor, leading to permanent stimulation of the cAMP pathway thus mimicking part of the TSH response.

1: Factors studied and methods employed

We limited our study to factors which are known to be involved in thyroid differentiation or growth. Thyroglobulin and calcitonin are differentiation markers for the follicular and C cell respectively. Insulin like growth factor 1 (IGF1) is known to be of key importance in human thyroid cell growth in vitro (Williams et al., 1987) and to be involved in thyroid neoplasia (Williams et al., 1988, Tode et al., 1989). The receptor for hepatocyte growth factor (met), the ligand for which is a potent mitogen for thyroid epithelial cells (Dremier et al., 1994), has been shown to be overexpressed in thyroid carcinomas (Di Renzo et al., 1988). Another key oncogene in papillary carcinoma, ret, was also studied, as was epidermal growth factor, which has been shown to promote thyroid follicular cell growth, but not differentiation, in vitro (Roger and Dumont 1984). Where possible all of the factors were studied in both man and mouse. However, some available antibodies (for example those for EGF and IGF1 receptor) did not show sufficient cross-species reactivity.

1.1: Immunocytochemistry

Immunocytochemistry was used to localise peptides for thyroglobulin, calcitonin and ret on sections of thyroid tumours from both mouse and man. IGF1 receptor and met were also localised in human tumours and EGF in mouse only. All antibodies were commercially available rabbit polyclonal antibodies with the exception of the IGF1 receptor antibodies which were mouse monoclonals kindly supplied by Professor K Siddle, University of Cambridge. A dilution profile was carried out for each antibody on a known positive control tissue. The following dilutions were used on thyroid sections; thyroglobulin 1:10000, calcitonin 1:2000, ret 1:100 (following pretreatment in a pressure cooker for 2 minutes in 0.1M citrate buffer), met 1:100, EGF 1:500, IGF1 receptor 1:500. Sections were incubated overnight at 4C and bound antibody was localised using either an indirect peroxidase method or streptavidin biotin complex. Diaminobenzidine was used as the reporter molecule. Serial sections were incubated with control antibodies or in the absence of antibody as negative controls. A positive control tissue was used as an internal quality control on each experimental run to ensure consistency between experiments.

1.2 In situ hybridisation

In situ hybridisation using digoxigenin oligoprobes was used to localise mRNA for thyroglobulin, calcitonin and IGF1 mRNA in human and mouse sections. EGF mRNA was localised in mouse sections only. The technique uses an alkaline phosphatase linked antibody to localise bound probe followed by enzyme hisochemistry for alkaline phosphatase using NBT as the reporter molecule (Thomas et al., 1993). Single probes labelled at both 5' and 3' ends were used for thyroglobulin IGF1 and EGF. A cocktail of three probes was used to localise calcitonin mRNA. Serial sections were hybridised with a probe complementary to EBER 1 mRNA or in the absence of labelled probe as negative controls. A known positive tissue was included for each probe on each experimental run to ensure consistency between experiments.

1.3: RT-PCR

We have also developed a reverse transcriptase PCR (RT-PCR) technique to demonstrate both ret translocation and ret expression in sections of formalin-fixed paraffin embedded material. We used primers which bridged the fusion point of the H4 gene and the tyrosine kinase end of the ret proto-oncogene to demonstrate the expression of the PTC1 transcript (Williams and Williams 1995) and primers to the tyrosine kinase region of the ret gene to demonstrate expression of the this part of the oncogene whether translocated or not. mRNA extracted from a cell line known to express the PTC1 fusion product was used as a positive control. Negative controls included tissue known to be negative for the ret gene product, reagent only, and primer excluded controls.

2:   Material studied
2.1   Human
Paraffin embedded formalin fixed material from 50 cases of thyroid tumours with sufficient material for research studies were obtained from the files of Addenbrooke's hospital in Cambridge. 4 mm serial sections were cut and mounted on silane coated slides.

2.2   Mouse
2.2.1   Study 1
Forty two mouse pups were injected with 2.5 mCi ^{131}I i.p. at three days of age. Eight other mouse pups were given no injection. All mice were maintained on normal rat and mouse maintenance diet and given a cocktail of 0.2% aminotriazole and 0.5% sodium perchlorate in the drinking water from weaning. We have previously shown that this goitrogenic regime produces tumours in mice within 9 - 10 months (Thomas and Williams 1992). After 9 months all mice were killed using sodium pentabarbitone and the thyroids removed and fixed in buffered formalin for 48 hours prior to routine processing to paraffin wax. 4 mm serial sections were cut and mounted on silane coated slides.

2.2.2   Study 2
A total of 33 thyroids from transgenic mice which constitutively express the pA2 receptor and 36 control mice of the same sex and strain were received from the Brussels group. Twenty two of the transgenic mice and 22 of the control mice had received a single dose of 0.5 mCi ^{131}I i.p. three days after birth. The remaining 11 transgenics and 14 non transgenic mice served as non irradiated controls. All mice were killed between 6 and 7 months of age and tissue was processed as above.

3:   Results: Human
3.1   Histology
Nine of the 50 tumours studied were classified as thyroid adenomas, 3 showed predominantly macrofollicular architecture, two predominantly microfollicular, two were trabecular and two were composed of both trabeculae and follicles. Thirteen tumours showed the morphological features of follicular carcinomas. Four of these tumours showed a solid poorly differentiated pattern of growth while nine were trabecular or follicular in structure including one which was widely invasive. Five tumours were classified as oxyphil carcinomas, 3 with follicular architecture and 2 with a mixture of papillae and follicles. The remaining 23 tumours showed the morphological features of papillary carcinoma.

Seventeen of the papillary carcinomas showed predominantly papillary architecture, while 6 were composed entirely or almost entirely of follicles. Five of the tumours with predominantly papillary architecture showed widespread heavy lymphocytic infiltrate within the fibroblastic core of papillae. The infiltrate appeared to be non destructive and consisted mainly of plasma cells. The remaining tumours showed little or no lymphoid infiltrate.

3.2   Immunocytochemistry
All control sections gave the expected negative results. Both IGF1 receptor antibodies gave similar staining on tissue sections. All tumours were positive for thyroglobulin and negative for calcitonin on immunocytochemistry. Normal C cells, where

present in the background normal thyroid removed with the tumour, showed positive staining for calcitonin.

3.2.1   Papillary carcinomas

Papillary carcinomas showed a focal positivity for thyroglobulin with storngly positive cells lying next to negative epithelial cells.

Papillary carcinomas showed a markedly different pattern of expression of the three tyrosine kinase receptors. Approximately 50% (13/23) showed moderately strong to strong cytoplasmic positivity for met, with stronger staining towards the periphery of the tumour. Membrane staining was also observed at the tumour periphery and in islands of tumour within the normal background thyroid, which was negative for both met and ret expression. The majority (19/23) of papillary carcinomas were strongly positive for ret expression. The ret localisation was not diffuse; in most cases it was a focal dot like positivity at the base of the cell. Occasionally the dot-like positivity was seen within intranuclear inclusions. In a minority of tumours there were areas of linear positivity at the apical cell membrane. In solid areas, there was positive staining around the whole circumference of the cell. A minority of papillary carcinomas were strongly or moderately strongly positive for IGF1 receptor . These results are summarised in Table 1.

Table 1:　　Semi quantitative analysis of tyrosine kinase receptor expression by ICC in thyroid tumours

	IGF1 receptor				c-met receptor				c-ret			
	0	+	++	+++	0	+	++	+++	0	+	++	+++
Papillary Ca (n=23)	0	18	2	3	4	6	12	1	2	2	5	14
Follicular Ca (n=13)	1	12	0	0	10	3	0	0	11	1	0	1
Follicular adenoma (n=9)	2	7	0	0	6	3	0	0	5	2	2	0
Oxyphil Ca (n=5)	1	1	3	0	2	2	1	0	3	2	0	0

No significant differences between expression of the three receptors were observed between papillary carcinomas of the follicular variant and classical subtypes, but a striking difference was observed in the subgroup of classical papillary carcinomas with a widespread lymphoplasmacytic infiltrate within the fibroblastic core of the papillae. The tumours in the latter group were strongly positive for IGF1 receptor (Figure 1A), but showed weak to negative staining for both ret and met. These results are summarised in Table 2.

Table 2:　　Tyrosine kinase receptor expression in different subgroups of papillary carcinoma

	IGF1 receptor				c-met receptor				c-ret			
	0	+	++	+++	0	+	++	+++	0	+	++	+++
Classical PTC (n=12)	0	12	0	0	0	6	16	0	0	0	3	9
Foll variant (n=6)	0	6	0	0	1	1	3	1	0	0	3	3
Classical PTC with LI (n=5	0	0	2	3	3	1	1	0	2	2	1	0

3.2.3   Follicular adenomas and carcinomas
Follicular carcinomas and adenomas showed weak to moderate diffuse positivity for thyroglobulin in epithelial cells with stronger positivity in the follicular lumen where lumina were present.

The majority of the follicular adenomas were entirely negative for met expression (6/9), and positive for IGF1 receptor (7/9). Two adenomas showed focal ret positivity, and two more widespread ret positivity. Two patterns of staining were observed, a focal dot like positivity at the base of the cell, and basal membrane staining. The two adenomas which showed widespread positivity for ret were solid trabecular adenomas.

The majority of follicular carcinomas (10/13) were entirely negative for met. The four positive carcinomas showed only weak diffuse positivity for met; no membrane staining was observed. The majority (11/13) of the follicular carcinomas showed no ret staining, one showed weak diffuse cytoplasmic positivity. The remaining tumour which was trabecular in structure, was strongly positive for ret, with membrane staining encircling the cells in over 50% of the of the tumour, including islands of tumour within the normal thyroid, which was negative for ret expression.

3.2.4   Oxyphil carcinomas
Four of the five oxyphil carcinomas studied showed moderate epithelial cytoplasmic positivity for IGF1 receptor and apical membrane staining for ret on follicular epithelial cells was observed in two of the five tumours studied. However, the dot-like basal staining which was characteristic of papillary carcinomas was not observed in oxyphil tumours. Staining for met was weak and diffuse in 4 of these tumours. One tumour was negative for all three receptors.

3.3   In situ hyridisation
All the tumours studied were positive on hybridisation with oligo dt and negative when hybridised with the probe for EBER 1 mRNA. All tumours were positive for thyroglobulin and negative for calcitonin. Where present in normal thyroid adjacent to the tumour, C cells were positive for calcitonin. Follicular tumours, both adenomas and carcinomas were more strongly and uniformly positive for thyroglobulin mRNA than papillary carcinomas. Papillary carcinomas showed a characteristic focal staining pattern, but this did not correlate cell for cell with the pattern seen on immunocytochemistry.

Five of the thirteen follicular carcinomas and all of the papillary carcinomas have so far been studied for IGF1 mRNA expression. Studies of the expression of IGF1 in oxyphil carcinomas and in adenomas are currently being performed.

Normal thyroid follicular epithelium removed with the tumours showed considerable intercellular heterogeneity for IGF-I mRNA positivity by in situ hybridisation. Positive follicular cells were usually restricted to smaller, more active follicles lined by tall columnar epithelium. Normal stroma contained no demonstrable IGF-I mRNA. The semi quantitative results for both the normal and the neoplastic thyroid are shown in Table 3.

4 of the 5 cases of follicular carcinoma showed a consistent uniform and high IGF-I mRNA expression throughout the tumour follicular cells (Figure 2), compared with a much lower and heterogeneous hybridisation signal in the follicular cells of the surrounding normal tissue. A serial section hybridised with a probe to EBER 1 mRNA was negative. The single case with a relatively weaker expression was a widely invasive carcinoma, which showed only scattered isolated strongly positive cells. These cells , when reviewed on the H and E stained section were compatible with apoptotic cells. Tumour stromal cells were negative.

Eighteen of the 23 papillary carcinomas studied lacked any demonstrable IGF-I mRNA in the stroma. Of these 18, 5 showed weak and 13 moderate positivity in the follicular epithelium for IGF-I mRNA by in situ hybridisation. There was no correlation between morphology and the level of IGF-I mRNA staining. Moderate positivity was observed in scattered lymphocytes in areas of thyroiditis in the surrounding normal tissue. This was confined to only a small proportion of lymphocytes within areas of thyroiditis. The remaining five papillary carcinomas showed a heavy stromal lymphoplasmacytic infiltrate which was strongly positive for IGF-I mRNA (Figure 1B). The positivity was confined to cells identified as plasma cells by their morphology and by their content of light chain

mRNAs in serial sections. The plasma cell mRNA positivity for IGF-I was uniformly strong, in contrast to that seen in areas of thyroiditis. The overlying follicular epithelium showed only weak to moderate staining. Further studies using digoxigenin labelled oligoprobes for kappa and lambda light chain mRNA revealed that the lymphoplasmacytic infiltrate was polyclonal .

Table 3:   IGF1 and IGF1 receptor expression in thyroid carcinomas

	IGF1 mRNA		IGF1 receptor	
	Epithelium	Stroma	Epithelium	Stroma
Normal thyroid (n=7)	+/-	-	+/-	-
Follicular Carcinoma (n=4)	+++	-	-	-
Follicular Carcinoma (n=1)	-	-	-	-
Papillary Carcinoma (n=18)	+/+++	-	+	-
Papillary Carcinoma with Lymphoid infiltrate (n=5)	+	+++	+++	-

4.4   Ret expression by RT-PCR
Twenty three papillary carcinomas have been studied for expression of the ret oncogene using RT-PCR for the tyrosine kinase domain of the ret gene. 13 of these tumours showed ret expression, which has been verified by direct sequencing. Studies of follicular carcinomas and adenomas are currently under way.

4:   Results: Mouse
4.1.1   Histology Study 1
Follicular tumours were found in all of the mice given ^{131}I at three days of age. Usually the majority of the gland was occupied by tumour, making analysis of the changes in oncogene expression in neoplasia difficult to interpret. A smaller number of focal lesions were found in mice given goitrogen only (Figure 3). Several of the lesions observed in both the radiated and non irradiated mice were cystic in structure with papillary projections into the lumen. However, the classical nuclear features associated observed in human papillary carcinoma were absent.

4.1.2   Histology Study 2
Multiple follicular tumours were observed in all transgenic mice. In animals which had received radiation, the majority of the gland was composed of neoplastic lesions and normal architecture was completed distorted. In non irradiated transgenic mice the lesions were more focal, but of the same morphology as in the irradiated transgenic animals. Several of the lesions were cystic, but the projecting epithelium was more solid than that seen in the mice from study 1. Again, the characteristic nuclear features of human papillary carcinomas were not present. No tumours were observed in non transgenic mice, irrespective of radiation exposure.

4.2   Immunocytochemistry and in situ hybridisation
Normal thyroid follicular epithelium, where present in animals harbouring tumours and in non tumour bearing animals was weakly positive for thyroglobulin peptide on immunocytochemistry and strongly positive for thyroglobulin mRNA. Follicular lumina were positive for thyroglobulin peptide and negative for mRNA. Normal C cells, where present, were positive for calcitonin peptide and mRNA and the majority were positive for ret peptide on immunocytochemistry. The majority of thyroid epithelial cells were negative for IGF1 mRNA and EGF mRNA and peptide.
All tumours regardless of irradiation or transgenic status of the animal were negative for calcitonin, and showed reduced levels of thyroglobulin positivity (Figure 4). Neighbouring normal thyroid follicular epithelium was strongly positive for thyroglobulin. There was no significant difference between the background thyroid and tumour epithelium

with respect to IGF1 mRNA and EGF mRNA and peptide positivity. All tumours were also negative for ret expression by immunocytochemistry.

5:   Discussion

We have so far studied only a very small number of tumours from adult patients with a known history of radiation treatment. However, we have studied tumours from children exposed to radioactive fallout after the Chernobyl accident, and have shown that there are no significant differences in the expression of the oncogenes and differentiation markers used in this study (Bogdanova et al., submitted and Williams et al., unpublished observations). This research is currently being funded under COSU contract CT94 0084. These results together with those from the mouse studies reported here suggest that radiation may not cause any particular changes in the frequency of the expression of the oncogenes so far studied. However, we cannot exclude the posssibility that there may be other oncogenes, not yet studied, which will show different patterns of expression.

The results reported here clearly show that the pattern of oncogene expression in human thyroid carcinomas is related to morphology and may therefore reflect differing aetiologies for the different tumour types. Papillary carcimomas show more frequent expression of the ret and met oncogenes by immunocytochemistry, with ret showing a specific intracellular pattern of staining which may be related to translocation of the oncogene. IGF1 mRNA expression is increased in some if not all follicular carcinomas, whereas papillary carcinomas appear to show a lower expression of IGF1 mRNA. However, we have identified a subset of papillary carcinomas which harbour a non destructive lymphoplasmacytic infiltrate which show high levels of IGF1 mRNA in the infiltrate and expression of IGF1 receptor on the follicular epithelium. These tumours are predominantly negative for met and ret expression, suggesting that a activation of a different growth factor mechanism may be stimulating their growth. This may involve production of an antigen by the follicular epithelium which induces the IGF1 producing infiltrate. Follicular tumours show a very low frequency of ret expression by immunocytochemistry and this appears to be restricted to one particular morphological subgroup, the trabecular tumours. Oxyphil carcinomas show features of both papillary and follicular carcinomas.

The mouse tumours studied here show a quite different pattern of oncogene and differentiation marker expression from the human tumours studied. Increased IGF1 production does not appear to play a role at least in the development of the early benign lesions we have studied and does not seem to be involved in the aggressive growth of the lesions induced in transgenic animals. However, we cannot exclude a role for IGF1 in tumour growth. The action of IGF1 is modulated by growth factor binding proteins, and we have not yet studied these in either human or murine thyroid. We found no evidence of expression of the ret peptide in follicular cells in normal or neoplastic thyroid in the mouse, although C cells were positive. This may in part be a reflection of the fact that morphologically at least the murine tumours appear to be follicular rather than papillary.

The most interesting finding in the mouse was the apparent tumour specific decrease in the expression of thyroglobulin both at the mRNA and the peptide level in both irradiated transgenic and normal mice given goitrogen and in non irradiated transgenic mice. This is somewhat surprising in the transgenic animals where the transgene expression is linked to a thyroglobulin promoter.

In conclusion, we have studied a variety of differentiation markers and oncogenes in both human and murine tumours. Expression of these factors can be linked to morphology in the human. The pattern of expression of these factors in the murine tumours suggests that they may serve to be a better model of human follicular than papillary neoplasms. Tumours induced in irradiated mice show a similar pattern both morphologically and immunocytochemically with respect to the factors studied here, which suggests that radiation increases the frequency of tumours, rather than changes the type of tumours produced by other mechanisms. This suggestion is supported by the finding that radiation linked tumours in man are also associated with a similar pattern of oncogene change to those in non radiation induced tumours. While radiation may differ from chemical carcinogens in the exact nature of the mutations induced, it appears that the increased mutagenesis leads to an increased rate of mutation in those oncogenes which are involved in non-radiation inuced thyroid neoplasia,

rather than leading to mutation in new oncogenes involving different growth pathways and different morphologies.

6: References

Baverstock K, Egloff B, Pinchera A, Ruchti C, Williams D (1992) Nature 359: 21-22
Bogdanova T, Bragarnik M, Tronko ND, Egloff B, Harach HR, Thomas GA, Williams ED (1995) submitted
Di Renzo MF, Olivero M, Ferro S, et al., (1992) Oncogene 7: 2549-2553
Doniach I (1974) Br J Cancer 30: 487 - 495
Dremier S, Tatou M, Coulonval K, Nakamura T, Matsumoto K, Dumont JE (1994) Endocrinol 135: 135-140
Eng C, Smith DP, Mulligan LM et al., (1994) Human Mol Genet 3: 237-241
Furmanchuk AW, Averin JI, Egloff B, Ruchti C, Abelin T, Schappi W, Korotkevich EA (1992) Histopathology 21: 401-408
Hemplemann LH (1968) Science 160: 159-163
Manenti G, Pilotti S, Re FC, Della Porta G, Pierotti MA (1994) Eur J Cancer 30A 987-993
Roger P and Dumont JE (1984) Mol Cell Endocrinol 36: 79-93
Santoro M, Sabino N, Ishizaka Y et al., (1993) Br J cancer 68: 460-464
Shore RE (1992) Radiation Res 131: 98-111
Thomas GA, Williams ED (1992) Carcinogenesis 13, 1039-1042
Thomas GA, Davies HG, Williams ED (1993) J Clin Pathol 46: 171-174
Tode B, Serio M, Rotella CM et al., (1989) J Endocrinol Metab 69: 639-647
Williams DW, Wynford-Thomas DW, Williams ED (1987) Mol Cell Endocrinol 51: 33-40
Williams GH, Williams ED (1995) J Pathol

6   Papers arising jointly out of this grant and BMHI 92 0081

Takahashi MH, Thomas GA, Williams ED (1995) Evidence for mutual interdependence of epithelium and stroma in a subset of papillary carcinomas. Br J Cancer in press
Thomas GA, Takahashi MH, Davies HG, Hooton N, Williams ED (1995) Morphology and cellular localisation of three tyrosine kinase receptors in differentiated thyroid tumours. submitted.

rather than leading to mutation in new oncogenes involving different growth pathways and different morphologies.

6: References

Baverstock K, Egloff B, Pinchera A, Ruchti C, Williams D (1992) Nature 359: 21-22

Bogdanova T, Bragarnik M, Tronko ND, Egloff B, Harach HR, Thomas GA, Williams ED (1995) submitted

Di Renzo MF, Olivero M, Ferro S, et al., (1992) Oncogene 7: 2549-2553

Doniach I (1974) Br J Cancer 30: 487 - 495

Dremier S, Tatou M, Coulonval K, Nakamura T, Matsumoto K, Dumont JE (1994) Endocrinol 135: 135-140

Eng C, Smith DP, Mulligan LM et al., (1994) Human Mol Genet 3: 237-241

Furmanchuk AW, Averin JI, Egloff B, Ruchti C, Abelin T, Schappi W, Korotkevich EA (1992) Histopathology 21: 401-408

Hemplemann LH (1968) Science 160: 159-163

Manenti G, Pilotti S, Re FC, Della Porta G, Pierotti MA (1994) Eur J Cancer 30A 987-993

Roger P and Dumont JE (1984) Mol Cell Endocrinol 36: 79-93

Santoro M, Sabino N, Ishizaka Y et al., (1993) Br J cancer 68: 460-464

Shore RE (1992) Radiation Res 131: 98-111

Thomas GA, Williams ED (1992) Carcinogenesis 13, 1039-1042

Thomas GA, Davies HG, Williams ED (1993) J Clin Pathol 46: 171-174

Tode B, Serio M, Rotella CM et al., (1989) J Endocrinol Metab 69: 639-647

Williams DW, Wynford-Thomas DW, Williams ED (1987) Mol Cell Endocrinol 51: 33-40

Williams GH, Williams ED (1995) J Pathol

7: Papers arising jointly out of this grant and BMHI 92 0081

Takahashi MH, Thomas GA, Williams ED (1995) Evidence for mutual interdependence of epithelium and stroma in a subset of papillary carcinomas. Br J Cancer in press

Thomas GA, Takahashi MH, Davies HG, Hooton N, Williams ED (1995) Morphology and cellular localisation of three tyrosine kinase receptors in differentiated thyroid tumours. submitted.
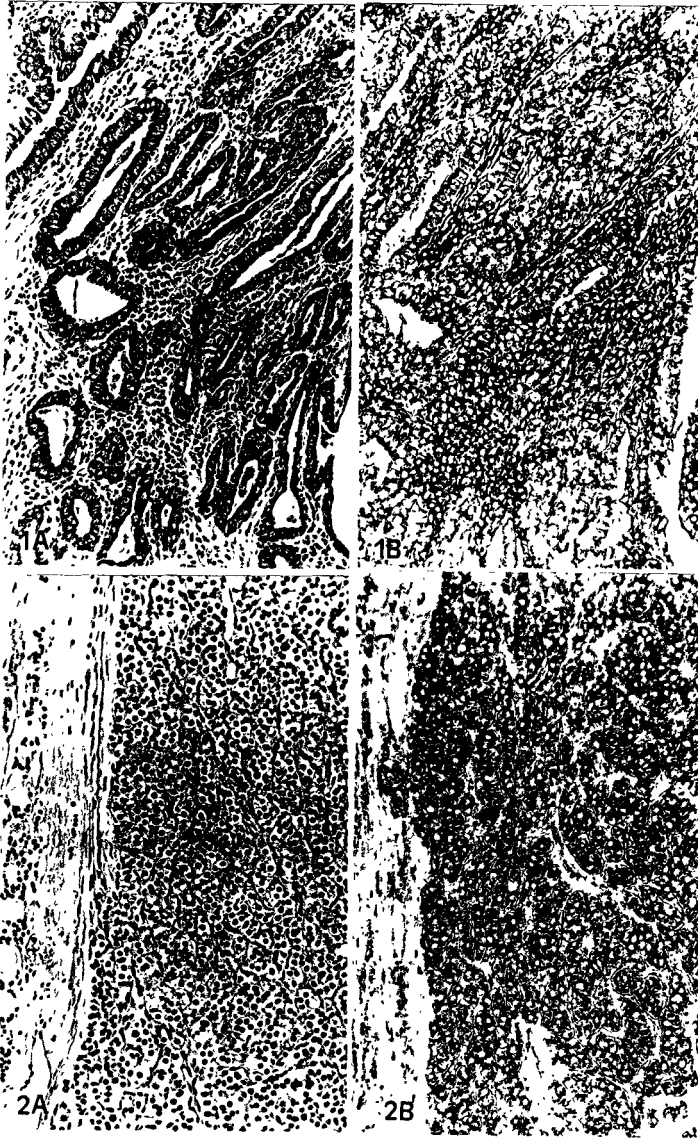
Figure 1:
Human Papillary Carcinoma.
Figure 1A shows strong immunoreactivity for IGF1 protein in a epithelial cells of a papillary carcinoma with a heavy lymphoplasmacytic infiltrate.
Figure 1B shows strong positivity for IGF1 mRNA in the lymphoid infiltrate.

Figure 2:
Human Follicular Carcinoma.
Figure 1A is a section stained with Haematoxylin and Eosin showing a solid trabecular follicular carcinoma.
Figure 2B shows uniform positivity for IGF1 mRNA in the tumour epithelial cells.
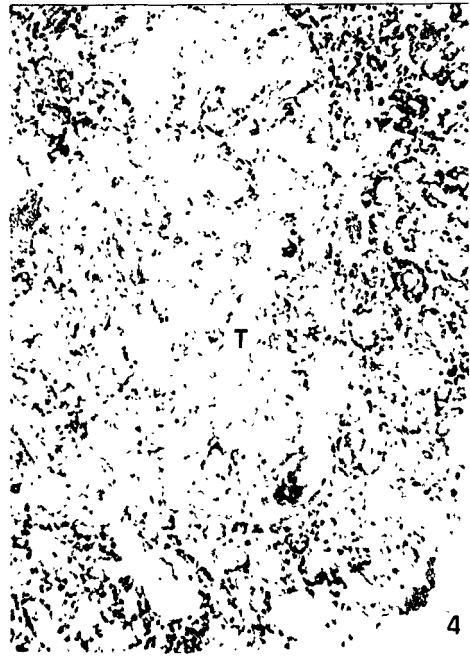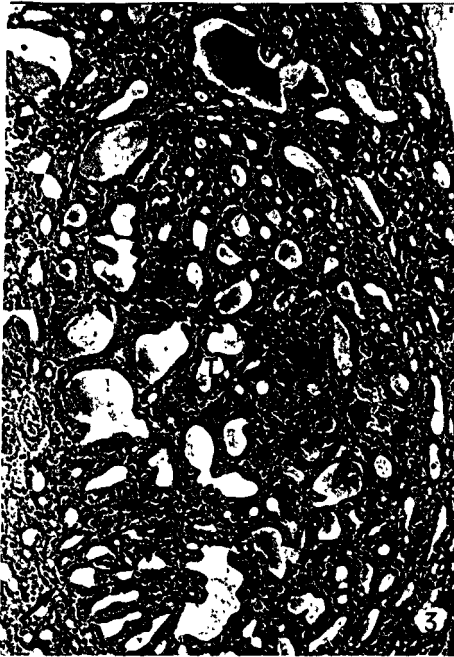
Figure 3:
A section stained with haematoxylin and eosin from a normal mouse treated with goitrogen only showing a discrete thyroid adenoma (arrowed).

Figure 4:
Section from the same tumour as in Figure 3, hybridised with a digoxiegnin labelled oligoprobe complementary to thyroglobulin mRNA. The tumour shows a decrease in positivity for thyroglobulin mRNA relative to the background thyroid.

Figure 5:
A section from a transgenic mouse treated with radioiodine hybridised with an oligoprobe complementary to thyroglobulin mRNA. Even in this very small lesion there is a marked decrease in thyroglobulin mRNA.

-

Final Report
1992 - 1994 (1995)

Contract: FI3PCT920015   **Duration: 1.9.92 to 30.6.95**   **Sector: B31**

Title: Effects of protracted exposures to low doses of radiations during the prenatal development of the central nervous system.

1)	Reyners	CEN/SCK, Brussels & Mol
2)	Coffigny	CEA-FAR & Bruyères le Chatel
3)	Ferrer	Hosp. Principes de Espana
4)	Saunders	NRPB
5)	Janeczko	Univ. Jagiellonian

1. Summary of Project Global Objectives and Achievements.

OBJECTIVES.

1. The 1992 basic project setup. A protracted (chronic) prenatal exposure to the neutrons of the Cf-252 was planned in order to assess the radiosensitivity of the foetal brain to low dose-rate irradiations. The interest for such an, up to now overlooked, situation had arisen during the last period of a preceding EC project (Bi7-003) over *in utero* brain exposure. It had been found that, in contrast with current radiobiological observations, the susceptibility of the foetal brain to a prenatal irradiation (PI) did not decrease **when the dose-rate was attenuated** during a protracted exposure (PPI). This raised the question of defining the minimal dose limit of such an unexpected phenomenon.
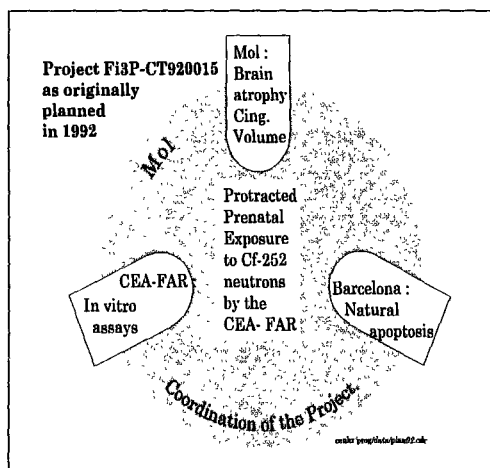
Scale. A large scale PPI (340 rats involved) was organized at the CEA-FAR which was, at that time, the only contractant laboratory with an available neutron source. High LET particles were requested due to the fact that we aimed *to focus* on the lowest damage limits attainable during any PPI.

Assays. CEA H. Coffigny exposed a large population of pregnant rats from day 12 to d16 post-conception (d12-16pc) and the brains of the offspring were distributed to the 3 laboratories participating to the project in 1993. Mol collected the female ones when aged 3 months in order to assess a general brain atrophy (until now, the most sensitive criterion to PI) but also to investigate for more subtle internal lesions (anatomical and cytological). CEA-FAR collected the male brains shortly after birth in an attempt to evaluate *in vitro* the behaviour of certain neurotransmitters but also the residual ability of the nerve cells to elaborate or maintain their dendritic
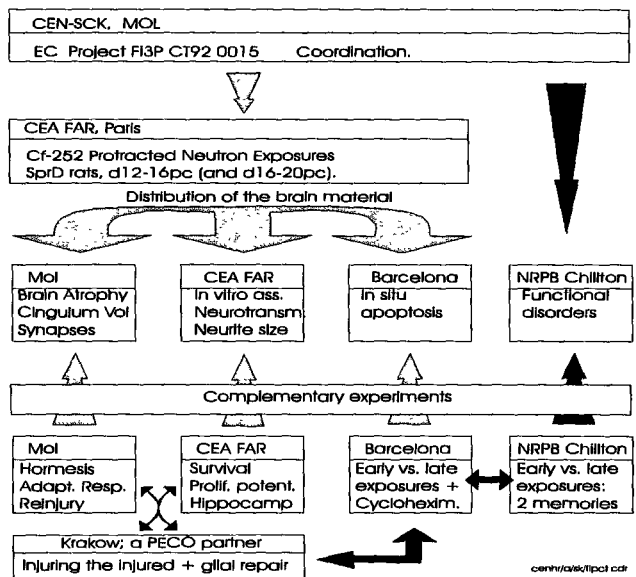
arborization. The role of Barcelona was to evaluate the influence of the added radioinduced cell death on the natural cell death which occurs massively in the normal perinatal brain.

2. Global achievements: minimal effects. From the point of view of the nuclear fission safety, the neutron PPI was a success. I. Ferrer could **not** reveal any modification of the natural cell death pattern even after the maximal dose used of 28 cGy given in 4 days. H. Coffigny, after enormous difficulties in cultivating the nerve cells, was finally able to recognize the optimal conditions for that; he introduced the **BrdU and vimentin** immunolabelling which have recently provided new informations on the high proliferativity of the API and PPI glial elements. At Mol, on the other hand, the **neutron-induced brain atrophy was found significant** down to the dose of 1 cGy per day during the 4 day exposure. This observation was confirmed later on when the above neutron PPI experiment was reproduced at the IRMM Euratom facility at Geel; for that purpose, the Van de Graaff generator was maintained in non-stop activity for 4 days providing a beam of 600 keV neutrons, identical to the very aggressive ones already used in a former acute PI experiment (Int.J.Rad. Biol., 1992). However, in spite of the clear cerebral atrophy, internal abnormalities were not easily recognized: the statistical analysis of the cingulum volume carried out in more than 300 brain sections from 64 CEA- FAR SprD female rats only showed a significant involution after the highest dose considered in the experiment: 7 cGy per day.

More tools. The efforts dedicated by the 3 laboratories to reveal brain abnormalities in the above neutron experiment were at the origin of further assays. Barcelona focused on relatively higher dose damages and in particular, on the modelization of a characteristic brain abnormality: **ectopia**. H. Coffigny using immunocytochemistry, is now able to recognize nervous from glial cells at very undifferentiated stages in the prenatal brain: he also claims for the presence in this material of **glial subclasses** based on their differential radiosensitivity. Mol has also improved immunocytochemical assays and is particularly intending to **quantify** the antibody markers by *in situ* gold labelling in 1 µm-thin tissue sections. They also evaluated alternative PI models (split-dose, exposures on day 18 for hormesis) in a continuous attempt to evaluate and assess the exacerbated radiosensitivity of the foetal brain. The final design of the project is given in the diagram nearby which also features the actions of 2 newcomer laboratories.

3. New assessments incorporated. The relatively late entry of 2 other

Effects of protracted exposures to low doses of radiations on the prenatal brain: End structure of the project.

CEN-SCK, MOL			
EC Project FI3P CT92 0015	Coordination.		

CEA FAR, Paris
Cf-252 Protracted Neutron Exposures
SprD rats, d12-16pc (and d16-20pc).

Distribution of the brain material

Mol	CEA FAR	Barcelona	NRPB Chilton
Brain Atrophy Cingulum Vol Synapses	In vitro ass. Neurotransm. Neurite size	In situ apoptosis	Functional disorders

Complementary experiments

Mol	CEA FAR	Barcelona	NRPB Chilton
Hormesis Adapt. Resp. Reinjury	Survival Prolif. potent. Hippocamp	Early vs. late exposures + Cyclohexim.	Early vs. late exposures: 2 memories

Krakow; a PECO partner
Injuring the injured + glial repair

centr/a/sk/fipct cdr

laboratories was certainly beneficial: it not only allowed to broaden the scope of the current inquiries but has also already provided results of particular interest. NRPB brought functional evaluations whereas Krakow University provided an original assay of PI brain reaction to a postnatal mechanical trauma. Some of the observations they report here are stimulating and even unexpected.

Z. Sienkiewicz (NRPB, in cooperation with A. Saunders) noticed that API, carried out at different days of the pregnancy, acted upon **different types of memories** (spatial memory impaired at d18pc; visual memory damaged at d15pc): these views are in agrrement with data from Coffigny and Ferrer who also point out to very different brain responses according to the timing of the irradiation. In Mol, an exposure of the rat at d18pc (using 18 cGy X-API) was however unable to cause any measurable cerebral atrophy (in contrast with the significant action of the same dose at d15pc).

Krakow K. Janeczko reports on the postnatal glial response to a stab wound in PI rats: his data reveal that the **proliferativity of adult glial** cells is surprisingly, but significantly, increased in PI animals; recent observations at the CEA-FAR corroborate this unexpected finding. A variant of the Krakow model of submitting PI animals to a second stress (the first one is PI) has been introduced at Mol (here the second stress is a second irradiation) in an attempt to reveal possible subliminal and undetectable foetally radioinduced damages by means of the superimposed second injury.

4. Conclusions. The rather limited project of 1992 has grown out into a panel of investigations encompassing many aspects of the particular radiobiology of the foetal brain. This task group will still be reinforced in the future by molecular biology assessments. The support of the Nuclear Fission Safety Programme of the EC has been essential in implementing such a powerful tool which is not to found elsewhere than in Europe presently. The multinational collaboration also appeared as a very stimulating way of tackling with the innumerable and uneasy problems of the central nervous system in its development and in defense. One is never enough in trying to evaluate the inner capabilities of the brain, the ultimate scientific challenge.

Mol, 30-9-95

Signed:

H. Reyners   CEN/SCK, Brussels & Mol
H. Coffigny   CEA-FAR & Bruyères le Chatel
I. Ferrer   Hosp. Principes de Espana
A. Saunders   NRPB
K. Janeczko   Univ. Jagiellonian

Abnormal neurone architecture after radial glia destruction
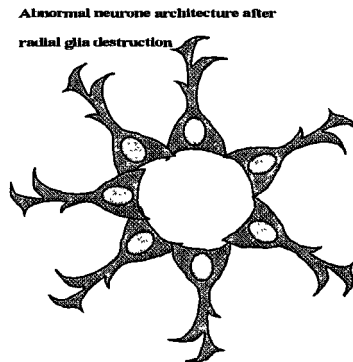
Head of project 1: Dr. Reyners

II. Objectives for the reporting period:

The **main objective** of the investigations reported hereafter was the study of a large population (n=64) of female rats which had been exposed from day 12 post conception (d12pc) to d16pc to the neutrons of a Cf-252 source at Arcueil (FR). We had in mind to assess the importance of the **brain atrophy** caused by a **protracted** neutron exposure, and to evaluate whether the effects of such irradiation, first discovered in our previous EC contract, could be traced down to **very low dose** levels (<10 cGy). This assessment also opened a series of satellite topics and questions which are summarized in the 10 points of Table I (next page). Each of them is considered in more detail within the following pages. A synopsis of the experiments in also provided at the end of the report.

III. Progress achieved excluding publications (grouped at the end of the 5 reports):

1. THRESHOLD.
Question: Can a 5 cGy protracted prenatal irradiation (PPI) induce brain atrophy ?
Answers: Positive for neutrons (Negative for gamma rays).

Introduction: Why *protracted* **exposures of rat embryos?** Deleterious effects of protracted prenatal irradiations of the foetal rat brain were first recognized and reported during our preceding participation to the Nuclear Fission Safety Programme (EC contract Bi7-0003C). The data as published in IJRB 1992 revealed that the Cingulum Volume was for any mode of irradiation, PPI or acute prenatal irradiation (API), and for any dose used, a more sensitive criterion than brain atrophy. However, in that work, the PPI were carried out with a "very" high dose (800 mGy) of Co-60 gamma rays and were given from d14-20pc, a period of the pregnancy which is posterior to the peak of corticogenesis and then certainly less critical. As a consequence of these first observations, it was assumed that protracted high LET irradiations (neutrons) given during a more radiosensitive (d12-16pc) period would possibly reveal brain atrophy and cingulum losses down to lower dose ranges (< 0.2 Gy).

Methods: 1. Which experimental setup ? A large experimental setup was organized in cooperation with CEA-FAR H. Coffigny. A population of pregnant outbred Sprague- Dawley rats (from IFFA-Credo) was irradiated from d12pc to d16pc with Cf-252 neutrons at the ETCA, a military facility at Arcueil, near Paris. The CEA was in charge for the dosimetry and the determination of the exact position of the aluminum cages. A pilot experiment (37 rats) had been carried out at the end of 1991 but the large irradiation took place in Sept 1992. At 3 months after birth, 64 female offspring were perfused with glutaraldehyde; their brains were collected at the CEA and transferred to Mol for the final tissue processing: the main quantitative evaluation focused on the involution of their Cingulum Volume after the neutron PPI; a part of the samples was also sent to Hospital de Llobregat I. Ferrer for parallel neuropathological investigations. Also, 12 female brains were perfused with buffered formaline *(3%)* alone, for immunocytological tests at Mol. Male offspring were used by Coffigny for in vitro measurements.

Main abbreviations: PI: Prenatal Irradiations; API: Acute PI; PPI: Protracted PI.

TABLE 1

THE PARTICIPATION OF CEN-SCK, MOL, BELGIUM TO THE CEC 1992-1995 PROGRAMME ON
IN UTERO BRAIN IRRADIATION, IN 10 TOPICS: A READER'S DIGEST.

#	TOPICS and QUESTIONS.	Short ANSWERS
1	THRESHOLD. Will a 5 cGy protracted prenatal irradiation (PPI) induce a brain atrophy ?	YES when using protracted neutrons from d12 -16pc.
2	LOW DOSE RANGE. Are the high dose effects caused by acute prenatal irradiation (API) to be found in the low dose range ?	NO Severe brain alterations arise after high dose only.
3	ADAPTIVE RESPONSE. Are radiolesions decreased when low dose API is followed by a larger one ?	NO Confirming a low repair capabil. in foetal brain.
4	HORMESIS. Is there a beneficial effect of low dose (18 cGy) API at day 18 pc ?	NO Adult rat brain weight is not modified after this !
5	CRITICAL PERIOD OF THE RAT PREGNANCY. Is d12-16pc a more critical foetal period than d11-15pc ?	YES Unsuspectedly.
6	NEURONAL IMMUNOCYTOCHEMISTRY. Are synaptic transmission markers attenuated after PI ?	UNKNOWN A quantitative attempt.
7	NEURONAL ULTRASTRUCTURE. Does API deplete subsurface cisterns inside the neurons ?	YES A quantitative EM assay
8	AGING. Is there an increase of the effects of PI with age ?	NO After 5 to 10 cGy gamma.
9	BEHAVIOUR. Will brain flexibility compensate for a radioinduced mild mental retardation ?	UNKNOWN But does mild mental retardation exist ?
10	SUBTHRESHOLD EFFECTS. After very low dose PI, will rhe deleterious consequences of a subsequent injury to the brain be more pronounced ?	YES The effects of split-dose irradiations are addititive.

A remake of the Arcueil experiment was carried out later on at the Van de Graaff accelerator of the EC IRMM at Geel, Belgium (in cooperation with A. Crametz and E. Wattecamps) using the 600 keV neutrons which had been found very aggressive in a previous API session reported in IJRB 1992. For this purpose, pregnant inbred Lewis rats were exposed from d12-16pc and their male and female offspring was perfused when 3 month old.

2. Cingulum volume measurements. Using a computer based image analysis, the cingulum **areas** in 4 to 5 randomly selected transversal brain sections were measured per rat, together with an evaluation of the exact **positions** of the plane of these sections along the main antero-posterior axis of the rat brain (figure 2). The individual cingulum area measurements and their respective positions are only shown in figure 1. For each rat brain, both previous
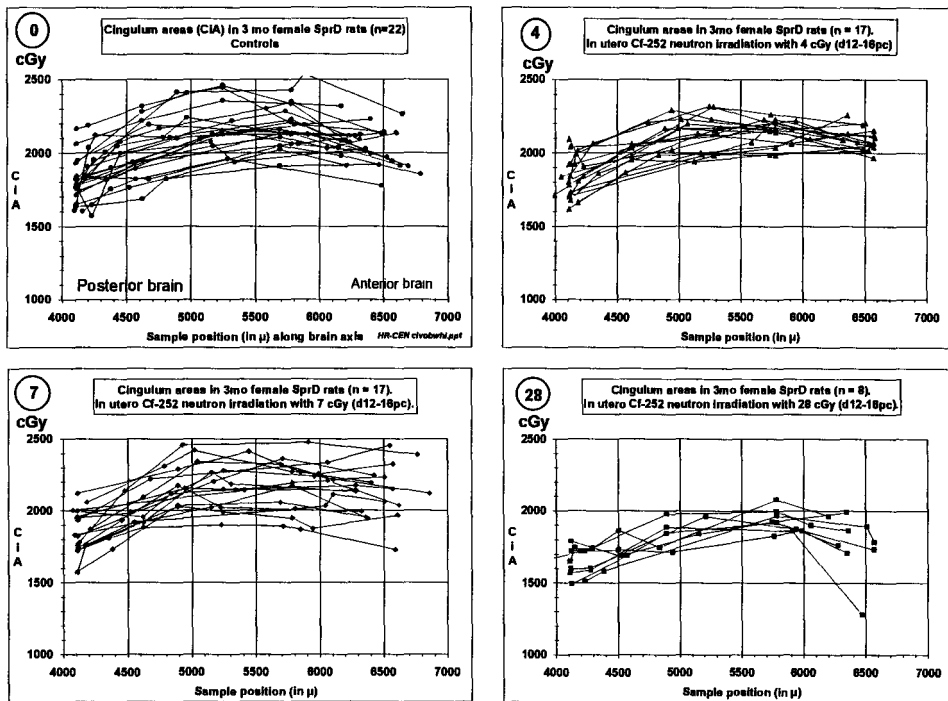
Figure 1: Relationships between position of sampling (along the antero-posterior axis of the rat brain) and the cingulum area (CiA, in ordinate) after 4 doses of prenatal Cf-252 neutron irradiation (0, 4, 7 and 28 cGy from d12-16pc). Each solid line corresponds to 1 SprD rat.

data were used to compute a single variable called the cingulum **volume** (CIVOL) which is the integral of the cingulum areas between two sample positions of reference. The correlation between CIVOL and BRW is plotted for all animals in figure 3.

Which effects ? Cingulum volume loss after low doses of Cf-252 neutrons. As mentioned above, 64 SprD rats were treated with a Cf-252 neutron exposure during 4 days and the cumulated doses were 0, 4, 7 and 28 cGy. A brain weight (BRW) loss was found significant down to the dose of 4 cGy (dose rate: 1 cGy / day; P Anova = *0.002*). Figure 3 shows the significant decrease of the brain weight associated to the reduction of the cingulum volume (Cingulum P Anova reaches a significance level of 0.0008 for the 4 neutron doses mentioned above but is insignificant for the 3 lower doses). This relatively poor sensitivity of the cingulum prompted us in implementing a second *in utero* exposure using a protracted exposure to the more *radio-efficient* 600 keV neutrons but also **inbred** rats (Lewis strain) in order to reduce the individual variability. These new irradiations confirmed brain atrophy after a dose-rate as little as 1 cGy of neutrons per day; however, in contrast with our assumptions, the slope of the dose-effect relationship (shown in progress report 1993-1994) was not steeper after the 600 keV Van de Graaff neutrons; for this reason, no time consuming quantitative evaluations of the cingulum were carried out on this material.
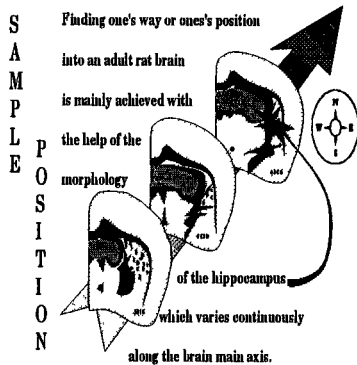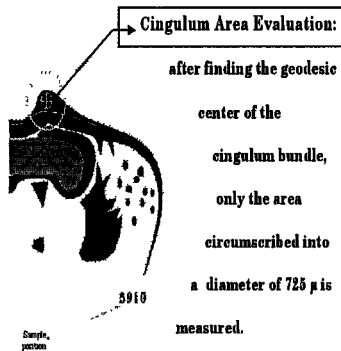
Figure 2: How to evaluate a cingulum area and the position of the brain samples ?

Which explanation ? Contrarily to our expectancies, the cingulum volume endpoint is not found so radiosensitive in chronic exposures as it was in acute ones as reported recently (Reyners et al., IJRB 1992). In spite of the large number (n=64) of rats involved, the effects of 4 and 7 cGy of neutrons given during the most critical period of the pregnancy remained insignificant in contrast with the decrease of the total brain weight (brain atrophy) which was significant down to the lowest dose assayed (4 cGy). It might be concluded from this that the radiosensitivity of the cingulum is restricted to a very small period of the cerebrogenesis, d15pc, and in consequence, is only present during 1/4 of the total chronic exposure time; in such conditions, 3/4 of the dose is wasted. An alternative explanation would be that the cingulum atrophy does not show below a certain threshold dose, at least for chronic exposures. These points should be considered further on in future work over early effects of PI.

3 mo SprD Cingulum Volume after protracted Cf-252 neutrons (d12-16pc).

CIVOL = 2.006e3+1.351*BRW+err.
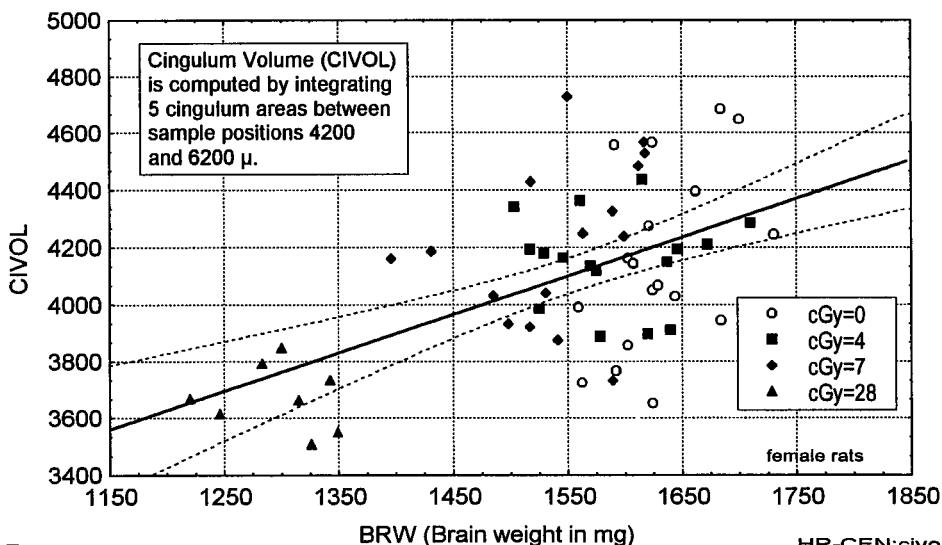
Figure 3.

HR-CEN:civol

2. LOW DOSE RANGE.
Q.: Can high dose PI effects be extrapolated to the low dose range situation ? A.: No

The facts and the theory: ectopia vs. ventriculomegaly. It is clear from our data and also from I. Ferrer's ones (this project) that a major consequence of prenatal irradiation, *ectopia*, is actually a non stochastic phenomenon. Ectopia is the formation of masses of nerve cells which become abnormally located between a dwarfed cerebral cortex and an apparently normal corpus callosum. This severe form of nervous dysgenesis is only observed after relatively high doses (Ferrer uses 2 Gy); in our material, it was only found above 0.5 Gy. Incidentally, ectopia was also observed in many (but not all) Japanese cases of severe mental retardation. To the best of our knowledge, the phenomenon is the best indication that certain damages associated with high doses **cannot** be extrapolated to the very low dose situation. It must however be pointed out that **not all radioinduced lesions are to be dealt with accordingly**: for instance, *ventriculomegaly*, an exaggerated dilation of the cerebral ventricles and a most frequent characteristic of prenatal irradiations was observed down to the lowest doses assayed in Mol (even after doses as low as 5 and 10 cGy gamma rays protracted from d12-16pc).

3. ADAPTIVE RESPONSE.
Q.: Is an adaptive response possible during corticogenesis ?   A.: No

Which experimental setup ? Split-dose prenatal X-irradiations were carried out using first, an exposure to 2 cGy and a second one to 25 cGy (after a 5 hour interval), both on d15pc Wistar foetuses. A similar group of animals was treated with the second exposure only in order to evaluate the effects of the first priming exposure. The female and male offsprings were sacrificed at 6 week old in order to check for the presence of adaptive responses (i.e. radioinduced repair enhancements) during the *foetal organogenesis of the brain*.

A model *without* an adaptive response. In agreement with recent work (Hays et al., 1993, Rad. Res.), no adaptive response was detected in the above situation: *although a radioinduced brain atrophy was evident, it remained similar in all rat brains,* had they or not received the first 2 cGy X-exposure.

Why did we look for an adaptive response ? The phenomenon of adaptive response is considered to be due to the stimulation or priming of the production of DNA repair enzymes whose presence at the time of a second irradiation would minimize the DNA damages produced then. *The lack of an adaptive response is in coping* with the surprisingly large effects of *low dose-rate* PPI observed in the foetal rat brain: the best explanation for these effects is based on the *absence of active repair* enzymes in the brain at its peak of development. The lack of adaptive response appears thus as *a supplementary argument* for the latter views.

4. HORMESIS.
Q.: Is there a beneficial effect of a low dose (18 cGy) API at day 18 pc ?   A.: No

Why 18 cGy API at d18pc ? Pilot experiments in 1991 (using only 6 sham-treated versus 6 irradiated rats) had indicated that acute 18 cGy X-irradiations carried out at d18pc had a positive (though statistically insignificant) influence on the brain weight (brain hypertrophy).

Absence of hormetic phenomenons. A remake of this experiment using as many as 25 female and 13 male sham treated animals versus 22 female and 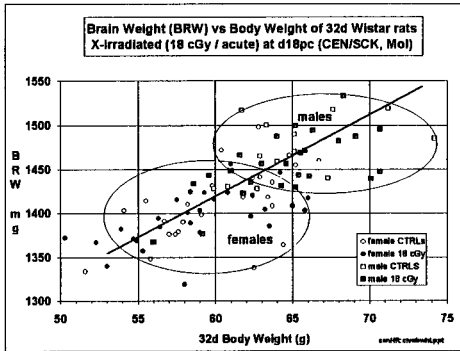21 male 18 cGy X-irradiated rats did not confirm the beneficial effect; however, it *did not reveal either any deficit* after irradiation (figure 4: neither male or female groups *can be separated* into treated vs. untreated). This absence of effect over a criterion as general as the brain weight does not totally exclude that certain areas (cerebral cortex) could be actually increased, possibly "at the expenses" of others (hippocampus). This latter view arises from some current cocontractor work in this project (Coffigny, Sienkiewicz) who indicate that the developing hippocampus is at risk at later times (d18pc) than the cerebral cortex.

Figure 4: Brain vs. body weight; API at d18pc.

5. CRITICAL PERIOD OF THE RAT PREGNANCY.
Q.: Is the period d12 -16pc more critical than d11 -15pc ?   **A.: Yes**

Why such an experiment ? In an attempt to reveal the lowest dose limits for the effects of PPI with gamma rays, it was assumed that a somewhat earlier exposure than the d12-16pc protocol, could be more deleterious to the brain Indeed, in previous tests, the effects of an acute 18 cGy exposure on d16pc had been found negligible (i.e.: wasted irradiation). In order to increase the concomitance between the irradiation and the period of major cerebral organogenesis and in consequence, the deleterious effects, a series of continuous exposures ranging from d11 to d15pc were carried out. Male and female Wistar offspring were checked for brain atrophy at 3 months of age and compared with previous d12-d16pc interval experiments. In contrast with the previsions, the *slope of this latter group dose-effect relationship remained much steeper* than the d11-d15pc one (figure 5; female data only). Brain atrophy was slightly (but not significantly) larger in male than in female brains (not shown).

Why a negative result ? It is assumed that some hours of exposure between day 15 and 16 were the most crucial for the effects of PPI.

6. NEURONAL IMMUNOCYTOCHEMISTRY.
Q.: Are synaptic transmission markers attenuated after PI ?   **A.: No**

Synaptophysin: a marker of the synaptic connections. Part of the CEA rat material was fixed for immunocytochemical studies in an attempt to evaluate the possible **loss** of synaptic connections in the prenatally irradiated animals. This intent raised not only from the above observations over the **general atrophy** of the brain but also from other data showing a dose related **disorganization of the dendritic arborization** and processes of the cortical neurons (Konermann, Adv. Rad. Biol., 1987).
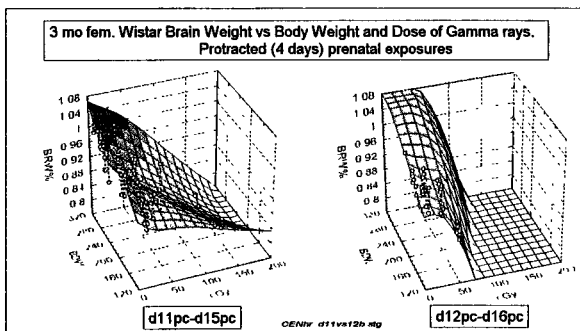
Figure 5. Steepness of dose-effect relationships.

The tissue samples were first searched for the presence of synaptophysin, by means of avidin-biotin immunocytochemistry and in 1994-5, with immunogold followed by silver latensification. In the cortex, *no clear loss was found* even after 28 cGy of neutrons from d12-16pc. In the hippocampus, *the synaptophysin decreased* in Ammon's horn (CA3) and in gyrus dentatus. However, the possible influence of the *sampling area* is still currently checked for this criterion.

7. NEURONAL ULTRASTRUCTURE.
Q.: Are neuron subsurface cisterns quantitatively depleted by PI ?   A.: Yes

The subsurface cisterns (SSC), an intraneuronal digital dosimeter. The subsurface cisterns organelles are found exclusively in neurons and represent a special form of endoplasmic reticulum (ER) which is easily spotted at the electron microscope (EM) level due to their electron dense membranes. The **function** of these organelles is still totally **unknown** although most of the authors assume they deal with electrophysiology. Alternatively, we proposed that SSC intervene in the **neoformation** and maintenance of the ER on morphological grounds (Reyners et al., 1977). In coping with this view, their *number* decreases with **age** in the rat brain. The SSC also decreased *in size* in the neurons of cortical layer II after 57 cGy gamma PPI from d12-16pc. This revealed that neuron perikaryons (and not only their external processes) also bear the marks of a prenatal irradiation. Unfortunately, SSC evaluation is an EM-based time consuming operation; it was not carried out after X-API nor after neutron PI; the dose response remains unknown but the moderate effects observed up to now, do not show SSC as very sensitive internal dosimeters.

8. AGING. Q.: Is there an increase of the effects of PI with age ?   A.: No

Aging does not amplify microcephaly. Very low PPI with gamma rays (5 and 10 cGy) had not induced a measurable brain atrophy **in the 3 month old rat** after an exposure during the critical d12-16pc period: this observation (Final EC report 1992) had been a first indication for the existence of a *threshold* in the dose-effect relationship of the developing brain after protracted *gamma* rays. It was however assumed that a very large lapse of time (30 months) could *amplify* the effects particularly in the rat model where the body (and the brain) *do never really stop* growing during the life span. An analysis of variance of the data obtained from 22 surviving animals is significant but the absence of a dose-effect relationship spoils such positive conclusion: it remained however that the responses of the 3 groups were much more separated than in the previous assessments at 3 months of age.

9. BEHAVIOUR. Q.: Will brain flexibility compensate for a radioinduced mild mental retardation ?   A.: Unknown.

Comment: This questions arises from the observation of the Japanese cases of severe mental retardation. Due to *a lack of clear evidence for mild mental retardation* (it is not found in their school scores or in QI measurements), it is assumed that mental retardation is only a severe occurrence and possibly a non stochastic (all-or-none) event. In such conditions, the brain is to be considered as able to manage the effects of small pathological changes   Does it ? This question introduces a future EC project which will feature a broad range of expertises.

	DOSES			CASES			EFFECTS	
d15	**d18**	**d3N**		**Mal**	**Fem**		**Mal**	**Fem**
0	0	0		15	18		0	0
20	0	0		12	12		−5.7	−7.8
0	50	0		19	17		−5.1	−5.2
0	0	50		13	8		−.4	−1.1
20	50	0		8	7		−11.2	−14.4
20	0	50		13	17		−6.2	−6
0	70	0		6	5		−10.2	−10.1
0	0	70		12	8		−1.6	−4.8
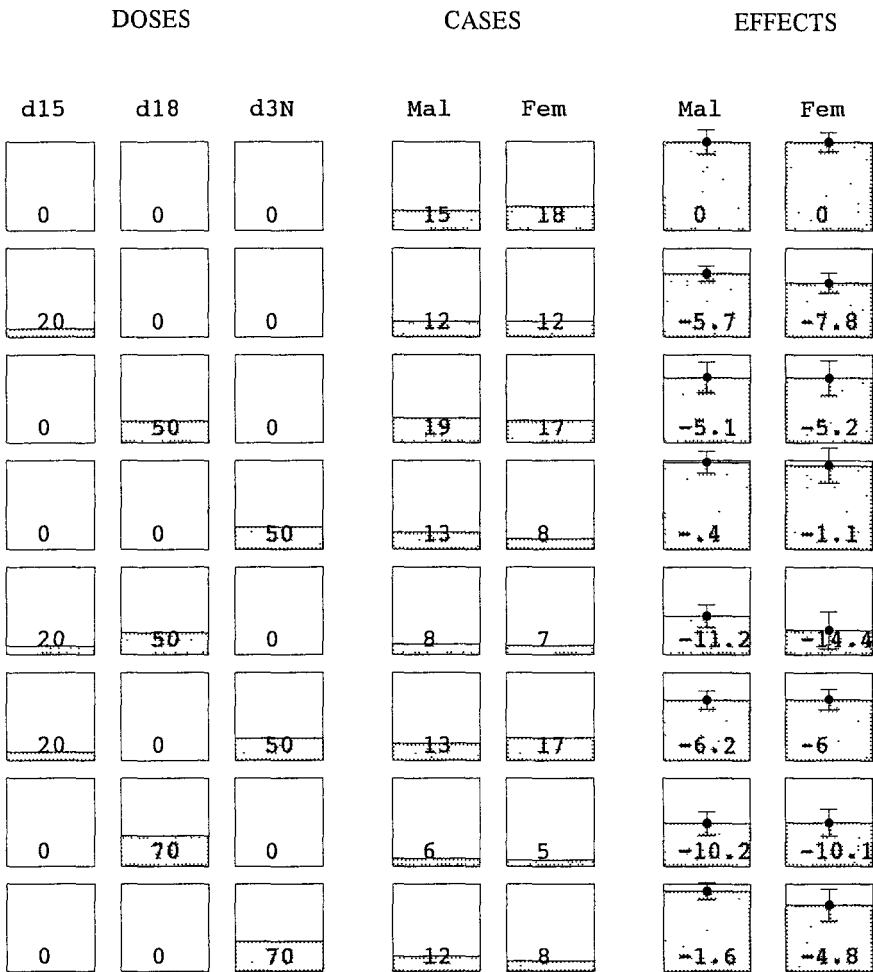
Figure 6: Split - dose (in cGy) API X-exposures, number of cases and effects on brain weight: an attempt to detect subthreshold effects (see next page).

10. SUBTHRESHOLD EFFECTS.   Q.: After very low dose API, will a subsequent injury to the brain induce more deleterious consequences ?   A.: Yes

Introduction: Injuring the injured. The question has arisen that possible subthreshold effects of a very low dose prenatal exposure could be spotted out or revealed if a supplementary stimulus is administered to the brain. This hypothesis has been evaluated in different ways during the current project : K. Janeczko used a mechanical injury (a specific stab wound) and in Mol, the stimulus was a second X-irradiation.

Methods: Split-dose irradiations. Figure 6 not only shows the different types of exposures which were carried out but also the number of animals and the brain weight loss observed. The second dose of radiation was always 50 cGy and given either on d18pc (i.e. 3 days after the first exposure on d15pc) or on d3N (= postnatal day 3, i.e. 9 days after the 1st irradiation on day 15 pc). Appropriate control exposures were also carried out (figure 6).

Results: Hyperadditivity. When a second 50 cGy exposure was given after an earlier one of 20 cGy, the effect of such split-dose exposure was at least equal and even slightly larger than the *sum* of the effects measured in animals receiving a single exposure to these doses. However, in the present conditions, the supplementary exposure to a foetally irradiated brain did not allow to reveal any possible subliminal damages. The results of figure 6 were presented at the Radiation Research meeting (Wurzburg, Aug. 95). To our surprise, they were in contrast with similar data presented there by B. Kimmler who claims for an hypoadditivity. In his trials, the interval between the 2 exposures was shorter than ours and for this reason, the exposure is rather similar to a fractionated one; in these circumstances, the US scientist advocates for a certain **repair capability** at the level of the foetal brain, a conclusion which is not only in contrast with the observations from the present split-dose experiments but also with the large effects we obtained after protracted low dose-rate exposures. It is worth pointing out already here that the problem of **repair** in the prenatal brain will be central to a new EC project starting this year and involving assays ranging from molecular to behavioural

Normal genesis of the cerebral

cortex architecture

Abnormal neurone architecture after

radial glia destruction

Prenatal

Irradiation

H. Reyners, 1995

CS   CS   CS
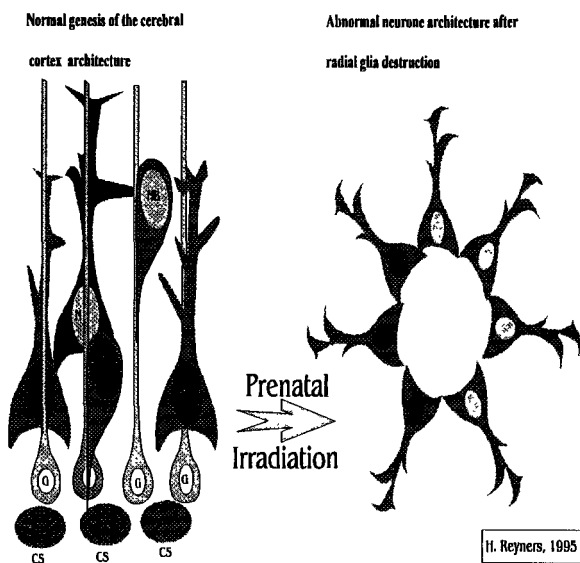
Synopsis of prenatal exposures and main assays carried out at, or for Mol, during project Fi3P-CT92-0015.

Protract. Cf-252 Neutron expo from d12-16 or d16-20pc — Topic 1

Expo at Arcueil Dec 1991	Produced: 36 and 37 female (from 25 offspring to 27-3-1992)	Brain collection at 3 months	GOAL: Pilot protracted neutron experiments.

Protracted Cf-252 Neutron Exposures from d12-16pc — Topic 1

Expo at Arcueil Sep 1992	Produced: 75 female offspring	Brain collection at 5month old from 9-12 to 12-12-1992	GOAL: Main Neutron expmt.: assays dealing with brain atrophy, cingulum volume measuremt, synaptophysin quant, immunodetect.

Adaptive response in foetal rat brain at d15pc. — Topic 3

Expo at Mol from 17/6 to 29/6/1994 (5 sessions).	Offspring: 21 fem. + 17 male	Brain collection at 6 wk old (from 11/8/ to 23/8/1994)	GOAL: The absence of Adaptive Response would confirm poor foetal brain repair.

Protracted 600 keV Neutron Exposures from d12-16pc — Topic 1

Expo at EC IRMM, Geel from 22 to 26/11/1993	Produced: 25 male + 65 female offspring	Brain collection at 3 month old (1/3/1994)	GOAL: Main Neutron expmt.: comparison with Cf-252-protracted neutron exposure.

Protracted low dose Gamma Expos. from d12-16pc (Co-60). — Topic 8

Expo at Mol during Feb 92 (4 sessions)	Female offspring maintained for survival.	Brain collec. at 30-mo -old, on 2/8/94: 22 fem. rats treated with 0, 5 & 10 cGy	GOAL: Will AGING reveal subthreshold brain damages ?

Protracted Co-60 Gamma Expos from d12-16pc — Topic 1

Expo at Mol, from 7/2 to 8/3/1994	Produced: 40 female + 36 male offspring	Brain collection at 3 months from 19/5/1994 to 14/6	GOAL: comparison with Cf-252-protracted neutron exposure.

Subthresholds — Topic 10

Expo at Mol, from 18/11/94 to 8/5/95 (>16 sessions)	>150 Male & Fem. offspring	Brain fixed from 6/4 to 14/9/95	GOAL: Do split-dose exposures during foetogenesis produce more damage ?

Hormesis in foetal rat brain at d18pc ?. — Topic 4

Expo at Mol, from 24/1 to 21/3/1994 (6 sessions)..	Offspring: 66 fem. + 50 male	Brain collection at 1 month old(from 28/2/ to 25/4/1994)	GOAL: can a small dose at d18pc induce a brain overgrowth ?

Protracted Co-60 Gamma Expos. (d11-15pc window) — Topic 5

Doses: 0, 25, 50 and 200 cGy. latter dose mainly for cancerogenesis.

1992	1993	1994	1995

Head of project 2: Dr. Coffigny

II. Objectives for the reporting period:

- Evaluation of *in vitro* survival of rat nerve cells from mesencephalic, striatal, cortical and hippocampal (pyramidal) areas isolated after gamma irradiation.
- Evaluation of *in vitro* and *in vivo* survival of hippocampal granular cells of the gyrus dentatus after irradiation.
- Assessment of the proportions of cultured mesencephalic and striatal cells of different types after a range of exposure doses. Measurements of the length of the neurites.
- *In vitro* survival of cortical GFAP-positive astroglial cells.
- *In vitro* proliferative potential of glial cells cultured in selective conditions from either newborn rats foetally X-irradiated with 1 Gy on d15pc or d21pc or from cells freshly isolated.

III. Progress achieved:

1. **Mesencephalic (M), striatal (S), cortical (C) and hippocampal (H) nerve cells survival.**

The first two structures (M and S) were taken from 14 day-old and the last two from 17 day-old rat fetuses. C and H cells were isolated by enzymatic and mechanical treatments but M and S cells by mechanical treatment only. Cobalt-60 gamma doses were 0.25, 0.50, 0.75 and 1.50 Gy *specific ones were 1.00 (C and H) and 3.00 Gy (M and S)*. The cells from all 4 structures were cultured 3 days in serum free medium before the observations. C and H cells were tested for viability after 4 hours incubation with a solution of MTT (tetrazolium salt); this molecule is metabolized by mitochondrial dehydrogenases to form a formazan dye which absorbance was measured at 540 nm. Survival of M and S cells was assessed by counting the trypan blue negative cells.
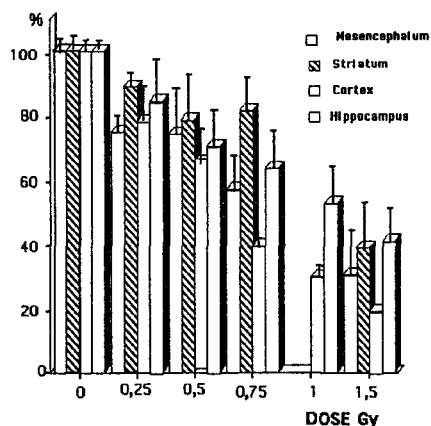
Figure 1: Survival of mesencephalic, striatal, cortical and hippocampal cells cultured three days after a range of irradiation doses.

The threshold value of mesencephalic, hippocampal and cortical cells is below 0.25 Gy and for striatal cells it is between 0.25 and 0.50 Gy indicating relatively more radioresistance in these cells (figure 1); the large proportion of GABA cells in the latter structure could possibly counteract a glutamic excito-toxicity release after irradiation.

The survival decrease of cortex cells beyond 0.75 Gy (figure 1) could be due to the presence of different types of cells in the culture. On day 17 of gestation, the granular cells of layer IV and the pyramidal cells of layer V are in optimum conditions for initiating culture. However, when granular cells begin to differentiate, the pyramidal cells are still mitotically active. The death of the latter elements could explain the relative radiosensitivity of cortex cells beyond 0.75 Gy.

2. *In vitro* and *in vivo* survival of hippocampal granular cells of the gyrus dentatus_

In vitro: The gyrus dentatus granular cells were isolated by enzymatic and mechanical treatments from 8 day-old rats, irradiated with 0.25, 0.50, 0.75, 1.00 and 1.50 Gy and cultured 3 days in serum free medium. The cell survival was measured by the MTT test as mentioned above. A 20% cell survival decrease was observed after the highest dose; a threshold of 0.75 Gy is also observed.
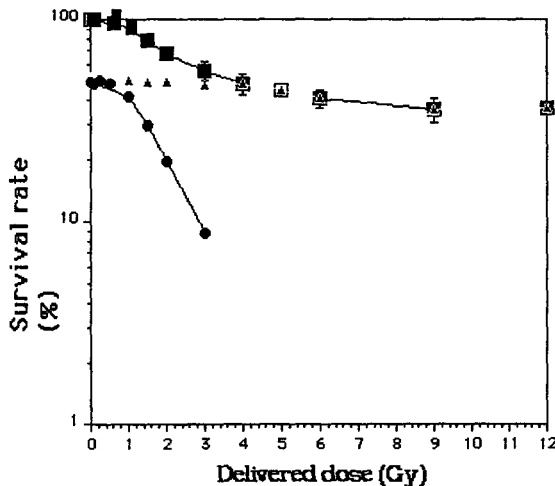
figure 2: Survival rate as a function of dose delivered at 6 hours after irradiation in the gyrus dentatus.

■   Graph corresponding to the two cells populations.

▲   The most radioresistant cells population with a D0 = 22,7 Gy

●   The least radioresistant cells population with a D0 = 1,2 Gy

In vivo: 14 day-old rat were whole-body irradiated in a range of 0.25 to 12 Gy. Six hours later, their brains were fixed by transcardiac perfusion with a 4% formaldehyde solution and processed for histological observation. A threshold value of 0.5 Gy was determined. The heterogeneous aspect of the dose-effect curve indicates the presence of 2 cellular subpopulations (figure 2).

The relative radioresistance of the postnatal gyrus dentatus granular cells *in vivo* and *in vitro* in comparison with the prenatal nerve cells *in vitro* (part 1) could be the consequence of the large amount of differentiated and differentiating -non mitotic- glial cells present after birth which could be considered as radioprotective for these neurons.

3. **Proportion of cultured mesencephalic and striatal cells in the different cell classes after a range of exposure doses and measurement of the longest neurite.**

Previously, we had observed a decrease of survival and of the neurotransmitter uptake in the mesencephalic and striatal cell population in relationship with radiation doses in the range 0 - 3.00 Gy (final report 1992). Nerve cells were now classified as monopolar, bipolar, tripolar and multipolar. Their longest neurite was measured on micrographs.

The ratio of monopolar, bipolar, tripolar and multipolar nerve cells of both structures was not clearly modified (Table 1 and 2).

% MESENCEPHALIC CELLS ANALYZED

dose (Gy)	0	0.25	0.50	0.75	1.50	3.00
monopolar	42.6	45	48.6	46.9	34.9	51.4
bipolar	21.9	20.8	24.8	25	17.4	17.1
tripolar	20	11.7	13.3	11.7	18.6	14.3
multipolar	15.5	22.5	13.3	16.4	29.1	17.1

Table 1: Percentage of each type of mesencephalic cells in culture for different radiation doses .

% STRIATAL CELLS ANALYZED

dose (Gy)	0	0.25	0.50	0.75	1.50	3.00
monopolar	31.9	28.9	32.7	32.1	28.1	26.3
bipolar	24.9	21.9	23	24.5	17.5	23.7
tripolar	21.8	23.9	18.1	22.5	27.5	16.9
multipolar	21.4	25.4	26.2	20.9	26.9	33.1

Table 2: Percentage of each type of striatal cells in culture for different radiation doses.
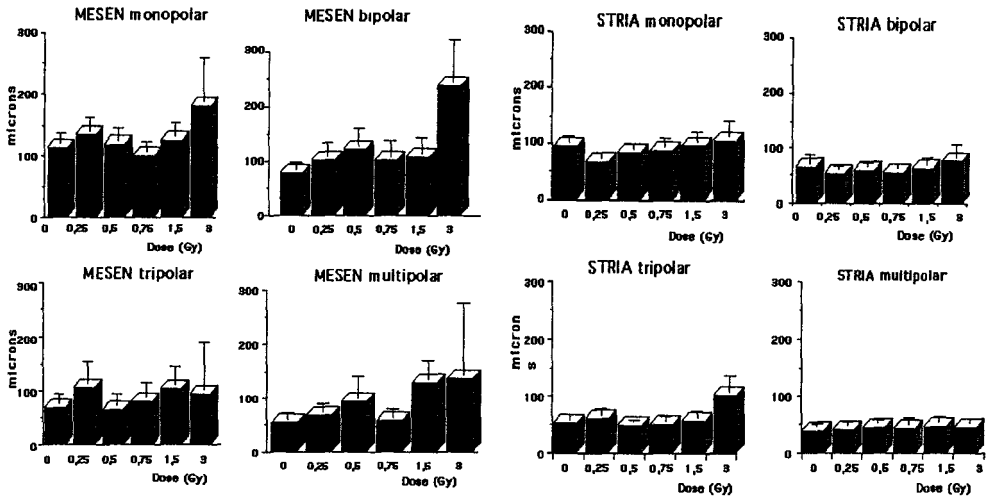
Figure 3: Length (μm) of the longest neurite of mesencephalic cell in each category versus the dose of irradiation (Gy).
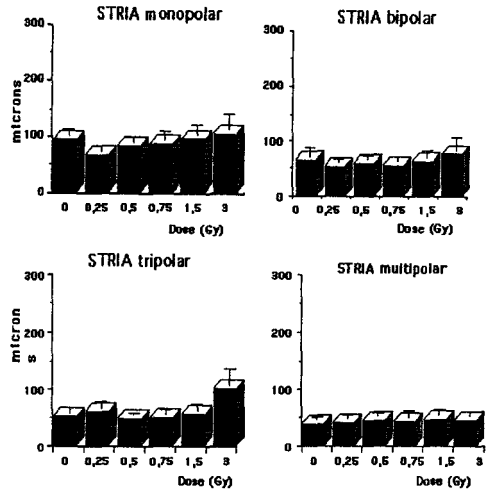
Figure 4: Length (μm) of the longest neurite of striatal cell in each category versus the dose of irradiation (Gy).

The mesencephalic neurite length was not obviously modified by the irradiation except for the *increase* after the highest dose in bipolar cells; the increase in mono- and multipolar cells is not significant (figure 3). The mesencephalic neurite lengths are shorter than the striatal ones.

No significant change of the length of the striatal neurites was observed except after 3 Gy in tripolar cells (figure 4). Again, a neurite length *increase* occurred after a dose of 3 Gy (in a population reduced to 10 to 20% of the control one). Only cells with long processes seemed to survive. The dopaminergic cells of the mesencephalum which normally send long process toward the striatum *in vivo* were not identified among these cells (using an antibody against tyroxine hydroxylase). The long neurite cells could possibly send and receive messages and growth factors from more neighbouring cells than cells with short processes, inducing a relative radioresistance.

4. In vitro survival of cortical GFAP+ glial cells

This experiment was carried out on cortical cells described in the first topic. Neurons were identified usung the MAP2 primary antibody and glial cells by GFAP positivity. A second antibody anti-Ig labeled with FITC or Texas Red revealed the cells positive for the first marker. The number of glial cells per 500 neurons was counted.

The proportion of glial cells increased with increasing radiation doses (Figure 5) indicating a neuronal death and a better survival of glial cells. The absence of dose relationship of glial cells survival could indicate glial cell death after 1.50 Gy.
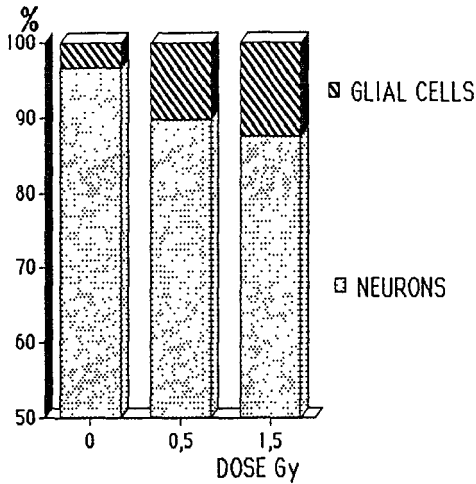
Figure 5: percentage of cortical neurones and
glial cells versus irradiation dose.

5. In vitro proliferative potential of glial cells after 1 Gy irradiation on d15pc or d21pc vs. irradiation of freshly isolated cells.

Pregnant rats were irradiated with 1 Gy on d15pc or d21pc. On day 1 after birth, the cortex was homogenized and cells isolated and cultured. At 30% of confluency, the medium was changed to 0.1% fetal calf serum (FCS) for 48 hours in order to synchronize cells in G1. FCS was increased to 10% to drive the cells into the S phase and 20 hours later, a pulse of 3H thymidine, or BrdU, was added to the medium for 6 hours. The radioactivity in washed cells was measured and BrdU+, GFAP+ cells were counted in 5 microscopic fields. The MTT survival test was carried out in all cultures.

The culture conditions with 10% FCS promoted survival of GFAP+ glial cells but death of the MAP2+ neurons. In other conditions, the glial cells would be more radioresistant than the neurons (part 4). Indeed, among cells irradiated freshly after isolation, the glial cells (GFAP+) survived as well as the controls (MTT test) and represented 99% of the cell population of the culture. The cell cycle arrest with 0.1% FCS was effective: only 7% of cells became BrdU+. After return to 10% FCS, 35% of glial cells were BrdU+ in the controls. The proliferative activity of glial cells measured by the radioactivity or BrdU counting of cells cultured after irradiation at seeding was similar to the control values (figure 6). The proliferative activity of cells from fetuses irradiated on d15pc was about twice the control values and on d21pc, about 50% higher (figure 6).
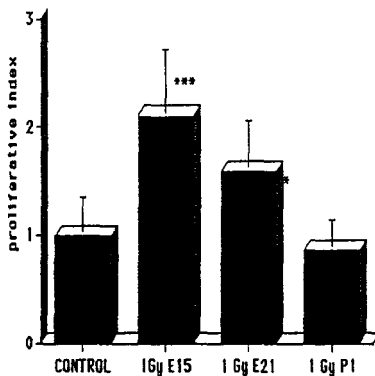
Figure 6: proliferative index with control values = 1 of glial cells after 1 Gy exposure on day 15 or 21 of gestation or on cells freshly isolated.

The increase of proliferative activity after irradiation on day 15 of gestation was very important; at that time, glial cells act mainly as progenitors whilst neurons are actively dividing. The increase in activity is lower on d21pc when the glial cells start dividing and neurons become mitotically inactive and differentiating. On day one after birth, isolated cells were irradiated when glial cells and neurons had lost their close relationships and no effect was observed. We can assume that the exposure on day 15, at the most radiosensitive period for the cortex, kills a great number of neurons which may release factors that stimulate progenitor glial cells to proliferate. On d21pc, both the decrease of the neuron radiosensitivity and of the number of progenitor glial cells (sensitive to growth factors released) could reduce the proliferative activity of the glial cells *in vitro*.

This increase of the proliferative glial activity after a prenatal irradiation is worth to be evaluated more carefully: it may be the source of serious consequences.
- the glioma incidence could be enhanced.
- a postnatal brain injury could recruit more reactive glial cells to proliferate. This later point is in agreement with the pioneer work of Dr Krzyztof Janeczko, the PECO participant to this contract, who observed *in vivo* important glial cell proliferations at the site of neonatal brain injury in animals which had been prenatally irradiated.

Head of project 3: Dr. Ferrer

II. Objectives for the reporting period:

1. Study of late effects in the CNS, and cellular mechanisms involved in these late effects, following prenatal ionizing radiation.
2. Morphological and biochemical study of radioinduced cell death in developing brain..
3. Maturation of glial cells in rats irradiated during the first postnatal days.
Methods. Immunohistochemistry, autoradiography, optical and electron microscopy, in situ labelling of nuclear DNA fragmentation, and agarose gel electrophoresis of extracted DNA.

III. Progress achieved excluding publications (grouped at the end of the report):

1. Cortical malformations induced following prenatal brain irradiation in the rat. Cellular mechanisms involved in late effects.

Different human cortical malformations were reproduced by irradiating prenatal rats at appropriate stages of gestation, they were analyzed here, by means of immunohistochemistry, optical or electron microscopy and autoradiography. Our attention was focused on disorders of the radial glial cells, abnormal cell migration and organization. For this purpose, Sprague-Dawley rats, were irradiated at different gestation ages with a single dose of 2 Gy X- or gamma rays. Their offspring was examined at different embryonic and postnatal ages.

Irradiation at embryonic day 14 (E14), which corresponds to the beginning of proliferation of neuroblasts committed to the cerebral cortex, results in a disruption of the germinal zone and the formation of ectopic germinal rosettes in the periventricular region However, certain cells in the germinal zone may maintain a capacity to produce a layered though dwarfed cortex if the radial glial fibers are preserved and the inside- outside gradient of neuroblast migration is not altered. On the other hand, the periventricular rosettes eventually transform into large subcortical ectopic masses resulting from abnormal migration patterns The true cortex and the subcortical ectopic masses are interconnected by multiple afferent and efferent fibers. Moreover, the ectopic masses send long fibers running via the corpus callosum to different subcortical targets (Fig. 1)

Irradiation at E15, E17 or E19, which corresponds to the bulk of the migration period of the cortical neuroblasts, results in the late formation of cortical cellular columns separated by poorly cellularized columns. This striking pattern is produced because germinal cells are not equally sensitive to radiation at a given time point. In fact, sensitive groups of germinal cells alternate with resistant groups of cells Migration of neuroblasts to their definitive positions in the cerebral cortex follows the normal inside- outside pattern (Fig. 2   ).

Irradiation at E16, just at the time when radial glial cells develop in the rat brain and neuroblasts committed to the upper cortical layers start migration, results in a cerebral cortex composed of four layers:
a.   the first layer is the molecular layer,
b.   the second layer is a cellular layer formed by neurons normally occupying layers VI and V of the normal cortex,
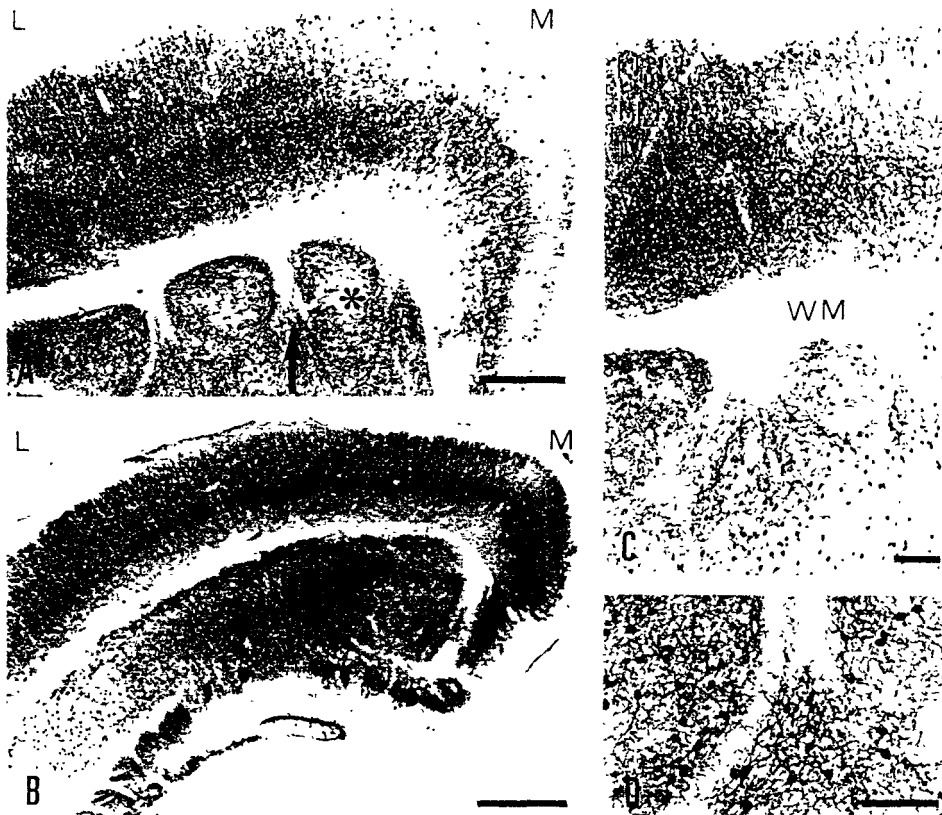
Figure 1 · Parvalbumin immonoreactivity in the cerebral cortex of rat (postnatal day 30: P30) irradiated at embryonic day 14 (E14) with 2 Gy irradiation.
A. Anterior coronal section showing a laminated true cerebral cortex and an inner large cortical mass (asterisk), formed by nodules separated by tracts of fibres (arrow).
B. Posterior coronal section (occipital cortex) showing a normal distribution of parvalbumin-immunoreactive cells in the true cortex and a large ectopic mass of neurons (asterisk), which is partly composed of parvalbumin-immunoreactive neurons distributed at random.
C. High magnification to show the borders, the ectopic mass and the white matter (WM); II-VI, cellular layers of the laminated cortex.
D. Parvalbumin immunoreactive neurons in the ectopic mass with a typical multipolar morphology. L, lateral regions; M, medial regions. A-C, bar = 500 µm; D, bar = 50 µm.

c.   the third layer is a sparsely cellular layer in continuity with the subcortical white matter,
d.   the fourth layer is an inner cellular layer composed of neurons which had failed to migrate to their normal positions in layers II, III and IV.

This abnormality is the consequence of the abnormal number and configuration of radial glial fibers which obstructs the normal migration of cortical neuroblasts to the upper cortical layers.
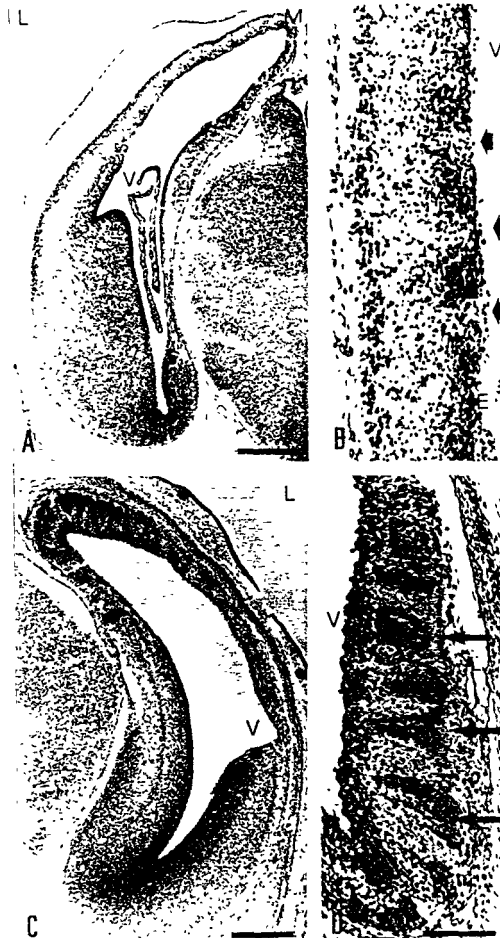
Figure 2: Coronal sections of embryo brains irradiated at E15 (2 Gy).
A and B: 6 h after X-exposure, dead cells in germinal layer are found in groups (arrows) separated by patches of preserved neuroepithelial cells.
C and D: 24 h later, columns of migrating cells (arrows) separated by low cell density zones are observed in the cortical mantle. V, ventricle; M, medial region; L, lateral region; NE, neuroepithelium. Nissl Stain. A and C, bar = 400 μm; D bar = 100 μm (also valid for B).

The present results are not only interesting in the study of radiation- induced deleterious effects on the developing brain but also may help to increase our understanding of normal and abnormal mechanisms commanding cortical histogenesis. The present models are phenocopies of common cortical malformations in human infants: irradiation at E14 is a good model for the study of large subcortical neuronal ectopias, irradiation at E15, E17 or E18 in the rat reproduces abnormal cortical nodules in children afflicted with some forms of mental retardation. Finally, irradiation at E16 in the rat is reproducible model of human lissencephaly type I.

2. Morphological and biochemical abnormalities associated to ionizing radiation induced cell death in the developing brain.

We have also examined sensitive cells and vulnerable phases of the cell cycle to ionizing radiation during the development of the nervous system, and have focused on basic morphologic and biochemical aspects of cell death Our study has demonstrated that germinal cells, neurons and glial cells are sensitive cells to ionizing radiation, and that this process is mediated through protein synthesis. Furthermore, radiation- induced cell death in the developing nervous system has the morphology of apoptosis and is associated with internucleosomal DNA fragmentation, whereas individual dying cells are stained with the method of in situ labelling of nuclear DNA fragmentation.
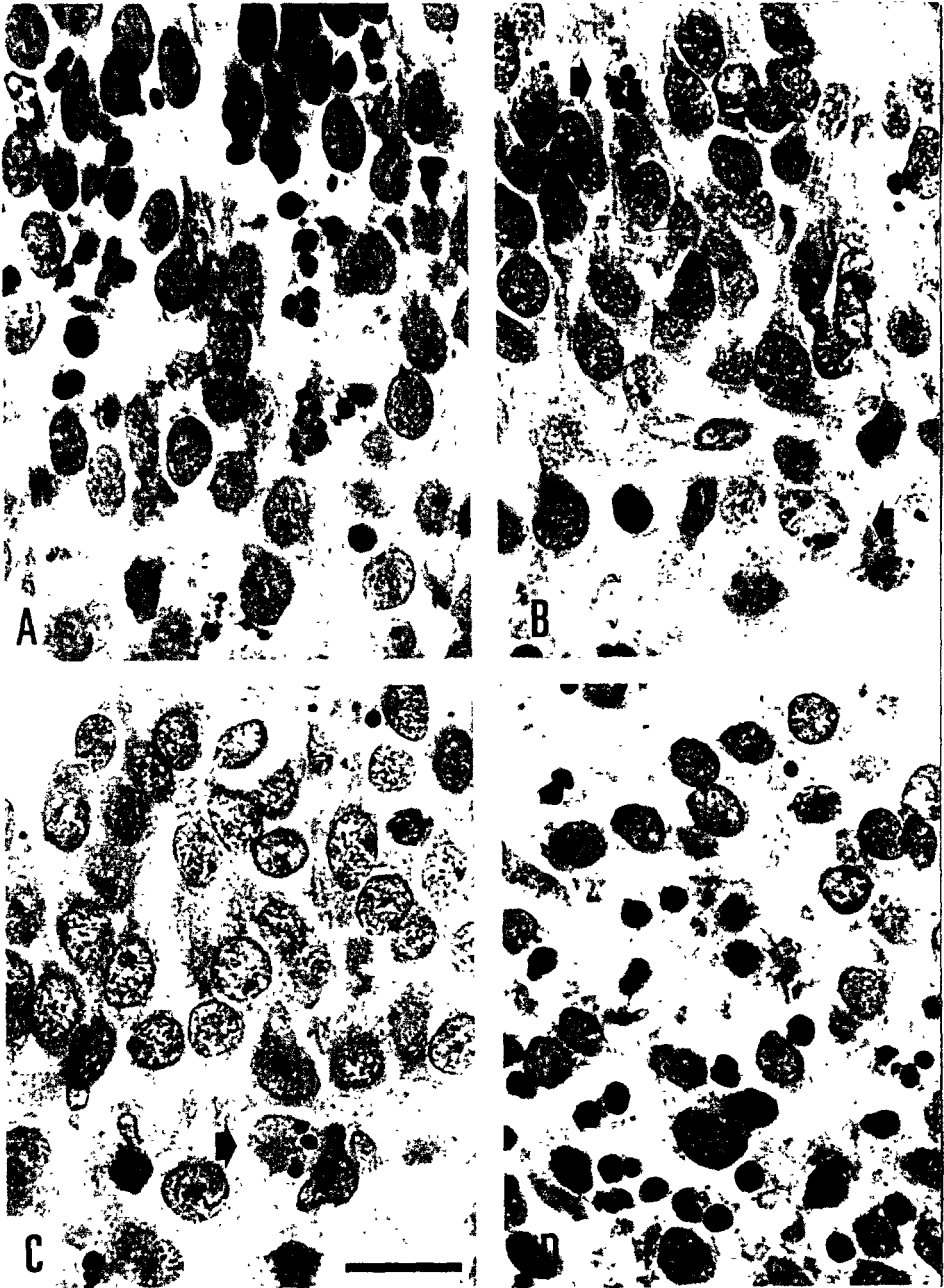
Figure 3: Large numbers of dying cells (characterized by their extremely condensed, often fragmented, nucleus: arrows) are observed in the subiculum (A), CA1 (B), CA3 regions of the hippocampus (C) and hilus of the dentate gyrus (D) in the 1 day old rat 6 h after 2 Gy X-irradiation. Haematoxylin - eosin. Bar = 20 μm.
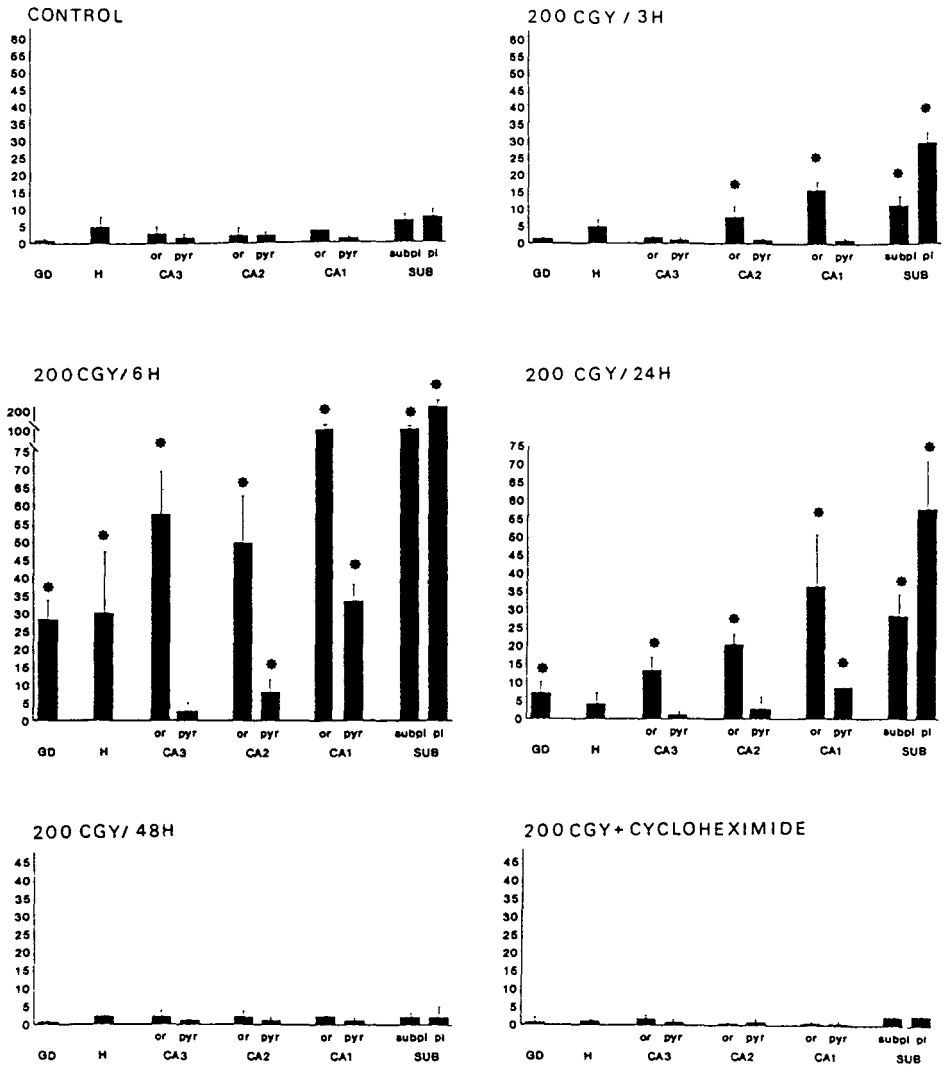
Figure 4: Number of dying cells (mean values ± SD) in the hippocampal complex in control and 1 d-old X-irradiated rats killed at different intervals (3, 6, 24 and 48 h) after irradiation, and in X-irradiated rats receiving 2 g/g body weight of cycloheximide at the time of irradiation, and killed 6 h later. GD, dentate gyrus; H, hilus; CA3, CA2, CA1, areas of the hippocampus; SUB, subiculum; or, stratum oriens; pyr, strat. pyramidale; pl: cortical plate (cellular layer); subpl, cortical subplate (future subcortical white matter). Asterisks indicate p < 0.0001 in relation to the corresponding values in controls (Mann-Whitney U-test).

First of all, the cells vulnerable to ionizing radiation were identified as well as their regional distribution in the developing cerebellum and hippocampus of the newborn rat following a single exposure of 2 Gy X- or gamma rays. The vulnerable cells are: 1. the germinal cells of the hilus of the fascia dentata of the hippocampus and of external germinal layer in the
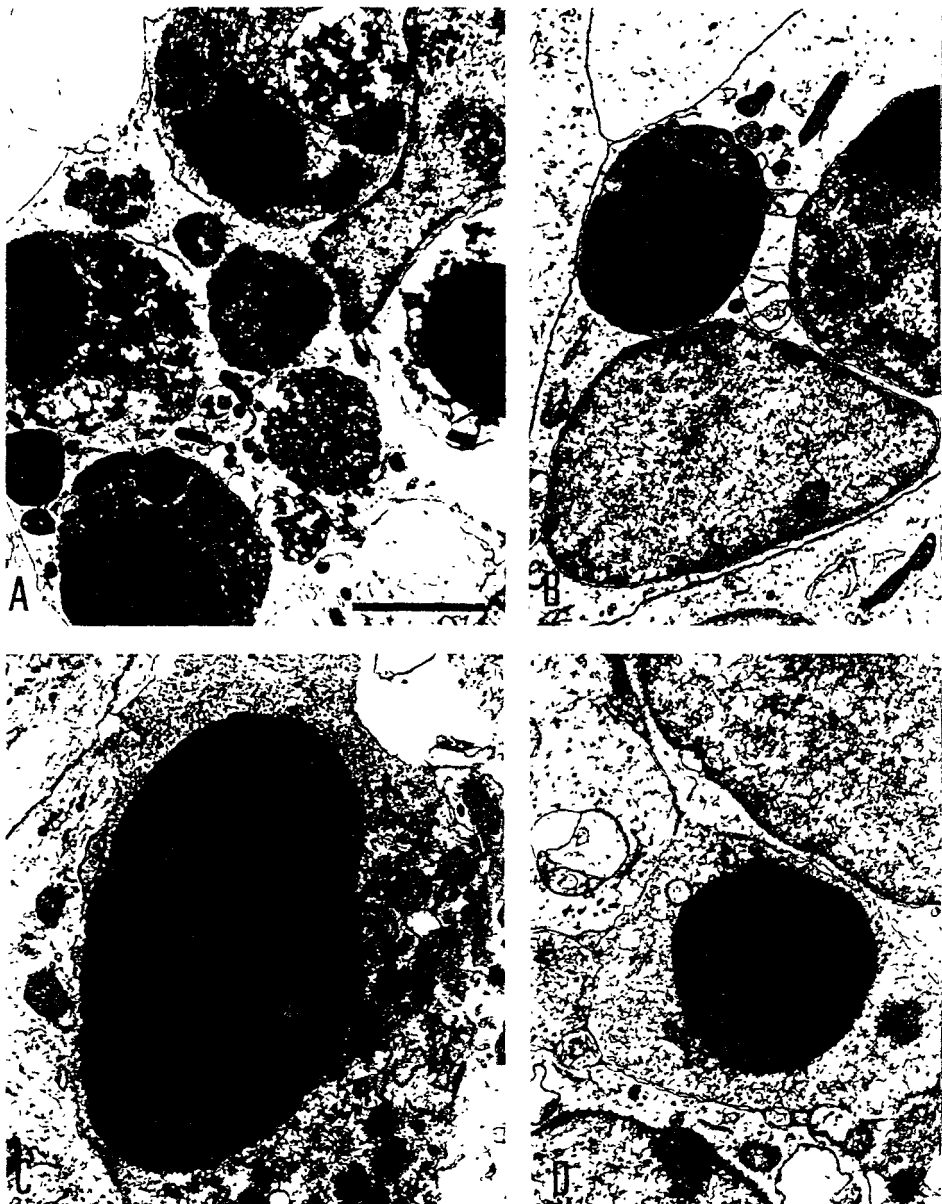
Figure 5 : Dying cells observed with the electron microscope, in the subiculum (A), stratum pyramidale of CA1 (B) and CA2 (C), and stratum oriens of CA1 in the 1 day old rat, 6 h after X-irradiation with a single dose of 2 Gy. Bar = 1μm.

cerebellum; 2. neurons of the CA1, CA2 and CA3 region of the hippocampus; 3. granule neurons of the internal granular layer of the cerebellum; 4. glial cells of the hippocampus, white matter of the cerebellum, and some Bergmann glia. Interestingly, these cellular populations are also particularly vulnerable to naturally occurring cell death. This observation enables the speculation that naturally occurring cell death and radiation- induced cell death during development share common mechanisms (Fig. 3).

On the basis of these studies, a study of morphological and biochemical aspects of cell death was implemented in both normal and pathological conditions. For this purpose, the morphology of dying cells was examined by means of optic and electronic microscopy (Fig 5); different biochemical methods assessed the nature of the dying process. The in situ labelling of nuclear DNA fragmentation is based on the incorporation of biotin-dUTP at the sites of DNA breaks through the action of a terminal deoxynucleotydil transferase. The dUTP is visualized with avidin-biotin- peroxidase. The method permits to detect DNA fragmentation in individual cells. Another method is the agarose gel electrophoresis of extracted DNA. This method is particularly useful since it enables the identification of DNA fragments multiples of 180-200 base pairs which form a ladder pattern on agarose gels characteristic of apoptotic cell death.

It is clear now, and for the first time, that naturally occurring cell death in the telencephalon of the rat has the morphological and biochemical properties of apoptosis. Furthermore, the radiation- induced cell death in the developing rat brain also has the morphology of apoptosis and is associated with a ladder pattern of internucleosomal DNA fragmentation in agarose gel electrophoresis. Dying cells were fairly well visualized with the method of in situ labelling of nuclear DNA fragmentation. Finally, it was also shown that radiation- induced cell death stops after an injection of cycloheximide, a protein synthesis inhibitor, if given at the time of irradiation; this shows that radiation- induced cell death is an active process mediated through protein synthesis (Fig. 4).

These findings represent an important step in our understanding of the mechanisms involved in both the naturally occurring and the radioinduced cell death in the developing brain. They are also a starting point in the study of the molecular cascade leading to apoptosis in the perinatal brain.

3. Maturation of glial cells in rats irradiated during the first postnatal days.

Finally, we have studied the long term effects of a perinatal brain irradiation on the maturation of glial cells in the rat brain. The purpose in this case was to investigate the possibility that the recovery of glial cell populations may depend on the developmental stage. Our results have shown a delayed maturation of oligodendroglia following irradiation in 3 day old rats but not in 1 day old ones, thus suggesting a series of vulnerable windows during the process of gliogenesis in the postnatal rat.

Head of project 4: Dr. Saunders

II. Objectives for the reporting period

The overall objectives of the behavioural project were to investigate the effects of low doses of radiation on functions of the central nervous system. Specifically, they were to identify and describe the functional deficits induced in adult animals following acute exposure to ionising radiation during the development of the cerebral cortex and hippocampus, and to assess the dose-response relationships for these effects. Deficits were assessed using both conventional and novel behavioural techniques. *Two main objectives were proposed.* The first was an investigation of the **decrement in radial arm maze performance** by adult mice following exposure during proliferation of the granule cells of the hippocampus. Animals were exposed to various doses in order to describe the most appropriate dose-response relationship. The second was to develop a programme of study using food-reinforced training tasks in order to examine **decrements in cortical function** and to investigate the dose-response relationship. The studies were seen in helping to better evaluate the radiation risks to humans, and to increase the available information on the effects of prenatal exposure on changes in cognitive function.

III. Progress achieved including publications

Deficits in behaviour and impairments in cognitive function induced by prenatal exposure to ionising radiation are of considerable importance to radiological protection. It is known that exposure of unborn humans during corticogenesis is associated with an increased incidence of severe mental retardation, and with reductions in both intelligence and performance at school, although the precise aetiology and dose-response relationships for these endpoints remain uncertain. Given the rather limited human database, consisting mostly of information derived from the Japanese A-bomb survivors, animal experiments appear to provide the only viable alternative means to explore and describe these relationships in detail, and to help evaluate the radiation risks to humans.

Comparatively little is known about low dose effects on specific memory function in animals and the effects of protracted irradiation. The functional changes assessed by behavioural tasks represent in many ways the analogue of the changes in learning ability observed in exposed humans, and offer clear insight into these processes. Likewise, morphological changes represent the long-term modifications within the central nervous system that are responsible for the observed changes in behaviour.

The behavioural project was concerned with evaluating specific functional changes resulting from acute prenatal irradiation (API). During the 2 year period of the project, considerable progress was made in defining these behavioural deficits. Effects on learned behaviour in adults were investigated using two types of task. The first used a **radial arm maze** to assess *spatial memory and learning*. Performance in this maze is sensitive to insult to the hippocampus and its

associated cortex, areas of the brain recognised as important in mnemonic functions in humans, primates and rodents. It is widely used in many branches of neuroscience for nearly 20 years. The second task used a novel form of operant chamber, called a **9-hole box,** and used a serial choice reaction time task, called the 5-choice task, to investigate *effects on attention and visual discrimination.* This task has not been used before in studies of the effects of radiation, nor has it been used with mice: previous studies have used rats.

1. Studies of spatial memory

Structure of the assay. The radial arm maze consists of eight identical arms that radiate out from an elevated, central arena. Simple guillotine doors allow or deny entrance between the arena and each of the arms. The animal is required to obtain the food pellets located at the end of each arm within a specified number of attempts or designated time. Normal animals use the extramaze cues within the laboratory to define the location of each of the arms, and remember which arms have been visited. These visual cues were provided by the variety of devices and equipment housed within the testing laboratory, including the distinct illumination provided by the overhead fluorescent lighting. A single food reward was placed in the food well in each arm, and a correct response was scored the first time an arm was visited during each trial, while an incorrect response was scored at each subsequent visit. The animals have to learn the rule not to re-visit arms on any day. In our studies, each session lasted for up to 15 minutes a day, and animals received 10 sessions in total. The animals in the maze were under constant observation to allow the behaviour of the animals to be recorded, and the doors were opened and closed manualy at the appropriate times (via a remote system).

Effects and the age at exposure. In previous studies, we have shown that animals irradiated late in gestation and early after birth (on gestational day 18 or postnatal day 1) show deficits in learning this task, but animals irradiated *earlier* in gestation (on gestational day 13 or 15) or *later* as very young animals (on postnatal day 10) do not show such deficits.

Threshold. In additional studies, we have investigated the association between dose on gestational day 18 and deficit in performance as adult. Using doses of between 0.1 Gy and 1.0 Gy the association was best described by a linear, no threshold relationship. On every day of training, the association between dose and performance was linear, but the exact relationship gradually changed from day to day. However it is possible that a "functional" threshold existed since only with doses above about 0.25 Gy were the deficits in performance large enough to allow the behaviour of the exposed animals to be distinguished from that of the controls. These studies were published in the International Journal of Radiation Biology.

Radioinduced sensory impairment ? It was considered possible that the animals exposed to radiation were not exhibiting a deficit in spatial memory, but their reduced performance was the result of some sensory, and particularly **visual, impairment,** perhaps in the eye itself or maybe in the visual areas of the brain. The observed changes in behaviour could then be the result of either

poor perception or discrimination of the landmarks within the laboratory used as extramaze cues to run the maze. Therefore another experiment was performed to control for this possibility.

Testing mouse vision. The same radial arm maze was used, but was placed in a darkened room and the light from a small electric lamp was used to indicate the presence of a food reward within an arm of the maze. These lamps were placed above the entrance to each the arms of the maze and were controlled by a remote manual switchbox. For each trial, four arms were randomly chosen, each baited with a food reward and their cue lights illuminated. The animals were required to visit these arms twice in a single trial, so after the first visit, the arm was baited again. The cue light was turned off after the second pellet had been retrieved. Careful arrangement of the maze within the laboratory allowed the arms to be quickly and quietly rebaited by hand without any apparent disturbance to the animals. In this task, visiting an illuminated arm was scored as a correct response, while visiting an arm with its cue light turned off was scored as an incorrect response. Hence animals could revisit arms, but only if the cue light was illuminated. Importantly, the animals do not have to try and remember the locations of the food using (spatial) memory. Indeed it is assumed that the lack of ambient light will severely impair or stop navigation using extramaze signals: in essence, this is a simple visual discrimination task.

No visual deficit. It was found that the animals irradiated on gestational day 18 that previously could not learn the spatial task, now showed excellent acquisition of the visual discrimination task, and animals irradiated on gestational day 15 which could learn the spatial task failed to learn the new one. Animals irradiated on gestational day 13 could learn both the spatial and discrimination tasks. These data are shown below in figures 4.1 and 4.2: values are means of groups of 10 animals; standard errors are shown as vertical lines. It is considered unlikely that an animal that could previously use the extramaze cues to navigate within the maze could now not perceive and respond to the light stimulus: the former are rather subtle, but the latter are very obvious.

The multiple facettes of memory. Overall, the results of these studies appear consistent with current theories of localisation of memory within the mammalian brain. For example, spatial memory appears to be a good example of a broad range of memory abilities that are dependent on the integrity of the hippocampus and related cortical areas, such as the entorhinal cortex, parahippocampal cortex and perirhinal cortex. In contrast, it is considered that the brain structures important in acquiring simple habits, such as the light/dark discrimination, involve the corticostriatal system, and specifically the cortex and the caudate and putamen. With exposures late in gestation, radiation-induced effects can be presumed to occur in the hippocampal formation, whereas exposures a little earlier in gestation are more likely to effect cortical and striatal areas which appear to develop at roughly the same time. With exposures earlier in gestation neither cortical or striatal areas would be not be maximally affected, and no deficits on these tasks were seen. The dissociation of results illustrates that deficits in vision, or the inability to perform the instrumental aspects of the tasks cannot be considered as explanations of these experiments: in all instances the maze and the necessary responses to obtain the food are the same, but the memory systems required for correct performance of the tasks are different. Comparable results have been shown to occur in adult rats with specific brain lesions within the hippocampus, caudate or amygdala. This study are currently being written for submission to the International Journal of Radiation Biology.
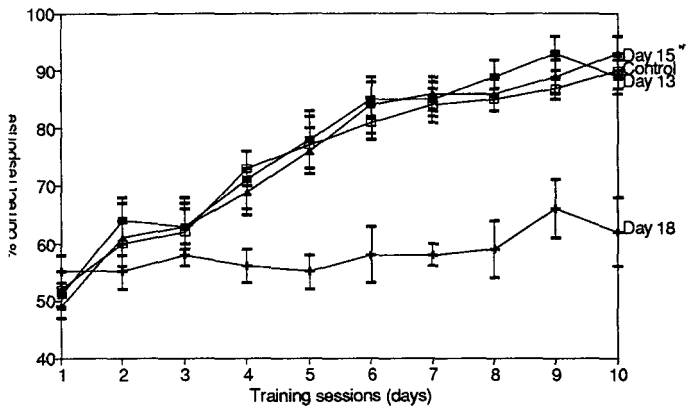
Figure 4.1 Effect of prenatal irradiation on performance of a spatial memory task in the radial arm maze.
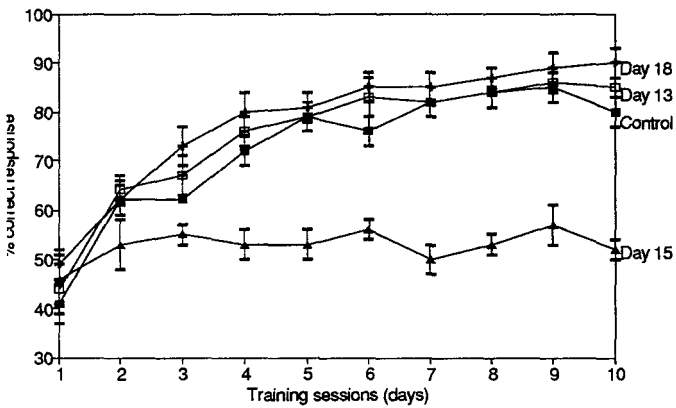

Figure 4.2 Effect of prenatal irradiation on performance of a light/dark visual discrimination task in the radial arm maze.

2. Studies of cortical function

The assay.   These studies used a novel form of operant chamber for mice that contains an assembly of 5 small, response holes, and animals were trained on a food-reinforced, serial reaction time task (called the 5-choice task).   Each chamber is also equipped with response levers to investigate effects using standard schedules of reinforcement.   The task used is analogous to Leonard's serial reaction time task in humans and (larger versions of) this equipment have been used to study deficits of memory and attention in rats with specific brain lesions.   The task is considered sensitive to damage to the cortex.

Animals were required to make a response by poking their noses into one of the holes within the chamber following a visual stimulus within that hole: a small light was illuminated for a short period.   If the correct response was performed within the set time, a 20 mg food pellet was delivered to the food magazine located on the front wall of the box, equidistant from the array of response holes.   Collection of the reward from the food magazine started the next trial.   The animals were therefore required to shuttle between the response holes and the magazine to keep responding and collecting the food.   An incorrect response, or missed response caused a period of time-out during which no rewards could be obtained.   In addition, the small house light was not illuminated during this time.   Registration and latency of all responses and delivery of stimuli and food pellets were computer   controlled.   The use of this system also allows a systematic manipulation of all of the various task parameters.

Individual variability. Preliminary studies using this apparatus revealed that the responses of mice were somewhat variable: a few mice were able to learn the response quickly and well, other mice could not learn the task even with extended training.   This suggested that the experimental protocol used in published studies with rats was not ideal for mice and initial studies to optimise the protocol were undertaken. These included using different flavours of food and different food formulations, as well as altering the various task parameters.   The results of these manipulations suggested that the animals would learn the task, but the task parameters could only be changed very slowly.   Changing the pellet types and pellet formulations appeared to have only rather modest effects: no single pellet or type gave significantly better results than the others.   Overall these modifications helped reduced variability both within and between animals, although the variation within some groups could be larger than within other groups.

The trial. An extensive experiment was then undertaken using CD1 mice to investigate the existence of a critical period for deficits in performance in the 5-choice task following API. Pregnant animals were exposed at up to 1 Gy either before, during, or after peak corticogenesis. The progeny were culled to achieve a constant litter size.   Male offspring were kept until three months old, and following a period of weight reduction (to ensure motivation to respond) eight animals from each exposure condition were trained on the task.   Training consisted of a single session of 30 minutes for each animal each work-day for a minimum of 50 days using the protocol established from the preliminary studies.   At first the stimulus was presented for a long period (6000 cs) and this was gradually reduced (to 100 cs) and at the same time, the period within which a response was required was also reduced (from 6000 cs to 500 cs).

No dose-effect relationship. The performances of the animals for the last 10 days of the experiment are shown in figure 4.3 for animals exposed on gestational day 15, 16 or 18 and in figure 4.4 for animals exposed on gestational day 13, 14 or 15. Results are expressed as mean and standard error. Data from the earlier part of the experiment are not presented as they represent the initial acquisition phase of the task. The performance scores of all the groups were low, and as can be seen from the figures, the animals exhibited a large degree of variation both within groups and between days. These data fail to show any clear radiation-induced effects: statistical analysis confirmed that there were no overall differences between the groups. It is possible that the poor performance and variation contributed towards the absence of finding any effect. The results of a number of operant studies performed by other investigators suggest that some effect is likely following exposure at 1 Gy during peak corticogenesis.
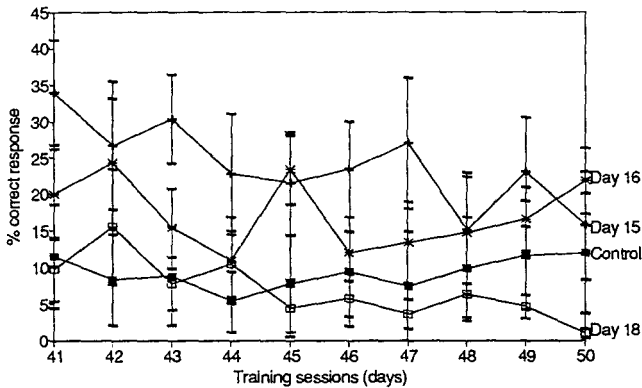
Figure 4.3 Effects of PI late in gestation on final performance in the 5-choice task.
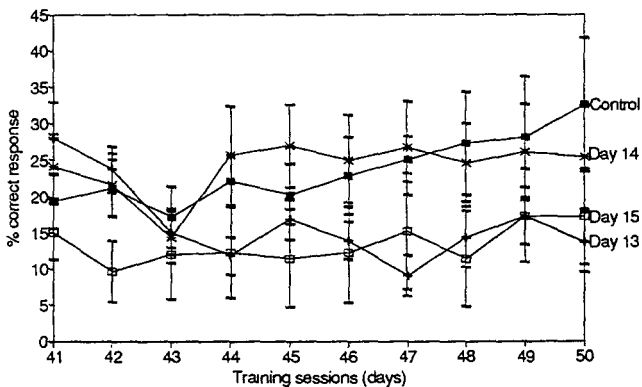
Figure 4.4 Effects of PI earlier in gestation on final performance in the 5-choice task.

A new experimental design. Therefore it was concluded that the initial experimental protocol was still not ideal for the mice and an extensive experiment was performed to optimise this protocol further in order to decrease the variability in response. This used unexposed animals and was performed over a 4 month period. It was considered essential to get the experimental protocol for this task finalised before performing further experiments with exposed animals. It was likely that only subtle modifications were necessary to the existing protocol. It would only be possible to explore the dose response relationship and to investigate the effects of protracted exposures once the protocol was completed.

GLP. In these studies, task variables such as the intertrial interval (ITI), limited hold (LH) and stimulus duration were slowly modified, and the apparent difficulty of the task slowly increased over a prolonged period. More importantly, however, a different strain of mouse was used. In the initial studies, the CD1 mouse was used, and although this strain is generally excellent in performing behavioural tasks, it was possible that this strain was not ideal for this particular task. Therefore the non-agouti, C57BL/6J mouse was used here. This strain is widely recognised as highly proficient in many behavioural tasks, and has been used in operationally similar tasks. Also two small water troughs were placed in the chambers, equidistant from the response holes and by the side of the food magazine. This allowed the animals to drink between trials. It was possible that the performance in previous experiments was limited by a need for water.

Training the trainees. On the first training session, using a long stimulus presentation of 6000 cs and a short ITI of 200 cs, all the animals performed well. Nevertheless, their response rate began to change and fall in the next session, a phenomenon which has been observed in previous experiments. Lengthening the ITI (to the standard duration of 500 cs), however, once again increased performance and decreased variability. The duration the stimulus was presented was gradually reduced over several sessions, and this caused little drop in performance. Most animals were making a more than acceptable number of trials, and were being correct in a high percentage of these (upwards of about 75%). In very few trials did the animals respond in an incorrect hole: they either made a correct response, or missed the trial. A missed trial occurred when the animal failed to make any response either during the stimulus or limited hold. However the longer ITI produced a large number of (incorrect) premature responses in many animals. These occurred when an animal was unable to withhold responding before a response light was illuminated. This behaviour was often accompanied by making large numbers of perseverative responses, and these occurred when the animal keeps making repeated responses. However as the stimulus length was shortened, the number of missed trials increased, although overall number of correct responses was maintained at a very high level (80 - 90% or more). At the same time, the response latency gradually decreased, as animals attempted to respond during the duration of the stimuli. About halfway through the training schedule, with only very few exceptions, all animals were making at least 50 trials a day with above 75% correct responses. The task parameters had by now been reduced to their target values, including a stimulus duration of 50 cs. The animals were now making far less premature or perseverative responses. Such performance was considered acceptable and necessary.

Towards a usable and efficient protocol . The final phase of this investigation involved trying to maximise the performance of the animals, and to reduce or even, eliminate, the missed responses. Various manipulations were tried on specific probe trials, and then performance was

re-established over the next few sessions. These results confirmed that half hour sessions of 100 trials appear optimal, and that an average animal can consume about 50 pellets in one session. Also it was felt that a stimulus duration of 50 cs, an ITI of 500 cs and a LH of 500 cs were acceptable target values. For example, a shorter ITI (of 250 cs) may eliminate premature responding, but it also increased the incidence of missed trials. A longer ITI (of around 1000 cs) increased the number of premature responses without much affect on the number of missed responses. A long stimulus duration (of 150 cs or more) produced less errors and decreased the number of missed trials, but did not increase the number of correct trials.

Weight watching. This experiment also confirmed that tight control of the weights of the animals was a crucial factor. If the animals were not very close to their target weights (that is, reduced to 80% of their free feeding weight, adjusted for growth), they were often unresponsive in the task. However, a weight loss of even a little greater than the target could severely affect the animals and make them slow and sluggish.

In summary, far more difficulty was encountered using this 5-choice task than had been anticipated, and to obtain a usable and efficient protocol took considerable effort. Mice appear more difficult to train on this task than rats, and hence we were unable to investigate the dose response relationship for the task or the effects of protracted exposures to low doses during the lifetime of the present project.

The particulars of the experimental protocol should be of interest to neuroscientists investigating behavioural defects in mice deficient in some specific gene (so-called knock-out animals) and it is hoped to publish these details.
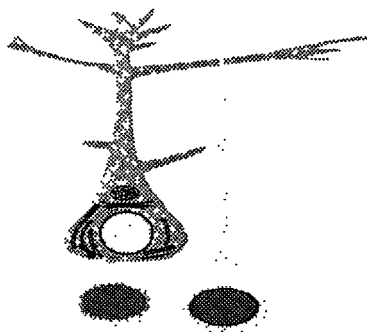
FINAL RESEARCH REPORT of a PECO PROJECT
for the period from 30 June, 1994 to 30 June, 1995

Project Title: "Effects of prenatal or early postnatal irradiation of the central nervous system."

Head of project: Krzysztof Janeczko, Ph.D.
Department of Neuroanatomy, Institute of Zoology, Jagiellonian University,
Ingardena 6,
30 060 Krakow, Poland.
tel: (48 12) 336377, ext. 465. Telefax: (48 12) 226306. E-mail: jane@zuk.iz.uj.edu.pl

I. State of art:

Irradiation of the brain during the period of early development (prenatal or early postnatal) causes irreversible changes in the structure and functional capacity of the brain. Effects of high-dose irradiation on the brain have already been a subject of extensive investigations. However, consequences of low-dose irradiation of developing brain delineate a relatively new research area. Assessment of the consequences is still of capital meaning for radiation security services and, therefore, needs further experimental exploration.

Irradiation-induced changes in the brain structure, even though they are critical for brain function, may exist below the level of detection of experimental techniques. However, it may be supposed that, under some experimental conditions, the changes may become detectable.
The purpose of the present research project was to investigate effects of early low-dose gamma irradiation on the response of brain tissue to injury.

Deficits in cell production and in protein synthesis caused by prenatal or early postnatal irradiation of the developing brain tissue may cause changes in its reactivity to injury. It may be reflected by reactive behaviour of cells different from that observed when the normal, non irradiated brain is injured. The influence of the prenatal brain irradiation on its reactivity to injury has never been examined systematically. This is why the present project focuses on this problem.

II. Objectives for the reporting period:

The two main purposes of that initial part of the experiment were:
1. To evaluate and compare changes in astrocyte GFAP-immunoreactivity following injury in irradiated and control brains.

2. To get an evidence that the intensity of injury-induced astrocyte proliferation in irradiated brains has changed. Also to determine the prenatal period of the highest vulnerability to gamma irradiation.

First of all the range of irradiation-induced changes in the brain anatomy had to be assessed in relation to the irradiation dose and the developmental stage when brains were irradiated. An early prenatal 100 cGy irradiation caused reduction of the brain size (especially at E13, E15 and E17). In consequence, the lesion size was reduced in an attempt to cover relatively similar areas in treated versus control brains.

III. Progress achieved

The research programme investigates the effects of a prenatal irradiation with low doses of 60-Cobalt gamma (10 cGy, 25 cGy or 100 cGy) on the astrocyte response in the brain mechanically injured at the postmitotic stage of development (in 6-day or 30-day-old rats).

For this, pregnant Wistar rats were irradiated on prenatal (E13, E15, E17 or E19) or early postnatal days (P0 or P2). After delivery, a lesion (stab wound) was made in the left cerebral hemisphere of newborn and postmitotic brains. Thereafter, the rats were injected with 3H-thymidine (10 µCi/g body weight) at 1 hour or at 1, 2, 4, 8 or 30 days after the injury and killed 4 hours after the injection.

The intensity of injury-induced proliferation of GFAP-immunopositive astrocytes was examined as previously described (see: Janeczko, 1989, 1994).

Brain paraffin sections were first immunostained to visualize GFAP in astrocytes then autoradiographed and examined microscopically to record changes in the distribution of GFAP-positive astrocytes labelled with 3H-thymidine. Their total number and distribution in experimental versus control brains were recorded and compared. The examination was carried out within the lesion area in the cerebral hemisphere and within the corresponding area in control brains.

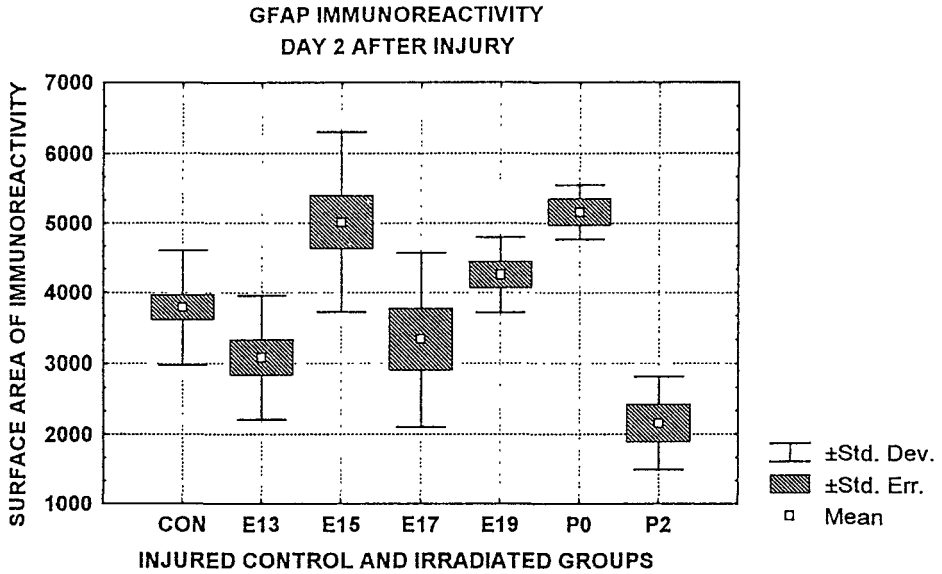## 1. Changes in the astrocyte GFAP-immunoreactivity.

This was measured using a computerized image analysis system (Visual Diagnostic, UK) acquired thanks to the support of the PECO project. In immunostained sections of irradiated brains the total immunoreactive area within 200 x 200µm unit squares adjacent to the lesion site was counted and compared with corresponding areas in injured but non-irradiated control brains. A part of histological material is still under examination or is to be examined. Therefore, the results are of still preliminary.

Image analysis did not reveal any statistically significant change in the GFAP-immunoreactivity (Graph 1). No changes could ever be associated with the foetal age at the time of irradiation. The results suggest that prenatal irradiation does not influence GFAP-immunoreactivity and/or GFAP content in reactive astrocytes.

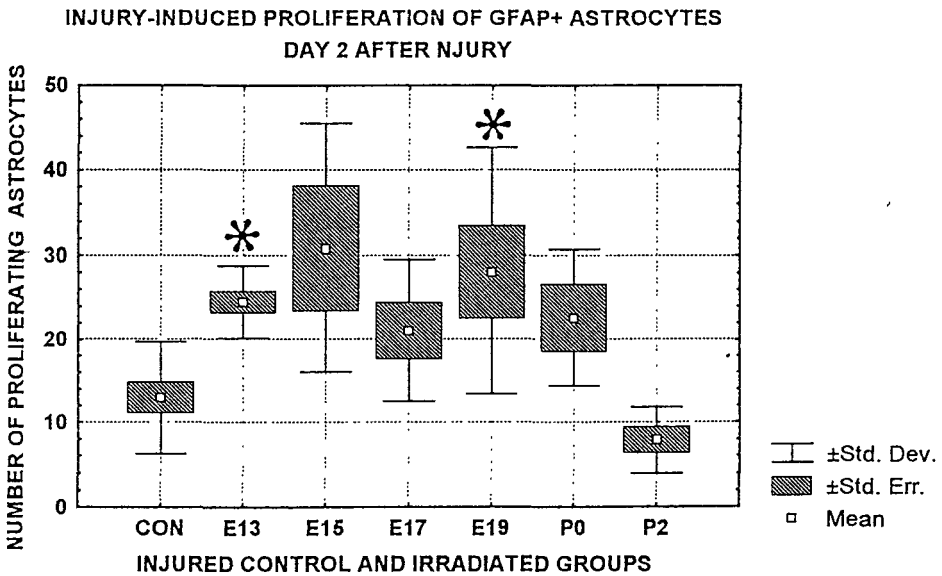## 2. Changes in the intensity of injury-induced astrocyte proliferation.

In contrast, statistically significant changes were revealed only in brains after the highest gamma dose used: 100 cGy. All the significant changes were obtained after examination of brains on the 2nd day following injury and these data are presented hereafter.

Graph 1.

GFAP IMMUNOREACTIVITY
DAY 2 AFTER INJURY

(The surface area of immunoreactivity is expressed in μm^2 per 200x200μm unit area)

Graph 2.

INJURY-INDUCED PROLIFERATION OF GFAP+ ASTROCYTES
DAY 2 AFTER NJURY

(Asterisks indicate statistically significant differences)

A considerable increase of the astrocyte proliferative activity was revealed in brains irradiated on E13 and E19 on the second day after the mechanical injury (Graph 2, E13 - $P<0.05$, E19 - $P<0.02$; one way ANOVAS). Until now, no significant changes were detected at the other stages. Graph 2 demonstrates the profile of an apparent age-dependent relation between the time of irradiation and the intensity of astrocyte proliferation. The profile suggests that effects of perinatal irradiation are minimal and that brain irradiation performed within the period of cerebrogenesis leads to the maximal increase in proliferative reactivity of astrocytes. Graphs 1 and 2 show that the numbers of proliferating astrocytes do not correlate with changes in GFAP-immunoreactivity of the injured brain tissue.

The results presented here may represent a first evidence that after a "low-dose" gamma irradiation given at early developmental stages, the reactivity of brain tissue to injury is changed. However, the data obtained will be verified by further examinations including 3H-thymidine autoradiography combined with immunocytochemical identification of astrocytes with the S-100 protein marker. A considerable amount of histological material from irradiated animals injured on postnatal days 0 and 6 is still under examination: the results will be communicated to all cocontractants of the main project in the near future via the Project Journal.

At present, the basis for this increased reactivity of astrocytes can only be a matter of speculations. Continuation of this research, especially comparisons of the astrocyte response in brains injured at different postnatal age, may give valuable insights about the developmental determinants of the detected phenomenon.

Recent references:

Janeczko, K. 1989. Spatio-temporal patterns of astroglial proliferation in rat brain injured at postmitotic stage of postnatal development. A combined immunocytochemical and autoradiographic study. Brain Research, 456: 280-285.

Janeczko, K. 1994. Age-dependent changes in the proliferative response of S-100 protein positive glial cells to injury in the rat brain. Int. J. Devl. Neuroscience, 12: 431-440.

PUBLICATIONS (n= 27) OF THE 5 GROUPS.

1992

Ferrer I, Reyners H, Gianfelici de Reyners E, Coffigny H (1992) **X-irradiation increases cell death in the cerebral cortex and subcortical white matter of developing rats and its effect is inhibited by cycloheximide.** 24th Congress of the European Society of Radiobiology, ESRB, Erfurt, Oct 4-8. Book of abstracts, p 44

Reyners H, Gianfelici de Reyners E, Coffigny H, Ferrer I (1992) **Protracted prenatal exposure with low doses of gamma rays and neutrons: late consequences in the central nervous system.** 24th Congress of the European Society of Radiobiology, ESRB, Erfurt, Oct 4-8. Book of abstracts, p 43

Reyners H, Gianfelici de Reyners E, Poortmans F, Crametz A, Maisin J-R (1992) **Brain atrophy after foetal exposure to very low doses of ionizing radiations.** International Journal of Radiation Biology, 62: 619-626

1993

Coffigny H, Beauvallet M, Ferrer I, Reyners H, Gianfelici de Reyners E, Court L (1993) **Comparison of the effects of gamma irradiation on rat mesencephalic and striatal nerve cells in culture.** 25th congress of the European Society of Radiobiology, ESRB, Stockholm, June 10-14. Book of abstracts, P02:03

Ferrer I (1993) **Experimentally-induced cortical malformations in rats.** Child's Nervous System 9: 403-407

Ferrer I, Alcantara S, Marti E (1993) **A four-layered lissencephalic cortex induced by prenatal X-irradiation in the rat.** Neuropathol. Appl. Neurobiol. 19: 74-81

Ferrer I, Alcantara S, Zujar MJ, Cinos C (1993) **Structure and pathogenesis of cortical nodules induced by prenatal X-irradiation in the rat.** Acta Neuropathol. 85: 205-212

Ferrer I, Santamaria J, Alcantara S, Zujar MJ, Cinos C(1993) **Neuronal ectopic masses induced by prenatal irradiation in the rat.** Virchows Archiv A Pathol. Anat. 422: 1-6

Ferrer I, Reyners H, Gianfelici de Reyners E and Coffigny H (1993) **Cell vulnerability in X-ray-induced apoptosis in the developing cerebral cortex.** 25th Congress of the European Society for Radiation Biology, ESRB. Stockholm, Sweden, June 10-14. Book of abstracts, P11:04

Ferrer I, Serrano T, Alcantara S, Tortosa A, Graus F (1993) **X-ray-induced cell death in the developing hippocampal complex involves neurons and requires protein synthesis.** J. Neuropathol. Exp. Neurol. 52: 370-378

Ferrer I, Serrano T, Rivera R, Olivé M, Zujar MJ, Graus F(1993) **Radiosensitive populations and recovery in X-ray-induced apoptosis in the developing cerebellum.** Acta Neuropathol. 86: 491-500

Reyners H, Coffigny H, Lemaire G, Ferrer I, Gianfelici de Reyners E (1993) **La radiosensibilité du cerveau foetal aux faibles doses et aux faibles débits de dose d'irradiation externe.** 1er Colloque "Radiobiologie: Aspect biologiques et bases physicochimiques", Jul 11-16, Book of abstracts. Univ. Sherbroke Publ., Book of Abstracts, p 84

Reyners H, Ferrer I, Coffigny H (1993) **Effects of radiation on the development of the central nervous system.** EEC radiation protection programme 1990-1991. Contract Bi7-003. Progress report EEC, p 1009-1016

Reyners H, Gianfelici de Reyners E, Coffigny H, Ferrer I (1993) **Quantitative histological assessment after low dose rate neutron irradiation during the corticogenesis of the foetal rat brain.** 25th Congress of the European Society of Radiobiolog, ESRB Stockholm, June 10-14. Book of Abstracts, P02:17

Reyners H, Gianfelici de Reyners E, Hopewell JW (1993) **Early vascular indicators of the radiation syndrome in the adult rat brain.** 25th Congress of the European Society of Radiobiolog, ESRB Stockholm, June 10-14. Book of Abstracts, L08:03

Reyners H, van Ravestyn L, Gianfelici de Reyners E (1993) **Neurologie du retard mental sévère causé par une irradiation prénatale.** Ann. Ass. Bel. Radioprotection 18: 151-157

1994

Ferrer I, Tortosa A, Blanco R, Martin F, Macaya A, Serrano T, Planas AM (1994) **Naturally occurring cell death in the cerebral cortex. Evidence of apoptosis-associated internucleosomal DNA fragmentation.** Neurosci. Lett. 182: 77-79

Janeczko, K (1994) **Age dependent changes in the proliferative response of S-100 protein positive glial cells to injury in the rat brain.** Int. J. Devl. Neuroscience, 12: 431-440

Reyners H, Ferrer I, Coffigny H (1994) **Effects of protracted exposures to low doses of radiations during the prenatal development of the central nervous system.** EEC radiation protection research action 1992-1994. Contract Fi3P-CT92-0015, Report "EUR 15238 en". p 413-418 EEC, Brussels.

Reyners H, Ferrer I, Coffigny H (1994) **Effects of radiation on the development of the central nervous system.** Contract Bi7-003 sector B31. Final report. In: EC radiation Protection Programme 1990-1991. EUR 15295 ed. Vol. 2. Ed: European Commission, Brussels, p 1233-1247.

Sienkiewicz, Z J, Haylock, R G E, and Saunders, R D, (1994) **Prenatal irradiation and spatial memory in mice: Investigation of dose-response relationship.** Int. J. Radiat. Biol., 65: 611-618.

1995

Coffigny H, Dormont D, Court L (1995) **In vitro nerve cell survival of four rat fetal brain structures after gamma irradiation.** In: "Radiation research 1895-1995" Congress Proceedings. 10th International Congress of Radiation Research, Würzburg, Germany, Aug

27- Sep 1. U. Hagen, H. Jung and C. Streffer editors, Würzburg, Volume 1, Congress Abstracts, p 413

Ferrer I, Macaya A, Blanco R, Olivé M, Cinos C, Munell F, Planas AM (1995) **Evidence of internucleosomal DNA fragmentation, and identification of dying cells in X-ray-induced cell death in the developing brain.** Int. J. Devl. Neurosci. 13: 21-28

Luccioni C, Reillaudou M, Beaumatin J, Coffigny H, Lefrançois D, Bardot V, Dutrillaux B, (1995) **Comparison of rat glial cells transformation after radiation or chemical exposure.** In: "Radiation research 1895-1995" Congress Proceedings. 10th International Congress of Radiation Research, Würzburg, Germany, Aug 27- Sep 1. U. Hagen, H. Jung and C. Streffer editors, Würzburg, Volume 1, Congress Abstracts, p 247

Reyners H, Coffigny H, Ferrer I (1995) **Effects of protracted exposures to low doses of radiations during the prenatal development of the central nervous system.** Contract Fi3P-CT92 0015. In: Nuclear Fission Safety Programme 1990-1994. Radiation Protection Research Action 1992-1994. Vol. Report EUR 16003. Ed: European Commission, Brussels, p 979-992

Reyners,H, Gianfelici de Reyners E, Calvo W, Ferrer I, Hopewell JW, Keyeux A, van der Kogel A (1995) **Les effets à retardement de l'irradiation focalisée du cerveau du rat adulte: données nouvelles et perspectives.** 2d Colloque Radiobiologie Fondamentale et Appliquée. Spa, Jul 9-13. Book of Abstracts, n° 18

Reyners H, Gianfelici de Reyners E, Coffigny H and Crametz A (1995) **Protracted low dose irradiations of the foetal rat brain.** In: "Radiation research 1895-1995" Congress Proceedings. 10th International Congress of Radiation Research, Würzburg, Germany, Aug 27- Sep 1. U. Hagen, H. Jung and C. Streffer editors, Würzburg, Volume 1, Congress Abstracts, p 415

1995-6

Ferrer I, Borras D (in press) **Effects of X-irradiation on glial cells in the developing rat brain.** J. Anat.

Guillemin G, Boussin F, Le Grand R, Croitoru J, Coffigny H. and Dormont D (in press) **Granulocyte macrophage colony stimutating factor stimulates in vitro proliferation of astrocytes derived from simian mature brains.** Glia .

Sienkiewicz, Z J, Haylock, R G E, and Saunders, R D. **Differential learning impairments produced by prenatal exposure to ionising radiation in mice.** Manuscript in preparation.

Sienkiewicz, Z J, and Saunders, R D. **The 5-choice task in mice.** Manuscript in preparation.

Contract : F13PCT920064c   **Duration: 1.7.92 to 30.6.95**   **Sector: B33**

Title: Dosimetry and effects of parental, fetal and neonatal exposure to incorporated radionuclides and external radiation.

1)	Harrison	NRPB
2)	Henshaw	Univ. Bristol
3)	Van den Heuvel	VITO
4)	Lord	Inst. Paterson
5)	Visser	TNO - Delft
6)	Tejero	Univ. Madrid - Compultense
7)	Bueren	CIEMAT
8)	Archimbaud	CEA - Bruyères-le-Châtel

I. Summary of Project Global Objectives and Achievements

I.I Objectives

1) Measurements of natural alpha emitters in human fetal tissues. Studies of the distribution of ^{210}Po in fetal bone in relation to structural changes during growth and the distribution of target cells. Studies of the transfer of ^{85}Sr, ^{210}Po, ^{210}Pb, ^{141}Ce, ^{106}Ru, ^{239}Pu and ^{241}Am to the embryo and fetus in rodents. Measurements of the transfer of ^{210}Po, ^{237}Np, ^{239}Pu and ^{241}Am to the baboon fetus in late gestation. The use of animal and human data to estimate doses to the human fetus and child after maternal intakes of radionuclides.

2) Studies of the effects of external irradiation and ^{239}Pu and ^{241}Am contamination on murine haemopoietic development *in utero* and after birth, using cellular and molecular techniques; including studies to distinguish between effects directly on haemopoietic cells and on the regulatory microenvironment, the sorting and characterisation of stem cells, the use of genetically labelled stem cells to study differentiation in normal and irradiated marrow, measurements of stable cytogenetic abnormalities in marrow from neonates after *in utero* irradiation, measurements of the effect of radiation on expression of haemopoietic growth factors, and studies of long-term effects on granulocyte function. Associated studies of the effects of *in vitro* exposure of haemopoietic tissues at different developmental stages to alpha-particle irradiation from ^{210}Po.

3) Studies in mice of the effect of paternal exposure to ^{239}Pu or ^{241}Am prior to conception to investigate possible instability in developing haemopoiesis and its regulatory microenvironment in offspring.

4) Analysis of data from an effects study in which ^{241}Am was administered to pregnant mice and tumour incidences in the offspring were determined.

5) Study the apoptotic response in the rat cerebellum after external irradiation and irradiation from incorporated radionuclides.

I.II Progress achieved

I.II.I Biokinetics and dosimetry

A detailed investigation has been undertaken at UB of the distribution of natural alpha radioactivity within the human fetus, using autopsy samples obtained from various stages of development from 18 weeks to stillborn. Samples from 117 cases have been collected, mainly from the Bristol area but including samples from West Cumbria. Alpha-activity in tissue samples, largely due to ^{210}Po, has been measured using the track detector, TASTRAK. A new method of background assessment has been devised which has enabled resolution of low activity concentrations in fetal soft tissues. For measurements on samples from the Bristol area, the recorded values were 0.073 ± 0.018, 0.058 ± 0.013 and 0.021 ± 0.006 Bq kg^{-1}, for thymus, spleen and liver, respectively. Concentrations in fetal vertebrae were greater, with values ranging from the detection limit to about 0.6 Bq kg^{-1}. Values for samples from Cumbria were similar or lower. The results suggest a correlation between fetal age and increasing concentrations of ^{210}Po in bone. Atomic absorption spectroscopy has been used to determine the calcium content of fetal vertebrae samples to provide information on increasing calcification with skeletal development. Studies of the distribution of alpha dose from ^{210}Po in relation to target cells in fetal bone are in progress. Smaller marrow spaces between trabuculae will lead to irradiation of a greater proportion of the marrow from ^{210}Po on bone surfaces or within bone mineral. CD34 and CD38 anitibody markers are being used to identify target cells.

Measurements have been made at NRPB of concentrations of ^{210}Po and other alpha-emitters in fetal tissues obtained from second trimester terminations carried out in the Oxford area and in west Cumbria. No correlation was observed between ^{210}Po concentration and either geographical location or maternal age, with values of about 4 - 60 mBq kg^{-1}. Measurements of $^{239/240}$Pu were also undertaken, by mass specrometry; overall, typical fetal concentrations were a few µ Bq kg^{-1}, about two orders of magnitude lower than typical average values for adult members of the UK population.

Studies at NRPB of the transfer of ^{210}Po to the fetus in rats and guinea pigs have been reported previously (Final Contract report: Bi6-347d). Other sources of ^{210}Po in the fetus are transfer after formation from ^{210}Pb accumulated in maternal skeleton and in-growth after transfer of ^{210}Pb. For ^{210}Pb administered to rats and guinea pigs during pregnancy, transfer was largely influenced by skeletal formation in the fetus and showed significant increases shortly before birth. Measurements of the transfer of ^{210}Po to the rat fetus after administration of ^{210}Pb to the mothers at 6 months prior to conception showed that the concentration of ^{210}Po in the yolk sac during haemopoiesis were about an order of magnitude greater than for the parent ^{210}Pb, with low concentrations of both radionuclides in the fetus. By birth, the relative concentrations of ^{210}Po in the yolk sac and placenta were about two orders of magnitude greater than the corresponding ^{210}Pb concentrations but transfer to the fetus was similar for the two nuclides. Studies of the transfer of ruthenium and cerium to the fetus in rodents have been completed. Retention by the fetus was greatest after administration in late gestation with fetus to mother concentration (C_f/C_m) ratios of about 0.2 for Ru and 0.01 for Am compared with previously reported values of about 0.1 for Pu and 0.02 for Am. Retention by the rat yolk sac during haemopoiesis was high for Ru as for Pu but considerably lower for Ce as for Am. After administration one month prior to conception, retention by the rat fetus was two orders of magnitude lower for all four elements than after short-term administration during pregnancy.

CEA and NRPB have studied the transfer of ^{210}Po, ^{239}Pu and other actinides to the fetus in late gestation in a primate species, the baboon. Results for two mothers and fetuses are complete, measurements having been made 7 days after intravenous injection at 5 months of gestation. The fetus accounted for 4% of injected ^{239}Pu, 0.4% of ^{241}Am, and about 1% of ^{210}Po and ^{237}Np with corresponding retention in the placenta of 10%, 2%, 1% and 0.3%, respectively. Results for ^{239}Pu and ^{210}Po show similar concentrations in fetal and maternal bone contrary to previous results for rodents which showed lower transfer to the fetus. For ^{241}Am and ^{237}Np, concentrations in fetal bone were a factor of ten or more lower than in maternal bone.

Autoradiographic studies using a beta emitter, ^{241}Pu have been undertaken to obtain information on the microdistribution of Pu in relation to sensitive cells in the yolk sac and other tissues. At 11 days of gestation, when haemopoiesis is established in the yolk sac, the greatest concentrations of ^{241}Pu were in the columnar epithelium of the endodermal layer with less activity associated with the primitive erythroblasts arising from the mesodermal layer.

Studies at CEA, designed to estimate doses delivered to fetal tissues and organs during development, have involved measurement of the skeletal distribution of different radionuclides with differing energies, and analysis of biological effects. The studies have been focussed on the uptake of radionuclides by the skull with the aim of studying effects on the brain. Studies of the distribution of ^{141}Ce in fetal and neonatal rats showed that the skeleton accounted for 60 - 85% of total fetal or neonatal activity at one day after administration. The proportion of retained activity in the fetal and neonatal liver was in the range 10 - 40% of total body activity. During the fetal period, the liver : skeleton ratio decreased, reaching a minimum at birth and increasing with neonatal age. Other organs, including the brain, did not accumulate significant ^{141}Ce activity. Measurements of the distribution of ^{141}Ce between different bones of the skeleton showed that the ribs and the spinal column both accounted for about 10 - 15% of total skeletal activity. The skull accounted for about 5 - 10% of total activity. Variations with developmental stage were observed which will affect doses to the brain and other tissues. Results for ^{85}Sr show that retention was mainly in the skeleton, with the ribs, skull, femora and spinal column accounting for 40 - 50% of retained activity. The was no significant difference between different stages of contamination. The skull accumulated 10 - 12% of the total body activity.

Measurements have been made of apoptotic response in the cerebellum of rats in order to assess the dose delivered from incorporated radionuclides. The mean duration of the apoptotic process gradually increased with dose from 6-9 hours after 0.25 Gy to more than 24 hours after 3 Gy. At doses up to 1 Gy, the maximum frequency was observed after 6 hours; a linear dose-response relationship was established for measurements at this time. Comparisons of the effect of external irradiation and irradiation from incorporated ^{89}Sr showed that administration of 500 kBq ^{89}Sr was equivalent to a dose of about 0.5 Gy.

The information obtained in studies of the transfer of radionuclides to the fetus is being used in current ICRP work on the estimation of doses to the human fetus.

I.II.II Effects on haemopoiesis

MBL/ITRI-TNO have undertaken studies to facilitate the separation and characterisation of haemopoietic stem cells using a combination of cell separation techniques, reverse transcriptase - polymerase chain reaction and cell culture methods. Stem cells were sorted and enriched several hundred fold from adult mouse bone marrow. About 0.4% of low-density bone marrow cells were

found to be wheat germ agglutinin positive and monoclonal antibody 15-1.1 negative, and 5% of these were Rhodamine 123 negative. Of this 0.02% of total bone marrow, 10% were found to be Rhodamine-123 negative in the presence of verapamil. This cell fraction was shown to contain the long term repopulation stem cells. The expression of a number of genes by these cells has been studied. The homing of these cells after transplantation into mice was more effective in unirradiated than in irradiated animals (8.5 Gy gamma) but proliferation was more rapid in the irradiated animals.

CIEMAT have investigated whether irradiation with doses as low as 0.5 Gy (X-rays) will induce persistent haemopoietic damage at particular stages of murine development. Mice were irradiated on day 4, 13 or 17 of *in utero* development, 2 or 8 days after birth or as young adults. Data showed that only in the case of *in utero* irradiation on day 13 or 17 were long-term haemopoietic changes observed, as shown by a reduction in the granulo-macrophage lineage. To confirm whether these results were also reproduced in the most primitive self-renewing lympho-haemopoietic stem cells, bone marrow from irradiated animals was mixed with genetically distinguishable normal marrow and transplanted into myeloblated mice. Data showed that not only the committed and pluripotent progenitors, but also the self-renewing lympho-haemopoietic stem cells were persistently damaged at long times after irradiation of the fetus with doses of 1 - 3 Gy. By the use of Ly 5.1/Ly 5.2 congenic mice, the induction of haemopoietc abnormalities was confirmed in both the myeloid and the T and B lymphoid lineages. In order to follow the differentiation fate of individual stem cell clones after irradiation, cells were labelled with retroviral vectors. Efficient procedures of gene transfer were developed so that individual clones could be followed for periods of longer than a year in primary, secondary and tertiary recipients. Experiments in which genetically labelled stem cells were seeded into normal and irradiated stromas have not yet revealed differences in the dynamics of stem cell clones.

With the aim of obtaining information relating to the molecular basis of persistent haemopoietic deficiencies observed after irradiation, analyses of the expression of haemopoietic growth factors (HGFs) have been undertaken at CIEMAT, initially in animals irradiated with high doses of X-rays (7 Gy). RNA samples extracted from the bone marrow and long-term cultures established with marrow from normal and irradiated mice were hybridised with probes for IL-1, IL-3, G-CSF, M-CSF and SCF. No reproducible differences could be established between samples harvested from the control and treated samples. ELISA analyses of IL-1, IL-3, IL-6 and GM-CSF were done with serum obtained from individual mice which had been exposed to radiation. In this case, up to 50% of the irradiated animals showed over-expression of some of the tested HGFs. No direct relationship has been established between HGF expression and CFU-GM numbers

In studies of methods to ameliorate the effect of radiation exposure on the haemopoietic system, comparisons are being made of expansion of murine bone marrow cells using different combinations of HGFs. While expansion with ILs 3 and 6 showed an earlier haemopoietic recovery of recipients than that observed in mice transplanted with unexpanded bone marrow cells, a greater effect was observed with other combinations involving ILs 1, 3, 6 and SCF. Using purified CD34 cells from human cord blood and mobilised peripheral blood, CFU-GM expansions as high as 500 fold have been achieved in the presence of hILs 3, 6 and SCF.

Studies at PICR on the effects of *in utero* exposure of mice to ^{239}Pu at 4, 13 or 17 d gestation or direct administration of ^{239}Pu to neonatal or weanling progeny have shown life-long deficits in marrow haemopoietic stem cell numbers, though not in mature, functional cell output. Results for the concentration of ^{239}Pu in tissues at different stages suggest that sensitivity to changes in

stem cell numbers varied by a factor of 100 between 4 d gestation and post-natal contamination. Although the haemopoietic outcome was similar in all cases, the mechanisms of radiation damage were different. Contamination at 4 d gestation resulted in direct stem cell damage, while contamination at 13 d caused damage to the haemopoietic regulatory microenvironment which limited the growth of the stem cell population. In all cases, however, end cell production was maintained by increased stem cell proliferation and it is suggested that this may potentially be a feature vulnerable to a secondary insult. Although normal in number, the functional activity of the granulocytes produced in these deficient microenvironments was greatly increased. In terms of long-term haemopoietic damage, a very large RBE - in excess of 100 - was assigned to the *in utero* incorporated ^{239}Pu. This was based on foetal liver incorporation of ^{239}Pu versus appropriate γ-ray doses giving comparable tissue disturbance in the adult offspring. This end-point was considered more appropriate than direct killing of isolated cells *in vitro*.

Studies at VITO have shown haemopoietic damage in mice after *in utero* contamination with ^{241}Am either by injection on day 14 of gestation or infusion in early or late gestation (mothers given 450 Bq g^{-1}). The dose to the femur in offspring was estimated as 4 to 20 mGy. Changes in the number of haemopoietic progenitor cells (CFU-GM) and a disturbance of the stromal haemopoietic microenvironemt were observed in all groups until at least 1.5 years after birth. No difference in growth factor production (GM - CSF, TNF - α, TGF - β, IL - 1) in the haemopoietic cultures could be demonstrated.

Studies were undertaken at VITO to determine the effect on haemopoietic and stromal stem cells after paternal contamination of BALB/c mice with ^{241}Am (3, 6, or 30 kBq) prior to conception. No changes in bone marrow cellularity and haemopoietic stem cells (CFU-s, day 14) were seen up to 6 months after birth. Changes in the number of haemopoietic progenitors (CFU-GM) and stromal stem cells (CFU-f) were observed; CFU-f numbers were generally increased. The stromal microenvironment, as evaluated by the capacity to establish *in vitro* long-term bone marrow cultures (LTBMCs), appeared to be disturbed. Male contamination with ^{239}Pu before mating has been shown to have long-term consequences on the bone marrow of their progeny, again directed primarily via the regulatory microenvironment (PICR). Defects are not consistently predictable but increasing chromosome damage has been recorded in the bone marrow and there is some suggestion of modifications to growth factor production.

In order to identify radiosensitive stages during development, experiments using in vitro alpha-irradiation with ^{210}Po were initiated. The radiosensitivity to ^{210}Po of the stromal microenvironment derived from bone marrow and liver of one-day old mice, adult bone marrow and fetal liver were compared. At concentrations of 5 and 10 Bq ml^{-1} of culture medium, cultures derived from adult and neonatal marrow showed a decreased haemopoietic activity compared to control cultures. At lower doses, the results were equivocal; in the majority of cases, no effect on CFU-GM yield was observed.

At UCM, studies of long-term radiation effects on murine stromal cell metabolism and granulocyte function have included *in utero* X-irradiation at 4 d or 13 d of gestation (1 Gy) and irradiation of adults (5 Gy). In adults, persistent increases in glucose-6-P-dehydrgenase (G6PD) activity were observed in granulocytes from LTBMCs at long times after irradiation. Characterization of the cytokine content of LTBMC supernatants demonstrated an overproduction of GM-CSF, IL-3 and IL-6. Increases in superoxide anion production, G6PD activity and protein levels were observed when granulocytes from control cultures were incubated with LTBMC supernatants from irradiated mice. Therefore, it was concluded that HGFs released

after irradiation are responsible for the enhancement observed in granulocyte function. In addition, a significant reduction in ATP levels was observed when control granulocytes were incubated with Fischer's medium compared with the incubations in LTBMC supernatants from irradiated mice, suggesting a protective effect on granulocyte apoptosis by the HGFs released. There was reduced cellularity in stromal adherent layers in LTBMCs but increased metabolism which could be involved in HGF production.

An increase in GM-CFC numbers and a decrease in LTBMC granulocyte production was observed at 12 months after *in utero* irradiation on d13 but not d4. However, at 3 months after birth the number of GM-CFCs was similar in both groups and controls. The results suggest that irradiation at d13 may result in a reduced number of pluripotent progenitor cells in the first weeks after birth and subsequent overproduction in the immediate committed progeny. The analysis of granulocytes from both treatments, suggest that the residual haemopoietic damage was not expressed as alterations in the function of these cells unlike the results obtained with 5 Gy irradiated adult mice. Characterization of LTBMC supernatants revealed GM-CSA in 13d and increases in IL-6 levels in both 4d and 13d.

Studies have been conducted at NRPB to compare the effects on haemopoietic progenitor cells of CBA/H mice following low dose x-irradiation (0.5 Gy) at day 7 or day 14 of gestation, and administration of ^{239}Pu on day 6 or 13. Femoral bone marrow samples from neonates and their mothers have been examined for the presence of stable cytogenetic abnormalities by G-band analysis. Although more time-consuming than the previously used technique of marker chromosome analysis, G-banding provides more definitive data. The results have shown a significant increase in stable chromosome abnormalities in x-ray and ^{239}Pu exposed mothers and offspring. There was no significant difference between the levels of damage in mothers and offspring in both cases. Unstable cytogenetic damage was observed in the marrow of ^{239}Pu exposed mothers but not offspring or x-irradiated animals. This unstable damage may be the result of persistent irradiation of haemopoietic cells from ^{239}Pu retained in bone.

A life-span effects study using Balb/c mice has been undertaken at VITO. Female mice were given ^{241}Am on day 14 of pregnancy (100, 500 or 1500 Bq g^{-1}) and offspring were separated from their mothers at birth. The adults showed a significantly shortened survival and increased incidence of osteosarcoma (to 40 - 50%). There was also a significant increase in osteosarcoma, all bone tumours, all sarcomas and all leukaemias in the offspring, although incidence appeared to be independent of dose. Estimates of the number of osteosarcoma per Gy varied between 0.01 and 0.2 for adults and 0.6 and 6 for offspring. Thus, it might be inferred that offspring were about 10 times more sensitive to osteosarcoma induction. Offspring had longer survival times than controls, possibly due to a lower incidence of early lung disease.

Head of project 1: Dr. Harrison

II. Objectives

To undertake the following studies:
1) measurements of natural alpha emitters and $^{239/240}$Pu in human fetal tissues;
2) studies of the transfer of radionuclides, principally ^{210}Po, ^{210}Pb, ^{141}Ce and ^{106}Ru, to the embryo and fetus in rodents;
3) studies with CEA on the transfer of ^{210}Po, ^{237}Np, ^{239}Pu and ^{241}Am to the baboon fetus;
4) autoradiographic studies of the distribution of ^{244}Pu and other nuclides in the rodent yolk sac;
5) the application of animal and human data in the estimation of doses to the human fetus and child after maternal intakes of radionuclides;
6) comparison of the effects of *in utero* exposure to ^{239}Pu or to external irradiation on murine haemopoietic development after birth, using clonogenic and cytogenetic techniques.

III. Progress achieved

III.I Human data

Measurements have been made of the concentration of Pu in human fetal tissue obtained from second trimester terminations carried out in the Oxford area and in Cumbria. These determinations have been undertaken using standard chemical separation techniques and sensitive detection systems, such as alpha spectrometry and thermal ionisation mass spectrometry. Typical fetal tissue concentrations of a few μBq kg^{-1} were recorded; placental concentrations were of the same order of magnitude. These concentrations are approximately two orders of magnitude lower than those typically found in tissues of adult members of the UK population. No differences were observed in concentrations of Pu in fetal tissue obtained from West Cumbria and Oxfordshire. Therefore, it would appear that the enhanced levels of Pu in the West Cumbrian environment, as a result of discharges from the Sellafield nuclear fuel reprocessing plant, do not result in a measurable increase in Pu concentrations in fetuses of pregnant females from this area.

Measurements have also been made of concentrations of naturally-occurring radionuclides in human fetal tissues and their distribution between fetus and placenta. Measurements of ^{210}Pb, ^{210}Po, ^{238}U and ^{232}Th in tissues from Oxfordshire are complete; analyses on samples from Cumbria are continuing.
Results obtained show similar concentrations of ^{210}Pb and ^{210}Po at 4 - 60 mBq kg^{-1} for fetal tissue and 8 to 140 mBq kg^{-1} for placental tissue. Corresponding values for ^{238}U and ^{232}Th were in the range 0.1 to 9 mBq kg^{-1}. The results do not show any correlation between ^{210}Po concentration and either geographical location or maternal age.

III.II Animal studies - biokinetics/dosimetry

Previous studies at NRPB on the transfer of the alpha-emitters, ^{210}Po, ^{238}Pu and ^{241}Am, to the embryo and fetus in rats and guinea pigs, together with the available human and primate data, have been used to estimate doses to haemopoietic tissue. The animal data suggest that in each case the main determinants of leukaemogenic risk from *in utero* exposure in humans are likely to

be irradiation of the yolk sac in early gestation and bone marrow during the fetal growth period. It was concluded that *in utero* doses to haemopoietic tissue from ^{210}Po will exceed those from ^{239}Pu and ^{241}Am at elevated environmental levels of actinide exposure (eg. near to Sellafield). However, important dosimetric uncertainties remained, including the distribution of dose within the irradiated tissues and species differences in transfer, particularly during the fetal growth period.

Figure 1 shows autoradiographs of the distribution of ^{210}Po in the embryo at the egg cylinder stage of embryonic development in the rat. From these early stages of development, ^{210}Po as well as ^{238}Pu have been shown to concentrated in the developing yolk sac. The distribution of alpha dose from ^{239}Pu within fetal tissues, and particularly the yolk sac, is being studied using the beta emitter, ^{241}Pu, to determine the cellular location of the element. Autoradiographs of ^{241}Pu in rat yolk sac during haemopoiesis (day 11) show concentration in the endodermal layer with less activity associated with the mesodermal layer where the primitive erythroblasts are formed (Figure 2). By late gestation, the endodermal layer has a fully developed columnar epithelium; autoradiographs show retention of ^{241}Pu in pinocytotic vesicles in the epithelial cells.

With CEA, the transfer of ^{210}Po, ^{239}Pu and other actinides to the fetus in late gestation has been studied in a primate species, the baboon. Results for two mothers and fetuses are complete, measurements having been made 7 days after intravenous injection at 5 months of gestation. The fetus accounted for about 4% of injected ^{239}Pu, 0.4% of ^{241}Am, and about 1% of ^{210}Po and ^{237}Np with corresponding retention in the placenta of 9%, 3%, 4% and 1%, respectively (Table 1). Results for ^{239}Pu and ^{210}Po show similar concentrations in fetal and maternal bone, contrary to previous results for rodents which showed lower transfer to the fetus. For ^{241}Am and ^{237}Np, concentrations in fetal bone were a factor of ten or more lower than in maternal bone. Concentrations in fetal liver were more than an order of magnitude lower than in maternal liver for all four nuclides.

Table 1. Retention of ^{210}Po, ^{237}Np, ^{239}Pu and ^{241}Am in the baboon fetus at 5 months of gestation after maternal administration as the citrates 7 days previously.

Tissue	% injected activity (% injected activity g^{-1})			
	^{210}Po	^{237}Np	^{239}Pu	^{241}Am
Placenta	4.0	0.9	9.1	2.5
Fetus (total)	0.8	1.3	3.8	0.35
Fetal femora	0.01 (0.001)	0.05 (0.006)	0.3 (0.03)	0.02 (0.002)
Fetal liver	0.09 (0.005)	0.01 (0.0007)	0.13 (0.007)	0.01 (0.0007)
Maternal femora	0.32 (0.002)	3.7 (0.02)	3.4 (0.02)	3.7 (0.02)
Maternal liver	16.6 (0.06)	3.1 (0.01)	29.6 (0.1)	27.5 (0.1)

Sources of ^{210}Po in the fetus, as well as transfer from current maternal intakes, include transfer after formation from ^{210}Pb accumulated in maternal skeleton and in-growth after transfer of ^{210}Pb. For ^{210}Pb administered to rats and guinea pigs during pregnancy, transfer was largely influenced by skeletal formation in the fetus and showed significant increases shortly before birth. Retention in the yolk sac was low throughout gestation. Retention in the rat neonate at birth after administration on day 19 of gestation was about 1% of admininistered activity per animal and for the guinea pig fetus in late gestation retention was about 3% of administered activity per fetus. The corresponding fetus/neonate : mother concentration (C_f/C_m) ratios were 0.6 in the rat and 0.8 in the guinea pig. Measurements have also been made of the transfer of ^{210}Po to the rat fetus after administration of ^{210}Pb to the mothers at 6 months prior to conception. Transfer of ^{210}Po in the yolk sac on day 13 of gestation was about an order of magnitude greater than for the parent ^{210}Pb, with low concentrations of both in the fetus. By birth, the relative concentrations of ^{210}Po in the yolk sac and placenta were about two orders of magnitude greater than the corresponding ^{210}Pb concentrations but transfer to the fetus was similar for the two nuclides. C_f/C_m ratios for both nuclides were less than 0.04 from day 13 of gestation onwards with values of 0.002 - 0.006 by birth.

Studies have been extended to other radionuclides, including ^{106}Ru and ^{141}Ce. The information obtained in these studies is being used in current ICRP work on the estimation of doses to the human fetus.

Ruthenium as ^{106}Ru in citrate solution was administered intravenously to rats at different stages of pregnancy and to guinea pigs either before conception or in late pregnancy. The results for rats showed that retention in the fetus measured at 3 days after administration increased from about 0.0002% of injected activity per fetus on day 13 of gestation to about 0.05% at birth (Table 2). The corresponding C_f/C_m concentration ratios were about 0.1 in each case. For transfer on day 13 of gestation, the retention of ^{106}Ru by each fetoplacental unit was about 0.2% of administered activity, with 40% of transferred activity in the decidua, 30% in the yolk sac, 30% in the placenta and 1% in the fetus. Concentrations were greatest in the yolk sac at about 1% g^{-1} compared with 0.01% g^{-1} in the fetus.

Table 2. The retention of ^{106}Ru, ^{141}Ce, ^{238}Pu and ^{241}Am in rat fetal tissues on day 13 of gestation after administration on day 10

Nuclide	% injected activity x10^3 (% g^{-1} x 10^3)			Cf/Cm
	Yolk sac	Placenta	Fetus	
^{106}Ru	7±0.3[a] (970±70)	7±0.4 (210±7)	0.2±0.01 (10±0.4)	0.1
^{141}Ce	0.07±0.001 (12±0.7)	0.4±0.02 (16±0.6)	0.02±0.002 (0.8±0.08)	0.004
^{238}Pu	4±0.8 (325±70)	5±0.5 (100±10)	0.04±0.01 (1.3±0.4)	0.003
^{241}Am	0.1±0.02 (8±2)	1±0.1 (26±1)	0.002±0.001 (0.1±0 2)	0.0002

[a] $\bar{x}$ ± SE, n=3-5; analysis of pooled tissues for 3-5 dams with 9 3±0.2 fetuses per dam.

Retention of ^{106}Ru in the guinea pig fetus in late gestation at 7 days after administration (days 50 - 57) was 0.2% injected activity per fetus corresponding to a C_f/C_m ratio of 0.2 (Table 3). Transfer to each fetoplacental unit was 2% of injected ^{106}Ru with 50% of transferred activity retained in the yolk sac, 35% in the placenta and 10% in the fetus. Total retention in three to four fetoplacental unit was therefore 6 - 8% compared with 14% in other tissues of the mother. Concentrations were greatest for the yolk sac at 0.3% g^{-1}, with values of 0.04% g^{-1} for the placenta and 0.004% g^{-1} for the fetus. For administration 4 weeks prior to conception, the level of ^{106}Ru retained in the fetus on day 57 of gestation was two orders of magnitude lower than after short-term administration with a C_f/C_m ratio of about 0.004.

Table 3. The retention of ^{106}Ru, ^{141}Ce, ^{238}Pu and ^{241}Am in guinea pig fetal tissues on day 57 of gestation after administration on day 50

	% injected activity x10^3 (% g^{-1} x 10^3)			
Nuclide	Yolk sac	Placenta	Fetus	Cf/Cm
^{106}Ru	280±60[a] (320±70)	200±20 (40±1)	200±20 (4±0.2)	0.2
^{141}Ce	12±1 (14±1)	310±30 (41±0.8)	50±5 (1±0.1)	0.01
^{238}Pu	100±30 (130±30)	630±50 (160±16)	280±50 (5±0.3)	0.06
^{241}Am	4±1 (5±2)	430±30 (110±40)	120±40 (2±0.7)	0.02

[a] $\bar{x}$ ± SE, n=3-5; analysis of pooled tissues for 3-5 dams with 3.6±0.1 fetuses per dam.

Cerium as ^{141}Ce chloride was administered to rats either before conception or at different stages during pregnancy and to guinea pigs in late gestation. Results for rats show that transfer measured 3 days after administration increased from about 3.10^{-5}% injected activity per fetus on day 13 to 0.001% on day 18 and 0.01% shortly before birth (Table 2). The corresponding C_f/C_m ratio increased from 0.004 to 0.02. For transfer measured on day 13, the retention of ^{141}Ce by each fetoplacental unit was about 0.001% of injected activity, with 60% of incorporated activity in the decidua, 7% in the yolk sac, 40% in the placenta and 2% in the fetus. Concentrations in the yolk sac and placenta were 0.01 - 0.02% g^{-1} compared with about 0.001% g^{-1} for the fetus. For transfer shortly before birth, the retention of ^{141}Ce by each fetoplacental unit was 0.2% of injected activity, with 33% of incorporated activity in the decidua, 36% in the yolk sac, 20% in the placenta and 9% in the fetus. Concentrations in the yolk sac, placenta and decidua were 0.5% g^{-1}, 0.1% g^{-1} and 0.4% g^{-1}, respectively, compared with 0.003% g^{-1} in the fetus.

Retention of ^{141}Ce in the guinea pig fetus in late gestation at 7 days after administration was about 0.05% administered activity per fetus, with a C_f/C_m ratio of 0.01 (Table 3). Retention in each fetoplacental unit was 0.4% of injected ^{141}Ce with 3% in the yolk sac, 80% in the placenta and 12% in the fetus.

Comparison of results for the transfer of ^{106}Ru and ^{141}Ce to the fetus in rats and guinea pigs with previous results for ^{238}Pu and ^{241}Am (Tables 2 and 3) showed that in each case the overall percentage transfer to the fetus increased with gestational age and generally the concentration in the fetus increased despite the increasing mass of the fetus. The greatest transfer values and C_f/C_m ratios were measured in guinea pigs in late gestation (day 57) during the period of fetal growth. Retention in the guinea pig fetus was in the range 0.05 - 0.3% injected activity per fetus for the four nuclides with C_f/C_m ratios in the order Ru > Pu > Am = Ce. Concentrations of ^{106}Ru and ^{238}Pu in the rat yolk sac during haemopoiesis were about two orders of magnitude greater than corresponding concentrations in the fetus; concentrations of ^{141}Ce and ^{241}Am were considerably lower. Following preconception administration, retained fetal activity levels in late gestation were typically two orders of magnitude lower for all four nuclides in rats and guinea pigs, compared to short-term administration during pregnancy. This applies to measurements of concentrations of ^{238}Pu, ^{241}Am and ^{106}Ru in the guinea pig fetus on day 57 after administration one month prior to conception and ^{141}Ce retention in the rat fetus on day 21 after administration one month prior to conception.

III.III Effects on Haemopoiesis

Studies at PICR (Contractor No.4: Dr. Lord) have shown long-term deficits in haemopoietic stem cells in the marrow of offspring of mice after *in utero* exposure to ^{239}Pu with important differences between exposures in early and late gestation. The aim of work at NRPB has been to compare effects on haemopoietic progenitor cells of CBA mice following *in utero* exposure to low dose x-irradiation (0.5 Gy) or administration of ^{239}Pu. Femoral bone marrow samples from neonates and their mothers were examined for the presence of stable cytogenetic abnormalities and concurrent clonogenic assays of primitive haemopoietic progenitor cells were also performed.

Following *in utero* x-irradiation (0.5 Gy) at day 7 or day 14 of gestation, a significant increase in stable chromosomal abnormalities was observed by G-banding in bone marrow samples from neonates, taken 2 to 4 weeks after birth. Applying the same technique to maternal marrow taken at the same time showed a similar level of stable chromosomal abnormalities, not significantly different from that in neonates. Previous marker chromosome results had indicated that, following *in utero* x-irradaition, neonates had a higher level of cytogenetic damage than their mothers. The G-banding technique can be taken to be more definitive, allowing the full range of radiation-induced chromosome changes to be identified. *In vitro* clonogenic assays of primitive haemopoietic progenitor cells gave results suggesting significant suppression of colony formation in marrow from neonates after irradiation on either day 7 or day 14. However, repeat assays showed variable levels of clonogenic activity in control un-irradiated marrow and theses studies were not pursued.

As with x-irradiation, *in utero* exposure to ^{239}Pu by intraperitoneal injection of pregnant females on day 6 or day 13 of pregnancy (3 kBq ^{239}Pu per mouse) led to a significant increase in stable chromosomal abnormalities, as assessed by G-banding, in both neonates and their mothers. Again there was no significant difference in the levels of stable cytogenetic damage observed in neonates and their mothers.

There were also no significant differences between the levels of stable cytogenetic damage seen in the *in utero* x-irradiated and ^{239}Pu exposed animals. In none of the individual animals

studied was there any evidence of preferential growth and clonal dominance of cytogenetically aberrant cells that might reflect the early phases of radiation-induced haemopoietic neoplasia.

In contrast to the stable cytogenetic damage seen following *in utero* irradiation, an increase in unstable cytogenetic damage was found in the bone marrow cell population of the ^{239}Pu exposed mothers but not in the offspring. This unstable damage may be the result of persistent irradiation of haemopoietic cells received from ^{239}Pu deposited in bones of the exposed mothers. In neonates, the level of ^{239}Pu retained in the rapidly growing skeleton was low and doses to marrow cells would be very low.

Studies of the distribution of ^{239}Pu in the mouse and calculation of doses to haemopoietic tissues are not yet complete. Available data indicate that the dose to maternal marrow may be about 0.1 - 0.5 Gy, delivered over the period from administration during pregnancy to 2 to 4 weeks after birth. For *in utero* exposure of the embryo and fetus doses to the haemopoietic tissue of the yolk sac and fetal liver are estimated from incomplete data to be around an order of magnitude lower than maternal bone marrow doses.

III.IV Publications

Bradley EG and Prosser SL (1993) Radionuclides in human fetal tissues. Radiol. Prot. Bull. **148**, 28-31.

Cox R, Kendall, GM, Muirhead, CR, Stradling, GN, Harrison, JD and Lloyd, DC (1993) Biomedical Effects Department Progress Report for the year to February 1993. NRPB-M422.

Cox, R, Muirhead, CR, Stradling, GN, Harrison, JD and Lloyd, DC (1994) Biomedical Effects Department Progress Report for the year to February 1994. NRPB-M491.

Cox, R, Muirhead, CR, Stradling, GN, Harrison, JD,
Lloyd, DC, Bouffler, SD and Silver, ARJ (1994) Biomedical Effects Department Progress Report for the year to February 1995. NRPB-M574.

Haines, JW, Harrison, JD, Pottinger, HE and Phipps, AW. (1995) Transfer of polonium to the embryo and fetus of rats and guinea pigs. Int. J. Radiat. Biol. **67**, 381-390.

Levack, V.M., Pottinger, H. and Harrison, J.D. (1995) The placental transfer of ruthenium in rats and guinea pigs. Int. J. Radiat. Biol. **66**, 809-814.

Levack, V.M., Pottinger, H., Ham, G.J. Harrison, J.D. and Pacquet, F. (1994) The fetal transfer of ruthenium, cerium, plutonium and americium. IRPA Regional Congress on Radiological Protection, Portsmouth, 1994. Nuclear Technology Publishing, pp. 161-164.

Morgan, A, Harrison, JD and Stather, JW (1992) Estimates of fetal doses from ^{239}Pu. Health Phys. **63**, 552-559.

Prosser, SL, McCarthy, WM and Lands, C. (1994) The plutonium content of human fetal tissue and implications for fetal dose. Radiat. Prot. Dosim. **55**, 1-5.

Figure 1a. A photographic emulsion autoradiograph of ^{210}Po in a 9.5 day rat egg cylinder showing greater concentration in cells of the developing yolk sac.

Figure 1b. ^{210}Po in a 9.5 day rat egg cylinder at higher magnification. A - ectoplacental cone, B - amniotic cavity, C - developing yolk sac, D - developing fetus, E - extraembryonic coelom, F - ectoplacental cavity

Figure 2. A photographic emulsion autoradiograph of 241Pu in a 9.5 day rat egg cylinder showing a higher concentration of plutonium tracks in the endodermal layer of the developing yolk sac. A - extraembryonic endodermal portion of the visceral yolk sac, B - extraembryonic mesoderm, C - extraembryonic ectoderm, D - developing fetus.

Figure 1a.

Figure 1b.

Figure 2

50 μm
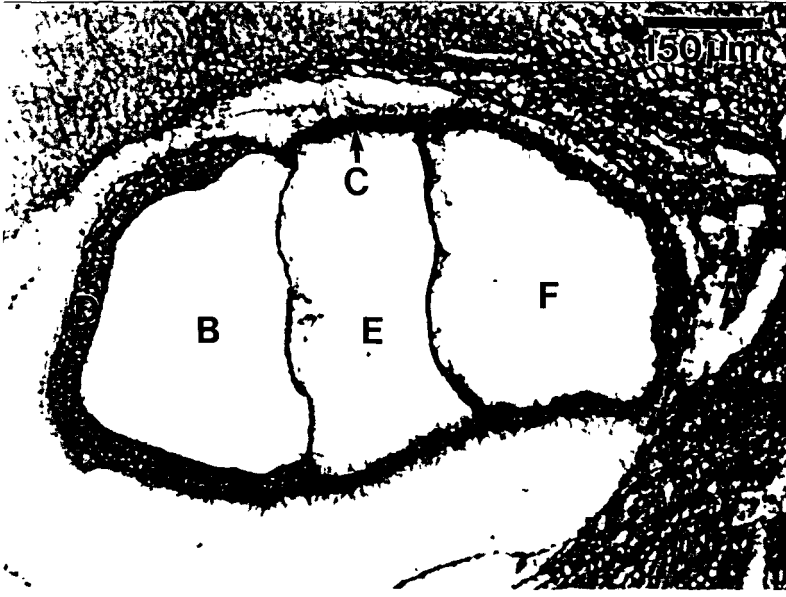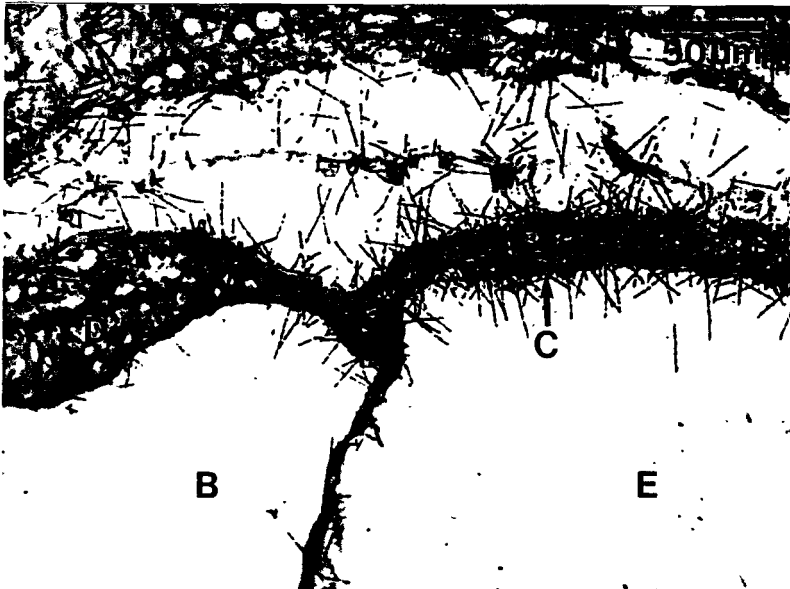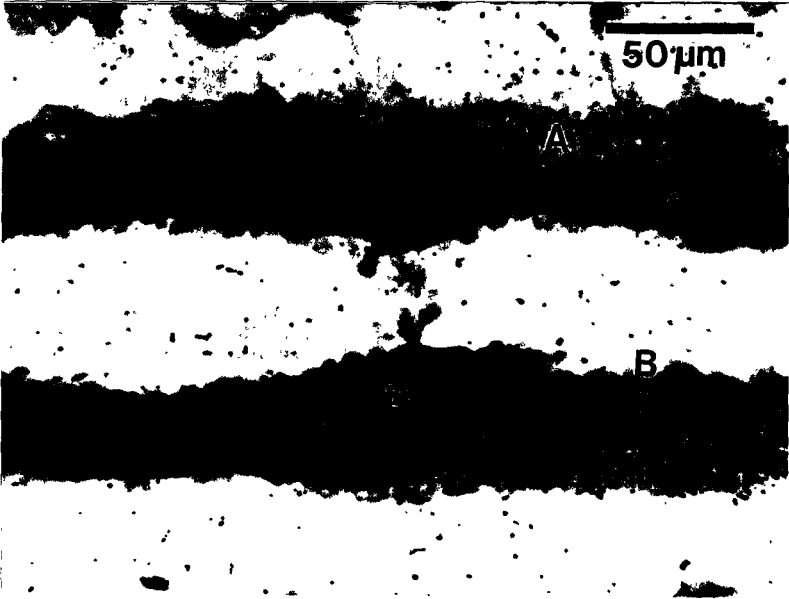
Head of project 2: Dr. Henshaw

II. Objectives

The research has investigated the transplacental transfer and fetal dosimetry of natural alpha-emitters. The first part of the programme concentrated on experimental measurements of natural alpha-activity in fetal organs using autopsy tissues from the Bristol area and from West Cumbria close to the site of the British Nuclear Fuels reprocessing plant at Sellafield. The latter part of the project was focused on more detailed investigation of the dose to target cells in the fetal skeleton.

III. Progress achieved

III.I. Fetal tissue measurements

Autopsy samples, 102 cases from Bristol and 15 from West Cumbria were obtained. Each case comprised small pieces, typically < 5g each, of fetal thymus, spleen, liver and vertebrae. Corresponding placenta samples were obtained in most cases. The samples were analysed by alpha-particle autoradiography using TASTRAK alpha-sensitive plastic. The plastic was pre-etched for background removal against which tissue samples were then loaded for up to two years. After storage the position of the tissue on the plastic was recorded photographically and the plastics were then processed by etching 6.25 M NaOH at 75° C for 6 hours. The autoradiographs were then scanned by eye under an optical microscope. In all, three person-years of microscope scanning were required to accumulate the track count data to date. This aspect of the work is ongoing and not all collected samples have yet been analysed.

The activity recorded on the plastic autoradiographs was in most cases close to detection threshold. By their nature, background levels on plastic autoradiographs vary from plastic to plastic. In this work background levels were estimated in two ways. One approach was to use control autoradiographs stored alongside the tissue loaded plastics. A second approach was developed from an understanding of the nature of the origin of the background tracks. Most background tracks are introduced into the body of the plastic during manufacture from radon emissions from trace ^{226}Ra in the casting glass. The level of these background tracks can be estimated from the number of larger tracks revealed by the pre-etch process. With these two approaches an average background level of 4.7 tracks cm^{-2} was determined, but with the ability to estimate the local background levels on each individual autoradiograph.

The frequency distribution of activities in fetal organs and placenta for the Bristol samples is given in figure 1
In the Bristol samples average activity concentrations in the fetal thymus, spleen and liver were 0.073 ± 0.018, 0.058 ± 0.013 and 0.021 ± 0.006 Bq kg^{-1} respectively. In placenta concentrations were within the noise fluctuations of background tracks and therefore below detection limit. Levels in fetal vertebrae were higher, and ranged up to 0.60 Bq kg^{-1}. Two cases (arrowed in figure 1) showed elevated levels in all fetal organs, although the reasons for this were not identified.

Levels in fetal tissues from West Cumbria, close to the BNFL reprocessing plant at Sellafield, were lower than in Bristol samples and mostly below detection limit. In all cases the dominant
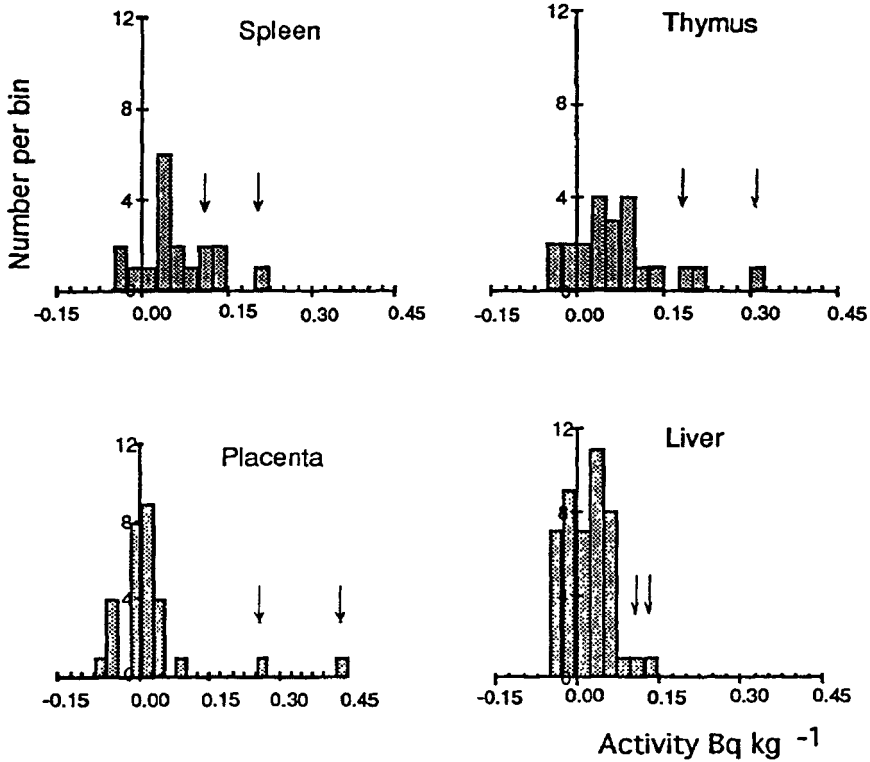
activity present could be attributed to naturally occurring ^{210}Pb-supported ^{210}Po. No evidence for the presence of plutonium was found.

In the fetal vertebrae activity concentration showed evidence of an increase with gestational age although, as indicated in figure 2, this was of borderline statistical significance at the 5% level. However, a separate measurement of the calcium concentration, illustrated in figure 3, showed stronger evidence of an increase with gestational age. On this basis we postulate that the ^{210}Pb-supported ^{210}Po concentration in the fetal skeleton is simply proportional to the calcium concentration.
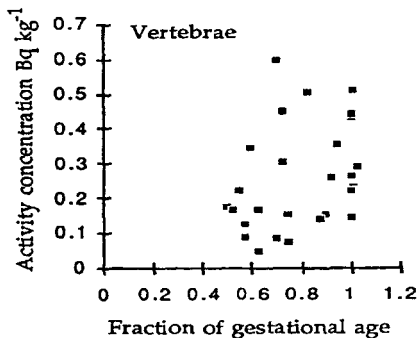
Fig 2
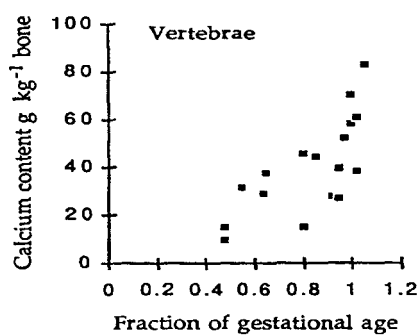
Fig 3

Table 1. Summary of activity concentrations in fetal organs

Fetal organ	Activity concentration Bq kg^{-1}/ ($\sigma/\sqrt{n}$)/number of cases
Thymus	0.073 (0.018) **22**
Spleen	0.058 (0.013) **18**
Liver	0.021 (0.006) **43**
Placenta	Not Detected
Vertebrae	<0.050 - 0.510 **23**

Correlation with the Severn Estuary

Bristol is situated close to the Severn Estuary which is known to contain high levels of industrial pollution including ^{210}Po (Hamilton and Clifton 1979, Hamilton et al 1979). The samples obtained from Bristol hospitals were from mothers who lived at various distances from the estuary. We therefore looked at the level of alpha-activity concentration in fetal vertebrae as a function of distance from the estuary.
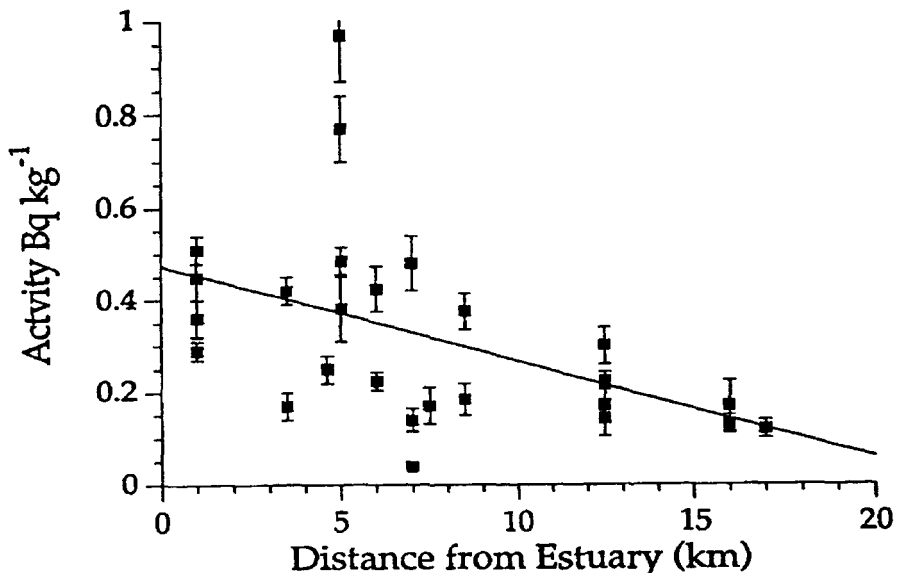
This revealed a statistically significant association of increased activity concentration close to the estuary. This is illustrated in figure 4. Outside the CEC project evidence is emerging of a similar correlation in both the deciduous and permanent teeth from local children.

Assessment of the level of direct human intake of ^{210}Pb from inhalation exposure dietary and other sources.

The above results, if confirmed in more detailed studies, imply enhanced intake of ^{210}Pb/^{210}Po by inhalation. We have examined the likely relative contribution from airborne and dietary intake of ^{210}Pb.

A summary of average levels of direct ^{210}Pb intake from the principle sources of air, drinking water and food was given by Jaworowski (1969), and is reproduced in table 2. In this highly generalised comparison, inhalation accounts for 20%, and the diet for 80% of ^{210}Pb entering the blood ("transfer compartment"). Of note is the high fraction of ^{210}Pb reaching the blood from air inhalation, compared with the other routes of intake.

Table 2. Average human intakes of ^{210}Pb from the principle environmental sources (from Jaworowski 1969).

Sources of ^{210}Pb	Daily intake of ^{210}Pb, Bq	Fraction of ^{210}Pb intake reaching the blood	^{210}Pb activity reaching the blood, Bq day^{-1}	% of ^{210}Pb reaching the blood from each source
Air	1.1×10^{-2}	0.29	3.2×10^{-3}	20
Drinking water	1.9×10^{-3}	0.08	1.5×10^{-4}	0.8
Food	0.19	0.08	$1\ 5 \times 10^{-2}$	80

These values are derived from a mean outdoor ^{210}Pb concentration of 5.2×10^{-4} Bq m^3, and an inhalation rate of 20 m^3 day^{-1} for the average person. The value for daily dietary intake of 0 18 Bq of ^{210}Pb was taken from a wide ranging study of the normal western diet (Globel, 1966). A study of the diet in the UK yielded an average ^{210}Pb daily dietary intake of 0 082 Bq (Smith-Briggs et al., 1986). Substituting this value for the UK, the relative amounts of ^{210}Pb reaching the blood from inhalation and diet would become 32% and 66% respectively.

Studies with stable lead have shown variability in intake and retention of Pb from inhalation, which could result in still higher relative contribution of ^{210}Pb from inhalation in some individuals. A significant variation has been demonstrated in the retention of inhaled Pb both between individuals, and under the influence of physical factors, which include aerosol particle size, ventilation rate and the solubility of the Pb compound within the aerosol (Taylor, 1986).

In summary, the higher fractional uptake to blood from inhalation intake of Pb, compared to dietary intake, means that while diet remains the predominant source of ^{210}Pb intake under average conditions, the contribution from inhaled ^{210}Pb could be significant in some cases. For the population of the UK, there is likely to be more potential variation in Pb and ^{210}Pb intake by inhalation than in dietary intake Within this variation it is quite possible that, in a significant subset of individuals, ^{210}Pb intakes to blood by inhalation could be comparable to and even predominate over dietary intakes.

III.II. Fetal dosimetry
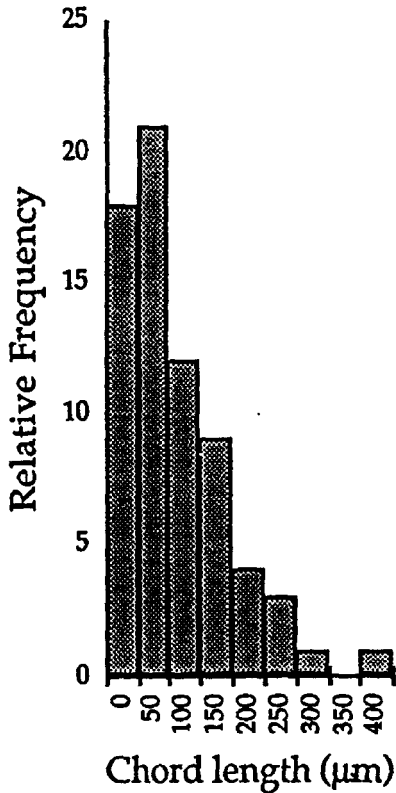
The latter part of the project was focused on more detailed investigation of the dose to target cells in the fetal skeleton. Work has started to determine the chord length distribution in fetal trabecular bone. Unlike the adult, the chord lengths in the fetus are comparatively small, in the range 30-400 μm, as illustrated in figure 5. This means that in some cases a substantial proportion of a given marrow space will lie within alpha-particle range of a bone surface. In the fetus, the trabecular bone structure exhibits differing degrees of calcification and this also varies with gestational age. X-ray micro probe analysis is being used as a technique to map local calcium concentration in fetal bone as an indicator of local $^{210}Pb/^{210}Po$ concentration.

Figure 5

Work has started to identify and measure the number and spatial distribution of potential target cells in the human fetus. The monoclonal antibody CD38 attaches to lymphoid stem cells, activated T-cells and plasma cells The two latter types of cells are produced during clonal proliferation of mature T- and B-cells during immune response. It is rare for them to be found in fetal bone marrow. CD34, is an antibody to a cell adhesion molecule present on stem cells and progenitor cells of the myeloid cell differentiation lines, but also on capillary endothelial cells and it consequently shows abundant staining in fetal bone marrow.

We are currently generating a series of slides stained using CD38 with a microwave antigen retrieval technique. We have prepared pairs of serial sections, one stained using CD38, the adjoining section stained using CD34. In this way, we may identify the CD34$^+$CD38$^+$ cells for study, which are the lymphoid stem cells. Although rare, any activated T-cells and plasma cells are identified as CD34$^-$CD38$^+$.

The histologically prepared slides are analysed by a colour image analysis system developed for this work in this laboratory. The image analysis software program has the capability of creating overlay images which identify haemopoietic tissue, fat cells (in the case of adult bone marrow), bone and stem cells. Further adjustments almost completed, will enable the program to calculate the alpha-radiation dose to haemopoietic tissue and to stem cells from ^{210}Pb-supported ^{210}Po at bone surfaces.

III.III. Publications

Henshaw D L, Allen J E, Keitch P A, Salmon P L and Oyedepo C *The microdistribution of ^{210}Po with respect to bone surfaces in adults, children and fetal tissues at natural exposure levels* In: "Health Effects of Internally Deposited Radionuclides: Emphasis on Radium and Thorium" (Eds: G van Kaick, A Karaoglou & A M Kellerer) Published by World Scientific EUR 15877 EN (1995) ISBN: 981-02-2015-4.

III.IV. References

Alexander F E, McKinney P A and Cartwright R A; *Leukaemia incidence, social class and estuaries: an ecological analysis.* Journal of Public Health Medicine 1991, Vol. 12 No. 2. 109-117.

Bradley E J and Prosser S L *Radiological Protection Bulletin* No. 148 (1993) 2 31. NRPB, Chilton, UK

Fews A P and Henshaw D L, *Alpha-particle autoradiography in CR-39: A technique for quantitative assessment of alpha-emitters in biological tissue.* Phys. Med. Biol. 28 (1983) 459-474.

Globel, B. (1966). Physicist Thesis, Institut fur Biophysiks der Universitat des Saarlandes, Saarbruken.

Gross, S. B. (1981). *Human oral and inhalation exposure to lead - Summary of the Kehoe Balance experiments* J Toxicol. & Environ. Health 8, 333-377.

Henshaw D L, Allen *J* E, Keitch P A and Randle P H *The spatial distribution of naturally occurring ^{210}Po and ^{226}Ra in children s teeth.* Int. J. Radiat Biol Vol 66, No. 6, 81-826, (1994)

Hamilton E I and Clifton R J. 1979. Isotopic abundance of lead in estuarine sediments, Swansea Bay, Bristol Channel *Estuarine and Coastal Marine Science* vol 8, pp271-78.

Hamilton E I, Watson P G, Cleary J J and Clifton R J. 1979. The Geochemistry of recent sediments of the Bristol Channel - Severn Estuary System. *Marine Geology* vol 31, pp139-182.

Henshaw D L, Eatough J P and Richardson R B, *"Radon: A causative factor in the induction of myeloid leukaemia and other cancers in adults and children?"* The Lancet **335** (1990)1008-1012.

Henshaw D L, Allen J E, Keitch P A, Salmon P L and Oyedepo C *The microdistribution of Po with respect to bone surfaces in adults, children and fetal tissues at natural exposure levels* In: "Health Effects of Internally Deposited Radionuclides: Emphasis on Radium and Thorium" (Eds: G van Kaick, A Karaoglou & A M Kellerer) Published by World Scientific EUR 15877 EN (1995) ISBN: 981-02-201-4.

Jaworowski, Z. (1969). Atomic Energy Rev. 7, 3-5.

Salmon P L, Henshaw D L, Allen J E, Keitch P A and Fews A P *TASTRAK spectroscopy of natural ^{210}Po alpha activity at bone surfaces: evidence for a concentrated surface deposit less than 2 µm deep.* Radiation Research Vol. 140, 63-71, (1994).

Smith-Briggs, J. L., Bradley E. J. and Potter M. D., (1986). Sci Tot. Environ. 54, pp. 127133.

Taylor, A. (1986). Rev. Environ. Health 6, (1-4), 1-83.

Head of project 3 :   Dr. R. Van Den Heuvel

II. Objectives

-      To determine radiosensitive stages during pre- and postnatal development for the response of both stromal and haemopoietic marrow cells. As well as maternal contamination (acute and chronic administration of ^{241}Am during pregnancy and/or lactation), attention was given to the effect of paternal contamination on the offspring. Effects of *in vitro* exposure of haemopoietic tissues at different developmental ages to alpha-particle irradiation from ^{210}Po was studied.
-      To search for sensitive parameters to detect radiation damage. Growth factor production in long-term haemopoietic cultures from mice after paternal and maternal contamination with ^{241}Am and in cultures exposed *in vitro* to ^{210}Po was studied.
-      To estimate the average radiation dose in the femur of the offspring by measuring the Am-uptake and metabolism studies following acute (single injection) and chronic (osmotic pump implantation) radiocontamination of the dams.
-      To analyse survival data from a large scale whole animal contamination experiment.

III. Progress achieved

III.I. *In vivo* effects of ^{241}Am on haemopoietic tissue

1. After various regimes of ^{241}Am administration in mice (paternal contamination pre-conception, protracted contamination during gestation, contamination at 14 days of gestation and/or during lactation), effects on the bone marrow were studied in the offspring (14 kBq ^{241}Am administered to the dams; 3,6,30 kBq to the fathers). Haemopoietic and stromal stem cell studies were continued in order to identify the most radiosensitive periods during development. To simulate the situation of continuous chronic intake of radionuclides from the environment, osmotic pumps containing ^{241}Am were implanted into pregnant mice for continuous exposure during organogenesis and the fetal period.

Effects on the haemopoietic and stromal cell population after maternal and paternal contamination were evaluated to 1 5 year after birth. After protracted contamination of pregnant mice between the 14-19th day of gestation no long-term effects on bone marrow cellularity, CFU-GM and CFU-f yield were seen in the offspring. The stromal microenvironment, as evaluated by its capacity to establish *in vitro* long-term bone marrow cultures, was damaged. The CFU-GM output in cultures from offspring of contaminated mice was decreased compared to the CFU-GM output in cultures from non-contaminated offspring. Female offspring after paternal contamination before conception (30 kBq to the father) showed no change in total bone marrow cellularity, an increase in CFU-GM numbers and a decreased CFU-f yield compared to offspring from non-contaminated fathers. Using long-term bone marrow cultures, damage to the stromal microenvironment was observed. Results showed that after both paternal and maternal contamination with ^{241}Am, there was persistent long term damage to the stromal microenvironment in the offspring.

Studies in which adult mice were exposed to ^{241}Am also showed that bone marrow cells can be considered as sensitive targets for chronic low level α-irradiation. Effects on haemopoietic and stromal cells were demonstrated after contamination of female mice with ^{241}Am at a dose level which causes bone tumours in more than 50% of the animals (50 Bq ^{241}Am/g mouse).

The radiation induced changes were persistent up to 20 months after ^{241}Am injection. Colony forming assays *in vitro* showed a decrease in the stromal stem cell (CFU-f) number as well as in the yield of granulocyte-macrophage progenitors (CFU-GM). The regulatory role of the stroma in haemopoiesis was assessed by measuring the CFU-GM production in long-term bone marrow cultures in which haemopoiesis is maintained *in vitro*. Results showed a decreased production of CFU-GM in cultures derived from exposed mice.

III.II. *In vitro* effects of ^{210}Po on haemopoietic tissue

2. In order to identify radiosensitive stages during development, experiments using *in vitro* alpha-irradiation with ^{210}Po were initiated. The sensitivity of different haemopoietic tissues (adult bone marrow, neonatal bone marrow, bone marrow and spleen from 18-day-old fetus and 15-day fetal liver) to *in vitro* α-irradiation from ^{210}Po was compared. Polonium-210 (0,27,55,110,220 Bq/ml) was added to the tissue culture medium of short-term clonal assays for haemopoietic progenitors (CFU-GM) and stromal stem cells (CFU-f). Results indicated no difference in radiosensitivity to α-particle irradiation of the fetal and neonatal tissues compared to adult bone marrow.

The radiosensitivity to ^{210}Po of the stromal microenvironment derived from bone marrow and liver of one-day-old mice, adult bone marrow and fetal liver was also compared. Long-term cultures from the respective organs were started. In order to assess the effects of α-irradiation on the buildup of the stromal microenvironment, half of the cultures were initiated in the presence of ^{210}Po and were exposed during the first 3 weeks of culture. The other half of the cultures were initiated in the absence of ^{210}Po. Haemopoietic stem cells were seeded onto the stromal layer and the haemopoietic capacity of the microenvironment was evaluated by measuring the CFU-GM yield With ^{210}Po concentrations of 5 and 10 Bq per ml tissue culture medium, cultures derived from adult and neonatal bone marrow showed a decreased haemopoietic activity compared to control cultures. At lower concentrations (between 0.5 and 5 Bq ^{210}Po/ml) results were somewhat equivocal. In the majority of the cases no effects on CFU-GM yield were seen. In several experiments, decreases and sometimes increases in the CFU-GM yield were detected. The different results were probably due to dose effects. We have demonstrated that ^{210}Po concentrates *in vitro* in the extracellular matrix and in the cells. By this the local dose to the target cells can differ between experiments and is a variable which we do not have under control.

III.III. Effects of ^{210}Po and ^{241}Am on haemopoietic growth factor production

3 Pregnant Balb/c mice were contaminated with ^{241}Am (14 kBq per mouse) by different procedures (acute and chronic administration of ^{241}Am) and male mice were contaminated before conception (3,6,30 kBq per mouse). At different time points after birth, long-term bone marrow cultures were initiated from the offspring after maternal or paternal exposure. Cell-free supernatants from these cultures and from cultures exposed *in vitro* to ^{210}Po were collected. With the aim of characterising these conditioned media, assays to detect haemopoietic growth factors were performed

GM/CSF (granulocyte-macrophage Colony Stimulating Factor) was measured by assay of CFU-GM growth. None of the supernatants were able to stimulate CFU-GM growth. TNF-α (Tumor Necrosis Factor alpha) was measured by bioassay using WEHI fibrosarcoma cells and TGF-ß (Transforming Growth Factor beta) was measured by a bioassay using the mink lung

epithelial cell line, Mv1Lu. Differences in TNF-α and TGF-ß production were only noticed in cultures from mice after paternal contamination with 30 kBq compared to cultures from control mice. At the lower dose levels no differences in growth factor production were seen. Interleukin-1 was measured by ELISA and could not be demonstrated in the conditioned media.

III.IV. Estimates of doses from ^{241}Am

4. Pregnant BALB/c mice and age and sex matched nulliparous contols were contaminated with ^{241}Am (13 kBq per mouse) by two different procedures : (1) a single intraperitoneal injection at the 14th day of gestation, and (2) continuous administration between the 7th and 14th day of gestation and between the 14th and 19th day of gestation. Continuous administration was achieved by implanting osmotic pumps filled with ^{241}Am which released the ^{241}Am activity at a constant rate Five days after the termination of contamination, ^{241}Am incorporation was measured in the tissues of adults and in the liver and the femur of newborn and one-month-old mice. Pregnancy results in higher ^{241}Am concentrations in bone but lower concentrations in the liver of the mothers. Protracted administration of ^{241}Am compared to a single injection resulted in a lower concentration of ^{241}Am in the livers of pregnant mice, their nulliparous controls and from newborn mice. The higher ^{241}Am concentration in the femur at birth after protracted exposure after 14 days of gestation compared to protracted exposure before 14 days of gestation could reflect the increased placental transfer of ^{241}Am with advancing gestational age. Radiation doses to the femur were estimated as between 4 and 20 mGy. Changes in the number of haemopoietic progenitor cells (CFU-GM) and a disturbance of the stromal haemopoietic micro-environment were noticed at these dose levels in all groups until at least 6 months after birth.

III.V. Life-time studies of tumour induction by ^{241}Am

5. Survival data from a large scale whole animal contamination experiment were analysed. Pregnant Balb/c mice were given 100, 500 or 1500 Bq/g of ^{241}Am/g at day 14 of pregnancy. The offspring were separated from the mothers at birth and followed until death. Survival and tumour occurrence were studied In addition, adult females and males were also studied for the effects of ^{241}Am following treatment with 45-213 Bq/g.

Methods

For the studies on adults, male and female mice respectively of 11 or 14 weeks age were injected intraperitoneally with different doses of the ^{241}Am solution as indicated in table 1. For the studies on the offspring, 12 week old pregnant mice were injected intravenously on day 14 of gestation The mice were housed individually until delivery on day 19 of gestation. The day of birth was defined as day zero Litters were reared by non-contaminated dams. Sham-injected pregnant mice with litters exchanged after birth were used as controls. All pups were weaned at an age of 21 days. No difference in litter size was noted between contaminated and non-contaminated mothers at the doses used.

The mice were observed daily until death when radiography of the skeleton and autopsy were performed Routine histological analysis was carried out on liver, lung, both kidneys, spleen, abdominal lymph nodes, adrenals, the left femur, female sex organs or testes and the gastrointestinal tract Other tissues were analysed only when they appeared abnormal on

autopsy. The diseases observed were classified in the following way : malignant bone tumors (osteosarcoma), benign bone tumors, liver tumors, lung tumors, myeloid leukaemia, adrenal gland carcinoma, deterministic lung diseases. In addition, all malignant tumors, all bone tumors (osteosarcoma, skeletal fibrosarcoma, angiosarcoma, fibromyosarcoma and benign bone tumors), all sarcomas and all leukemias (myeloid leukaemia, thymoma, reticulosarcoma) were pooled for analysis.

Times of survival and times of death from different causes in a group were evaluated by the Kaplan-Meier procedure. Differences between groups were assessed for causes of death by means of the Cox-Mantel log-rank (Mantel 1966, Cox 1972), the Breslow (Gart *et al.* 1986) (Breslow 1970) and the Peto tests. Possible causes of death were analysed by the Peto test. For the Cox and the Breslow tests, a share-ware programme from the Ludwig institute (KMSURV) was used. The other programmes used were developed or modified in our laboratory.

Results

Table 1 presents the Kaplan-Meier analysis of the data from the experiments on adult mice with the total number of animals and the number of animals with histo-pathological diagnoses in the first row. The following rows show the product limit estimates for mean times of survival and their standard errors with respect to all causes of death and to specific diseases causing death as well as the percentages of animals dying from this cause. It should be pointed out that the cut-off chosen for the determination of the mean survival times in all groups and for all diseases was 1200, i.e. the survival time of the animal with the longest life span among all groups studied. This value has been chosen in preference to a cut-off of the animal dying at the latest time in a given group in order to make comparison of mean survival times between groups more meaningful. However, this procedure and the fact that times of death in several groups with relatively small incidences of a disease are spread over a considerable part of the lifespan can result in the apparent incongruity that mean survial times from diseases are longer than the total mean survival time.

Table 1 shows a significantly ($p < 10^{-3}$) shortened survival at all ^{241}Am doses with only small, although significant, differences among the treated animals; this results in a significant deviation from linearity (Peto test). As expected, osteosarcomas, all bone tumors and all sarcomas increase significantly ($p < 10^{-3}$) with dose but again, as for survival, the dose response deviates significantly from linearity. Indeed, doses in this experiment have been rather high, apparently within the region of saturation, in order to obtain sufficient exposure of the offspring. Malignant tumours in the exposed animals increase at the lower dose then decrease at higher ones. This causes a significant Cox and Breslow tests ($p < 10^{-3}$) and Peto test ($p < 10^{-3}$). Adrenal carcinomas increase significantly at the lowest dose resulting in positive Cox and Breslow tests ($p < 10^{-4}$) and a doubtful Peto test (only non-linearity significant). Although, this appears to suggest a reduction in leukamias after treatment, this is not significant in any statistical test used and is attributable to shortened survival of all treated groups. It should be pointed out that the results of the different statistical tests used do not always agree, especially if the difference between groups occurred during the early period, and/or the disease studied occurred at the same time earlier and less often. This is due to the fact that the weight given to the different periods of life differs among the tests (Gart *et al.* 1986).

The adult males have a significantly shortened survival and increased incidence of osteosarcoma, all bone tumors and all sarcomas. Deterministic lung diseases occur significantly earlier. A statistical comparison between males and females with respect to osteosarcoma is not feasible although there is a suggestion that males are more resistant to osteosarcoma induction by ^{241}Am than females.

When considering the Kaplan-Meier survival data (table 2) and survival curves it appears that the animals whose mother were contaminated survive longer but the tests diverge (males : Breslow and Cox tests p < 5 10^{-3} with the Peto test only suggesting non linearity; females : Cox and Peto test non-significant, Breslow test p = 0 05). The reason for this abnormality could be the larger percentage of controls dying early from deterministic lung disease (significance tests similar as for survival). The significance tests also tend to be uneven for osteosarcoma, all bone tumors and all sarcomas. Thus in both males and females, the Cox and Breslow tests are highly significant for osteosarcoma (Cox p = 0.004, Breslow p = 0.002 for females, and p = 0.002 and p = 0.001 respectively for males) whereas the Peto test, at the most, suggests non-linearity (p = 0 015 in males, 0.06 in females). P values for all bone tumors and for all sarcomas are similar to those for osteosarcoma. Combining female and male groups with the same doses does not much improve the significance values since the tumors are not in the same dose group in both sexes; thus, only the tendency to non-linearity is underligned. All malignant tumors in males also show significant differences between groups (Cox, Breslow p < 10^{-2}, with significant p = 0.01 non linearity from the Peto test) Female display only some deviation from non linearity (p = 0.02) for malignant tumors with the other tests being not significant. All leukaemias show significant differences in males (Cox and Breslow tests p < 10^{-2} with significant non linearity from the Peto test) and females (Cox, Breslow and Peto tests p between 0.01 and 0.05).

Discussion

As expected, adult mice treated with ^{241}Am have a shortened survival and an increased incidence of osteosarcoma (all bone tumours and all sarcomas) from the lowest dose (0.8 kBq/mouse). It is more difficult to appraise the situation in the offspring, there appears to be less early mortality due to fewer deterministic lung diseases in the offspring of ^{241}Am treated animals. For osteosarcoma, a strong indication, supported by several, but not all, significance tests, exists that this disease is more frequent in the offspring of mice treated with ^{241}Am on day 14 of pregnancy although no significant relation exists between the dose applied and the incidence of osteosarcoma. The data also suggest an effect of the ^{241}Am treatment with respect to the incidence of leukaemia.

A comparison of effects in adult and foetal mice is difficult in view of the uncertainties of dose distribution on a microscopic scale and their changes with time after injection, the lack of an overlap of the doses in both sets of experiments and the non-linearity of the dose-effect relationships. Nevertheless, if such a comparison is carried out on the basis of calculated cumulative doses to the femur, the offspring appear to be more sensitive to the induction of osteosarcoma. The number of osteosarcoma per mouse Gy varied for contamination of adult mice between 0.2 and 0 01. The number of osteosarcoma per Gy in the offspring varied between 0 6 and 7 with no significant differences between sexes However, it is not clear from the data whether the dose effect curve in the offspring had already attained a point of saturation.

In summary, adults treated with ^{241}Am showed significantly shortened survival and increased incidence of osteosarcoma (to 40-50%). The data also suggest that female mice are more susceptible to induction of osteosarcoma than male mice. There was also a significant increase in osteosarcoma, all bone tumours, all sarcomas and all leukemias in the offspring from the contaminated mothers, although this appeared to occur independently of dose. Calculations of the numbers of osteosarcomas induced per Gy varied for contamination of adult mice between 0.2 and 0.01 and for the offspring between 6 and 0.6. Thus, offspring seemed to be about 10 times more at risk if osteosarcomas induced per mouse Gy are compared. Surprisingly, offspring from mothers treated with ^{241}Am displayed a longer survival time than controls, possibly due to fewer deterministic lung diseases appearing early in life.

Table 1 . Percentage of mice dying from a disease and Kaplan-Meier estimates of survival for the three experiments on adult animals treated with ^{241}Am.

		Female adults				Male adults	
		0 Bq/g 0 kBq/mouse	45 Bq/g 0.8 kBq/mouse	90 Bq/g 16 kBq/mouse	213 Bq/g 3.8 kBq/mouse	0 Bq/g 0 kBq/mouse	103 Bq/g 2.5 kBq/mouse
No animals		31 (29)*	46 (43)	15 (14)	62 (59)	30 (28)	59 (58)
Survival days	Mean survival time	794 ± 38	595 ± 21	479 ± 36	463 ± 11	780 ± 41	471 ± 12
Osteosarcoma	Mean survival time	0	773 ± 50	758 ± 43	547 ± 17	0	1006 ± 94
	incidence %		44	43	39		8 6
All bone tumours	Mean survival time	1079	773 ± 50	758 ± 120	547 ± 17	0	1006 ± 94
	incidence %	3 4	44	43	39		8.6
Lung carcinoma	Mean survival time	1083 ± 52	975 ± 112	0	0	985 ± 52	1116 ± 82
	incidence %	17	9 3			36	3 4
Adrenal carcinoma	Mean survival time	0	1074 ± 53	0	0	0	0
	incidence %		6.7				
All malignant tumous	Mean survival time	913 ± 30	658 ± 28	759 ± 122	544 ± 16	891 ± 40	972 ± 88
	incidence %	58	72	43	41	61	15
All leukemias	Mean survival time	1127 ± 46	1087 ± 88	0	1159	1016 ± 40	1171
	incidence %	31	6.7		1.7	21.4	17
All sarcomas	Mean survival time	994 ± 34	766 ± 49	758 ± 122	547 ± 17	0	993 ± 92
	incidence %	10	46	43	39		10
Deterministic lung diseases	Mean survival time	927 ± 41	880 ± 55	669 ± 132	731 ± 66	953 ± 59	499 ± 13
	incidence %	10	23	43	44	39	71

Kaplan Meier estimates were calculated for a cut-off of 1200 days.

* with histological diagnoses

Table 2 : Percentage of mice dying from a disease and Kaplan-Meier estimates of survival for the experiments on mice treated *in utero* with 241 Am.

		Female offspring				Male offspring			
		0 Bq/g 0 kBq/mouse	100 Bq/g 2.85 kBq/mouse	500 Bq/g 13.68 kBq/mouse	1500 Bq/g 40.94 kBq/mouse	0 Bq/g 0 kBq/mouse	100 Bq/g 2.85 kBq/mouse	500 Bq/g 13.68 kBq/mouse	1500 Bq/g 40.94 kBq/mouse
No animals		50 (46)*	46 (45)	45 (41)	56 (49)	91 (81)	51 (46)	59 (55)	81 (77)
Survival days	Mean survival time	692 ± 44	734 ± 39	756 ± 44	726 ± 38	701 ± 41	798 ± 41	743 ± 43	797 ± 38
Osteosarcoma	Mean survival time incidence %	0	1163 ± 36 44	1178 24	1170 ± 28 41	0	0	1188 ± 21 18	0
All bone tumours	Mean survival time incidence %	0	1163 ± 36 44	1189 24	1178 ± 28 41	1185 ± 15 2.5	1188 22	1188 ± 21 18	0
Lung carcinoma	Mean survival time incidence %	1072 ± 39 15	1064 ± 48 16	1095 ± 37 15	1088 ± 40 14	1076 ± 23 27	1067 ± 34 26	1041 ± 32 25	1055 ± 24 32
Adrenal carcinoma	Mean survival time incidence %	0	1179 2.2	0	1168 ± 30 4.1	1178 ± 14 3.7	1187 2.2	0	0
All malignant tumours	Mean survival time incidence %	913 ± 27 54	840 ± 29 71	928 ± 32 58	888 ± 31 65	984 ± 23 57	965 ± 27 72	936 ± 27 64	979 ± 25 65
All leukemias	Mean survival time incidence %	968 ± 30 35	923 ± 35 38	1043 ± 41 27	978 ± 30 39	1108 ± 24 18	1076 ± 23 30	1034 ± 26 31	1075 ± 19 29
All sarcomas	Mean survival time incidence %	1182 2.2	1082 ± 47 11	1125 ± 37 9.8	1138 ± 33 8.2	1172 ± 15 4.9	1136 ± 22 11	1150 ± 26 7.3	1192 1.3
Deterministic lung diseases	Mean survival time incidence %	880 ± 60 41	925 ± 58 29	984 ± 54 27	961 ± 54 29	912 ± 47 38	1010 ± 52 26	958 ± 52 31	983 ± 43 31

Kaplan Meier estimates were calculated for a cut-off of 1200 days.

* with histological diagnoses

Publications

Van Den Heuvel R., Vander Plaetse F., Leppens H. and Schoeters G.
^{241}Am distribution and retention in pregnant mice, in their offspring and in non-pregnant mice : comparisons between continuous Am administration and single injection.
Radiat. Prot. Dosim. (1992), 41, 137-142

Van Den Heuvel R.
Effects on the bone marrow in offspring of ^{241}Am contaminated mice.
Eulep Newsletter (1992), 67, 5.

Van Den Heuvel R.
Effects of radioactive irradiationn on fetal and young organism.
Annalen van de Belgische Vereniging voor stralingsbescherming (1992), 17, 193-212.

Schoeters G.E.R., Vander Plaetse F., Leppens H. Van Den Heuvel R.
Response of murine stromal bone marrow cultures to α-particle irradiation *in vivo* and *in vitro* at osteosarcomogenic α-radiation doses.
Toxic In Vitro (1993), 7(4), 547-550.

Van Den Heuvel R., Schoeters G., Leppens H.
Bone marrow damage after α-exposure of mice to ^{241}Am is assessed using *in vitro* cell culture techniques.
Toxicology letters (1994), 74(1), 89.

Van Den Heuvel R., Leppens H., Geyzen K., Schoeters G.
Growth factor production in cultures from murine pre- and postnatal haemopoietic organs.
Journal of Experimental & Clinical Cancer Research (1995) 14 (1), 60-62.

Van Den Heuvel R , Gerber G.B., Leppens H., Vander Plaetse F., Schoeters G.
Long-term effects on tumour incidence and survival from ^{241}Am exposure of Balb/c mice *in utero* and during adulthood.
Int. J. Radiat. Biol. (1995) in press

Head of project 4:   Dr. Lord

II. Objectives

1. To study the relative effects of ^{239}Pu, injected at different stages of embryonic, foetal and neonatal development, on long-term haemopoiesis both at stem cell and peripheral blood levels.

2. To estimate RBE of ^{239}Pu injected during foetal development, in long-term haemopoiesis.

3. To study the contribution of the haemopoietic regulatory micro environment to the above effects.

4. To study the effects of preconceptual paternal ^{239}Pu contamination on haemopoiesis: progenitor cell numbers and cytogenetic disturbances.

5. As a preliminary to the assessment of dose distribution from bone incorporated, α-emitting radionuclides among potential leukaemogenic and osteosarcomogenic target cells:- to define the spatial distributions of such cells in the bone marrow.

III. Progress achieved

III.I. <u>Plutonium-239 Contamination during Development</u>

Plutonium-239 has been injected into pregnant mice at 4, 13, 17 d gestation or weanling offspring (30 Bq g^{-1}) or neonatal offspring (10 Bq per mouse). This latter dose was based on the amount of plutonium transferred, by birth, following mid-term contamination with 30 Bq g^{-1}. Measurements of ^{239}Pu incorporation into the various tissues of the foetus and neonate were made at sequential times following contamination. Plutonium-239 was shown to concentrate primarily in the foetal liver (3.6% of injected activity - IA per gm) and ultimately in the skeleton (0.63% IA.g^{-1}), though significant quantities also appeared transiently in the intestine and kidneys. Table 1 shows primary uptake figures for contamination at 13 d gestation.

Calculated from the incorporation data, it is clear that retention of plutonium varies widely, depending on the time of contamination (Table 2). At 4 wks after birth, the concentration in the liver varies by a factor of 2500 and in the femur by 500, the neonate appearing to retain the highest concentration. Nevertheless, damage to the long-term post-natal haemopoietic stem cell (CFU-S) population growth is similar: eg. 4 d v 13 d contamination (Figure 1) despite a hundred fold difference in incorporation levels at birth (Table 3). Contamination later than 13 d results in slightly less haemopoietic damage despite the higher uptake and retention.

Table 1:   Transfer of ^{239}Pu from Maternal to Foetal and Neonatal Tissues

Day of Assay	% Injected Activity (% IA)			
	Placenta	**Membranes**	**Liver**	**Femur**
14 d gest.	1.03 (8)	0.89 (37)	0.03 (1.3)	-
16 d gest.	0.83 (7)	1.33 (51)	0.13 (2.4)	-
1 d post-partum	-	-	0.18 (3.6)	0.01 (0.6)
9 d post-partum	-	-	0.20 (1.9)	0.007 (0.4)

Figures in parentheses are tissue concentrations (% IA.g^{-1})

Table 2: **Relative Tissue Concentration of ^{239}Pu Retention Following Contamination at Different Stages of Haemopoiesis**

	Time of Contamination				
	4 d gest.	**13 d gest.**	**17 d gest.**	**Neonate**	**Weanling**
Liver[*]	1	10	20	2500	500
Femur[**]	1	4	40	510	430

[*] At 4 wks old. The factor 10 at 13 d gestation is equivalent to 1.8 Bq g^{-1}.

[**] Average from 4 to 55 wks old. The factor 4 at 13 d gestation is equivalent to 1.5 Bq g^{-1}.

Table 3: **^{239}Pu in Day-Old Neonate Compared to that in its Mother**

	Time of Contamination (d. gestation)		
	4	**13**	**17**
Concentration (Bq g^{-1})	0.06	5.2	5.3[*]
% Concentration in Mother	0.2	17.4	17.8

[*] This concentration increases slightly due to additional uptake via lactation in the weaning period.
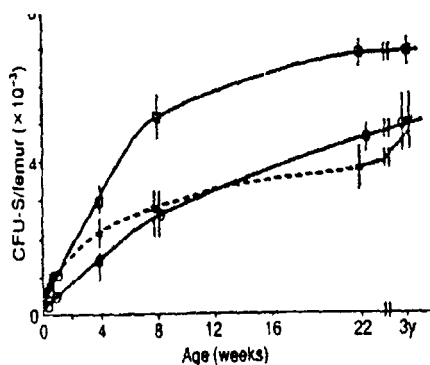
Growth of CFU-S following Pu-239 in utero
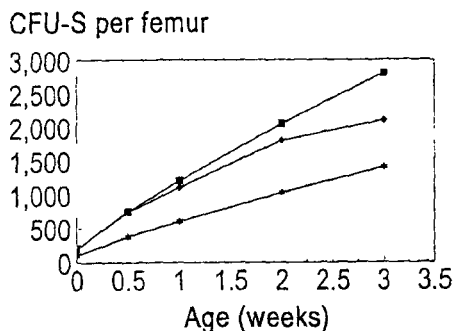
Figure 1

Figure 2

Figure 1: Growth of the femoral CFU-S population after birth in normal mice (□) and in offspring of mice contaminated with ^{239}Pu at 4 d gestation (○) or 13 d gestation (*).

Figure 2: Growth of the femoral CFU-S population after birth in normal mice (■) and in offspring of mice contaminated with ^{239}Pu at 4 d gestation (*) or 13 d gestation (♦) .

A more detailed look at the early growth pattern for CFU-S shows (Figure 2) that following contamination at 13 d, the animal is born with a normal complement of stem cells which amplify their population at a slower rate than normal. By contrast, 4 d contamination - despite its lower incorporation, radiation dose is likely to be higher due to more localised concentrations - results in birth with a reduced (50%) number of stem cells which grow at a normal rate.

This implies different mechanisms of damage induction which were shown to hinge on the balance of cell/regulatory micro environmental damage. Measurement of micro environmental damage in terms of generating an osseous capsule containing marrow from marrow implanted in the kidney capsule showed (Table 4) that following contamination at 4 d gestation, the ossicle was normal but damage caused at 13 d contamination was such that the micro environment of the capsule could support only 50% of normal haemopoietic stem cell growth. This means that mid-term contamination results in damage to the developing micro environment which ultimately limits the growth rate of a (probably) largely undamaged stem cell population. By contrast, the lower incorporation of plutonium is sufficient (perhaps by virtue of high local concentrations) to damage the embryonic stem cell but not to damage the later developing micro environment.

Table 4: Quality of the Haemopoietic Micro environment in Mice Contaminated with ^{239}Pu *In Utero*

Donor Marrow		CFU-S/Renal Ossicle
Age (Weeks)	^{239}Pu (d. gestation)	
4	Control	2350
	4	2470
4	Control	1380
	4	620
8	Control	4620
	13	1930

In all cases, the reduced stem cell numbers were compensated by higher stem cell proliferation rates and increased numbers of their progeny, the lineage committed progenitor cells. This process of adaptation resulted in a normal output of mature functional cells to the peripheral blood and the animals remained ostensibly healthy.

Complementary to these studies on the micro environment were experiments carried out in conjunction with Contractor No.6, Dr C. Tejero. These studies involved measurement of functional activity of granulocytes produced in the long-term after various radiological procedures including ^{239}Pu contamination at 4 and 13 d gestation and of repeated doses of external radiation. It was demonstrated that superoxide anion production by granulocytes was significantly enhanced in all cases where micro environmental damage had previously been demonstrated. For example, Table 5 shows the superoxide anion production in granulocytes from 2½ year old mice whose mothers had been treated with ^{239}Pu. Coincident with the deficient micro environment shown above, production in the granulocytes from mice treated at 13 d gestation was increased more than 2 fold. Measurements on micro environmental control and growth factor production confirmed this correlation.

Table 5: **Superoxide Anion Production in Granulocytes Obtained from LTBMC from 2.5 yr Old Offspring of Mice Treated with ^{239}Pu**

	nmol O_2^-/min/10^6 cells
Control	2.0 ± 0.1
^{239}Pu @ 4 d g	1.7 ± 0.1
^{239}Pu @ 13 d g	4.3 ± 0.4 (p < 0.01)

It is concluded from this phase of work that there is gross variation in the sensitivity of developing haemopoietic tissue - at the stem cell level - to ^{239}Pu contamination delivered at different stages of the development process. This variation should clearly be taken into account in any dosimetric and risk models developed.

III.II. RBE for ^{239}Pu in Haemopoiesis
In view of long-term damage to haemopoiesis as a result of ^{229}Pu contamination *in utero*, a measure of effectiveness on the tissue was considered more appropriate than one of direct kill on specific cells (ie. stem cells). One specific disturbance recorded in the tissue, and reflecting the dynamic and kinetic performance of the tissue, was of an altered spatial distribution of the stem cells in the marrow of adult mice which had been contaminated *in utero* (Figure 3). In these mice, the normal high concentration of CFU-S close to the bone surface was abrogated and this represented the 40% deficit in CFU-S numbers recorded in '1' above
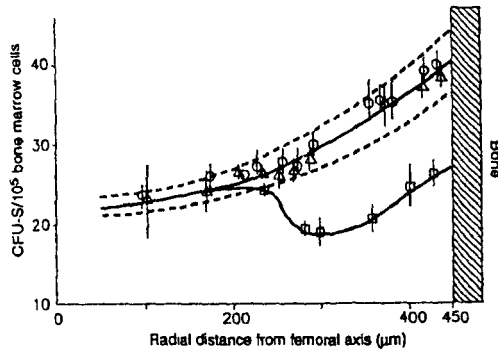
Figure 3: Distribution of CFU-S across the radial axis of a control mouse femur. The position of the ordinate represents the central longitudinal axis of the femur. CFU-S$_8$ (O) and CFU-S$_{12}$ (Δ) in control mice: mean CFU-S$_8$ and CFU-S$_{11}$ ($\square$) in offspring of mice injected with 30 Bq g^{-1} ^{239}Pu at day 13 of gestation. Concentrations of CFU-S$_8$ and CFU-S$_{12}$ were not significantly different, and the mean curve ($\pm$ standard deviation) for normal marrow corresponds to a regression line fitting mean CFU-S per 10^5 cells = 21.86 + 0.94 r^2 where r = distance from axis in μm x 10^{-2}. The ^{239}Pu data are similarly the mean for 8- and 11-day CFU-S obtained in three series of experiments.

From incorporation data an average radiation dose to the foetal liver of approximately 10-14 mGy over the 6 days from contamination at 13 d to birth was calculated. This was the only significant radiation dose to haemopoietic tissue at that or any subsequent stage.

These experiments set out to determine external γ-ray doses which would recreate both the 40% shortfall in CFU-S in the adult and the same altered spatial distribution. 13 day pregnant mice were thus exposed to external whole body γ-rays from a ^{60}Co source for 6 days. They were then allowed to give birth and their offspring assayed at 8 wks of age for femoral CFU-S numbers and spatial distribution. CFU-F (fibroblastoid CFU, a component of the haemopoietic micro environment) were also recorded.

In preliminary experiments, γ-ray dose rates up to 0.15 Gy per day did not affect the CFU-S distribution and the dose rate was ultimately increased to 0.6 Gy per day.

Table 6: **Cellularity, CFU-S and CFU-F Content of Femur (% Control)**

Treatment	Cells	CFU-S	CFU-F
0.15 Gy/d γ-rays (13 d g - birth)	89 ± 4	81 ± 5	89 ± 6
0.6 Gy/d γ-rays (13 d g - birth)	80 ± 3	67 ± 2	67 ± 4
30 Bq/g [239]Pu injected at 13 d g	86 ± 4	60 ± 5	(a) 72 ± 12*
			(b) 42 ± 2

* CFU-F were not assayed for [239]Pu contamination. Instead, cellularity (a) and CFU-S (b) content of renal ossicles are shown (see '1' above).

Table 6 shows that 0 15 Gy/d continuous γ-irradiation had little effect on cellularity, CFU-S or CFU-F content. The higher dose rate of 0.6 Gy per day produced changes comparable with those induced by [239]Pu. Similarly, in terms of spatial distributions of CFU-S, the higher dose rate was required to approximate the [239]Pu picture (Figure 4).
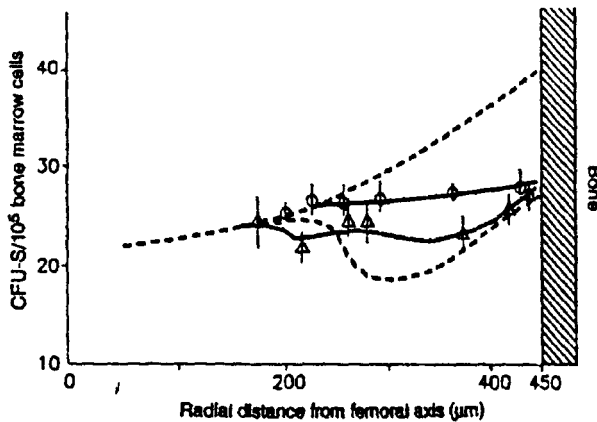
Figure 4: Distribution of CFU-S across the radial axis of a femur from an 8-week-old mouse. The mean control and [239]Pu distributions are transposed from Fig. 1 (- - -). The other curves are for mice given 0.15 Gy (○) or 0.6 Gy (△) γ-rays per day of whole-body continuous γ-radiation *in utero* for 6 days from 13 days of gestation. Mean data for CFU-S$_8$ and CFU-S$_{12}$, which were not distinguishable, are presented.

Similar levels of CFU-S damage resulted from 6 daily acute doses of 0.3 Gy (but not 0.1 Gy) over the same foetal development phase, or from a single acute dose of 1.8 Gy (but not 0.6 Gy) given at day 15 of gestation (Figure 5).
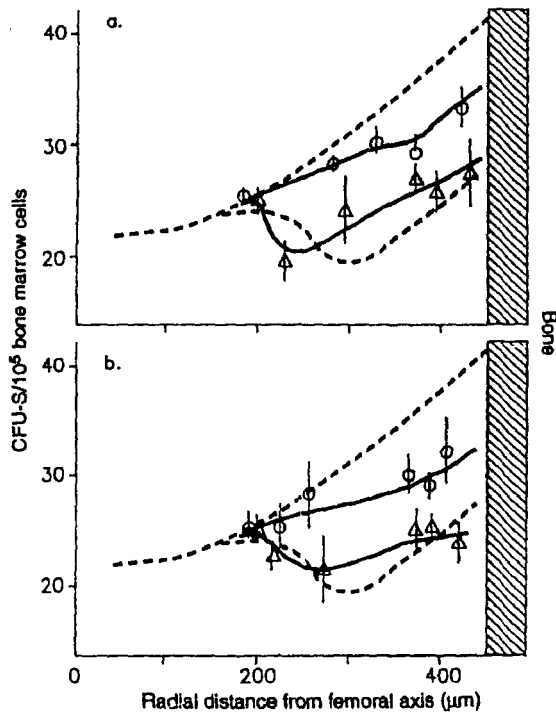

Figure 5: Femoral distribution of CFU-S as in Fig.1 for control and ^{239}Pu-contaminated mice. Experimental mice were given (a) six daily acute doses of 0.1 Gy (O) or 0.3 Gy (△) γ-rays at 0.6 Gy/min from day 13 of gestation, (b) a single acute dose of 0.6 Gy (O) or 1.8 Gy (△) γ-rays at 0.6 Gy/min on day 15 of gestation. Mean data for CFU-S$_8$ and CFU-S$_{12}$, which were not distinguishable, are presented.

Compared with the radiation dose from incorporated ^{239}Pu (10-14 mGy over 6 d) these cumulative doses of 3.6 Gy continuous γ-irradiation or 1.8 Gy acute γ-rays, these results imply an effective α-particle RBE for long-term haemopoietic tissue damage of 250-360 (continuous γ-rays) or 130-180 (acute γ-rays).

Direct measurements of RBE based on acute kill of isolated cells in suspension have frequently been in the region of 1 or 2 and ICRP recommendations give an α-particle weighting of 20. These results indicate, however, that for *in vivo* contamination and for the long-term effects on tissue function, the α-particle RBE can be very high. It must be appreciated that the value may be tissue dependent.

III.III. Tissue v Micro environment
It was concluded from the ^{239}Pu studies on contamination at mid-term gestation that the

damage to developing haemopoietic tissue was at least partly dependent on damage to the haemopoietic regulatory micro environment   This part of the study was designed to determine the relative contributions of these complementary components to long-term damage in haemopoiesis.

For simplicity, we used the newly determined equivalent γ-ray dose of 1.8 Gy given at 15 d gestation (see Section 2) in place of [239]Pu injected at 13 d gestation.

Making observations on their adult offspring, we again confirmed the long-term effects of this approach, CFU-S and CFU-F running respectively at 62-69% and 53-82% of normal over the period 8-21 wks after birth (Table 7).

Table 7:   CFU-S and CFU-F in Offspring of Normal and Irradiated Pregnant Female Mice

Age (weeks)	Offspring	CFU-S/Femur	CFU-F/Femur
8-9	Normal	3119 ±265 (6)	238 ± 31 (2)
	Irradiated	2169 ± 199 (6)	195 ± 14 (2)
21	Normal	4180 ± 643 (4)	112 ± 14 (4)
	Irradiated	2584 ± 277 (4)	59 ± 21 (4)

means ± s.e for (n) experiments.

The same CFU-S deficit was also exposed by sublethal irradiation of the offspring, 59-71% of endogenous CFU-S surviving 5-6 Gy whole body γ-irradiation (Table 8).

Table 8:   Endogenous CFU-S in Normal or Irradiated Offspring After Sub-lethal Irradiation

γ-ray dose	Endogenous Colonies per Spleen	
	Normal	Irradiated
6 Gy	6.9 ± 1.0 (15)	4.1 ± 0.9 (10)
5 Gy	18.9 ± 1.2 (14)	13.4 ± 0.7 (15)

mean ± s.e. for (n) experiments

The main part of the experiment was to study the growth of haemopoietic stem cells (CFU-S) in the femur of heavily irradiated recipient mice following a bone marrow transplant   Thus, femoral CFU-S were assayed 5 to 30 days after transplantation in the following groups.

1. Normal Offspring BM into Standard (15 Gy) Normal Recipients (NBM → SR)
2. Normal Offspring BM into Recipient Offspring (15 Gy) of Irradiated Mothers (NBM → IOR)
3. BM from Offspring Irradiated Mothers into Standard (15 Gy) Normal Recipients (IOBM → SR)
4. BM from Offspring of Irradiated Mothers into Recipient Offspring (15 Gy) of Irradiated Mothers (IOBM → IOR)

Comparison of Groups 1 with 3 and 2 with 4 show the relative capacity of CFU-S from NBM and IOBM to grow in similar recipients. Comparison of Groups 1 with 2 and 3 with 4 show the relative capacity of the N (S) and IO micro environment to host a similar graft. The results are shown in Figure 6.
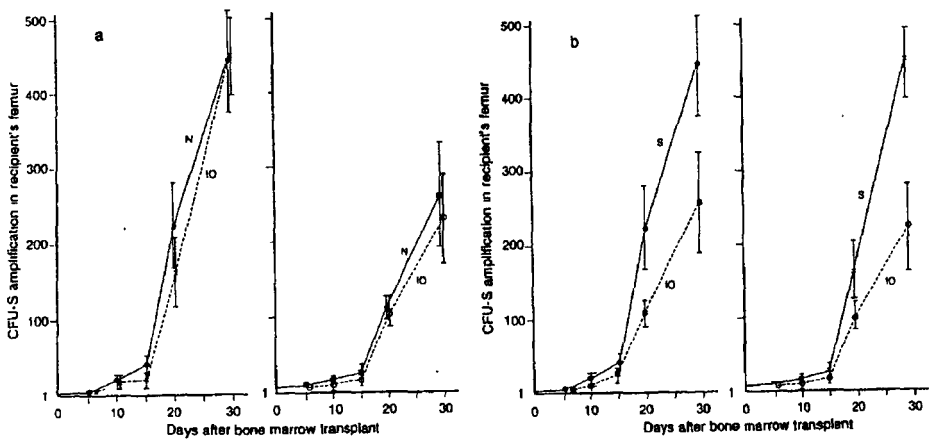

Figure 6: Growth of transplanted CFU-S in irradiated hosts. Part a: Comparison of bone marrow from normal mice (NBM) with that from offspring of irradiated pregnant mice (IOBM) in standard (SR, left panel) or irradiated-offspring (IOR, right panel) recipients. Part b: Comparison of the capacity of standard (SR) or irradiated offspring (IOR) used as transplant recipients, to host the growth of bone marrow CFU-S from normal mice (NBM, left panel) or offspring of irradiated pregnant mice (IOBM, right panel). (●) NBM → SR; (■) NBM → IOR; (X) IOBM → SR; (○) IOBM → IOR.

The results show that bone marrow from normal and irradiated offspring grows equally well in either standard or irradiated offspring recipients (Fig. 6a) but that each grows about twice as efficiently in standard recipients as it does in irradiated offspring recipients.

Assay of CFU-F in the same recipients 30 days after transplant showed that IOR mice contained only 30% of the CFU-F in the SR mice (Table 9). The higher level of CFU-F in the normal donor marrow does not compensate the deficit in the recipients' stroma and the component of the micro environment is clearly not transplantable - at least not sufficiently to manifest growth within 1 month.

We conclude that ^{239}Pu contamination (30 Bq g^{-1}) at mid-term pregnancy, or an equivalent dose of γ-radiation, damages the developing, regulatory stromal micro environment but not measurably the developing haemopoiesis which it supports.

This damage then limits the long-term development and function of its otherwise normal haemopoietic tissue.

The altered kinetic circumstances (see Section 1) of the haemopoietic tissues might render it more susceptible to secondary damage and/or late development of haemopoietic (or osteotic) malignant diseases.

Table 9: CFU-F per Femur, 30 d after BM Transplant

Transplantation Group		CFU-F per Recipient Femur (% control)
Donor	Recipient	
NBM	SR	100
NBM	IOR	30.5 ± 8.0
IOBM	SR	93.3 ± 17.1
IOBM	IOR	29.5 ± 7.2

mean (3 experiments) ± s.e.

III.IV. Preconceptual Paternal ^{239}Pu Contamination

This study was designed to test the hypothesis that prior contamination of the male with an α-emitting radionuclide might have detrimental effects on developing haemopoietic tissue in his offspring.

Male mice were injected with ^{239}Pu (64, 128 or 256 Bq g^{-1}) at 4, 12 or 24 wks before mating with normal females. Their offspring were weaned and haemopoiesis assessed as above at 6-8 wks of age. All mice were assayed individually. Tables 10-12 show the results.

Table 10: Femoral Haemopoiesis in Offspring

Cells per femur	Normalised Mean Control	^{239}Pu @ - 4 wks		^{239}Pu @ - 12 wks	
		64 Bq g^{-1}	128 Bq g^{-1}	64 Bq g^{-1}	128 Bq g^{-1}
CFU-S	5000	4800	4700	5100	4100[1]
CFU-F	500	440	380[2]	490	300[3]
GM-CFC	15000	12600	14800	17400	16500
Cells (x10^{-6})	20.0	19.9	21.2	20.2	19.4

[1] p = 0.004;   [2] p = 0.06;   [3] p = 0.005

Table 11: Femoral Haemopoiesis in Offspring

Cells per femur	^{239}Pu @ - 4 wks 256 Bq g^{-1}	^{239}Pu @ - 12 wks 256 Bq g^{-1}	^{239}Pu @ - 24 wks		
			64 Bq g^{-1}	128 Bq g^{-1}	256 Bq g^{-1}
CFU-S	6200	3800	5200	5400	4900
CFU-F	1390	870	2580	460	660
GM-CFC	18300	11100	16500	15900	16100
Cells (x 10^{-6})	22.2	16.0	20.8	21.0	21.6

In general, bone marrow cellularity and the committed progenitor cells (GM-CFC) were normal. CFU-S numbers were reduced when the father had received ^{239}Pu at 12 wks before mating. CFU-F (and corresponding renal ossicle assays) showed considerably more variability,

particularly at the highest dose level where some effects on fertility had been recorded (smaller litters and reduced mating activity). The most consistent deviation from normal was seen in the groups receiving 128 Bq g^{-1}, 12 wks before mating, where CFU-S and, particularly, CFU-F were significantly reduced.

Table 12: Haemopoiesis in Renal Ossicles

	Normal	^{239}Pu @ - 4 wks			^{239}Pu @ - 12 wks			^{239}Pu @ - 24 wks		
		64	128	256	64	128	256	64	128	256
Cells/ossicle (x 10^{-6})	5.0	5.7	5.8	2.3	6.7	3.9	6.4	4.5	4.0	2.7
CFU-S/10^5 cells	12.0	11.2	15.2	3.8	11.7	9.6	7 1	5.3	8.4	10.4
CFU-S per ossicle	600	577	736	84	758	390	524	243	336	277

A larger scale study has more recently been set up using 128 and 256 Bq g^{-1}, 12 weeks before mating and the offspring assessed at 6, 12 and 20 wks of age.

Haemopoietic cells were largely unaffected but CFU-F numbers were particularly erratic compared to normal. Cytogenetic studies have (for the first time and as yet incomplete) been included and are showing increasing chromosome aberrations in the femoral marrow. No change has been observed in the cytogenetics of splenic lymphocytes.

Haemopoietic growth factors (GFs) are products of the haemopoietic micro environment. Consequently, a preliminary screen on GFs in the sera of some of these mice (carried out by Dr J A Bueren - Contractor No.7) has been incorporated. As with CFU-F, more variability appeared in the individual mice. For GM-CSF, 1 out of 7 mice (128 Bq g^{-1}) and 4/13 (256 Bq g^{-1}) gave readings higher than the average control IL-1 levels remained normal while IL-6 levels fluctuated wildly, even in the control animals. These results are inconclusive at the moment though indications of increased GM-CSF levels coupled with primary variability in the micro environmental components may well be compatible with the changes in granulocyte activity under similar circumstances (see Section 1).

We conclude that preconceptual paternal contamination with ^{239}Pu can induce transmissible damage which becomes manifest, variably, in assays of the micro environment which in turn could foreseeably misregulate blood production in the haemopoietic tissue.

III.V. Spatial Distribution of Haemopoietic Progenitor Cells in Mouse Femur
It has previously been shown that the marrow cells conform to a specific microanatomical distribution in the bone marrow spaces. This throws doubt on the reliability of dosimetric models for α-emitters in bone which assume a random and uniform distribution of potential target cells in red marrow Among the target cells, and in addition to the pluripotent stem cells, are the lineage restricted, committed progenitor cells which respond to a variety of specific growth factors. Preliminary to dosimetric comparisons correlating radiation dose and

target cell distributions we have now mapped out the spatial distributions of cells which respond to granulocyte colony stimulating factor (G-CSF), granulocyte-macrophage (GM)-CSF, macrophage (M)-CSF and interleukin-3 (IL-3).

Our standard axial/marginal fractionation technique was used to obtain cells from different locations across a cross section of femoral marrow and their responses to the individual growth factors assessed. This allowed a map of the locations of responding cells to be drawn. The results are shown in Figure 7.

IL-3 v GM-CSF v G-CSF v M-CSF (Corrected)

Cols per 10^{-5} BM Cells (y-axis: 40 to 180)

Radial distance from femoral axis (um) (x-axis: 0 to 500)
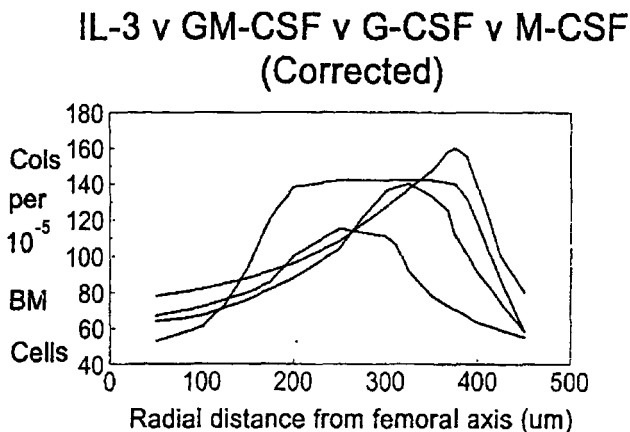
Figure 7: Distribution of *in vitro* CFC responding to IL-3 (I), GM-CSF (GM), G-CSF (G) and M-CSF (M) in the mouse femur. A radial distance of 450 μm represents the bone surface and 0 μm is the central longitudinal axis of femoral shaft.

IL-3, which stimulates relatively primitive cells including some of the multipotent progenitors, stimulates cells closest to the bone surface (R = 450 μm) while GM-CSF and G-CSF respectively stimulate progressively more mature progenitors. M-CSF, with properties overlapping those of GM- and G-CSF appears to have a wide range of responsive cells.

These distributions together with those previously obtained will be linked with α-emitting radiation dose distributions in the marrow, obtained from autoradiographs available at NRPB (Dr J D Harrison - Contractor No.1). This will allow a better assessment of risk to those cells which are potential targets for development of haematological and osseous tissue disorders.

Publications
Mason TM, Humphreys ER and Lord BI (1991). Int. J. Radiat. Biol. 59, 467-478. Alpha-particle irradiation of haemopoietic tissue in pre- and post-natal mice. 1: Distribution of plutonium-239 after mid-term contamination.

Mason TM, Lord BI, Molineux G and Humphries ER (1992). Int. J. Radiat. Biol. 61, 393-403. Alpha-irradiation of haemopoietic tissue in pre- and post-natal mice. 2: Effects of mid-term contamination with [239]Pu *in utero*.

Lord BI, Mason TM and Humphreys ER (1992). Radiat. Protect. Dosim. 41, 163-167.
Age-dependent uptake and retention of ^{239}Pu: Its relationship to haemopoietic damage.

Jiang T-N, Lord BI and Hendry JH (1994). Radiat. Res. 137, 380-384.
Alpha-particles are extremely damaging to developing haemopoiesis compared to gamma irradiation.

Yang F-T, Lord BI and Hendry JH (1995). Radiat. Res. 141, 309-313.
Gamma irradiation of the fetus damages the developing hemopoietic micro environment rather than the haemopoietic progenitor cells.

Lord BI, Humphreys ER and Stones VA (1995).
In: Health Effects of Internally Deposited Radionuclides. Eds. G van Kaick, A Karaoglou and A M Keller. World Scientific Pub. Co. Singapore, p. 341-345. Preconceptual paternal plutonium-239 contamination: development of haemopoiesis in the offspring.

Gaitan S, Tejero C, Humphreys ER and Lord BI (1993). Exp. Hemat. 21, 1227-1232.
A relationship between residual stromal damage in hemopoietic tissue and the functional activity of granulocytes.

Cui Y-F, Lord BI, Woolford LB and Testa NG (1995). In preparation.
The relative spatial distributions of *in vitro*-CFCs in the bone marrow, responding to specific growth factors.

Head of project 5: Dr. Visser

II. Objectives for the reporting period

Hemopoietic stem cells of normal bone marrow are analyzed and sorted by a combination of cell separation techniques, reverse transcriptase - polymerase chain reaction (RT-PCR) and cell culture methods. Sorting of the hemopoietic stem cells (PHSC) will be performed by combining density gradient centrifugation and fluorescence-activated cell sorting (FACS) for wheat germ agglutinin (WGA) positive, monoclonal antibody 15-1.1 negative cells with medium to low forward scatter and low perpendicular light scatter intensities. Subpopulations of this cell fraction will be sorted using Rhodamine 123, a mitochondrion specific dye which is pumped out of cells with a high expression of the multi drug resistance efflux pump, the P-gp. The action of this pump can be blocked by verapamil, and, therefore, we will further study the sorted fractions wih and without verapamil. The resulting fractions will be analyzed again for long- and short term hemopoietic reconstitution. In addition, the molecular characteristics of these candidate stem cells will be analyzed by RT-PCR with cDNA of the sorted cells.

The interactions between stromal cells and stem cells will be studied by analysis of the homing of sorted candidate stem cells. For this purpose sorted stem cell fractions are stained with the hydrophobic membrane dye PKH-26 and transplanted into irradiated and non-irradiated recipients. The stained stem cells and their progeny are subsequently traced back in the various organs, and analyzed.

These studies are performed in collaboration with Dr. A. Belyavsky (Engelhardt Institute of Molecular Biology, Moscow, Russia) and with Drs. J. Landegent and W. Fibbe (Dept. of Hematology, Academic Hospital Leiden, The Netherlands).

III. Progress achieved

PHSC were sorted and enriched several hundred fold from adult mouse bone marrow. About 0.4 % of low-density bone marrow cells are WGA-positive and 15-1.1-negative, and 5 % of these are Rh123-negative. This 0.02 % of total bone marrow can be further subdivided by Rhodamine 123 staining in the presence of verapamil: 0.002 % of total bone marrow is also Rh123-negative with verapamil. This double negative Rh123$^-$Vp$^-$ cell fraction was found to contain the long term repopulation stem cells, but not the short-term repopulating cells. Therefore they did not provide their recipients with radioprotection. By adding cell fractions which were shown to contain short-term repopulating radioprotective cells it could be shown that less than 30 Rh123$^-$Vp$^-$ cells are needed for restoring hemopoiesis in lethally irradiated mice.

The RT-PCR experiments with these Rh123$^-$Vp$^-$ cells indicated that they have a very high expression of our newly discovered cdc-2 related gene, crk1, whereas the Rh123-dull and positive sorted fractions had no or a low expression. A number of other interesting genes were found to be expressed specifically in these very rare and very early hemopoietic cells, amongst these were a putative leucine-zipper molecule (TSC-22) which is induced by the stem cell inhibitor TGFb. And also the expression of CTLA-2a, a protease regulator was found in the PHSC fraction only. A number of other genes were found both in the Rh123$^-$Vp$^-$ PHSC fraction and in the Rh123$^-$Vp$^+$ fraction, but not in other cells. These may be differentiation stage specific and useful to distinguish radioprotective cells from PHSC.

The homing of the candidate stem cells was studied by transplantation of PKH-26 stained stem cell fractions into lethelly irradiated (8.5 Gy total body g-irradiation) and in non-irradiated syngeneic recipients. The proliferation of the homed stem cells could be followed for three days by analysis of the PKH-26 positive cells in the variuous organs. It was found, that the stem cells homed better in non-irradiated than in irradiated recipients, however, their proliferation after homing was slower.

Publications

Zijlmans et al. Modification of rhodamine staining by verapamil in sorted stem cell populations allows identification of a fraction highly enriched for cells providing radioprotection and long term repopulating ability. Blood (1993) vol. 82, no 10, Suppl. 1 to, abstract 41.

Ershler, M A, Nagorskaya, T V, Visser, J W M, and Belyavsky, A V. Novel CDC2-related protein kinases in murine haemopoietic stem cells. Gene (1993), 124, 305-306.

Corso, A, Hogeweg-Platenburg, M G C, De Vries, P, and Visser, J W M. A protocol for the enrichment of different types of CFU-S from mouse fetal liver, Haematologica (1993), 78, 5-11.

Visser, J W M, Rozemuller, H, DeJong, M O, and Belyavsky, A. The expression of cytokine receptors by purified haemopoietic stem cells. Stem Cells (1993), 11(suppl 2), 49-55/

Visser, J W M, and Hogeweg-Platenburg, M G C. Identification and isolation of bone marrow stem cells. In: low Cytometry, NATO ASI Series Vol. H 67 (JacqueminSablon, A., ed) (1993). pp 141154. SpringerVerlag Berlin, Heidelberg.

Head of Project 6: Dr. Tejero

II. Objectives

In this project we have extended our investigations into haemopoietic residual damage produced by X-rays (5 Gy) in adult mice. Therefore, our main objectives were:
- To analyze the impaired oxidative metabolism of granulocytes from adult animals by means of glucose uptake, glycolytic flux and ATP levels.
- To correlate the enhancement of superoxide anion production in granulocytes from adult mice, described in the last project, with the oxidation of glucose via the hexose monophosphate shunt and G6PD activity.
- To evaluate the role of the stroma, by means of analyzing cellular metabolic parameters (protein levels, G6PD activity) and characterization of the release of cytokines (IL-3, GMCSF, IL-6) and their influence on granulocyte function. Analysis of granulocyte DNA fragmentation is being undertaken.
- In order to evaluate a correlation between radiation-induced haemopoietic residual damage and gestational age, we have extended our studies to include 4 and 13 days postconception irradiated animals (1 and 3 Gy X-rays).
- To determine long-term bone marrow recovery after these treatments, quantifying cellularity and precursor cells.
- To assess granulocyte function (O_2^-, G6PD activity and ATP levels) after these treatments
- To study the role of stroma determining the release of HGFs.

III. Progress achieved

III.I. IRRADIATION of ADULT MICE (5 Gy X-rays)

Granulocytes

Granulocytes from long-term bone marrow cultures (LTBMC) showed a significant increase in G6PD activity with respect to control animals at 6 (fig 1), 9 and 12 months postirradiation. The higher capacity of this enzyme is related to the enhancement of the hexose monophosphate shunt (HMPS) in response to PMA that has also been demonstrated in these cells (fig 2). Since superoxide anion is generated by a NADPH-dependent oxidase system, the increase in HMPS and G6PD activity is associated with the higher requirement for NADPH to facilitate the increased production of this oxyradical, observed previously. Furthermore, protein levels were higher in granulocytes from irradiated animals than in age matched controls at 6 (fig 3), 9 and 12 months post-irradiation This result suggests an increase in protein expression as a consequence of irradiation.

The levels of ATP were reduced in LTBMC granulocytes from irradiated animals at 4 and 12 months post-irradiation (35% and 67% lower than controls, respectively). No significant differences between controls and treated animals were observed in glucose uptake (Km, Vmax) and glycolytic flux. Therefore, the reduction in ATP levels was probably largely the result of higher energy consumption in increased protein synthesis rather than impaired transport and/or oxidation of glucose via glycolysis

In bone marrow cells, no significant effects were observed on glucose uptake, glycolytic flux, HMPS and G6PD activity. However, the ATP levels in cells from 12 months post-irradiation mice were significantly lower than controls. An increase in protein levels was also observed. The maintenance of a normal blood cells number from a reduced number of precursor cells in irradiated mice could be the reason for the lower levels of ATP in these cells.

Characterization of LTBMC supernatants

Previous results demonstrated that LTBMC cell-free supernatants were capable of stimulating GM-CFC growth. With the aim of characterizing the activity of supernatants, neutralization experiments with anti rmGM-CSF and ELISA assays were performed. The results showed a total inhibition of activity with 48 µg anti rmGM-CSF per ml (table 1) and the increase of IL-3, GM-CSF and IL-6 levels (fig 4).

Role of HGFs in granulocyte function

With the aim of confirming whether HGFs released after irradiation are responsible of the priming of granulocytes, cells from control animals were incubated at $37°C$ with LTBMC supernatants of irradiated animals.

After 3 hours incubation, the superoxide anion production was higher in the presence of supernatant from irradiated mice. The levels of this oxyradical were similar to those obtained with 16 ng/10^6 cells of mr GM-CSF (fig 5). Furthermore, G6PD activity and protein levels were also increased at 3, 6 (fig 6) and 15 hours of incubation in the presence of supernatant. Similar results were obtained with 18 ng/ml of rm GM-CSF. These results indicate that the overproduction of HGFs, as a consequence of irradiation, primes granulocytes promoting modifications in non-specific host defence mechanisms.

Since it has been reported that HGFs inhibit apoptosis in granulocytes, we have investigated this parameter by incubating LTBMC control cells with or without supernatants from LTBMC irradiated mice. The significant reduction of ATP levels, observed when control granulocytes were incubated 15 hours in Fischer's medium compared with the incubations in LTBMC supernatants from irradiated animals, suggest a protective effect of HGFs released after irradiation. Quantitative and qualitative analysis of DNA is being undertaken to determine the grade of DNA fragmentation.

Stromal cells

We observed a reduction in stromal cellularity from LTBMC adherent layers at 9 and 12 months (fig 7) post-irradiation. However, protein levels were higher in adherent cells harvested from LTBMC of irradiated mice (fig 8).

Since HMPS is the pathway that provides the NADPH needed for cellular biosynthetic processes, we have determined levels of G6PD activity in stromal cells. The results showed an enhancement of the enzymatic activity in cells from irradiated mice of about 70% and 40% at 9 and 12 months (fig 9) post-irradiation respectively.

Therefore, total body irradiation with 5 Gy X-rays produce a residual stromal damage and an increase in the cellular metabolism that could assist the extra production of HGFs.

III.II. IRRADIATION OF MICE AT 4 AND 13 DAYS OF GESTATION

3 Gy

After irradiation of pregnant females with 3 Gy, we observed deaths, malformations and growth retardation in the offspring. Therefore we abandoned our studies with this experimental animal model.

1 Gy

Femoral contents of GM-CSF

We have quantified the femoral cellularity and no differences were obtained between both treatment models and control mice. However, a remarkable increase of GM-CFC number was observed in the13d irradiation group at 12 months after birth, when cells were stimulated both with wehi-3b and several concentrations of rm GM-CSF (fig 10). The plateau of the dose-response curve was obtained between 5 and 7 ng/ml. However, at 3 months there were no significant differences between irradiation groups and controls. These results may be due to a reduced pluripotent progenitor cell population in the first weeks after birth and subsequent overproduction in the immediate committed progeny.

Wehi-3b plus rm GM-CSF produced a recruitment in GM-CFC precursors, resulting in an increase in colony numbers of about 47% with respect to both CSFs (fig 11). Moreover, combination of wehi-3b: 10%, rm GM-CSF: 7ng/ml and IL6: 7ng/ml shows an enhanced proliferation of the growth of GM-CFC colonies from the 13d group at 12 months post-irradiation. It is possible that the unusually large colonies obtained could be the result of the stimulation of a more ancestral precursor which may require double signalling before proliferation is initiated.

Granulocytes

Granulocyte production from LTBMC was significantly reduced in both irradiation groups at 6 (fig 12) and 9 months post-irradiation. However, at 12 months post-irradiation, the reduction was only observed in the 13d group. This decreased granulocyte production after 13d irradiation at the foetal stage might be a reflection of direct damage to the microenvironment. Taking account of the results obtained by Lord et al (Project No. 4), it seems likely that the decreased number of granulocytes produced at 3 and 6 months after irradiation at the 4d embryonic stage could be the effect of a deficiency in pluripotent progenitor cell population when mice were born.

Superoxide anion production, G6PD activity and protein levels were similar in LTBMC granulocytes from control and from both irradiated groups at different times post-irradiation. These results suggest that the residual haemopoietic damage was not expressed as alterations in granulocyte function in contrast with the results obtained with 5 Gy irradiated adult mice.

With regard to ATP levels, a significant reduction was observed in the 13d group at 6 months post-irradiation (fig 13).

The parameters analyzed in bone marrow cells (G6PD activity, ATP and protein levels) indicated no differences between irradiated and control mice.

LTBMC supernatant characterization

LTBMC supernatants from the 13d gestation group were capable of stimulating the growth of colonies to a significantly greater extent than control supernatants (fig 14). Supernatants from both 4d and 13d groups showed an increase of IL-6 levels, determined by ELISA (fig 15).

Publications

- GAITAN, S.; CUENLLAS, E; SANCHO, P; BUEREN, J.A. and TEJERO, C. (1992) Mechanisms towards compensation of long term haemopoietic injury in mice after 5 Gy irradiation: "in vivo" and "in vitro" enhancement of superoxide anion production by granulocytes. *Bioscience. Rep.* 12, 281-292

- GAITAN, S., TEJERO, C., CUENLLAS, E and LORD. B.I. Residual stroma damage in mice expressed as a priming of granulocytes. 21st Annual Meeting International Society for Experimental Hematology. Providence, Rhode Island, 1992. *Exp. Hematol.* 20, pg. 815

- CUENLLAS,E., ESCRIBANO, S., GAITAN S, and TEJERO, C. Prime mice granulocytes after total body irradiation with 5 Gy X-rays. Haemopoietic Cell Growth Factors. 38th Harden Conference. The Biochemical Society. Wye, Ashford (Kent) 1992. Abs. 22

-ESCRIBANO, S., CUENLLAS, E., GAITAN, S., and TEJERO, C. Over production of GM-CSF after total body irradiation with 5 Gy (X-rays). Enhancement of G6PD activity in mice granulocytes. 24th Annual Meeting of the European Society for Radiation Biology. Erfurt,1992. Abs. 182.

- GRANDE, T.; GAITAN, S.; TEJERO, C. and BUEREN, J.A. (1993) Residual haemopoietic damage in adult and 8 day-old mice exposed to 7 Gy of X-Rays. *Int. J. Radiat. Biol.* 63, 59-67.

- GAITAN, S.; TEJERO, C. HUMPHREYS, E. and LORD, B.I. (1993) Residual stromal damage in hemopoietic tissue results in granulocytes expressing an overproduction of superoxide anion. *Exp. Hematol* 21, 1227-1232.

- ESCRIBANO, S., GAITAN, S., CUENLLAS, E. y TEJERO, C. Granulocyte-macrophage colony stimulating factor released after mice total body irradiation: its role in granulocyte function. 22nd Meeting International Society for Experimental Hematology. Rotterdam, 1993. *Exp. Hematol.* 21, pg 1145.

- CUENLLAS, E , ESCRIBANO, S., GAITAN, S. Y TEJERO, C. Daño residual radioinducido en el estroma hematopoyético de ratón: parámetros metabólicos. V Congreso de la Asociación de Investigación sobre el Cancer (ASEICA). Las Palmas de Gran Canaria, 1993. *Oncología.* 16, pg 325.

- ESCRIBANO, S., CUENLLAS, E., GAITAN, S., TEJERO, C. Hematopoiesis residual damage after irradiation in pregnant mice. Granulocyte functionality. 23rd Annual Meeting of

the International Society for Experimental Hematology. Minneapolis, Minnesota, 1994. *Exp. Hematol.* 22, pg 810.

- GAITAN, S., ESCRIBANO, S., SANCHO, P., CUENLLAS, E. and TEJERO C.
Metabolismo de granulocitos como expresión del daño hematopoyético residual radioinducido. XIX Congreso de la Sociedad Española de Bioquímica y Biología Molecular. Córdoba, September, 1995.

- ESCRIBANO, S., CUENLLAS, E., GAITAN, S., TEJERO, C. (1995)
Long-term haemopoietic injury in mice by X-rays (1 Gy) at different post-conceptional stages. In preparation.

- GAITAN, S., ESCRIBANO, S., SANCHO, P., CUENLLAS, E. and TEJERO C. (1995)
Glucose metabolism in bone marrow cells and granulocytes of adult mice after X-rays (5 Gy) irradiation: relationship with granulocyte functionality. In preparation.

FIG. 1: GRANULOCYTES

G6PD ACTIVITY

(UI/10^6 cells).10^{-3}

5 Gy   6th MONTH

control
irradiated

FIG. 2: GRANULOCYTES

HMPS

pmol CO_2/min/10^6 cells

5 Gy   4th MONTH

PMA 1ug/ml

control
irradiated
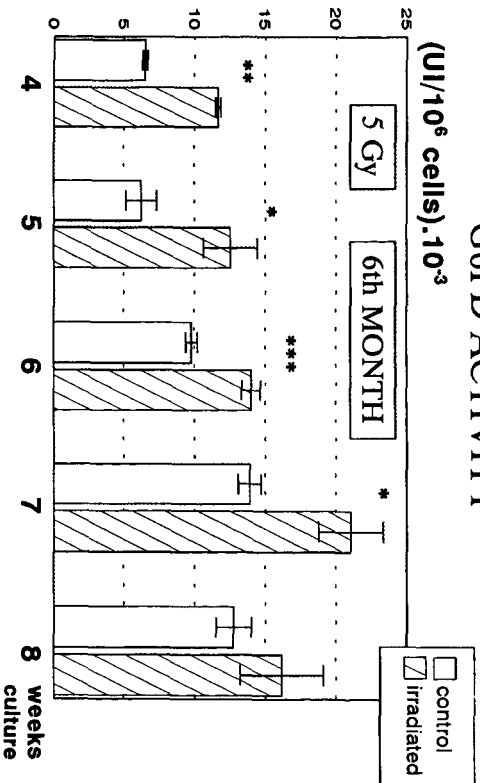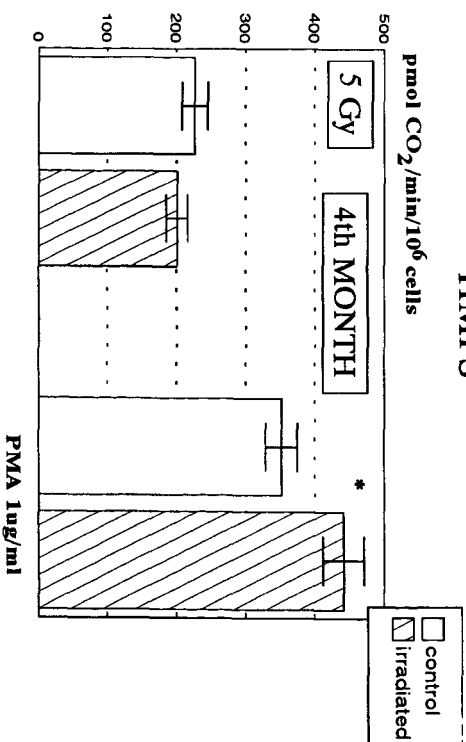
FIG. 3: GRANULOCYTES

PROTEIN LEVELS

mg prot/10^6 cells

5 Gy   6th MONTH

weeks culture

control
irradiated
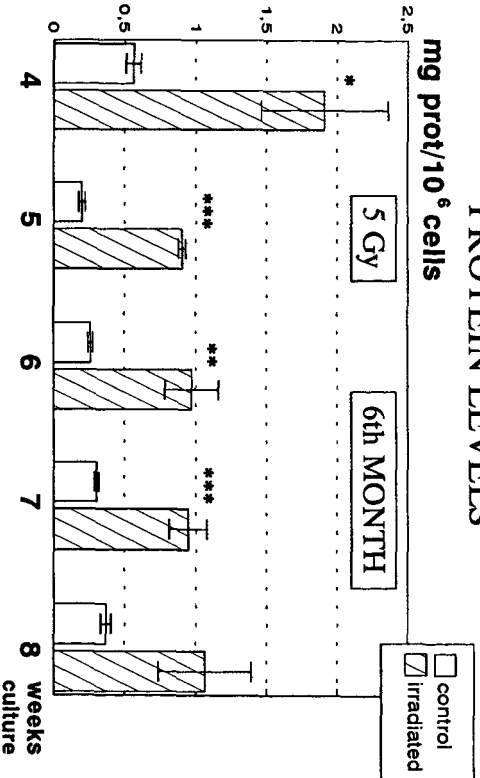
TABLE 1: NEUTRALIZATION ASSAY

	% Supernatant (4x)	anti GM-CSF (µg/ml)	% Inhibition
C	40	16	0
	20	24	0
	20	48	0
R	40	16	38,85
	20	24	70,21
	20	48	100,00

FIG. 4: LTBMC SUPERNATANS
ELISA DETERMINATION

IL-6

(x10e3)pg/ml supernatant

5Gy

2x   6m

*

4x

**

4x   8m

*

IL-3

pg/ml supernatant(8x)

5Gy

6m

GM-CSF

pg/ml supernatant(8x)

5Gy

6m

months
postirradiation

control
irradiated

FIG. 5:
Superoxide anion production

nmol O₂⁻/min/10⁸ cells

IRRADIATED
CONTROL
mrGM-CSF

***

After 3 hours incubation

FIG. 6: G6PD Activity

%IU/10⁶ cells

IRRADIATED
CONTROL

time
(hours)
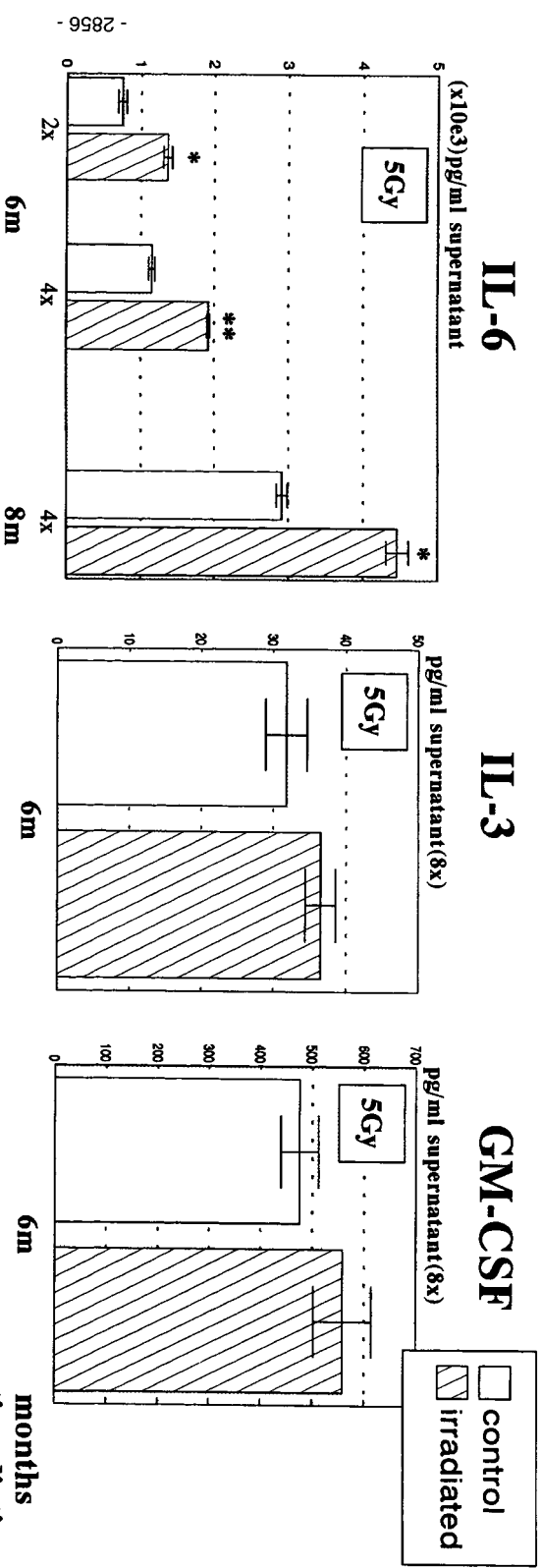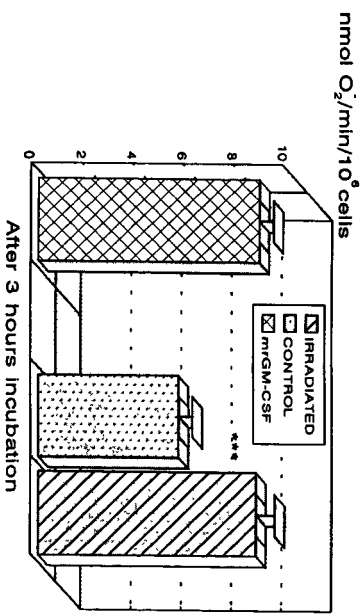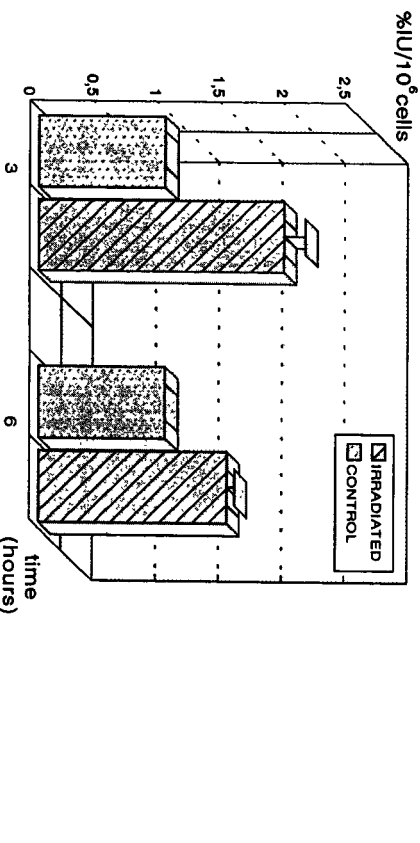
FIG. 7: STROMAL CELLS
Adherent cells cuantification

(Adherent cells/flask).10⁻⁴

FIG 9: STROMAL CELLS
G6PD ACTIVITY

(UI/10⁶ adherent cells). 10⁻³

FIG 8: STROMAL CELLS
Protein levels

mg protein/10⁶ cells

FIG 10: BONE MARROW

GM-CFC colonies/3.10 ^{4} cells
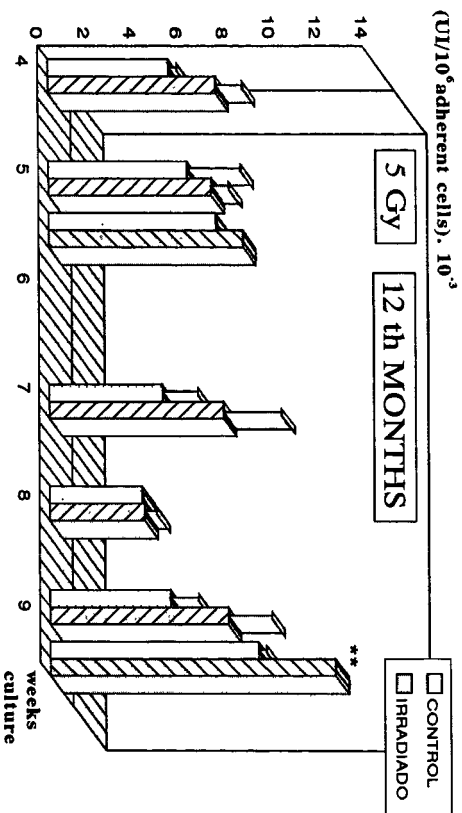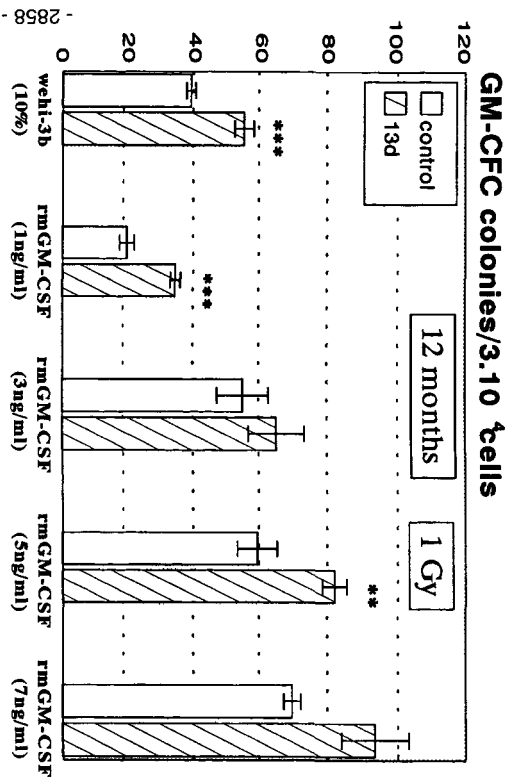
FIG 11: EFFECTS WEHI-3b + GM-CSF

% REDUCTION GM-CFC
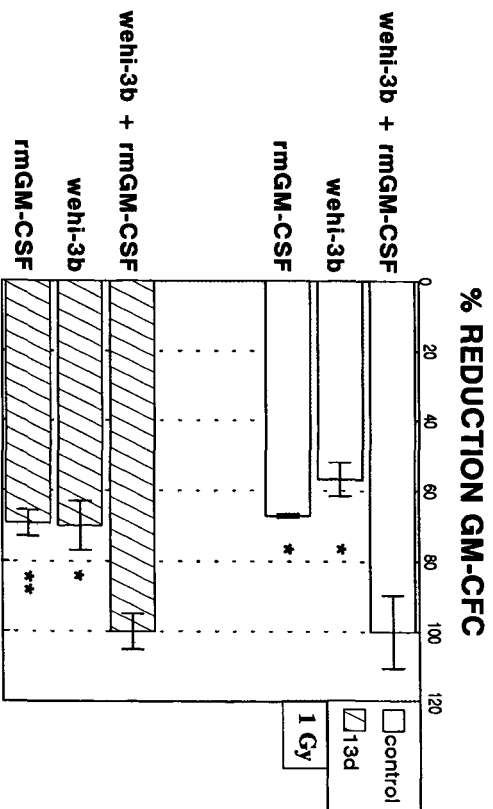
FIG 12: LTBMC PRODUCTION

(x10⁶)nonadherent cells/flask

FIG 13: GRANULOCYTES ATP LEVELS

(x10⁻³)μmol/10⁶ cells
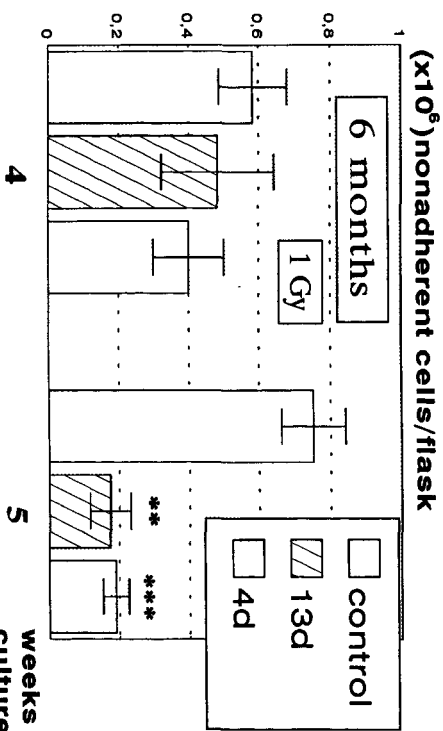
FIG 14: LTBMC SUPERNATANT
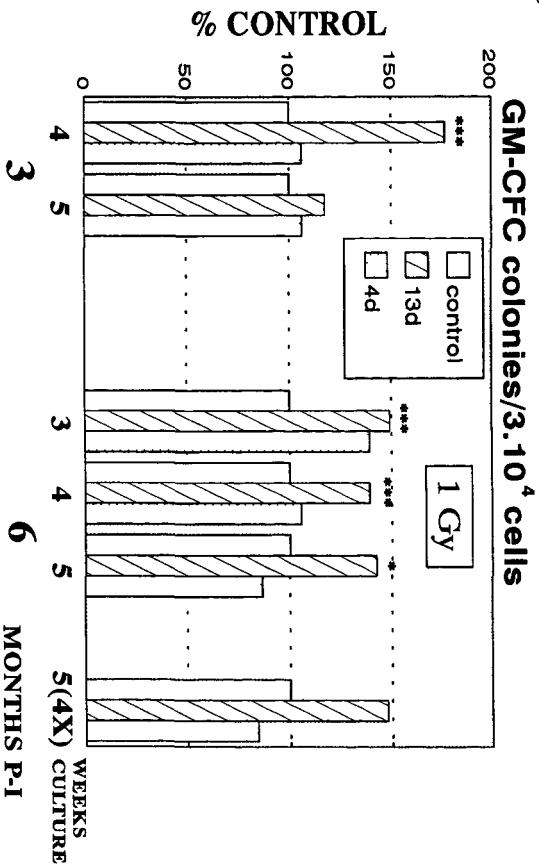
GM-CFC colonies/3.10⁴ cells

FIG. 15: LTBMC SUPERNATANT

ELISA: IL-6

pg/ml supernatant(4x)
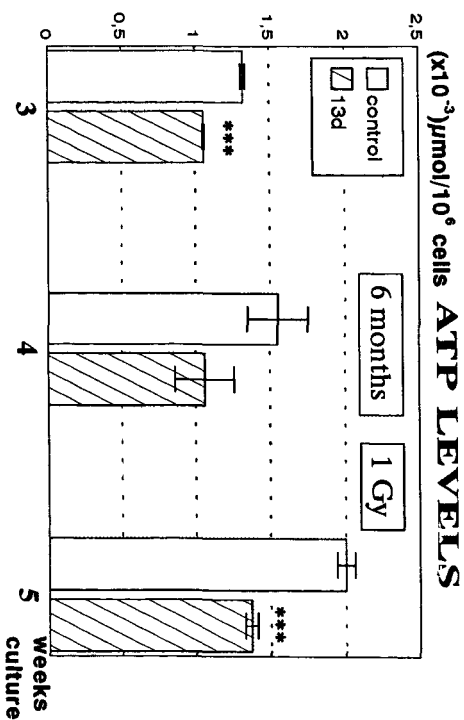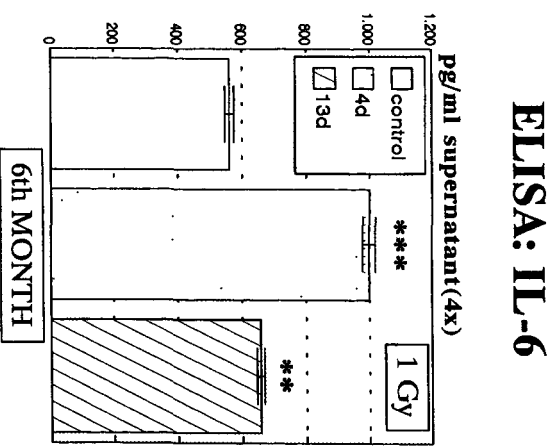
Head of project 7: Dr. Bueren

II. Objectives

1.- To evaluate the radiation sensitivity of the different stages of the mouse development for the induction of persistent deficiencies in the content of hematopoietic progenitors and stem cells.

2.- To study the self-renewal and differentiation potential of lympho-hematopoietic stem cells exposed to external low LET radiation.

3.- To investigate the mechanisms involved in the induction of long-term hematopoietic deficiencies produced as a result of irradiation.

4.- To evaluate the efficacy of methods based on hematopoietic stimulation with polysaccharides and on the transplantation of *ex vivo* expanded bone marrow in the treatment of mice exposed to high doses of radiation.

III. Progress achieved

1. We have investigated whether a relatively low dose of 500 mGy of X rays given at different stages of pre- and postnatal development induced significant changes in the content of femoral hematopoietic progenitors during a one-year period after irradiation *(Grande and Bueren 1995)*. Data showed that in the case of 4 day-old embryos as well as in 2 day-old, 8 day-old and 12 week-old mice, this dose was below the threshold capable of inducing a long-term hematopoietic impairment in the mouse hematopoietic system. Nevertheless, in two groups of irradiated animals, significant long-term changes in the proportion of femoral CFU-GMs were observed (Figure 1), revealing for the first time a long-term hematopoietic dysfunction in mice exposed to a relatively low dose of 500 mGy of X rays, which was characterized by the following points:

- The hematopoietic deficiency was only observed in mice irradiated during the later stages of *in utero* growth (days 13 and 17 of gestation).
- It was only manifested in the long-term after irradiation (beginning with the 9th month of life).
- The dysfunction was characterized by a reduction in the proportion of femoral CFU-GMs, but not in the bulk of femoral bone marrow cells, represented by the femoral cellularity.

The observation that this defect was only produced in mice which had been irradiated at the 13th and 17th day postconception is consistent with the notion that this period of the development is particularly sensitive to the induction of long-term hematopoietic failures. We cannot for the moment presume the existence of a direct relationship between our observations and the radiation-induction of stochastic effects such as leukaemia, since both the target cell and the nature of the initial damaging events are probably different in each case.

To determine whether the effects produced in the most primitive lympho-hematopoietic self-renewing stem cells were consistent with data obtained in the clonogenic progenitors, bone marrow of animals irradiated at different stages of growth was harvested at different post-irradiation times, mixed with genetically distinguishable normal bone marrow cells (BMC), and then transplanted into myeloablated mice. Data showed that not only the clonogenic

progenitors, but also the self-renewing lympho-hematopoietic stem cells were persistently damaged long-term after irradiation with doses of 1 to 3 Gy. Consistent with data obtained in the clonogenic assays, the late stages of *in utero* embryonic growth were characterized by a particular sensitivity to external low LET irradiation. By the use of Ly 5.1/Ly 5.2 clonogenic mice, the induction of the hematopoietic abnormalities was confirmed both in the myeloid and the T and B lineages *(manuscript in preparation)*.
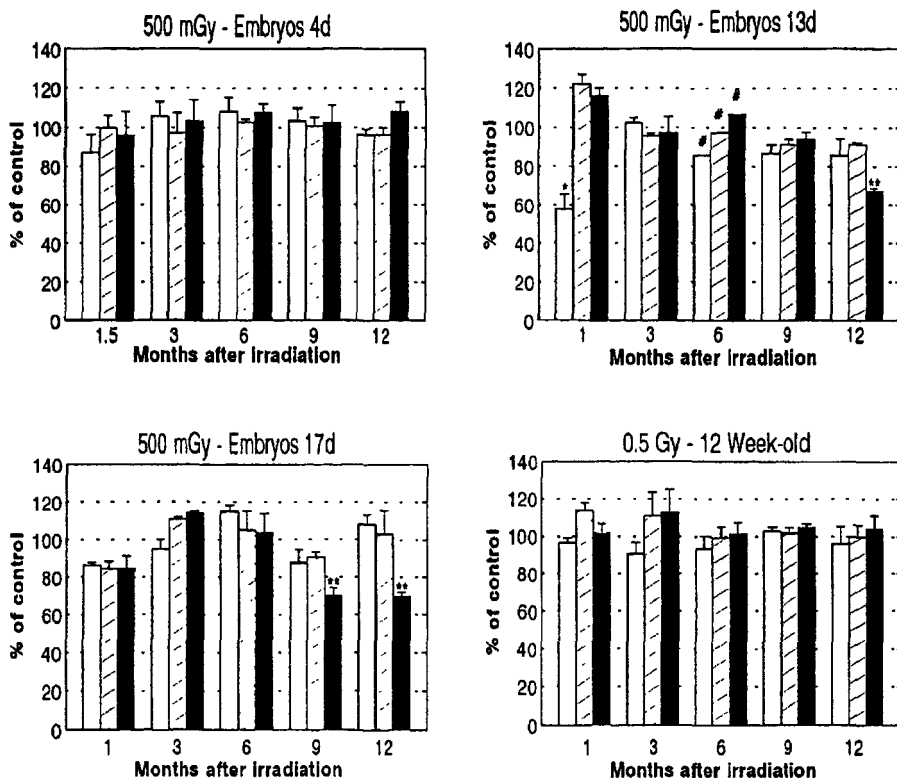
Figure 1. Long-term hematopoietic influence of an acute 500mGy dose of X rays given at different stages of the mouse development Each bar represents the mean and standard error of data obtained in the irradiated mice with respect to their age-matched control group, each consisting of two to eight individual animals. #: Only one animal was analyzed. Significantly different from the control. *p<0.05; **p<0.01 □:Cells per femur; □:CFU-S/10^5 BMCs; ■·CFU-GM/10^5 BMCs. *(Modified from Grande and Bueren, 1995)*.

2. Failures in the self-renewal capacity of stem cells from mice which had been irradiated were routinely observed, in agreement with other studies (B.I.Lord et al). The role that the stromal cells played was investigated by means of the ectopic implantation of irradiated bone marrow into the renal capsule of non-irradiated mice. Bone marrow implants from donor irradiated mice developed ossicles that were incapable of sustaining normal values of host hematopoietic progenitors, indicating that radiation mediates a long-term damage in the hematopoietic

lodging capacity of the stromal cells. The analysis of the number of CFU-S generated per ossicle-derived spleen colony, revealed, however, that the irradiation of hematopoietic stromas resulted in an improved self-renewal capacity of lodged unirradiated CFU-S precursors (Table 1). These data strongly suggested that the impairment in the self-renewal capacity observed in the CFU-S population long-term after irradiation was not a result of stromal damage, which on the contrary may generate a stimulatory response to facilitate the preservation of the low numbers of primitive precursors that survive the irradiation *(Grande and Bueren 1994)*.

In order to follow the differentiation fate of individually irradiated stem cell clones, these were genetically labelled by their transduction with retroviral vectors. Because of limitations in the infectivity of these cells, efficient procedures of gene transfer were first developed *(Bernad et al. 1994)* which allowed us to follow individual clones of stem cells for periods longer than a year in primary as well as in secondary and in tertiary recipients. Experiments in which genetically labelled stem cells were seeded into normal and irradiated stromas have not revealed, for the moment, differences in the dynamics of the stem cell clones.

Table 1. Analysis of the content of hematopoietic progenitors (CFU-S and CFU-GM) and self-renewal capacity of CFU-S in renal ossicles generated by bone marrow implants from normal and 7 Gy-irradiated mice.

Donor of bone marrow implant	Cells/ossicle ($x10^{-6}$)	CFU-GM/10^5 cells	CFU-S/10^5 cells	CFU-S/Colony
Normal	2.4 ± 0.4	$125.6 \pm 14\,7$	28.0 ± 2.2	23.1 ± 3.0
7 Gy	4.3 ± 2.7	$79.1 \pm 10.4^{**}$	$12\,9 \pm 0.7^{***}$	$46.6 \pm 14.8^{*}$

Bone marrow shafts were obtained one year after 7 Gy irradiation of mice. Ossicles were removed 12-15 weeks after marrow implantation. Data show the mean ± SEM from 4-7 ossicles. Differences from control (normal implant) were statistically different (* $0.05<p<0.1$; ** $p<0.05$; *** $p<0.005$). *(Modified from Grande and Bueren, 1994)*.

3. To evaluate the role that Hematopoietic Growth Factors played in the hematopoietic abnormalities described above, Northern blot and ELISA analyses were carried out individually on bone marrow cells and serum of irradiated mice RNA samples extracted from bone marrow and from long-term bone marrow cultures established from normal and irradiated mice were hybridized with probes for IL-1, IL-3, IL-6, G-CSF, M-CSF and SCF. No reproducible differences could be established between samples harvested from the control and the treated groups of animals. ELISA analyses of IL-1, IL-3, IL-6 and GM-CSF were done with serum obtained from individual mice which had been exposed to radiation In this case, up to a 50%

of the irradiated animals showed over expression in some of the tested HGFs. In an attempt to establish a direct relationship between these observations and the hematopoietic abnormalities observed in the irradiated mice, parallel analyses of HGFs expression and CFU-GMs content were performed individually. No direct relationships could be established, however, between the serum levels of HGFs and the CFU-GM content in the bone marrow.

4. With the aim of rescuing mice exposed to high doses of radiation we investigated the efficacy of methods based on hematopoietic stimulation with polysaccharides and on the transplantation of bone marrow grafts which had been expanded *ex vivo* with ILs 3 and 6 in culture.

The radioprotective effects of a protein-associated polysaccharides named AM5 were studied following i.v. injection in mice. A faster recovery of spleen CFU-GMs was observed in mice treated with 0.4 mg/Kg of AM5 3 days or 1 day prior to a sublethal irradiation, and at this time AM5 produced a significant survival enhancement from 10 to 90% in mice irradiated with 7.6 Gy X rays. This effect was correlated with an increase in the number of leucocytes during the initial radiation response *(Real et al 1992)*. Northern blots of LTBMC-adherent layers treated with AM5 revealed a significant mRNA expression for IL-1, GM-CSF, G-CSF, in contrast with adherent layers from untreated cultures which only expressed, in detectable levels, M-CSF and SCF. Our results strongly suggested that the hematopoietic stimulation induced by AM5 was mediated by the modulated expression of endogenous hematopoietic growth factors (*Güenechea et al, 1995*).

Using a different approach, we investigated whether the *ex vivo* expansion of BM grafts under IL-3/IL-6 stimulation accelerated, with respect to freshly harvested BM, the early hematopoietic recovery of heavily irradiated animals. The results showed that the number of CFU-GM and CFU-S_{12} progenitors in the graft was significantly increased (56 fold and 14 fold, respectively), as a result of a 3 day incubation in the presence of ILs 3 and 6. Daily analyses of animals transplanted with 5×10^4 BM cells, either freshly harvested or expanded for 3 days, showed that the expanded grafts consistently allowed a faster hematopoietic recovery of recipients. Differences between both groups of transplanted animals were most evident when the number of either femoral or splenic CFU-GMs were compared, with increases close to 70 fold at the fifth day of engraftment (Fig. 2A). Similarly, mice transplanted with expanded grafts showed a hastened recovery in the cellularity of both organs, that was most significant during the second week following transplantation (with maximal increases of 15 and 40 fold in the BM and spleen, respectively) (Fig. 2B). Differences in peripheral leukocyte numbers between both groups of recipients were much less remarkable than those observed in the hematopoietic organs, although from the nadir period to the eleventh day post-transplantation differences ranging from 2 to 6 fold were apparent, consistent with a higher rate of survival of the mice (fig. 2C, 2D) . Finally, the high degree of exogenous lympho-hematopoietic reconstitution observed in recipients 4 and 9 months after transplantation with 10^5 5FU treated BM cells - either freshly harvested or following a 3 day-expansion - revealed the preservation of the long-term repopulating capacity of expanded grafts (*Serrano et al. 1994*).
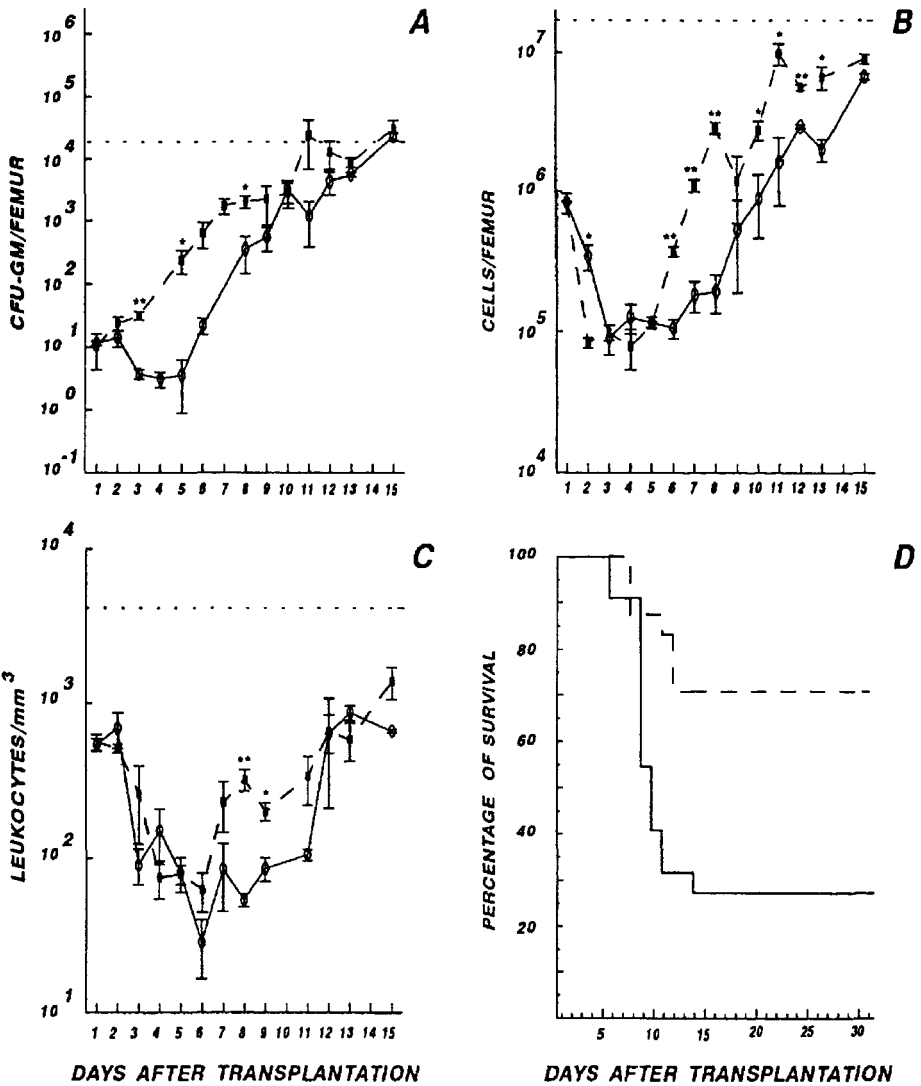
Figure 2: Comparison of the early hematopoietic engraftment (femoral CFU-GM content, panel A; femoral cellularity, panel B; peripheral leucocyte numbers, panel C) and the survival of mice transplanted with 5×10^4 5FU treated bone marrow cells (panel D), prior to (●) and after a 3-day expansion (■) under IL-3/IL-6 stimulation. Each point represents the mean value ± s.e. obtained from 3 mice individually analysed, corresponding to one representative experiment. Dotted lines represent normal values observed in untreated mice. *p<0.05; **p<0.01 (*Modified from Serrano et al, 1994*).

Similar procedures of expansion (hILs 3,6 and SCF) for human cord blood and mobilized peripheral blood have recently been initiated. In these experiments early hematopoietic progenitors were purified by mini MACS cell sorting. This procedure generated an almost pure (>90% purity) population of CD34$^+$ progenitors which were subsequently cultured in the presence of hematopoietic growth factors (Figure 3a). The incubation of the CD34$^+$ population in the presence of IL3, IL-6 and the SCF expanded the CFU-GM population by two to three orders of magnitude (Figure 3b). These increases suggest that *ex vivo* expansion strategies will also be helpful in the treatment of severely irradiated humans.
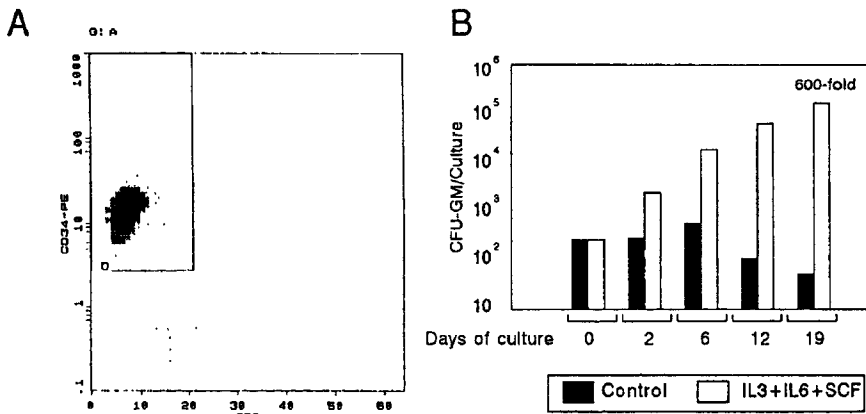
Figure 3: Purification of CD34$^+$ cells from cord blood (A) and *ex vivo* expansion of CFU-GM progenitors in the presence of IL3, IL-6 and SCF (B)

References and Publications:

Radioprotection mediated by the haemopoietic stimulation conferred by AM5: a protein-associated polysaccharides. (1992) Real A, Güenechea G, Bueren JA and Maganto G. **Int.J.Radiat.Biol. 62:65-72**

Mechanisms towards compensation of long-term haemopoietic injury in mice after 5Gy irradiation: In vivo and in vitro enhancement of superoxide anion production by granulocytes. (1992). Gaitan S, Cuenllas E, Sancho P, Bueren JA and Tejero C. **Biosci.Rep.12:281-291**

Residual hematopoietic damage in adult and 8 day-old mice exposed to 7 Gy of X rays. (1993). Grande T, Gaitan S, Tejero C and Bueren JA. **Int.J.Radiat.Biol. 63:59-67**

Involvement of the bone marrow stroma in the residual hematopoietic damage induced by irradiation. (1994) Grande T and Bueren JA. **Exp.Hematol. 22:1283-1287**

Ex vivo expansion and selection of transduced bone marrow: An efficient methodology for gene-transfer to murine lympho-hematopoietic stem cells. (1994). Bernad A, Varas F, Gallego, JM, Almendral JM and Bueren JA. **Br. J. Hematol 87:6-17**

Accelerated and long-term hematopoietic engraftment in mice transplanted with ex vivo expanded bone marrow grafts. (1994) Serrano F, Varas F, Bernad A and Bueren JA. **Bone Marrow Transpl 14:855-862**

AM5, a protein-associated polysaccharides stimulates hematopoiesis and modulates the expression of endogenous hematopoietic growth in murine long-term bone marrow cultures. (1995) Güenechea G, Bueren JA, Maganto G, Tuduri, Guerrero A, Pivel JP and Real A. **Stem Cells 13:175-185**

Long-term hematopoietic analysis of mice irradiated with 500mGy of X rays at different stages of development. (1995) Grande T and Bueren JA. **Radiation Research.** In press

The relevance of myeloablative conditioning in the engraftment of limiting numbers of normal and genetically marked lymho-hematopoietic stem cells. Varas F, Bernad A, almendral JM and Bueren JA. Submitted

Meetings:

Analysis of long-term hematopoietic effects in mice irradiated with 0.5 Gy-X rays during early stages of development (1992). Grande T and Bueren JA. Meeting of the Europ. Soc. for Radiat. Biol Erfurt

Radiation-protection conferred by a biological response modifier of polysaccharidic nature (AM218) (1992). Güenechea G, Albella B, Real A, Bueren JA and Maganto G. Meeting of the Europ. Soc. for Radiat. Biol. Erfurt

Analysis of the self-renewal capacity of CFU-S precursors long-term after 7Gy irradiation (1993). Grande T and Bueren JA. 22nd Meeting of the Int. Soc.for Exp. Hematol. Rotterdam

Analysis of the murine hematopoietic engraftment following transplantation of ex vivo expanded bone marrow (1993). Varas F, Serrano F, Bernad A and Bueren JA. 8th Symposium of Molecular Biology of Hematopoiesis Basel

An improved selection method for retroviral gene transfer to long-term repopulating hematopoietic stem cells (1993). Bernad A, Varas F, Gallego JM, Almendral JM and Bueren JA. Gene Therapy. Keystone Symposia. Colorado

Effect of AM218, a polycarboxilic polysaccharides, on peripheral blood cells recovery in potentially lethally irradiated mice (1993). Albella B, Real A, Güenechea, Bueren JA and Maganto. 22nd Meeting of the Int. Soc. for Exp. Hematol. Rotterdam

Hematopoietic growth factors expression in murine long term bone marrow cultures after in vitro treatment with AM5, a protein-associated polysaccharides (1993). Güenechea G, Real A, Bueren JA and Maganto G. 8th Symposium Mol. Biol. of Hematopoiesis. Basel

Late hematopoietic effects in mice irradiated with 0.5 Gy - X rays during embryonic stages of development (1994). Grande T. and Bueren J.A.Meeting of the Europ. Soc. for Radiat. Biol. Amsterdam

Ex vivo expansion of murine bone marrow: Applications in experimental bone marrow transplantation and retrovirally mediated gene-transfer (1994). Bueren J.A, Bernad A, Varas F, Gallego JM, Almendral JM. First Meeting of the European Haematology Association. Brussels

Radiation-protection and hematological recovery induced by three structurally related polysaccharides (1994). Albella B, Güenechea G, Real A, Tuduri P, Maganto G and Bueren JA. Meeting of the Europ. Soc. for Radiat. Biol. Amsterdam

Long-term hematopoietic deficiencies in mice irradiated at different stages of embryonic development (1994). Grande T and Bueren J.A. European Stem Cell Club Meeting. Barcelona

Polysaccharidic compounds stimulate and radioprotect the hematopoietic system in mice through the release of endogenous hematopoietic growth factors (1994). Real A, Albella B, Güenechea G, Pivel JP, Maganto G and Bueren J.A. European Stem Cell Club Meeting. Barcelona

Head of project 8: Dr. F. Paquet

II. Objectives

(1) To measure the skeletal distribution of ^{141}Ce and ^{85}Sr
(2) To assess the induced biological effects in the cerebellum
(3) To compare these effects with those observed after external irradiation
(4) To determine the dose absorbed in the cerebellum

III. Progress achieved

III.I. Skeletal distribution of ^{141}Ce and ^{85}Sr

The objectives in this first part of the study were to define the skeletal distribution of ^{141}Ce and ^{85}Sr in rats after contamination at both *in utero* and juvenile stages. These stages were chosen because the development of the cerebellum continues after birth.

a) Skeletal distribution of ^{141}Ce

First, pregnant female rats (Sprague Dawley) were contaminated at different stages of gestation, from day 17 p.c. to day 21 (i.e. E17, E18, E19, E20). For each stage, three animals were killed 24 h after contamination and three at day 21. The embryos were dissected and the main organs and skeletal pieces were removed for radiological measurements by gamma counting and for autoradiographic studies. Second, juvenile rats were used and were contaminated at 1,3,5,7 or 9 days after birth. For each stage, four animals were sacrificed at T = 5h; T + 24h and T + 72h. The dissections and radioactivity measurement were done in the same way as after *in utero* contamination.

The distribution of ^{141}Ce occurred mainly in the skeleton. This part of the body accumulated 60 to 85% of the total radioactivity (Fig 1). The liver of the embryos/juveniles accumulated between 10 to 40% of the total radioactivity, depending on the stage of contamination. During the fetal period, the ratio liver / skeleton decreased as the development of the fetus progressed with a minimum at the day of birth. In the same way, this ratio increased with juvenile development, i.e. as the time elapsed from birth increased. Other organs, like kidneys or brain did not accumulate cerium significantly. The study of the distribution in the different parts of the skeleton showed that the ribs and the spinal column concentrated each between 10 and 15% of the skeletal radioactivity, depending on the stage of contamination. The skull concentrated 5 to 10% of the radioactivity and the two femora approximately 3%. A large part of the radioactivity was included in other parts of skeleton which were not separated (mandible, tibia, humerus, etc..). Nevertheless, the distribution in the skeleton seemed not to be homogenous and some variations were noticeable as the stage of contamination increased.

Conclusions:
 The distribution of ^{141}Ce in the different organs of the rat and in the different parts of the skeleton depended on the developmental stage of the animal when contaminated. The skeleton accumulated ^{141}Ce preferentially during the late stages of fetal development, corresponding to the calcification period. Within the skeleton, the skull played an important role, as a source for irradiation of the brain during development. This part of the skeleton accumulated 5 to 10% of

the skeletal radioactivty (i.e. 3 to 8% of the total radioactivity) and had a high specific activity (% IA / g).

b) Skeletal distribvtion of ^{85}Sr

For ^{85}Sr, the methodology employed was the same as for ^{141}Ce. Juvenile rats were contaminated at 1,3,5,7 or 9 days after birth and sacrified either 5 hr, 24 hr or 72 hr later. The skull, ribs, spinal column, femora, liver, kidneys and remaining carcass were analysed by gamma spectrometry.

The distribution of ^{85}Sr occurred mainly in the skeleton (Fig 2). The total ribs + skull+ femora + spinal column accounted for 40-50 % of the total radioactivity. There was no significal difference between the different stages of contamination. The skull accumulated 10-12% of the total body radioactivity, resulting in significant irradiation of the brain.

The localization of both radionuclides in the skull can lead to morphological changes in the brain or in the cerebellum during development. For that reason, it has been interesting to evaluate the microscopical alterations induced, including apoptosis, and to try to correlate them with the radiation dose absorbed.

III.II. Biological effects induced after internal and external contamination

The apoptotic response in the cerebellum was studied in order to assess the dose delivered to that organ after internal or external contamination. Cerebellum is a very sensitive model because of its low spontaneous frequency of apoptosis.

In a first preliminary study, we have studied the distribution of apoptosis in the external granular layer (EGL) of the cerebellum after whole body irradiation of 14 day old rats by gamma rays from ^{60}Co. The animals were killed at different post-irradiation times or at different times after the begining of the continuous exposure. Light microscopy studies were undertaken after 2h-immersion of the central nervous system in a mixture of acetic acid/ethanol (1/3) and storage in ethanol. A sagittal slice of cerebellum was embedded in epoxy resin and 1-μm thick sections were observed after azur staining. A total of at least 500 apoptotic or normal cells were counted. The distribution of apoptotic cells and mitosis were determined according to cell position within the external granular layer (EGL). For this analysis, only EGL areas with 5-6 cells depth were considered. Samples from one or more animals in each group were prepared for electron microscopy study. These animals were anaesthetized as previously described and perfused transcardially for 20 min using a solution of 1% glutaraldehyde, 1% paraformaldehyde in 0.12 M phosphate buffer, pH: 7.3, containing 0.002% CaCl2. The cerebellums were then collected, fixed for 1 hour in the same solution and then kept overnight in the 0.12 M phosphate buffer solution containing 8 % glucose. A thin sagittal slice was then prepared, cut into four section that were post fixed in 1% OsO_4 for 2 hours and embedded in araldite. Thin sections were observed with a CM20 Philips electron microscope after standard uranyl acetate and lead citrate staining.

After acute exposure to 0.25, 0.5, 1.5 and 3 Gy (1 8cGy/min), the mean duration of the apoptotic process gradually increased with dose from 6-9 hours after 0.25 Gy to more than 24 hours after 3 Gy (Fig 3). Up to 1 Gy, maximal frequency was found 6 hours after exposure and, at this post irradiation time, a linear increase in apoptosis with dose was observed. No

effect of dose rate on apoptosis induction could be demonstrated 6 hours after delivering 1 Gy at dose rate from 2.2 to 18 cGy/min. Continuous irradiation at 1.8 cGy/h induced a gradual increase of apoptosis that remained at a plateau value of about 3 % from 15 to 29 h (controls: 0.12%; S.D.: 0.07) and then gradually decreased to 1% at 53 h (Fig. 4). Apoptosis occuring 3 h after acute irradiation, confined to proliferative cells, was only observed for doses of 1.5 and 3 Gy.

In another study, experiments were performed after intraperitoneal contamination of animals with 200, 500 and 1000 kBq of [89]Sr. The animals were sacrified 24 hrs later and the cerebellum was studied as described above. The apoptotic response was determined and compared with that obtained after external irradiation (Fig. 4). The results showed that the apoptotic response was comparable after whole body contamination with 500 kBq of ^{89}Sr and after whole body irradiation with 52cGy (Fig. 5).
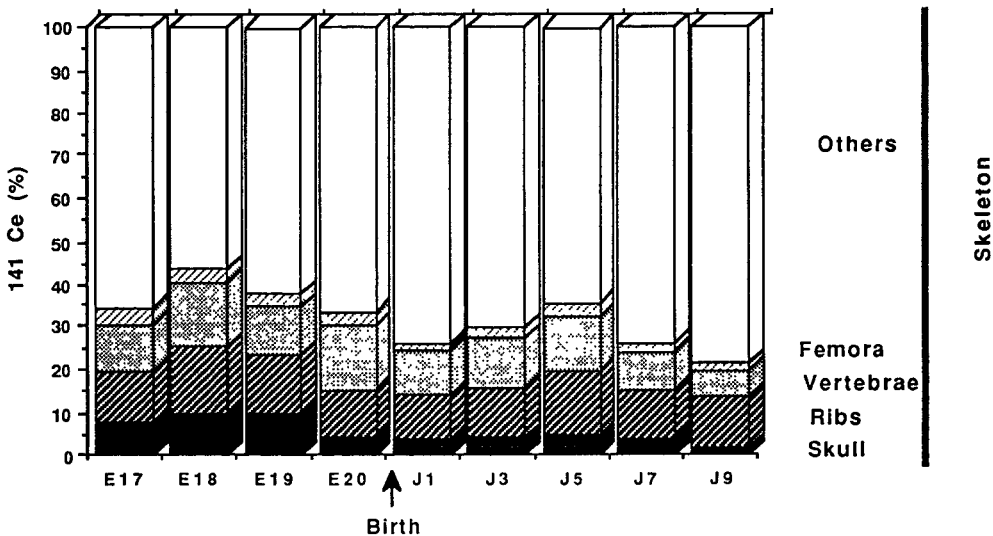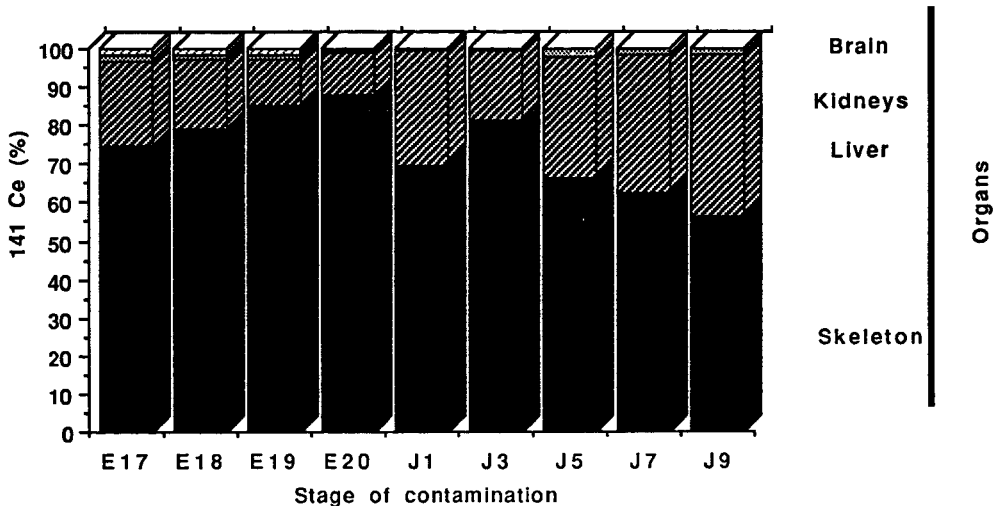
Studies are continuing, and some results have to be obtained with different contamination doses and for other organs including brain and gut. Nevertheless, it has been demonstrated with the results obtained that apoptosis could be used as an biological indicator of internal irradiation, resulting from internal contamination.

Publications:

Fritsch P., Richard-LeNaour H., Denis S., Menetrier F., 1994. Kinetics of radiation-induced apoptosis in the cerebellum of 14 day-old rats after acute or during continuous exposure. Int. J. Radiat. Biol., 66 (1): 111-117.
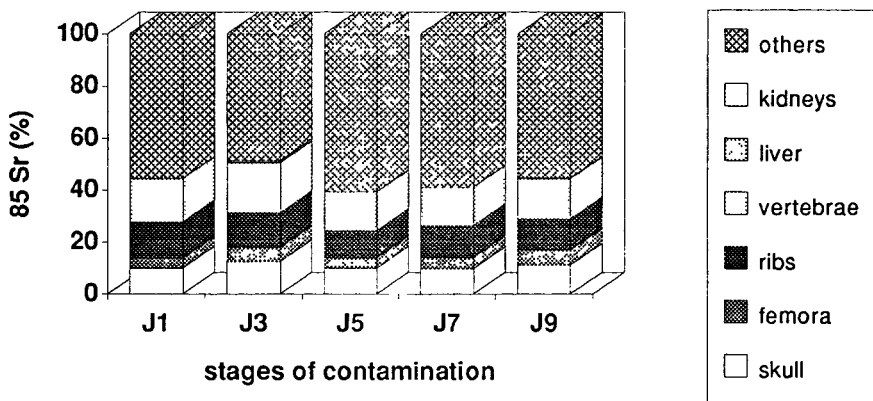
Fritsch P., Richard-LeNaour H. Paquet F., Grillon G., 1995 . Apoptosis scoring for biological dosimetry during histogenesis of the rat cerebellum. Scanning Microscopy. (submitted).
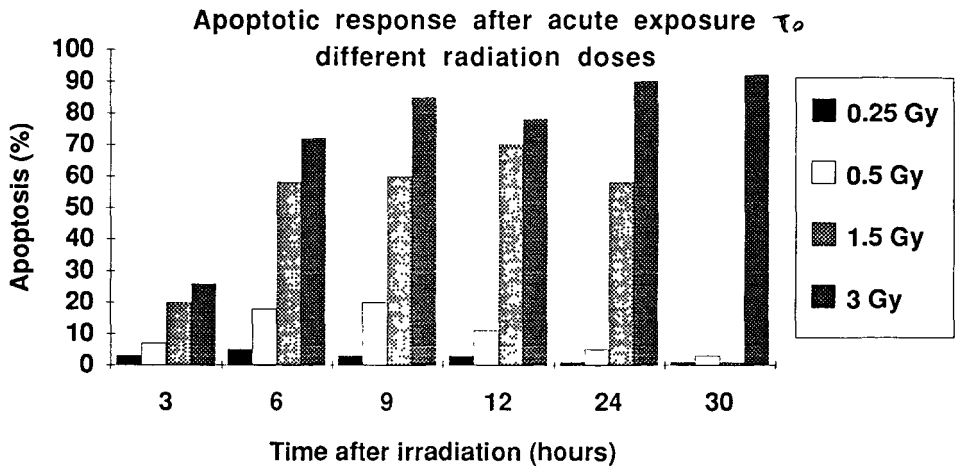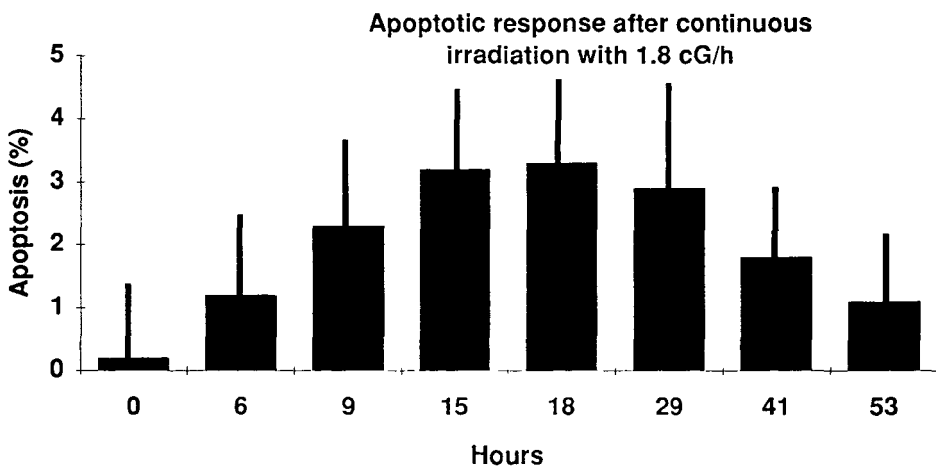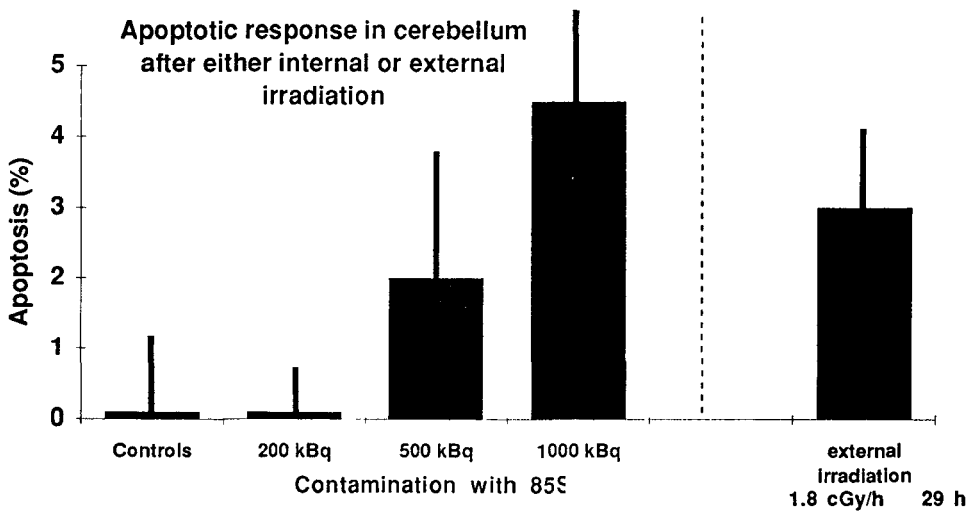CEC Contract PL 920085 - B33

Sacrifice T + 24 hours

Sacrifice T + 24 hrs

Organotropism of 85Sr after juvenile contamination

85 Sr (%)

100
80
60
40
20
0

J1   J3   J5   J7   J9

stages of contamination

- others
- kidneys
- liver
- vertebrae
- ribs
- femora
- skull

Apoptotic response after acute exposure το different radiation doses

Apoptotic response after continuous irradiation with 1.8 cG/h

Apoptotic response in cerebellum after either internal or external irradiation

Apoptosis (%)

Controls 200 kBq 500 kBq 1000 kBq external irradiation 1.8 cGy/h 29 h

Contamination with 85S

CORDIS

The Community Research and Development Information Service

Your European R&D Information Source

CORDIS represents a central source of information crucial for any organisation - be it industry, small and medium-sized enterprises, research organisations or universities - wishing to participate in the exploitation of research results, participate in EU funded science and technology programmes and/or seek partnerships.

CORDIS makes information available to the public through a collection of databases. The databases cover research programmes and projects from their preparatory stages through to their execution and final publication of results. A daily news service provides up-to-date information on EU research activities including calls for proposals, events, publications and tenders as well as progress and results of research and development programmes. A partner search facility allows users to register their own details on the database as well as search for potential partners. Other databases cover Commission documents, contact information and relevant publications as well as acronyms and abbreviations.

By becoming a user of CORDIS you have the possibility to:

• Identify opportunities to manufacture and market new products

• Identify partnerships for research and development

• Identify major players in research projects

• Review research completed and in progress in areas of your interest

The databases - nine in total - are accessible on-line free of charge. As a user-friendly aid for on-line searching, Watch-CORDIS, a Windows-based interface, is available on request. The databases are also available on a CD-ROM. The current databases are:

News (English, German and French version) - Results -
Partners - Projects - Programmes - Publications -
Acronyms - Comdocuments - Contacts

CORDIS on World Wide Web

The CORDIS service was extended in September 1994 to include the CORDIS World Wide Web (WWW) server on Internet. This service provides information on CORDIS and the CORDIS databases, various software products, which can be downloaded (including the above mentioned Watch-CORDIS) and the possibility of downloading full text documents including the work programmes and information packages for all the research programmes in the Fourth Framework and calls for proposals.

The CORDIS WWW service can be accessed on the Internet using browser software (e.g. Netscape) and the address is: http://www.cordis.lu/

The CORDIS News database can be accessed through the WWW.

Contact details for further Information

If you would like further information on the CORDIS services, publications and products, please contact the CORDIS Help Desk :

CORDIS Customer Service   Telephone: +352-401162-240
B.P. 2373   Fax: +352-401162-248
L-1023 Luxembourg   E-mail: helpdesk@cordis.lu
                            WWW: http://www.cordis.lu/

The final report of the 1992-94 period of the radiation protection programme outlines the research work carried out during the whole contractual period under all contracts between the European Commission and research groups in the Member States. More than 450 scientists collaborated on this programme.
Results of more than 500 projects are reported. They are grouped into three sectors:

1. Human exposure to radiation and radioactivity, which includes:
    1.1. Measurement of radiation dose and its interpretation
    1.2. Transfer and behaviour of radionuclides in the environment
2. Consequences of radiation exposure to Man; assessment, prevention and treatment, which includes:
    2.1. Stochastic effects of radiation
    2.2. Non-stochastic effects of radiation
    2.3. Radiation effects on the developing organism
3. Risks and management of exposure, which includes:
    3.1. Assessment of human exposure and risks
    3.2. Optimization and management of radiation protection

Within the framework programme, the aim of this scientific research is to improve the conditions of life with respect to work and protection of man and his environment and to assure safe production of energy, i.e.:

(i) to improve methods necessary to protect workers and the population by updating the scientific basis for appropriate standards;
(ii) to prevent and counteract harmful effects of radiation;
(iii) to assess radiation risks and provide methods to cope with the consequences of radiation accidents.

Venta • Salg • Verkauf • Πωλήσεις • Sales • Vente • Vendita • Verkoop • Venda • Myynti • Försäljning

BELGIQUE/BELGIË

Moniteur belge/Belgisch Staatsblad
Rue de Louvain 40-42/Leuvenseweg 40-42
B-1000 Bruxelles/Brussel
Tel (32-2) 552 22 11
Fax (32-2) 511 01 84

Jean De Lannoy
Avenue du Roi 202/Koningslaan 202
B-1060 Bruxelles/Brussel
Tél (32-2) 538 51 69
Fax (32-2) 538 08 41
E-mail jean de lannoy@infoboard be
URL http://www.jean-de-lannoy be

Librairie européenne/Europese Boekhandel
Rue de la Loi 244/Wetstraat 244
B-1040 Bruxelles/Brussel
Tel (32-2) 295 26 39
Fax (32-2) 735 08 60

DANMARK

J H Schultz Information A/S
Herstedvang 10-12
DK-2620 Albertslund
Tlf (45) 43 63 23 00
Fax (45) 43 63 19 69
E-mail schultz@schultz dk
URL http://www.schultz dk

DEUTSCHLAND

Bundesanzeiger Verlag
Breite Straße 78-80
Postfach 10 05 34
D-50667 Köln
Tel (49-221) 20 29-0
Fax (49-221) 202 92 78
E-mail vertneb@bundesanzeiger de
URL http://www.bundesanzeiger de

ΕΛΛΑΔΑ/GREECE

G. C Eleftheroudakis SA
International Bookstore
Panepistimiou 17
GR-10564 Athina
Tel (30-1) 331 41 80/1/2/3
Fax (30-1) 323 98 21
E-mail elebooks@netor gr

ESPAÑA

Mundi Prensa Libros, SA
Castelló, 37
E-28001 Madrid
Tel (34-1) 431 33 99
Fax (34-1) 575 39 98
E-mail libreria@mundiprensa es
URL http://www.mundiprensa es

Boletín Oficial del Estado
Trafalgar, 27
E-28010 Madrid
Tel (34-1) 538 21 11 (Libros)/
          384 17 15 (Suscripciones)
Fax (34-1) 538 21 21 (Libros)/
          384 17 14 (Suscripciones)
E-mail webmaster@boe es
URL http://www boe es

FRANCE

Journal officiel
Service des publications des CE
26, rue Desaix
F-75727 Paris Cedex 15
Tél (33) 140 58 77 01/31
Fax (33) 140 58 77 00

IRELAND

Government Supplies Agency
Publications Section
4-5 Harcourt Road
Dublin 2
Tel (353-1) 661 31 11
Fax (353-1) 475 27 60

ITALIA

Licosa SpA
Via Duca di Calabria, 1/1
Casella postale 552
I-50125 Firenze
Tel (39-55) 64 54 15
Fax (39-55) 64 12 57
E-mail licosa@ftbcc it
URL http://www.ftbcc it/licosa

LUXEMBOURG

Messageries du livre SARL
5, rue Raiffeisen
L-2411 Luxembourg
Tel (352) 40 10 20
Fax (352) 49 06 61
E-mail mdl@pt lu

Abonnements

Messageries Paul Kraus
11, rue Christophe Plantin
L-2339 Luxembourg
Tel (352) 49 98 88-8
Fax (352) 49 98 88-444
E-mail mpk@pt lu
URL http://www.mpk lu

NEDERLAND

SDU Servicecentrum Uitgevers
Externe Fondsen
Postbus 20014
2500 EA Den Haag
Tel (31-70) 378 98 80
Fax (31-70) 378 97 83
E-mail sdu@sdu nl
URL http://www sdu nl

ÖSTERREICH

**Manz'sche Verlags- und
Universitatsbuchhandlung GmbH**
Siebenbrunnengasse 21
Postfach 1
A-1050 Wien
Tel (43-1) 53 16 13 34/40
Fax (43-1) 53 16 13 39
E-mail auslieferung@manz co at
URL http://www austria EU net 81/manz

PORTUGAL

Imprensa Nacional-Casa da Moeda, EP
Rua Marquês de Sá da Bandeira, 16 A
P-1050 Lisboa Codex
Tel (351-1) 353 03 99
Fax (351-1) 353 02 94, 384 01 32

Distribuidora de Livros Bertrand Ld [a]
Rua das Terras dos Vales, 4/A
Apartado 60037
P-2701 Amadora Codex
Tel (351-1) 495 90 50, 495 87 87
Fax (351-1) 496 02 55

SUOMI/FINLAND

**Akateeminen Kirjakauppa/Akademiska
Bokhandeln**
Pohjoisesplanadi 39/
Norra esplanaden 39
PL/PB 128
FIN-00101 Helsinki/Helsingfors
P /tfn (358-9) 121 41
F /fax (358-9) 121 44 35
E-mail akatilaus@stockmann mailnet fi
URL http://booknet cultnet fi/aka/index htm

SVERIGE

BTJ AB
Traktorvägen 11
S-221 82 Lund
Tfn (46-46) 18 00 00
Fax (46-46) 30 79 47
E-post btjeu-pub@btj se
URL http://www btj se/media/eu

UNITED KINGDOM

**The Stationery Office Ltd
International Sales Agency**
51 Nine Elms Lane
London SW8 5DR
Tel (44-171) 873 90 90
Fax (44-171) 873 84 63
E-mail jill speed@theso co uk
URL http://www the-stationery-office co uk

ISLAND

Bokabud Larusar Blöndal
Skolavördustig, 2
IS-101 Reykjavik
Tel (354) 551 56 50
Fax (354) 552 55 60

NORGE

NIC Info A/S
Ostenjoveien 18
Boks 6512 Etterstad
N-0606 Oslo
Tel (47-22) 97 45 00
Fax (47-22) 97 45 45

SCHWEIZ/SUISSE/SVIZZERA

OSEC
Stampfenbachstraße 85
CH-8035 Zürich
Tel (41-1) 365 53 15
Fax (41-1) 365 54 11
E-mail ulembacher@osec ch
URL http://www osec ch

BÅLGARIJA

Europress-Euromedia Ltd
59, Bld Vitosha
BG-1000 Sofia
Tel (359-2) 980 37 66
Fax (359-2) 980 42 30

ČESKÁ REPUBLIKA

NIS CR — prodejna
Konviktská 5
CZ-113 57 Praha 1
Tel (420-2) 24 22 94 33, 24 23 09 07
Fax (420-2) 24 22 94 33
E-mail nkposp@dec nis cz
URL http://www.nis cz

CYPRUS

Cyprus Chamber of Commerce & Industry
Griva-Digeni 38 & Deligiorgi 3
Mail orders
PO Box 1455
CY-1509 Nicosia
Tel (357-2) 44 95 00, 46 23 12
Fax (357-2) 36 10 44
E-mail cy1691_eic_cyprus@vans infonet com

MAGYARORSZAG

Euro Info Service
Európa Haz
Margitsziget
PO Box 475
H-1396 Budapest 62
Tel (36-1) 111 60 61, 111 62 16
Fax (36-1) 302 50 35
E-mail euroinfo@mail matav hu
URL http://www euroinfo hu/index htm

MALTA

Miller Distributors Ltd
Malta International Airport
PO Box 25
LQA 05 Malta
Tel (356) 66 44 88
Fax (356) 67 67 99

POLSKA

Ars Polona
Krakowskie Przedmiescie 7
Skr pocztowa 1001
PL-00-950 Warszawa
Tel (48-22) 826 12 01
Fax (48-22) 826 62 40, 826 53 34, 826 86 73
E-mail ars_pol@bevy hsn com pl

ROMÂNIA

Euromedia
Str G-ral Berthelot Nr 41
RO-70749 Bucuresti
Tel (40-1) 210 44 01, 614 06 64
Fax (40-1) 210 44 01, 312 96 46

SLOVAKIA

**Slovak Centre of Scientific and Technical
Information**
Namestie slobody 19
SK-81223 Bratislava 1
Tel (421-7) 531 83 64
Fax (421-7) 531 83 64
E-mail europ@tbb1 sltk stuba sk

SLOVENIA

Gospodarski Vestnik
Zaloznska skupina d d
Dunajska cesta 5
SLO-1000 Ljubljana
Tel (386) 611 33 03 54
Fax (386) 611 33 91 28
E-mail belicd@gvestnik si
URL http://www gvestnik si

TURKIYE

Dunya Infotel AS
Istiklâl Cad No 469
TR-80050 Tünel-Istanbul
Tel (90-212) 251 91 96
Fax (90-212) 251 91 97

AUSTRALIA

Hunter Publications
PO Box 404
3167 Abbotsford, Victoria
Tel (61-3) 94 17 53 61
Fax (61-3) 94 19 71 54

CANADA

Subscriptions only/Uniquement abonnements

Renouf Publishing Co. Ltd
5369 Chemin Canotek Road Unit 1
K1J 9J3 Ottawa, Ontario
Tel (1-613) 745 26 65
Fax (1-613) 745 76 60
E-mail renouf@fox nstn ca
URL http://www renoufbooks com

EGYPT

The Middle East Observer
41, Sherif Street
Cairo
Tel (20-2) 393 97 32
Fax (20-2) 393 97 32

HRVATSKA

Mediatrade Ltd
Pavla Hatza 1
HR-10000 Zagreb
Tel (385-1) 43 03 92
Fax (385-1) 43 03 92

INDIA

EBIC India
3rd Floor, Y B Chavan Centre
Gen J Bhosale Marg
400 021 Mumbai
Tel (91-22) 282 60 64
Fax (91-22) 285 45 64
E-mail ebic@giasbm01 vsnl net in

ISRAËL

ROY International
17, Shimon Hatarssi Street
PO Box 13056
61130 Tel Aviv
Tel (972-3) 546 14 23
Fax (972-3) 546 14 42
E-mail royil@netvision net il

Sub-agent for the Palestinian Authority

Index Information Services
PO Box 19502
Jerusalem
Tel (972-2) 627 16 34
Fax (972-2) 627 12 19

JAPAN

PSI-Japan
Asahi Sanbancho Plaza #206
7-1 Sanbancho, Chiyoda-ku
Tokyo 102
Tel (81-3) 32 34 69 21
Fax (81-3) 32 34 69 15
E-mail psijapan@gol com
URL http://www.psi-japan com

MALAYSIA

EBIC Malaysia
Level 7, Wisma Hong Leong
18 Jalan Perak
50450 Kuala Lumpur
Tel (60-3) 262 62 98
Fax (60-3) 262 61 98
E-mail ebic-kl@mol net my

PHILIPPINES

EBIC Philippines
19th Floor, PS Bank Tower Sen
Gil J Puyat Ave cor Tindalo St
Makati City
Metro Manila
Tel (63-2) 759 66 80
Fax (63-2) 759 66 90
E-mail eccpcom@globe com ph

RUSSIA

CCEC
60-letiya Oktyabrya Av 9
117312 Moscow
Tel (70-95) 135 52 27
Fax (70-95) 135 52 27

SOUTH AFRICA

Safto
5th Floor Export House,
CNR Maude & West Streets
PO Box 782 706
2146 Sandton
Tel (27-11) 883 37 37
Fax (27-11) 883 65 69

SOUTH KOREA

Kyowa Book Company
1 F1 Phyung Hwa Bldg
411-2 Hap Jeong Dong, Mapo Ku
121-220 Seoul
Tel (82-2) 322 67 80/1
Fax (82-2) 322 67 82
E-mail kyowa2@ktnet co kr

THAILANDE

EBIC Thailand
Vanissa Building 8th Floor
29 Soi Chidlom
Ploenchit
10330 Bangkok
Tel (66-2) 655 06 27
Fax (66-2) 655 06 28
E-mail ebicbkk@ksc15 th com

UNITED STATES OF AMERICA

Bernan Associates
4611-F Assembly Drive
MD20706 Lanham
Tel (800) 274 44 47 (toll free telephone)
Fax (800) 865 34 50 (toll free fax)
E-mail query@beman com
URL http://www.beman com

**ANDERE LANDER/OTHER COUNTRIES/
AUTRES PAYS**

Bitte wenden Sie sich an ein Buro Ihrer
Wahl / Please contact the sales office of
your choice / Veuillez vous adresser au
bureau de vente de votre choix

NOTICE TO THE READER

Information on European Commission publications in the areas of research and innovation can be obtained from:

◆ **CORDIS, the Community R&D Information Service**

For more information, contact:
CORDIS Customer Service, BP 2373, L-1023 Luxembourg
Tel. (352) 40 11 62-240, Fax (352) 40 11 62-248, e-mail: helpdesk@cordis.lu
or visit the website at http://www.cordis.lu/

◆ **euro abstracts**

The European Commission's periodical on research publications, issued every two months. For a subscription (1 year: ECU 65) please write to the sales office in your country.